FROM TRADITIONAL TO MODERN: PROGRESS OF MOLDS AND YEASTS IN FERMENTED-FOOD PRODUCTION

EDITED BY: Wanping Chen, Jae-Hyuk Yu, Kap-Hoon Han, Jun-ichi Maruyama, Xucong Lv and Van-Tuan Tran

PUBLISHED IN: Frontiers in Microbiology

frontiers Research Topics

ISSN 1664-8714
ISBN 978-2-88974-880-8
DOI 10.3389/978-2-88974-880-8

About Frontiers

Frontiers is more than just an open-access publisher of scholarly articles: it is a pioneering approach to the world of academia, radically improving the way scholarly research is managed. The grand vision of Frontiers is a world where all people have an equal opportunity to seek, share and generate knowledge. Frontiers provides immediate and permanent online open access to all its publications, but this alone is not enough to realize our grand goals.

Frontiers Journal Series

The Frontiers Journal Series is a multi-tier and interdisciplinary set of open-access, online journals, promising a paradigm shift from the current review, selection and dissemination processes in academic publishing. All Frontiers journals are driven by researchers for researchers; therefore, they constitute a service to the scholarly community. At the same time, the Frontiers Journal Series operates on a revolutionary invention, the tiered publishing system, initially addressing specific communities of scholars, and gradually climbing up to broader public understanding, thus serving the interests of the lay society, too.

Dedication to Quality

Each Frontiers article is a landmark of the highest quality, thanks to genuinely collaborative interactions between authors and review editors, who include some of the world's best academicians. Research must be certified by peers before entering a stream of knowledge that may eventually reach the public - and shape society; therefore, Frontiers only applies the most rigorous and unbiased reviews.
Frontiers revolutionizes research publishing by freely delivering the most outstanding research, evaluated with no bias from both the academic and social point of view. By applying the most advanced information technologies, Frontiers is catapulting scholarly publishing into a new generation.

What are Frontiers Research Topics?

Frontiers Research Topics are very popular trademarks of the Frontiers Journals Series: they are collections of at least ten articles, all centered on a particular subject. With their unique mix of varied contributions from Original Research to Review Articles, Frontiers Research Topics unify the most influential researchers, the latest key findings and historical advances in a hot research area! Find out more on how to host your own Frontiers Research Topic or contribute to one as an author by contacting the Frontiers Editorial Office: frontiersin.org/about/contact

FROM TRADITIONAL TO MODERN: PROGRESS OF MOLDS AND YEASTS IN FERMENTED-FOOD PRODUCTION

Topic Editors:
Wanping Chen, University of Göttingen, Germany
Jae-Hyuk Yu, University of Wisconsin-Madison, United States
Kap-Hoon Han, Woosuk University, South Korea
Jun-ichi Maruyama, The University of Tokyo, Japan
Xucong Lv, Fuzhou University, China
Van-Tuan Tran, Vietnam National University, Hanoi, Vietnam

Citation: Chen, W., Yu, J.-H., Han, K.-H., Maruyama, J.-i., Lv, X., Tran, V.-T., eds. (2022). From Traditional to Modern: Progress of Molds and Yeasts in Fermented-Food Production. Lausanne: Frontiers Media SA.
doi: 10.3389/978-2-88974-880-8

Table of Contents

frontiers in Microbiology

EDITORIAL
published: 17 March 2022
doi: 10.3389/fmicb.2022.876872

Editorial: From Traditional to Modern: Progress of Molds and Yeasts in Fermented-Food Production

Wanping Chen[1]*, *Xucong Lv*[2], *Van-Tuan Tran*[3], *Jun-ichi Maruyama*[4], *Kap-Hoon Han*[5] and *Jae-Hyuk Yu*[6,7]

[1] Department of Molecular Microbiology and Genetics, Georg-August-Universität Göttingen, Göttingen, Germany, [2] College of Biological Science and Technology, Fuzhou University, Fuzhou, China, [3] Department of Microbiology, National Key Laboratory of Enzyme and Protein Technology, University of Science, Vietnam National University, Hanoi, Vietnam, [4] Department of Biotechnology, The University of Tokyo, Tokyo, Japan, [5] Department of Pharmaceutical Engineering, Woosuk University, Wanju, South Korea, [6] Department of Bacteriology, University of Wisconsin-Madison, Madison, WI, United States, [7] Department of Systems Biotechnology, Konkuk Institute of Science and Technology, Konkuk University, Seoul, South Korea

Keywords: fermented food, mold, yeast, *Aspergillus, Saccharomyces*, Koji

Editorial on the Research Topic

From Traditional to Modern: Progress of Molds and Yeasts in Fermented-Food Production

INTRODUCTION

Molds (filamentous fungi) and yeasts have been used for the production of foods and beverages throughout the world since ancient times (Venturini Copetti, 2019). For example, yeasts widely contribute to various alcoholic fermentations, such as beer and wine, and non-alcoholic fermentations, such as bread and coffee (Maicas, 2020; Iorizzo et al., 2021). In western countries, *Penicillium* spp. are used for ripening cheeses and meats (Chávez et al., 2011). In the Orient, there are also a variety of fermented foods produced by molds and/or yeasts, which have profoundly shaped the eating habits of the locals. For example, *Aspergillus oryzae* is widely applied for brewing soy sauce, douche, miso, sake, and doenjang etc. (Hong and Kim, 2020; Daba et al., 2021).

Despite the great economic, cultural, and social values of traditional fungal fermentations in food production, these have strong regional characteristics. Therefore, this Research Topic tried to offer a collection of articles associated with different types of fermentation products and processes from different regions, which could provide a global perspective for molds and yeasts in fermented food production. Based on the research content, the articles in this collection could be divided into the following sections.

CHARACTERIZATION AND IMPROVEMENT OF FERMENTATION PROCESS

Tan et al. optimized the production of the soursop kombucha by response surface method, and determined the effects of different storage conditions on the quality, metabolites, and biological activity. This study revealed that prolonged storage conditions have a high potential to improve the quality, metabolites content, biological activity, and the Halal status of the soursop kombucha.

Liu et al. evaluated the effect of different starter cultures on the ripening of dry fermented sausages and found that the lactic acid bacteria could rapidly reduce the pH value of the products and inhibit *Enterobacter putrefaciens* to ensure safety, while the yeasts contributed more in flavor formation and effective inhibition of lipid oxidation.

OPEN ACCESS

Edited and reviewed by:
Giovanna Suzzi,
University of Teramo, Italy

***Correspondence:**
Wanping Chen
chenwanping1@foxmail.com

Specialty section:
This article was submitted to Food Microbiology, a section of the journal Frontiers in Microbiology

Received: *15 February 2022*
Accepted: *21 February 2022*
Published: *17 March 2022*

Citation:
Chen W, Lv X, Tran V-T, Maruyama J-i, Han K-H and Yu J-H (2022) Editorial: From Traditional to Modern: Progress of Molds and Yeasts in Fermented-Food Production. Front. Microbiol. 13:876872. doi: 10.3389/fmicb.2022.876872

Xiao et al. investigated the effect of three yeasts on the Kazak cheese quality and flavor, and the results showed that the texture of cheese added with yeasts was more brittle, suggesting that yeasts are important auxiliary starters for cheese production.

Lee et al. used *Aspergillus cristatus* for the liquid-state and solid-state fermentation of *Panax notoginseng* and examined the contents of protopanaxadiol and protopanaxatriol representing antioxidant activity and skin anti-aging. The results suggested that fermentation of *P. notoginseng* by *A. cristatus* could enhance the quality and availability of bioactive compounds associated with skin anti-aging.

Qin et al. studied the contribution of four non-*Saccharomyces* yeast strains *Issatchenkia terricola* SLY-4, *Pichia kudriavzevii* F2-24, *P. kudriavzevii* F2-16, and *Metschnikowia pulcherrima* HX-13 with β-glucosidase activity to the flavor and quality of wine making. The results showed that in general, the sensory evaluation score of adding non-*Saccharomyces* yeast-fermented wine was better than that of *Saccharomyces cerevisiae*.

Fan et al. isolated a *Clavispora lusitaniae* strain capable of producing a large amount of ethyl caproate from Daqu, a crude fermentation starter for Baijiu, and optimized the fermentation conditions for ethyl caproate production. The results also revealed that this strain can produce many flavor compounds important for high-quality Baijiu and has potential applications in improving the flavor and quality of Baijiu.

Yuan and Chen designed a double-sided petri dish to characterize the cocultivation of *Monascus* spp. and *Aspergillus niger* inspired by black-skin-red-koji. The results indicate that the designed petri dish might be an efficient tool for the investigation of microbial interaction in the laboratory.

Farh et al. cultured *Saccharomyces fibuligera* strains used for the production of *makgeolli* (Korean rice wine) under different pH conditions, and investigated the effect on their enzyme production and gene expression. The results showed that the decrease in pH induced a dimorphic lifestyle switch from yeast cell formation to hyphal growth in *S. fibuligera* and caused a decrease in carbohydrate hydrolyzing enzyme production, and marked changes in the expression of genes related to enzyme production and pH adaptation.

Yang et al. investigated the effects of *Flos sophorae immaturus* on the stability of *Monascus* pigments, the flavor profiles, and the sensory characteristics of Hongqu Huangjiu. The study suggested that the addition of *Flos sophorae immaturus* could be a new strategy for improving the stability of photosensitive pigments and adjusting the aroma of Hongqu Huangjiu.

Chen et al. prepared an artificial starter culture by using the core microbial species of JIUYAO to produce Chinese rice wine and compared its fermentation activity and flavor profiles with traditional JIUYAO and a commercial starter culture. The results showed that the fermentation activity and flavor profiles of the artificial starter resembled those of traditional JIUYAO.

MICROBIOTA OF QU AND FERMENTATION PROCESS

The microbiota of fermented meat products is closely linked with their characteristics (Van Reckem et al., 2019). Chen et al. studied the microbial community structure of Mianning ham and found that *Penicillium lanosum*, *Penicillium nalgiovense*, *Debaryomyces hansenii*, *Staphylococcus equorum*, and *Erwinia tasmaniensis* were isolated from the surfaces of the hams by the traditional culture method, while *Aspergillus*, *Penicillium,* and *Wallemia* were the dominant genera by Illumina high-throughput sequencing. Moreover, the authors identified a total of 60 flavor substances in the hams. Wang et al. summarized and compared the microbial diversity of Chinese ham, sausage, preserved meat, pressed salted duck, preserved fish, and air-dried meat, which is a useful review for the microbial compositions of fermented meat products in China. Wang et al. studied the correlation between the microbial communities and volatile flavor compounds of 15 Suan zuo rou (a traditional fermented pork product) samples from three regions in Guizhou province, and revealed that *Brochothrix*, *Candida*, *Debaryomyces*, *Kazachstania*, *Lactobacillus*, *Leuconostoc*, *Pediococcus*, *Pichia*, *Staphylococcus*, *Weissella*, and *Wickerhamomyces* were highly correlated with 48 volatile flavor compounds.

Qu (Koji) is usually composed of cooked grains inoculated with a fermentation culture and used as the fermentation starter in the production of many Oriental fermented foods (Zhu and Tramper, 2013). The investigation of Qu microbiota could contribute to the understanding on how the fermentation starts. Zhao et al. analyzed the microbiota of three typical traditional Xiaoqu from the Guizhou province in China by metagenomic sequencing, and revealed that *Lactobacillus*, *Bacillus*, *Acinetobacter*, *Leuconostoc*, and *Weissella* were the dominant bacterial genera, while *Aspergillus*, *Saccharomyces*, *Pichia*, *Rhizopus*, and *Phycomyces* are the predominant fungal genera. Zhang et al. explored the microbial shifts in high-temperature Daqu during maturation, and revealed that the predominant bacteria shifted from *Saccharopolyspora* (outer) and *Staphylococcus* (inner) to *Kroppenstedtia* (both outer and inner), while the predominant fungi shifted from *Thermoascus* (both outer and inner) to *Byssochlamys* (outer) and *Fusarium* (inner).

Baijiu is a good representative to study the succession of complex microbiota during fermentation. Hao et al. analyzed the microbial community structure in the initial fermentation of Maotai-flavor Baijiu by high-throughput sequencing and found that *Lactobacillus*, *Pichia*, and *Saccharomyces* were the dominant microorganisms in the initial fermentation. It also suggested that reducing sugar was the key driving factor for microbial succession in the heap fermentation, while acidity, alcohol, and temperature were the main driving forces in pit fermentation. Hu et al. tracked the changes of microbial community in the production of rice-flavor Baijiu by high-throughput sequencing technology and revealed that the dominant bacteria were *Lactobacillus*, while the core fungi were *Saccharomyces* and *Rhizopus*. It inferred that compared to other flavor types of Baijiu, the fewer microbial species but prominent microorganisms may be the main reason for the small variety of flavor substances in rice-flavor Baijiu. Kang et al. investigated the shifts in microbial community diversity of Fuyu-flavor Baijiu from the pretreatment of raw materials to the end of saccharification by high-throughput sequencing and revealed that *Lactobacillus*, *Weissella*, and *Bacillus* in the bacterial community and *Rhizopus*, *Candida*, *Pichia*, and *Aspergillus* in

the fungal community are predominant during raw material pretreatment and saccharification processes. It further indicated that during the saccharification process, the cooling grains and rice husks were the main contributors to the bacterial community composition, and Qu was the main contributor to the shaping of the fungal community structure.

In addition, Zhu et al. investigated the succession of fungal communities on Cabernet Sauvignon grapes from an organic vineyard in Xinjiang at different developmental stages and found that *Aspergillus*, *Malassezia*, *Metschnikowia*, and *Udeniomyces* were predominant during the unripe stage, whereas *Cladosporium*, *Cryptococcus*, *Erysiphe*, and *Vishniacozyma* were dominant in the ripe stages. Ma et al. investigated the dynamic changes of the microbial population and volatile compounds during the spontaneous fermentation of *Petit Manseng* sweet wine and found that *Candida* and *Mortierella* were dominant genera in the fermentation and contributed to the formation of fermentative aroma compounds.

FUNCTIONAL COMPONENTS PRODUCED BY FERMENTATION FUNGI

Cui et al. deleted or overexpressed 2,3-butanediol dehydrogenase (BDH) coding genes BDH1 and BDH2 to evaluate the effect on the content of acetoin and 2,3,5,6-tetramethylpyrazine in *S. cerevisiae*. This work provides a novel method to improve the quality and beneficial health attributes of Baijiu by increasing 2,3,5,6-tetramethylpyrazine production in *S. cerevisiae* by genetic engineering.

Dai et al. isolated and characterized an aromatic strain of *Zygosaccharomyces rouxi* from the chili sauce. They identified the aromatic alcohol with a rose honey scent as 2-phenylethanol and inferred its possible biosynthetic pathway.

Zhang et al. compared the fermentation broths of *Monascus purpureus* with and without glutamic acid supplementation using a metabolomic profiling approach to identify key metabolites and metabolic pathways for improving the yield of monacolin K. The results suggested that the citric acid cycle is closely related with monacolin K yield.

Husakova et al. tested the activity of red yeast rice extract on germination of *Clostridium* and *Bacillus* spores. The results revealed that the extract added to the medium at a concentration of 2% v/v could fully suppress *Clostridium beijerinckii* spore germination, while the addition of 4% v/v extract to the medium containing 1.3% w/w NaCl could fully inhibit *Bacillus subtilis* spore germination.

Wu et al. investigated the difference in the composition of *Monascus* azaphilone pigments between functional Qu and coloring Qu and analyzed their relationships with antioxidant activity. The results indicated that the seven *Monascus* yellow pigments may be the key active components for coloring Qu to have a more potent antioxidant capacity than functional Qu.

Jiang et al. summarized the types, structures, and biosynthetic pathways of glycosphingolipids in filamentous fungi, and the roles of glycosphingolipids in fungal growth, spore formation, and environmental stress response. Furthermore, this review proposed the advantage, potential development, and application of glucosylceramides and galactosylceramides from filamentous fungi *Aspergillus* spp. in health foods and cosmetics.

EVALUATION AND SAFETY CONTROL OF FERMENTED PRODUCTS

Zhao et al. explored the flavor characteristics of three kinds of Japanese soy sauce and identified a total of 173 volatile flavor substances and 160 taste compounds. The results revealed that alcohols and aldehydes were in high abundance in Japanese soy sauce, but pyrazines and esters were only a small portion.

Xu et al. summarized the origin, evolution, and control technology of undesirable metabolites (e.g., ochratoxin A, ethyl carbamate, and biogenic amines) in wine. This review also highlighted current wine industry practices of minimizing the number of biotoxins in wine.

Yang et al. summarized the aspects that may affect the formation of Huangjiu flavor compounds. This review also discussed the selection of appropriate raw materials and the improvement of fermentation technologies to promote the flavor quality of Huangjiu. In addition, this review investigated the effects of microbial community composition, metabolic function of predominant microorganisms, and dynamics of microbial community on the flavor quality of Huangjiu.

GENETIC RESEARCH OF FERMENTATION FUNGI

Jin et al. reviewed the advances in basic research and genetic engineering technologies of the fermentation strain *A. oryzae*, which could open up more effective ways and research space for the breeding of *A. oryzae* production strains in the future. The review of Tanaka and Gomi presented the current knowledge on the regulation of hydrolase gene expression, including carbon catabolite repression, in *A. oryzae*.

Yang et al. studied the role of three kinases, Elm1, Tos3, and Sak1, in the maltose metabolism of baker's yeast in lean dough. The results, for the first time, revealed that Elm1, rather than Tos3 and Sak1, might be the dominant regulator in the maltose metabolism of baker's yeast.

Liu et al. predicted the boundary of the biosynthetic gene cluster of *Monascus* azaphilone pigments (MonAzPs) in *Monascus ruber* M7 by a combination of computational and transcriptional analyses. Then, gene knockouts and analysis of MonAzPs production of the mutants were used to validate the prediction, revealing that the biosynthetic gene cluster consists of 16 genes.

PHYLOGENETIC, PHYSIOLOGICAL, AND GENOMIC FEATURES OF FERMENTATION SPECIES

He et al. isolated a *Monascus sanguineus* strain, and speculated that this strain may be a natural nothospecies based on the morphological characteristics and the phylogenetic relationship

of *Monascus* species. This study provides new insights into how *Monascus* evolved. Zhou et al. found that *Monascus* has good tolerance to lactic acid and ethanol, while the microbial community was repressed at the condition, and then designed a novel restrictive medium for *Monascus* enrichment from Hongqu based on the synergistic stress of lactic acid and ethanol. This work has great application value for the isolation of *Monascus* strain from Hongqu and the better development of its germplasm resources.

Han et al. performed a population genomic analysis of massive *S. cerevisiae* isolates, and suggested that the wild and domesticated populations of *S. cerevisiae* are separated and the domesticated population diverges into two distinct groups associated with solid- and liquid-state fermentations from a single ancestor. This study improves the understanding on the genetic diversity of *S. cerevisiae* strains and how they evolved.

Chacón-Vargas et al. performed a population genomic analysis of *A. oryzae* isolates, especially focusing on the comparison of industrial strains *A. oryzae* 14160 and RIB 40, and revealed substantial genome and phenotypic variation especially for alpha-amylase genes within *A. oryzae*. This study provides insights into the adaptive evolution of *A. oryzae* during domestication.

OPINIONS, PERSPECTIVES, AND REVIEWS ON FUNGAL FERMENTATION INDUSTRY AND RESEARCH

Red mold rice is the fermentation product of *Monascus* spp. and widely used as a food colorant, brewing starter, and monacolin K supplement (Chen et al., 2015). In the opinion of Wang et al., it summarized the current research themes on *Monascus* and proposed some future issues on red mold rice production, the correlation of *Monascus* polyketide biosynthetic pathways and their regulation, and the relationship between *Monascus* development and secondary metabolism. In the perspective of Yanli and Xiang, it summarized the bioactive components of functional red mold rice (FRMR) and their functions, and proposed the efficient strategies for FRMR production, and future directions and challenges of FRMR application.

Sake is a Japanese traditional fermented alcoholic drink, which is brewed using koji mold *A. oryzae* to convert the starch in rice into sugar, and sake yeast *S. cerevisiae* further convert into ethanol (Zhang et al., 2020). In the opinion of Nishida, it highlights the bacterial roles in Sake that is considered exclusively mold/yeast-based. In addition, the opinion points out that bacteria should also be considered for the complete safety assessment of Sake.

In the perspective of Carrau and Henschke, it explained the concept of "friendly" yeasts for developing wine starters that do not suppress desirable native microbial flora at the initial steps of fermentation, summarized the roles of non-Saccharomyces yeasts, and proposed that inoculation of *Hanseniaspora vineae* strains could develop ideal conditions for flavor expression of the microbial terroir without the risk of undesirable strains.

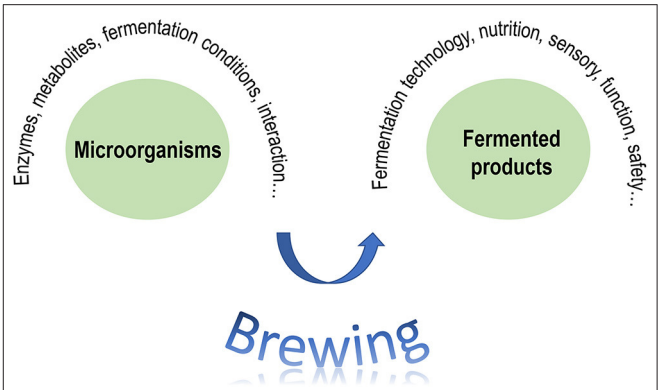

FIGURE 1 | The main research aspects on food fermentation.

Cheese is an ancient traditional fresh or fermented dairy product but with a complex microbial community structure, diverse processing technologies, and flavors. The review of Zheng et al. summarized the research progress on the general processing technology and key control points of natural cheese, the biochemical pathways of cheese flavor formation, the diversity, and the role of yeasts in cheese. This review provides important advances in understanding the effects of different cheese-making techniques and microbial diversity on cheese flavor and quality.

Molds and yeasts play an irreplaceable role in the formation of flavor substances and the production of functional components in traditional Chinese fermented foods. The review of Yang et al. summarized the research progress of molds and yeasts in traditional Chinese fermented foods, including the diversity, population structure and interaction of molds and yeasts, and discussed their application development prospects in related industries.

CONCLUSIONS AND PERSPECTIVES

In general, the research mainly includes two aspects (**Figure 1**). The first aspect revolves around fermentation microorganisms to address their enzymes, metabolites, fermentation conditions, interaction, dynamic changes, etc. The other aspect centers on fermented products to study their fermentation technology, nutrition, sensory, safety, etc. The main purpose is to connect the behaviors of fermentation microorganisms and the properties of fermented products.

Although this Research Topic focused on molds and yeasts, the brewing processes from microorganisms to products in most cases are complex and involve a plethora of strains including bacteria. For example, as revealed by many studies in the topic, the microbiota of Qu and Baijiu fermentation process cooperatively involved a high number of fungi and bacteria. In the previous studies, most of research attention has been focused on some key microorganisms. However, as proposed in the opinion of Nishida and perspective of Carrau and Henschke, more attention may need to be paid to the synergy of the microbiome other than several key microorganisms. Hopefully,

with the development of new technologies, especially the emerging omics tools like metagenomics, metatranscriptomics, metaproteomics, and microbiomics, further studies will provide a more comprehensive and vivid perspective on food fermentation.

AUTHOR CONTRIBUTIONS

WC drafted the manuscript. All authors contributed to the final version and approved it for publication.

REFERENCES

Chávez, R., Fierro, F., García-Rico, R. O., and Laich, F. (2011). "Mold-fermented foods: *Penicillium* spp. as ripening agents in the elaboration of cheese and meat products," in *Mycofactories,* ed A. L. Leitão (Emirate of Sharjah: Bentham Science Publisher), 73–98.

Chen, W., He, Y., Zhou, Y., Shao, Y., Feng, Y., Li, M., et al. (2015). Edible filamentous fungi from the species *Monascus*: early traditional fermentations, modern molecular biology, and future genomics. *Compr. Rev. Food Sci. Food Saf.* 14, 555–567. doi: 10.1111/1541-4337.12145

Daba, G. M., Mostafa, F. A., and Elkhateeb, W. A. (2021). The ancient koji mold (*Aspergillus oryzae*) as a modern biotechnological tool. *Bioresour. Bioprocess.* 8:52. doi: 10.1186/s40643-021-00408-z

Hong, H. H., and Kim, M. K. (2020). Physiochemical quality and sensory characteristics of koji made with soybean, rice, and wheat for commercial doenjang production. *Foods* 9:975. doi: 10.3390/foods9080975

Iorizzo, M., Coppola, F., Letizia, F., Testa, B., and Sorrentino, E. (2021). Role of yeasts in the brewing process: tradition and innovation. *Processes* 9:839. doi: 10.3390/pr9050839

Maicas, S. (2020). The role of yeasts in fermentation processes. *Microorganisms* 8:1142. doi: 10.3390/microorganisms8081142

Van Reckem, E., Geeraerts, W., Charmpi, C., Van Der Veken, D., De Vuyst, L., and Leroy, F. (2019). Exploring the link between the geographical origin of European fermented foods and the diversity of their bacterial communities: the case of fermented meats. *Front. Microbiol.* 10:2302. doi: 10.3389/fmicb.2019.02302

Venturini Copetti, M. (2019). Yeasts and molds in fermented food production: an ancient bioprocess. *Curr. Opin. Food Sci.* 25, 57–61. doi: 10.1016/j.cofs.2019.02.014

Zhang, K., Wu, W., and Yan, Q. (2020). Research advances on sake rice, koji, and sake yeast: a review. *Food Sci. Nutr.* 8, 2995–3003. doi: 10.1002/fsn3.1625

Zhu, Y., and Tramper, J. (2013). Koji – where East meets West in fermentation. *Biotechnol. Adv.* 31, 1448–1457. doi: 10.1016/j.biotechadv.2013.07.001

Conflict of Interest: The authors declare that the research was conducted in the absence of any commercial or financial relationships that could be construed as a potential conflict of interest.

frontiers in Microbiology

ORIGINAL RESEARCH
published: 29 October 2020
doi: 10.3389/fmicb.2020.597454

Zygosaccharomyces rouxii, an Aromatic Yeast Isolated From Chili Sauce, Is Able to Biosynthesize 2-Phenylethanol *via* the Shikimate or Ehrlich Pathways

Jun Dai[1,2,3†], Ke Li[1†], Na Song[1], Wanting Yao[1], Huili Xia[1], Qiao Yang[2], Xiaoling Zhang[2], Xin Li[1], Zhi Wang[1], Lan Yao[1], Shihui Yang[3] and Xiong Chen[1]*

[1] Key Laboratory of Fermentation Engineering (Ministry of Education), National "111" Center for Cellular Regulation and Molecular Pharmaceutics, Hubei Provincial Cooperative Innovation Center of Industrial Fermentation, College of Bioengineering, Hubei University of Technology, Wuhan, China, [2] ABI Group, College of Marine Science and Technology, Zhejiang Ocean University, Zhoushan, China, [3] State Key Laboratory of Biocatalysis and Enzyme Engineering, School of Life Sciences, Hubei University, Wuhan, China

OPEN ACCESS

Edited by:
Xucong Lv,
Fuzhou University, China

Reviewed by:
Chongde Wu,
Sichuan University, China
Sheng Yin,
Beijing Technology and Business University, China

***Correspondence:**
Xiong Chen
cx163_qx@163.com

[†] These authors have contributed equally to this work and share first authorship

Specialty section:
This article was submitted to Food Microbiology, a section of the journal Frontiers in Microbiology

Received: 21 August 2020
Accepted: 06 October 2020
Published: 29 October 2020

Citation:
Dai J, Li K, Song N, Yao W, Xia H, Yang Q, Zhang X, Li X, Wang Z, Yao L, Yang S and Chen X (2020) Zygosaccharomyces rouxii, an Aromatic Yeast Isolated From Chili Sauce, Is Able to Biosynthesize 2-Phenylethanol via the Shikimate or Ehrlich Pathways. Front. Microbiol. 11:597454. doi: 10.3389/fmicb.2020.597454

We isolated an aromatic strain of yeast (M2013310) from chili sauce. Assembly, annotation, and phylogenetic analysis based on genome sequencing, identified M2013310 as an allodiploid yeast that was closely related to *Zygosaccharomyces rouxii*. During fermentation, M2013310, produced an aromatic alcohol with a rose-honey scent; gas chromatography tandem mass spectrometry identified this alcohol as 2-phenylethanol. The concentration of 2-phenylethanol reached 3.8 mg/L, 1.79 g/L, and 3.58 g/L, in M3 (NH_4^+), M3 (NH_4^+ + Phe), and M3 (Phe) culture media, after 72 h of fermentation, respectively. The mRNA expression levels of *ARO8* encoding aromatic aminotransferases I and *ARO10* encoding phenylpyruvate decarboxylase by M2013310 in M3 (Phe) were the lowest of the three different forms of media tested. These results indicated that M2013310 can synthesize 2-phenylethanol via the Shikimate or Ehrlich pathways and the production of 2-phenylethanol may be significantly improved by the over-expression of these two genes. Our research identified a promising strain of yeast (M2013310) that could be used to improve the production of 2-phenylethanol.

Keywords: aroma-producing strain, *Zygosaccharomyces rouxii*, 2-phenylethanol, Shikimate pathway, Ehrlich pathway

INTRODUCTION

The *Zygosaccharomyces* genus consists of six different species: *Z. bailii*, *Z. bisporus*, *Z. kombuchaensis*, *Z. lentus*, *Z. mellis*, and *Z. rouxii* (Zuehlke et al., 2013). *Z. rouxii* is a halotolerant and osmotolerant species of yeast that is most phylogenetically related to *Saccharomyces cerevisiae* (Kobayashi and Hayashi, 1998; Solieri et al., 2013; Guo et al., 2020). It is known that *Z. rouxii* has different genomic forms, including haploid and allodiploid forms, at least (Kinclová et al., 2001; Solieri et al., 2013; Watanabe et al., 2017). *Z. rouxii* CBS732 is a haploid strain featuring one copy of each gene (Montigny et al., 2000; Kinclová et al., 2001). ATCC 42981, isolated from miso paste, features a mosaic genome with two copies of many genes and represents a sterile allodiploid (Kinclová et al., 2001; Bizzarri et al., 2016). Generally, the *Z. rouxii* strain of yeast is applied during

the fermentation process used to make soy sauce and miso paste (Kobayashi and Hayashi, 1998; Dakal et al., 2014) and can produce a range of different volatile compounds, including ethanol, ethyl propanoate, 1-butanol, ethyl 2-methylpropanoate, 4-hydroxy-2-ethyl-5-methyl-3(2H)-furanone (HEMF), and 2-phenylethanol (Lee et al., 2014).

2-Phenylethanol (2-PE) is a higher aromatic alcohol that is characterized by its rose-honey-like fragrance and has been utilized as a fragrance ingredient in a range of different products, including cosmetics, perfumes, beer, olive oil, tea, and coffee (Scognamiglio et al., 2012; Chreptowicz et al., 2016). Furthermore, 2-PE plays an important role in the pharmaceutical industry because it can exert antibacterial effects on Gram-negative bacteria, coccus, bacillus, and some fungi (Fraud, 2003). Natural forms of 2-PE are extracted from aromatic essential plant oils, including rose, jasmine, or hyacinth; however, it is difficult to satisfy market demand and the commercial price of this extraction process is high (approximately $1,000/kg). Over recent years, the majority of global 2-PE production involved a chemical process that is far less extensive ($5/kg). However, this chemical process is limited by the fact that it involves benzene and styrene (known carcinogens) and produces byproducts that are difficult to remove (Etschmann et al., 2002; Hua and Xu, 2011). Therefore, 2-PE is now synthesized mostly by microbial fermentation; this is far more cost-effective and provides much simpler and more efficient options for product purification. Bacteria such as *Enterobacter* sp. CGMCC 5087 (Zhang et al., 2014), and fungi such as *Aspergillus oryzae* (Masuo et al., 2015), are able to successfully produce 2-PE, but with relatively low yield.

The microorganisms that are most efficient at producing 2-PE are yeasts, including *S. cerevisiae, Kluyveromyces marxianus*, *Kluyveromyces lactis, Pichia fermentans*, *Candida glycerinogenes*, and *Z. rouxii* (Etschmann et al., 2003; Kim et al., 2014; Lu et al., 2016; Chreptowicz et al., 2018; Martínez-Avila et al., 2019). Yeasts are known to predominantly biosynthesize 2-PE *via* the Shikimate or Ehrlich pathways (**Figure 4**) (Wang et al., 2019). The Shikimate pathway is a long pathway with multiple branches and a variety of inhibitory feedback mechanisms (Etschmann et al., 2002); this pathway is associated with low yields of 2-PE. However, when using amino acids as the sole source of nitrogen, the Ehrlich pathway is far more efficient; consisting of three steps, this pathway is very effective in synthesizing 2-PE.

In the present study, we isolated an aromatic strain of yeast (M2013310) from chili sauce. This yeast produced a rose-honey-like fragrance during fermentation. The strain was identified as *Z. rouxii* and was able to synthesize 2-PE. Next, we used L-Phe or ammonium sulfate as nitrogen sources to help us to investigate the pathways responsible for the biosynthesis of 2-PE in this particular strain.

MATERIALS AND METHODS

Isolation of Yeast Strains and Culture Conditions

Strain M2013310 was isolated from chili sauce in our laboratory. First, the sauce sample was serially diluted with a sterile 0.85% (w/v) NaCl solution. These dilutions were then screened on yeast extract-peptone-glucose (YEPD; 10 g/L of yeast extract, 20 g/L of peptone, and 20 g/L of glucose) agar plates prepared with 15 g/L of agar and 180 g/L of NaCl. After incubation for 7 days at 30°C, individual colonies were isolated and purified by repeated streaking. Isolates were maintained on YEPD agar slants and kept at 4°C before preservation by freeze-drying. Yeast isolates were routinely sub-cultured in YEPD at 30°C for 72 h with shaking at 200 rpm.

Strain M2013310 was cultivated in 50 mL of YEPD medium and activated in 250 mL flasks at 30°C with shaking at 200 rpm. Subsequently, 2.5 mL of secondary activated cells grown to mid-log phase and inoculated into M3 (Phe) based on Mierzejewska et al. (2017), M3 (NH_4^+), and M3 (NH_4^+ + Phe) culture media (**Table 1**), respectively. These were incubated at 30°C with shaking at 200 rpm for 6 h, 12 h, 24 h, 36 h, 48 h, or 72 h (in triplicate).

Morphological and Physiological Analysis

Isolates were characterized using established criteria for spore formation and the physiological tests described by Kurtzman et al. (2011). Cell morphology was examined by optical microscopy. Sugar fermentation and assimilation tests were also performed using the VITEK system with YST cards, in accordance with the manufacturer's instructions (bioMérieux). The effects of various culture media on cell growth were examined in test tubes containing 10 ml of liquid medium; these were inoculated with approximately 10^5 cells/mL. Tubes were then incubated under both static and shaking conditions (200 rpm) for 7 days. The ability of the isolates to grow at different temperatures (4, 8, 16, 20, 28, 34, 37, and 40°C) was then evaluated using YEPD medium. In order to test the effects of high sugar concentrations on growth, we supplemented the YEPD medium with different amounts of glucose (200 g/L, 400 g/L, and 600 g/L) and incubated these cultures at 28°C. We also investigated growth in modified YEPD (mYEPD), which lacked glucose but contained fructose (20 g/L), at 28°C. Cell density was monitored by measuring OD_{600}.

Genome Sequencing, Assembly, and Annotation

Genomic DNA was extracted from strain M2013310 from pure cultures and sequenced on a PacBio single-molecule real-time (SMRT) Sequel sequencer. *De novo* genome assembly of the PacBio reads was then carried out using the hierarchical genome-assembly process (HGAP4) with default parameters, including consensus polishing with Quiver (Chin et al., 2013). Augustus (version 3.3) was used for gene prediction (Stanke and Morgenstern, 2005), and non-coding RNA was identified by sequence alignment with the Rfam database (version 12.0) (Gardner et al., 2009). Gene functional annotation was performed by aligning the protein sequences to the National Center for Biotechnology Information Non-redundant protein sequences (NCBI NR), Clusters of orthologous groups for eukaryotic complete genomes (KOG), and Kyoto Encyclopedia of Genes

TABLE 1 | The compositions of the cell culture media used to produce 2-PE in this study.

	Glucose (g/L)	Sucrose (g/L)	YNB (g/L)	l-Phe (g/L)	$(NH_4)_2SO_4$ (g/L)	$MgSO_47H_2O$ (g/L)
M3 (Phe)	30	8	1.7	9	–	0.5
M3 (Phe + NH_4^+)	30	8	1.7	4.5	2.25	0.5
M3 (NH_4^+)	30	8	1.7	–	4.5	0.5

Yeast nitrogen base (YNB) without amino acids and ammonium sulfate (BD Co., Ltd.).

and Genomes (KEGG) databases, using BLASTP v2.3.0+ with an E-value cut-off of 1×10^{-5}.

Phylogenetic Analysis

Orthologous and paralogous gene families were assigned from six species (*Z. rouxii*, *Z. bailii*, *Z. parabailii*, *S. cerevisiae*, *S. eubayanus*, and *S. arboricola*) by OrthoFinder (Emms and Kelly, 2015) with default parameters. Gene families that contained only one gene for each species were selected to construct a phylogenetic tree. The protein sequences of each gene family were independently aligned by Muscle v3.8.3 (Edgar, 2004) and then concatenated into one super-sequence. The phylogenetic tree was constructed by maximum likelihood (ML) using PhyML v3.0 (Guindon et al., 2010; Darriba et al., 2011).

Determination of Volatile Flavor Components

Gas chromatography tandem mass spectrometry (1200 L GC/MS-MS; Varian Company, United States) was used to detect volatile flavor components. Chromatography included a DB-WAX (30 m × 0.25 mm × 0.25 μm) capillary column. Helium was used as a carrier gas (flow rate: 0.8 mL/min). The initial temperature was 40°C; this was maintained for 4 min. A 6°C/min rate was then used to reach 160°C, and a 10°C/min rate to reach 220°C; this was maintained for 6 min. Mass spectrometry involved an interface temperature of 250°C, an ion source temperature of 200°C, the EI ionization mode, an electron energy of 70 eV, a detection voltage of 350 V, and an emission current of 200 μA.

The Growth of *Z. rouxii* M2013310 in the Presence of Exogenous 2-PE

In brief, 2.5 mL of the secondary activated strain of *Z. rouxii* M2013310 was inoculated into 50 mL of fresh YEPD medium in five 250 mL flasks and cultivated at 30°C with shaking at 200 rpm. When the cultures achieved an OD_{600} of 0.8, we added 2-PE to five of the flasks to a final concentration of 1, 2, 3, 4, 5 g/L. The sixth flask acted as a control and did not contain 2-PE. Cultures were incubated for 24 h, 48 h, or 72 h (in triplicate) and growth was monitored by the measurement of OD_{600} measurement.

Growth, Glucose Assays, L-Phe, and 2-PE Fermentation Analysis

In brief, 5 ml of each culture was centrifuged at 8000 rpm for 3 min at 4°C. We then discarded the supernatant and added an equivalent volume of deionized water. The OD_{600} was then determined using a spectrophotometer. Glucose consumption was determined by the DNS method (Deed et al., 2018). One milliliter of culture was centrifuged for 10 min at 12000 rpm at 4°C. The remaining supernatant was then used to determine the concentration of 2-PE and L-Phe, which were both quantified by high performance liquid chromatography (Thermo Fisher Scientific) with a C-18 column. A solvent, consisting of ultra-pure water/methanol (40/60), or ultra-pure water/methanol (50/50), was applied for the analysis of 2-PE or L-Phe, respectively, with a constant flow rate of 0.6 mL/min or 1 mL/min. We then estimated the concentrations of 2-PE and L-Phe at 210 nm and 260 nm, respectively.

Quantitative Real-Time PCR (qRT-PCR)

Total RNA was isolated from yeast cells with a total RNA extraction kit (Tiangen Biochemical Technology Co., Ltd.). We then used qRT-PCR to determine the relative mRNA expression levels of *GAP1*, *ARO8*, *ARO9*, *ARO10*, or *ENO1*. The reaction mixture for reverse transcription included 1μg of total RNA, 4 μL of 4 × gDNA wiper Mix, 4 μL of 5 × HiscriptIIqRT SuperMix II, and RNase free ddH_2O (Vazyme Biotech Co., Ltd.). PCR was performed at 50°C for 15 min and 85°C for 5 s. A 20 μL reaction mixture was prepared for each qPCR reaction and contained 10 μL of ChamQ Universal SYBR qPCR Master Mix, gene-specific primers (**Table 2**), 1 μL of Temple DNA/cDNA, and RNase free ddH_2O. PCR was then performed at 95°C for 30 s, with 40 cycles of 95°C for 10 s and 60°C for 30 s, 95°C for 15 s, 60°C for 1 min, and 95°C for 15 s, using a QuantStudio 3 real-time PCR system (Thermo Fisher Scientific). Delta cycle threshold (ΔC_T) values were calculated by the C_Ts of the target genes minus the C_T of *ENO1*, which was used as a housekeeping gene. $\Delta\Delta C_T$ values were calculated by ΔC_T values from the experimental samples – the C_T of the control sample. Fold changes were calculated using the $2^{-\Delta\Delta CT}$ method (Livak and Schmittgen, 2001).

RESULTS AND DISCUSSION

Phenotypic Characteristics

After 3 days of growth at 28°C in YEPD broth, cells from strain M2013310 were observed to adopt an ovoid or slightly elongated shape. These cells were 2.6–2.7 × 4.1–5.0 μm in diameter, non-flagellated, non-gliding, and appeared in pairs or in small groups. Colonies on YEPD agar were white in color, opaque, and circular, with regular margins after incubation for 3 days at 30°C. Growth occurred with 0–24% NaCl (w/v) at 6–34°C and at a pH of 4.0–7.0. Sugar fermentation and assimilation tests showed that the cultures were positive for leucine-arylamidase activity, D-glucose

TABLE 2 | The primers used in this study.

Primers	Sequences
ENO F	5′-CGGTATGGACTGTGCTTCTTCTG-3′
ENO R	5′-GGATGGGTCGCTGTTAGGGTTCTT-3′
ARO9 F	5′-GGTATGCCCAATGCTGGCTTC-3′
ARO9 R	5′-CACTAGCGGCCTCATACCCTCAGTG-3′
ARO10 F	5′-TTACGCTGCTGATGGTTATTCTCGC-3′
ARO10 R	5′-CGGCAACACCATTTATCGCAC-3′
GAP1 F	5′-AAAGATTGCTATTGCTACCGCCAG-3′
GAP1 R	5′-AACGCAGTACCAGACCCAAC-3′
ARO8 F	5′-GCTCAAGGTGTTACTACCATTCC-3′
ARO8 R	5′-GACGTACCAGTTGGGTTTTGAC-3′

TABLE 3 | The assembly of the genome for strain M2013310.

Assembly feature	CCTCC M2013310
Assembled sequence (bp)	18,600,657
No. of scaffolds	38
Sequence depth	303.70
Maximum contig length (bp)	1,922,742
N50 length (bp)	1,437,955
N90 length (bp)	819,506
GC content in Genome (%)	39.9

assimilation, D-mannose assimilation, and xylitol assimilation. However, the cultures were negative for L-lysine-arylamidase, tyrosine arylamidase, β-*N*-acetyl-glucosaminidase, γ-glutamyl-transferase, PNP-*N*-acetyl-beta-D-galactosaminidase, urease, α-glucosidase, esculin hydrolyze, L-malate assimilation, erythritol assimilation, glycerol assimilation, arbutine assimilation, amygdalin assimilation, D-galactose assimilation, gentiobiose assimilation, lactose assimilation, methyl-A-D-glucopyranoside assimilation, D-cellobiose assimilation, D-maltose assimilation, D-raffinose assimilation, D-melibiose assimilation, D-melezitose assimilation, L-sorbose assimilation, L-rhamnose assimilation, D-sorbitol assimilation, sucrose assimilation, D-turanose assimilation, D-trehalose assimilation, nitrate assimilation, L-arabinose assimilation, D-galacturonate assimilation, L-glutamate assimilation, D-xylose assimilation, DL-lactate assimilation, acetate assimilation, citrate (sodium) assimilation, glucuronate assimilation, L-proline assimilation, 2-keto-D-gluconate assimilation, *N*-acetyl-glucosamine assimilation, and D-gluconate assimilation. Morphological and physiological results demonstrated that strain M2013310 was characteristic of the species *Z. rouxii* (James, 2011).

High-Quality Genome Assembly and Gene Annotation

We generated 7.3 gigabase (Gb) PacBio single-molecule real-time (SMRT) sequences with a mean read length of 3.9 kb. These PacBio SMRT sequences was assembled into 38 contigs with a total length of 18.6 Mb, an N50 length of 1.4 Mb, and an N90 length of 0.8 Mb (**Table 3**), via the hierarchical genome-assembly process (HGAP4).

TABLE 4 | The general features of strain M2013310, *Z. rouxii* CBS732, and *S. cerevisiae* S288c genomes.

Strain	CCTCC M2013310	*Z. rouxii* CBS732	*S. cerevisiae* S288c
Ploidy	(∼2n)	n	n
Genome size (Mb)	18.6	9.7	12.3
GC content in genome (%)	39.9	39.1	38.3
Total number of CDS	9,043	4,991	5,769
GC content in CDS (%)	40.7	40.2	40.3
Average CDS length (bp)	1,507	1,491	1,464

The GC content in the genome of strain M2013310 was similar to that of *S. cerevisiae* S288c and *Z. rouxii* CBS732 (**Table 4**). Furthermore, the gene density and mean GC content in the sequence coding for amino acids in protein (CDS) of the M2013310 genome are similar with those described for other hemiascomycetous yeasts, including *S. cerevisiae* S288c and *Z. rouxii* CBS732 (**Table 4**). In total, 9,043 genes were predicted to be present in the genome of M2013310. This is approximately twice that of the genes annotated for *Z. rouxii* CBS732 (4,991 genes), 89.5% of these genes were considered to be duplicated genes (8,097 genes) as the proteins encoded share >70% identity and >70% coverage at the amino acid level (**Supplementary Table S1**). The total genome size of strain M2013310 (18.6 Mb) was well above the size expected for a haploid genome (type strain *Z. rouxii* CBS732, 9.7 Mb). These results indicated that the genome of M2013310 could be diploid. The 9,043 genes identified in strain M2013310 were functionally annotated using KOG function categories (Tatusov et al., 1997) (**Figure 1** and **Supplementary Table S2**). Analysis showed that the highest number of genes were assigned to the functional categories of 'general function prediction only' (869 genes), 'posttranslational modification, protein turnover, chaperones' (702 genes), and 'translation, ribosomal structure and biogenesis' (558 genes). In addition, 493 genes were assigned to unknown functions. The vast majority of the proteins in strain M2013310 exhibited homologs with proteins found in yeast species which are phylogenetically close to species of *Z. rouxii,* including *Z. bailii*, *Torulaspora delbrueckii*, *S. cerevisiae*, and other yeasts of the *Saccharomycetaceae* family. These results showed that M2013310 may be an allodiploid yeast.

Phylogenic Analysis Based on Genome Sequences

The phylogenetic position of M2013310 was evaluated by analyzing eight reference genome sequences from related yeast strains. The phylogenetic tree shows that all strains of the *Saccharomyces* genus and *Zygosaccharomyces rouxii* formed a very tight cluster adjacent to other *Zygosaccharomyces* species. The M2013310 strain formed a branch with *Z. rouxii* CBS732 and both species showed separation from the clade that was phylogenetically linked to *Saccharomyces* species (**Figure 2**). These results showed that M2013310 is more closely related to *Z. rouxii* species, which had also been proved by phylogenetic tree based on 26S rDNA (**Supplementary Figure S1**).

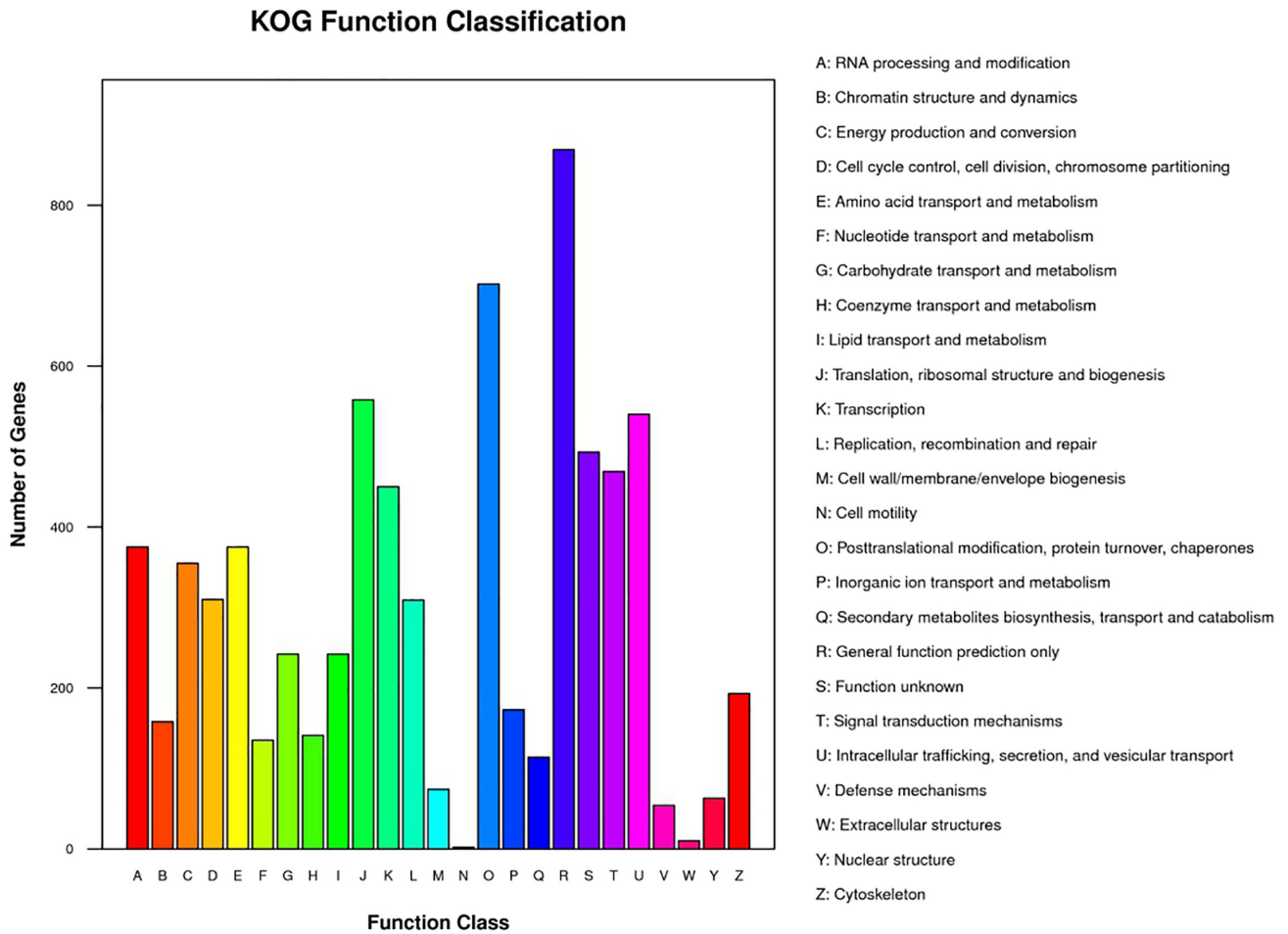

FIGURE 1 | KOG function categories for strain M2013310.

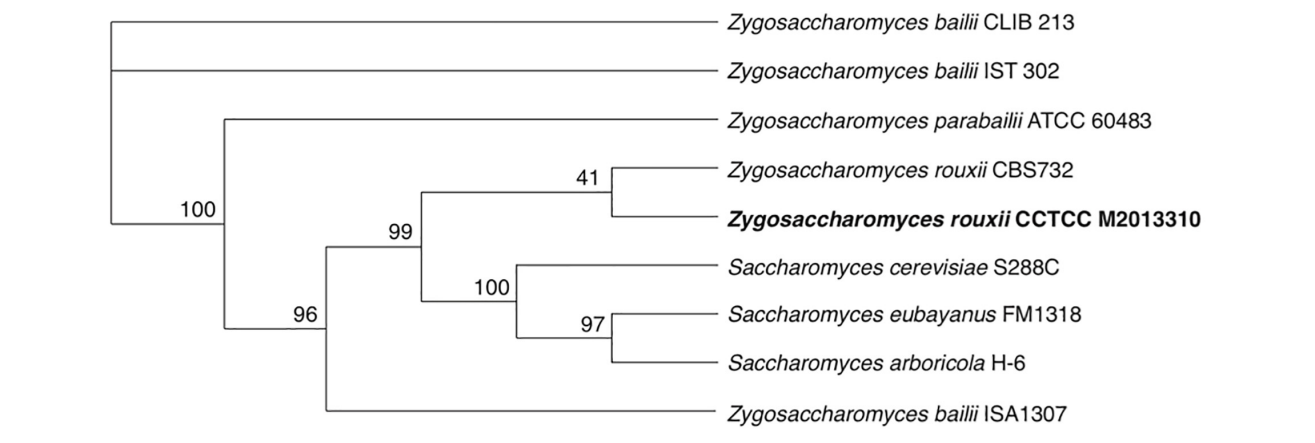

FIGURE 2 | A phylogenetic tree for strain M2013310, as constructed using Orthofinder based on single-copy orthologs.

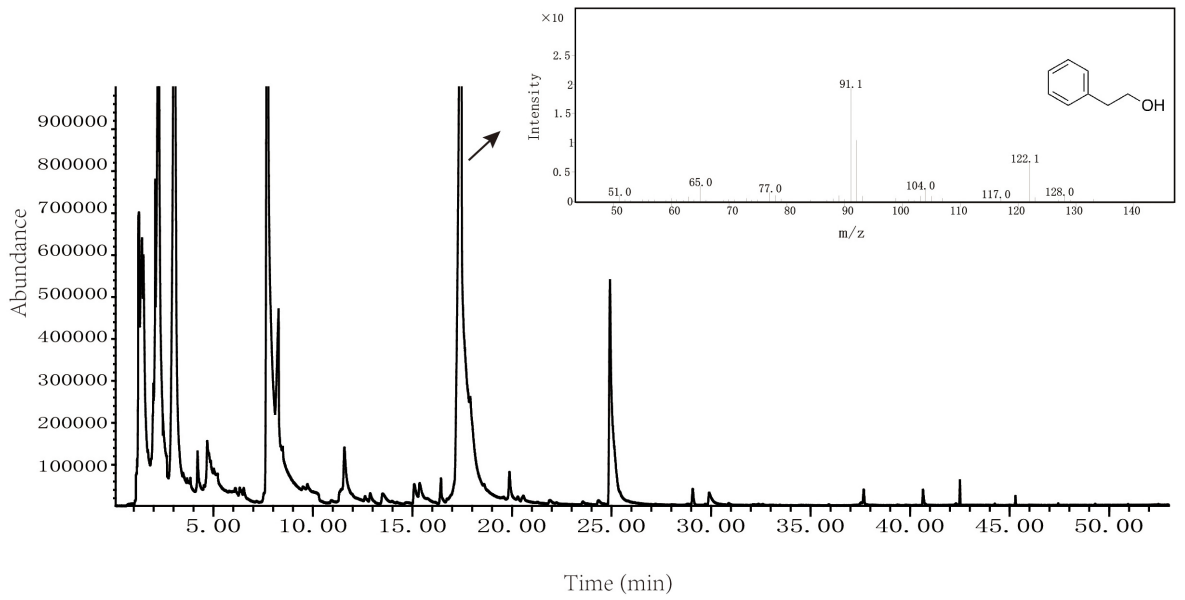

FIGURE 3 | Volatile flavor compounds produced by *Z. rouxii* M2013310.

Determination of Volatile Flavor Components

Volatile flavor compounds produced by *Z. rouxii* M2013310 were analyzed by solid phase micro extraction-mass spectrometry; the resultant spectrum is show in **Figure 3**. We also used spectrometry to identify total ion chromatograms for the volatile flavor components of *Z. rouxii* M2013310, including 16 types of alcohols, 2 types of phenols, 9 types of esters, 6 types of aldehydes, 8 types of ketones, 11 types of acids, 8 types of heterocyclic compounds, and 4 types of alkanes. Some important alcohol compounds (acetic acid, 2-phenylethyl ester, 3-methyl-1-butanol, and 2-phenylethanol) were detected in 7.2%, 11%, 13.2%, and 24.3%, of the total number of volatile flavor compounds, respectively (**Supplementary Table S4**). These results indicated that *Z. rouxii* M2013310 was capable of producing 2-PE.

Analysis of the Pathway Used to Synthesize 2-Phenylethanol

KEGG pathway analysis showed that *Z. rouxii* M2013310 harbors the glycolysis, tricarboxylic acid (TCA), Shikimate, and Ehrlich pathways (**Figure 4** and **Supplementary Table S3**) (Kanehisa et al., 2013). In the presence of preferred nitrogen sources, 2-PE was produced by *de novo* synthesis via the Shikimate pathway. Phosphoenolpyruvate (PEP), and erythrose-4-phosphate (E4P), arising from the glycolysis and pentose-phosphate pathways, respectively, are catalyzed to synthesize 1 by *AROF*, *AROG* and *AROH*, which encode 3-deoxy-7-phosphoheptulonate synthase. Phenylpyruvate is then synthesized via a series of reactions and finally converted into 2-PE. The major limitation of the Shikimate pathway is that the glycolysis and pentose-phosphate pathways are mainly directed into the TCA cycle for cell growth rather than for the synthesis of 2-PE. In comparison, the yield of 2-PE is significantly improved when 2-PE is bio-transformed from L-Phe *via* the Ehrlich pathway. The *ARO9* gene encodes aromatic aminotransferases II while the *ARO8* gene encodes aromatic aminotransferases I; these enzymes catalyze the conversion of L-Phe to phenylpyruvate. However, the by-product of this process, glutamate, is produced during the transamination reaction. *GUDB*, *ROCG*, *GDH2* and *GDHA* encode glutamate dehydrogenase, and enzyme that catalyzes glutamate to synthesize a-ketoglutarate that is directed into the TCA, thus repressing the synthesis of 2-PE *via* the Ehrlich pathway. The *ARO10* gene encodes phenylpyruvate decarboxylase, a rate-limiting enzyme, which catalyzes the decarboxylation of phenylpyruvate to phenylacetaldehyde. *ADH* encode alcohol dehydrogenases that catalyze the reduction of phenylacetaldehyde to form 2-PE (Hazelwood et al., 2008).

The production of 2-PE is highly dependent on the source of nitrogen. Different sources of nitrogen can influence the expression of crucial genes by nitrogen catabolite repression (NCR) (Cooper, 2002). The uptake of non-preferred nitrogen will result in NCR; this will significantly diminish in the presence of preferred nitrogen sources, thus affecting the expression of the general amino acid permease GAP1p that is used to transport aromatic amino acid L-Phe into yeast cells (Sáenz et al., 2014; Wang Z. et al., 2017). *ARO8*, *ARO9*, and *ARO10*, are the predominant research targets for the Ehrlich pathway. *ARO8* is responsible for the biosynthesis of phenylalanine and tyrosine (Iraqui et al., 1998). The expression of *ARO9* is induced by aromatic amino acids; while *ARO9* and *ARO10* are NCR-sensitive genes; their expression levels are regulated by GATA factors consisting of Gln 3 and Gat 1 (Broach, 2012; Lee and Hahn, 2013). Therefore, when using L-Phe as a sole source of nitrogen, yeasts such as *S. cerevisiae* can achieve maximized yields of 2-PE. The identification of the 2-PE biosynthesis pathway, and the roles

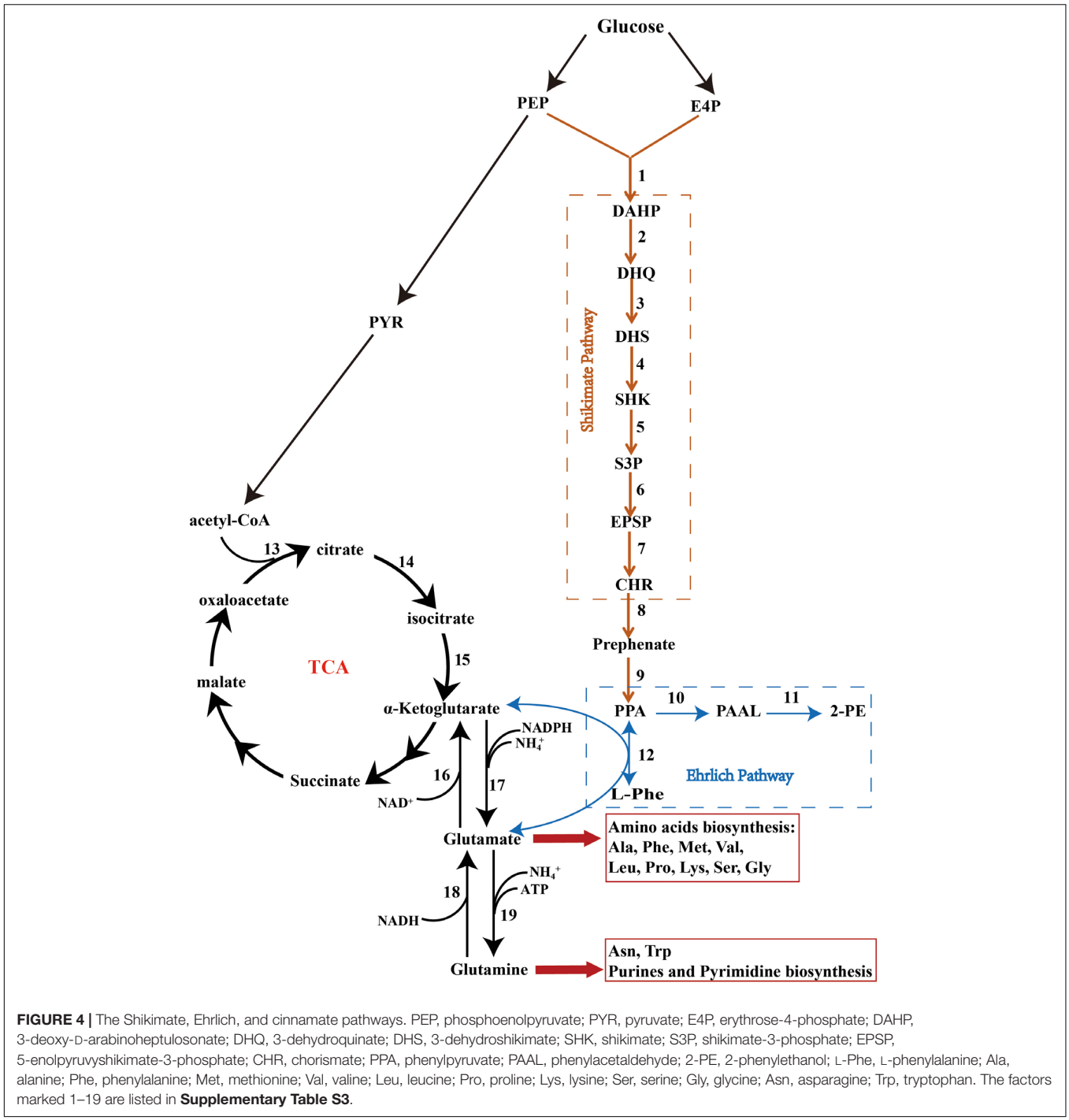

FIGURE 4 | The Shikimate, Ehrlich, and cinnamate pathways. PEP, phosphoenolpyruvate; PYR, pyruvate; E4P, erythrose-4-phosphate; DAHP, 3-deoxy-D-arabinoheptulosonate; DHQ, 3-dehydroquinate; DHS, 3-dehydroshikimate; SHK, shikimate; S3P, shikimate-3-phosphate; EPSP, 5-enolpyruvyshikimate-3-phosphate; CHR, chorismate; PPA, phenylpyruvate; PAAL, phenylacetaldehyde; 2-PE, 2-phenylethanol; L-Phe, L-phenylalanine; Ala, alanine; Phe, phenylalanine; Met, methionine; Val, valine; Leu, leucine; Pro, proline; Lys, lysine; Ser, serine; Gly, glycine; Asn, asparagine; Trp, tryptophan. The factors marked 1–19 are listed in **Supplementary Table S3**.

of specific genes in this pathway, will play an important role in improving the production of 2-PE in a range of commercial sectors.

The Effect of Exogenous 2-PE on the Growth of *Z. rouxii* M2013310

Previous research has shown that 2-PE can enhance reactive oxygen species (ROS) accumulation, lipid peroxidation, and cell membrane damage, thus significantly inhibiting the production of 2-PE (Wang et al., 2020). The 2-PE yield of strain can be improved by the application of *in situ* product removal (ISPR) to alleviate the toxicity of 2-PE (Mierzejewska et al., 2017; Chreptowicz et al., 2018; Hua et al., 2010). Furthermore, the tolerance of strain to 2-PE plays an important role in alleviating product inhibition. To study the tolerance of *Z. rouxii* M2013310 with regards to 2-PE, we cultivated this yeast strain in YEPD supplemented with exogenous 2-PE to final concentrations of

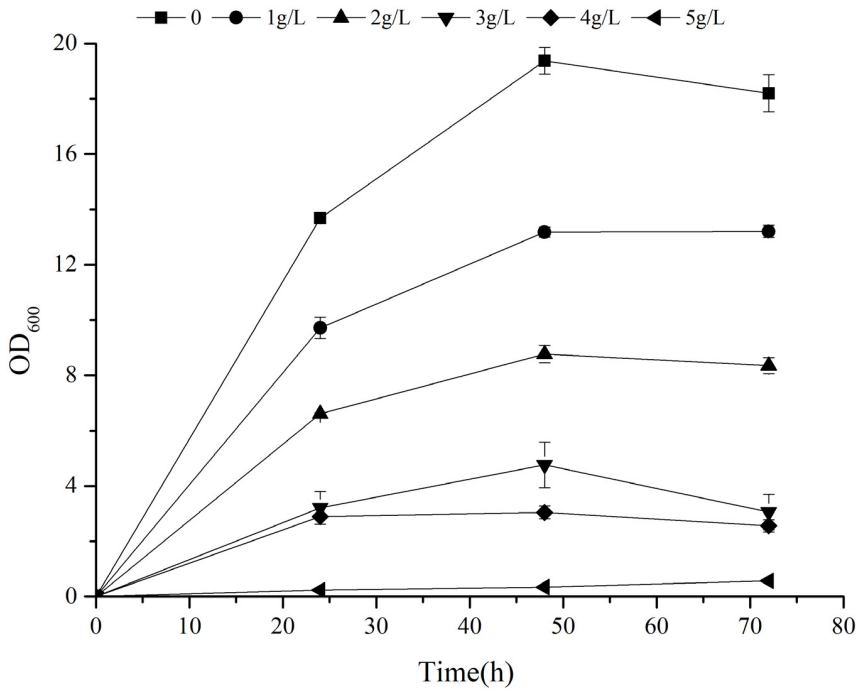

FIGURE 5 | The effect of exogenous 2-PE on the growth of *Z. rouxii* M2013310.

1 g/L, 2 g/L, 3 g/L, 4 g/L and 5 g/L. After 72 h of fermentation, the cell density in the control group control was 7.11- and 32- fold higher than the density of cells in YEPD containing 4 g/L and 5 g/L 2-PE. At concentration of 5 g/L, the growth of the strain was significantly inhibited (**Figure 5**). These results showed that *Z. rouxii* M2013310 is tolerant to 2-PE up to a concentration of 4 g/L.

The Effect of Different Nitrogen Sources on Growth and 2-PE Biosynthesis in *Z. rouxii* M2013310

To further investigate the pathway used to synthesize 2-PE, we inoculated *Z. rouxii* M2013310 into three different culture media: M3 (Phe), M3 (NH_4^+), and M3 (Phe + NH_4^+). The M3 (Phe) and M3 (NH_4^+) media use L-Phe and ammonium sulfate as the sole source of nitrogen, respectively. When cultured in M3 (Phe) media, *Z. rouxii* M2013310 used Ehrlich pathway to biotransform L-Phe into 2-PE. When grown in M3 (NH_4^+) media, the yeast produced 2-PE by *de novo* synthesis (Etschmann et al., 2002, 2004). When grown in M3 (Phe) and M3 (NH_4^+) media, *Z. rouxii* M2013310 entered the stationary phase at 36 h; OD_{600} reached 13.4 and 11.25, respectively. However, the production of 2-PE in M3 (Phe) was 942-fold higher than that in M3 (NH_4^+). The highest yield of 2-PE, without the application of in suit product removal (ISPR), was 3.58 g/L in M3 (Phe) medium. This strain exhibited a four-fold higher capacity to produce 2-PE than *Z. rouxii* CBS 5717 (Etschmann et al., 2003). Collectively, these data indicate that the biotransformation of L-Phe to 2-PE is a key process in the production of 2-PE.

Data relating to cell density and glucose consumption for the yeast were similar when cultivated in either M3 (Phe) or M3 (Phe + NH_4^+) medium, thus indicating that the co-existence of ammonium sulfate and L-Phe did not affect the growth of *Z. rouxii* M2013310. The concentration of 2-PE in M3 (Phe) was two-fold higher than that in M3 (Phe + NH_4^+) after 72 h of fermentation; we anticipated that the production of 2-PE would have continued to increase after this timepoint. During the adaptive period and the log phase, the strains grown in M3 (Phe) and M3 (Phe + NH_4^+) synthesized 2.3 g/L and 1.28 g/L of 2-PE, respectively. The 2-PE synthesis ability in M3 (Phe) and M3 (Phe + NH_4^+) was 64 mg/L/h and 36 mg/L/h, respectively. The consumption of L-Phe was 2.67 g/L and 1.45 g/L, respectively, with a consumption rate of 74 mg/L/h and 40 mg/L/h. After 36 h of fermentation, yeast cells entered the stationary phase and the consumption of L-Phe decreased notably. The consumption of L-Phe was 0.33 g/L and 0.29 g/L after 36 h and 72 h of culture, respectively, with a consumption rate of 9.2 mg/L/h and 8.1 mg/L/h (**Figures 6A,B**). The concentration of 2-PE in M3 (Phe) and M3 (Phe + NH_4^+) increased, to 1.28 g/L and 0.51 g/L, respectively, producing 35.5 mg/L/h and 14.2 mg/L/h of 2-PE, respectively. In M3 (Phe) and M3 (Phe + NH_4^+) media, the yield of 2-PE was 5.3- and 2.3-fold higher than the maximum theoretical concentration of the product that could be achieved by the bioconversion of the remaining L-Phe after 36 h of fermentation. This indicated that there may be additional enzymes that are activated to promote the biotransformation of intermediates in the Ehrlich pathway to synthesize 2-PE, or that the strain also synthesized 2-PE via the Shikimate pathway. These remain for future

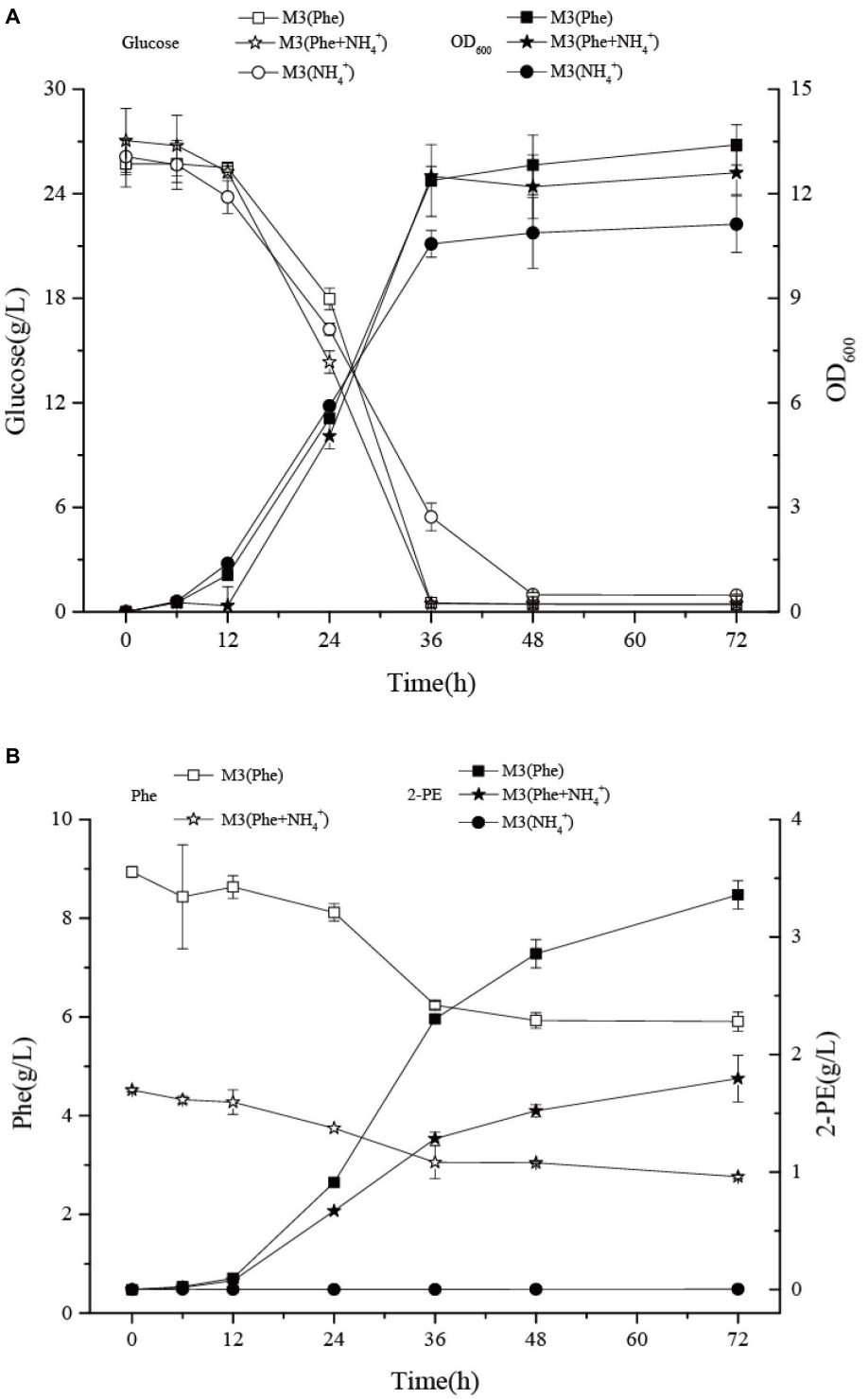

FIGURE 6 | The effects of different nitrogen sources on the growth **(A)** and 2-PE synthesis of *Z. rouxii* M2013310 **(B)**.

studies to determining the concentration of phenylpyruvate and phenylacetaldehyde and the activity of related enzyme (Wang P. et al., 2017; Wang Z. et al., 2017). The transformation ratio of the non-genetically modified strain of *Z. rouxii* M2013310 was 0.53 mol/mol. Furthermore, a strain of *S. cerevisiae* S288c (0.5 mol/mol) that over-expresses *ARO8* and *ARO10* (Yin et al., 2015), exhibited a clear advantage with regards to 2-PE production.

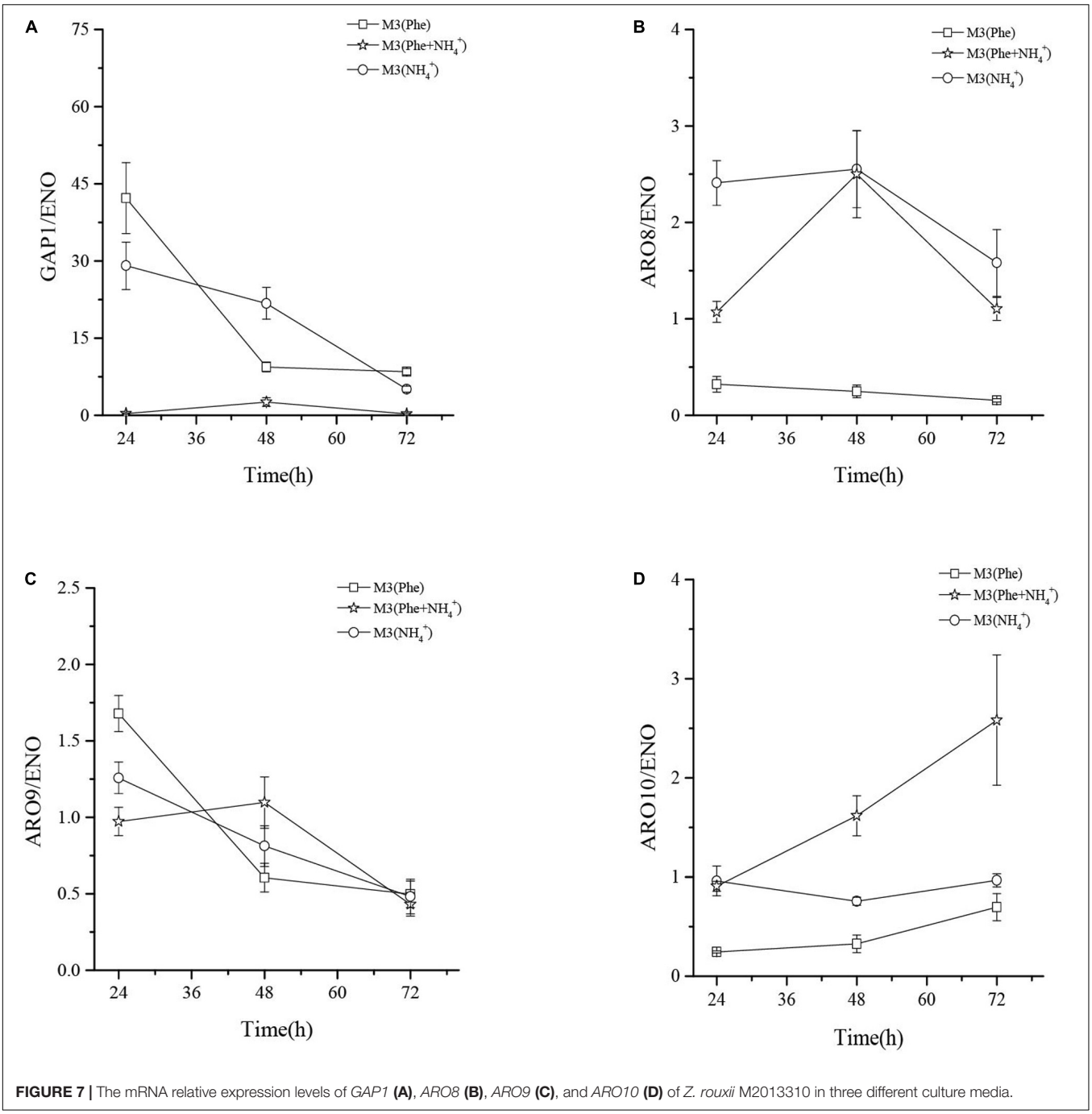

FIGURE 7 | The mRNA relative expression levels of *GAP1* **(A)**, *ARO8* **(B)**, *ARO9* **(C)**, and *ARO10* **(D)** of *Z. rouxii* M2013310 in three different culture media.

The Relative Expression Levels of *GAP1*, *ARO8*, *ARO9*, and *ARO10,* in *Z. rouxii* M2013310 When Cultured in Different Media

qRT-PCR analysis showed that the mRNA levels of general amino acid permease (*GAP1*) in M3 (Phe) and M3 (NH_4^+) were 124- and 86-fold higher than that in M3 (Phe + NH_4^+) after 24 h of fermentation. When L-Phe and ammonium sulfate were used as nitrogen sources, GAP1p activity fell rapidly although L-Phe uptake and bioconversion continued (**Figure 6B**). These results suggested that GAP1p was not the only permease involved in L-Phe uptake (Sáenz et al., 2014).

The mRNA levels of *ARO9* were similar when compared in three different culture media, thus indicating that the concentration of ammonium ions in the media had little effect on the expression of *ARO9*. The expression levels of *ARO8* mRNA in M3 (NH_4^+) and M3 (Phe + NH_4^+) were similar after 48 h of fermentation and the mRNA levels of *ARO8* in the

two types of culture media were 10-fold higher than that in M3 (Phe). The mRNA levels of *ARO10* (2-keto acid decarboxylase) in M3 (NH_4^+) were significantly higher than those in M3 (Phe + NH_4^+) and M3 (Phe) media. The expression levels of *ARO8* and *ARO10* mRNA in M3 (Phe) were lower than in the other two media. However, when comparing the concentration of 2-PE after fermentation of the strain in three different media, we found that the highest concentration of 2-PE was produced by the strain grown in M3 (Phe) media (**Figure 7**). This data suggests that this strain of yeast may bio-transform L-Phe to 2-PE via an alternative pathway, or these crucial enzymes (ARO8p, ARO10p, and GAP1p) may be regulated by other genes such as *AGP1, BAP2,* and *PDC* (Kim et al., 2014; Sáenz et al., 2014). However, this hypothesis needs to be verified by future research studies.

CONCLUSION

In the present study, we used PacBio sequencing technology to characterize the biological properties and genomic features of *Z. rouxii* M2013310, a strain of yeast, that we isolated from chili sauce. In addition, we found that *Z. rouxii* M2013310 was capable of synthesizing 2-PE in YEPD medium. We used three different types of culture media to investigate the pathway by which *Z. rouxii* M2013310 synthesizes 2-PE. The highest concentration of 2-PE synthesized by *Z. rouxii* M2013310 was 3.58 g/L in the M3 (Phe) medium. Transamination and decarboxylation are essential for 2-PE synthesis via the Ehrlich pathway. Similarly, *ARO8*, *ARO9*, and *ARO10*, genes are all crucial L-Phe biotransformation. The mRNA levels of *ARO8* and *ARO10* in *Z. rouxii* M2013310 grown in M3 (Phe) were lower than when the same yeast strain was grown in M3 (NH_4^+) or M3 (Phe + NH_4^+) media. Our data suggest that the Ehrlich pathway may not be the only pathway involved in the synthesis of 2-PE in M3 (Phe) medium of *Z. rouxii* M2013310, although this requires further verification. We identified a promising target strain (*Z. rouxii* M2013310) that can be used to improve the commercial production of 2-PE, which is firstly proposed.

ACCESSION NUMBERS

Zygosaccharomyces rouxii M2013310 has been deposited in China Center for Type Culture Collection under the number: CCTCC M2013310. The assembly and raw sequencing data have been deposited in GenBank under BioProject accession PRJNA577023, WHVI01000000 for genome assembly data, and SRR10260307 for genomic PacBio sequencing data.

DATA AVAILABILITY STATEMENT

The datasets presented in this study can be found in online repositories. The names of the repository/repositories and accession number(s) can be found in the article/**Supplementary Material**.

AUTHOR CONTRIBUTIONS

JD and XC conceived the research. KL, NS, WY, HX, QY, XZ, XL, ZW, LY, and SY conducted all experiments. JD and KL wrote the manuscript. All authors edited and approved the manuscript.

FUNDING

This work was supported by the National Natural Science Foundations of China (Grant Nos. 31871789 and 41876114), Open Funding Project of the State Key Laboratory of Biocatalysis and Enzyme Engineering (Grant No. SKLBEE2018013), the Natural Science Foundation of Hubei Provincial Department of Education (Grant No. B2016046), and the Natural Science Foundation of Zhejiang Province (Grant No. LY18D060007).

SUPPLEMENTARY MATERIAL

The Supplementary Material for this article can be found online at: https://www.frontiersin.org/articles/10.3389/fmicb.2020.597454/full#supplementary-material

REFERENCES

Bizzarri, M., Giudici, P., Cassanelli, S., and Solieri, L. (2016). Chimeric sex-determining chromosomal regions and dysregulation of cell-type identity in a sterile *Zygosaccharomyces* allodiploid yeast. *PLoS One* 11:e0152558. doi: 10.1371/journal.pone.0152558

Broach, J. R. (2012). Nutritional control of growth and development in yeast. *Genetics* 192, 73–105. doi: 10.1534/genetics.111.135731

Chin, C., Alexander, D. H., Marks, P., Klammer, A. A., Drake, J., Heiner, C., et al. (2013). Nonhybrid, finished microbial genome assemblies from long-read SMRT sequencing data. *Nat. Methods* 10, 563–569. doi: 10.1038/nmeth.2474

Chreptowicz, K., Sternicka, M. K., Kowalska, P. D., and Mierzejewska, J. (2018). Screening of yeasts for the production of 2-phenylethanol (rose aroma) in organic waste-based media. *Lett. Appl. Microbiol.* 66, 153–160. doi: 10.1111/lam.12835

Chreptowicz, K., Wielechowska, M., Główczyk-Zubek, J., Rybak, E., and Mierzejewska, J. (2016). Production of natural 2-phenylethanol: from biotransformation to purified product. *Food Bioprod. Process.* 100, 275–281. doi: 10.1016/j.fbp.2016.07.011

Cooper, T. G. (2002). Transmitting the signal of excess nitrogen in *Saccharomyces cerevisiae* from the Tor proteins to the GATA factors: connecting the dots. *FEMS Microbiol. Rev.* 26, 223–238. doi: 10.1016/S0168-6445(02)00071-72

Dakal, T. C., Solieri, L., and Giudici, P. (2014). Adaptive response and tolerance to sugar and salt stress in the food yeast *Zygosaccharomyces rouxii*. *Int. J. Food Microbiol.* 185, 140–157. doi: 10.1016/j.ijfoodmicro.2014.05.015

Darriba, D., Taboada, G. L., Doallo, R., and Posada, D. (2011). ProtTest 3: fast selection of best-fit models of protein evolution. *Bioinformatics* 27, 1164–1165. doi: 10.1093/bioinformatics/btr088

Deed, R. C., Hou, R., Kinzurik, M. I., Gardner, R. C., and Fedrizzi, B. (2018). The role of yeast ARO8, ARO9 andARO10 genes in the biosynthesis of 3-(methylthio)-1-propanol from L-methionine during fermentation in synthetic grape medium. *FEMS Yeast Res.* 19, foy109. doi: 10.1093/femsyr/foy109

Edgar, R. C. (2004). MUSCLE: multiple sequence alignment with high accuracy and high throughput. *Nucleic Acids Res.* 32, 1792–1797. doi: 10.1093/nar/gkh340

Emms, D. M., and Kelly, S. (2015). OrthoFinder: solving fundamental biases in whole genome comparisons dramatically improves orthogroup inference accuracy. *Genome Biol.* 16:722. doi: 10.1186/s13059-015-0721-722

Etschmann, M. M. W., Sell, D., and Schrader, J. (2002). Biotechnological production of 2-phenylethanol. *Appl. Microbiol. Biot.* 59, 1–8. doi: 10.1007/s00253-002-0992-x

Etschmann, M. M. W., Sell, D., and Schrader, J. (2003). Screening of yeasts for the production of the aroma compound 2-phenylethanol in a molasses-based medium. *Biotechnol. Lett.* 25, 531–536. doi: 10.1023/A:1022890119847

Etschmann, M. M. W., Sell, D., and Schrader, J. (2004). Medium optimization for the production of the aroma compound 2-phenylethanol using a genetic algorithm. *J. Mol. Cataly. B Enzym.* 29, 187–193. doi: 10.1016/j.molcatb.2003.10.014

Fraud, S. (2003). Aromatic alcohols and their effect on Gram-negative bacteria, cocci and mycobacteria. *J. Antimicrob. Chemoth.* 51, 1435–1436. doi: 10.1093/jac/dkg246

Gardner, P. P., Daub, J., Tate, J. G., Nawrocki, E. P., Kolbe, D. L., Lindgreen, S., et al. (2009). Rfam: updates to the RNA families database. *Nucleic Acids Res.* 37, D136–D140. doi: 10.1093/nar/gkn766

Guindon, S., Dufayard, J., Lefort, V., Anisimova, M., Hordijk, W., and Gascuel, O. (2010). New algorithms and methods to estimate maximum-likelihood phylogenies: assessing the performance of PhyML 3.0. *Syst. Biol.* 59, 307–321. doi: 10.1093/sysbio/syq010

Guo, H., Qiu, Y., Wei, J., Niu, C., Zhang, Y., Yuan, Y., et al. (2020). Genomic insights into sugar adaptation in an extremophile yeast *Zygosaccharomyces rouxii*. *Front. Microbiol.* 10:3157. doi: 10.3389/fmicb.2019.03157

Hazelwood, L. A., Daran, J., van Maris, A. J. A., Pronk, J. T., and Dickinson, J. R. (2008). The ehrlich pathway for fusel alcohol production: a century of research on *Saccharomyces cerevisiae* metabolism. *Appl. Environ. Microb.* 74, 2259–2266. doi: 10.1128/AEM.02625-2627

Hua, D., Lin, S., Li, Y., Chen, H., Zhang, Z., Du, Y., et al. (2010). Enhanced 2-phenylethanol production from L-phenylalanine viain situ product adsorption. *Biocatal. Biotransform.* 28, 259–266. doi: 10.3109/10242422.2010.500724

Hua, D., and Xu, P. (2011). Recent advances in biotechnological production of 2-phenylethanol. *Biotechnol. Adv.* 29, 654–660. doi: 10.1016/j.biotechadv.2011.05.001

Iraqui, I., Vissers, S., Cartiaux, M., and Urrestarazu, A. (1998). Characterisation of *Saccharomyces cerevisiae* ARO8 and ARO9 genes encoding aromatic aminotransferases I and II reveals a new aminotransferase subfamily. *Mol Gen Genet* 257, 238–248. doi: 10.1007/s004380050644

James, S. A. S. M. (2011). "*Zygosaccharomyces* Barker (1901)," in *The Yeasts, A Taxonomic Study*, eds C. P. Kurtzman, J. W. Fell, and T. Boekhout, (New York: NY: Elsevier Science Publishers), 937–947.

Kanehisa, M., Goto, S., Sato, Y., Kawashima, M., Furumichi, M., and Tanabe, M. (2013). Data, information, knowledge and principle: back to metabolism in KEGG. *Nucleic Acids Res.* 42, D199–D205. doi: 10.1093/nar/gkt1076

Kim, B., Cho, B., and Hahn, J. (2014). Metabolic engineering of *Saccharomyces cerevisiae* for the production of 2-phenylethanol via Ehrlich pathway. *Biotechnol. Bioeng.* 111, 115–124. doi: 10.1002/bit.24993

Kinclová, O., Potier, S., and Sychrová, H. (2001). The *Zygosaccharomyces rouxii* strain CBS732 contains only one copy of the HOG1 and the SOD2 genes. *J. Biotechnol.* 88, 151–158. doi: 10.1016/S0168-1656(01)00274-277

Kobayashi, M., and Hayashi, S. (1998). Supplementation of NaCl to starter culture of the soy yeast *Zygosaccharomyces rouxii*. *J. Ferment. Bioeng.* 85, 642–644. doi: 10.1016/S0922-338X(98)80021-80024

Kurtzman, C. P., Fell, J. W., Boekhout, T., and Robert, V. (2011). Methods for isolation, phenotypic characterization and maintenance of yeasts. *Yeasts* 1, 87–110. doi: 10.1016/b978-0-444-52149-1.00007-0

Lee, K., and Hahn, J. (2013). Interplay of Aro80 and GATA activators in regulation of genes for catabolism of aromatic amino acids in *Saccharomyces cerevisiae*. *Mol. Microbiol.* 88, 1120–1134. doi: 10.1111/mmi.12246

Lee, K. E., Lee, S. M., Choi, Y. H., Hurh, B. S., and Kim, Y. S. (2014). Comparative volatile profiles in soy sauce according to inoculated microorganisms. *Biosci. Biotechnol. Biochem.* 77, 2192–2200. doi: 10.1271/bbb.130362

Livak, K. J., and Schmittgen, T. D. (2001). Analysis of relative gene expression data using real-time quantitative PCR and the 2-ΔΔCT Method. *Methods* 25, 402–408. doi: 10.1006/meth.2001.1262

Lu, X., Wang, Y., Zong, H., Ji, H., Zhuge, B., and Dong, Z. (2016). Bioconversion of L-phenylalanine to 2-phenylethanol by the novel stress-tolerant yeast *Candida glycerinogenes* WL2002-5. *Bioengineered* 7, 418–423. doi: 10.1080/21655979.2016.1171437

Martínez-Avila, O., Sánchez, A., Font, X., and Barrena, R. (2019). Fed-batch and sequential-batch approaches to enhance the bioproduction of 2-Phenylethanol and 2-Phenethyl acetate in solid-state fermentation residue-based systems. *J. Agric. Food Chem.* 67, 3389–3399. doi: 10.1021/acs.jafc.9b00524

Masuo, S., Osada, L., Zhou, S., Fujita, T., and Takaya, N. (2015). Aspergillus oryzae pathways that convert phenylalanine into the flavor volatile 2-phenylethanol. *Fungal Genet. Biol.* 77, 22–30. doi: 10.1016/j.fgb.2015.03.002

Mierzejewska, J., Tymoszewska, A., Chreptowicz, K., and Krol, K. (2017). Mating of 2 laboratory *Saccharomyces cerevisiae* strains resulted in enhanced production of 2-Phenylethanol by biotransformation of L-phenylalanine. *J. Mol. Microb. Biotech.* 27, 81–90. doi: 10.1159/000455169

Montigny, J., Straub, M., Potier, S., Tekaia, F., Dujon, B., Wincker, P., et al. (2000). Genomic Exploration of the Hemiascomycetous Yeasts: *Zygosaccharomyces rouxii*. *FEBS Lett.* 487, 52–55. doi: 10.1016/S0014-5793(00)02279-2271

Sáenz, D. A., Chianelli, M. S., and Stella, C. A. (2014). L-Phenylalanine Transport in *Saccharomyces cerevisiae*: participation ofGAP1, BAP2, andAGP1. *J. Amino Acids* 2014, 1–9. doi: 10.1155/2014/283962

Scognamiglio, J., Jones, L., Letizia, C. S., and Api, A. M. (2012). Fragrance material review on phenylethyl alcohol. *Food Chem. Toxicol.* 50, S224–S239. doi: 10.1016/j.fct.2011.10.028

Solieri, L., Chand Dakal, T., Croce, M. A., and Giudici, P. (2013). Unravelling genomic diversity of *Zygosaccharomyces rouxii* complex with a link to its life cycle. *FEMS Yeast Res.* 13, 245–258. doi: 10.1111/1567-1364.12027

Stanke, M., and Morgenstern, B. (2005). AUGUSTUS: a web server for gene prediction in eukaryotes that allows user-defined constraints. *Nucleic Acids Res.* 33, W465–W467. doi: 10.1093/nar/gki458

Tatusov, R. L., Koonin, E. V., and Lipman, D. J. (1997). A genomic perspective on protein families. *Science* 278, 631–637. doi: 10.1126/science.278.5338.631

Wang, P., Yang, X., Lin, B., Huang, J., and Tao, Y. (2017). Cofactor self-sufficient whole-cell biocatalysts for the production of 2-phenylethanol. *Metab. Eng.* 44, 143–149. doi: 10.1016/j.ymben.2017.09.013

Wang, Z., Bai, X., Guo, X., and He, X. (2017). Regulation of crucial enzymes and transcription factors on 2-phenylethanol biosynthesis via Ehrlich pathway in *Saccharomyces cerevisiae*. *J. Ind. Microbiol. Biot.* 44, 129–139. doi: 10.1007/s10295-016-1852-1855

Wang, Y., Zhang, H., Lu, X., Zong, H., and Zhuge, B. (2019). Advances in 2-phenylethanol production from engineered microorganisms. *Biotechnol. Adv.* 37, 403–409. doi: 10.1016/j.biotechadv.2019.02.005

Wang, Y., Zhang, Z., Lu, X., Zong, H., and Zhuge, B. (2020). Transcription factor Hap5 induces gsh2 expression to enhance 2-phenylethanol tolerance and production in an industrial yeast Candida glycerinogenes. *Appl. Microbiol. Biot.* 104, 4093–4107. doi: 10.1007/s00253-020-10509-y

Watanabe, J., Uehara, K., Mogi, Y., and Tsukioka, Y. (2017). Mechanism for restoration of fertility in hybrid *Zygosaccharomyces rouxii* generated by interspecies hybridization. *Appl. Environ. Microb.* 83:e01187-17. doi: 10.1128/AEM.01187-1117

Yin, S., Zhou, H., Xiao, X., Lang, T., Liang, J., and Wang, C. (2015). Improving 2-phenylethanol production via ehrlich pathway using genetic engineered *Saccharomyces cerevisiae* strains. *Curr. Microbiol.* 70, 762–767. doi: 10.1007/s00284-015-0785-y

Zhang, H., Cao, M., Jiang, X., Zou, H., Wang, C., Xu, X., et al. (2014). De-novo synthesis of 2-phenylethanol by *Enterobacter* sp. *CGMCC* 5087. *BMC Biotechnol.* 14:30. doi: 10.1186/1472-6750-14-30

Zuehlke, J. M., Petrova, B., and Edwards, C. G. (2013). Advances in the control of wine spoilage by *Zygosaccharomyces* and dekkera brettanomyces. *Annu. Rev. Food Sci. Trans.* 4, 57–78. doi: 10.1146/annurev-food-030212-182533

Conflict of Interest: The authors declare that the research was conducted in the absence of any commercial or financial relationships that could be construed as a potential conflict of interest.

frontiers in Microbiology

REVIEW
published: 13 November 2020
doi: 10.3389/fmicb.2020.580247

Flavor Formation in Chinese Rice Wine (Huangjiu): Impacts of the Flavor-Active Microorganisms, Raw Materials, and Fermentation Technology

Yijin Yang[1,2†], Wuyao Hu[1†], Yongjun Xia[1], Zhiyong Mu[1], Leren Tao[2], Xin Song[1], Hui Zhang[3], Bin Ni[3] and Lianzhong Ai[1]*

[1] Shanghai Engineering Research Center of Food Microbiology, School of Medical Instrument and Food Engineering, University of Shanghai for Science and Technology, Shanghai, China, [2] School of Energy and Power Engineering, University of Shanghai for Science and Technology, Shanghai, China, [3] Shanghai Jinfeng Wine Co., Ltd., Shanghai, China

Huangjiu (Chinese rice wine) has been consumed for centuries in Asian countries and is known for its unique flavor and subtle taste. The flavor compounds of Huangjiu are derived from a wide range of sources, such as raw materials, microbial metabolic activities during fermentation, and chemical reactions that occur during aging. Of these sources, microorganisms have the greatest effect on the flavor quality of Huangjiu. To enrich the microbial diversity, Huangjiu is generally fermented under an open environment, as this increases the complexity of its microbial community and flavor compounds. Thus, understanding the formation of flavor compounds in Huangjiu will be beneficial for producing a superior flavored product. In this paper, a critical review of aspects that may affect the formation of Huangjiu flavor compounds is presented. The selection of appropriate raw materials and the improvement of fermentation technologies to promote the flavor quality of Huangjiu are discussed. In addition, the effects of microbial community composition, metabolic function of predominant microorganisms, and dynamics of microbial community on the flavor quality of Huangjiu are examined. This review thus provides a theoretical basis for manipulating the fermentation process by using selected microorganisms to improve the overall flavor quality of Huangjiu.

Keywords: Huangjiu (Chinese rice wine), flavor compounds, microbial community, raw material, fermentation technology, yeast starter, fungi

OPEN ACCESS

Edited by:
Xucong Lv,
Fuzhou University, China

Reviewed by:
Huaxi Yi,
Ocean University of China, China
Sylvester Holt,
INSERM U1081 Institut de recherche sur le cancer et le Vieillissement, France

****Correspondence:***
Lianzhong Ai
ailianzhong@hotmail.com

† These authors have contributed equally to this work

Specialty section:
This article was submitted to Food Microbiology, a section of the journal Frontiers in Microbiology

Received: *05 July 2020*
Accepted: *22 September 2020*
Published: *13 November 2020*

Citation:
Yang Y, Hu W, Xia Y, Mu Z, Tao L, Song X, Zhang H, Ni B and Ai L (2020) Flavor Formation in Chinese Rice Wine (Huangjiu): Impacts of the Flavor-Active Microorganisms, Raw Materials, and Fermentation Technology. Front. Microbiol. 11:580247. doi: 10.3389/fmicb.2020.580247

INTRODUCTION

Huangjiu (Chinese rice wine), which is brewed with cereal grain, yeast, and *Qu* (a saccharification starter, which is similar to the "*koji*" starter used for making Japanese sake), has a history dating back more than 5,000 years (Varela et al., 2015). Huangjiu has been widely consumed in Asia because of its desirable flavor (Yu et al., 2019). According to the report released by the National Statistics Bureau of China[1], consumption of alcoholic beverages in China exceeded 800 billion Yuan in 2019, whereas the market share of the Huangjiu industry is significantly smaller than other alcoholic beverages (such as Chinese Baijiu and beer) in China. The lack of flavor diversity and individuation in Huangjiu is responsible for the phenomenon.

[1] http://lwzb.stats.gov.cn/pub/lwzb/gzdt

As an alcoholic beverage, aroma is the most important factor governing the perceived quality of Huangjiu and consumer preference. Based on aroma types, Huangjiu is divided into traditional-aroma Huangjiu, light-aroma Huangjiu, and special-aroma Huangjiu. Different raw materials and fermentation technologies result in varied aromas of Huangjiu. The production of these three different types of Huangjiu is shown in **Figure 1**. Generally, Huangjiu is produced by three major processes: selection and pretreatment (soaking) of raw materials, alcoholic fermentation, and post-process treatment. The brewing processes not only affect the fermentation efficiency of Huangjiu, but also largely determine the overall flavor quality of Huangjiu. During soaking, the acid-producing microorganisms use the water-soluble nutrients of rice to grow and produce various acids, which acidify the rice (Adeniran et al., 2012). The acidified rice that contributes to the low pH during initial fermentation can inhibit the growth of miscellaneous bacteria and is conducive to the successful alcoholic fermentation. During the alcoholic fermentation stage, the Huangjiu is firstly fermented at 28°C for 5 days (primary fermentation) and then at 10–15°C for 10–20 days (secondary fermentation; Yang et al., 2019). Primary fermentation assists the growth of yeast, which ferments sugars to ethanol, while secondary fermentation performed under low temperatures increases the accumulation of aroma compounds (Luo et al., 2008; Cao et al., 2010). Finally, the post-process treatment involves sterilization to inactivate microorganisms, thus ensuring the safety and shelf life of Huangjiu, while aging promotes the condensation of acids with alcohols to form esters, which improve the flavor profile of Huangjiu. However, conventional sterilization methods (e.g., boiling at 80–95°C for 15–30 min) lead to large nutritional losses, significant flavor changes, and poor vinosity, all of which are key limitations in the current Huangjiu industry (Yang et al., 2019).

The aroma of Huangjiu is the result of various volatile flavor compounds. Therefore, as the nature, range, and relative concentrations of these compounds change, so do does the aroma and flavor characteristics of Huangjiu. Currently, more than 900 kinds of volatile flavor compounds have been detected in Huangjiu, mainly including esters, alcohols, ketones, aldehydes, phenols, and acids (Chen et al., 2018). As Huangjiu is brewed using a variety of microorganisms co-fermenting under an open environment, the microbial community of Huangjiu during brewing plays a decisive role in the production of flavor compounds (Zhu et al., 2015). Microorganisms detected during Huangjiu brewing are yeast, bacteria, and filamentous fungi; of these, yeast and filamentous fungi contribute the most aroma components due to their involvement in saccharification, liquefaction, and alcoholic fermentation (Huang et al., 2018; Chen C. et al., 2020). Changes in the raw materials or fermentation process directly influence the composition of microbial communities and thereby alter the flavor profile of the resulting Huangjiu. Thus, studying the microbial community composition and changes in the community structure during brewing will improve our understanding of the formation of Huangjiu flavor compounds and lay a theoretical foundation for producing more diverse flavors in Huangjiu.

In this review, we summarize the research on the selection and pretreatment of raw materials, alcoholic fermentation, post-process treatment, and microorganisms that influence the formation of flavor compounds during Huangjiu brewing. We focus on the research that examines the effect of microbial community composition, metabolic function of predominant microorganisms, and changes of microbial community on the flavor quality of Huangjiu. This review will assist brewers in producing Huangjiu with high flavor quality and diversity.

SELECTION AND PRETREATMENT OF RAW MATERIALS TO IMPROVE HUANGJIU FLAVOR

Raw materials greatly contribute to the flavor by providing microorganisms with precursors of flavor compounds that are crucial for the aroma of Huangjiu (Xu et al., 2018; Chen T. et al., 2020). Rice starch and proteins are correspondingly degraded by microbial enzymes and mostly converted into glucose and amino acids, which effects not only the growth of microorganisms, but also that of the metabolites of microorganisms (**Figure 2**). Different grains contain different proportions of starch, protein, and fat, so that the resultant Huangjiu exhibits different flavor characteristics. In addition, the pretreatment of raw material (soaking) also has an important effect on the flavor quality of Huangjiu.

Selection of Grains Appropriate for Huangjiu Fermentation

Grains vary significantly in bitterness, color, and freshness (Shekhawat et al., 2017). Desirable grains used for fermentation need to have a high content of amylopectin, and low contents of protein and fat. The microcrystalline structure of amylopectin in rice is more disordered than that of amylose (Area et al., 2019). Thus, grains containing a high amylopectin content are preferentially used by microorganisms to produce flavor compounds during Huangjiu brewing. Rice varieties also differ in their physicochemical properties, such as the starch granule size, the relative proportion of amylose and amylopectin, and the chain length distribution of polysaccharide (Ahmed et al., 2015). Glutinous rice is considered as the best for producing Huangjiu with a high flavor quality as it contains up to 98% amylopectin (Pachuau et al., 2017). However, due to the high cost and strong taste of the resulting wine, glutinous rice is used for brewing traditional-aroma Huangjiu, such as Hong Qu Huangjiu and some Shaoxing Huangjiu, but is rarely used for brewing light-aroma Huangjiu. Rao et al. (2014) used Yangzhou rice (a type of japonica rice) to ferment Huangjiu and observed that this rice had a higher rate of water absorption than glutinous rice, which resulted in less raw rice remaining after processing. As the use of Yangzhou rice yields Huangjiu with a high concentration of amino acids and a refreshing, lighter flavor, Yangzhou rice is considered a good substitute for glutinous rice in Huangjiu brewing.

The 2-phenylethyl alcohol, which has a unique and pleasant rose-like aroma in Huangjiu, is substantially affected by the raw materials used (Chen et al., 2009; Martínez-Avila et al., 2018). Compared to rice, sorghum and maize produced higher

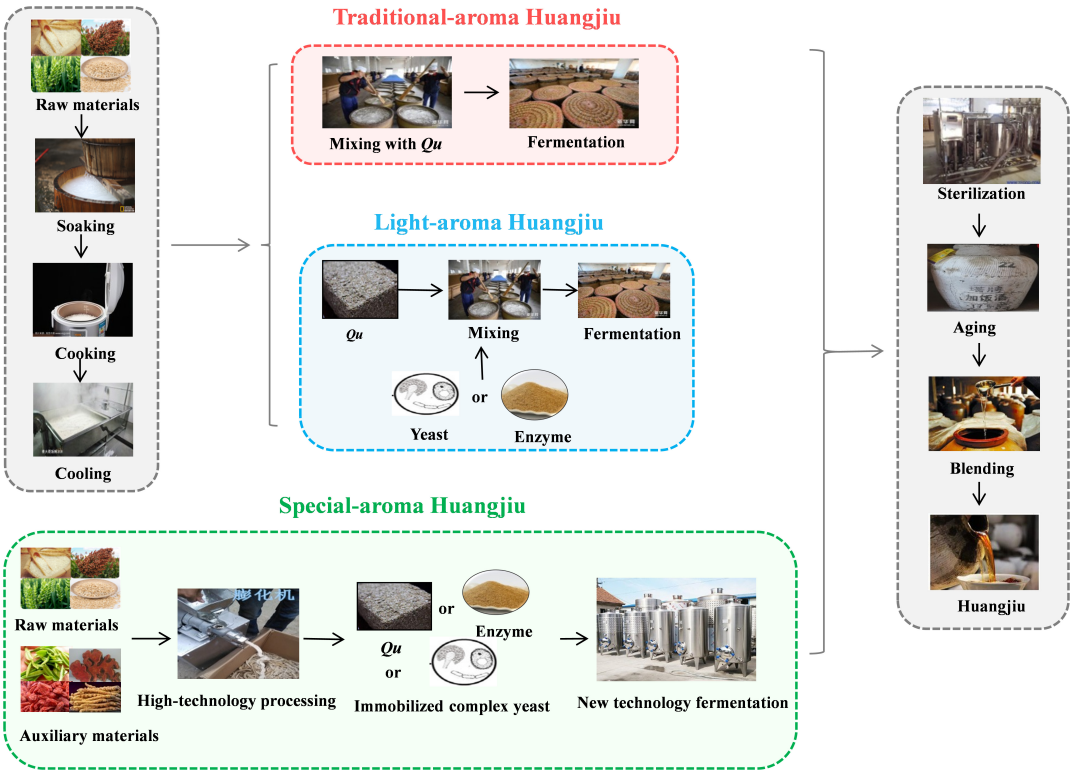

FIGURE 1 | The brewing process of Huangjiu with different aroma types.

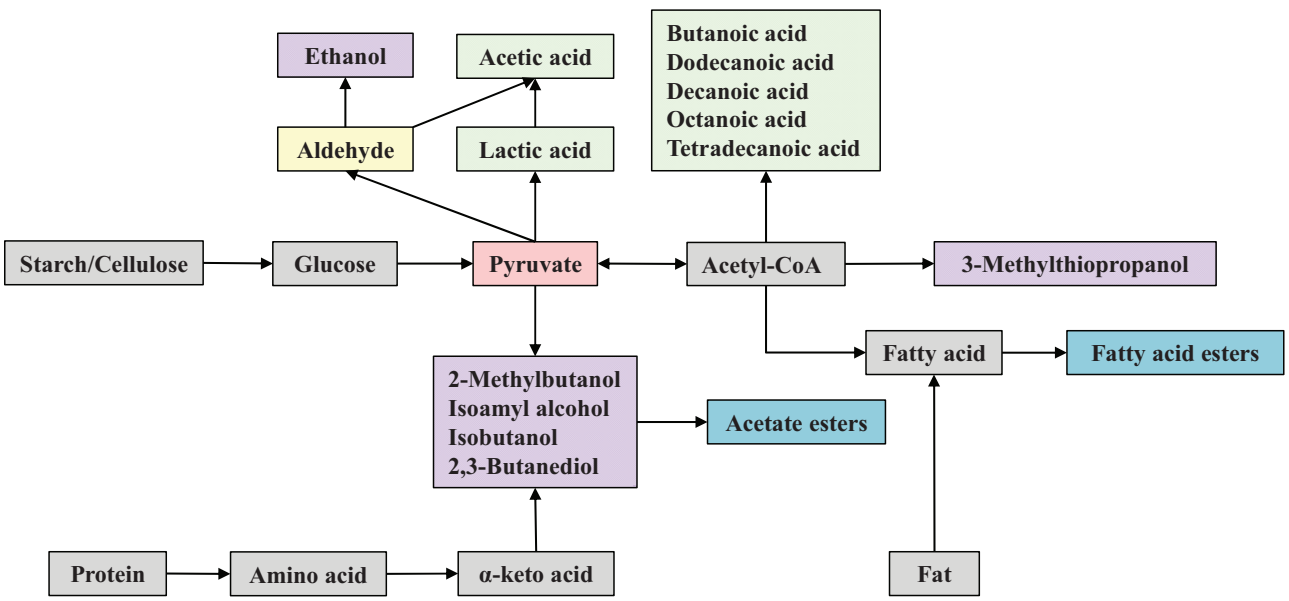

FIGURE 2 | Metabolism of major flavor compounds during Huangjiu brewing.

contents of 2-phenylethyl alcohol for Huangjiu brewing. This was attributable to the high content of L-phenylalanine in sorghum and maize, as L-phenylalanine is the substrate for the generation of 2-phenylethyl alcohol and its content in raw materials positively affects the yield of 2-phenylethyl alcohol (Cao et al., 2010; Pineda et al., 2012). When the toxic analog of L-phenylalanine—fluorinated L-phenylalanine is used as a substrate, selecting yeast mutants with resistance to fluorinated L-phenylalanine also allows the increased production of 2-phenylethyl alcohol (Akita et al., 1990;

Dueñas-Sánchez et al., 2014; Cordente et al., 2018). In addition, the tannin content of raw materials has been shown to affect the flavor of the resulting Huangjiu. Jia et al. (2018) observed that Huangjiu brewed with sorghum varieties containing different contents of tannin exhibited different flavor characteristics. The differences in fungi community structure induced by different tannin contents may be responsible for the results (Shi et al., 2011).

As consumers demand a diverse range of products, Huangjiu brewing is no longer limited to using commonly consumed grains. The development of new raw materials, such as loquat leaf, oatmeal, barley, and bitter buckwheat, as well as the fungus *Cordyceps militaris*, have become popular topics in Huangjiu brewing research (Yue et al., 2012; Chen and Xu, 2013; Wang et al., 2013; Li H. et al., 2014). Raw materials for Huangjiu brewing are selected not only according to the drinking habits of people in different regions and for economic reasons, but also for enhancing the taste and flavor of Huangjiu. Auxiliary materials can be applied to strengthen the specific flavor characteristics and health benefits of the resultant Huangjiu.

Effective Soaking Conditions for Rice

Soaking is one of the most important processes during Huangjiu brewing and directly affects the initial fermentation acidity and flavor quality of the resulting wines. The soaking process involves water absorption-mediated expansion of rice, partial decomposition of starch, and acidification of rice (Ji et al., 2013). The total acidity, the concentration of lactic acid, and the lactic acid bacteria (LAB) count in the water after rice soaking are important indicators for evaluating the quality and flavor of Huangjiu.

In traditional brewing of Huangjiu, the rice may be soaked for several weeks, while in modern brewing, soaking is performed for only a few days (Chen et al., 2018; Lv et al., 2018). However, even in modern brewing, a successful soaking process needs to rely on the empirical knowledge of winemakers. The soaking acidity needs to reach a value ranging from 2 g/L to 5 g/L (or soaking 1–3 days in summer and soaking 2–5 days in winter) using modern techniques. Gong et al. (2020) evaluated the effect of different soaking times on rice used for Huangjiu brewing, concluding that the total acidity and amino nitrogen of soaking increased slowly at first, then increased rapidly and finally became stable, while the reducing sugar content exhibited the opposite tendency. Nevertheless, there is still no specific standard regulations for rice soaking, which may result in the inconsistency of quality in terms of taste and flavor among different batches of Huangjiu. In future, standardized soaking procedures should be established to ensure the between-batch flavor stability of Huangjiu.

EFFECTS OF ALCOHOLIC FERMENTATION ON THE FLAVOR OF HUANGJIU

The principal metabolic process in Huangjiu brewing is the alcoholic fermentation, which consists in the biotransformation of rice nutrients into a wide variety of metabolites responsible for aroma and flavors (Querol et al., 2018). During alcoholic fermentation, fermentation starters of yeast and saccharification starters of *Qu* involved in the principal metabolic process are applied to improve the quality of Huangjiu. However, the starter strains may be sensitive to environmental conditions during the long fermentation period and thus developing high-efficiency fermentation techniques that are suitable with the growth of strains are also necessary.

Fermentation Starter of Yeast

Within yeast species, *Saccharomyces* strains are the main group that can survive and contribute to wine fermentation. Yeast fermentation not only produces ethanol, but also generates a range of volatile flavor compounds, which result in the specific flavor characteristic of Huangjiu (Fleet, 2003; Chen and Xu, 2012; Cai et al., 2018). As microbial composition during Huangjiu fermentation is complex, a purebred yeast starter is typically used to provide a growth advantage by preventing the excessive proliferation of bacteria, as this can lead to rancidity. However, Yang et al. (2017) found that fermentation performed with inoculation of a single *Saccharomyces* strain leads to a less mellow flavor and taste than that of Huangjiu fermented with two *Saccharomyces* strains. The exception is *Hong Qu* Huangjiu, which is fermented with *Hong Qu* and *Bai Qu* containing a variety of yeasts instead of purebred yeast. But the undefined number of different yeasts makes the brewing of *Hong Qu* Huangjiu uncontrollable. The use of mixed *Saccharomyces* strains has been proven as an effective strategy to improve the flavor profiles and diversity of Huangjiu (Yang et al., 2017). With the knowledge that *non-Saccharomyces* species actively participate during the alcoholic fermentation, the co-fermentation of selected non-*Saccharomyces* with *S. cerevisiae* has been a new strategy to produce beer or grape wine products with more complex aromatic and flavor characters (Escribano-Viana et al., 2018; Zdaniewicz et al., 2020). In this regard, more and more attention should be paid to the use of controlled mixed fermentation with selected *S. cerevisiae* and non-*Saccharomyces* yeasts to change the sensory characteristics of Huangjiu.

During Huangjiu fermentation, due to nutrients consumption and an accumulation of stressful factors that affect the yeast fermentation (**Figure 3**), the alcoholic fermentation sometimes remains stuck in the secondary fermentation, thus lowering the quality of the resultant wine (Longo et al., 2020). Among those factors, ethanol stress is the greatest challenge for yeast striving to survive and ferment, as yeast contributes to high ethanol concentration [14–20% (v/v) in the final fermentation mash of Huangjiu], which is also toxic to yeast cells (Chen and Xu, 2012; Snoek et al., 2016). Furthermore, nutrients' competition among the complex microbial community during secondary fermentation of Huangjiu makes yeast confront higher stress levels. Thus, acquiring yeasts with a high fermentation performance is always desirable to winemakers, as this can theoretically result in more complete fermentation and a higher flavor quality of the resulting wine (Steensels and Verstrepen, 2014). The improvement of fermentation performance and sensory characteristics by yeast has focused on *S. cerevisiae* strains isolated from the natural environment or fermentation foods,

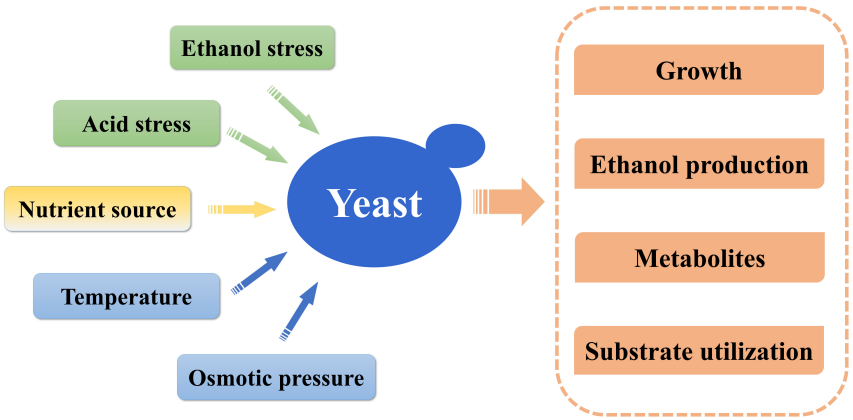

FIGURE 3 | Factors affecting the fermentation of yeasts.

along with some directed evolution, mutagenesis, and strain hybridization. Xie et al. (2010) and Yang et al. (2013) screened *S. cerevisiae* strains with a quick fermentation ability and high stress tolerance, which could effectively improve the fermentation efficacy of Huangjiu. *S. cerevisiae* hybrid created by the strategies of directed evolution and protoplast fusion displayed higher flavor production and oenological performance in Huangjiu brewing (Yang et al., 2018). Yeast isolates screened with specific flavor compounds production, such as 2-phenylethanol (De Lima et al., 2018), Isoamyl alcohol ester (Asano et al., 1999), and ethyl caproate (Arikawa et al., 2000; Takahashi et al., 2017), have also been frequently reported in Japanese sake. Screening yeast strains for flavor formation in Huangjiu is a technique that is just now beginning to be used, although it is one that has been widely developed for Japanese sake. The innovative screening strategies of Japanese sake are worth learning from for Huangjiu in the future.

Apart from traditional screening, genetic modification techniques are also capable of creating new yeast strains with specific metabolic profiles for alcoholic fermentation (Krogerus et al., 2017). Ding et al. (2015) enhanced deacidification activity in *Schizosaccharomyces pombe* using genome shuffling, and Dong et al. (2019) increased production of acetate ester in *S. cerevisiae* using a "self-cloning" integration strategy. Ohashi et al. (2020) reported that the removal of feedback inhibition of NAGK activity resulted in the significantly higher production of ornithine in sake and sake cake by gene expression. Although the methods mentioned above can be used in developing new yeasts with novel properties for alcoholic fermentation, genetically modified yeasts are generally not permitted in the production of alcoholic beverages at present. Therefore, only novel strains and innovations discovered by natural breeding will be of immediate use.

Saccharification Stater of *Qu*

As for the saccharification starter of *Qu*, it could be made either by natural inoculation and artificial inoculation (Ji et al., 2018). Generally, *Qu* is prepared by the spontaneous fermentation of raw materials and inoculated with fungal, yeasts, and bacteria to secrete enzymes such as glucoamylase and protease (Mo et al., 2009). Artificial inoculation of *Qu* is often made by purebred fungus, while natural inoculation of *Qu* contains abundant microorganisms. Based on the color of fungal spores, *Qu* is classified as yellow *Wheat Qu*, red *Hong Qu*, and yellow *Hong Qu*. Aside from *Hong Qu*, in which the dominant fungal species is *Monascus* spp., the other artificial *Qu* are cultivated with *Aspergillus* spp. Of these, the commonly used *Qu* is raw *Wheat Qu* (RWQ), which is made by natural inoculation, and cooked *Wheat Qu* (CWQ), which is made by artificial inoculation. To make RWQ, wheat is squashed and squeezed into bricks, followed by piling up in the natural environment for at least 2 months (Ji et al., 2018). Although RWQ contains abundant microorganisms that may be conducive to generating more flavor compounds, it could not guarantee effective microbial composition and quantity, rendering control of the brewing process difficult and the quality of RWQ inconsistent. CWQ, which is inoculated only with *Aspergillus flavus*, can improve the saccharification rate as well as the fermentation efficiency, and thus has been widely utilized for industrial Huangjiu production. However, purebred CWQ produces weak-flavored Huangjiu, and thus, a combination of CWQ and RWQ is generally applied in the Huangjiu industry. Moreover, to reduce costs and improve efficiency, manufacturers also explore different combinations of *Qu* and enzymes as saccharification starters. Currently, high-temperature α-amylase, medium-temperature α-amylase, composite glucoamylase, and acidic protease are the most commonly used industrial enzymes. The rapid pace of development in enzyme engineering means that an increasing number of enzymes will be available for Huangjiu production.

Microorganisms in *Qu* produce large amounts of cellular metabolic enzymes that subsequently produce small molecules throughout Huangjiu fermentation, which contribute to flavor formation in the final product (Yang et al., 2017). Due to variations in the production process and raw materials for *Qu*, the microorganisms contained therein also vary. Yu et al. (2012) studied the volatile flavor compounds of different traditional Huangjiu and their representative fungus in *Wheat Qu*, and results showed that *Wheat Qu* not only acted as a saccharifying

agent, but also increased the activity of yeast and the formation of aroma compounds. In other words, the aroma of Huangjiu can be adjusted according to the amount of *Qu* used in fermentation, implying that differences in the amount of *Qu* could lead to significant differences in the ultimate flavor profile of the wine.

Different Brewing Techniques for Huangjiu Fermentation

Traditional Huangjiu is successively produced by saccharification and fermentation stages. The fermentation allows starch to be completely hydrolyzed to glucose so that sugar is no longer produced during the fermentation phase, resulting in a decrease in the sugar concentration. However, the high osmotic pressure created by the high initial concentration of glucose inhibits the growth of yeast and thus limits the fermentation rate of Huangjiu (Snoek et al., 2016). Hence, simultaneous saccharification and fermentation, which could improve fermentation efficiency and reduce energy consumption, is applied in the production of modern Huangjiu (Wang et al., 2014). During synchronous fermentation, the sugar produced by amylase-mediated starch hydrolysis is immediately utilized by *Saccharomyces*. This effectively promotes fermentation, and thus increases ethanol yield, which significantly shortens the required entire fermentation time and reduces the possibility of external microbial contamination (Xu et al., 2015). Gong et al. (2013) examined the effects of different brewing processes on physicochemical indicators and the concentration of higher alcohols in Huangjiu. The results showed that the ethanol concentration in Huangjiu fermented by successive steps of saccharification and fermentation was lower than that in Huangjiu from simultaneous fermentation, which was due to the inhibition of yeast activity and a lack of nutrients. In terms of higher alcohols, similar results were also observed between the two fermentation processes. This is because yeast is inhibited by the high concentration of sugar in the pre-fermentation period and thus produces lower content of higher alcohols. That is, during post-fermentation in the two-step process, low concentrations of carbon and nitrogen sources were present, which inhibited yeast activity, resulting in the lack of α-keto acid formation (Takagi, 2019). The resulting large concentrations of ketone acids could not be converted into amino acids, which in turn could not be converted into higher alcohols via the Erlich pathway (Avalos et al., 2013).

Compared with Huangjiu made from conventionally fermented steamed rice with *Qu* and yeast, it has been found that rice liquefied by enzymes and then fermented with *Qu* and yeast exhibited a higher fermentation efficiency (Li et al., 2013). Applying the method of enzyme liquefaction, the pretreatment processes of rice soaking and cooking were both excluded. Bechman et al. (2012) reported that using the liquefaction method to produce Huangjiu could increase the content of higher alcohols and decrease the content of sugar. Furthermore, the content of amino nitrogen was also higher than wine fermented by simultaneous fermentation. This may be attributable to the liquefaction of raw material, which would disperse protein particles throughout the fermented mash, where they are more easily utilized by proteases to increase the amino nitrogen level (Arroyo-Lopez et al., 2009). Although the liquefaction method simplifies the fermentation process and increases the utilization rate of raw materials, the finished wine is less palatable. Hence, the liquefaction method has not been widely applied in the Huangjiu industry.

To prevent environmental pollution of water from soaking, Wei et al. (2017) proposed an innovative brewing technique which involved adding *Lactobacillus* to make up for the total acid originally produced by soaking. Besides, the metabolic reaction of *Lactobacillus* could contribute to the flavor profiles of alcoholic beverages (e. g., malolactic fermentation in grape wine), though the role of *Lactobacillus* in the lavor development of rice wine has not been investigated systematically (Rhee et al., 2011; Oguro et al., 2017). The method could not only save water resources and reduce environmental pollution, but also decrease the content of biogenic amine, which might have deleterious effects on human health if the content is too high (del Rio et al., 2020). Compared to Huangjiu brewed using the rice soaking process, Huangjiu produced with the addition of *Lactobacillus* exhibited a higher content of esters and a lower content of alcohols, which led to a more soft-tasting Huangjiu after a shorter aging time (Regueiro et al., 2017; Wei et al., 2017). Moreover, as there is no standard method for rice soaking, which means that there is inconsistent quality between different batches of Huangjiu, this eco-friendly and simplified brewing technique may be widely applied in the future.

POST-PROCESS TREATMENT TO ENSURE SAFETY AND ENHANCE AROMA

Sterilization Techniques

Post-process sterilization is a critical step during Huangjiu production, since it can partially prevent micro-organism contamination, which affects the shelf life and safety of Huangjiu products. Thermal sterilization (boiling at 80–95°C for 15–30 min) is commonly used in the Huangjiu industry. However, this conventional boiling technique not only leads to large nutritional losses, but also significant flavor changes (Xu et al., 2015). Moreover, during boiling, glucose, proteins, polyphenols, and other substances tend to undergo non-enzymatic browning, which affects the flavor and color of the final Huangjiu product (Li X. et al., 2014; Xu et al., 2016). Over the past decades, many studies have been conducted attempting to overcome the limitations of traditional boiling, and a series of non-thermal sterilization technologies have been developed for Huangjiu (Chang, 2003; Yang et al., 2019). Notably, high hydrostatic pressure (HHP) technology inactivates foodborne spoilage and pathogenic microorganisms without causing the significant loss of sensory and nutritional value of food products. Moreover, Tian et al. (2016) concluded that HHP could shorten the aging time of Huangjiu significantly and improve wine quality. In another study reported by

Yang et al. (2019), it was found that HHP treatment appeared to be more beneficial for the total amount of aroma-active volatiles in Huangjiu than thermal treatment. Thus, non-thermal sterilization techniques, such as HHP processing, can effectively enhance the flavor profiles of Huangjiu, but the high cost of HHP equipment limits the wide use of this technique in the Huangjiu industry. As wineries are focused on how to improve the flavor quality of their wine products, non-thermal sterilization techniques will become prominent sterilization techniques in the future.

Formation of Key Flavor Compounds During Aging

As fresh wine has an insufficient aroma and a rough taste, it usually requires a period of storage, commonly known as aging, to reduce its pungency and render it more palatable, full-bodied, and well-balanced in flavor (Tao et al., 2014). Huangjiu is commonly stored in traditional pottery jars for 1 to 3 years during the aging process, with high-quality Huangjiu aged for longer periods (Fan and Xu, 2012). Due to the high energy consumption and uncontrollability of this natural aging process, it has failed to meet the market demand. Consequently, stainless-steel pots are currently used for Huangjiu aging. However, the flavor characteristics of Huangjiu aged in a pottery jar are considerably different from those of Huangjiu aged in a stainless-steel pot at an industrial scale (Huang et al., 2020). Therefore, understanding the key flavor compounds and their formation mechanisms is crucial for optimization of the aging process of Huangjiu. Chen et al. (2019) reported that vanillin, 3-methylbutanol, sotolon, and benzaldehyde contributed substantially to the overall aroma of aged Huangjiu. During aging, the content of aldehydes, ketones, lactones, and phenolic flavor compounds changed consistently with aging time. The concentrations of key aroma compounds such as benzaldehyde, 3-methylbutanol, 1,1-diethoxyethane, sotolon, and vanillin increased significantly with the aging time, while those of other key aroma compounds, such as 4-vinylguaiacol and methional, decreased significantly with aging time. However, the formation mechanisms of these key flavor compounds remain to be elucidated.

Aging involves two processes: physical maturation and chemical maturation (Tao et al., 2014). During physical maturation, the hydrogen bonding among flavor compounds of Huangjiu and the volatilization of heterogeneous volatile compounds may contribute to the final flavor characteristic of Huangjiu (Cao et al., 2018; Wang et al., 2019). As for chemical maturation aging, a variety of chemical reactions, such as oxidation, esterification, and hydrolysis reactions, may affect the composition of flavor compounds, and thus are responsible for the flavor quality of Huangjiu. Generally, spiciness, roughness, and bitterness, which are associated with the "unpleasant" flavor characteristics, are prominent in fresh wine due to its excessive ethanol content (Jones P. R. et al., 2008). After aging, the increased acidity promoted proton exchange between water and ethanol and thus strengthened the hydrogen-bonding structure in alcoholic beverages (Nose et al., 2004, 2005). This reduced the freedom degree of ethanol molecules and produced a softer tasting Huangjiu. Furthermore, alcohol, aldehydes and other substances in wine may be oxidized to acid, which can then react with alcohols to afford esters and thus enhance the aroma of Huangjiu (Shen et al., 2011). Currently, there are many other new techniques that have been proposed for aging, such as microwave aging and biological aging (Roldán et al., 2017; Zhong et al., 2020). Nevertheless, these techniques have different effects on the aroma and taste of the resultant Huangjiu (Zhang et al., 2005), which is also a major challenge for the Huangjiu industry.

RELATIONSHIP BETWEEN MICROBIAL COMMUNITY AND HUANGJIU FLAVOR

The composition of microbial communities in Huangjiu is complicated. This is due to microorganisms derived from the yeast starter and *Qu*, the open fermentation environment, and the introduction of environmental microorganisms by the re-use of rice soaking water, which increases the diversity and complexity of the microbial communities in Huangjiu (Chen C. et al., 2020). Owing to the interaction of microorganisms in different fermentation stages of Huangjiu, different types and contents of flavor compounds are produced (**Figure 2**), which greatly affect the flavor characteristic of Huangjiu. Generally, alcohols account for more than 50% of the total flavor compounds content in Huangjiu, with esters being the second most abundant flavor compounds (Chen et al., 2018). Alcohols are mainly generated by yeast metabolism, and although they usually have a low odor activity value, their high concentration means they play a key role in the process (Yang et al., 2018). Esters constitute one of the most important classes of flavor compounds because they are largely responsible for the desired fruity, candy, and perfume-like aroma associated with Huangjiu (Hu et al., 2018). Esters can form from alcohols and acids in the absence of enzymes and microorganisms. However, this manner of ester formation is apparently too slow to account for the large amounts of ester normally found in alcoholic beverages. Thus, the enzymic formation of esters by microorganism metabolism is the main manner through which to accumulate esters for Huangjiu. As most of the flavor compounds are produced by the common metabolism of multiple microorganisms, the compositions of the microbial community directly affect the metabolic function of microorganisms and the production of flavor compounds during Huangjiu brewing.

Metabolic Function of Dominant Microorganisms During Huangjiu Brewing

Microorganisms that have been detected in Huangjiu are listed in **Table 1**, with yeast, molds, and bacteria being the main types that have been identified during Huangjiu brewing. Chen and Xu (2012) found that the dominant flavor compounds in Huangjiu, including alcohols, some esters, and volatile acids, were mainly produced by yeast fermentation. During Huangjiu brewing,

TABLE 1 | Microorganisms detected in Huangjiu during brewing by HTS technology.

Microbes	Genus level	Sample origin	References	Identified methods
Bacterium	*Saccharopolyspora*	SXRW	Xie et al., 2013	Illumina sequencing
	Streptomyces	SXRW	Xie et al., 2013	Illumina sequencing
	Mycobacterium	SXRW	Xie et al., 2013	Illumina sequencing
	Arthrobacter	SXRW	Xie et al., 2013	Illumina sequencing
	Actinosynnema	SXRW	Xie et al., 2013	Illumina sequencing
	Amycolatopsis	SXRW	Xie et al., 2013	Illumina sequencing
	Kocuria	SXRW	Xie et al., 2013	Illumina sequencing
	Rhodococcus	SXRW	Xie et al., 2013	Illumina sequencing
	Bacillus	SXRW	Lv et al., 2013; Xie et al., 2013	Illumina sequencing
	Staphylococcus	SXRW	Xie et al., 2013	Illumina sequencing
	Lactobacillus	SXRW	Lv et al., 2013; Xie et al., 2013	Illumina sequencing
	Pantoea	SXRW	Lv et al., 2013; Xie et al., 2013	Illumina sequencing
	Burkholderia	WYQRW and GTQRW	Li et al., 2018	16S rRNA genes
	Erwinia	WYQRW and GTQRW	Li et al., 2018	16S rRNA genes
	Klebsiella	WYQRW and GTQRW	Lv et al., 2013; Li et al., 2018	16S rRNA genes
	Ochrobactrum	WYQRW and GTQRW	Li et al., 2018	16S rRNA genes
	Shewanella	WYQRW and GTQRW	Li et al., 2018	16S rRNA genes
	Agrobacterium	WYQRW and GTQRW	Li et al., 2018	16S rRNA genes
	Acinetobacter	WYQRW and GTQRW	Li et al., 2018	16S rRNA genes
	Lactococcus	WYQRW and GTQRW	Lv et al., 2013; Li et al., 2018	16S rRNA genes
	Brevibacillus	WYQRW	Huang et al., 2018	16S rRNA genes
	Gluconacetobacter	WYQRW	Huang et al., 2018	16S rRNA genes
	Pseudomonas	WYQRW	Lv et al., 2013; Huang et al., 2018	16S rRNA genes
	Raoultella	WYQRW	Huang et al., 2018	16S rRNA genes
	Serratia	WYQRW	Huang et al., 2018	16S rRNA genes
	Sphingomonas	WYQRW	Huang et al., 2018	16S rRNA genes
	Staphylococcus	WYQRW	Huang et al., 2018	16S rRNA genes
	Thermus	WYQRW	Huang et al., 2018	16S rRNA genes
	Weissella	WYQRW	Lv et al., 2013; Huang et al., 2018	16S rRNA genes
	Enterobacter	ZJRW	Fang et al., 2015	Illumina sequencing
	Acidovorax	ZJRW	Fang et al., 2015	Illumina sequencing
	Propionibacterium	ZJRW	Fang et al., 2015	Illumina sequencing
Fungi	*Monascus purpureus*	WYQRW and GTQRW	Li et al., 2018	ITS1 regions
	Saccharomyces sp	WYQRW and GTQRW	Li et al., 2018	ITS1 regions
	Aspergillus niger	WYQRW and GTQRW	Li et al., 2018	ITS1 regions
	Eurotionmycetes sp	WYQRW and GTQRW	Li et al., 2018	ITS1 regions
	Fusarium pseudensiforme	WYQRW and GTQRW	Li et al., 2018	ITS1 regions
	Rhizopus microsporus	WYQRW and GTQRW	Li et al., 2018	ITS1 regions
	Aspergillus sp	WYQRW and GTQRW	Jia et al., 2018; Li et al., 2018	ITS1 regions
	Agaricomycetes sp	WYQRW and GTQRW	Li et al., 2018; Rui et al., 2019	ITS1 regions
	Cunninghamella	WYQRW	Huang et al., 2018	ITS1 regions
	Cladosporium cladosporioides	ZJRW	Yu et al., 2012	Illumina sequencing
	Alternaria alternata	ZJRW	Yu et al., 2012	Illumina sequencing
	Penicillium sp	ZJRW	Yu et al., 2012	Illumina sequencing
	Clavispora lusitaniae	ZJRW	Yu et al., 2012	Illumina sequencing
	Issatchenkia orientalis	ZJRW	Yu et al., 2012	Illumina sequencing
Yeast	*Geotrichum*	WYQRW	Huang et al., 2018	ITS1 regions
	Debaryomyces	WYQRW	Huang et al., 2018	ITS1 regions
	Issatchenkia	WYQRW	Huang et al., 2018	ITS1 regions
	Meyerozyma	WYQRW	Huang et al., 2018	ITS1 regions
	Rhodotorula	WYQRW	Huang et al., 2018	ITS1 regions

(Continued)

TABLE 1 | Continued

Microbes	Genus level	Sample origin	References	Identified methods
	Wickerhamomyces	WYQRW	Huang et al., 2018	ITS1 regions
	Blastobotrys	WYQRW	Huang et al., 2018	ITS1 regions
	Candida	WYQRW	Huang et al., 2018	ITS1 regions
	Clavispora	WYQRW	Huang et al., 2018	ITS1 regions

SXRW, Shao Xing Huangjiu; WYQRW, Wuyi Hong Qu Huangjiu; GTQRW, Gutian Hong Qu Huangjiu; and ZJRW, Zhen Jiang Huangjiu.

S. cerevisiae is not the only yeast that can contribute to the flavor of wine. *Non-Saccharomyces* yeasts also contribute positively to the brewing process as they produce certain additional aromatic compounds that improve the flavor and aroma of wine (Zot et al., 2008; Jolly et al., 2014). A *Saccharomyces*-yeast used for Huangjiu production should exhibit a strong fermentation ability, reproduce rapidly, generate a high concentration of alcohol with less foaming, and be strongly resist to bacterial contamination. In recent years, *AS.2.1392* (original 501, Shanghai Jinfeng brewery), *M85* (Wuxi brewery), and *zmyl-6* (Zhejiang Institute of Microbiology and Shaoxing brewery) have been demonstrated to show excellent fermentation performances, and have been popular in Huangjiu production. In terms of *non-Saccharomyces* yeast, *Debaryomyces*, *Issatchenkia*, *Meyerozyma*, *Rhodotorula*, *Wickerhamomyces*, *Blastobotrys*, *Candida,* and *Clavispora* are the most commonly identified *non-Saccharomyces yeasts* in Huangjiu (**Table 1**). When amino acids constitute the major nitrogen source, *non-Saccharomyces* yeasts convert tryptophan and L-phenylalanine into tyrosol, tryptizol, and 2-phenylethyl alcohol via Ehrlich pathway metabolism (Hazelwood et al., 2008; de Jesús Rodríguez-Romero et al., 2020). These alcohols not only affect the flavor and taste of wine, but are also involved in the growth regulation of yeast (Avbelj et al., 2015). Aromatic alcohols could act as quorum-sensing molecules, as they are recognized by other yeast cells when secreted into the extracellular medium, which induces the pseudo-filamentous growth of yeast (Chen and Fink, 2006). Canonico et al. (2019) found that using non-*Saccharomyces* yeast strains in sequential fermentation with *S. cerevisiae* could produce a Chardonnay wine with reduced ethanol concentration and acceptable chemical volatile profiles. Binati et al. (2020) reported that the use of selected non-*Saccharomyces* strains in conjunction with *S. cerevisiae* positively modulated some relevant chemical parameters and improved the aromatic intensity of Pinot Grigio grape wine. Although non-*Saccharomyces* yeasts can provide a means for increasing aroma and flavor diversity in fermented beverages, it is rarely selected and applicated in rice wine brewing, let alone in Huangjiu. Screening novel non-*Saccharomyces* isolates and evaluating their contribution to the sensory characteristics of rice wine will help to differentiate the final products.

Molds produce many enzymes involved in cellular metabolism and the resultant small molecules contribute to the formation of esters (Cai et al., 2018). The molds in Huangjiu are mainly derived from *Qu*, and the dominance of different molds in different samples of *Qu* results in the unique local flavor of Huangjiu (Mo et al., 2009). Researchers have screened functional saccharification and fermentation mold strains from *Qu* in different regions of China and found that *Rhizopus* and *Aspergillus* play crucial roles. *Rhizopus* produces a variety of enzymes, such as high-activity amylase and saccharification enzymes, which play an important role in the saccharification process of Huangjiu (Lücke et al., 2019). At the same time, some *Rhizopus* spp. can process alcohols under certain conditions and thus produce flavor compounds, such as 2-phenethyl alcohol, and the esters ethyl caproate, and ethyl lactate (Londoño-Hernández et al., 2017). *Aspergillus* can produce acidic proteases and carboxypeptidases during Huangjiu brewing. These proteases hydrolyze the proteins in rice into nitrogen sources, such as peptides and amino acids, that can be easily used by yeast (Chen T. et al., 2020). They can be used as nutrients for yeast growth or as precursors for the synthesis of flavor compounds (Chang et al., 2015). Generally, *Aspergillus* is the most abundant filamentous fungus and is present in various fermentation stages of *Wheat Qu* Huangjiu (Rui et al., 2019). Ji et al. (2018) reported that filamentous molds showed significant differences in Huangjiu fermented with different *Wheat Qu*. Fungal community structure and diversity are affected by organic acids, suggesting that the metabolites of filamentous molds may contribute significantly to the formation of major flavor compounds in Huangjiu. Furthermore, Huangjiu fermentation often increases the contents of ethanol and organic acid due to the lack of sufficient oxygen, which may ultimately lead to the death of bacteria or the loss of the metabolic activity of *Aspergillus*.

Compared with yeast and mold, few studies about the function of bacteria in Huangjiu have been reported. However, the number of different types of bacteria in the microbial community of Huangjiu far exceed the number of types of yeast and mold. Both the traditional PCR-DGGE method and high-throughput sequencing (HTS) analysis have shown that *Bacillus sp.* and LAB are the main bacterial genera present during Huangjiu brewing (Lv et al., 2013; Cai et al., 2018; Huang et al., 2018). A significant change in the bacterial community occurs during brewing, especially in the abundance of *Bacillus* and *Lactobacillus* species. *Bacillus* secrete various hydrolases, which may generate nitrogen-containing flavor compounds, such as pyrazines (Bednarek et al., 2019). *Bacillus* spp. survive as spores in unfavorable environments, which helps these organisms to produce flavor compounds under high ethanol conditions during the secondary fermentation of Huangjiu. LAB produce various antibacterial substances that inhibit pathogens and toxin-producing spoilage organisms (Castellano et al., 2008; Jones R. J. et al., 2008). Organic acids produced by LAB provide precursor substances for the generation of flavor compounds. Wang et al. (2014) reported that

the presence of LAB was positively related to the presence of organic acids during Huangjiu brewing.

Dynamics of Microbial Community During Huangjiu Brewing

The brewing process of Huangjiu is comprised of two stages: primary fermentation at 28°C for 5 days and secondary fermentation at 15°C for 10–20 days under an open environment. The microbial community interacts with the open fermentation environment, and thus changes constantly during Huangjiu brewing. Both fungal and bacterial communities varied significantly in different fermentation periods of Huangjiu (Huang et al., 2018). Numerous studies on the microbial communities of *Wheat Qu* Huangjiu and *Hong Qu* Huangjiu have been reported, as well as on *Qu* and other traditional starters (Wang et al., 2014; Hong et al., 2016; Huang et al., 2018; Ji et al., 2018; Shuang et al., 2019; Chen C. et al., 2020).

At the initial fermentation, owing to the sufficiency of nutrients and a favorable environment, fungal microorganisms grow rapidly to generate a complex fungal community (Yasuda et al., 2012). With the release of some compounds that are harmful to the growth of microorganisms and the consumption of nutrients, the diversity of the fungal community gradually decreases (Kobayashi et al., 2014). During the final stage of fermentation, the populations of some fungal microorganisms increase, which is largely ascribable to the utilization of residual nutrients released during the autolysis of dead cells. Although the diversity of fungal communities changes during the fermentation period, the changes in the dominant genera and their relative abundance are not significant. *Saccharomyces*, *Saccharomycopsis*, *Rhizopus*, *Monascus*, *Pichia*, *Wickerhamomyces*, *Candida*, and *Aspergillus* have been found to be the predominant genera during the traditional fermentation process of *Hong Qu* Huangjiu, while *Aspergillus*, *Thermomyces,* and *Rhizopus* play a dominant role in the brewing of *Wheat Qu* Huangjiu (Huang et al., 2018; Liu et al., 2019). Ji et al. (2018) found that *Aspergillus* species were more abundant in *Wheat Qu* than in various fermentation mashes, and that their abundance continually decreased until the end of *Wheat Qu* Huangjiu fermentation. Normally, the major flavor compounds in Huangjiu are generated by the metabolism of fungal microorganisms (Chen and Xu, 2012; Xie et al., 2012). Mu et al. (2016) found that the production of ethanol and higher alcohols was due to the metabolism of yeast. Furthermore, higher alcohols and organic acids reacted to form esters, and alcohols were oxidized to aldehydes, resulting in an increase of ester and aldehyde contents. During secondary fermentation, the ethanol-producing ability of yeast is reduced by the presence of high concentrations of ethanol and low pH, so that the production of alcohols, esters, and aldehydes is also decreased.

The bacterial communities in Huangjiu has previously been overlooked, however, these organisms not only affect the fermentation efficiency, but also play a decisive role in the flavor quality of Huangjiu. The diversity of bacterial community increases at the initial fermentation and then gradually becomes stable, and the changing environmental conditions may be responsible (Wang et al., 2014). The presence of sufficient nutrients and oxygen and a low content of ethanol are all conducive to the growth of microorganisms during primary fermentation. Conversely, the low temperature and high content of ethanol during secondary fermentation inhibits the growth of microorganisms. The diversity of the bacterial community is much greater than that of the fungal community during Huangjiu brewing (Huang et al., 2018; Chen C. et al., 2020). In the early stages of this research area, studies on the fermented mash of Shaoxing Huangjiu were conducted based on traditional isolation methods, but researchers obtained different results. Zhang et al. (2013) found that *Lactobacillus brevis* occurred during the entire brewing process of Huangjiu, while Hu et al. (2009) identified that *Bacillus subtilis* appeared throughout the whole fermentation process. The limitations of traditional isolation methods mean that they cannot fully reflect the composition of bacterial communities in Huangjiu brewing. Using PCR-DGGE and HTS technologies, researchers confirmed that a number of uncultured bacteria exist in the fermentation broth of Huangjiu, and also delineated their functional metabolism characteristics (Lv et al., 2013; Huang et al., 2019; Shuang et al., 2019). At the genus level, *Bacillus*, *Saccharopolyspora*, *Staphylococcus*, *Lactobacillus*, *Leuconostoc*, *Lactococcus*, *Weissella*, *Pseudomonas*, *Thermoactinomyces*, and *Enterobacteria* were the most abundant bacteria in Shaoxing Huangjiu and Shanghai Huangjiu (both were *Wheat Qu* Huangjiu, but used different types of *Qu*; Ji et al., 2018). As for *Hong Qu* Huangjiu, Huang et al. (2018) reported that *Lactobacillus*, *Bacillus*, *Leuconostoc*, *Lactococcus*, *Raoultella*, *Staphylococcus*, *Pediococcus*, and *Weissella* were the predominant genera. Although there are many different types of *Qu*, LAB play a crucial role in flavor generation of all Huangjiu. The bacterial community is dominated by the genus of *Bacillus*, *Staphylococcus*, and *Thermoactinomyces* during the primary fermentation of Huangjiu, but these are replaced by LAB during secondary fermentation, due to the facultative anaerobic and acid-tolerant features of most LAB (Hong et al., 2016; Shuang et al., 2019; Chen C. et al., 2020). The organic acids produced by LAB increase the acidity and lower the pH value, which inhibits the excessive growth of miscellaneous bacteria to prevent the rancidity of Huangjiu. The autolysis of bacteria also produces peptides, a small amount of amino acids, and other ingredients, which contribute to the aroma and taste of Huangjiu. Based on metagenomics and multivariate statistical analysis, Chen C. et al. (2020) found that *Pediococcus* and *Weissella* showed a strong correlation with the acid-producing ability of microbial communities in Shaoxing rice wine. Huang et al. (2018) found that the generation of fruit-flavored esters were strongly associated with *L. brevis* and *L. alimentarius*, as well as *Bacillus* and *Lactobacillus,* which contributed substantially to the formation of fatty acid ethyl esters.

SUMMARY AND PERSPECTIVES

Huangjiu is a national drink in China, and is thus the most promising wine for exportation. However, the consumer acceptance and market share of Huangjiu are significantly lower than that of Baijiu and beer due to its limited flavor

diversity and individuation. As the fermentation of Huangjiu involves multiple microorganisms under an open environment, manipulation of the fermentation process become difficult. Thus, understanding the nature of the microbial communities involved in different fermentation processes is of great significance to improve the flavor quality and economic competitiveness of Huangjiu products. In recent decades, the raw materials, brewing process, and microbial communities of Huangjiu have been comprehensively investigated. The characteristic flavor compounds, the predominant micro-organisms, and their metabolic functions during Huangjiu brewing are now clearer than before. Moreover, many functional strains have been isolated and microbes that were considered uncultivable in the past have now been isolated and cultured.

The contribution of microorganisms to flavor compound mixtures are studied mainly by HTS and multivariate statistics analysis. However, the relationship between microorganisms and flavor compounds based on correlation analysis cannot reveal the function of specific microbes in the fermentation process of Huangjiu. Furthermore, the interaction between microorganisms during Huangjiu brewing also remains to be elucidated. In future, with the further development of HTS technology and the combined application of multi-omics technologies (metagenomics, proteomics, flavoromics, and metabolomics), the aroma-producing microorganisms of microbial communities during Huangjiu brewing may be identified and applicated in the production of high-quality, flavorful Huangjiu. In addition, the investigation of interactions between aroma-generating microorganisms and their adaption to changes in the fermentation environment will provide a more theoretical basis for manipulating the fermentation process, such as by using selected microorganisms to improve the overall flavor quality of Huangjiu.

AUTHOR CONTRIBUTIONS

YY: investigation, software, visualization, and writing – original draft. WH: resources, methodology, and visualization. YX: conceptualization, project administration, and writing – review and editing. ZM: resources, visualization, and writing – review and editing. LT: visualization and investigation. XS: writing – review and editing and visualization. HZ: writing – review and editing. BN: writing – review and editing. LA: supervision, writing – original draft, and writing – review and editing. All authors contributed to the article and approved the submitted version.

FUNDING

This study was financially supported by the Shanghai Agriculture Applied Technology Development Program (2019-02-08-00-07-F01152), the Key Project of Special Development Fund in National Self-innovative Pilot Area (201705-PD-LJZ-B2074-007), the Shanghai Engineering Research Center of food microbiology program (19DZ2281100), and the Technical Standard Project of Huangjiu in 2018 (18DZ2200200).

REFERENCES

Adeniran, O., Atanda, O., Edema, M., and Oyewole, O. (2012). Effect of lactic acid bacteria and yeast starter cultures on the soaking time and quality of "ofada" rice. *Food Nutr. Sci.* 3, 207–211. doi: 10.4236/fns.2012.32030

Ahmed, J., Al-Jassar, S., and Thomas, L. (2015). A comparison in rheological, thermal, and structural properties between indian basmati and egyptian giza rice flour dispersions as influenced by particle size. *Food Hydrocol.* 48, 72–83. doi: 10.1016/j.foodhyd.2015.02.012

Akita, O., Ida, T., Obata, T., and Hara, S. (1990). Mutants of *Saccharomyces cerevisiae* producing a large quantity of β-phenethyl alcohol and β-phenethyl acetate. *J. Ferment. Bioeng.* 69, 125–128. doi: 10.1016/0922-338X(90)90200-G

Area, M. R., Rico, M., Montero, B., Barral, L., Bouza, R., López, J., et al. (2019). Corn starch plasticized with isosorbide and filled with microcrystalline cellulose: Processing and characterization. *Carbohydr. Polym.* 206, 726–733. doi: 10.1016/j.carbpol.2018.11.055

Arikawa, Y., Yamada, M., Shimosaka, M., Okazaki, M., and Fukuzawa, M. (2000). Isolation of sake yeast mutants producing a high level of ethyl caproate and/or isoamyl acetate. *J. Biosci. Bioeng.* 90, 675–677. doi: 10.1016/S1389-1723(00)90016-1

Arroyo-Lopez, F. N., Orlic, S., Querol, A., and Barrio, E. (2009). Effects of temperature, pH and sugar concentration on the growth parameters of *Saccharomyces cerevisiae*, *S. kudriavzevii* and their interspecific hybrid. *Int. J. Food Microbiol.* 131, 120–127. doi: 10.1016/j.ijfoodmicro.2009.01.035

Asano, T., Inoue, T., Kurose, N., Hiraoka, N., and Kawakita, S. (1999). Improvement of isoamyl acetate productivity in sake yeast by isolating mutants resistant to econazole. *J. Biosci. Bioeng.* 87, 697–699. doi: 10.1016/S1389-1723(99)80137-6

Avalos, J. L., Fink, G. R., and Stephanopoulos, G. (2013). Compartmentalization of metabolic pathways in yeast mitochondria improves the production of branched-chain alcohols. *Nat. Biotechnol.* 31, 335–341. doi: 10.1038/nbt.2509

Avbelj, M., Zupan, J., Kranjc, L., and Raspor, P. (2015). Quorum-sensing kinetics in *Saccharomyces cerevisiae*: a symphony of ARO genes and aromatic alcohols. *J. Agric. Food Chem.* 63, 8544–8550. doi: 10.1021/acs.jafc.5b03400

Bechman, A., Phillips, R. D., and Chen, J. (2012). Changes in selected physical property and enzyme activity of rice and barley koji during fermentation and storage. *J. Food Sci.* 77, 318–322. doi: 10.1111/j.1750-3841.2012.02691.x

Bednarek, M., Szwengiel, A., Florez, A. B., Czarnecki, Z., and Mzyo, B. (2019). Effect of different starter cultures on chemical and microbial parameters of buckwheat honey fermentation. *Food Microbiol.* 82, 294–302. doi: 10.1111/j.1750-3841.2012.02691.x

Binati, R. L., Junior, W. J. L., Luzzini, G., Slaghenaufi, D., Ugliano, M., and Torriani, S. (2020). Contribution of non-*Saccharomyces* yeasts to wine volatile and sensory diversity: a study on *Lachancea thermotolerans*. *Int. J. Food Microbiol.* 318:108470. doi: 10.1016/j.ijfoodmicro.2019.108470

Cai, H., Zhang, T., Zhang, Q., Luo, J., Cai, C., and Mao, J. (2018). Microbial diversity and chemical analysis of the starters used in traditional chinese sweet rice wine. *Food Microbiol.* 73, 319–326. doi: 10.1016/j.fm.2018.02.002

Canonico, L., Solomon, M., Comitini, F., Ciani, M., and Varela, C. (2019). Volatile profile of reduced alcohol wines fermented with selected non-*Saccharomyces* yeasts under different aeration conditions. *Food Microbiol.* 84:103247. doi: 10.1016/j.fm.2019.103247

Cao, J., Liu, K., Zhang, A., Yan, W., Zheng, Y., and Zeng, Q. (2018). ^{1}H-NMR and viscosity studies of hydrogen bonding of chinese rice wine. *CyTA-J. Food* 16, 776–785. doi: 10.1080/19476337.2018.1473497

Cao, Y., Xie, G. F., Wu, C., and Lu, J. (2010). A study on characteristic flavor compounds in traditional chinese rice wine-guyue longshan rice wine. *J. Inst. Brew.* 116, 182–189. doi: 10.1002/j.2050-0416.2010.tb00416.x

Castellano, P., Belfiore, C., Fadda, S., and Vignolo, G. (2008). A review of bacteriocinogenic lactic acid bacteria used as bioprotective cultures in fresh

meat produced in Argentina. *Meat Sci.* 79, 483–499. doi: 10.1016/j.meatsci.2007.10.009

Chang, A. C. (2003). The effects of gamma irradiation on rice wine maturation. *Food Chem.* 83, 323–327. doi: 10.1016/S0308-8146(03)00050-5

Chang, P., Scharfenstein, L. L., Solorzano, C. D., Abbas, H. K., Hua, S. S. T., Jones, W. A., et al. (2015). High sequence variations in the region containing genes encoding a cellular morphogenesis protein and the repressor of sexual development help to reveal origins of *aspergillus oryzae*. *Int. J. Food Microbiol.* 200, 66–71. doi: 10.1016/j.ijfoodmicro.2015.01.021

Chen, C., Liu, Y., Tian, H., Ai, L., and Yu, H. (2020). Metagenomic analysis reveals the impact of JIUYAO microbial diversity on fermentation and the volatile profile of Shaoxing-jiu. *Food Microbiol.* 86:103326. doi: 10.1016/j.fm.2019.103326

Chen, T., Wu, F., Guo, J., Ye, M., Hu, H., Guo, J., et al. (2020). Effects of glutinous rice protein components on the volatile substances and sensory properties of chinese rice wine. *J. Sci. Food Agric.* 100, 3297–3307. doi: 10.1002/jsfa.10343

Chen, H., and Fink, G. R. (2006). Feedback control of morphogenesis in fungi by aromatic alcohols. *Genes Dev.* 20, 1150–1161. doi: 10.1101/gad.1411806

Chen, S., Luo, T., Xu, Y., Fan, W., and Zhao, G. (2009). Effects of yeast strains and raw materials on β-pheonylethanol production in chinese rice wines. *China Brew.* 28, 23–26.

Chen, S., Wang, C., Qian, M., Li, Z., and Xu, Y. (2019). Characterization of the key aroma compounds in aged chinese rice wine by comparative aroma extract dilution analysis, quantitative measurements, aroma recombination, and omission studies. *J. Agric Food Chem.* 67, 4876–4884. doi: 10.1021/acs.jafc.9b01420

Chen, S., and Xu, Y. (2012). The influence of yeast strains on the volatile flavour compounds of chinese rice wine. *J. Inst. Brew.* 116, 190–196. doi: 10.1002/j.2050-0416.2010.tb00417.x

Chen, S., and Xu, Y. (2013). Effect of 'wheat Qu' on the fermentation processes and volatile flavour-active compounds of chinese rice wine (Huangjiu). *J. Inst. Brew.* 119, 71–77. doi: 10.1002/jib.59

Chen, S., Xu, Y., and Qian, M. C. (2018). Comparison of the aromatic profile of traditional and modern types of Huang Jiu (chinese rice wine) by aroma extract dilution analysis and chemical analysis. *Flavour Frag. J.* 33, 263–271. doi: 10.1002/ffj.3440

Cordente, A. G., Solomon, M., Schulkin, A., Francis, I. L., Barker, A., Borneman, A. R., et al. (2018). Novel wine yeast with ARO4 and TYR1 mutations that overproduce 'floral' aroma compounds 2-phenylethanol and 2-phenylethyl acetate. *Appl. Microbiol. Biotechnol.* 102, 5977–5988. doi: 10.1007/s00253-018-9054-x

de Jesús Rodríguez-Romero, J., Aceves-Lara, C. A., Silva, C. F., Gschaedler, A., Amaya-Delgado, L., and Arrizon, J. (2020). 2-Phenylethanol and 2-phenylethylacetate production by nonconventional yeasts using tequila vinasses as a substrate. *Biotechnol. Rep.* 25:e00420. doi: 10.1016/j.btre.2020.e00420

De Lima, L. A., Diniz, R. H. S., De Queiroz, M. V., Fietto, L. G., and Da Silveira, W. B. (2018). Screening of yeasts isolated from brazilian environments for the 2-phenylethanol (2-PE) production. *Biotechnol. Bioproc. Eng.* 23, 326–332. doi: 10.1007/s12257-018-0119-6

del Rio, B., Redruello, B., Fernandez, M., Martin, M. C., Ladero, V., and Alvarez, M. A. (2020). The biogenic amine tryptamine, unlike β-phenylethyamine, shows in vitro cytotoxicity at concentrations that have been found in foods. *Food Chem.* 331:127303. doi: 10.1016/j.foodchem.2020.127303

Ding, S., Zhang, Y., Zhang, J., Zeng, W., Yang, Y., Guan, J., et al. (2015). Enhanced deacidification activity in *Schizosaccharomyces pombe* by genome shuffling. *Yeast* 32, 317–325.

Dong, J., Hong, K. Q., Zhang, C. Y., Dong, S. S., Li, X., Chen, Y. F., et al. (2019). Increased acetate ester production of polyploid industrial brewer's yeast strains via precise and seamless "self-cloning" integration strategy. *Iran. J. Biotechnol.* 17:e1990. doi: 10.21859/ijb.1990

Dueñas-Sánchez, R., Pérez, A. G., Codón, A. C., Benítez, T., and Rincón, A. M. (2014). Overproduction of 2-phenylethanol by industrial yeasts to improve organoleptic properties of bakers' products. *Int. J. Food Microbiol.* 180, 7–12. doi: 10.1016/j.ijfoodmicro.2014.03.029

Escribano-Viana, R., González-Arenzana, L., Portu, J., Garijo, P., López-Alfaro, I., López, R., et al. (2018). Wine aroma evolution throughout alcoholic fermentation sequentially inoculated with non-*Saccharomyces*/*Saccharomyces* yeasts. *Food Res. Int.* 112, 17–24. doi: 10.1016/j.foodres.2018.06.018

Fan, W., and Xu, Y. (2012). Characteristic aroma compounds of chinese dry rice wine by gas chromatography-olfactometry and gas chromatography-mass spectrometry. *ACS Symposium Ser.* 1104, 277–301.

Fang, R. S., Dong, Y. C., Chen, F., and Chen, Q. H. (2015). Bacterial diversity analysis during the fermentation processing of traditional Chinese yellow rice wine revealed by 16S rDNA 454 pyrosequencing. *J. Food Sci.* 80, M2265–M2271. doi: 10.1111/1750-3841.13018

Fleet, G. H. (2003). Yeast interactions and wine flavor. *Int. J. Food Microbiol.* 86, 11–22. doi: 10.1016/S0168-1605(03)00245-9

Gong, M., Zhou, Z., Jin, J., Yu, Y., Liu, S., Han, X., et al. (2020). Effects of soaking on physicochemical properties of four kinds of rice used in Huangjiu brewing. *J. Cereal Sci.* 91:102855. doi: 10.1016/j.jcs.2019.102855

Gong, Y. P., Zhou, J. D., Qian, B., Ren, J., and Jiang, Y. J. (2013). Study on the influence of different brewing processes on physical and chemical indicators and higher alcohol content of yellow wine. *China Brew.* 32, 37–43.

Hazelwood, L. H., Daran, J. M. G., Van Maja, and Dickinson, J. R. (2008). The ehrlich pathway for fusel alcohol production: a century of research on *Saccharomyces cerevisiae* metabolism. *Appl. Environ. Microbiol.* 74, 2259–2266. doi: 10.1128/AEM.02625-07

Hong, X. T., Chen, J., Liu, L., Wu, H., Tao, H. O., Xie, G. F., et al. (2016). Metagenomic sequencing reveals the relationship between microbiota composition and quality of chinese rice wine. *Sci. Rep.* 6, 26621–26633. doi: 10.1038/srep26621

Hu, K., Jin, G. J., Mei, W. C., Li, T., and Tao, Y. S. (2018). Increase of medium-chain fatty acid ethyl ester content in mixed *H. uvarum*/*S. cerevisiae* fermentation leads to wine fruity aroma enhancement. *Food Chem.* 239, 495–501. doi: 10.1016/j.foodchem.2017.06.151

Hu, Z. M., Xie, G. F., Wu, C., Cao, Y., and Lu, J. (2009). Research on prokaryotic microbes in mash during yellow rice wine big pot fermentation. *Liquor Making Sci. Technol.* 8, 58–61.

Huang, Z., Zeng, Y., Liu, W., Wang, S., Shen, C., and Shi, B. (2020). Effects of metals released in strong-flavor baijiu on the evolution of aroma compounds during storage. *Food Sci. Nutr.* 8, 1904–1913. doi: 10.1002/fsn3.1475

Huang, Z. R., Guo, W. L., Zhou, W. B., Li, L., Xu, J. X., Hong, J. L., et al. (2019). Microbial communities and volatile metabolites in different traditional fermentation starters used for *Hong Qu* glutinous rice wine. *Food Res. Int.* 121, 593–603. doi: 10.1016/j.foodres.2018.12.024

Huang, Z. R., Hong, J. L., Xu, J. X., Li, L., Guo, W. L., Pan, Y. Y., et al. (2018). Exploring core functional microbiota responsible for the production of volatile flavour during the traditional brewing of Wuyi Hong Qu glutinous rice wine. *Food Microbiol.* 76, 487–496. doi: 10.1016/j.fm.2018.07.014

Ji, Z. W., Huang, G. D., Mao, J., and Fu, W. J. (2013). Effect of rice immersion time ton he quality of rice wine. *Food Equip.* 29, 49–52.

Ji, Z. W., Jin, J. S., Yu, G. S., Mou, R., Mao, J., Liu, S. P., et al. (2018). Characteristic of filamentous fungal diversity and dynamics associated with wheat Qu and the traditional fermentation of chinese rice wine. *Int. J. Food Sci. Technol.* 53, 1611–1621. doi: 10.1111/ijfs.13743

Jia, L. X., Hui, J. W., Zhi, W. W., Fu, P. Z., Xin, L., Zheng, P. L., et al. (2018). Microbial dynamics and metabolite changes in chinese rice wine fermentation from sorghum with different tannin content. *Sci. Rep.* 8, 39–46. doi: 10.1038/s41598-018-23013-1

Jolly, N. P., Varela, C., and Pretorius, I. S. (2014). Not your ordinary yeast: *non-Saccharomyces* yeasts in wine production uncovered. *FEMS Yeast Res.* 14, 215–237. doi: 10.1111/1567-1364.12111

Jones, P. R., Gawel, R., Francis, I. L., Francis, I. L., and Waters, E. J. (2008). The influence of interactions between major white wine components on the aroma, flavour and texture of model white wine. *Food Qual. Preference* 19, 596–607. doi: 10.1016/j.foodqual.2008.03.005

Jones, R. J., Hussein, H. M., Zagorec, M., Brightwell, G., and Tagg, J. R. (2008). Isolation of lactic acid bacteria with inhibitory activity against pathogens and spoilage organisms associated with fresh meat. *Food Microbiol.* 25, 228–234. doi: 10.1016/j.fm.2007.11.001

Kobayashi, K., Hattori, T., Honda, Y., and Kirimura, K. (2014). Oxalic acid production by citric acid-producing *Aspergillus niger* overexpressing the oxaloacetate hydrolase gene oahA. *J. Ind. Microbiol. Biotechnol.* 41, 749–756. doi: 10.1007/s10295-014-1419-2

Krogerus, K., Magalhães, F., Vidgren, V., and Gibson, B. (2017). Novel brewing yeast hybrids: creation and application. *Appl. Microbiol. Biotechnol.* 101, 65–78. doi: 10.1007/s00253-016-8007-5

Li, H., Jiao, A., Xu, X., Wu, C., et al. (2013). Simultaneous saccharification and fermentation of broken rice: an enzymatic extrusion liquefaction pretreatment for Chinese rice wine production. *Bioproc. Biosyst. Eng.* 36, 1141–1148. doi: 10.1007/s00449-012-0868-0

Li, H., Wei, B., Wu, C., Zhang, B., Xu, X., Jin, Z., et al. (2014). Modelling and optimisation of enzymatic extrusion pretreatment of broken rice for rice wine manufacture. *Food Chem.* 150, 94–98. doi: 10.1016/j.foodchem.2013.10.146

Li, X., Wang, P., Wu, D., and Lu, J. (2014). Effects of sterilization temperature on the concentration of ethyl carbamate and other quality traits in chinese rice wine. *J. Inst. Brew.* 120, 512–515. doi: 10.1002/jib.169

Li, Z. Y., Feng, C. X., and Luo, X. G. (2018). Revealing the influence of microbiota on the quality of pu-er tea during fermentation process by shotgun metagenomic and metabolomic analysis. *Food Microbiol.* 76, 405–415. doi: 10.1016/j.fm.2018.07.001

Liu, S. P., Chen, Q. L., Zou, H. J., Yu, Y. J., Zhou, Z. L., Mao, J., et al. (2019). A metagenomic analysis of the relationship between microorganisms and flavor development in Shaoxing mechanized Huangjiu fermentation mashes. *Int. J. Food Microbiol.* 303, 9–18. doi: 10.1016/j.ijfoodmicro.2019.05.001

Londoño-Hernández, L., Ramírez-Toro, C., Ruiz, H. A., Ascacio-Valdés, J. A., Aguilar-Gonzalez, M. A., Rodríguez-Herrera, R., et al. (2017). *Rhizopus oryzae*-Ancient microbial resource with importance in modern food industry. *Int. J. Food Microbiol.* 257, 110–127. doi: 10.1016/j.ijfoodmicro.2017.06.012

Longo, R., Carew, A., Sawyer, S., Kemp, B., and Kerslake, F. (2020). A review on the aroma composition of *Vitis vinifera L. Pinot noir* wines: origins and influencing factors. *Crit. Rev. Food Sci. Nutr.* 2020, 1–16. doi: 10.1080/10408398.2020.1762535

Lücke, F. K., Fritz, V., Tannhäuser, K., and Arya, A. (2019). Controlled fermentation of rapeseed presscake by *Rhizopus*, and its effect on some components with relevance to human nutrition. *Food Res. Int.* 120, 726–732. doi: 10.1016/j.foodres.2018.11.031

Luo, T., Fan, W., and Xu, Y. (2008). Characterization of volatile and semi-volatile compounds in chinese rice wines by headspace solid phase microextraction followed by gas chromatography-mass spectrometry. *J. Inst. Brew.* 114, 172–179. doi: 10.1002/j.2050-0416.2008.tb00323.x

Lv, R., Chantapakul, T., Zou, M., Li, M., Zhou, J., Ding, T., et al. (2018). Thermal inactivation kinetics of *Bacillus cereus* in chinese rice wine and in simulated media based on wine components. *Food Control* 89, 308–313. doi: 10.1016/j.foodcont.2018.01.029

Lv, X. C., Huang, R. L., Chen, F., Zhang, W., Rao, P. F., and Ni, L. (2013). Bacterial community dynamics during the traditional brewing of Wuyi Hong Qu glutinous rice wine as determined by culture-independent methods. *Food Control* 34, 300–306. doi: 10.1016/j.foodcont.2013.05.003

Martínez-Avila, O., Sánchez, A., Font, X., and Barrena, R. (2018). Bioprocesses for 2-phenylethanol and 2-phenylethyl acetate production: current state and perspectives. *Appl. Microbiol. Biotechnol.* 102, 9991–10004. doi: 10.1007/s00253-018-9384-8

Mo, X., Fan, W., and Xu, Y. (2009). Changes in volatile compounds of chinese rice wine wheat *Qu* during fermentation and storage. *J. Inst. Brew.* 115, 300–307. doi: 10.1002/j.2050-0416.2009.tb00385.x

Mu, R., Mao, J., Meng, X. Y., and Liu, Y. Y. (2016). Analysis of fungi diversity and volatile flavor compounds in chinese rice wine fermentation process. *J. Food Sci. Biotechnol.* 35, 303–309.

Nose, A., Hojo, M., Suzuki, M., and Ueda, T. (2004). Solute effects on the interaction between water and ethanol in aged whiskey. *J. Agric. Food Chem.* 52, 5359–5365. doi: 10.1021/jf0400516

Nose, A., Myojin, M., Hojo, M., Ueda, T., and Okuda, T. (2005). Proton nuclear magnetic resonance and raman spectroscopic studies of japanese sake, an alcoholic beverage. *J. Biosci. Bioeng.* 99, 493–501. doi: 10.1263/jbb.99.493

Oguro, Y., Nishiwaki, T., Shinada, R., Kobayashi, K., and Kurahashi, A. (2017). Metabolite profile of koji amazake and its lactic acid fermentation product by *Lactobacillus sakei* UONUMA. *J. Biosci. Bioeng.* 124, 178–183. doi: 10.1016/j.jbiosc.2017.03.011

Ohashi, M., Nasuno, R., Isogai, S., and Takagi, H. (2020). High-level production of ornithine by expression of the feedback inhibition-insensitive N-acetyl glutamate kinase in the sake yeast *Saccharomyces cerevisiae*. *Metab. Eng.* 62, 1–9. doi: 10.1016/j.ymben.2020.08.005

Pachuau, L., Dutta, R. S., Roy, P. K., Kalita, P., and Lalhlenmawia, H. (2017). Physicochemical and disintegrant properties of glutinous rice starch of mizoram, *india*. *Int. J. Biol. Macromol.* 95, 1298–1304. doi: 10.1016/j.ijbiomac.2016.11.029

Pineda, A., Carrasco, J., Pena-Farfal, C., Henriquez-Aedo, K., and Aranda, M. (2012). Preliminary evaluation of biogenic amines content in chilean young varietal wines by HPLC. *Food Control* 23, 251–257. doi: 10.1016/j.foodcont.2011.07.025

Querol, A., Pérez-Torrado, R., Alonso-del-Real, J., Minebois, R., Stribny, J., Oliveira, B. M., et al. (2018). New trends in the uses of yeasts in oenology. *Adv. Food Nutr. Res.* 85, 177–210. doi: 10.1016/bs.afnr.2018.03.002

Rao, Q. S., Yang, Z. Q., Gao, L., Song, Y. L., and Fang, W. M. (2014). Effect of raw rice on antioxidant activity of finished yellow wine. *China Brew.* 33, 75–77.

Regueiro, J., Negreira, N., and Simal-Gándara, J. (2017). Challenges in relating concentrations of aromas and tastes with flavor features of foods. *Crit. Rev. Food Sci. Nutr.* 57, 2112–2127. doi: 10.1080/10408398.2015.1048775

Rhee, S. J., Lee, J. E., and Lee, C. H. (2011). Importance of lactic acid bacteria in asian fermented foods. *Microb. Cell Fact.* 10:S5. doi: 10.1186/1475-2859-10-S1-S5

Roldán, A. M., Lloret, I., and Palacios, V. (2017). Use of a submerged yeast culture and lysozyme for the treatment of bacterial contamination during biological aging of sherry wines. *Food Control* 71, 42–49. doi: 10.1016/j.foodcont.2016.06.016

Rui, Y., Wan, P., Chen, G. J., Xie, M. H., Sun, Y., Zeng, X. X., et al. (2019). Analysis of bacterial and fungal communities by Illumina MiSeq platforms and characterization of *Aspergillus cristatus* in fuzhuan brick tea. *LWT Food Sci. Technol.* 110, 168–174. doi: 10.1016/j.lwt.2019.04.092

Shekhawat, K., Bauer, F. F., and Setati, M. E. (2017). Impact of oxygenation on the performance of three non-*Saccharomyces* yeasts in co-fermentation with *Saccharomyces cerevisiae*. *Appl. Microbiol. Biotechnol.* 101, 2479–2491. doi: 10.1007/s00253-016-8001-y

Shen, F., Ying, Y., Li, B., Zheng, Y., and Hu, J. (2011). Prediction of sugars and acids in Chinese rice wine by mid-infrared spectroscopy. *Food Res. Int.* 44, 1521–1527. doi: 10.1016/j.foodres.2011.03.058

Shi, S., Zhang, L., Wu, Z. Y., Zhang, W. X., Deng, Y., and Li, J. M. (2011). Analysis of the fungi community in multiple- and single-grains zaopei from a luzhou-flavor liquor distillery in western china. *World J. Microbiol. Biotechnol.* 27, 1869–1874. doi: 10.1007/s11274-010-0645-7

Shuang, P. L., Qing, L. C., Hui, J. A., Yong, J. Y., Zhi, L. Z., Jian, M., et al. (2019). A metagenomic analysis of the relationship between microorganisms and flavor development in shaoxing mechanized huangjiu fermentation mashes. *Int. J. Food Microbiol.* 303, 9–18. doi: 10.1016/j.ijfoodmicro.2019.05.001

Snoek, T., Verstrepen, K. J., and Voordeckers, K. (2016). How do yeast cells become tolerant to high ethanol concentrations? *Curr. Genet.* 62, 475–480. doi: 10.1007/s00294-015-0561-3

Steensels, J., and Verstrepen, K. J. (2014). Taming wild yeast: potential of conventional and nonconventional yeasts in industrial fermentations. *Annu. Rev. Microbiol.* 68, 61–80.

Takagi, H. (2019). Metabolic regulatory mechanisms and physiological roles of functional amino acids and their applications in yeast. *Biosci. Biotechnol. Biochem.* 83, 1449–1462. doi: 10.1080/09168451.2019.1576500

Takahashi, T., Ohara, Y., and Sueno, K. (2017). Breeding of a sake yeast mutant with enhanced ethyl caproate productivity in sake brewing using rice milled at a high polishing ratio. *J. Biosci. Bioeng.* 123, 707–713. doi: 10.1016/j.jbiosc.2017.01.014

Tao, Y., García, J. F., and Sun, D. W. (2014). Advances in wine aging technologies for enhancing wine quality and accelerating wine aging process. *Crit. Rev. Food Sci. Nutr.* 54, 817–835. doi: 10.1080/10408398.2011.609949

Tian, Y., Huang, J., Xie, T., Huang, L., Zhuang, W., Zheng, Y., et al. (2016). Oenological characteristics, amino acids and volatile profiles of *hongqu* rice wines during pottery storage: effects of high hydrostatic pressure processing. *Food Chem.* 203, 456–464. doi: 10.1016/j.foodchem.2016.02.116

Varela, C., Dry, P. R., Kutyna, D. R., Francis, I. L., Henschke, P. A., Curtin, C. D., et al. (2015). Strategies for reducing alcohol concentration in wine. *Aust. J. Grape Wine Res.* 21, 670–679. doi: 10.1111/ajgw.12187

Wang, J. G., Sheng, Y. G., Huang, Y. Y., Lu, W. J., and Xue, C. (2013). Development of oatmeal red yeast rice wine. *China Brew.* 32, 152–154.

Wang, N., Chen, S., and Zhou, Z. (2019). Characterization of volatile organic compounds as potential aging markers in chinese rice wine using multivariable statistics. *J. Sci. Food Agric.* 99, 6444–6454. doi: 10.1002/jsfa.9923

Wang, P., Mao, J., Meng, X., Li, X., Liu, Y., and Feng, H. (2014). Changes in flavour characteristics and bacterial diversity during the traditional fermentation of chinese rice wines from shaoxing region. *Food Control* 44, 58–63. doi: 10.1016/j.foodcont.2014.03.018

Wei, X. L., Liu, S. P., Yu, J. S., Yu, Y. J., Zhu, S. H., Zhou, Z. L., et al. (2017). Innovation chinese rice wine brewing technology by bi-acidification to exclude rice soaking process. *J. Biosci. Bioeng.* 123, 460–465. doi: 10.1016/j.jbiosc.2016.11.014

Xie, G. F., Li, W. J., Lu, J., Cao, Y., Fang, H., and Zou, H. J. (2012). Isolation and identification of representative fungi from shaoxing rice wine wheat Qu using a polyphasic approach of culture-based and molecular-based methods. *J. Inst. Brew.* 113, 272–279. doi: 10.1002/j.2050-0416.2007.tb00287.x

Xie, G. F., Wang, L., Gao, Q., Yu, W., Hong, X., Zhao, L., et al. (2013). Microbial community structure in fermentation process of Shaoxing rice wine by Illumina-based metagenomic sequencing. *J. Sci. Food Agric.* 93, 3121–3125. doi: 10.1002/jsfa.6058

Xie, G. F., Zheng, Z. Q., Ma, J., and Fu, J. W. (2010). Screening of yeast strains for quick fermentation in chinese rice wine brewing. *China Brew.* 8, 12–14.

Xu, E., Wu, Z., Wang, F., Li, H., Xu, X., Jin, Z., et al. (2015). Impact of high-shear extrusion combined with enzymatic hydrolysis on rice properties and chinese rice wine fermentation. *Food Bioprocess Technol.* 8, 589–604. doi: 10.1007/s11947-014-1429-0

Xu, E., Wu, Z., Wang, F., Long, J., Xu, X., and Jin, Z. (2016). Effect of 'wheat Qu' addition on the formation of ethyl carbamate in chinese rice wine with enzymatic extrusion liquefaction pretreatment. *J. Inst. Brew.* 122, 55–62. doi: 10.1002/jib.290

Xu, J., Wu, H., Wang, Z., Zheng, F., Lu, X., Li, Z., et al. (2018). Microbial dynamics and metabolite changes in chinese rice wine fermentation from sorghum with different tannin content. *Sci. Rep.* 8, 1–11. doi: 10.1038/s41598-018-23013-1

Yang, L. J., Jiang, Y. J., and Li, Y. D. (2013). Screening, identification and fermentation characteristics of a chinese rice wine yeast strain with high stress tolerance. *Chin. J. Food Sci.* 13, 71–77.

Yang, Y., Xia, Y., Lin, X., Wang, G., Zhang, H., Xiong, Z., et al. (2018). Improvement of flavor profiles in chinese rice wine by creating fermenting yeast with superior ethanol tolerance and fermentation activity. *Food Res. Inter.* 108, 83–92. doi: 10.1016/j.foodres.2018.03.036

Yang, Y. J., Xia, Y. J., Wang, G. Q., Tao, L. R., Yu, J. S., and Ai, L. Z. (2019). Effects of boiling, ultra-high temperature and high hydrostatic pressure on free amino acids, flavor characteristics and sensory profiles in chinese rice wine. *Food Chem.* 275, 407–416. doi: 10.1016/j.foodchem.2018.09.128

Yang, Y. J., Xia, Y. J., Wang, G. Q., Yu, J. S., and Ai, L. Z. (2017). Effect of mixed yeast starter on volatile flavor compounds in chinese rice wine during different brewing stages. *LWT Food Sci. Technol.* 78, 373–381. doi: 10.1016/j.lwt.2017.01.007

Yasuda, M., Tachibana, S., and Kuba-Miyara, M. (2012). Biochemical aspects of red koji and tofuyo prepared using *Monascus* fungi. *Appl. Microbiol. Biotechnol.* 96, 49–60. doi: 10.1007/s00253-012-4300-0

Yu, H. Y., Xie, T., Xie, J. R., Ai, L. Z., and Tian, H. X. (2019). Characterization of key aroma compounds in chinese rice wine using gas chromatography-mass spectrometry and gas chromatography-olfactometry. *Food Chem.* 293, 8–14. doi: 10.1016/j.foodchem.2019.03.071

Yu, L. J., Ding, F., and Ye, H. (2012). Analysis of characteristic flavor compounds in chinese rice wines and representative fungi in wheat *Qu* samples from different regions. *J. Inst. Brew.* 118, 114–119. doi: 10.1002/jib.13

Yue, Ch, Tian, J. J., Ge, Z. Q., and Yang, J. H. (2012). Research and development of loquat leaf cordyceps militaris rice wine. *China Brew.*31, 186–189.

Zdaniewicz, M., Satora, P., Pater, A., and Bogacz, S. (2020). Low lactic acid-producing strain of *Lachancea thermotolerans* as a new starter for beer production. *Biomolecules* 10:256. doi: 10.3390/biom10020256

Zhang, F. J., Zhu, X. M., Xue, J., Wang, Y. J., Wang, D. L., Zhou, J. D., et al. (2013). Study on bacterial communities and their fermenting properties in brewing process of yellow rice wine. *Liquor Making Sci. Technol.* 12, 32–35.

Zhang, W. X., Qiao, Z. W., Toru, S., Tang, Y. Q., Hu, C., Shigeru, M., et al. (2005). Analysis of the bacterial community in zaopei during production of chinese luzhou-flavor liquor. *J. Inst. Brew.* 111, 215–222. doi: 10.1002/j.2050-0416.2005.tb00669.x

Zhong, Y., Xiang, X., Chen, T., Liu, Y., Ye, J., Luo, S., et al. (2020). Accelerated aging of rice by controlled microwave treatment. *Food Chem.* 323:126853. doi: 10.1016/j.foodchem.2020.126853

Zhu, J., Lin, J., Palomec, L., and Wheeldon, I. (2015). Microbial host selection affects intracellular localization and activity of alcohol-o-acetyltransferase. *Microb. Cell Fact.* 14, 1–10. doi: 10.1186/s12934-015-0221-9

Zot, K., Miot-Sertier, C., Claisse, O., Lonvaud-Funel, A., and Masneuf-Pomarede, I. (2008). Dynamics and diversity of non-*Saccharomyces* yeasts during the early stages in winemaking. *Int. J. Food Microbiol.* 125, 197–203. doi: 10.1016/j.ijfoodmicro.2008.04.00

Conflict of Interest: HZ and BN were employed by the company of Shanghai Jinfeng Wine Co., Ltd.

The remaining authors declare that the research was conducted in the absence of any commercial or financial relationships that could be construed as a potential conflict of interest.

frontiers in Microbiology

CORRECTION
published: 25 February 2021
doi: 10.3389/fmicb.2021.636810

Corrigendum: Flavor Formation in Chinese Rice Wine (Huangjiu): Impacts of the Flavor-Active Microorganisms, Raw Materials, and Fermentation Technology

Yijin Yang[1,2†], Wuyao Hu[1†], Yongjun Xia[1], Zhiyong Mu[1], Leren Tao[2], Xin Song[1], Hui Zhang[3], Bin Ni[3] and Lianzhong Ai[1]*

[1] Shanghai Engineering Research Center of Food Microbiology, School of Medical Instrument and Food Engineering, University of Shanghai for Science and Technology, Shanghai, China, [2] School of Energy and Power Engineering, University of Shanghai for Science and Technology, Shanghai, China, [3] Shanghai Jinfeng Wine Co., Ltd., Shanghai, China

Keywords: Huangjiu (Chinese rice wine), flavor compounds, microbial community, raw material, fermentation technology, yeast starter, fungi

OPEN ACCESS

Approved by:
Frontiers Editorial Office, Frontiers Media SA, Switzerland

***Correspondence:**
Lianzhong Ai
ailianzhong@hotmail.com

†These authors have contributed equally to this work

Specialty section:
This article was submitted to Food Microbiology, a section of the journal Frontiers in Microbiology

Received: *02 December 2020*
Accepted: *03 February 2021*
Published: *25 February 2021*

Citation:
Yang Y, Hu W, Xia Y, Mu Z, Tao L, Song X, Zhang H, Ni B and Ai L (2021) Corrigendum: Flavor Formation in Chinese Rice Wine (Huangjiu): Impacts of the Flavor-Active Microorganisms, Raw Materials, and Fermentation Technology. Front. Microbiol. 12:636810. doi: 10.3389/fmicb.2021.636810

A Corrigendum on

Flavor Formation in Chinese Rice Wine (Huangjiu): Impacts of the Flavor-Active Microorganisms, Raw Materials, and Fermentation Technology
by Yang, Y., Hu, W., Xia, Y., Mu, Z., Tao, L., Song, X., et al. (2020). Front. Microbiol. 11:580247. doi: 10.3389/fmicb.2020.580247

In the original article, there was a mistake in **Figure 2** as published. "2-Methy-butanol" has been corrected as "2-Methylbutanol," and "Isoamylol" has been corrected as "Isoamyl alcohol." The corrected **Figure 2** appears below.

The authors apologize for this error and state that this does not change the scientific conclusions of the article in any way. The original article has been updated.

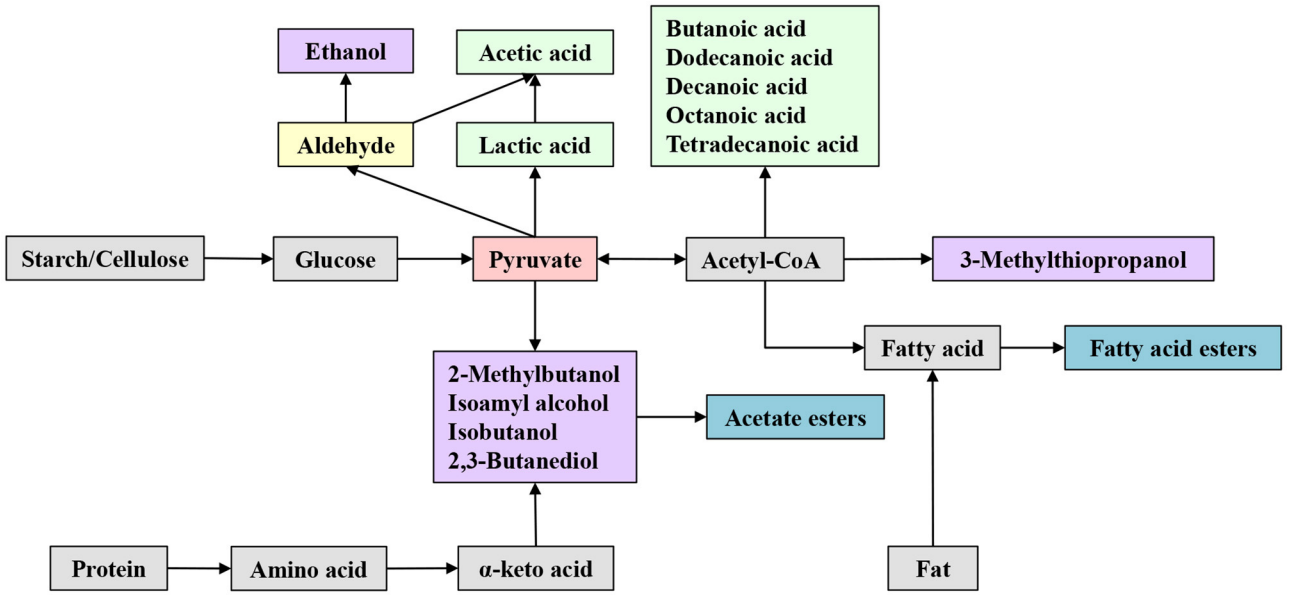

FIGURE 2 | Metabolism of major flavor compounds during Huangjiu brewing.

frontiers in Microbiology

PERSPECTIVE
published: 25 November 2020
doi: 10.3389/fmicb.2020.606959

Perspectives on Functional Red Mold Rice: Functional Ingredients, Production, and Application

Feng Yanli[1,2,3,4]* *and Yu Xiang*[1,2,3,4]

[1] Hubei Key Laboratory of Edible Wild Plants Conservation and Utilization, Hubei Normal University, Huangshi, China, [2] Hubei Engineering Research Center of Typical Wild Vegetables Breeding and Comprehensive Utilization Technology, Hubei Normal University, Huangshi, China, [3] National Demonstration Center for Experimental Biology Education, Hubei Normal University, Huangshi, China, [4] College of Life Sciences, Hubei Normal University, Huangshi, China

Monacolin K (MK) is a secondary metabolite of the *Monascus* species that can inhibit cholesterol synthesis. Functional red mold rice (FRMR) is the fermentation product of *Monascus* spp., which is rich in MK. FRMR is usually employed to regulate serum cholesterol, especially for hypercholesterolemic patients who refuse statins or face statin intolerance. The present perspective summarized the bioactive components of FRMR and their functions. Subsequently, efficient strategies for FRMR production, future challenges of FRMR application, and possible directions were proposed. This perspective helps to understand the present situation and developmental prospects of FRMR.

Keywords: functional red mold rice, monacolins, functional ingredients, production, application, *Monascus* spp.

OPEN ACCESS

Edited by:
Wanping Chen,
Georg-August-University Göttingen, Germany

Reviewed by:
Bo-Bo Zhang,
Shantou University, China
Chan Zhang,
Beijing Technology and Business University, China
Yang Hua,
Tianjin University of Science and Technology, China

****Correspondence:***
Feng Yanli
fengyanli@hbnu.edu.cn

Specialty section:
This article was submitted to Food Microbiology, a section of the journal Frontiers in Microbiology

Received: *16 September 2020*
Accepted: *29 October 2020*
Published: *25 November 2020*

Citation:
Yanli F and Xiang Y (2020) Perspectives on Functional Red Mold Rice: Functional Ingredients, Production, and Application. Front. Microbiol. 11:606959. doi: 10.3389/fmicb.2020.606959

INTRODUCTION

Red mold rice (RMR), also called red koji or red yeast rice is the fermentation product of *Monascus* spp. (Farkouh and Baumgärtel, 2019). It is widely used as a colorant, supplement, and starters in the food industry in Asian countries. RMR contains multiple beneficial metabolites, such as *Monascus* pigments, monacolin K (MK), and γ-aminobutyric acid. RMR also contains some enzymes, for instance, protease and amylase (De Backer, 2017; Chen et al., 2019; Jiang et al., 2019). However, a mycotoxin-citrinin produced by *Monascus* spp. can induce health risks (He et al., 2020b). Nowadays, RMR has three main product types on the market depending on its application, as follows: coloring RMR, brewing RMR, and functional red mold rice (FRMR). Coloring RMR is the RMR with a color value higher than 1,000 U/g according to the National Food Safety Standard of China (GB 1886.19–2015). Brewing RMR is the RMR that possesses strong saccharifying power and esterifying power, which is used as a fermentation starter in the food industry based on the Light Industry Standard of the People's Republic of China (QB/T 5188–2017). FRMR is the RMR with a natural MK of more than 0.4% according to the Light Industry Standard of the People's Republic of China (QB/T 2847–2007). MK is chemically identical to lovastatin, which is a lipid-lowering drug and shows evident effects on inhibiting 3-hydroxy-3-methylglutaryl-CoA (HMG-CoA) reductase that catalyzes the rate-limiting step of cholesterol biosynthesis (De Backer, 2017; Bruno et al., 2018). Therefore, FRMR is a commonly consumed food supplement by hypercholesterolemia patients, especially for statin-intolerant community (Mazzanti et al., 2017; Xiong et al., 2019).

However, some issues related to FRMR should be taken into consideration. Firstly, MK has a large number of analogs with different lipid-lowering effects and complex conversion relationships (Kimura et al., 1990; Li et al., 2017; Beltrán et al., 2019). For instance, 84 monacolins (MLs) have been monitored in RMR sample (Li et al., 2017). FRMR available from market contains

different contents of MK and different MLs in each FRMR sample (Dujovne, 2017). Therefore, it is inappropriate to define the functions of FRMR by merely depending on its MK content. Secondly, MK possesses specific active forms and has multiple functions. MK is an inactive lactone, which needs to be converted into its active β-hydroxy acid form (MKA) for the lipid-lowering activity (Yang and Hwang, 2006). Moreover, some other functions of MLs have also been reported, including promoting bone formation, being an antioxidant, and suppressing cancer cell proliferation (Wong and Rabie, 2008; Kurokawa et al., 2017; Nagabhishek and Madankumar, 2019; del Gaudio et al., 2020). Thirdly, a great number of metabolites besides MLs are available from FRMR. The functions of the beneficial metabolites such as *Monascus* pigments and γ-aminobutyric acid should be understood and evaluated, while using FRMR as a food supplement or as an alternative drug to the chemical statins. Meanwhile, the toxic metabolite produced by some *Monascus* strains, citrinin, should not only be studied but should also be carefully controlled (Farkouh and Baumgärtel, 2019). Furthermore, the side effects of MLs such as myopathies and liver injury need to be evaluated (Mazzanti et al., 2017). For the efficient application of FRMR, MK contents of FRMR should be standardized, and the functions and safety of FRMR need to be evaluated.

To obtain sufficient MK in FRMR, parameters for FRMR production in solid- and liquid-state fermentation such as initial moisture, pH, and nitrogen source have been optimized (Hp, 2012; Feng et al., 2014; Lin et al., 2017; Huang et al., 2018). Moreover, the screening of *Monascus* strains with high-MK production has also been carried out (Suh et al., 2007; Wang et al., 2011). Novel substrates have been utilized for FRMR production and enriching its product types, such as *Dioscorea*, *Finger millet*, and *Saccharina japonica* (Lee et al., 2007; Venkateswaran and Vijayalakshmi, 2010; Suraiya et al., 2018). All these strategies head for high-quality FRMR. The natural and environmental-friendly production of FRMR with sufficient MK is also prospected.

In the present perspective, we focus on the MLs in FRMR and their differences with lovastatin; strategies for efficient production of FRMR, the current situation of FRMR application, and the corresponding future directions for a wide application were proposed.

FUNCTIONAL SUBSTANCES IN FRMR

Monacolins are the main bioactive substances in FRMR. MK was chemically identified as lovastatin and was first isolated from the cultures of *Monascus ruber* No. 1005 as a hypocholesterolemic agent in 1979 (Endo, 1979). MK is a polyketide compound synthesized by polyketide synthase (PKS) in *Monascus* spp. MK biosynthetic pathway and gene cluster in *Monascus* spp. are similar to those of lovastatin from *Aspergillus terreus* (Zhang et al., 2020). The MK gene cluster including nine genes named *mok A-mok I* was isolated from the genome of *Monascus pilosus*, and functions of the genes have been carried out (Chen et al., 2008; Zhang et al., 2017b). Overexpression of key genes (*mokC*, *mokD*, *mokE*, and *mokI*) in *the Monascus purpureus* azaphilone polyketide pathway can be used to improve MK production (Zhang et al., 2019).

Monacolins are chemical analogs of MK that share a similar basic skeleton, with difference in the substituent groups. MLs are mainly divided into lactone ring form and free acidic form (Li et al., 2017). At least 84 MLs have been identified, though not all of the MLs have been studied (Li et al., 2017). MLs, for instance, monacolin L, monacolin J, dihydromonacolin L, monacolin X, and compactin, etc., in both the lactone and acid forms have attracted more attention, owing to their high contents in FRMR and their well-known beneficial bioactivities (Endo and Hasumi, 1985; Endo, 1985a,b; Endo et al., 1986; Dhale et al., 2007a,b; Zhu et al., 2012; Hachem et al., 2020). With the progress in research on these compounds, more and more MLs have been isolated and characterized. The structures and functions of MLs O-S, α, β-dehydromonacolin S, 3α- hydroxy-3,5-dihydromonacolin L, 3b-hydroxy-3,5-dihydro monacolin L, α, β-hydromonacolin Q, monacolin T, monacolin U, 6a-O-methyl-4,6-dihydromonacolin L and 6a-O-ethyl-4,6- dihydromonacolin L have been explored (Li et al., 2004; Liu et al., 2013; Zhang et al., 2016, 2018a). It is interesting that an unusual aromatic monacolin analog, monacophenyl, was isolated from RMR (Liu et al., 2011). In view of this, one of the most important key points for taking full advantage of FRMR is exploring its functions and side effects.

Besides MLs, other functional substances such as pigments, ergosterol, γ-aminobutyric acid, and polysaccharides, also play a certain role in the function of FRMR (Wang et al., 2014; Liang et al., 2019). For instance, ergosterol showed remarkable lipid-lowering efficiency. Moreover, three *Monascus* azaphilone pigments of monascin, monasfluore B, and ankaflavin were discovered as ligands of lipase (Fang et al., 2017; Liang et al., 2019).

FUNCTIONS OF FRMR

Functional red mold rice is widely consumed as a lipid-lowering product due to it containing MLs. Among the most commonly studied MLs, MK and its dihydro derivatives are the most active compounds for lowering lipid levels (Avula et al., 2014). However, MK exists in the inactive form naturally and undergoes reduction to its β-hydroxy acid (MKA) active form (Beltrán et al., 2019). MK in the lactone form gets absorbed from the gastrointestinal tract and gets converted into MKA in liver and non-hepatic tissues (Ertürk et al., 2003). In addition, the transformation process of MK into MKA spontaneously occurs at neutral pH, without the participation of gut microbiota. However, the lipid-lowering effect is mediated by the gut microbiota by catabolizing MKA to other compounds (Beltrán et al., 2019). *In vitro* experiments also indicated that MK could be completely converted into MKA only in alkaline solutions (Yang and Hwang, 2006).

Monacolins are usually obtained by consuming FRMR as a food supplement or from FRMR in combination with other bioactive compounds (Yang and Mousa, 2012; Heinz et al., 2016; D'Addato et al., 2017; Iskandar et al., 2020). An efficient and better tolerance in hypercholesterolemic patients was seen

when FRMR was combined with other bioactive compounds. For instance, combining FRMR with guggulipid extract, chromium picolinate, berberine, and coenzyme Q_{10} showed a better tolerance and efficiency (Yang and Mousa, 2012; Di Pierro et al., 2016; Cicero et al., 2017; D'Addato et al., 2017; Stefanutti et al., 2017; Mazza et al., 2018; Formisano et al., 2019; Wang et al., 2019; Iskandar et al., 2020).

Besides the lowering lipid effects, the physiological functions of MLs like promoting bone formation, attenuating arterial thrombosis, and anticancer have also been confirmed (Wong and Rabie, 2008; Tseng et al., 2011; Tien et al., 2016; Xu et al., 2017; Wang et al., 2019). New bone formation in bone defects *in vivo* and bone cell formation *in vitro* can be stimulated and increased using RMR extract (Wong and Rabie, 2008). In addition, apoptosis on gastric cancer was induced by MLs and other components by scavenging the mitochondrial reactive oxygen species (Kurokawa et al., 2017). Monacolin X is known to attenuate the cell proliferation, migration, and ROS stress-mediated apoptosis in breast cancer cells, which provides a scope for the functional research of MLs (Nagabhishek and Madankumar, 2019). Another important function of FRMR is its strong antioxidant effect, which needs to be taken into consideration (Lee et al., 2009; Mohan-Kumari et al., 2011).

EFFICIENT PRODUCTION OF FRMR

Optimization for Production of Monacolins

Optimization of the fermentation parameters for MK production has attracted much interest since its discovery (Tsukahara et al., 2009; Panda et al., 2010; Hp, 2012; Dikshit and Tallapragada, 2016). Liquid state fermentation (LSF) has not yielded constant results and higher production. Therefore, solid-state fermentation (SSF) is gaining an increasing popularity for multiple industrially important products such as pigments, enzymes, and antibiotics, besides MLs. SSF has been widely employed in the industrial production of FRMR, due to its advantages like maximum substrate utilization, better process control, lower chances of contamination, and easy downstream processing (Praveen and Savitha, 2012). Therefore, fermentation parameters of SSF for FRMR production, such as moisture content, fermentation temperature, and inoculum concentration have been studied extensively and discussed herewith. Generally, adjusting the moisture content to 35% (*w*/*w*) and maintaining an environmental humidity at 55∼65% is beneficial for the MK production (Subhagar et al., 2009; Feng et al., 2014). Fermentation temperature is another vital parameter for MK production. The temperature-shift cultivation is more advantageous for the MK production, when compared with the constant temperature fermentation. *Monascus* spp. are generally cultured at 30°C for their growth and at lower temperature such as 25°C or even 23°C for MK production (Tsukahara et al., 2009; Lin et al., 2017). In addition, the inoculum concentration also shows an influence on *Monascus* fermentation and MK production (Subhagar et al., 2009). Appropriate inoculum size starts the fermentation quickly and maintains the fermentation process at a good rate for metabolite production. There is a significant relation between the inoculum size and the spore concentrations of the inoculum, for instance, by adjusting them to 13% (*v*/*w*) and 10^6 CFU/ml, respectively (Feng et al., 2014). For the speedy growth of *Monascus* spp. and avoiding contamination by other microorganisms, lactic acid and acetic acid are usually added to adjust the pH of the fermentation substrates (Xu et al., 2005; Feng et al., 2014). The methods for improving the MK production by *Monascus* strains have been screened by chemical mutagenesis or genetic engineering technology (Yang et al., 2005b; Suh et al., 2007; Wang et al., 2011). A mutant KU609 with high MK and no citrinin production has been obtained from the wild-strain *Monascus* isolate number 711 by subjecting to γ-irradiation (Suh et al., 2007). The binary vector pCAMBIA3300-*gpdA-hph-trpC* with hygromycin B phosphotransferase (*hph*) was constructed and transformed into *Monascus albidus* 9901 by *Agrobacterium tumefaciens*-mediated transformation. Two transformants H1 and H2 were selected, and the MK yields of H1 and H2 fermentation products were increased by 42.15 and 40.34%, respectively, compared with that of *Monascus albidus* 9901 (Wang et al., 2011). Moreover, the mutagenic treatment of ultrasonic wave was also employed to screen *Monascus* strain producing more MK (Yang et al., 2005b). However, the biological characteristic stability of mutants should be well studied, before commencing the industrial production of FRMR.

Besides the optimization of fermentation parameters, some novel fermentation patterns have also been employed to enhance the MK production (Panda et al., 2010; Zhang et al., 2013; Seenivasan et al., 2020). Metabolic footprinting concept has been used to improve the MK production. A strong glycolytic flux pattern was observed in the shake culture, tricarboxylic acids such as, citric acid, succinic acid, and oxalic acid, apart from glycerol and ethanol are most probably utilized for enhancing production of MK (Seenivasan et al., 2020). A co-culture of *M. purpureus* and *M. ruber* or *M. purpureus* and *Monascus kaoliang* showed positive effects on MK production (Panda et al., 2010; Suraiya et al., 2018). On the other hand, agar was tried as a carrier and the MK production of 2,047.03 mg/L was obtained, when the agar concentration, particle size, and glycerol concentration were 4%, 4 × 4 × 4 mm and 18%, respectively (Zhang et al., 2013). To meet the individual needs of consumers, novel FRMR needs to be developed.

Novel Nutritious Substrates for FRMR Production

Novel substrates have been used for *Monascus* fermentation to enrich the types and functions of FRMR, for instance, soybean flour, finger millet, and Thai glutinous rice (Chairote et al., 2010; Venkateswaran and Vijayalakshmi, 2010; Feng et al., 2014; **Table 1**). Among the substrates mentioned, substrates rich in starch or protein, for example, soybean flour and *Dioscorea* are more suitable for *Monascus* fermentation and MK production (**Table 1**). Moreover, combining novel

TABLE 1 | Substrates used for FRMR production.

Substrates	Addition	Fermentation mode	Fermentation time (day)	Strain	MK (mg/g)/ detection method	References
Finger millet	Substrate	SSF	7	*M. purpureus*	0.370/HPLC	Venkateswaran and Vijayalakshmi, 2010
Adlay	Substrate	SSF	7	*M. purpureus*	1.120/HPLC	Yang et al., 2005a
Dioscorea	Substrate	SSF	10	*M. purpureus* NTU 301	2.584/HPLC	Lee et al., 2006
Soybean powder	40%	SSF	14	*M. pilosus* MS-1	18.733/HPLC	Feng et al., 2014
Saccharina japonica	Approximately 48.5%	SSF	14.49	*M. purpureus* KCCM 60168	13.980/HPLC	Suraiya et al., 2018
Mixed grains	Substrate	SSF	15	*M. pilosus* K-1140	2.310/HPLC	Pyo and Seo, 2010
Wheat bran	Approximately 25%	SSF	16	*M. sanguineus*	20.040/UV	Dikshit and Tallapragada, 2016
Millet	Substrate	SSF	20	*Monascus ruber*	7.120/HPLC	Zhang et al., 2018b
Soybean	Substrate	SSF	21	*M.* sp. K	0.892/HPLC	Hong et al., 2012
Thai rice varity *Oryza sativa* L. cv. RD6	Substrate	SSF	21	*M. purpureus* CMU001	33.790/HPLC	Chairote et al., 2010

SSF, solid-state fermentation.

substrates with rice or with different grains together showed a higher MK production, than using them as sole substrate (Feng et al., 2014; Suraiya et al., 2018). However, it generally needs 2∼3 weeks of fermentation to obtain FRMR with MK content of more than 10.00 mg/g. Long-term fermentation of FRMR will increase its risk of contamination (Chairote et al., 2010; Dikshit and Tallapragada, 2016; Suraiya et al., 2018). Therefore, strategies for improving the MK production and further shortening the fermentation period need an urgent attention, especially in consideration to environmentally friendly and natural means. Improving MK production during a fixed conventional fermentation cycle, for example, 14 or 21 days, which equate to shorten the fermentation periods to obtain the required MK contents of FRMR. So, irritants have been used to improve MK production for the rapid fermentation of FRMR (Zhang et al., 2019; Zhen et al., 2019; Peng et al., 2020).

Improving Monacolin Production Using Irritants

For efficient production of FRMR, some nutritional and non-nutritional irritants, such as glycerol, glutamic acid, NaCl, and Chinese medicines have been used in medium or substrates, in order to improve the MK production (Lu et al., 2013; Zhang et al., 2019; Zhen et al., 2019; Peng et al., 2020) (**Table 2**). Generally, higher yield of MK with low cost is expected for commercial purposes. Most of the irritants mentioned above confirm to this expectation. When 10 mM glutamic acid was used in the medium, MK production increased 4.8-fold; the expressions of *mokC* and *mokG* and permeability of cell membrane were also increased (Zhang et al., 2017a, 2019). Trace of linoleic acid also achieved the likely results, which was attributed to the fact that linoleic acid increased the cyclic AMP concentration and activated protein kinase that enhanced the MK production (Huang et al., 2018).

MK can be enhanced by glycerol both in LSF and SSF with varying concentrations of glycerol (Lu et al., 2013; Feng et al., 2015). MK yields of fermentation broth and mycelia could be enhanced significantly, when glycerol concentration was adjusted to 6 g/L ($p < 0.05$). Concentration of MLs increased and mainly existed in the mycelia after adding glycerol, compared with that of control (Feng et al., 2015). The maximum MK yield of 2.401 mg/g in mycelia was obtained, when the glycerol concentration was 40 g/L (Feng et al., 2015). Furthermore, the maximal MK yield of 12.900 mg/g was obtained, when 26% glycerol was used in SSF, with bagasse as a carrier (Lu et al., 2013). As an environmentally friendly substance, which could be obtained from byproducts of biodiesel, the comprehensive utilization of glycerol needs to be explored in a future study (Carabajal et al., 2020).

However, most of the irritants are used in LSF instead of SSF at the present research stage. It is inferred that the low addition of the irritants can easily modulate the MK production in LSF, due to rapid mixing and quick fermentation. Irritants used in SSF needs a further study in future research.

STRATEGIES FOR BETTER APPLICATION OF FRMR

It is well known that MK from FRMR acts as an inhibitor of cholesterol synthesis. Lovastatin and several other statins are marketed as drugs whereas FRMR is offered as a food supplement. Statins can cause side effects such as muscle damage and kidney failure, hence the side effects of FRMR need a critical consideration (Xue et al., 2017). In addition, the quantities of MK in FRMR remain widely variable (Yang and Mousa, 2012). Therefore, it is imperative to evaluate whether FRMR or MLs can be safe and efficient food supplement.

Content Variability and Quality Standardization of FRMR

Functional red mold rice promotes the maintenance of normal blood low-density lipoprotein (LDL) cholesterol concentrations due to the presence of MLs (De Backer, 2017). FRMR containing

TABLE 2 | Irritants used for improving MK production.

Irritants	Addition	Fermentation mode	Fermentation time (day)	Strain	MK/detection method	References
Glycerol	40 g/L	LSF	7	*M. pilosus* MS-1	2.401 mg/g/HPLC (MK yield of mycelia)	Feng et al., 2015
NaCl	0.02 M	LSF	10	*M. purpureus* SKY219	Approximately 90 μg/mL/HPLC (MK yield of fermentation broth)	Zhen et al., 2019
Dioscorea	1%	LSF	12	*M. purpureus* NTU 568	27.9 mg/g/HPLC (MK yield of mycelia)	Lee et al., 2007
Glutamic acid	10 mM	LSF	12	*Monascus* M1	215 μg/mL/HPLC (MK yield of fermentation broth)	Zhang et al., 2017a
Citri Reticulatae Pericarpium, *Poria cocos*, and *Radix Angelicae dahuricae*	3.75% Citri Reticulatae Pericarpium, 2.55% *Poria cocos*, and 2.01% *Radix*	SSF	12	*M. ruber* M2-1	3.6 mg/g/HPLC	Peng et al., 2020
Sodium nitrate	1%	SSF	14	*M. purpureus* CCRC 31615	0.378 mg/g/HPLC	Su et al., 2003
Glutamic acid	10 mM	LSF	15	*Monascus* C8	Approximately 450 μg/mL/HPLC (MK yield of fermentation broth)	Zhang et al., 2019
Linoleic acid	512 μM	LSF	15	*M. ruber* cicc 5006	Approximately 150 μg/mL/HPLC (MK yield of fermentation broth)	Huang et al., 2018
Glycerol	26%	SSF	20	*M. purpureus* 9901	12.900 mg/g/HPLC	Lu et al., 2013
Soybean hull	Approximately 50%	LSF	30	*M. pilosus* KCCM 60084	0.02 mg/g/HPLC (MK yield of fermentation product)	Simu et al., 2018

LSF, liquid-state fermentation, SSF, solid-state fermentation.

5∼7 mg MK is considered to be an efficient cholesterol-lowering agent equivalent to 20∼40 mg of pure lovastatin (Burke, 2015). Standardized FRMR formulation with 10 mg MLs consumed daily has shown to reduce LDL cholesterol by approximately 20% (McCarty et al., 2015). In 2011, the European Food Safety Authority (EFSA) concluded the existance of a causal relationship between the consumption of lovastatin from FRMR and "maintaining normal LDL cholesterol levels." To obtain the claimed effect, a dose of ≥10 mg lovastatin everyday was prescribed (Efsa Panel on Dietetic Products Nutrition, and Allergies. (NDA), 2011). However, the results of percent of MK in 28 brands of RMR showed a large variability. No presence of MK was detected in two brands of RMR, and MK range in the other 26 RMR brands ranged more than 60-fold. The quantity of MK consumed per day would range more than 120-fold, compared with the recommended intake claimed by the manufacturers (Cohen et al., 2017). Some other studies indicate similar results (Heber et al., 2001; Gordon et al., 2010; Song et al., 2012). In addition, the quantity of MK in RMR supplements notified to the health authorities by the manufacturers varies by 30-fold, which is attributed to the variation in the strain and the fermentation process (De Backer, 2017). The large variation of MK content in RMR supplements could induce large difference in the lipid regulating effects within individuals, which in turn could problems to the efficiency and safety of the RMR supplements. Hence, standardization must be rigorously ensured, as in many cases, the content labeling of RMR supplement is erroneous. The MK content in RMR supplements varies due to the production of RMR with different strains and fermentation process (Patel, 2016; Dujovne, 2017). However, it is worth mentioning that MK in 0.1∼0.2% range in RMR is efficient and free of side effects (Halbert et al., 2010). Based on this, effective analytical tools such as chromatography and mass spectrometry can be used to identifiy the discrepancies. In addition, a statement on the product label is required which assures that a toxin-free, non-augmented, standardized amount of MLs would be advantageous to consumers, which will allow more predictable efficacy and better safety (Nguyen et al., 2017).

FRMR available from markets is with various MK contents, for instance, 0.4, 0.8, 1.0, 1.2, 1.5, 2.0, 2.5, and 3%. FRMR with different MK contents varies in price, and the price of FRMR is usually positively correlated with its MK content (Song et al., 2019). For instance, the price of FRMR with MK content of 2% available from the market is about US$50 per 1 kg. In addition, FRMR with different product types also varies in price[1]. Therefore, in order to meet drug quality standards, commercial

[1]https://www.walgreens.com/store/c/red-yeast-rice/ID=361661-tier3

lovastatin is illegally added to common RMR to imitate FRMR (Song et al., 2019). In view of this, the Hongqu Health Food Standard in 2007 (Taiwan Guardian Food No.0960406448) and the EFSA are currently reassessing the safety of a 10-mg dose of MK as a food supplement (Poli et al., 2018; Song et al., 2019). For the accuracy of MK content, many standards for MLs detection have been established. However, there is no clear requirement for inspection of MK in FRMR according to most of the standards. Some criteria clarify that the required content of MK lactone in FRMR is generally not less than 0.4%, while just a few of them mention the content requirements of MK lactone and acid forms (Poli et al., 2018; Song et al., 2019). The Standard for Chinese Medicine Yinpian Processing of Sichuan Province (2015) requires that MK lactone should serve as the quality control of FRMR and the lowest MK content should be 0.4%, which is in accordance with the standard of the "Functional red yeast rice QB/T 2847–2007." The Standard for Chinese Medicine Yinpian Processing of Zhejiang Provine (2015) indicated that the total of MK lactone and acid in FRMR should be more than 0.3%, and the peak area of acid MK must not be less than 5% of the lactone MK peak area.

In order to distinguish commercial lovastatin from MK, some efficient detection methods such as UHPLC-QQQ-MS, UHPLC-Q-TOF-MAS, and stable isotope ration analysis (^{13}C-NMR) have been employed to authenticate the FRMR (Zhu et al., 2013; Perini et al., 2017). Moreover, it is demonstrated that the analysis of δ^{13}C with isotope ratio mass spectrometry could authenticate the FRMR (Song et al., 2019). All the aforementioned strategies relate to standardize the MK content in RMR and authenticate the FRMR, thereby laying the foundation for standardization of FRMR.

Safety Evaluation of FRMR

Functional red mold rice has always been used as an alternative lipid-lowering therapy for patients who are unable to tolerate the statin therapy, due to statin-associated myalgias (Gordon and Becker, 2011). However, the variability of MK content, potential of toxic byproducts, and no clinical data on the FRMR dietary supplement indicate that the patients should be cautious before FRMR is standardized (Venhuis et al., 2016). As of date, some side effects of FRMR have been reported, such as myopathy, erectile dysfunction, and liver injury, etc. (Polsani et al., 2008; Childress et al., 2013; Mazzanti et al., 2017; Liu and Chen, 2018). On the other hand, among dyslipidemic patients with low to moderate cardiovascular risk, FRMR induces less muscle fatigue symptoms and exerts comparable lipid-lowering effects, when compared with simvastatin in single-center randomized pilot trials (Xue et al., 2017). Therefore, safety evaluation of FRMR is an urgent and important subject.

It has been confirmed that the safety profile of FRMR is similar to that of statins (Mazzanti et al., 2017). Therefore, the composition and formulation of FRMR dietary supplement is particularly important due to the presence of MLs; besides, MK may also act as HMG-CoA-reductase inhibitors (Li et al., 2004). For instance, compactin is likely to be only half as effective, with respect to HMG-CoA reductase inhibition as MK (Heber et al., 2001; Li et al., 2004). Therefore, the bioavailability of the individual MLs is difficult to determine, in the presence of MK. It may be useful to specify a total MLs content in the form of monacolin equivalents. This hypothesis suggests that FRMR can be considered an unregistered medicine (Farkouh and Baumgärtel, 2019).

In addition, citrinin is a confirmed nephrotoxic and teratogenic agent present in FRMR, which is another obstacle for using FRMR as food supplement or medicine. Therefore, *Monascus* strains with high MK production and low even undetectable citrinin have been screened (Li et al., 2020). Additives such as soybean isoflavones and NaCl were also used to reduce citrinin production (Huang et al., 2019; Zhen et al., 2019; He et al., 2020a). Meanwhile, detection of citrinin in FRMR is also a matter of great concern and HPLC is usually used to detect citrinin in FRMR (Li et al., 2020). For the efficient detection of citrinin in FRMR, immunoaffinity column is employed for citrinin extraction according to the Chinese National Standards for Determination of Citrinin in Food (GB 5009.222–2016). Moreover, additive pharmacological effects may be expected for other MLs present (Venhuis et al., 2016). It should be suggested that the consumers taking FRMR should do a blood test for cholesterol before taking the FRMR dietary supplement. It should also be noted that taking FRMR and statins at the same time can easily lead to overdosing and side effects. Without active postmarket surveillance for adverse drug reactions, the valuable signals of product safety are lost. If the current regulatory status for pharmacologically effective FRMR dietary supplements do not permit adequate warnings and active monitoring of adverse drug reactions, then their regulatory status may not be appropriate (Venhuis et al., 2016).

Based on this, some strategies like the continuous monitoring of "natural" dietary supplement safety through spontaneous reports, long-term trials, appropriate information to clinicians and consumers, and timely submission of suspect reports to regulatory agencies, should be carried out (Mazzanti et al., 2017). Moreover, three important points need to be taken into consideration: (1) Recognizing that FRMR contains a statin-like compound; (2) carefully recommending FRMR to statin-intolerant patients with a history of myositis or myopathy; (3) Documenting all alternative medicines, such as FRMR, taken by patients, in order to weigh the benefit-to-risk of co-administration of other drugs (Polsani et al., 2008). Overall, the real-world vigilance should be strengthened at different levels, including consumers, clinicians and policy-makers to promote the proper use and harmonize the regulatory status of FRMR (Raschi et al., 2018; Farkouh and Baumgärtel, 2019).

CONCLUSION

Functional red mold rice has been used as a folk medicine by people suffering from hyperlipidemia. However, besides MK, other MLs, pigments, and citrinin in FRMR show multiple activities, sometimes even resulting in toxicity to the consumers.

For improving the MK content and optimizing the product type of FRMR, fermentation parameters should be optimized and the used of novel substrates or irritants should be employed for FRMR production. Standardization of MK contents in FRMR and evaluation of FRMR safety should be studied in detail. Based on this, a better application of FRMR as a safe and effective lipid-lowering agent can be actualized.

DATA AVAILABILITY STATEMENT

The original contributions presented in the study are included in the article/supplementary material, further inquiries can be directed to the corresponding author.

AUTHOR CONTRIBUTIONS

FY drafted the main parts of the manuscript. YX contributed to parts of the manuscript. Both authors approved the manuscript.

FUNDING

This work was supported by Key Project of Research Project of the Education Department of Hubei Province in China (No. D20192502), Open Fund of Hubei Key Laboratory of Edible Wild Plants Conservation and Utilization (No. EWPL201807), and Research Innovation Team Project of Hubei Normal University (2019CZ07).

REFERENCES

Avula, B., Cohen, P. A., Wang, Y. H., Sagi, S., Feng, W., Wang, M., et al. (2014). Chemical profiling and quantification of monacolins and citrinin in red yeast rice commercial raw materials and dietary supplements using liquid chromatography-accurate QToF mass spectrometry: chemometrics application. *J. Pharmaceut. Biomed.* 100, 243–253. doi: 10.1016/j.jpba.2014.07.039

Beltrán, D., Frutos-Lisón, M. D., Espín, J. C., and García-Villalba, R. (2019). Re-examining the role of the gut microbiota in the conversion of the lipid-lowering statin monacolin K (lovastatin) into its active β-hydroxy acid metabolite. *Food Funct.* 10, 1787–1791. doi: 10.1039/C8FO02594K

Bruno, A., Pandolfo, G., Crucitti, M., Troili, G. M., Spina, E., Zoccali, R. A., et al. (2018). Red Yeast Rice (RYR) supplementation in patients treated with second-generation antipsychotics. *Complement. Ther. Med.* 37, 167–171. doi: 10.1016/j.ctim.2018.03.007

Burke, F. (2015). Red yeast rice for the treatment of dyslipidemia. *Curr. Atheroscler. Rep.* 17:495.

Carabajal, M. D., Glorio, A., Marcipar, I. S., and Lagier, C. M. (2020). Determination of free and total glycerol in biodiesel by spot analysis. *Microchem. J* 158:105148. doi: 10.1016/j.microc.2020.105148

Chairote, E. O., Lumyong, S., and Chairote, G. (2010). Study on cholesterol lowering compounds in red yeast rice prepared form thai glutinous rice. *Asian J. Food Agro Ind.* 3, 217–228.

Chen, W., Feng, Y., Molnár, I., and Chen, F. (2019). Nature and nurture: confluence of pathway determinism with metabolic and chemical serendipity diversifies *Monascus azaphilone* pigments. *Nat. Prod. Rep.* 36, 561–572. doi: 10.1039/C8NP00060C

Chen, Y., Tseng, C., Liaw, L., Wang, C., Chen, I., Wu, W., et al. (2008). Cloning and characterization of monacolin K biosynthetic gene cluster from *Monascus pilosus*. *J. Agric. Food Chem.* 56, 5639–5646. doi: 10.1021/jf800595k

Childress, L., Gay, A., Zargar, A., and Ito, M. K. (2013). Review of red yeast rice content and current Food and Drug Administration oversight. *J. Clin. Lipidol.* 7, 117–122. doi: 10.1016/j.jacl.2012.09.003

Cicero, A. F. G., Fogacci, F., Rosticci, M., Parini, A., Giovannini, M., Veronesi, M., et al. (2017). Effect of a short-term dietary supplementation with phytosterols, red yeast rice or both on lipid pattern in moderately hypercholesterolemic subjects: a three-arm, double-blind, randomized clinical trial. *Nutr. Metab.* 14, 61–67. doi: 10.1186/s12986-017-0214-2

Cohen, P. A., Avula, B., and Khan, I. A. (2017). Variability in strength of red yeast rice supplements purchased from mainstream retailers. *Eur. J. Prev. Cardiol.* 24, 1431–1434. doi: 10.1177/2047487317715714

D'Addato, S., Scandiani, L., Mombelli, G., Focanti, F., Pelacchi, F., Salvatori, E., et al. (2017). Effect of a food supplement containing berberine, monacolin K, hydroxytyrosol and coenzyme Q10 on lipid levels: a randomized, double-blind, placebo controlled study. *Drug Des. Dev. Ther.* 2017, 1585–1592. doi: 10.2147/DDDT.S128623

De Backer, G. G. (2017). Food supplements with red yeast rice: more regulations are needed. *Eur. J. Prev. Cardiol.* 24, 1429–1430. doi: 10.1177/2047487317716500

del Gaudio, F., Guerrera, I. C., Riccio, R., and Monti, M. C. (2020). Quantitative proteomics discloses monacolin K-induced alterations in triple-negative breast cancer cell proteomes and phosphoproteomes. *Mol. Omics* 16, 19–30. doi: 10.1039/C9MO00140A

Dhale, M., Divakar, S., Kumar, S. U., and Vijayalakshmi, G. (2007a). Isolation and characterization of dihydromonacolin-MV from *Monascus purpureus* for antioxidant properties. *Appl. Microbiol. Biotechnol.* 73, 1197–1202. doi: 10.1007/s00253-006-0578-0

Dhale, M. A., Divakar, S., Umesh-Kumar, S., and Vijayalakshmi, G. (2007b). Characterization of dehydromonacolin-MV2 from *Monascus purpureus* mutant. *J. Appl. Microbiol.* 103, 2168–2173. doi: 10.1111/j.1365-2672.2007.03457.x

Di Pierro, F., Putignano, P., Ferrara, T., Raiola, C., Rapacioli, G., and Villanova, N. (2016). Retrospective analysis of the effects of a highly standardized mixture of Berberis aristata, Silybum marianum, and monacolins K and KA in patients with dyslipidemia. *Clin. Pharm. Adv. Appl.* 2017, 1–7. doi: 10.2147/CPAA.S120032

Dikshit, R., and Tallapragada, P. (2016). Statistical optimization of lovastatin and confirmation of nonexistence of citrinin under solid-state fermentation by *Monascus sanguineus*. *J. Food Drug Anal.* 24, 433–440. doi: 10.1016/j.jfda.2015.11.008

Dujovne, C. A. (2017). Red yeast rice preparations: are they suitable substitutions for statins? *Am. J. Med.* 130, 1148–1150. doi: 10.1016/j.amjmed.2017.05.013

Efsa Panel on Dietetic Products Nutrition, and Allergies. (NDA) (2011). Scientific opinion on the substantiation of health claims related to monacolin K from red yeast rice and maintenance of normal blood LDL-cholesterol concentrations (ID 1648, 1700) pursuant to Article 13(1) of Regulation (EC) No 1924/2006. *EFSA J* 9:2304.

Endo, A. (1979). Monacolin K, a new hypocholesterolemic agent produced by a *Monascus* species. *J. Antibiot.* 32, 852–854. doi: 10.7164/antibiotics.32.852

Endo, A. (1985b). Monacolins J and L, new inhibitors of cholesterol biosynthesis produced by *Monascus ruber*. *J. Antibiot.* 38, 420–422. doi: 10.7164/antibiotics.38.420

Endo, A. (1985a). Compactin (ML-236B) and related compounds as potential cholesterol-lowering agents that inhibit HMG-CoA reductase. *J. Med. Chem.* 28, 401–405. doi: 10.1021/jm00382a001

Endo, A., and Hasumi, K. (1985). Dihydromonacolin L and monacolin X, new metabolites those Inhibit cholesterol biosynthesis. *J. Antibiot* 38, 321–327. doi: 10.7164/antibiotics.38.321

Endo, A., Komagata, D., and Shimada, H. (1986). Monacolin M, a new inhibitor of cholesterol biosynthesis. *J. Antibiot.* 39, 1670–1673. doi: 10.7164/antibiotics.39.1670

Ertürk, S., Önal, A., and Müge Çetin, S. (2003). Analytical methods for the quantitative determination of 3-hydroxy-3-methylglutaryl coenzyme A reductase inhibitors in biological samples. *J. Chromatogr. B* 793, 193–205. doi: 10.1016/S1570-0232(03)00314-3

Fang, Y. X., Song, H. P., Liang, J. X., Li, P., and Yang, H. (2017). Rapid screening of pancreatic lipase inhibitors from Monascus-fermented rice by ultrafiltration

liquid chromatography-mass spectrometry. *Anal. Methods* 238:111879. doi: 10.1039/C7AY00777A

Farkouh, A., and Baumgärtel, C. (2019). Mini-review: medication safety of red yeast rice products. *Int. J. Gen. Med.* 2019, 167–171. doi: 10.2147/ijgm.s202446

Feng, Y. L., Shao, Y. C., Zhou, Y. X., and Chen, F. S. (2014). Production and optimization of monacolin K by citrinin-free *Monascus pilosus* MS-1 in solid-state fermentation using non-glutinous rice and soybean flours as substrate. *Eur. Food Res. Technol.* 239, 629–636. doi: 10.1007/s00217-014-2259-z

Feng, Y. L., Shao, Y. C., Zhou, Y. X., and Chen, F. S. (2015). Effects of glycerol on pigments and monacolin K production by the high-monacolin K-producing but citrinin-free strain, *Monascus pilosus* MS-1. *Eur. Food Res. Technol.* 240, 635–643. doi: 10.1007/s00217-014-2365-y

Formisano, E., Pasta, A., Cremonini, A. L., Favari, E., Ronca, A., Carbone, F., et al. (2019). Efficacy of nutraceutical combination of monacolin K, berberine, and silymarin on lipid profile and PCSK9 plasma level in a cohort of hypercholesterolemic patients. *J. Med. Food* 23, 658–666. doi: 10.1089/jmf.2019.0168

Gordon, R., and Becker, D. (2011). The role of red yeast rice for the physician. *Curr. Atheroscler. Rep.* 13, 73–80. doi: 10.1007/s11883-010-0145-0

Gordon, R. Y., Cooperman, T., Obermeyer, W., and Becker, D. J. (2010). Marked variability of monacolin levels in commercial red yeast rice products: buyer beware! Arch. *Intern. Med.* 170, 1722–1727. doi: 10.1001/archinternmed.2010.382

Hachem, R., Assemat, G., Balayssac, S., Martins-Froment, N., Gilard, V., Martino, R., et al. (2020). Comparative chemical profiling and monacolins quantification in red yeast rice dietary supplements by 1H-NMR and UHPLC-DAD-MS. *Molecules* 25, 317–349. doi: 10.3390/molecules25020317

Halbert, S., French, B., and Gordon, R. (2010). Tolerability of red yeast rice (2,400 mg twice daily) versus pravastatin (20 mg twice daily) in patients with previous statin intolerance. *Am. J. Cardiol.* 105, 198–204. doi: 10.1016/j.amjcard.2009.08.672

He, S., Liu, X., Wang, Y., Xie, J., Gao, H., Li, X., et al. (2020a). Metabolomics analysis based on UHPLC-Q-TOF-MS/MS reveals effects of genistein on reducing mycotoxin citrinin production by *Monascus aurantiacus* Li AS3.*4384*. *LWT* 130:109613. doi: 10.1016/j.lwt.2020.109613

He, S., Wang, Y., Xie, J., Gao, H., Li, X., and Huang, Z. (2020b). 1H NMR-based metabolomic study of the effects of flavonoids on citrinin production by Monascus. *Food Res. Int.* 137:109532. doi: 10.1016/j.foodres.2020.109532

Heber, D., Lembertas, A., Lu, Q., Bowerman, S., and Go, V. (2001). An analysis of nine proprietary Chinese red yeast rice dietary supplements: implications of variability in chemical profile and contents. *J. Altern. Complement. Med.* 7, 133–139. doi: 10.1089/107555301750164181

Heinz, T., Schuchardt, J. P., Möller, K., Hadji, P., and Hahn, A. (2016). LDL-cholesterol-lowering effect of monacolin K from red yeast rice extract – results of a randomized, placebo-controlled intervention study. *Nutr. Res.* 36, 1162–1170. doi: 10.1016/j.nutres.2016.07.005

Hong, S., Lee, I., Kim, S., and Imm, J. Y. (2012). Improved functionality of soft soybean curd containing Monascus fermented soybean ethanol extract. *Food Sci. Biotechnol.* 21, 701–707. doi: 10.1007/s10068-012-0091-4

Hp, M. K. (2012). Optimization of monacolin K production by *Monascus purpureus* MTTC 410 in submerged fermentation. *Int. J. Food Eng.* 8, 1–12. doi: 10.1515/1556-3758.1420

Huang, J., Liao, N., and Li, H. (2018). Linoleic acid enhance the production of moncolin K and red pigments in *Monascus ruber* by activating mokH and mokA, and by accelerating cAMP-PkA pathway. *Int. J. Biol. Macromol* 109, 950–954. doi: 10.1016/j.ijbiomac.2017.11.074

Huang, Z., Zhang, L., Gao, H., Wang, Y., Li, X., Huang, X., et al. (2019). Soybean isoflavones reduce citrinin production by *Monascus aurantiacus* Li AS3.*4384* in liquid state fermentation using different media. *J. Sci. Food Agri.* 99, 4772–4780. doi: 10.1002/jsfa.9723

Iskandar, I., Harahap, Y., Wijayanti, T. R., Sandra, M., Prasaja, B., and Cahyaningsih, P. (2020). Efficacy and tolerability of a nutraceutical combination of red yeast rice, guggulipid, and chromium picolinate evaluated in a randomized, placebo-controlled, double-blind study. Complement. *Ther. Med* 48:102282. doi: 10.1016/j.ctim.2019.102282

Jiang, Y., Lv, X., Zhang, C., Zheng, Y., Zheng, B., Duan, X., et al. (2019). Microbial dynamics and flavor formation during the traditional brewing of Monascus vinegar. *Food Res. Int.* 125:108531. doi: 10.1016/j.foodres.2019.108531

Kimura, K., Komagata, D., Murakawa, S., and Endo, A. (1990). Biosynthesis of monacolins: conversion of monacolin J to monacolin K (mevinolin). *J. Antibiot.* 43, 1621–1622. doi: 10.7164/antibiotics.43.1621

Kurokawa, H., Ito, H., and Matsui, H. (2017). *Monascus purpureus* induced apoptosis on gastric cancer cell by scavenging mitochondrial reactive oxygen species. *J. Clin. Biochem. Nutr.* 61, 189–195. doi: 10.3164/jcbn.17-27

Lee, C. L., Hung, H. K., Wang, J. J., and Pan, T. M. (2007). Improving the ratio of monacolin K to citrinin production of *Monascus purpureus* NTU 568 under dioscorea medium through the mediation of pH value and ethanol addition. *J. Agr. Food Chem.* 55, 6493–6502. doi: 10.1021/jf0711946

Lee, C. L., Wang, J. J., Kuo, S. L., and Pan, T. M. (2006). Monascus fermentation of dioscorea for increasing the production of cholesterol-lowering agent—monacolin K and antiinflammation agent—monascin. *Appl. Microbiol. Biotechnol.* 72, 1254–1262. doi: 10.1007/s00253-006-0404-8

Lee, Y. L., Yang, J. H., and Mau, J. L. (2009). Antioxidant properties of ethanolic and methanolic extracts from Monascus-fermented soybeans. *J. Food Biochem.* 33, 707–727. doi: 10.1111/j.1745-4514.2009.00246.x

Li, M. N., Li, C. R., Gao, W., Li, P., and Yang, H. (2017). Highly sensitive strategy for identification of trace chemicals in complex matrix: Application to analysis of monacolin analogues in monascus-fermented rice product. *Anal. Chim. Acta* 982, 156–167. doi: 10.1016/j.aca.2017.05.030

Li, Y., Zhang, F., Wang, Z., and Hu, Z. (2004). Identification and chemical profiling of monacolins in red yeast rice using high-performance liquid chromatography with photodiode array detector and mass spectrometry. *J. Pharm. Biomed. Anal.* 35, 1101–1112. doi: 10.1016/j.jpba.2004.04.004

Li, Z., Liu, Y., Li, Y., Lin, F., and Wu, L. (2020). Screening and identification of *Monascus* strains with high-yield monacolin K and undetectable citrinin by integration of HPLC analysis and pksCT and ctnA genes amplification. *J. Appl. Microbiol.* 129, 1410–1418. doi: 10.1111/jam.14689

Liang, J. X., Zhang, Q. Q., Huang, Y. F., Pang, H. Q., Liu, X. G., Gao, W., et al. (2019). Comprehensive chemical profiling of monascus-fermented rice product and screening of lipid-lowering compounds other than monacolins. *J. Ethnopharmacol.* 238:111879. doi: 10.1016/j.jep.2019.111879

Lin, L., Wang, C., Li, Z., Wu, H., and Chen, M. (2017). Effect of temperature-shift and temperature-constant cultivation on the monacolin K biosynthetic gene cluster expression in *Monascus* sp. *Food Technol. Biotechnol.* 55, 40–47. doi: 10.17113/ftb.55.01.17.4729

Liu, M. T., Li, J. J., Shang, X. Y., Li, S., Li, L. L., Luan, N., et al. (2011). Structure elucidation and complete NMR spectral assignment of an unusual aromatic monacolin analog from *Monascus purpureus*-fermented rice. *Magn. Reson. Chem.* 49, 129–131. doi: 10.1002/mrc.2714

Liu, M. T., Wang, A. L., Sun, Z., Li, J. J., Wu, X. L., Liu, Y. X., et al. (2013). Cytotoxic monacolin analogs from *Monascus purpureus*-fermented rice. *J. Asian Nat. Prod. Res.* 15, 600–609. doi: 10.1080/10286020.2013.790379

Liu, Z., and Chen, P. (2018). A case of erectile dysfunction induced by red yeast rice in lipidlowering therapy. *Phytother. Res.* 32, 953–954. doi: 10.1002/ptr.6025

Lu, L. P., Zhang, B. B., and Xu, G. R. (2013). Efficient conversion of high concentration of glycerol to monacolin K by solid-state fermentation of *Monascus purpureus* using bagasse as carrier. *Bioproce. Biosyst. Eng.* 36, 293–299. doi: 10.1007/s00449-012-0784-3

Mazza, A., Lenti, S., Schiavon, L., Di Giacomo, E., Tomasi, M., Manunta, R., et al. (2018). Effect of Monacolin K and CO_{Q10} supplementation in hypertensive and hypercholesterolemic subjects with metabolic syndrome. *Biomed. Pharmacother.* 105, 992–996. doi: 10.1016/j.biopha.2018.06.076

Mazzanti, G., Moro, P. A., Raschi, E., Da Cas, R., and Menniti-Ippolito, F. (2017). Adverse reactions to dietary supplements containing red yeast rice: assessment of cases from the Italian surveillance system. *Brit. J. Clin. Pharmacol.* 83, 894–908. doi: 10.1111/bcp.13171

McCarty, M., O'Keefe, J., and DiNicolantonio, J. (2015). Red yeast rice plus berberine: practical strategy for promoting vascular and metabolic health. *Altern. Ther. Health Med.* 21, 40–45.

Mohan-Kumari, H. P., Dhale, M. A., Akhilender Naidu, K., and Vijayalakshmi, G. (2011). Antioxidant effect of red mould rice in hypercholesterolemic Wistar male rats. *Cell Biochem. Funct.* 29, 597–602. doi: 10.1002/cbf.1793

Nagabhishek, S. N., and Madankumar, A. (2019). A novel apoptosis-inducing metabolite isolated from marine sponge symbiont *Monascus* sp. *NMK7*

attenuates cell proliferation, migration and ROS stress-mediated apoptosis in breast cancer cells. *RSC Adv.* 9, 5878–5890. doi: 10.1039/C8RA09886G

Nguyen, T., Karl, M., and Santini, A. (2017). Red yeast rice. *Foods* 6:19. doi: 10.3390/foods6030019

Panda, B., Javed, S., and Ali, M. (2010). Optimization of fermentation parameters for higher lovastatin production in red mold rice through co-culture of *Monascus purpureus* and *Monascus ruber*. *Food Bioprocess Tech.* 3, 373–378. doi: 10.1007/s11947-008-0072-z

Patel, S. (2016). Functional food red yeast rice (RYR) for metabolic syndrome amelioration: a review on pros and cons. *World J. Microb. Biot.* 32:87. doi: 10.1007/s11274-016-2035-2

Peng, L., Ai-lati, A., Liu, S., Ji, Z., Mao, J., and Che, X. (2020). Effects of Chinese medicines on monacolin K production and related genes transcription of *Monascus ruber* in red mold rice fermentation. *Food Sci. Nutr.* 8, 2134–2142. doi: 10.1002/fsn3.1511

Perini, M., Carbone, G., and Camin, F. (2017). Stable isotope ratio analysis for authentication of red yeast rice. *Talanta* 174, 228–233. doi: 10.1016/j.talanta.2017.05.057

Poli, A., Barbagallo, C. M., Cicero, A. F. G., Corsini, A., Manzato, E., Trimarco, B., et al. (2018). Nutraceuticals and functional foods for the control of plasma cholesterol levels. *An intersociety position paper*. *Pharmacol. Res.* 134, 51–60. doi: 10.1016/j.phrs.2018.05.015

Polsani, V. R., Jones, P. H., Ballantyne, C. M., and Nambi, V. (2008). A case report of myopathy from consumption of red yeast rice. *J. Clin. Lipidol.* 2, 60–62. doi: 10.1016/j.jacl.2007.12.005

Praveen, V., and Savitha, J. (2012). Solid state fermentation: an effective method for lovastatin production by fungi over submerged fermentation. *J. Biotechnol. Pharm. Res.* 3, 15–21.

Pyo, Y. H., and Seo, S. Y. (2010). Simultaneous production of natural statins and coenzyme Q10 by *Monascus pilosus* fermentation using different solid substrates. *Food Sci. Biotechnol.* 19, 1635–1641. doi: 10.1007/s10068-010-0231-7

Raschi, E., Girardi, A., Poluzzi, E., Forcesi, E., Menniti-Ippolito, F., Mazzanti, G., et al. (2018). Adverse events to food supplements containing red yeast rice: cmparative analysis of FAERS and CAERS reporting systems. *Drug Safety* 41, 745–752. doi: 10.1007/s40264-018-0661-3

Seenivasan, A., Satya Eswari, J., Sankar, P., Gummadid, S. N., Pandae, T., and Venkateswarluf, C. (2020). Metabolic pathway analysis and dynamic macroscopic model development for lovastatin production by Monascus purpureus using metabolic footprinting concept. *Biochem. Eng. J.* 154:107437. doi: 10.1016/j.bej.2019.107437

Simu, S. Y., Castro-Aceituno, V., Lee, S., Ahn, S., Lee, H. K., Hoang, V. A., et al. (2018). Fermentation of soybean hull by *Monascus pilosus* and elucidation of its related molecular mechanism involved in the inhibition of lipid accumulation. An in sílico and in vitro approach. *J. Food Biochem.* 42:e12442. doi: 10.1111/jfbc.12442

Song, F., El-Demerdash, A., Lee, S. S., and Smith, R. (2012). Fast screening of lovastatin in red yeast rice products by flow injection tandem mass spectrometry. *Pharm. Biomed. Anal. Chem.* 57, 76–81. doi: 10.1016/j.jpba.2011.08.039

Song, J., Luo, J., Ma, Z., Sun, Q., Wu, C., and Li, X. (2019). Quality and authenticity control of functional red yeast rice—a review. *Molecules* 24:1944. doi: 10.3390/molecules24101944

Stefanutti, C., Mazza, F., Mesce, D., Morozzi, C., Di Giacomo, S., Vitale, M., et al. (2017). *Monascus purpureus* for statin and ezetimibe intolerant heterozygous familial hypercholesterolaemia patients: a clinical study. *Atherosclerosis Supp.* 30, 86–91. doi: 10.1016/j.atherosclerosissup.2017.05.021

Su, Y. C., Wang, J. J., Lin, T. T., and Pan, T. M. (2003). Production of the secondary metabolites γ-aminobutyric acid and monacolin K by Monascus. *J. Ind. Microbiol. Biot.* 30, 41–46. doi: 10.1007/s10295-002-0001-5

Subhagar, S., Aravindan, R., and Viruthagiri, T. (2009). Response surface optimization of mixed substrate solid state fermentation for the production of lovastatin by *Monascus purpureus*. *Eng. Life Sci.* 9, 303–310. doi: 10.1002/elsc.200900022

Suh, S. H., Rheem, S., Mah, J.-H., Lee, W., Byun, M.-W., and Hwang, H.-J. (2007). Optimization of production of monacolin K from γ-irradiated *Monascus* mutant by ue of response surface methodology. *J. Med. Food* 10, 408–415. doi: 10.1089/jmf.2006.097

Suraiya, S., Kim, J. H., Tak, J. Y., Siddique, M. P., Young, C. J., Kim, J. K., et al. (2018). Influences of fermentation parameters on lovastatin production by *Monascus purpureus* using *Saccharina japonica* as solid fermented substrate. *LWT* 92, 1–9. doi: 10.1016/j.lwt.2018.02.013

Tien, A. J., Chueh, T. H., Hsia, C. P., and Chien, C. T. (2016). Monascus adlay and monacolin K attenuates arterial thrombosis in rats through the inhibition of ICAM-1 and oxidative stress. *Kidney Blood Press. Res.* 41, 815–827. doi: 10.1159/000452584

Tseng, Y. H., Yang, J. H., Chen, C. H., and Mau, J. L. (2011). Quality and antioxidant properties of Anka-enriched bread. *J. Food Process. Pres.* 35, 518–523. doi: 10.1111/j.1745-4549.2010.00497.x

Tsukahara, M., Shinzato, N., Tamaki, Y., Namihira, T., and Matsui, T. (2009). Red yeast rice fermentation by selected *Monascus* sp. with deep-red color, lovastatin production but no citrinin, and effect of temperature-shift cultivation on lovastatin production. *Appl. Biochem. Biotechnol.* 158, 476–482. doi: 10.1007/s12010-009-8553-8

Venhuis, B. J., van Hunsel, F., van de Koppel, B. S., Keizers, B. P. H. J., Jeurissena, S. M. F., and De Kaste, D. (2016). Pharmacologically effective red yeast rice preparations marketed as dietary supplements illustrated by a case report. *Drug Test. Anal.* 8, 315–318. doi: 10.1002/dta.1929

Venkateswaran, V., and Vijayalakshmi, G. (2010). Finger millet (Eleusine coracana) — an economically viable source for antihypercholesterolemic metabolites production by Monascus purpureus. *J. Food Sci. Technol.* 47, 426–431. doi: 10.1007/s13197-010-0070-9

Wang, L., Wang, W., and Xu, G. (2011). Promotion of monacolin K production by *Agrobacterium tumefaciens*-mediated transformation in *Monascus albidus* 9901. *Curr. Microbiol.* 62, 501–507. doi: 10.1007/s00284-010-9735-x

Wang, P., Chen, D., Jiang, D., Dong, X., Chen, P., and Lin, Y. (2014). Alkali extraction and in vitro antioxidant activity of Monascus mycelium polysaccharides. *J. Food Sci. Technol.* 51, 1251–1259. doi: 10.1007/s13197-012-0618-y

Wang, T. J., Lien, A. S. Y., Chen, J. L., Lin, C. H., Yang, Y. S., and Yang, S. H. (2019). A randomized clinical efficacy trial of red yeast rice (Monascus pilosus) against hyperlipidemia. *Am. J. Chinese Med.* 47, 323–335. doi: 10.1142/S0192415X19500150

Wong, R., and Rabie, B. (2008). Chinese red yeast rice (*Monascus purpureus*-fermented rice) promotes bone formation. *Chin. Med. U.K.* 3, 1–6. doi: 10.1186/1749-8546-3-4

Xiong, Z., Cao, X., Wen, Q., Chen, Z., Cheng, Z., Huang, X., et al. (2019). An overview of the bioactivity of monacolin K / lovastatin. *Food Chem. Toxicol.* 131:110585. doi: 10.1016/j.fct.2019.110585

Xu, B., Wang, Q., and Sung, C. (2017). Telomerase inhibitory effects of red pigment rubropunctatin and statin monacolin L isolated from red yeast rice. *Genes* 8, 129–138. doi: 10.3390/genes8050129

Xu, B. J., Wang, Q. J., Jia, X. Q., and Sung, C. K. (2005). Enhanced lovastatin production by solid state fermentation of *Monascus ruber*. *Biotechnol. Bioproc. E.* 10, 78–84. doi: 10.1007/bf02931187

Xue, Y., Tao, L., Wu, S., Wang, G., Qian, L., Li, J., et al. (2017). Red yeast rice induces less muscle fatigue symptom than simvastatin in dyslipidemic patients: a single center randomized pilot trial. *BMC Cardiovasc. Disord.* 17:127. doi: 10.1186/s12872-017-0560-z

Yang, C. W., and Mousa, S. A. (2012). The effect of red yeast rice (*Monascus purpureus*) in dyslipidemia and other disorders. *Complement. Ther. Med.* 20, 466–474. doi: 10.1016/j.ctim.2012.07.004

Yang, D. J., and Hwang, L. S. (2006). Study on the conversion of three natural statins from lactone forms to their corresponding hydroxy acid forms and their determination in Pu-Erh tea. *J. Chromatogr. A* 1119, 277–284. doi: 10.1016/j.chroma.2005.12.031

Yang, J. H., Tseng, Y. H., Chang, H. L., Lee, Y. L., and Mau, J. L. (2005a). Storage stability of monascal adlay. *Food Chem.* 90, 303–309. doi: 10.1016/j.foodchem.2004.03.053

Yang, S., Zhang, H., Li, Y., Qian, J., and Wang, W. (2005b). The ultrasonic effect on biological characteristics of *Monascus* sp. *Enzyme Microb. Tech.* 37, 139–144. doi: 10.1016/j.enzmictec.2005.02.005

Zhang, B., Liu, T. X., Wang, A. L., Li, J. J., Wang, X., Luan, N., et al. (2018a). Four new monacolin analogs from *Monascus purpureus*-fermented

rice. *J. Asian Nat. Prod. Res.* 20, 209–216. doi: 10.1080/10286020.2017.1396978

Zhang, B. B., Lu, L. P., Xia, Y. J., Wang, Y. L., and Xu, G. R. (2013). Use of agar as carrier in solid-state fermentation for Monacolin K production by *Monascus*: A novel method for direct determination of biomass and accurate comparison with submerged fermentation. *Biochem. Eng. J.* 80, 10–13. doi: 10.1016/j.bej.2013.09.007

Zhang, B. B., Xing, H. B., Jiang, B. J., Chen, L., Xu, G. R., Jiang, Y., et al. (2018b). Using millet as substrate for efficient production of monacolin K by solid-state fermentation of *Monascus ruber*. *J. Biosci. Bioeng.* 125, 333–338. doi: 10.1016/j.jbiosc.2017.10.011

Zhang, C., Chai, S., Hao, S., Zhang, A., Zhu, Q., Zhang, H., et al. (2019). Effects of glutamic acid on the production of monacolin K in four high-yield monacolin K strains in Monascus. *Appl. Microbiol. Biotechnol.* 103, 5301–5310. doi: 10.1007/s00253-019-09752-9

Zhang, C., Liang, J., Yang, L., Chai, S., Zhang, C., Sun, B., et al. (2017a). Glutamic acid promotes monacolin K production and monacolin K biosynthetic gene cluster expression in Monascus. *AMB Expr.* 7:22. doi: 10.1186/s13568-016-0311-z

Zhang, C., Liang, J., Yang, L., Sun, B., and Wang, C. (2017b). De novo RNA sequencing and transcriptome analysis of *Monascus purpureus* and analysis of key genes involved in monacolin K biosynthesis. *PLoS One* 12:e0170149. doi: 10.1371/journal.pone.0170149

Zhang, Y., Chen, Z., Wen, Q., Xiong, Z., Cao, X., Zheng, Z., et al. (2020). An overview on the biosynthesis and metabolic regulation of monacolin K/lovastatin. *Food Funct.* 11, 5738–5748. doi: 10.1039/D0FO00691B

Zhang, Z., Ali, Z., Khan, S. I., and Khan, I. A. (2016). Cytotoxic monacolins from red yeast rice, a Chinese medicine and food. *Food Chem.* 202, 262–268. doi: 10.1016/j.foodchem.2015.12.039

Zhen, Z., Xiong, X., Liu, Y., Zhang, J., Wang, S., Li, L., et al. (2019). NaCl inhibits citrinin and stimulates Monascus pigments and monacolin K production. *Toxins* 11:118. doi: 10.3390/toxins11020118

Zhu, L., Han, Q. B., Ho, A., Hsiao, W. L., and Jiang, Z. H. (2013). Characterization and simultaneous determination of immunosuppressive decalins in red yeast rice by ultra-high-performance liquid chromatography hyphenated with mass spectrometry. *J. Chromatogr. A* 1303, 54–61. doi: 10.1016/j.chroma.2013.06.045

Zhu, L., Yau, L. F., Lu, J. G., Zhu, G. Y., Wang, J. R., Han, Q. B., et al. (2012). Cytotoxic dehydromonacolins from red yeast rice. *J. Agr. Food Chem.* 60, 934–939. doi: 10.1021/jf203579f

Conflict of Interest: The authors declare that the research was conducted in the absence of any commercial or financial relationships that could be construed as a potential conflict of interest.

frontiers in Microbiology

ORIGINAL RESEARCH
published: 26 November 2020
doi: 10.3389/fmicb.2020.596306

Increasing Yield of 2,3,5,6-Tetramethylpyrazine in Baijiu Through *Saccharomyces cerevisiae* Metabolic Engineering

*Dan-Yao Cui[1,2], Ya-Nan Wei[1,2], Liang-Cai Lin[1,2], Shi-Jia Chen[1,2], Peng-Peng Feng[1,2], Dong-Guang Xiao[1,2], Xue Lin[1] and Cui-Ying Zhang[1,3]**

[1] State Key Laboratory of Food Nutrition and Safety, Key Laboratory of Industrial Fermentation Microbiology, Ministry of Education, Tianjin Industrial Microbiology Key Laboratory, College of Biotechnology, Tianjin University of Science & Technology, Tianjin, China, [2] Tianjin Engineering Research Center of Microbial Metabolism and Fermentation Process Control, Tianjin, China, [3] Key Laboratory of Wuliangye-flavor Liquor Solid-state Fermentation, China National Light Industry, Yibin, China

OPEN ACCESS

Edited by:
Xucong Lv,
Fuzhou University, China

Reviewed by:
Yi Wang,
Auburn University, United States
Choowong Auesukaree,
Mahidol University, Thailand
Liaoyuan Zhang,
Fujian Agriculture and Forestry University, China

***Correspondence:**
Cui-Ying Zhang
cyzhangcy@tust.edu.cn

Specialty section:
This article was submitted to Food Microbiology, a section of the journal Frontiers in Microbiology

Received: 19 August 2020
Accepted: 28 October 2020
Published: 26 November 2020

Citation:
Cui D-Y, Wei Y-N, Lin L-C, Chen S-J, Feng P-P, Xiao D-G, Lin X and Zhang C-Y (2020) Increasing Yield of 2,3,5,6-Tetramethylpyrazine in Baijiu Through Saccharomyces cerevisiae Metabolic Engineering. Front. Microbiol. 11:596306. doi: 10.3389/fmicb.2020.596306

Baijiu is a traditional distilled beverage in China with a rich variety of aroma substances. 2,3,5,6-tetramethylpyrazine (TTMP) is an important component in Baijiu and has the function of promoting cardiovascular and cerebrovascular health. During the brewing of Baijiu, the microorganisms in *jiuqu* produce acetoin and then synthesize TTMP, but the yield of TTMP is very low. In this work, 2,3-butanediol dehydrogenase (BDH) coding gene *BDH1* and another *BDH2* gene were deleted or overexpressed to evaluate the effect on the content of acetoin and TTMP in *Saccharomyces cerevisiae*. The results showed that the acetoin synthesis of strain α5-D1B2 was significantly enhanced by disrupting *BDH1* and overexpressing *BDH2*, leading to a 2.6-fold increase of TTMP production up to 10.55 mg/L. To further improve the production level of TTMP, the α-acetolactate synthase (ALS) of the pyruvate decomposition pathway was overexpressed to enhance the synthesis of diacetyl. However, replacing the promoter of the *ILV2* gene with a strong promoter (*PGK1p*) to increase the expression level of the *ILV2* gene did not result in further increased diacetyl, acetoin and TTMP production. Based on these evidences, we constructed the diploid strains AY-SB1 (Δ*BDH1:loxP*/Δ*BDH1:loxP*) and AY-SD1B2 (Δ*BDH1:loxP-PGK1p-BDH2-PGK1t*/Δ*BDH1:loxP-PGK1p-BDH2-PGK1t*) to ensure the fermentation performance of the strain is more stable in Baijiu brewing. The concentration of TTMP in AY-SB1 and AY-SD1B2 was 7.58 and 9.47 mg/L, respectively, which represented a 2.3- and 2.87-fold increase compared to the parental strain. This work provides an example for increasing TTMP production in *S. cerevisiae* by genetic engineering, and highlight a novel method to improve the quality and beneficial health attributes of Baijiu.

Keywords: ***Saccharomyces cerevisiae*, 2,3,5,6-tetramethylpyrazine, acetoin, Baijiu, *BDH1*, *BDH2***

INTRODUCTION

Baijiu is an alcoholic beverage that is widely consumed in China (Du et al., 2011). Cereals (sorghum corn, rice, wheat, peas, and millet) and fermentation starter are the main raw materials for brewing Baijiu. The fermentation starter of Baijiu is also known as *jiuqu*, including *daqu*, *xiaoqu*, *fuqu*, and other *jiuqu*. Baijiu brewed from different *jiuqu* will have significant differences in content of aroma and flavor substances. Therefore, Baijiu is classified into five types according to its aroma: strong aroma type, light aroma type, soy sauce aroma type, sweet honey aroma type, and miscellaneous aroma type (Wang et al., 2014). Esters and alcohols are the main flavor substances and their content will affect the quality of Baijiu. Although the kinds of pyrazine are lower than these two volatile flavor compounds, pyrazine is also one of the important aroma compounds in Baijiu (Liu and Sun, 2018). Fan et al. (2007) identified 27 pyrazines in Baijiu by gas chromatography-mass spectrometry (GC-MS), including 2,5-dimethylpyrazine, 2,3,5-trimethylpyrazine, and 2,3,5,6-tetramethylpyrazine (TTMP).

2,3,5,6-Tetramethylpyrazine was originally extracted from the herb of Chuan qiong (*Ligusticum wallichii*), a traditional Chinese medicinal plant (Xiao et al., 2006). TTMP has been previously found to have a beneficial effect on cardiovascular and cerebrovascular health (Xiao et al., 2018; Chen et al., 2020). Moreover, recent studies have shown that TTMP has a positive therapeutic effect on several diseases, including hepatocellular carcinoma and spinal cord injury, and especially with regards to heart toxicity caused by ethanol (Shin et al., 2013; Cao et al., 2015). During Baijiu fermentation, TTMP may be produced via the microbial metabolism and acetoin is the precursor of TTMP (Meng et al., 2016; Xu et al., 2018). First, acetoin is used as a substrate to react with ammonium (or ammonia) to form α-hydroxyimine (Xiao et al., 2014). Subsequently, α-hydroxyimine is converted to 2-amino-3-butanone, which condense to form TTMP spontaneously (Xu et al., 2018; Zhang et al., 2019). It has been reported that the content of TTMP also increased with a gradually increased concentration of acetoin, suggesting that acetoin is a precursor of TTMP (Rizzi, 1988; Chen et al., 2010; Zhu et al., 2010; Meng et al., 2020).

In terms of *Saccharomyces cerevisiae,* pyruvate is converted into α-acetolactate by α-acetolactate synthase (ALS), which is encoded by the *ILV2* gene (*YMR108W*) (Brat et al., 2012). In *S. cerevisiae,*α-acetolactate is decarboxylated into diacetyl spontaneously when the cells are cultured in an aerobic environment (Dulieu and Poncelet, 1999). Diacetyl is then reduced into acetoin by 2,3-butanediol dehydrogenase (BDH), which is encoded by the *BDH1* gene (*YAL060W*) (Ehsani et al., 2009; Kim et al., 2013; Wess et al., 2019). Acetoin is converted into 2,3-butanediol under the control of BDH. The *BDH1* gene plays an important role in the synthesis of acetoin and 2,3-butanediol. The *BDH2* gene (*YAL061W*) is adjacent to *BDH1*, Bdh2p is 51% similar to the Bdh1p (González et al., 2010; Li P. et al., 2017). The overexpression of the *BDH2* gene improved the tolerance of yeast cells to vanillin (Ishida et al., 2016, 2017). Although the function of BDH in the synthesis of 2,3-butanediol has been extensively studied, its effect on TTMP production has not been reported yet (Kim et al., 2013; Choi et al., 2016; Yang and Zhang, 2018).

2,3,5,6-Tetramethylpyrazine has been proved to be effective in the treatment of a variety of diseases and beneficial to human health (Hao et al., 2013). However, the content of TTMP in Baijiu is low, so it is interesting to increase the concentration of TTMP in Baijiu. This study is the first to genetically *S. cerevisiae* engineer strains to increase the content of TTMP in Baijiu. The biosynthetic pathway of TTMP and metabolic regulation strategy is shown in **Figure 1**. In α-type haploid strain, BDH coding gene *BDH1* and another gene *BDH2* were deleted or overexpressed to elucidate their role in TTMP production. Then, recombinant diploid strains were constructed to ensure the fermentation performance during Baijiu brewing. The results demonstrated that overexpression of *BDH2* and deletion of *BDH1* can effectively increase the accumulation of acetoin and then enhance the content of TTMP. The concentrations of ester and higher alcohol produced by the diploid strains were not affected by the genetic modification. In addition, we found that overexpression of the ALS coding gene *ILV2* had no significant effect on the production of acetoin and TTMP. Overall, the diploid strains showed significant potential for industrial applications.

MATERIALS AND METHODS

Strains and Medium

The strains and plasmids used in this study are listed in **Table 1**. *S. cerevisiae* was grown in YPD medium at 30°C. Then, 1,000 μg/mL G418 (Promega, Madison, WI, United States) was added to the YPD medium to select the right transformants. The YPG medium (10 g/L yeast extract, 20 g/L peptone, 20 g/L galactose) was used to eliminate the *KanMX* resistance gene, as the selection marker for the yeast strain. *Escherichia coli* was grown in LB medium at 37°C. Ampicillin (100 μg/mL) was added to the LB medium as required. The YPD, LB, and YPG mediums were mixed with 2% agar powder for plating.

Construction of Recombinant Strains

The primers used in this study are listed in **Supplementary Table 1**. The plasmid pUG6 was used to obtain the *loxP-KanMX-loxP* fragment, with the *KanMX* gene used as the selection marker for the yeast strain. To construct the *BDH1* gene deletion strain (α5-TB1) and *BDH2* gene deletion strain (α5-TB2), the plasmid pUG6 was used as the template to obtain the *KanMX-B1* and *KanMX-B2* fragments using the primers B1C-U/B1C-D and B2C-U/B2C-D, respectively. Homologous recombination was used to assemble the fragments into the parental strain α5.

The *ILV2* expression cassette was composed of the homologous sequence fragments of the *ILV2* gene, *ILV2A* and *ILV2B*, the *PGK1* promoter and terminator, the *ILV2* gene, and the *KanMX* gene. The cassette containing the *ILV2* gene was under the control of the *PGK1* promoter and *PGK1p* terminator. The strain α5-VI2 was obtained as follows: the *ILV2A-loxP-KanMX-loxP-PGK1p* and *PGK1t-ILV2B* fragments were obtained through PCR using the

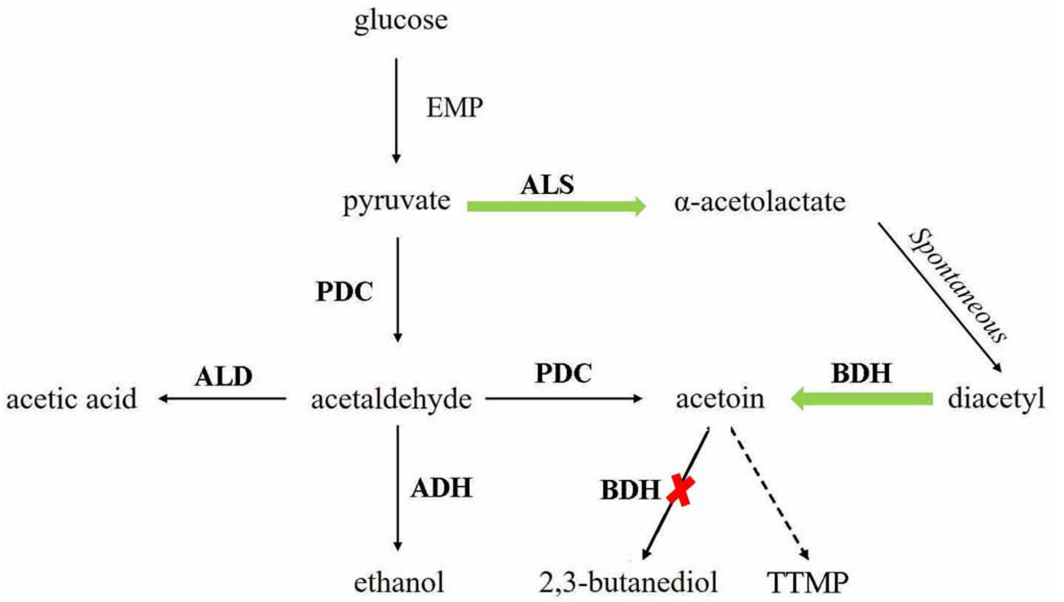

FIGURE 1 | TTMP and acetoin pathway construction in *Saccharomyces cerevisiae*. The *green arrows* indicate the enhanced pathways. The *red cross mark* indicates the disrupted pathways. ALS, α-acetolactate synthase, encoded by *ILV2*; PDC, pyruvate decarboxylase, encoded by *PDC1*, *PDC5*, and *PDC6*; ALD, acetaldehyde dehydrogenase, encoded by *ALD6*; ADH, alcohol dehydrogenase, encoded by *ADH1*, *ADH3*, and *ADH5*; BDH, 2,3-butanediol dehydrogenase, encoded by *BDH1*.

TABLE 1 | Strains and plasmids used in the current study.

Strains or plasmids	Relevant characteristic	Source
Strains		
	Escherichia coli	
DH5α	*sup*E44 Δ*lac*U169 (φ 80*lacZ*ΔM15) *hsd*R17 *rec*A1*end*A1*gyr*A96 *thi*1 *rel*A	Stratagene (Santa Clara, CA, United States)
	Saccharomyces cerevisiae	
AY15	Commercial liquor yeast strain	Tianjin Industrial Microbiology Key Laboratory
a8	*MATa*, haploid yeast strain from AY15	Li W. et al., 2017
α5	*MAT*α, haploid yeast strain from AY15	Li W. et al., 2017
α5-TB1	*MAT*α, Δ*BDH1:loxP*	This study
α5-VB1	*MAT*α, Δ*BDH1:loxP-PGK1*$_p$*-BDH1-PGK1*$_t$	This study
α5-TB2	*MAT*α, Δ*BDH2:loxP*	This study
α5-VB2	*MAT*α, Δ*BDH2:loxP-PGK1*$_p$*-BDH2-PGK1*$_t$	This study
α5-D1B2	*MAT*α, Δ*BDH1:loxP-PGK1*$_p$*-BDH2-PGK1*$_t$	This study
α5-VI2	*MAT*α, Δ*ILV2:loxP -PGK1p-ILV2-PGK1t*	This study
AY-B1	*MAT*α*/MATa*, Δ*BDH1:loxP/BDH1*	This study
AY-SB1	*MAT*α*/MATa*, Δ*BDH1:loxP/*Δ*BDH1:loxP*	This study
AY-D1B2	*MAT*α*/MATa*, Δ*BDH1:loxP-PGK1*$_p$*-BDH2-PGK1*$_t$*/BDH1*	This study
AY-SD1B2	*MAT*α*/MATa*, Δ*BDH1:loxP-PGK1*$_p$*-BDH2-PGK1*$_{t\,/}$Δ*BDH1:loxP-PGK1*$_p$*-BDH2-PGK1*$_t$	This study
Plasmids		
pUG6	*E. coli/S. cerevisiae* shuttle vector, containing *Amp* marker and *loxP-KanMX-loxP* cassette	Gueldener et al., 2002
Yep352	*URA3* marker, *Amp* marker ori control vector	Invitrogen (Carlsbad, CA, United States)
pSH-Zeocin	*Zeo* marker, Cre expression vector	Li W. et al., 2017
YEPI2KPB1	*Amp* marker, *Kan* marker, containing *ILV2A-loxP-KanMX-loxP–PGK1*$_p$*-BDH1-PGK1*$_t$*-ILV2B*	Shi et al., 2016
Yep-KPB2	*Amp* marker, *Kan* marker, containing *loxP-KanMX-loxP-PGK1p–BDH2-PGK1t*	Shi et al., 2017

primers L1-F/L1-R and L2-F/L2-R, respectively, from the plasmid YEPI2KPB1. The fragment of the *ILV2* gene was obtained using the primers ILV2-F/ILV2-R from the α5 yeast genome.

The construction of the α5-VB1, α5-VB2, and α5-D1B2 strain was similar to that of α5-ILV2. The recombinant fragments and corresponding PCR primers of the constructed strains are listed in **Supplementary Table 2**. The α5 yeast strain was transformed

using lithium acetate/PEG according to the standard protocol (Gietz and Woods, 2002). The transformant cells were grown on a YPD-G418 plate for 48 h at 30°C. The recombinant strains were then verified using PCR with different primers. Finally, the resistance gene *KanMX* of the recombinant strains α5-TB1, α5-VB1, α5-TB2, α5-VB2, α5-D1B2, and α5-VI2 were removed using the Cre/*loxP* procedure.

Construction of the Diploid Recombinants

To obtain diploid recombinant strains, the a-type and α-type haploid strains were hybridized. These two type strains were cultured in test tubes until the logarithmic growth phase in YPD medium. They were then hybridized in fresh YPD medium for 8 h. The diploid recombinants were tested with MAT-F/MAT-a/MAT-α as primers.

The a-type strain a8 was hybridized with α-type haploid recombinant strain α5-TB1 and α5-D1B2 to obtain the diploid recombinant strains AY-B1 and AY-D1B2, respectively. The *KanMX-B1S* fragment was amplified using PCR with the primers B1C-2U/B1C-2D from the plasmid pUG6. The *B12A-KanMX-PGKp-BDH2-PGKt-B12B* fragment was amplified using the primers B12C-U/B12C-D from the α5-D1B2 strain. The *KanMX-B1S* and *B12A-KanMX-PGK1p-BDH2-PGK1t-B12B* fragments were transferred into the AY-B1 and AY-D1B2 strains to delete the *BDH1* gene of the a8 strain, respectively. The resulting diploid strains were verified by PCR using the corresponding primers. The *KanMX* gene of the resulting diploid strains was eliminated using the Cre/*loxP* procedure, to obtain the AY-SB1 and AY-SD1B2 strains.

Fermentation Experiments

Corn-semi-solid medium was used to simulate industrial Baijiu fermentation (Li W. et al., 2017). The corn-semi-solid medium was prepared by gelatinizing a mixture of 60 g of corn flour and 130 mL of water at 65°C for 20 min in a 250-mL conical bottle. Then the mixture was liquefied at 90°C for 90 min with thermostable α-amylase (10 U/g corn weight, 2×10^5 U/mL) and subsequently saccharified at 60°C for 30 min with a saccharifying enzyme (150 U/g corn weight, 10×10^5 U/mL). The resulting medium was cooled to 30°C at room temperature. The strains were cultured in a test tube with 8° Bx medium (6 mL) for 24 h. The culture was then added to 12° Bx medium (54 mL) for 16 h. Finally, 15 mL of the strain culture was inoculated into corn-semi-solid fermentation medium for 4 days. The content of residual sugar was measured using Fehling's reagent.

GC and HPLC Analysis

The contents of flavor substances (esters, higher alcohols, diacetyl, and TTMP) were detected by gas chromatography (GC) using an Agilent 7890C GC (Agilent, Palo Alto, CA, United States) equipped with an G4513A autosampler, injector, and flame ionization detector (FID) (Cui et al., 2018). HP-INNOWax polyethylene glycol (30 m × 320 μm, i.e., 0.5 μm coating thickness) was used for separation. N-Butyl acetate was used as the internal standard. An internal calibration curve was established utilizing authentic standards to detected the content of the compound. The chemicals were purchased from Merck (Darmstadt, Germany).

High-performance liquid chromatography (HPLC) was used to measure the production of acetoin and 2,3-butanediol. The fermentation broth was diluted to an appropriate concentration and filtered using a 0.22-μm filter. Agilent 1260HPLC equipped with a Bio-Rad HPX-87H column was used, according to the detection method reported by Li P. et al. (2018).

Real-Time Quantitative PCR

The transcript levels of the *BDH1*, *BDH2*, and *ILV2* genes in the strains were detected using quantitative real-time PCR (RT-qPCR). The *ACT1* gene was used as the reference gene. The primers ACT1-F/ACT1-R, BDH1-F/BDH1-R, BDH2-F/BDH2-R, and ILV2-F/ILV2-R were used to amplify the *ACT1*, *BDH1*, *BDH2*, and *ILV2* genes, respectively. Yeast Processing Reagent (Takara Biotechnol, Dalian, China) was used to extract yeast total RNA, and then reverse transcribed using a PrimeScript™ RT reagent Kit with gDNA Eraser (Perfect Real Time) (Takara Biotechnol, Dalian, China). TB Green PreMix Ex Taq II (Tli RNAseH Plus) (Takara Biotechnol, Dalian, China) was used to detect changes in gene expression levels by RT-qPCR. The PCR amplification program includes 95°C pre-denaturation 30 s, 95°C denaturation 5 s, 60°C annealing polymerization 30 s, melting curve stage 15 s, 60°C 1 min. Real-time PCR was performed using a StepOnePlus real-time PCR system (Applied Biosystems/Thermo Fisher Scientific, Foster City, CA, United States). The $2^{-\Delta\Delta Ct}$ method was used for quantitative analysis.

Enzyme Assays

The enzyme activities of BDH and ALS were determined as previously described (Calam et al., 2016; Murashchenko et al., 2016). The protein concentration was determined using a TaKaRa Bradford Protein Assay Kit (Takara Biotechnology, Dalian, China). The ALS reaction mixture contained 40 mM pyruvate, 1 mM thiamine diphosphate, 1 mM $MgCl_2$, 10 μM FAD, and 100 mM potassium phosphate buffer (pH 7.0). The enzyme activity unit was defined as the amount of acetoin catalyzed by 1 mg enzyme within 1 min under reaction conditions. The BDH reaction mixture contained 10 mM acetoin, 0.1 mM NADH, and 100 mM potassium phosphate buffer (pH 7.0). Acetoin and NADH were used as substrates to measure the activity of BDH. The BDH enzyme unit was defined as 1 μmol of NAD^+ produced from NADH per min.

Determination of the Growth Curve

The method used to calculate the growth curve was obtained from Li W. et al. (2018). Briefly, the yeast strain was grown in YPD medium for 12 h up until the stationary phase. Then, the yeast culture was inoculated into fresh YPD medium and cultured in a shaking flask for 24 h. The optical density (OD_{600}) was measured every 1 h to obtain the data needed to draw the growth curve.

Statistical Analysis

Data are provided as the mean ± standard error. The differences between the recombinant strains and host strain were analyzed using Student's *t*-test. A *p*-value <0.05 was considered statistically significant.

RESULTS AND DISCUSSION

Effects of *BDH1* Deletion or Overexpression on Production of TTMP in *Saccharomyces cerevisiae*

The *BDH1* gene encodes BDH and plays an important role in the synthesis of 2,3-butanediol and acetoin (Kim et al., 2013). To determine the effect of *BDH1* gene on TTMP production, we constructed *BDH1* deletion strain α5-TB1 and *BDH1* overexpression strain α5-VB1. The TTMP content in the strain α5-TB1 was 1.94-fold higher than that of strain α5 (**Table. 2**). As the precursor, acetoin production by strain α5-TB1 was 3.77-fold greater than that of α5. Meanwhile, 2,3-butanediol produced by strain α5-TB1 was reduced by 77.33%. The recombinant strain α5-VB1 yielded a 74.85% decrease in acetoin compared to the parental strain. Hence, the production of TTMP by recombinant strain α5-VB1 decreased slightly. The production of 2,3-butanediol by α5-VB1 was increased to 2,702.16 mg/L, which was 1.44-fold greater than that generated by α5. Moreover, deletion or overexpression of *BDH1* gene did not affect the fermentation performance (ethanol production, CO_2 emission, residual sugar, and growth curve) of the strain (**Table. 3** and **Supplementary Figure 1A**).

The expression of *BDH1* at the transcriptional level in strains α5-VB1 and α5-TB1 was also measured by RT-qPCR. As shown in **Figure 2A**, the relative expression of the *BDH1* gene in the recombinant α5-VB1 strain was 16.38-fold that of α5. In strain α5-TB1, the *BDH1* relative expression level was approximately zero. The expression of *BDH2* in α5-VB1 and α5-TB1 were 0.45- and 0.72-fold that of α5. Compared with the parental α5 strain, the level of BDH enzyme activity in the α5-VB1 strain were significantly improved. As shown in **Figure 3**, the specific activity of BDH in the parental strain α5 at 25°C was 0.264 U/mg. The activity of BDH in the recombinant α5-VB1 and α5-TB1 strains was 1.32 and 0.027 U/mg, respectively. This result is consistent with the transcription assay shown in **Figure 2A**. In our study,

TABLE 2 | The concentrations of TTMP and other metabolites produced by haploid strains.

Strains[a]	TTMP (mg/L)	Acetoin (mg/L)	Diacetyl (mg/L)	2,3-Butanediol (mg/L)
α5	4.04 ± 0.12	601.02 ± 25.23	30.85 ± 1.52	1, 866.73 ± 19.96
α5-Vl2	4.15 ± 0.15	595.65 ± 35.6	34.06 ± 1.14	1, 884.81 ± 24.09
α5-VB1	3.06 ± 0.18	151.1 ± 14.56**	29.41 ± 1.59	2, 702.16 ± 37.43**
α5-TB1	7.85 ± 0.12**	2, 268.85 ± 50.12**	34.89 ± 2.55**	422.28 ± 13.77**
α5-VB2	5.48 ± 0.12**	1, 054.85 ± 26.21**	27.16 ± 0.51**	1, 515.81 ± 21.92**
α5-TB2	4.12 ± 0.13	504.38 ± 13.83**	31.34 ± 1.49	1, 667.66 ± 23.36**
α5-D1B2	10.55 ± 0.2**	2, 934.53 ± 48.57**	28.37 ± 0.58**	606.21 ± 15.43**

[a]*Haploid strain: α5 (parental strain), α5-Vl2 (ILV2 overexpression), α5-VB1 (BDH1 overexpression), α5-TB1 (BDH1 deletion), α5-VB2 (BDH2 overexpression), α5-TB2 (BDH2 deletion), and α5-D1B2 (BDH1 deletion and BDH2 overexpression). The strains were fermented by corn-semi-solid medium at 30°C for 4 days. Values are means ± standard deviations from at least three independent tests. Statistical significance is denoted as **P < 0.01 and *P < 0.05.*

TABLE 3 | Fermentation Performances of recombinant strains.

Strains	Weight loss of CO_2 (g)	Ethanol (%, v/v, 20°C)	Residual reducing sugars (g/100 mL)
Haploid strain			
α5	23.3 ± 0.2	15.2 ± 0.1	3.76 ± 0.18
α5-Vl2	22.9 ± 0.2	14.9 ± 0.1	3.87 ± 0.12
α5-VB1	23.0 ± 0.3	15.5 ± 0.1	3.87 ± 0.16
α5-TB1	22.8 ± 0.2	15.2 ± 0.1	3.92 ± 0.11
α5-VB2	23.1 ± 0.2	15.0 ± 0.2	4.14 ± 0.15
α5-TB2	22.8 ± 0.3	15.4 ± 0.2	3.71 ± 0.18
α5-D1B2	22.9 ± 0.3	15.1 ± 0.1	3.86 ± 0.12
Diploid strain			
AY15	23.3 ± 0.3	15.4 ± 0.2	3.17 ± 0.12
AY-B1	23.2 ± 0.1	15.2 ± 0.1	3.28 ± 0.19
AY-SB1	23.1 ± 0.4	15.1 ± 0.3	3.26 ± 0.16
AY-D1B2	23.4 ± 0.2	15.6 ± 0.2	2.63 ± 0.22
AY-SD1B2	23.1 ± 0.3	15.2 ± 0.1	3.06 ± 0.14

The strains were fermented by corn-semi-solid medium at 30°C for 4 days. Values are means ± standard deviations from at least three independent tests.

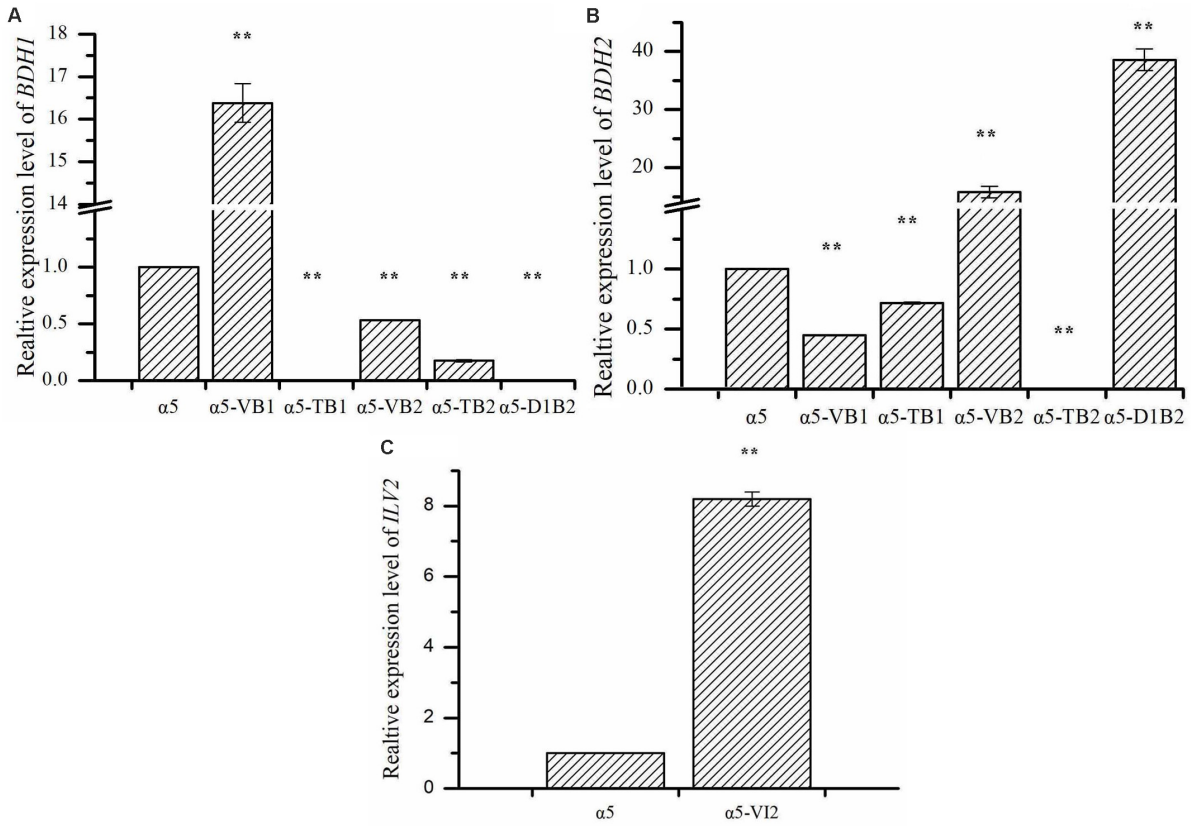

FIGURE 2 | The relative expression levels of *BDH1*, *BDH2*, *and ILV2*. **(A)** The relative expression of *BDH1* in strain α5, α5-VB1, α5-TB1, α5-VB2, α5-TB2, and α5-D1B2. **(B)** The relative expression of *BDH2* in strain α5, α5-VB1, α5-TB1, α5-VB2, α5-TB2, and α5-D1B2. **(C)** The relative expression of *ILV2* in strain α5 and α5-VI2. Data represent the mean of three independent biological replicates. Error bars represent the SD of the average values. Statistical significance is denoted as $^{**}P < 0.01$ and $^{**}P < 0.05$.

the enzyme activity of BDH was almost reduced to zero after knocking out the *BDH1* gene. This indicates that the *BDH1* gene is the main BDH encoding gene, which supports the conclusion that the expression of *BDH2* gene is not related to BDH activity (González et al., 2001, 2010).

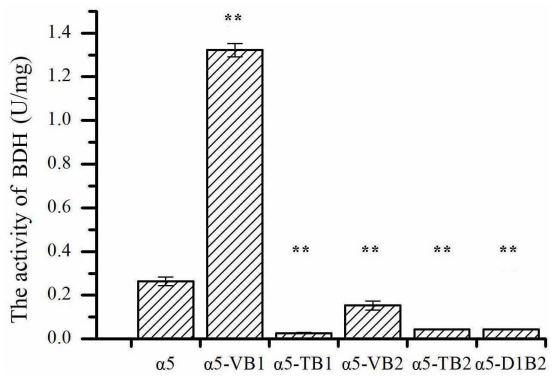

FIGURE 3 | The specific activities of 2,3-butanediol dehydrogenase (BDH). Data represent the mean of three independent biological replicates. Error bars represent the SD of the average values. Statistical significance is denoted as $^{**}P < 0.01$ and $^{**}P < 0.05$.

In the present work, *YAL060W* gene was considered to encode BDH, namely *BDH1* (González et al., 2000, 2001). Many subsequent reports focused on the regulating the production of glycerin, isobutanol, and 2,3-butanediol in laboratory strain of *S. cerevisiae* (Ehsani et al., 2009; Kim et al., 2014; Wess et al., 2019). However, the Bdh1p activity of industrial *S. cerevisiae* strain may be different from that of laboratory strain. The results of Kuang et al. (2020) demonstrated that the reduction of acetaldehyde, glycolaldehyde and furfural by Bdh1p from industrial strain was better than that of Bdh1p from laboratory strain. Therefore, we further deleted and overexpressed *BDH1* gene in industrial strain α5, resulting in strain α5-TB1 and α5-VB1, respectively. The production of acetoin indicates that the deletion of *BDH1* gene is beneficial to the synthesis of acetoin. After knocking out the *BDH1* gene, the relative expression level of the *BDH1* gene and the enzyme activity of the BDH decreased, which resulted in the pyruvate flux was successfully redirected toward acetoin pathway (Bae et al., 2016). With the accumulation of acetoin, the TTMP produced during the fermentation of Baijiu has also increased, which is consistent with the previous research

conclusions (Hao et al., 2013; Zhang et al., 2019; Zhong et al., 2020).

Many reports have focused on reducing or eliminating the production of glycerol and ethanol by knocking out the *ADH1-5*, *PDC1*, *PDC5*, *GPD1*, and *GPD2* genes, which redirect metabolic flux to 2,3-butanediol or acetoin for high-yield production (Kim et al., 2013; Kim and Hahn, 2015; Bae et al., 2016). However, although the content of acetoin in *S. cerevisiae* strain with *ADH1-5* gene deletion was increased, the yield of ethanol was significantly reduced, which was unfavorable for Baijiu fermentation. Moreover, the simultaneous knockout of *PDC1* and *PDC5* genes would affect the fermentation performance of the engineered strain (Oud et al., 2012). In addition, the introduction of acetoin biosynthetic pathway (ALS and α-acetolactate decarboxylase) from *Bacillus subtilis* into *S. cerevisiae* can also significantly increase the concentration of acetoin (Kim and Hahn, 2015; Jia et al., 2017). However, the insertion of heterogeneous genes may pose a hidden danger to the safety of the strain (Gibson et al., 2018). Therefore, these strategies are not suitable for the construction of high-yield TTMP-producing Baijiu industrial strain.

Effects of *BDH2* Deletion or Overexpression on Production of TTMP in *Saccharomyces cerevisiae*

The amino acid sequence of Bdh2p is 51% identical to that of Bdh1p, but the effect of Bdh2p on the production of acetoin and TTMP have not been reported yet. We determined the effect of *BDH2* overexpression or deletion on TTMP production in *S. cerevisiae*. The concentration of TTMP in the α5-TB2 (*BDH2* deletion) and α5-VB2 (*BDH2* overexpression) strains was 4.12 and 5.48 mg/L, respectively (**Table. 2**). The recombinant strain α5-TB2 yielded a 16.07% decrease in acetoin compared with the initial α5 strain. Overexpression of the *BDH2* gene increased the production of acetoin by 1.75-fold compared with the original strain. The production of 2,3-butanediol by the α5-TB2 and α5-VB2 strains was 10.62 and 18.75% decrease compared to that produced by α5, respectively. The deletion or overexpression of *BDH2* gene did not have an impact on fermentation performance in Baijiu fermentation (**Table 3** and **Supplementary Figure 1A**).

The expression of *BDH2* at the transcriptional level in α5-TB2 and α5-VB2 was also measured by RT-qPCR. The *BDH2* relative expression level in α5-TB2 was approximately zero. The expression of *BDH2* in α5-VB2 was 15.84-fold higher than that of α5 (**Figure 2B**). Under the control of *PGK1p* promoter, the relative expression level of *BDH2* gene was increased significantly. Moreover, the *BDH1* gene expression level and BDH activity were detected in strains α5-TB2 and α5-VB2. As shown in **Figure 2A**, the relative expression of the *BDH1* gene in the recombinant α5-VB2 and α5-TB2 strains was 0.53- and 0.17-fold that of α5. The BDH enzyme activity was also decreased significantly. Obviously, the decrease of BDH enzyme activity of strain α5-VB2 and α5-TB2 was closely related to the expression level of *BDH1* gene. This means that overexpression or deletion of *BDH2* gene affected the transcription level of *BDH1* gene firstly, and then decreased the enzyme activity of BDH. Therefore, the enzyme activity of BDH depends on the transcription level of *BDH1* gene, and has no obvious relationship with *BDH2* gene.

Many recent reports focus on the use of *BDHs* gene to regulate yeast tolerance to vanillin and acetaldehyde. Ishida et al. (2017) found that *BDH2* gene overexpression improved the tolerance of *S. cerevisiae* to vanillin, and this effect was stronger than that of overexpression of *BDH1*. In reduction of acetaldehyde, the activities of Bdh2p were significantly higher than Bdh1p (Kuang et al., 2020). However, few literatures have reported that the overexpression of *BDH2* gene can improve the synthesis of acetoin and TTMP. In our study, we confirmed that overexpression of *BDH2* could reduce the content of diacetyl, thereby increasing the production of acetoin and TTMP. As shown in **Figure 2**, we found that knocking out or overexpressing the *BDH1* gene will reduce the expression level of the *BDH2* gene. Similarly, the expression level of *BDH1* gene was also reduced to different degrees in *BDH2* deletion or overexpression strains. In the study of González et al. (2010), the same phenomenon occurred when the *BDH1* or *BDH2* gene was deleted. Due to the changes in the transcription level of *BDH1* and *BDH2* genes, the activity of BDH enzymes was also regulated to different degrees. Based on these data, we speculate that there is a potential association between the Bdh1p and Bdh2p in *S. cerevisiae*. But the functions of Bdh1p and Bdh2p were different: Bdh1p was related to the synthesis of 2,3-butanediol, while Bdh2p was related to the synthesis of acetoin. Under the catalysis of Bdh2p, diacetyl is converted into acetoin, increasing the concentration of TTMP. Hence, the diacetyl content produced by the strain α5-VB2 was lower than that of parental strain α5 and the yield of acetoin increased by 1.74-fold. In contrast, the acetoin production was decreased due to the deletion of *BDH2* gene in the α5-TB2 strain. If the main enzyme that converts diacetyl to acetoin is Bdh1p, then the content of acetoin should be increased, but this is contrary to our experimental results. In our study, the acetoin content produced by strain α5-VB1 (*BDH1* overexpression) decreased by 74.85% compared with the strain α5, while the production of 2,3-butanediol increased significantly. Therefore, the main function of Bdh1p is related to the synthesis of 2,3-butanediol. However, the specific mechanism between Bdh1p and Bdh2p is still unclear and needs further research. It is the first report that overexpression of the *BDH2* gene can increase the concentration of TTMP produced in Baijiu fermentation.

Increasing Production of TTMP by *BDH1* Deletion and *BDH2* Overexpression in *Saccharomyces cerevisiae*

Based on the results of TTMP productions in the strains α5-TB1, α5-VB1, α5-TB2, and α5-VB2, *BDH1* gene deletion and *BDH2* gene overexpression may improve the content of TTMP. Therefore, we constructed the recombinant strain α5-D1B2. The constructed α5-D1B2 strain with a 4.88-fold increase in acetoin production and a 2.63-fold increase in TTMP titer compared to the parental strain (**Table. 2**). Owing to the combined action of the *BDH1* deletion and *BDH2* overexpression, the final concentrations of diacetyl and 2,3-butanediol were markedly decreased. The fermentation performance of the α5-D1B2

strain was similar to that of parental strain (**Table 3** and **Supplementary Figure 1A**).

Due to the deletion of *BDH1* gene, the relative expression level of *BDH1* was almost zero (**Figure 2A**). As shown in **Figure 2B**, the expression of *BDH2* in α5-D1B2 were 38.56-fold that of α5. The expression level of *BDH2* gene was higher than that of single overexpression of *BDH2* gene (strain α5-VB2). It seems that the expression level of *BDH2* gene is influenced by *BDH1* gene, which confirmed our hypothesis that the functions of Bdh1p and Bdh2p are closely related. These changes demonstrated that the combination of *BDH1* gene deletion and *BDH2* gene overexpression could increase the concentration of TTMP significantly, which was the most effective strategy in this study.

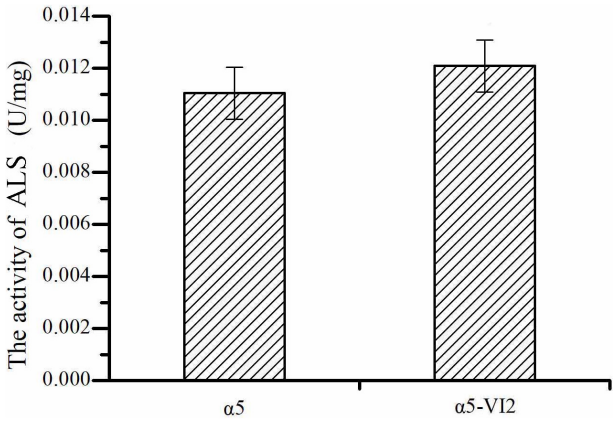

FIGURE 4 | The activities of α-acetolactate synthase (ALS). Data represent the mean of three independent biological replicates. Error bars represent the SD of the average values.

No Influence of ILV2 Overexpression on Production of TTMP in *Saccharomyces cerevisiae*

In *S. cerevisiae*, α-acetolactate is decarboxylated into diacetyl spontaneously. This means that the strategy of enhancing the "α-acetolactate – diacetyl" pathway by genetic engineering could not be used to increase the content of diacetyl. Since pyruvate produced α-acetolactate under the catalysis of ALS, we focused on enhancing this pathway to increase the content of diacetyl (Espinosa-Cantú et al., 2018). In order to determine the accumulation effect of increasing the expression level of ALS on diacetyl production, thereby increasing the content of acetoin and TTMP, we improved the catalytic reaction of the α-acetolactate biosynthetic pathway by overexpressing the *ILV2* gene, resulting in strain α5-VI2. As shown in **Table. 2**, the diacetyl content in the parental strain α5 and recombinant strain α5-VI2 was 30.85 and 34.06 mg/L, respectively. Except that the content of diacetyl was slightly increased, no other metabolites were affected by *ILV2* overexpression. As shown in **Table 3** and **Supplementary Figure 1A**, the performances of strain α5-VI2 did not change significantly in comparison to the parental strain α5.

The relative expression level of *ILV2* gene was determined by RT-PCR. As shown in **Figure 2C**, the relative expression level of *ILV2* was increased significantly, which was 8.21-fold higher than that of the parental strain a5. As shown in **Figure 4**, the specific activities of ALS in the α5 and α5-VI2 strains were 0.0111 and 0.0121 U/mg, respectively. The overexpression of *ILV2* gene had little effect on the activity of the ALS. Further promoting of α-acetolactate biosynthesis by overexpressing *ILV2* did not significantly improve the concentration of TTMP.

During the fermentation of beer and wine, high concentration of diacetyl was often considered to affect quality of alcoholic beverages (Bartowsky and Henschke, 2004; Humia et al., 2019). In previous studies, we tried to regulate the content of diacetyl by controlling the expression level of *ILV2* gene. Shi et al. (2016) reduced the diacetyl content during beer fermentation by 17.83% by knocking out the *ILV2* gene in brewer's yeast strain. Meanwhile, the content of diacetyl was decreased by 61.93% in recombinant brewer's yeast, which deleting *ILV2* gene and overexpressing acetohydroxyacid reductoisomerase encoding gene *ILV5* (Shi et al., 2017). These results indicated that the expression of *ILV2* gene is related to diacetyl biosynthesis. However, in this study, the biosynthesis of diacetyl needs to be improved and then increased the content of acetoin.

The *ILV2* gene overexpression slightly increased diacetyl production, but had no significant influence on the content of TTMP, acetoin, 2,3-butanediol. Although the expression level of the *ILV2* gene increased, it did not significantly affect the activity of the ALS. It has been known that ALS consists of two subunits, the catalytic subunit (Ilv2p) and the regulatory subunit (Ilv6p). A previous study revealed that Ilv2p activity is negatively regulated by the regulatory subunit Ilv6, which may be one of the reasons for affecting the enzyme activity of Ilv2p (Dasari and Kölling, 2011; Takpho et al., 2018). Diacetyl production was also regulated by the expression level of *ILV6* gene. Li P. et al. (2018) reduced the expression level of *ILV6* gene in *Saccharomyces uvarum* by 40% and then diacetyl production was reduced by 25.71%. In lager brewers' yeast with single and double deletion of *ILV6*, the *ILV6* expression was reduced by 13% and 40%, respectively, and the concentration of diacetyl was significantly reduced. However, the enzyme activity of ALS had not been significantly reduced, which was similar to our experimental results (Duong et al., 2011). It has been reported that the *ILV6* transcription level of native strain with high diacetyl production is higher than that of native strain with low production (Gibson et al., 2015). Meanwhile, overexpression of the *ILV6* gene of *S. cerevisiae* not only enhanced the content of diacetyl, but also increased the transcription level of *ILV2* gene. These results suggest that an effective strategy to increase ALS enzyme activity may be to simultaneously overexpress the genes encoding the regulatory and catalytic subunits, which are *ILV6* and *ILV2* genes.

Moreover, the acetohydroxyacid reductoisomerase (Ilv5p) catalyzes the degradation of α-acetolactate to produce dihydroxy isovalerate, hence the content of diacetyl is also regulated by Ilv5p (Omura, 2008; van Bergen et al., 2016; Shi et al., 2017). In our study, the diacetyl content of strains overexpressing the *ILV2* gene was only slightly increased, which may be related to the decomposition of a part of α-acetolactate by Ilv5p.

Furthermore, the conversion of α-acetolactate to diacetyl is a rate-limiting step in *S. cerevisiae* (Kim et al., 2017). This may mean that α-acetolactate needs a large amount of accumulation to significantly increase the concentration of diacetyl. However, α-acetolactate is toxic to *S. cerevisiae* cells and affects the growth performance of the strain (Park and Hahn, 2019). In addition, too high content of diacetyl results in an unwanted buttery flavor, the balance of Baijiu flavor will be broken and the quality of Baijiu will also be decreased. In general, the strategy of promoting the synthesis of acetoin and TTMP by excessively increasing the content of diacetyl is not entirely ideal for Baijiu. Therefore, it is necessary to precisely control the concentration of α-acetolactate and diacetyl to maintain the balance between diacetyl and Baijiu flavor.

Production of TTMP by Recombinant Diploid Strains

The TTMP content of haploid strains α5-TB1 (*BDH1* deletion) and α5-D1B2 (*BDH1* deletion and *BDH2* overexpression) significantly increased compared with the parental strain α5. In order to investigate the fermentation performance of the strain during Baijiu brewing, four diploid strains (AY-B1, AY-SB1, AY-D1B2, and AY-SD1B2) were constructed based on strains α5-TB1 and α5-D1B2. The production of TTMP and acetoin by diploid strains was investigated by simulating alcohol fermentation experimentally. The data obtained by GC and HPLC are shown in **Table. 4**. The content of TTMP and acetoin in the parental AY15 strain were 3.29 and 581.13 mg/L, respectively. Compared to the AY15 strain, the AY-B1 strain (*BDH1* single-allele-deletion diploid) yielded a 10.94 and 24.07% increase in TTMP and acetoin production, respectively. The AY-SB1 strain (*BDH1* double-allele-deletion diploid) yielded a 130.39% increase in TTMP and a 271.57% increase in acetoin.

The diploid strain AY-D1B2 represents *BDH1* single-allele-deletion and *BDH2* single-allele-overexpression. The production of TTMP and acetoin by the AY-D1B2 strain was 4.48 and 909.73 mg/L, respectively. Strain AY-D1B2 yielded a 36.17% increase in TTMP and a 56.54% increase in acetoin. The diploid strain AY-SD1B2 was *BDH1* double-allele-deletion and *BDH2* double-allele-overexpression. The TTMP and acetoin content represented a 2.87- and 4.97-fold increase compared to strain AY15. As shown in **Table. 3** and **Supplementary Figure 1B**, the fermentation performance of the AY-B1, AY-SB1, AY-D1B2, and AY-SD1B2 were similar to that of parental strain AY15. The production of acetoin and TTMP produced by AY-SD1B2 was the highest among the four diploid strains, while the double-allele-deletion of *BDH1* and the double-allele-overexpression of *BDH2* had the greatest impact on acetoin and TTMP production. In addition, regardless of whether this was the result of the deletion or overexpression of *BDH1* and *BDH2*, the content of acetoin was positively correlated with TTMP production.

Diploid strains of *S. cerevisiae* are widely used for fermentation in the food industry, including bread making and wine brewing. The diploid strain of *S. cerevisiae* is used as a stable source of fermentation in Baijiu brewing. To ensure the fermentation performance of the strain, it is necessary to hybridize the haploid strains into diploid strains. Diploid strains AY-SB1 (*BDH1* double-allele-deletion) and AY-SD1B2 (*BDH1* double-allele-deletion and *BDH2* double-allele-overexpression) were found to produce high levels of acetoin, which resulted in increased TTMP production. Moreover, compared with the original strain AY15, there were no significant differences regarding the growth curve, the fermentation performance, or the production of esters or higher alcohols. It is worth noting that the *BDH1* double-allele-deletion and *BDH2* double-allele-overexpression were the most efficient in terms of increased TTMP production. This study provides an important reference for the application genetic engineering to *S. cerevisiae* in order to increase the yield of TTMP in Baijiu and other alcoholic beverages, thereby improving their beneficial health attributes.

Production of Ester and Higher Alcohol by Recombinant Diploid Strains

To analyze the effects of the modification of *BDH1* and *BDH2* genes on the flavor substances, we detected the contents of esters and higher alcohols in diploid strains. The production of ester and higher alcohol was detected as a result of corn-semi-solid medium fermentation. As shown in **Figure 5**, the production of ethyl acetate by the AY15, AY-B1, AY-SB1, AY-D1B2, and AY-SD1B2 strains was 24.51, 19.44, 23.87, 27.98, and 24.92 mg/L, respectively. The AY-D1B2 strain showed a 23.71% decrease in the production of 2-phenylethanol. There were no significant changes in terms of the content of other higher alcohols in the fermentation samples of AY-B1, AY-SB1, AY-D1B2, and AY-SD1B2. These

TABLE 4 | The concentrations of TTMP and other metabolites produced by diploid strains.

Strains[a]	TTMP (mg/L)	Acetoin (mg/L)	Diacetyl (mg/L)	2,3-Butanediol (mg/L)
AY15	3.29 ± 0.11	581.13 ± 54.13	27.43 ± 1.36	1, 825.34 ± 30.81
AY-B1	3.65 ± 0.12	721.02 ± 49.42*	29.14 ± 1.58	1, 259.41 ± 30.02**
AY-SB1	7.58 ± 0.17**	2, 159.34 ± 160.73**	37.32 ± 2.55**	620.55 ± 16.23**
AY-D1B2	4.48 ± 0.11	909.72 ± 96.89**	28.62 ± 1.5	1, 868.59 ± 28.72
AY-SD1B2	9.47 ± 0.21**	2, 893.96 ± 184.93**	35.52 ± 2.47**	508.12 ± 15.84**

[a]*Diploid strain: AY-B1 (BDH1 single-allele-deletion), AY-SB1 (BDH1 double-allele-deletion), AY-D1B2 (BDH1 single-allele-deletion and BDH2 single-allele-overexpression), and AY-SD1B2 (BDH1 double-allele-deletion and BDH2 double-allele-overexpression). The strains were fermented by corn-semi-solid medium at 30°C for 4 days. Values are means ± standard deviations from at least three independent tests. Statistical significance is denoted as **P < 0.01 and *P < 0.05.*

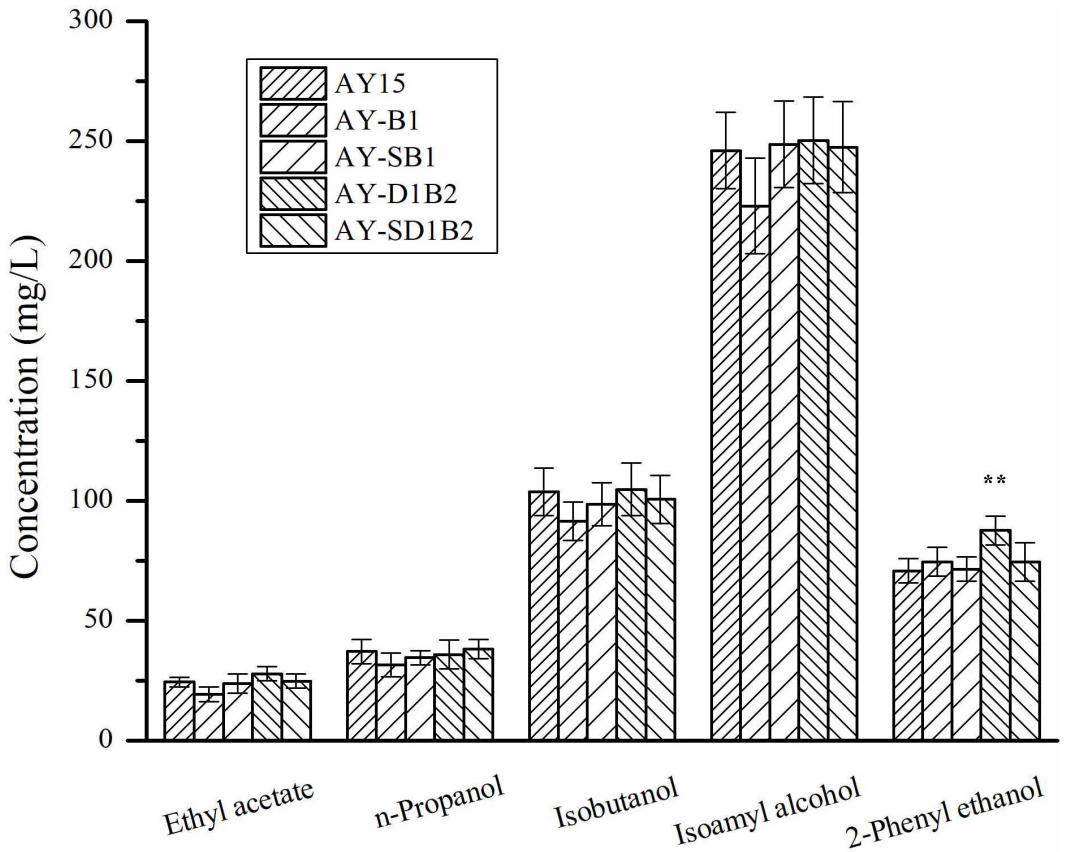

FIGURE 5 | The content of esters and higher alcohols in diploid strains. Data represent the mean of three independent biological replicates. Error bars represent the SD of the average values. Statistical significance is denoted as $^{**}P < 0.01$ and $^{**}P < 0.05$.

results indicated that the modification of *BDH1* and *BDH2* did not affect the flavor substance content produced by the diploid strain.

CONCLUSION

2,3,5,6-Tetramethylpyrazine is a type of pyrazine that has a nutty aroma, and is a key flavor compound of Baijiu (Zhu et al., 2007). During Baijiu fermentation, acetoin is converted to TTMP spontaneously rather than as an enzymatic reaction, which is one of the reasons for the low TTMP content in Baijiu (Xiao et al., 2014; Zhang et al., 2019). In this study, we focus on regulating the expression levels of *BDH1* and *BDH2* genes to control the content of acetoin and TTMP. The results proved that knockout of *BDH1* or overexpression of *BDH2* can promote the synthesis of acetoin, and then increase the concentration of TTMP. In our research, knocking out *BDH1* and overexpressing *BDH2* in *S. cerevisiae* is the best strategy to increase the concentration of TTMP. It is important that the fermentation performance and the content of esters and higher alcohols produced by diploid strains (AY-B1, AY-SB1, AY-D1B2, and AY-SD1B2) with high TTMP production were not negatively affected. This study provides an important reference for the application genetic engineering to *S. cerevisiae* in order to increase the yield of TTMP in Baijiu and other alcoholic beverages, thereby improving their beneficial health attributes.

DATA AVAILABILITY STATEMENT

The original contributions presented in the study are included in the article/**Supplementary Material**, further inquiries can be directed to the corresponding author.

AUTHOR CONTRIBUTIONS

D-YC, D-GX, and C-YZ conceived and designed research. D-YC, Y-NW, and P-PF conducted experiments. L-CL, XL, and C-YZ analyzed data. D-YC and S-JC wrote the manuscript. D-GX, L-CL, and C-YZ revised and reviewed the manuscript. All authors read and approved the manuscript.

FUNDING

The current study was financially supported by the National Key Research and Development Program of China

(2016YFD0400500), National Natural Science Foundation of China (31571809), the Key Laboratory of Wuliangye-flavor Liquor Solid-state Fermentation, China National Light Industry (No. 2019JJ005), Public Service Platform Project for Selection and Fermentation Technology of Industrial Microorganisms (17PTGCCX00190) and the Innovative Research Team of Tianjin Municipal Education Commission (TD13-5013). The Project Supported by the Foundation (No. 2018KF001) of Key Laboratory of Industrial Fermentation Microbiology of Ministry of Education and Tianjin Key Lab of Industrial Microbiology (Tianjin University of Science & Technology).

SUPPLEMENTARY MATERIAL

The Supplementary Material for this article can be found online at: https://www.frontiersin.org/articles/10.3389/fmicb.2020.596306/full#supplementary-material

Supplementary Figure 1 | Growth curve of haploid strains and diploid strains.

Supplementary Table 1 | Primers used in this study.

Supplementary Table 2 | The recombinant fragments and corresponding PCR primers.

REFERENCES

Bae, S. J., Kim, S., and Hahn, J. S. (2016). Efficient production of acetoin in *Saccharomyces cerevisiae* by disruption of 2,3-butanediol dehydrogenase and expression of NADH oxidase. *Sci. Rep.* 6:27667. doi: 10.1038/srep27667

Bartowsky, E. J., and Henschke, P. A. (2004). The 'buttery' attribute of wine–diacetyl–desirability, spoilage and beyond. *Int. J. Food Microbiol.* 96, 235–252. doi: 10.1016/j.ijfoodmicro.2004.05.013

Brat, D., Weber, C., Lorenzen, W., Bode, H. B., and Boles, E. (2012). Cytosolic re-localization and optimization of valine synthesis and catabolism enables increased isobutanol production with the yeast *Saccharomyces cerevisiae*. *Biotechnol. Biofuels* 5:65. doi: 10.1186/1754-6834-5-65

Calam, E., González-Roca, E., Fernández, M. R., Dequin, S., Parés, X., Virgili, A., et al. (2016). Enantioselective synthesis of vicinal (R,R)-diols by *Saccharomyces cerevisiae* butanediol dehydrogenase. *Appl. Environ. Microbiol.* 82, 1706–1721. doi: 10.1128/aem.03717-15

Cao, J., Miao, Q., Miao, S., Bi, L., Zhang, S., Yang, Q., et al. (2015). Tetramethylpyrazine (TMP) exerts antitumor effects by inducing apoptosis and autophagy in hepatocellular carcinoma. *Int. Immunopharmacol.* 26, 212–220. doi: 10.1016/j.intimp.2015.03.028

Chen, J. C., Chen, Q. H., Guo, Q., Ruan, S., Hui, R., He, G. Q., et al. (2010). Simultaneous determination of acetoin and tetramethylpyrazine in traditional vinegars by HPLC method. *Food Chem.* 122, 1247–1252.

Chen, Y., Lu, W., Yang, K., Duan, X., Li, M., Chen, X., et al. (2020). Tetramethylpyrazine, a promising drug for treatment of pulmonary hypertension. *Br. J. Pharmacol.* 177, 2743–2764. doi: 10.1111/bph.15000

Choi, E. J., Kim, J. W., Kim, S. J., Seo, S. O., Lane, S., Park, Y. C., et al. (2016). Enhanced production of 2,3-butanediol in pyruvate decarboxylase-deficient *Saccharomyces cerevisiae* through optimizing ratio of glucose/galactose. *Biotechnol. J.* 11, 1424–1432. doi: 10.1002/biot.201600042

Cui, D. Y., Zhang, Y., Xu, J., Zhang, C. Y., Li, W., and Xiao, D. G. (2018). PGK1 promoter library for the regulation of acetate ester production in *Saccharomyces cerevisiae* during Chinese Baijiu fermentation. *J. Agric. Food Chem.* 66, 7417–7427. doi: 10.1021/acs.jafc.8b02114

Dasari, S., and Kölling, R. (2011). Cytosolic localization of acetohydroxyacid synthase Ilv2 and its impact on diacetyl formation during beer fermentation. *Appl. Environ. Microbiol.* 77, 727–731. doi: 10.1128/aem.01579-10

Du, H., Fan, W., and Xu, Y. (2011). Characterization of geosmin as source of earthy odor in different aroma type Chinese liquors. *J. Agric. Food Chem.* 59, 8331–8337. doi: 10.1021/jf201171b

Dulieu, C., and Poncelet, D. (1999). Spectrophotometric assay of α-acetolactate decarboxylase. *Enzyme Microb. Technol.* 25, 537–542. doi: 10.1016/S0141-0229(99)00079-4

Duong, C. T., Strack, L., Futschik, M., Katou, Y., Nakao, Y., Fujimura, T., et al. (2011). Identification of Sc-type ILV6 as a target to reduce diacetyl formation in lager brewers' yeast. *Metab. Eng.* 13, 638–647. doi: 10.1016/j.ymben.2011.07.005

Ehsani, M., Fernández, M. R., Biosca, J. A., Julien, A., and Dequin, S. (2009). Engineering of 2,3-butanediol dehydrogenase to reduce acetoin formation by glycerol-overproducing, low-alcohol *Saccharomyces cerevisiae*. *Appl. Environ. Microbiol.* 75, 3196–3205. doi: 10.1128/aem.02157-08

Espinosa-Cantú, A., Ascencio, D., Herrera-Basurto, S., Xu, J., Roguev, A., and Krogan, N. J. (2018). Protein moonlighting revealed by noncatalytic phenotypes of yeast enzymes. *Genetics* 208, 419–431. doi: 10.1534/genetics.117.300377

Fan, W., Xu, Y., and Zhang, Y. (2007). Characterization of pyrazines in some Chinese liquors and their approximate concentrations. *J. Agric. Food Chem.* 55, 9956–9962. doi: 10.1021/jf071357q

Gibson, B., Krogerus, K., Ekberg, J., Monroux, A., Mattinen, L., Rautio, J., et al. (2015). Variation in α-acetolactate production within the hybrid lager yeast group *Saccharomyces pastorianus* and affirmation of the central role of the ILV6 gene. *Yeast* 32, 301–316. doi: 10.1002/yea.3026

Gibson, B., Vidgren, V., Peddinti, G., and Krogerus, K. (2018). Diacetyl control during brewery fermentation via adaptive laboratory engineering of the lager yeast *Saccharomyces pastorianus*. *J. Ind. Microbiol. Biotechnol.* 45, 1103–1112. doi: 10.1007/s10295-018-2087-4

Gietz, R. D., and Woods, R. A. (2002). Transformation of yeast by lithium acetate/single-stranded carrier DNA/polyethylene glycol method. *Methods Enzymol.* 350, 87–96. doi: 10.1016/s0076-6879(02)50957-5

González, E., Fernández, M. R., Larroy, C., Parés, X., and Biosca, J. A. (2001). Characterization and functional role of *Saccharomyces cerevisiae* 2,3-butanediol dehydrogenase. *Chem. Biol. Interact.* 130-132, 425–434. doi: 10.1016/s0009-2797(00)00282-9

González, E., Fernández, M. R., Larroy, C., Solà, L. S., Pericàs, M. A., Parés, X., et al. (2000). Characterization of a (2R,3R)-2,3-butanediol dehydrogenase as the *Saccharomyces cerevisiae* YAL060W gene product disruption and induction of the gene. *J. Biol. Chem.* 275, 35876–35885. doi: 10.1074/jbc.M003035200

González, E., Fernández, M. R., Marco, D., Calam, E., Sumoy, L., Parés, X., et al. (2010). Role of *Saccharomyces cerevisiae* oxidoreductases Bdh1p and Ara1p in the metabolism of acetoin and 2,3-butanediol. *Appl. Environ. Microbiol.* 76, 670–679. doi: 10.1128/AEM.01521-09

Gueldener, U., Heinisch, J., Koehler, G. J., Voss, D., and Hegemann, J. H. (2002). A second set of loxP marker cassettes for Cre-mediated multiple gene knockouts in budding yeast. *Nucleic Acids Res.* 30:e23. doi: 10.1093/nar/30.6.e23

Hao, F., Wu, Q., and Xu, Y. (2013). Precursor supply strategy for tetramethylpyrazine production by *Bacillus subtilis* on solid-state fermentation of wheat bran. *Appl. Biochem. Biotechnol.* 169, 1346–1352. doi: 10.1007/s12010-012-0083-0

Humia, B. V., Santos, K. S., Barbosa, A. M., Sawata, M., Mendonça, M. D. C., and Padilha, F. F. (2019). Beer molecules and its sensory and biological properties: a review. *Molecules* 24:1568. doi: 10.3390/molecules24081568

Ishida, Y., Nguyen, T., and Izawa, S. (2017). The yeast *ADH7* promoter enables gene expression under pronounced translation repression caused by the combined stress of vanillin, furfural, and 5-hydroxymethylfurfural. *J. Biotechnol.* 252, 65–72. doi: 10.1016/j.jbiotec.2017.04.024

Ishida, Y., Nguyen, T. T., Kitajima, S., and Izawa, S. (2016). Prioritized expression of *BDH2* under bulk translational repression and its contribution to tolerance to severe vanillin stress in *Saccharomyces cerevisiae*. *Front. Microbiol.* 7:1059. doi: 10.3389/fmicb.2016.01059

Jia, X., Liu, Y., and Han, Y. (2017). A thermophilic cell-free cascade enzymatic reaction for acetoin synthesis from pyruvate. *Sci. Rep.* 7:4333. doi: 10.1038/s41598-017-04684-8

Kim, S., and Hahn, J. S. (2015). Efficient production of 2,3-butanediol in *Saccharomyces cerevisiae* by eliminating ethanol and glycerol production and redox rebalancing. *Metab. Eng.* 31, 94–101. doi: 10.1016/j.ymben.2015.07.006

Kim, S. J., Kim, J. W., Lee, Y. G., Park, Y. C., and Seo, J. H. (2017). Metabolic engineering of *Saccharomyces cerevisiae* for 2,3-butanediol production.

Appl. Microbiol. Biotechnol. 101, 2241–2250. doi: 10.1007/s00253-017-8172-1

Kim, S. J., Seo, S. O., Jin, Y. S., and Seo, J. H. (2013). Production of 2,3-butanediol by engineered *Saccharomyces cerevisiae*. *Bioresour. Technol.* 146, 274–281. doi: 10.1016/j.biortech.2013.07.081

Kim, S. J., Seo, S. O., Park, Y. C., Jin, Y. S., and Seo, J. H. (2014). Production of 2,3-butanediol from xylose by engineered *Saccharomyces cerevisiae*. *J. Biotechnol.* 192, 376–382. doi: 10.1016/j.jbiotec.2013.12.017

Kuang, X., Ouyang, Y., Guo, Y., Li, Q., Wang, H., Abrha, G. T., et al. (2020). New insights into two yeast BDHs from the PDH subfamily as aldehyde reductases in context of detoxification of lignocellulosic aldehyde inhibitors. *Appl. Microbiol. Biotechnol.* 104, 6679–6692. doi: 10.1007/s00253-020-10722-9

Li, P., Gao, Y., Wang, C., Zhang, C. Y., Guo, X., and Xiao, D. (2018). Effect of *ILV6* deletion and expression of aldB from *Lactobacillus plantarum* in *Saccharomyces uvarum* on diacetyl production and wine flavor. *J. Agric. Food Chem.* 66, 8556–8565. doi: 10.1021/acs.jafc.8b02356

Li, P., Guo, X., Shi, T., Hu, Z., Chen, Y., Du, L., et al. (2017). Reducing diacetyl production of wine by overexpressing *BDH1* and *BDH2* in *Saccharomyces uvarum*. *J. Ind. Microbiol. Biotechnol.* 44, 1541–1550. doi: 10.1007/s10295-017-1976-2

Li, W., Chen, S. J., Wang, J. H., Zhang, C. Y., Shi, Y., Guo, X. W., et al. (2018). Genetic engineering to alter carbon flux for various higher alcohol productions by *Saccharomyces cerevisiae* for Chinese Baijiu fermentation. *Appl. Microbiol. Biotechnol.* 102, 1783–1795. doi: 10.1007/s00253-017-8715-5

Li, W., Wang, J. H., Zhang, C. Y., Ma, H. X., and Xiao, D. G. (2017). Regulation of *Saccharomyces cerevisiae* genetic engineering on the production of acetate esters and higher alcohols during Chinese Baijiu fermentation. *J. Ind. Microbiol. Biotechnol.* 44, 1–12. doi: 10.1007/s10295-017-1907-2

Liu, H., and Sun, B. (2018). Effect of fermentation processing on the flavor of Baijiu. *J. Agric. Food Chem.* 66, 5425–5432. doi: 10.1021/acs.jafc.8b00692

Meng, W., Ding, F., Wang, R. M., and Wang, T. F. (2020). Enhanced production of tetramethylpyrazine in *Bacillus licheniformis* BL1 through aldC over-expression and acetaldehyde supplementation. *Sci. Rep.* 10:3544. doi: 10.1038/s41598-020-60345-3

Meng, W., Xiao, D., and Wang, R. (2016). Enhanced production of tetramethylpyrazine in *Bacillus licheniformis* BL1 by bdhA disruption and 2,3-butanediol supplementation. *World J. Microbiol. Biotechnol.* 32:46. doi: 10.1007/s11274-015-1992-1

Murashchenko, L., Abbas, C., Dmytruk, K., and Sibirny, A. (2016). Overexpression of the truncated version of *ILV2* enhances glycerol production in *Saccharomyces cerevisiae*. *Yeast* 33, 463–469. doi: 10.1002/yea.3161

Omura, F. (2008). Targeting of mitochondrial *Saccharomyces cerevisiae* Ilv5p to the cytosol and its effect on vicinal diketone formation in brewing. *Appl. Microbiol. Biotechnol.* 78, 503–513. doi: 10.1007/s00253-007-1333-x

Oud, B., Flores, C. L., Gancedo, C., Zhang, X., Trueheart, J., Daran, J. M., et al. (2012). An internal deletion in *MTH1* enables growth on glucose of pyruvate-decarboxylase negative, non-fermentative *Saccharomyces cerevisiae*. *Microb. Cell Fact.* 11:131. doi: 10.1186/1475-2859-11-131

Park, S. H., and Hahn, J. S. (2019). Development of an efficient cytosolic isobutanol production pathway in *Saccharomyces cerevisiae* by optimizing copy numbers and expression of the pathway genes based on the toxic effect of α-acetolactate. *Sci. Rep.* 9:3996. doi: 10.1038/s41598-019-40631-5

Rizzi, G. P. (1988). Formation of pyrazines from acyloin precursors under mild conditions. *J. Agric. Food Chem.* 36, 349–352. doi: 10.1021/jf00080a026

Shi, T. T., Li, P., Chen, S. J., Chen, Y. F., Guo, X. W., and Xiao, D. G. (2017). Reduced production of diacetyl by overexpressing *BDH2* gene and *ILV5* gene in yeast of the lager brewers with one *ILV2* allelic gene deleted. *J. Ind. Microbiol. Biotechnol.* 44, 397–405. doi: 10.1007/s10295-017-1903-6

Shi, T. T., Li, P., Zhou, Z., and Xiao, D. G. (2016). Diacetyl content reduction in industrial brewer's yeast through *ILV2* disruption and *BDH1* expression. *Eur. Food Res. Technol.* 242, 919–926. doi: 10.1007/s00217-015-2598-4

Shin, J. W., Moon, J. Y., Seong, J. W., Song, S. H., Cheong, Y. J., Kang, C., et al. (2013). Effects of tetramethylpyrazine on microglia activation in spinal cord compression injury of mice. *Am. J. Chin. Med.* 41, 1361–1376. doi: 10.1142/s0192415x13500912

Takpho, N., Watanabe, D., and Takagi, H. (2018). High-level production of valine by expression of the feedback inhibition-insensitive acetohydroxyacid synthase in *Saccharomyces cerevisiae*. *Metab. Eng.* 46, 60–67. doi: 10.1016/j.ymben.2018.02.011

van Bergen, B., Cyr, N., Strasser, R., Blanchette, M., Sheppard, J. D., and Jardim, A. (2016). α,β-Dicarbonyl reduction is mediated by the *Saccharomyces* Old Yellow Enzyme. *FEMS Yeast Res.* 16:fow059. doi: 10.1093/femsyr/fow059

Wang, X., Fan, W., and Xu, Y. (2014). Comparison on aroma compounds in Chinese soy sauce and strong aroma type liquors by gas chromatography–olfactometry, chemical quantitative and odor activity values analysis. *Eur. Food Res. Technol.* 239, 813–825. doi: 10.1007/s00217-014-2275-z

Wess, J., Brinek, M., and Boles, E. (2019). Improving isobutanol production with the yeast by successively blocking competing metabolic pathways as well as ethanol and glycerol formation. *Biotechnol. Biofuels* 12:173. doi: 10.1186/s13068-019-1486-8

Xiao, Z., Hou, X., Xin, L., Xi, L., and Zhao, J. (2014). Accelerated green process of tetramethylpyrazine production from glucose and diammonium phosphate. *Biotechnol. Biofuels* 7:106. doi: 10.1186/1754-6834-7-106

Xiao, Z., Zhao, L., Tian, L., Wang, L., and Zhao, J. Y. (2018). GC-FID determination of tetramethylpyrazine and acetoin in vinegars and quantifying the dependence of tetramethylpyrazine on acetoin and ammonium. *Food Chem.* 239:726. doi: 10.1016/j.foodchem.2017.07.015

Xiao, Z. J., Xie, N. Z., Liu, P. H., Hua, D. L., and Xu, P. (2006). Tetramethylpyrazine production from glucose by a newly isolated *Bacillus mutant*. *Appl. Microbiol. Biotechnol.* 73, 512–518. doi: 10.1007/s00253-006-0491-6

Xu, Y., Jiang, Y., Li, X., Sun, B., Teng, C., Yang, R., et al. (2018). Systematic characterization of the metabolism of acetoin and its derivative ligustrazine in *Bacillus subtilis* under micro-oxygen conditions. *J. Agric. Food Chem.* 66, 3179–3187. doi: 10.1021/acs.jafc.8b00113

Yang, Z., and Zhang, Z. (2018). Production of (2R, 3R)-2,3-butanediol using engineered *Pichia pastoris*: strain construction, characterization and fermentation. *Biotechnol. Biofuels* 11:35. doi: 10.1186/s13068-018-1031-1

Zhang, L., Cao, Y., Tong, J., and Xu, Y. (2019). An alkylpyrazine synthesis mechanism involving l-threonine-3-dehydrogenase describes the production of 2,5-dimethylpyrazine and 2,3,5-trimethylpyrazine by *Bacillus subtilis*. *Appl. Environ. Microbiol.* 85, e1807–e1819. doi: 10.1128/aem.01807-19

Zhong, H., Shen, J., Meng, Z., Zhao, J. Y., and Xiao, Z. (2020). Tetramethylpyrazine production from edible materials by the probiotic *Bacillus coagulans*. *Prep. Biochem. Biotechnol.* 50, 935–942. doi: 10.1080/10826068.2020.1774777

Zhu, B. F., Xu, Y., and Fan, W. L. (2010). High-yield fermentative preparation of tetramethylpyrazine by *Bacillus* sp. using an endogenous precursor approach. *J. Ind. Microbiol. Biotechnol.* 37, 179–186. doi: 10.1007/s10295-009-0661-5

Zhu, S., Xin, L., Ji, K., Guo, K., Li, Y., Wu, C., et al. (2007). Characterization of flavor compounds in Chinese liquor Moutai by comprehensive two-dimensional gas chromatography/time-of-flight mass spectrometry. *Anal. Chim. Acta* 597, 340–348. doi: 10.1016/j.aca.2007.07.007

Conflict of Interest: The authors declare that the research was conducted in the absence of any commercial or financial relationships that could be construed as a potential conflict of interest.

frontiers in Microbiology

ORIGINAL RESEARCH
published: 04 December 2020
doi: 10.3389/fmicb.2020.603481

Influence of Storage Conditions on the Quality, Metabolites, and Biological Activity of Soursop (*Annona muricata.* L.) Kombucha

*Wee Ching Tan[1], Belal J. Muhialdin[1,3] and Anis Shobirin Meor Hussin[2,3]**

[1] Department of Food Science, Faculty of Food Science and Technology, Universiti Putra Malaysia, Serdang, Malaysia,
[2] Department of Food Technology, Faculty of Food Science and Technology, Universiti Putra Malaysia, Serdang, Malaysia,
[3] Halal Products Research Institute, Universiti Putra Malaysia, Serdang, Malaysia

Kombucha is a slightly alcoholic beverage produced using sugared tea via fermentation using the symbiotic culture of bacteria and yeast (SCOBY). This study aimed to optimize the production of soursop kombucha and determine the effects of different storage conditions on the quality, metabolites, and biological activity. The response surface method (RSM) results demonstrated that the optimum production parameters were 300 ml soursop juice, 700 ml black tea, and 150 g sugar and 14 days fermentation at 28°C. The storage conditions showed significant ($P < 0.05$) effects on the antioxidant activity including the highest antioxidant activity for the sample stored for 14 days at 25°C in light and the highest total phenolic content (TPC) for the sample stored for 7 days at 4°C in the dark. No significant effects were observed on the antimicrobial activity of soursop kombucha toward *Escherichia coli* and *Staphylococcus aureus*. The microbial population was reduced from the average of 10^6 CFU/ml before the storage to 10^4 CFU/ml after the storage at 4 and 25°C in dark and light conditions. The metabolites profiling demonstrated significant decline for the sucrose, acetic acid, gluconic acid, and ethanol, while glucose was significantly increased. The storage conditions for 21 days at 25°C in the dark reduced 98% of ethanol content. The novel findings of this study revealed that prolonged storage conditions have high potential to improve the quality, metabolites content, biological activity, and the Halal status of soursop kombucha.

Keywords: antioxidant activity, Halal, fermented tea, beverages and biological samples, health promoting

OPEN ACCESS

Edited by:
Wanping Chen,
Georg-August-University Goettingen, Germany

Reviewed by:
Viduranga Y. Waisundara,
Australian College of Business and Technology - Kandy Campus, Sri Lanka
Bin Wang,
Shihezi University, China

***Correspondence:**
Anis Shobirin Meor Hussin
shobirin@upm.edu.my

Specialty section:
This article was submitted to Food Microbiology, a section of the journal Frontiers in Microbiology

Received: *07 September 2020*
Accepted: *02 November 2020*
Published: *04 December 2020*

Citation:
Tan WC, Muhialdin BJ and Meor Hussin AS (2020) Influence of Storage Conditions on the Quality, Metabolites, and Biological Activity of Soursop (Annona muricata. L.) Kombucha. Front. Microbiol. 11:603481. doi: 10.3389/fmicb.2020.603481

INTRODUCTION

Kombucha is a slightly alcoholic beverage produced via the fermentation of sugared tea using symbiotic culture of bacteria and yeast (SCOBY) for 7–21 days (Leal et al., 2018). Kombucha has a slight sweet, sourly, and refreshing taste with high acceptability by the consumers worldwide (Teoh et al., 2004). Several studies reported that kombucha demonstrated biological activities such as antimicrobial, antioxidant, anticancer, antidiabetic, and anti-inflammatory activities (Villarreal-soto et al., 2018; Gaggìa et al., 2019; Ivanišová et al., 2019). The biological activity of kombucha has strong interaction with the SCOBY that is also known as "tea fungus." The SCOBY contains symbiotic culture of yeast (*Brettanomyces*, *Zygosaccharomyces*, *Saccharomyces*, and *Pichia*) and

acetic acid bacteria (*Acetobacter xylinum*) (Bellut et al., 2020). The yeast's role is mainly to hydrolyze the sugar (sucrose) in the tea to glucose and fructose and convert it to ethanol, while the bacteria utilize the ethanol to produce acetic acid (Kulshrestha et al., 2013). The final product will have low pH and broad range of bioactive compounds with different biological activities (Teoh et al., 2004). Kombucha was reported as a rich source of different metabolites including organic acids (acetic and glucuronic), vitamins (B1, B2, and B12), and slight ethanol (Villarreal-Soto et al., 2019). In addition, phenolic compounds were reported to be found in black tea kombucha including gallic acid, caffeine, rutin, quercetin, and catechin (Barbosa et al., 2020).

Kombucha is traditionally produced using black tea and table sugar (sucrose) as the main ingredients. Thus, great numbers of studies were carried out to modify the substrates by adding fruit juices to enhance the biological activities and improve the flavor profile (Akbarirad et al., 2017; Yavari et al., 2018). Tropical fruit juices are rich in phenolic compounds and have the potential to increase the phenolic compound content and biological activities of fruit-based kombucha. In a recent study, snake fruit juice kombucha was fermented for 14 days and demonstrated high antidiabetic activity as determined in an *in vivo* study (Zubaidah et al., 2019). In another study, apple juice [150 ml/l (*v*/*v*)] was added to black tea to produce fruit-based kombucha, and the result was a significantly higher total phenol content compared to the control kombucha without apple juice (Liamkaew et al., 2016). Watawana et al. (2015) observed enhanced antioxidant activity and phenolic content for a coffee beverage fermented using kombucha SCOBY. In another study, kombucha SCOBY significantly enhanced the antioxidant activity of coconut water fermented for 7 days (Watawana et al., 2016). Soursop (*Annona muricata* L.) is an exotic tropical fruit that is found abundantly in the Southeast Asia region (Pinto et al., 2005). Soursop fruit is aromatic and juicy and has white flesh, creamy texture, pleasant characteristic, and sour taste (Lutchmedial et al., 2004). Soursop fruit was reported as a rich source of bioactive compounds such as acetogenins, alkaloids, and phenolic compounds (George et al., 2015). Ho et al. (2020) produced an alcoholic beverage with strong antioxidant activity using soursop juice and a combination of two starter culture including mushroom (*Pleurotus pulmonarius*) and yeast (*Saccharomyces cerevisiae*).

According to Villarreal-Soto et al. (2019), fermentation process conditions have a significant impact on the bioactive compounds in kombucha in relation to their biological activities. Thus, the optimization of fermentation conditions is very critical to produce kombucha that is rich in bioactive metabolites. In addition, the storage conditions including time, light, and duration can have a significant impact on the quality, metabolites, and the biological activities of kombucha. To the best of the authors' knowledge, no studies were carried out to optimize the production of soursop kombucha and determine the effects of storage conditions on the final product. Therefore, the aim of this was to optimize the production of soursop kombucha and determine the effects of different storage conditions including temperature, light, and time on the quality, metabolites, and biological activities of soursop kombucha.

MATERIALS AND METHODS

Materials

Fresh and ripen soursop (*Annona muricata* L.) fruits were purchased from NSK Trade City in Selayang, Selangor. The kombucha starter culture was obtained from the Food Bioprocessing Laboratory, Faculty of Food Science and Technology, Universiti Putra Malaysia (UPM). Table refined sugar of food grade was purchased from *Gula Prai*, Malayan Sugar Manufacturing Co. Berhad, Malaysia, and black tea from BOH, Malaysia.

Sample Preparation

The soursop fruits were washed under running tap water, peeled, deseeded, and cut into small size cubes. The fruits (500 g) were mixed (1:1, *w*/*w*) with water using a blender (Kenwood, England) (Abbo et al., 2006). Black tea was prepared by adding 5 g of tea leaves in 1 l of boiling water and infused for 5 min. The soursop juice was pasteurized at 65°C for 30 min. The fruit and tea were mixed at different concentrations including 300:700, 500:500, and 700:300 ml (*v*/*v*). The mixtures were added into sterile glass jar and sugar was added at different concentrations including 50, 100, and 150 g/l (*w*/*v*). The sugared mixtures were inoculated with kombucha starter [1:10 (*w*/*w*)] and incubated for 7, 14, and 21 days at 28 ± 2°C. Samples of the soursop kombucha were collected at days 7, 14, and 21 to conduct analysis following a previous method (Zubaidah et al., 2018). The optimum condition for the production of soursop kombucha was based on parameters such as antioxidant activity [2,2-diphenyl-1-picrylhydrazyl (DPPH) and ferric reducing antioxidant power (FRAP)], antimicrobial activity (*Escherichia coli* and *Staphylococcus aureus*), and microbiological analysis [total plate count, yeast and mold, and availability of lactic acid bacteria (LAB)]. Optimized soursop kombucha was chosen for the storage study to determine the effects of temperature (4 and 25°C) and dark and light conditions on the physiochemical properties, metabolites, and biological activity of soursop kombucha. Samples were collected at days 7, 14, and 21 to carry out the different analyses. The samples were prepared in triplicate and subjected to freeze drying for 48 h (LaboGene, Denmark).

Physicochemical Properties

The pH was measured by a calibrated electric pH meter (JENWAY 3505, Essex, England). The total soluble solids (TSS) were measured using a refractometer (Atago N1, Tokyo, Japan).

Proton Nuclear Magnetic Resonance Metabolomics Analysis

The soursop kombucha freeze-dried samples (10 mg) were mixed with 0.375 ml of methanol-D4 and 0.375 ml of KH_2PO_4 buffer in D_2O (pH 6.0) containing 1% TSP as internal standard for relative quantification of the identified metabolites. The mixture was vortexed for 1 min and sonicated at 30°C for 15 min in an ultra-sonicator (Branson, United States). The solution was centrifuged at 13,000 rpm for 10 min, and 600 μl of

supernatant was transferred to a nuclear magnetic resonance tube for proton nuclear magnetic resonance (^{1}H-NMR) analysis (Muhialdin et al., 2020b). Spectra were recorded at 25°C with frequency of 500 MHz on a Varian Unity INOVA 500 MHz Spectrometer (Varian Inc., CA). Each sample was subjected to 64 scans and recorded with an acquisition time of 193 s, with a pulse width of 10 ppm and a relaxation delay of 1 s. The spectra were automatically phased and bucketed using Chenomx software, with standard bins of δ 0.05 ranging from region δ 0.50 to 10.00. The analysis was required to remove residual methanol region (δ 3.28–3.33) and water region (δ 4.70–4.96). Two-dimensional ^{1}H–^{1}H J-resolved and was employed to identify metabolites. Partial least square analysis (PLS) and principal component analysis (PCA) were performed using SIMCA-P software (Umetrics AB, Umeå, Sweden).

Free Radical Scavenging (DPPH) Assay

The free radical scavenging activity of soursop kombucha was evaluated by DPPH assay following the method done by Chu and Chen (2006). The soursop kombucha (25 μl) was mixed with 225 μl of 1 mmol/l DPPH solution in 96-well micro-titter plates and incubated in the dark at room temperature for 30 min before proceeding to the measurement of absorbance at 517 nm using a spectrophotometer (Shimadzu, UVmini-1240, Tokyo, Japan). The control was water and DPPH solution. The scavenging capacity of soursop kombucha was calculated as follows:

$$\text{Scanvenging activity (\%)} = \frac{A_{\text{control}} - A_{\text{sample}}}{A_{\text{control}}} \times 100(1) \quad (1)$$

whereas A_{blank} was the control reading and A_{sample} was the sample reading.

Ferric Reducing Antioxidant Power Assay

The antioxidant activity was measured by FRAP assay described by Benzie and Szeto (1999). FRAP reagent was prepared by mixing acetate buffer (300 mmol/l, pH 3.6), a solution of 10 μM 2,4,6-tripyridyl-s-triazine (TPTZ) in 40 mmol/l HCl, and 20 mmol/l $FeCl_3$ at 10:1:1 (*v*/*v*/*v*). The reagent (300 μl) and kombucha (10 μl) were mixed thoroughly in 96-well micro-titter plates and incubated in dark condition for 30 min, and the absorbance was measured at 593 nm using a spectrophotometer (Shimadzu, UVmini-1240, Tokyo, Japan). The standard curve was prepared by ferrous sulfate solution ($FeSO_4{\cdot}7H_2O$) with the range of concentration from 0.1 to 1.0 mmol/l. The FRAP reading was expressed as mmol Fe(II)/ml.

Total Phenolic Content (TPC)

The TPC of soursop kombucha was measured following a previous method (Chu and Chen, 2006). Fermented soursop kombucha (0.05 ml) was mixed to 2 ml of 2% sodium carbonate and kept for 2 min. Folin–Ciocalteu reagent (0.1 ml) was then mixed with the solution and incubated for 30 min in the dark, and the absorbance was measured at 750 nm using a spectrophotometer (Shimadzu, UVmini-1240, Tokyo, Japan). The standard curve was plotted using gallic acid with the concentration range of 0–100 mmol/l, and TPC-value was expressed as μg GAE/ml (Muhialdin et al., 2019).

Microbial Growth Inhibition

The antimicrobial activity of soursop kombucha samples was evaluated against pathogenic bacteria including *Escherichia coli* 0157:H7 and *Staphylococcus aureus* ATCC6538 using the microtiter plate assay (Muhialdin et al., 2020b). The sample (100 μl) was pipetted into the wells of microtiter plates and mixed with 100 μl of nutrient broth containing 10^6 CFU/ml. The nutrient broth (200 μl) containing the tested bacteria was pipetted into the wells of microtiter plates as control. The plates were incubated at 37°C for 24 h. The growth of inhibition of targeted bacteria was measured at OD_{600} using the BioTek EL × 800 ELISA reader. The percentage growth of *E. coli* and *S. aureus* was calculated according to the following formula:

$$\text{inhibition\%} = \frac{(\text{24h negative control} - \text{24h negative control}) - (\text{24h sample} - \text{0h sample})}{\text{0h negative conrtrol}} \times 100 \quad (2)$$

Microbial Load Evaluation

Total plate counts of the soursop kombucha samples were done using the standard plate count procedure according to the Bacteriological Analytical Manual-Food and Drug Administration (BAM-FDA) protocol (Maturin and Peeler, 2001). Briefly, 1 ml of the samples was mixed with 9 ml of sterile 0.1% peptone water (10^{-1} dilution) followed by serial dilutions 10^{-2}–10^{-6}. A total of 100 μl of each dilution was inoculated into Plate Count Agar (PCA) (Merck, United States) and spread evenly using a sterile plate spreader. The agar dishes were incubated at 37°C for 24 h and then the colonies were counted and reported as colony-forming units/ml (CFU/ml).

Yeast and mold counts of the kombucha samples were done using the standard plate count procedure according to the BAM-FDA protocol (Maturin and Peeler, 2001) following the previous procedure: 100 μl of each dilution was inoculated into Malt Extract Agar (Oxoid) and spread evenly using a sterile plate spreader. The Petri dishes were incubated at 30°C for 72 h and then the colonies of yeast and mold were counted and reported as colony-forming units/ml (CFU/ml).

LAB count in the soursop kombucha samples was done following the standard according to the BAM-FDA protocol (Maturin and Peeler, 2001). Each dilution (100 μl) was inoculated into Petri dishes with De Man, Rogosa, and Sharpe (MRS) agar (Merck, United Kingdom) and spread evenly using a sterile plate spreader. The Petri dishes were incubated upside down at 37°C for 48 h in anaerobic jar, and the colonies were counted and reported as colony-forming units/ml (CFU/ml).

Data Processing and One-Way Analysis of Variance Data Analysis

The data was analyzed using Minitab version 17 (Minitab, Inc., United States). The statistical differences between the samples and controls were evaluated by one-way analysis of variance (ANOVA) with Tukey's multiple comparison to identify significant differences ($P < 0.05$) among means for all samples. Results were shown as the mean of three triplicates ± SD.

RESULTS AND DISCUSSION

Optimization of Soursop Kombucha Production

The response surface method (RSM) was carried out for 15 run orders, and the response was based on the microbial growth inhibition percentage against *Escherichia coli* and *Staphylococcus aureus*, DPPH, and FRAP for the different soursop kombuchas at different concentrations of fruit and sugar and storage time (**Table 1**). The predicted optimized conditions for soursop kombucha fermentation were found to be 300 ml soursop juice, 700 ml black tea, and 150 g sugar and 14 days fermentation at 28°C (**Figure 1**). The predicted conditions were validated, and no significant differences were observed between the actual and predicted conditions. The optimum conditions were applied to prepare the samples for the effect of storage study.

^{1}H-NMR Identification for Metabolites Changes

The sucrose concentration was significantly ($P < 0.05$) reduced from day 7 until day 21 of storage at different conditions (**Table 2**). In comparison, fructose and glucose concentrations significantly increased in correlation with the storage time. The observed fructose and glucose changes were due to the breakdown of sucrose by the bacteria and yeasts in the soursop kombucha into monosaccharides. Villarreal-soto et al. (2018) reported that sucrose is hydrolyzed into glucose and fructose during the fermentation due to the enzymatic activity of different microorganisms including yeast and bacteria. The hydrolysis is catalyzed by the enzyme invertase secreted from yeasts and bacteria into the fermentation substrates (Rasu Jayabalan et al., 2014). However, fructose concentration was significantly lower compared to glucose at all the storage conditions (**Table 2**). The difference is may be due to the preference of the yeast cells to rapidly utilize fructose as source of energy (Neffe-skocińska et al., 2017). In this study, the sugar concentration changes are mainly due to the activity of the soursop kombucha microorganisms that originated from the SCOBY that was used for the fermentation process (Leal et al., 2018).

On the other hand, acetic acid, malic acid, and gluconic acid were all present in soursop kombucha (**Table 2**). A previous study reported that the chemical compositions in kombucha include organic acids such as acetic acid, malic acid, and gluconic acid (Ramachandran et al., 2006). Acetic acid in soursop kombucha samples increased from days 7 to 21 for samples stored under room temperature. The increased content is due to the presence of *Acetobacter* bacteria in the soursop kombucha samples that produce acetic acid. Acetic acid bacteria are the dominant aerobic microorganisms in kombucha that utilize alcohol as substrate to produce acetic acid. In the presence of oxygen, acetic acid bacteria have the ability to keep producing acetic acid in the soursop kombucha beverage (Villarreal-soto et al., 2018). Cvetković et al. (2008) reported that acetic acid bacteria function to produce a new cellulose layer and metabolize ethanol to produce organic acids. Acetaldehyde is converted into ethanol, whereas acetaldehyde hydrate is being converted into acetic acid facilitated by the enzyme acetaldehyde dehydrogenase (Jayabalan et al., 2007). On the other hand, malic acid content was stable in all soursop kombucha along the storage period at different conditions. Malic acid is one

TABLE 1 | Response surface methodology (RSM) of soursop kombucha at different concentrations of fruit and sugar and fermentation times.

Nos.	Fruit (%)	Sugar (%)	Time (days)	*E. coli* inhibition (%)	*S. aureus* inhibition (%)	DPPH (%)	FRAP [mmol Fe(II)/mL]
1	70	10	7	0	0	63.92	358.03
2	50	15	7	0	0	66.11	355.11
3	30	15	14	68.8	69.74	68.68	372.75
4	70	15	14	0	0	60.32	357.05
5	50	10	14	82.09	79.38	72.86	352.05
6	30	5	14	77.14	74.85	77.04	344.83
7	50	5	7	78.52	78.13	67.35	349.97
8	70	5	14	0	0	64.33	348.72
9	30	10	21	0	78.8	77.91	358.02
10	50	5	21	0	0	69.05	384.41
11	70	10	21	0	0	71.65	352.75
12	50	15	21	0	0	74.79	337.05
13	50	10	14	0	0	70.87	344.41
14	30	10	7	75.44	70.52	81.05	373.02
15	50	10	14	50.08	60.78	80.7	357.33

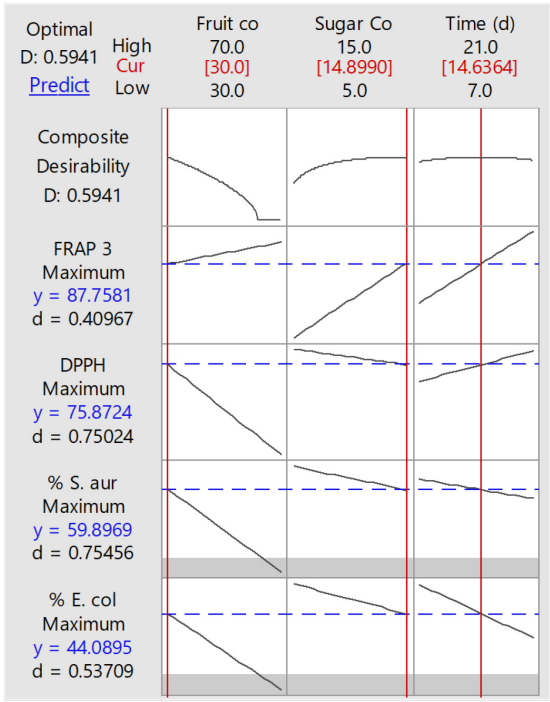

FIGURE 1 | Response surface methodology (RSM) results of optimized conditions to produce soursop kombucha.

of the dominant organic acids that can be found commonly in kombucha (Jayabalan et al., 2007). In addition, gluconic acid concentration decreased in correlation to the storage period from 0 h to day 21. Gluconic acid is produced by *Gluconobacter* bacteria which prefer the utilization of glucose during fermentation (Rasu Jayabalan et al., 2014). In another study, *Komagataeibacter xylinus* was reported as the dominant species in *Acetobacter* that acts to oxidize glucose to gluconic acid (Villarreal-soto et al., 2018). Gluconic acid is one of the healthy promoting metabolites found in kombucha made up of sucrose and black tea under optimized fermenting conditions (Chen and Liu, 2000; Malbaša et al., 2002; Jayabalan et al., 2007). Gluconic acid is converted to 2-ketogluconate and finally to 2,5-diketogluconic acid during oxidation by gluconic acid dehydrogenase and 2-ketogluconate dehydrogenase enzymes, respectively (Ramachandran et al., 2006).

The ethanol concentration in soursop kombucha samples gradually declined from 0 h until day 21 (**Table 2**). The sample at 0 h showed the highest ethanol concentration of 3.284 mmol/l, whereas the sample 21RD stored for 21 days at room temperature in the dark showed the lowest ethanol concentration (0.062 mmol/l) (**Figure 2**). Ethanol is produced by the yeast in kombucha from the sugar substrates via the glycolysis pathway, as sucrose is hydrolyzed into glucose and fructose and catalyzed by an enzyme secreted by yeasts. Ethanol produced during the fermentation process can be converted into acetic acid by acetic acid bacteria (Villarreal-soto et al., 2018). Acetic acid bacteria will then reduce the ethanol concentration via utilizing ethanol as source of carbon (Battikh et al., 2012). The observed reduction in the ethanol content indicated that different storage conditions can improve the quality of soursop kombucha for the concerned religious consumers. Beverages containing high ethanol concentrations are called non-Halal according to the Islamic regulations, as ethanol is limited to less than 1% (Alzeer and Abou Hadeed, 2016). The best storage conditions to decrease ethanol were 21 days, room temperature, and in dark storage. These storage conditions are recommended in this study to reduce ethanol content for Muslim consumers.

Antioxidant Activities

Bioactive compounds present in fermented foods and beverages have the key role for the antioxidant activity. The soursop

TABLE 2 | The effect of different storage conditions on the major metabolite changes of soursop kombucha samples and their concentration (mmol/l) as determined using ^{1}H-NMR metabolomics-based analysis.

Sample	Sucrose δ 5.40 (d)	Fructose δ 3.823 (m)	Glucose δ 4.58 (d)	Acetic acid δ 1.98 (s)	Malic acid δ 2.7 (d)	Gluconic acid δ 4.18 (d)	Ethanol δ 1.17 (t)
Control (0 h)	11.51	21.01	4.60	0.33	0.13	6.59	3.28
7RL	1.01	13.39	13.05	0.15	0.12	1.11	1.02
7RD	1.12	13.67	17.21	0.11	0.12	1.00	1.00
7CL	1.06	13.77	16.19	0.16	0.10	1.13	1.04
7CD	1.16	13.90	18.70	0.22	0.12	1.13	1.02
14RL	0.81	14.43	19.65	0.23	0.12	0.90	1.07
14RD	0.81	18.12	20.61	0.34	0.13	1.03	1.95
14CL	1.00	16.37	20.62	0.18	0.12	1.19	0.45
14CD	1.05	17.04	20.47	0.23	0.13	1.17	0.67
21RL	0.54	16.29	25.92	0.64	0.11	0.66	0.14
21RD	0.19	15.86	25.56	0.63	0.11	0.28	0.06
21CL	0.01	15.31	24.41	0.07	0.12	0.70	0.37
21CD	0.01	15.15	23.07	0.07	0.11	0.71	0.26

7, 14, and 21 days are storage times.R, room temperature; C, chilled temperature; L, light condition; D, dark condition.

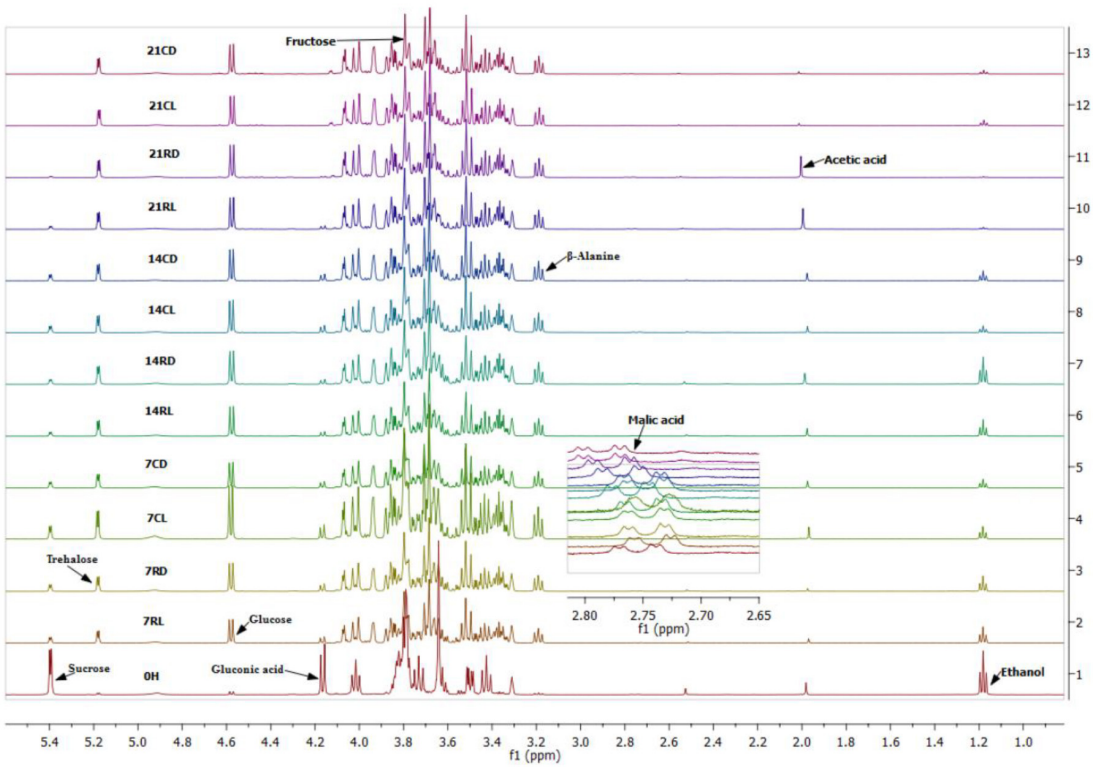

FIGURE 2 | Proton nuclear magnetic resonance (^{1}H-NMR) spectra of soursop kombucha at different storage conditions. Full spectra of δ 1.0–5.5 ppm. Identified ^{1}H-NMR signals: sucrose, fructose, glucose, acetic acid, malic acid, gluconic acid, and ethanol. 7, 14, and 21 days are storage times. R, room temperature; C, chilled temperature; L, light condition; D dark condition.

TABLE 3 | The antioxidant activity measured using DPPH, FRAP, and TPC assays of soursop kombucha during the storage at different conditions.

Sample	DPPH (%)	FRAP [mmol Fe(II)/ml]	TPC (μg GAE/mL)
7RL	89.12 ± 0.04^{ab}	430.25 ± 0.02^{a}	39.55 ± 0.25^{bc}
7RD	88.46 ± 0.04^{ab}	424.56 ± 0.01^{a}	41.99 ± 0.12^{abc}
7CL	87.56 ± 0.03^{ab}	410.67 ± 0.01^{a}	46.94 ± 0.07^{a}
7CD	89.22 ± 0.03^{ab}	414.83 ± 0.01^{a}	46.96 ± 0.07^{a}
14RL	90.76 ± 0.01^{a}	429.83 ± 0.01^{a}	37.90 ± 0.07^{c}
14RD	88.98 ± 0.01^{ab}	425.11 ± 0.02^{a}	37.97 ± 0.08^{c}
14CL	88.88 ± 0.02^{ab}	419.00 ± 0.01^{a}	39.14 ± 0.06^{bc}
14CD	87.98 ± 0.03^{ab}	434.69 ± 0.00^{a}	38.81 ± 0.10^{c}
21RL	86.12 ± 0.02^{ab}	422.89 ± 0.00^{a}	42.21 ± 0.11^{abc}
21RD	85.71 ± 0.02^{b}	420.67 ± 0.01^{a}	43.07 ± 0.15^{abc}
21CL	87.15 ± 0.02^{ab}	419.14 ± 0.01^{a}	41.69 ± 0.13^{abc}
21CD	86.02 ± 0.03^{ab}	432.80 ± 0.04^{a}	45.56 ± 0.13^{ab}

Data are expressed as mean ± SD of three replicates (n = 4). Means with different superscript letters in columns show significant difference using Tukey's test ($P < 0.05$) for different storage conditions. 7, 14, and 21 days are storage times.R, room temperature; C, chilled temperature; L, light condition; D, dark condition.

kombucha exhibited good antioxidant activity at all the storage conditions for days 7, 14, and 21 (**Table 3**). The scavenging ability of DPPH for soursop kombucha declined in the following order: 14RL > 7CD > 7RL > 14RD > 14CL > 7RD > 14CD > 7CL > 21CL > 21RL > 21CD > 21RD. Soursop kombucha stored for 14 days at room temperature and exposed to light conditions (14RL) exhibited the highest antioxidant activity (90.76%), while 21 days at room temperature and dark conditions (21RD) showed the lowest antioxidant activity (85.71%). The results did not show any significant differences in DPPH radical scavenging assay ($P \geq 0.05$). The DPPH inhibition percentage was 90% and above which indicates high antioxidant activity exhibited by soursop kombucha at all the storage conditions. The SCOBY plays an important role in affecting the composition of the produced kombucha due to the unique microflora present in different SCOBY (Chen and Liu, 2000). Another study reported

that the utilization of different SCOBY as starter in kombucha resulted in variable antioxidant activities (Malbaša et al., 2011). The findings of this study agree with the previous studies as modifying the conditions showed significant impact on the antioxidant activity.

The sample 14CD showed the highest FRAP-value of 434.69 μl GAE/ml, while 7CL has the lowest FRAP-value of 410.67 ± 0.013 mmol Fe(II)/ml (**Table 3**). The result showed that the prolonged storage has no significant effects on the FRAP-values ($P \geq 0.05$) (**Table 3**). However, the results revealed that all soursop kombuchas have high antioxidant properties as the results expressed high ferric reducing antioxidant power, with a range of 410.67–434.69 mmol Fe(II)/ml. The results of the FRAP assay are based on reducing Fe^{3+} in ferric-tripyridyltriazine to Fe^{2+}, and it is commonly used to evaluate antioxidant activity (Kim et al., 2013). A previous study reported that the lipophilic antioxidant is the main antioxidant compounds in soursop pulp with hydrogen donation as the mechanism of action (Gordillo et al., 2012). The strong antioxidant activity may be a result of the bioactive metabolites from soursop juice that contributed to the antioxidant property of soursop kombucha. The results showed that the soursop kombucha stored at different conditions had different TPC concentrations. In comparison to all samples, TPC in sample 7CD was the highest measuring at 46.96 μg GAE/ml. There was only a slight difference observed between the samples. The result showed no significant changes in the TPC ($P \geq 0.05$). Phenolic compounds perform antioxidant activity and are recognized for their function in reducing free radical activity and oxidative stress. Yeasts and bacteria in SCOBY produce an enzyme that acts in the conversion of polyphenolic complex into simpler phenolic components. The increased phenol content could be due to biotransformation that modifies a specific functional group into composing substances facilitated by enzymes. Enzymes are used in biotransformation to escalate specific biological activities (Srihari and Satyanarayana, 2012). Bhanja et al. (2009) reported phenol as one of the organic compounds that has a strong correlation to the antioxidant activity: the greater the amount of phenols being produced during fermentation as metabolites, the greater is the antioxidant activity. In a previous study, prolonged fermentation periods increased the TPC and antioxidant activity with no effects on the pH-value and the sensory characteristics (Muhialdin et al., 2019).

Antimicrobial Activity

The highest percentages of microbial growth inhibition against *E. coli* and *S. aureus* were 99.83 and 100.00% (**Table 4**). The results showed that storage conditions have no significant ($P \geq 0.05$) effects on the antimicrobial activity of soursop kombucha. The results indicated the stability of the strong antimicrobial activity of soursop kombucha at prolonged storage due to the presence of organic acids (Muhialdin et al., 2020a). In a previous study, kombucha demonstrated antibacterial activity toward a broad range of pathogens due to the presence of organic acids (Greenwalt et al., 1998). The results of this study showed similar findings as acetic acid was found at high concentrations in the soursop kombucha. Acetic acid has the ability to penetrate into gram-positive bacteria cells more easily than gram-negative bacteria due to its lipophilic characteristics (Naidu, 2000). Protons are released when acetic acid undergoes disassociation, and this causes the increment in acidity. The cell membrane function of targeted bacteria will be disrupted once the contact is established with the protons. Acetic acid denatures enzyme activity and disrupts the permeability of the cell membrane. Acetic acid in soursop kombucha is therefore affecting the antimicrobial activity of this fermented beverage. Dufresne and Farnworth (2000) observed that ethanol and acetic acid contents inhibit the growth of pathogens and are related with antimicrobial activity in their study. In another study, the antimicrobial activity of kombucha was reported against *Candida* spp. as compared with the common black tea that showed low antimicrobial activity (Battikh et al., 2012).

TABLE 4 | The effects of different storage conditions on the antimicrobial activity of soursop kombucha toward *Escherichia coli* and *Staphylococcus aureus* expressed as growth inhibition percentage.

	Microbial growth inhibition (%)	
Samples	***Escherichia coli***	***Staphylococcus aureus***
7RL	99.83 ± 0.00^{a}	98.41 ± 0.00^{f}
7RD	99.57 ± 0.00^{a}	98.14 ± 0.00^{de}
7CL	99.65 ± 0.00^{a}	98.76 ± 0.00^{a}
7CD	99.91 ± 0.00^{a}	99.56 ± 0.00^{bc}
14RL	98.96 ± 0.03^{a}	99.65 ± 0.02^{bc}
14RD	99.57 ± 0.00^{a}	98.58 ± 0.00^{ef}
14CL	95.66 ± 0.00^{a}	100.00 ± 0.00^{a}
14CD	99.74 ± 0.00^{a}	98.58 ± 0.00^{def}
21RL	99.13 ± 0.00^{a}	98.14 ± 0.00^{bc}
21RD	99.57 ± 0.00^{a}	98.50 ± 0.00^{b}
21CL	99.13 ± 0.00^{a}	97.70 ± 0.00^{b}
21CD	98.78 ± 0.010^{a}	97.70 ± 0.001^{b}

Data are expressed as mean ± SD of three replicates (n = 4). Means with different superscript letters in columns show significant difference using Tukey's test ($P < 0.05$) for different storage conditions. 7, 14, and 21 days are storage periods.R, room temperature; C, chilled temperature; L, light condition; D, dark condition.

Microbiological Analysis

The microbial load for soursop kombucha was determined for the total plate count, yeast, and LAB counts (**Table 5**). The results showed that all microorganisms were decreasing during the 21 days of storage for all the conditions. According to Fifteenth schedule, Regulation 39 on the Microbiological Standard in Food Regulation 1985, the maximum level of total plate count has to be at or less than 10^5/ml for ready-to-eat foods and beverages. The results showed that the aerobic bacteria count significantly declined from 7 (2.98×10^6 CFU/ml) to 21 days (2.80×10^4 CFU/ml). The result indicated that prolonged storage can enhance the safety of the soursop kombucha. The microbial load declined to 10^5 after storage for 14 days which is highly safe for the consumers. The reduction of the aerobic bacteria could be due to the high acidic environment and the depletion of the nutrients. Watawana et al. (2015) reported that the increased acidity during storage of fermented beverages reduces oxygen content and the number of aerobic bacteria viable cells. The

TABLE 5 | The effect of different storage conditions on the microbiological load in the soursop kombucha.

Soursop kombucha	Total plate count (CFU/ml)	Yeast count (CFU/ml)	Lactic acid bacteria count (CFU/ml)
7RL	2.24×10^6	2.91×10^5	1.39×10^6
7RD	2.98×10^6	2.04×10^6	2.12×10^6
7CL	2.61×10^5	9.80×10^5	4.00×10^5
7CD	2.90×10^5	9.10×10^5	2.20×10^5
14RL	1.35×10^5	4.10×10^5	2.90×10^5
14RD	1.18×10^5	1.50×10^5	1.20×10^5
14CL	1.30×10^5	1.20×10^5	2.40×10^5
14CD	2.95×10^5	3.60×10^5	4.60×10^5
21RL	2.80×10^4	3.70×10^4	3.40×10^4
21RD	7.20×10^4	1.63×10^5	1.03×10^5
21CL	9.30×10^4	6.30×10^4	3.70×10^4
21CD	1.20×10^5	1.59×10^5	1.59×10^5

Data are expressed as mean ± SD of three replicates (n = 4). Means with different superscript letters in columns show significant difference using Tukey's test ($P < 0.05$) for different storage conditions. 7, 14, and 21 days are storage times.R, room temperature; C, chilled temperature; L, light condition; D, dark condition; CFU, colony-forming unit.

results of this study agreed with the previous study, and the pH of the soursop kombucha declined during the prolonged storage. The count for yeast was decreasing during the storage period, significantly for the samples exposed to light at room temperature for 21 days storage (**Table 5**). The reduction in yeast count could be due to the reduction in sugar concentration that is required for yeast growth and cell production. Abbo et al. (2006) reported that low sugar concentration, low pH, and storage at 28°C limited the growth of yeast in soursop juice. The effects of light exposure and storage temperature exhibited unexpected effects on the availability of LAB cells. The exposure to light significantly reduced the cell count for the LAB to 3.40×10^4 at room temperature and 3.70×10^4 at chilled temperature. According to Trisnawita et al. (2018), the storage condition at chilled temperature (4°C) showed no significant effects on the LAB cells after prolonged storage for 28 days. Thus, the availability of LAB significantly declined at 28°C for 28 days. In another study, a beverage containing LAB stored at 25°C showed significant reduction in the LAB cell count (Begum et al., 2015). The reduction of LAB cell count in beverages was attributed to several reasons including dehydration of cells, high water activity, low pH-value, and depletion of the nutrients in the substrate (Trisnawita et al., 2018). Nevertheless, the LAB cell count showed no strong interaction with storage temperature, but an interaction was observed for light exposure.

CONCLUSION

This is the first study to develop and optimize the production of soursop kombucha. The developed beverage showed strong antioxidant and antimicrobial activities and high phenolic content. The different storage conditions demonstrated slight effects on the biological activities and significant effects on the metabolites of the soursop kombucha. Sucrose was significantly declined and glucose was significantly increased. The storage of soursop kombucha for 21 days at room temperature in dark conditions degraded 98% of the ethanol content. The microbial load for aerobic and anaerobic bacteria and yeast showed significant decline and high interaction with light exposure. The results revealed that prolonged storage for 21 days has high potential to improve the quality and metabolite content for soursop kombucha. Moreover, storing soursop kombucha for 21 days at room temperature with dark conditions can significantly improve the Halal status for consumers with religious concerns and allergies to alcohols. Further study is highly recommended to determine the consumer preference and acceptability for commercialization of soursop kombucha.

DATA AVAILABILITY STATEMENT

The original contributions presented in the study are included in the article/supplementary material, further inquiries can be directed to the corresponding author/s.

AUTHOR CONTRIBUTIONS

WT performed the fermentation experiments, analyses, and statistics and wrote the manuscript. BM designed the experiments, performed NMR analysis, bioinformatics analysis, and reviewed the manuscript draft. AM supervised the project. All authors checked and approved the manuscript.

FUNDING

This work was supported by the Universiti Putra Malaysia within the framework of a Grant Putra (GP-IPS/2018/9620100).

ACKNOWLEDGMENTS

We would like to thank the Department of Food Technology, Faculty of Food Science and Technology, Universiti Putra Malaysia for their support and permission for using the research facilities.

REFERENCES

Abbo, M. S., Olurin, T. O., and Odeyemi, G. (2006). Studies on the storage stability of soursop (*Annona muricata* L.) juice. *Afr. J. Biotechnol.* 5, 1808–1812.

Akbarirad, H., Mazaheri Assadi, M., Pourahmad, R., and Mousavi Khaneghah, A. (2017). Employing of the different fruit juices substrates in vinegar kombucha preparation. *Curr. Nutr. Food Sci.* 13, 303–308. doi: 10.2174/1573401313666170214165641

Alzeer, J., and Abou Hadeed, K. (2016). Ethanol and its Halal status in food industries. *Trends Food Sci. Technol.* 58, 14–20. doi: 10.1016/j.tifs.2016.10.018

Barbosa, C. D., Baqueta, M. R., Santos, W. C. R., Gomes, D., Alvarenga, V. O., Teixeira, P., et al. (2020). Data fusion of UPLC data, NIR spectra and physicochemical parameters with chemometrics as an alternative to evaluating kombucha fermentation. *LWT Food Sci. Technol.* 133:109875. doi: 10.1016/j.lwt.2020.109875

Battikh, H., Bakhrouf, A., and Ammar, E. (2012). Antimicrobial effect of Kombucha analogues. *LWT Food Sci. Technol.* 47, 71–77. doi: 10.1016/j.lwt.2011.12.033

Begum, A. A., Jakaria, D. M., Anisuzzaman, S. M., Islam, M., and Mahmud, S. A. (2015). Market assessment and product evaluation of probiotic containing dietary supplements available in bangladesh market. *J. Pharm.* 2015:763796. doi: 10.1155/2015/763796

Bellut, K., Krogerus, K., and Arendt, E. K. (2020). *Lachancea fermentati* strains isolated from kombucha: fundamental insights, and practical application in low alcohol beer brewing. *Front. Microbiol.* 11:764. doi: 10.3389/fmicb.2020.00764

Benzie, I. F., and Szeto, Y. T. (1999). Total antioxidant capacity of teas by the ferric reducing/antioxidant power assay. *J. Agric. Food Chem.* 47, 633–636. doi: 10.1021/jf9807768

Bhanja, T., Kumari, A., and Banerjee, R. (2009). Enrichment of phenolics and free radical scavenging property of wheat koji prepared with two filamentous fungi. *Bioresour. Technol.* 100, 2861–2866. doi: 10.1016/j.biortech.2008.12.055

Chen, C., and Liu, B. Y. (2000). Changes in major components of tea fungus metabolites during prolonged fermentation. *J. Appl. Microbiol.* 89, 834–839. doi: 10.1046/j.1365-2672.2000.01188.x

Chu, S., and Chen, C. (2006). Effects of origins and fermentation time on the antioxidant activities of kombucha. *Food Chem.* 98, 502–507. doi: 10.1016/j.foodchem.2005.05.080

Cvetković, D., Sinisa, M., Djurić, M., Savic, D., and Velićanski, A. (2008). Specific interfacial area as a key variable in scaling-up Kombucha fermentation. *J. Food Eng.* 85, 387–392. doi: 10.1016/j.jfoodeng.2007.07.021

Dufresne, C., and Farnworth, E. (2000). Tea, Kombucha, and health: a review. *Food Res. Int.* 33, 409–421. doi: 10.1016/S0963-9969(00)00067-3

Gaggìa, F., Baffoni, L., Galiano, M., Nielsen, D. S., Jakobsen, R. R., Castro-Mejía, J. L., et al. (2019). Kombucha beverage from green, black and rooibos teas: a comparative study looking at microbiology, chemistry and antioxidant activity. *Nutrients* 11:1. doi: 10.3390/nu11010001

George, V. C., Kumar, D. N., Suresh, P. K., and Kumar, R. A. (2015). Antioxidant, DNA protective efficacy and HPLC analysis of Annona muricata (soursop) extracts. *J. Food Sci. Technol.* 52, 2328–2335. doi: 10.1007/s13197-014-1289-7

Gordillo, J. C., Ortiz, D., Larrahondo, J. E., Mejía, M. S., and Pachon, H. (2012). Actividad antioxidante en guanábana (Annona muricata l.): una revisión bibliográfica. *Boletin Latinoamericano y del Caribe de Plantas Medicinales y Aromáticas* 11, 111–126.

Greenwalt, C. J., Ledford, R. A., and Steinkraus, K. H. (1998). Determination and characterization of the antimicrobial activity of the fermented tea kombucha. *LWT Food Sci. Technol.* 31, 291–296. doi: 10.1006/fstl.1997.0354

Ho, C. W., Lazim, A., Fazry, S., Hussain Zaki, U. K. H., Massa, S., and Lim, S. J. (2020). Alcoholic fermentation of soursop (*Annona muricata*) juice via an alternative fermentation technique. *J. Sci. Food Agric.* 100, 1012–1021. doi: 10.1002/jsfa.10103

Ivanišová, E., Meńhartová, K., Terentjeva, M., Harangozo, L., Kćntor, A., and Kaèániová, M. (2019). The evaluation of chemical, antioxidant, antimicrobial and sensory properties of kombucha tea beverage. *J. Food Sci. Technol.* 57, 1840–1846. doi: 10.1007/s13197-019-04217-3

Jayabalan, R., Malbaša, R. V., Lončar, E. S., Vitas, J. S., and Sathishkumar, M. (2014). A review on kombucha tea—microbiology, composition, fermentation, beneficial effects, toxicity, and tea fungus. *Comprehensive Rev. Food Sci. Food Saf.* 13, 538–550. doi: 10.1111/1541-4337.12073

Jayabalan, R., Marimuthu, S., and Swaminathan, K. (2007). Changes in content of organic acids and tea polyphenols during kombucha tea fermentation. *Food Chem.* 102, 392–398. doi: 10.1016/j.foodchem.2006.05.032

Kim, J., Jung, Y., Song, B., Bong, Y. S., Ryu, D., Lee, K. S., et al. (2013). Discrimination of cabbage (*Brassica rapa* ssp pekinensis) cultivars grown in different geographical areas using H-1 NMR-based metabolomics. *Food Chem.* 137, 68–75. doi: 10.1016/j.foodchem.2012.10.012

Kulshrestha, S., Tyagi, P., Sindhi, V., and Yadavilli, K. S. (2013). Invertase and its applications–a brief review. *J. Pharm. Res.* 7, 792–797. doi: 10.1016/j.jopr.2013.07.014

Leal, J. M., Suárez, L. V., Jayabalan, R., Oros, H., and Escalante-aburto, A. (2018). A review on health benefits of kombucha nutritional compounds and metabolites. *CyTA J. Food* 16, 390–399. doi: 10.1080/19476337.2017.1410499

Liamkaew, R., Chattrawanit, J., and Danvirutai, P. (2016). Kombucha production by combinations of black tea and apple juice. *Sci. Technol. RMUTT J.* 6, 139–146.

Lutchmedial, M., Ramlal, R., Badrie, N., and Chang-Yen, I. (2004). Nutritional and sensory quality of stirred soursop (*Annona muricata* L.) yoghurt. *Int. J. Food Sci. Nutr.* 55, 407–414. doi: 10.1080/09637480400002800

Malbaša, R., Lončar, E., and Kolarov, L. (2002). L-lactic, L-ascorbic, total and volatile acids contents in dietetic kombucha beverage. *Roumanian Biotechnol. Lett.* 7, 891–895.

Malbaša, R., Lončar, E., Vitas, J., and Ćanadanović-Brunet, J. (2011). Influence of starter cultures on the antioxidant activity of kombucha beverage. *Food Chem.* 127, 1727–1731. doi: 10.1016/j.foodchem.2011.02.048

Maturin, L., and Peeler, J. T. (2001). *BAM: Aerobic Plate Count*. Dhule: Bacteriological Analytical Manual US Food and Drug Administration.

Muhialdin, B. J., Kadum, H., and Hussin, A. S. M. (2020a). Metabolomics profiling of fermented cantaloupe juice and the potential application to extend the shelf life of fresh cantaloupe juice for six months at 8° C. *Food Control* 2020:107555. doi: 10.1016/j.foodcont.2020.107555

Muhialdin, B. J., Kadum, H., Zarei, M., and Hussin, A. S. M. (2020b). Effects of metabolite changes during lacto-fermentation on the biological activity and consumer acceptability for dragon fruit juice. *LWT Food Sci. Technol.* 121:108992. doi: 10.1016/j.lwt.2019.108992

Muhialdin, B. J., Osman, F. A., Muhamad, R., Wan Sapawi, C. W. N. S. C., Anzian, A., Voon, W. W. Y., et al. (2019). Effects of sugar sources and fermentation time on the properties of tea fungus (kombucha) beverage. *Int. Food Res. J.* 26, 481–487.

Naidu, A. S. (ed.) (2000). *Natural Food Antimicrobial Systems*. Boca Raton, FL: CRC press.

Neffe-skocińska, K., Sionek, B., and ścibisz, I. (2017). Acid contents and the effect of fermentation condition of Kombucha tea beverages on physicochemical, microbiological and sensory properties. *CyTA J. Food* 15, 601–607. doi: 10.1080/19476337.2017.1321588

Pinto, A. D. Q., Cordeiro, M. C. R., De Andrade, S. R. M., Ferreira, F. R., Filgueiras, H. D. C., Alves, R. E., et al. (2005). Annona species. Embrapa Cerrados-Livro científico (ALICE).

Ramachandran, S., Fontanille, P., Pandey, A., and Larroche, C. (2006). Gluconic acid: properties, applications and microbial production. *Food Technol. Biotechnol.* 44, 185–195.

Srihari, T., and Satyanarayana, U. (2012). Changes in free radical scavenging activity of Kombucha during fermentation. *J. Pharm. Sci. Res.* 4, 1978–1981.

Teoh, A. L., Heard, G., and Cox, J. (2004). Yeast ecology of Kombucha fermentation. *Int. J. Food Microbiol.* 95, 119–126. doi: 10.1016/j.ijfoodmicro.2003.12.020

Trisnawita, Y., Silalahi, J., and Sinaga, S. M. (2018). The effect of storage condition on viability of lactic acid bacteria in probiotic product. *Asian J. Pharm. Clin. Res.* 11:84. doi: 10.22159/ajpcr.2018.v11s1.26574

Villarreal-soto, S. A., Beaufort, S., Bouajila, J., Souchard, J., and Taillandier, P. (2018). Understanding kombucha tea fermentation: a review. *J. Food Sci.* 83, 580–588. doi: 10.1111/1750-3841.14068

Villarreal-Soto, S. A., Beaufort, S., Bouajila, J., Souchard, J. P., Renard, T., Rollan, S., et al. (2019). Impact of fermentation conditions on the production of bioactive compounds with anticancer, anti-inflammatory and antioxidant properties in kombucha tea extracts. *Process Biochem.* 83, 44–54. doi: 10.1016/j.procbio.2019.05.004

Watawana, M. I., Jayawardena, N., Gunawardhana, C. B., and Waisundara, V. Y. (2016). Enhancement of the antioxidant and starch hydrolase inhibitory activities of king coconut water (*Cocos nucifera* var. aurantiaca) by fermentation with kombucha 'tea fungus'. *Int. J. Food Sci. Technol.* 51, 490–498. doi: 10.1111/ijfs.13006

Watawana, M. I., Jayawardena, N., and Waisundara, V. Y. (2015). Enhancement of the functional properties of coffee through fermentation by "tea fungus" (kombucha). *J. Food Process. Preserv.* 39, 2596–2603. doi: 10.1111/jfpp.12509

Yavari, N., Mazaheri-Assadi, M., Mazhari, Z. H., Moghadam, M. B., and Larijani, K. (2018). Glucuronic acid rich kombucha-fermented pomegranate juice. *J. Food Res.* 7, 61–69. doi: 10.5539/jfr.v7n1p61

Zubaidah, E., Ifadah, R. A., Kalsum, U., Lyrawati, D., Putri, W. D. R., Srianta, I., et al. (2019). Anti-diabetes activity of Kombucha prepared from different snake fruit cultivars. *Nutr. Food Sci.* 49, 333–343. doi: 10.1108/NFS-07-2018-0201

Zubaidah, E., Julian, F., Rizki, F., Srianta, I., and Blanc, P. J. (2018). Biocatalysis and agricultural biotechnology potential of snake fruit (*Salacca zalacca* (Gaerth.) Voss) for the development of a beverage through fermentation with the kombucha consortium. *Biocatal. Agric. Biotechnol.* 13, 198–203. doi: 10.1016/j.bcab.2017.12.012

Conflict of Interest: The authors declare that the research was conducted in the absence of any commercial or financial relationships that could be construed as a potential conflict of interest.

frontiers in Microbiology

ORIGINAL RESEARCH
published: 16 December 2020
doi: 10.3389/fmicb.2020.614208

Evaluation of the Effect of Auxiliary Starter Yeasts With Enzyme Activities on Kazak Cheese Quality and Flavor

Jing Xiao[1†], Yu Chen[2†], Jie Li[2], Xuewei Shi[2], Li Deng[2] and Bin Wang[2]*

[1] College of Information Science and Technology, Shihezi University, Shihezi, China, [2] Food College, Shihezi University, Shihezi, China

To investigate the effect of yeasts on Kazak cheese quality and flavor, three isolated yeasts (*Kluyveromyces marxianus* A2, *Pichia kudriavzevii* A11, and *Pichia fermentans* A19) were used to ferment cheeses and designated as StC, LhC, and WcC, respectively. The cheese fermented with a commercial lactic acid starter without adding yeast was used as control named LrC. The results showed that the texture of cheese added with yeasts were more brittle. *K. marxianus* A2 contributed to the formation of free amino acids and organic acids, especially glutamate and lactic acid. Moreover, *K. marxianus* A2 provides cheese with onion, oily, and floral aromas. Furthermore, *P. kudriavzevii* A11 promotes a strong brandy, herbaceous, and onion flavor. Although no significant aroma change was observed in PfC, it promoted the production of acetic acid, isoamyl acetate, and phenethyl acetate. These results indicate that yeasts are important auxiliary starters for cheese production.

Keywords: Kazak cheese, yeasts, physicochemical indicators, volatile compounds, flavor

OPEN ACCESS

Edited by:
Wanping Chen,
Georg-August-University Goettingen, Germany

Reviewed by:
Chen Chen,
Shanghai Institute of Technology, China
Huaxi Yi,
Ocean University of China, China
Xiuyan Zhang,
Huazhong Agricultural University, China

***Correspondence:**
Bin Wang
binwang0228@shzu.edu.cn

† These authors have contributed equally to this work

Specialty section:
This article was submitted to Food Microbiology, a section of the journal Frontiers in Microbiology

Received: *05 October 2020*
Accepted: *18 November 2020*
Published: *16 December 2020*

Citation:
Xiao J, Chen Y, Li J, Shi X, Deng L and Wang B (2020) Evaluation of the Effect of Auxiliary Starter Yeasts With Enzyme Activities on Kazak Cheese Quality and Flavor. Front. Microbiol. 11:614208. doi: 10.3389/fmicb.2020.614208

INTRODUCTION

Xinjiang is a multiethnic region in China. The Kazakhs, one of the primary minority nationalities in Xinjiang of China, produce Kazak cheeses with a unique craftsmanship (Zheng et al., 2018b). Kazak cheese is prepared from raw cow's milk without adding an exogenous lactic acid bacteria (LAB) starter during the traditional production process, which can be identified with several stages: boiling, milk fermentation in goatskin bags, dehydration, shaping, and after-ripening (Zheng et al., 2018b, 2020). Furthermore, milk is believed to contain a large number of microorganisms, such as *Lactococcus*, *Staphylococcus*, *Corynebacterium*, *Brevibacterium*, *Clostridiisalibacter*, *Saccharomyces*, *Trichosporon*, and *Kluyveromyces* (Sun et al., 2014; Ryssel et al., 2015). The process with diverse and dynamic conditions led to the diversity of microorganism types. Some microorganisms with probiotic characteristics are preserved in ripened Kazak cheese (Zheng et al., 2018a). In the Kazakh diet, cheeses act as an excellent carrier for viable probiotic microorganisms and provide high levels of vitamins, calcium, oligosaccharides, and iron, compared with yogurt, milk powder, and condensed milk.

Lactic acid bacteria, such as *Lactobacillus* and *Lactococcus*, are identified as the main bacterial genera in the cheese fermentation process (Gao et al., 2017). During Kazak cheese making, milk is spontaneously fermented in a goatskin bag at room temperature (approximately 30°C) for 15 days, producing a high concentration of lactic acid (Zheng et al., 2018b). The increased lactic acid promotes a low pH value. The casein micelles demineralize to coagulate when the pH reaches the

isoelectric point of casein (Fox et al., 2017; Kamimura et al., 2019). Recent studies have shown that except for LAB, a large number of yeasts also play an important role in cheese fermentation (Yuvaşen et al., 2018), such as *Pichia kudriavzevii*, *Kluyveromyces marxianus*, and *K. lactis* in Kazak artisanal cheese (Zheng et al., 2018a); *Yarrowia lipolytica*, *Debaryomyces hansenii*, and *P. fermentans* in artisanal short-ripened Galician cheeses (Atanassova et al., 2016); and *Torulaspora delbrueckii* and *Saccharomyces cerevisiae* in traditional Serbian cheeses (Zivkovic et al., 2015). It is believed that the LAB that become dominant during cheese fermentation originate from milk (Paxson, 2008), whereas yeasts are primarily derived from the storage environment and the fermentation process (Gonçalves Dos Santos et al., 2017). One study showed that *P. kudriavzevii*, *K. marxianus*, and *K. lactis*, which could provide a unique flavor to Kazak cheese, may originate from the environment, such as the milking, curd, storage, and ripening environment (Zheng et al., 2018b).

Yeasts exist in various fermented food because of their ability to adapt to low pH, high salt concentration, and low temperature storage conditions during milk fermentation (Chaveslopez et al., 2012). Besides, some yeasts can inhibit the growth of some enteric pathogens. For example, *K. lactis,* and *K. marxianus*, isolated from the Tomme d'orchie French cheese are able to inhibit the growth of *Listeria monocytogenes*, *Candida albicans*, and some *Bacillus* spp. (Ceugniez et al., 2015). During cheese fermentation, some yeasts, such as *D. hansenii*, *S. cerevisiae*, and *Y. lipolytica*, are beneficial to enhance the nutrition of cheese by releasing proteases, lipases, or β-galactosidases to convert proteins, lipids, and lactose of milk into small molecules (amino acids, fatty acids, and organic acids; Akpınar et al., 2011; Golić et al., 2013; Cardoso et al., 2015). Furthermore, *Y. lipolytica*, *K. lactis*, and *D. hansenii* also contribute to the formation of the texture and unique flavor of cheese by producing high concentrations of methyl ketone, butanoic acid, branched chain aldehydes, acetaldehyde, ethanol, and acetic acid esters (Atanassova et al., 2016; Juan et al., 2016). *K. lactis* also produce high levels of acetaldehyde, ethanol, branched chain aldehydes and alcohols, and acetic acid esters, which are the primary components of aroma and flavor in acid curd Cebreiro cheese (Atanassova et al., 2016).

Currently, flavors (Bergamaschi and Bittante, 2018), microorganisms (Yunita and Dodd, 2018; Yuvaşen et al., 2018), and their relationships (Bezerra et al., 2017; van Mastrigt et al., 2018) in cheese have become a research hotspot due to cheese providing excellent nutritional value with high digestibility and low allergenic potential (Bezerra et al., 2017). However, there is little research focusing on contribution of yeast to cheese flavors. In this study, to investigate the contribution of yeast to cheese flavor and quality, three yeasts, isolated from traditional Kazak cheese with protease, lipase, or β-galactosidase activity, were used to ferment cheese through co-fermentation with a commercial LAB starter. The physicochemical characteristics, free amino acids (FAAs), organic acids, texture, and volatile aromatic compounds in the ripened cheeses were investigated. The results will lay the theoretical foundation for the improvement of cheese flavor.

MATERIALS AND METHODS

Isolation and Identification of Yeasts in Kazak Cheese

A total of 28 mature Kazak cheese samples were collected from local ethnic minority farmhouses in Xinjiang: Mulei regions (5 cheese), Yili (5), Altay (5), Balikun (5), and Tacheng (8) and stored at 4°C before the separation operation. The isolation method of yeasts was conducted as described by Zheng et al. (2018b) with some modification. First, 5 *g* cheese and 50 ml of sterile 0.9% sodium chloride solution were mixed and then homogenized in a rotary shaker (ZWYR-C2402; Shanghai Zhicheng Co., Ltd., Shanghai, China) for 30 min at 28°C. After being serially diluted, 100 μl of the corresponding dilutions was added to YPD (1% yeast extract, 2% peptone, and 2% glucose, 2% agar) agar-solidified medium (in triplicate) and then placed in a 28°C incubator (LRH-70; Shanghai Yiheng Technology Co., Ltd., Shanghai, China) to cultivate for 24 h. Single colonies were purified and stored in YPD broth with 30% glycerol at −20°C. Strains were identified by comparing sequences in the GenBank database[1].

Screening of Yeasts With Protease, Lipase, or β-Galactosidase Activities

According to the method described by Ozturkoglu-Budak et al. (2016), strains with protease activity can produce opaque hydrolyzed circles on YPD agar medium containing 2% skim milk. Quantitative measurements of protease activity were based on the method described by Mageswari et al. (2017) with modifications. First, 100 μl cell-free supernatants were mixed with 100 μl of 1% casein, which was dissolved in a 50 mM borax–NaOH buffer solution (pH 10) and incubated at 40°C for 10 min. The reaction was stopped by adding 200 μl of 0.4 M trichloroacetic acid. A blank control sample was also prepared by adding trichloroacetic acid before adding the enzyme solution. The test and blank solution were then centrifuged at 8,000 rpm for 5 min, after which 100 μl of filtrate was mixed with 500 μl 0.4 M Na_2CO_3 solution and 100 μl Folin–Ciocalteu reagent, and incubated at 40°C for 20 min. Finally, the absorbance was measured at a wavelength of 680 nm, and the enzymatic activity was calculated based on a tyrosine standard curve.

Strains with lipase activity were screened by adding 10% tributyrin (Yuanye Biotechnology Co., Ltd., Shanghai, China) to YPD, where a transparent circle will form around colonies with lipase activity. The method described by Konkit and Kim (2016) was used to assess lipase activity with some adjustments. First, 4 ml 12% olive oil and 5 ml 25 mM phosphate buffer solution (pH 7.0) were added to an Erlenmeyer flask and incubated at 40°C for 10 min. Then, 1.0 ml enzyme solution was added to the above mixture followed by an incubation at 37°C for 15 min. Finally, 15 ml 95% ethanol was added to the above mixture, which was then thoroughly mixed. Lipase activity was determined by titration with 50 mM NaOH after adding 3 drops of phenolphthalein to each sample and blank solutions.

[1]https://blast.ncbi.nlm.nih.gov/blast.cgi

Strains with β-galactosidase activity were screened by adding 20 mg/ml 5-bromo-4-chloro-3-indolyl-β-D-galactopyranoside (Sangon Biological Technology Co., Ltd., Shanghai, China) to YPD agar plates, where colonies testing positive for β-galactosidase activity turned blue. Measurement of β-galactosidase activity was based on the method of Souza et al. (2018). Furthermore, 50 μl enzyme solution was added to 50 μl 20 mM *o*-nitrophenyl-β-D-galactopyranoside substrate solution (Sangon Biological Technology), and the mixture was then incubated for 10 min at 37°C in a water bath (HH-1 Digital Thermostatic Water Bath; Junteng Electronic Instrument Co., Ltd., Shandong, China). The reaction was stopped by adding 200 μl 0.5 M sodium carbonate solution. Phosphate buffer without the enzyme solution was used as a blank control. The absorbance of the solutions was measured at 420 nm in a microplate reader (UV-1750; Shimadzu Corporation, Kyoto, Japan).

Cheese Making and Sampling

A total of 120 L raw cow's milk (Garden Dairy Co., Ltd., Xinjiang, China) was pasteurized at 75°C for 15 s and divided into four 30-L vats to make four different cheeses after cooled to 35°C. All the batches were first mixed with 1×10^6 cfu/ml commercial LAB starter (Ci Enkang Biotechnology Co., Ltd., Jiangsu, China) for acidification. Then, *K. marxianus* A2 (file number in the GenBank database: MN985331.1), *P. fermentans* A19 (MN985333.1), and *P. kudriavzevii* A11 (MN985332.1) were added at a cell concentration of approximately 1×10^6 cfu/ml to co-ferment with the commercial LAB starter. Before being added to the batches, the three yeasts were activated in a sterile medium consisting of 12% reconstituted skim milk, then incubated at 28°C for pre-ripening with 48 h. A batch without added yeast was used as a control. Then, all the batches were stirred for 10 min at 35°C and curdled at this temperature for 2 h. The curd was cut into 5-mm pieces to discharge the whey, and then was filtered with gauze and pressed in a mold to further remove the whey. Finally, the cheese was immersed in a 2% (*w*/*v*) salt solution for 1 h, then cut into small pieces and dried at 25°C for 2 days. All the cheese samples were stored in sterile bags under the same conditions (25°C, 65 ± 1% relative humidity).

For physicochemical and microbiological analysis, the cheeses were removed aseptically, transferred to sterile bags, and stored under the same conditions (25°C, 65 ± 1% relative humidity). Volatile compound analysis was performed at 10-day intervals for 40 days, and the cheese samples were frozen at −80°C and wrapped in vacuum plastic pouches.

Physicochemical and Microbiological Analysis

The moisture of cheese was measured by direct drying in a laboratory oven at 105°C according to the Chinese national standard GB 5009.3-2016. Total protein was determined via the Kjeldahl method (follow the Chinese national standards GB 5009.5-2016) with Kjeldahl instruments (KjeIMaster K-375; BÜCHI Labortechnik AG, Switzerland). The determination of salt was performed with reference to the national standard GB 5009.42-2016. The pH was measured with a calibrated electronic digital pH meter (PHS-3C, Shanghai, China). The fat contents were determined by Soxhlet extraction following the Chinese national standard GB 5009.6-2016. Acidity was determined by the titration method according to the Chinese national standard GB 5413.34-2010. All samples were analyzed in triplicate.

Microbiological analysis was performed as Atanassova described with plate count method (Atanassova et al., 2016). Enumeration of the total viable microorganisms was performed on agar plates prepared with toxoid. LAB were cultured on MRS agar plates (peptone 10 g/L, beef powder 10 g/L, yeast extract 5 g/L, glucose 20 g/L, dipotassium hydrogen phosphate 2 g/L, diammonium hydrogen citrate 2 g/L, sodium acetate 5 g/L, magnesium sulfate 0.2 g/L, manganese sulfate 0.04 g/L, agar 14 g/L, and Tween 80 1 ml) containing natamycin and incubated at 35°C for 48 h under anaerobic conditions. Yeasts were enumerated on YPD medium containing 100 mg of chloramphenicol and after incubating at 28°C for 48 h.

Determination of Free Amino Acids

The FAA levels in cheese samples were measured according to the method of Zhou et al. (2018). First, 2 *g* cheeses and 10 ml 6 M hydrochloric acid solution were transferred to a hydrolysis tube, evacuated, sealed, and then hydrolyzed at 110°C for 24 h. The hydrolysate was filtered into a volumetric flask and brought to the appropriate volume with distilled water. Then, 2 ml of the hydrolysate was dried, dissolved with 2 ml sodium citrate buffer solution (pH 2.2), and then filtered through a 0.22-μm filter for analysis. The FAA contents were determined using a fully automatic amino acid analyzer (LBA800; Tianjin Rambo Co., Ltd., Tianjin, China; Niro et al., 2017). The total FAAs were identified and quantified based on the retention times and peak areas of a standard FAA mixture (Yuanye Biotechnology).

Determination of Organic Acids

To pretreat the sample according to Murtaza et al. (2017), 2 *g* cheese was mixed with 10 ml water and centrifuged. Then, the supernatant was transferred to a 50-ml volumetric flask and the cheese precipitate was repeatedly extracted to the same volumetric flask. After being brought to a constant volume with ethanol, 10 ml of the above solutions was transferred to a distillation flask and rotated at 80°C to dryness, with a second drying step performed after adding 5 ml of ethanol. Finally, the dried sample residue was dissolved in 1 ml phosphoric acid solution, then filtered through a 0.22-μm filter and assayed via HPLC.

Organic acids were determined according to Belguesmia et al. (2014). A high-performance liquid chromatography instrument (HPLC, Shimadzu LC-2010, Tokyo, Japan) equipped with a 5-μm 250 × 4.6 mm Spursil C18 (LC) column (Dima Technology Co., Ltd., Guangzhou, China.) was used. The UV detector was set at 210 nm and the column oven at 40°C. The mobile phase was methanol and 0.1% phosphoric acid, and the isocratic elution was performed at a volume ratio of 3:97 with a flow rate of 0.7 ml/min. The sample volume injected was 20 μl. Quantification of organic acid contents in the samples was carried out by generating calibration curves of external standards, including tartaric acid,

lactic acid, succinic acid, malic acid, and citric acid (Yuanye Biotechnology Co., Ltd., Shanghai, China).

Determination of Texture

Texture properties were measured using a TA texture analyzer (TA.XTPlus; Stable Micro System Co., United Kingdom) and a P/36R cylindrical probe (TA15/1000, 458 Å, 36 mm diameter) by reference to the method of Bekele et al. (2019). The test mode was TPA, the compression rate was 5 mm/s, the test speed was 1 mm/s, the speed after test was 5 mm/s, the trigger force was 5 *g*, the interval between measurements was 5 s, the deformation of the samples was 50%, and two consecutive determinations were performed for each sample. Before the test, the cheese was removed from the refrigerator at 4°C and equilibrated for 1 h at room temperature, and were then cut into 2-cm pieces for measurement. The calculation of texture properties was based on the method described by Rehman et al. (2018).

Determination of Volatile Aromatic Compounds

The volatile profiles of the cheeses were determined by headspace-solid phase microextraction gas chromatography–mass spectrometry (HS-SPME/GC–MS) according to the method of Ocak et al. (2015). First, 2 *g* cracked cheese was added to a 15-ml headspace vial with a PTFE silicone lined magnetic cap and 1 μl 40 μg/kg 2-octanol was used as an internal control. Volatile aromatic compounds were extracted with an aging DVB/CAR/PDMS fiber (50/30 μm; Agilent Technologies, Palo Alto, CA, United States). The SPME fiber was first desorbed for 5 min in the injection port at 230°C before use to reduce the carryover from the previous analysis, after which the SPME needle was introduced into the septum in the vial cap, and the fibers were exposed to the headspace for 40 min at 40°C to extract volatile compounds (Li et al., 2020; Zheng et al., 2020).

Analyses were performed with a gas chromatography system (Agilent 7890B; Agilent Technologies) consisting of an HP Innowax column (60 m × 0.25 mm × 0.25 μm). The following oven temperature program was used: 50°C maintained for 3 min and then increased at a rate of 2°C/min to 100°C maintaining for 25 min, and finally an increase at 10°C/min to 230°C maintaining for 3 min. Helium was used as carrier gas at a flow rate of 1 ml/min, and the electron impact mode was set at 70 eV. Identification was based on comparing the retention time (RT) with those published in the National Institute of Standards and Technology (NIST, https://webbook.nist.gov) mass spectral library, where only compounds with a matching score ≥ 800 were retrieved and recorded (Panseri et al., 2014). Retention index (RI) of each compound was calculated with the retention time according to using a series of *n*-alkanes (C_8–C_{40}). Moreover, calculated RI was matched with a reference value according to NIST database (Panseri et al., 2014; Xu et al., 2019). The concentrations of the volatile compound were calculated with semi-quantitative method by multiplying the internal standard concentration and the ratio of the peak area of the volatile compound in the sample to the internal standard peak area, as shown in the following formula (Lugaz et al., 2005; Zheng et al., 2018b):

$$\mathrm{RCVC} = (\mathrm{PAVC}/\mathrm{PAIS}) \times \mathrm{CIS}$$

RCVC: relative concentration of volatile compounds;
PAVC: peak area of volatile compounds;
PAIS: peak area of internal standard;
CIS: concentration of internal standard.

To evaluate which compounds were responsible for the aroma of Kazak cheeses, odor activity values (OAVs) were obtained by dividing the concentration of each compound by the respective odor threshold (in water) reported in the literature for the aroma analysis (Gemert, 2011; Li et al., 2020).

Statistical Analysis

One-way ANOVA ($p < 0.05$) and Duncan's tests were performed with SPSS version 22 (IBM Corp., Armonk, NY, United States) for physicochemical, amino acid, organic acid, texture, and volatile compound analysis. A heat map was generated to show the trends in flavors during the five storage periods in different cheeses following R version 3.5.3. The effects of different yeasts on the aroma profiles were evaluated by principal component analysis (PCA) using SIMCA 14.1 (Umetrics, Sweden).

RESULTS AND DISCUSSION

Screening of Yeasts With Enzymatic Activity and Cheese Making

In this study, a total of 86 yeast strains were screened from the Kazak cheeses produced from different regions in Xinjiang, which could be classified as *K. lactis* (9 strains), *K. marxianus* (28 strains), *P. kudriavzevii* (21 strains), *T. delbrueckii* (3 strains), *Candida parapsilosis* (2 strains), *P. fermentans* (15 strains), *Lodderomyces elongisporus* (5 strains), and *Clavispora lusitaniae* (3 strains). Among these strains, *K. marxianus* and *P. kudriavzevii* were the dominant species, followed by *P. fermentans* (**Supplementary Table 1**). Only 16 yeasts exhibited high protease, lipase, or β-galactosidase activities. Based on the enzymatic activity results (**Supplementary Figure 1**), both *K. marxianus* A2 and *P. fermentans* A19 were observed to possess protease, β-galactosidase, and lipase activities, whereas *P. kudriavzevii* A11 had only protease and β-galactosidase activity (**Supplementary Table 2**). In addition, *K. marxianus* A2 had the highest protease activity (135 U/ml), *P. kudriavzevii* A11 possessed the highest β-galactosidase activity (375 U/ml), and *P. fermentans* A19 had the highest lipase activity (227 U/ml). Based on the dominant flora and enzymatic activities, *K. marxianus* A2, *P. kudriavzevii* A11, and *P. fermentans* A19 were selected as representative strains to manufacture cheeses, referred to hereafter as KmC, PkC, and PfC, respectively.

Physicochemical and Microbiological Analysis of Kazak Cheese

The physicochemical characteristics of the Kazak cheeses are shown in **Table 1**. Also, the results showed that no differences

TABLE 1 | Physicochemical parameters and microbial counts (log cfu/g) in four Kazak cheeses.

Composition	Control	KmC	PkC	PfC
Protein (%)	21.27 ± 1.82^{a}	22.62 ± 1.90^{a}	23.28 ± 1.93^{a}	21.52 ± 1.86^{a}
Moisture (%)	26.55 ± 1.08^{b}	28.61 ± 1.03^{ab}	29.48 ± 1.15^{a}	29.15 ± 1.27^{a}
Fat (%)	29.35 ± 2.53^{a}	28.75 + 2.78^{a}	29.21 ± 2.49^{a}	28.97 ± 2.65^{a}
Salt (%)	1.94 ± 0.07^{a}	1.92 ± 0.06^{a}	1.91 ± 0.05^{a}	1.92 ± 0.08^{a}
pH	4.98 ± 0.75^{a}	5.48 ± 0.93^{a}	5.25 ± 0.79^{a}	4.95 ± 0.82^{a}
Acidity (%)	1.25 ± 0.07^{a}	1.13 ± 0.04^{b}	0.96 ± 0.06^{c}	0.92 ± 0.05^{c}
Total viable counts	9.5 ± 0.05^{a}	9.3 ± 0.04^{c}	9.5 ± 0.03^{a}	9.4 ± 0.02^{b}
LABs	9.2 ± 0.02^{a}	9.0 ± 0.05^{c}	9.1 ± 0.03^{b}	8.9 ± 0.03^{d}
Yeasts	nd	2.8 ± 0.02^{c}	3.1 ± 0.04^{a}	2.9 ± 0.03^{b}

[1]Data are mean ± SD of three replicate analyses (n = 3). [a–c]Means with different superscripts within the same row are significantly (P < 0.05) different. [nd]Means not detected.

in the protein, fat, and salt contents or pH values were observed between the four cheeses, whereas significant differences in moisture and acidity were observed. Among the four types of cheese, the moisture content of the control cheese was the lowest (26.55%), whereas those in PkC were the highest (29.48%). The observed moisture contents were consistent with the characteristics of Kazak cheese as a hard cheese, which is different from that of other cheeses (Cichosz et al., 2014; Cuffia et al., 2017). Salt acts as a preservative in cheese, inhibiting the growth of spoilage microorganisms and contributing to the flavor of the cheese (Guinee, 2004). In the four assayed cheeses, the average salt content was 1.9%, with almost no loss observed in this study. These results suggested that the physicochemical indicators of cheese primarily depend on the milk material and the LAB starter. The addition of the three types of yeasts had no significant differences on the physicochemical properties of the cheeses, including the protein, fat, and salt contents and pH value.

The highest microbial counts (9.5 log cfu/g) and LAB (9.2 log cfu/g) were determined in the control cheeses (**Table 1**), whereas the total viable microbes counts (9.3 log cfu/g) and yeast counts (2.8 log cfu/g) determined in the KmC made with *K. marxianus* A2 were lower than those observed in the PkC and PfC samples after 40 days of ripening, respectively. The average number of viable yeasts (3.1 log cfu/g) observed in PkC was significantly higher than those in other cheeses. The results indicate that the yeasts survived during the cheese-making process as previously observed in raw-milk Tetilla cheese (Centeno et al., 2017).

Free-Amino-Acid Analysis

In cheese, the abundances of yeasts, such as *Metschnikowia reukaufii*, *Y. lipolytica*, *Metschnikowia pulcherrima*, and *P. kudriavzevii* (Akpınar et al., 2011; Zheng et al., 2018b), have been shown affect the release of proteases, which was vital for the formation of FAAs from proteins.

In the four Kazak cheeses made in this study, the most abundant FAA was Glu, whereas the contents of Cys were the lowest (**Figure 1**). These results agree with previously reported data for Manchego cheese (Poveda et al., 2004), which was related to a number of synthetic pathways for Glu,

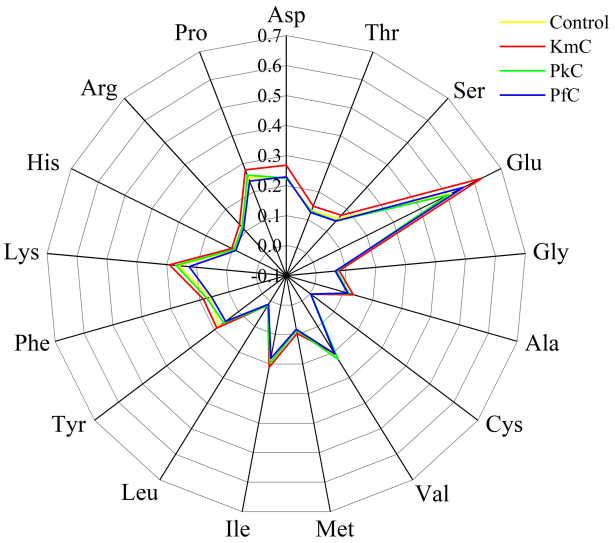

FIGURE 1 | Amino acid contents in four cheeses. The letters in the rose wind direction figure indicate 17 kinds of amino acids.

such as the EMP pathway, HMP pathway, TCA cycle, and transamination reaction.

The total FAA contents in the four cheeses were different due to the addition of the yeasts used to ferment the cheese. In the KmC, a total FAA content of up to 3.13 *g*/100 *g* was observed, indicating that *K. marxianus* A2 contributes to the formation of FAAs (**Supplementary Table 3**). Furthermore, among the 17 amino acids measured, except for Val and Leu, the amino acid contents in the KmC were significantly higher than those observed in the other cheeses. This fact may be attributed to the high protease activity of *K. marxianus* A2. In contrast, the total FAA contents in the PfC were the lowest among the assayed cheeses (2.70 *g*/100 *g*). FAAs play an important role in the formation of cheese flavor, like *P. cactophila* and *K. lactis* were helpful to the production of 2-phenylethanol and isoamyl alcohol (Celinska et al., 2018). These results indicate that the addition of *K. marxianus* A2, which had the highest protease activity, resulted in significantly higher FAA contents than those observed in the other cheeses.

Organic Acid Analysis

Organic acids are the primary source of acidic taste in foods (Lugaz et al., 2005; Da Conceicao Neta et al., 2007). The levels of tartaric acid, lactic acid, malic acid, succinic acid, and citric acid were investigated, and slight differences were observed in the contents of organic acids between the four cheese samples (**Supplementary Table 4**).

Among the several organic acids assayed, the concentration of lactic acid was significantly higher than that of the other organic acids, especially in the KmC with content up to 38.77 g/kg, whereas only 15.38 g/kg was detected in the PfC (**Figure 2**). A high lactic acid content would help lower the pH and subsequently affect the coagulation of casein. Besides, lactic acid also affects the flavor of cheese by altering the

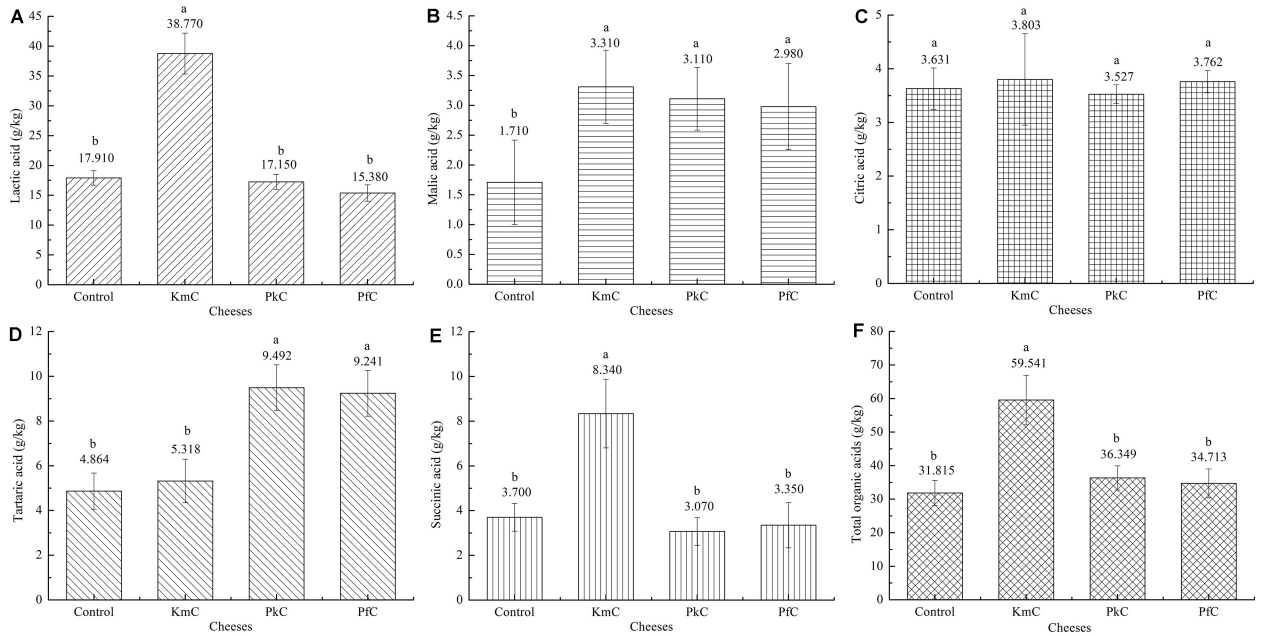

FIGURE 2 | Organic acid contents in four cheeses. The letters control, KmC, PkC, and PfC represent cheeses fermented by a commercial lactic acid starter, a commercial lactic acid starter with *K. marxianus* A2, *P. fermentans* A19, and *P. Kudriavzevii* A11, respectively. **(A–F)** Represent lactic acid, malic acid, citric acid, tartaric acid, succinic acid and tatal organic acids, respectively. The letters in the column chart indicate whether the difference among data was statistically significant.

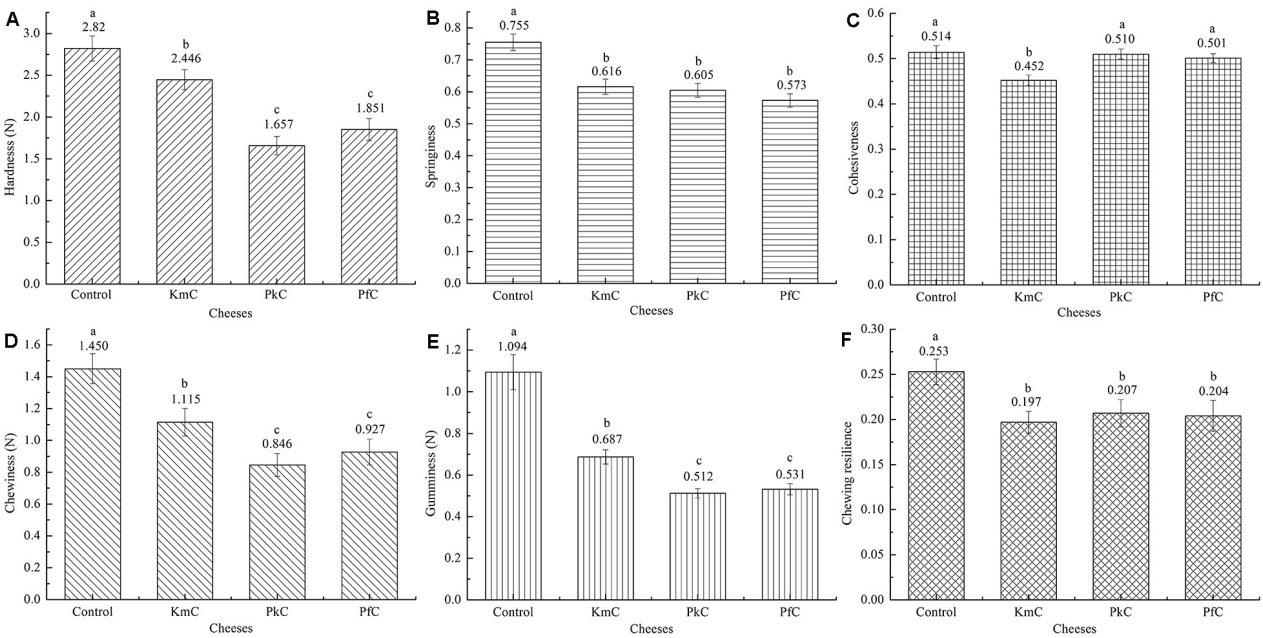

FIGURE 3 | Texture analysis of four cheeses. The letters control, KmC, PkC, and PfC represent cheeses fermented by a commercial lactic acid starter, a commercial lactic acid starter with *K. marxianus* A2, *P. fermentans* A19, and *P. Kudriavzevii* A11, respectively. The letters in the column chart indicate whether the difference among data was statistically significant. **(A–F)** Represent hardness, springiness, cohesiveness, chewiness, gumminess and chewing resilience, respectively.

enzymatic activity and promoting the retention of coagulant in the curd (McSweeney, 2004). In addition, malic acid, citric acid, and succinic acid were also present at high levels in the KmC, while *P. kudriavzevii* A11 and *P. fermentans* A19 both promoted the generation of tartaric acid, the levels of which in the corresponding cheeses were as high as 9.49 and 9.24 *g*/kg, respectively. Because glycolytic and lipolytic activities greatly promote organic acids (Izco et al., 2002), as well as an important

TABLE 2 | Concentrations of volatile compounds in Kazak cheeses sampled at 40 days (μg/kg).

Compound	Calculated RI	IA	Control	KmC	PkC	PfC
Alcohols						
Ethanol	932	MS	434.46 ± 9.6^{b}	81.29 ± 2.5^{d}	898.64 ± 17.8^{a}	271.76 ± 7.5^{c}
Isobutanol	1092	MS	24.36 ± 3.5^{b}	21.73 ± 1.6^{b}	50.92 ± 1.6^{a}	9.38 ± 0.6^{c}
Isoamylol	1209	MS	290.25 ± 7.3^{b}	7.90 ± 0.7^{d}	649.08 ± 12.4^{a}	52.20 ± 1.2^{c}
Pentanol	1250	MS, RI	4.37 ± 0.3^{b}	92.30 ± 1.9^{a}	5.97 ± 0.8^{b}	4.69 ± 0.2^{b}
4-Methyl-hexan-2-ol	1327	MS	1.16 ± 0.3^{b}	195.04 ± 6.3^{a}	4.97 ± 0.3^{b}	2.46 ± 0.1^{b}
1-Hexanol	1355	MS	5.19 ± 0.4^{c}	14.40 ± 1.7^{b}	20.94 ± 0.2^{a}	5.97 ± 0.5^{c}
3-Octanol	1393	MS, RI	1.87 ± 0.1^{c}	40.22 ± 3.2^{a}	5.75 ± 0.4^{b}	0.90 ± 0.1^{c}
2-Ethylhexanol	1491	MS, RI	1.27 ± 0.2^{b}	1963.82 ± 35.7^{a}	2.12 ± 0.1^{b}	nd
2,3-Butanediol	1543	MS, RI	322.98 ± 1.8^{c}	4071.46 ± 43.8^{a}	416.49 ± 8.6^{b}	117.34 ± 2.8^{d}
1-Octanol	1557	MS, RI	3.62 ± 0.6^{c}	7.62 ± 0.3^{a}	6.48 ± 0.9^{b}	3.55 ± 0.3^{c}
Isobutoxypropanol	1582	MS	44.61 ± 1.3^{b}	695.07 ± 38.2^{a}	51.64 ± 1.5^{b}	18.14 ± 0.9^{b}
4-Methyl-2-pentenal	1604	MS	1.98 ± 0.1^{b}	27.80 ± 1.7^{a}	2.57 ± 0.2^{b}	nd
1-Non-anol	1660	MS, RI	2.50 ± 0.2^{bc}	11.57 ± 2.5^{a}	4.13 ± 0.4^{b}	1.52 ± 0.1^{c}
1,3-Butanediol	1576	MS, RI	nd	1186.32 ± 32.6	nd	nd
Methionol	1719	MS, RI	2.58 ± 0.1^{b}	1196.36 ± 28.5^{a}	3.96 ± 0.2^{b}	1.33 ± 0.3^{b}
α-Cumyl alcohol	1773	MS, RI	0.41 ± 0.1^{b}	6.49 ± 0.7^{a}	nd	0.66 ± 0.1^{b}
Phenylethanol	1906	MS, RI	128.63 ± 3.6^{b}	222.00 ± 4.3^{a}	1.23 ± 0.1^{d}	9.71 ± 0.4^{c}
2-Methylheptan-2-ol	1053	MS	Nd	8.75 ± 0.5	10.27 ± 0.9	nd
Aldehydes						
Hexanal	1083	MS, RI	0.64 ± 0.1^{c}	36.69 ± 2.7^{a}	30.32 ± 2.4^{b}	2.13 ± 0.3^{c}
2-Heptenal	1322	MS, RI	0.86 ± 0.1^{c}	5.08 ± 0.4^{a}	2.07 ± 0.3^{b}	0.99 ± 0.1^{c}
Non-anal	1391	MS, RI	5.94 ± 0.8^{c}	58.71 ± 0.6^{a}	15.24 ± 2.6^{b}	13.93 ± 0.3^{b}
Decanal	1498	MS, RI	nd	1.27 ± 0.2^{b}	2.01 ± 0.2^{a}	1.52 ± 0.1^{b}
3-Butanolal	2423	MS	0.34 ± 0.1^{c}	1.41 ± 0.1^{a}	1.06 ± 0.1^{b}	0.90 ± 0.1^{b}
Acids						
Acetic acid	1449	MS, RI	465.28 ± 26.3^{c}	187.14 ± 17.5^{d}	815.79 ± 45.2^{a}	728.22 ± 33.6^{b}
Isobutyric acid	1570	MS, RI	98.11 ± 10.4^{c}	56.73 ± 2.1^{d}	195.13 ± 20.7^{a}	167.41 ± 14.2^{b}
Butanoic acid	1625	MS, RI	64.82 ± 9.4^{d}	383.31 ± 21.8^{a}	158.28 ± 17.3^{b}	111.51 ± 7.7^{c}
2-Methylcaproic acid	1757	MS, RI	55.18 ± 6.9^{c}	8.47 ± 1.5^{d}	159.84 ± 14.8^{b}	285.36 ± 26.3^{a}
Pentanoic acid	1733	MS, RI	0.90 ± 0.1^{c}	6.49 ± 0.7^{a}	1.84 ± 0.3^{b}	1.61 ± 0.4^{bc}
2-Methylvalerate	1764	MS	1.98 ± 0.2^{b}	nd	1.73 ± 0.1^{b}	5.87 ± 0.2^{a}
Hexanoic acid	1846	MS, RI	69.60 ± 6.3^{c}	nd	142.98 ± 7.3^{a}	120.94 ± 5.7^{b}
Heptanoic acid	1950	MS, RI	1.42 ± 0.2^{b}	387.68 ± 37.4^{a}	0.56 ± 0.1^{b}	0.33 ± 0.1^{b}
Non-anoic acid	2171	MS, RI	0.41 ± 0.1^{b}	1.13 ± 0.1^{b}	1.28 ± 0.2^{b}	51.59 ± 2.5^{a}
Octanoic acid	2060	MS, RI	25.07 ± 1.5^{a}	16.09 ± 2.8^{b}	0.17 ± 0.1^{d}	8.15 ± 1.1^{c}
Benzoic acid	2412	MS, RI	6.28 ± 1.8^{b}	13.97 ± 1.5^{a}	16.41 ± 2.1^{a}	nd
Esters						
Ethyl acetate	888	MS, RI	620.10 ± 48.4^{a}	493.96 ± 42.9^{b}	690.90 ± 37.4^{a}	267.28 ± 26.4^{c}
Isobutyl acetate	1012	MS, RI	4.97 ± 1.1^{c}	22.30 ± 1.6^{b}	4.13 ± 1.3^{c}	30.06 ± 2.9^{a}
Ethyl butanoate	1035	MS, RI	12.59 ± 1.2^{c}	178.53 ± 5.1^{a}	30.65 ± 1.8^{b}	nd
Isoamyl acetate	1122	MS, RI	571.08 ± 16.4^{b}	36.69 ± 1.7^{c}	573.21 ± 34.1^{b}	1931.13 ± 41.7^{a}
Ethyl hexanoate	1233	MS, RI	35.83 ± 2.9^{b}	23.57 ± 2.8^{c}	73.97 ± 6.3^{a}	15.02 ± 2.8^{d}
Hexyl acetate	1272	MS	2.32 ± 0.2^{c}	10.02 ± 1.4^{a}	nd	7.63 ± 1.2^{b}
Ethyl tert-butylacetate	1334	MS	0.97 ± 0.1^{b}	2.54 ± 0.6^{a}	2.46 ± 0.2^{a}	1.09 ± 0.1^{b}
Ethyl propanoate	1365	MS	0.26 ± 0.1^{b}	nd	3.07 ± 1.1^{a}	0.85 ± 0.2^{b}
Ethyl lactate	1427	MS	26.23 ± 5.2^{b}	8.19 ± 0.03^{d}	67.78 ± 2.1^{a}	17.86 ± 3.2^{c}
Ethyl caprylate	1435	MS, RI	55.70 ± 3.9^{a}	39.94 ± 1.9^{c}	47.34 ± 0.8^{b}	25.01 ± 2.7^{d}
Propyleneacetate	1526	MS, RI	1.91 ± 0.1^{b}	147.06 ± 3.2^{a}	4.91 ± 1.1^{b}	1.75 ± 0.1^{b}
Glycol diacetate	1535	MS, RI	4.03 ± 0.8^{b}	45.02 ± 2.1^{a}	4.30 ± 1.2^{b}	1.23 ± 0.2^{c}
Ethyl caprate	1638	MS, RI	3.44 ± 0.6^{b}	4.80 ± 1.7^{b}	3.91 ± 1.8^{b}	15.54 ± 2.5^{a}
Phenethyl acetate	1815	MS, RI	212.17 ± 24.7^{c}	1750.72 ± 57.2^{a}	154.59 ± 25.8^{c}	319.56 ± 16.4^{b}

(Continued)

TABLE 2 | Continued

Compound	Calculated RI	IA	Control	KmC	PkC	PfC
Phenethyl butyrate	1958	MS, RI	2.88 ± 0.8^{b}	208.45 ± 24.8^{a}	1.40 ± 0.3^{b}	0.28 ± 0.1^{b}
D-(-)-Pantolactone	2029	MS, RI	0.49 ± 0.1^{b}	18.21 ± 1.9^{a}	0.50 ± 0.1^{b}	nd
5-Decanolide	2194	MS, RI	1.46 ± 0.2^{c}	7.34 ± 0.3^{a}	nd	2.27 ± 0.2^{b}
Ketones						
2-Heptanone	1078	MS, RI	13.97 ± 3.2^{b}	14.54 ± 2.8^{b}	49.30 ± 4.2^{a}	15.40 ± 0.8^{b}
Acetoin	1284	MS, RI	85.55 ± 9.4^{b}	8.47 ± 1.9^{d}	154.31 ± 5.8^{a}	47.32 ± 6.3^{c}
6-Methyl-5-hepten-2-one	1338	MS, RI	0.93 ± 0.1^{c}	13.27 ± 2.6^{a}	9.04 ± 0.3^{b}	8.62 ± 1.4^{b}
2-Non-anone	1390	MS, RI	12.18 ± 1.2^{c}	54.90 ± 4.2^{a}	27.41 ± 3.9^{b}	28.94 ± 2.8^{b}

[1]Data are mean ± SD of three replicate analyses (n = 3). [a–d]Means with different superscripts within the same row are significantly ($P < 0.05$) different. [2]Control, KmC, PkC, and PfC represent samples collected on 40 days. [nd]Means not detected. IA, identification approach.

carbon source for microbial growth (Akalin et al., 2002), yeasts with enzymatic activity greatly promoted the production of organic acids through metabolism. Importantly, different organic acids produce different sour tastes. For example, citric acid provides a smooth sour taste and a fresh sensation, while malic acid provides a soft sour taste (Park et al., 2017).

The contents of malic acid and tartaric acids in the control cheese, which was only fermented by commercial LAB, were lower than those observed in the KmC, PkC, and PfC samples. Furthermore, the total organic acid contents in the KmC, PkC, and PfC samples (59.54, 36.35, and 34.71 g/kg) were also higher than that observed in the control. These results indicate that the addition of yeasts was beneficial to the formation of organic acids in cheese. Moreover, the differences of contents in organic acids depended largely on the yeasts used.

Texture Analysis

Analysis of the textural characteristics of the four cheeses showed that the hardness, springiness, cohesiveness, chewiness, gumminess, and chewing resilience were different (**Figure 3**).

All of the texture indicators, except for cohesiveness, in the KmC, PkC, and PfC samples were lower than those observed in the control, which may be related to acidification caused by the LAB starter (**Supplementary Table 5**). It is recognized that the pH, acidity, and moisture in food affect the cheese texture during the cheese fermentation process. However, a vital factor to the texture of cheeses is related to the proteolytic activity (Murtaza et al., 2014). The high contents of lactic acid promoted the hydration of casein, which further promotes the solubilization of proteins making the cheese less brittle (Dalié et al., 2010; Delavenne et al., 2012). The hardness, springiness, chewiness, and gumminess of the KmC were the highest among the cheeses assayed. These results indicate that the addition of yeasts led to a softer cheese texture compared with that of the control, which was highly related to the contents of lactic acid in the cheese.

Volatile Compound Analysis

Fifty-five volatile compounds were detected in the cheeses, including 18 alcohols, 5 aldehydes, 11 acids, 17 esters, and 4 ketones (**Table 2**). Significant differences ($P < 0.05$) were observed for the amounts of flavor compounds between cheeses (**Supplementary Figure 3**). Among the four cheeses, alcohols and esters were the primary compound types, followed by acids (**Figure 4**), with large amounts of alcohols detected, such as ethanol, isoamylol, and 2,3-butanediol. Similarly, ethyl acetate, isoamyl acetate, and phenethyl acetate were abundant esters. These results were associated with alcohols and free fatty acids because of the reaction of esterification and alcoholysis that presented in cheeses (Bertuzzi et al., 2017). Acetic acid, isobutyric acid, butanoic acid, 2-methylcaproic acid, and hexanoic acid were the dominant acids of cheeses. Other volatile compounds such as methyl ketones were also detected. These volatiles can be produced by the esterification of an alcohol with a free carboxylic acid (Alewijn et al., 2005) or β-oxidation of fatty acids (Collins et al., 2003). As shown in **Figure 4**, we also observed that the level of esters, alcohols, and ketones were significantly different between the control cheese and PkC. However, in the KmC, the ester contents decreased, whereas that of alcohols gradually increased. In the PfC, the levels of alcohols tended to first increase and then decrease, whereas the changes in ester levels exhibited the opposite trend. The aforementioned results indicate that the addition of yeasts altered the composition and contents of volatile compounds, especially alcohols, esters, and acids.

Dynamic Changes in Volatile Compounds and Aroma Evaluation in Cheeses

The aromatic profiles of the four Kazak cheeses on different days (0, 10, 20, 30, 40 days) were determined, and the relationships between the different yeast strains and the composition of the volatile compounds were analyzed via PCA. The results showed that PC1 and PC2 could explain 26.3 and 22% of the observed variance, respectively (**Figure 5**). The differences between selected yeasts and the volatile compounds produced could be easily distinguished by the concentrations of isoamylol (A3), 1-hexanol (A6), 2,3-butanediol (A9), methionol (A15), decanal (B4), 3-butanolal (B5), heptanoic acid (C8), ethyl acetate (D1), and ethyl hexanoate (D5; **Supplementary Figure 2**).

A heat map was used to compare the trends in the levels of 55 flavor compounds observed during the five ripening periods. According to the clustering results, these compounds could be divided into four categories (I, II, III, and IV) that contained 15, 10, 18, and 12 aromatic compounds, respectively (**Figure 6**). The results showed that not only the LAB contributed to the flavor

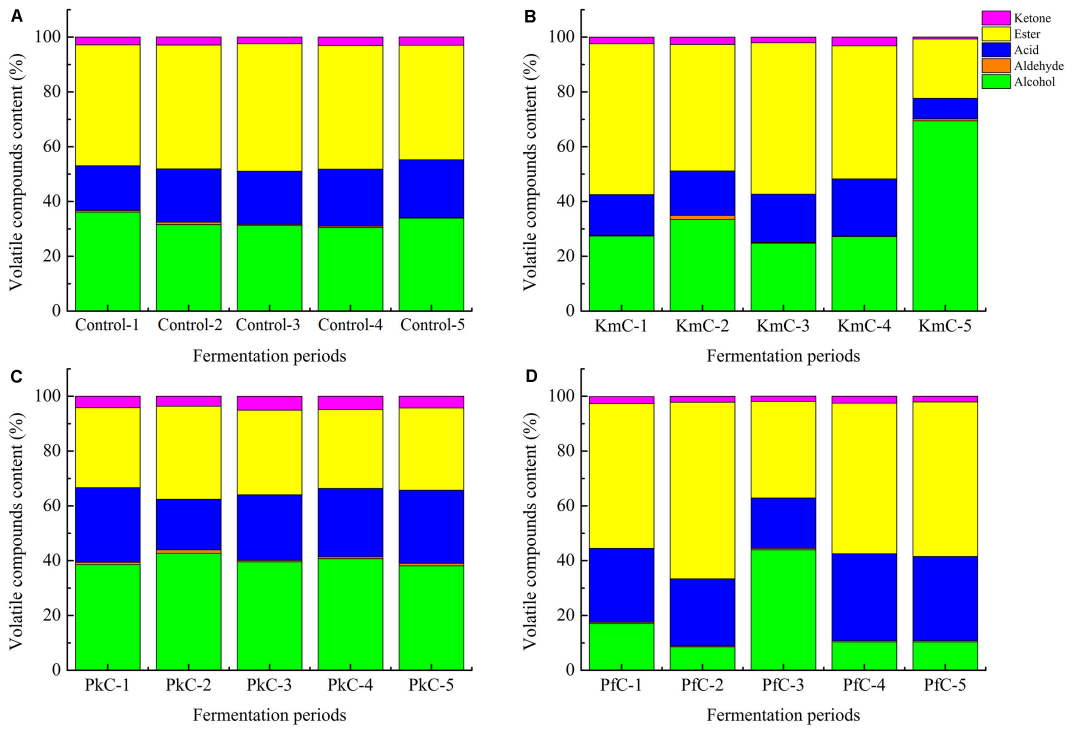

FIGURE 4 | Classification of flavor compounds in Kazak cheese. The letters control **(A)**, KmC **(B)**, PkC **(C)**, and PfC **(D)** represent cheeses fermented by a commercial lactic acid starter, a commercial lactic acid starter with *K. marxianus* A2, *P. fermentans* A19, and *P. Kudriavzevii* A11, respectively. 1–5 represent 0, 10, 20, 30, and 40 days of fermentation time.

of the cheese but also *K. marxianus* A2, *P. kudriavzevii* A11, and *P. fermentans* A19 strains were associated with proteolysis, lipolysis, or lactose degradation. *K. marxianus* A2 contributed to the formation of compounds in categories I and II, *P. kudriavzevii* A11 had an important effect on the compounds in category III, whereas *P. fermentans* A19 primarily promoted the contents of compounds in category IV. These results indicate that adding yeasts could alter the flavor of cheeses and that *K. marxianus* A2, *P. kudriavzevii* A11, and *P. fermentans* A19 were good producers of flavor compounds.

Yeast can effectively produce many secondary metabolites that are crucial to the quality of cheese, including carbonyl compounds, sulfur compounds, fatty acid derivatives, phenolic compounds, and higher alcohols, which have been directly related to the aroma of cheeses (Dzialo et al., 2017). Volatile compounds with OAV > 1 were divided into six aromas, comprising fruity, herbaceous, floral, fatty/oily, brandy, and onion. Volatile compounds in the KmC, PfC, and PkC samples exhibited a richer flavor than that of the control (**Figure 7**). Among the identified volatile compounds, the OAV of ethyl acetate was the highest, especially in the PkC, followed by the control, KmC, and PfC, which indicates that fruity aroma was abundant in the four cheeses. Furthermore, except for hexanal, all other volatile compounds detected possessed a specific fruity aroma. High OAVs were also observed for isoamyl acetate (64.37), which has a banana odor in PfC and 2,3-butanediol (42.81) possesses an onion odor quality in KmC (**Supplementary**

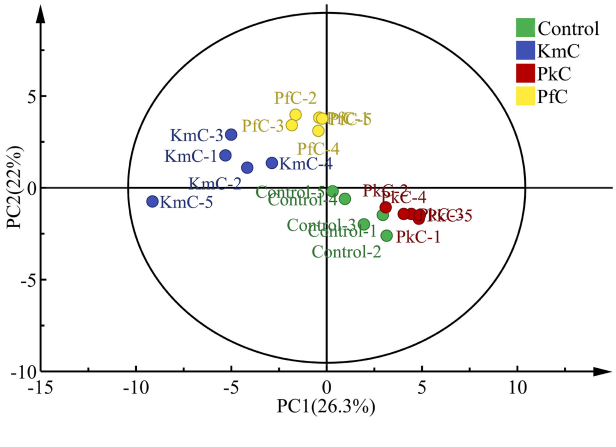

FIGURE 5 | Principal component analysis of four Kazak cheeses according to the determined volatile compounds. The letters control, KmC, PkC, and PfC represent cheeses fermented by a commercial lactic acid starter, a commercial lactic acid starter with *K. marxianus* A2, *P. fermentans* A19, and *P. Kudriavzevii* A11, respectively. 1–5 represent 0, 10, 20, 30, and 40 days of fermentation time.

Table 6). Furthermore, non-anal with oily, rose, and citrus-like notes, ethyl butanoate with an apple aroma, and ethyl hexanoate with brandy, orange, and sour odor notes in the KmC had OAVs of 7.34, 9.92, and 4.71, respectively. OAVs higher than one were

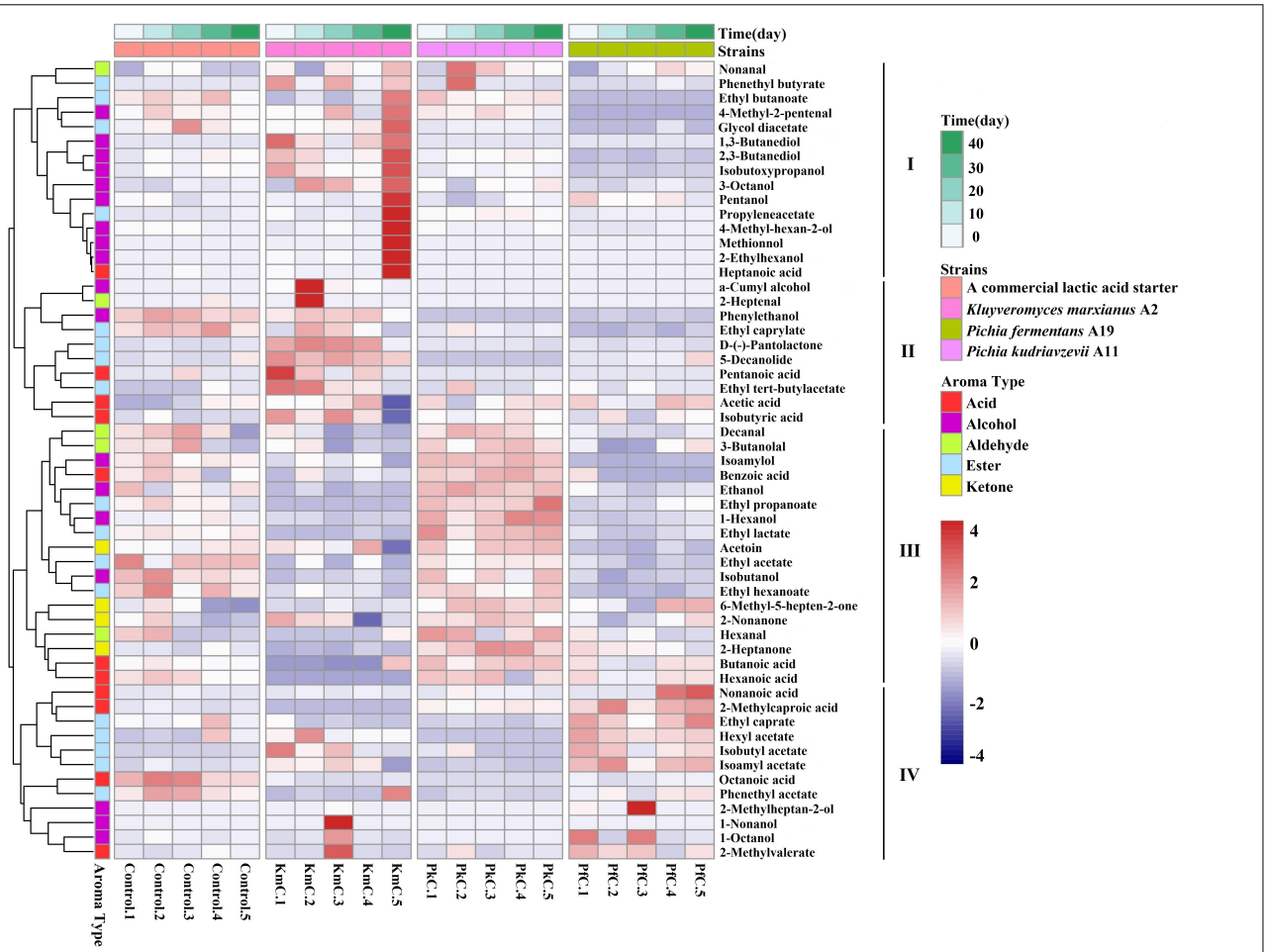

FIGURE 6 | Correlation analysis between five fermentation periods of strains. The letters control, KmC, PkC, and PfC represent cheeses fermented by a commercial lactic acid starter, a commercial lactic acid starter with *K. marxianus* A2, *P. fermentans* A19, and *P. Kudriavzevii* A11, respectively. 1–5 represent 0, 10, 20, 30, and 40 days of fermentation time.

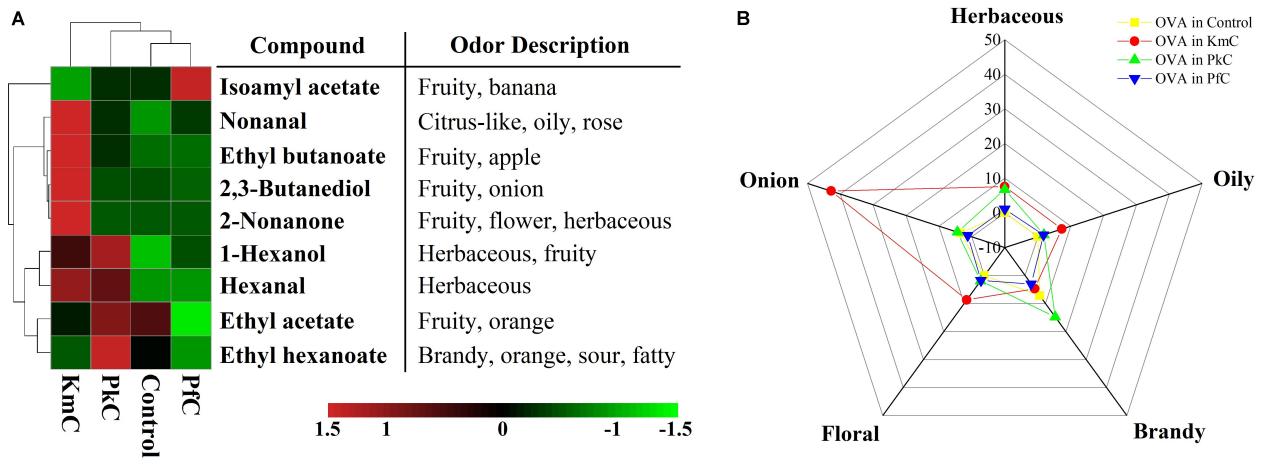

FIGURE 7 | Aroma profile of four Kazak cheeses. **(A)** Odor description and odor activity value (OAV) of aroma compounds in Kazak cheese. **(B)** The letters control, KmC, PkC, and PfC represent cheeses fermented by a commercial lactic acid starter, a commercial lactic acid starter with *K. marxianus* A2, *P. fermentans* A19, and *P. Kudriavzevii* A11, respectively.

also determined for 1-hexanol, hexanal, and 2-non-anone in the different cheeses. Evaluation of aroma characteristics other than fruity flavor showed that the cheese produced with *K. marxianus* A2 possessed a strong onion, oily, and floral aroma, whereas *P. kudriavzevii* A11 contributed to the formation of brandy, herbaceous, and onion flavors in the PkC, and no significant aroma changes were observed in PfC made with *P. fermentans* A19 (**Figure 7B**).

CONCLUSION

The results of this study showed that yeasts were primary microbial components in Kazak cheese and contributed to cheese quality and flavors. In general, adding yeast had no effect on the physicochemical parameters like pH value or protein, fat, and salt contents of cheeses, except for moisture and acidity. The cheeses made with added yeasts were more brittle than that of control cheese. Furthermore, the yeast added in this study had complex and diverse effects on cheese flavors. *K. marxianus* A2 contributed to the formation of FAA and organic acids in cheese, especially Glu and lactic acid. Besides, this yeast also promoted the contents of 2-ethylhexanol, 2,3-butanediol, isobutoxypropanol, 1,3-butanediol, methionol, and phenethyl acetate, providing onion, oily, and floral aromas to the cheese. In contrast, *P. kudriavzevii* A11 contributed to the accumulation of ethanol, isoamylol, acetic acid, ethyl acetate, and isoamyl acetate, promoting a strong brandy, herbaceous, and onion flavor. Thus, the addition of yeasts increases the flavors and distinctiveness of Kazak cheese, indicating that yeasts are important auxiliary starters for cheese production.

DATA AVAILABILITY STATEMENT

The raw data supporting the conclusions of this article will be made available by the authors, without undue reservation.

AUTHOR CONTRIBUTIONS

YC did the experiment, collected test data, and drafted the article. JX and YC analyzed data and submitted amendments to the article. XS, LD, and JL conceived and designed the study. BW revised the article. All authors contributed to the article and approved the submitted version.

FUNDING

We are grateful for the financial support from Shihezi University (No. CXBJ202004), the National Natural Science Foundation of China (Nos. 31960465 and 31660453), and Xinjiang Production and Construction Corps (Nos. 2019AB025, 2020AB014, 2020GY07, and 20GY01).

SUPPLEMENTARY MATERIAL

The Supplementary Material for this article can be found online at: https://www.frontiersin.org/articles/10.3389/fmicb.2020.614208/full#supplementary-material

REFERENCES

Akalin, A. S., Gonc, S., and Akbas, Y. (2002). Variation in organic acids content during ripening of Pickled white cheese. *J. Dairy Sci.* 85, 1670–1676. doi: 10.3168/jds.S0022-0302(02)74239-2

Akpınar, O., Uçar, F., and Yalçın, H. T. (2011). Screening and regulation of alkaline extracellular protease and ribonuclease production of Yarrowia lipolytica strains isolated and identified from different cheeses in Turkey. *Ann. Microbiol.* 61, 907–915. doi: 10.1007/s13213-011-0213-x

Alewijn, M., Sliwinski, E. L., and Wouters, J. T. M. (2005). Production of fat-derived (flavour) compounds during the ripening of gouda cheese. *Int. Dairy J.* 15, 733–740. doi: 10.1016/j.idairyj.2004.09.009

Atanassova, M. R., Fernández-Otero, C., Rodríguez-Alonso, P., Fernández-No, I. C., Garabal, J. I., and Centeno, J. A. (2016). Characterization of yeasts isolated from artisanal short-ripened cows' cheeses produced in Galicia (NW Spain). *Food Microbiol.* 53, 172–181. doi: 10.1016/j.fm.2015.09.012

Bekele, B., Hansen, E. B., Eshetu, M., Ipsen, R., and Hailu, Y. (2019). Effect of starter cultures on properties of soft white cheese made from camel (*Camelus dromedarius*) milk. *J. Dairy Sci.* 102, 1108–1115. doi: 10.3168/jds.2018-15084

Belguesmia, Y., Rabesona, H., Mounier, J., Pawtowsky, A., Blay, G. L., Barbier, G., et al. (2014). Characterization of antifungal organic acids produced by *Lactobacillus* harbinensis K.V9.3.1Np immobilized in gellan–xanthan beads during batch fermentation. *Food Control* 36, 205–211. doi: 10.1016/j.foodcont.2013.08.028

Bergamaschi, M., and Bittante, G. (2018). From milk to cheese: evolution of flavor fingerprint of milk, cream, curd, whey, ricotta, scotta, and ripened cheese obtained during summer Alpine pasture. *J. Dairy Sci.* 101, 3918–3934. doi: 10.3168/jds.2017-13573

Bertuzzi, A. S., Kilcawley, K. N., Sheehan, J. J., Osullivan, M. G., Kennedy, D., Mcsweeney, P. L. H., et al. (2017). Use of smear bacteria and yeasts to modify flavour and appearance of Cheddar cheese. *Int. Dairy J.* 72, 44–54. doi: 10.1016/j.idairyj.2017.04.001

Bezerra, T. K. A., Arcanjo, N. M. D. O., Garcia, E. F., Gomes, A. M. P., Queiroga, R. D. C. R. D. E., De Souza, E. L., et al. (2017). Effect of supplementation with probiotic lactic acid bacteria, separately or combined, on acid and sugar production in goat 'coalho' cheese. *LWT* 75, 710–718. doi: 10.1016/j.lwt.2016.10.023

Cardoso, V. M., Borelli, B. M., Lara, C. A., Soares, M. A., Pataro, C., Bodevan, E. C., et al. (2015). The influence of seasons and ripening time on yeast communities of a traditional Brazilian cheese. *Food Res. Int.* 69, 331–340. doi: 10.1016/j.foodres.2014.12.040

Celinska, E., Bonikowski, R., Bialas, W., Dobrowolska, A., Sloma, B., Borkowska, M., et al. (2018). Pichia cactophila and kluyveromyces lactis are highly efficient microbial cell factories of natural amino acid-derived aroma compounds. *Molecules* 23:97. doi: 10.3390/molecules23010097

Centeno, J. A., Garabal, J. I., Docampo, F., Lorenzo, J. M., and Carballo, J. (2017). Recovering traditional raw-milk Tetilla cheese flavour and sensory attributes by using Kocuria varians and *Yarrowia* lipolytica adjunct cultures. *Int. J. Food Microbiol.* 251, 33–40. doi: 10.1016/j.ijfoodmicro.2017.03.014

Ceugniez, A., Drider, D., Jacques, P., and Coucheney, F. (2015). Yeast diversity in a traditional French cheese "Tomme d'orchies" reveals infrequent and frequent species with associated benefits. *Food Microbiol.* 52, 177–184. doi: 10.1016/j.fm.2015.08.001

Chaveslopez, C., Tofalo, R., Serio, A., Paparella, A., Sacchetti, G., and Suzzi, G. (2012). Yeasts from Colombian Kumis as source of peptides with Angiotensin I converting enzyme (ACE) inhibitory activity in milk. *Int. J. Food Microbiol.* 159, 39–46. doi: 10.1016/j.ijfoodmicro.2012.07.028

Cichosz, G., Aljewicz, M., and Nalepa, B. (2014). Viability of the *Lactobacillus rhamnosus* HN001 probiotic strain in Swiss- and Dutch-Type cheese and Cheese-Like products. *J. Food Sci.* 79, 1181–1188. doi: 10.1111/1750-3841.12458

Collins, Y. F., Mcsweeney, P. L. H., and Wilkinson, M. G. (2003). Evidence of a relationship between autolysis of starter bacteria and lipolysis in Cheddar cheese during ripening. *J. Dairy Res.* 70, 105–113. doi: 10.1017/S0022029902005915

Cuffia, F., George, G., Renzulli, P., Reinheimer, J., Meinardi, C. A., and Burns, P. (2017). Technological challenges in the production of a probiotic pasta filata soft cheese. *LWT* 81, 111–117. doi: 10.1016/j.lwt.2017.03.039

Da Conceicao Neta, E. R., Johanningsmeier, S. D., Drake, M. A., and McFeeters, R. F. (2007). A chemical basis for sour taste perception of acid solutions and fresh-pack dill pickles. *J. Food Sci.* 72, S352–S359. doi: 10.1111/j.1750-3841.2007.00400.x

Dalié, D. K. D., Deschamps, A. M., and Richard-Forget, F. (2010). Lactic acid bacteria – Potential for control of mould growth and mycotoxins: a review. *Food Control* 21, 370–380. doi: 10.1016/j.foodcont.2009.07.011

Delavenne, E., Mounier, J., Déniel, F., Barbier, G., and Le Blay, G. (2012). Biodiversity of antifungal lactic acid bacteria isolated from raw milk samples from cow, ewe and goat over one-year period. *Int. J. Food Microbiol.* 155, 185–190. doi: 10.1016/j.ijfoodmicro.2012.02.003

Dzialo, M. C., Park, R., Steensels, J., Lievens, B., and Verstrepen, K. J. (2017). Physiology, ecology and industrial applications of aroma formation in yeast. *FEMS Microbiol. Rev.* 41(Suppl._1), S95–S128. doi: 10.1093/femsre/fux031

Fox, P. F., Guinee, T. P., Cogan, T. M., and McSweeney, P. L. H. (2017). "Fresh cheese products: principals of manufacture and overview of different varieties*," in *Fundamentals of Cheese Science*, (Boston, MA: Springer), 543–588.

Gao, M. L., Hou, H. M., Teng, X. X., Zhu, Y. L., Hao, H. S., and Zhang, G. L. (2017). Microbial diversity in raw milk and traditional fermented dairy products (Hurood cheese and Jueke) from Inner Mongolia. *China. Genet. Mol. Res.* 16:gmr16019451. doi: 10.4238/gmr16019451

Gemert, L. J. V. (2011). *Compilations of Odour Threshold Values in Air, Water and Other Media (second Enlarged and Revised Edition). No. 1*. Utrecht: Oliemans Punter & Partners.

Golić, N., Čadež, N., Terzić-Vidojević, A., Šuranská, H., Beganović, J., Lozo, J., et al. (2013). Evaluation of lactic acid bacteria and yeast diversity in traditional white pickled and fresh soft cheeses from the mountain regions of Serbia and lowland regions of Croatia. *Int. J. Food Microbiol.* 166, 294–300. doi: 10.1016/j.ijfoodmicro.2013.05.032

Gonçalves Dos Santos, M. T. P., Benito, M. J., Córdoba, M. D. G., Alvarenga, N., and Ruiz-Moyano Seco de Herrera, S. (2017). Yeast community in traditional Portuguese Serpa cheese by culture-dependent and -independent DNA approaches. *Int. J. Food Microbiol.* 262, 63–70. doi: 10.1016/j.ijfoodmicro.2017.09.013

Guinee, T. P. (2004). Salting and the role of salt in cheese. *Int. J. Dairy Technol.* 57, 99–109. doi: 10.1111/j.1471-0307.2004.00145.x

Izco, J. M., Tormo, M., and Jiménez-Flores, R. (2002). Rapid simultaneous determination of organic acids, free amino acids, and lactose in cheese by capillary electrophoresis. *J. Dairy Sci.* 85, 2122–2129. doi: 10.3168/jds.S0022-0302(02)74290-2

Juan, B., Zamora, A., Quevedo, J. M., and Trujillo, A.-J. (2016). Proteolysis of cheese made from goat milk treated by ultra high pressure homogenisation. *LWT* 69, 17–23. doi: 10.1016/j.lwt.2015.12.013

Kamimura, B. A., De Filippis, F., Sant'Ana, A. S., and Ercolini, D. (2019). Large-scale mapping of microbial diversity in artisanal Brazilian cheeses. *Food Microbiol.* 80, 40–49. doi: 10.1016/j.fm.2018.12.014

Konkit, M., and Kim, W. (2016). Activities of amylase, proteinase, and lipase enzymes from Lactococcus chungangensis and its application in dairy products. *J. Dairy Sci.* 99, 4999–5007. doi: 10.3168/jds.2016-11002

Li, J., Huang, Q., Zheng, X., Ge, Z., Lin, K., Zhang, D., et al. (2020). Investigation of the lactic acid bacteria in kazak cheese and their contributions to cheese fermentation. *Front. Microbiol.* 11:228. doi: 10.3389/fmicb.2020.00228

Lugaz, O., Pillias, A. M., Boireau-ducept, N., and Faurion, A. (2005). Time-intensity evaluation of acid taste in subjects with saliva high flow and low flow rates for acids of various chemical properties. *Chem. Senses* 30, 89–103. doi: 10.1093/chemse/bji004

Mageswari, A., Subramanian, P., Chandrasekaran, S., Karthikeyan, S., and Gothandam, K. M. (2017). Systematic functional analysis and application of a cold-active serine protease from a novel Chryseobacterium sp. *Food Chem.* 217, 18–27. doi: 10.1016/j.foodchem.2016.08.064

McSweeney, P. L. H. (2004). Biochemistry of cheese ripening. *Int. J. Dairy Technol.* 57, 127–144. doi: 10.1111/j.1471-0307.2004.00147.x

Murtaza, M. A., Huma, N., Sameen, A., Murtaza, M. S., Mahmood, S., Mueen-ud-Din, G., et al. (2014). Texture, flavor, and sensory quality of buffalo milk Cheddar cheese as influenced by reducing sodium salt content. *J. Dairy Sci.* 97, 6700–6707. doi: 10.3168/jds.2014-8046

Murtaza, M. A., Huma, N., Shabbir, M. A., Murtaza, M. S., and Anees-ur-Rehman, M. (2017). Survival of micro-organisms and organic acid profile of probiotic Cheddar cheese from buffalo milk during accelerated ripening. *Int. J. Dairy Technol.* 70, 562–571. doi: 10.1111/1471-0307.12406

Niro, S., Succi, M., Tremonte, P., Sorrentino, E., Coppola, R., Panfili, G., et al. (2017). Evolution of free amino acids during ripening of Caciocavallo cheeses made with different milks. *J. Dairy Sci.* 100, 9521–9531. doi: 10.3168/jds.2017-13308

Ocak, E., Javidipour, I., and Tuncturk, Y. (2015). Volatile compounds of Van Herby cheeses produced with raw and pasteurized milks from different species. *J. Food Sci. Technol.* 52, 4315–4323. doi: 10.1007/s13197-014-1458-8

Ozturkoglu-Budak, S., Wiebenga, A., Bron, P. A., and de Vries, R. P. (2016). Protease and lipase activities of fungal and bacterial strains derived from an artisanal raw ewe's milk cheese. *Int. J. Food Microbiol.* 237, 17–27. doi: 10.1016/j.ijfoodmicro.2016.08.007

Panseri, S., Chiesa, L. M., Zecconi, A., Soncini, G., and De Noni, I. (2014). Determination of volatile organic compounds (VOCs) from wrapping films and wrapped PDO Italian cheeses by using HS-SPME and GC/MS. *Molecules* 19, 8707–8724. doi: 10.3390/molecules19078707

Park, J.-M., Shin, J.-A., Lee, J. H., and Lee, K.-T. (2017). Development of a quantitative method for organic acid in wine and beer using high performance liquid chromatography. *Food Sci. Biotechnol.* 26, 349–355. doi: 10.1007/s10068-017-0047-9

Paxson, H. (2008). Post-pasteurian cultures: the microbiopolitics of raw-milk cheese in the United States. *Cult. Anthropol.* 23, 15–47. doi: 10.1111/j.1548-1360.2008.00002.x

Poveda, J. M., Cabezas, L., and McSweeney, P. L. H. (2004). Free amino acid content of Manchego cheese manufactured with different starter cultures and changes throughout ripening. *Food Chem.* 84, 213–218. doi: 10.1016/S0308-8146(03)00204-8

Rehman, R.-U., Wang, Y., Wang, J., and Geng, W. (2018). Physicochemical analysis of Mozzarella cheese produced and developed by the novel EPS-producing strain Lactobacillus kefiranofaciens ZW3. *Int. J. Dairy Technol.* 71, 90–98. doi: 10.1111/1471-0307.12445

Ryssel, M., Johansen, P., Al-Soud, W. A., Sørensen, S., Arneborg, N., and Jespersen, L. (2015). Microbial diversity and dynamics throughout manufacturing and ripening of surface ripened semi-hard Danish Danbo cheeses investigated by culture-independent techniques. *Int. J. Food Microbiol.* 215, 124–130. doi: 10.1016/j.ijfoodmicro.2015.09.012

Souza, C. J. F., Garciarojas, E. E., and Favarotrindade, C. S. (2018). Lactase (β-galactosidase) immobilization by complex formation: impact of biopolymers on enzyme activity. *Food Hydrocoll.* 83, 88–96. doi: 10.1016/j.foodhyd.2018.04.044

Sun, Z., Liu, W., Bao, Q., Zhang, J., Hou, Q., Kwok, L., et al. (2014). Investigation of bacterial and fungal diversity in tarag using high-throughput sequencing. *J. Dairy Sci.* 97, 6085–6096. doi: 10.3168/jds.2014-8360

van Mastrigt, O., Gallegos Tejeda, D., Kristensen, M. N., Abee, T., and Smid, E. J. (2018). Aroma formation during cheese ripening is best resembled by Lactococcus lactis retentostat cultures. *Microb. Cell Fact.* 17:104. doi: 10.1186/s12934-018-0950-7

Xu, M., Jin, Z., Lan, Y., Rao, J., and Chen, B. (2019). HS-SPME-GC-MS/olfactometry combined with chemometrics to assess the impact of germination on flavor attributes of chickpea, lentil, and yellow pea flours. *Food Chem.* 280, 83–95. doi: 10.1016/j.foodchem.2018.12.048

Yunita, D., and Dodd, C. E. R. (2018). Microbial community dynamics of a blue-veined raw milk cheese from the United Kingdom. *J. Dairy Sci.* 101, 4923–4935. doi: 10.3168/jds.2017-14104

Yuvaşen, A., Macit, E., and Dertli, E. (2018). Microbial species playing roles for the production of traditional Kasar cheese during pre-maturation period. *LWT* 91, 406–413. doi: 10.1016/j.lwt.2018.01.075

Zheng, X., Ge, Z., Lin, K., Zhang, D., Chen, Y., Xiao, J., et al. (2020). Dynamic changes in bacterial microbiota succession and flavour development during milk fermentation of Kazak artisanal cheese. *Int. Dairy J.* 113:104878. doi: 10.1016/j.idairyj.2020.104878

Zheng, X., Liu, F., Li, K., Shi, X., Ni, Y., Li, B., et al. (2018a). Evaluating the microbial ecology and metabolite profile in Kazak artisanal cheeses from Xinjiang. *China. Food Res. Int.* 111, 130–136. doi: 10.1016/j.foodres.2018.05.019

Zheng, X., Liu, F., Shi, X., Wang, B., Li, K., Li, B., et al. (2018b). Dynamic correlations between microbiota succession and flavor development involved in the ripening of Kazak artisanal cheese. *Food Res. Int.* 105, 733–742. doi: 10.1016/j.foodres.2017.12.007

Zhou, L., Tang, Q., Wasim Iqbal, M., Xia, Z., Huang, F., Li, L., et al. (2018). A comparison of milk protein, fat, lactose, total solids and amino acid profiles of three different buffalo breeds in Guangxi. *China. Ital. J. Anim. Sci.* 17, 873–878. doi: 10.1080/1828051X.2018.1443288

Zivkovic, M., Cadez, N., Uroic, K., Miljkovic, M., Tolinacki, M., Dousova, P., et al. (2015). Evaluation of probiotic potential of yeasts isolated from traditional cheeses manufactured in Serbia and Croatia. *J. Intercult. Ethnopharmacol.* 4, 12–18. doi: 10.5455/jice.20141128051842

Conflict of Interest: The authors declare that the research was conducted in the absence of any commercial or financial relationships that could be construed as a potential conflict of interest.

frontiers in Microbiology

ORIGINAL RESEARCH
published: 17 December 2020
doi: 10.3389/fmicb.2020.610471

Metabolomics Analysis of the Effect of Glutamic Acid on Monacolin K Synthesis in *Monascus purpureus*

Chan Zhang[1,2]*, *Nan Zhang*[1], *Mengxue Chen*[1], *Haijiao Wang*[1], *Jiachen Shi*[1], *Bei Wang*[1,2], *Baoguo Sun*[1,2] and *Chengtao Wang*[1,2]*

[1] Beijing Advanced Innovation Center for Food Nutrition and Human Health, Beijing Technology & Business University, Beijing, China, [2] Beijing Engineering and Technology Research Center of Food Additives, Beijing Technology & Business University, Beijing, China

Monacolin K is a secondary metabolite produced by *Monascus* with beneficial effects on health, including the ability to lower cholesterol. We previously showed that the yield of monacolin K was significantly improved when glutamic acid was added to the fermentation broth of *Monascus purpureus* M1. In this study, we analyzed *M. purpureus* in media with and without glutamic acid supplementation using a metabolomic profiling approach to identify key metabolites and metabolic pathway differences. A total of 817 differentially expressed metabolites were identified between the two fermentation broths on day 8 of fermentation. Pathway analysis of these metabolites using the KEGG database indicated overrepresentation of the citric acid cycle; biotin metabolism; and alanine, aspartate, and glutamate metabolic pathways. Six differentially expressed metabolites were found to be related to the citric acid cycle. The effect of citric acid as an exogenous additive on the synthesis of monacolin K was examined. These results provide technical support and a theoretical basis for further studies of the metabolic regulatory mechanisms underlying the beneficial effects of monacolin K and medium optimization, as well as genetic engineering of *Monascus* M1 for efficient monacolin K production.

Keywords: monacolin K, monascus, metabolomics, citric acid, glutamic acid

OPEN ACCESS

Edited by:
Wanping Chen,
Georg-August-University Goettingen, Germany

Reviewed by:
Yanli Feng,
Hubei Normal University, China
Li Li,
Yangtze University, China

***Correspondence:**
Chan Zhang
zhangchan@th.btbu.edu.cn
Chengtao Wang
hongqumei@126.com

Specialty section:
This article was submitted to Food Microbiology, a section of the journal Frontiers in Microbiology

Received: *25 September 2020*
Accepted: *12 November 2020*
Published: *17 December 2020*

Citation:
Zhang C, Zhang N, Chen M, Wang H, Shi J, Wang B, Sun B and Wang C (2020) Metabolomics Analysis of the Effect of Glutamic Acid on Monacolin K Synthesis in Monascus purpureus. Front. Microbiol. 11:610471. doi: 10.3389/fmicb.2020.610471

INTRODUCTION

Monascus is a common saprophytic fungus with practical applications in the food, brewing, and medical industries in China (Lin et al., 2008; Pérez-Jiménez et al., 2018). *Monascus* species, such as *M. ruber*, *M. fuliginosus*, *M. albidus*, *M. rubiginosus*, *M. serorubescens*, and *M. purpureus* are widely known to produce various secondary metabolites with polyketide structures, such as pigments (Krairak et al., 2000), monacolin K (Endo, 1979), citrinin (Blanc et al., 1995), and γ-aminobutyric acid (Diana et al., 2014). Extensive studies of physiological substances in *Monascus* have led to the discovery of various metabolites with high nutritional and pharmaceutical value (Li et al., 2011; Stefanutti et al., 2017).

Among these metabolites, monacolin K is widely used as a drug for the treatment of hyperlipidemia (Anagnostis et al., 2018; Lee et al., 2018). Monacolin K can effectively suppress the activity of a key enzyme in cholesterol biosynthesis (HMG-CoA) as a competitive inhibitor and can regulate blood lipid abnormalities (Su et al., 2003). Moreover, it can suppress breast cancer cell proliferation (Patel, 2016) and facilitate apoptosis in malignant thyroid cells

(Chen et al., 2014). However, its use is limited by low yields and high production costs. Therefore, it is important to improve the production of monacolin K by *Monascus*. Generally, the yield of monacolin K is improved by two approaches. First, high monacolin K-producing strains can be produced by genetic engineering technology (Liu et al., 2019) and mutation breeding (Chen et al., 2008). Second, fermentation conditions of *Monascus*, such as medium components and conditions, can be optimized (Kalaivani and Rajasekaran, 2014). The regulatory mechanism of monacolin K has not been fully resolved. Metabolomics techniques are used to analyze the differences in key metabolites involved in the synthesis of monacolin K, which is a better analytical method.

Metabolomics is a new qualitative and quantitative method for comprehensive analyses of small molecule metabolites (<1.5 kDa) produced by an organism in a specific physiological period (Zhang et al., 2016); this approach is widely used in the food, medical, and agricultural fields (Vongsangnak et al., 2011; Johanningsmeier et al., 2016). Metabolites serve as direct indicators of biological activity and are therefore, useful for detecting correlations with phenotypes (Patti et al., 2012). Both targeted (Dudley et al., 2010) and untargeted metabolomics approaches can characterize metabolites that accumulate differentially in biological samples (Nordström et al., 2008). Filamentous fungi produce numerous secondary metabolites that are not directly involved in growth or reproduction (Keller et al., 2005). Increasing studies have focused on the characterization of filamentous fungi by metabolite profiling and metabolomics. Liquid chromatography high-resolution mass spectrometry (LC-HRMS) and gas chromatography mass spectrometry (GC-MS) were used by (Kang et al., 2011) to categorize *Trichoderma* species according to their secondary metabolite profiles (Kang et al., 2011). Identifying unknown bioactive compounds produced by filamentous fungi is also a major research goal (Wiemann et al., 2013). Several compounds that are correlated with co-cultivation of *Streptomyces coelicolor* and *Aspergillus niger* have been identified by nuclear magnetic resonance (NMR)-based metabolomics (Wu et al., 2015). A variety of volatile organic compounds associated with the catabolism of branched chain amino acids have been detected by solid phase microextraction (SPME)-GC-MS (Roze, 2010). Major differences between *Escherichia coli* strains grown under different conditions have been examined at the levels of amino acids, fatty acids, and precursor metabolites by GC-MS (Carneiro et al., 2012).

Despite this increase in metabolomics studies of filamentous fungi, this technology has not been used to investigate changes in the metabolome of *Monascus* during different growth phases. Previous analyses showed that glutamic acid can enhance the production of monacolin K in *Monascus* M1 (Zhang et al., 2017). In this study, the fermentation broths prepared using two types of medium were collected at different time points for metabolomic profiling by ultra-performance liquid chromatography quadrupole time-of-flight mass spectrometry (UPLC-Q-TOF-MS). The composition of metabolites and molecular mechanism by which glutamic acid regulates monacolin K production were investigated.

METHODS AND MATERIALS

Fungal Strain and Culture Conditions

Monascus purpureus M1 was obtained from the Chinese General Microbiological Culture Collection Center (strain number, CGMCC 3.0568, Beijing, China). *M. purpureus* M1 is a wild-type strain that stably produces monacolin K. It was grown on potato dextrose agar at 30°C for 4 days and cultured with 50 mL of seed medium containing 30 g/L glucose, 15 g/L soybean powder, 1 g/L $MgSO_4 \cdot 7H_2O$, 2 g/L KH_2PO_4, 70 g/L glycerol, 2 g/L $NaNO_3$, and 10 g/L peptone at neutral pH. The cultures were incubated at 30°C for 48 h with shaking at 200 rpm. Two types of fermentation medium were used. The original fermentation medium contained 20 g/L rice powder, 1 g/L $MgSO_4 \cdot 7H_2O$, 2 g/L $ZnSO_4 \cdot 7H_2O$, 2.50 g/L KH_2PO_4, 90 g/L glycerol, 5 g/L $NaNO_3$, and 10 g/L peptone at a neutral pH. For the glutamic acid fermentation medium, the original fermentation medium was supplemented with 10 mM glutamic acid. The seed culture (5 mL) was then inoculated into these two types of fermentation media (50 mL). The cultures were incubated at 30°C for 2 days with shaking at 150 rpm, followed by incubation at 25°C for 10 days with shaking at 150 rpm.

Determination of Monacolin K

To evaluate the yield of monacolin K, the fermentation broth (5 mL) was added to 15 mL of 75% methanol (v/v) and sonicated for 20 min, and the supernatant was passed through a 0.45 μm filter. High-performance liquid chromatography (HPLC) using an Inertsil ODS-3 C18 column (150 mm × 4.6 mm × 5 μm) was used to detect the yield. The mobile phase was ddH_2O (with 0.1% H_3PO_4) /methanol (1:3, v/v) and was run at 1 mL/min. An ultraviolet detector was used at a wavelength of 237 nm, detection temperature of 30°C, and injection volume of 10 μL.

Sample Collection and Preparation

The fermentation medium was collected at 0, 8, and 12 days in two different cultures and stored at−80°C until analysis. NG0, NG8, and NG12 indicate the fermentation medium without glutamic acid on days 0, 8, and 12, respectively; G8 and G12 indicate the fermentation medium with glutamic acid on days 8 and 12. A volume of 300 μL of 80% methanol was added to 100 μL of each sample followed by ultrasonication for 10 min; ultrasonication was stopped for 10 s every 5 s. The samples were vortexed for 1–3 min and left standing for 10 min at 4°C. To separate the methanol/water layers, the samples

TABLE 1 | Gradient elution conditions in LC.

Time (min)	Mobile phase A (%)	Mobile phase B (%)
0	98	2
1	98	2
13	10	90
16	10	90
16.1	98	2
20	98	2

were centrifuged for 10 min at 13,000 rpm. The supernatant was dried to a powder by vacuum drying and dissolved in methanol.

UPLC-Q-TOF-MS

Liquid chromatography (LC) separation was performed using an Agilent ZORBAX Eclipse Plus C18 column (100 × 2.1 mm, 3.5 μm; Agilent Technologies, Santa Clara, CA, USA). The injected sample volume was 20 μL for each run in the full loop injection mode, and the column temperature was 25°C. The flow rate of the mobile phase was 0.5 ml/min, where mobile phases A and B were 0.1% formic acid in ddH_2O and acetonitrile, respectively. The program for elution gradient is described in **Table 1**.

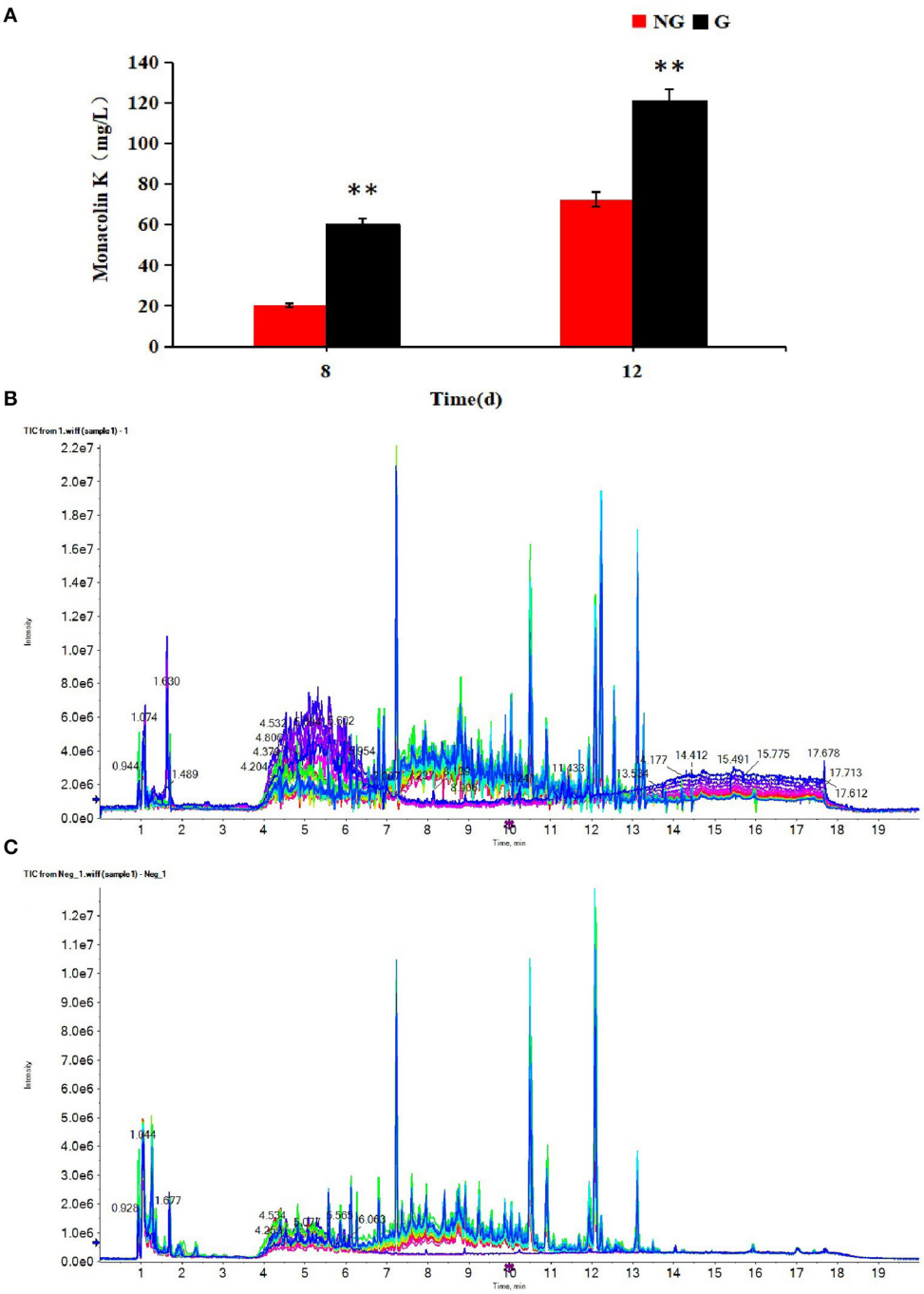

FIGURE 1 | (A) Effect of glutamic acid on monacolin K production in *Monascus*, **(B)** the TIC diagrams of positive, **(C)** and negative ions for all samples. **(B,C)** Indicate that all samples were available. $^{**}p < 0.01$.

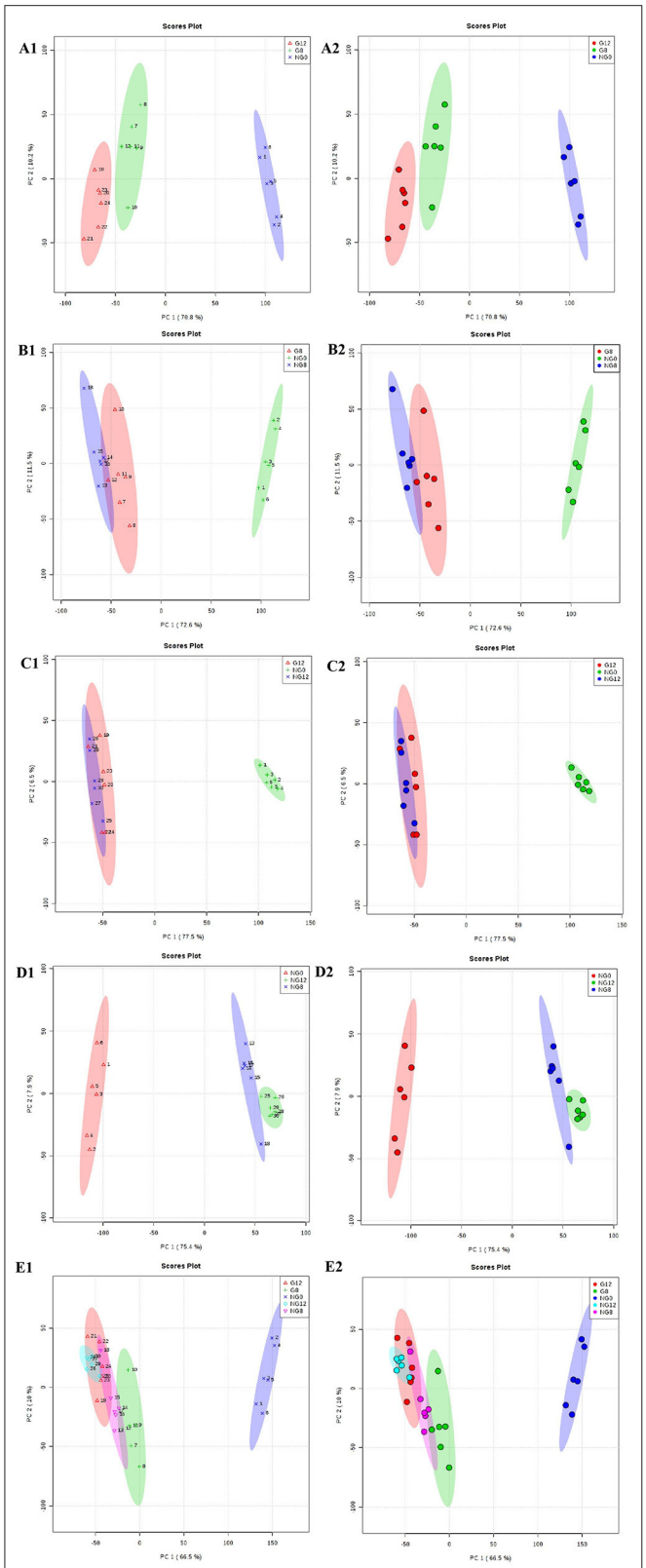

FIGURE 2 | PCA score plots. **(A1,A2)** NG0-G8-G12; **(B1,B2)** NG0-G8-NG8; **(C1,C2)** NG0-G12-NG12; **(D1,D2)** NG0-NG8-NG12; **(E1,E2)** G8-G12-NG0-NG8-NG12. The middle point represents the sample number, and the contribution rate of PC1 and PC2 in the score chart is shown. The area within the middle ellipse represents the 95% confidence interval.

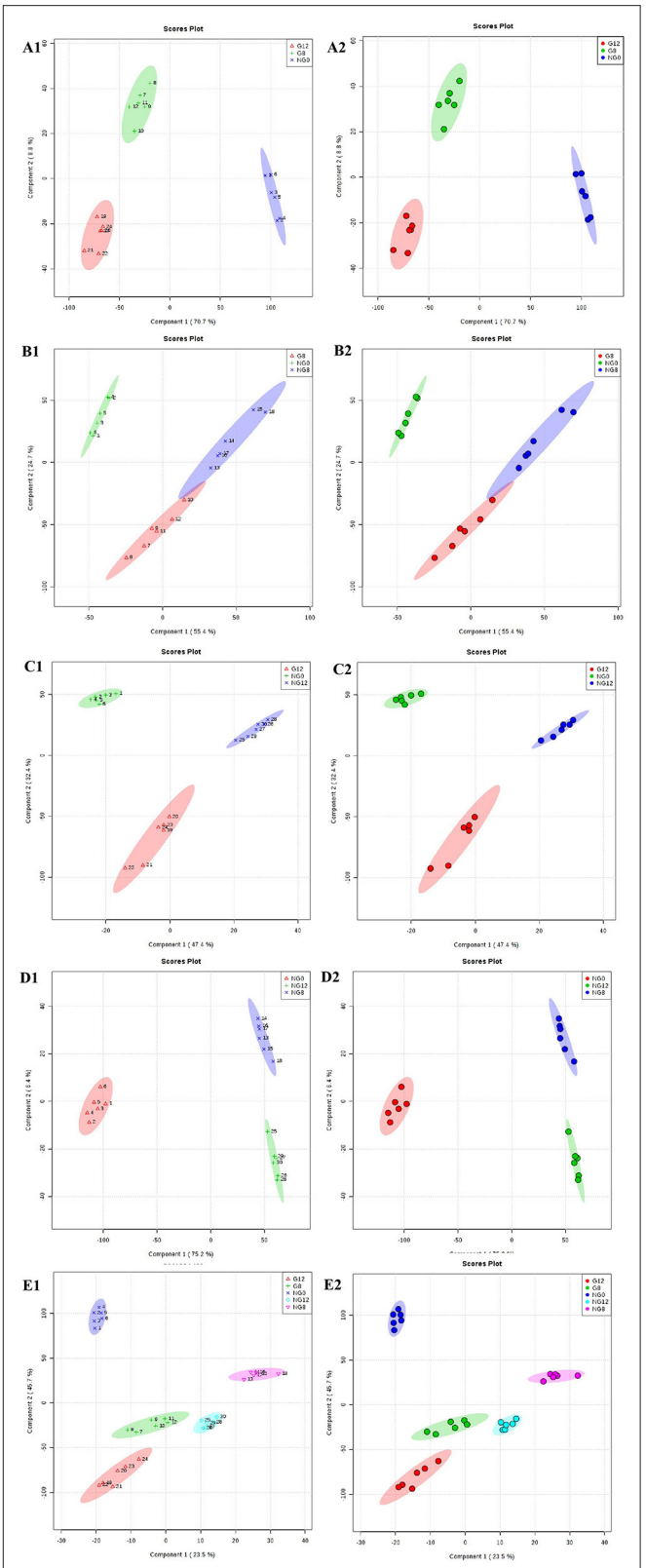

FIGURE 3 | PLS-DA score plots. **(A1,A2)** NG0-G8-G12; **(B1,B2)** NG0-G8-NG8; **(C1,C2)** NG0-G12-NG12; **(D1,D2)** NG0-NG8-NG12; **(E1,E2)** G8-G12-NG0-NG8-NG12. The contribution rate of PC1 and PC2 in the score chart is shown. The area inside the middle ellipse represents the 95% confidence interval.

MS was performed using Triple TOF 5600+, an orthogonal accelerated TOF-MS (AB Sciex, Redwood City, CA, USA) equipped with an electrospray ion source. Data were acquired in positive and negative-V-geometry mode for each LC-MS analysis. The capillary voltages were set to 2,500 and 3,000 V, cone gas flow rate 50 L/h, desolvation gas flow rate 600 L/h, source temperature 120°C, and desolvation temperature 500°C. The scan range of mass-to-charge (m/z) was 50 to 1,500 in full scan mode and data were collected in centroid mode. Independent reference lock-mass ions obtained by Analyst TF 1.6 and MarkerView 1.2.1 were used to ensure mass accuracy during data acquisition.

The differentially expressed metabolite ions were identified by searches against the HMDB (http://www.hmdb.ca/spectra/ms/search) databases (Wishart et al., 2008). The mass tolerance for the HMDB database search was set to 0.05 Da. The chromatographic retention behavior was also considered in order to reduce false-positive matches.

Statistical Analysis

MarkerView was used for peak identification, peak filtering, and peak alignment of raw mass spectrometry data. The qualitative m/z and a two-dimensional data matrix of peak areas were obtained. MetaboAnalyst 3.0 was used to normalize samples with different requirements for comparison. Differentially expressed metabolites among groups were visualized by principal component analysis (PCA), partial least squares discriminant analysis (PLS-DA), and orthogonal partial least squares-discriminant analysis (OPLS-DA). The false discovery rate method was used to correct for multiple comparisons. Data are presented as the mean ± SD.

Multivariate analyses, including unsupervised PCA and supervised PLS-DA, were implemented in MetaboAnalyst 4.0 (http://www.metaboanalyst.ca/MetaboAnalyst/). PLS-DA models were cross-validated by the 10-fold method with unit variance scaling. The parameter R^2 was used to evaluate the fitting of the PLS-DA models, and Q^2 was used to assess predictive ability. Negative or very low Q^2 values indicate that the differences between groups were not significant. The PLS-DA model removes variation in the X matrix that is not correlated with the Y matrix. Thus, only one predictive component is generally used for discrimination between two classes.

Comparisons in the intensities of integrated regions between two groups were performed using the two-tailed Welch's t-test implemented in MetaboAnalyst 4.0, and $p < 0.05$ was considered statistically significant. A volcano plot was generated based on a combination of fold change values and t-tests, and significantly different peaks among the three groups were used for multivariate pattern recognition. Moreover, peaks that were consistently upregulated or downregulated were identified; the intensity data for these regions were used in box-plot, hierarchical cluster, and metabolic pathway analyses.

Pathway Analysis

Differences in chemical metabolites were evaluated using the MetaboAnalyst 4.0 web portal for pathway analysis and visualization (http://www.metaboanalyst.ca/). Additional metabolite set enrichment analysis was performed (http://www.metaboanalyst.ca/). Pearson's correlation coefficients were calculated to evaluate the relationships between biomarkers ($p < 0.05$, impact >0.01).

Verification of Fermentation Experiment

Fermentation experiments were carried out on the characteristic substances selected by the metabolome to verify their functions. According to the compounds involved in the tricarboxylic acid cycle, this study chose to add malic acid, fumaric acid, α-ketoglutarate, and citric acid to the common medium. Based on the preliminary exploration of the optimal concentration in our laboratory, the concentration of the above-mentioned substances was determined. For the malic acid-fermentation medium, fumaric acid-fermentation medium, α-ketoglutarate-fermentation medium, and citric acid-fermentation medium, the original fermentation medium was separately supplemented with 3 g/L malic acid, 0.60 g/L fumaric acid, 10 g/L α-ketoglutarate, 1 g/L citric acid. The culture conditions were the same as 2.1.

RESULTS

Glutamic Acid Influences Monacolin K Yield

Monacolin K production was detected at 8 and 12 days in two different cultures. As shown in **Figure 1A**, the monacolin K yield using the M1 strain was higher in a glutamic acid-containing medium than in an ordinary medium on days 8 and 12, with increases of 2.90 and 1.70-fold, respectively.

Multivariate Statistical Analysis

The profiles of metabolites in medium detected by UPLC-Q-TOF-MS were analyzed by multivariate statistical methods, including PCA, PLS-DA, and OPLS-DA. The TIC diagrams of all samples in positive and negative ion mode are shown in **Figures 1B,C**.

Through PCA analysis, inspect the distribution of samples, verify the rationality of the experimental design and the uniformity of biological replicate samples. The PCA analysis results were shown in **Figure 2**. The middle point in **Figure 2** represents the sample number, and the contribution rate of PC1 and PC2 in the score chart is shown in **Figure 2**. The area within the middle ellipse represents the 95% confidence interval. It could be seen from **Figure 2** that the samples of the same group were relatively concentrated in two-dimensional space, indicating that the selection of these indicators was representative and the biological repetition was good.

The PLS-DA results are shown in **Figure 3**; this analysis was performed to visualize the differentiation among the three groups (NG0, G8, and G12) (**Figures 3A1,A2**). The selection of indicators was representative, and repeatability among biological replicates was acceptable. Components within groups were relatively concentrated, and the NG0-G8-NG8 groups (**Figures 3B1,B2**), NG0-G12-NG12 groups (**Figures 3C1,C2**), NG0-NG8-NG12 groups (**Figures 3D1,D2**), and G8-G12-NG0-NG8-NG12 groups (**Figures 3E1,E2**) showed similar results. The

contribution rate of PC1 and PC2 in the score chart was shown in **Figure 3**. The area inside the middle ellipse represents the 95% confidence interval.

At the same time, VIP value (variable importance in projection) was a variable importance factor. Generally, VIP >1 can be considered as a difference. The PLS-DA-vip score as shown

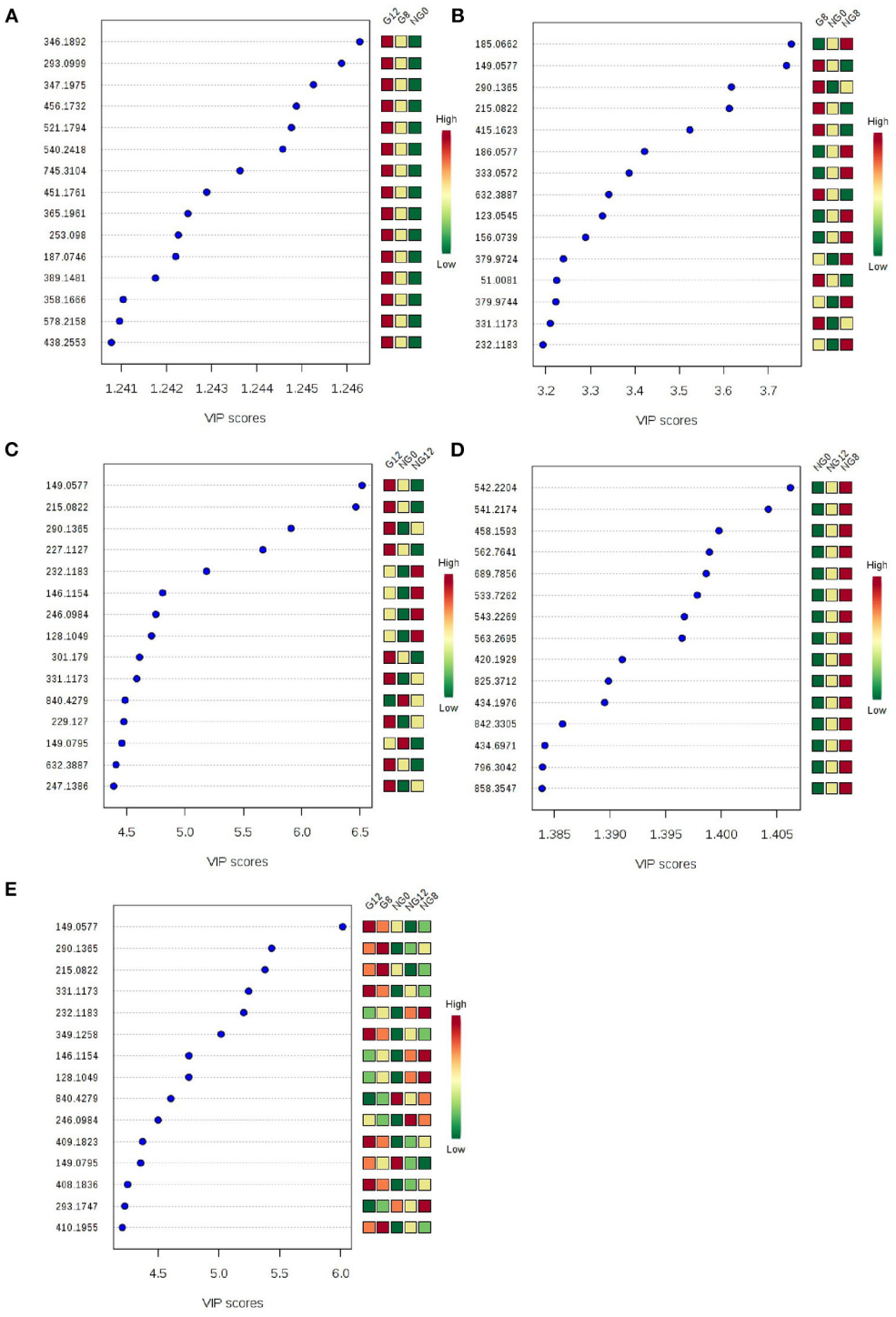

FIGURE 4 | PLS-DA-vip score of samples. **(A)** NG0-G8-G12; **(B)** NG0-G8-NG8; **(C)** NG0-G12-NG12; **(D)** NG0-NG8-NG12; **(E)** G8-G12-NG0-NG8-NG12. Part of the molecular weight list of VIP >1, the abscissa represents the VIP score value, the ordinate represents the molecular weight information of m/z, and the red and green on the right represent the expression level of m/z in the two groups.

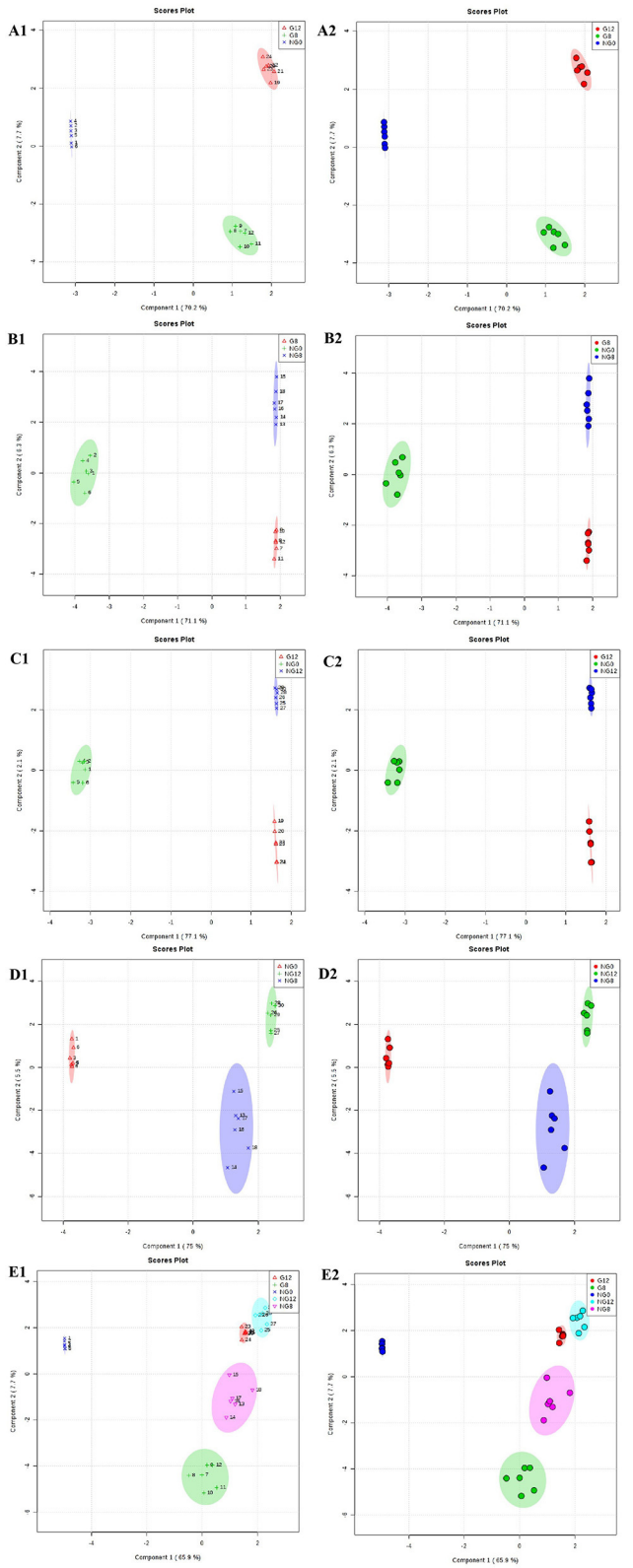

FIGURE 5 | OPLS-DA score plots for the data sets. **(A1,A2)** NG0-G8-G12; **(B1,B2)** NG0-G8-NG8; **(C1,C2)** NG0-G12-NG12; **(D1,D2)** NG0-NG8-NG12; **(E1,E2)** G8-G12-NG0-NG8-NG12. The OPLS-DA model shows significant differences among the different groups.

in **Figure 4**. Part of the molecular weight list of VIP >1, the abscissa represents the VIP score value; the ordinate represents the molecular weight information of m/z. **Figures 4A–E** showed that all the samples were different.

Furthermore, OPLS-DA was used to filter uncorrelated signals related to model classification. As shown in **Figures 5E1,E2**, OPLS-DA models showed a distinct separation between NG0-NG8-NG12-G8-G12 groups. Accordingly, there were significant differences among groups, and six repeated data points in each group were highly aggregated, indicating good repeatability. In addition, the components for different groups were separated with significant differences (**Figures 5A–D**).

Difference Analysis

In the analysis of ANOVA volcano graph, the *p*-value needed to be considered at the same time. After the ANOVA test data was converted into a negative logarithm base 10, the graph was shown in **Figure 6**. The NG0-G8-G12 groups (**Figure 6A**), NG0-G8-NG8 groups (**Figure 6B**), NG0-G12-NG12 groups (**Figure 6C**), NG0-NG8-NG12 groups (**Figure 6D**), and G8-G12-NG0-NG8-NG12 groups (**Figure 6E**) showed similar results. The red point represented $p < 0.05$, which meant there was a significant difference.

In the cluster analysis, all the metabolites obtained were subjected to two-way clustering of samples and metabolites, and the method used was hierarchical clustering. In **Figure 7**, the abscissa represented the sample number, and the ordinate represented the molecular weight of each metabolite. From the results shown in **Figure 7A**, it can be seen that G12 and G8 have similar metabolic profiles and were clustered together. G8-NG8 (**Figure 7B**), G12-NG12 (**Figure 7C**), NG12-NG8 (**Figure 7D**), and G12-G8-NG12-NG8 (**Figure 7E**) also had similar metabolic profiles.

Identification of Metabolites

After analysis of the metabolomics profiles of different groups, differential metabolites were selected based on VIP scores. A total of 2,509 differential metabolites were detected between NG8 and G8. Through the use of a fold-change >2, VIP >1, and $p < 0.05$, 817 differentially expressed metabolites were selected. More than 18 differential metabolites were screened according to superclass classification. A superclass pie chart of differential metabolites between NG8 and G8 is shown in **Figure 8A**. The metabolites included "lipids and lipid-like molecules" ($n = 185$, 23%); "phenylpropanoids and polyketides" ($n = 140$, 17%); "organoheterocyclic compounds" ($n = 136$, 17%); "organic acids and derivatives" ($n = 108$, 17%); "benzenoids" ($n = 85$, 10%); and "organic oxygen compounds" ($n = 82$, 10%).

A total of 2,488 differential metabolites was detected between NG12 and G12. Using a fold-change > 2, VIP > 1, and $p < 0.05$ as criteria, 628 differential metabolites were selected. More than 17 types of differential metabolites were screened according to superclass classification. A superclass pie chart of differential metabolites between NG12 and G12 is shown in **Figure 8B**. The metabolites included "lipids and lipid-like molecules" ($n = 147$, 23%); "phenylpropanoids and polyketides" ($n = 100$, 16%); "organoheterocyclic compounds" ($n = 98$, 16%); "organic acids

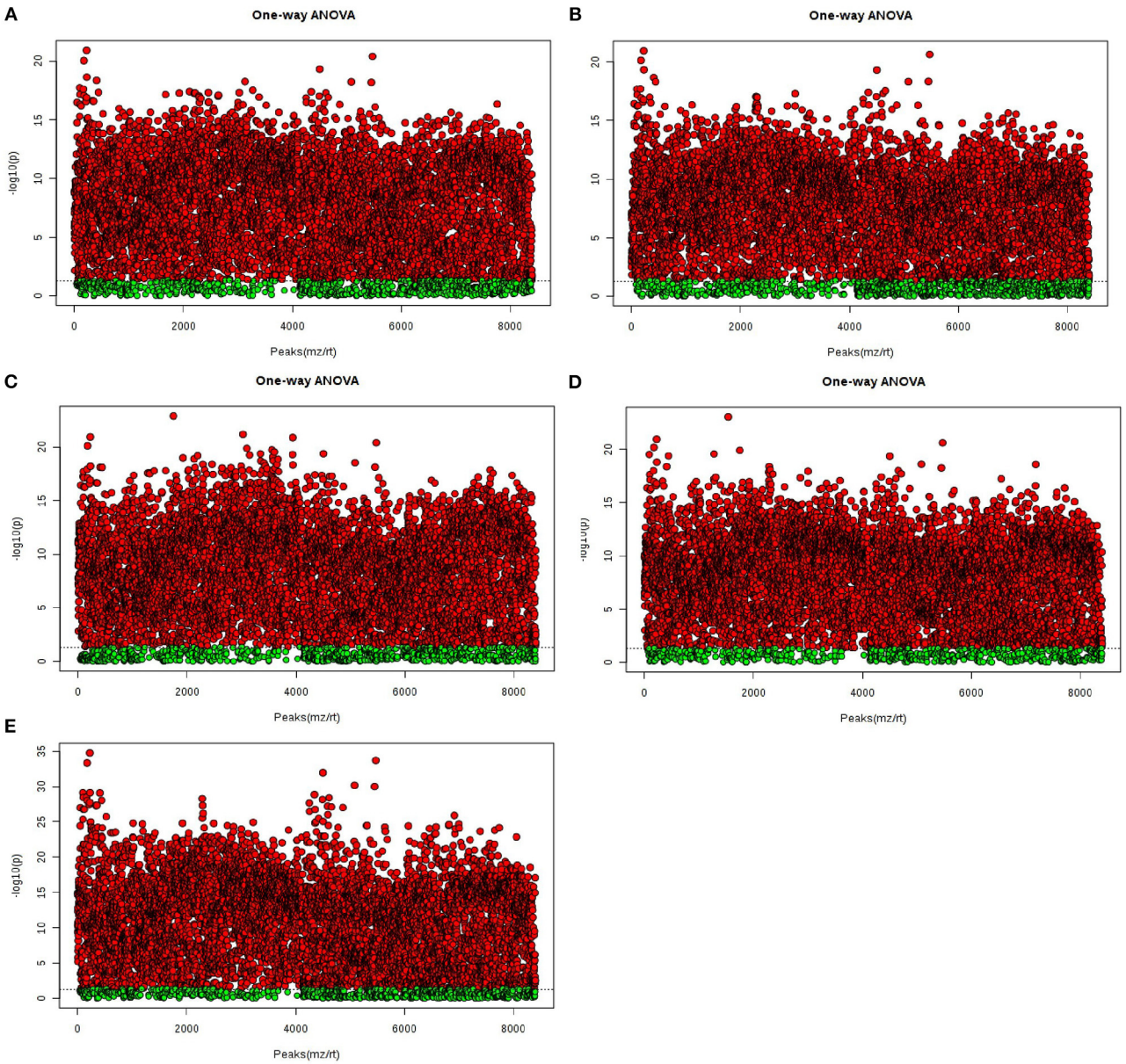

FIGURE 6 | The ANOVA volcano maps of samples. **(A)** NG0-G8-G12; **(B)** NG0-G8-NG8; **(C)** NG0-G12-NG12; **(D)** NG0-NG8-NG12; **(E)** G8-G12-NG0-NG8-NG12. The red point represents $p < 0.05$, which means there is a significant difference.

and derivatives" ($n = 77$, 14%); "benzenoids" ($n = 77$, 12%); and "organic oxygen compounds" ($n = 58$, 9%).

A total of 817 differential metabolites were putatively identified (VIP $>$ 1, $p < 0.05$) between NG8 and G8 and subsequently categorized in subclasses, including fatty acids and conjugates, amino acids, peptides, and analogs. Six differential metabolites were classified as fatty acids and conjugates (**Table 2**). A variety of metabolites were produced during the growth of microorganisms. Among them, fatty acids and conjugates were very common. Molds, bacteria, yeast, and some algae can produce lipid metabolites. Particularly, molds can produce many types of fatty acids, including many beneficial polyunsaturated fatty acids. *Monascus* is rich in polyunsaturated fatty acids, and unsaturated fatty acids may enhance the cholesterol-inhibiting effects of monacolin K. Fatty acids in *Monascus* mainly include C18:1, C18:2, C16:0, C18:0, and C16:1 (Dr et al., 1989). The pathway for the production of polyketide secondary metabolites by *Monascus* is related to the fatty acid production pathway because acetyl-CoA is a common initial substance for these two pathways. Acetyl-CoA is synthesized in the early fermentation period of *Monascus* and acetyl-CoA is mainly used to synthesize lipid compounds. At the end of fermentation, the fatty acid

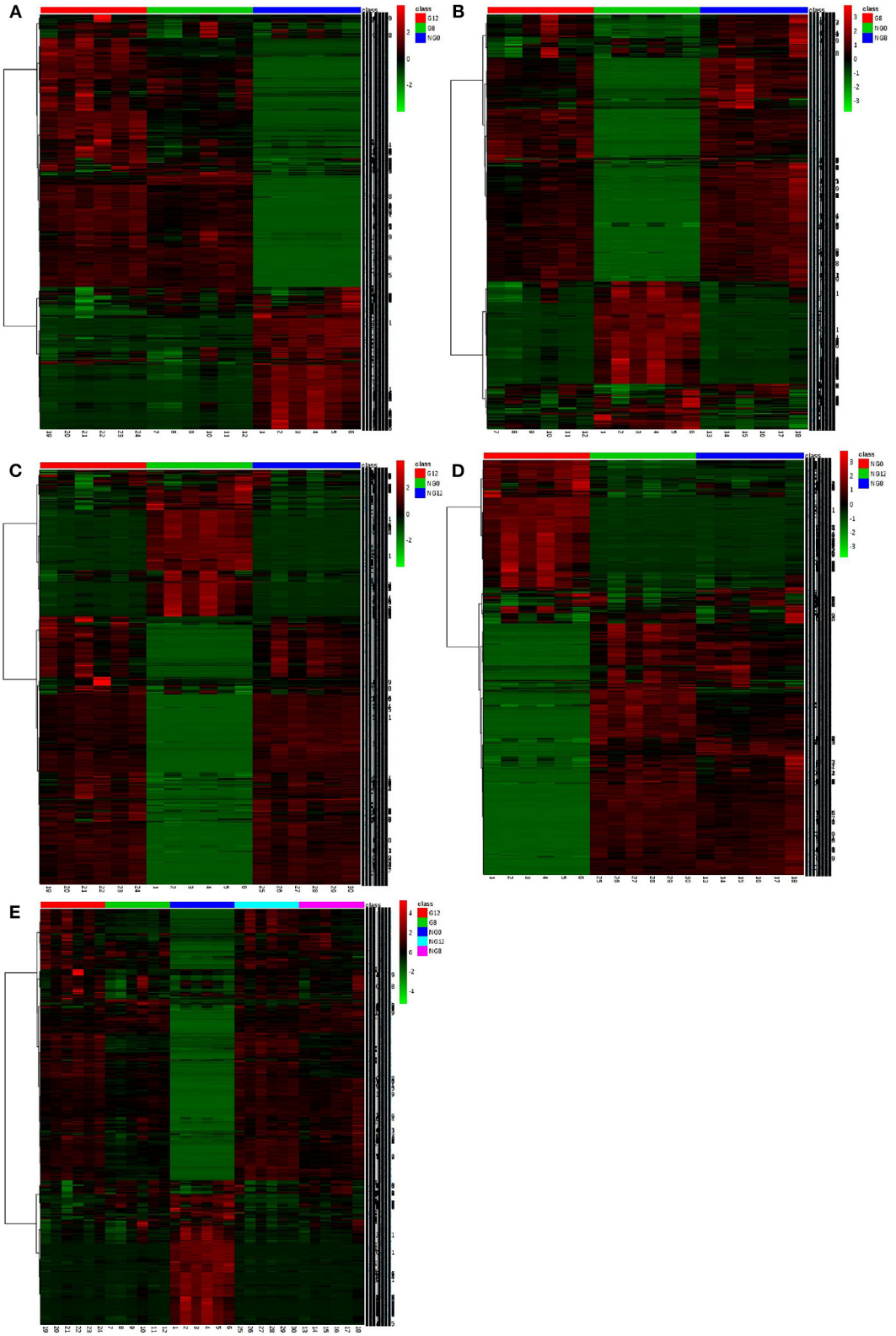

FIGURE 7 | The cluster maps of samples. **(A)** NG0-G8-G12; **(B)** NG0-G8-NG8; **(C)** NG0-G12-NG12; **(D)** NG0-NG8-NG12; **(E)** G8-G12-NG0-NG8-NG12. The abscissa represents the sample number, and the ordinate represents the molecular weight of each metabolite.

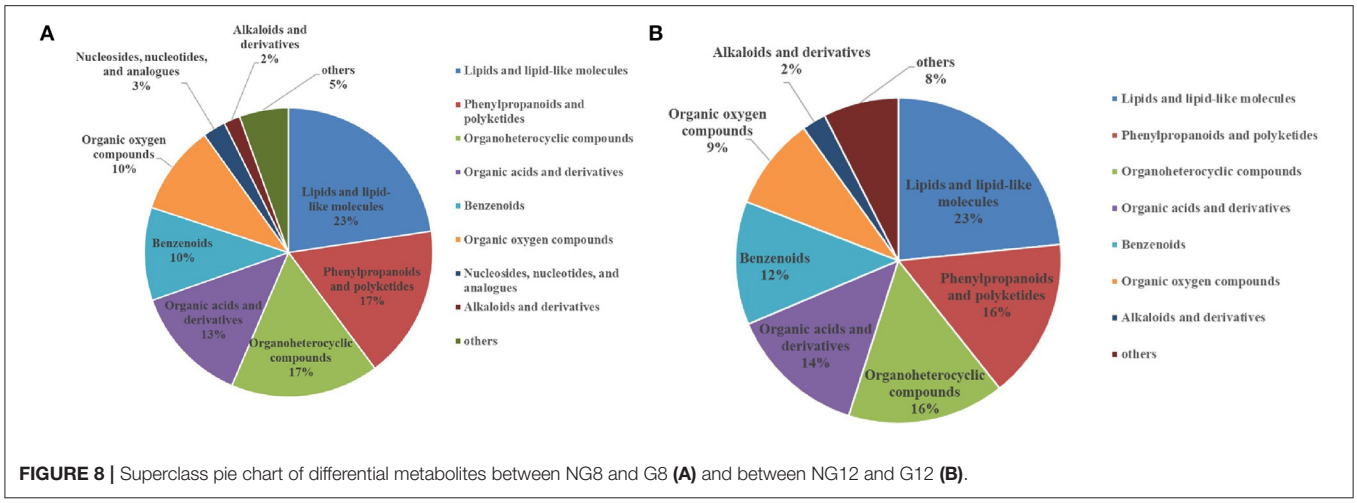

FIGURE 8 | Superclass pie chart of differential metabolites between NG8 and G8 **(A)** and between NG12 and G12 **(B)**.

TABLE 2 | Differential metabolites of fatty acids and conjugates among NG0-G8-NG8.

Compound name	Query mass	VIP	Formula	Peak area in NG0	Peak area in G8	Peak area in NG8
3-Dehydroxycarnitine	146.1154	2.5433	$C_7H_{15}NO_2$	55,558	97,272	121,302
Mevalonic acid	149.0795	2.3703	$C_6H_{12}O_4$	239,155	269,756	126,102
2-Hydroxyadipic acid	161.0456	1.6775	$C_6H_{10}O_5$	1,057,921	798,989	694,349
Petroselinic acid	280.2348	1.8957	$C_{18}H_{33}O_2$	901	19,043	37,173
Oleic acid	281.2466	1.8399	$C_{18}H_{34}O_2$	6737	13,077	29,831
12-Oxo-20-carboxy-leukotriene B4	363.18	2.447	$C_{20}H_{28}O_6$	17,560	34,749	78,353

contents were low; acetyl-CoA is mainly used to synthesize *Monascus* pigments (Somashekar and Joseph, 2000). As shown in differential metabolites of fatty acids and conjugates among NG0-G8-NG8 (**Table 2**), the contents of petroselinic acid and oleic acid decreased following the addition of glutamic acid. Acetyl-CoA was presumably mainly used to synthesize secondary metabolites in *Monascus*.

KEGG Pathway Analysis of Differential Metabolites

The pathway analysis of differential metabolites was performed using the KEGG database. As shown in **Figure 9**, many metabolic pathways were identified in this analysis. Among them, citric acid cycle, biotin metabolism, alanine, aspartate, and glutamate metabolism, one carbon pool by folate, sphingolipid metabolism, d-glutamine and d-glutamate metabolism, pyrimidine metabolism, d-arginine and d-ornithine metabolism, valine, leucine, isoleucine biosynthesis, pantothenate, and CoA biosynthesis were potential target pathways with a high impact and low false discovery rate.

Fermentation Test Results

The citric acid cycle is a cyclic reaction system composed of a series of enzymatic reactions, with the condensation reaction of acetyl-CoA and oxaloacetic acid as the initial reaction. Because acetyl-CoA is the common key substance of the citric acid cycle and monacolin K synthesis, it is speculated that the regulatory pathways of the citric acid cycle and monacolin K influence each other to a large extent. Therefore, we combined the differential metabolites obtained through metabolomics with the compounds involved in the citric acid cycle as screening conditions, and we selected malic acid, fumaric acid, α-ketoglutarate, and citric acid for fermentation experiment verification. In order to verify the above speculation, malic acid, fumaric acid, α-ketoglutarate, and citric acid were added to the original medium, and the change in the production of monacolin K cultured in the original medium was detected. **Figure 10A** shows that malic acid, fumaric acid, and citric acid have a promoting effect on the production of monacolin K. Among them, malic acid and fumaric acid had significant effects, and α-ketoglutarate inhibited the production of monacolin K. It was speculated that the accumulation of α-ketoglutarate inhibited the synthesis of acetyl-CoA, thereby inhibiting the production of monacolin K. The addition of the above four kinds of substances in the citric acid cycle had a certain influence on the synthesis of monacolin K, which also proved the mutual influence and effect of the citric acid cycle and the synthesis of monacolin K (**Figure 10B**).

DISCUSSION

The PCA and supervised PLS-DA were used in the multivariate analyses for this study. The PCA was a statistical analysis method for mastering the main contradictions of things. It could analyze the main influencing factors from multiple things, reveal the

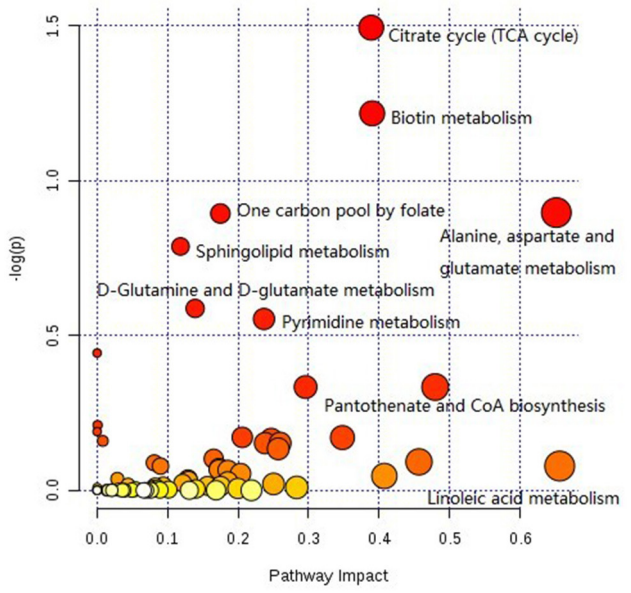

FIGURE 9 | KEGG pathway analysis diagram.

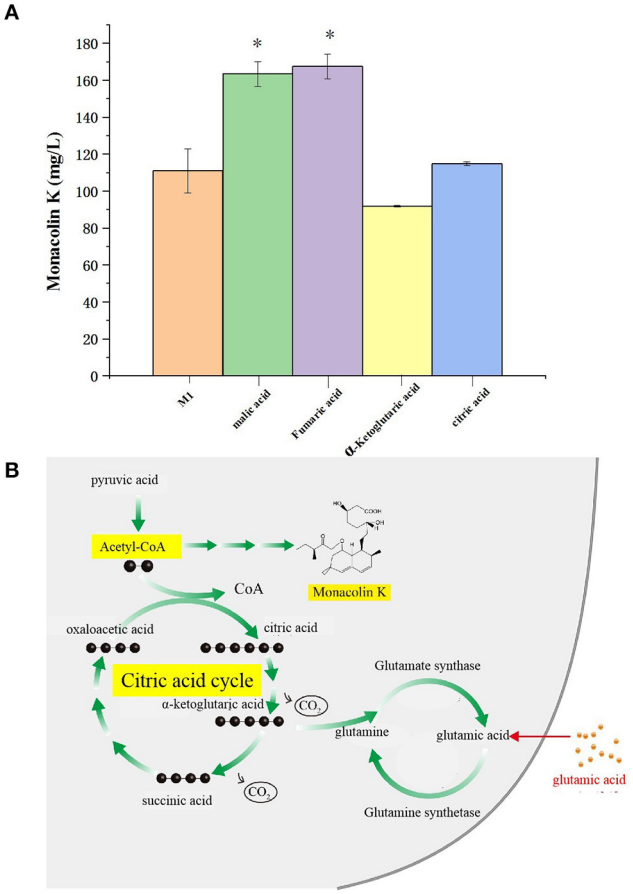

FIGURE 10 | (A) Effect of differential metabolite on the yield of monacolin K (* represents $p < 0.05$) and **(B)** schematic diagram to summarize the proposed model for the relationship among the citric acid cycle, acetyl-CoA, monacolin K, and any other metabolites.

essence of things, and simplify complex problems. The purpose of calculating the principal components was to project high-dimensional data into a lower-dimensional space to simplify the data and reduce the dimensionality. PCA is a multivariate statistical method that converts multiple variables into a few principal components (i.e., comprehensive variables) through dimensionality reduction technology. It is an unsupervised pattern recognition method.

Another common method of pattern recognition is the "supervised" pattern recognition method, which is a multivariate statistical method that first uses a set of samples or classifications with known results to establish a mathematical model and then uses several sets of independent and effective data to evaluate. PLS-DA has more obvious advantages than principal component analysis, that is, PLS has one more dependent variable "response" matrix than principal component analysis (PCA), so it has a predictive function.

The citric acid cycle is a key process in most plants, animals, fungi, and many bacteria (Enrique et al., 1996; Korla and Mitra, 2014; Wang et al., 2019). It consists of eight steps catalyzed by several enzymes. The citric acid cycle is initiated when acetyl-CoA reacts with oxaloacetate to form citrate. Acetyl-CoA is a common substance in the citric acid cycle and monacolin K biosynthetic pathways (Hajjaj et al., 1999). Accordingly, these two pathways may interact. Biotin participates extensively in the metabolic pathways of the three major nutrients as a coenzyme of acetyl-CoA. Under ammonium restriction, different proteins affecting the production of *Monascus* pigments mainly impact the glycolytic pathway, citric acid cycle, and fatty acid metabolic pathways.

A total of 6 differential metabolites related to the citric acid cycle were identified (fold-change > 2, VIP > 1, $p < 0.05$) between NG8 and G8, including fumaric acid, L-malic acid, oxoglutaric acid, *cis*-aconitic acid, citric acid, and thiamine pyrophosphate. The citric acid cycle acts as a central link between the metabolism of carbohydrates, lipids, and amino acids (Buchanan and Arnon, 1990). The metabolism of carbohydrates, lipids, and amino acids can produce acetyl-CoA, the initial substance in both the citric acid cycle and monacolin K biosynthetic pathways, as indicated above. Citric acid can promote the synthesis of monacolin K and influence the mycelial growth of *Monascus*. According to the previous experimental results, the addition of citric acid to the medium can increase the surface wrinkles of mycelium, and when the concentration of citric acid is 0.1%, the production of monacolin K is significantly increased, which is 2.7 times higher than that of the original medium. In addition, oxoglutaric acid is an intermediate metabolite in the citric acid cycle and a precursor for the synthesis of glutamic acid. In our study, the yield of monacolin K increased following the addition of glutamic acid. As shown in **Table 3**, the peak areas of fumaric acid, L-malic acid, *cis*-aconitic acid, citric acid, and thiamine pyrophosphate

TABLE 3 | Differential metabolites of the citric acid cycle between G8-NG8.

Compound name	Query mass	VIP	Delta (ppm)	Subclass	KEGG ID	Peak area in G8	Peak area in NG8
Fumaric acid	114.9919	2.7177	103	Dicarboxylic acids and derivatives	C00122	222,940	346,850
L-Malic acid	133.0141	1.1576	1	Beta hydroxy acids and derivatives	C00149	6832	7701
Oxoglutaric acid	145.0146	1.5621	3	Gamma-keto acids and derivatives	C00026	12,330	16,923
cis-Aconitic acid	173.0074	1.5026	10	Tricarboxylic acids and derivatives	C00417	12,083	10,545
Citric acid	191.0201	1.5945	2	Tricarboxylic acids and derivatives	C00158	40,736	64,824
Thiamine pyrophosphate	424.0083	1.5915	69	Pyrimidines and pyrimidine derivatives	C00068	18,584	20,018

decreased after the addition of glutamic acid. We hypothesized that the addition of glutamic acid inhibited the citric acid cycle, and more acetyl-CoA was used in the synthesis of monacolin K.

A total of 12 differential metabolites related to monacolin K were identified (fold change > 2, VIP > 1, $p < 0.05$) between NG8-G8-NG12-G12, including farnesyl pyrophosphate, natamycin, alpha-solanine, geranylgeranyl-PP, flavin mononucleotide, fumaric acid, L-malic acid, oxoglutaric acid, *cis*-aconitic acid, citric acid, dTDP-d-glucose, and 4,6-dideoxy-4-oxo-dTDP-d-glucose. Among these, farnesyl pyrophosphate, and geranylgeranyl-PP are non-fatty intermediate products in cholesterol synthesis (Takahashi, 1982). HMG-CoA reductase is an early rate-limiting enzyme in cholesterol synthesis, and monacolin K is a competitive inhibitor of HMG-CoA reductase (Chen and Hu, 2005; Niknejad et al., 2007). This is the first untargeted metabolomic profiling analysis of *Monascus* under different culture conditions by UPLC-Q-TOF-MS. In pathway analysis of differential metabolites using the KEGG database, we identified the citric acid cycle, biotin metabolism, alanine, aspartate, and glutamate metabolism as key pathways underlying differences among groups. Six differential metabolites related to the citric acid cycle were detected, including fumaric acid, L-malic acid, oxoglutaric acid, *cis*-aconitic acid, citric acid, and thiamine pyrophosphate. Five substances other than *cis*-aconitic acid decreased with the addition of glutamic acid. This study improves our understanding of secondary metabolites in *Monascus* in different culture conditions and benefits of *Monascus* in the food and pharmaceutical industries. Combined application of different "-omics" approaches, such as proteomics, metabolomics, and transcriptomics, can provide a more comprehensive view of the biochemical response in future studies.

DATA AVAILABILITY STATEMENT

The original contributions presented in the study are included in the article/supplementary materials, further inquiries can be directed to the corresponding author/s.

AUTHOR CONTRIBUTIONS

CZ, BS, and CW managed the project. NZ, MC, HW, and BW performed fungal culture, the secondary metabolites analysis, and the metabolomics results analysis in this work. HW and JS interpreted the analysis results and wrote the paper. All authors reviewed the manuscript.

FUNDING

This work was supported by the Beijing Natural Science Foundation (Grant No. KZ201810011015), Beijing Nova Program (Grant No. Z181100006218021), Support Project of High-level Teachers in Beijing Municipal Universities in the Period of the 13th Five-Year Plan (Grant No. CIT&TCD201804023), Quality Construction of Talent Cultivation—First-class Professional Construction (City Level)—Food Science and Engineering (Grant No. PXM2019_014213_000010), National Natural Science Foundation of China (Grant Nos. 31301411, and 32072345), National Key Research and Development Program (Grant Nos. 2016YFD0400802, 2016YFD0400502-02), The construct of innovation service ability—Science and Technology Achievement Transformation—Upgrade project (Grant No. PXM 2016-014213-000034), Beijing Municipal Science and Technology Project (Grant No. Z171100002217019), and Beijing Excellent Talents Training Project (Grant No. 2016000020124G025).

ACKNOWLEDGMENTS

Miss Anan Zhang (Beijing Technology & Business University, 11 Fucheng Road, Haidian District, Beijing, China) was thanked for the contribution of metabolomics results analysis in this study.

REFERENCES

Anagnostis, P., Paschou, S. A., Goulis, D. G., Athyros, V. G., Karagiannis, A. (2018). Dietary management of dyslipidaemias. Is there any evidence for cardiovascular benefit? *Maturitas* 108, 45–52. doi: 10.1016/j.maturitas.2017.11.011

Blanc, P. J., Laussac, J. P., Le Bars, J., Le Bars, P., Loret, M. O., Pareilleux, A., et al. (1995). Characterization of monascidin A from *Monascus* as citrinin. *Int. J. Food Microbiol.* 27, 201–213. doi: 10.1016/0168-1605(94)00167-5

Buchanan, B. B., and Arnon, D. I. (1990). A reverse KREBS cycle in photosynthesis: consensus at last. *Photosynthesis Res.* 24, 47–53. doi: 10.1007/BF00032643

Carneiro, S., Villas, B. S., Ferreira, E., and Rocha, I. (2012). Influence of the RelA activity on *E. coli* metabolism by metabolite profiling of glucose-limited chemostat cultures. *Metabolites* 2, 717–732. doi: 10.3390/metabo2040717

Chen, F., and Hu, X. (2005). Study on red fermented rice with high concentration of monacolin K and low concentration of citrinin. *Int. J. Food Microbiol.* 103, 331–337. doi: 10.1016/j.ijfoodmicro.2005.03.002

Chen, H. H., Chen, Y. Y., Yeh, Z. J., Jiang, C. M., and Wu, M. C. (2014). Immune-stimulated antitumor effect of different molecular weight polysaccharides from *Monascus purpureus* on human leukemic U937 cells. *CyTA J. Food.* 12, 134–140. doi: 10.1080/19476337.2013.805818

Chen, Y. P., Tseng, C. P., Liaw, L. L., Wang, C. L., Chen, I. C., Wu, W. J., et al. (2008). Cloning and characterization of monacolin K biosynthetic gene cluster from *Monascus pilosus*. *J. Agric. Food Chem.* 56, 5639–5646. doi: 10.1021/jf800595k

Diana, M., Quílez, J., and Rafecas, M. (2014). Gamma-aminobutyric acid as a bioactive compound in foods: a review. *J. Func. Foods*. 10, 407–420. doi: 10.1016/j.jff.2014.07.004

Dr, J. N., Yasuhiro, S., Jun, K., and Hiroshi, I. (1989). Cellular fatty acids composition of the genus *Monascus*. *J. Basic Microbiol*. 29, 369–374. doi: 10.1002/jobm.3620290615

Dudley, E., Yousef, M., Wang, Y., and Griffiths, W. J. (2010). Targeted metabolomics and mass spectrometry. *Adv. Protein Chem. Struc. Biol*. 80, 45–83. doi: 10.1016/B978-0-12-381264-3.00002-3

Endo, A. (1979). Monacolin K, a new hypocholesterolemic agent produced by a *Monascus* species. *J. Antibiot*. 32, 852–854. doi: 10.7164/antibiotics.32.852

Enrique, M. H., Waddell, T. G., and Cascante, M. (1996). The puzzle of the Krebs citric acid cycle: assembling the pieces of chemically feasible reactions, and opportunism in the design of metabolic pathways during evolution. *J. Mol. Evol*. 43, 293–303. doi: 10.1007/pl00006089

Hajjaj, H., Klaebe, A., Loret, M. O., Goma, G., Blanc, P. J., and Francois, J. (1999). Biosynthetic pathway of citrinin in the filamentous fungus *Monascus ruber* as revealed by 13C nuclear magnetic resonance. *Appl. Environ. Microbiol.* 65, 311–314. doi: 10.1128/AEM.65.1.311-314.1999

Johanningsmeier, S. D., Harris, G. K., and Klevorn, C. M. (2016). Metabolomic technologies for improving the quality of food: practice and promise. *Ann. Rev. Food Sci. Technol.* 7, 413–438. doi: 10.1146/annurev-food-022814-015721

Kalaivani, M., and Rajasekaran, A. (2014). Improvement of monacolin K/citrinin production ratio in *Monascus purpureus* using UV mutagenesis. *Nutrafoods* 13, 79–84. doi: 10.1007/s13749-014-0021-6

Kang, D., Kim, J., Choi, J. N., Liu, K. H., and Lee, C. H. (2011). Chemotaxonomy of *Trichoderma* spp. using mass spectrometry-based metabolite profiling. *J. Microbiol. Biotechnol.* 21, 5–13. doi: 10.4014/jmb.1008.08018

Keller, N. P., Turner, G., and Bennett, J. W. (2005). Fungal secondary metabolism—from biochemistry to genomics. *Nat. Rev. Microbiol.* 3:937. doi: 10.1038/nrmicro1286

Korla, K., and Mitra, C. K. (2014). Modelling the krebs cycle and oxidative phosphorylation. *J. Biomol. Struc. Dyn*. 32, 242–256. doi: 10.1080/07391102.2012.762723

Krairak, S., Yamamura, K., Irie, R., Nakajima, M., Shimizu, H., Chim-Anage, P., et al. (2000). Maximizing yellow pigment production in fed-batch culture of *Monascus sp. J. Biosci. Bioeng.* 90, 363–367. doi: 10.1016/S1389-1723(01)80002-5

Lee, C. L., Wen, J. Y., Hsu, Y. W., and Pan, T. M. (2018). The blood lipid regulation of Monascus-produced monascin and ankaflavin via the suppression of low-density lipoprotein cholesterol assembly and stimulation of apolipoprotein A1 expression in the liver. *J. Microbiol. Immunol. Infect*. 51, 27–37. doi: 10.1016/j.jmii.2016.06.003

Li, X. M., Shen, X. H., Duan, Z. W., and Guo, S. R. (2011). Advances on the pharmacological effects of red yeast rice. *Chin. J. Nat. Med*. 9, 161–166. doi: 10.3724/SP.J.1009.2011.00161

Lin, Y. L., Wang, T. H., Lee, M. H., and Su, N. W. (2008). Biologically active components and nutraceuticals in the monascus-fermented rice: a review. *Appl. Microbiol. Biotechnol.* 77:965. doi: 10.1007/s00253-007-1256-6

Liu, J., Lei, M., Zhou, Y., and Chen, F. (2019). A comprehensive analysis of the small GTPases Ypt7 involved in the regulation of fungal development and secondary metabolism in *Monascus ruber* M7. *Front. Microbiol.* 10:452. doi: 10.3389/fmicb.2019.00452

Niknejad, N., Morley, M., and Dimitroulakos, J. (2007). Activation of the integrated stress response regulates lovastatin-induced apoptosis. *J. Biol. Chem.* 282, 29748–29756. doi: 10.1074/jbc.M705859200

Nordström, A., Want, E., Northen, T., Lehtiö, J., and Siuzdak, G. (2008). Multiple ionization mass spectrometry strategy used to reveal the complexity of metabolomics. *Anal. Chem*. 80, 421–429. doi: 10.1021/ac701982e

Patel, S. (2016). Functional food red yeast rice (RYR) for metabolic syndrome amelioration: a review on pros and cons. *World J. Microbiol. Biotechnol*. 32:87. doi: 10.1007/s11274-016-2035-2

Patti, G. J., Yanes, O., and Siuzdak, G. (2012). Metabolomics: the apogee of the omics trilogy: Innovation. *Nat. Rev. Mol. Cell. Biol.* 13, 263–269. doi: 10.1038/nrm3314

Pérez-Jiménez, F., Pascual, V., Meco, J. F., Pérez Martínez, P., Delgado Lista, J., Domenech, M., et al. (2018). Document of recommendations of the SEA 2018. Lifestyle in cardiovascular prevention. *Clín. Investig. Arterioscler.* 30, 280–310. doi: 10.1016/j.artere.2018.11.001

Roze, L. V. (2010). Volatile profiling reveals intracellular metabolic changes in *Aspergillus parasiticus*: veA regulates branched chain amino acid and ethanol metabolism. *BMC Biochem*. 11:33. doi: 10.1186/1471-2091-11-33

Somashekar, D., and Joseph, R. (2000). Inverse relationship between carotenoid and lipid formation in Rhodotorula gracilis according to the C/N ratio of the growth medium. *World J. Microbiol. Biotechnol.*16, 491–493. doi: 10.1023/A:1008917612616

Stefanutti, C., Mazza, F., Mesce, D., Morozzi, C., Di Giacomo, S., Vitale, M., et al. (2017). *Monascus purpureus* for statin and ezetimibe intolerant heterozygous familial hypercholesterolaemia patients: a clinical study. *Atheroscler. Suppl*. 30, 86–91. doi: 10.1016/j.atherosclerosissup.2017.05.021

Su, Y. C., Wang, J. J., Lin, T. T., and Pan, T. M. (2003). Production of the secondary metabolites γ-aminobutyric acid and monacolin K by *Monascus*. *J. Indus. Microbiol. Biotechnol*. 30, 41–46. doi: 10.1007/s10295-002-0001-5

Takahashi, I. (1982). Prenyltransferases of bacillus subtilis: undecaprenyl pyrophosphate synthetase and geranylgeranyl pyrophosphate synthetase. *J. Biochem.* 92, 1527–1537. doi: 10.1093/oxfordjournals.jbchem.a134077

Vongsangnak, W., Hansen, K., and Nielsen, J. (2011). Integrated analysis of the global transcriptional response to α-amylase over-production by *Aspergillus oryzae*. *Biotechnol. Bioeng.* 108, 1130–1139. doi: 10.1002/bit.23033

Wang, W., Li, S., Li, Z., Zhang, J., Fan, K., Tan, G., et al. (2019). Harnessing the intracellular triacylglycerols for titer improvement of polyketides in Streptomyces. *Nat. Biotechnol.* 38, 76–83. doi: 10.1038/s41587-019-0335-4

Wiemann, P., Sieber, C. M., von Bargen, K. W., Studt, L., Niehaus, E. M., Espino, J. J., et al. (2013). Deciphering the cryptic genome: genome-wide analyses of the rice pathogen *Fusarium fujikuroi* reveal complex regulation of secondary metabolism and novel metabolites. *PLoS Pathog*. 9:e1003475. doi: 10.1371/journal.ppat.1003475

Wishart, D. S., Knox, C., Guo, A. C., Eisner, R., Young, N., Gautam B., et al. (2008). HMDB: a knowledgebase for the human metabolome. *Nucleic Acids Res.* 37, D603–D610. doi: 10.1093/nar/gkn810

Wu, C., Zacchetti, B., Ram, A. F., van Wezel, G. P., Claessen, D., and Hae Choi, Y. (2015). Expanding the chemical space for natural products by Aspergillus-Streptomyces co-cultivation and biotransformation. *Sci. Rep*. 5:10868. doi: 10.1038/srep10868

Zhang, C., Liang, J., Yang, L., Chai, S., Zhang, C., Sun, B., et al. (2017). Glutamic acid promotes monacolin K production and monacolin K biosynthetic gene cluster expression in monascus. *AMB Express* 7:22. doi: 10.1186/s13568-016-0311-z

Zhang, Y., Sun, S., Xing, X., Du, Z., Guo, Q., and Yu, W. (2016). Detection and identification of leachables in vaccine from plastic packaging materials using UPLC-QTOF MS with self-built polymer additives library. *Anal. Chem.* 88, 6749–6757. doi: 10.1021/acs.analchem.6b01027

Conflict of Interest: The authors declare that the research was conducted in the absence of any commercial or financial relationships that could be construed as a potential conflict of interest.

frontiers in Microbiology

HYPOTHESIS AND THEORY
published: 22 December 2020
doi: 10.3389/fmicb.2020.614910

Monascus sanguineus May Be a Natural Nothospecies

Yatao He[1,2†], Junlin Liu[1†], Qian Chen[1], Senning Gan[1], Ting Sun[1] and Shengdong Huo[1*]*

[1] College of Life Science and Engineering, Northwest Minzu University, Lanzhou, China, [2] Center for Life Sciences, School of Life Sciences, Yunnan University, Kunming, China

The genus *Monascus* has important economic and ecological values. In 2016, we isolated a strain *M. sanguineus*. After studying the phylogenetic relationship of *Monascus*, we believe that *M. sanguineus* is an independent species and speculate that it is a natural nothospecies. Recently, the morphological characteristics and sequences of seven genes (ITS, LSU, β-tubulin, calmodulin, RNA polymerase II subunit, β-ketoacyl synthase, and mating-type locus 1-1) of 15 *Monascus* strains were analyzed, including sequencing of multiple clones of five protein genes in four *M. sanguineus* strains. Two types of haplotypes (A and B) were observed in the five protein genes of *M. sanguineus*. Haplotype A was closely related to *M. ruber*, and haplotype B may be derived from an unknown *Monascus* species. The results demonstrated that *M. sanguineus* including type strains may be a natural nothospecies. This study laid the foundation for further exploration of the *M. sanguineus* genome, and the study may be of significant importance for the *Monascus* fermentation industry.

Keywords: *Monascus sanguineus*, phylogeny, morphology, nothospecies, fungi, natural pigment, industrial strain

OPEN ACCESS

Edited by:
Wanping Chen,
Georg-August-University Goettingen, Germany

Reviewed by:
Yanchun Shao,
Huazhong Agricultural University, China
Jiao Liu,
Hubei Academy of Agricultural Sciences, China

***Correspondence:**
Yatao He
hyt@mail.ynu.edu.cn
Shengdong Huo
huoshd@xbmu.edu.cn

[†]These authors have contributed equally to this work and share first authorship

Specialty section:
This article was submitted to Food Microbiology, a section of the journal Frontiers in Microbiology

Received: *07 October 2020*
Accepted: *24 November 2020*
Published: *22 December 2020*

Citation:
He Y, Liu J, Chen Q, Gan S, Sun T and Huo S (2020) Monascus sanguineus May Be a Natural Nothospecies. Front. Microbiol. 11:614910. doi: 10.3389/fmicb.2020.614910

INTRODUCTION

Monascus spp. are filamentous fungi first described by a French scientist Van Tieghem (1884). Having medicinal as well as edible uses, *Monascus* has been used in China for nearly 2000 years. Its use can be dated back to the Han dynasty (BC 202–AD 220). As a characteristic species, *Monascus*-fermented rice (also known as red yeast rice, a rice-based fermentation product) is widely consumed throughout East Asia and has a profound impact on local life and culture. *Monascus* has received worldwide attention because of its diverse products and rich beneficial metabolites. Its distribution ranges from the Korean Peninsula to the Malay Archipelago, and it is even spread globally (Lee and Pan, 2011, 2012; Shi and Pan, 2012; Chen et al., 2015). In industrial production, *Monascus* has three principal applications or products: starter culture (as a starter in various food fermentations), *Monascus*-fermented rice (as a food supplement), and functional food, which are widely used in brewing, food coloring, and healthcare industries. *Monascus* is an important source of numerous types of hydrolytic enzymes required in fermentation of foods (including red rice wine, red rice vinegar, Chinese spirits, fish paste, and fermented tofu). The beneficial secondary metabolites produced by *Monascus* mainly include *Monascus* pigments (food colorants and condiments), biofunctional components (including monacolins, γ-amino butyric acid, and dimerumic acid) (Feng et al., 2012; Hsu and Pan, 2012; Vendruscolo et al., 2014; Mérillon and Ramawat, 2017), and citrinin (safety disputed because of renal toxicity) (Kim et al., 2010; Li et al., 2012, 2015). More than one billion people have been estimated to eat *Monascus*-fermented products daily, with the most popular product being *Monascus*-fermented rice (Yang et al., 2015). Additionally, researchers have

found that *Monascus* has a mutually beneficial symbiotic relationship with some bees, indicating its important ecological value (Menezes et al., 2015; Barbosa et al., 2017).

The genus *Monascus* belongs to the family Aspergillaceae and order Eurotiales. It contains 36 species; however, many of them are considered synonymous (Shao et al., 2011, 2014). Based on the study by Barbosa et al. (2017), we preliminarily unified the phylogenetic relationships of the species within the genus *Monascus* and confirmed that *Monascus* includes the *Rubri* and *Floridani* sections. The *Rubri* section consists of three species and three varieties; the *Floridani* section consists of seven species, and additionally, one species speculated to be a natural nothospecies was found (He et al., 2018). In this study, to improve the phylogenetic relationship within *Monascus* and identify the parents of suspected nothospecies, we analyzed the sequences of the internal transcribed spacer (ITS), large subunit (LSU), beta-tubulin (*BenA*), calmodulin (*CaM*), RNA polymerase II subunit (*RPB2*), beta-ketoacyl synthase (*pksKS*), and mating-type locus 1-1 (*MAT1-1*) in 15 strains of *Monascus*. Based on a polyphasic approach combining sequence data with macroscopic and microscopic characters, it is speculated that *M. sanguineus* may be a natural nothospecies; *M. ruber* is one of its parents, and the other parent may be an unknown species.

MATERIALS AND METHODS

Strains

The strain *M. sanguineus* (CGMCC 3.19000 = RJL03) was isolated from the medicinal plant *Rehmannia glutinosa*. *M. purpureus* (Han01) was isolated from the commercially available Fujian (China) red yeast rice. The strain *M. sanguineus* (SICC 3.292) was purchased from the Sichuan Center of Industrial Culture Collection (SICC,[1], China), and the remaining 12 *Monascus* strains were purchased from the China General Microbiological Culture Collection Center (CGMCC,[2], China).

Cultivation and Morphological Analyses

For observing the colonial morphology, the 15 strains (**Table 1**) were cultured in three points on potato dextrose agar (PDA), malt extract agar (MEA), and Czapek yeast extract agar (CYA) plates at 30°C for 7 days. Macroscopic characteristics such as soluble pigments, color of the mycelium, and obverse and reverse colony colors were studied. Single colony diameters were measured after incubation for 7 days, and the average growth rate was calculated. The hyphae were observed by the transparent tape method using an optical microscope. A drop of lactophenol cotton blue stain was placed on a glass slide. The hyphae were adhered to a transparent tape. Ethanol was added dropwise to the surface of the hyphae, and they were placed on the slide with the drop of stain. The stain solution was added dropwise on the surface of the tape, which was later covered with a coverslip. Scanning electron microscopy revealed that the strains were cultured by insert coverslip. After the hyphae were climbed, the coverslips were gently removed for treatment. The coverslips with hyphae were fixed in 2.5% glutaraldehyde for more than 4 h and further rinsed 3 times with phosphate buffer. The coverslips with samples were dehydrated with graded concentrations of ethanol (50, 70, 80, 90, 95, and 100%) for 20 min for each concentration, transferred to pure isoamyl acetate for 1 h, and coated with gold–palladium. After pretreatment of the samples, morphological characteristics such as size, shape, and pigmentation of conidia, conidiophores, ascomata, asci, and ascospores were observed under the BME Biooptical microscope (Shanghai Leica Microsystems Co., Ltd., China) and SM-5600LV low vacuum scanning electron microscope (Japan Electronic Co., Ltd., Japan).

DNA Extraction, Amplification, Cloning, and Sequencing

Strains were grown on MEA for 7–14 days prior to DNA extraction. Genomic DNA was extracted using Fungi Genomic DNA Extraction Kit (Beijing Solarbio Science and Technology Co., Ltd., China) as per the manufacturer's instructions. DNA was amplified through polymerase chain reaction (PCR) using seven pairs of primers for seven genes (**Supplementary Table 1**). According to our study, cloning of PCR products was not required except for five protein genes in four *M. sanguineus* strains. At least 10 clones were randomly selected for each sample using the blue–white selection system, and both regular and clones were sequenced (Sangon Biotech Co., Ltd., Shanghai, China).

Sequence Alignment and Phylogenetic Analyses

Contings were assembled using the forward and reverse sequences with the SeqMan v.7.1.0. Analysis of homology of amplified products was studied using Blastn. Further, the sequences generated in this study were submitted to GenBank via the web tool BankIt or Sequin program. Sequence datasets were generated by combining the 197 newly generated sequences and 44 sequences that we deposited from GenBank (**Supplementary Table 2**). Sequence alignments were performed in MAFFT[3] and were manually optimized using MEGA 7. The best substitution model for each partition was inferred with the program MrModeltest 2.3. Phylogenetic trees were constructed through maximum likelihood (ML) analysis in raxmlGUI 1.5 using the GTRGAMMA substitution model and 1000 bootstrap replicates. Bayesian inference (BI) in MrBayes v.3.2.1 was performed using the Markov Chain Monte Carlo (MCMC) algorithm. Sequence format conversion was performed using Mesquite 3.10. Individual alignments were concatenated using Sequence Matrix v.1.7.8 for multilocus phylogenetic analyses. Each gene was analyzed separately, and further, two sequences with the highest rate of the two haplotypes were selected.

[1] http://www.sc-sicc.org.cn/

[2] http://www.cgmcc.net/

[3] https://mafft.cbrc.jp/alignment/server/

TABLE 1 | Strains used in this study.

Species	Strain numbers	Substrate	Location and date
Monascus ruber	CBS 135.60 = CGMCC 3.4701 ^{NT}	Soil	India, 1884
M. ruber	CGMCC 3.2093	Fermented grain	Guizhou, China, 1961
M. ruber	FWB13	Red yeast rice	Fujian, China, 2015
M. ruber var. albidulus	CGMCC 3.568 ^{T}	Fermented wheat grain	Liaoning, China, 1952
M. purpureus	CBS 109.07 = CGMCC 3.5833 ^{T}	Fermented rice grain	Indonesia, 1895
M. purpureus	YY-1	Food coloring Commercial strain	China, Unknown
M. purpureus	Han01	Red yeast rice	Fujian, China, 2018
M. purpureus var. rutilus	CGMCC 3.2636 ^{T}	Fermented grain	Fujian, China, 1961
M. purpureus var. aurantiacus	CGMCC 3.4384 ^{T}	Fermented grain	Anhui, China, 1980
M. sanguineus	IMI 356821 = CGMCC 3.5845 ^{T}	River sediment	Iraq, 1995
M. sanguineus	SICC 3.292	Fermented grain	Sichuan, China, 1960
M. sanguineus	CGMCC 3.2848	Fermented grain	Guangdong, China, 1970
M. sanguineus	CGMCC 3.19000 = RJL03	Tuber of *Rehmannia glutinosa*	Henan, China, 2016
M. floridanus	CBS 142228 = CGMCC 3.5843 ^{T}	Sand pine roots	United States, 1987
M. pallens	CBS 142229 = CGMCC 3.5844 ^{T}	River sediment	Iraq, 1995
M. lunisporas	CBS 142230 = CGMCC 3.7951 ^{T}	Moldy feed for race horses	Japan, 1998
M. argentinensis	CBS 109402 = CGMCC 3.7882 ^{T}	Soil	Argentina, 2004
M. mellicola	CBS 142364 ^{T}	Honey of *Melipona scutellaris*	Brazil, 2017
M. recifensis	CBS 142365 ^{T}	Pollen of *Melipona scutellaris*	Brazil, 2017
M. flavipigmentosum	CBS 142366 ^{T}	Inside nest of *Melipona scutellaris*	Brazil, 2017
Penicillium eremophilus	CBS 123361 ^{T}	Moldy prunes	Australia, 1988
P. verrucosum	CBS 603.74 ^{T}	Unknown source	Belgium, 1901
P. polonicum	CBS 222.28 ^{T}	Soil	Poland, 1927

T, type strain; NT, neotype strain; CBS, Culture collection of the Westerdijk Fungal Biodiversity Institute (formerly known as Centraalbureau voor Schimmelcultures), The Netherlands; CGMCC (AS), China General Microbiological Culture Collection Center (formerly known as Chinese Academy of Sciences), China; SICC, Sichuan Center of Industrial Culture Collection, China; IMI, International Mycological Institute, United Kingdom.

Data partitioning was performed to construct a multigene phylogenetic tree.

RESULTS AND DISCUSSION

Evidence for *M. sanguineus* as a Natural Nothospecies

Our analysis revealed two well-supported sections (*Rubri* and *Floridani*) in *Monascus*. Seven lineages are present in the section *Floridani* and these lineages are treated as separate species. *M. purpureus*, *M. sanguineus*, and *M. ruber* are located in the section *Rubri*. Also, the results of this study demonstrated that four *M. sanguineus* strains including the type strain may be natural nothospecies (not found in previous research data). Additionally, two types of haplotypes (A and B) were found after cloning and sequencing of five protein genes. Haplotype A was closely related to *M. ruber*. Haplotype B may be derived from an unknown *Monascus* species (**Figure 1** and **Supplementary Figure 1**). Haplotype B had a much higher red-pigment-producing ability than its suspected parent *M. ruber*, but its growth rate was lower than that of *M. ruber*. Thus, it was speculated that the yet unknown parent (*Monascus* sp.) of haplotype B confers the ability to produce red pigment. Additionally, the heterozygosity of the four *M. sanguineus* strains was notably different. For example, we had not cloned haplotype A of the strain CGMCC 3.5845; all SNPs were only observed at the corresponding sites in the direct sequencing of the five protein genes, and the two types of haplotypes between each hybrid strain were not completely consistent. For example, the results of cloning and sequencing demonstrated that the β-tubulin (*BenA*) gene of strain CGMCC 3.2848 had five haplotypes A and five haplotypes B (**Supplementary Figure 2**). For better understanding, an example of yeast (*Saccharomyces*) can be considered, which is similar to the *M. sanguineus* hybrid and has been studied in detail. The allopolyploid hybrid *S. pastorianus* was once considered the synonym of its parent strain *S. cerevisiae*; however, the parent strain *S. eubayanus*, with its most important low-temperature fermentation characteristics, was discovered after a long period (Bing et al., 2014; Wendland, 2014). Simple tests, such as DAPI staining to examine karyotypes and qPCR to assess fold changes in gene copy number, can be used to analyze the difference between chromosome ploidy in *M. sanguineus* and *M. ruber* (Waalwijk et al., 2018). It is speculated that in the previous study, the ribosomal ITS and LSU gene sequences could not distinguish between the hybrids *M. ruber* and *Monascus* sp., probably because in the chromosome of the hybrid, the chromosome containing the ribosomal RNA gene (rDNA) cluster from the *M. ruber* parent was substantially lost or reduced in length after hybridization. Referring to this example, to reflect the characteristics of *M. sanguineus* as a hybrid, we describe it as an independent species (*M. sanguineus*). The official DNA barcode for the fungal ITS region can recognize all *Monascus* species (including *M. purpureus* and *M. sanguineus*), but larger

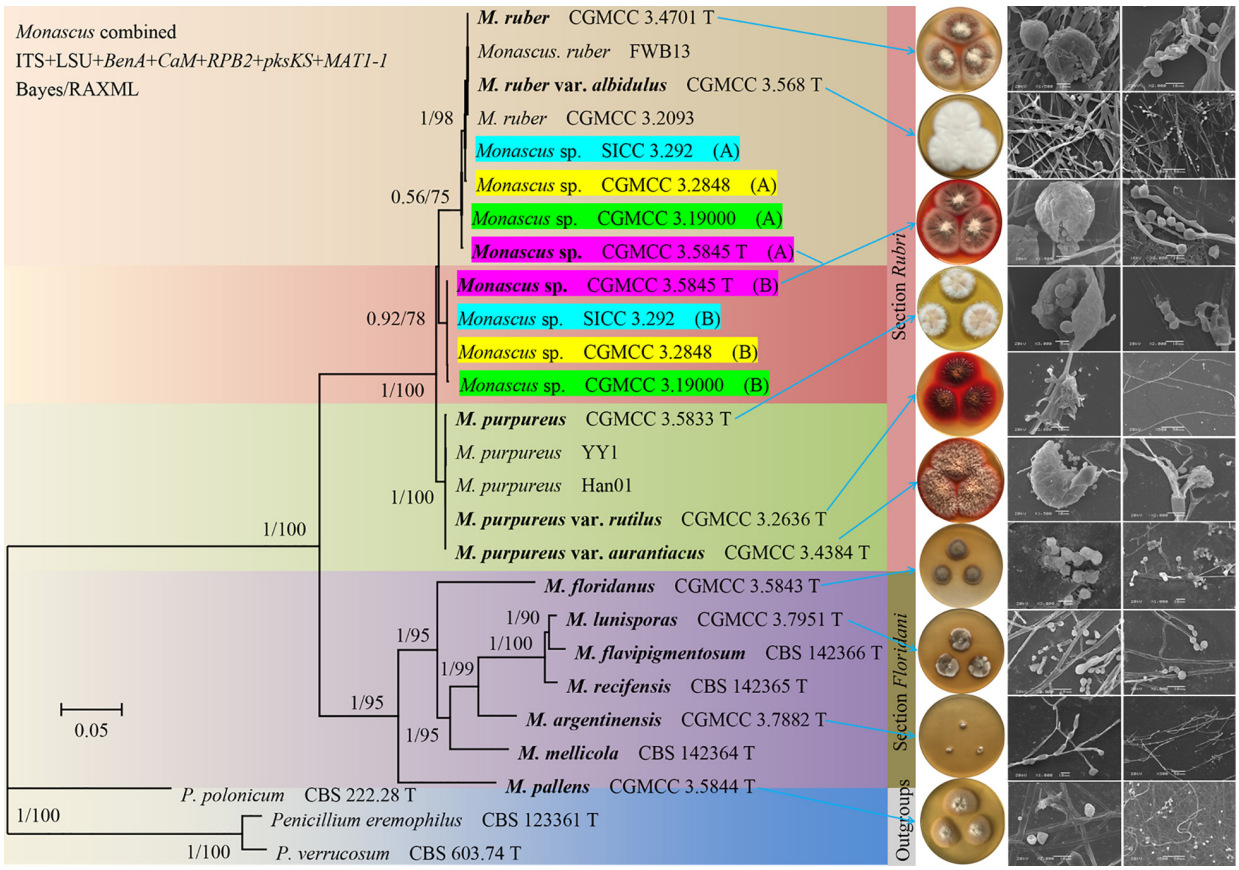

FIGURE 1 | Phylogeny of *Monascus*. Phylogenetic tree constructed from Bayesian analysis of the concatenated sequences of five protein genes (*BenA*, *CaM*, *RPB2*, *pksKS*, and *MAT1-1*) and two ribosomal RNA genes (ITS and LSU) with a total length of 6,983 bp. Posterior probabilities from Bayesian analysis/bootstrap percentages from 1,000 replicates of maximum likelihood analysis are shown on major branches. The right side of the figure is the cultural characters and scanning electron microscope structural of the strains indicated by the arrow. For the sake of illustration, the *M.* sp. CGMCC 3. 5845 (A) in the figure are manually supplemented.

sequence variations can be observed in the *BenA* gene. Therefore, we suggest that the *BenA* gene can be used as a secondary barcode for the identification of *Monascus* species, besides the methods based on morphological features (Barbosa et al., 2017).

Natural hybridization is very common in flowering plants. Approximately 25% of plant species are reported to hybridize with other species (Arnold, 1992; Mallet, 2005). Natural hybridization plays an important role in speciation, genetic exchange, and adaptive evolution. However, it can also lead to the extinction of rare species or generate super invasive species (Hegarty and Hiscock, 2007; Zhuang et al., 2019). *M. sanguineus* (CGMCC 3.5845) was first isolated from the sediments of the Arab River in Iraq in 1995 (Cannon et al., 1995) and was later reported in an Indian plant *Punica granatum* (Rashmi and Padmavathi, 2014). The SICC 3.292 strain was isolated from fermented grain in Sichuan Province in 1960, and the RJL03 strain was isolated from the plant *Rehmannia glutinosa* in our laboratory (He et al., 2019). Four *M. sanguineus* strains from different sources used in this study showed hybridization, indicating that hybrids may not have occurred by artificial breeding but by natural hybridization. However, the origin of its formation still needs to be studied. *M. sanguineus* was considered to be the synonym species of *M. purpureus*. This study demonstrated that *M. ruber* may be one of its parents, and there are some significant differences among the four *M. sanguineus* strains. We compared the morphological characteristics of two different *M. sanguineus* strains (CGMCC 3.5845 and CGMCC 3.2848) with *M. ruber* (CGMCC 3.4701) and *M. purpureus* (CGMCC 3.5833); the results showed that the morphological structure of the ascomata, ascospores, and conidium of the two hybrid strains was different from that of *M. ruber* and *M. purpureus*, but it was close to that of *M. ruber* (**Table 2**). Additionally, a significant difference was observed between the two hybrids; the three *M. sanguineus* strains grew faster than the type strain CGMCC 3.5845 (**Supplementary Figures 3**, **4**).

Urgent Need to Study the *M. sanguineus* Genome

With the sequencing of the *M. pilosus* genome in 2004, the study on *Monascus* has entered the era of genomics (data not

TABLE 2 | Morphological characteristics of some tested strains of *Monascus*.

Strain	Ascomata (μ m)	Ascospore (μ m)	Conidium (μ m)		Mycelium (μ m)	Growth rate (mm/d)
CGMCC 3.4701	Hyaline or orange 25–40	Ellipsoidal 4.5–5.5 × 5.5–7	Rough reticulate, globose to obpyriform 8–14 × 10–18	Single or up to 9 conidia in chain	Hyaline or light brown, Oleous 3–6	4.66
CGMCC 3.5833	Hyaline or reddish 25–65	Ellipsoidal 4–5.5 × 5–7	Smooth, globose to obpyriform 8–10 × 10–12	Single or up to 5 conidia in chain	Hyaline or light brown, Oleous 3–5	3.07
CGMCC 3.5845	Brown 32–60	Ellipsoidal 6–8 × 5.5	Rough reticulate, globose to obpyriform 10–14 × 8–10	Single or up to 10 conidia in chain	Hyaline or reddish, no oleous 3–4	2.80
CGMCC 3.2848	Brown or reddish 32–70	Ellipsoidal 6–7.5 × 4–5	Rough reticulate, globose to obpyriform 8–16.5 × 7.5–14	Single or up to 10 conidia in chain	Hyaline or reddish, no oleous 3–6	4.56

shown). Genomic sequencing of *M. ruber* (M7, NRRL 1597) and *M. purpureus* (NRRL 1596, YY-1) was completed. The average genome size was found to be 24.04 Mb, containing 7 or 8 chromosomes. The sketch genome coverage rate was approximately 95.6%. This gave us a deeper understanding of the physiology of *Monascus* and revealed new methods for strain improvement (Chen et al., 2015; Yang et al., 2015; Ding et al., 2016). However, only a few genes have been sequenced in *M. sanguineus*, and characteristics of the whole genome (genome size, chromosome number, and precise structure) remain undiscovered. We suggest that first, the genome of *M. sanguineus* should be sequenced, its ploidy should be determined, and comparative genomics studies should be conducted to compare its genomic sequence with that of other *Monascus* species (especially *M. ruber* and *M. purpureus*). Further, the structural features of two subgroups of hybrids (A and B subgenomes), the homology of the *M. sanguineus* subgroup and *M. sanguineus* should be analyzed, and it should be determined whether *M. ruber* is the ancestor of the *M. sanguineus* subgroup A while investigating the donor parent of subgroup B. In addition to its economic value, *Monascus* genomics research plays an important role in recognizing structural variability, integrating phenotype–genotype association, understanding the origin and evolution of the *Monascus* genome, and elucidating the genetic structure of some important traits. A comparative genomic study of *Monascus* species will enrich the knowledge about *Monascus* genetics and biology. Additionally, as an industrial strain, *Saccharomyces* has been studied in more detail; hence, the related research cases can be assessed in the study of *Monascus* genomics.

Monascus fermentation and its applications are the driving forces for research on *Monascus*. This study demonstrated that *M. sanguineus* may be a natural hybrid; we suggest to describe it as an independent species, and sequence analysis of its whole genome should be performed. In recent years, to analyze the regulation of secondary metabolites in *Monascus*, molecular biological studies such as those related to genes (clusters) of the main secondary metabolites of *Monascus*, biosynthetic pathways, and regulatory mechanism have made significant progress (Chen et al., 2017). At present, we can improve the production of beneficial metabolites of *Monascus* through strain selection, optimization of fermentation conditions, and genetic modification and effectively eliminate or reduce the content of citrinin in *Monascus* products. The completion of *Monascus* genome sequencing will greatly promote the studies on various aspects of *Monascus*, by which we can better understand the fermentation characteristics of different strains and molecular mechanisms underlying metabolite production and clarify the breeding and genetic transformation of *Monascus* strains. This will be beneficial for the *Monascus* fermentation industry. During the era of molecular biology, the aim was to establish the connection between *Monascus* genetics and biological performance. The studies on *Monascus* genomics will eventually boost *Monascus* research to a global level with clear goals. In the foreseeable future, the combination of genomics and molecular biology techniques will play a major role in *Monascus* research (Chen et al., 2015).

DATA AVAILABILITY STATEMENT

The datasets presented in this study can be found in online repositories. The names of the repository/repositories and accession number(s) can be found in the article/**Supplementary Material**.

AUTHOR CONTRIBUTIONS

YH and JL conceived and designed the experiment. YH, QC, SG, and TS carried out the experiment and performed the analysis. YH wrote the manuscript. JL and SH revised the manuscript. All authors discussed the results and commented on the manuscript.

FUNDING

This work was supported by the Laboratory Open Project of Northwest Minzu University (SYSKF-2018157); the National Trainning Program of Innovation and Entrepreneurship for Undergraduates (201810742120); and the Fundamental Research Funds for the Central Universities (31920190204).

ACKNOWLEDGMENTS

We gratefully thank Peijie Han (Institute of Microbiology, Chinese Academy of Sciences, China) for his help during the

research and TopEdit (www.topeditsci.com) for English language editing of this manuscript.

SUPPLEMENTARY MATERIAL

The Supplementary Material for this article can be found online at: https://www.frontiersin.org/articles/10.3389/fmicb.2020.614910/full#supplementary-material

Supplementary Figure 1 | Single gene phylogenetic trees of the ITS, LSU, *BenA*, *CaM*, *RPB2*, *pksKS*, and *MAT1-1* gene regions of species from *Monascus*.

Supplementary Figure 2 | Two haplotypes of the *BenA* gene of four *M. sanguineus* strains (only inconsistent sequences are retained after alignment).

Supplementary Figure 3 | Cultural characters of 15 *Monascus* strains cultured on MEA, PDA, and CYA media at 30°C for 7 days.

Supplementary Figure 4 | Mean growth rates (mm/d) of 15 *Monascus* strains cultured on PDA, MEA and CYA media at 30°C for 7 days.

Supplementary Table 1 | Genes sequenced and primers for PCR.

Supplementary Table 2 | GenBank accession numbers of sequences used in the molecular study.

REFERENCES

Arnold, M. L. (1992). Natural hybridization as an evolutionary process. *Annu. Rev. Ecol. Evol. S.* 85, 1893-1896. doi: 10.1146/annurev.es.23.110192.001321

Barbosa, R. N., Leong, S. L., Vinnere-Pettersson, O., Chen, A. J., Souza-Motta, C. M., Frisvad, J. C., et al. (2017). Phylogenetic analysis of *Monascus*, and new species from honey, pollen and nests of stingless bees. *Stud. Mycol.* 86, 29-51. doi: 10.1016/j.simyco.2017.04.001

Bing, J., Han, P., Liu, W., Wang, Q., and Bai, F. (2014). Evidence for a Far East Asian origin of lager beer yeast. *Curr. Biol.* 24, R380-R381. doi: 10.1016/j.cub.2014.04.031

Cannon, P. F., Abdullah, S. K., and Abbas, B. A. (1995). Two new species of *Monascus* from Iraq, with a key to known species of the genus. *Mycol. Res*. 99, 659-662. doi: 10.1016/s0953-7562(09)80523-6

Chen, W., Chen, R., Liu, Q., He, Y., He, K., Ding, X., et al. (2017). Orange, Red, Yellow: Biosynthesis of Azaphilone Pigments in *Monascus* Fungi. *Chem. Sci.* 8, 4917-4925. doi: 10.1039/c7sc00475c

Chen, W., He, Y., Zhou, Y., Shao, Y., Feng, Y., Li, M., et al. (2015). Edible filamentous fungi from the species *Monascus*: early traditional fermentations, modern molecular biology, and future genomics. *Compr. Rev. Food Sci. F.* 14, 555-567. doi: 10.1111/1541-4337.12145

Ding, X., Chen, W., and Chen, F. (2016). Karyotype analysis and chromosome localization of pigment and citrinin biosynthesis gene clusters of *Monascus ruber* M7. *Mycosystema* 35, 309-16. doi: 10.13346/j.mycosystema.140287

Feng, Y., Shao, Y., and Chen, F. (2012). *Monascus* pigments. *Appl. Microbiol. Biot.* 96, 1421-1440. doi: 10.1007/s00253-012-4504-3

He, Y., Gao, D., Gan, S., Sun, T., Cai, K., and Liu, J. (2019). Isolation and identification of a red pigment producer endophytic fungus *Monascus sanguineus* from *Rehmannia glutinosa* Libosch. *J. Zhejiang Univ.* 45, 1-7. doi: 10.3785/j.issn.1008-9209.2018.02.022

He, Y., Ran, Q., Liu, Y., Lan, Q., and Liu, J. (2018). Phylogenetic relationship of the genus *Monascus* in China based on multi-gene sequence analysis. *Mycosystema* 37, 1154-1169. doi: 10.13346/j.mycosystema.180091

Hegarty, M., and Hiscock, S. (2007). Polyploidy: Doubling up for Evolutionary Success. *Curr. Biol.* 17, R927-R929. doi: 10.1016/j.cub.2007.08.060

Hsu, W. H., and Pan, T. M. (2012). *Monascus purpureus*-fermented products and oral cancer: a review. *Appl. Microbiol. Biot.* 93, 1831-1842. doi: 10.1007/s00253-012-3891-9

Kim, J. Y., Kim, H. J., Oh, J. H., and Lee, I. (2010). Characteristics of *monascus* sp. isolated from *monascus* fermentation products. *Food Sci. Biotechnol.* 19, 1151-1157. doi: 10.1007/s10068-010-0164-1

Lee, C. L., and Pan, T. M. (2011). Red mold fermented products and Alzheimer's disease: a review. *Appl. Microbiol. Biot.* 91, 461-469. doi: 10.1007/s00253-011-3413-1

Lee, C. L., and Pan, T. M. (2012). Benefit of *Monascus*-fermented products for hypertension prevention: a review. *Appl. Microbiol. Biot.* 94, 1151-1161. doi: 10.1007/s00253-012-4076-2

Li, Y. P., Tang, X., Wu, W., Xu, Y., Huang, Z. B., and He, Q. H. (2015). The ctnG gene encodes carbonic anhydrase involved in mycotoxin citrinin biosynthesis from *Monascus* aurantiacus. *Food Addit. Contam. B* 32, 577-583. doi: 10.1080/19440049.2014.990993

Li, Y., Zhou, Y. C., Yang, M. H., and Ou-Yang, Z. (2012). Natural occurrence of citrinin in widely consumed traditional Chinese food red yeast rice, medicinal plants and their related products. *Food Chem.* 132, 1040-1045. doi: 10.1016/j.foodchem.2011.11.051

Mallet, J. (2005). Hybridization as an invasion of the genome. *Trends Ecol. Evol.* 20, 229-237. doi: 10.1016/j.tree.2005.02.010

Menezes, C., Vollet-Neto, A., Marsaioli, A. J., Zampieri, D., Fontoura, I. C., Luchessi, A. D., et al. (2015). A Brazilian social bee must cultivate fungus to survive. *Curr. Biol.* 25, 2851-2855. doi: 10.1016/j.cub.2015.09.028

Mérillon, J., and Ramawat, K. G. (2017). *Fungal Metabolites*. Switzerland: Springer International Publishing, 821-851.

Rashmi, D., and Padmavathi, T. (2014). Statistical optimization of pigment production by *Monascus sanguineus* under stress condition. *Prep. Biochem. Biotech.* 44, 68-79. doi: 10.1080/10826068.2013.792097

Shao, Y., Lei, M., Mao, Z., Zhou, Y., and Chen, F. (2014). Insights into *Monascus* biology at the genetic level. *Appl. Microbiol. Biot.* 98, 3911-3922. doi: 10.1007/s00253-014-5608-8

Shao, Y., Xu, L., and Chen, F. (2011). Genetic diversity analysis of *Monascus* strains using SRAP and ISSR markers. *Mycoscience* 52, 224-233. doi: 10.1007/s10267-010-0087-y

Shi, Y. C., and Pan, T. M. (2012). Red mold, diabetes, and oxidative stress: a review. *Appl. Microbiol. Biot.* 94, 47-55. doi: 10.1007/s00253-012-3957-8

Van Tieghem, M. (1884). *Monascus*, genre nouveau de l'ordre des Ascomycetes. *Bull. Soc. Bot. Fr.* 31, 226-231. doi: 10.1080/00378941.1884.10828230

Vendruscolo, F., Tosin, I., Admir José, G., Schmidell, W., and Ninow, J. L. (2014). Antimicrobial activity of *Monascus* pigments produced in submerged fermentation. *J. Food Process. Pres.* 38, 1860-1865. doi: 10.1111/jfpp.12157

Waalwijk, C., Taga, M., Zheng, S. L., Proctor, R. H., Vaughan, M. M. (2018). Karyotype evolution in fusarium. *IMA Fungus* 9, 13-26. doi: 10.5598/imafungus.2018.09.01.02

Wendland, J. (2014). Lager yeast comes of age. *Eukaryotic Cell* 13, 1256-1265. doi: 10.1128/EC.00134-14

Yang, Y., Liu, B., Du, X., Li, P., Liang, B., Cheng, X., et al. (2015). Complete genome sequence and transcriptomics analyses reveal pigment biosynthesis and regulatory mechanisms in an industrial strain, *Monascus purpureus* YY-1. *Sci. Rep.* 5:8331. doi: 10.1038/srep08331

Zhuang, W., Chen, H., Yang, M., Wang, J., Pandey, M.K., Zhang, C., et al. (2019). The genome of cultivated peanut provides insight into legume karyotypes, polyploid evolution and crop domestication. *Nat. Genet.* 51, 865-76. doi: 10.1038/s41588-019-0402-2

Conflict of Interest: The authors declare that the research was conducted in the absence of any commercial or financial relationships that could be construed as a potential conflict of interest.

frontiers in Microbiology

ORIGINAL RESEARCH
published: 06 January 2021
doi: 10.3389/fmicb.2020.579808

Chemical Characteristics of Three Kinds of Japanese Soy Sauce Based on Electronic Senses and GC-MS Analyses

Guozhong Zhao[1,2], Yixu Feng[2], Hadiatullah Hadiatullah[2], Fuping Zheng[1] and Yunping Yao[2]**

[1] Beijing Advanced Innovation Center for Food Nutrition and Human Health, Beijing Technology and Business University, Beijing, China, [2] State Key Laboratory of Food Nutrition and Safety, Key Laboratory of Food Nutrition and Safety, Ministry of Education, College of Food Science and Engineering, Tianjin University of Science & Technology, Tianjin, China

OPEN ACCESS

Edited by:
Xucong Lv,
Fuzhou University, China

Reviewed by:
Aly Farag El Sheikha,
Jiangxi Agricultural University, China
Guoliang Yan,
China Agricultural University, China
Li Li,
South China University of Technology, China

***Correspondence:**
Fuping Zheng
zhengfp@btbu.edu.cn
Yunping Yao
yaoyunping1314@tust.edu.cn;
yaoyunping1314@163.com

Specialty section:
This article was submitted to Food Microbiology, a section of the journal Frontiers in Microbiology

Received: *03 July 2020*
Accepted: *24 November 2020*
Published: *06 January 2021*

Citation:
Zhao G, Feng Y, Hadiatullah H, Zheng F and Yao Y (2021) Chemical Characteristics of Three Kinds of Japanese Soy Sauce Based on Electronic Senses and GC-MS Analyses. Front. Microbiol. 11:579808. doi: 10.3389/fmicb.2020.579808

Japanese soy sauce has become more acceptable by Chinese consumers due to its umami taste. However, the volatile flavor compounds and taste characters have not been fully clarified. This study aimed to explore the flavor characteristics of three kinds of Japanese soy sauce, including Koikuchi Shoyu, Usukuchi Shoyu, and Amakuchi Shoyu. The secret of volatile flavor substances was investigated by Gas Chromatography-Mass Spectrometry (GC-MS) and electronic nose, while taste compounds were investigated by silylation GC-MS and electronic tongue (E-tongue). A total of 173 volatile flavor substances and 160 taste compounds were identified. In addition, 28 aroma compounds with odor activity values (OAV) $\geq$ 1 were considered as the typical flavors. We found that alcohols and aldehydes were in high abundance in Japanese soy sauce, but only a small portion of pyrazines and esters were. Based on electronic nose and GC-MS analysis, Koikuchi Shoyu gives more contribution to aroma compounds, while Usukuchi Shoyu and Amakuchi Shoyu give the sourness and sweetness features based on E-tongue and silylation GC-MS analysis. In this study, 50 kinds of sugars were detected that contributed to the sweetness of soy sauce. This study will provide new insight into the flavor characteristics of Japanese soy sauce that potentially contribute to the innovation and development of soy sauce.

Keywords: soy sauce, flavor, taste, GC-MS, aroma

INTRODUCTION

Soy sauce, produced mainly in China or Japan, is widely consumed as a food condiment or seasoning in Asian countries and other neighboring countries, to improve the appetite, desirable flavor, and digestion. The quality of soy sauce may determine its acceptability to consumers, which has given manufacturers a new challenge. Nowadays, Japanese soy sauce has attracted more attention due to its unique and high-quality flavor. The fermentation method of soy sauce has been modified in Japan, but it is still traditional in China today. Japanese soy sauce has improved the brewing process, which has been introduced in some factories in China.

Soy sauce is commonly made from soybeans and wheat, fermented by *Aspergillus oryzae* for koji, with the addition of 18% saline water for moromi. Lactobacilli and yeast are selectively used during moromi fermentation (Kataoka, 2005). Three typical varieties of Japanese soy sauce favored in different areas of Japan, such as Koikuchi Shoyu (eastern Japan), Usukuchi Shoyu (midwestern Japan), and Amakuchi Shoyu (southern Japan), are well recognized by Chinese consumers. Furthermore, these kinds of soy sauce can be easily purchased in China from offline or online markets, such as Taobao. Koikuchi Shoyu is dark-colored with a slightly fruity flavor and is made from a high percentage of soybeans, which reduces fishy and meaty smells in cooking. It is suitable for stew meat and barbecue seasoning. Usukuchi Shoyu has a lighter color and saltier taste than Koikuchi Shoyu. It is commonly used for udon noodle soup, chawanmushi, and simmered seasoning (nimono). Amakuchi Shoyu is a light-colored and sweet soy sauce that represents an ideal match with seafood seasoning. However, the differences in flavor compounds lead to a complicated usage scale of these kinds of soy sauce.

Several important aroma compounds of soy sauce have been detected. 5(or 2)-ethyl-4-hydroxy-2(or 5)-methyl-3(2*H*)-furanone (4-HEMF), a caramel-like aroma, is one of the most essential aroma compounds in soy sauce, and it was also detected in Koikuchi Shoyu and Usukuchi Shoyu (Kaneko et al., 2012). Volatile phenols such as 4-vinylguaiacol (4-VG) and 4-ethylguaiacol (4-EG) are produced by *Candida versatilis* during moromi fermentation (Suezawa and Suzuki, 2007). In our previous study, some typical fragrant compounds with aromatic rings, such as phenylacetaldehyde, 2-phenylethanol, and phenylethyl acetate, accounted for a large proportion of the flavors of traditional Chinese-type soy sauce (Zhao et al., 2020). To date, over 400 flavor compounds have been detected in soy sauce, and other more important flavors are continually being discovered (Meng et al., 2014). The flavor and taste compounds of the three kinds of Japanese soy sauce were not fully clarified in the previous study. Therefore, this investigation of the flavor and taste is necessary and will help us to improve the flavor of our products. The research will contribute to the innovation of traditional industries in China.

In this study, an electronic nose and electronic tongue (E-tongue), combined with GC-MS, were used to determine the secret of volatile flavor substances and taste compounds of Koikuchi Shoyu, Usukuchi Shoyu, and Amakuchi Shoyu, which could uncover the mystery of Japanese soy sauce for different kinds of dishes.

MATERIALS AND METHODS

Materials

Three kinds of Japanese soy sauce were purchased online (Taobao) and divided into three groups. Koikuchi Shoyu was named S1, Usukuchi Shoyu S2, and Amakuchi Shoyu S3. GC-grade of 2-octanol and N,O-bis(trimethylsilyl)trifluoroacetamide and trimethylchlorosilane (BSTFA + 1% TMCS, 99:1) were purchased from Sigma (Sigma Aldrich Co., St. Louis, MO, United States). N, N-dimethylformamide (DMF) (99%) was purchased from damas-beta (Adamas Reagent, Ltd.). Heptadecanoic acid (98%) was purchased from Alfa Aesar (Ward-Hill, MA, United States).

Electronic Nose Analysis

Portable electronic nose 3 (PEN 3, Airsense Co., Germany), which assembles 10 sensors for different application targets, was applied for detection. A soy sauce sample (5 ml) was carefully transferred into the sealed bottle for electronic nose (E-nose) detection and then soaked in a water bath (50°C) for 20 min. The cleaning process was maintained for 220 s to exclude impurities. After being cleaned to the baseline, the samples were detected and persisted for 120 s until sensors reached stable values. The headspace flavor compounds were pumped into the sensor chamber at a constant rate of 300 ml/min. The cleaning procedure was repeated after completion of the detection. Each sample was carried out in triplicate.

GC-MS Analysis

A soy sauce sample (5 ml) was carefully transferred into a bottle with sufficient headspace (20 ml) with a small magnetic stir bar. Compound 2-octanol was selected and injected into the bottle as the internal standard substance. Then, the bottle was soaked in a water bath (60°C) with a magnetic stirring apparatus (250 rpm) (IKA, RCT Basic, Staufen, Germany). After 30 min balancing, the cap seal was punctured by a 50/30 μm DVB/CAR/PDMS extraction fiber (Supelco, Inc., Bellefonte, PA, United States), which was exposed above the soy sauce sample for absorption for 30 min. Then, the solid-phase microextraction (SPME) fiber was removed and inserted into the heated injector of GC-MS (QP2010 Ultra, Shimadzu Co., Kyoto, Japan) with 15 min desorption time. The separation was performed with a low-polarity Rtx-5ms column (30 m × 0.25 mm × 0.25 μm) (Restek Co., Bellefonte, PA, United States). The column temperature was programed at 40°C for 3 min and then increased to 150°C at a rate of 4°C/min for 1 min. At the final stage, the temperature was increased to 250°C at a rate of 8°C/min for 6 min with the nitrogen as the carrier (N2 99.99%, 3.5 ml/min). The ionization voltage of the mass spectrometer (MS) was set at 70 eV. The test voltage was 0.8 kV, and the scan area was 29–500 u. Flavor compounds were identified based on RI by comparing the experimental spectra of reference standards with matches in the standard NIST 17 library. The similarity of flavor compounds was detected over 80% of the standard spectra library.

Electronic Tongue Analysis

Electronic tongue Taste-Sensing system SA 402B (Intelligent Sensor Technology Co. Ltd., Japan) equipped with five test sensors (CA0, C00, AE1, CT0, and AAE) and two reference electrodes Cai was used in this study following Cai et al. (2020). The taste sensors were, namely, CA0 specific for sourness, C00 for bitterness and aftertaste bitterness (aftertaste-b), AE1 for astringency and aftertaste astringency (aftertaste-a), CT0 for saltiness, and AAE for umami and richness (aftertaste of umami). The sensor array was initially immersed into a sample (30 ml) as the reference solution, then continuously treated into other sample solutions for 120 s. The sensor array was rinsed with

a sensor cleaning solution containing 5% ethanol until a stable potential was obtained. Each sample was carried out in triplicate.

Silylation Derivatization Procedure and GC-MS Detection

A soy sauce sample (50 μl) was transferred into a 1.5 ml EP tube and frozen for 6 h at -80°C, and then treated by vacuum freeze-drying for 12 h. DMF (100 μl) (Sigma, United States) was added to dissolve the freeze-dried sample. The mixture was treated by an ultrasonic oscillator (YH-200DH, Shanghai, China) for 15 min and then vibrated with a vortex oscillator (Vortex-Genie 2, United States) for 5 min to make the sample fully dissolved. Finally, the sample was centrifuged at 12,000 rpm for 3 min. The supernatant (50 μl) was transferred into a new EP tube and then mixed with 100 μl N,O-Bis(trimethylsilyl)trifluoroacetamide with 1% trimethylchlorosilane (BSTFA + 1%TMCS, 99:1) (Sigma, United States) and 5 μl heptadecanoic acid solution (the internal standard substance, dissolved in DMF solution, 10 mg/ml). After being heated in the water bath (70°C) for 2 h, 1 μl sample was absorbed after cooling down to the room temperature for GC-MS analysis (Agilent Technologies, Santa Clara, CA, United States). Helium was used as a carrier gas at a constant flow rate of 1 ml/min. Oven temperature was maintained at 70°C for 8 min, programed at 3°C/min to 190°C and then raised to 300°C with a rate of 10°C/min and held for 11 min. The MS was operated in electron impact mode with the electron energy set at 70 eV and a scan range of 43–1,000 m/z (scan rate: 4.37 scans/sec, gain factor: 1, resulting EM voltage: 1,188 V). The temperatures of MS source and quadrupole were set at 230 and 150°C, respectively. The components of the compounds were preliminarily identified according to the published data, retention time, and mass spectra of real compounds. The substances with a similarity of more than 70% were selected.

Statistical Analysis

All tests were conducted in triplicate; significant differences were tested by analysis of variance (ANOVA) using SPSS 17.0 (SPSS Statistics, Chicago, IL, United States) at $p < 0.05$, and Tukey's test was applied to compare average values. Data analysis of the electronic nose was based on pattern recognition software (Win Muster) provided by the PEN3 e-nose device (Schwerin, Germany). Principal component analysis (PCA) was also achieved by using SPSS 17.0. PLSR analysis was based on Unscrambler 10.4 (CAMO ASA, Oslo, Norway). The rest of the other figures were drawn by Origin 8.5 (OriginLab, MA, United States).

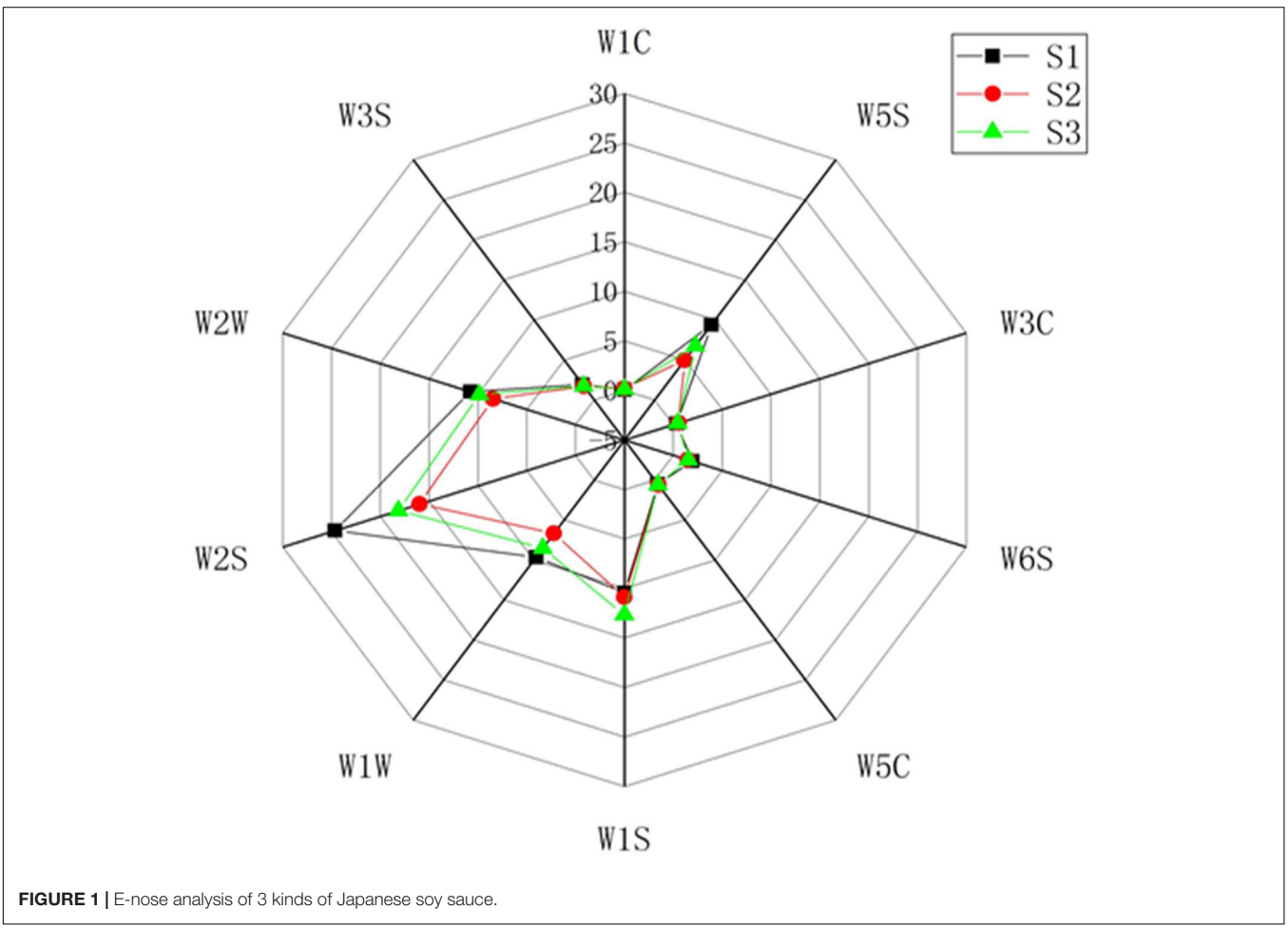

FIGURE 1 | E-nose analysis of 3 kinds of Japanese soy sauce.

RESULTS AND DISCUSSION

Koikuchi Shoyu Showed Significant Contribution in Aroma by E-Nose Analysis

The total volatile compounds of soy sauce samples were distinguished by E-nose (**Figure 1**). PCA and loading analysis (LDA) were used to discriminate these samples according to the differences between volatile compounds and signal intensities. The migration of different samples along principal components 1 and 2 (PC1 and PC2) accounted for 96.04 and 3.36% of the total variance, respectively (**Supplementary Figure 1A**). The measurement results overlapped; however, the degree of separation between the samples was noticeable. These three groups of samples were clearly distinguished by LDA, which showed the significant differences among S1, S2, and S3 (**Supplementary Figure 1B**). The 10 important sensors were compared by LDA, which is useful for identifying the important sensors according to the values of loading parameters for a particular principal component, which might be responsible for discrimination in the current pattern file (Gao et al., 2017). W2S, W1S, W1C, W5S, W1W, and W2W had much greater influence on the current pattern file than the others, with the contribution of W2S being the most obvious sensor for characterization (**Supplementary Figure 1C**). The results showed that Koikuchi Shoyu had more advantages in aroma than two other Japanese soy sauce, Usukuchi Shoyu and Amakuchi Shoyu. The W2S sensor was more sensitive in S1 than others to compounds such as alcohols, aldehydes, and ketones, indicating that more oxygenated compounds exist in Koikuchi Shoyu. W5S was sensitive to nitrogen oxides, which are also indicated in Koikuchi Shoyu. The relatively high response values of W1W and W2W in S1 indicate that sulfides play a vital role in Koikuchi shoyu. Low sensitivity to methane or methyl substances was found in Koikuchi shoyu, but its benefit remains in the aroma.

Aroma Compounds Were More Typical in Koikuchi Shoyu by GC-MS Analysis

A total of 173 volatile flavor compounds were detected, including 35 alcohols, 60 esters, 26 aldehydes, 10 acids, 22 ketones, 8 phenols, 4 ethers, and 8 heterocycles (**Supplementary Table 1**). Significant differences in the contents of volatile compounds were found among these soy sauces. Alcohols were the most abundant volatile compounds in S1 and S3, followed by esters

TABLE 1 | Flavor compounds with OAV ≥ 1 in soy sauce.

CAS	Compounds	Concentration (mg/l)			Odor threshold	OAV		
		S1	S2	S3		S1	S2	S3
112-53-8	1-Dodecanol	0.04	0.14	0.20	0.016	2.28	8.84	12.64
123-51-3	Isoamylol	1.40	0.43	0.75	0.004	351.11	108.20	186.34
137-32-6	2-Methylbutan-1-ol	0.64		0.41	0.0159	40.42		25.75
24347-58-8	(R,R)-butane-2,3-diol	3.90	0.20	0.78	0.0951	41.03	2.15	8.18
505-10-2	3-(Methylthio)-1-propanol	0.22			0.12323	1.81		
60-12-8	Phenylethyl alcohol	2.07	2.19	1.66	0.56423	3.67	3.89	2.94
71-41-0	1-Pentano1		0.19	0.15	0.1502		1.29	1.03
104-61-0	gamma-Nonanolactone	0.03	0.03		0.0097	3.13	3.48	
105-54-4	Ethyl butyrate	0.00			0.0009	4.23		0.00
108-64-5	Ethyl isovalerate	0.01			0.00001	721.85		
141-78-6	Ethyl acetate	1.37	0.36	2.51	0.005	273.53	71.24	502.49
544-35-4	Linoleic acid ethyl ester	0.24	2.03	11.65	0.45	0.53	4.51	25.88
106-32-1	Octanoic acid, ethyl ester		0.03		0.0193		1.59	
111-62-6	Ethyl oleate		0.19	1.32	0.87		0.21	1.51
105-57-7	Acetal	0.04		0.11	0.0049	8.10		22.89
112-31-2	Decanal	0.01	0.04	0.04	0.003	3.36	12.82	13.25
122-78-1	Benzeneacetaldehyde	1.35	1.24	1.06	0.0063	213.62	196.75	168.71
3268-49-3	Methional	0.11			0.00045	251.92		
590-86-3	Isovaleraldehyde	1.44	0.90	1.64	0.0011	1307.73	819.42	1491.83
66-25-1	Hexanal	0.01			0.005	1.13		
78-84-2	Isobutyraldehyde	0.89		0.62	0.0015	596.35		413.57
96-17-3	2-Methylbutyraldehyde	1.57	0.55	1.92	0.001	1565.32	552.94	1922.52
124-19-6	Nonanal		0.02		0.0011		22.61	
27538-09-6	HEMF	0.11	0.08	0.07	0.00115	93.53	66.37	64.48
4485-09-0	4-Nonanone		0.31		0.0082		38.26	
2785-89-9	4-Ethylguaiacol	1.94	1.16	0.69	0.0695	27.82	16.65	9.99
7786-61-0	2-Methoxy-4-vinylphenol	6.58	4.56	1.44	0.01202	547.32	379.65	120.10
90-05-1	Guaiacol	0.07	0.06		0.00048	151.30	115.86	

and aldehydes. In all, 28 aroma compounds with OAV ≥ 1 were focused and analyzed by PCA (**Table 1**). **Figure 2** showed the two-dimensional score plot (PC1 and PC2), which accounted for 58.8 and 41.2% of the variation, respectively. Flavor compounds were clearly separated, and some typical flavor substances closely related to the three kinds of Japanese soy sauce were revealed. As shown in **Figure 2**, S1 had a significant correlation with HEMF, 4-EG, 2,3-butanediol, 3-methylthio-1-propanol, ethyl butyrate, ethyl isovalerate, methional, and hexanal, while S2 was correlated with octanoic acid ethyl ester, 4-non-anone, and nonanal. Only two flavors of linoleic acid ethyl ester and ethyl oleate were closely related to S3.

4-Hydroxy-2(or 5)-ethyl-5-(or 2)-methyl-3(2H)-furanone and 2-methylbutyraldehyde give the caramel-like aroma and malty aroma, respectively, and were detected in all these samples with high OAV (Lee et al., 2006). These substances could enhance the flavor performance of soy sauce when used in cooking. Another typical aroma compound, ethyl butyrate, a short-chain ester, plays a significant role in soy sauce as aroma constituents with fruity flavors (pineapple, passion fruit, and strawberry), which can enrich the flavor of soy sauce (Rodriguez-Nogales et al., 2005; Kaneko et al., 2012). Ethyl isovalerate was a derivative of valeric acid found in fruits with a fruity odor reminiscent of blueberry (Mahmood et al., 2013). And 3-methylthio-1-propanol contributed a unique burnt, caramel-like, garlic, and cooked potato aroma to the soy sauce. Hexanal was positively associated with the cooked grain aroma (Silva et al., 2010). These aroma compounds may contribute a significant reason that S1 is favorably used for stew meat and barbecue condiment.

The Comparison of Aroma Compounds in Japanese Soy Sauce and Chinese Traditional Soy Sauce Based on the Literature

The advantage of the flavor compounds in Koikuchi Shoyu is described in the previous study (Kaneko et al., 2012). Lots of alcohols were detected in Japanese soy sauce (**Supplementary Table 1**), more than in Chinese traditional soy sauce. The content of ethanol in Japanese soy sauce is much higher than Chinese traditional soy sauce (average >three times). The varieties of aldehydes in Japanese soy sauce are highly related to the artificially inoculated strains. The formation of the branched aldehydes, such as isobutyraldehyde, isovaleraldehyde, and benzeneacetaldehyde with floral and malty flavors, is probably related to the transamination of the amino acids by yeast or lactic acid bacteria (Gocke et al., 2007). Pyrazines,

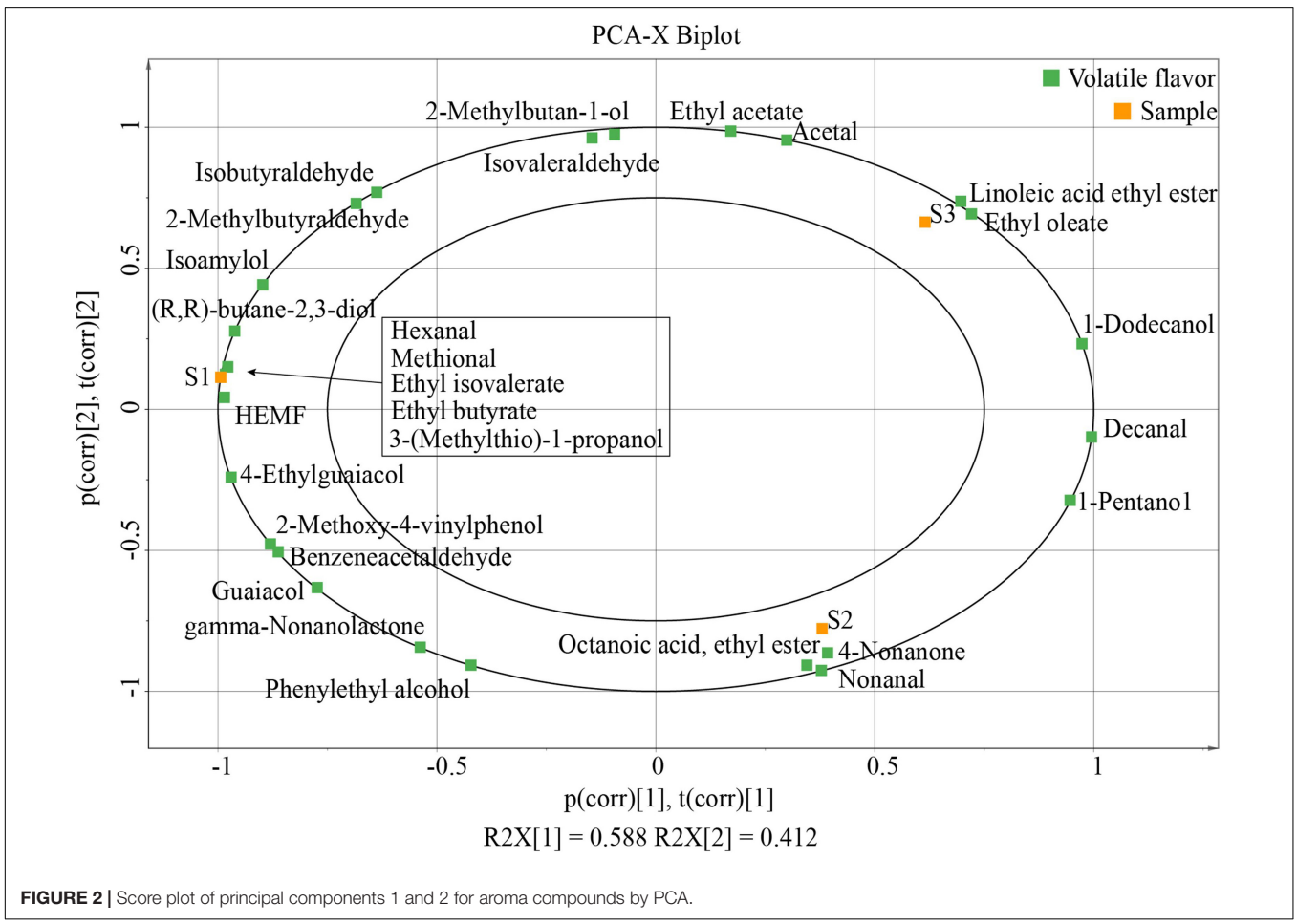

FIGURE 2 | Score plot of principal components 1 and 2 for aroma compounds by PCA.

such as 2,6-dimethylpyrazine, trimethylpyrazine, 2-ethyl-6-methylpyrazine, 3-ethyl-2,5-dimethylpyrazine, and 2-methylpyrazine—the special compounds with the burnt flavor in Chinese traditional soy sauce—were relatively higher than in Japanese soy sauce (Zhao et al., 2020). These compounds may be attributed to the high temperature during moromi fermentation. Esters were also found in Chinese traditional soy sauce in abundance, such as ethyl lactate and triethyl citrate that give it a fruity flavor. In addition, some esters, such as phenethyl acetate and ethyl phenylacetate, were unique to Chinese soy sauce (Ding et al., 2019). Esters are commonly recognized as important flavor and fragrance molecules in soy sauce due to their typically fruity smell and high volatility.

Sourness and Sweetness as the Indicators of Soy Sauce by E-Tongue Analysis

Electronic tongue quantitatively analyzed the six basic soy sauce tastes, sourness, bitterness, astringency, saltiness, umami, and sweetness, by using artificial lipid membrane sensor technology (Kobayashi et al., 2010). Sensor work time was estimated at 200 s to reach the optimum state for effective evaluation of the differences of soy sauce samples (Haddi et al., 2014). The box-plot of all variable sensors is shown in **Figure 3**. We can see that the soy sauce samples included in this study display great differences in the two indicators of sourness and sweetness, and extremely different values were reached at 4.93 and 5.45, respectively, which indicate that sourness and sweetness are the main factors in distinguishing these three types of soy sauce by taste attribute. The results may be closely related to taste of sugars, amino acids, fatty acids or organic acids.

Overview of the Silylation GC-MS Analysis

In this study, a non-targeted analysis of taste components was performed by silylation GC-MS. A total of 160 non-volatile compounds were detected, including 10 amino acids, 8 amines, 36 organic acids, 50 sugars, 21 esters, 20 alcohols, and 6 ketones (**Supplementary Table 2**). This method was desirable for its simplicity, precision, and speed, especially for semiquantitative and qualitative analysis. The significant differences in organic acids and sugars were consistent with the results of E-tongue, indicating that fermentation technologies or fermented strains affect the metabolic carbohydrate features during soy sauce fermentation (EI Sheikha and Hu, 2020). Stearic acid and palmitic acid were found to be major components in soy sauce, which are identified as saturated fatty acids and mainly come from soybean oil. Generally, the oxides of fatty acids lead to unpleasant flavor and taste, but the complex system of soy sauce includes various substances that cover each other up or affect the flavor jointly. Therefore, the high levels of fatty acids may lead to a fuller flavor.

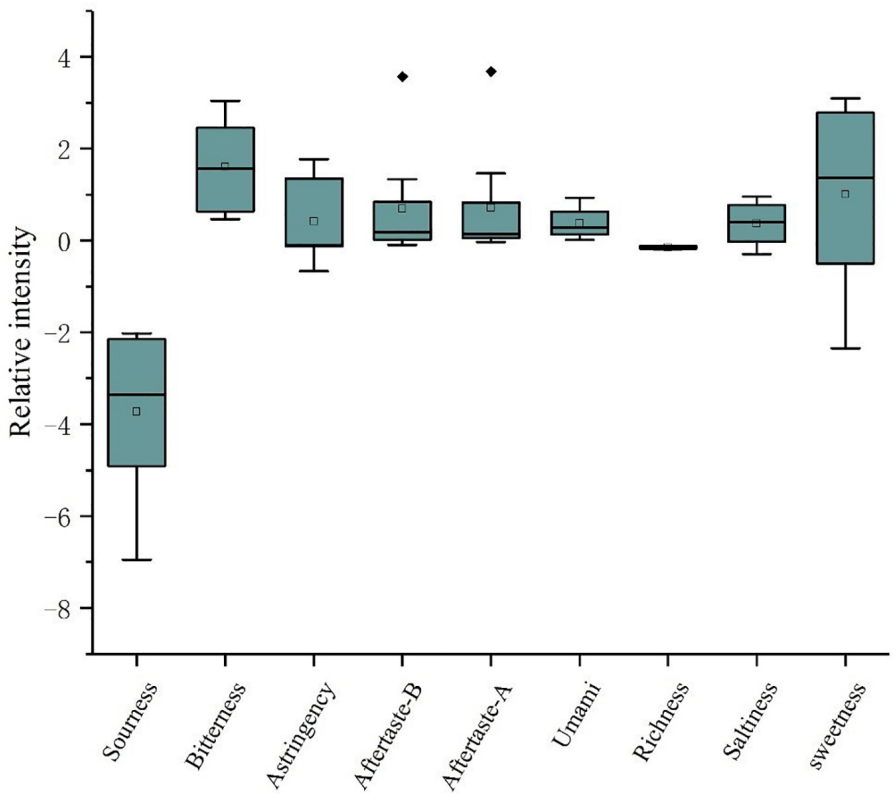

FIGURE 3 | Box-plot figure of the relative intensities of taste indexes measured by E-tongue in Japanese soy sauce.

Non-volatile Acid Compounds in Soy Sauce by Silylation GC-MS Analysis

A total of 33 organic acids were found in soy sauce by silylation GC-MS. Although the total organic acid content in S1 was lower than in S2 and S3, the varieties of organic acids were abundant in S1. Lactic acid, a common acidic agent and taste regulator, was the predominant organic acid in soy sauce samples. The lactic acid content was 6008.52 mg/l in S2, which was over 2.4 times more than S3 and over 6 times more than S1. Lactic acid can be produced by the fermentation of sugars (sucrose, glucose, fructose and so on) using lactic acid bacteria or yeast. Succinic acid was rich in S1 and S3, which enhanced umami taste to these two kinds of soy sauce. The 2-keto-L-gulonic acid content in S2 was 3,068 mg/l, but it was not detected in S1 and S3. The high content of 2-keto-L-gulonic acid also indicated that the different stains worked during soy sauce fermentation. S2 and S3 are usually used for seafood condiments to reduce the fishy smell because of their unique acids.

Usukuchi Shoyu and Amakuchi Shoyu Accounted for Far More Sugars Than Koikuchi Shoyu by Silylation GC-MS Analysis

Sweetness is another key indicator to distinguish the three kinds of soy sauce. Fifty types of sugars were detected in this study. Sugars were typical taste compounds due to their abundant content—49.9, 52.2, and 45.3% of S1, S2, and S3, respectively. Sugars favorably contribute to the sweetness of soy sauce. The sugar content of S2 was prominent at 83,668 mg/l, and S3 accounted for 51,709 mg/l, whereas S1 was much lower. D-melibiose's content highly contributed to the taste of S2, accounting for 23,353 mg/l, but only 6,037 mg/l in S3 and none

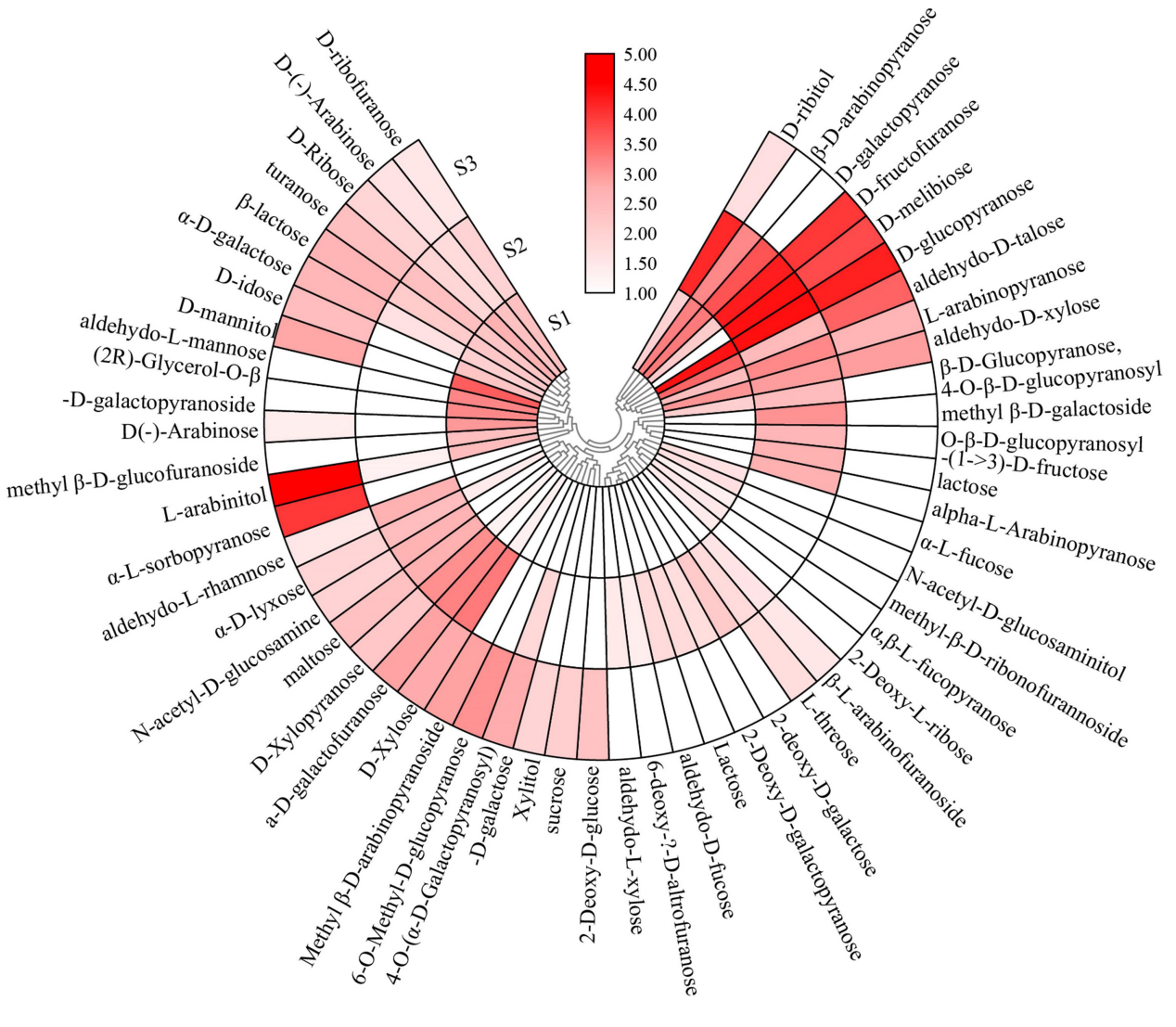

FIGURE 4 | The heat map of sugars detected in Japanese soy sauce.

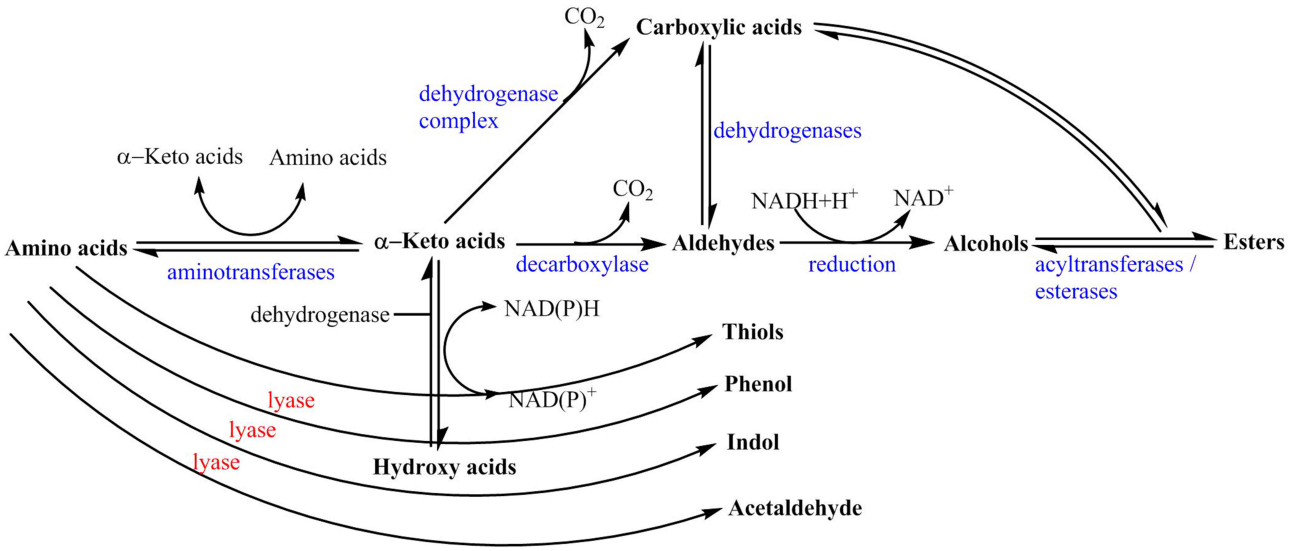

FIGURE 5 | Conversion relationships between amino acids and other aroma compounds.

in S1. D-fructofuranose accounted for more ratios in S2 and S3 (**Figure 4**). D-fructofuranose can be obtained by enzymatic transformation of glucose and hydrolysis of sucrose.

Sugars such as L-arabinopyranose and D-xylose are mainly obtained from wheat bran, the raw material of soy sauce, and showed higher content in S2 than others. Some sugars may be released from enzymolysis. D-ribofuranose was distributed through all the Japanese soy sauce samples with a lower content that released from the hydrolysis of polysaccharides (Wesener et al., 2015). Turanose, a structural isomer of sucrose, is a high-quality functional sweetener (Wang et al., 2012). In addition, rare sugars, such as D-xylopyranose, α-D-lyxose, and α-D-galactose, were also detected in this study, which plays important role in the diet, health care, medicine, and other fields. D-xylopyranose and α-D-lyxose were prominent in S2, but α-D-galactose was more abundant in S3.

The Relationship Between Amino Acids and Aromas in Soy Sauce

Amino acids are essential taste compounds released by proteolysis of the raw materials (Zhao et al., 2016). Amino acids, such as glycine, alanine, and threonine, provide a sweet taste. In this study, glycine and alanine contents in S1 and S3 were higher than in S2, but not threonine. The possible interaction of glycine, alanine, and threonine may also lead to a strong taste of soy sauce (Heyer et al., 2003). Lysine in S2 tastes sweet/bitter. While phenylalanine, valine, leucine, and serine taste bitter (Yu et al., 2015). GABA (4-aminobutyric acid), a non-protein amino acid and bioactive component, was detected in S1 and S2 (Dhakal et al., 2012). The content of GABA in S2 was seven times higher than in S1. The results showed that L-pyroglutamic acid (L-PGA) contents were higher in S1 and S3, but not L-glutamic acid. L-PGA is a tasteless compound converted from L-glutamine by a non-enzymatic pathway (Kim and Lee, 2008), which yields a faster browning process in soy sauce (Wegener et al., 2017). In this study, the presence of L-PGA may be generated due to heat treatment during silylation.

Amino acids are the main sources of aroma substances that are closely related to some alcohols and aldehydes. As shown in **Figure 5**, amino acids can be deaminated by aminotransferase to a-keto acids, which act as the precursors of higher alcohols. Also, amino acids can be converted to aldehydes by decarboxylase. For example, leucine can be converted to a-ketoisocaproic acid by amiotransferase, then converted to 3-methylbutanal by decarboxylase, and finally reduced to 3-methylbutanol by Ehrlich pathway (Smit et al., 2004). Simultaneously, valine, phenylalanine, and threonine can be degraded to 2-methylpropanal, phenylacetaldehyde, phenylethanol, 2-methylbutyraldehyde, and 2-methylbutanol. Additionally, amino acids also have close relationships with the formation of volatile compounds such as pyrazines. In this study, 2, 6-dimethylpyrazine, 2-ethyl-6-methylpyrazine, and trimethylpyrazine were obtained by the conversion of serine, threonine, and lysine. In addition, 2-phenylethanol, important volatile alcohol, can be degraded from phenylalanine by amino acid decarboxylases.

CONCLUSION

Soy sauce has become a worldwide condiment for its unique flavor and taste for cooking. But some differences existed between soy sauce samples for different fermentation technologies, strains, or raw materials. Alcohols and aldehydes is highly abundant in Japanese soy sauce, which has only a modest range of pyrazines and esters. Based on the electronic nose and GC-MS analysis, Koikuchi Shoyu contributes more to flavor compounds. Usukuchi Shoyu and Amakuchi Shoyu have sourness and sweetness features according to E-tongue and silylation

GC-MS analysis. Additionally, 50 kinds of sugars were detected that provide the sweetness of soy sauce. This study will provide remarkable knowledge about flavor and taste improvement of soy sauce, which potentially can improve the quality of soy sauce in the future.

DATA AVAILABILITY STATEMENT

The original contributions presented in the study are included in the article/**Supplementary Materials**, further inquiries can be directed to the corresponding authors.

AUTHOR CONTRIBUTIONS

GZ: writing, reviewing, editing, and supervision. YF: writing of the first draft and investigation. HH: methodology. FZ and YY: conceptualization and project administration. All authors contributed to the article and approved the submitted version.

FUNDING

This work was supported by the National Natural Science Foundation of China (No. 31972194) and Shanxi Province Key R&D Plan (No. 201703D211001-06-02).

SUPPLEMENTARY MATERIAL

The Supplementary Material for this article can be found online at: https://www.frontiersin.org/articles/10.3389/fmicb.2020.579808/full#supplementary-material

REFERENCES

Cai, W., Tang, F., Guo, Z., Guo, X., Zhang, Q., Zhao, X., et al. (2020). Effects of pretreatment methods and leaching methods on jujube wine quality detected by electronic senses and HS-SPME–GC–MS. *Food Chem.* 330:127330. doi: 10.1016/j.foodchem.2020.127330

Dhakal, R., Bajpai, V. K., and Baek, K. H. (2012). Production of GABA (γ-aminobutyric acid) by microorganisms: a review. *Braz. J. Microbiol.* 43, 1230–1241. doi: 10.1590/S1517-83822012000400001

Ding, L., Wang, H., Wang, X., Pan, Z., and Zhao, G. (2019). Analysis of volatile aroma substances of Japanese soy sacue and Chinese soy sauce under different simulated conditions. *China Brew.* 38, 144–151. doi: 10.11882/j.issn.0254-5071.2019.06.028

EI Sheikha, A. F., and Hu, D. M. (2020). Molecular techniques reveal more secrets of fermented foods. *Crit. Rev. Food Sci. Nutr.* 60, 11–32. doi: 10.1080/10408398.2018.1506906

Gao, L., Liu, T., An, X., Zhang, J., Ma, X., and Cui, J. (2017). Analysis of volatile flavor compounds influencing Chinese-type soy sauces using GC-MS combined with HS-SPME and discrimination with electronic nose. *J. Food Sci. Technol.* 54, 130–143. doi: 10.1007/s13197-016-2444-0

Gocke, D., Nguyen, C. L., Pohl, M., Stillger, T., Walter, L., and Müller, M. (2007). Branched-chain keto acid decarboxylase from *Lactococcus lactis* (KdcA), a valuable thiamine diphosphate-dependent enzyme for asymmetric C-C bond formation. *Adv. Synth. Catal.* 349, 1425–1435. doi: 10.1002/adsc.200700057

Haddi, Z., Mabrouk, S., Bougrini, M., Tahri, K., Sghaier, K., Barhoumi, H., et al. (2014). E-Nose and e-Tongue combination for improved recognition of fruit juice samples. *Food Chem.* 150, 246–253. doi: 10.1016/j.foodchem.2013.10.105

Heyer, B. R., Taylor-Burds, C. C., Tran, L. H., and Delay, E. R. (2003). Monosodium glutamate and sweet taste: generalization of conditioned taste aversion between glutamate and sweet stimuli in rats. *Chem. Senses* 28, 631–641. doi: 10.1093/chemse/bjg056

Kaneko, S., Kumazawa, K., and Nishimura, O. (2012). Comparison of key aroma compounds in five different types of Japanese soy sauces by aroma extract dilution analysis (AEDA). *J. Agric. Food Chem.* 60, 3831–3836. doi: 10.1021/jf300150d

Kataoka, S. (2005). Functional effects of Japanese style fermented soy sauce (shoyu) and its components. *J. Biosci. Bioeng.* 100, 227–234. doi: 10.1263/jbb.100.227

Kim, J. S., and Lee, Y. S. (2008). A study of chemical characteristics of soy sauce and mixed soy sauce: chemical characteristics of soy sauce. *Eur. Food Res. Technol.* 227, 933–944. doi: 10.1007/s00217-007-0808-4

Kobayashi, Y., Habara, M., Ikezazki, H., Chen, R., Naito, Y., and Toko, K. (2010). Advanced taste sensors based on artificial lipids with global selectivity to basic taste qualities and high correlation to sensory scores. *Sensors* 10, 3411–3443. doi: 10.3390/s100403411

Lee, S., Seo, B., and Kim, Y. S. (2006). Volatile compounds in fermented and acid-hydrolyzed soy sauces. *J. Food Sci.* 71, C146–C156. doi: 10.1111/j.1365-2621.2006.tb15610.x

Mahmood, I., Ahmad, I., Chen, G., and Huizhou, L. (2013). A surfactant-coated lipase immobilized in magnetic nanoparticles for multicycle ethyl isovalerate enzymatic production. *Biochem. Eng. J.* 73, 72–79. doi: 10.1016/j.bej.2013.01.017

Meng, Q., Hatakeyama, M., and Sugawara, E. (2014). Formation by yeast of 2-furanmethanethiol and ethyl 2-mercaptopropionate aroma compounds in Japanese soy sauce. *Biosci. Biotechnol. Biochem.* 78, 109–114. doi: 10.1080/09168451.2014.877820

Rodriguez-Nogales, J. M., Roura, E., and Contreras, E. (2005). Biosynthesis of ethyl butyrate using immobilized lipase: a statistical approach. *Process Biochem.* 40, 63–68. doi: 10.1016/j.procbio.2003.11.049

Silva, J. B. d, Felberg, I., Carrão-Panizzi, M. C., Lee, S. Y., and Prudencio, S. H. (2010). Relationships among sensory analysis, isoflavone and hexanal contents of soymilk powder. *Braz. Arch. Biol. Technol.* 53, 1197–1204. doi: 10.1590/S1516-89132010000500025

Smit, B. A., Engels, W. J. M., Wouters, J. T. M., and Smit, G. (2004). Diversity of L-leucine catabolism in various microorganisms involved in dairy fermentations, and identification of the rate-controlling step in the formation of the potent flavour component 3-methylbutanal. *Appl. Microbiol. Biotechnol.* 64, 396–402. doi: 10.1007/s00253-003-1447-8

Suezawa, Y., and Suzuki, M. (2007). Bioconversion of ferulic acid to 4-vinylguaiacol and 4-ethylguaiacol and of 4-vinylguaiacol to 4-ethylguaiacol by halotolerant yeasts belonging to the genus Candida. *Biosci. Biotechnol. Biochem.* 71, 1058–1062. doi: 10.1271/bbb.60486

Wang, R., Bae, J. S., Kim, J. H., Kim, B. S., Yoon, S. H., Park, C. S., et al. (2012). Development of an efficient bioprocess for turanose production by sucrose isomerisation reaction of amylosucrase. *Food Chem.* 132, 773–779. doi: 10.1016/j.foodchem.2011.11.035

Wegener, S., Kaufmann, M., and Kroh, L. W. (2017). Influence of l-pyroglutamic acid on the color formation process of non-enzymatic browning reactions. *Food Chem.* 232, 450–454. doi: 10.1016/j.foodchem.2017.04.046

Wesener, D. A., Wangkanont, K., McBride, R., Song, X., Kraft, M. B., Hodges, H. L., et al. (2015). Recognition of microbial glycans by human intelectin-1. *Nat. Struct. Mol. Biol.* 22, 603–610. doi: 10.1038/nsmb.3053

Yu, H. Y., Zhao, J., Li, F., Tian, H., and Ma, X. (2015). Characterization of Chinese rice wine taste attributes using liquid chromatographic analysis, sensory evaluation, and an electronic tongue. *J. Chromatogr. B Analyt.*

Technol. Biomed. Life Sci. 997, 129–135. doi: 10.1016/j.jchromb.2015.05.037

Zhao, C. J., Schieber, A., and Gänzle, M. G. (2016). Formation of taste-active amino acids, amino acid derivatives and peptides in food fermentations – a review. *Food Res. Int.* 89(Pt 1), 39–47. doi: 10.1016/j.foodres.2016.08.042

Zhao, G., Ding, L. L., Hadiatullah, H., Li, S., Wang, X., Yao, Y., et al. (2020). Characterization of the typical fragrant compounds in traditional Chinese-type soy sauce. *Food Chem.* 312:126054. doi: 10.1016/j.foodchem.2019.126054

Conflict of Interest: The authors declare that the research was conducted in the absence of any commercial or financial relationships that could be construed as a potential conflict of interest.

frontiers in Microbiology

ORIGINAL RESEARCH
published: 08 January 2021
doi: 10.3389/fmicb.2020.611260

Functional Characteristics of *Lactobacillus* and Yeast Single Starter Cultures in the Ripening Process of Dry Fermented Sausage

*Yingli Liu, Zhen Wan, Kalekristos Woldemariam Yohannes, Qinglin Yu, Ziyan Yang, Hongyan Li, Jie Liu and Jing Wang**

China-Canada Joint Lab of Food Nutrition and Health (Beijing), Beijing Advanced Innovation Center for Food Nutrition and Human Health (BTBU), Beijing Engineering and Technology Research Center of Food Additives, Beijing Technology & Business University (BTBU), Beijing, China

Dry fermented sausage is popular among the world because of its rich nutrition and unique flavor. Starter cultures play an important role in the quality of dry fermented sausage. In this study, probiotics lactic acid bacteria *Lactobacillus delbrueckii* N102, *Latilactobacillus sakei* H1-5, *Debaryomyces hansenii* Y4-1, and *Wickerhamomyces anomalus* Y12-3 were isolated from food-borne materials. The physicochemical properties, microbial populations, TBARS, lipolysis, proteolysis, and volatile flavor compounds of dry fermented sausages with different starter cultures were evaluated comparatively during the ripening process. The results showed that both *L. delbrueckii* N102 and *L. sakei* H1-5 grow well and could rapidly reduce the pH value of the products. At the same time, they could significantly reduce the number of *Enterobacter putrefaciens*, so as to ensure the safety of the products. In addition, the strains N102 promoted the formation of flavor compounds 2,3-butanedione, 3-hydroxy-2-butanone, and carnosine, whereas taurine content of batch H1-5 was significantly increased, while yeast y4-1 and y12-3 could also grow faster in sausage and promoted the esters and alcohols formation such as ethyl acetate and linalool, with the formation of γ-aminobutyric acid by y4-1. Compared with lactic acid bacteria, yeasts showed to contribute more in flavor formation and effective inhibition of lipid oxidation. The starter cultures played different roles in flavor contribution and had obvious differentiation in the ripening process of dry fermented sausage.

Keywords: starter culture, lipid oxidation, protein hydrolysis, volatile compound, functional differences, dry fermented sausage

OPEN ACCESS

Edited by:
Xucong Lv,
Fuzhou University, China

Reviewed by:
Qingli Dong,
University of Shanghai for Science and Technology, China
Jinxuan Cao,
Ningbo University, China
Peijun Li,
Hefei University of Technology, China

****Correspondence:***
Jing Wang
wangjing@th.btbu.edu.cn

Specialty section:
This article was submitted to Food Microbiology, a section of the journal Frontiers in Microbiology

Received: *28 September 2020*
Accepted: *08 December 2020*
Published: *08 January 2021*

Citation:
Liu Y, Wan Z, Yohannes KW, Yu Q, Yang Z, Li H, Liu J and Wang J (2021) Functional Characteristics of Lactobacillus and Yeast Single Starter Cultures in the Ripening Process of Dry Fermented Sausage. Front. Microbiol. 11:611260. doi: 10.3389/fmicb.2020.611260

INTRODUCTION

Fermented sausage refers to the fermented meat products with stable microbial characteristics, typical fermentation flavor and long shelf life, which is made by mixing minced meat (often referring to pork or beef) with fat, sugar, salt, spices and other ingredients into the casing after microbial fermentation (Villani et al., 2007). Because of the variety and quantity of meat and raw materials, as well as the different fermentation and drying conditions, the sensory characteristics of products are diverse. Almost every country has its own traditional fermented sausage, For example: salami in Italy, dauerwurst in Germany, charqui in Spain, Chouriço de vinho in Portugal, and Harbin sausage in China. In order to improve the quality and safety of the final product

and standardize the production process, exogenous microorganisms are often used as starter in the production of traditional or naturally dried fermented sausage. Studies have shown that the starter culture is mainly composed of *coagulase-negative cocci* (CNC), yeast, and *lactic acid bacteria* (LAB), such as *Latilactobacillus sakei*, *Latilactobacillus curvatus*, and *Lactiplantibacillus plantarum* (Cocolin et al., 2011).

Lactic acid bacteria plays a leading role in the sausage fermentation process. The main function of LAB is to reduce the pH of the matrix through production of lactic acid from the fermentation of sugars. A reduction in pH is necessary for fibrillar proteins to coagulate, resulting in improved firmness and cohesiveness of the final product, facilitating slicing (Drosinos et al., 2007). Montel et al. (1998) found that lactobacillus can give sausage special flavor by utilizing acetic acid, formic acid, and succinic acid generated by carbohydrate. Moreover, LAB species inhibit the multiplication of pathogenic and spoilage bacteria, mainly due to the production of organic acids or other antimicrobial metabolites, such as hydrogen peroxide, diacetyl, and peptides known as bacteriocins (Almeida da Costa et al., 2018). Bacteriocins have been shown to provide added control against pathogens in fermented sausages (Barbosa et al., 2015).

Yeast in dry fermented sausages produce a protection against the detrimental effect of oxygen and facilitate the drying process by protecting the sausage against fluctuation in humidity, which will produce changes in sausage appearance. Yeast can affect the color and flavor of sausage by their oxygen-scavenging and lipolytic activities, in addition to, it can utilize fermentation products such as lactic acid and contribute to increase more aroma compounds (Flores et al., 2015). Flores et al. (2004) first reported effect on VOCs and aroma by yeast starter cultures (*D. hansenii*) in fermented sausages due to the inhibition of lipid oxidation products (linear aldehydes) and promotion of ethyl ester compounds. Cano-Garcia et al. (2014a) found that inoculation of *D. hansenii* strains in fermented sausages can reduce lipid oxidation and produce flavor substances.

In the previous research, LAB and yeast with excellent characters were isolated from Chinese *Laminaria japonica* and traditional fermented foods (Chu et al., 2015; Liu et al., 2015). The purpose of these studies was to evaluate the improvement of the quality of dry fermented sausages and the contribution to flavor by inoculating them into sausages fermentation.

MATERIALS AND METHODS

Bacterial Cultures and Culture Media

Autochthonous starter cultures are used for making dry fermented sausage. These strains included *L. delbrueckii* N102, *L. sakei* H1-5, *D. hansenii* Y4-1, and *W. anomalus* Y12-3 were previously isolated from Chinese *Laminaria japonica* and traditional fermented foods (Chu et al., 2015; Liu et al., 2015). *L. delbrueckii* N102 and *L. sakei* H1-5 have been proved to have strong acid production capacity and antimicrobial ability. *D. hansenii* Y4-1 and *W. anomalus* Y12-3 have been shown to contribute to good flavor formation. LAB were stored in glycerin and Man-Rogosa-Sharpe (MRS, Oxoid) broth medium mixture at −80°C until use, whereas yeasts were stored at −20°C on the yeast peptone dextrose (YPD, Oxoid) agar plate until use.

Dry Fermented Sausage Manufacturing

The sausage was divided into following five batches: batch control without inoculation, batch N102 inoculated with about 10^7 CFU g^{-1} of *L. delbrueckii* N102, batch H1-5 inoculated with about 10^7 $CFUg^{-1}$ of *L. sakei* H1-5, batch Y4-1 inoculated with about 10^6CFUg^{-1} of *D. hansenii* Y4-1, batch Y12-3 inoculated with about 10^6 $CFUg^{-1}$ of *W. anomalus* Y12-3. The sausage formulation (200 g of meat-mixture for each sausage) include 70% lean pork, 30% fat, 3.5% NaCl, 0.2% glucose, 0.3% sucrose, 0.05% sodium ascorbate, 0.1% garlic powder, 0.3% white pepper, and 0.3% black pepper. Mix lean meat, fat, and ingredients with a blender at 4°C and add different starter cultures (Huang et al., 2020; Xiao et al., 2020).

Subsequently, the sausage mixture was filled into a natural casing (sheep small intestine) and placed in a fermentation chamber. All the sausages were fermented for 22 h at 22°C with 85% relative humidity (RH) and for 20 h at 20°C with 65% RH. Then the sausages are ripened for 18 h at 19°C with 67% RH, 22 h at 18°C with 69% RH, 18 h at 17°C with 71% RH, 21 h at 15°C with 73% RH, 21 h at 14°C with 76% RH, 16 h at 12°C with 77% RH and kept at 11°C with 37% RH until the end of 23 days.

From each batch, a 500 g portion of meat mixture (0 day) and three sausages at 5, 10, 16, and 23 days were randomly collected. 50 g portion of each sausage was minced and used for moisture and pH tests and a 25 g portion was taken for microbiological analysis. In addition, the remaining minced sausage was vacuum packaged and frozen at −20°C for subsequent analyses (TBARS, free fatty acids measurement, free amino acids measurement, sarcoplasmic proteins analysis, myofibrillar protein analysis). Also, 10 g sausage was wrapped in aluminum foil, vacuum packaged, and stored at −80°C for volatile compound analysis. Finally, sensory analysis was carried out at 23 days of the drying process. Results were expressed as the mean of three replicates per 100 g of dry matter at each processing time and batch.

Measurement of pH Value

Measurement of pH was performed using a pH meter (Mettler Toledo Instruments Co., Ltd., Shanghai, China) in a homogenate prepared with 225 mL distilled water and 25 g samples.

Determination of Water Content and Mobility

According to the method of Zhang et al. (2017), the change of water during sausage ripening was determined by LF-NMR.

Measurement of Microbial Population

Shred dry fermented sausage samples (25 g) under aseptic conditions were added to 225 mL sterile saline and the samples were evenly oscillated. Microbiota were separated and counted using different selective media. The total number of bacteria was counted by incubation with Plate Count Agar (PCA, Oxoid) at 30°C for 72 h; LAB were counted in an anaerobic culture at 30°C for 48 h using Man-Rogosa-Sharpe agar (MRS, Oxoid)(Xiao et al.,

2018); *Micrococci* and *Staphylococci* were counted on mannitol salt agar (MSA, Oxoid) at 30°C for 48–72 h; *Enterobacteriaceae* were counted on violet red bile glucose agar (VRBG, Oxoid) at 37°C for 24 h. The yeast was counted on yeast peptone dextrose agar (YPD, Oxoid) at 28°C for 5 days.

Extraction of Myofibrillar and Sarcoplasmic Protein

The method of Mauriello et al. (2002), with some modifications to extract sarcoplasmic and myofibrillar proteins was used. The sample dilute with phosphate buffer (0.02 M, pH 6.5) was homogenized (4,000 rpm) for 4 min, then centrifuged at 10,000 × *g* for 20 min at 4°C. Supernatant filtered and sterilized was the sarcoplasmic protein extraction. The pretreatment of myofibrillar protein was the same as that of sarcoplasmic protein except that in the last step. The precipitate diluted with phosphate buffer (0.03 M, pH 6.5) containing 0.1% (v/v) Triton X-100 was homogenized (4,000 rpm) for 4 min, then centrifuged at 10,000 × *g* for 20 min at 4℃, for three times. The precipitate was suspended in phosphate buffer (0.1 M, pH 6.5, 0.7 M KI) with 0.02% (v/v) NaN_3, homogenized (4,000 rpm) for 4 min at 4℃ and centrifuged at 10,000 × *g* for 20 min at 4℃. The supernatant was sterilized by filtration, which was the myofibrillar protein extraction. All extracts are stored at 4℃ until use.

Sarcoplasmic and myofibrillar proteins were analyzed by sodium dodecyl sulfate-polyacrylamide gel electrophoresis (SDS-PAGE) to evaluate the degree of proteolysis (Laemmli, 1970). SDS-PAGE was performed using a 12% acrylamide dissolution gel, a 6% acrylamide stacking gel and Mini-Protean Tetra System (Bio-Rad). The proteins used as standards were high molecular weight standard protein Marker (Sigma, MW-SDS-200). The polygels were scanned with a gel imager (Bio-Rad).

Measurement of Free Amino Acids

Free amino acids were extracted by the method of Casaburi et al. (2007) and determined reverse phase by HPLC as described and determined by Bidlingmeyer et al. (1987).

Thiobarbituric Acid Reactive Substances

The TBARS of sausages was analyzed according to the method of Wang and Xiong (2005). The TBARS value was expressed as mg of malondialdehyde/100 g sausage.

Measurement of Free Fatty Acids

The extraction of lipids and the separation of free fatty acids were carried out by referring to the method of Bligh and Dyer (1959). After methyl esterification of free fatty acids, the determination of free fatty acid content and composition by gas chromatography was carried out according to the method of Navarro et al. (1997).

Analysis of Volatile Compounds

Volatile compounds were extracted by solid-phase micro-extraction (SPME) (Wen et al., 2019). Four grams of sausage was placed in a 20 ml headspace extraction flask, equilibrated at 60°C for 30 min and then extracted with a 50 μm layer DVD/PDMS for 30 min at 60°C. After sample extraction was complete, the fibers were drawn into the needle and transferred to the injection of the GC-MS system for desorption at 250°C for 5 min. GC-MS analysis was performed on model 7890A of Agilent Technologies (Paolo Alto, CA, United States) gas chromatograph, and model 5975C of mass spectrometry detector was selected. GC conditions: TRACE TR-5 GC column (30 m, 0.25 mm × 0.25 μm); the initial column temperature was maintained at 40°C for 5 min, then raised to 100°C at 5°C/min and held isothermal 10 min, then from 100℃ to 180°C at a rate of 5°C/min, and finally, the temperature was raised to 240°C for 10 min a rate of 15°C/min. The carrier gas is helium and the flow rate was 1 mL min^{-1}. MS conditions: ionization voltage 70 eV; ion source temperature 280℃; mass scan range: 30–300 mass units (Martin et al., 2003). The peak components were determined through the search of NIST14 standard library, and the flavor component was determined by the matching degree greater than 80%. The relative content was expressed as the percentage of the peak area of each component to the total peak.

Sensory Analysis

Twelve experienced panelists were chosen to evaluate the sensory properties. The evaluations were conducted in a sensory panel room at 25°C. The sausage sample was cut into slices (3 mm thick) and placed in a white plastic dish. The samples were blind-coded with 3-digit random numbers and evaluated three times. Unsalted crackers and water were used to cleanse the palate between samples. The following sensory characteristics were evaluated: color, aroma, chewiness, acid taste, and overall acceptability. The intensity or degree of an attribute was expressed by a seven-point descriptive scale from 1 (low intensity) to 7 (high intensity): color (7 = red and shiny; 1 = dark and dull), aroma (7 = strong; 1 = light), chewiness (7 = hard; 1 = soft), acid taste (7 = strong acid taste; 1 = light acid taste), and overall acceptability (7 = high; 1 = low).

Statistical Analysis

All experimental data were repeated three times and the results were expressed as mean and standard deviation. The data were analyzed by one-way ANOVA using the SPSS 13.0 software for Windows (SPSS Chicago, IL, United States) and means were compared by Duncan's multiple comparison range test. Values were considered significantly different at $P < 0.05$. Biplot based on principal component analysis (PCA) was performed using the SIMCA software (version 14.1, Umeå, Sweden) for volatile compounds data.

RESULTS

Effects of Different Starter Cultures on pH Value Changes of Dry Fermented Sausage

As shown in **Figure 1**, the pH values of fermented sausages significantly decreased at the first 5 days in all batches ($P < 0.05$). The initial pH value was about 5.8. After 12 days fermentation, the pH of control, N102, H1-5, Y4-1, and Y12-3 were reduced

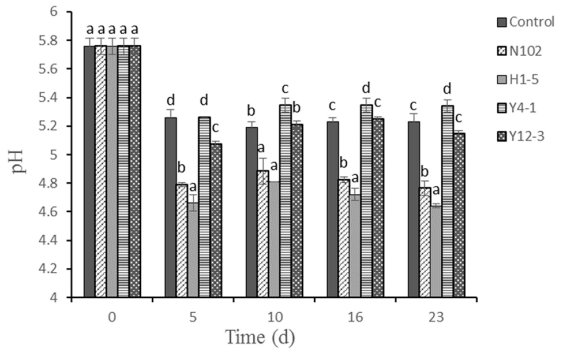

FIGURE 1 | Evolution of pH value during the ripening of the different samples of sausage non-inoculated and inoculated with various starter cultures. Error bars refer to the standard deviations obtained from triplicate sample analysis. Different letters (a–d) indicate significant differences among different batches at the same fermentation time ($P < 0.05$). N102, *L. delbrueckii*; H1-5, *L. sakei*; Y4-1, *D. hansenii*; Y12-3, *W. anomalus*.

to 5.23, 4.76, 4.64, 5.30, and 5.14, respectively. The pH values of N102 and H1-5 batches were lower than the control throughout the sausage ripening process ($P < 0.05$) and its pH was below 5.0. However, the pH of the batch inoculated with yeast was not significant compared with the control during sausage ripening. The pH of all batches increased on the 10th to 16th day of drying, and the change in pH decreased slightly after 23 days fermentation.

Effects of Different Starter Cultures on Water State of Dry Fermented Sausage

The state of water in sausages was investigated by low-field nuclear magnetic resonance (LF-NMR). **Figure 2** shows the change in the percentage of water state at different fermentation time during the dry fermented sausage making, the proportion of immobilized water is up to 88.55%, the content of free water is 9.52%, and the content of bound water is at least 1.93%. The proportion of bound water in each batches increased with the drying of the sausage. In the first 10 days, the proportion of bound water in each batches did not exceed 2.28%, while in the late drying stage, the proportion accounted for more than 20% in all samples, of which, in 16 days and 23 days of ripening, the content of bound water of the batch inoculated with H1-5, Y4-1, and Y12-3 was significantly lower than that of the control ($P < 0.05$). In the first 10 days, the proportion of immobilized water was still the highest. In the late stage of drying, the proportion of immobilized water of the batches inoculated with H1-5, Y4-1, and Y12-3 was significantly higher than that in the control ($P < 0.05$). The proportion of free water in each batch decreased from 9.52% at the beginning to less than 1% at the end.

Effects of Different Starter Cultures on Microbial Population of Dry Fermented Sausage

The changes in microbiota are shown in **Figure 3**. During the ripening of sausage, LAB were dominant bacteria in all batches, and the number was much higher than other bacteria. The number of LAB reached the maximum at 8.79, 8.69, 8.25, 8.18, and 8.23 log cfu g^{-1} after 5 days fermentation, in the batches inoculated with starter cultures N102, H1-5, Y4-1, Y12-3, and the control, respectively. The growth rate of *Micrococci* and *Staphylococci* increased in the early stage of processing and showed a downward trend in the later stage. In batches N102 and H1-5, the numbers of *Micrococci* and *Staphylococci* were lower than other batches, probably because LAB lowered the pH of the sausage and inhibited their growth. As spoilage bacteria in meat products, the number of *Enterobacteriaceae* showed a downward trend in all batches. In batches N102 and H1-5, the number of *Enterobacteriaceae* was significantly lower than that of other batches, indicating that *L. delbrueckii* N102 and *L. sakei* H1-5 had a significant inhibitory effect on the growth of *Enterobacteriaceae*. The initial yeast quantity for batches Y4-1 and Y12-3 was 6 log cfu/g, which was consistent with the quantity of starter added. The number of yeasts in batches Y4-1 and Y12-3 showed an upward trend in the early stage of processing, and reached the maximum values of 8.26 and 7.75 log cfu/g on the 5th day, which was significantly higher than other batches of about 5 log cfu/g. At end of sausage ripening, the amount of yeast then showed a downward trend, with the number of final products being about 6 log cfu g^{-1} of the batch inoculated with Y4-1 and Y12-3, while the number of other batches was about 4.95 log cfu g^{-1}.

Effects of Different Starter Cultures on Proteolysis of Dry Fermented Sausage

Degradation of myofibrillar and sarcoplasmic proteins in each batch was analyzed by SDS-PAGE technique. The degradation of sarcoplasmic proteins is shown in the **Figure 4A**. In the batch inoculated with N102 and H1-5, from the fermentation stages to the ripening of sausage, the protein bands of 157, 97, 45, and 29 kD gradually weakened and disappeared during the fermentation and ripening stage. Compared to the other three batches, the 25 kD protein band of the N102 and H1-5 batches were weaker in color. The protein bands of only 97 and 45 kD were weakened in the control and the Y4-1 and Y12-3 batches. The low protein bands below 20 kD of the batch inoculated Y12-3 were weaker in color than the other batches. As shown in **Figure 4B**, actin and myosin were significantly degraded in each batch, as well as the heavy chain of myosin.

Effects of Different Starter Cultures on Free Amino Acids of Dry Fermented Sausage

In order to evaluate the effect of the starter cultures on proteolysis, the free amino acids in the meat mixture of 0 day and in all batches of sausages ripening were determined. The results are shown in **Figure 5**. The main amino acids in the meat mixture used for sausage processing were carnosine, anserine, leucine, alanine, glycine; and the content of cysteine, ornithine, and citrulline was at least about 0.5 mg/100 g meat. At the end of ripening, the total amino acid content of each batch was significantly higher than the sausage at the beginning

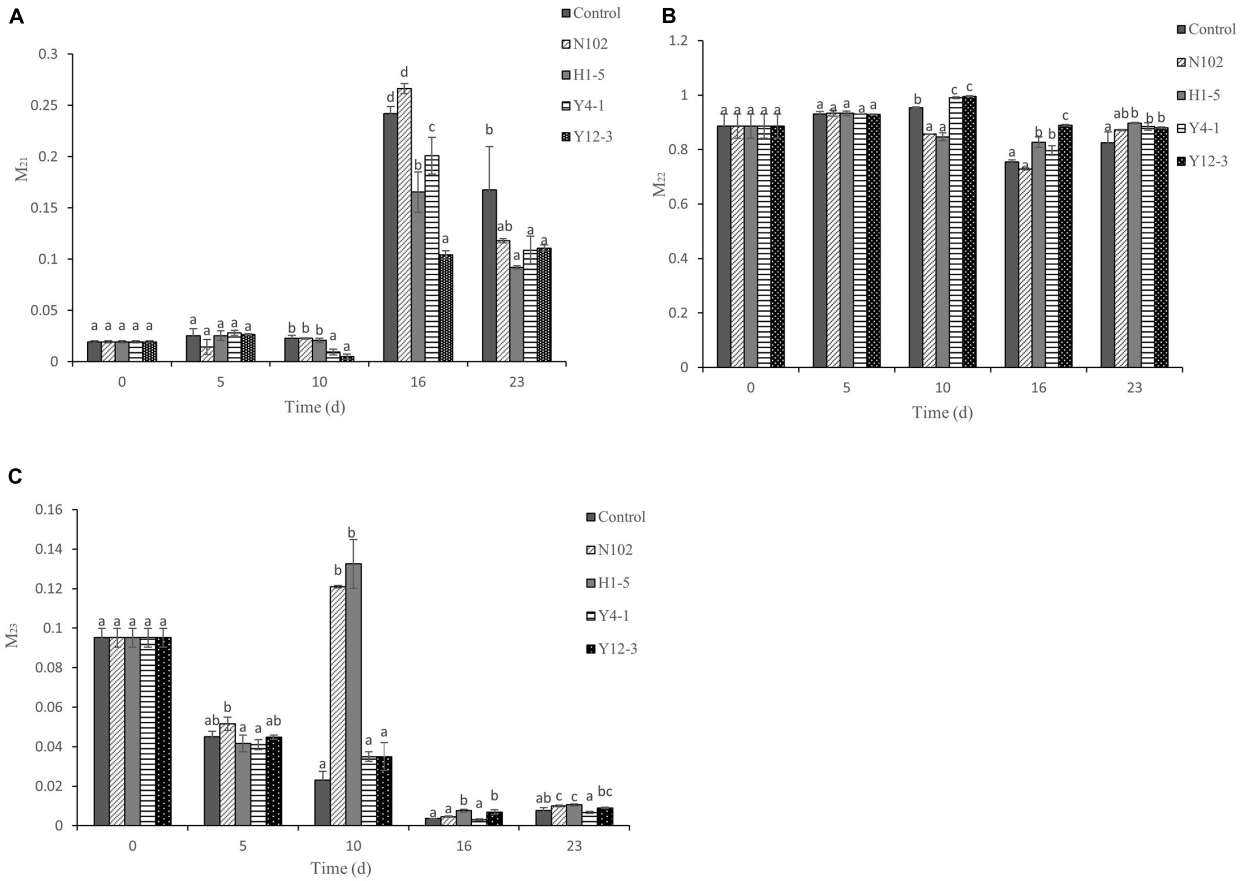

FIGURE 2 | Relative area percentages of hydration water **(A)**, immobilized water **(B)**, and free water **(C)** populations. Error bars refer to the standard deviations obtained from triplicate sample analysis. Different letters (a–d) indicate significant differences among different batches at the same fermentation time ($P < 0.05$). N102, *L. delbrueckii*; H1-5, *L. sakei*; Y4-1, *D. hansenii*; Y12-3, *W. anomalus.*

of processing ($P < 0.05$) (from 509.38 at 0 days to 1028.52, 1263.04, 1196.57, 1072.65, 1093.63 mg/100 g sausage in control sausage and in the batches inoculated with N102, H1-5, Y4-1, and Y12-3, respectively, at end of ripening). At the same stage, the total amino acid content of the batch inoculated with N102, H1-5, Y4-1, and Y12-3 was higher than that of the control($P < 0.05$), indicating that these starter cultures may contribute to the formation of free amino acids. At end of sausage ripening, the content of threonine, tyrosine and carnosine in the batch inoculated with N102 was significantly higher than that in the control ($P < 0.05$); the contents of taurine, citrulline, glycine, glutamine, aspartic acid, alanine, tyrosine, lysine, and leucine in the batch inoculated with H1-5 was significantly higher than that in the control ($P < 0.05$); In addition, the contents of tyrosine, taurine and leucine in batch H1-5 were significantly higher than those in other batches ($P < 0.05$). Lysine, proline, tyrosine, citrulline, ornithine, and γ-aminobutyric acid in the batch inoculated with Y4-1 were significantly higher than that in the control ($P < 0.05$), Moreover, the contents of ornithine and proline were significantly higher than those of other batches ($P < 0.05$). The content of 2-aminobutyric acid, citrulline, and threonine in the batch inoculated with Y12-3 was significantly higher than that in the control ($P < 0.05$). However, the content of arginine in each batch at the end of fermentation was lower than that at 0 days. In general, Val, Leu, Phe, Glu, Ala, Car, and Ans were the most abundant amino acids in the all batches.

Effects of Different Starter Cultures on Free Fatty Acids of Dry Fermented Sausage

The effects of various starter cultures on lipid hydrolysis were evaluated by determining the content of free fatty acids. The results are shown in **Table 1**. The content of saturated fatty acids (C14:0, C16:0, and C18:0), monounsaturated fatty acids (C16:1, C18:1), polyunsaturated fatty acids (C18:2, C18:3, C20:2, C20:3, and C20:4) were determined at 0 days and the ripening period of all batches. At the end of ripening, the total free fatty acids content was significantly higher than the free fatty acids content of the sausage at the beginning of processing ($P < 0.05$)(from 257.00 at 0 days to 1037.97, 685.64, 1019.21, 873.21, and 736.73 mg/100 g sausage in control sausage and in the batches inoculated with N102, H1-5, Y4-1, and Y12-3, respectively, at end of ripening). Palmitic acid, oleic acid, and linoleic acid were the three highest

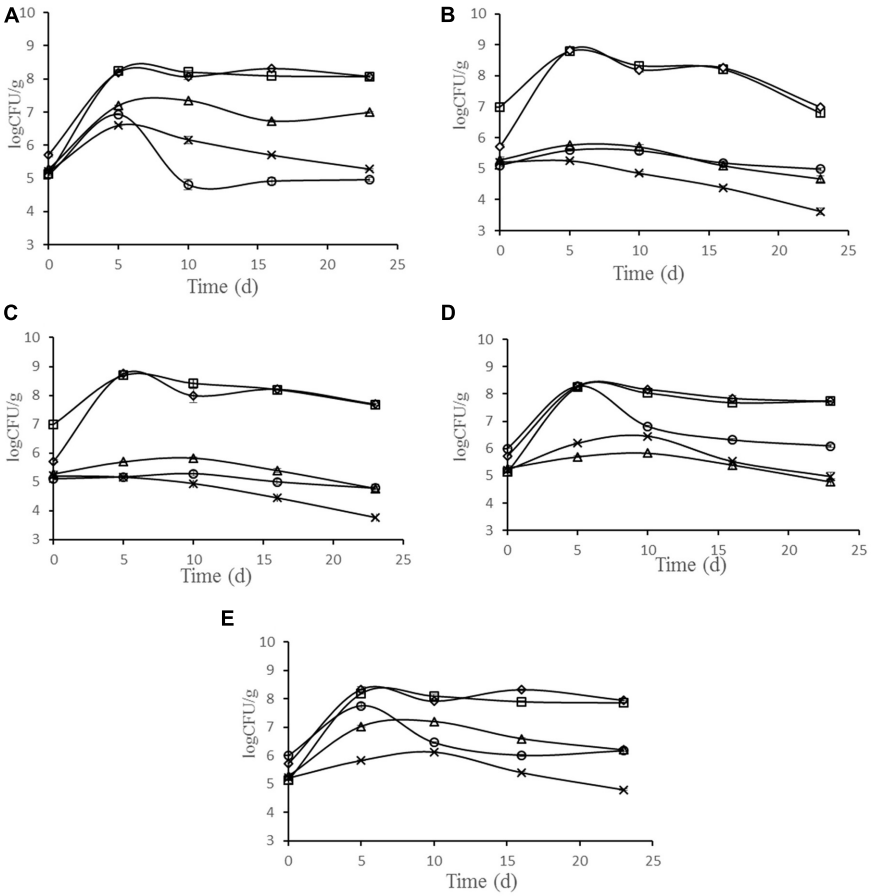

FIGURE 3 | Evolution of microbial populations during the ripening of different samples of sausages non-inoculated and inoculated with various starter cultures. Error bars refer to the standard deviations obtained from triplicate sample analysis. **(A)** control (uninoculated) sausage; **(B)** sausage inoculated with the strain *L. delbrueckii* N102; **(C)** sausage inoculated with the strain *L. sakei* H1-5; **(D)** sausage inoculated with the strain *D. hansenii* Y4-1; **(E)** sausage inoculated with the strain *W. anomalus* Y12-3. (□) LAB; (△) *Micrococci* and *Staphylococci*; (×) *Enterobacteriaceae*;(○)Yeast; (◇)Total bacterial plate.

free fatty acids in all samples. All samples had the highest monounsaturated fatty acid content, followed by saturated fatty acids and polyunsaturated fatty acids at the end of ripening.

Effects of Different Starter Cultures on Lipid Oxidation of Dry Fermented Sausage

TBARS evaluates the degree of oxidation of sausages during processing by measuring the amount of secondary products (such as malondialdehyde) produced during the oxidation process. The results are shown in **Figure 6**. In all batches, the TBARS value gradually increased with the sausage ripening time, reaching a maximum of 0.94, 0.57, 0.70, 0.41, and 0.47 mg MDA/kg sausage in control sausage, N102, H1-5, Y4-1, and Y12-3, respectively, at end of ripening. The TBARS value of the batch added to the starter cultures was significantly lower than that of the control ($P < 0.05$), indicating that the starter cultures could inhibit the oxidation of lipids. Among them, the TBARS value of the batch inoculated with Y4-1 and Y12-3 was lower than that of the other batch, indicating that the yeast may have an inhibitory effect on lipid oxidation.

Effects of Different Starter Cultures on Flavor Compounds of Dry Fermented Sausage

A total of 59 flavor substances were detected in 5 batch samples, including 29 substances in the control, 25 substances in the batch inoculated with N102, 24 flavor substances in the batch inoculated with H1-5, and 40 substances in the batches inoculated with Y4-1 and Y12-3, respectively. According to the results shown in **Table 2**, the main volatile substances can be divided into ketones, acids, esters, aldehydes, alcohols, terpenes and some other substances. Terpenes are mainly produced by adding black pepper, white pepper and garlic powder to sausage (Guadayol et al., 1997). The 2, 3-butanediol was detected in all five batches of sausages with high content. Batch N102 and batch H1-5 detected less alcohol content and categories than the control and yeast batches. The ethanol content of batch Y4-1 was significantly higher than that of other batches. 2-phenylethanol was detected

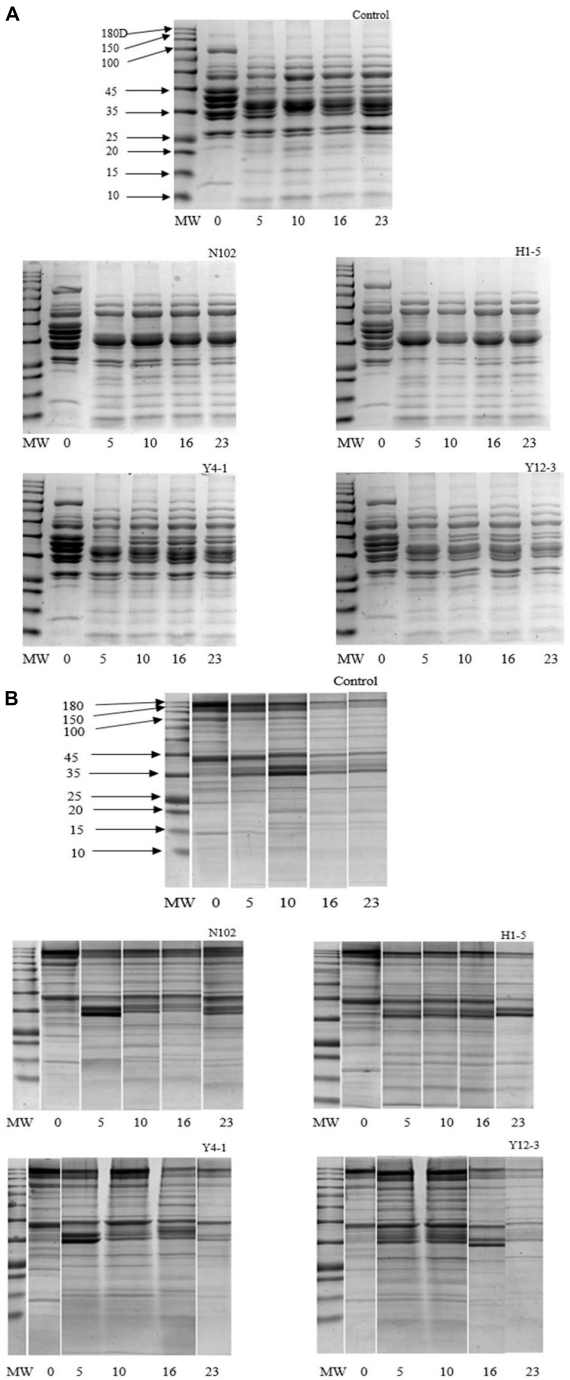

FIGURE 4 | SDS-PAGE analyses of sarcoplasmic proteins **(A)** and myofibrillar protein **(B)** degradation during the ripening of the different samples of sausages non-inoculated and inoculated with various starter cultures. MW refers to the molecular weights of a protein standard; 0–23 refer to fermentation time (days). N102, *L. delbrueckii*; H1-5, *L. sakei*; Y4-1, *D. hansenii*; Y12-3, *W. anomalus*.

in batch Y4-1 and batch Y12-3, and linalool was detected in batch Y12-3, which had an important effect on the flavor of sausage. Butyric acid was detected in all batches and the batches inoculated with Y4-1 and Y12-3 had higher levels of butyric acid, which is an important flavor substance. The isobutyric acid was detected in the batch inoculated with Y4-1 and 2-methylbutyric acid was detected only in the batch inoculated with N102. Only ethyl lactate and 2-methyl-1-butylethyl ester were detected in the batch inoculated with H1-5and N102, and the total ester substances in this two batches were lower than those in the control. The ethyl acetate content of the batches inoculated Y4-1 and Y12-3 was significantly higher than that of the control. Further, seven types of ester substances were detected in the Y4-1 batch, which indicated the strain Y4-1 contributed to the formation of ester substances. The content of ethyl lactate and ethyl isovalerate in the batch Y12-3 was higher than that in the control. The presence of benzaldehyde was detected in all samples, which is a unique flavor component of the fermented meat product. In addition to the batch inoculated with Y4-1, the other batches had the highest content of hexanal, which had an apple aroma and improved the flavor. The content of hexanal in the batch H1-5 and batch Y12-3 was higher than that in the control. Only 3-hydroxy-2-propanone was detected in the control, which did not appear in other batches. The contents of 2,3-butanedione and 3-hydroxy-2-butanone in the batches inoculated with N102 and H1-5 were very high. The presence of 3-hydroxy-2-butanone was detected in the batches inoculated with Y4-1 and Y12-3.

Principal Component Analysis of Volatile Compounds

In an attempt to further understand the difference in the volatile profile between the different inoculated strains of sausage, a total of 33 significantly different volatiles between two batches of sausages were used for the PCA. The first two principle components explained 83.30 and 10.47% of the overall variance, respectively (**Figure 7**). The first principal component (PC1) was the most important variable and positively correlated with most of the volatile compounds except for ten kinds of volatile compounds, 2-methyl-1-butyl acetate, 4-isopropyltoluened and 3-methyl-1-butanol. As shown in **Figure 7B**, inoculate lactobacillus, yeast, and control batches of sausages were well-differentiated along PC1.

Sensory Evaluation

The sensory scores, including color, aroma, chewiness, acid taste, and overall acceptability, are presented in **Figure 8**. The acidity of sausages in batches N102 and H1-5 is significantly higher than other batches. The sensory evaluation team members generally think that the Y4-1 batch of sausages is more aromatic (Fadda et al., 1999). The aroma scores of the Y4-1 batch of sausages were significantly higher than the other batches, which also correspond to the analysis results of volatile compound analysis. Compared with the control batch, the overall acceptability of sausages inoculated with starter was improved to varying degrees.

DISCUSSION

Fermented sausages are the result of biochemical, microbiological, physical and sensorial changes occurring

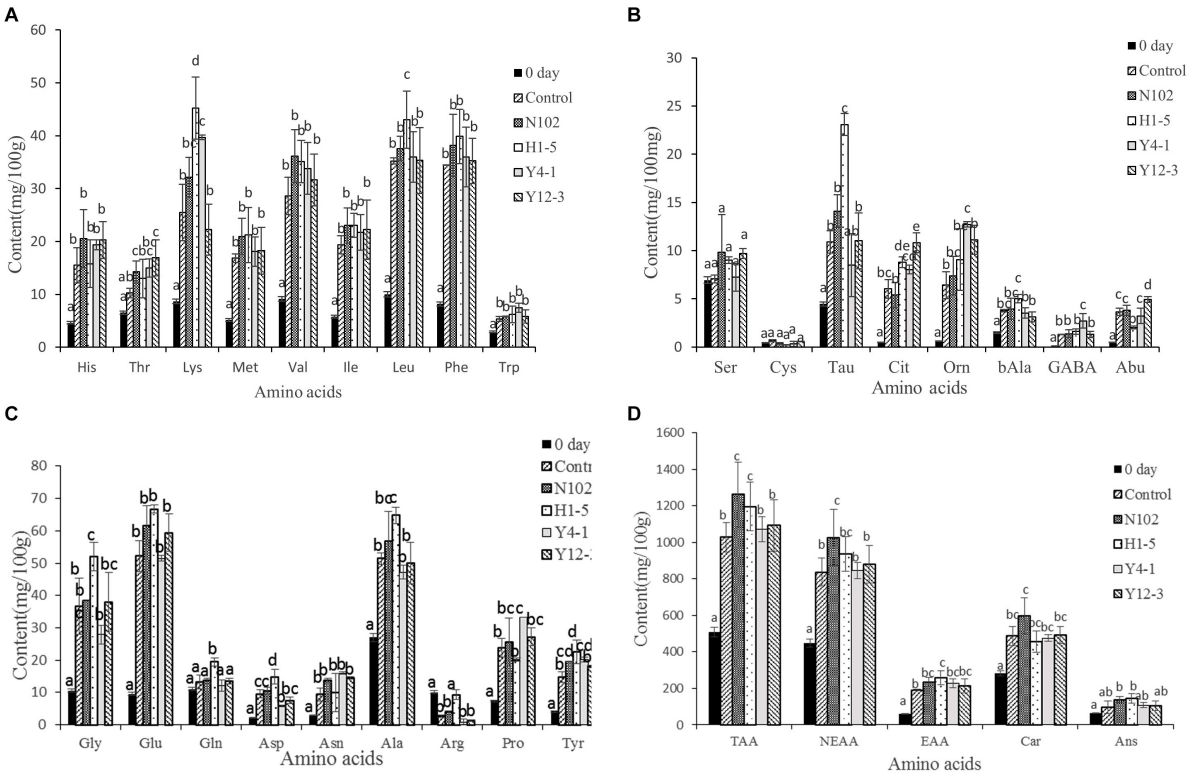

FIGURE 5 | Free amino acids content of the different samples of sausages non-inoculated and inoculated with various starter cultures. Concentration of His, Thr, Lys, Met, Val, Ile, Leu, Phe and Trp **(A)**; Concentration of Ser, Cys, Tau, Cit, Orn, bAla, GABA and Abu **(B)**; the concentration of Gly, Glu, Gln, Asp, Asn, Ala, Arg, Pro and Tyr **(C)**; Concentration of TAA, NEAA, EAA, Car and Ans **(D)**. Error bars refer to the standard deviations obtained from triplicate sample analysis, expressed as mg free amino acid/100 g dry-matter sample. Different letters (a–d) indicate significant differences among the values ($P < 0.05$). TAA, total amino acids; NEAA, nonessential amino acids; EAA, essential amino acid. N102, *L. delbrueckii*; H1-5, *L. sakei*; Y4-1, *D. hansenii*; Y12-3, *W. anomalus*.

TABLE 1 | Changes in free fatty acids (FFA) of the different samples of sausages non-inoculated and inoculated with various starter cultures.

Time (day)	**0**	**28**				
FFA	**Control**	**Control**	**N102**	**H1-5**	**Y4-1**	**Y12-3**
Myristic	3.79 ± 1.01^{a}	13.63 ± 1.27^{d}	8.33 ± 0.64^{b}	11.71 ± 0.60^{c}	11.54 ± 0.08^{c}	9.38 ± 1.47^{bc}
Palmitic	73.28 ± 25.91^{a}	202.56 ± 10.53^{d}	143.48 ± 0.93^{b}	194.92 ± 6.99^{cd}	179.63 ± 12.54^{bcd}	150.37 ± 35.20^{bc}
Stearic	40.42 ± 19.59^{a}	87.25 ± 3.11^{b}	67.31 ± 0.92^{ab}	87.55 ± 4.09^{b}	80.80 ± 7.64^{b}	66.04 ± 14.83^{ab}
Arachidic	2.08 ± 0.81^{a}	10.19 ± 0.63^{c}	6.81 ± 1.25^{b}	10.75 ± 0.42^{c}	8.82 ± 0.21^{bc}	6.99 ± 1.79^{b}
Palmitoleic	4.39 ± 0.83^{a}	23.41 ± 1.39^{c}	14.14 ± 1.48^{b}	23.38 ± 0.04^{c}	19.50 ± 0.69^{c}	18.35 ± 4.56^{bc}
Octadecenoic	90.72 ± 26.09^{a}	445.10 ± 20.24^{c}	278.99 ± 25.22^{b}	439.35 ± 8.57^{c}	357.55 ± 19.46^{bc}	304.23 ± 6.62^{b}
Linoleic	38.62 ± 7.25^{a}	227.69 ± 15.05^{c}	148.29 ± 11.12^{b}	225.96 ± 0.86^{c}	190.02 ± 5.09^{bc}	159.31 ± 6.74^{b}
g-linolenic	0.50 ± 0.07^{a}	4.01 ± 0.57^{d}	2.51 ± 0.53^{b}	3.58 ± 0.18^{cd}	3.43 ± 0.20^{bcd}	2.97 ± 0.35^{bc}
Eicosadienoic	1.67 ± 0.49^{a}	9.32 ± 0.83^{c}	7.13 ± 1.74^{bc}	9.40 ± 0.42^{c}	7.38 ± 0.14^{bc}	5.82 ± 1.27^{b}
Eicosatrienoic	0.00^{a}	0.75 ± 0.01^{d}	0.46 ± 0.00^{b}	0.57 ± 0.03^{c}	0.56 ± 0.02^{c}	0.00^{a}
Arachidonic	2.64 ± 0.13^{a}	14.08 ± 1.22^{c}	8.19 ± 0.29^{b}	12.02 ± 0.84^{bc}	13.97 ± 0.10^{c}	13.27 ± 4.95^{bc}
SFA	119.56 ± 47.32^{a}	313.63 ± 15.53^{c}	225.93 ± 3.73^{b}	304.94 ± 12.09^{bc}	280.80 ± 20.30^{bc}	232.79 ± 53.29^{bc}
MUFA	95.11 ± 26.92^{a}	468.50 ± 21.63^{c}	293.13 ± 26.70^{b}	462.73 ± 8.60^{c}	377.05 ± 20.15^{bc}	322.58 ± 11.18^{b}
PUFA	42.33 ± 6.27^{a}	255.84 ± 17.66^{c}	166.58 ± 13.68^{b}	251.54 ± 1.13^{c}	215.36 ± 5.16^{bc}	181.36 ± 13.31^{b}
Total FFA	257.00 ± 80.51^{a}	1037.97 ± 54.82^{c}	685.64 ± 44.11^{b}	1019.21 ± 21.82^{c}	873.21 ± 45.61^{bc}	736.73 ± 77.78^{b}

The results are expressed as mg/100 g dry matter and are means of three replicates ± standard deviations. Different lowercase letters (a–d) indicate significant differences among the values ($P < 0.05$). SFA, saturated fatty acids; MUFA, monounsaturated fatty acids; PUFA, polyunsaturated fatty acids. N102, L. delbrueckii; H1-5, L. sakei; Y4-1, D. hansenii; Y12-3, W. anomalus.

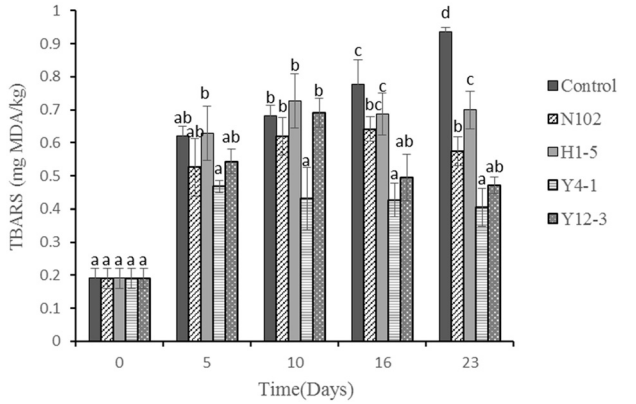

FIGURE 6 | Thiobarbituric acid reactive substances (TBARS) (mg MDA/kg meat) during the ripening of the different samples of sausages non-inoculated and inoculated with various starter cultures. Different letters (a–d) indicate significant differences among different batches at the same fermentation time ($P < 0.05$). N102, *L. delbrueckii*; H1-5, *L. sakei*; Y4-1, *D. hansenii*; Y12-3, *W. anomalus*.

in a meat mixture during ripening in defined conditions of temperature and relative humidity (Villani et al., 2007). Starter cultures are crucial in regulating the quality of fermented sausages. In this study, *L. delbrueckii* N102, *L. sakei* H1-5, *D. hansenii* Y4-1, and *W. anomalus* Y12-3 were selected from traditional fermented foods and inoculated into fermented sausages as starter cultures. The aim was to investigate the effects of different types of starter cultures on the microbial population, fat oxidation, lipolysis, proteolysis, and flavor compounds of the fermented sausage.

The decrease in pH of fermented sausages is due to the production of various organic acids such as lactic acid and acetic acid by LAB (Ammor and Mayo, 2007). Lower pH can inhibit the growth of harmful bacteria and contribute to product safety and extend the shelf life of the product (Osterlie and Lerfall, 2005; Flores and Toldra, 2011). The pH of the sausages inoculated with LAB was significantly lower than that of the control ($P < 0.05$), indicating that *L. delbrueckii* N102 and *L. sakei* H1-5 had strong acid-producing ability and produced more organic acids. This means that *L. delbrueckii* N102 and *L. sakei* H1-5 may help enhance the safety of dry fermented sausages. The pH rise in the middle and late stages of processing is mainly due to the action of microbes and enzymes of the meat tissue, which produces some basic ammonia and amines in the fermented sausage. However, yeast can raise the pH by using lactic acid (Flores et al., 2015). The LAB in each batches are the dominant bacteria, which is consistent with the results of Casaburi et al. (2016). It was found by microbial counts that the number of *Staphylococci* and *Micrococci* in the N102 and H1-5 batches were lower than that of the other batches, probably because *L. delbrueckii* N102 and *L. sakei* H1-5 reduced the pH and inhibited its growth (Casaburi et al., 2008). LAB ensure the safety of the product by reducing the pH of the sausage to inhibit the growth of *Enterobacteriaceae*.

Changes in the state of water in sausages affect product stability and shelf life and sensory qualities such as texture and juiciness by affecting microbial growth and enzyme activity (Fernández et al., 2000; Olivares et al., 2010). In meat products, bound water is an important part of the macromolecule compound; the immobilized water is located in the myofibril network, and the free water is outside the myofibril network (Bertram et al., 2004; Straadt et al., 2007). The change of the immobilized water and the free water is due to the effect of drying rather than fermentation; therefore, their content drops significantly during the late drying period. In sausage processing, the proportion of bound water increases because the structure of the protein changes due to oxidation, and muscle protein is hydrolyzed by bacteria or enzymes (Berardo et al., 2015).

Lactobacillus delbrueckii N102 and *L. sakei* H1-5 showed a strong ability to degrade sarcoplasmic proteins. This conclusion is consistent with the findings of Fadda et al. (1999), which showed that strains of *L. curvatus* and *L. sakei* were capable of hydrolyzing 97, 45, 37, and 26 kDa sarcoplasmic fractions. Protein degradation is one of the main reactions in the process of fermented sausages. It is generally believed that cathepsins play a major role in initiating proteolysis, while microbial enzymes play a weak role and play a role mainly in the late stage of sausage ripening (Berardo et al., 2017); of course, sausage processing also affects protein degradation. Due to the strong hydrolysis of protein by muscle and microbial peptidase, a large number of peptides and free amino acids are produced, which can be involved in the production of fermented sausage flavor. Many free amino acids are precursors to flavoring substances or are themselves flavoring substances. For example, glutamic acid contributes to umami, and the increase in content may be due to deamination of glutamine (Demasi et al., 1990); alanine contributes to sweetness (Ordonez et al., 1999). Branched-chain amino acids (valine, leucine, isoleucine) play an important role in the formation of flavor (Chen et al., 2016), and their content is significantly increased in all samples ($P < 0.05$), of which the leucine content in batch inoculated with H1-5 is the highest. The batch inoculated with *L. sakei* H1-5 has the highest levels of leucine and alanine which is consistent with the study of Flores and Toldra (2011). They believe that *L. sakei* has high exopeptidase activity, and it can produce a large amount of free amino acids (mainly leucine and alanine). The arginine content is reduced compared to day 0 because it can be utilized by the arginine deiminase (ADI) pathway (Mainar et al., 2017; Zagorec and Champomier-Verges, 2017). Taurine has excellent antioxidant activity (Gallego et al., 2018), which is highest in the H1-5 batch. In addition, hydrophobic amino acids (Ala, Phe, Val, Pro, Gly, Leu, and Ile), Glu, and His may also have antioxidant activity (Gallego et al., 2018). At the end of ripening, the dipeptides including carnosine and anserine were produced and have significant biological activity, which are higher than 200 mg/100 g, and the carnosine content of batch inoculated with N102 is significantly higher than that of the control ($P < 0.05$).

Endogenous enzymes found in meat tissues, such as lipases, esterases, and phospholipases, play an important role in the lipolysis process. Acid lipase activity can be activated by reducing water activity and increasing salt content (Motilva and Toldra, 1993). At lower pH, endogenous enzymes in muscle tissue are more efficient at degrading fat (Zanardi et al., 2004). The content

TABLE 2 | Volatile compounds identified and quantified by SPME–GC–MS of the different samples of sausages non-inoculated and inoculated with various starter cultures.

Volatile compounds	Strains				
	Control	N102	H1-5	Y4-1	Y12-3
Aldehydes					
Benzaldehyde	0.44 ± 0.02^{a}	0.45 ± 0.02^{a}	0.34 ± 0.02^{b}	0.17 ± 0.01^{c}	0.46 ± 0.02^{a}
Hexanal	1.62 ± 0.08^{c}	0.78 ± 0.04^{d}	2.56 ± 0.13^{b}	n. d.	4.43 ± 0.22^{a}
Nonana	0.10 ± 0.01^{a}	n. d.	n. d.	n. d.	0.08 ± 0.01^{a}
Heptanal	n. d.	0.12 ± 0.01^{b}	n. d.	n. d.	0.21 ± 0.01^{a}
Total	2.16 ± 0.11^{c}	1.35 ± 0.07^{d}	2.9 ± 0.15^{b}	0.17 ± 0.01^{e}	5.18 ± 0.26^{a}
Alcohols					
1-pentanol	0.19 ± 0.01^{b}	0.24 ± 0.01^{b}	0.15 ± 0.01^{b}	n. d.	0.31 ± 0.02^{a}
4-isopropyltoluene	2.65 ± 0.13^{a}	n. d.	n. d.	1.51 ± 0.08^{c}	1.78 ± 0.10^{b}
1-hexanol	0.11 ± 0.01^{a}	n. d.	n. d.	0.03	0.13 ± 0.01^{a}
2-ethyl-1-hexanol	0.14 ± 0.01^{a}	0.06 ± 0.01^{c}	n. d.	0.03^{d}	0.09^{b}
2,3-butanediol	5.31 ± 0.27^{a}	1.64 ± 0.08^{c}	1.76 ± 0.09^{c}	5.77 ± 0.2^{a}	3.6 ± 0.18^{b}
Isobutanol	1.19 ± 0.06^{a}	n. d.	n. d.	0.08^{c}	0.74 ± 0.04^{b}
3-methyl-1-butanol	n. d.	0.58 ± 0.03^{c}	0.38 ± 0.02^{d}	0.89 ± 0.04^{a}	0.81 ± 0.04^{b}
Ethanol	n. d.	n. d.	0.46 ± 0.02^{c}	14.28 ± 0.71^{a}	1.55 ± 0.08^{b}
2-phenylethanol	n. d.	n. d.	n. d.	0.04 ± 0.01^{a}	0.05 ± 0.01^{a}
Linalool	n. d.	n. d.	n. d.	n. d.	0.12 ± 0.01^{a}
Total	9.59 ± 0.48^{b}	2.52 ± 0.13^{c}	2.75 ± 0.14^{c}	22.63 ± 1.13^{a}	9.18 ± 0.46^{b}
Ketones					
3-hydroxy-2-butanone	9.15 ± 0.46^{a}	n. d.	n. d.	n. d.	n. d.
2-butanone	n. d.	1.30 ± 0.07^{a}	n. d.	n. d.	n. d.
2,3-butanedione	n. d.	21.50 ± 1.08^{a}	9.36 ± 0.47^{a}	n. d.	n. d.
2,3-octanedione	n. d.	37.26 ± 1.86^{a}	27.06 ± 1.35^{b}	3.83 ± 0.19^{d}	4.77 ± 0.24^{c}
2-heptenone	n. d.	n. d.	n. d.	n. d.	0.03
Total	9.15 ± 0.46^{c}	60.06 ± 3.00^{a}	36.42 ± 1.82^{b}	3.83 ± 0.19^{e}	4.8 ± 0.24^{d}
Acids					
Acetic acid	21.1 ± 1.06^{a}	16.71 ± 0.84^{b}	23.21 ± 1.16^{a}	21.73 ± 1.09^{a}	22.29 ± 1.11^{a}
Propionic acid	0.3 ± 0.02^{a}	n. d.	n. d.	0.18 ± 0.01^{c}	0.24 ± 0.01^{b}
Butyric acid	0.52 ± 0.03^{c}	0.34 ± 0.02^{d}	0.53 ± 0.03^{c}	0.62 ± 0.03^{b}	0.83 ± 0.04^{a}
Hexanoic acid	0.25 ± 0.01^{c}	0.19 ± 0.01^{d}	0.13 ± 0.01^{e}	2.41 ± 0.12^{a}	0.36 ± 0.02^{b}
Isobutyric acid	n. d.	0.41 ± 0.02^{b}	0.41 ± 0.02^{b}	2.17 ± 0.11^{a}	n. d.
2-methylbutanoic acid	n. d.	0.98 ± 0.05^{a}	n. d.	n. d.	n. d.
Isovaleric acid	n. d.	n. d.	0.94 ± 0.05^{a}	n. d.	n. d.
Pentanoic acid	n. d.	n. d.	n. d.	0.02	n. d.
Octanoic acid	n. d.	n. d.	n. d.	n. d.	0.08
Total	22.17 ± 1.11^{c}	18.63 ± 0.93^{d}	25.22 ± 1.26^{b}	27.13 ± 1.36^{a}	23.8 ± 1.19^{c}
Esters					
Ethyl acetate	13.66 ± 0.68^{b}	n. d.	n. d.	21.64 ± 1.08^{a}	22.01 ± 1.10^{a}
Ethyl 3-methylbutanoate	0.27 ± 0.01^{b}	n. d.	n. d.	0.28 ± 0.01^{b}	0.70 ± 0.04^{a}
Ethyl hexanoate	0.12 ± 0.01^{c}	n. d.	n. d.	0.02^{b}	0.20 ± 0.01^{a}
Ethyl lactate	0.20 ± 0.01^{d}	0.20 ± 0.01^{d}	0.37 ± 0.02^{b}	0.28 ± 0.01^{c}	0.93 ± 0.05^{a}
2-methyl-1-butyl acetate	n. d.	n. d.	4.82 ± 0.24^{a}	0.73 ± 0.04^{b}	n. d.
Ethyl pentanoate	n. d.	n. d.	n. d.	0.73 ± 0.04^{a}	n. d.
Methylbutyl acetate	n. d.	n. d.	n. d.	0.26 ± 0.01^{a}	n. d.
Total	14.25 ± 0.71^{b}	0.2 ± 0.01^{d}	5.19 ± 0.26^{c}	23.94 ± 1.19^{a}	23.84 ± 1.19^{a}
Terpenes					
α-pinene	0.83 ± 0.04^{c}	1.32 ± 0.07^{b}	1.44 ± 0.07^{a}	0.58 ± 0.03^{d}	n. d.
β-pinene	1.40 ± 0.07^{a}	1.03 ± 0.05^{b}	1.45 ± 0.07^{a}	0.88 ± 0.04^{c}	0.92 ± 0.05^{c}
δ-3-carene	17.91 ± 0.90^{a}	7.53 ± 0.38^{d}	11.30 ± 0.57^{b}	10.01 ± 0.50^{c}	11.36 ± 0.57^{b}
Sabinene	1.79 ± 0.09^{a}	0.27 ± 0.01^{d}	0.59 ± 0.03^{c}	0.77 ± 0.04^{b}	0.74 ± 0.04^{b}

(Continued)

TABLE 2 | Continued

Volatile compounds	Strains				
	Control	N102	H1-5	Y4-1	Y12-3
D-limonene	8.18 ± 0.41^{a}	3.07 ± 0.1^{e}	3.58 ± 0.18^{d}	3.96 ± 0.20^{c}	5.47 ± 0.27^{b}
Terpinolene	0.18 ± 0.01^{a}	n. d.	n. d.	0.04	n. d.
α-terpinene	n. d.	n. d.	n. d.	0.03^{a}	n. d.
α-cubebene	0.14 ± 0.01^{a}	0.04	n. d.	0.03^{b}	0.12 ± 0.01^{a}
β-caryophyllene	4.74 ± 0.24^{a}	1.59 ± 0.08^{d}	1.25 ± 0.06^{e}	2.28 ± 0.11^{c}	3.92 ± 0.10^{b}
β-selinene	0.13 ± 0.01^{a}	n. d.	n. d.	n. d.	0.15 ± 0.01^{a}
Alloaromadendrene	n. d.	n. d.	n. d.	0.04^{b}	0.07^{a}
Isocaryophyllene	n. d.	n. d.	n. d.	n. d.	0.14 ± 0.01^{a}
1-isopropenyl-4-methylbenzene	n. d.	n. d.	n. d.	n. d.	0.08^{a}
δ-elemene	n. d.	n. d.	n. d.	n. d.	0.35 ± 0.02^{a}
Caryophyllene	n. d.	n. d.	0.70 ± 0.04^{a}	n. d.	n. d.
Phenylethylene	n. d.	n. d.	n. d.	0.12 ± 0.02^{a}	n. d.
Total	35.3 ± 1.77^{a}	14.85 ± 0.74^{e}	20.31 ± 1.02^{c}	18.74 ± 0.94^{d}	23.32 ± 1.17^{b}
Others					
Toluene	2.03 ± 0.10^{b}	1.4 ± 0.07^{c}	0.69 ± 0.03^{e}	1.07 ± 0.05^{d}	2.43 ± 0.12^{a}
2-acetyl-1-pyrroline	0.33 ± 0.02^{a}	n. d.	n. d.	0.02^{c}	0.03^{b}
4-isopropyltoluene	n. d.	0.92 ± 0.05^{b}	1.09 ± 0.05^{a}	0.77 ± 0.04^{c}	n. d.
Dimethyl trisulfide	n. d.	0.08^{a}	n. d.	0.05^{b}	0.08^{a}
4-methylphenol	n. d.	n. d.	n. d.	n. d.	0.02^{a}
2,6-dimethyl pyrazine	n. d.	n. d.	n. d.	0.03^{a}	n. d.
Total	2.36 ± 0.12^{b}	2.4 ± 0.12^{b}	1.78 ± 0.08^{d}	1.94 ± 0.09^{c}	2.56 ± 0.12^{a}

The results are means of three replicates ± standard deviations. n. d., not detected.

of free fatty acids is affected by many factors, such as raw meat, processing time, and ingredients, so sausages release different free fatty acids due to various differences (Lorenzo and Franco, 2012). In addition, the FFA composition ratio of the fat tissue of all sausages was similar at the end of fermentation. In other words, during the fermentation process, bacterial fermentation increased the degree of hydrolysis of fats and oils and produced FFAs, but did not change the hydrolysis mode (Chen et al., 2016). It has been reported that hydrogen peroxide is produced by LAB metabolism, which also caused the lipid oxidant to increase. In our experiment, the TBARS value of the batch inoculated with Y4-1 and Y12-3 was lower than that of the other batch, indicating that the yeast may have an inhibitory effect on lipid oxidation. Meanwhile, Flores et al. (2004) found that the fermentation of sausage by inoculation with *D. hansenii* inhibited the oxidation of lipids and facilitated the formation of ethyl esters.

Flavor is one of the important qualities of fermented sausage. The carbohydrates in fermented sausages are metabolized by LAB to produce organic acids such as lactic acid, acetic acid, formic acid, propionic acid, butyric acid, and 3-methyl-butyric acid. Yeast in fermented sausages promotes the drying process of sausages (Lucke, 2000), and it also has proteolytic and lipolytic activities that affect the flavor of the product (Flores et al., 2004). The 2,3-butanediol was detected in all five batches of sausages with high content. Most alcohols are derived from the metabolism of carbohydrates by microorganisms such as ethanol and 2,3-butanediol, which are less stable, but can form diacetyl with 3-hydroxy-2-butanone to improve the overall flavor of the sausage (Mateo et al., 1996). Martin et al. (2003) reported that high concentrations of cyclic alcohol and aromatic alcohol can be produced when inoculating yeast. This result is consistent with the effect of strains Y4-1 and Y12-3 on the production of alcohols. Among the acid substances in all batches, the content of acetic acid is the highest, which is mainly formed by the metabolism of carbohydrates by LAB. In addition, the metabolism of fat and amino acids also produces acetic acid. Hexanoic acid content of the batch Y4-1 was the highest, probably due to the higher ethanol content of the Y4-1 batch reacting with butyric acid to form hexanoic acid. The batch inoculated with H1-5 detected higher isovaleric acid, which may be derived from the degradation of amino acids, which is consistent with H1-5 strains contributing to the release of amino acids. Acidic substances are important and representative flavor substances in fermented sausages and play an important role in the formation of esters. At the same time, the acid substance can improve the flavor complexity of the product and promote the fermentation sausage to form its unique sensory flavor characteristics. The source of aldehydes is mainly the oxidation of fats. The detection amount of aldehydes in the y4-1 inoculation batch was lower, especially hexanal and nonanal, which was corresponding to the results of TBARS discussed above, further confirming that Y4-1 may have antioxidant activity. Some branched aldehydes are derived from the Strecker degradation reaction of the corresponding amino acids and microbial action and the aldehydes of C5-C9 usually come from fat oxidation and have a fatty odor. Ketones contribute to lactic aroma notes, mainly due to the butter aroma

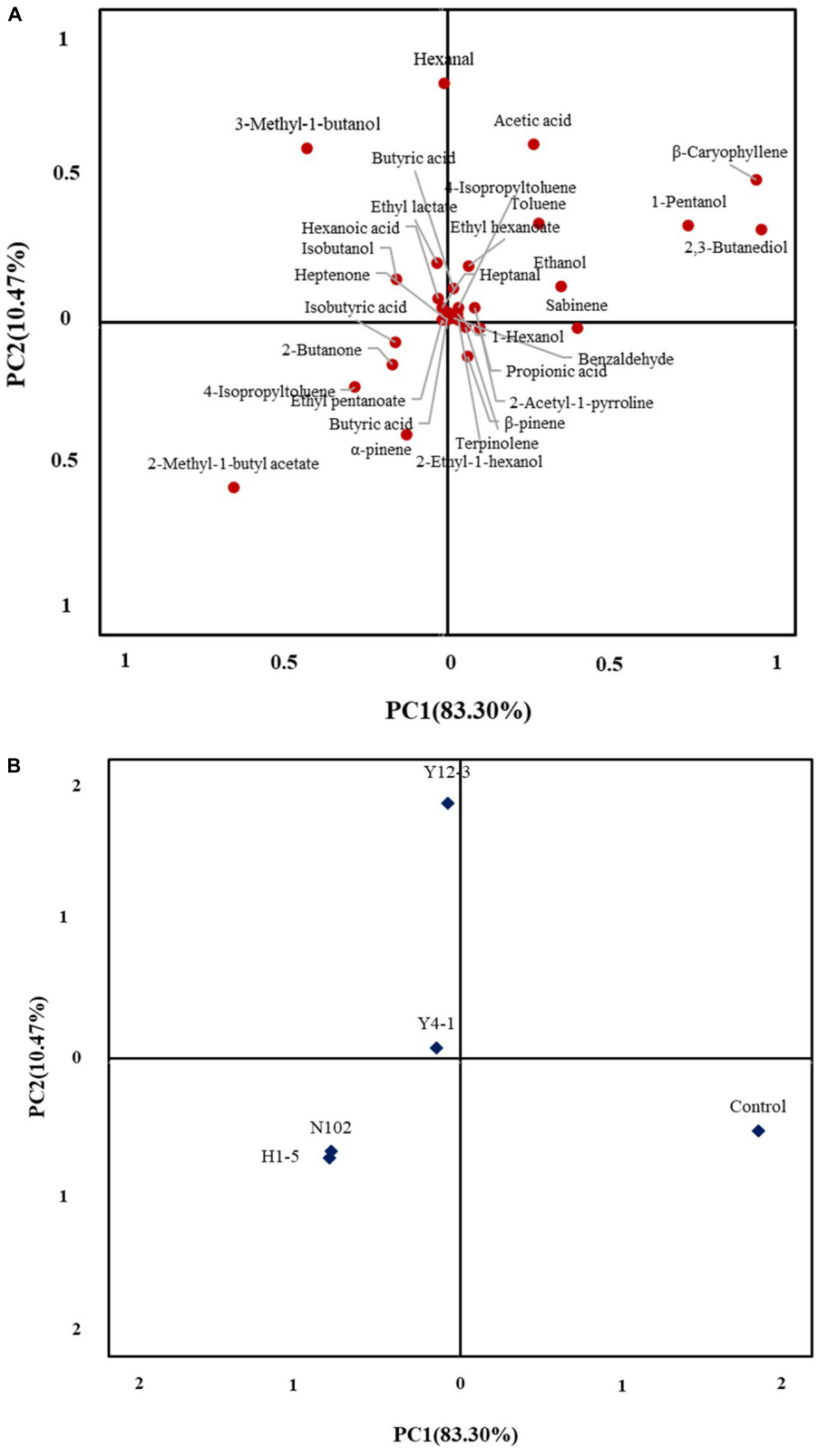

FIGURE 7 | Principal component analysis loading plot **(A)** of volatile compound and principal component analysis score plot **(B)** of dry fermented sausages inoculated with different starter cultures.

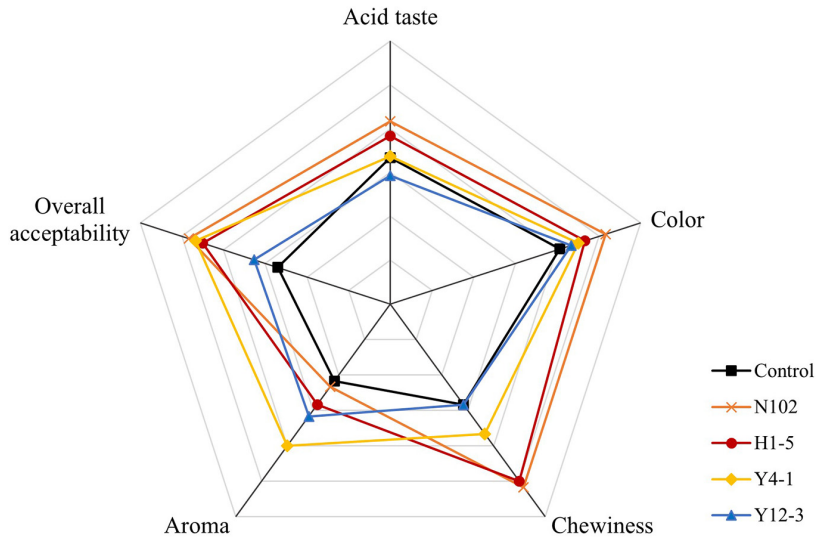

FIGURE 8 | Sensory evaluation of the fermented sausages with different starter cultures.

produced by 2,3-butanedione, as well as other aroma notes such as mushroom and herbs. The 3-hydroxy-2-butanone and 2,3-octanedione detected in the HG sample were linked to citrate and lactose metabolism through the action of LAB and could also be generated through amino acid catabolism (Kieronczyk et al., 2004; Hu et al., 2020). The ester substance is necessary for the formation of the flavor of the fermented sausage, as the ethyl ester substance imparts a fruity and creamy aroma to the product, which is an important substance for promoting the formation of the flavor of the fermented sausage. Ethyl esters, usually present in fermented meat products, may arise from the action of inoculated yeast strains. The first reported effect on VOCs and aroma by yeast inoculation (*D. hansenii*) in fermented sausages indicated the promotion of ethyl ester compounds. Jesus Andrade et al. (2010) inoculated different *D. hansenii* strains isolated from dry cured hams in dry fermented sausages (Jesus Andrade et al., 2009) to study the effect on VOCs production. Similarly, Cano-Garcia et al. (2014b) believe that *D. hansenii* strains contribute to the esters in sausages. As the result of volatile compound analysis and principal component analysis showed, the flavor characteristics of LAB and yeast are obviously different. The strains Y4-1 and Y12-3 may contribute to the formation of esters, Yeast y4-1 and y12-3 can promote the esters formation such as ethyl lactate, ethyl hexanoate. Due to the presence of some pyruvate decarboxylases and alcohol dehydrogenases in yeasts (Dura et al., 2004), the alcohol content of the batches inoculated with yeast is higher. This aliphatic alcohol has not been described as essential in the aroma development of dry-cured meat products but it is the precursor of several esters (Molimard and Spinnler, 1996). This may be the reason why yeast promotes the production of esters. LAB were more inclined to produce butyric acid and isobutyric acid, which are produced through carbohydrate metabolism. The sensory analysis results also show that *D. hansenii* Y4-1 can enhance the flavor quality of dry fermented sausages. Compared with LAB, yeast, especially Y4-1, shows that the content of aldehyde compounds produced is lower, and the overall volatile flavor components are more abundant. This indicates that y4-1 may have the effect of inhibiting lipid oxidation and promoting the formation of dry fermented sausage flavor.

In conclusion, based on the understanding of the effect of single starter on the quality of dry fermented sausage, the functional differences between strains in sausage were further clarified, and the two starter cultures of LAB and yeast have their own advantages in acid production, bacteriostasis, protein degradation, antioxidant and flavor substance formation, which cannot be completely replaced by each other. However, considering the influence of strain on free amino acids and flavor, *L. sakei* H1-5 is better than *L. delbrueckii* N102. In addition, considering the long-term storage time of the product, antioxidant is also an important quality factor. Therefore, *D. hansenii* y4-1 is better than *W. anomalus* y12-3, which can be used for subsequent dry fermented sausage production and further sales. Of course, considering the combination of factors, it is necessary to further explore the overall impact of LAB and yeast cooperatively on the quality of salami sausage.

DATA AVAILABILITY STATEMENT

The original contributions presented in the study are included in the article/supplementary material, further inquiries can be directed to the corresponding author/s.

AUTHOR CONTRIBUTIONS

YL designed and drafted the manuscript. ZW carried out the physicochemical properties test and sausage making. KY

performed the analysis of microbial population's part. QY performed the analysis of volatile flavor compounds. ZY carried out the TBARS test. HL and JL provided helpful feedback and revised the manuscript. JW assisted in securing funding and managed the project. All authors contributed to the article and approved the submitted version.

FUNDING

This work was supported by the National Key R&D Program of China (2018YFD0401200), Beijing Excellent Talents Funding for Youth Scientist Innovation Team (2016000026833TD01), and High-level Teachers in Beijing Municipal Universities (IDHT20180506).

REFERENCES

Almeida da Costa, W. K., de Souza, G. T., Brandao, L. R., de Lima, R. C., Garcia, E. F., Lima, M.d.S, et al. (2018). Exploiting antagonistic activity of fruit-derived *Lactobacillus* to control pathogenic bacteria in fresh cheese and chicken meat. *Food Res. Int.* 108, 172–182. doi: 10.1016/j.foodres.2018.03.045

Ammor, M. S., and Mayo, B. (2007). Selection criteria for lactic acid bacteria to be used as functional starter cultures in dry sausage production: an update. *Meat Sci.* 76, 138–146. doi: 10.1016/j.meatsci.2006.10.022

Barbosa, M.d.S, Todorov, S. D., Ivanova, I., Chobert, J.-M., Haertle, T., and Gombossy de Melo Franco, B. D. (2015). Improving safety of salami by application of bacteriocins produced by an autochthonous *Lactobacillus curvatus* isolate. *Food Microbiol.* 46, 254–262. doi: 10.1016/j.fm.2014.08.004

Berardo, A., Claeys, E., Vossen, E., Leroy, F., and De Smet, S. (2015). Protein oxidation affects proteolysis in a meat model system. *Meat Sci.* 106, 78–84. doi: 10.1016/j.meatsci.2015.04.002

Berardo, A., Devreese, B., De Maere, H., Stavropoulou, D. A., Van Royen, G., Leroy, F., et al. (2017). Actin proteolysis during ripening of dry fermented sausages at different pH values. *Food Chem.* 221, 1322–1332. doi: 10.1016/j.foodchem.2016.11.023

Bertram, H. C., Kristensen, M., and Andersen, H. J. (2004). Functionality of myofibrillar proteins as affected by pH, ionic strength and heat treatment – a low-field NMR study. *Meat Sci.* 68, 249–256. doi: 10.1016/j.meatsci.2004.03.004

Bidlingmeyer, B. A., Cohen, S. A., Tarvin, T. L., and Frost, B. (1987). A new, rapid, high-sensitivity analysis of amino acids in food type samples. *J. Assoc. Off. Anal. Chem.* 70, 241–247. doi: 10.1093/jaoac/70.2.241

Bligh, E. G., and Dyer, W. J. (1959). A rapid method of total lipid extraction and purification. *Can. J. Biochem. Physiol.* 37, 911–917.

Cano-Garcia, L., Belloch, C., and Flores, M. (2014a). Impact of *Debaryomyces hansenii* strains inoculation on the quality of slow dry-cured fermented sausages. *Meat Sci.* 96, 1469–1477. doi: 10.1016/j.meatsci.2013.12.011

Cano-Garcia, L., Rivera-Jimenez, S., Belloch, C., and Flores, M. (2014b). Generation of aroma compounds in a fermented sausage meat model system by *Debaryomyces hansenii* strains. *Food Chem.* 151, 364–373. doi: 10.1016/j.foodchem.2013.11.051

Casaburi, A., Aristoy, M. C., Cavella, S., Di Monaco, R., Ercolini, D., Toldra, F., et al. (2007). Biochemical and sensory characteristics of traditional fermented sausages of Vallo di Diano (Southern Italy) as affected by the use of starter cultures. *Meat Sci.* 76, 295–307. doi: 10.1016/j.meatsci.2006.11.011

Casaburi, A., Di Martino, V., Ferranti, P., Picariello, L., and Villani, F. (2016). Technological properties and bacteriocins production by *Lactobacillus curvatus* 54M16 and its use as starter culture for fermented sausage manufacture. *Food Control* 59, 31–45. doi: 10.1016/j.foodcont.2015.05.016

Casaburi, A., Di Monaco, R., Cavella, S., Toldra, F., Ercolini, D., and Villani, F. (2008). Proteolytic and lipolytic starter cultures and their effect on traditional fermented sausages ripening and sensory traits. *Food Microbiol.* 25, 335–347. doi: 10.1016/j.fm.2007.10.006

Chen, Q., Kong, B., Han, Q., Liu, Q., and Xu, L. (2016). The role of bacterial fermentation in the hydrolysis and oxidation of sarcoplasmic and myofibrillar proteins in Harbin dry sausages. *Meat Sci.* 121, 196–206. doi: 10.1016/j.meatsci.2016.06.012

Chu, X., Guo, L., Ye, Z., Cao, L., Liu, Y., and Lin, J. (2015). Screening and identification of lactic acid bacteria with degrading nitrite and cholesterol from *Laminaria japonica*. *Sci. Technol. Food Ind.* 36, 163–167, 177. doi: 10.13386/j.issn1002-0306.2015.03.025

Cocolin, L., Dolci, P., and Rantsiou, K. (2011). Biodiversity and dynamics of meat fermentations: the contribution of molecular methods for a better comprehension of a complex ecosystem. *Meat Sci.* 89, 296–302. doi: 10.1016/j.meatsci.2011.04.011

Demasi, T. W., Wardlaw, F. B., Dick, R. L., and Acton, J. C. (1990). Nonprotein nitrogen (NPN) and free amino acid contents of dry, fermented and nonfermented sausages. *Meat Sci.* 27, 1–12. doi: 10.1016/0309-1740(90)90024-z

Drosinos, E. H., Paramithiotis, S., Kolovos, G., Tsikouras, I., and Metaxopoulos, I. (2007). Phenotypic and technological diversity of lactic acid bacteria and *Staphylococci* isolated from traditionally fermented sausages in Southern Greece. *Food Microbiol.* 24, 260–270. doi: 10.1016/j.fm.2006.05.001

Dura, M. A., Flores, M., and Toldra, F. (2004). Effect of growth phase and dry-cured sausage processing conditions on *Debaryomyces* spp. generation of volatile compounds from branched-chain amino acids. *Food Chem.* 86, 391–399. doi: 10.1016/j.foodchem.2003.09.014

Fadda, S., Sanz, Y., Vignolo, G., Aristoy, M. C., and Vilardell, F. T. (1999). Hydrolysis of pork muscle sarcoplasmic proteins by *Lactobacillus curvatus* and *Lactobacillus sake*. *Appl. Environ. Microbiol.* 65, 578–584. doi: 10.1128/AEM.65.2.578-584.1999

Fernández, M., Ordóñez, J. A., Bruna, J. M., Herranz, B., and Hoz, L. D. L. (2000). Accelerated ripening of dry fermented sausages. *Trends Food Sci. Technol.* 11, 201–209. doi: 10.1016/S0924-2244(00)00077-7

Flores, M., Corral, S., Cano-Garcia, L., Salvador, A., and Belloch, C. (2015). Yeast strains as potential aroma enhancers in dry fermented sausages. *Int. J. Food Microbiol.* 212, 16–24. doi: 10.1016/j.ijfoodmicro.2015.02.028

Flores, M., Dura, M. A., Marco, A., and Toldra, F. (2004). Effect of *Debaryomyces* spp. on aroma formation and sensory quality of dry-fermented sausages. *Meat Sci.* 68, 439–446. doi: 10.1016/j.meatsci.2003.04.001

Flores, M., and Toldra, F. (2011). Microbial enzymatic activities for improved fermented meats. *Trends Food Sci. Technol.* 22, 81–90. doi: 10.1016/j.tifs.2010.09.007

Gallego, M., Mora, L., Escudero, E., and Toldra, F. (2018). Bioactive peptides and free amino acids profiles in different types of European dry-fermented sausages. *Int. J. Food Microbiol.* 276, 71–78. doi: 10.1016/j.ijfoodmicro.2018.04.009

Guadayol, J. M., Caixach, J., Ribé, J., Cabañas, J., and Rivera, J. (1997). Extraction, separation and identification of volatile organic compounds from paprika oleoresin (Spanish type). *J. Agric. Food Chem.* 45, 1868–1872. doi: 10.1021/jf960266i

Hu, Y., Zhang, L., Liu, Q., Wang, Y., Chen, Q., and Kong, B. (2020). The potential correlation between bacterial diversity and the characteristic volatile flavour of traditional dry sausages from Northeast China. *Food Microbiol.* 91:103505. doi: 10.1016/j.fm.2020.103505

Huang, P., Shao, X., Zhu, M., Xu, B., Chen, C., and Li, P. (2020). Sucrose enhances colour formation in dry sausages by up-regulating gene expression of nitric oxide synthase in *Staphylococcus vitulinus*. *Int. J. Food Microbiol.* 315:108419. doi: 10.1016/j.ijfoodmicro.2019.108419

Jesus Andrade, M., Jose Cordoba, J., Ma Casado, E., Cordoba, M. G., and Rodriguez, M. (2010). Effect of selected strains of *Debaryomyces hansenii* on the volatile compound production of dry fermented sausage "salchichon". *Meat Sci.* 85, 256–264. doi: 10.1016/j.meatsci.2010.01.009

Jesus Andrade, M., Jose Cordoba, J., Sanchez, B., Casado, E. M., and Rodriguez, M. (2009). Evaluation and selection of yeasts isolated from dry-cured Iberian ham by their volatile compound production. *Food Chem.* 113, 457–463. doi: 10.1016/j.foodchem.2008.07.080

Kieronczyk, A., Skeie, S., Langsrud, T., Le Bars, D., and Yvon, M. (2004). The nature of aroma compounds produced in a cheese model by glutamate dehydrogenase positive *Lactobacillus* INF15D depends on its relative aminotransferase activities towards the different amino acids. *Int. Dairy J.* 14, 227–235. doi: 10.1016/j.idairyj.2003.07.001

Laemmli, U. K. (1970). Cleavage of structural proteins during the assembly of the head of bacteriophage T4. *Nature* 227, 680–685. doi: 10.1038/227680a0

Liu, Y., Li, W., Zhang, H., Wang, J., and Sun, B. (2015). Screening of aroma-producing yeast strains from traditional fermented food and research on their aroma-production and fermentation characteristics. *J. Chin. Inst. Food Sci. Technol.* 15, 63–70. doi: 10.16429/j.1009-7848.2015.04.008

Lorenzo, J. M., and Franco, D. (2012). Fat effect on physico-chemical, microbial and textural changes through the manufactured of dry-cured foal sausage lipolysis, proteolysis and sensory properties. *Meat Sci.* 92, 704–714. doi: 10.1016/j.meatsci.2012.06.026

Lucke, F. K. (2000). Utilization of microbes to process and preserve meat. *Meat Sci.* 56, 105–115. doi: 10.1016/s0309-1740(00)00029-2

Mainar, M. S., Stavropoulou, D. A., and Leroy, F. (2017). Exploring the metabolic heterogeneity of coagulase-negative *Staphylococci* to improve the quality and safety of fermented meats: a review. *Int. J. Food Microbiol.* 247, 24–37. doi: 10.1016/j.ijfoodmicro.2016.05.021

Martin, A., Cordoba, J. J., Benito, M. J., Aranda, E., and Asensio, M. A. (2003). Effect of *Penicillium chryso* genum and *Debaryomyces hansenii* on the volatile compounds during controlled ripening of pork loins. *Int. J. Food Microbiol.* 84, 327–338. doi: 10.1016/s0168-1605(02)00474-9

Mateo, J., Dominguez, M. C., Aguirrezabal, M. M., and Zumalacarregui, J. (1996). Taste compounds in chorizo and their changes during ripening. *Meat Sci.* 44, 245–254. doi: 10.1016/s0309-1740(96)00098-8

Mauriello, G., Casaburi, A., and Villani, F. (2002). Proteolytic activity of *Staphylococcus xylosus* strains on pork myofibrillar and sarcoplasmic proteins and use of selected strains in the production of 'Naples type' salami. *J. Appl. Microbiol.* 92, 482–490. doi: 10.1046/j.1365-2672.2002.01551.x

Molimard, P., and Spinnler, H. E. (1996). Compounds involved in the flavor of surface mold-ripened cheeses: origins and properties. *J. Dairy Sci.* 79, 169–184. doi: 10.3168/jds.S0022-0302(96)76348-8

Montel, M. C., Masson, F., and Talon, R. (1998). Bacterial role in flavour development. *Meat Sci.* 49S1, S111–S123.

Motilva, M. J., and Toldra, F. (1993). Effect of curing agents and water activity on pork muscle and adipose subcutaneous tissue lipolytic activity. *Z. Lebensm. Unters. Forsch.* 196, 228–232. doi: 10.1007/BF01202737

Navarro, J. L., Nadal, M. I., Izquierdo, L., and Flores, J. (1997). Lipolysis in dry cured sausages as affected by processing conditions. *Meat Sci.* 45, 161–168. doi: 10.1016/s0309-1740(96)00118-0

Olivares, A., Luis Navarro, J., Salvador, A., and Flores, M. (2010). Sensory acceptability of slow fermented sausages based on fat content and ripening time. *Meat Sci.* 86, 251–257. doi: 10.1016/j.meatsci.2010.04.005

Ordonez, J. A., Hierro, E. M., Bruna, J. M., and de la Hoz, L. (1999). Changes in the components of dry-fermented sausages during ripening. *Crit. Rev. Food Sci. Nutr.* 39, 329–367. doi: 10.1080/10408699991279204

Osterlie, M., and Lerfall, J. (2005). Lycopene from tomato products added minced meat: effect on storage quality and colour. *Food Res. Int.* 38, 925–929. doi: 10.1016/j.foodres.2004.12.003

Straadt, I. K., Rasmussen, M., Andersen, H. J., and Bertram, H. C. (2007). Aging-induced changes in microstructure and water distribution in fresh and cooked pork in relation to water-holding capacity and cooking loss – a combined confocal laser scanning microscopy (CLSM) and low-field nuclear magnetic resonance relaxation study. *Meat Sci.* 75, 687–695. doi: 10.1016/j.meatsci.2006.09.019

Villani, F., Casaburi, A., Pennacchia, C., Filosa, L., Russo, F., and Ercolini, D. (2007). Microbial ecology of the soppressata of Vallo di Diano, a traditional dry fermented sausage from southern Italy, and in vitro and in situ selection of autochthonous starter cultures. *Appl. Environ. Microbiol.* 73, 5453–5463. doi: 10.1128/aem.01072-07

Wang, L. L., and Xiong, Y. L. L. (2005). Inhibition of lipid oxidation in cooked beef patties by hydrolyzed potato protein is related to its reducing and radical scavenging ability. *J. Agric. Food Chem.* 53, 9186–9192. doi: 10.1021/jf051213g

Wen, R., Hu, Y., Zhang, L., Wang, Y., Chen, Q., and Kong, B. (2019). Effect of NaCl substitutes on lipid and protein oxidation and flavor development of Harbin dry sausage. *Meat Sci.* 156, 33–43. doi: 10.1016/j.meatsci.2019.05.011

Xiao, Y., Li, P., Zhou, Y., Ma, F., and Chen, C. (2018). Effect of inoculating *Lactobacillus pentosus* R3 on N-nitrosamines and bacterial communities in dry fermented sausages. *Food Control* 87, 126–134. doi: 10.1016/j.foodcont.2017.12.025

Xiao, Y., Liu, Y., Chen, C., Xie, T., and Li, P. (2020). Effect of *Lactobacillus plantarum* and *Staphylococcus xylosus* on flavour development and bacterial communities in Chinese dry fermented sausages. *Food Res. Int.* 135:109247. doi: 10.1016/j.foodres.2020.109247

Zagorec, M., and Champomier-Verges, M.-C. (2017). *Lactobacillus sakei*: a starter for sausage fermentation, a protective culture for meat products. *Microorganisms* 5:56. doi: 10.3390/microorganisms5030056

Zanardi, E., Ghidini, S., Battaglia, A., and Chizzolini, R. (2004). Lipolysis and lipid oxidation in fermented sausages depending on different processing conditions and different antioxidants. *Meat Sci.* 66, 415–423. doi: 10.1016/s0309-1740(03)00129-3

Zhang, Q. Q., Li, W., Li, H. K., Chen, X. H., Jiang, M., and Dong, M. S. (2017). Low-field nuclear magnetic resonance for online determination of water content during sausage fermentation. *J. Food Eng.* 212, 291–297. doi: 10.1016/j.jfoodeng.2017.05.021

Conflict of Interest: The authors declare that the research was conducted in the absence of any commercial or financial relationships that could be construed as a potential conflict of interest.

frontiers in Microbiology

ORIGINAL RESEARCH
published: 26 January 2021
doi: 10.3389/fmicb.2020.623775

Flavor Composition and Microbial Community Structure of Mianning Ham

*Lin Chen†, Zhengli Wang†, Lili Ji, Jiamin Zhang, Zhiping Zhao, Rui Zhang, Ting Bai, Bo Hou and Wei Wang**

Key Lab of Meat Processing of Sichuan Province, Chengdu University, Chengdu, China

Mianning ham, a traditional Chinese dry-cured ham, is protected by national geographical indications. To understand the surface and internal flavor composition and microbial community structure of Mianning ham, solid phase microextraction-gas chromatography (SPME-GC-MS) technology and Illumina high-throughput sequencing were utilized. The results showed that a total of 60 flavor substances were identified in the hams. Forty-nine kinds of flavorings were identified on the surface, including 14 aldehydes, 6 ketones, 10 alcohols, 5 esters, 7 hydrocarbons, 5 acids, and 2 other compounds. Thirty-six kinds of internal flavorings were identified, including 13 aldehydes, 4 ketones, 6 alcohols, 3 esters, 5 hydrocarbons, 4 acids and 1 other type. Decanal (34.91 μg/g) was the most prevalent compound on the surface, followed by n-hexanol (24.99 μg/g), n-hexanal (20.20 μg/g), and n-octyl (16.14 μg/g). n-Hexanal (20.74 μg/g) was the most common compound internally, followed by non-aldehyde (5.70 μg/g), 1-octene-3-alcohol (3.54 μg/g), and inverse-2-octenal (2.77 μg/g). *Penicillium lanosum, Penicillium nalgiovense, Debaryomyces hansenii, Staphylococcus equorum*, and *Erwinia tasmaniensis* were isolated from the surfaces of the hams by the traditional culture method. By Illumina high-throughput sequencing, three fungal phyla were identified. Ascomycota was the dominant phylum followed by Basidiomycota. At the genus level, 11 fungi were identified, of which *Aspergillus* was the dominant fungus, followed by *Penicillium* and *Wallemia*. These findings provide fundamental knowledge regarding the microorganisms and flavor compounds in Mianning ham, which will help industrial processors develop effective strategies for standardizing quality parameters.

Keywords: Mianning ham, volatile flavor compound, high-throughput sequencing, fungal community diversity, colony screening, quality

OPEN ACCESS

Edited by:
Wanping Chen,
Georg August University of Göttingen, Germany

Reviewed by:
Jinxuan Cao,
Ningbo University, China
Peijun Li,
Hefei University of Technology, China

***Correspondence:**
Wei Wang
wangwei8619@163.com

† These authors have contributed equally to this work

Specialty section:
This article was submitted to Food Microbiology, a section of the journal Frontiers in Microbiology

Received: *30 October 2020*
Accepted: *30 December 2020*
Published: *26 January 2021*

Citation:
Chen L, Wang Z, Ji L, Zhang J, Zhao Z, Zhang R, Bai T, Hou B and Wang W (2021) Flavor Composition and Microbial Community Structure of Mianning Ham. Front. Microbiol. 11:623775. doi: 10.3389/fmicb.2020.623775

INTRODUCTION

Mianning ham is a famous fermented meat product in Mianning, Sichuan province in southwest China, and is protected by national geographical indications. Mianning hams are made by traditional local techniques and are salty, delicious, rich in aroma, and bright in color. Mianning ham is characterized by plump muscles and small legs, generally weighing 4 ∼ 6 kg (Yang, 1979).

The production technology of Mianning ham includes material selection, repair, curing, washing, and drying, fermentation, and storage. In the production process, plump, fresh, and healthy hind legs should be selected. After four salt applications, the total amount of salt is 9∼10% of the leg weight. After salting, the surface oil and excess salt are washed with clean water, the ham is hung in a ventilated area indoors, and natural fermentation is allowed to occur (Yu, 2004).

Flavor is an important index to evaluate the quality of ham. The flavor of ham comes from the oxidative decomposition of endogenous enzymes during natural fermentation and extracellular enzymes and metabolites secreted by microorganisms (Harkouss et al., 2015; Mu et al., 2019). The microorganisms in ham mainly come from the meat itself, auxiliary materials that are added, the processing environment and manual contact (Comi et al., 2004) and include lactobacillus, staphylococcus, micrococcus, mold, and yeast (Wang, 2008). Microorganisms play an important role in the formation of ham flavor. Microorganisms can degrade the protein of ham muscle and promote the formation of its quality characteristics. At present, there is no report on the flavor composition and microorganisms of Mianning ham. Therefore, the study of the surface and internal flavor composition and microbial community structure of these hams is of great significance for theoretical research and development of the Mianning ham industry.

MATERIALS AND METHODS

Sample Preparation and Sampling

Ten Mianning hams were selected from a batch of hams produced at a processing plant in Mianning (China) and ripened for 24 months. A 0.2-cm-thick piece of Mianning ham surface meat was cut with a sterile scalpel and taken as the surface (BM) sample. Then, a 1 ∼ 1.5-cm-thick piece of ham surface was removed with a scalpel, and sterile scissors or scalpels were used to collect a meat sample from a depth of 3 ∼ 4 cm as an internal (NB) sample (Zhen, 2004). Then, the samples were stored at −20°C for subsequent analysis.

Physical and Chemical Index Measurements

The pH and a_w were measured in triplicate according to the methods described by Wang et al. (2018). The water, nitrite, malondialdehyde, protein, and fat contents were measured in triplicate according to the methods described by Li et al. (2020). The L^* (brightness), a^* (redness), and b^* (yellowness) values were measured in triplicate according to the methods described by Pan (2016).

Flavor Compound Analysis

The surface and internal samples of Mianning ham were cut into pieces, and 3.00 g was accurately weighed into a 15 mL headspace bottle. Then, 1 μL 2,4,6-trimethylpyridine was added to the headspace bottle as an internal standard, and the bottle was sealed (Bai et al., 2018; Zhang et al., 2020). The extraction method for the flavoring substances was headspace solid-phase microextraction (SPME). The pretreatment conditions of the sample were set by the CTC automatic sampler: the heating chamber temperature was 75°C, the heating time was 45 min, the sample extraction time was 20 min, and the analysis time was 5 min. The flavor substances were analyzed with gas chromatography-mass spectrometry (GC-MS).

Gas chromatography conditions: an HP-5 MS UI chromatographic column (30 m × 0.25 mm, 0.25 m) was used; the pressure was 32.0 kPa; the column flow velocity was 1.0 mL/min; the carrier gas was helium, and splitless injection was performed. The temperature of the injection port was 250°C.

Column temperature program: the starting temperature was 40°C for 15 min; the temperature was increased to 160°C at 3°C/min and maintained for 0 min; then, the temperature was increased to 230°C at 4°C/min and maintained for 5 min.

Mass spectrometry conditions: an electron ionization source (EI) was used; the electron energy was 70 eV; the ion source temperature was 230°C; the temperature of the four-stage rod was 150°C; the quality scanning range was 35 ∼ 500 m/z; and the detector voltage was 350 V.

Qualitative analysis: the resulting sample chromatograms were integrated, and the volatile compounds corresponding to the peaks on the matched chromatogram were retrieved from the NIST14. L library at a matching degree of 80%.

Quantitative analysis: the relative contents of each component were obtained by normalizing the peak areas of the total ion flow chromatograms.

Microbial Separation Count

Under aseptic conditions, 12.5 g surface and internal samples were weighed and placed in a sterile homogenizer, 112.5 mL sterile normal saline was added, and the homogenizer was used to beat the samples for 4 min at 5 T/sec to make a 10^{-1} diluent. Then, bacterial solutions of 10^{-2}, 10^{-3}, and 10^{-4} were successively obtained according to the 10-fold dilution method. Then, 0.1 ml of each bacterial dilution was inoculated with the smear method into the following media: plate count agar medium (PCA) with incubation at 36°C for 48 h; MRS agar medium at 36°C for 72 h; mannitol fermentation medium at 36°C for 24 h; and bengal red culture medium at 28°C for 5 days.

Isolation and Identification of Microorganisms

Plates with microbial community numbers between 30∼300 CFU were selected, and a single colony was selected to be smeared and purified on a sterilized plate for growth. The culture temperature and time were the same as before. Individual colonies were observed and preliminarily identified by microscopy after Gram staining. After the preliminary identification, the characteristic colonies were selected for further culture.

The genomic DNA of bacteria and fungi was extracted according to the instructions of the genomic DNA extraction kit. The bacterial 16S rRNA gene was amplified

with universal primers: upstream primer 27F (5′-AGAGTTTGATCCTGGCTCAG-3′) and downstream primer 1492R (5′-GGTTACCTTGTTACGACTT-3′). The general primers for fungal ITS gene amplification were as follows: upstream primer ITS1 (5′-TCCGTAGGTGAACCTGCGG-3′) and downstream primer ITS4 (5′-TCCTCCGCTTATTATTGATATGC-3′). The PCR mixture (50 μL) was mixed for 30 s and contained the following: Taq PCR Master Mix 25 L, template DNA 2 μL, primers 2 μL each, and sterile ddH_2O 19 μL. PCR conditions were as follows: predenaturation at 94°C for 4 min; followed by 30 cycles of denaturation at 94°C for 30 s, annealing at 45°C for 30 s, and elongation at 72°C for 90 s; and final elongation at 72°C for 10 min. The PCR amplification products were determined by 1% agarose gel electrophoresis and then pooled on the device for sequencing. BLAST was used to analyze the homology of genes through the NCBI database, and the sequences of different species with high homology with the target gene sequences were obtained. The bacterial colony characteristics and morphology were comprehensively considered to confirm the identities of the strains.

Fungal Diversity Analysis

Total microbial DNA of the samples was extracted with the HiPure Soil DNA kit according to the manufacturer's protocol. Then, the DNA concentration and purity were determined by a NanoDrop microspectrophotometer. The extraction quality of DNA was determined by 2% agarose gel electrophoresis. The purified DNA was used for amplification of fungal ITS genes. ITS 3-kyo2 (F) (5′-GATGAAGAACGYAGYRAA-3′) and ITS4 (R) (5′-TCCTCCGCTTATTATTGATATGC-3′) were used as primers for PCR amplification of the fungal ITS2 region.

The first round PCR amplification system (50 μL) included the following: 5 μL 10 × KOD buffer, 5 μL 2 mM dNTPs, 3 μL 25 mM $MgSO_4$, 1.5 μL 10 μM forward primer, 1.5 μL 10 μM reverse primer, 1 μL KOD enzyme, 100 ng DNA template, and distilled water to final volume. The amplification procedure was as follows: predenaturation at 94°C for 2 min, 30 cycles of denaturation at 98°C for 10 s, annealing at 62∼66°C for 30 s, and extension at 68°C for 30 s, and final extension at 68°C for 5 min. PCR products were purified by AMPure XP Beads. After purification, the PCR products were quantified with Qubit 3.0. The second round PCR amplification system (50 μL) contained the following: 5 μL 10 × KOD buffer, 5 μL 2 mM dNTPs, 3 μL 25 mM MgSO4, 1 μL 10 μM connector primer, 1 μL 10 μM PCR universal primer, 1 μL KOD enzyme, and 100 ng DNA template. The reaction was brough to final volume with distilled water. The amplification procedure was as follows: predenaturation at 94°C for 2 min, 30 cycles of denaturation at 98°C for 10 s, annealing at 65°C for 30 s, and extension at 68°C for 30 s, and final extension at 68°C for 5 min.

AMPure XP beads were used to purify the second round of amplification products. ABI StepOnePlus Real-Time PCR System (Life Technologies, origin United States) was used for quantitative analysis. According to Novaseq 6000 PE 250 model pooling, PCR amplification products were pooled on the device used for sequencing (Hirokazu et al., 2012). The QIIME platform and RDP Classifier were used to compare the representative OTU sequences, and the Silva taxonomy database was used to annotate the species classification information. The composition of each sample community was calculated according to the comparative data. The species diversity of samples was determined by alpha diversity analysis (Wang et al., 2019). The Ace, Chao1, Shannon and Simpson indexes of each sample at the 97% similarity level were evaluated by using Mothur software.

Statistical Analysis

Microsoft Excel 2019 was used for data statistics, and IBM SPSS 25.0 was used for *t*-tests of the variance. The results showed that $P > 0.05$ was not significant. $0.05 > P > 0.01$ was significant and marked with *; $P < 0.01$ was extremely significant and marked with **.

RESULTS AND DISCUSSION

Physical and Chemical Index Analyses

The physical and chemical indexes of the surface (BM) and internal (NB) of Mianning ham are shown in **Table 1**. Physical and chemical properties are closely related to the quality of ham. Studies have shown that when the pH value of ham is >6.0 ∼ 6.2, there is a high risk of microbial contamination (Ramona et al., 2018); when the pH value is <6.0, the ham has an ideal texture and color; and when the pH value is <5.6, the ham has a more acidic taste (Gou et al., 2008). The surface pH value of the Mianning ham was 5.76 ± 0.01, and the internal pH value was 5.77 ± 0.02, which was close to the pH value of Panxian ham (5.73 ± 0.02) (Mu et al., 2020). The pH value plays an important role in presenting the umami taste of ham and has an obvious effect on the formation of flavor (Ma, 2014). During the processing, due to the REDOX reaction of myoglobin, the L^* (brightness) of the surface was significantly lower than internal, the a^* (redness) of the surface was extremely significantly lower than internal, and there was no significant difference in b^* (yellowness). Because the ham of

TABLE 1 | Physical and chemical indexes of Mianning ham.

Physicochemical indexes	BM	NB
pH	5.76 ± 0.01	5.77 ± 0.02
Color deviation		
L^*	37.21 ± 0.28	41.82 ± 0.29*
a^*	2.76 ± 0.41	11.67 ± 0.71**
b^*	7.82 ± 1.37	10.38 ± 1.01
Moisture content (g/100 g)	22.6 ± 0.681	36.7 ± 0.889**
a_w	0.735 ± 0.001	0.772 ± 0.004**
Fat (g/100 g)	39.0 ± 1.0	19.6 ± 1.1**
Protein (g/100 g)	32 ± 0.58	24 ± 3.1**
Malondialdehyde (mg/kg)	5.4 ± 0.31	1.7 ± 0.10**
Nitrite (mg/kg)	6.3 ± 0.58	0.3 ± 0.00**

*BM is the surface sample of Mianning ham, NB is the internal sample of Mianning ham (the same below). Variance t-test: P > 0.05 was not non-significant, 0.05 > P > 0.01 was significant and marked with *; P < 0.01 was extremely significant and marked with **.*

Mianning is preserved by hanging naturally, the tissue of the ham is hard outside and soft inside. The surface moisture content was 22.6 ± 0.681 g/100 g, and the internal moisture content was 36.7 ± 0.889 g/100 g. Thus, the surface moisture content was significantly lower than the internal moisture content. A low moisture content is of great significance to prevent spoilage and improve the quality of ham. Fan et al. (2019) found that the moisture content of Jinhua ham was 39.1 ± 0.37 g/100 g, that of Xuanwei ham was 45.2 ± 0.79 g/100 g, that of Rugao ham was 41.1 ± 0.09 g/100 g, and that of Xuanwei ham was 43.1 ± 0.12 g/100 g. In contrast, the moisture content of the Mianning ham was relatively low. Low water activity is conducive to the preservation of ham; when $a_W < 0.85$, most of the bacteria stop growing, while mold and a small amount of salt-consuming bacteria can also grow; the surface a_W of Mianning ham was 0.735 ± 0.001, and the internal a_W was 0.772 ± 0.004. Zhang et al. (2009) found that the a_W of Xuanwei ham was 0.758, which was close to the a_W of Mianning ham in this study. The content of fat and protein on the surface was 39.0 ± 1.0 g/100 g and 32 ± 0.58 g/100 g, respectively, and the content of fat and protein internal was 19.6 ± 1.1 g/100 g and 24 ± 3.1 g/100 g, respectively. The content of fat and protein on the surface was significantly higher than internal. The content of malondialdehyde on the surface of Mianning ham was 5.4 ± 0.31 mg/kg, and the content of malondialdehyde inside the ham was 1.7 ± 0.10 mg/kg. Malondialdehyde is the final product of fat oxidation. The surface of the ham had sufficient contact with oxygen, which made it more easily oxidized. The nitrite contents on the surface and internal areas of Mianning ham were 6.3 ± 0.58 and 0.3 ± 0.00 mg/kg, respectively, which were all within the range of nitrite residue limits (<30 mg/kg) of meat products in China. The nitrite content on the surface was significantly higher than the internal nitrite content. The reason for this finding may be that the pickling materials were all applied on the surface of the ham; only part of the nitrite enters into the ham, and the nitrite that enters into the ham is further degraded under the action of lactic acid (Guo, 2017). Dang found that the nitrite content of Nuodeng ham was 0.2 mg/kg after 1 year, close to the internal nitrite content of Mianning ham (Dang, 2018). Fan et al. (2019) found that the nitrite content of Xuanwei ham was 5.97 ± 0.05 mg/kg, close to the surface value of the Mianning ham.

Flavor Compound Analysis

The flavor compound data from the Mianning hams are shown in **Table 2**. Using the SPME-GC-MS method, 49 species flavor compounds were detected on the surface, including 14 aldehydes, 6 ketones, 10 alcohols, 5 esters, 7 hydrocarbons, 5 acids, and 2 other compounds. Thirty-six compounds were detected internally: 13 aldehydes, 4 ketones, 6 alcohols, 3 esters, 5 hydrocarbons, 4 acids, and 1 other compound. There were more kinds of flavor compounds on the surface than internal areas, among which aldehydes and alcohols were the predominant flavor compounds in Mianning ham. Decanal (34.91 μg/g) was the most abundant at the surface, followed by 1-hexanol (24.99 μg/g), hexanal (20.20 μg/g), and octanol (16.14 μg/g). Hexanal (20.74 μg/g) was the most abundant internally, followed by nonanal (5.70 μg/g), 1-octen-3-ol (3.54 μg/g), and (E)-2-octenal (2.77 μg/g). The types of flavor compounds on the surface were more abundant than those in the internal area. The reasons for this difference may be associated with the degree of oxidation on the surface. The surface is in full contact with air, and the degree of oxidation is high (the malondialdehyde content is high). Therefore, a wide variety of flavor substances are formed. The amount of each flavor substance relative to the standard substances was calculated, according to the amount of standard substance added to the ham and compared with the chromatographic peak area of flavor compounds and standard substances. The results showed that the contents of flavor compounds differed among the surface and internal areas. The reason for this difference may be related to the different degrees of oxidation between the surface and internal. A total of 60 flavor compounds were detected in the Mianning hams, and there were 26 common flavor compounds on the surface and internal areas. Using the SPME-GC-MS method, Mu et al. (2019) detected 51 kinds of flavor compounds in Panxian ham, and Tan et al. (2019) detected 56 kinds of flavor compounds in Jinhua Jinzi ham, 53 kinds of flavor compounds in Xuanwei Puji ham, and 57 kinds of flavor compounds in Changshou Rugao ham.

A large number of studies have found that the complex flavor system of meat is composed of components with flavor and aroma activity (Donald, 1998). Volatile flavor substances determine the flavor characteristics of ham and can be divided into two categories: the first class is simple compounds such as hydrocarbons, alcohols, aldehydes, ketones, acids, esters, etc.; the other is heterocyclic compounds containing oxygen, sulfur, and nitrogen atoms, such as furan and its derivatives, thiophene and its derivatives, etc. (Li et al., 2016). The formation pathways of ham flavor compounds include the decomposition of sulfur-containing amino acids, fatty acids, thiamine, the Maillard reaction between sugars and amino acids, microbial action, etc. (Guo et al., 2019; Zhang et al., 2019).

Microbial Separation Count

After pure culture of surface and internal samples, it was found through plate counting results (**Table 3**) that the number of microorganisms on the surface was above 10^6 CFU/g. The number of molds and yeasts was the largest and played an important role in the formation of ham flavor and quality. This is consistent with the research results of Li et al. (2003), in which the number of *Staphylococcus*, *Micrococcus*, and molds on the surface of Xuanwei ham was above 10^6 CFU/g. In this experiment, the internal samples were examined twice according to the microbial culture standard in China, but no microorganisms were cultured. It may be that the high salt content (9∼10%) and low a_W in the ham inhibited the growth of microorganisms.

Isolation and Identification of Microorganisms

Plate count agar, MRS, mannitol, and Bengal red plates were used to isolate and culture the characteristic bacteria from the ham surfaces, and a total of five strains were isolated and numbered

TABLE 2 | Types and contents of flavor compounds in Mianning ham.

Compound	RT	Name	CAS	Absolute content (μg/g)	
				BM	NB
Aldehydes					
1	4.684	Hexanal	66-25-1	20.20 ± 4.44	20.74 ± 1.61
2	10.128	Heptanal	111-71-7	6.73 ± 1.02	1.88 ± 0.30
3	15.741	Benzaldehyde	100-52-7	0.48 ± 0.12	0.64 ± 0.03
4	20.59	Octanal	124-13-0	16.14 ± 1.98	2.44 ± 0.22
5	23.441	Benzeneacetaldehyde	122-78-1	1.92 ± 0.06	1.29 ± 0.34
6	24.774	(E)-2-Octenal	2548-87-0	3.27 ± 0.14	2.77 ± 0.54
7	27.946	Nonanal	124-19-6	34.91 ± 3.23	5.70 ± 1.19
8	31.059	(E)-2-Nonenal	18829-56-6	5.01 ± 0.36	1.98 ± 0.34
9	33.588	Decanal	112-31-2	8.79 ± 1.31	0.26 ± 0.13
10	33.897	(E,E)-2,4-Nonadienal	5910-87-2	0.90 ± 0.34	0.89 ± 0.51
11	36.339	(E)-2-Decenal	3913-81-3	7.28 ± 0.03	2.02 ± 0.76
12	37.843	2,4-Dodecadienal	13162-47-5	0.62 ± 0.10	–
13	38.869	(E,E)-2,4-decadienal	25152-84-5	1.84 ± 0.90	1.76 ± 0.11
14	40.921	Dihydro-5-pentyl-2(3H)-furanone	104-61-0	4.05 ± 0.14	0.34 ± 0.01
15	41.037	2-Undecenal	2463-77-6	4.52 ± 0.21	–
16	58.214	Hexadecanal	629-80-1	–	0.75 ± 0.03
Ketones					
17	9.359	2-Heptanone	110-43-0	6.67 ± 0.25	–
18	9.376	5-Methyl-2-hexanone	110-12-3	–	1.20 ± 0.22
19	19.634	2-Octanone	111-13-7	2.06 ± 0.17	–
20	25.743	3,5-Octadien-2-one	38284-27-4	–	2.16 ± 0.51
21	26.652	8-Nonen-2-one	5009-32-5	–	0.27 ± 0.08
22	27.165	3,5-Octadien-2-one	38284-27-4	–	2.36 ± 0.05
23	27.196	2-Nonanone	821-55-6	4.58 ± 1.98	–
24	35.174	1,4-Cyclooctanedione	55794-45-1	0.51 ± 0.05	–
25	36.462	Cyclodecanone	1502-06-3	0.56 ± 0.06	–
26	41.486	3,6-Dimethyl-octan-2-one	118452-32-7	0.36 ± 0.03	–
Alcohols					
27	8.100	1-Hexanol	111-27-3	24.99 ± 0.57	2.23 ± 0.37
28	17.874	1-Heptanol	111-70-6	4.18 ± 1.91	0.63 ± 0.03
29	18.644	1-Octen-3-ol	3391-86-4	1.78 ± 0.16	3.54 ± 0.10
30	25.772	(Z)-2-Nonen-1-ol	41453-56-9	1.08 ± 0.20	–
31	28.208	Phenylethyl Alcohol	60-12-8	1.07 ± 0.76	–
32	31.968	(S)-(+)-5-Methyl-1-heptanol	57803-73-3	4.33 ± 0.96	–
33	35.634	Z-2-Dodecenol	69064-36-4	–	0.23 ± 0.04
34	36.462	2-Methyl-1-decanol	18675-24-6	–	0.26 ± 0.04
35	38.781	3,4-Di[1-butenyl]-tetrahydrofuran-2-ol	1000131-84-0	0.35 ± 0.08	–
36	40.035	4,4,6-Trimethyl-cyclohex-2-en-1-ol	1000144-64-7	3.22 ± 0.32	0.66 ± 0.20
37	42.646	2-Butyl-1-octanol	3913-02-8	1.59 ± 1.49	–
38	46.056	E-2-Hexadecacen-1-ol	1000131-10-1	0.61 ± 0.00	–
Ester					
39	24.950	n-Caproic acid vinyl ester	3050-69-9	–	1.83 ± 0.58
40	25.985	Formic acid, octyl ester	112-32-3	5.67 ± 0.45	0.90 ± 0.14
41	34.736	Nitric acid, nonyl ester	20633-13-0	0.49 ± 0.11	–
42	36.077	5-Butyldihydro-2(3H)-furanone	104-50-7	1.14 ± 0.10	–
43	38.193	Heptadecyl prop-1-en-2-yl ester carbonic acid	1000382-90-2	0.43 ± 0.09	–
Hydrocarbons					
44	3.815	2-(1,1-Dimethylethyl)-3-methyl-oxirane	53897-30-6	1.75 ± 0.09	1.41 ± 0.04
45	15.951	1-Chloro-octane	111-85-3	2.49 ± 0.55	–
46	22.450	3-Ethyl-2-methyl-1,3-hexadiene	61142-36-7	–	0.35 ± 0.06
47	35.739	(Z)-5-Tridecene	25524-42-9	0.49 ± 0.03	–

(Continued)

TABLE 2 | Continued

Compound	RT	Name	CAS	Absolute content (μg/g)	
				BM	NB
48	38.513	Decyl-oxirane	2855-19-8	0.36 ± 0.17	–
49	41.043	1-Octadecyne	629-89-0	–	2.23 ± 0.05
50	42.605	2-(1-Methylpropyl)-bicyclo[2.2.1]heptane	74663-93-7	–	0.71 ± 0.13
51	45.245	2-Methyltetracosane	1560-78-7	0.46 ± 0.12	–
52	46.784	Pentadecane	629-62-9	2.13 ± 0.13	0.22 ± 0.07
53	50.672	Hexadecane	544-76-3	0.84 ± 0.04	–
Acids					
54	22.176	Hexanoic acid	142-62-1	1.24 ± 0.42	1.76 ± 0.88
55	27.631	Heptanoic acid	111-14-8	0.74 ± 0.17	–
56	32.964	Octanoic acid	124-07-2	2.95 ± 1.26	1.28 ± 0.30
57	37.353	Nonanoic acid	112-05-0	1.30 ± 0.07	0.32 ± 0.03
58	41.830	n-Decanoic acid	334-48-5	4.14 ± 0.22	1.04 ± 0.26
Other					
59	7.429	Syn-3-methyl-butyl aldoxime	5780-40-5	0.37 ± 0.03	–
60	19.448	2-pentyl-Furan	3777-69-3	4.43 ± 0.58	0.74 ± 0.04
61	19.693	2,4,6-trimethyl-Pyridine	108-75-8	6.67 ± 0.00	6.67 ± 0.00

The symbol "–" denotes the substance was not detected.

MN1, MN2, MN3, MN4, and MN5. After observation of the presence of a single colony, Gram staining was used, and the colonies were then examined under the microscope. The bacterial colony characteristics and morphology are shown in **Table 4**. The isolated bacteria were all round colonies with neat middle raised edges. MN1 and MN2 had broom-like branches and were preliminarily determined to be molds. MN4 was a G^+ bacteria, with a white color and a grape-like pattern and was preliminarily determined to be Staphylococcus.

The isolated bacteria were subjected to ITS and 16S rRNA sequencing, and the identification results (**Table 5**) showed that MN1 was *Penicillium lanosum*, MN2 was *Penicillium nalgiovense*, MN3 was *Debaryomyces hansenii*, MN4 was *Staphylococcus equorum*, and MN5 was *Erwinia tasmaniensis*. *P. nalgiovense* is a rare species found in Shennongjia of Hubei province, Deyang of Sichuan province, Dujiangyan of Sichuan province, and Guiyang of Guizhou province. It has been reported from moldy pork, soil, pot lids and paper boxes. He et al. (2008) found that the molds in Jinhua ham mainly included *Penicillium italium*, *Penicillium simum*, *Penicillium citrate*, *Aspergillus sagrada*, and *Aspergillus flavus*. Zou et al. (2020) found that fungi in Jinhua ham mainly included *Aspergillus pseudoglaucus*, *Aspergillus penicillioides*, *Phialosimplex caninus*, *Yamadazyma triangularis*,

TABLE 3 | Microbes in Mianning ham.

	Colony number (CFU/g)	Lactic acid bacteria (CFU/g)	Micrococcus and Staphylococcus (CFU/g)	Mold and yeast (CFU/g)
BM	2.4×10^6	1.5×10^6	2.1×10^6	2.8×10^6
NB	–	–	–	–

The symbol "–" denotes the microbes was not detected.

TABLE 4 | Colony characteristics and morphology of isolated strains from Mianning ham.

Name	Colony characteristics	Mycelial morphology
MN1	White, round, middle raised edge is neat	Broom-like branches, three-whorled, double-whorled or irregular, conidia spherical
MN2	Grayish white, round, middle raised edge is neat	Broom-like branches, three-whorled, double-whorled or irregular, conidia spherical
MN3	Reddish, round, middle raised edge is neat, matte	The bacteria are large, oval in shape
MN4	Milky white, round, smooth surface, middle raised edge is neat	G^+, globular, singly, in pairs or in a grape-like pattern
MN5	White, smooth surface, round, middle raised edge is neat	G^-, short rod-shaped, singly, in pairs or in irregular clumps

TABLE 5 | Identification results of five strains isolated from Mianning ham.

Name	Identification results
MN1	*Penicillium lanosum*
MN2	*Penicillium nalgiovense*
MN3	*Debaryomyces hansenii*
MN4	*Staphylococcus equorum*
MN5	*Erwinia tasmaniensis*

TABLE 6 | Alpha diversity indexes of fungi in Mianning hams.

Samples	Reads	Observed OTUs	Shannon	Simpson	Chao1	Ace	Good's coverage
BM	95,733	41	0.31	0.07	45.00	51.20	1.00
NB	97,820	43	0.70	0.16	45.14	46.32	1.00

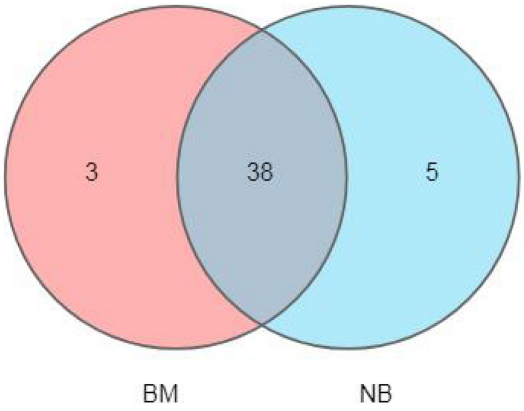

FIGURE 1 | Venn diagram of fungal diversity of Mianning hams.

Candida glucosophila, *Wallemia sebi*, etc. Dang (2018) found that the fungi on the surface of Nuodeng ham included *Scopulariopsis*, *Epicoccum*, *Pithoascus*, *Phallu, Valsa*, *Hypochnicium*, *Pithoascus Aspergillus, Cercospora, Isaria, Penicillium*, and so on. No *P. lanosum* was detected in any of these famous hams, but *P. lanosum* was the dominant fungus in Mianning ham. At present, there are few reports on *P. lanosum*, and its effect on quality characteristics and flavor formation in ham needs to be further studied. In this study, only five kinds of microorganisms were isolated. This kind of result may be related to sample freezing treatment.

OTU Diversity and Taxonomic Annotation

The alpha diversity index of fungi in Mianning ham is shown in **Table 6**. After raw reads were obtained by sequencing, low-quality reads were filtered. Then, they were assembled and refiltered to obtain effective data for OTU clustering (Nicholas et al., 2013). A total of 95,733 high-quality ITS gene sequences were recovered from the surface, with a total length of 33,296,274 bp. The sequences were clustered into 41 OTUs with 97% consistency. A total of 97,820 high-quality ITS gene sequences were recovered internally, with a total length of 34,140,823 bp. The sequences were clustered into 43 OTUs with 97% consistency. There was a small difference in the number of OTUs from the surface and internal samples, indicating a small difference in the diversity of fungi on the surface and internal areas. Both the surface and internal fungal coverage rates were 1.00, indicating that the sequencing depth was sufficient to reflect the fungal community contained in the samples. The fungal abundance on the surface of the ham was higher than that on the internal, and the fungal diversity on the internal was higher than that on the surface.

A Venn diagram (**Figure 1**) was used to analyze and compare the common and unique OTUs among and within groups to preliminarily understand the OTU characteristics among groups. Forty-one OTUs were detected on the surface, and 43 OTUs were detected internally. There were 38 common OTUs, accounting for the vast majority of the OTUs. This result indicates that the difference in the fungal community composition on the surface and internal areas is small, but the internal microbial diversity is higher than that on the surface.

Microbial Community Composition

Dominant species largely determine the ecological and functional structures of the microbial community. Understanding the species composition of the community at all levels can allow for effective interpretation of the formation, changes and ecological impacts of the community structure. In this experiment, the fungal community composition on the surface and internal eukaryotes of Mianning ham at the phylum and genus levels was statistically analyzed. The fungal abundance was visualized in the form of a stack diagram (**Figure 2**). Three phyla were detected in the surface and internal fungal communities, of which Ascomycota was the dominant phylum, accounting for 99.72 (surface) and 97.49% (internal) of the total fungal population, respectively, followed by Basidiomycota. A total of 11 genera were detected at the genus level. *Penicillium* and *Wallemia* were found to be the dominant fungal genera, accounting for 99.19 (surface) and 99.20% (internal) of the total fungal population, respectively. The dominant phylum of Panxian ham is Ascomycota, and the dominant genera are *Aspergillus* and *Penicillium*, similar to those of Mianning hams (Mu et al., 2019).

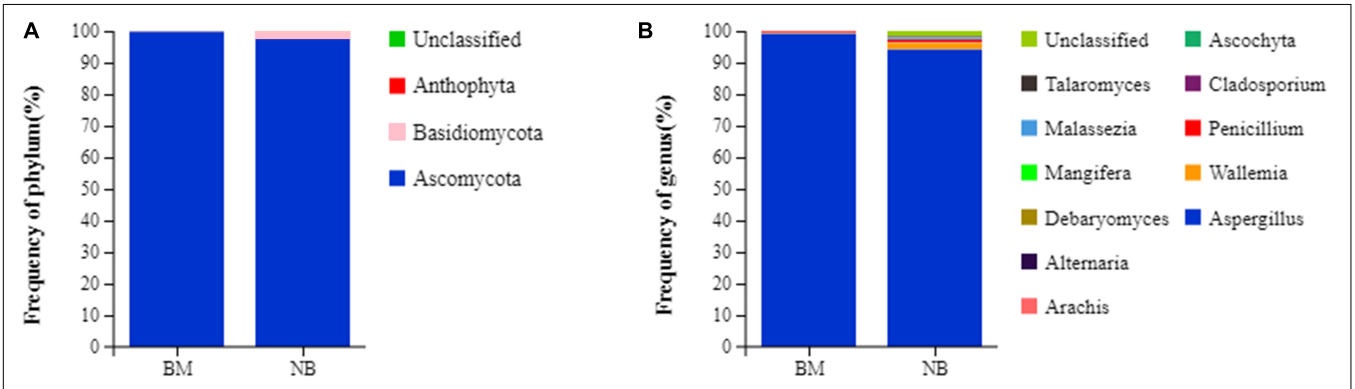

FIGURE 2 | Relative abundance of fungal community proportions at the phylum **(A)** and genus **(B)** levels in Mianning ham.

CONCLUSION

Mianning ham is a specialty meat product of Sichuan province. No detailed reports have been published on Mianning ham. This study revealed the physical and chemical characteristics, microbial contents, dominant bacteria, flavor substances, and fungal community composition of Mianning ham, providing a theoretical reference for further research on these hams.

The physical and chemical indexes of Mianning ham were within the range of food safety standards, and the pH value was approximately 5.76, which promotes the presentation of flavor. A low moisture content and a_W are important for the preservation of Mianning ham. Mianning ham is rich in flavor compounds. A total of 60 flavor compounds were detected by SPME-GC-MS technology, 49 of which were detected on the surface and 36 in the internal. There were more kinds of flavor compounds on the surface than internally, among which aldehydes and alcohols were the most abundant. Five kinds of bacteria were isolated from Mianning ham by the traditional culture method. The identification results showed that MN1 was *P. lanosum*, MN2 was *P. nalgiovense*, MN3 was *D. hansenii*, MN4 was *S. equorum*, and MN5 was *E. tasmaniensis.* By Illumina high-throughput sequencing, the fungal diversity index showed that the internal fungal diversity was higher than that of the surface of the Mianning ham. Three fungal phyla were detected, of which Ascomycota was the dominant phylum, followed by Basidiomycota. Eleven fungal genera were detected, of which *Aspergillus* was the dominant genus, followed by *Penicillium* and *Wallemia*.

DATA AVAILABILITY STATEMENT

The datasets presented in this study can be found in online repositories. The names of the repository/repositories and accession number(s) can be found below: NCBI SRA (https://www.ncbi.nlm.nih.gov/sra/PRJNA679145).

AUTHOR CONTRIBUTIONS

ZW: experiment and writing—review and editing. LJ, TB, BH, and JZ: formal analysis. RZ: validation. LC: writing—original draft preparation and funding acquisition. WW: supervision. All authors contributed to the article and approved the submitted version.

FUNDING

This work was supported by the Applied Basic Research Program of Sichuan Province (2019YJ0670).

ACKNOWLEDGMENTS

We thank Genedenovo Co., Ltd. (Guangzhou, China) for technical assistance in carrying out the analyses. We would also like to thank AJE (www.aje.cn) for English language editing.

REFERENCES

Bai, T., Li, X. Y., Hou, B., Chen, L., and Wang, W. (2018). Effects of complex microbial strains on volatile flavor components of Air-dried rabbits. *Chin. Condiment* 43, 38–43. doi: 10.3969/j.issn.1000-9973.2018.11.007

Comi, G., Orlic, S., Redzepovic, S., Urso, R., and Iacumin, L. (2004). Moulds isolated from Istrian dried ham at the pre-ripening and ripening level. *Int.J. Food Microbiol.* 96, 29–34. doi: 10.1016/j.ijfoodmicro.2004.03.005

Dang, X. J. (2018). *Study on the chemical composition and surface microbial diversity for Nuodeng ham*. Master's thesis, Yunnan: Yunnan University.

Donald, S. M. (1998). Flavour formation in meat and meat products: a review. *Food Chem.* 62, 415–424. doi: 10.1016/s0308-8146(98)00076-4

Fan, L., Qiu, C. K., and Cai, Y. C. (2019). Physical and chemical properties changes of Xuanwei ham during its processing. *China Food Addit.* 30, 120–125.

Fan, L., Qiu, C. K., and Chen, M. (2019). Comparative analysis of physical and chemical indexes of four famous hams in China. *Meat Indust.* 2019, 9–13.

Gou, P., Morales, R., Serra, X., Guardia, M. D., and Arnau, J. (2008). Effect of a 10-day ageing at 30°C on the texture of dry-cured hams processed at temperatures up to 18°C in relation to raw meat pH and salting time. *Meat Sci.* 80, 1333–1339. doi: 10.1016/j.meatsci.2008.06.009

Guo, X. X. (2017). *Effects of antioxidant, cooking and storage conditions on qualities and nitrite conversion pathways in ham*. Master's thesis, Shandong: Shandong Agricultural University.

Guo, X., Lu, S. L., Wang, B., and Wang, Q. L. (2019). Progress on flavor analysis of Chinese traditional ham. *Cereals Oils* 32, 18–21.

Harkouss, R., Astruc, T., Lebert, A., Gatellier, P., Loison, O., Safa, H., et al. (2015). Quantitative study of the relationships among proteolysis, lipid oxidation, structure and texture throughout the dry-cured ham process. *Food Chem.* 166:013. doi: 10.1016/j.foodchem.2014.06.013

He, Z. F., Zhen, Z. Y., Li, H. J., Zhou, G. H., and Zhang, J. H. (2008). Microorganisms flora ftudy on Jinhua ham fermentation. *Food Sci.* 1, 190–195.

Hirokazu, T., Tanabe, A. S., Yamamoto, S., and Hirotoshi, S. (2012). High-Coverage ITS Primers for the DNA-Based Identification of Ascomycetes and Basidiomycetes in Environmental Samples. *PLoS One* 7:0040863. doi: 10.1371/journal.pone.0040863

Li, F., Feng, X., Zhang, D. N., Li, C. B., Xu, X. L., Zhou, G. H., et al. (2020). Physical properties, compositions and volatile profiles of Chinese dry-cured hams from different regions. *J.Food Measure. Charact.* 14, 492–504. doi: 10.1007/s11694-019-00158-9

Li, J., Yang, X. H., Xia, H. S., and Peng, X. L. (2016). Reviews on volatile flavor of Jinhua ham. *Chin. Qinghai J. Anim. Vet. Sci.* 46, 55–57.

Li, P. L., Shen, Q. W., Lv, Y. N., Jiang, Z. J., and Ma, C. W. (2003). Analysis of main of microorganisms in Xuanwei ham. *Chinese J. Microecol.* 12–13. doi: 10.13381/j.cnki.cjm.2003.05.007

Ma, Y. M. (2014). *The change rule of protein in mutton and ham and its effect on its quality*. Master's thesis, Shihezi: Shihezi University.

Mu, Y., Su, W., and Mu, Y. C. (2019). Analysis of microbial diversity and key volatile flavor compounds of Panxian dry-cured ham. *Food Res. Dev.* 40, 77–85. doi: 10.12161/j.issn.1005-6521.2019.15.013

Mu, Y., Su, W., and Mu, Y. C. (2020). Characterisation of microorganisms and volatile flavor compounds of deep spoiled Panxian dry-cured ham. *Food Sci.* 2020, 20191111–20191143. doi: 10.7506/spkx1002-6630-20191111-143

Nicholas, A. B., Sathish, S., Jeremiah, J. F., Dirk, G., Jeffrey, I. G., Rob, K., et al. (2013). Quality-filtering vastly improves diversity estimates from Illumina amplicon sequencing. *Nat. Methods* 10, 57–59. doi: 10.1038/nmeth.2276

Pan, Y. X. (2016). Study on color control technology of smoked ham. Master's thesis.

Ramona, B. N. D., Anne, M., Monika, G., Agnes, W., Herbert, S., and Jochen, W. (2018). Recent advances in cured raw ham manufacture. *Sci. Nutrit.* 58, 610–630. doi: 10.1080/10408398.2016.1208634

Tan, Y. Z., Zhou, G. H., Xu, S. L., Liu, Y., Li, C. B., and Zhang, D. N. (2019). Volatile compounds in subcutaneous fat of three brands of dry-cured hams. *Food Sci.* 40, 185–192. doi: 10.7506/spkx1002-6630-20180725-304

Wang, L. (2008). Reviews on effects of microorganisms in dry-cured ham. *Meat Res.* 16–18.

Wang, X. H., Wang, S. H., and Zhao, H. (2019). Unraveling microbial community diversity and succession of Chinese Sichuan sausages during spontaneous fermentation by high-throughput sequencing. *J. Food Sci. Technol.* 56, 3254–3263. doi: 10.1007/s13197-019-03781-y

Wang, X. H., Zhang, Y. L., Ren, H. Y., and Zhang, Y. (2018). Comparison of bacterial diversity profiles and microbial safety assessment of salami, Chinese dry-cured sausage and Chinese smoked-cured sausage by high-throughput sequencing. *LWT-Food Sci. Technol.* 90, 108–115. doi: 10.1016/j.lwt.2017.12.011

Yang, H. S. (1979). Preliminary evaluation on the quality of Yun ham and Mianning ham. *Chin. J. Anim. Sci.* 1979, 16–19.

Yu, H. J. (2004). Production of Mianning ham. *Rural Cult. Technol.* 21:35.

Zhang, J., Pan, D. D., Zhou, G. G., Wang, Y., Dang, Y. L., He, J., et al. (2019). The Changes of the Volatile Compounds Derived from Lipid Oxidation of Boneless Dry-Cured Hams During Processing. *Eur. J. Lipid Sci. Technol.* 121: 201900135.

Zhang, X., Wang, W., Bai, T., Ji, L. L., Kang, J., and Zhang, J. M. (2020). Determination and principal component analysis of the volatile flavor substances during the processing of sichuan light fermented sausage. *Mod. Food Sci. Technol.* 2020:0383. doi: 10.13982/j.mfst.1673-9078.2020.10.0383

Zhang, Y., Xu, G. H., He, C. Y., and Zhang, L. W. (2009). Studies on the changes of physical and chemical index during the processing of Xuanwei ham. *J. Henan Inst. Sci. Technol.* 37, 39–41.

Zhen, Z. Y. (2004). *A study of the microbial flora of Jinhua ham*. Master's thesis, Chongqing: Southwest Agricultural University.

Zou, Y. L., Liu, S. Y., Wang, G. Y., Pu, Y. H., Ge, C. R., and Liao, G. Z. (2020). Analysis of fungal community structure in Xuanwei ham by PCR-DGGE. *Food Ferment. Indust.* 46, 269–274. doi: 10.13995/j.cnki.11-1802/ts.022394

Conflict of Interest: The authors declare that the research was conducted in the absence of any commercial or financial relationships that could be construed as a potential conflict of interest.

frontiers in Microbiology

ORIGINAL RESEARCH
published: 01 February 2021
doi: 10.3389/fmicb.2020.617030

Integrative Metagenomics–Metabolomics for Analyzing the Relationship Between Microorganisms and Non-volatile Profiles of Traditional *Xiaoqu*

Chi Zhao[1,2], *Wei Su*[1,2]*, *Yu Mu*[1,2], *Yingchun Mu*[1] and *Li Jiang*[1]

[1] School of Liquor and Food Engineering, Guizhou University, Guiyang, China, [2] Guizhou Key Laboratory for Storage and Processing of Agricultural and Animal Products, Guizhou University, Guiyang, China

Xiaoqu, one of three traditional *jiuqu* in China, is a saccharifying and fermenting agent used in *Xiaoqu jiu* brewing, with different ingredient compositions and preparation techniques used in various regions. The yield and quality of *Xiaoqu jiu* are significantly affected by the metabolites and microbiota of *Xiaoqu*; however, the associated relationship remains poorly understood. This study aimed to analyze this relationship in three typical traditional *Xiaoqu* from the Guizhou province in China. The non-volatile metabolites of *Xiaoqu* were detected using gas chromatography time-of-flight mass spectrometry, whereas the classification and metabolic potential of the microbiota were investigated using metagenomic sequencing. Results show that Firmicutes, Proteobacteria, and Actinobacteria represent the dominant bacterial phyla, with *Lactobacillus*, *Bacillus*, *Acinetobacter*, *Leuconostoc*, and *Weissella* found to be the dominant bacterial genera. Meanwhile, Ascomycota, Mucoromycota, and Basidiomycota are the dominant fungal phyla with *Aspergillus*, *Saccharomyces*, *Pichia*, *Rhizopus*, and *Phycomyces* being the predominant fungal genera. Functional annotation of the microbiota revealed a major association with metabolism of carbohydrates, cofactors, and vitamins, as well as amino acids. A total of 39 significantly different metabolites (SDMs) were identified that are involved in 47 metabolic pathways, primarily that of starch and sucrose; glycine, serine, and threonine; glyoxylate and dicarboxylate; pyruvate; as well as biosynthesis of pantothenate and CoA. Further, based on Spearman's correlation analysis, *Aspergillus*, *Saccharomyces*, *Lactobacillus*, *Acetobacter*, *Weissella*, *Pantoea*, *Desmospora*, and *Bacillus* are closely correlated with production of physicochemical indexes and SDMs. Moreover, the metabolic network generated for the breakdown of substrates and formation of SDMs in *Xiaoqu* was found to primarily center on the metabolism of carbohydrates and the tricarboxylic acid cycle. These results provide insights into the functional microorganisms and metabolic patterns present in traditional Guizhou *Xiaoqu* and might guide researchers in the production of stable and efficient *Xiaoqu* in the future.

Keywords: traditional *Xiaoqu*, metabolomics, metagenomics, non-volatile metabolite, functional microorganism, metabolic pathway

OPEN ACCESS

Edited by:
Xucong Lv,
Fuzhou University, China

Reviewed by:
Jyoti Prakash Tamang,
Sikkim University, India
Song Yang,
Qingdao Agricultural University, China
Rina Wu,
Shenyang Agricultural University, China

***Correspondence:**
Wei Su
suwei1886@163.com

Specialty section:
This article was submitted to Food Microbiology, a section of the journal Frontiers in Microbiology

Received: *13 October 2020*
Accepted: *18 December 2020*
Published: *01 February 2021*

Citation:
Zhao C, Su W, Mu Y, Mu Y and Jiang L (2021) Integrative Metagenomics–Metabolomics for Analyzing the Relationship Between Microorganisms and Non-volatile Profiles of Traditional Xiaoqu. Front. Microbiol. 11:617030. doi: 10.3389/fmicb.2020.617030

INTRODUCTION

Chinese *Xiaoqu jiu* accounts for approximately one sixth of the total liquor production in China and is widely distributed throughout the southern regions, including Guizhou, Sichuan, and Hubei provinces (Wang J. et al., 2018; Wang M. Y. et al., 2019). It is brewed using raw materials, such as rice, corn, wheat, sorghum, and *Xiaoqu*, which is a complex saccharifying and fermenting agent. Due to differences in ecological characteristics and technological parameters employed in the production of *Xiaoqu jiu*, various starters are employed in different regions, such as *Ragi* in Indonesia (Siebenhandl et al., 2001), *Men* in Vietnam (Dung et al., 2006), *Marcha* in India and Nepal (Sha et al., 2017), *Dombea* in Cambodia (Sokny et al., 2018), and *Nuruk* in Korea (Kim et al., 2019). *Xiaoqu*, specifically, is produced by solid-state fermentation comprising soaking, grinding, molding, powder coating, cultivating, ripening, and drying of rice and rice bran (Liu and Sun, 2018). During this procedure, numerous microbes, enzymes, aroma precursors, and significant aroma constituents are enriched, contributing to the style and quality of the final distillate (Gou et al., 2015).

Microorganisms are the key factors contributing to the delicate balance between stability, quality, and productivity of *Xiaoqu jiu*, making analysis of the core functional microorganisms the basis for realizing modern standardized *Xiaoqu* production (Wang X. D. et al., 2019). However, in most regions of Asia, including India (Bora et al., 2016), Thailand (Chuenchomrat et al., 2008), Korea (Son et al., 2018), and China (Zhao et al., 2020), *Xiaoqu* and *Xiaoqu jiu* are manufactured under conditions of spontaneous fermentation in an open environment based on operation skills and individual experiences. This often leads to inconsistent quality between batches and potential food safety concerns (Zheng and Han, 2016). The application of a standardized *Xiaoqu* protocol represents an effective way to regulate the fermentation process and regulate *Xiaoqu jiu* quality. Hence, investigation into the functional activity of microorganisms present in *Xiaoqu* is important.

With the development of detection technology, increasing focus has been placed on investigating the phenotypic correlation between microorganisms and metabolites with fermented products (Elhalis et al., 2020; Lv et al., 2020). Previous studies using amplicon sequencing technology identified *Weissella*, *Aspergillus*, *Rhizopus*, *Staphylococcus*, *Saccharomyces*, and *Candida* as the dominant microorganisms in traditional *Xiaoqu* starters in Sichuan, Hubei, and Huaxi (Wu H. et al., 2017; Tang et al., 2019; Wang M. Y. et al., 2019); *Aspergillus*, *Saccharomycetales*, *Streptomyces*, *Bacillus*, *Enterococcus*, and *Weissella* in Korean *Nuruk* (Bal et al., 2017); and *Weissella*, *Pediococcus*, *Lactobacillus*, *Saccharomyces*, *Saccharomycopsis*, and *Rhizopus* in Cambodia *Dombea* (Sokny et al., 2018). However, species may contain similar hypervariable regions, or the specific fragments that distinguish them may be outside the amplicon region, thereby creating PCR bias (Illeghems et al., 2012; Melanie et al., 2015). Compared with amplicon sequencing, metagenomic sequencing, which randomly generates small microbial gene fragments, reportedly offers an advantage for species identification (Liu et al., 2020) and may provide additional insights into the metabolic potential of the microbiome at the genetic and functional levels (Walsh et al., 2017). Indeed metagenomic sequencing has been widely applied for the identification of functional microorganisms in fermented foods, including wine (Liu et al., 2019), vinegar (Wu L. et al., 2017), cheese (Escobar-Zepeda et al., 2016), pickles (Jung et al., 2011), cocoa beans (Agyirifo et al., 2019), and fermented sausages (Ferrocino et al., 2017). Furthermore, metabolomics analysis based on gas chromatography (GC), mass spectrometry (MS), high-performance liquid chromatography (HPLC), and nuclear magnetic resonance revealed the metabolite profiles of *jiuqu* (Tang et al., 2019; Wang N. et al., 2019) and Baijiu (Huo et al., 2020; Jia et al., 2020; Liu and Miao, 2020). However, former studies on *Xiaoqu* have primarily focused on microorganisms and volatile flavors (Liu and Sun, 2018; Tang et al., 2019; Chen C. et al., 2020), whereas the correlation between microorganisms and non-volatile metabolites requires further investigation.

Therefore, herein, we used gas chromatography time-of-flight mass spectrometry (GC-TOF-MS)-based metabolomics and metagenomic approaches to analyze the distribution and metabolic potential of the microbial community, and non-volatile metabolites of three typical traditional *Xiaoqu* originating in Guizhou. Additionally, we investigated potential correlations between major microbiota with significantly different metabolites (SDMs) and physicochemical indexes. Finally, we evaluated the relationship between substrate decomposition and SDM formation in the microbial community using metabolic network analysis. Our results might provide a theoretical basis for the development of a standardized production procedure for *Xiaoqu*.

MATERIALS AND METHODS

Sample Collection

Nine *Xiaoqu* samples were collected in August 2019 from three representative *Xiaoqu*-producing distilleries located in Huishui (HS), Anshun (AS), and Kaili (KL) in the Guizhou province, China. Samples were collected from the upper, middle, and bottom layers of the relevant *Xiaoqu* storeroom. From each layer, individual 40-g samples were collected from five separate points in the middle or surrounding edges (**Supplementary Figure 1**). All samples collected from each point in all three layers were then evenly combined into one mixture, from which a 150-g sample was collected using quartile method to eliminate sampling error. This process was repeated three times for each distillery. Samples were immediately transported to the laboratory, placed in sterile bags, and stored at −80°C for further analyses.

Determination of Physical and Chemical Properties

The pH, moisture, water activity (a_w), as well as the saccharifying, fermenting, esterifying, and liquefying power of *Xiaoqu* samples were determined according to general methods of analysis for *Daqu* (Ministry of Light Industry of China, 2011). All experiments were performed in triplicate.

Genomic DNA Extraction

Xiaoqu sample (0.5 g) was weighed and placed in a triangle bottle containing 10 ml of sterilized phosphate buffer solution (pH 7.4), and 30 sterilized glass beads. After sealing, the bottle was shaken at 5°C for 1.5 h and stirred with a glass bar every 30 min. The mixture was then filtered using sterilized gauze (Shanghai, China). The filtrate was centrifuged at 4°C and 12,000 rpm for 10 min to obtain the precipitate. Subsequently, the PowerSoil DNA Isolation Kit (Carlsbad, California, USA) was used to extract total DNA from the precipitate. DNA was analyzed using 1% agar-gel electrophoresis and spectrophotometry (260/280 nm optical density ratio) and was stored at −80°C for further processing.

Library Construction and High-Throughput Sequencing

A total of 1 μg of DNA per sample was used as input material to generate sequencing libraries using the NEBNext® Ultra™ DNA Library Prep Kit for Illumina (NEB Inc., Ipswich, MA, USA) following the manufacturer's recommendations, with added index codes to attribute sequences to each sample. Briefly, DNA samples were fragmented by sonication to a size of 350 bp, end-polished, A-tailed, and ligated with the full-length adaptor for Illumina sequencing and further PCR amplified. PCR products were purified (AMPure XP system) and libraries were analyzed for size distribution using the Agilent 2100 Bioanalyzer (Palo Alto, California, USA) and quantified using real-time PCR. Clustering of the index-coded samples was performed on a cBot Cluster Generation System according to the manufacturer's instructions. Library preparations were then sequenced on an Illumina PE-150 (San Diego, California, USA) and paired-end reads were generated.

Quality Control

To obtain valid sequences for subsequent analysis, raw reads were generated for quality control according to the following steps: (1) removal of adapter sequence (parameter ILLUMINACLIP:adapters_PATH:2:30:10); (2) scanning of sequence (4 bp sliding window size); if the average quality score was <20 or 30 (99% accuracy), the subsequent sequence (parameter SLIDINGWINDOW:4:20 or 30) was removed; (3) removal of sequences with a final length <50 bp (parameter MINLEN:50).

Taxonomic Assignment and Functional Annotation

The MetaPhlAn2[1] (Truong et al., 2015) analysis tool was used to compare clean reads with unique species markers to determine the microflora composition. Finally, the normalized species abundance was calculated based on read number and marker length obtained from the comparison. Furthermore, using the HUMAnN2[2] (Franzosa et al., 2018) software, clean reads were compared with the protein database (UniRef 90) based on DIAMOND[3]. Failed reads were filtered out and relative abundance of each protein was quantified. According to the corresponding relationship between the UniRef 90 ID and the KEGG (Kyoto encyclopedia of genes and genomes) database ID, the relative abundances of corresponding functions from the KEGG database were determined (Zhu et al., 2010; Kim et al., 2016).

Extraction of Metabolites and Gas Chromatography Time-of-Flight Mass Spectrometry Analysis

A 20 ± 1 mg *Xiaoqu* sample, 500 μl of precooled extraction mixture [3:1 methanol/chloroform (v:v)], and 10 μl of internal standard substance (Adonito, 0.5 mg/ml stock solution) were added to a 2-ml PE tube and vortexed for 30 s. After homogenization for 4 min in a 45-Hz ball mill, the mixture was sonicated for 5 min in ice water. After centrifugation at 12,000 rpm and 4°C for 15 min, 100 μl of supernatant was placed in a 2-ml PE tube and vaporized in a vacuum concentrator. Subsequently, 60 μl of 20 mg/ml methoxyamination hydrochloride in pyridine solution was added to the sample and incubated at 80°C for 30 min. Next, the sample was derivatized using 80 μl of BSTFA reagent (1% templated mesoporous carbons, v/v) at 70°C for 1.5 h. All samples were analyzed using GC-TOF-MS after cooling to 25°C.

GC-TOF-MS results were obtained using an Agilent 7890 gas chromatograph (Palo Alto, California, USA) coupled with a time-of-flight mass spectrometer (St. Joseph, MI, USA) equipped with a DB-5MS capillary column (30 × 250 m inner diameter, 0.25 m film thickness; J&W Scientific, Folsom, CA, USA). Consecutively, 1-μl sample aliquots were injected in the splitless mode. Helium was used as the carrier gas, with a 3 ml min^{-1} front inlet purge flow, and a 1 ml min^{-1} gas flow rate through the column. The injection, transfer line, and ion source temperatures were 280, 280, and 250°C, respectively. Mass spectra was generated in the electron impact mode at 70 eV, using full-scan range of 50–500 m/z at a rate of 12.5 spectra per second after a solvent delay of 6.25 min.

Metabolome Data Processing

Raw data analysis, including peak extraction, baseline adjustment, deconvolution, alignment, and integration were completed using the Chroma TOF (V 4.3x, LECO) software. The LECO-Fiehn Rtx5 database was used for identification of metabolites by matching the mass spectrum and retention index.

Metabolic Profile Associated With SDMs

The KEGG database, MetaboAnalyst database, and literature data were used to collect and collate information on the SDM formation pathways and associated catalytic enzymes. The metabolic network of SDMs and microorganisms was established through gene comparisons with metagenomics sequencing data.

[1]http://huttenhower.sph.harvard.edu/metaphlan2
[2]http://huttenhower.sph.harvard.edu/humann2
[3]http://ab.inf.uni-tuebingen.de/software/diamond/

Multivariate Statistical Analysis

All statistical analyses were performed using SPSS 25.0 software (IBM Inc., Chicago, IL, USA). Significant differences were determined using one-way analysis of variance (ANOVA), with $p < 0.05$ considered statistically significant. Principal component analysis (PCA) and orthogonal partial least squares discriminant analysis (OPLS-DA) were performed to analyze the GC-TOF-MS dataset using SIMCA 14.1 software (Umetrics, Umea, Sweden). Meanwhile, to avoid overfitting the model and to evaluate the model feasibility, the OPLS-DA replacement test was carried out. Based on the OPLS-DA model and ANOVA, the variable importance in projection (VIP) and p values were calculated and SDMs (VIP > 1, $p < 0.05$) were identified. The peak area of SDMs was visualized using the R software (version 3.6.1, Cambridge, Massachusetts, USA) and pheatmap package. Pathway and enrichment analyses were conducted by MetaboAnalyst 4.0[4]. The microbial taxonomic data were primarily analyzed using Origin (version 2019b, Origin Lab Inc., Hampton, MS, USA), and R software with the ggplot2 package was used for analyzing gene data related to KEGG pathways. Correlations between representative microorganisms with physicochemical properties and SDMs were calculated using the Spearman's rank correlation, and visualized via heatmap using R 3.6.1. Finally, integrated metabolomics and metagenomics datasets were used to generate network pathways for microbial metabolism and metabolite formation using the MetaboAnalyst 4.0[4] and KEGG pathway[5] databases. Each sample was verified in triplicate.

RESULTS AND DISCUSSION

Analyses of Fermentation Characteristics

In general, the key factors for evaluating the quality and fermentation performances of *Xiaoqu* are its physicochemical properties (Zhang et al., 2012). Nevertheless, different process parameters and geographic regions could variably influence the physicochemical properties of *jiuqu* and thus are of vital significance (Tang et al., 2019). The various physiochemical properties for all examined samples are presented in **Table 1**. The moisture content of *jiuqu* must remain at ∼13% to facilitate storage (Yan et al., 2015). However, we observed that the moisture contents of the three *Xiaoqu* samples were below 13%. Among these, AS *Xiaoqu* had a significantly higher moisture content, compared to the others ($p < 0.05$).

The water activity, fermenting power, saccharifying power, esterifying power, and liquefying power in KL *Xiaoqu* were significantly higher than those of other samples, with the lowest values observed in AS *Xiaoqu* ($p < 0.05$). Fermentability is positively correlated with the ability to convert fermentable sugars into ethanol (Fan et al., 2018). The saccharification power refers to the ability to convert starch in *jiuqu* raw materials into sugars (Zheng et al., 2012). Meanwhile, the esterification power of *jiuqu* has been strongly linked to that of ester compounds in Baijiu (Xiong et al., 2014). Additionally, the order of acidity was HS (0.38 ± 0.01 mmol g^{-1}) > KL (0.52 ± 0.00 mmol g^{-1}) > AS (0.38 ± 0.01 mmol g^{-1}). Currently, acidity is not only considered an important index to evaluate the degree of *jiuqu* maturity, but also an objective criteria used in *jiuqu* preparation (Yan et al., 2016).

Overview of Metagenomic Data

A total of 227,943,215 raw reads, averaging 7.60 Gb in size and 150 bp in length, were generated from DNA extracted from nine *Xiaoqu* samples (**Supplementary Table 1**). We noted that the sequence GC content (%) in the datasets ranged from 36 to 41%, reflecting the predominance of microbiota with low GC content in samples (Briggs et al., 2012). After performing quality control, the percentage of high-quality reads was 95.13, 95.37, and 95.05% in AS, HS, and KL samples, respectively. Moreover, the average clean data size was 7.23 Gb, accounting for 95.18% of the original data, with the proportion of bases having a quality score higher than 20 and 30 being >98 and >95%, respectively.

Taxonomic Analysis

Based on the annotation information of MetaPhlAn2, reads were assigned to different phyla and genera. At the phylum level, three dominant bacterial phyla and three dominant fungal phyla were identified in the nine *Xiaoqu* samples, including Firmicutes (84.41%), Proteobacteria (15.06%), and Actinobacteria (0.49%) and Ascomycota (79.70%), Mucoromycota (18.85%), and Basidiomycota (1.42%), respectively. The abundances of Firmicutes and Proteobacteria were 70.71, 91.97, and 90.56% and 29.29, 6.65, and 9.24% in AS, HS, and KL, respectively, whereas Actinobacteria was only detected in HS with an abundance of 1.39% (**Figure 1A**). Additionally, the abundances of Ascomycota and Mucoromycota were 70.85, 71.96, and 96.30% and 26.86, 26.20, and 3.49% in AS, HS, and KL, respectively (**Figure 1B**). However, Basidiomycota was predominantly dominant in AS (2.28%) and HS (1.77%; **Figure 1B**). Firmicutes, Proteobacteria, and Actinobacteria were previously identified as the dominant bacteria in *Xiaoqu* (Wu H. et al., 2017), *Xiaoqu jiu* (Dong et al., 2020), and strong-flavored Baijiu fermentation ecosystems (Zou et al., 2018). Meanwhile, Ascomycota, Mucoromycota, and Basidiomycota occupy a major position in the brewing process of black glutinous rice wine (Zhao et al., 2020), Indian dry starters (Anupma and Tamang, 2020), and strong-flavor Baijiu Daqu (Guan et al., 2015). It was, therefore, suggested that Firmicutes, Proteobacteria, Actinobacteria, Ascomycota, Mucoromycota, and Basidiomycota play a vital role in the quality and flavor of traditional *jiuqu* and fermented wine.

A total of 468 bacteria genera and 143 fungi genera were detected and classified. **Figure 1C** illustrates the overview of 15 bacteria genera with relative abundance >0.01 from the nine *Xiaoqu* samples, and their composition, which accounts for 98.73% of the total abundance, at the bacteria genus level. The dominant bacterial genera (>0.1 relative abundance) were *Bacillus*, *Lactobacillus*, *Weissella*, *Leuconostoc*, and *Acinetobacter*, which belong to Firmicutes and Proteobacteria phyla. More specifically, *Bacillus* had a dominant abundance in AS (30.23%) and KL (48.50%), whereas its abundance was only 0.27% in HS. This genus secretes various hydrolases (including amylases, proteases, lipases, etc.) and also produces a wide range of volatile

[4]www.metaboanalyst.ca
[5]egg.jp/kegg/pathway.html

TABLE 1 | Differences in physicochemical properties of three traditional *Xiaoqu* samples.

Sample ID[A]	Acidity (g/kg)	Water activity (a_w)	Moisture (%)	Fermenting power (g/1 g · 72 h)	Esterifying power (mg/50 g · 7 days)	Saccharifying power (mg/g · h)	Liquefying power (g/g · h)
AS	0.38 ± 0.01^{c}	0.59 ± 0.00^{b}	10.7 ± 0.12^{a}	1.31 ± 0.01^{b}	52.04 ± 1.42^{b}	952.27 ± 1.64^{b}	0.96 ± 0.12^{b}
HS	0.79 ± 0.01^{a}	0.48 ± 0.01^{c}	9.00 ± 0.07^{b}	1.02 ± 0.06^{c}	11.91 ± 0.67^{c}	847.07 ± 1.32^{c}	0.84 ± 0.02^{c}
KL	0.52 ± 0.00^{b}	0.63 ± 0.01^{a}	6.33 ± 0.14^{c}	3.23 ± 0.04^{a}	114.07 ± 0.41^{a}	1508.80 ± 1.31^{a}	1.12 ± 0.03^{a}

[A]*AS, Anshun; HS, Huishui; KL, Kaili. Values are presented as mean ± standard error (n = 3).* [a–c]*Different letters in the same row represent significant differences (P < 0.05).*

compounds, including pyrazine, aldehydes, and ketones, during fermentation (Li H. et al., 2014; Li Z. M. et al., 2014; Wang et al., 2017; Jin et al., 2019). Moreover, the abundance of *Lactobacillus* and *Weissella* was predominant in HS (72.44 and 12.90%) and KL (17.98 and 21.43%), whereas *Leuconostoc* and *Acinetobacter* were dominant in AS, accounting for 26.05 and 22.13%, respectively. We also detected several lactic acid bacteria (LAB), including *Lactobacillus*, *Weissella*, and *Leuconostoc*, consistent with the results reported for Wuyi Qu and Gutian Qu, which are traditional *jiuqu* used in rice wine processing (Liu et al., 2018). LAB, as functional microorganisms, play a crucial role in the food industry of China (de Paiva et al., 2016) and reportedly produce bacteriocins through fermentation while accumulating organic acids via consumption of fermentable sugars. Hence, LAB can provide a lower pH condition that inhibits the propagation of pathogenic bacteria during the brewing process (Johan and Magnusson, 2005; Cappello et al., 2016), thereby facilitating enhanced sensory and nutritional values of the end-product (Frédéric and Luc, 2004). Similarly, *Acinetobacter* inhibits the growth of other microorganisms by acidifying the environment and producing biosurfactants, having a favorable degradation effect on nitrite (Al Atrouni et al., 2016). However, most *Acinetobacter* species are conditionally pathogenic bacteria. Thus, the AS *Xiaoqu* sample with its high abundance of *Acinetobacter* should be further investigated in the context of *Xiaoqu* production and the final liquor brewing process.

Microbial taxonomic assignment identified 12 fungal genera present in the nine *Xiaoqu* samples at abundances >0.01 (**Figure 1D**), which accounted for 95.45% of the total fungal genera abundance. The dominant fungi (>0.1 abundance) identified were *Aspergillus*, *Saccharomyces*, *Pichia*, *Rhizopus*, and *Phycomyces*, belonging to Ascomycota and Mucoromycota phyla. In particular, *Aspergillus* was dominant in AS, HS, and KL, accounting for 62.99, 11.46, and 66.03% of the abundance, respectively, whereas *Saccharomyces and Pichia* were only detected in KL and HS with an abundance of 26.87 and 46.97%, respectively. *Aspergillus* represented the main fungus while *Saccharomycopsis* and *Pichia* were the major yeast groups. As the most effective ethanol producer, *Saccharomyces* represents one of the core functional strains with strong fermentation capacity in liquor brewing (Wu Q. et al., 2012). However, *Pichia* primarily has an esterification role, which can enhance the ester aroma of liquor and contribute to the high ester and phenylethanol content in *Daqu* (Wang et al., 2011). Additionally, *Aspergillus* is a genus of functional aerobic microorganisms, which can survive under conditions of low humidity and high temperature (Ma et al., 2014). Thus, it is often detected in starters, such as Maotai flavor *Daqu* (Gan et al., 2019), Luzhou-flavor *Daqu* (He et al., 2019), sweet wine starter (Cai et al., 2018), and *Monascus* starter (Huang Z. R. et al., 2018), in which it secretes various enzymes and metabolic products (Wu et al., 2009). Additionally, the abundances of *Rhizopus* and *Phycomyces* were 13.64 and 11.26% and 13.24 and 10.90% in AS and HS, respectively. *Rhizopus*, a strong amylase producer that degrades starch during *Xiaoqu jiu* production (Tang et al., 2019; Dong et al., 2020), was previously identified as the main fungi in Wuyi Qu (Liu et al., 2018). Conclusively, the microbiota detected in these *Xiaoqu* samples demonstrated significant differences in their structure and diversity, which might be due to differences in geographical environment, raw materials, and preparation technology (Du et al., 2019).

Distribution of Genes Associated With KEGG Pathways in *Xiaoqu*

To explore the metabolic potential of the *Xiaoqu* microbiome, genes were annotated and classified using the KEGG database. **Table 2** illustrates the biological metabolic pathways of functional genes, which included metabolism (58.16%), genetic information processing (12.57%), human diseases (10.92%), organismal systems (8.29%), cellular processes (5.76%), and environmental information processing (3.85%). As each category can be divided into subclasses, a total of 47 subtypes are presented in **Figure 2**, with metabolism of carbohydrates, cofactors and vitamins, and amino acids found to predominate (relative abundance >7%), followed by the other amino acid metabolism, transport, global and overview map, lipid metabolism, xenobiotics biodegradation and metabolism, and energy metabolism (relative abundance >4%). These results agree with those reported for Shaoxing *huang jiu*, a traditional rice wine in China (Liu et al., 2019).

Carbohydrates are a primary component of cell structure and energy supply and play a key role in regulation of microbial activity during fermentation. We found that the metabolism of carbohydrates accounted for the largest proportion of microbial functional genes, consistent with that reported by Xie et al. (2020) in *da-jiang*, a popular Chinese traditional fermented soybean food. Moreover, cofactors provide redox carriers for biosynthesis and decomposition reactions and are paramount in the intracellular transfer of microorganism energy (Wang et al., 2013). Therefore, regulation of cofactor abundance might be

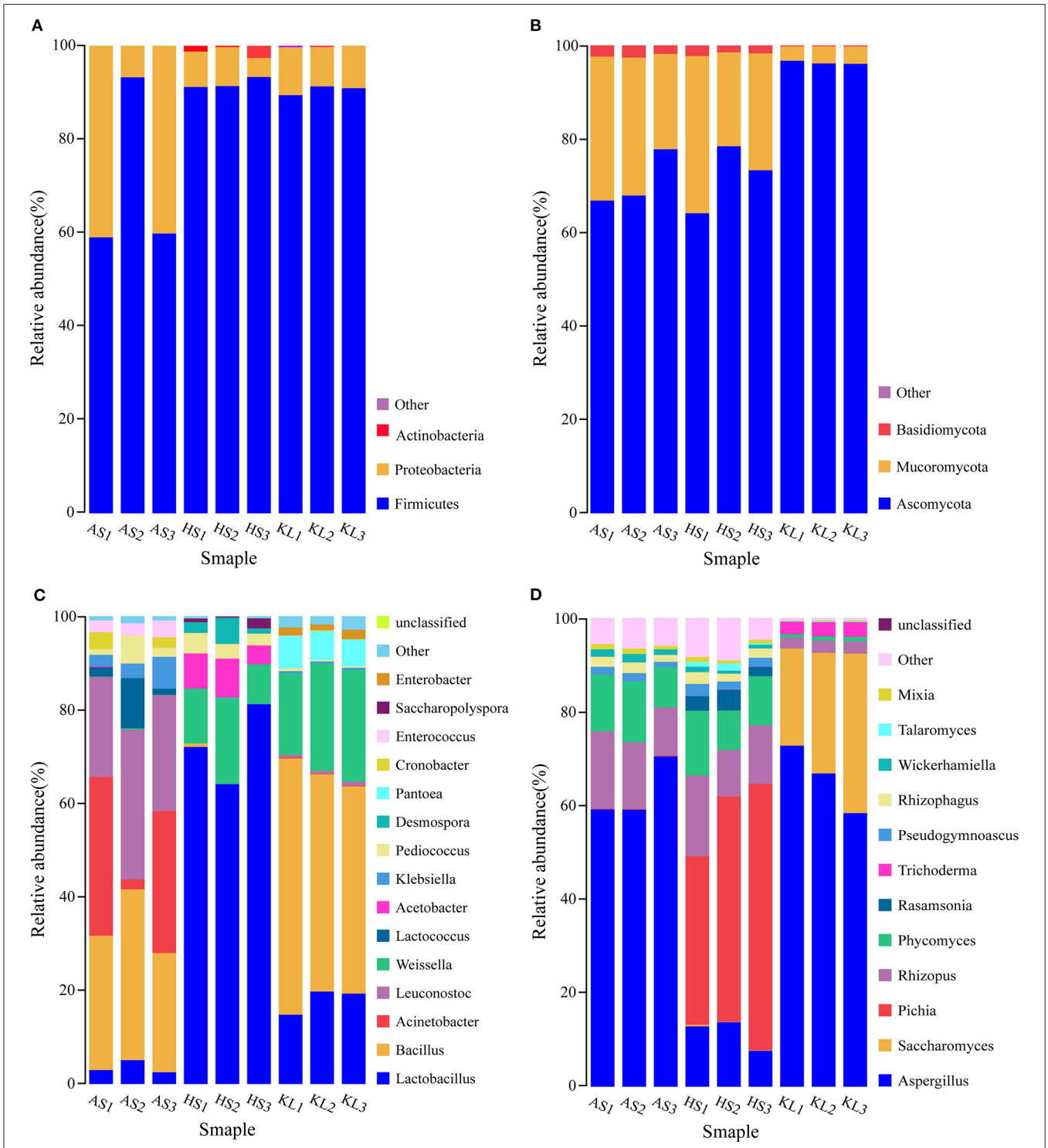

FIGURE 1 | Relative abundance of bacteria **(A)** and fungi **(B)** at the phylum level and of bacteria **(C)** and fungi **(D)** at the genus level in *Xiaoqu* samples. AS, HS, and KL indicate traditional *Xiaoqu* in Guizhou: AS, Anshun; HS, Huishui; KL, Kaili.

beneficial for efficient production of target metabolites (Chen et al., 2017). As small molecule organic compounds, vitamins often participate in metabolism in the form of cofactors. In addition, the metabolism of amino acids is a cardinal process in enhancing product flavor and quality (Huang X. N. et al., 2018). Meanwhile, the higher abundance of genes associated

TABLE 2 | Relative abundance (%) of genes associated with KEGG pathways (at level 1) in three traditional *Xiaoqu* samples.

KEGG pathway	AS	HS	KL	Total[a]
Metabolism	18.68	20.92	18.56	58.16
Genetic information processing	3.58	5.18	3.81	12.57
Human diseases	4.53	2.89	3.50	10.92
Organismal systems	3.51	1.84	2.94	8.29
Cellular processes	1.75	1.16	2.85	5.76
Environmental information processing	1.14	1.17	1.54	3.85

AS, Anshun; HS, Huishui; KL, Kaili. [a]*Total proportion of samples in six biometabolic pathways.*

with carbohydrate, cofactor, vitamin, and amino acid metabolism indicates that starch, vitamins, and proteins serve as critical flavor precursors.

We also observed a small number of genes related to human diseases. Other researchers found similar results in fermented food, such as turbid rice wine (a Korean rice wine) (Kim et al., 2015), sweet and fermenting brewery wort (Menz et al., 2010), and traditional fermented foods in the northeast region of India (Keisam et al., 2019). According to Bolotin et al. (1999) and Olano et al. (2001), the mere existence of these undesired genes may not be represent pathogenicity of these fermented products. Further, Liu et al. (2019) and Jiang et al. (2020) found that genes related to human diseases gradually decrease during fermentation due to the inhibitory effect of LAB, yeast, ethanol, and other factors. Therefore, the safety of *Xiaoqu* is considered to be reliable.

Analyses of Non-volatile Metabolites

The results of typical GC-TOF-MS total ion chromatography of the nine samples are shown in **Supplementary Figure 2**, in which 797 peaks were extracted, and 795 peaks were retained after quality control. According to the degree of match (similarity $\geq$800) between the substances of the qualitative analysis and the substances in the standard library (Wu S. M. et al., 2012), we identified 59 reliable metabolites (**Supplementary Table 2**) from 795 metabolites. Subsequently, we conducted a series of multivariate pattern recognition analysis. The PCA score plot implied an obvious separation among groups and superior reliability within each group, with the variance of PC1 and PC2 being 47.6 and 41.2%, respectively (**Figure 3A**). Our PCA loading plot demonstrated that Z1 and Z3 mainly influenced the separation by PC 1 (47.6% of the total variance), while fumaric acid and Z2 contributed to the separation by PC 2 (41.2% of the total variance) (**Figure 3B**). It is obvious from the loading plot that the substances that distinguish AS, HS, and KL samples correspond to Z1, Z2, and Z3 regions, respectively. To better understand the metabolites that trigger the differences between groups, we performed OPLS-DA analysis to filter orthogonal variables that were irrelevant to categorical variables in the metabolites, and analyzed non-orthogonal variables and orthogonal variables separately to obtain more reliable model information (Trygg and Wold, 2002). Based on the results of the OPLS-DA score plots (**Supplementary Figures 3A–C**), samples were all within the 95% Hotelling's T-Squared Ellipse, illustrating that no outlier existed among the analyzed samples. The R^2Y and Q^2 values of the three models approached 1, indicating that they could efficiently account for the difference between samples (Lee et al., 2019). To assess the robustness and predictive ability of the OPLS-DA model, we carried out sevenfold cross-validation and permutation verification ($n = 200$; permutations experiments). The R^2Y and Q^2 values were both smaller than those of the original model (**Supplementary Figures 3D–F**), which was indicative of robustness and the absence of overfitting in the OPLS-DA models, thus offering an additional explanation for differences observed among AS, KL, and HS *Xiaoqu*.

Note that when 59 reliable metabolites (similarity $\geq$800) appeared with the same name and a distinct digital number, we selected the substance with a high degree of match for future analysis (Kind et al., 2009). Meanwhile, SDMs were identified based on their VIP scores $>$ 1.0 of OPLS-DA and $p < 0.05$ of ANOVA. In this way, we identified 39 metabolites as SDMs (**Supplementary Table 3**), including 12 carbohydrates, 10 organic acids, 7 fatty acids, 3 amino acids, 2 sugar alcohols, 2 nucleic acids, and 3 other compounds. We then calculated the Euclidean distance matrix using the quantitative values of SDMs, and 39 SDMs with the same characteristics were clustered though the complete linkage method, which were displayed in a heatmap to identify their group differences (**Figure 4**). In addition, to clarify the potential differential metabolic processes of *Xiaoqu*, we applied MetaboAnalyst 4.0 for SDM pathway enrichment. **Supplementary Figure 4** demonstrates the existence of SDMs in 28 metabolic pathways. Subsequently, an impact value $>$0.1 was applied to determine the most relevant pathways (Chen et al., 2018), and five major metabolic pathways, namely, "starch and sucrose metabolism," "glycine, serine, and threonine metabolism," "glyoxylate and dicarboxylate metabolism," "biosynthesis of pantothenate and CoA," and "pyruvate metabolism" were identified. Interestingly, "metabolism of carbohydrates," "metabolism of cofactors and vitamins," and "metabolism of amino acids" mentioned in the obtained metagenomic data correspond to "starch and sucrose metabolism," "biosynthesis of pantothenate and CoA," and "glycine, serine, and threonine metabolism" in the metabonomics data, respectively. The high matching between the data results not only shows the feasibility of the method, but also verifies the metabolic pathway of *Xiaoqu*.

Carbohydrates and organic acids were found to be the kernel metabolites leading to differences in AS and KL, respectively. However, carbohydrates, organic acids, amino acids, and fatty acids were also found to represent differential metabolites in the clustering of integrated HS *Xiaoqu*. Carbohydrates enter the tricarboxylic acid (TCA) cycle through the glycolysis pathway for the synthesis of organic acids, amino acids, and other flavor metabolites during the fermentation process, and provide energy for microbial growth via the carbohydrate metabolism pathway (Gu et al., 2017). Herein, we observed that the SDMs included several carbohydrates in AS *Xiaoqu*, such as cellobiose, sucrose, and 1-kestose. Previous studies inferred that cellobiose was the end-product of the endo-β-glucanase gene in Luzhou-flavor *Daqu* (Ali et al., 2018), having a positive effect on extracellular

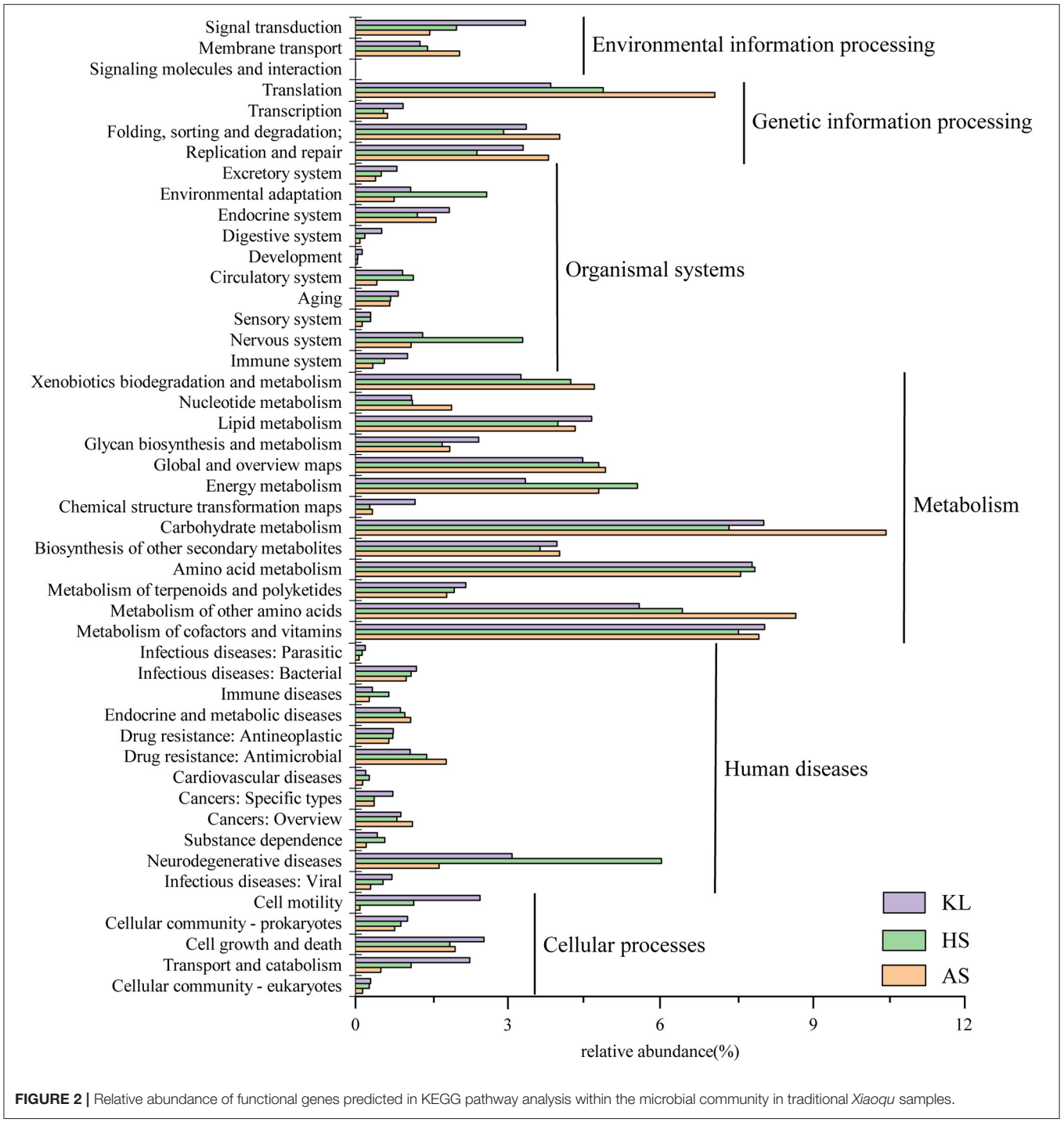

FIGURE 2 | Relative abundance of functional genes predicted in KEGG pathway analysis within the microbial community in traditional *Xiaoqu* samples.

β-glucosidase production (Swangkeaw et al., 2009). Additionally, we identified fructose, melibiose, trehalose, glucose, ribose, and raffinose as the major carbon compounds in HS *Xiaoqu*. Among these, trehalose has a prominent protective effect on biological cells, and thus can serve as a natural storage carbon source and a protective agent to protect biomolecular structures from destruction (Kim et al., 2011). Besides, glucose and raffinose form stable mixtures with bisulfite under certain conditions (Harbertson et al., 2013). Meanwhile, sugar reportedly exerts minimal effects on the direct sensory attributes of Baijiu as it is primarily involved in metabolism during the fermentation process, with a low content present in the final product (<2% of the total non-volatile profile) (Fang et al., 2019; Tan et al., 2019).

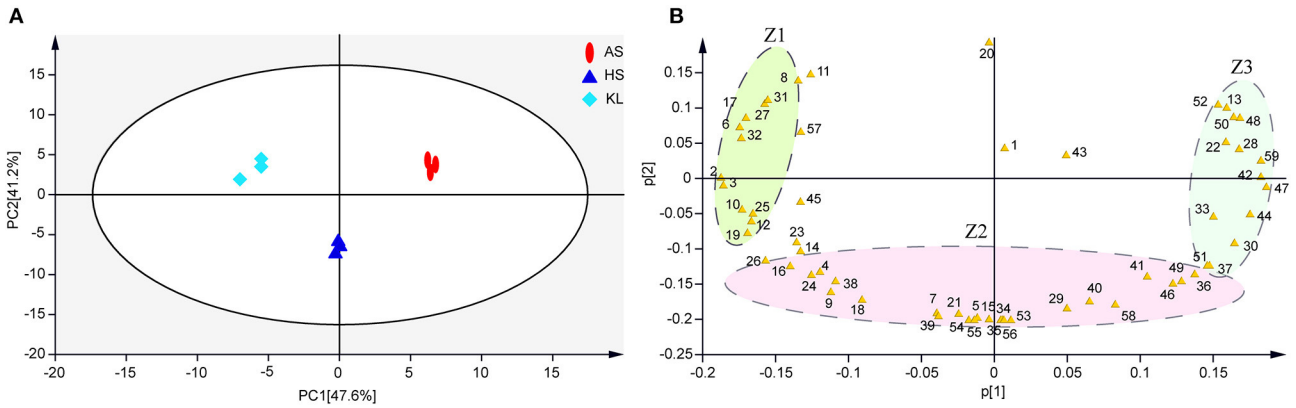

FIGURE 3 | (A,B) Metabolite principal component analysis of samples. Colored ellipses indicate 95% confidence intervals for metabolites in each sample. AS, Anshun; HS, Huishui; KL, Kaili. 1–59, Reliable metabolite numbers in traditional *Xiaoqu* samples (**Supplementary Table 2**).

Organic acids are not only paramount aroma and taste substances in liquor, but also flavor precursors. The appropriate content of organic acids can make the liquor body elegant and delicate or mellow and soft with a long aftertaste (Xu et al., 2018). We found that succinic acid, lactic acid, fumaric acid, and glycolic acid represented the distinguishable SDMs in KL *Xiaoqu*. Succinic acid, a main product of the TCA cycle, is known as the "wine skeleton" (Zhang et al., 2017) and, when combined with lactic acid, provides the unique sourness and umami taste to the final product. Additionally, lactic acid is the central precursor of ethyl lactate, which is the key flavoring component in liquor (Cai et al., 2019; Liu and Miao, 2020). Meanwhile, fumaric acid improves the stability and freshness of wine and decreases the level of SO_2 (Morata et al., 2018). Furthermore, methylmalonic acid, 2-furoic acid, 3-phenyllactic acid, and 3-hydroxypropionic acid were clustered in HS *Xiaoqu*. The decarboxylation of 2-furoic acid was confirmed as an alternative pathway in the formation of furan in heat-treated foods (Delatour et al., 2019), whereas 3-phenyllactic acid, which is widely present in fermented foods, has highly effective and broad-spectrum antimicrobial activity (Xu et al., 2020). However, we did not observe any dominant organic acids in AS *Xiaoqu*.

Among the key HS *Xiaoqu* metabolites, we identified three amino acids, namely, proline, glycine, and oxoproline. Among them, proline is reportedly beneficial for providing balance and softness in the taste of wine (Hu B. R. et al., 2020). Moreover, isoamylol, phenylethanol, and β-phenylethanol form from the amino acids leucine, phenylalanine, and phenylalanine, respectively, and are crucial flavor precursors (Chen Y. et al., 2020), contributing to the sweet, fresh, and bitter taste of wine (Procopio et al., 2015; Yin et al., 2017). Meanwhile, as major nitrogen sources for the survival of microorganisms, amino acids are closely related to the growth of microorganisms and production of metabolites (Park et al., 2013; Yang et al., 2018) and can interact with carbohydrates via the Maillard reaction to produce aromatic substances (Wang W. Y. et al., 2018). We also identified four SDMs, namely, linoleic acid, stearic acid, arachidic acid, and d-glyceric acid, as the major fatty acids in HS *Xiaoqu*. These fatty acids are involved in the composition of liquor flavor in liquor and are also associated with various health-related functions. For instance, linoleic acid and stearic acid, which are present in myrtle liqueur (Correddu et al., 2019), Maotai flavor liquor (Cai et al., 2019), and cacao liquor (Osakabe et al., 1998), have been reported to exhibit antitumor, antiobesity, antidiabetic, and anti-inflammatory properties (Jaudszus et al., 2016). Moreover, arachidic acid, a C20 saturated fatty acid, was implicated in the incidence of atherosclerosis and coronary heart disease (Rivellese et al., 2003). Generally, regarding their non-volatile profiles, the features of these samples were shown to be sufficiently different, indicating that the non-volatile components of *Xiaoqu* might be impacted by several factors, including microbial abundance, raw materials, or physical location.

Correlation Analysis of Representative Microbiota With Physicochemical Properties and SDMs

It is generally accepted that the differences in microbiota play a major role not only in the flavor and taste, but also in the formation of metabolites. Therefore, we explored the relationship of the seven physicochemical indexes, 39 SDMs, and the top 15 genera in the relative abundance of all species in the nine *Xiaoqu* samples using Spearman's algorithm. To further clarify the associated relationships, we carried out clustering heatmap using the R software.

As illustrated in **Figure 5**, *Aspergillus* was found to be positively associated with the esterifying power, saccharifying power, fermenting power, water activity, benzoic acid, 4-hydroxybenzoic acid, 4-hydroxypyridine, and 3,6-anhydro-d-galactose, whereas it was negatively associated with seven carbohydrates, including raffinose, glucose, melibiose, fructose, trehalose, ribose, and cellobiose. Moreover, *Aspergillus* as the pivotal mold detected in *jiuqu* likely plays a key role in the saccharification, fermentation, and esterification of wine (Wu et al., 2009; Liang et al., 2016), as it secretes a variety of extracellular enzymes, including proteolytic enzymes and

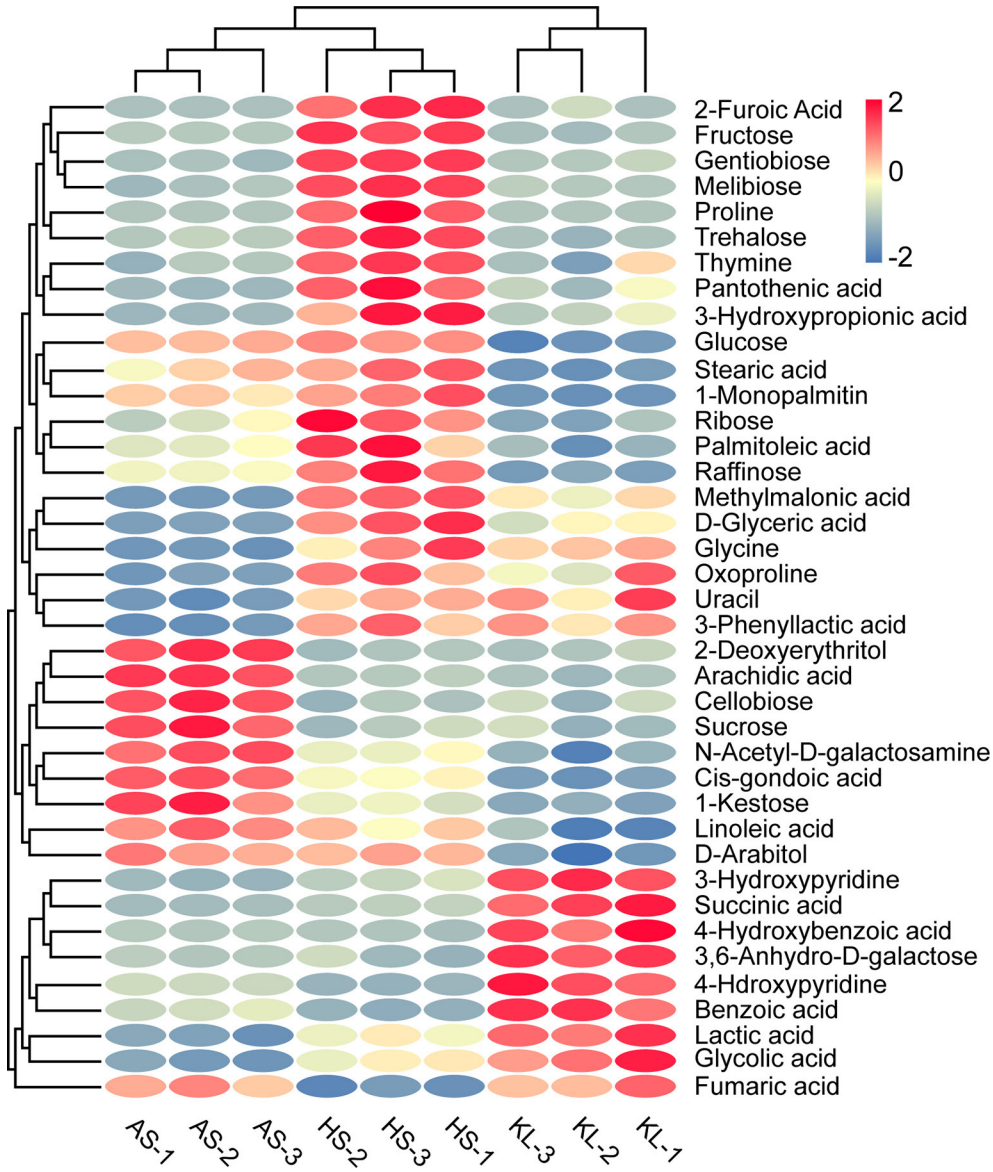

FIGURE 4 | Heatmap of significantly different metabolites in combination with cluster analysis in traditional *Xiaoqu*. Dark red oval indicates higher concentration of non-volatile compounds; dark blue oval indicates lower concentration.

starch hydrolytic enzymes, thereby leading to the production of flavor metabolites and flavor precursors (Wicklow et al., 2007; Jing et al., 2014). These results support the conclusion that *Aspergillus* promotes formation of hydrolase, sugar, and acid in *Xiaoqu*. Furthermore, *Saccharomyces* was positively correlated with the esterifying power, saccharifying power, fermenting power, succinic acid, and glycolic acid, whereas it was negatively associated with fructose, trehalose, ribose, cellobiose, palmitoleic acid, stearic acid, and 1-monopalmitin. Yeast can convert carbohydrates into ethanol, producing a series of key flavor compounds, such as acids, esters, and higher alcohols (Li H. et al., 2014; Li Z. M. et al., 2014; Liu et al., 2017; Fan et al., 2019). Therefore, it was not surprising that the *Saccharomyces* genus exhibited this type of correlation (**Figure 5**). Note that *Lactobacillus* exhibited a significant and positive correlation with acidity, methylmalonic acid, d-glyceric acid, 2-furoic acid, methylmalonic acid, pantothenic acid, gentiobiose, oxoproline, glycine, and proline (**Figure 5**; $p < 0.05$). Moreover, LAB can produce a large amount of organic acids, amino acids, and fatty acids (Ho et al., 2014; Huang X. N. et al., 2018; Jin et al., 2019; Zang et al., 2020), which was supported by the current study results. Moreover, by reducing acidity, LAB can also inhibit the growth and reproduction of pathogenic bacteria during the fermentation system (Cappello et al., 2016; Huang et al., 2019). In our study, *Acetobacter* was positively correlated with acidity (**Figure 5A**), which was consistent with

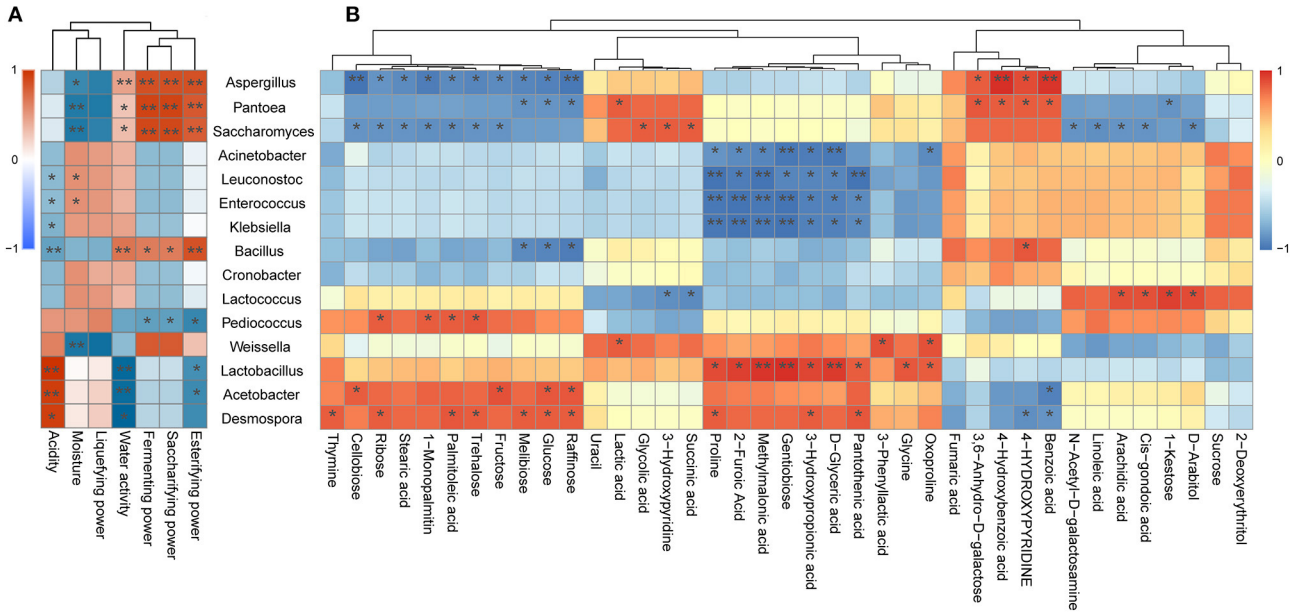

FIGURE 5 | (A) Correlation between physicochemical properties and representative microbial taxa identified in the three traditional *Xiaoqu*. **(B)** Correlation between significantly different metabolites and representative microbial taxa identified in the three traditional *Xiaoqu*. Red represents a positive correlation; blue represents a negative correlation. $^{*}p < 0.05$, $^{**}p < 0.001$.

previous reports that described *Acetobacter* as one of the major contributors to acidity in the Shanxi aged fermented vinegar and Luzhou-flavor liquor pit mud (Li et al., 2016; Jiang et al., 2019). *Acetobacter* was also found to be positively correlated with four carbohydrates, namely, cellobiose, fructose, raffinose, and glucose (**Figure 5B**). In fact, *Acetobacter* contains amylase activity and can hydrolyze starch from raw materials into sugar compounds (Ye et al., 2019). Besides, *Bacillus* is significantly positively correlated with esterifying power, saccharifying power, fermenting power, and water activity (**Figure 5A**). A previous study found that *Bacillus* could degrade cellulose, starch, and protein into substances available for subsequent fermentation and promote the production of alcohols (Tang et al., 2019), which agrees with our results.

It is worth noting that *Acinetobacter*, *Enterococcus*, and *Klebsiella* showed significant negative correlations with most SDMs (**Figure 5**; $P < 0.05$). Members of the *Acinetobacter, Enterococcus*, and *Klebsiella* genera are recognized as synthetic acetoin bacteria during fermentation (Molinari et al., 2003; Chen et al., 2010), thus posing a health risk to consumers (Liu and Sun, 2018). Fortunately, it was demonstrated that *Weissella* exerts strong antagonism against these undesirable microorganisms (**Supplementary Table 4**), which was supported by the conclusion that *Weissella* enhances the production of acids and alcohols to inhibit the growth of pathogenic bacteria (Chen C. et al., 2020). Moreover, pathogenic microorganisms only represent a small portion of the microbial community in the early steps of black glutinous rice wine fermentation (Jiang et al., 2020). Likewise, Liu et al. (2019) and Mu et al. (2020) reported that these undesirable microorganisms disappeared during fermentation. Hence, further research is required to determine the mechanism by which pathogenic bacteria become destroyed. Besides, we find that *Pantoea* and *Desmospora* exhibited significant and positive correlation with most SDMs (**Figure 5**; $P < 0.05$). Although the roles of members from these genera in the fermentation of *Xiaoqu* wine have not yet been fully elucidated, they have been studied extensively in other fields. For example, the genus *Pantoea*, belonging to the family *Enterobacteriaceae*, represents a genus comprising common endophytes of rice (Megías et al., 2016). Members from this genus are commonly used as biological control agents due to their excellent antimicrobial production capacity (Walterson et al., 2014). Meanwhile, *Desmospora* may represent a new member of the DTEase family of enzymes with highest substrate specificity toward d-psicose (Zhang et al., 2013). This genus was isolated from a deep-sea sediment and was recently detected in traditional fermentation of Chinese Fen-Maotai-flavored liquor in pottery jars (Zhang et al., 2015; Hu X. X. et al., 2020).

Construction of the Metabolic Network

To better understand the relationship between microorganisms and metabolites, we used metabolomics, metagenomics, and related network data to predict the metabolic network associated with substrate decomposition and SDM formation in Guizhou *Xiaoqu* (**Figure 6**). Starch, cellulose, protein, and fat were the raw materials of *Xiaoqu* and the main substrates for metabolite formation. Meanwhile, melibiose in raw materials, as well as raffinose, sucrose, fructose, and glucose degraded from starch and cellulose in rice and rice bran by microorganisms, serve as alternative carbon sources for the production of organic

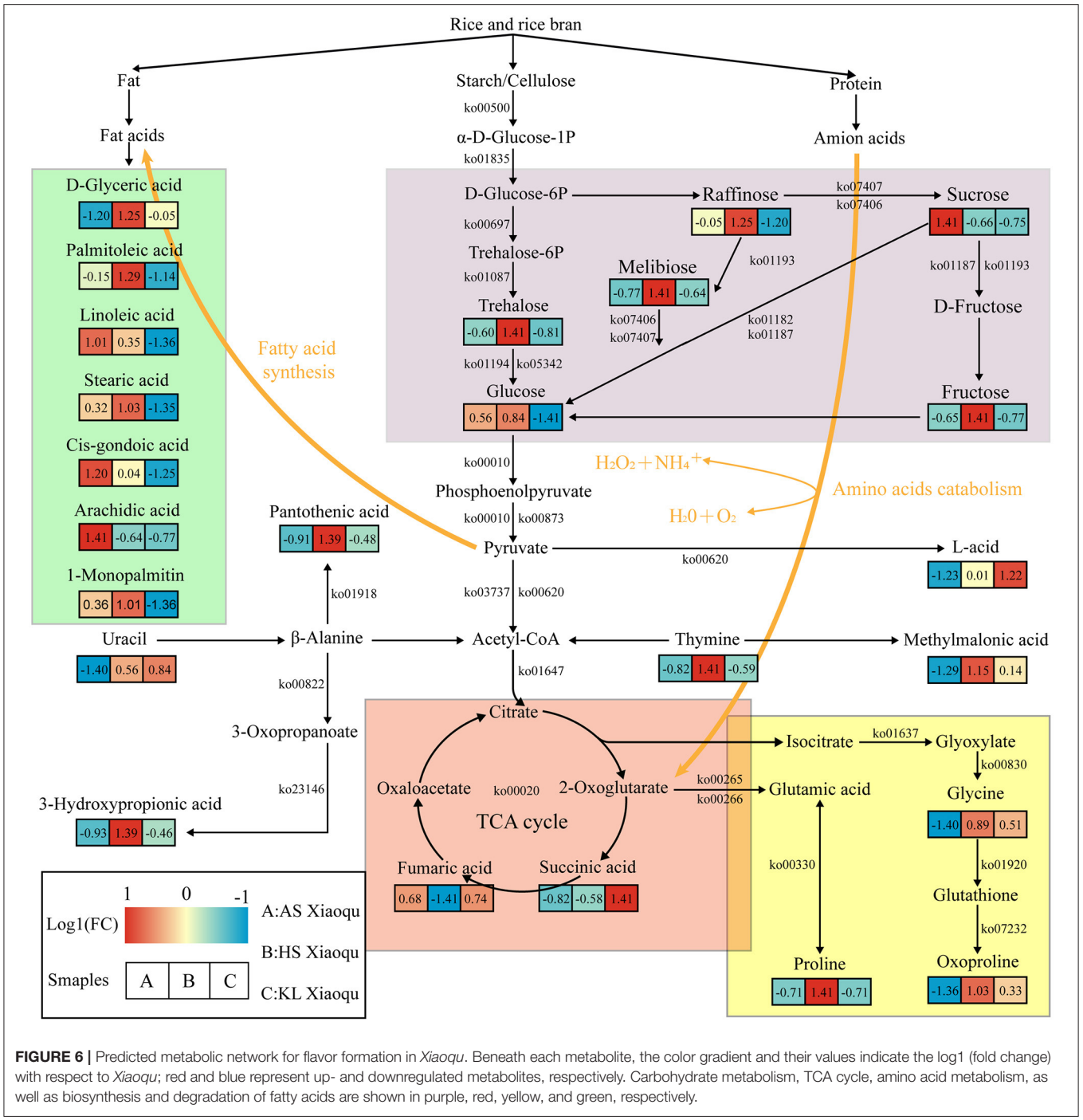

FIGURE 6 | Predicted metabolic network for flavor formation in *Xiaoqu*. Beneath each metabolite, the color gradient and their values indicate the log1 (fold change) with respect to *Xiaoqu*; red and blue represent up- and downregulated metabolites, respectively. Carbohydrate metabolism, TCA cycle, amino acid metabolism, as well as biosynthesis and degradation of fatty acids are shown in purple, red, yellow, and green, respectively.

acids, amino acids, and fatty acids Wu L. et al., 2017; Jin et al., 2019. Pyruvate and acetyl-CoA are further produced by microbial degradation as central compounds of the metabolic network. Acetyl-CoA participates in the TCA cycle and fatty acid biosynthesis. Moreover, organic acids, including succinic and fumaric acid, that are generated through the TCA cycle are further converted into proline, glycine, and oxoproline (He et al., 2019), all of which were abundant in HS and KL *Xiaoqu*, and which may serve as nitrogen sources for microbial growth during fermentation and as flavor precursors (Fairbairn et al., 2017). The nucleic acids in the raw materials of *Xiaoqu*, including uracil and thymine, can also be used as a nitrogen source during the fermentation of *Xiaoqu*. Specifically, uracil can be degraded to acetyl-CoA, 3-hydroxypropionic acid, and pantothenic acid during the fermentation of HS *Xiaoqu* (Zhu et al., 2020), whereas thymine can be degraded to acetyl-CoA and methylmalonic acid in KL *Xiaoqu*. Besides, pyruvate can be degraded to lactic acid in KL *Xiaoqu* (Ai et al., 2019). Fatty acids, including d-glyceric acid, palmitoleic acid, linoleic acid, stearic acid, cis-gondoic acid, arachidic acid, and 1-monopalmitin, produced by acetyl-CoA

through the fatty acid biosynthesis pathway or fat degradation, were also identified as major compounds in AS and HS *Xiaoqu* (Mu et al., 2020). In summary, the metabolism of carbohydrates and TCA cycle appear to play a paramount role in the formation of non-volatile compounds in *Xiaoqu*.

CONCLUSION

Using metagenomics and metabolomics analyses, we investigated potential correlations between the microbial community and metabolites produced in traditional *Xiaoqu* collected in Guizhou, China. Our metabolomics data results were highly consistent with those of the metagenomics data. Eight microbial genera, namely, *Aspergillus*, *Saccharomyces*, *Lactobacillus*, *Acetobacter*, *Weissella*, *Pantoea*, *Desmospora*, and *Bacillus*, were positively correlated with physicochemical indexes and SDMs. Besides, we established the flavor metabolic network in the microbiota of Guizhou *Xiaoqu* and revealed the decomposition profile for substrates and formation of SDMs in metabolic pathways. Further isolation and identification of functional strains in *Xiaoqu* is warranted, including characterization of the functions and fermentation mechanisms of these strains using multiomics methods, such as macro transcriptomics and metaproteomics. These findings provide insights for the use of specific functional strains to provide biological enhancement, as well as improved yield stability and quality in *Xiaoqu* wine production.

DATA AVAILABILITY STATEMENT

The datasets presented in this study can be found in online repositories. The names of the repository/repositories and accession number(s) can be found in the article/**Supplementary Material**.

AUTHOR CONTRIBUTIONS

CZ and WS contributed to the experimental design, performed the statistical analysis, and wrote the manuscript. CZ, WS, YuM, YiM, and LJ contributed to manuscript revision, read, and approved the submitted version. All authors contributed to the article and approved the submitted version.

FUNDING

The research was financially supported by the National Natural Science Foundation of China under Grant No. 31860441 and by the Guizhou Science and Technology Program [QKHPTRC (2020) 5004].

ACKNOWLEDGMENTS

The authors thank Novogene Bioinformatics Technology Co., Ltd. (Beijing, China) and Biomarker Technologies Co, Ltd. (Beijing, China) for technical assistance in carrying out the analyses. We would like to thank Editage (www.editage.cn) for English language editing.

SUPPLEMENTARY MATERIAL

The Supplementary Material for this article can be found online at: https://www.frontiersin.org/articles/10.3389/fmicb.2020.617030/full#supplementary-material

REFERENCES

Agyirifo, D. S., Wamalwa, M., Otwe, E. P., and Galyuon, I. (2019). Metagenomics analysis of cocoa bean fermentation microbiome identifying species diversity and putative functional capabilities. *Heliyon* 5:e02170. doi: 10.1016/j.heliyon.2019.e02170

Ai, M., Qiu, X., Huang, J., We, C. D., Jin, Y., and Zhou, R. Q. (2019). Characterizing the microbial diversity and major metabolites of Sichuan bran vinegar augmented by *Monascus purpureus*. *Int. J. Food Microbiol.* 292, 83–90. doi: 10.1016/j.ijfoodmicro.2018.12.008

Al Atrouni, A., Joly-Guillou, M. L., Hamze, M., and Kempf, M. (2016). Reservoirs of *non-baumannii Acinetobacter* species. *Front. Microbiol.* 7:49. doi: 10.3389/fmicb.2016.00049

Ali, B., Yi, Z. L., Fang, Y., Chen, L. C., He, M. Z., Liu, D. Y., et al. (2018). Characterization of a fungal thermostable endoglucanase from Chinese nong-flavor *Daqu* by metatranscriptomic method. *Int. J. Biol. Macromol.* 121, 183–190. doi: 10.1016/j.ijbiomac.2018.09.173

Anupma, A., and Tamang, J. P. (2020). Diversity of filamentous fungi isolated from some amylase and alcohol-producing starters of India. *Front. Microbiol.* 11:905. doi: 10.3389/fmicb.2020.00905

Bal, J., Yun, S. H., Yeo, S. H., Kim, J. M., Kim, B. T., and Kim, D. H. (2017). Effects of initial moisture content of Korean traditional wheat-based fermentation starter *Nuruk* on microbial abundance and diversity. *Appl. Microbiol. Biotechnol.* 101, 2093–2106. doi: 10.1007/s00253-016-8042-2

Bolotin, A., Mauger, S., Malarme, K., Ehrlich, S. D., and Sorokin, A. (1999). Low-redundancy sequencing of the entire *Lactococcus lactis* il1403 genome. *Antonie Van Leeuwe.* 76, 27–76. doi: 10.1023/A:1002048720611

Bora, S. S., Keot, J., Das, S., Sarma, K., and Barooah, M. (2016). Metagenomics analysis of microbial communities associated with a traditional rice wine starter culture (Xaj-pitha) of Assam, India. *3 Biotech* 6:153. doi: 10.1007/s13205-016-0471-1

Briggs, G. S., Smits, W. K., and Soultanas, P. (2012). Chromosomal replication initiation machinery of low-G plus C-content *Firmicutes*. *J. Bacteriol.* 194, 5162–5170. doi: 10.1128/JB.00865-12

Cai, H., Zhang, T., Zhang, Q., Luo, J., Cai, C., and Mao, J. (2018). Microbial diversity and chemical analysis of the starters used in traditional Chinese sweet rice wine. *Food Microbiol.* 73, 319–326. doi: 10.1016/j.fm.2018.02.002

Cai, X. M., Shen, Y., Chen, M. Y., Zhong, M. Y., Zhou, Y. L., and Luo, A. M. (2019). Characterisation of volatile compounds in Maotai flavour liquor during fermentation and distillation. *J. Inst. Brew.* 125, 453–463. doi: 10.1002/jib.581

Cappello, M. S., Zapparoli, G., Logrieco, A., and Bartowsky, E. J. (2016). Linking wine lactic acid bacteria diversity with wine aroma and flavour. *Int. J. Food Microbiol.* 243, 16–27. doi: 10.1016/j.ijfoodmicro.2016.11.025

Chen, C., Liu, Y., Tian, H. X., Ai, L. Z., and Yu, H. Y. (2020). Metagenomic analysis reveals the impact of JIUYAO microbial diversity on fermentation and the volatile profile of Shaoxing-jiu. *Food Microbiol.* 86:103326. doi: 10.1016/j.fm.2019.103326

Chen, J. C., Chen, Q., Guo, Q., Ruan, S., Ruan, H., and He, G. (2010). Simultaneous determination of acetoin and tetramethylpyrazine in

traditional vinegars by HPLC method. *Food Chem*. 122, 1247–1252. doi: 10.1016/j.foodchem.2010.03.072

Chen, X., Liu, J., Luo, Q., and Liu, L. (2017). Manipulation of cofactor balance in microorganisms. *Chin. J. Biotechnol*. 33, 16–26. doi: 10.13345/j.cjb.160232

Chen, Y., Zhang, W., Yi, H., Wang, B., and Shi, X. (2020). Microbial community composition and its role in volatile compound formation during the spontaneous fermentation of ice wine made from vidal grapes. *Process Biochem*. 92, 365–377. doi: 10.1016/j.procbio.2020.01.027

Chen, Y. R., Ma, Z. H., Zhong, J., Li, L. Q., Min, L. S., Xu, L. M., et al. (2018). Simultaneous quantification of serum monounsaturated and polyunsaturated phosphatidylcholines as potential biomarkers for diagnosing non-small cell lung cancer. *Sci. Rep*. 8:7137. doi: 10.1038/s41598-018-25552-z

Chuenchomrat, P., Assavanig, A., and Lertsiri, S. (2008). Volatile flavour compounds analysis of solid state fermented Thai rice wine (Qu). *ScienceAsia* 34, 199–206. doi: 10.2306/scienceasia1513-1874.2008.34.199

Correddu, F., Maldini, M., Addis, R., Petretto, G. L., Palomba, M., Battacone, G., et al. (2019). Myrtus communis liquor byproduct as a source of bioactive compounds. *Foods*. 8:237. doi: 10.3390/foods8070237

de Paiva, I. M., Steinberg, R. D., Lula, I. S., Souza-Fagundes, E. M., Mendes, T. D., Valenzuela Bell, M. J., et al. (2016). *Lactobacillus kefiranofaciens* and *Lactobacillus satsumensis* isolated from Brazilian kefir grains produce alpha-glucans that are potentially suitable for food applications. *LWT Food Sci. Technol*. 72, 390–398. doi: 10.1016/j.lwt.2016.05.010

Delatour, T., Huertas-Pérez, J. F., Dubois, M., Theurillat, X., and Stadler, R. H. (2019). Thermal degradation of 2-furoic acid and furfuryl alcohol as pathways in the formation of furan and 2-methylfuran in food. *Food Chem*. 303:125406. doi: 10.1016/j.foodchem.2019.125406

Dong, W. W., Yang, Q., Liao, Y. X., Liu, Y. C., Hu, Y. L., Peng, N., et al. (2020). Characterisation and comparison of the microflora of traditional and pure culture *Xiaoqu* during the Baijiu liquor brewing process. *J. Inst. Brew*. 126, 213–220. doi: 10.1002/jib.597

Du, H., Wang, X., Zhang, Y., and Xu, Y. (2019). Exploring the impacts of raw materials and environments on the microbiota in Chinese *Daqu* starter. *Int. J. Food Microbiol*. 297, 32–40. doi: 10.1016/j.ijfoodmicro.2019.02.020

Dung, N. T. P., Rombouts, F. M., and Nout, M. J. R. (2006). Functionality of selected strains of moulds and yeasts from vietnamese rice wine starters. *Food Microbiol*. 23, 331–340. doi: 10.1016/j.fm.2005.05.002

Elhalis, H., Cox, J., and Zhao, J. (2020). Ecological diversity, evolution and metabolism of microbial communities in the wet fermentation of australian coffee beans. *Int. J. Food Microbiol*. 321:108544. doi: 10.1016/j.ijfoodmicro.2020.108544

Escobar-Zepeda, A., Sanchez-Flores, A., and Baruch, M. Q. (2016). Metagenomic analysis of a mexican ripened cheese reveals a unique complex microbiota. *Food Microbiol*. 57, 116–127. doi: 10.1016/j.fm.2016.02.004

Fairbairn, S., McKinnon, A., Musarurwa, H. T., Ferreira, A. C., and Bauer, F. F. (2017). The impact of single amino acids on growth and volatile aroma production by *Saccharomyces cerevisiae* strains. *Front. Microbio*. 8:2554. doi: 10.3389/fmicb.2017.02554

Fan, G. S., Fu, Z. L., Teng, C., Wu, Q. H., Liu, P. X., Yang, R., et al. (2019). Comprehensive analysis of different grades of roasted-sesame-like flavored *Daqu*. *Int. J. Food Prop*. 22, 1205–1222. doi: 10.1080/10942912.2019.1635154

Fan, G. S., Sun, B. G., Fu, Z. L., Xia, Y. Q., Huang, M. Q., Xu, C. Y., et al. (2018). Analysis of physicochemical indices, volatile flavor components, and microbial community of a light-flavor *Daqu*. *J. Am. Soc. Brew. Chem*. 76, 209–218. doi: 10.1080/03610470.2018.1424402

Fang, C., Wei, H., Wei, J., and Xu, Y. (2019). Compositional differences and similarities between typical Chinese Baijiu and Western liquor as revealed by mass spectrometry-based metabolomics. *Metabolites* 9:2. doi: 10.3390/metabo9010002

Ferrocino, I., Bellio, A., Giordano, M., Macori, G., Romano, A., Rantsiou, K., et al. (2017). Shotgun metagenomics and volatilome profile of the microbiota of fermented sausages. *Appl. Environ. Microbiol*. 84, e02120–e02117. doi: 10.1128/AEM.02120-17

Franzosa, E. A., McIver, L. J., Rahnavard, G., Thompson, L. R., Schirmer, M., Weingart, G., et al. (2018). Species-level functional profiling of metagenomes and metatranscriptomes. *Nat. Methods* 15, 962–968. doi: 10.1038/s41592-018-0176-y

Frédéric, L., and Luc, D. V. (2004). Lactic acid bacteria as functional starter cultures for the food fermentation industry. *Trends Food Sci. Technol*. 15, 67–78. doi: 10.1016/j.tifs.2003.09.004

Gan, S. H., Yang, F., Sahu, S. K., Luo, R. Y., and Liu, H. (2019). Deciphering the composition and functional profile of the microbial communities in Chinese Moutai liquor. *Front. Microbiol*. 10:1540. doi: 10.3389/fmicb.2019.01540

Gou, M., Wang, H. Z., Yuan, H. W., Zhang, W. X., Tang, Y. Q., and Kida, K. (2015). Characterization of the microbial community in three types of fermentation starters used for Chinese liquor production. *J. Inst. Brew*. 121, 620–627. doi: 10.1002/jib.272

Gu, E. J., Kim, D. W., Jang, G. J., Song, S. H., Lee, J. I., Lee, S. B., et al. (2017). Mass-based metabolomic analysis of soybean sprouts during germination. *Food Chem*. 217, 311–319. doi: 10.1016/j.foodchem.2016.08.113

Guan, T. M., Yang, Z., Ou, M. Y., and Zhang, J. X. (2015). Storage period affecting dynamic succession of microbiota and quality changes of strong-flavor Baijiu Daqu. *LWT Food Sci. Technol*. doi: 10.1016/j.lwt.2020.110544

Harbertson, J. F., Yuan, C., Mireles, M. S., Hanlin, R. L., and Downey, M. O. (2013). Glucose, fructose and sucrose increase the solubility of protein-tannin complexes and at high concentration, glucose and sucrose interfere with bisulphite bleaching of wine pigments. *Food Chem*. 138, 556–563. doi: 10.1016/j.foodchem.2012.10.141

He, G., Huang, J., Zhou, R., Wu, C., and Jin, Y. (2019). Effect of fortified *Daqu* on the microbial community and flavor in Chinese strong-flavor liquor brewing process. *Front. Microbiol*. 10:56. doi: 10.3389/fmicb.2019.00056

Ho, V. T. T., Zhao, J., and Fleet, G. (2014). Yeasts are essential for cocoa bean fermentation. *Int. J. Food Microbiol*. 174, 72–87. doi: 10.1016/j.ijfoodmicro.2013.12.014

Hu, B. R., Gao, J., Xu, S. C., Zhu, J. Y., Fan, X. M., and Zhou, X. Y. (2020). Quality evaluation of different varieties of dry red wine based on nuclear magnetic resonance metabolomics. *Appl. Biol. Chem*. 63:24. doi: 10.1186/s13765-020-00509-x

Hu, X. X., Huang, Y. G., Jiang, X., Zhu, J. H., and Jin, L. (2020). Bacterial community structure and diversity during fermentation of Chinese Fen-Maotai-flavored liquor in pottery jars. *Food Sci*. 8, 130–138. doi: 10.7506/spkx1002-6630-20190314-175

Huang, X. N., Yu, S. Z., Han, B. Z., and Chen, J. Y. (2018). Bacterial community succession and metabolite changes during sufu fermentation. *LWT Food Sci. Technol*. 97, 537–545. doi: 10.1016/j.lwt.2018.07.041

Huang, Z. R., Guo, W. L., Zhou, W. B., Li, L., Xu, J. X., and Hong, J. L. (2019). Microbial communities and volatile metabolites in different traditional fermentation starters used for Hong Qu glutinous rice wine. *Food Res. Int*. 121, 593–603. doi: 10.1016/j.foodres.2018.12.024

Huang, Z. R., Hong, J. L., and Xu, J. X. (2018). Exploring core functional microbiota responsible for the production of volatile flavour during the traditional brewing of Wuyi Hong Qu glutinous rice wine. *Food Microbiol*. 76, 487–496. doi: 10.1016/j.fm.2018.07.014

Huo, J. Y., Wu, J. H., Sun, B. G., Zhao, M., Sun, W. Z., Sun, J. Y., et al. (2020). Isolation, purification, structure characterization of a novel glucan from Huangshui, a byproduct of Chinese Baijiu, and its immunomodulatory activity in LPS-stimulated THP-1 cells. *Int. J. Biol. Macromol*. 161, 406–416. doi: 10.1016/j.ijbiomac.2020.06.028

Illeghems, K., Vuyst, L. D., Papalexandratou, Z., and Weckx, S. (2012). Phylogenetic analysis of a spontaneous cocoa bean fermentation metagenome reveals new insights into its bacterial and fungal community diversity. *PLoS ONE* 7:e38040. doi: 10.1371/journal.pone.0038040

Jaudszus, A., Mainz, J. G., Pittag, S., Dornaus, S., Dopfer, C., Roth, A., et al. (2016). Effects of a dietary intervention with conjugated linoleic acid on immunological and metabolic parameters in children and adolescents with allergic asthma a placebo-controlled pilot trial. *Lipids Health Dis*. 15:21. doi: 10.1186/s12944-016-0187-6

Jia, W., Li, Y. L., Du, A., Fan, Z. B., Zhang, R., Shi, L., et al. (2020). Foodomics analysis of natural aging and gamma irradiation maturation in Chinese distilled Baijiu by UPLC-orbitrap-MS/MS. *Food Chem*. 315:126308. doi: 10.1016/j.foodchem.2020.126308

Jiang, L., Su, W., Mu, Y., and Mu, Y. (2020). Major metabolites and microbial community of fermented black glutinous rice wine with different starters. *Front. Microbiol*. 11:593. doi: 10.3389/fmicb.2020.00593

Jiang, Y. J., Lv, X. C., Zhang, C., Zheng, Y. M., Zheng, B. D., Duan, X., et al. (2019). Microbial dynamics and flavor formation during the traditional brewing of *Monascus* vinegar. *Food Res. Int*. 125:108531. doi: 10.1016/j.foodres.2019.108531

Jin, Y., Li, D. Y., Ai, M., Tang, Q. X., Huang, J., Ding, X. F., et al. (2019). Correlation between volatile profiles and microbial communities: a metabonomic approach to study Jiang-flavor liquor *Daqu*. *Food Res. Int*. 121, 422–432. doi: 10.1016/j.foodres.2019.03.021

Jing, Z., Cheng, J., Jin, J., Su, J., and Bai, Y. (2014). Revegetation as an efficient means of improving the diversity and abundance of soil eukaryotes in the loess plateau of China. *Ecol. Eng*. 70, 169–174. doi: 10.1016/j.ecoleng.2014.05.011

Johan, S., and Magnusson, J. (2005). Antifungal lactic acid bacteria as biopreservatives. *Trends Food Sci. Technol*. 16, 70–78. doi: 10.1016/j.tifs.2004.02.014

Jung, J. Y., Lee, S. H., Kim, J. M., Park, M. S., Bae, J. W., Hahn, Y., et al. (2011). Metagenomic analysis of kimchi, a traditional Korean fermented food. *Appl. Environ. Microbiol*. 77, 2264–2274. doi: 10.1128/AEM.02157-10

Keisam, S., Tuikhar, N., Ahmed, G., and Jeyaram, K. (2019). Toxigenic and pathogenic potential of enteric bacterial pathogens prevalent in the traditional fermented foods marketed in the northeast region of India. *Int. J. Food Microbiol.* 296, 21–30. doi: 10.1016/j.ijfoodmicro.2019.02.012

Kim, H. R., Kim, J. H., Bai, D. H., and Ahn, B. H. (2011). Identification and characterization of useful fungi with α-amylase activity from the Korean traditional *Nuruk*. *Mycobiology* 39, 278–282. doi: 10.5941/MYCO.2011.39.4.278

Kim, J., Kim, M. S., Koh, A. Y., Xie, Y., and Zhan, X. (2016). Fmap: functional mapping and analysis pipeline for metagenomics and metatranscriptomics studies. *BMC Bioinformatics* 17:420. doi: 10.1186/s12859-016-1278-0

Kim, S. A., Yun, S. J., Jeon, S. H., Kim, N. H., Kim, H. W., Cho, T. J., et al. (2015). Microbial composition of turbid rice wine (Makgeolli) at different stages of production in a real processing line. *Food Control* 53, 1–8. doi: 10.1016/j.foodcont.2015.01.002

Kim, S. J., Cho, H., Ahn, J. H., Weon, H. Y., Joa, J. H., Kim, J. S., et al. (2019). *Paenibacillus nuruki* sp. nov., isolated from Nuruk, a Korean fermentation starter. *J. Microbiol*. 57, 836–841. doi: 10.1007/s12275-019-9118-3

Kind, T., Wohlgemuth, G., Lee, D. Y., Lu, Y., Palazoglu, M., Shahbaz, S., et al. (2009). FiehnLib: mass spectral and retention index libraries for metabolomics based on quadrupole and time-of-flight gas chromatography/mass spectrometry. *Anal. Chem*. 81, 10038–10048. doi: 10.1021/ac9019522

Lee, J. H. J., Jayaprakasha, G. K., Avila, C. A., Crosby, K. M., and Patil, B. S. (2019). Metabolomic studies of volatiles from tomatoes grown in net-house and open-field conditions. *Food Chem*. 25, 282–291. doi: 10.1016/j.foodchem.2018.09.091

Li, H., Lian, B., Ding, Y. H., Nie, C. C., and Zhang, Q. M. (2014). Bacterial diversity in the central black component of Maotai *Daqu* and its flavor analysis. *Ann. Microbiol*. 64, 1659–1669. doi: 10.1007/s13213-014-0809-z

Li, S., Li, P., Liu, X., Luo, L., and Lin, W. (2016). Bacterial dynamics and metabolite changes in solid-state acetic acid fermentation of Shanxi aged vinegar. *Appl. Microbiol. Biotechnol*. 100, 4395–4411. doi: 10.1007/s00253-016-7284-3

Li, Z. M., Bai, Z. H., Wang, D. L., Zhang, W. J., Zhang, M., Lin, F., et al. (2014). Cultivable bacterial diversity and amylase production in three typical *Daqus* of Chinese spirits. *Int. J. Food Sci. Technol*. 49, 776–786. doi: 10.1111/ijfs.12365

Liang, H. P., Luo, Q. C., Zhang, A., Wu, Z. Y., and Zhang, W. X. (2016). Comparison of bacterial community in matured and degenerated pit mud from Chinese Luzhou-flavour liquor distillery in different regions. *J. Inst. Brew*. 112, 48–54. doi: 10.1002/jib.296

Liu, H. L., and Sun, B. G. (2018). Effect of fermentation processing on the flavor of Baijiu. *J. Agric. Food Chem*. 66, 5425–5432. doi: 10.1021/acs.jafc.8b00692

Liu, P. L., and Miao, L. H. (2020). Multiple batches of fermentation promote the formation of functional microbiota in Chinese Miscellaneous-flavor Baijiu fermentation. *Front. Microbiol*. 11:75. doi: 10.3389/fmicb.2020.00075

Liu, P. L., Xiong, X. M., Wang, S., and Miao, L. H. (2017). Population dynamics and metabolite analysis of yeasts involved in a Chinese Miscellaneous-flavor liquor fermentation. *Ann. Microbiol*. 67, 553–565. doi: 10.1007/s13213-017-1286-y

Liu, S., Chen, Q., Zou, H., Yu, Y., and Zhang, S. (2019). A metagenomic analysis of the relationship between microorganisms and flavor development in Shaoxing mechanized Huangjiu fermentation mashes. *Int. J. Food Microbiol*. 303, 9–18. doi: 10.1016/j.ijfoodmicro.2019.05.001

Liu, Z., Wang, Z., Lv, X., Zhu, X., and Ni, L. (2018). Comparison study of the volatile profiles and microbial communities of Wuyi Qu and Gutian Qu, two major types of traditional fermentation starters of Hong qu glutinous rice wine. *Food Microbiol*. 69, 105–115. doi: 10.1016/j.fm.2017.07.019

Liu, Y. X., Qin, Y., Chen, T., Lu, M., and Bai, Y. (2020). A practical guide to amplicon and metagenomic analysis of microbiome data. *Protein Cell*. 1–16. doi: 10.1007/s13238-020-00724-8

Lv, X. R., Li, Y., Cui, T. Q., Sun, M. T., Bai, F. L., Li, X. P., et al. (2020). Bacterial community succession and volatile compound changes during fermentation of shrimp paste from Chinese Jinzhou region. *LWT Food Sci. Technol*. 122:108998. doi: 10.1016/j.lwt.2019.108998

Ma, K. D., Maeda, T., You, H. Y., and Shirai, Y. (2014). Open fermentative production of L-lactic acid with high optical purity by thermophilic *Bacillus coagulans* using excess sludge as nutrient. *Bioresour. Technol*. 151, 28–35. doi: 10.1016/j.biortech.2013.10.022

Megías, E., Megías, M., Ollero, F. J., and Hungria, M. (2016). Draft genome sequence of *Pantoea ananatis* strain AMG521, a rice plant growth-promoting bacterial endophyte isolated from the guadalquivir marshes in Southern Spain. *Genome Announc*. 4, e01681–e01615. doi: 10.1128/genomeA.01681-15

Melanie, S., Ijaz, U. Z., Rosalinda, D., Neil, H., Sloan, W. T., and Christopher, Q. (2015). Insight into biases and sequencing errors for amplicon sequencing with the illumina miseq platform. *Nucleic Acids Res*. 43:e37. doi: 10.1093/nar/gku1341

Menz, G., Vriesekoop, F., Zarei, M., Zhu, B. F., and Aldred, P. (2010). The growth and survival of food-borne pathogens in sweet and fermenting brewers' wort. *Int. J. Food Microbiol.* 140, 19–25. doi: 10.1016/j.ijfoodmicro.2010.02.018

Ministry of Light Industry of China (2011). *General Methods of Analysis for DAQU (QB/T 4257 2011)*. Beijing: China Light Industry Press.

Molinari, F., De Faveri, D., Torre, P., Perego, P., and Converti, A. (2003). Carbon material balances and bioenergetics of 2,3-butanediol bio-oxidation by *Acetobacter hansenii*. *Enzyme Microb. Technol*. 33, 708–719. doi: 10.1016/S0141-0229(03)00218-7

Morata, A., Bañuelos, M. A., Lopez, C., Song, C. L., Vejarano, R., Loira, I., et al. (2018). Use of fumaric acid to control pH and inhibit malolactic fermentation in wines. *Food Addit. Contam. A* 37, 1–11. doi: 10.1080/19440049.2019.1684574

Mu, Y., Su, W., Mu, Y. C., and Jiang, L. (2020). Combined application of high-throughput sequencing and metabolomics reveals metabolically active microorganisms during Panxian ham processing. *Front. Microbiol*. 10:3012. doi: 10.3389/fmicb.2019.03012

Olano, A., Chua, J., Schroeder, S., Minari, A., La Salvia, M., and Hall, G. (2001). *Weissella confusa* (Basonym: *Lactobacillus confusus*) bacteremia: a case report. *J. Clin. Microbiol*. 39, 1604–1607. doi: 10.1128/JCM.39.4.1604-1607.2001

Osakabe, N., Yamagishi, M., Sanbongi, C., Natsume, M., Takizawa, T., and Osawa, T. (1998). The antioxidative substances in cacao liquor. *J. Nutr. Sci. Vitaminol*. 44, 313–321. doi: 10.3177/jnsv.44.313

Park, H. J., Lee, S., Song, S., and Kim, Y. S. (2013). Characterization of volatile components in Makgeolli, a traditional Korean rice wine, with or without pasteurization, during storage. *Molecules* 18, 5317–5325. doi: 10.3390/molecules18055317

Procopio, S., Sprung, P., and Becker, T. (2015). Effect of amino acid supply on the transcription of flavour-related genes and aroma compound production during lager yeast fermentation. *LWT Food Sci. Technol*. 63, 289–297. doi: 10.1016/j.lwt.2015.03.007

Rivellese, A. A., Maffettone, A., Vessby, B., Uusitupa, M., Hermansen, K., Berglund, L., et al. (2003). Effects of dietary saturated, monounsaturated and n-3 fatty acids on fasting lipoproteins, ldl size and post-prandial lipid metabolism in healthy subjects. *Atherosclerosis* 167, 149–158. doi: 10.1016/S0021-9150(02)00424-0

Sha, S. P., Jani, K., Sharma, A., Anupma, A., Pradhan, P., Shouche, Y., et al. (2017). Analysis of bacterial and fungal communities in Marcha and Thiat, traditionally prepared amylolytic starters of India. *Sci. Rep.* 7:10967. doi: 10.1038/s41598-017-11609-y

Siebenhandl, S., Lestario, L. N., Trimmel, D., and Berghofer, E. (2001). Studies on tape ketan-an Indonesian fermented rice food. *Int. J. Food Sci. Nutr*. 52, 347–357. doi: 10.1080/09637480120057585

Sokny, L., Hasika, M., Cédric, T., Bernard, T., Georges, D., Marie-Laure, F., et al. (2018). Impact of microbial composition of cambodian traditional dried starters (Dombea) on flavor compounds of rice wine: combining amplicon sequencing with HP-SPME-GCMS. *Front. Microbiol.* 8:894. doi: 10.3389/fmicb.2018.00894

Son, E. Y., Lee, S. M., Kim, M., Seo, J. A., and Kim, Y. S. (2018). Comparison of volatile and non-volatile metabolites in rice wine fermented by Koji inoculated with *Saccharomycopsis fibuligera* and *Aspergillus oryzae*. *Food Res. Int.* 109, 596–605. doi: 10.1016/j.foodres.2018.05.008

Swangkeaw, J., Vichitphan, S., Butzke, C. E., and Vichitphan, K. (2009). The characterisation of a novel *Pichia anomala* β-glucosidase with potentially aroma-enhancing capabilities in wine. *Ann. Microbiol.* 59, 335–343. doi: 10.1007/BF03178336

Tan, Y. W., Zhong, H. P., Zhao, D., Du, H., and Xu, Y. (2019). Succession rate of microbial community causes flavor difference in strong-aroma Baijiu making process. *Int. J. Food Microbiol.* 311:108350. doi: 10.1016/j.ijfoodmicro.2019.108350

Tang, Q., He, G., Huang, J., Wu, C., Jin, Y., and Zhou, R. (2019). Characterizing relationship of microbial diversity and metabolite in Sichuan *Xiaoqu*. *Front. Microbiol.* 10:696. doi: 10.3389/fmicb.2019.00696

Truong, D. T., Franzosa, E. A., Tickle, T. L., Scholz, M., Weingart, G., Pasolli, E., et al. (2015). Metaphlan2 for enhanced metagenomic taxonomic profiling. *Nat. Methods* 12, 902–903. doi: 10.1038/nmeth.3589

Trygg, J., and Wold, S. (2002). Orthogonal projections to latent structures (o-pls). *J. Chemometr.* 16, 119–128. doi: 10.1002/cem.695

Walsh, A. M., Crispie, F., Claesson, M. J., and Cotter, P. D. (2017). Translating omics to food microbiol. *Annu. Rev. Food Sci. Technol.* 8, 113–134. doi: 10.1146/annurev-food-030216-025729

Walterson, A. M., Smith, D. D. N., and Stavrinides, J. (2014). Identification of a *Pantoea* biosynthetic cluster that directs the synthesis of an antimicrobial natural product. *PLoS ONE* 9:e96208. doi: 10.1371/journal.pone.0096208

Wang, H. Y., Gao, Y. B., Fan, Q. W., and Xu, Y. (2011). Characterization and comparison of microbial community of different typical Chinese liquor *Daqus* by PCR-DGGE. *Lett. Appl. Microbiol.* 53, 134–140. doi: 10.1111/j.1472-765X.2011.03076.x

Wang, J., Zhong, Q. P., Yang, Y. Y., Li, H. R., Wang, L., Tong, Y. G., et al. (2018). Comparison of bacterial diversity between two traditional starters and the round-koji-maker starter for traditional cantonese Chi-flavor liquor brewing. *Front. Microbiol.* 9:1053. doi: 10.3389/fmicb.2018.01053

Wang, M. Y., Zhao, Q. S., Su, C., and Yang, J. G. (2019). Analysis of the microbial community structure during brewing of Sichuan *Xiaoqu* Baijiu. *J. Am. Soc. Brew. Chem.* 77, 210–219. doi: 10.1080/03610470.2019.1605033

Wang, N., Jia, G., Wang, C., Chen, M., and Guo, Q. (2019). Structural characterisation and immunomodulatory activity of exopolysaccharides from liquid fermentation of *Monascus purpureus* (Hong Qu). *Food Hydrocoll.* 103:105636. doi: 10.1016/j.foodhyd.2019.105636

Wang, P., Wu, Q., Jiang, X. J., Wang, Z. Q., Tang, J. L., and Xu, Y. (2017). *Bacillus licheniformis* affects the microbial community and metabolic profile in the spontaneous fermentation of *Daqu* starter for Chinese liquor making. *Int. J. Food Microbiol.* 250, 59–67. doi: 10.1016/j.ijfoodmicro.2017.03.010

Wang, W. Y., Liu, R. L., Shen, Y., and Lian, B. (2018). The potential correlation between bacterial sporulation and the characteristic flavor of Chinese Maotai liquor. *Front. Microbiol.* 9:1435. doi: 10.3389/fmicb.2018.01435

Wang, X. D., Qiu, S. Y., Li, P., and Ban, S. D. (2019). Analysis of microbial community structure in traditional and automated Moutai-flavor *Daqu*. *J. Am. Soc. Brew. Chem.* 77, 140–146. doi: 10.1080/03610470.2019.1569886

Wang, Y. P., San, K. Y., and Bennett, G. N. (2013). Cofactor engineering for advancing chemical biotechnology. *Curr. Opin. Biotechnol.* 24, 994–999. doi: 10.1016/j.copbio.2013.03.022

Wicklow, D. T., Mcalpin, C. E., and Yeoh, Q. L. (2007). Diversity of *Aspergillus oryzae* genotypes (rflp) isolated from traditional soy sauce production within Malaysia and Southeast Asia. *Mycoence* 48, 373–380. doi: 10.1007/S10267-007-0383-3

Wu, H., Zhang, S., Ma, Y., Zhou, J., Luo, H., and Yang, J. (2017). Comparison of microbial communities in the fermentation starter used to brew *Xiaoqu* liquor. *J. Inst. Brew.* 123, 113–120. doi: 10.1002/jib.388

Wu, L., Lu, Z., Zhang, X., Wang, Z., and Xu, Z. (2017). Metagenomics reveals flavour metabolic network of cereal vinegar microbiota. *Food Microbiol.* 62, 23–31. doi: 10.1016/j.fm.2016.09.010

Wu, Q., Xu, Y., and Chen, L. (2012). Diversity of yeast species during fermentative process contributing to Chinese Maotai-flavour liquor making. *Lett. Appl. Microbiol.* 55, 301–307. doi: 10.1111/j.1472-765X.2012.03294.x

Wu, Z. Y., Zhang, W. X., Zhang, Q. S., Hu, C., Wang, R., and Liu, Z. H. (2009). Developing new sacchariferous starters for liquor production based on functional strains isolated from the pits of several famous luzhou-flavor liquor brewers. *J. Inst. Brew.* 115, 111–115. doi: 10.1002/j.2050-0416.2009.tb00354.x

Wu, S. M., Feng, B., Cheng, J. H., Li, H. J., Fang, J. J., Yan, X. Z., et al. (2012). GC/TOF-MS-based analytical method of endogenous metabolites for mouse serum. *Chem. J. Chin. Univ.-Chin.* 33, 1188–1194. doi: 10.3969/j.issn.0251-0790.2012.06.013

Xie, M. X., An, F. Y., Zhao, Y., Wu, R. N., and Wu, J. R. (2020). Metagenomic analysis of bacterial community structure and functions during the fermentation of *da-jiang*, a Chinese traditional fermented food. *LWT Food Sci. Technol.* 129:109450. doi: 10.1016/j.lwt.2020.109450

Xiong, X. M., Yan, N. F., Huang, Y. N., Hu, Q. Q., Yang, T. Y., Zhang, M. C., et al. (2014). Analysis of the difference in physiochemical indexes and microbial quantity of Baiyunbian high-temperature *Daqu* produced by different techniques. *Liquor Making Sci. Technol.* 21–23. doi: 10.13746/j.njkj.2014.01.008

Xu, J., Wu, H., Wang, Z. W., Zheng, F. P., Lu, X., Li, Z. P., et al. (2018). Microbial dynamics and metabolite changes in Chinese rice wine fermentation from sorghum with different tannin content. *Sci. Rep.* 8:4639. doi: 10.1038/s41598-018-23013-1

Xu, J. J., Fu, L. J., Si, K. L., Yue, T. L., and Guo, C. F. (2020). 3-Phenyllactic acid production by free-whole-cells of *Lactobacillus crustorum* in batch and continuous fermentation systems. *J. Appl. Microbiol.* 129, 335–344. doi: 10.1111/jam.14599

Yan, Z. K., Meng, Q. Y., Wang, X. Z., and Du, J. (2016). Analysis on physicochemical indexes and cultivation technology of traditional Xifeng *Daqu* sensory evaluation. *Liquor Making.* 43, 51–55.

Yan, Z. K., Feng, Y. F., Meng, Q. Y., Wang, X. Z., Gou, J. Y., Fang, H. Z., et al. (2015). Research on the perspective of microbial diversity and physicochemical properties of Xifeng-*Daqu's* culturable microorganisms. *Liquor Making* 42, 36–41. doi: 10.3969/j.issn.1002-8110.2015.03.013

Yang, Y., Xia, Y., Wang, G., Tao, L., Yu, J., and Ai, L. (2018). Effects of boiling, ultra-high temperature and high hydrostatic pressure on free amino acids, flavor characteristics and sensory profiles in Chinese rice wine. *Food Chem.* 275, 407–416. doi: 10.1016/j.foodchem.2018.09.128

Ye, F. Y., Xiao, L., Liang, Y. N., Zhou, Y., and Zhao, G. H. (2019). Spontaneous fermentation tunes the physicochemical properties of sweet potato starch by modifying the structure of starch molecules. *Carbohydr. Polym.* 213, 79–88. doi: 10.1016/j.carbpol.2019.02.077

Yin, H., He, Y., Deng, Y., Dong, J., Lu, J., and Chen, L. (2017). Application of placket-burman experimental design for investigating the effect of wort amino acids on flavor-active compounds production during lager yeast fermentation. *J. Inst. Brew.* 123, 300–311. doi: 10.1002/jib.424

Zang, J. H., Xu, Y. S., Xia, W. S., Regenstein, J. M., Yu, D. W., Yang, F., et al. (2020). Correlations between microbiota succession and flavor formation during fermentation of Chinese low-salt fermented common carp (*Cyprinus carpio* L.) inoculated with mixed starter cultures. *Food Microbiol.* 90:103487. doi: 10.1016/j.fm.2020.103487

Zhang, C. L., Ao, Z. H., Chui, W. Q., Shen, C. H., Tao, W. Y., and Zhang, S. Y. (2012). Characterization of the aroma-active compounds in *Daqu*: a tradition Chinese liquor starter. *Eur. Food Res. Technol.* 234, 69–76. doi: 10.1007/s00217-011-1616-4

Zhang, W. L., Fang, D., Zhang, T., Zhou, L., Jiang, B., and Mu, W. M. (2013). Characterization of a metal-dependent d-psicose 3-epimerase from a novel strain, Desmospora sp 8437. *J. Agric. Food Chem.* 61, 11468–11476. doi: 10.1021/jf4035817

Zhang, X., Lan, Y., Zhu, B., Xiang, X., Duan, C., and Shi, Y. (2017). Changes in monosaccharides, organic acids and amino acids during cabernet sauvignon wine aging based on a simultaneous analysis using gas chromatography-mass spectrometry. *J. Sci. Food Agric.* 98, 104–112. doi: 10.1002/jsfa.8444

Zhang, Y., Li, J., Tian, X. P., and Zhang, S. (2015). *Marinithermofilum abyssi* gen. nov., sp nov and *Desmospora profundinema* sp nov., isolated from a deep-sea sediment, and emended description of the genus *Desmospora* Yassin et al. 2009. *Int. J. Syst. Evol. Microbiol.* 65, 2622–2629. doi: 10.1099/ijs.0.000314

Zhao, C., Su, W., Mu, Y. C., Jiang, L., and Mu, Y. (2020). Correlations between microbiota with physicochemical properties and volatile flavor components

in black glutinous rice wine fermentation. *Food Res. Int*. 138:109800. doi: 10.1016/j.foodres.2020.109800

Zheng, X. W., and Han, B. Z. (2016). Baijiu, Chinese liquor: history, classification and manufacture. *J. Ethnic Foods* 3, 19–25. doi: 10.1016/j.jef.2016.03.001

Zheng, X. W., Yan, Z., Han, B. Z., Zwietering, M. H., Samson, R. A., Boekhout, T., et al. (2012). Complex microbiota of a Chinese "Fen" liquor fermentation starter (Fen-*Daqu*), revealed by culture-dependent and culture-independent methods. *Food Microbiol*. 31, 293–300. doi: 10.1016/j.fm.2012.03.008

Zhu, D., Wei, Y. F., Yin, J. Y., Liu, D. Z., Ang, E. L., Zhao, H. M., et al. (2020). A pathway for degradation of uracil to acetyl coenzyme a in *Bacillus megaterium*. *Appl. Environ. Microbiol.* 86, e02837–e02819. doi: 10.1128/AEM.02837-19

Zhu, W. H., Lomsadze, A., and Borodovsky, M. (2010). Ab initio gene identification in metagenomic sequences. *Nucleic Acids Res*. 38:e132. doi: 10.1093/nar/gkq275

Zou, W., Zhao, C. Q., and Luo, H. B. (2018). Diversity and function of microbial community in Chinese strong-flavor Baijiu ecosystem: a review. *Front. Microbiol*. 9:671. doi: 10.3389/fmicb.2018.00671

Conflict of Interest: The authors declare that the research was conducted in the absence of any commercial or financial relationships that could be construed as a potential conflict of interest.

frontiers in Microbiology

ORIGINAL RESEARCH
published: 17 February 2021
doi: 10.3389/fmicb.2021.631250

Adaptive Gene Content and Allele Distribution Variations in the Wild and Domesticated Populations of *Saccharomyces cerevisiae*

*Da-Yong Han[1,2], Pei-Jie Han[1], Karl Rumbold[3], Anbessa Dabassa Koricha[1,2,4], Shou-Fu Duan[1,2], Liang Song[1,2], Jun-Yan Shi[1,2], Kuan Li[1], Qi-Ming Wang[1] and Feng-Yan Bai[1,2]**

[1] State Key Laboratory of Mycology, Institute of Microbiology, Chinese Academy of Sciences, Beijing, China, [2] College of Life Sciences, University of Chinese Academy of Sciences, Beijing, China, [3] School of Molecular and Cell Biology, University of the Witwatersrand, Johannesburg, South Africa, [4] Department of Biology, College of Natural Sciences, Jimma University, Jimma, Ethiopia

Recent studies on population genomics of *Saccharomyces cerevisiae* have substantially improved our understanding of the genetic diversity and domestication history of the yeast. However, the origin of the domesticated population of *S. cerevisiae* and the genomic changes responsible for ecological adaption of different populations and lineages remain to be fully revealed. Here we sequenced 64 African strains from various indigenous fermented foods and forests in different African countries and performed a population genomic analysis on them combined with a set of previously sequenced worldwide *S. cerevisiae* strains representing the maximum genetic diversity of the species documented so far. The result supports the previous observations that the wild and domesticated populations of *S. cerevisiae* are clearly separated and that the domesticated population diverges into two distinct groups associated with solid- and liquid-state fermentations from a single ancestor. African strains are mostly located in basal lineages of the two domesticated groups, implying a long domestication history of yeast in Africa. We identified genes that mainly or exclusively occur in specific groups or lineages and genes that exhibit evident group or lineage specific allele distribution patterns. Notably, we show that the homing endonuclease VDE is generally absent in the wild but commonly present in the domesticated lineages of *S. cerevisiae*. The genes with group specific allele distribution patterns are mostly enriched in functionally similar or related fundamental metabolism processes, including the evolutionary conserved TOR signaling pathway.

Keywords: ***Saccharomyces cerevisiae*, domestication, population genomics, adaptive evolution, homing endonuclease VDE**

OPEN ACCESS

Edited by:
Wanping Chen,
Georg-August-Universität Göttingen, Germany

Reviewed by:
Li-Lin Du,
National Institute of Biological Sciences (NIBS), China
Jose Paulo Sampaio,
New University of Lisbon, Portugal

***Correspondence:**
Feng-Yan Bai
baify@im.ac.cn

Specialty section:
This article was submitted to Food Microbiology, a section of the journal Frontiers in Microbiology

Received: *19 November 2020*
Accepted: *26 January 2021*
Published: *17 February 2021*

Citation:
Han D-Y, Han P-J, Rumbold K, Koricha AD, Duan S-F, Song L, Shi J-Y, Li K, Wang Q-M and Bai F-Y (2021) Adaptive Gene Content and Allele Distribution Variations in the Wild and Domesticated Populations of Saccharomyces cerevisiae. Front. Microbiol. 12:631250. doi: 10.3389/fmicb.2021.631250

INTRODUCTION

The budding yeast *Saccharomyces cerevisiae* is used worldwide in baking and alcoholic beverage production and the earliest evidence for wine-like beverage fermentation dates back to Neolithic times about 9,000 years ago (McGovern et al., 2004). *S. cerevisiae* is also the most extensively studied eukaryote as a model in physiology, genetics, and cellular and molecular biology. *S. cerevisiae* was once considered a domesticated species with distribution limited in man-made environments

(Martini, 1993; Vaughanmartini and Martini, 1995; Naumov, 1996; Camperio-Ciani et al., 2004). Recent studies have shown that *S. cerevisiae* widely distributes in nature and occurs in highly diversified substrates from human-associated environments as well as habitats remote from human activity (e.g., primeval forests) (Wang et al., 2012). Thus, the species has been becoming a powerful system in the studies of population and evolution genomics, ecology and biogeography. The genomes of more than 2,500 *S. cerevisiae* strains have been sequenced independently by different laboratories in the world (Libkind et al., 2020), aiming to illuminate the natural and domestication histories of the yeast and evolutionary forces shaping its biodiversity. Population genetics and genomics studies have shown that the wild and domesticated populations of *S. cerevisiae* are clearly separated. The genetic diversity of the species is mainly contributed by the wild lineages found in China or Far East Asia (Wang et al., 2012; Liti, 2015; Duan et al., 2018). This area also harbors the oldest lineages of the species documented so far. Therefore, an out-of-China origin hypothesis of *S. cerevisiae* has been proposed (Wang et al., 2012; Duan et al., 2018; Peter et al., 2018). However, it remains unclear whether *S. cerevisiae* was first domesticated in Asia and the domesticated strains were later introduced to other continents, or whether wild *S. cerevisiae* immigrated from Asia to other continents and was then domesticated independently in different places (Steensels et al., 2019). Liti et al. (2009) and Peter et al. (2018) showed close relationships of different domesticated lineages with different wild relatives and thus suggested that multiple independent domestication events lead to the origin of different domesticated lineages of *S. cerevisiae*. Separate domestication events have also been proposed in previous studies based on different strain and data sets (Fay and Benavides, 2005; Legras et al., 2007; Ezeronye and Legras, 2009; Liti et al., 2009; Schacherer et al., 2009; Goddard et al., 2010; Pontes et al., 2020). Specifically, Almeida et al. (2015) showed that the European Wine lineage originated from the Mediterranean oak (MO) lineage. On the other hand, our recent study showed that the domesticated lineages documented worldwide so far share a common ancestor which was likely formed by outcrossing between diverse wild isolates, implying a single domestication event scenario (Duan et al., 2018).

Specific wild and domesticated lineages of *S. cerevisiae* have been recognized in different studies employing strains with different origins and sample sizes (Liti et al., 2009; Wang et al., 2012; Gallone et al., 2016; Duan et al., 2018; Peter et al., 2018; Pontes et al., 2020). The fine phylogenetic relationships among the lineages recognized in different studies remain to be resolved. For example, the CHN-IX lineage containing strains from a subtropical primeval forest located in central China was recognized as the oldest lineage of *S. cerevisiae* in Duan et al. (2018), while a lineage represented by a few strains from Taiwan was resolved as the most basal lineage of the species in Peter et al. (2018). It is unclear if the two lineages belong to a same lineage or, if not, which is older. A specific lineage of *S. cerevisiae* from fermented milk products collected in west China and Mongolia was identified in Duan et al. (2018). A distinct lineage from French dairy products was also identified in Legras et al. (2018) and Peter et al. (2018). It is uncertain whether the Asian and European milk strains belong to a single lineage or share a recent common ancestor due to the same or similar niche.

We have shown that all the domesticated lineages belong to two major monophyletic groups associated with liquid- and solid-state fermentations, respectively (Duan et al., 2018). The liquid-state fermentation (LSF) group is mainly consisted of European industrial strains and the solid-state fermentation (SSF) group contains strains mainly from Asia. Thus, the two groups are also called the European and Asian clades, respectively (Steensels et al., 2019). However, the separation of the two domesticated groups were not recognized in other studies on population genetics and genomics of *S. cerevisiae* (Fay and Benavides, 2005; Liti et al., 2009; Schacherer et al., 2009; Cromie et al., 2013; Strope et al., 2015; Gallone et al., 2016; Legras et al., 2018; Peter et al., 2018; Pontes et al., 2020). It is uncertain if worldwide domesticated strains can simply be assigned to the two groups and if the separation of the two groups is primarily caused by geography or ecology. Addition of more strains associated with indigenous fermented foods from other continents, especially Africa, will be helpful to resolve the problems. Africa is rich of fermented foods and has a long history of fermented food production (Ashenafi, 2008; Koricha et al., 2020). Indeed, an African origin hypothesis of domesticated yeast was proposed in Fay and Benavides (2005). Distinct lineages associated with cocoa and palm wine fermentation in West Africa have been identified (Cromie et al., 2013; Tapsoba et al., 2015; Ludlow et al., 2016; Duan et al., 2018; Peter et al., 2018). However, African populations of *S. cerevisiae* were poorly represented in previous studies in terms of strain numbers and geographic and ecological origins. The diversity and evolution of both wild and domesticated *S. cerevisiae* in Africa remain largely unknown.

In recent years, we isolated a set of *S. cerevisiae* strains from indigenous fermented foods and forests in different African countries and sequenced their genomes. We also sequenced more domesticated *S. cerevisiae* strains associated with solid-state fermentation in China. In this study, we combined the newly sequenced *S. cerevisiae* strains with a set of previously sequenced strains representing the maximum genetic diversity and all lineages of the species documented so far in the world. Our integrated phylogenomic and population genomic analyses reveal new distinct lineages from Africa which are mostly located in basal domesticated lineages. We confirm the separation of the wild and domesticated population and the divergence of the LSF and SSF groups of the domesticated population from a single ancestor. We find the correlation of gene content variation with population, group, and lineage delimitation and identified genes that show group or lineage specific patterns in terms of content or allele distribution. The results provide new insights into the domestication history of *S. cerevisiae*.

MATERIALS AND METHODS

S. cerevisiae Isolates

A total of 126 *S. cerevisiae* isolates were sequenced in this study, including 64 isolates from different African countries, 52 isolates associated with Baijiu (Chinese liquor) and ten

isolates associated with Huangjiu (rice wine) fermentation from different regions in China (**Supplementary Table 1**). The genome sequence data from a total of 486 isolates sequenced in other studies (Gallone et al., 2016; Duan et al., 2018; Peter et al., 2018) are included. These isolates represent different lineages of *S. cerevisiae* with different ecological and geographic origins (**Supplementary Table 1**). The newly sequenced isolates were isolated using either the dilution plating method from fermented food and beverage samples as described in Duan et al. (2018) or the enrichment method from natural samples as described in Wang et al. (2012). Yeast isolates were identified as described in Wang et al. (2012).

Genome Resequencing, Assembly, and Annotation

The genome DNA of each isolate was extracted using a standard Zymolyase protocol (Amberg et al., 2005). For the isolates sequenced in this study, a paired-end library with an average insert size of 300 bp was prepared and was sequenced using the Illumina Hiseq 2000 platform with 2 × 150 bp reads. The sequence coverages ranged from 109× to 242× (average = 184×; median = 187×). For each library, low-quality and ambiguous reads were trimmed using Trimmomatic (v0.30) (Bolger et al., 2014). The program SPAdes (v3.10.0) (Bankevich et al., 2012) was used to assemble clean reads with K = 21, 33, 55, and 77, and the best assembly strategy was selected automatically. AUGUSTUS (v2.5.5) (Stanke et al., 2004) was employed for gene prediction from the final assemblies generated by PAGIT with *S. cerevisiae* S288c as the model using the following parameters (genemodel = complete, protein = on). Then, the BLAST (Altschul et al., 1990) program was used to annotate the gene function through searching for homologous sequences in GenBank.

Reference-Based Alignment and Variant Calling

The clean paired reads obtained were mapped to the S288c (R64-1-1) genome using the BWA (Li and Durbin, 2009) program with default settings. SAMTools (v1.361) (Li, 2011) was employed to convert the alignment results into the BAM format, and Picard Tools (v1.56)[1] was used to sort the reads and remove duplicated sequences. VarScan (v2.3.9) (Koboldt et al., 2012) was applied for extracting the variant bases with following parameters (min-coverage = 15, min-avg-qual = 25, min-var-freq = 0.2). In addition, the Genome Analysis Toolkit (GATK v2.7.2) (McKenna et al., 2010) program was used to detect the variable sites, with the 'stand_call_conf' and the 'stand_emit_conf' were set to 40.0 and 30.0, respectively. The high-quality SNPs extracted were the consistent variation sites obtained from VarScan and GATK. The variation sites with a coverage depth ≥ 15 were remained for subsequent analyses and final SNP extraction. The variation sites of an isolates with a coverage depth greater than four times of the sequence depth of the isolate were probably resulted from sequencing errors or duplicate sequences and thus were removed according to Lam et al. (2010). The variation sites were kept only when at least 80% of the reads were positive for homogeneous sites and at least 20% of the reads were positive for heterogeneous sites.

Among the 486 isolates sequenced in previous studies, variation sites were obtained by the following approaches: SNPs of 244 isolates sequenced in Peter et al. (2018) were extracted from the published Matrix.gvcf.gz file; SNPs of 191 isolates selected from Duan et al. (2018) were offered by the author; SNPs of the rest 51 isolates sequenced in Gallone et al. (2016) were extracted from the assembled genome files deposited in GenBank using show-snps in the MUMmer software (Kurtz et al., 2004) with default setting. A total of 1,537,415 SNPs were obtained from the 612 isolates compared. We then filtered out the sites missing in more than 1% isolates using the tirmAl (Capella-Gutierrez et al., 2009) software and finally obtained a set of 1,382,078 SNPs across all isolates employed.

Phylogenomics, Structure, and Population Genetics Analyses

Phylogenetic trees were constructed based on the whole genome SNPs, including both homozygous and heterozygous sites. The sequence alignment was subjected to maximum likelihood analysis using the FastTree program (Price et al., 2009). The repeated random haplotype sampling (RRHS) strategy with 100 repetitions was applied as described in Lischer et al. (2014). The 100 ML trees generated were then summarized in a majority rule consensus tree with mean branch lengths and bootstrap values using the SumTrees program (Sukumaran and Holder, 2010). ADMIXTURE (v1.23) (Alexander et al., 2009) was used to detect and quantify the number of populations and the degree of admixture in all 612 isolates. The set of 1,382,078 biallelic segregating sites identified above was filtered further by removing the SNPs with a minor allele frequency (MAF) < 0.01 and the SNPs in linkage-disequilibrium, using PLINK (v1.07) (Purcell et al., 2007) with a window size of 50 SNPs advanced by 5 SNPs at a time and an r2 threshold of 0.5 described in Gallone et al. (2016). ADMIXTURE was run on a filtered set of 239,507 segregating sites, the best-fit K value from 2 to 60 was determined by the cross-validation (CV) procedure of the program and the value with a minimum CV error was selected. The same set of 239,507 SNPs was used to perform a principal component analysis (PCA) as implemented in the SNPRelate (v1.26.0) program (Zheng et al., 2012).

The nucleotide diversity (π, the average number of nucleotide differences per site) and the nucleotide polymorphism (θ, the proportion of nucleotide sites that are expected to be polymorphic) of the collection of the 612 isolates and each population or group were calculated using the software Variscan (v2.0.6) (Hutter et al., 2006) with the NumNuc parameter being adjusted for each group for including at least 80% of isolates within the group and parameters 'CompleteDeletion = 0, FixNum = 0, RunMode = 12, and WindowType = 0' were selected.

[1]https://sourceforge.net/projects/picard/

Gene Prediction and Gene Content Venn and PCA Analyses

In the study of Peter et al. (2018), a total of 7,796 ORFs were identified from the pan genome of *S. cerevisiae*, including 4,940 core ORFs and 2,856 variable ORFs. In this study, ORFs from the genomes of 368 isolates that were not employed in Peter et al. (2018) were predicted using Augustus (v2.5.5) (Stanke et al., 2004) with parameters mentioned above in genome annotation, then all predicted ORFs were aligned to the 7,796 ORFs using BLAST with the following parameters: gapopen 5, gapextend 5, penalty 5, reward 1, evalue 10, word_size 11, and no_greedy. A predicted ORF with an alignment identity of over 95% and an over 75% mapping length to one of the 7,796 ORFs identified in Peter et al. (2018) were regarded as a known ORF. Finally, 92 new ORFs were identified and a total of 7,888 ORFs were recognized as pan genome of *S. cerevisiae* in this study.

Then the assembled genome of each isolate employed in this study was executed BLAST search against the 7,888 ORFs with the parameters mentioned above in the novel ORFs prediction process. The presence of an ORF in an isolate was determined by the threshold of 95% alignment identity and 75% mapping length. To avoid the effects of rare ORFs and prediction bias, we removed the ORFs which were present in less than 1% of all the isolates compared. Finally, 6,999 ORFs were remained for Venn and PCA analyses based on the presence or absence of each of these ORFs in each strain compared. Venn diagram analysis was performed using the R package VennDiagram (Chen and Boutros, 2011). The package Python-TSNE[2] was used to reduce the dimensionality of the gene contents of the isolates compared.

The functions of ORFs which are not present in the genome of S288c were estimated by annotations in the Pfam database (Finn et al., 2014) and online protein BLAST search[3].

Allele Distribution Analysis

From the 1,382,078 SNPs employed in phylogenomic analysis, the sites which were shared by less than 1% isolates were filtered out and 595,790 sites were remained. Then 10,000 SNPs were randomly selected from the remained sites by custom python script. Finally, we excluded the sites that exist in less than 80% isolates of any lineages, resulting in 7,348 sites for further analyses. The alleles were ordered by the groups and lineages, and then visualized using ggplot2 (Wickham, 2016). Group specific alleles were defined as the alleles that were shared by more than 90% isolates in one domesticated group but not shared by more than 90% isolates in the other domesticated group. BEDTools (Quinlan and Hall, 2010) was used to map group specific SNPs to genes annotated in *S. cerevisiae* S288c.

Gene Ontology (GO) enrichment analysis was implemented using Metascape (Zhou et al., 2019) and the GO terms with corrected $P < 0.01$ were considered as significantly enriched. Enrichment networks were then constructed based on functional similarities of the terms which were measured using an algorithm adopts Kappa statistics (Huang et al., 2009). The algorithm quantitatively measures the degree of the agreement how genes share the similar annotation terms, resulting in Kappa similarities ranging from 0 to 1. Enrichment networks were created by representing each enriched term as a node and connecting pairs of nodes with Kappa similarities above 0.3 (Zhou et al., 2019).

Data Processing, Statistical Analyses, and Visualization

Primary data processing and conversion were performed using the Python project (v3.7.0)[4]. Standard statistical analyses were conducted in R project (v3.3.5)[5] with custom scripts under available packages in the project. Figtree (v1.44)[6] and iTOL (Letunic and Bork, 2016) were used for visualizing phylogenetic trees. R package ggplot2 (Wickham, 2016) was employed for visualizing other results.

RESULTS

The Population Structure of *S. cerevisiae* Is Primarily Shaped by Ecology

In this study we sequenced 126 isolates, including 64 African strains from various indigenous fermented foods and forests in Ethiopia, Mauritius, Nigeria, and South Africa and 52 strains associated with Baijiu (Chinese liquor) fermentation and 10 strains associated with Huangjiu (rice wine) fermentation from China (**Supplementary Table 1**). A total of 486 previously sequenced strains representing all lineages that were recognized in previous studies (Gallone et al., 2016; Duan et al., 2018; Peter et al., 2018) were selected for an integrated phylogenomic analysis (**Supplementary Table 1**). In agreement with Duan et al. (2018), three major groups were resolved in the phylogenetic tree constructed from the whole genome SNPs, covering a total of 1,382,078 sites (**Supplementary Figure 1**). The wild and the domesticated populations were clearly separated. The domesticated strains were clustered into two major groups associated mainly with liquid- and solid-state fermentation, respectively (**Supplementary Figure 1**). The lineages are defined and named in this study based on a combined consideration of phylogenetic clustering, ecological and geographic origins, population structures and definitions and names used in previous studies. A total of 42 lineages are recognized in this study and 14 lineages are recognized in each of the Wild, the SSF, and the LSF groups. Distinct sub-lineages in the Wine/Europe and Beer 1 lineages are also recognized as in Peter et al. (2018) and Gallone et al. (2016) (**Figure 1**, **Supplementary Table 1**, and **Supplementary Figures 1,2**).

The wild group recognized in this study mainly consists of forest strains from China, other Far East countries (including Japan, Malaysia, and Russia), and North and South America (**Figure 1** and **Supplementary Figures 1,2**). The CH-IX lineage from a primeval forest in Central China and the Taiwanese lineage from soil which were recognized as the oldest lineage of *S. cerevisiae* in Duan et al. (2018) and

[2]https://pypi.org/project/tsne/

[3]https://blast.ncbi.nlm.nih.gov/Blast.cgi

[4]https://www.python.org/

[5]https://ww-w.rproject.org/

[6]http://tree.bio.ed.ac.uk/software/figtree

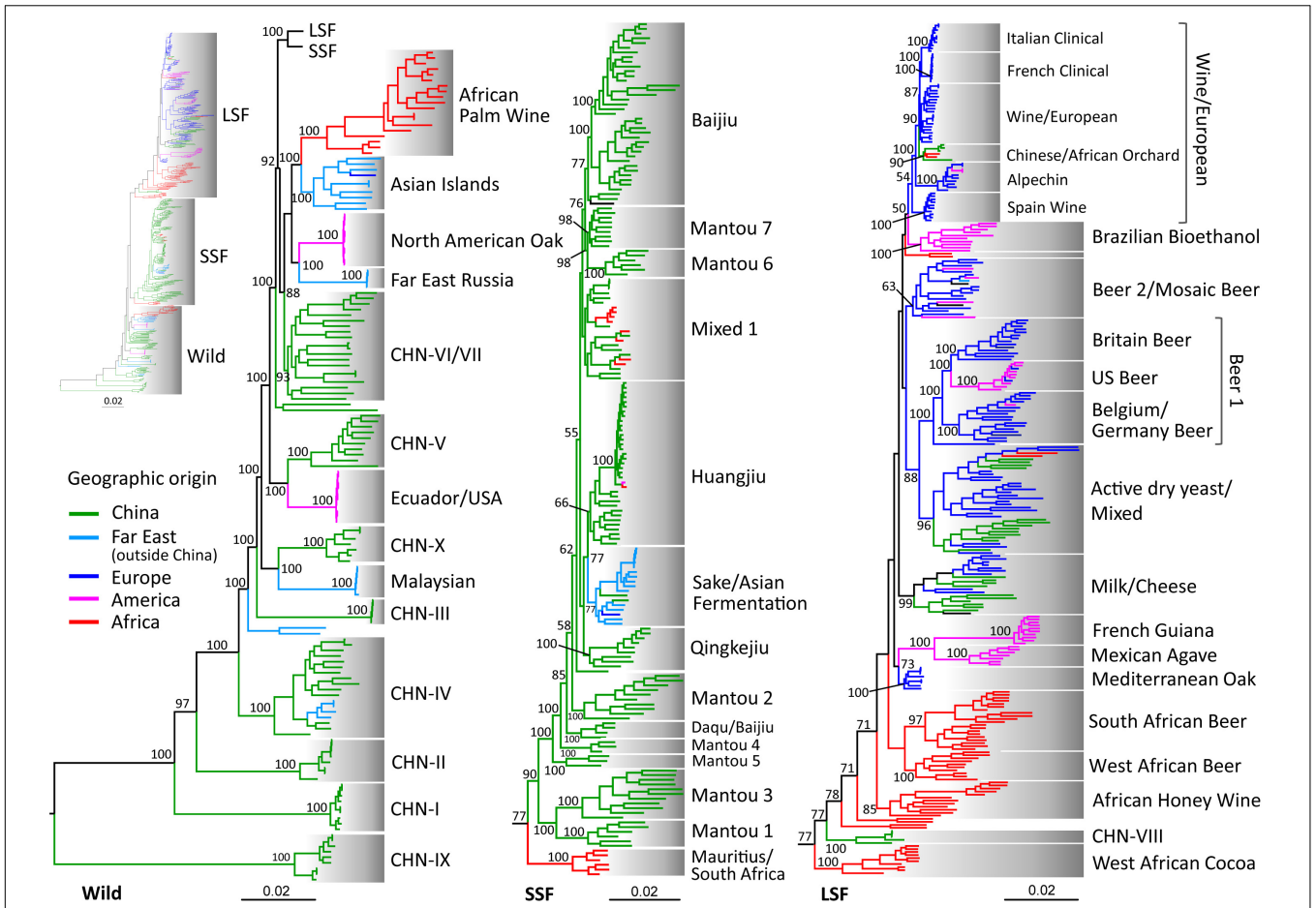

FIGURE 1 | Phylogeny of wild and domesticated isolates of *S. cerevisiae* inferred from maximum likelihood analysis based on 1,382,078 genome-wide SNPs from 612 isolates with worldwide origins. The tree is rooted by lineage CHN-IX and the bootstrap support values to lineages and major clades above 50% are shown. Strain branches are colored according to geographic origins. LSF, liquid-state fermentation; SSF, solid-state fermentation. Scale bar, 0.02 substitutions per site.

Peter et al. (2018), respectively, were clustered together (**Figure 1** and **Supplementary Table 1**). Differing from Pontes et al. (2020) which combined the North America-Japan group (Almeida et al., 2015), the Far East Russia group (Peter et al., 2018) and the China VI–VII group (Duan et al., 2018) in one lineage (Clade 17), these groups are all resolved as distinct lineages in the Wild group this study (**Figure 1** and **Supplementary Figure 2**). The Ecuador/United States lineage consisted of strains from trees, fruit, flowers, and insects was closely related with the CHN-V lineage from South China forests. The North American Oak lineage formed a sister clade of the Far East Russia lineage (**Figure 1**). We did not identify any new wild lineages or wild isolates belonging to basal wild lineages of *S. cerevisiae* from Africa. The Asian Islands lineage containing strains from trees, unspecified fermentation environment and palm wine in Indonesia, Pakistan, Philippines, and Sri Lanka (Peter et al., 2018) formed a sister clade of the African Palm Wine lineage containing strains from Burkina Faso, Djibouti, and Nigeria. These two lineages are mostly from spontaneous fermentation environments and closely related with the domesticated population (**Figure 1** and **Supplementary Figures 1,2**).

The LSF group recognized in our previous study (Duan et al., 2018) is substantially expanded by additional strains from different continents. The European industrial strains for beer, bread and wine production compared in Gallone et al. (2016) and Peter et al. (2018) were included in this group. Interestingly, African strains clustered in this group were mostly located in basal lineages. The strains from honey wine collected in Ethiopia formed a distinct basal lineage. The strains associated with beer brewing in Africa form other two strongly supported basal lineages. One is formed by beer strains from South African and the other by beer strains from West African countries, including Chad, Ghana, Ivory Coast and Nigeria (**Figure 1** and **Supplementary Table 1**). The African beer lineages were clustered together, but they are not statistically supported. Strains associated with cocoa fermentation in West Africa formed a root lineage of the LSF group. The strains from Mexican agave distillery and French Guiana form two closely related lineages. The Mediterranean oak (MO) lineage, which was regarded as the ancestor of European wine strains (Almeida et al., 2015),

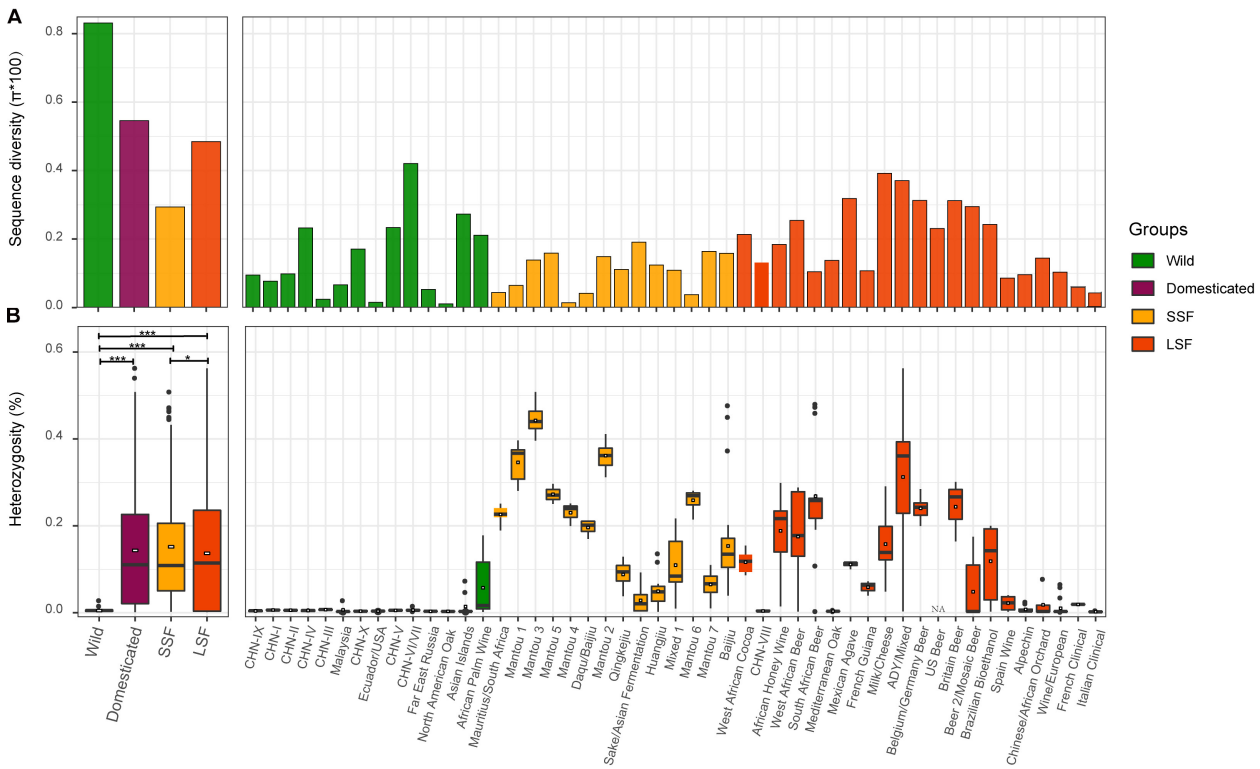

FIGURE 2 | Sequence diversity **(A)** and heterozygosity **(B)** of different populations, groups and lineages of *S. cerevisiae*. Sequence diversity **(A)** is calculated from genome-wide SNPs, and heterozygosity **(B)** is expressed as the ratio of heterozygous SNPs to the consensus genome size of each isolate. LSF, liquid-state fermentation; SSF, solid-state fermentation. *, $P < 0.05$; ***, $P < 0.001$.

shows a close relationship to the two South American lineages with a moderate support. The strains in the Milk lineage recognized in Duan et al. (2018) and the French dairy lineage recognized in Legras et al. (2018) and Peter et al. (2018) merge in a distinct lineage (**Figure 1**). In agreement with Peter et al. (2018), the strains used in Brazilian bioethanol production form a distinct lineage with a weakly supported close relationship to the Wine/European lineage. Six sub-lineages are recognized in the Wine/European lineage (**Figure 1** and **Supplementary Table 1**). The Spain wine, Alpechin, French clinical, and Italian clinical strains form well-supported sub-lineages, respectively. Four strains from Orchard in Northwest China and two strains from oak tree in South Africa form another sub-lineage.

As shown in Duan et al. (2018), the SSF group is mainly consisted of domesticated strains from China. The Sake/Asian Fermentation lineage recognized in Peter et al. (2018) is closely related with the Huangjiu (rice wine) lineage recognized in Duan et al. (2018). A nature strain from Ecuador, South America, and a soil strain from Algeria, Africa, formed a branch within the Huangjiu lineage. Three strains from cow milk and four strains from forest in South Africa and one strain from tree in Mauritius locate in a mixed lineage consisted of strains associated with various solid-state fermentation processes in China (**Figure 1** and **Supplementary Table 1**). Five African strains from fruit trees and juice collected in Mauritius and South Africa formed a lineage basal to the SSF group, but with a moderate support.

After removing the SNPs with a minor allele frequency of < 0.05 and those in linkage-disequilibrium according to Gallone et al. (2016), a principle component analysis (PCA) was performed based on 239,507 sites. The result shows that the typical wild and domesticated strains are also clearly separated (**Supplementary Figure 3**). The most ancient lineages CHN-IX, CHN-I, and CHN-II are clearly separated from the other wild strains. The LSF and SSF groups are also clearly separated. The Mauritius/South Africa lineage which is located basal to the SSF group in the phylogenetic tree (**Figure 1**) is located between the wild and SSF groups. Some strains in the West African Cocoa and CHN-VIII lineages, which are resolved as the basal lineages of the LSF group, are located between the wild and LSF groups (**Supplementary Figure 3**).

Variations in Sequence Diversity and Heterozygosity

Though the domesticated population is substantially expanded compared to our previous study Duan et al. (2018), especially the LSF group, the sequence diversity of the wild population ($\pi = 8.08 \times 10^{-3}$) is still higher (1.48-fold) than that of the domesticated population ($\pi = 5.46 \times 10^{-3}$) (**Figure 2A**). Within the domesticated population, the sequence diversity of the LSF group ($\pi = 4.85 \times 10^{-3}$) is higher (1.65-fold) than that of the SSF group ($\pi = 2.94 \times 10^{-3}$). At the lineage level, the

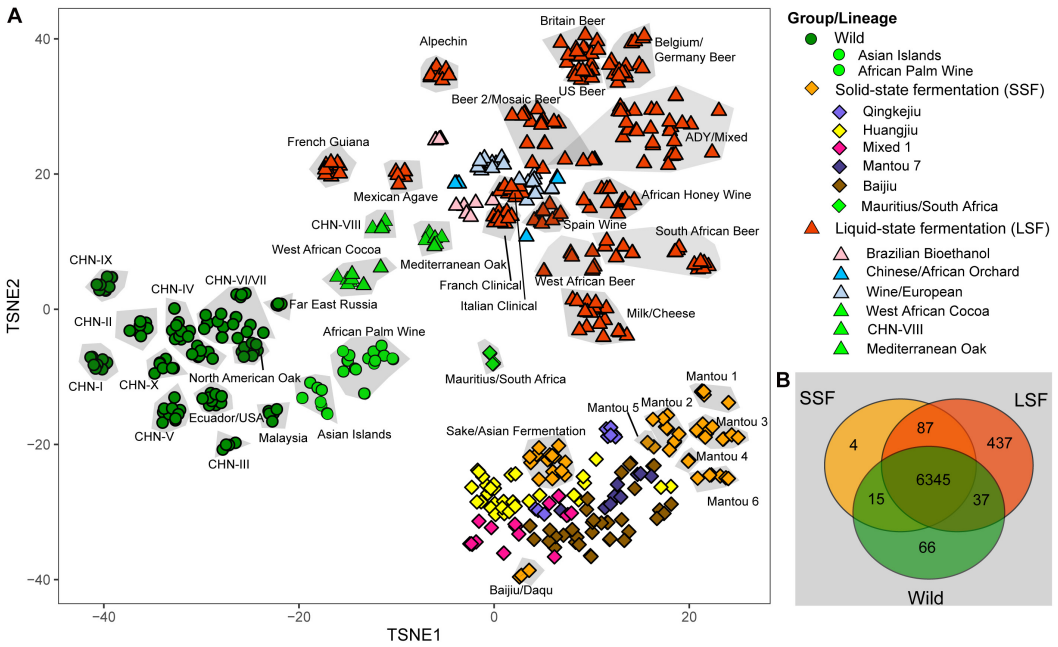

FIGURE 3 | Gene content variations in the genomes of *S. cerevisiae* isolates. **(A)** Principal component analysis (PCA) based on the presence or absence of each gene in each isolate. When the isolates belonging to the same lineage form a distinct clustered, they are included in the same gray block. The lineages with isolates that are not clustered together are marked using different colors. **(B)** Venn diagram based on gene contents. The numbers of genes which are shared by different groups or occur exclusively in single groups are shown.

wild lineage CHN-VI/VII ($\pi = 4.21 \times 10^{-3}$) exhibited the highest genetic diversity, followed by the domesticated lineage milk/cheese ($\pi = 3.92 \times 10^{-3}$) (**Figure 2B**).

As shown in our previous study (Duan et al., 2018), the wild and domesticated strains exhibited a hallmark difference in heterozygosity (**Figure 2C**). The wild isolates are generally homozygous with an average heterozygous site ratio of 0.005%, being significantly lower than that of the domesticated isolates (0.143%, $P < 0.001$). The average heterozygosity of the LSF group (0.137%) is slightly lower than that (0.152%) of the SSF group ($P = 0.039$). Different lineages in both groups exhibited remarkably different degree of heterozygosity (**Figure 2D**). Isolates with exceptionally high heterozygosity are mostly from Africa. For example, the two isolates exhibiting the highest heterozygosity (0.54% and 0.56% heterozygous site ratio, respectively) are Ethiopian honey wine strains located in the Active dry yeast/Mixed lineage in the LSF group (**Figure 2D** and **Supplementary Table 1**). However, on average, the three lineages formed by strains associated with Mantou (steamed bread) fermentation in China possessed the highest heterozygosity (0.346–0.443%) among the domesticated lineages (**Figure 2B**). It is worth noting that though the forest strains in the CHN-VIII and the Mediterranean Oak lineages are clustered in the LSF group in the phylogenetic tree (**Figure 1**), they exhibited as low heterozygosity as the wild strains (**Figure 2D**). The strains in the Wine/European lineage exhibited relatively low heterozygosity compared to other domesticated lineages. It is consistent with the observation that the Wine/European lineage contains the highest proportion of homozygous isolates among domesticated lineages of *S. cerevisiae* (Peter et al., 2018).

Gene Content Variations Recapitulate Population Differentiation

A total of 7,888 ORFs, including 92 ORFs that were not identified by Peter et al. (2018), were identified in the isolates compared in this study. After excluding the ORFs that exist in only single strains or shared by less than 1% of the strains compared, we identified 6,999 ORFs from the 612 isolates for further analyses. PCA analysis based on the presence or absence of each of the ORFs in each strain showed that the Wild and the two domesticated LSF and SSF groups were also clearly separated (**Figure 3A**). The strains from the same lineages were also generally clustered together, except a few domesticated lineages, including three lineages in the LSF group and five lineages in the SSF group (**Figure 3A**). Six lineages, including the Asian Island, African Palm Wine, Mauritius/South Africa, West African Cocoa, CHN-VIII and MO, were located between the wild and domesticated groups (**Figure 3A**).

We then tried to find genes that exist only in specific groups or lineages by Venn analysis. A total of 6,345 genes were shared by the three main groups and 69, 4 and 436 genes were found only in the Wild, SSF and LSF groups, respectively (**Figure 3B**). Genes in the regions A, B, and C, which were obtained by HGT and first found in the wine yeast strain EC1118 (Novo et al., 2009), were found to be LSF group specific genes. The genes in the regions A, B, and C were

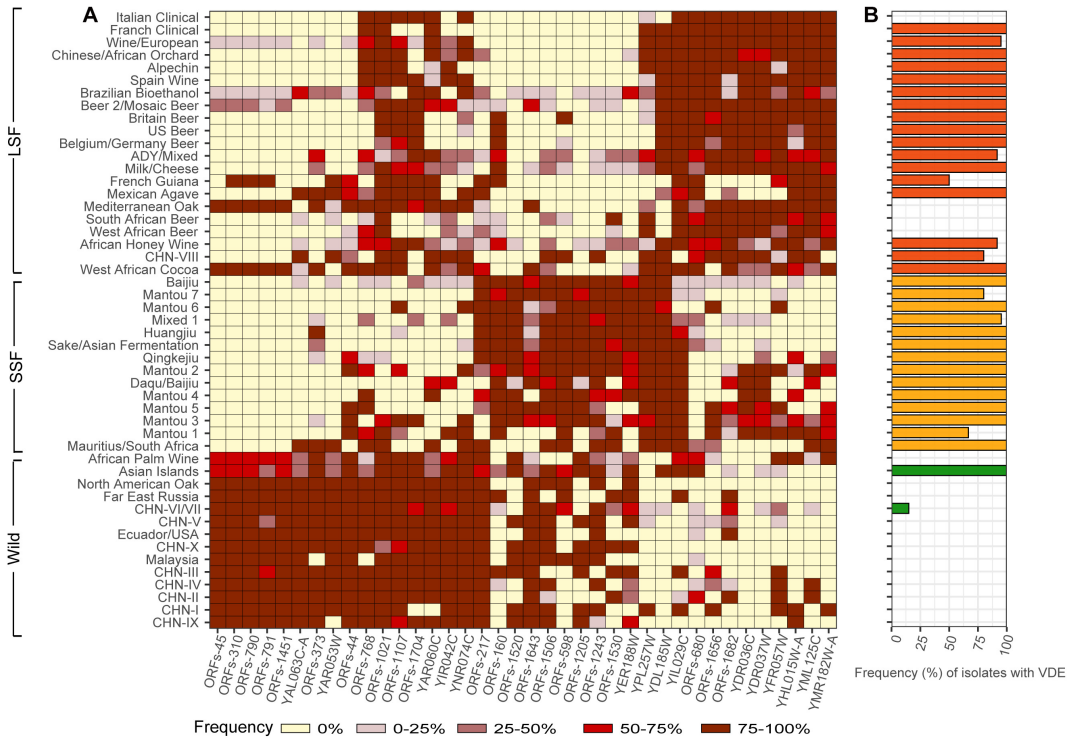

FIGURE 4 | Distribution of selected genes in different populations, groups and lineages of *S. cerevisiae*. **(A)** Frequencies of isolates in different lineages harboring the genes listed at the bottom. These genes are shared by the majority (>90%) of the isolates in one group but occur in limited isolates (<10%) in another group. Frequency ranges are depicted using different colors as shown at the bottom. **(B)** Frequencies of isolates harboring the homing endonuclease VDE in gene *VMA1* in different lineages in the wild (dark green), liquid- (red) and solid-state fermentation (orange) groups.

completely absent in the wild strains compared in this study (**Supplementary Figure 4**). They are also absent in the SSF group, except in two strains (AHQ and BEF) in the Sake/Asian Fermentation lineage which have five genes of region B and three genes of region C, respectively (**Supplementary Figure 4**). Genes in Region A were detected in only four strains of the Beer2/Mosaic Beer lineage. Region B genes were detected in 45% isolates and 90% lineages of the LSF group. Region C genes distributed in 26% strains and 40% lineages of the LSF group (**Supplementary Figure 4**).

From the group specific genes, we identified 347 lineage specific genes (existing in only single lineages) from 15 lineages (**Supplementary Table 2**). Among these genes, 261 were introgressed from *S. paradoxus* (**Supplementary Table 2**). Notably, the Alpechin (waste from olive oil production) lineage has as many as 214 unique genes and 203 (94.9%) of them were introgressed from *S. paradoxus* (**Supplementary Table 2**). This result is in agreement with the finding that the *S. cerevisiae* lineage associated with processed olives results from a hybridization between *S. cerevisiae* and *S. paradoxus* (Pontes et al., 2019). The majority of the lineage specific genes in the French Guiana (92.9%) and the Mexican Agave (57.1%) lineages also originate from *S. paradoxus* (**Supplementary Table 2**), implying a similar hybridization history of the two yeast lineages in South America.

The group specific genes identified by the Venn analysis occurs in only limited lineages or strains of the group and we did not identify group specific genes that were shared by more than 50% of the strains in each group. We then tried to find genes that are shared by the majority (>90%) of the strains in one group but occur in limited strains (<10%) in another group. We finally identified 38 genes which are shared by the majority of the strains in the same groups (**Figure 4A**). These genes all fall in the set of variable OFRs defined in Peter et al. (2018) except YDL185W (*VMA1*). These genes likely contribute to the adaptation of different groups to the wild or different fermentation environments, but the functions of many of these genes are still unclear (**Supplementary Table 3**).

The gene YDL185W (*VMA1*) is worth noting. This gene harbors an intein VDE (*VMA1*-derived endonuclease) which is a nuclear homing endonuclease that has been found from several yeast species (Koufopanou et al., 2002). Two versions of *VMA1*, with and without VDE, respectively, distribute in the *S. cerevisiae* strains compared. Up to 90.6% strains in the wild population do not harbor VDE (**Figure 4B**). Specifically, the strains in the basal wild lineages completely lack VDE. Only three strains in lineage CHN-VI/VII mostly from secondary forests and one Mosaic isolate (YN3 from soil) and the ten strains in the Asian Islands lineage closely related with the domesticated populations have VDE. On the other hand, VDE commonly exists in domesticated strains and 97.2% SSF and 79.4% LSF isolates have VDE. In the majority of the domesticated lineages recognized, 100% strains tested

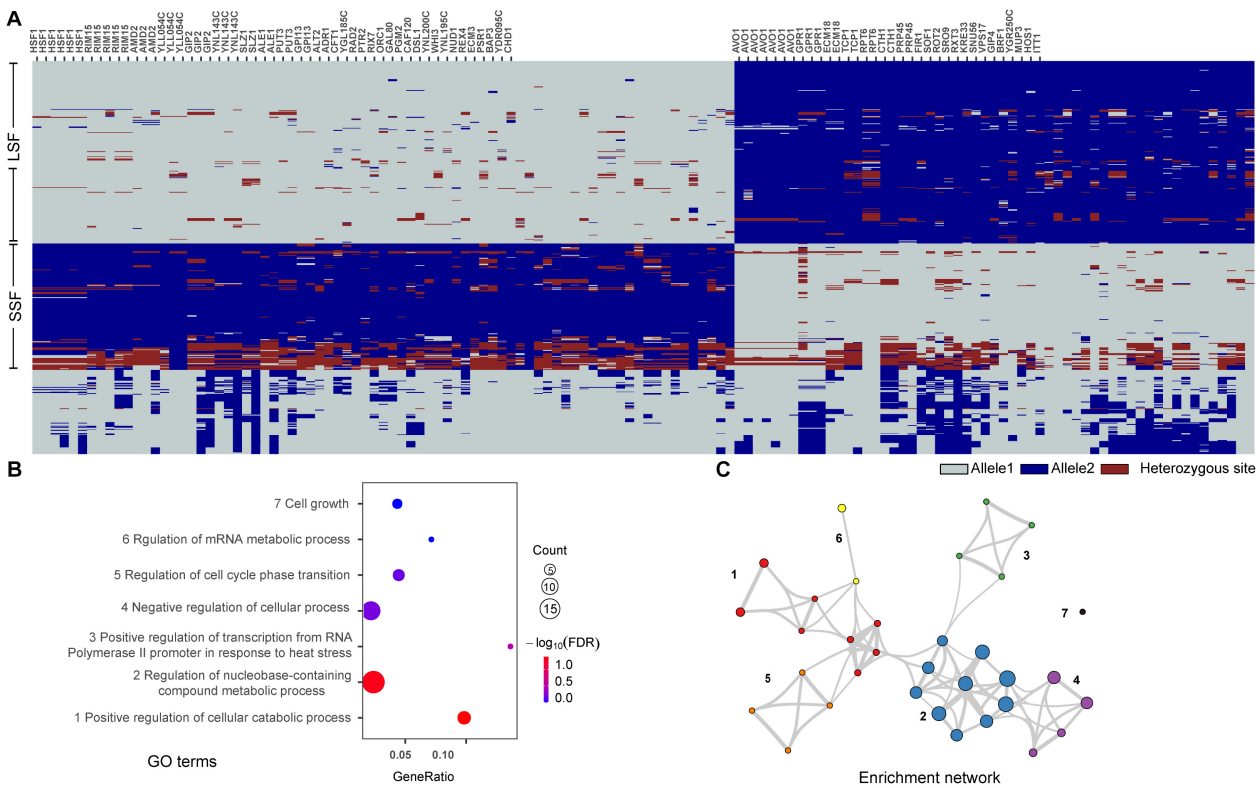

FIGURE 5 | Functions of genes with group specific allele distribution patterns in different domesticated groups of *S. cerevisiae*. **(A)** Distribution patterns of selected SNPs with alleles that were shared by more than 90% isolates in one domesticated group but not shared by more than 90% isolates in the other group. The genes with known functions harboring the SNPs are listed at the top. **(B)** GO terms enriched with the genes with group specific allele distribution patterns. **(C)** Enrichment networks show the intra- and intercluster functional similarities of the enriched GO terms shown in **(B)**. Enrichment networks are created by representing each enriched term as a node and connecting pairs of nodes with Kappa similarities above 0.3. The sizes of the nodes are proportional to the numbers of input genes fall into the terms.

contain VDE. Only three domesticated lineages (South African Beer, West African Beer and Italian Clinical) do not have VDE (**Figure 4B**).

Group- and Lineage-Specific Sequence Divergence of Core Genes

In order to investigate sequence divergence of core genes of the species, we performed SNP distribution and enrichment analysis. We randomly selected 10,000 SNPs from the total SNPs identified and then excluded the sites that exist in less than 80% isolates of any lineages, resulting in 7,348 sites for further analyses. We found evident group and lineage specific allele distribution patterns (**Supplementary Figure 5**). The alleles shared by the strains in the LSF and SSF groups were clearly different. In addition, the majority of the lineages possessed lineage specific alleles. Notably, all wild lineages except lineage CHN-VI/VII have evident lineage specific alleles and the basal lineages CHN-IX, CHN-I and CHN-II have more lineage specific alleles than others. In the domesticated population, the LSF group possessed more evident lineage specific alleles than the SSF group. Many lineage-specific alleles in the domesticated population were heterozygous (**Supplementary Figure 5**).

To figure out genes harboring group specific alleles, we selected SNPs with alleles that were shared by more than 90% isolates in one domesticated group but not shared by more than 90% isolates in the other domesticated group for enrichment analysis. A total of 134 sites were identified and 88 of them were mapped to 54 known genes annotated in *S. cerevisiae* S288c (**Figure 5** and **Supplementary Table 4**). The alleles containing these SNP sites showed clearly different distribution patterns between the wild and the domesticated populations and between the two domesticated groups (**Figure 5A** and **Supplementary Table 4**). Gene Ontology (GO) enrichment analysis using the Metascape tool (Zhou et al., 2019) showed that the 54 genes were enriched in seven terms, including positive regulation of cellular catabolic process, regulation of nucleobase-containing compound metabolic process, positive regulation of transcription from RNA polymerase II promoter in response to heat stress, negative regulation of cellular process, regulation of cell cycle phase transition, regulation of mRNA metabolic process, and cell growth (**Figure 5B**). Interestingly, six of the seven GO terms formed an enrichment network resulted from the Metascape analysis based on quantitative measurements of the functional similarities of the GO terms (**Figure 5C**) (Zhou et al., 2019). The result suggests that

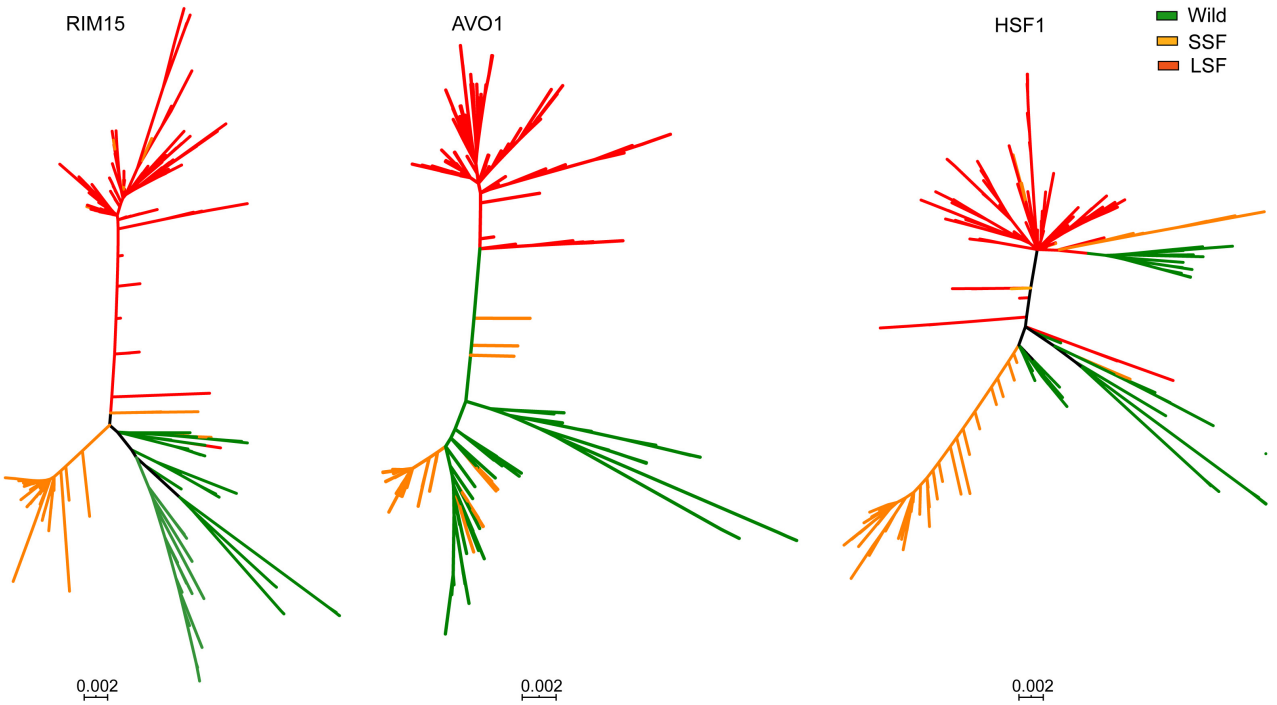

FIGURE 6 | Unrooted phylogenetic trees of 612 worldwide isolates of *S. cerevisiae* constructed from the sequences of genes *AVO1*, *HSF1,* and *RIM15*, respectively. Isolate branches are colored according to the positions of the isolates clustered in the wild, liquid-state (LSF) and solid-state fermentation (SSF) groups in the tree constructed from the whole genome SNPs as shown in **Supplementary Figure 1**.

the genes with group specific alleles are generally similar or correlated in function.

Among the 54 genes identified, genes *HSF1*, *RIM15*, and *AVO1* harboring the highest number (5–7) of group specific SNPs each in the LSF and SSF groups (**Figure 5A**). Phylogenetic analyses based on the sequences of these genes showed that the topologies of the single gene trees are similar with that of the tree constructed from the whole genome SNPs (**Figure 6**). The three main groups recognized based on the whole genome SNP analysis were largely resolved in the single gene trees. The result suggests that the sequence divergence of these genes correlates well with the divergence of the domesticated groups and likely contribute to the ecological adaption of the groups.

DISCUSSION

The present phylogenomic analysis on a set of worldwide *S. cerevisiae* strains representing the maximum genetic diversity of the species documented so far confirms our previous conclusion that the divergence and population structure of the species are primarily shaped by ecology (Duan et al., 2018). Wild and domesticated populations are clearly separated, supporting our hypothesis that the domesticated population probably originated from a single domestication event (Duan et al., 2018). The separation of the two main groups generally associated with solid-state and liquid-state fermentation, respectively, in the domesticated population remains clear after more African strains are included. The LSF group includes native lineages from Africa, America, Asia, and Europe (**Figure 1** and **Supplementary Figures 1,2**). Though the SSF group includes strains mainly from Far East Asian countries, a few African strains are located in this group. Solid-state fermentation is also employed in fermented food production in Africa, for examples, teff (*Eragrostis tef*) dough and false banana (*Ensete ventricosum*) starchy pulp (bulla) fermentation (Ashenafi, 2008; Koricha et al., 2020). It is reasonable to expect to find more isolates belonging to the SSF group from Africa.

Lineages within the wild and domesticated population are shaped by both ecology and geography. Geography seems to play a main role in the wild population. Wild strains from forests in North and South America are located in the wild population together with forest strains from Far East Asia, but they form distinct lineages. Strains from Far East countries other than China also form separate lineages from Chinese strains. Ecology seems to be the main driving force for the divergence of domesticated strains. Within each of the two domesticated groups, strains used for different food and beverage fermentation usually formed distinct lineages, while those associated with the same fermentation environments usually cluster together, regardless of their geographic origins. For example, strains from fermented milk products in Asia and Europe are located together in a single lineage. Geography may also play a role in the diversification of domesticated strains, especially for the strains associated with Mantou fermentation (**Figure 1**) and beer brewing (Gallone et al., 2016). The strains associated with

Mantou fermentation from different regions or provinces of China form several distinct lineages (Mantou 1 to Mantou 7). The beer strains from South Africa form a lineage separate from that formed by the beer strains from west African countries (**Figure 1**). However, the role of ecological factor for the differentiation of the African beer strains cannot be excluded, because the raw materials and fermentation processes may be different in different African countries.

The types of substrates involved in the liquid- (grape juice, wort, milk, etc.) and solid-sate (dough, sorghum grain, barley grain, cooked rice, etc.) fermentations are diversified and should contribute to the diversification of the yeast strains involved within each of the two groups. The clear separation of the LSF and SSF yeast groups suggests that there should be a common selective pressure for the divergence of the two groups. The main difference between the two types of fermentation is the water contents of the fermentation substrates. The water contents are usually 80–90% and 40–60% in the liquid- and solid-state fermentation, respectively. The water contents in the substrates of Huangjiu and Sake (cooked rice in semi-solid state) is usually 70–80%, but the starter (Jiuqu) of Huangjiu, which provides yeasts and other microbes for the fermentation process, is prepared through solid-state fermentation of wheat grain with a water content of about 40–50%. The Sake yeast, which is usually inoculated in pure culture at the beginning of fermentation, probably originated from Huangjiu yeast as shown in Duan et al. (2018) and the present study (**Figure 1**).

Within each of the Wild, LSF and SSF groups recognized in the phylogenetic tree based on genome SNPs (**Figure 1**), there are lineages that are not from typical environments of the groups. These lineages include the Asian Island lineage with strains from palm wine and the African Palm Wine lineage in the wild group; the Mauritius/South Africa lineage with strains from fruit trees and juice in the SSF group; and the CHN-VIII lineage with strains from fruit and secondary forests, the West African Cocoa lineage, and the MO lineage in the LSF group. In the PCA analysis based on the gene content, they are located between the wild and domesticated groups (**Figure 3A**), implying that these lineages probably represent transitional forms between the wild and domesticated populations of *S. cerevisiae*. Interestingly, Pontes et al. (2020) detected domestication signatures from one tree bark and one fruit strain of the CHN-VIII lineage. It is also possible that the strains in the MO lineage, which locates in the middle of the LSF group, are escapees from a certain liquid-state fermentation environment.

We have proposed a China/Far East Asia origin hypothesis of the domesticated population of *S. cerevisiae* based on our previous study with limited African strains (Duan et al., 2018). However, the present study shows that African strains are located in basal lineages of the LSF and SSF groups, implying an alternative African origin hypothesis of the domesticated population of *S. cerevisiae*, as proposed by Fay and Benavides (2005). To resolve the problem, more wild and domesticated African strains need to be sampled and sequenced. Africa is one of the origin centers of domesticated plants in the world and is rich in diversified fermented foods and beverages, in which *S. cerevisiae* is usually among the essential functional microorganisms (Koricha et al., 2020). The present study shows that *S. cerevisiae* strains from different fermented food samples in different African countries form distinct lineages, suggesting a potentially high genetic diversity of the domesticated population of *S. cerevisiae* in Africa.

The distribution and diversity of wild population of *S. cerevisiae* in Africa remain largely unknown. Though *S. cerevisiae* strains from forests in different African countries have been isolated, but they are not located in the wild population of the species. Four strains (SAN30 to SAN33) isolated from a forest in South Africa are located in a mixed lineage together with some strains from Daqu (starter of Baijiu) in the SSF group. However, their high degree of heterozygosity suggests that they are probably recent escapees or contaminants from fermented environment. It is still unclear whether wild strains belonging to basal wild lineages exist in Africa or not. Survey of wild *S. cerevisiae* in primeval forests in Africa will certainly be helpful to determine the origin place of the yeast in the world.

Differing from our single domestication event hypothesis, the multiple independent domestication events hypothesis (Liti et al., 2009; Peter et al., 2018) predicts that different domesticated lineages in different continents will have separate local wild ancestors. The wild ancestor (the MO lineage) of the Wine lineage was specified in Almeida et al. (2015). However, the close relationship between the Wine and the MO lineages as shown in Almeida et al. (2015) is not supported in the present study and in Pontes et al. (2020). When more isolates with more diversified origins were added to the phylogenetic tree, the MO lineage was separated from the Wine lineage and clustered together with two South American lineages Mexican Agave and French Guiana (**Figure 1** and **Supplementary Figures 1,2**). The close relationship of the MO lineage with the South American lineages was also shown in Pontes et al. (2020). Multiple domesticated and wild lineages have been identified from each of the Asian and American continents; however, close relationships between the domesticated and wild lineages within each of the two continents are not observed. In contrast, as discussed above, the wild and domesticated lineages are respectively located in the same groups, regardless of their geographic origins (**Figure 1** and **Supplementary Figures 1,2**). This result is apparently consistent with the single domestication event scenario. Further systematic investigation of indigenous wild and domesticated *S. cerevisiae* in Africa will also be of great value for testing the origin hypotheses of the domesticated lineages of *S. cerevisiae*.

Previous studies have revealed extensive genomic changes associated with ecological adaptation of domesticated *S. cerevisiae*, including heterozygosity, gene contraction or expansion, SNP accumulation and foreign gene acquisition through HGT or introgression (Magwene et al., 2011; Gallone et al., 2016; Steenwyk and Rokas, 2017; Duan et al., 2018; Peter et al., 2018; Pontes et al., 2020). However, hallmark genomic differences between the SSF

and LSF groups have not been shown, though they are phylogenetically separated. In this study, we found more genomic variations between the wild and domesticated populations and between the domesticated SSF and LSF groups. We identified group and lineage specific genes which are likely associated with ecological adaption of the yeast (**Figure 4** and **Supplementary Tables 2,3**). The specific roles or contribution of these genes to the adaption of different groups and lineages remain to be addressed, for the functions of the majority of these genes are largely unknown (**Supplementary Table 3**).

The clearly different distribution pattern of the homing intein VDE between the wild and domesticated populations of *S. cerevisiae* is interesting. The VDE coding gene is one of the homing endonuclease genes (HEGs) and appears to be specifically adapted for horizontal transmission (Koufopanou et al., 2002; Koufopanou and Burt, 2005). One possible explanation to the dominance of VDE in the domesticated but absent in the wild lineages of *S. cerevisiae* observed in this study is that VDE may have invaded into the initial domesticated ancestor formed by the single domestication event as proposed by Duan et al. (2018). Another possible explanation is that the invasion of VDE perhaps occurred recently in a fermentation environment and then spread among domesticated strains of *S. cerevisiae* through human assisted admixtures. Okuda et al. (2003) previously identified two subfamilies of VDE from nine of the 10 *S. cerevisiae* strains compared. The more extensive genomic resources available today for *S. cerevisiae* should allow a more thorough investigation of the intraspecific diversity of VDE in *S. cerevisiae*. We plan to carry out such studies in the future.

VDE and other intein-encoded HEGs are usually considered to be nonessential genes with no known function and susceptible to degeneration if they become fixed in a population (Koufopanou et al., 2002; Koufopanou and Burt, 2005). Little evidence for positive selection for intein-encoded HEGs by the host organism has been shown (Posey et al., 2004; Naor et al., 2016). However, a previous study shows that VDE is involved in the regulation of the high affinity glutathione transporter gene *GSH11* in *S. cerevisiae* (Miyake et al., 2003). The expression of *GSH11* is enhanced by rapamycin, an inhibitor of the TOR (target of rapamycin) signaling pathway, in a VDE-dependent manner under conditions of sulfur starvation (Miyake et al., 2003). Whether VDE is functional or plays a role in the adaptation of domesticated strains of *S. cerevisiae* as implied in this study remains to be revealed.

The evident group and lineage specific distribution of alleles of core genes of *S. cerevisiae* suggests that mutation or accumulation of SNPs plays an important role in the adaptation of different group or lineages to natural and specific fermentation environments (**Figure 5** and **Supplementary Figure 5**). The genes with group specific allele distribution patterns are enriched in fundamental metabolism processes which are functionally similar or closely related (**Figure 5**). The clear difference in allele distribution of core genes in the domesticated LSF and SSF groups suggests that accumulation of SNPs not only play an important role in genome evolution of wild isolates as shown in Peter et al. (2018), but also in genome evolution and ecological adaptation of domesticated isolates. The genes *AVO1* and *HSF1* enriched with the highest number of group specific SNPs are involved in TOR signaling system. *AVO1* is an essential gene and involve in the regulation of cell growth and TOR signaling as a part of TORC2 complex. *HSF1* encodes a heat shock transcription factor which activates multiple genes in response to highly diverse stresses and negatively regulates TOR signaling pathway. Interestingly, the homing intein VDE with a group specific distribution pattern is also related with TOR signaling system as discussed above. In addition, the translocation of VDE is stimulated and stabilized by nitrogen starvation and inactivation of the TOR regulatory system as shown in Nagai et al. (2003). TOR signaling is an evolutionary conserved pathway that controls multiple cellular processes upon various intracellular and extracellular stimuli (Takahara and Maeda, 2013; Tatebe and Shiozaki, 2017). The present study suggests a possible role of TOR signaling pathway in the adaptation of wild and domesticated yeast strains to different natural and fermentation environments, through fixed mutations in genes involved in the pathway.

DATA AVAILABILITY STATEMENT

This datasets used in this study be found here: https://www.ncbi.nlm.nih.gov/bioproject/PRJNA680387.

AUTHOR CONTRIBUTIONS

F-YB and D-YH conceived and designed the project. F-YB, Q-MW, P-JH, KR, AK, and D-YH performed sampling and yeast isolation and identification. D-YH and J-YS isolated DNA for genome sequencing. D-YH, KL, LS, and S-FD performed the bioinformatics analyses. F-YB and D-YH analyzed the data and wrote the manuscript. All authors contributed to the article and approved the submitted version.

FUNDING

This study was supported by the grants from the Chinese Academy of Sciences (Grants Nos. QYZDJ-SSW-SMC013 and 153211KYSB20160029), the Ministry of Science and Technology of China (Grant No. KY201701011 from the Science and Technology Partnership Program), and the National Natural Science Foundation of China (Grant No. 31461143027).

SUPPLEMENTARY MATERIAL

The Supplementary Material for this article can be found online at: https://www.frontiersin.org/articles/10.3389/fmicb.2021.631250/full#supplementary-material

REFERENCES

Alexander, D. H., Novembre, J., and Lange, K. (2009). Fast model-based estimation of ancestry in unrelated individuals. *Genome Res.* 19, 1655–1664. doi: 10.1101/gr.094052.109

Almeida, P., Barbosa, R., Zalar, P., Imanishi, Y., Shimizu, K., Turchetti, B., et al. (2015). A population genomics insight into the Mediterranean origins of wine yeast domestication. *Mol. Ecol.* 24, 5412–5427. doi: 10.1111/mec.13341

Altschul, S. F., Gish, W., Miller, W., Myers, E. W., and Lipman, D. J. (1990). Basic local alignment search tool. *J. Mol. Biol.* 215, 403–410. doi: 10.1016/s0022-2836(05)80360-2

Amberg, D. C., Burke, D. J., and Strathern, J. N. (2005). *Methods in Yeast Genetics: A Cold Spring Harbor Laboratory Course Manual*. New York, NY: Cold Spring Press.

Ashenafi, M. (2008). A review on the microbiology of indigenous fermented foods and beverages of Ethiopia. *Ethiop. J. Biol. Sci.* 5, 189–245. doi: 10.4314/ejbs.v5i2.39036

Bankevich, A., Nurk, S., Antipov, D., Gurevich, A. A., Dvorkin, M., Kulikov, A. S., et al. (2012). SPAdes: a new genome assembly algorithm and its applications to single-cell sequencing. *J. Comput. Biol.* 19, 455–477. doi: 10.1089/cmb.2012.0021

Bolger, A. M., Lohse, M., and Usadel, B. (2014). Trimmomatic: a flexible trimmer for illumina sequence data. *Bioinformatics* 30, 2114–2120. doi: 10.1093/bioinformatics/btu170

Camperio-Ciani, A., Corna, F., and Capiluppi, C. (2004). Evidence for maternally inherited factors favouring male homosexuality and promoting female fecundity. *Proc. Biol. Sci.* 271, 2217–2221. doi: 10.1098/rspb.2004.2872

Capella-Gutierrez, S., Silla-Martinez, J. M., and Gabaldon, T. (2009). trimAl: a tool for automated alignment trimming in large-scale phylogenetic analyses. *Bioinformatics* 25, 1972–1973. doi: 10.1093/bioinformatics/btp348

Chen, H., and Boutros, P. C. (2011). VennDiagram: a package for the generation of highly-customizable Venn and Euler diagrams in R. *BMC Bioinform.* 12:35. doi: 10.1186/1471-2105-12-35

Cromie, G. A., Hyma, K. E., Ludlow, C. L., Garmendia-Torres, C., Gilbert, T. L., May, P., et al. (2013). Genomic sequence diversity and population structure of *Saccharomyces cerevisiae* assessed by RAD-seq. *G3 (Bethesda)* 3, 2163–2171. doi: 10.1534/g3.113.007492

Duan, S. F., Han, P. J., Wang, Q. M., Liu, W. Q., Shi, J. Y., Li, K., et al. (2018). The origin and adaptive evolution of domesticated populations of yeast from Far East Asia. *Nat. Commun.* 9:2690. doi: 10.1038/s41467-018-05106-7

Ezeronye, O. U., and Legras, J. L. (2009). Genetic analysis of *Saccharomyces cerevisiae* strains isolated from palm wine in eastern Nigeria. comparison with other African strains. *J. Appl. Microbiol.* 106, 1569–1578. doi: 10.1111/j.1365-2672.2008.04118.x

Fay, J. C., and Benavides, J. A. (2005). Evidence for domesticated and wild populations of *Sacchoromyces cerevisiae*. *PLoS Genet.* 1:66–71. doi: 10.1371/journal.pgen.0010005

Finn, R. D., Bateman, A., Clements, J., Coggill, P., Eberhardt, R. Y., Eddy, S. R., et al. (2014). Pfam: the protein families database. *Nucleic Acids Res.* 42, 222–230. doi: 10.1093/nar/gkt1223

Gallone, B., Steensels, J., Prahl, T., Soriaga, L., Saels, V., Herrera-Malaver, B., et al. (2016). Domestication and divergence of *Saccharomyces cerevisiae* beer yeasts. *Cell* 166, 1397–1410.e16. doi: 10.1016/j.cell.2016.08.020

Goddard, M. R., Anfang, N., Tang, R. Y., Gardner, R. C., and Jun, C. (2010). A distinct population of *Saccharomyces cerevisiae* in New Zealand: evidence for local dispersal by insects and human-aided global dispersal in oak barrels. *Environ. Microbiol.* 12, 63–73. doi: 10.1111/j.1462-2920.2009.02035.x

Huang, D. W., Sherman, B. T., and Lempicki, R. A. (2009). Systematic and integrative analysis of large gene lists using DAVID bioinformatics resources. *Nat. Protoc.* 4, 44–57. doi: 10.1038/nprot.2008.211

Hutter, S., Vilella, A. J., and Rozas, J. (2006). Genome-wide DNA polymorphism analyses using VariScan. *BMC Bioinform.* 7:409. doi: 10.1186/1471-2105-7-409

Koboldt, D. C., Zhang, Q., Larson, D. E., Shen, D., McLellan, M. D., Lin, L., et al. (2012). VarScan 2: somatic mutation and copy number alteration discovery in cancer by exome sequencing. *Genome Res.* 22, 568–576. doi: 10.1101/gr.129684.111

Koricha, A. D., Han, D. Y., Bacha, K., and Bai, F. Y. (2020). Diversity and distribution of yeasts in indigenous fermented foods and beverages of Ethiopia. *J. Sci. Food Agric.* 100, 3630–3638. doi: 10.1002/jsfa.10391

Koufopanou, V., and Burt, A. (2005). Degeneration and domestication of a selfish gene in yeast: molecular evolution versus site-directed mutagenesis. *Mol. Biol. Evol.* 22, 1535–1538. doi: 10.1093/molbev/msi149

Koufopanou, V., Goddard, M. R., and Burt, A. (2002). Adaptation for horizontal transfer in a homing endonuclease. *Mol. Biol. Evol.* 19, 239–246. doi: 10.1093/oxfordjournals.molbev.a004077

Kurtz, S., Phillippy, A., Delcher, A. L., Smoot, M., Shumway, M., Antonescu, C., et al. (2004). Versatile and open software for comparing large genomes. *Genome Biol.* 5:R12. doi: 10.1186/gb-2004-5-2-r12

Lam, H.-M., Xu, X., Liu, X., Chen, W., Yang, G., Wong, F.-L., et al. (2010). Resequencing of 31 wild and cultivated soybean genomes identifies patterns of genetic diversity and selection. *Nat. Genet.* 42, 1053–1059. doi: 10.1038/ng.715

Legras, J.-L., Galeote, V., Bigey, F., Camarasa, C., Marsit, S., Nidelet, T., et al. (2018). Adaptation of *S. cerevisiae* to fermented food environments reveals remarkable genome plasticity and the footprints of domestication. *Mol. Biol. Evol.* 35, 1712–1727. doi: 10.1093/molbev/msy066

Legras, J.-L., Merdinoglu, D., Cornuet, J.-M., and Karst, F. (2007). Bread, beer and wine: *Saccharomyces cerevisiae* diversity reflects human history. *Mol. Ecol.* 16, 2091–2102. doi: 10.1111/j.1365-294X.2007.03266.x

Letunic, I., and Bork, P. (2016). Interactive tree of life (iTOL) v3: an online tool for the display and annotation of phylogenetic and other trees. *Nucleic Acids Res.* 44, 242–245. doi: 10.1093/nar/gkw290

Li, H. (2011). A statistical framework for SNP calling, mutation discovery, association mapping and population genetical parameter estimation from sequencing data. *Bioinformatics* 27, 2987–2993. doi: 10.1093/bioinformatics/btr509

Li, H., and Durbin, R. (2009). Fast and accurate short read alignment with Burrows-Wheeler transform. *Bioinformatics* 25, 1754–1760. doi: 10.1093/bioinformatics/btp324

Libkind, D., Cadez, N., Opulente, D. A., Langdon, Q. K., Rosa, C. A., Sampaio, J. P., et al. (2020). Towards yeast taxogenomics: lessons from novel species descriptions based on complete genome sequences. *FEMS Yeast Res.* 20:foaa042. doi: 10.1093/femsyr/foaa042

Lischer, H. E. L., Excoffier, L., and Heckel, G. (2014). Ignoring heterozygous sites biases phylogenomic estimates of divergence times: implications for the evolutionary history of microtus voles. *Mol. Biol. Evol.* 31, 817–831. doi: 10.1093/molbev/mst271

Liti, G. (2015). The fascinating and secret wild life of the budding yeast *S. cerevisiae*. *Elife* 4:e05835. doi: 10.7554/eLife.05835

Liti, G., Carter, D. M., Moses, A. M., Warringer, J., Parts, L., James, S. A., et al. (2009). Population genomics of domestic and wild yeasts. *Nature* 458, 337–341. doi: 10.1038/nature07743

Ludlow, C. L., Cromie, G. A., Garmendia-Torres, C., Sirr, A., Hays, M., Field, C., et al. (2016). Independent origins of yeast associated with coffee and cacao fermentation. *Curr. Biol.* 26, 965–971. doi: 10.1016/j.cub.2016.02.012

Magwene, P. M., Kayikci, O., Granek, J. A., Reininga, J. M., Scholl, Z., and Murray, D. (2011). Outcrossing, mitotic recombination, and life-history trade-offs shape genome evolution in *Saccharomyces cerevisiae*. *Proc. Natl. Acad. Sci. U.S.A.* 108, 1987–1992. doi: 10.1073/pnas.1012544108

Martini, A. (1993). Origin and domestication of the wine yeast *Saccharomyces cerevisiae*. *J. Wine Res.* 4, 165–176. doi: 10.1080/09571269308717966

McGovern, P. E., Zhang, J. H., Tang, J. G., Zhang, Z. Q., Hall, G. R., Moreau, R. A., et al. (2004). Fermented beverages of pre- and proto-historic China. *Proc. Natl. Acad. Sci. U.S.A.* 101, 17593–17598. doi: 10.1073/pnas.0407921102

McKenna, A., Hanna, M., Banks, E., Sivachenko, A., Cibulskis, K., Kernytsky, A., et al. (2010). The genome analysis toolkit: a MapReduce framework for analyzing next-generation DNA sequencing data. *Genome Res.* 20, 1297–1303. doi: 10.1101/gr.107524.110

Miyake, T., Hiraishi, H., Sammoto, H., and Ono, B. I. (2003). Involvement of the VDE homing endonuclease and rapamycin in regulation of the *Saccharomyces cerevisiae GSH11* gene encoding the high affinity glutathione transporter. *J. Biol. Chem.* 278, 39632–39636. doi: 10.1074/jbc.M302084200

Nagai, Y., Nogami, S., Kumagai-Sano, F., and Ohya, Y. (2003). Karyopherin-mediated nuclear import of the homing endonuclease *VMA1*-derived

endonuclease is required for self-propagation of the coding region. *Mol. Cell. Biol.* 23, 1726–1736. doi: 10.1128/mcb.23.5.1726-1736.2003

Naor, A., Altman-Price, N., Soucy, S. M., Green, A. G., Mitiagin, Y., Turgeman-Grott, I., et al. (2016). Impact of a homing intein on recombination frequency and organismal fitness. *Proc. Natl. Acad. Sci. U.S.A.* 113, 4654–4661. doi: 10.1073/pnas.1606416113

Naumov, G. I. (1996). Genetic identification of biological species in the *Saccharomyces sensu stricto* complex. *J. Ind. Microbiol.* 17, 295–302. doi: 10.1007/bf01574704

Novo, M., Bigey, F., Beyne, E., Galeote, V., Gavory, F., Mallet, S., et al. (2009). Eukaryote-to-eukaryote gene transfer events revealed by the genome sequence of the wine yeast *Saccharomyces cerevisiae* EC1118. *Proc. Natl. Acad. Sci. U.S.A.* 106, 16333–16338. doi: 10.1073/pnas.0904673106

Okuda, Y., Sasaki, D., Nogami, S., Kaneko, Y., Ohya, Y., and Anraku, Y. (2003). Occurrence, horizontal transfer and degeneration of VDE intein family in Saccharomycete yeasts. *Yeast* 20, 563–573. doi: 10.1002/yea.984

Peter, J., De Chiara, M., Friedrich, A., Yue, J.-X., Pflieger, D., Bergstrom, A., et al. (2018). Genome evolution across 1,011 *Saccharomyces cerevisiae* isolates. *Nature* 556, 339–344. doi: 10.1038/s41586-018-0030-5

Pontes, A., Cadez, N., Goncalves, P., and Sampaio, J. P. (2019). A quasi-domesticate relic hybrid population of *Saccharomyces cerevisiae* x *S. paradoxus* adapted to olive brine. *Front. Genet.* 10:449. doi: 10.3389/fgene.2019.00449

Pontes, A., Hutzler, M., Brito, P. H., and Sampaio, J. P. (2020). Revisiting the taxonomic synonyms and populations of *Saccharomyces cerevisiae*-phylogeny, phenotypes, ecology and domestication. *Microorganisms* 8:903. doi: 10.3390/microorganisms8060903

Posey, K. L., Koufopanou, V., Burt, A., and Gimble, F. S. (2004). Evolution of divergent DNA recognition specificities in VDE homing endonucleases from two yeast species. *Nucleic Acids Res.* 32, 3947–3956. doi: 10.1093/nar/gkh734

Price, M. N., Dehal, P. S., and Arkin, A. P. (2009). FastTree: computing large minimum evolution trees with profiles instead of a distance matrix. *Mol. Biol. Evol.* 26, 1641–1650. doi: 10.1093/molbev/msp077

Purcell, S., Neale, B., Todd-Brown, K., Thomas, L., Ferreira, M. A. R., Bender, D., et al. (2007). Plink:a tool set for whole-genome association and population-based linkage analyses. *Am. J. Hum. Genet.* 81, 559–575. doi: 10.1086/519795

Quinlan, A. R., and Hall, I. M. (2010). BEDTools:a flexible suite of utilities for comparing genomic features. *Bioinformatics* 26, 841–842. doi: 10.1093/bioinformatics/btq033

Schacherer, J., Shapiro, J. A., Ruderfer, D. M., and Kruglyak, L. (2009). Comprehensive polymorphism survey elucidates population structure of *Saccharomyces cerevisiae*. *Nature* 458, 342–345. doi: 10.1038/nature07670

Stanke, M., Steinkamp, R., Waack, S., and Morgenstern, B. (2004). Augustus: a web server for gene finding in eukaryotes. *Nucleic Acids Res.* 32, 309–312. doi: 10.1093/nar/gkh379

Steensels, J., Gallone, B., Voordeckers, K., and Verstrepen, K. J. (2019). Domestication of industrial microbes. *Curr. Biol.* 29, 381–393. doi: 10.1016/j.cub.2019.04.025

Steenwyk, J., and Rokas, A. (2017). Extensive copy number variation in fermentation-related genes among *Saccharomyces cerevisiae* wine strains. *G3 (Bethesda)* 7, 1475–1485. doi: 10.1534/g3.117.040105

Strope, P. K., Skelly, D. A., Kozmin, S. G., Mahadevan, G., Stone, E. A., Magwene, P. M., et al. (2015). The 100-genomes strains, an *S.cerevisiae* resource that illuminates its natural phenotypic and genotypic variation and emergence as an opportunistic pathogen. *Genome Res.* 25, 762–774. doi: 10.1101/gr.185538.114

Sukumaran, J., and Holder, M. T. (2010). DendroPy: a python library for phylogenetic computing. *Bioinformatics* 26, 1569–1571. doi: 10.1093/bioinformatics/btq228

Takahara, T., and Maeda, T. (2013). Evolutionarily conserved regulation of TOR signalling. *J. Biochem.* 154, 1–10. doi: 10.1093/jb/mvt047

Tapsoba, F., Legras, J.-L., Savadogo, A., Dequin, S., and Traore, A. S. (2015). Diversity of *Saccharomyces cerevisiae* strains isolated from *Borassus akeassii* palm wines from Burkina Faso in comparison to other African beverages. *Int. J. Food Microbiol.* 211, 128–133. doi: 10.1016/j.ijfoodmicro.2015.07.010

Tatebe, H., and Shiozaki, K. (2017). Evolutionary conservation of the components in the TOR signaling pathways. *Biomolecules* 7:77. doi: 10.3390/biom7040077

Vaughanmartini, A., and Martini, A. (1995). Facts, myths and legends on the prime industrial microorganism. *J. Ind. Microbiol.* 14, 514–522. doi: 10.1007/bf01573967

Wang, Q. M., Liu, W. Q., Liti, G., Wang, S. A., and Bai, F. Y. (2012). Surprisingly diverged populations of *Saccharomyces cerevisiae* in natural environments remote from human activity. *Mol. Ecol.* 21, 5404–5417. doi: 10.1111/j.1365-294X.2012.05732.x

Wickham, H. (2016). *ggplot2: Elegant Graphics for Data Analysis*. Cham: Springer Press.

Zheng, X., Levine, D., Shen, J., Gogarten, S. M., Laurie, C., and Weir, B. S. (2012). A high-performance computing toolset for relatedness and principal component analysis of SNP data. *Bioinformatics* 28, 3326–3328. doi: 10.1093/bioinformatics/bts606

Zhou, Y., Zhou, B., Pache, L., Chang, M., Khodabakhshi, A. H., Tanaseichuk, O., et al. (2019). Metascape provides a biologist-oriented resource for the analysis of systems-level datasets. *Nat. Commun.* 10:1523. doi: 10.1038/s41467-019-09234-6

Conflict of Interest: The authors declare that the research was conducted in the absence of any commercial or financial relationships that could be construed as a potential conflict of interest.

frontiers in Microbiology

REVIEW
published: 23 February 2021
doi: 10.3389/fmicb.2021.644404

Advances in Genetic Engineering Technology and Its Application in the Industrial Fungus *Aspergillus oryzae*

Feng-Jie Jin, Shuang Hu, Bao-Teng Wang and Long Jin*

Co-Innovation Center for Sustainable Forestry in Southern China, College of Biology and the Environment, Nanjing Forestry University, Nanjing, China

The filamentous fungus *Aspergillus oryzae* is an important strain in the traditional fermentation and food processing industries and is often used in the production of soy sauce, soybean paste, and liquor-making. In addition, *A. oryzae* has a strong capacity to secrete large amounts of hydrolytic enzymes; therefore, it has also been used in the enzyme industry as a cell factory for the production of numerous native and heterologous enzymes. However, the production and secretion of foreign proteins by *A. oryzae* are often limited by numerous bottlenecks that occur during transcription, translation, protein folding, translocation, degradation, transport, secretion, etc. The existence of these problems makes it difficult to achieve the desired target in the production of foreign proteins by *A. oryzae*. In recent years, with the decipherment of the whole genome sequence, basic research and genetic engineering technologies related to the production and utilization of *A. oryzae* have been well developed, such as the improvement of homologous recombination efficiency, application of selectable marker genes, development of large chromosome deletion technology, utilization of hyphal fusion techniques, and application of CRISPR/Cas9 genome editing systems. The development and establishment of these genetic engineering technologies provided a great deal of technical support for the industrial production and application of *A. oryzae*. This paper reviews the advances in basic research and genetic engineering technologies of the fermentation strain *A. oryzae* mentioned above to open up more effective ways and research space for the breeding of *A. oryzae* production strains in the future.

Keywords: *Aspergillus oryzae*, fermentation industry, genetic engineering technology, cell factory, heterologous protein production

OPEN ACCESS

Edited by:
Wanping Chen,
Georg August University of Göttingen, Germany

Reviewed by:
Bin He,
Jiangxi Science and Technology Normal University, China
Moriyuki Kawauchi,
Kyoto University, Japan
Katsuya Gomi,
Tohoku University, Japan

****Correspondence:***
Feng-Jie Jin
jinfj@njfu.edu.cn

Specialty section:
This article was submitted to Food Microbiology, a section of the journal Frontiers in Microbiology

Received: *21 December 2020*
Accepted: *05 February 2021*
Published: *23 February 2021*

Citation:
Jin F-J, Hu S, Wang B-T and Jin L (2021) Advances in Genetic Engineering Technology and Its Application in the Industrial Fungus Aspergillus oryzae. Front. Microbiol. 12:644404. doi: 10.3389/fmicb.2021.644404

INTRODUCTION

Aspergillus oryzae is an important filamentous fungus that is widely applied in the traditional fermentation and food processing industries, such as soy sauce, soybean paste, and sake brewing. This long history of its widespread use in the food industry has led to *A. oryzae* being recognized by the Food and Drug Administration (FDA) of the United States as Generally Recognized as Safe (GRAS) organisms. Its safety is also supported by the World Health Organization (FAO/WHO) (Kobayashi et al., 2007).

In addition, *A. oryzae* has a strong capacity to secrete large amounts of hydrolytic enzymes (such as amylases and proteases); therefore, it has also been used in the enzyme industry as a cell factory for the production of numerous native and heterologous enzymes. In addition to protein secretion ability, *A. oryzae* also has a strong synthesis ability,

rapid growth, and easy culture, among its advantages. Compared to *Escherichia coli* and yeast *Saccharomyces cerevisiae*, *A. oryzae* has a strong posttranslational modification function; therefore, it is widely used to produce a variety of enzyme preparations (Lissau et al., 1998; Hama et al., 2008; Merz et al., 2015) and in recent years has also been used in the production of secondary metabolites (Yamada et al., 2014; Kan et al., 2019; Liu et al., 2019; Nagamine et al., 2019; Morishita et al., 2020; Oikawa, 2020a).

In the past few decades, research on *A. oryzae* has focused on breeding techniques and developing methods for brewing. Despite its considerable commercial importance, the study of fundamental biological processes in *A. oryzae* was delayed in comparison with the yeast *S. cerevisiae*. The main reasons are that *A. oryzae* is an imperfect fungus that does not have a sexual life cycle and forms multinucleate conidia, making classical genetic manipulation difficult to implement (Kitamoto, 2015). Therefore, it is difficult to study this organism using conventional genetic methods. The production and secretion of foreign proteins by *A. oryzae* are often limited by numerous bottlenecks during transcription, translation, protein folding, translocation, degradation, transport, secretion, etc. (Conesa et al., 2001; Ohno et al., 2011). The existence of these problems makes it difficult to achieve the desired target in heterologous protein production by *A. oryzae*.

In 2005, the genome sequence of *A. oryzae* RIB40 was deciphered (Machida et al., 2005), which marked the advent of the whole genome era of *A. oryzae*, and the combination of genetic engineering technology further promoted the development of *A. oryzae*. Subsequently, many other *A. oryzae* strains were sequenced, such as 3.042, which is extensively used for the production of both soy sauce and other fermented foods in China (Zhao et al., 2012). Comparative genomics analysis showed some strain-specific genes that encode putative proteins potentially involved in cell growth, salt tolerance, environmental resistance and flavor formation (Zhao et al., 2013). The 37-Mb genome of *A. oryzae* RIB40 was predicted to contain more than 12,000 genes, which is 7–9 MB larger than the genomes of *Aspergillus nidulans* and *Aspergillus fumigatus* (Galagan et al., 2005; Machida et al., 2005; Nierman et al., 2005). The completed genomic studies using expressed sequence tag analyses (Machida, 2002; Akao et al., 2007) combined with the development of genetic engineering technology have made it possible to overcome these deficiencies and promoted the study of heterologous protein production in *A. oryzae* and the breeding of new strains for industrial production (Vongsangnak et al., 2008; Zhu et al., 2013). Regarding genetic engineering to solve the bottleneck problems in heterologous protein production in *A. oryzae*, this article elaborated on several aspects, such as optimization of the genetic transformation system and the improvement of transformation efficiency, construction of protease gene-deleted strains, development of fusion expression strategies, optimization of exogenous gene expression systems, and development of other genetic engineering techniques to improve the production of foreign proteins. These advances in basic research and genetic engineering technology have greatly improved the production and application of *A. oryzae*.

DEVELOPMENT OF TRANSFORMATION SYSTEMS OF *A. ORYZAE*

In industrial applications, the establishment of a highly efficient genetic transformation system is a prerequisite for genetic manipulation and recombinant gene expression in *A. oryzae*. Compared to *E. coli* and yeast *S. cerevisiae*, the *A. oryzae* cell wall is hard and not easily broken, which is an obstacle for gene introduction into host cells in later genetic transformation experiments. Therefore, some rapid and convenient transformation methods, such as the electroporation and gene gun methods, are not suitable for *A. oryzae* genetic transformation due to their extremely low transformation efficiency. By contrast, another conventional genetic transformation method, which is a polyethylene glycol (PEG)/$CaCl_2$-mediated protoplast transformation system, was widely utilized in *A. oryzae*.

Development and Application of Selective Marker Genes

The application of recombinant DNA methodology in *A. oryzae* allows advanced molecular genetic analyses, which makes it possible to introduce DNA fragments into the host to produce heterologous proteins (Kitamoto, 2002). For effective molecular genetic analysis and protein production, suitable and stable hosts are needed as genetically engineered strains to transform the selected target genes. In previous research, several auxotrophic marker genes, such as *pyrG*, *argB*, *niaD*, and *sC* (Gomi et al., 1987; Mattern et al., 1987; Unkles et al., 1989; Yamada et al., 1997), and dominant selectable markers, such as *amdS* and *ptrA* (Gomi et al., 1991; Kubodera et al., 2000), have been developed and used in the genetic transformation of *A. oryzae*. Recently, a new pyrithiamine resistance marker gene, *thiI*, was also identified for use in genome editing by selecting mutants resistant to pyrithiamine from UV-mutagenized *A. oryzae* strains (Todokoro et al., 2020). In addition to these, a bleomycin resistance marker gene (*blmB*) and a carboxin resistance marker gene [*AosdhB*(cxr)] also were developed for *A. oryzae* transformation (Shima et al., 2009; Suzuki et al., 2009). However, all these transformation techniques only use a single gene as a selective marker gene; therefore, several multitransformation systems of *A. oryzae* containing multiple selective marker gene-defective strains were constructed, which could carry out gene engineering operations such as introduction or deletion of multiple genes in the same host. For this purpose, Yamada et al. (1997) further developed a double auxotrophic transformation system (*niaD*$^{-}$, *sC*$^{-}$) that can conduct two genetic manipulations in a single host strain. On this basis, triple auxotrophic mutants (*niaD*$^{-}$, *sC*$^{-}$, *adeA*$^{-}$/*adeB*$^{-}$) were further obtained from *A. oryzae* by UV mutagenesis, which added a new adenine auxotrophy (Jin et al., 2004a). In addition, a quadruple auxotrophic host transformation system was further developed by *argB* gene deletion combined with exploiting adenine auxotrophy (Jin et al., 2004b). Among these selection marker genes, the *pyrG* gene, which encodes an orotidine-5′-phosphate (OMP) decarboxylase, has been used for marker recycling that allows multiple genetic manipulations

in the *Aspergillus* species (Nielsen et al., 2006; Maruyama and Kitamoto, 2008) because *pyrG*-deficient strains can be positively selected by 5-fluoroorotic acid (5-FOA), which is converted to a toxic compound, to strains expressing *pyrG*. These selectable marker genes mentioned above are summarized in **Table 1**. In addition, the Cre-*loxP* site-specific recombination system, which has been widely applied in a number of organisms, such as bacterial, yeast, plant, and mammalian cells (Sauer, 1987; Gu et al., 1993; Sieburth et al., 1998), was also developed for multiple gene integrations and deletions in *A. oryzae* (Mizutani et al., 2012; Zhang et al., 2017). This system is used for site-specific recombination between two *loxP* sites mediated by a Cre recombination protein derived from bacteriophage P1 (Abremski et al., 1986).

Chromosomal Engineering Technology

One of the major reasons for the lag in basic research on *A. oryzae* is the low efficiency of homologous recombination transformation, which makes it difficult to obtain gene deletion strains. Takahashi et al. (2006) significantly improved the homologous recombination efficiency of *A. oryzae* by deleting non-homologous end-joining (NHEJ)-related genes such as *ku70* and *ku80*, thus enhancing the gene deletion efficiency of *A. oryzae*. Next, some studies also showed that the disruption of another NHEJ-related *ligD* gene significantly improved gene-targeting efficiency in *A. oryzae* (Maruyama and Kitamoto, 2008; Mizutani et al., 2008). With the significant improvement in the efficiency of homologous recombination, deletion technology of large chromosomal segments, including loop-out recombination and replacement-type recombination methods, has been developed (Takahashi et al., 2008, 2009), providing technical support for the further deletion of unnecessary and even harmful large chromosomal segments from the chromosomes in *A. oryzae*. Although *A. oryzae* is regarded as an industrially important fungus, its genome sequence still contains several gene clusters related to the synthesis of toxins, such as imperfect clustered genes related to aflatoxin biosynthesis and cyclopiazonic acid production. Although these toxic secondary metabolites are not normally synthesized, they are also at a certain risk, and these gene clusters can be deleted through the deletion technology of large chromosomal segments. On this basis, Jin et al. (2010) conducted a chromosome-shortening experiment, and most of the unnecessarily long DNA fragments and potential toxin synthesis-related gene clusters on chromosome 7 of *A. oryzae* were successfully removed, which not only promoted the production of amylase but also avoided the production of some byproducts that are possibly harmful to human health. By eliminating non-essential chromosomal segments and retaining only the genes that maintain basic physiological functions, we will gain a deeper understanding of the physiological characteristics of this organism and the essential gene functions for its industrial use. The development of these techniques pave a new way for the future production and utilization of *A. oryzae*.

In addition, *A. oryzae* was thought to undergo asexual reproduction, and no sexual stage has been reported; therefore, it has certain limitations in production and application. For instance, breeding better production strains cannot be achieved by sexual hybridization. To solve this problem, protoplast fusion technology was developed, and a further reduced chromosome *A. oryzae* mutant was constructed with a shortened chromosomes 7 and 8, both of which include a large number of non-syntenic blocks by using this protoplast fusion technique (Hara et al., 2012). The large chromosome segment deletion technique combined with the protoplast fusion technique has effectively solved the problem that has puzzled *A. oryzae* researchers for many years and provided a good technical means for better chromosome processing in the future to obtain the breeding of excellent *A. oryzae* production strains. In addition, using the large-scale chromosome deletion technique, a member of the basic helix-loop-helix (bHLH) transcription factor family, SclR, was identified and characterized (Jin et al., 2009, 2011b). Studies have shown that SclR cannot only promote sclerotia formation by promoting hyphal fusion but also effectively promote nucleus fusion between different strains (Wada et al., 2014), which provides a more feasible space for breeding excellent *A. oryzae* strains in the future. These studies indicated that the deletion technique of large chromosome segments is also of great value for the discovery and exploration of unknown functional genes.

Agrobacterium-Mediated Transformation System

Aspergillus oryzae is resistant to most common antifungal antibiotics that are often used as selective agents for transformation experiments of filamentous fungi (Suzuki et al., 2009); therefore, *A. oryzae* transformation systems were developed mainly based on nutritional selectable markers for complementation of auxotrophic strains (Gomi et al., 1987; Mattern et al., 1987). Currently, PEG-mediated protoplast transformation is the common method utilized for fungal transformation experiments (Liu and Friesen, 2012). The *Agrobacterium tumefaciens*-mediated transformation (ATMT) system is another method that was developed and used for genetic transformation in the *Aspergilli* species (Michielse et al., 2005). The approach usually requires a binary vector carrying T-DNA (transfer DNA), an *A. tumefaciens* strain that harbors a helper plasmid with *vir* (virulence) supporting the T-DNA transfer process, and a suitable recipient (Michielse et al., 2005; Frandsen, 2011). Using the ATMT method to transfer DNA into the fungal genome has been shown to be more efficient and simpler to implement in different filamentous fungi, while PEG-mediated protoplast transformation is more laborious and time-consuming for protoplast preparation (Idnurm et al., 2017; Weyda et al., 2017). Recently, the efficient approach was used to successfully construct uridine/uracil auxotrophic mutants by deleting the *pyrG* gene in different industrial fungus *A. oryzae* wild-type strains, and the genetic transformation efficiency by *A. tumefaciens* was higher and reached approximately 0.1% using the *pyrG* selectable marker and these auxotrophic mutants (Nguyen et al., 2016, 2017). These generated auxotrophic mutants were also used to successfully express the DsRed fluorescent reporter gene under the control of the *A. oryzae* alpha-amylase gene (*amyB*) promoter by the ATMT method. Furthermore, using the ATMT method,

TABLE 1 | Selectable marker genes used in *Aspergillus oryzae.*

Selectable marker gene	Description	References
niaD	The *niaD* gene encodes a nitrate reductase, and the *niaD*$^{-}$ mutants display chlorate resistance	Unkles et al., 1989
pyrG	The *pyrG* gene encodes an orotidine-5′-phosphate (OMP) decarboxylase, and *pyrG*-deficient strains can be positively selected by 5-fluoroorotic acid (5-FOA)	Mattern et al., 1987
argB	The *argB* gene encodes an ornithine carbamoyltransferase and allows the complementation of the arginine auxotrophic mutation	Gomi et al., 1987
sC	*sC* marker gene encodes an ATP sulfurylase, and the *sC*$^{-}$ mutants can be isolated by positive selection for selenate resistance	Yamada et al., 1997
adeA	The *adeA* gene encodes a phosphoribosylaminoimidazolesuccinocarboxamide synthase of purine biosynthetic pathway and could complement the adenine auxotrophic mutants	Jin et al., 2004a
adeB	The *adeB* gene encodes a phosphoribosylaminoimidazole carboxylase of purine biosynthetic pathway and could complement the adenine auxotrophic mutants	Jin et al., 2004a
amdS	The *amdS* gene encodes an acetamidase that is required for acetamide utilization	Gomi et al., 1991
ptrA	The *ptrA* is a pyrithiamine-resistant gene that was cloned from a pyrithiamine resistant mutant of *A. oryzae*	Kubodera et al., 2000
thiI	The *thiI* gene encodes a thiamine transporter gene, and its mutant showed pyrithiamine resistance	Todokoro et al., 2020
blmB	The *blmB* gene encodes bleomycin *N*-acetyltransferase from bleomycin-producing *Streptomyces verticillus* and is responsible for the bleomycin resistance	Suzuki et al., 2009
AosdhB(cxr)	*AosdhB* encodes a succinate dehydrogenase gene, and its mutation [*AosdhB*(cxr)] confers the carboxin resistance.	Shima et al., 2009

a useful dual selection marker system was developed for genetic manipulations in an industrial *A. oryzae* 3.042 strain by constructing a uridine/uracil auxotrophic mutant and pyrithiamine (PT) genes as selection markers (Sun et al., 2019). In summary, this ATMT method can simplify transformation procedures and improve the efficiency of genetic manipulations. This strategy can be applied in functional gene research and the production of recombinant proteins by the industrial fungus *Aspergillus* strains through genetic transformation systems based on nutrition markers.

CRISPR/Cas9-Based Genome Engineering

The increase in the number of whole genomes available for fungal species provided a wider range of possibilities for gene manipulation in filamentous fungi. In recent years, a versatile genomic editing technique, the CRISPR (clustered regularly interspaced short palindromic repeat)–Cas9 (CRISPR-related nuclease 9) system, has been rapidly developed and widely applied in filamentous fungi. The advance of this technology has revolutionized biological research and led to innovative applications in a wide range of fields, showing great prospects in the research and application of filamentous fungi (Song et al., 2019).

The CRISPR/Cas9 system is divided into two categories, including six types and 19 subtypes (Shmakov et al., 2017). Among them, the type II system is a simpler CRISPR system than other systems that have been widely used. The type II CRISPR/Cas9 system contains Cas9 (nuclease), mature crRNA (CRISPR associate RNA), tracrRNA (*trans*-activating crRNA), and RNaseIII. The crRNA and tracrRNA have been modified and linked into a single-guide RNA (sgRNA) (Jinek et al., 2012) that could efficiently guide the Cas9 nuclease to the target sequences to cut the DNA. Currently, CRISPR/Cas9 technology has been widely used for genome editing in yeasts/fungi, plants, mammalian cells, and others (Cong et al., 2013; van Erp et al., 2015; Schiml and Puchta, 2016). In fungi, the CRISPR/Cas9 genome editing system was first introduced into *S. cerevisiae* (DiCarlo et al., 2013) and then further applied to *Trichoderma reesei*, *Neurospora crassa*, and *Aspergillus nidulans* (Liu et al., 2015; Matsu-Ura et al., 2015; Nodvig et al., 2018). In addition, the CRISPR/Cas9 system was discovered in bacteria or archaea, and therefore, the Cas9-encoding gene usually needs to be fungal codon-optimized and a nuclear localization signal when the genome editing system is used in fungi (Generoso et al., 2016; Nodvig et al., 2018). In recent years, some studies have shown that the CRISPR/Cas9 technique has been used in the production of recombinant proteins in the *Aspergilli* species (Dong et al., 2020; Rojas-Sanchez et al., 2020).

To develop the CRISPR/Cas9 genome editing technique in *A. oryzae*, plasmids that express the Cas9 nuclease gene and sgRNAs were constructed and introduced into an *A. oryzae* strain for the mutagenesis of target genes (Katayama et al., 2016). In this study, the codon usage of *cas9* with a sequence encoding an SV40 nuclear localization signal at its 5′- and 3′-ends was optimized to improve the nuclear localization of Cas9 nuclease. The generated transformants contained mutations in which each target gene showed the expected phenotype. Mutation rates between 10 and 20% with 1 bp of deletion or insertion are the most common induced mutations, and genome editing technology will contribute to the efficient use of targeted mutagenesis in many *A. oryzae* industrial strains without a clear genetic background. To further improve the targeting efficiency in *A. oryzae* industrial strains, the *ligD* gene involved in NHEJ was mutated by employing the CRISPR/Cas9 system (Nakamura et al., 2017). The gene targeting efficiency of the generated *ligD* mutant was examined using the *ecdR* gene, which encodes a regulator involved in the early stage of conidiophore development in the *A. oryzae* (Jin et al., 2011a). The results

indicated that the deletion efficiency was significantly improved and reached approximately 60∼80% in the *ligD* mutants.

In addition to food fermentation and industrial production of recombinant proteins, *A. oryzae* has also been used for heterologous production of useful secondary metabolites; therefore, multiple steps of genetic manipulation are required.

An improved CRISPR/Cas9 approach that includes an *AMA1*-based autonomously replicating plasmid harboring the pyrithiamine resistance marker gene *ptrA* was further developed (Katayama et al., 2019). The conditional expression of the *Aoace2* gene in the *AMA1*-based plasmid significantly repressed the growth of fungi, which made it possible for forced plasmid recycling and allowed repeated genome editing. This study showed that the repeatable marker-free genome editing approach can effectively delete or integrate multiple genes in the industrial *A. oryzae* strain (Katayama et al., 2019). In the production experiment of human antibody (anti-TNFα antibody adalimumab) by *A. oryzae*, the CRISPR/Cas9 technique was used for the deletion of the *Aooch1* gene, which encodes a key enzyme for the hypermannosylation process, to detect the binding ability of the recombinant antibody with FcγRIIIa (Huynh et al., 2020). In addition, the CRISPR/Cas9 system was also used to delete *AoGld3,* which is one of 45 glycerol dehydrogenase genes in *A. oryzae,* to investigate its effect on the production of the secondary metabolite kojic acid. The result showed that the deletion of *AoGld3* resulted in the inhibition of kojic acid production by affecting the expression of *kojA* and *kojR*, which encode an enzyme and a transcription factor involved in the kojic acid biosynthesis (Fan et al., 2020). In addition, a platinum-fungal TALEN (Transcription activator-like effector nucleases) -based genome editing technique has also been developed for targeted gene mutations in *A. oryzae* (Mizutani et al., 2017). The platinum-fungal TALEN technique resulted in various different mutation patterns with almost half of deletions larger than 1 kb in the target region. Taken together, these genome editing technologies will greatly enhance the convenience of genetic manipulation in a wide range of industrial production strains and significantly contribute to efficient molecular breeding of these industrial strains.

STUDY ON HETEROLOGOUS GENE EXPRESSION AND PROTEIN SECRETION SYSTEMS

Aspergillus oryzae has attracted increasing attention due to its wide use as a cell factory in the study of exogenous gene expression and heterologous protein production in recent years. An understanding of how optimize the exogenous gene expression system is of great significance to the industrial application of *A. oryzae*. By analyzing the advantages and disadvantages of the exogenous gene expression system of *A. oryzae* and combining genetic engineering technology developed in recent years, the exogenous gene expression of *A. oryzae* can be improved by making full use of the advantages while avoiding the disadvantages.

Disruption of Proteinase Genes in *A. oryzae*

Compared with the production and secretion system of prokaryotes such as *E. coli*, exogenous genes expressed in *A. oryzae* undergo eukaryotic posttranslational modifications, including glycosylation and protein folding. Therefore, *A. oryzae* is considered as one of the most advantageous hosts for expressing recombinant proteins from higher eukaryotes (Fleissner and Dersch, 2010). The production of heterologous proteins is limited by many factors, such as the transcriptional level, translation level, secretory process, and extracellular degradation (Jeenes et al., 1991). Therefore, several bottleneck genes related to proteases, secretion pathways, cell polarity establishment, and metabolism must be manipulated to breed favorable hosts for heterologous protein production.

Among them, the strong protease activity of *A. oryzae* is the most important reason to inhibit the production of heterologous proteins because heterologous proteins are more easily broken down by proteases than the organism's own proteins. To improve the yield of heterologous proteins, researchers have tried various biological methods. For instance, downstream processing at low temperature, early separation of products from proteases, application of protease inhibitors, etc. can reduce hydrolysis; however, the effect is not optimistic because most heterologous proteins could be degraded in the process of protein production (Jin et al., 2007). Using a quadruple auxotrophic host (Jin et al., 2004b), Jin et al. (2007) expressed the heterologous human lysozyme (HLY) gene by disrupting an intracellular acid protease PepE and a tripeptidyl peptidase TppA genes, and the double disruption led to an increase (63%) in HLY production in comparison to the control. In this study, the *HLY* gene fused with an *A. oryzae* α-amylase (AmyB) gene was expressed, the Kex2 cleavage site was inserted between them, and HLY was successfully processed and dissociated from the native AmyB protein and secreted into the medium. In addition, a systematic deletion analysis of five proteinase genes (*pepA*, *pepE*, *tppA*, *alpA*, and *palB*) in the HLY-producing strain was performed, and comparative analysis indicated that deletion of the *tppA* gene resulted in the highest increase (36%) in lysozyme activity of the HLY-producing strain (Jin et al., 2007). On this basis, a quintuple protease gene disrupted strain (*tppA*, *pepE*, *dppIV*, *dppV*, and *nptB*) (Yoon et al., 2009) and an additional ten protease gene disrupted strain with five additional deleted genes (*alpA*, *pepA*, *AopepAa*, *AopepAd*, and *cpI*) (Yoon et al., 2011) were successively constructed using *pyrG* marker recycling combined with a highly efficient gene targeting background (△*ligD*). The results showed that the yield of HLY and bovine chymosin (CHY) protein in the ten protease gene disruptants was significantly enhanced, which was 3.2 and 3.8 times that of the control strains, respectively.

To further solve the bottlenecks limiting the production of heterologous protein by *A. oryzae*, another tripeptidyl peptidase gene, *AosedD*, which may be involved in the proteolytic degradation of recombinant proteins, was selected to construct its deletion strain for the production of heterologous proteins. In the *AosedD* deletion mutant, the production levels of recombinant HLY and CHY improved approximately 1.7- and 2.9-fold,

respectively, relative to their control strains (Zhu et al., 2012). The results show that AoSedD is one of the main proteases involved in the degradation of heterologous recombinant proteins in *A. oryzae*.

Optimization of Heterologous Protein Secretion Pathways

Another important bottleneck in the production of heterologous proteins in filamentous fungi is the secretion of the proteins (Conesa et al., 2001). The unfolded protein response (UPR) is an intracellular regulatory pathway that activates the genes involved in folding, quality control, transport, and other functions of secreted proteins. The overexpression of heterologous proteins may result in the overload of unfolded proteins in the endoplasmic reticulum (ER) (Ron and Walter, 2007). The response is accompanied by the transcription activation of ER protein folding- and secretion-related genes. Some studies have shown that heterologous protein production upregulates the expression of ER chaperone genes, such as *bipA* (a major endoplasmic reticulum chaperone protein gene), *prpA* (a PDI [protein disulfide isomerase]-related gene), and *clxA* (a calnexin homologue from *Aspergillus niger*) (Punt et al., 1998; Wang and Ward, 2000; Wang et al., 2003). To examine the effects of carrier fusion on the UPR and secretion of the target protein, a DNA microarray was used to analyze the transcriptional level of the *A. oryzae* whole genome using CHY as a model heterologous protein (Ohno et al., 2011). The production level of a carrier-fused CHY with α-amylase increased by approximately twofold in comparison with the non-carrier-fused CHY, and several genes involved in ER protein folding and secretion were significantly upregulated in the carrier fusion CHY strain by DNA microarray analysis. Similarly, the transcripts of *hacA*, which encodes the UPR transcription factor required for upregulation of the ER chaperone and foldase-encoding genes (Mulder et al., 2006), were effectively spliced in the carrier-fused CHY strain. These results suggest that carrier-fused CHY temporarily accumulated in the ER and remarkably induced UPR in the carrier-fused strain (Ohno et al., 2011). However, recent studies have shown that highly expressed endogenous secretory proteins can also evoke the UPR. This finding raises the possibility that unfolded or misfolded proteins are selectively recognized by quality control mechanisms in filamentous fungi (Yokota et al., 2017).

Protein trafficking through the secretory pathway depends on the production levels of foldases and chaperones, which play crucial roles in protein folding during secretion. Some studies have shown that the overexpression of ER foldase- and molecular chaperone-related genes partially alleviate ER overload. It has been reported that the overexpression of chaperone BipA and PDI genes improve the production of heterologous proteins (Moralejo et al., 2001; Lombrana et al., 2004). Among them, the overexpression of *bipA* increased thaumatin secretion by 2- to 2.5-fold compared to the control strain; conversely, homologous protein secretion was not influenced by its overexpression in *Aspergillus awamori*.

In addition, vacuolar protein sorting (VPS), autophagy, and ER-Golgi cargo receptors also affect the heterologous protein production of *A. oryzae* (Yoon et al., 2013; Hoang et al., 2015). Autophagy is a highly conserved intracellular degradation pathway in eukaryotes that can recycle intracellular components as a survival mechanism under nutritional starvation (Reggiori and Klionsky, 2002). Furthermore, autophagy was confirmed to deliver misfolded secreted proteins accumulated in the ER to vacuoles, which is an important process that adversely affects heterologous protein production in *A. oryzae* (Kimura et al., 2011). In a previous study, according to the homology analysis with *S. cerevisiae*, five putative autophagy-related genes: *Aoatg1*, encoding a kinase involved in autophagy induction; *Aoatg4* and *Aoatg8*, which are essential genes for the formation of autophagosomes and membrane fusion; *Aoatg13*, encoding a component of the AoAtg1 complex; and *Aoatg15*, encoding a lipase required for the breakdown of autophagic bodies, were selected and successfully deleted in *A. oryzae* (Yoon et al., 2013). Using CHY as a reporter heterologous protein, the production level of CHY in the *Aoatg1*, *Aoatg4*, and *Aoatg8* deletion strains was improved by 2. 3-, 3. 1-, and 2.5-fold, respectively, compared to the control strain.

In addition, homologs of several VPS genes, which play crucial roles in the secretory pathway, have been identified and characterized (Lemmon and Traub, 2000; Suzuki et al., 2003). Among them, VPS10 has been identified to encode a sorting receptor for the recognition and delivery of some vacuolar proteins in yeast (Cooper and Stevens, 1996). Although it was also found to target aberrant and recombinant proteins for vacuolar degradation, the effect of *VPS10* gene deletion on the production of heterologous proteins is unclear. Studies have shown that the *vps10* gene deletion resulted in missorting of vacuolar carboxypeptidase CpyA and was then secreted into the medium (Marcusson et al., 1994), indicating that Vps10 is necessary for sorting vacuolar proteins into vacuoles. The analysis of heterologous protein production indicated that the *Aovps10* deletion mutation elevated the maximum extracellular production levels of the heterologous proteins HLY and CHY by 2.2- and 3-fold, respectively (Yoon et al., 2010). These results revealed that AoVps10 is involved in the regulation of heterologous protein secretion and vacuolar protein degradation in *A. oryzae*.

Promoters and Endogenous Secretion Carrier Proteins for Heterologous Gene Expression

To improve the production of heterologous proteins, in addition to reducing the activity of proteases, a series of strong promoters were developed to induce the expression of heterologous genes (**Table 2**). In *A. oryzae*, the starch-inducible promoter of the alpha-amylase gene (P*amyB*) is one of the most commonly used promoters for the production of foreign proteins (Tsuchiya et al., 1992; Ward et al., 1992; Rey et al., 2003; Hoshida et al., 2005; Yamashita et al., 2011; Yin et al., 2015). The glucoamylase gene promoter (P*glaA*) and its improved promoter (P*glaA142*) were often used for the production and function analysis of recombinant proteins, such as *Candida antarctica* lipase B and *A. oryzae* recombinant tannase (Tamalampudi et al., 2007;

Tokuoka et al., 2008; Ichikawa et al., 2020). The constitutive *gpdA* gene promoter from *A. nidulans* (de Ruiter-Jacobs et al., 1989; te Biesebeke et al., 2006; Punya et al., 2013), thiamine-regulatable promoter of the thiamine thiazole synthase gene (P*thiA*) (Shoji et al., 2005), and the promoter of the translation-elongation factor 1 alpha gene (P*tef1*) (Kitamoto et al., 1998) were also used for homologous and heterologous protein production in *A. oryzae*. In addition, the glucoamylase-encoding gene (*glaB*) promoter was developed for recombinant protein production in solid-state fermentation of *A. oryzae* (Ishida et al., 2006), and the promoter of the oxidoreductase gene *kojA* involved in the kojic acid biosynthesis, was successfully used to induce the expression of the polyketide synthase gene (*wA*) by *A. oryzae* (Tamano et al., 2019). The promoters used for *A. oryzae* recombinant protein production are summarized in **Table 2**. In addition to these promoters, studies have shown that the alterations in 5′ untranslated region (5′ UTR) importantly improved the translation efficiency of heterologous proteins in *A. oryzae* (Koda et al., 2004, 2006). The results suggested that the 5′ UTR can be used in combination with various strong promoters to enhance the expression of heterologous proteins. Furthermore, the host endogenous high-secreted protein genes were also further developed for the fusion and expression of exogenous protein genes (Gasser and Mattanovich, 2007; Jin et al., 2007; Hoang et al., 2015). Current studies have shown that the fusion of exogenous protein genes into the end of the highly secreted endogenous protein genes of *A. oryzae* reduce the degradation of heterologous proteins by the protease of *A. oryzae* (Ohno et al., 2011). For example, when a reporter heterologous protein CHY was expressed with fused α-amylase (AmyB), which is one of the most abundantly expressed proteins in *A. oryzae* under starch-induced culture conditions, the production level increased by approximately twofold compared to the non-carrier fused CHY (Ohno et al., 2011). Another study showed that using the *A. oryzae* glucoamylase gene (*glaA*) as a carrier protein, carrier-fused recombinant chymosin was secreted at a high level and showed a fivefold higher chymosin production level compared with the control using the *glaA* promoter alone (Tsuchiya et al., 1994). Furthermore, a mite allergen Der f 7 gene was highly expressed by fusion with the *A. oryzae* glucoamylase carrier protein, and its expression level was further enhanced by codon optimization which is also an effective method for improving the production levels of heterologous proteins (Tokuoka et al., 2008; Tanaka et al., 2012).

Applications of Other Biotechnological Research Methods

Random mutations caused by ultraviolet radiation is a traditional method to improve the production capacity of heterologous proteins in filamentous fungi. Through the UV radiation mutation method, an *A. oryzae* superproductive mutant (AUT1-8) was isolated using HLY as a screening indicator (Nemoto et al., 2009). First, HLY-hyperproducing mutants were screened from the *tppA* and *pepE* disruptants through a halo assay based on HLY activity. Then, the plasmid containing the lysozyme gene was removed from the mutants, and the resulting strains were named AUT strains. The AUT1 strain showed production levels of heterologous proteins HLY and CHY that were 2.6 and 3.2 times higher than those of the control strains, respectively (Nemoto et al., 2009). By utilizing next-generation DNA sequencing technology and comparative genomics analysis, some potential protein production-related mutation sites were identified in the *A. oryzae* mutant (Jin et al., 2016). Among these genes, an *autA* gene (AO090120000003), which was predicted to encode a cytoplasmic protein with unknown function, including an alpha/beta hydrolase fold domain, was identified for the first time to be responsible for high-level heterologous protein production in the AUT1 strain. The HLY production level of the *autA* mutant or deletion strains was twofold higher than that of the control strain, especially in the early growth stage of cultivation. To further improve heterologous protein production, using the generated hyperproducing mutant strain of *A. oryzae*, AUT1, double deletion of the *Aovps10* and *AosedD* genes mentioned above was performed, which increased the yield of HLY and CHY by 2.1- and 1.6-fold, respectively, compared to the parental strain (Zhu et al., 2013). Thus, an excellent fungal host for the production of heterologous recombinant protein was generated by combining the mutation method with molecular breeding techniques.

Through ultraviolet radiation, Murthy and Kusumoto (2015) also obtained an *A. oryzae* mutant with a high acid protease yield, which was 5.6 times higher than that of the parent strain. In addition, through exposure to different doses of gamma irradiation, two maximum kojic acid overproduction mutants were attained from *A. flavus* HAk1 and *A. oryzae* HAk2, and the yield of kojic acid of the two mutants was 1.9- and 2.03-fold higher than that of their wild-type strains under malt extract sucrose culture conditions (Ammar et al., 2017).

The *A. oryzae* solid-state fermentation has been confirmed to produce high levels of hydrolases critical to the fermentation process. The genomic comparison and transcriptomic analysis revealed that the extracellular hydrolase genes were highly induced during solid-state cultivation in *A. oryzae* (Machida et al., 2008). Studies have shown that some proteinases and glycoside hydrolases have higher production level in solid-state fermentation than in submerged fermentation by *A. oryzae* (Zhao et al., 2019; Melnichuk et al., 2020). In addition, a glucoamylase gene *glaB* expressed exclusively in solid-state culture, therefore, as mentioned above, its promoter has been used for the production of recombinant proteins in solid-state fermentation of *A. oryzae* (Hata et al., 1998; Ishida et al., 2006). Recent studies have also shown that the transcription factor FlbC is involved in the GlaB production in solid-state culture (Tanaka et al., 2016; Gomi, 2019). These advances in molecular biology are expected to be better applied to the production of homologous and heterologous production in solid-state fermentation of *A. oryzae*. A transposable element known as a DNA sequence can change its relative position within the genome. According to their different mechanisms of transposition, transposable elements can be divided into two classes: retrotransposons, which replicate through an RNA intermediate and introduce into multiple loci of the genome, and DNA transposons, which transpose directly by a 'cut-and paste' mechanism through a DNA form (Daboussi,

TABLE 2 | Promoters used for the production of recombinant proteins in *Aspergillus oryzae*.

Promoter gene	Species	Description	Produced recombinant protein	References
amyB	*Aspergillus oryzae*	An alpha-amylase gene (*amyB*) promoter.	A mature human lysozyme (HLY);	Tsuchiya et al., 1992
			Recombinant human lactoferrin	Ward et al., 1992
			Thielavia terrestris glucoamylase	Rey et al., 2003
			Pycnoporus coccineus extracellular laccase	Hoshida et al., 2005
			Aspergillus fumigatus elastase inhibitor AFUEI	Yamashita et al., 2011
			A novel fungal α-amylase (PcAmy) gene from *Penicillium* sp.	Yin et al., 2015
			Leucine aminopeptidase A (*lapA*) from *A. oryzae*	Matsushita-Morita et al., 2011
glaA142	*A. oryzae*	An improved glucoamylase gene promoter P*glaA142*	*Candida antarctica* lipase B (CALB)	Tamalampudi et al., 2007
			Mite allergen Der f 7	Tokuoka et al., 2008
			A. oryzae enzymes (BglA, BglF, and BglJ)	Kudo et al., 2015
			A. oryzae recombinant tannase (*AotanB*)	Ichikawa et al., 2020
glaB	*A. oryzae*	A glucoamylase-encoding gene (*glaB*) promoter for recombinant protein production in solid-state fermentation of *A. oryzae*	*A. oryzae* glucoamylase A (*glaA*) and glucoamylase B (*glaB*)	Ishida et al., 2006
tef1	*A. oryzae*	Promoter of a translation-elongation factor 1 alpha gene, *tef1*	Polygalacturonase (*pgaA* and *pgaB*)	Kitamoto et al., 1998
melO	*A. oryzae*	The tyrosinase-encoding gene (*melO*) promoter	*E. coli* beta-glucuronidase (GUS)	Ishida et al., 2001
gpdA	*Aspergillus nidulans*	The constitutive *gpdA* promoter from *A. nidulans*	Bacterial beta-galactosidase (*lacZ*) and beta-glucuronidase (*uidA*)	de Ruiter-Jacobs et al., 1989
			GFP and DsRed fluorescent proteins	Nguyen et al., 2016
			Seven polyketide synthase (PKS) genes from *Xylaria* sp.	Punya et al., 2013
			Hemoglobin domains (HBD) isolated from *A. oryzae* and *Aspergillus niger*	te Biesebeke et al., 2006
thiA	*A. oryzae*	The thiamine-regulatable promoter of the thiamine thiazole synthase gene (P*thiA*)	Enhanced green fluorescent protein (EGFP)	Shoji et al., 2005
enoA142	*A. oryzae*	An improved enolase promoter (P-*enoA142*)	*Fusarium heterosporum* lipase (FHL)	Takaya et al., 2011
		An improved *enoA* promoter that harbored 12 tandem repeats of the *cis*-acting element (region III) of *A. oryzae*	Beta-glucuronidase (GUS)	Tsuboi et al., 2005
kojA	*A. oryzae*	A promoter of the secondary metabolism gene *kojA* involved in the kojic acid biosynthesis, for the production of other secondary metabolites by *A. oryzae*	A polyketide synthase (*wA*) of *A. oryzae*	Tamano et al., 2019
hlyA	*A. oryzae*	A hemolysin-like protein encoding gene (*hlyA*) promoter used for protein overexpression in *A. oryzae* grown in solid-state culture	*A. oryzae* endo-1,4-β-glucanase (CelA) and endoglucanase CelB; *Trichoderma reesei* endoglucanases (TrEgII and TrEgIII)	Bando et al., 2011
actB	*A. oryzae*	Promoter of an actin-encoding *actB* gene that can be highly induced by benomyl treatment	Antifungal compounds	Marui et al., 2010b
pgkA	*A. oryzae*	A constitutive phosphoglycerate kinase (PGK) gene promoter	PEP carboxylase (PPC) or PEP carboxykinase (PCK) genes from *E. coli*	Liu et al., 2017
sodM	*A. oryzae*	Promoter of manganese superoxide dismutase-encoding gene *sodM*	Beta-glucuronidase (GUS)	Ishida et al., 2004
			6-phosphofructokinase (*pfk*)	Liu et al., 2017

1997; Daboussi and Capy, 2003). Although the *A. oryzae* genome sequence database (Machida et al., 2005) showed that a DNA transposon and some retrotransposons have been identified, their transposition activities have not yet been detected. In recent years, an active class II DNA transposon, *crawler*, has been identified in an industrial production strain of *A. oryzae* (OSI1013) under appropriate conditions (Ogasawara et al., 2009). In addition, in a constructed chromosomally reduced mutant of *A. oryzae*, the copy number of a gene (AO090005001597), which is a part of an LTR retrotransposable element, increased significantly (Jin et al., 2014). The discovery of this phenomenon is expected to improve the production capacity of heterologous recombinant proteins by constructing multicopy exogenous protein production strains in *A. oryzae* in the future.

PRODUCTION OF SECONDARY METABOLITES IN *A. ORYZAE*

As a versatile fermentative strain, *A. oryzae* cannot only produce a large number of amylases and proteases but also produce useful secondary metabolites; however, the research progress in this area is relatively slow. Moreover, *A. oryzae*, as the host for fungal secondary metabolite production, has a significant advantage in identifying the function of secondary metabolic genes compared to other filamentous fungi such as *A. nidulans*, in which almost no production of endogenous secondary metabolites was found. With the development of a large number of *Aspergillus* genome sequences in recent years, the production of some metabolites can be predicted through a comparative genomics approach, among which only a small part of the related gene clusters of secondary metabolites have been identified (Ehrlich and Mack, 2014; Takeda et al., 2014; Kjaerbolling et al., 2020). For example, genomic comparison analysis has shown that *A. oryzae* retains a highly intact gene cluster that produces penicillin but has very low yields. By artificially regulating the overexpression of biosynthetic genes by strong promoters, the yield of penicillin was increased by 100 times in *A. oryzae* (Marui et al., 2010a). In addition to penicillin, *A. oryzae* also produces useful secondary metabolites such as kojic acid (Marui et al., 2011; Yamada et al., 2014; Ammar et al., 2017). In addition, using the Cre/*loxP*-mediated marker recycling system, hyperproduction of kojic acid was achieved in *A. oryzae* by introducing the oxidoreductase gene *kojA* and transporter gene *kojT* (Zhang et al., 2017).

Epigenetic manipulation through the gene disruption or drug treatment [e.g., histone deacetylase inhibitors trichostatin A (TSA) and suberoylanilide hydroxamic acid (SAHA)] is one of the trend for waking up silent secondary metabolite genes cluster. It has been reported that the addition of the histone deacetylase inhibitor SAHA markedly improved the diversity of secondary metabolites in filamentous fungi (Zhu et al., 2019). In *A. oryzae*, through screening a gene-disruption library of transcription factors, Shinohara et al. (2016) found that the production of some secondary metabolites including astellolide F (14-deacetyl astellolide B) were significantly increased by the disruption of *cclA*, which encodes a component of the histone 3 lysine 4 (H3K4) methyltransferase complex of proteins associated with Set1 complex. Kawauchi et al. (2013) also showed that the fungus-specific sirtuin HstD/AoHst4 could coordinate the production of secondary metabolites by regulating the expression of *laeA*, which encodes a global regulator importantly involved in the regulation of fungal development and secondary metabolism.

Some studies have shown that *A. oryzae* can also be used as a host for heterologous expression of biosynthetic gene clusters for useful secondary metabolites, such as diterpene aphidicolin, which is a specific inhibitor of DNA polymerase α, and plant polyketide curcumin (Fujii et al., 2011; Kan et al., 2019). In particularly, a host strain with quadruple selectable markers (Jin et al., 2004b) has also been efficiently used for heterologous production of some fungal natural products (e.g., phytotoxic metabolites, basidiomycete terpenes, and plant hormones) by reconstituting these biosynthetic gene clusters in *A. oryzae* (Nagamine et al., 2019; Takino et al., 2019; Oikawa, 2020a,b). Moreover, the overexpression of *laeA* gene was also found to promote the overexpression of two clusters of heterologous biosynthetic genes from *A. nidulans*, resulting in the production of the corresponding metabolite, monacolin K or terrequinone A (Sakai et al., 2012). In summary, although some progress has been made in the study of secondary metabolites of *Aspergillus* species in recent years (Sanchez et al., 2012; Amare and Keller, 2014; He et al., 2018; Caesar et al., 2020), there are still many unknown fields awaiting further discovery.

CONCLUSION

Decoding the *A. oryzae* genome sequence provides abundant and reliable genetic information for a deep understanding of its genetic background and production performance. Subsequently, the establishment and rapid development of new genetic engineering technology in *A. oryzae* opened up more ways for its breeding of production strains and the utilization of industrial production. In recent years, although the production capacity of some heterologous proteins and secondary metabolites has been improved to some extent, it is far from the expected goal.

At present, in addition to these bottlenecks in the production of heterologous proteins mentioned above, there are still some problems that need to be further overcome, such as: (1) How to ensure high activity in the enzyme extraction process; (2) In industrial production, some macromolecular substances, such as wheat bran, rice bran, silage, corn, and soybean meal are difficult to utilize by *A. oryzae*. Therefore, biotechnological improvements are being made to degrade and utilize these substrates, thereby reducing production costs and pollution caused by raw material waste; (3) The large amount of heterologous protein production has a certain adverse effect on *A. oryzae* itself. (4) In the late growth stage of *A. oryzae*, the introduction of some strong promoters, such as *amyB* and *glaA* promoters, will be inhibited by high-concentration products, such as glucose. A study has shown that deletion of single and double *creA*/*creB* genes, which encode regulation factors involved in carbon catabolite repression, significantly improved amylase activity in submerged cultures containing high concentrations of inducing sugars compared to the control strain (Ichinose et al., 2014).

In addition, although the whole genome sequence has been deciphered, the function of most genes in *A. oryzae* is still unclear, and there remains many restrictions on its production and utilization. Therefore, there are still a large number of unknown functional genes and fields that need to be discovered and explored. Recent advances in omics techniques, such as comparative transcriptomics, proteomics and metabolomics, have opened up a new perspective for future research on functional genes and the exploration of protein secretion pathways. In summary, there remains a great space for further research and exploration on combining genetic engineering technology with *A. oryzae* production and application to obtain the breeding of highly efficient production strains.

AUTHOR CONTRIBUTIONS

F-JJ wrote the main manuscript text. SH and B-TW contributed to certain sections. LJ contributed to overall editing and proofreading. All the authors approved the submitted version.

FUNDING

This study was supported by the National Natural Science Foundation of China (31570107) and Priority Academic Program Development of Jiangsu Higher Education Institutions (PAPD).

REFERENCES

Abremski, K., Wierzbicki, A., Frommer, B., and Hoess, R. H. (1986). Bacteriophage P1 Cre-loxP site-specific recombination. Site-specific DNA topoisomerase activity of the Cre recombination protein. *J. Biol. Chem.* 261, 391–396.

Akao, T., Sano, M., Yamada, O., Akeno, T., Fujii, K., Goto, K., et al. (2007). Analysis of expressed sequence tags from the fungus *Aspergillus oryzae* cultured under different conditions. *DNA Res.* 14, 47–57. doi: 10.1093/dnares/dsm008

Amare, M. G., and Keller, N. P. (2014). Molecular mechanisms of *Aspergillus flavus* secondary metabolism and development. *Fungal Genet. Biol.* 66, 11–18. doi: 10.1016/j.fgb.2014.02.008

Ammar, H. A. M., Ezzat, S. M., and Houseny, A. M. (2017). Improved production of kojic acid by mutagenesis of *Aspergillus flavus* HAk1 and *Aspergillus oryzae* HAk2 and their potential antioxidant activity. *3 Biotech.* 7:276. doi: 10.1007/s13205-017-0905-4

Bando, H., Hisada, H., Ishida, H., Hata, Y., Katakura, Y., and Kondo, A. (2011). Isolation of a novel promoter for efficient protein expression by *Aspergillus oryzae* in solid-state culture. *Appl. Microbiol. Biotechnol.* 92, 561–569. doi: 10.1007/s00253-011-3446-5

Caesar, L. K., Kelleher, N. L., and Keller, N. P. (2020). In the fungus where it happens: history and future propelling *Aspergillus nidulans* as the archetype of natural products research. *Fungal Genet. Biol.* 144:103477. doi: 10.1016/j.fgb.2020.103477

Conesa, A., Punt, P. J., van Luijk, N., and van den Hondel, C. A. (2001). The secretion pathway in filamentous fungi: a biotechnological view. *Fungal Genet. Biol.* 33, 155–171. doi: 10.1006/fgbi.2001.1276

Cong, L., Ran, F. A., Cox, D., Lin, S. L., Barretto, R., Habib, N., et al. (2013). Multiplex genome engineering using CRISPR/Cas systems. *Science* 339, 819–823. doi: 10.1126/science.1231143

Cooper, A. A., and Stevens, T. H. (1996). Vps10p cycles between the late-Golgi and prevacuolar compartments in its function as the sorting receptor for multiple yeast vacuolar hydrolases. *J. Cell Biol.* 133, 529–541. doi: 10.1083/jcb.133.3.529

Daboussi, M. J. (1997). Fungal transposable elements and genome evolution. *Genetica* 100, 253–260.

Daboussi, M. J., and Capy, P. (2003). Transposable elements in filamentous fungi. *Annu. Rev. Microbiol.* 57, 275–299. doi: 10.1146/annurev.micro.57.030502.091029

de Ruiter-Jacobs, Y. M., Broekhuijsen, M., Unkles, S. E., Campbell, E. I., Kinghorn, J. R., Contreras, R., et al. (1989). A gene transfer system based on the homologous pyrG gene and efficient expression of bacterial genes in *Aspergillus oryzae*. *Curr. Genet.* 16, 159–163. doi: 10.1007/BF00391472

DiCarlo, J. E., Norville, J. E., Mali, P., Rios, X., Aach, J., and Church, G. M. (2013). Genome engineering in *Saccharomyces cerevisiae* using CRISPR-Cas systems. *Nucleic Acids Res.* 41, 4336–4343. doi: 10.1093/nar/gkt135

Dong, L. B., Lin, X. T., Yu, D., Huang, L. G., Wang, B., and Pan, L. (2020). High-level expression of highly active and thermostable trehalase from *Myceliophthora thermophila* in *Aspergillus niger* by using the CRISPR/Cas9 tool and its application in ethanol fermentation. *J. Ind. Microbiol. Biotechnol.* 47, 133–144. doi: 10.1007/s10295-019-02252-9

Ehrlich, K. C., and Mack, B. M. (2014). Comparison of expression of secondary metabolite biosynthesis cluster genes in *Aspergillus flavus*. A. parasiticus, and A. oryzae. *Toxins* 6, 1916–1928. doi: 10.3390/toxins6061916

Fan, J., Zhang, Z., Long, C., He, B., Hu, Z., Jiang, C., et al. (2020). Identification and functional characterization of glycerol dehydrogenase reveal the role in kojic acid synthesis in *Aspergillus oryzae*. *World J. Microbiol. Biotechnol.* 36:136. doi: 10.1007/s11274-020-02912-4

Fleissner, A., and Dersch, P. (2010). Expression and export: recombinant protein production systems for *Aspergillus*. *Appl. Microbiol. Biotechnol.* 87, 1255–1270. doi: 10.1007/s00253-010-2672-6

Frandsen, R. J. (2011). A guide to binary vectors and strategies for targeted genome modification in fungi using *Agrobacterium tumefaciens*-mediated transformation. *J. Microbiol. Methods* 87, 247–262. doi: 10.1016/j.mimet.2011.09.004

Fujii, R., Minami, A., Tsukagoshi, T., Sato, N., Sahara, T., Ohgiya, S., et al. (2011). Total biosynthesis of diterpene aphidicolin, a specific inhibitor of DNA polymerase alpha: heterologous expression of four biosynthetic genes in *Aspergillus oryzae*. *Biosci. Biotechnol. Biochem.* 75, 1813–1817. doi: 10.1271/bbb.110366

Galagan, J. E., Calvo, S. E., Cuomo, C., Ma, L. J., Wortman, J. R., Batzoglou, S., et al. (2005). Sequencing of *Aspergillus nidulans* and comparative analysis with A. fumigatus and A. oryzae. *Nature* 438, 1105–1115. doi: 10.1038/nature04341

Gasser, B., and Mattanovich, D. (2007). Antibody production with yeasts and filamentous fungi: on the road to large scale? *Biotechnol. Lett.* 29, 201–212. doi: 10.1007/s10529-006-9237-x

Generoso, W. C., Gottardi, M., Oreb, M., and Boles, E. (2016). Simplified CRISPR-Cas genome editing for *Saccharomyces cerevisiae*. *J. Microbiol. Methods* 127, 203–205. doi: 10.1016/j.mimet.2016.06.020

Gomi, K. (2019). Regulatory mechanisms for amylolytic gene expression in the koji mold *Aspergillus oryzae*. *Biosci. Biotechnol. Biochem.* 83, 1385–1401. doi: 10.1080/09168451.2019.1625265

Gomi, K., Iimura, Y., and Hara, S. (1987). Integrative transformation of *Aspergillus oryzae* with a plasmid containing the *Aspergillus nidulans* argB gene. *Agric. Biol. Chem.* 51, 2549–2555.

Gomi, K., Kitamoto, K., and Kumagai, C. (1991). Cloning and molecular characterization of the acetamidase-encoding gene (amdS) from *Aspergillus oryzae*. *Gene* 108, 91–98. doi: 10.1016/0378-1119(91)90491-s

Gu, H., Zou, Y. R., and Rajewsky, K. (1993). Independent control of immunoglobulin switch recombination at individual switch regions evidenced through Cre-loxP-mediated gene targeting. *Cell* 73, 1155–1164. doi: 10.1016/0092-8674(93)90644-6

Hama, S., Tamalampudi, S., Suzuki, Y., Yoshida, A., Fukuda, H., and Kondo, A. (2008). Preparation and comparative characterization of immobilized *Aspergillus oryzae* expressing Fusarium heterosporum lipase for enzymatic biodiesel production. *Appl. Microbiol. Biotechnol.* 81, 637–645. doi: 10.1007/s00253-008-1689-6

Hara, S., Jin, F. J., Takahashi, T., and Koyama, Y. (2012). A further study on chromosome minimization by protoplast fusion in *Aspergillus oryzae*. *Mol. Genet. Genomics* 287, 177–187. doi: 10.1007/s00438-011-0669-1

Hata, Y., Ishida, H., Ichikawa, E., Kawato, A., Suginami, K., and Imayasu, S. (1998). Nucleotide sequence of an alternative glucoamylase-encoding gene (glaB) expressed in solid-state culture of *Aspergillus oryzae*. *Gene* 207, 127–134. doi: 10.1016/s0378-1119(97)00612-4

He, Y., Wang, B., Chen, W., Cox, R. J., He, J., and Chen, F. (2018). Recent advances in reconstructing microbial secondary metabolites biosynthesis in *Aspergillus* spp. *Biotechnol. Adv.* 36, 739–783. doi: 10.1016/j.biotechadv.2018.02.001

Hoang, H. D., Maruyama, J., and Kitamoto, K. (2015). Modulating endoplasmic reticulum-Golgi cargo receptors for improving secretion of carrier-fused heterologous proteins in the filamentous fungus *Aspergillus oryzae*. *Appl. Environ. Microbiol.* 81, 533–543. doi: 10.1128/AEM.02133-14

Hoshida, H., Fujita, T., Murata, K., Kubo, K., and Akada, R. (2005). Copper-dependent production of a *Pycnoporus coccineus* extracellular laccase in *Aspergillus oryzae* and *Saccharomyces cerevisiae*. *Biosci. Biotechnol. Biochem.* 69, 1090–1097. doi: 10.1271/bbb.69.1090

Huynh, H. H., Morita, N., Sakamoto, T., Katayama, T., Miyakawa, T., Tanokura, M., et al. (2020). Functional production of human antibody by the filamentous fungus *Aspergillus oryzae*. *Fungal. Biol. Biotechnol.* 7:7. doi: 10.1186/s40694-020-00098-w

Ichikawa, K., Shiono, Y., Shintani, T., Watanabe, A., Kanzaki, H., Gomi, K., et al. (2020). Efficient production of recombinant tannase in *Aspergillus oryzae* using an improved glucoamylase gene promoter. *J. Biosci. Bioeng.* 129, 150–154. doi: 10.1016/j.jbiosc.2019.08.002

Ichinose, S., Tanaka, M., Shintani, T., and Gomi, K. (2014). Improved alpha-amylase production by *Aspergillus oryzae* after a double deletion of genes involved in carbon catabolite repression. *Appl. Microbiol. Biotechnol.* 98, 335–343. doi: 10.1007/s00253-013-5353-4

Idnurm, A., Bailey, A. M., Cairns, T. C., Elliott, C. E., Foster, G. D., Ianiri, G., et al. (2017). A silver bullet in a golden age of functional genomics: the impact of Agrobacterium-mediated transformation of fungi. *Fungal Biol. Biotechnol.* 4:6. doi: 10.1186/s40694-017-0035-0

Ishida, H., Hata, Y., Kawato, A., and Abe, Y. (2006). Improvement of the glaB promoter expressed in solid-state fermentation (SSF) of *Aspergillus oryzae*. *Biosci. Biotechnol. Biochem.* 70, 1181–1187. doi: 10.1271/bbb.70.1181

Ishida, H., Hata, Y., Kawato, A., Abe, Y., and Kashiwagi, Y. (2004). Isolation of a novel promoter for efficient protein production in *Aspergillus oryzae*. *Biosci. Biotechnol. Biochem.* 68, 1849–1857. doi: 10.1271/bbb.68.1849

Ishida, H., Matsumura, K., Hata, Y., Kawato, A., Suginami, K., Abe, Y., et al. (2001). Establishment of a hyper-protein production system in submerged *Aspergillus oryzae* culture under tyrosinase-encoding gene (melO) promoter control. *Appl. Microbiol. Biotechnol.* 57, 131–137. doi: 10.1007/s002530100771

Jeenes, D. J., Mackenzie, D. A., Roberts, I. N., and Archer, D. B. (1991). Heterologous protein production by filamentous fungi. *Biotechnol. Genet. Eng. Rev.* 9, 327–367.

Jin, F. J., Hara, S., Sato, A., and Koyama, Y. (2014). Discovery and analysis of an active long terminal repeat-retrotransposable element in *Aspergillus oryzae*. *J. Gen. Appl. Microbiol.* 60, 1–6. doi: 10.2323/jgam.60.1

Jin, F. J., Katayama, T., Maruyama, J. I., and Kitamoto, K. (2016). Comparative genomic analysis identified a mutation related to enhanced heterologous protein production in the filamentous fungus *Aspergillus oryzae*. *Appl. Microbiol. Biotechnol.* 100, 9163–9174. doi: 10.1007/s00253-016-7714-2

Jin, F. J., Maruyama, J., Juvvadi, P. R., Arioka, M., and Kitamoto, K. (2004a). Adenine auxotrophic mutants of *Aspergillus oryzae*: development of a novel transformation system with triple auxotrophic hosts. *Biosci. Biotechnol. Biochem.* 68, 656–662. doi: 10.1271/bbb.68.656

Jin, F. J., Maruyama, J., Juvvadi, P. R., Arioka, M., and Kitamoto, K. (2004b). Development of a novel quadruple auxotrophic host transformation system by argB gene disruption using adeA gene and exploiting adenine auxotrophy in *Aspergillus oryzae*. *FEMS Microbiol. Lett.* 239, 79–85. doi: 10.1016/j.femsle.2004.08.025

Jin, F. J., Nishida, M., Hara, S., and Koyama, Y. (2011a). Identification and characterization of a putative basic helix-loop-helix transcription factor involved in the early stage of conidiophore development in *Aspergillus oryzae*. *Fungal Genet. Biol.* 48, 1108–1115. doi: 10.1016/j.fgb.2011.10.001

Jin, F. J., Takahashi, T., Matsushima, K., Hara, S., Shinohara, Y., Maruyama, J., et al. (2011b). SclR, a basic helix-loop-helix transcription factor, regulates hyphal morphology and promotes sclerotial formation in *Aspergillus oryzae*. *Eukaryot Cell* 10, 945–955. doi: 10.1128/EC.00013-11

Jin, F. J., Takahashi, T., Machida, M., and Koyama, Y. (2009). Identification of a basic helix-loop-helix-type transcription regulator gene in *Aspergillus oryzae* by systematically deleting large chromosomal segments. *Appl. Environ. Microbiol.* 75, 5943–5951. doi: 10.1128/AEM.00975-09

Jin, F. J., Takahashi, T., Utsushikawa, M., Furukido, T., Nishida, M., Ogawa, M., et al. (2010). A trial of minimization of chromosome 7 in *Aspergillus oryzae* by multiple chromosomal deletions. *Mol. Genet. Genomics* 283, 1–12. doi: 10.1007/s00438-009-0494-y

Jin, F. J., Watanabe, T., Juvvadi, P. R., Maruyama, J., Arioka, M., and Kitamoto, K. (2007). Double disruption of the proteinase genes, tppA and pepE, increases the production level of human lysozyme by *Aspergillus oryzae*. *Appl. Microbiol. Biotechnol.* 76, 1059–1068. doi: 10.1007/s00253-007-1088-4

Jinek, M., Chylinski, K., Fonfara, I., Hauer, M., Doudna, J. A., and Charpentier, E. (2012). A programmable Dual-RNA-Guided DNA endonuclease in adaptive bacterial immunity. *Science* 337, 816–821. doi: 10.1126/science.1225829

Kan, E., Katsuyama, Y., Maruyama, J. I., Tamano, K., Koyama, Y., and Ohnishi, Y. (2019). Production of the plant polyketide curcumin in *Aspergillus oryzae*: strengthening malonyl-CoA supply for yield improvement. *Biosci. Biotechnol. Biochem.* 83, 1372–1381. doi: 10.1080/09168451.2019.1606699

Katayama, T., Nakamura, H., Zhang, Y., Pascal, A., Fujii, W., and Maruyama, J. I. (2019). Forced recycling of an AMA1-based genome-editing plasmid allows for efficient multiple gene deletion/integration in the industrial filamentous fungus *Aspergillus oryzae*. *Appl. Environ. Microbiol.* 85:e01896-18. doi: 10.1128/AEM.01896-18

Katayama, T., Tanaka, Y., Okabe, T., Nakamura, H., Fujii, W., Kitamoto, K., et al. (2016). Development of a genome editing technique using the CRISPR/Cas9 system in the industrial filamentous fungus *Aspergillus oryzae*. *Biotechnol. Lett.* 38, 637–642. doi: 10.1007/s10529-015-2015-x

Kawauchi, M., Nishiura, M., and Iwashita, K. (2013). Fungus-specific sirtuin HstD coordinates secondary metabolism and development through control of LaeA. *Eukaryotic Cell* 12, 1087–1096. doi: 10.1128/Ec.00003-13

Kimura, S., Maruyama, J., Kikuma, T., Arioka, M., and Kitamoto, K. (2011). Autophagy delivers misfolded secretory proteins accumulated in endoplasmic reticulum to vacuoles in the filamentous fungus *Aspergillus oryzae*. *Biochem. Biophys. Res. Commun.* 406, 464–470. doi: 10.1016/j.bbrc.2011.02.075

Kitamoto, K. (2002). Molecular biology of the Koji molds. *Adv. Appl. Microbiol.* 51, 129–153. doi: 10.1016/s0065-2164(02)51004-2

Kitamoto, K. (2015). Cell biology of the Koji mold *Aspergillus oryzae*. *Biosci. Biotechnol. Biochem.* 79, 863–869. doi: 10.1080/09168451.2015.1023249

Kitamoto, N., Matsui, J., Kawai, Y., Kato, A., Yoshino, S., Ohmiya, K., et al. (1998). Utilization of the TEF1-alpha gene (TEF1) promoter for expression of polygalacturonase genes, pgaA and pgaB, in *Aspergillus oryzae*. *Appl. Microbiol. Biotechnol.* 50, 85–92. doi: 10.1007/s002530051260

Kjaerbolling, I., Vesth, T., Frisvad, J. C., Nybo, J. L., Theobald, S., Kildgaard, S., et al. (2020). A comparative genomics study of 23 *Aspergillus* species from section Flavi. *Nat. Commun.* 11:1106. doi: 10.1038/s41467-019-14051-y

Kobayashi, T., Abe, K., Asai, K., Gomi, K., Juvvadi, P. R., Kato, M., et al. (2007). Genomics of *Aspergillus oryzae*. *Biosci. Biotechnol. Biochem.* 71, 646–670. doi: 10.1271/bbb.60550

Koda, A., Bogaki, T., Minetoki, T., and Hirotsune, M. (2006). 5′ Untranslated region of the Hsp12 gene contributes to efficient translation in *Aspergillus oryzae*. *Appl. Microbiol, Biotechnol.* 70, 333–336. doi: 10.1007/s00253-005-0083-x

Koda, A., Minetoki, T., Ozeki, K., and Hirotsune, M. (2004). Translation efficiency mediated by the 5′ untranslated region greatly affects protein production in *Aspergillus oryzae*. *Appl. Microbiol. Biotechnol.* 66, 291–296. doi: 10.1007/s00253-004-1681-8

Kubodera, T., Yamashita, N., and Nishimura, A. (2000). Pyrithiamine resistance gene (ptrA) of *Aspergillus oryzae*: cloning, characterization and application as a dominant selectable marker for transformation. *Biosci. Biotechnol. Biochem.* 64, 1416–1421. doi: 10.1271/bbb.64.1416

Kudo, K., Watanabe, A., Ujiie, S., Shintani, T., and Gomi, K. (2015). Purification and enzymatic characterization of secretory glycoside hydrolase family 3 (GH3) aryl beta-glucosidases screened from *Aspergillus oryzae* genome. *J. Biosci. Bioeng.* 120, 614–623. doi: 10.1016/j.jbiosc.2015.03.019

Lemmon, S. K., and Traub, L. M. (2000). Sorting in the endosomal system in yeast and animal cells. *Curr. Opin. Cell Biol.* 12, 457–466. doi: 10.1016/s0955-0674(00)00117-4

Lissau, B. G., Pedersen, P. B., Petersen, B. R., and Budolfsen, G. (1998). Safety evaluation of a fungal pectinesterase enzyme preparation and its use in food. *Food Addit. Contam.* 15, 627–636. doi: 10.1080/02652039809374691

Liu, C., Minami, A., Ozaki, T., Wu, J., Kawagishi, H., Maruyama, J. I., et al. (2019). Efficient reconstitution of basidiomycota diterpene erinacine gene cluster in ascomycota host *Aspergillus oryzae* Based on Genomic DNA sequences. *J. Am. Chem. Soc.* 141, 15519–15523. doi: 10.1021/jacs.9b08935

Liu, J., Xie, Z., Shin, H. D., Li, J., Du, G., Chen, J., et al. (2017). Rewiring the reductive tricarboxylic acid pathway and L-malate transport pathway of *Aspergillus oryzae* for overproduction of L-malate. *J. Biotechnol.* 253, 1–9. doi: 10.1016/j.jbiotec.2017.05.011

Liu, R., Chen, L., Jiang, Y., Zhou, Z., and Zou, G. (2015). Efficient genome editing in filamentous fungus *Trichoderma reesei* using the CRISPR/Cas9 system. *Cell Discov.* 1:15007. doi: 10.1038/celldisc.2015.7

Liu, Z., and Friesen, T. L. (2012). Polyethylene glycol (PEG)-mediated transformation in filamentous fungal pathogens. *Methods Mol. Biol.* 835, 365–375. doi: 10.1007/978-1-61779-501-5_21

Lombrana, M., Moralejo, F. J., Pinto, R., and Martin, J. F. (2004). Modulation of Aspergillus awamori thaumatin secretion by modification of bipA gene expression. *Appl. Environ. Microbiol.* 70, 5145–5152. doi: 10.1128/AEM.70.9.5145-5152.2004

Machida, M. (2002). Progress of *Aspergillus oryzae* genomics. *Adv. Appl. Microbiol.* 51, 81–106. doi: 10.1016/s0065-2164(02)51002-9

Machida, M., Asai, K., Sano, M., Tanaka, T., Kumagai, T., Terai, G., et al. (2005). Genome sequencing and analysis of *Aspergillus oryzae*. *Nature* 438, 1157–1161. doi: 10.1038/nature04300

Machida, M., Yamada, O., and Gomi, K. (2008). Genomics of *Aspergillus oryzae*: learning from the history of Koji mold and exploration of its future. *DNA Res.* 15, 173–183. doi: 10.1093/dnares/dsn020

Marcusson, E. G., Horazdovsky, B. F., Cereghino, J. L., Gharakhanian, E., and Emr, S. D. (1994). The sorting receptor for yeast vacuolar carboxypeptidase Y is encoded by the VPS10 gene. *Cell* 77, 579–586. doi: 10.1016/0092-8674(94)90219-4

Marui, J., Ohashi-Kunihiro, S., Ando, T., Nishimura, M., Koike, H., and Machida, M. (2010a). Penicillin biosynthesis in *Aspergillus oryzae* and its overproduction by genetic engineering. *J. Biosci. Bioeng.* 110, 8–11. doi: 10.1016/j.jbiosc.2010.01.001

Marui, J., Yoshimi, A., Hagiwara, D., Fujii-Watanabe, Y., Oda, K., Koike, H., et al. (2010b). Use of the *Aspergillus oryzae* actin gene promoter in a novel reporter system for exploring antifungal compounds and their target genes. *Appl. Microbiol. Biotechnol.* 87, 1829–1840. doi: 10.1007/s00253-010-2627-y

Marui, J., Yamane, N., Ohashi-Kunihiro, S., Ando, T., Terabayashi, Y., Sano, M., et al. (2011). Kojic acid biosynthesis in *Aspergillus oryzae* is regulated by a Zn(II)(2)Cys(6) transcriptional activator and induced by kojic acid at the transcriptional level. *J. Biosci. Bioeng.* 112, 40–43. doi: 10.1016/j.jbiosc.2011.03.010

Maruyama, J., and Kitamoto, K. (2008). Multiple gene disruptions by marker recycling with highly efficient gene-targeting background (DeltaligD) in *Aspergillus oryzae*. *Biotechnol. Lett.* 30, 1811–1817. doi: 10.1007/s10529-008-9763-9

Matsushita-Morita, M., Tada, S., Suzuki, S., Hattori, R., Marui, J., Furukawa, I., et al. (2011). Overexpression and characterization of an extracellular leucine aminopeptidase from *Aspergillus oryzae*. *Curr. Microbiol.* 62, 557–564. doi: 10.1007/s00284-010-9744-9

Matsu-Ura, T., Baek, M., Kwon, J., and Hong, C. (2015). Efficient gene editing in *Neurospora crassa* with CRISPR technology. *Fungal Biol. Biotechnol.* 2:4. doi: 10.1186/s40694-015-0015-1

Mattern, I. E., Unkles, S., Kinghorn, J. R., Pouwels, P. H., and van den Hondel, C. A. (1987). Transformation of *Aspergillus oryzae* using the A. niger pyrG gene. *Mol. Gen. Genet.* 210, 460–461. doi: 10.1007/BF00327197

Melnichuk, N., Braia, M. J., Anselmi, P. A., Meini, M. R., and Romanini, D. (2020). Valorization of two agroindustrial wastes to produce alpha-amylase enzyme from *Aspergillus oryzae* by solid-state fermentation. *Waste Manag.* 106, 155–161. doi: 10.1016/j.wasman.2020.03.025

Merz, M., Eisele, T., Berends, P., Appel, D., Rabe, S., Blank, I., et al. (2015). Flavourzyme, an enzyme preparation with industrial relevance: automated nine-step purification and partial characterization of eight enzymes. *J. Agric. Food Chem.* 63, 5682–5693. doi: 10.1021/acs.jafc.5b01665

Michielse, C. B., Arentshorst, M., Ram, A. F., and van den Hondel, C. A. (2005). Agrobacterium-mediated transformation leads to improved gene replacement efficiency in *Aspergillus awamori*. *Fungal Genet. Biol.* 42, 9–19. doi: 10.1016/j.fgb.2004.06.009

Mizutani, O., Arazoe, T., Toshida, K., Hayashi, R., Ohsato, S., Sakuma, T., et al. (2017). Detailed analysis of targeted gene mutations caused by the Platinum-Fungal TALENs in *Aspergillus oryzae* RIB40 strain and a ligD disruptant. *J. Biosci. Bioeng.* 123, 287–293. doi: 10.1016/j.jbiosc.2016.09.014

Mizutani, O., Kudo, Y., Saito, A., Matsuura, T., Inoue, H., Abe, K., et al. (2008). A defect of LigD (human Lig4 homolog) for nonhomologous end joining significantly improves efficiency of gene-targeting in *Aspergillus oryzae*. *Fungal Genet. Biol.* 45, 878–889. doi: 10.1016/j.fgb.2007.12.010

Mizutani, O., Masaki, K., Gomi, K., and Iefuji, H. (2012). Modified Cre-loxP recombination in *Aspergillus oryzae* by direct introduction of Cre recombinase for marker gene rescue. *Appl. Environ. Microbiol.* 78, 4126–4133. doi: 10.1128/AEM.00080-12

Moralejo, F. J., Watson, A. J., Jeenes, D. J., Archer, D. B., and Martin, J. F. (2001). A defined level of protein disulfide isomerase expression is required for optimal secretion of thaumatin by *Aspegillus awamori*. *Mol. Genet. Genomics* 266, 246–253. doi: 10.1007/s004380100550

Morishita, Y., Sonohara, T., Taniguchi, T., Adachi, K., Fujita, M., and Asai, T. (2020). Synthetic-biology-based discovery of a fungal macrolide from *Macrophomina phaseolina*. *Org. Biomol. Chem.* 18, 2813–2816. doi: 10.1039/d0ob00519c

Mulder, H. J., Nikolaev, I., and Madrid, S. M. (2006). HACA, the transcriptional activator of the unfolded protein response (UPR) in *Aspergillus niger*, binds to partly palindromic UPR elements of the consensus sequence 5′-CAN(G/A)NTGT/GCCT-3'. *Fungal Genet. Biol.* 43, 560–572. doi: 10.1016/j.fgb.2006.02.005

Murthy, P. S., and Kusumoto, K. I. (2015). Acid protease production by *Aspergillus oryzae* on potato pulp powder with emphasis on glycine releasing activity: a benefit to the food industry. *Food Bioprod. Process.* 96, 180–188. doi: 10.1016/j.fbp.2015.07.013

Nagamine, S., Liu, C. W., Nishishita, J., Kozaki, T., Sogahata, K., Sato, Y., et al. (2019). Ascomycete *Aspergillus oryzae* is an efficient expression host for production of basidiomycete terpenes by using genomic DNA sequences. *Appl. Environ. Microbiol.* 85:e00409-19. doi: 10.1128/AEM.00409-19

Nakamura, H., Katayama, T., Okabe, T., Iwashita, K., Fujii, W., Kitamoto, K., et al. (2017). Highly efficient gene targeting in *Aspergillus oryzae* industrial strains under ligD mutation introduced by genome editing: strain-specific differences in the effects of deleting EcdR, the negative regulator of sclerotia formation. *J. Gen. Appl. Microbiol.* 63, 172–178. doi: 10.2323/jgam.2016.10.002

Nemoto, T., Watanabe, T., Mizogami, Y., Maruyama, J., and Kitamoto, K. (2009). Isolation of *Aspergillus oryzae* mutants for heterologous protein production from a double proteinase gene disruptant. *Appl. Microbiol. Biotechnol.* 82, 1105–1114. doi: 10.1007/s00253-008-1851-1

Nguyen, K. T., Ho, Q. N., Do, L. T. B. X., Mai, L. T. D., Pham, D. N., Tran, H. T. T., et al. (2017). A new and efficient approach for construction of uridine/uracil auxotrophic mutants in the filamentous fungus *Aspergillus oryzae* using *Agrobacterium tumefaciens*-mediated transformation. *World J. Microbiol. Biotechnol.* 33:107. doi: 10.1007/s11274-017-2275-9

Nguyen, K. T., Ho, Q. N., Pham, T. H., Phan, T. N., and Tran, V. T. (2016). The construction and use of versatile binary vectors carrying pyrG auxotrophic marker and fluorescent reporter genes for Agrobacterium-mediated transformation of *Aspergillus oryzae*. *World J. Microbiol. Biotechnol.* 32:204. doi: 10.1007/s11274-016-2168-3

Nielsen, M. L., Albertsen, L., Lettier, G., Nielsen, J. B., and Mortensen, U. H. (2006). Efficient PCR-based gene targeting with a recyclable marker for *Aspergillus nidulans*. *Fungal Genet. Biol.* 43, 54–64. doi: 10.1016/j.fgb.2005.09.005

Nierman, W. C., Pain, A., Anderson, M. J., Wortman, J. R., Kim, H. S., Arroyo, J., et al. (2005). Genomic sequence of the pathogenic and allergenic filamentous fungus *Aspergillus fumigatus*. *Nature* 438, 1151–1156. doi: 10.1038/nature04332

Nodvig, C. S., Hoof, J. B., Kogle, M. E., Jarczynska, Z. D., Lehmbeck, J., Klitgaard, D. K., et al. (2018). Efficient oligo nucleotide mediated CRISPR-Cas9 gene editing in *Aspergilli*. *Fungal Genet. Biol.* 115, 78–89. doi: 10.1016/j.fgb.2018.01.004

Ogasawara, H., Obata, H., Hata, Y., Takahashi, S., and Gomi, K. (2009). Crawler, a novel Tc1/mariner-type transposable element in *Aspergillus oryzae* transposes

under stress conditions. *Fungal Genet. Biol.* 46, 441–449. doi: 10.1016/j.fgb.2009.02.007

Ohno, A., Maruyama, J., Nemoto, T., Arioka, M., and Kitamoto, K. (2011). A carrier fusion significantly induces unfolded protein response in heterologous protein production by *Aspergillus oryzae*. *Appl. Microbiol. Biotechnol.* 92, 1197–1206. doi: 10.1007/s00253-011-3487-9

Oikawa, H. (2020a). Heterologous production of fungal natural products: reconstitution of biosynthetic gene clusters in model host *Aspergillus oryzae*. *Proc. Jpn. Acad. Ser. B Phys. Biol. Sci.* 96, 420–430. doi: 10.2183/pjab.96.031

Oikawa, H. (2020b). Reconstitution of biosynthetic machinery of fungal natural products in heterologous hosts. *Biosci. Biotechnol. Biochem,* 84, 433–444. doi: 10.1080/09168451.2019.1690976

Punt, P. J., van Gemeren, I. A., Drint-Kuijvenhoven, J., Hessing, J. G., van Muijlwijk-Harteveld, G. M., Beijersbergen, A., et al. (1998). Analysis of the role of the gene bipA, encoding the major endoplasmic reticulum chaperone protein in the secretion of homologous and heterologous proteins in black *Aspergilli*. *Appl. Microbiol. Biotechnol.* 50, 447–454. doi: 10.1007/s002530051319

Punya, J., Tachaleat, A., Wattanachaisaereekul, S., Haritakun, R., Boonlarppradab, C., and Cheevadhanarak, S. (2013). Functional expression of a foreign gene in *Aspergillus oryzae* producing new pyrone compounds. *Fungal Genet. Biol.* 50, 55–62. doi: 10.1016/j.fgb.2012.10.005

Reggiori, F., and Klionsky, D. J. (2002). Autophagy in the eukaryotic cell. *Eukaryot Cell* 1, 11–21. doi: 10.1128/ec.01.1.11-21.2002

Rey, M. W., Brown, K. M., Golightly, E. J., Fuglsang, C. C., Nielsen, B. R., Hendriksen, H. V., et al. (2003). Cloning, heterologous expression, and characterization of Thielavia terrestris glucoamylase. *Appl. Biochem. Biotechnol.* 111, 153–166. doi: 10.1385/abab:111:3:153

Rojas-Sanchez, U., Lopez-Calleja, A. C., Millan-Chiu, B. E., Fernandez, F., Loske, A. M., and Gomez-Lim, M. A. (2020). Enhancing the yield of human erythropoietin in *Aspergillus niger* by introns and CRISPR-Cas9. *Protein Exp. Purif.* 168:105570. doi: 10.1016/j.pep.2020.105570

Ron, D., and Walter, P. (2007). Signal integration in the endoplasmic reticulum unfolded protein response. *Nat. Rev. Mol. Cell Biol.* 8, 519–529. doi: 10.1038/nrm2199

Sakai, K., Kinoshita, H., and Nihira, T. (2012). Heterologous expression system in *Aspergillus oryzae* for fungal biosynthetic gene clusters of secondary metabolites. *Appl. Microbiol. Biotechnol.* 93, 2011–2022. doi: 10.1007/s00253-011-3657-9

Sanchez, J. F., Somoza, A. D., Keller, N. P., and Wang, C. C. (2012). Advances in *Aspergillus* secondary metabolite research in the post-genomic era. *Nat. Prod. Rep.* 29, 351–371. doi: 10.1039/c2np00084a

Sauer, B. (1987). Functional expression of the cre-lox site-specific recombination system in the yeast *Saccharomyces cerevisiae*. *Mol. Cell Biol.* 7, 2087–2096. doi: 10.1128/mcb.7.6.2087

Schiml, S., and Puchta, H. (2016). Revolutionizing plant biology: multiple ways of genome engineering by CRISPR/Cas. *Plant Methods* 12:8. doi: 10.1186/s13007-016-0103-0

Shima, Y., Ito, Y., Kaneko, S., Hatabayashi, H., Watanabe, Y., Adachi, Y., et al. (2009). Identification of three mutant loci conferring carboxin-resistance and development of a novel transformation system in *Aspergillus oryzae*. *Fungal Genet. Biol.* 46, 67–76. doi: 10.1016/j.fgb.2008.10.005

Shinohara, Y., Kawatani, M., Futamura, Y., Osada, H., and Koyama, Y. (2016). An overproduction of astellolides induced by genetic disruption of chromatin-remodeling factors in *Aspergillus oryzae*. *J. Antibiot.* 69, 4–8. doi: 10.1038/ja.2015.73

Shmakov, S., Smargon, A., Scott, D., Cox, D., Pyzocha, N., Yan, W., et al. (2017). Diversity and evolution of class 2 CRISPR-Cas systems. *Nat. Rev. Microbiol.* 15, 169–182. doi: 10.1038/nrmicro.2016.184

Shoji, J. Y., Maruyama, J., Arioka, M., and Kitamoto, K. (2005). Development of *Aspergillus oryzae* thiA promoter as a tool for molecular biological studies. *FEMS Microbiol. Lett.* 244, 41–46. doi: 10.1016/j.femsle.2005.01.014

Sieburth, L. E., Drews, G. N., and Meyerowitz, E. M. (1998). Non-autonomy of AGAMOUS function in flower development: use of a Cre/loxP method for mosaic analysis in *Arabidopsis*. *Development* 125, 4303–4312.

Song, R., Zhai, Q., Sun, L., Huang, E., Zhang, Y., Zhu, Y., et al. (2019). CRISPR/Cas9 genome editing technology in filamentous fungi: progress and perspective. *Appl. Microbiol. Biotechnol.* 103, 6919–6932. doi: 10.1007/s00253-019-10007-w

Sun, Y. L., Niu, Y. L., He, B., Ma, L., Li, G. H., Tran, V. T., et al. (2019). Dual selection marker transformation system using *Agrobacterium tumefaciens* for the industrial *Aspergillus oryzae* 3.042. *J. Microbiol. Biotechnol.* 29, 230–234. doi: 10.4014/jmb.1811.11027

Suzuki, S., Tada, S., Fukuoka, M., Taketani, H., Tsukakoshi, Y., Matsushita, M., et al. (2009). A novel transformation system using a bleomycin resistance marker with chemosensitizers for *Aspergillus oryzae*. *Biochem. Biophys. Res. Commun.* 383, 42–47. doi: 10.1016/j.bbrc.2009.03.108

Suzuki, T., Oiso, N., Gautam, R., Novak, E. K., Panthier, J. J., Suprabha, P. G., et al. (2003). The mouse organellar biogenesis mutant buff results from a mutation in Vps33a, a homologue of yeast vps33 and *Drosophila* carnation. *Proc. Natl. Acad. Sci. U.S.A.* 100, 1146–1150. doi: 10.1073/pnas.0237292100

Takahashi, T., Jin, F. J., and Koyama, Y. (2009). Nonhomologous end-joining deficiency allows large chromosomal deletions to be produced by replacement-type recombination in *Aspergillus oryzae*. *Fungal Genet. Biol.* 46, 815–824. doi: 10.1016/j.fgb.2009.07.009

Takahashi, T., Jin, F. J., Sunagawa, M., Machida, M., and Koyama, Y. (2008). Generation of large chromosomal deletions in koji molds *Aspergillus oryzae* and *Aspergillus sojae* via a loop-out recombination. *Appl. Environ. Microbiol.* 74, 7684–7693. doi: 10.1128/AEM.00692-08

Takahashi, T., Masuda, T., and Koyama, Y. (2006). Enhanced gene targeting frequency in ku70 and ku80 disruption mutants of *Aspergillus sojae* and *Aspergillus oryzae*. *Mol. Genet. Genomics* 275, 460–470. doi: 10.1007/s00438-006-0104-1

Takaya, T., Koda, R., Adachi, D., Nakashima, K., Wada, J., Bogaki, T., et al. (2011). Highly efficient biodiesel production by a whole-cell biocatalyst employing a system with high lipase expression in *Aspergillus oryzae*. *Appl. Microbiol. Biotechnol.* 90, 1171–1177. doi: 10.1007/s00253-011-3186-6

Takeda, I., Umemura, M., Koike, H., Asai, K., and Machida, M. (2014). Motif-independent prediction of a secondary metabolism gene cluster using comparative genomics: application to sequenced genomes of *Aspergillus* and ten other filamentous fungal species. *DNA Res.* 21, 447–457. doi: 10.1093/dnares/dsu010

Takino, J., Kozaki, T., Ozaki, T., Liu, C., Minami, A., and Oikawa, H. (2019). Elucidation of biosynthetic pathway of a plant hormone abscisic acid in phytopathogenic fungi. *Biosci. Biotechnol. Biochem.* 83, 1642–1649. doi: 10.1080/09168451.2019.1618700

Tamalampudi, S., Talukder, M. M., Hama, S., Tanino, T., Suzuki, Y., Kondo, A., et al. (2007). Development of recombinant *Aspergillus oryzae* whole-cell biocatalyst expressing lipase-encoding gene from *Candida antarctica*. *Appl. Microbiol/Biotechnol.* 75, 387–395. doi: 10.1007/s00253-006-0814-7

Tamano, K., Kuninaga, M., Kojima, N., Umemura, M., Machida, M., and Koike, H. (2019). Use of the kojA promoter, involved in kojic acid biosynthesis, for polyketide production in *Aspergillus oryzae*: implications for long-term production. *BMC Biotechnol.* 19:70. doi: 10.1186/s12896-019-0567-x

Tanaka, M., Tokuoka, M., Shintani, T., and Gomi, K. (2012). Transcripts of a heterologous gene encoding mite allergen Der f 7 are stabilized by codon optimization in *Aspergillus oryzae*. *Appl. Microbiol. Biotechnol.* 96, 1275–1282. doi: 10.1007/s00253-012-4169-y

Tanaka, M., Yoshimura, M., Ogawa, M., Koyama, Y., Shintani, T., and Gomi, K. (2016). The C2H2-type transcription factor, FlbC, is involved in the transcriptional regulation of *Aspergillus oryzae* glucoamylase and protease genes specifically expressed in solid-state culture. *Appl. Microbiol. Biotechnol.* 100, 5859–5868. doi: 10.1007/s00253-016-7419-6

te Biesebeke, R., Boussier, A., van Biezen, N., Braaksma, M., van den Hondel, C. A., de Vos, W. M., et al. (2006). Expression of *Aspergillus* hemoglobin domain activities in *Aspergillus oryzae* grown on solid substrates improves growth rate and enzyme production. *Biotechnol. J.* 1, 822–827. doi: 10.1002/biot.200600036

Todokoro, T., Bando, H., Kotaka, A., Tsutsumi, H., Hata, Y., and Ishida, H. (2020). Identification of a novel pyrithiamine resistance marker gene thiI for genome co-editing in *Aspergillus oryzae*. *J. Biosci. Bioeng.* 130, 227–232. doi: 10.1016/j.jbiosc.2020.04.013

Tokuoka, M., Tanaka, M., Ono, K., Takagi, S., Shintani, T., and Gomi, K. (2008). Codon optimization increases steady-state mRNA levels in *Aspergillus oryzae* heterologous gene expression. *Appl. Environ. Microbiol.* 74, 6538–6546. doi: 10.1128/AEM.01354-08

Tsuboi, H., Koda, A., Toda, T., Minetoki, T., Hirotsune, M., and Machida, M. (2005). Improvement of the *Aspergillus oryzae* enolase promoter (P-enoA)

by the introduction of cis-element repeats. *Biosci. Biotechnol. Biochem.* 69, 206–208. doi: 10.1271/bbb.69.206

Tsuchiya, K., Nagashima, T., Yamamoto, Y., Gomi, K., Kitamoto, K., Kumagai, C., et al. (1994). High level secretion of calf chymosin using a glucoamylase-prochymosin fusion gene in *Aspergillus oryzae*. *Biosci. Biotechnol. Biochem.* 58, 895–899. doi: 10.1271/bbb.58.895

Tsuchiya, K., Tada, S., Gomi, K., Kitamoto, K., Kumagai, C., Jigami, Y., et al. (1992). High level expression of the synthetic human lysozyme gene in *Aspergillus oryzae*. *Appl. Microbiol. Biotechnol.* 38, 109–114. doi: 10.1007/BF00169428

Unkles, S. E., Campbell, E. I., de Ruiter-Jacobs, Y. M. J. T., Broekhuijsen, M., Marco, J. A., Carrez, D., et al. (1989). The development of a homologous transformation system for *Aspergillus oryzae* based on the nitrate assimilation pathway: a convenient and general selection system for ?lamentous fungal transformation. *Mol. Gen. Genet.* 218, 99–104.

van Erp, P. B. G., Bloomer, G., Wilkinson, R., and Wiedenheft, B. (2015). The history and market impact of CRISPR RNA-guided nucleases. *Curr. Opin. Virol.* 12, 85–90. doi: 10.1016/j.coviro.2015.03.011

Vongsangnak, W., Olsen, P., Hansen, K., Krogsgaard, S., and Nielsen, J. (2008). Improved annotation through genome-scale metabolic modeling of *Aspergillus oryzae*. *BMC Genomics* 9:245. doi: 10.1186/1471-2164-9-245

Wada, R., Jin, F. J., Koyama, Y., Maruyama, J., and Kitamoto, K. (2014). Efficient formation of heterokaryotic sclerotia in the filamentous fungus *Aspergillus oryzae*. *Appl. Microbiol. Biotechnol.* 98, 325–334. doi: 10.1007/s00253-013-5314-y

Wang, H., Entwistle, J., Morlon, E., Archer, D. B., Peberdy, J. F., Ward, M., et al. (2003). Isolation and characterisation of a calnexin homologue, clxA, from *Aspergillus niger*. *Mol. Genet. Genomics* 268, 684–691. doi: 10.1007/s00438-002-0790-2

Wang, H., and Ward, M. (2000). Molecular characterization of a PDI-related gene prpA in *Aspergillus niger* var. awamori. *Curr. Genet.* 37, 57–64. doi: 10.1007/s002940050009

Ward, P. P., Lo, J. Y., Duke, M., May, G. S., Headon, D. R., and Conneely, O. M. (1992). Production of biologically active recombinant human lactoferrin in *Aspergillus oryzae*. *Biotechnology* 10, 784–789. doi: 10.1038/nbt0792-784

Weyda, I., Yang, L., Vang, J., Ahring, B. K., Lubeck, M., and Lubeck, P. S. (2017). A comparison of Agrobacterium-mediated transformation and protoplast-mediated transformation with CRISPR-Cas9 and bipartite gene targeting substrates, as effective gene targeting tools for *Aspergillus carbonarius*. *J. Microbiol. Methods* 135, 26–34. doi: 10.1016/j.mimet.2017.01.015

Yamada, O., Lee, B. R., and Gomi, K. (1997). Transformation system for *Aspergillus oryzae* with double auxotrophic mutations, niaD and sC. *Biosci. Biotechnol. Biochem,* 61, 1367–1369.

Yamada, R., Yoshie, T., Wakai, S., Asai-Nakashima, N., Okazaki, F., Ogino, C., et al. (2014). *Aspergillus oryzae*-based cell factory for direct kojic acid production from cellulose. *Micro.b Cell Fact.* 13:71. doi: 10.1186/1475-2859-13-71

Yamashita, N., Komori, Y., Okumura, Y., Uchiya, K., Matsui, T., Nishimura, A., et al. (2011). High-yields heterologous production of the novel Aspergillus fumigatus elastase inhibitor AFUEI in *Aspergillus oryzae*. *J. Biosci. Bioeng.* 112, 114–117. doi: 10.1016/j.jbiosc.2011.03.020

Yin, Y., Mao, Y., Yin, X., Gao, B., and Wei, D. (2015). Construction of a shuttle vector for heterologous expression of a novel fungal alpha-amylase gene in *Aspergillus oryzae*. *J. Microbiol. Biotechnol.* 25, 988–998. doi: 10.4014/jmb.1410.10022

Yokota, J. I., Shiro, D., Tanaka, M., Onozaki, Y., Mizutani, O., Kakizono, D., et al. (2017). Cellular responses to the expression of unstable secretory proteins in the filamentous fungus *Aspergillus oryzae*. *Appl. Microbiol. Biotechnol.* 101, 2437–2446. doi: 10.1007/s00253-016-8086-3

Yoon, J., Aishan, T., Maruyama, J., and Kitamoto, K. (2010). Enhanced production and secretion of heterologous proteins by the filamentous fungus *Aspergillus oryzae* via disruption of vacuolar protein sorting receptor gene Aovps10. *Appl. Environ. Microbiol.* 76, 5718–5727. doi: 10.1128/AEM.03087-09

Yoon, J., Kimura, S., Maruyama, J., and Kitamoto, K. (2009). Construction of quintuple protease gene disruptant for heterologous protein production in *Aspergillus oryzae*. *Appl. Microbiol. Biotechnol.* 82, 691–701. doi: 10.1007/s00253-008-1815-5

Yoon, J., Kikuma, T., Maruyama, J., and Kitamoto, K. (2013). Enhanced production of bovine chymosin by autophagy deficiency in the filamentous fungus *Aspergillus oryzae*. *PLoS One* 8:e62512. doi: 10.1371/journal.pone.0062512

Yoon, J., Maruyama, J., and Kitamoto, K. (2011). Disruption of ten protease genes in the filamentous fungus *Aspergillus oryzae* highly improves production of heterologous proteins. *Appl. Microbiol. Biotechnol,* 89, 747–759. doi: 10.1007/s00253-010-2937-0

Zhang, S., Ban, A., Ebara, N., Mizutani, O., Tanaka, M., Shintani, T., et al. (2017). Self-excising Cre/mutant lox marker recycling system for multiple gene integrations and consecutive gene deletions in *Aspergillus oryzae*. *J. Biosci. Bioeng.* 123, 403–411. doi: 10.1016/j.jbiosc.2016.11.001

Zhao, G., Ding, L. L., Pan, Z. H., Kong, D. H., Hadiatullah, H., and Fan, Z. C. (2019). Proteinase and glycoside hydrolase production is enhanced in solid-state fermentation by manipulating the carbon and nitrogen fluxes in *Aspergillus oryzae*. *Food Chem.* 271, 606–613. doi: 10.1016/j.foodchem.2018.07.199

Zhao, G., Yao, Y., Wang, C., Hou, L., and Cao, X. (2013). Comparative genomic analysis of *Aspergillus oryzae* strains 3.042 and RIB40 for soy sauce fermentation. *Int. J. Food Microbiol.* 164, 148–154. doi: 10.1016/j.ijfoodmicro.2013.03.027

Zhao, G. Z., Yao, Y. P., Qi, W., Wang, C. L., Hou, L. H., Zeng, B., et al. (2012). Draft genome sequence of *Aspergillus oryzae* strain 3.042. *Eukaryotic Cell* 11, 1178–1178. doi: 10.1128/Ec.00160-12

Zhu, J. X., Ding, L., and He, S. (2019). Discovery of a new biphenyl derivative by epigenetic manipulation of marine-derived fungus *Aspergillus versicolor*. *Nat. Prod. Res.* 33, 1191–1195. doi: 10.1080/14786419.2018.1465423

Zhu, L., Maruyama, J., and Kitamoto, K. (2013). Further enhanced production of heterologous proteins by double-gene disruption (DeltaAosedD DeltaAovps10) in a hyper-producing mutant of *Aspergillus oryzae*. *Appl. Microbiol. Biotechnol.* 97, 6347–6357. doi: 10.1007/s00253-013-4795-z

Zhu, L., Nemoto, T., Yoon, J., Maruyama, J., and Kitamoto, K. (2012). Improved heterologous protein production by a tripeptidyl peptidase gene (AosedD) disruptant of the filamentous fungus *Aspergillus oryzae*. *J. Gen. Appl. Microbiol.* 58, 199–209. doi: 10.2323/jgam.58.199

Conflict of Interest: The authors declare that the research was conducted in the absence of any commercial or financial relationships that could be construed as a potential conflict of interest.

frontiers in Microbiology

OPINION
published: 04 March 2021
doi: 10.3389/fmicb.2021.602380

Sake Brewing and Bacteria Inhabiting Sake Breweries

*Hiromi Nishida**

Department of Biotechnology, Toyama Prefectural University, Imizu, Japan

Keywords: bacterial flora, *koji*, *kuratsuki*, *Hatsuzoe*, *moto*, *Kocuria* sp., sake brewing

INTRODUCTION

Sake is a Japanese traditional fermented alcoholic drink. It is brewed using *koji* mold to convert the starch in rice into sugar, which is then converted into ethanol by sake yeast. Two eukaryotic microorganisms, *Aspergillus oryzae* and *Saccharomyces cerevisiae*, are used for sake brewing, leading to highly efficient ethanol fermentation. The final ethanol concentration is ∼20%, which is higher than that of beer and wine. The use of technology in the sake brewing process is remarkably high and involves parallel double fermentation. In contrast, beer is brewed using malt to convert the starch in barley into sugar, which is then converted into ethanol by beer yeast. In winemaking, wine yeast converts sugar from grapes into ethanol. Beer and wine processes can include also serial yeast-based double fermentation. It is well-known that bacteria, mainly lactic acid bacteria, can have a role in the production process of beer (sour beer) and wine (malolactic fermentation) (Berbegal et al., 2019; De Roos et al., 2020; Dysvik et al., 2020; Virdis et al., 2020). On the opposite, several alcoholic beverages, such as sake, are considered fermented only by eukaryotic microorganisms.

Beer, sake, and wine originated long before the discovery of microorganisms. Thus, these alcoholic drinks were produced without understanding the mechanism of ethanol fermentation. Surprisingly, sake undergoes pasteurization, called *hiire*, in the process of sake storage, and it has been recorded as performed 300 years before Pasteur reported the pasteurization method. The high level of biotechnology involved in sake brewing has been maintained for a long time. Sake breweries are widely distributed in Japan, and there may be much more to learn from the sake brewing process. Sake has different grades depending on the degree of polishing of rice. The highest grade (*Daiginjo*) is produced using polished rice with 50% or more removal of the outer layer of the grain. In addition, sake is distinguished by the addition of distilled alcohol. Sake without distilled alcohol is called *Junmaishu*. This opinion paper proposes Sake as a model matrix to highlight bacterial role in traditional beverages that are considered exclusively mold/yeast-based. In addition, the opinion underlines the importance of considering all microbial determinants for a complete safety assessment.

BACTERIAL DNA IN SAKE

Numerous microorganisms are present at the beginning of the sake production process because sake brewing is not performed under completely sterile conditions. The ethanol concentration increases with the growth of sake yeast. Although all (or most) microorganisms die due to the high ethanol concentration, their DNA is present in the final sake product. Thus, the DNA sequences in sake can be analyzed to determine and compare the microbial flora contained in sake (Bokulich et al., 2014; Koyanagi et al., 2016; Terasaki et al., 2017; Tsuji et al., 2018).

The bacterial DNA composition of sake is entirely different from that of the water used in sake production (Terasaki et al., 2018). That is, the bacterial DNA detected in sake is not derived from the water but rather from bacteria that have entered and probably briefly grown during the sake production process. Some lactic acid bacteria can survive at ethanol concentrations of 20%, and

OPEN ACCESS

Edited by:
Van-Tuan Tran,
Vietnam National University,
Hanoi, Vietnam

Reviewed by:
Vittorio Capozzi,
Italian National Research Council, Italy
Wanping Chen,
Georg-August-University
Goettingen, Germany

***Correspondence:**
Hiromi Nishida
nishida1966@gmail.com

Specialty section:
This article was submitted to Food Microbiology, a section of the journal Frontiers in Microbiology

Received: *03 September 2020*
Accepted: *27 January 2021*
Published: *04 March 2021*

Citation:
Nishida H (2021) Sake Brewing and Bacteria Inhabiting Sake Breweries. Front. Microbiol. 12:602380. doi: 10.3389/fmicb.2021.602380

they cause spoiling when they contaminate sake (Suzuki et al., 2008). We have detected a high rate of lactic acid bacteria DNA sequences in spoiled sakes. Thus, DNA sequence comparison can be used as a powerful tool to analyze bacterial flora composition in sake. However, we must bear in mind that the detection of bacterial DNA in sake does not necessarily indicate that these bacteria are still alive.

BACTERIAL FLORA IN *MOTO*

Different sakes generally comprise different chemical components (Akaike et al., 2020), and the diversity of chemical components in sake is lower than that of the bacterial flora (Akaike et al., 2020; Terasaki and Nishida, 2020). Specific bacteria appear to affect specific chemical components during the production of the fermentation starter *moto*. For example, the ornithine composition increases and the arginine composition decreases during the production process of the fermentation starter *yamahai-moto* (also known as *kimoto*; traditional fermentation starter), and ornithine-producing *Latilactobacillus sakei* has been isolated from *yamahai-moto* (Tsuji et al., 2018). The bacteriocins produced by *Lactococcus lactis* inhibit the growth of sake-spoiling bacteria (Taniguchi et al., 2010). Although *Bacillus* sp. and *Staphylococcus* sp. predominate the early stage of *kimoto* production, lactobacilli predominate the late stage (Bokulich et al., 2014). Additionally, bacterial flora composition differs between the fermentation starters *yamahai-moto* and *sokujo-moto* (Terasaki et al., 2017).

These findings suggest that bacterial flora in sake may influence the chemical components and quality of sake products. Thus, bacteria that have inhabited a sake brewery for a long time could enter the sake brewing process and may be related to the bacterial flora and the characteristics of that sake.

BACTERIAL ISOLATION FROM *HATSUZOE*

The fermentation starter *moto* is mixed with *koji*, steamed rice, and water, and this is generally a three-step process, including *Hatsuzoe* (the first step), *Nakazoe* (the second step), and *Tomezoe* (the third step). Because bacteria cannot be isolated from sake products, we isolated bacteria from samples of the first mixture (*Hatsuzoe*). There are many live bacteria in *Hatsuzoe* (the first mixture of *moto* and *koji*) that can be identified and classified based on their 16S rDNA sequences. We obtained 46 isolates from six *Hatsuzoe* (the first mixture of *moto* and *koji*) samples from Brewery Toyama 1 (Terasaki and Nishida, 2020). Of them, 23, 12, 6, 2, 2, and 1 belonged to the bacterial genera *Kocuria*, *Staphylococcus*, *Bacillus*, *Leifsonia*, *Microbacterium*, and *Enterococcus*, respectively (Terasaki and Nishida, 2020). The detection of DNA associable to bacteria belonging to these genera underlines the importance, among the future perspectives, of a complete microbial safety assessment in sake productions that includes also prokaryotic organisms. In fact, some of these taxonomic units encompass species/strains of interest for food fermentations, but also undesired species/strains in the food chains (e.g., Tamang et al., 2017; Hanchi et al., 2018; Wu et al., 2019).

We isolated *Kocuria* sp. from all six *Hatsuzoe* (the first mixture of *moto* and *koji*) samples from Brewery Toyama 1 (Terasaki and Nishida, 2020). We also analyzed 16S rDNA sequencing results from 44 clear sake samples, three cloudy sake samples, and 11 *sake-kasu* (sake lee) samples from 33 sake breweries. *Kocuria* DNA was only detected in two samples of cloudy sake and one of *sake-kasu*, all of which were from Brewery Toyama 1 (Terasaki and Nishida, 2020). Interestingly, *Kocuria* DNA was not detected in any clear sakes. Our findings indicate that *Kocuria* DNA was not present in the sake solution because *Kocuria* cells are difficult to lyse by ethanol (Fujita et al., 2006). Thus, the *Kocuria* isolates inhabit Brewery Toyama 1 (Terasaki and Nishida, 2020) and are *kuratsuki* (= living in a sake brewery) bacteria from the sake brewery.

KURATSUKI BACTERIA AND YEAST

In the past, different sake breweries used different yeast strains that inhabited their brewery, known as *kuratsuki* yeast. Today, sake brewing using *kuratsuki* yeast is rare. Many sake breweries buy and use selected sake yeasts that are managed by the Brewery Society of Japan (*Jozo-kyokai*). However, these yeasts were once established in selected sake breweries.

To our knowledge, no *kuratsuki* bacteria other than lactic acid bacteria had been reported prior to the publication of our paper (Terasaki and Nishida, 2020). Because it was thought that bacteria do not have a positive effect on the sake brewing process and cause negative effects, such as spoilage, *kuratsuki* bacteria have not been investigated. All or most *kuratsuki* yeasts are different strains of *Saccharomyces cerevisiae*. On the other hand, *kuratsuki* bacteria may differ at the genus or species level because *Kocuria* DNA was not detected in any other sake breweries except for Brewery Toyama 1 (Terasaki and Nishida, 2020). Thus, we hypothesize that *kuratsuki* bacteria have different functions in the sake production process in different sake breweries. We have sequenced the genomic DNA of the *Kocuria* isolates and are currently analyzing them. We believe that *kuratsuki* bacteria affect the sake quality, resulting in tastes and flavors that are specific to the brewery producing the sake.

Staphylococcus sp. and *Bacillus* sp. were isolated from 4/6 and 3/6 *Hatsuzoe* (the first mixture of *moto* and *koji*) samples, respectively, from Brewery Toyama 1 (Terasaki and Nishida, 2020), suggesting that these isolates may also be *kuratsuki* bacteria. Furthermore, *Staphylococcus* sp. and *Bacillus* sp. DNA were detected more frequently in sake than *Kocuria* DNA (Terasaki and Nishida, 2020). Thus, these DNAs are not specific to bacterial DNA in the sakes of Brewery Toyama 1 (Terasaki and Nishida, 2020) at the genus level. However, if the *Staphylococcus* sp. and *Bacillus* sp. isolates are specific to the sake brewery, their genomic sequences could differ at the species or strain level in each genus.

FUTURE PLAN

The *hiire* pasteurization process halts the activities of enzymes of *koji* mold and sake yeast during the sake production process. Although enzymes, such as amylase and alcohol dehydrogenase, are essential for sake brewing, sake cannot be produced using only rice and these enzymes. Microorganisms are essential for sake production because they produce flavor and taste and influence the sake quality. Although bacteria die at the final stage of sake production, recent studies have shown that bacteria in sake are alive and grow temporarily during the sake production process. Thus, in the production process of sake, a bacterium interacts with another bacterium and sake yeast. *Kuratsuki* bacteria may play a key role in the interaction among microorganisms and may influence the sake quality. We are studying the functions of *kuratsuki* bacteria during sake brewing using comparative genome analyses and co-culturing experiments with these bacteria and sake yeast. We plan to change the characteristics of sake and produce a unique sake with different tastes and flavors by exchanging the *kuratsuki* bacteria from different sake breweries during the production process. Interest in sake is increasing around the world. Some Sake products are Geographical Indications (GIs) (https://www.nta.go.jp/publication/pamph/sake/04.pdf). In effect, an increasing interest is recognized to autochthonous microorganisms in the production of fermented traditional products (Capozzi and Spano, 2011; Capozzi et al., 2012, 2020). This opinion paper claims a possible role for autochthonous bacteria isolated from the sake productions among the factors included in the product specifications. At the same time, it highlights the importance of a complete microbial safety assessment that involves also bacteria.

AUTHOR CONTRIBUTIONS

HN wrote the manuscript.

FUNDING

This study was supported by a fund of University collaboration acceleration project of Toyama Prefecture.

REFERENCES

Akaike, M., Miyagawa, H., Kimura, Y., Terasaki, M., Kusaba, Y., Kitagaki, H., et al. (2020). Chemical and bacterial components in sake and sake production process. *Curr. Microbiol.* 77, 632–637. doi: 10.1007/s00284-019-01718-4

Berbegal, C., Borruso, L., Fragasso, M., Tufariello, M., Russo, P., Brusetti, L., et al. (2019). A metagenomic-based approach for the characterization of bacterial diversity associated with spontaneous malolactic fermentations in wine. *Int. J. Mol. Sci.* 20:3980. doi: 10.3390/ijms20163980

Bokulich, N. A., Ohta, M., Lee, M., and Mills, D. A. (2014). Indigenous bacteria and fungi drive traditional kimoto sake fermentations. *Appl. Environ. Microbiol.* 80, 5522–5529. doi: 10.1128/AEM.00663-14

Capozzi, V., Fragasso, M., and Russo, P. (2020). Microbiological safety and the management of microbial resources in artisanal foods and beverages: the need for a transdisciplinary assessment to conciliate actual trends and risks avoidance. *Microorganisms* 8:306. doi: 10.3390/microorganisms8020306

Capozzi, V., Russo, P., and Spano, G. (2012). Microbial information regime in EU geographical indications. *World Pat. Inf.* 34, 229–231. doi: 10.1016/j.wpi.2012.04.001

Capozzi, V., and Spano, G. (2011). Food microbial biodiversity and "microbes of protected origin". *Front. Microbiol.* 2:237. doi: 10.3389/fmicb.2011.00237

De Roos, J., Verce, M., Weckx, S., and De Vuyst, L. (2020). Temporal shotgun metagenomics revealed the potential metabolic capabilities of specific microorganisms during lambic beer production. *Front. Microbiol.* 11:1692. doi: 10.3389/fmicb.2020.01692

Dysvik, A., La Rosa, S. L., Liland, K. H., Myhrer, K. S., Østlie, H. M., De Rouck, G., et al. (2020). Co-fermentation involving *Saccharomyces cerevisiae* and *Lactobacillus* species tolerant to brewing-related stress factors for controlled and rapid production of sour beer. *Front. Microbiol.* 11:279. doi: 10.3389/fmicb.2020.00279

Fujita, K., Hagishita, T., Kurita, S., Kawakura, Y., Kobayashi, Y., Matsuyama, A., et al. (2006). The cell structural properties of *Kocuria rhizophila* for aliphatic alcohol exposure. *Enzyme Microbial Technol.* 39, 511–518. doi: 10.1016/j.enzmictec.2006.01.033

Hanchi, H., Mottawea, W., Sebei, K., and Hammami, R. (2018). The genus *Enterococcus*: between probiotic potential and safety concerns—an update. *Front. Microbiol.* 9:1791. doi: 10.3389/fmicb.2018.01791

Koyanagi, T., Nakagawa, A., Kiyohara, M., Matsui, H., Tsuji, A., Barla, F., et al. (2016). Tracing microbiota changes in *yamahasi-moto*, the traditional Japanese sake starter. *Biosci. Biotechnol. Biochem.* 80, 399–406. doi: 10.1080/09168451.2015.1095067

Suzuki, K., Asano, S., Iijima, K., and Kitamoto, K. (2008). Sake and beer spoilage lactic acid bacteria—a review. *J. Inst. Brew.* 114, 209–223. doi: 10.1002/j.2050-0416.2008.tb00331.x

Tamang, J. P., Holzapfel, W. H., Shin, D. H., and Felis, G. E. (2017). Editorial: Microbiology of ethnic fermented foods and alcoholic beverages of the world. *Front. Microbiol.* 8:1377. doi: 10.3389/fmicb.2017.01377

Taniguchi, M., Ishiyama, Y., Takata, T., Nakanishi, T., Kaneoke, M., Watanabe, K., et al. (2010). Growth-inhibition of hiochi bacteria in namazake (raw sake) by bacteriocins from lactic acid bacteria. *J. Biosci. Bioeng.* 109, 570–575. doi: 10.1016/j.jbiosc.2009.11.015

Terasaki, M., Fukuyama, A., Takahashi, Y., Yamada, M., and Nishida, H. (2017). Bacterial DNA detected in Japanese rice wines and the fermentation starters. *Curr. Microbiol.* 74, 1432–1437. doi: 10.1007/s00284-017-1337-4

Terasaki, M., Miyagawa, S., Yamada, M., and Nishida, H. (2018). Detection of bacterial DNA during the process of sake production using *sokujo-moto*. *Curr. Microbiol.* 75, 874–879. doi: 10.1007/s00284-018-1460-x

Terasaki, M., and Nishida, H. (2020). Bacterial DNA diversity among clear and cloudy sakes, and *sake-kasu*. *Open Bioinf. J.* 13, 74–82. doi: 10.2174/1875036202013010074

Tsuji, A., Kozawa, M., Tokuda, K., Enomoto, T., and Koyanagi, T. (2018). Robust domination of *Lactobacillus sakei* in microbiota during traditional Japanese sake starter *yamahai-moto* fermentation and the accompanying changes in metabolites. *Curr. Microbiol.* 75, 1498–1505. doi: 10.1007/s00284-018-1551-8

Virdis, C., Sumby, K., Bartowsky, E., and Jiranek, V. (2020). Lactic acid bacteria in wine: technological advances and evaluation of their functional role. *Front. Microbiol*. doi: 10.3389/fmicb.2020.612118

Wu, S., Huang, J., Zhang, F., Wu, Q., Zhang, J., Pang, R., et al. (2019). Prevalence and characterization of food-related methicillin-resistant *Staphylococcus aureus* (MRSA) in China. *Front. Microbiol.* 10:304. doi: 10.3389/fmicb.2019.00304

Conflict of Interest: The author declares that the research was conducted in the absence of any commercial or financial relationships that could be construed as a potential conflict of interest.

frontiers in Microbiology

OPINION
published: 31 March 2021
doi: 10.3389/fmicb.2021.659907

From Traditional Application to Genetic Mechanism: Opinions on *Monascus* Research in the New Milestone

Jie Wang[†], *Yueyan Huang*[†] *and Yanchun Shao*[*]

College of Food Science and Technology, Huazhong Agricultural University, Wuhan, China

Keywords: red mold rice, *Monascus* species, secondary metabolism, development, ecological status

OPEN ACCESS

Edited by:
Van-Tuan Tran,
Vietnam National University,
Hanoi, Vietnam

Reviewed by:
Zhilong Wang,
Shanghai Jiao Tong University, China
Petra Patakova,
University of Chemistry and
Technology in Prague, Czechia
Bijinu Balakrishnan,
Ohio University, United States

***Correspondence:**
Yanchun Shao
yanchunshao@mail.hzau.edu.cn

[†]*These authors have contributed equally to this work*

Specialty section:
This article was submitted to Food Microbiology, a section of the journal Frontiers in Microbiology

Received: *28 January 2021*
Accepted: *17 February 2021*
Published: *31 March 2021*

Citation:
Wang J, Huang Y and Shao Y (2021) From Traditional Application to Genetic Mechanism: Opinions on Monascus Research in the New Milestone. Front. Microbiol. 12:659907. doi: 10.3389/fmicb.2021.659907

INTRODUCTION

Red mold rice (RMR), the fermented product of *Monascus* strains, also called Hongqu, red fermented rice (RFR), and red yeast rice (RYR), has been used as a food coloring agent, food preservative, and traditional medicine for about 2,000 years in China (Chen et al., 2015). There are also historical records regarding the use of RMR in other oriental countries (Chen et al., 2015). Due to regional and cultural differences, there are many other names for RMR, such as beni-koji, red koji, or anka in Japan and Rotschimmelreis in Europe (Chen et al., 2015). Although RMR has a long history of consumption, we didn't know the *Monascus* strain until it was isolated from RMR in 1884 (Tieghem, 1884). Since then, scholars have gradually turned their attention to *Monascus* strain and its metabolic products (Patakova, 2013; Shao et al., 2014). *Monascus* species have great abilities to produce polyketides, such as well-known *Monascus* azaphilone pigments (MonAzPs), monacolin K (MK), and citrinin. Genomic information mining shows that *Monascus* spp. have great potential to produce multiple secondary metabolites (Chen et al., 2015), attracting more and more attention worldwide. Based on current progress of RMR and *Monascus* species, this opinion puts forward the issues that need to be further studied and discussed.

THE CATEGORIES OF RMR AND THEIR APPLICATIONS

According to the applicable scope of RMR, it can be divided into three main categories, namely, color RMR (CRMR), functional RMR (FRMR), and brewing RMR (BRMR) (Feng and Yu, 2020). CRMR is the product rich in MonAzPs, which have been extensively used in the food industry as a natural food colorant. It is estimated that more than one billion people consume food containing MonAzPs-related products during their daily life (Yang et al., 2015). Currently, MonAzPs have become one of the fastest growing categories of natural food colorants in the Chinese market (Sun and Wang, 2019). Annual production of MonAzPs is estimated to exceed 20,000 metric tons in China alone (Yang et al., 2015). MonAzPs also possess a wide range of biological activities, making them potential as a functional food ingredient (Lin et al., 2017). In addition, MonAzPs have many promising applications in the cosmetics, textile, printing, and dyeing industries (Chen et al., 2019). FRMR is a product rich in MK. Since MK can reduce the synthesis of cholesterol by inhibiting the activity of HMG-CoA reductase to lower blood lipids, it has been developed as a blood lipid-lowering drug and health care product (Zhang et al., 2020). There are two forms of MK produced by *Monascus* strains containing the active β-hydroxy acid form that exerts pharmacological effects, as well as an inactive lactone form, which makes the side effects of MK less than currently reported statin-like drugs (Beltran et al., 2019; Zhang et al., 2020). BRMR is a kind of fermented product rich in esterification enzymes, which can be used to enhance the unique aroma

components of food. In China, it is mainly used for the enhancement of the aroma of liquor and soy sauce (Xu et al., 2021).

CURRENT RESEARCH AND FUTURE DIRECTION

Given large-scale utilization and economic importance of RMR, scholars make more efforts to study the *Monascus* species to improve the product quality. In an attempt to summarize the published articles, the themes regarding *Monascus* research can be clustered into six groups: (1) the classification and identification of *Monascus* strains; (2) the methods to improve useful metabolites but inhibit citrinin; (3) the isolation and identification of new metabolites; (4) the exploration of the functional activity of metabolites; (5) the biosynthetic pathway and genetic regulation of secondary metabolites and developmental process; and (6) genomic information mining. These studies have brought new life to the RMR. However, many issues about RMR and the *Monascus* species still need to be further discussed, which are summarized as followed.

The Production of RMR

The method of producing RMR by solid-state fermentation (SSF) has continued from ancient times to today in China (Chen et al., 2015). This method looks simple and does not require large equipment, but it is time-consuming and relies on manual labor (Chen et al., 2015). So it is difficult to control RMR quality among different batches. Comparatively, liquid-state (submerged) fermentation (LSF/SF) has the characteristics of short period, not easy to be contaminated, and a higher degree of automation, so it is more and more favored by manufacturers. This has been practiced in MonAzPs production and also been considered to produce MK (Silveira et al., 2013; Feng et al., 2016). But the confusing problem is that the content of MK produced by LSF is much lower than the yield by SSF. This phenomenon has also been observed in antibiotic-producing bacteria *Cylindrocarpon* sp. LL-Cyan426 and *Acremonium* sp. LL-Cyan416, which was attributed to the interface of SSF providing various exceptional habitations, such as the gradient of pH, O_2, and substrate concentrations as well as product concentrations for mycelia growth (Bigelis et al., 2006). If all kinds of RMR can be produced by LSF, the RMR fermentation industry will be bought to a new level.

Generally, *Monascus purpureus*, *Monascus ruber*, and *Monascus pilosus* are widely used as the producers of various types of RMR (Patel, 2016). In fact, since van Tieghem first isolated *Monascus* strains from RMR (Tieghem, 1884), more than 20 species of *Monascus* have been recorded (Li and Guo, 2003). These *Monascus* species come from a wide range of ecological environments, such as sand pine (Barnard and Cannon, 1987), the surface sediment samples of water (Cannon et al., 1995), soil (Celestino et al., 2014), honey, and nests of stingless bees (Barbosa et al., 2017), showing their high adaptability in complex environments. We know that *Monascus* strains for fermentation usually grow slowly and are easily contaminated. However, how do these *Monascus* strains survive in such a diverse natural environment? What is the ecological role of a *Monascus* strain in nature? There is no doubt that different environments should influence the genetic regulation and cell development even influence the secondary metabolites. So the exploration of these issues will help us to better understand and utilize *Monascus* resources.

Correlation of Polyketide Biosynthetic Pathway and Their Regulation

Currently, MonAzPs, MK, and citrinin are the most well-known secondary metabolites produced by *Monascus* strains, and their biosynthetic pathways had been explained by several research groups (Fu et al., 2007; Chen et al., 2008, 2017; Balakrishnan et al., 2014; He and Cox, 2016). But there is a complicated relationship among these compounds. Usually, the production of MonAzPs was often accompanied by the contamination of mycotoxin (citrinin), meaning that MonAzPs high-producing strains usually have strong abilities to synthesize citrinin (Wang et al., 2012). For this reason, scholars made great efforts to decrease or eliminate the production of citrinin in RMR and the related products through optimization of fermentation parameters and strain screening. Yet, it is still not clear why citrinin and MonAzPs always coexist in RMR.

It was proposed that the initial synthesis of citrinin shared the same precursor and biosynthetic steps with MonAzPs (Hajjaj et al., 1999). With the application of molecular biology tools, it has been demonstrated that MonAzPs and citrinin have their own independent biosynthetic pathways, and genes encoding these two biosynthetic pathways form separate gene clusters located on two different chromosomes (Balakrishnan et al., 2014; Li et al., 2015; Ding et al., 2016; He and Cox, 2016; Chen et al., 2017), which presents a new idea for people to control citrinin in RMR through knocking out the genes responsible for citrinin synthesis. However, this didn't achieve the desired expectations but even led to some results contradictory to our current understanding of biosynthetic pathways with respect to MonAzPs and citrinin. An example is that the deletion of specific genes involved in citrinin synthesis decreased the production of citrinin and MonAzPs (Li et al., 2015); another example is that the deletion of genes in the MonAzPs biosynthetic pathways resulted in decreased MonAzPs and citrinin (Liang et al., 2017). Therefore, it is currently hard to explain the puzzling phenomenon of MonAzPs and citrinin from the perspective of biosynthetic pathways. Interestingly, strains with high MK production rarely produce citrinin but can produce visible MonAzPs. So it is necessary to explore the relationship among these three polyketides at the genetic level.

The biosynthesis of secondary metabolites are regulated by multiple levels. It is well-known that certain regulatory factors, such as global regulator MrLaeA (Liu et al., 2016), components of G-protein signaling pathway, including MrFlbA (a regulator of G-protein alpha subunit) α, β, and γ subunits (Yang et al., 2012; Lei et al., 2019), and response regulator

MrSkn7 have been demonstrated to modulate the production of MonAzPs, MK, and citrinin (Shao et al., 2016). But it is a remarkable fact that the regulation trend of these regulators on MonAzPs and citrinin is consistent. Are there any regulators that provide reverse regulation of the production of MonAzPs and citrinin? This is also an interesting question worthy of investigation.

The Relationship Between Development and Secondary Metabolism

Secondary metabolism is always coupled with developmental processes (Chen et al., 2019). At present, the regulators reported in *Monascus* strains have played important regulatory roles in the production of MonAzPs and citrinin, and usually affected their growth, sexual, and asexual development (Yang et al., 2012; Liu et al., 2016; Shao et al., 2016; Lei et al., 2019). Do these regulators affect the secondary metabolic process by influencing the developmental process, or vice versa? This is a common problem with other filamentous fungi and a great challenge. If this question can be explained clearly, it will play an important guiding role in the rational improvement of industrial strains.

SUMMARY

Although RMR has been used as a traditional fermented food for nearly 2,000 years, we still lack a deep understanding of *Monascus* species at the genetic level. With the application of genome information mining and modern biotechnology, the genetic information of *Monascus* species will be continuously deciphered, which will help us make better use of *Monascus* resources.

AUTHOR CONTRIBUTIONS

JW and YH collected data and drafted part of the manuscript. YS drafted the manuscript and revised it. All authors commented on the manuscript.

FUNDING

This work was funded by the National Natural Science Foundation of China (No. 31671834) and the Fundamental Research Funds for the Central University (2662018PY090) to YS.

REFERENCES

Balakrishnan, B., Chen, C. C., Pan, Z. M., and Kwona, H. J. (2014). Mpp7 controls regioselective Knoevenagel condensation during the biosynthesis of *Monascus* azaphilone pigments. *Tetrahedron Lett.* 55, 1640–1643. doi: 10.1016/j.tetlet.2014.01.090

Barbosa, R. N., Leong, S. L., Vinnere-Pettersson, O., Chen, A. J., Souza-Motta, C. M., Frisvad, J. C., et al. (2017). Phylogenetic analysis of *Monascus* and new species from honey, pollen and nests of stingless bees. *Stud. Mycol.* 86, 29–51. doi: 10.1016/j.simyco.2017.04.001

Barnard, E. L., and Cannon, P. F. (1987). A new species of *Monascus* from pine tissues in Florida. *Mycologia* 79, 479–484. doi: 10.1080/00275514.1987.12025410

Beltran, D., Frutos-Lison, M. D., Espin, J. C., and Garcia-Villalba, R. (2019). Re-examining the role of the gut microbiota in the conversion of the lipid-lowering statin monacolin K (lovastatin) into its active beta-hydroxy acid metabolite. *Food Function* 10, 1787–1791. doi: 10.1039/C8FO02594K

Bigelis, R., He, H. Y., Yang, H. Y., Chang L. P., Greenstein, M. (2006). Production of fungal antibiotics using polymeric solid supports in solid-state and liquid fermentation. *J. Indus. Microbiol. Biotechnol.* 33, 815–826. doi: 10.1007/s10295-006-0126-z

Cannon, P. F., Abdullah, S. K., and Abbas, B. A. (1995). 2 new species of *Monascus* from Iraq, with a key to know species of the genus. *Mycol. Res.* 99, 659–662. doi: 10.1016/S0953-7562(09)80523-6

Celestino, J. D., de Carvalho, L. E., Lima, M. D., Lima, A. M., Ogusku, M. M., and de Souza, J. V. B. (2014). Bioprospecting of Amazon soil fungi with the potential for pigment production. *Process Biochem.* 49, 569–575. doi: 10.1016/j.procbio.2014.01.018

Chen, W., Feng, Y. L., Molnar, I., and Chen, F. S. (2019). Nature and nurture: confluence of pathway determinism with metabolic and chemical serendipity diversifies *Monascus* azaphilone pigments. *Nat. Product Rep.* 36, 561–572. doi: 10.1039/C8NP00060C

Chen, W. P., Chen, R. F., Liu, Q. P., He, Y., He, K., Ding, X. L., et al. (2017). Orange, red, yellow: biosynthesis of azaphilone pigments in *Monascus* fungi. *Chem. Sci.* 8, 4917–4925. doi: 10.1039/C7SC00475C

Chen, W. P., He, Y., Zhou, Y. X., Shao, Y. C., Feng, Y. L., Li, M., et al. (2015). Edible filamentous fungi from the species *Monascus*: early traditional fermentations, modern molecular biology, and future genomics. *Comprehens. Rev. Food Sci. Food Safety* 14, 555–567. doi: 10.1111/1541-4337.12145

Chen, Y. P., Tseng, C. P., Liaw, L. L., Wang, C. L., Chen, I. C., Wu, W. J., et al. (2008). Cloning and characterization of monacolin K biosynthetic gene cluster from *Monascus pilosus*. *J. Agri. Food Chem.* 56, 5639–5646. doi: 10.1021/jf800595k

Ding, X. L., Chen, W. P., and Chen, F. S. (2016). Karyotype analysis and chromosome localization of pigment and citrinin biosynthesis gene clusters of *Monascus ruber* M7. *Mygosystema* 35, 309–316. doi: 10.13346/j.mycosystema.140287

Feng, Y. L., Chen, W. P., and Chen, F. S. (2016). A *Monascus pilosus* MS-1 strain with high-yield monacolin K but no citrinin. *Food Sci. Biotechnol.* 25, 1115–1122. doi: 10.1007/s10068-016-0179-3

Feng, Y. L., and Yu, X. (2020). Perspectives on functional red mold rice: functional ingredients, production, and application. *Front. Microbiol.* 11:606959. doi: 10.3389/fmicb.2020.606959

Fu, G. M., Xu, Y., Li, Y. P., and Tan, W. H. (2007). Construction of a replacement vector to disrupt pksCT gene for the mycotoxin citrinin biosynthesis in *Monascus aurantiacus* and maintain food red pigment production. *Asia Pacific J. Clin. Nutr.* 16, 137–142. doi: 10.6133/APGCN.2007.16.S1.26

Hajjaj, H., Klaebe, A., Loret, M. O., Goma, G., Blanc, P. J., and Francois, J. (1999). Biosynthetic pathway of citrinin in the filamentous fungus *Monascus ruber* as revealed by 13C nuclear magnetic resonance. *Appl. Environ. Microbiol.* 65, 311–314. doi: 10.1128/AEM.65.1.311-314.1999

He, Y., and Cox, R. J. (2016). The molecular steps of citrinin biosynthesis in fungi. *Chem. Sci.* 7, 2119–2127. doi: 10.1039/C5SC04027B

Lei, M., Liu, J., Fang, Y., Shao, Y. C., Li, L., Yu, J. H., et al. (2019). Effects of different G-Protein alpha-subunits on growth, development and secondary metabolism of *Monascus ruber* M7. *Front. Microbiol.* 10:11. doi: 10.3389/fmicb.2019.01555

Li, Y. P., Tang, X., Wu, W., Xu, Y., Huang, Z. B., and He, Q. H. (2015). The *ctnG* gene encodes carbonic anhydrase involved in mycotoxin citrinin biosynthesis from *Monascus aurantiacus*. *Food Additiv. Contaminants A Chem. Anal. Control Exposure Risk Assessment* 32, 577–583. doi: 10.1080/19440049.2014.990993

Li, Z. Q., and Guo, F. (2003). *Morphology and Taxonomy of Monascus*. Beijing: Chinese Light Industry Press.

Liang, B., Du, X. J., Li, P., Guo, H., Sun, C. C., Gao, J. X., et al. (2017). *Orf6* gene encoded glyoxalase involved in mycotoxin citrinin biosynthesis

in *Monascus purpureus* YY-1. *Appl. Microbiol. Biotechnol.* 101, 7281–7292. doi: 10.1007/s00253-017-8462-7

Lin, C. H., Lin, T. H., and Pan, T. M. (2017). Alleviation of metabolic syndrome by monascin and ankaflavin: the perspective of *Monascus* functional foods. *Food Function* 8, 2102–2109. doi: 10.1039/C7FO00406K

Liu, Q. P., Cai, L., Shao, Y. C., Zhou, Y. X., Li, M., Wang, X. H., et al. (2016). Inactivation of the global regulator LaeA in *Monascus ruber* results in a species-dependent response in sporulation and secondary metabolism. *Fungal Biol.* 120, 297–305. doi: 10.1016/j.funbio.2015.10.008

Patakova, P. (2013). *Monascus* secondary metabolites: production and biological activity. *J. Indus. Microbiol. Biotechnol.* 40, 169–181. doi: 10.1007/s10295-012-1216-8

Patel, S. (2016). Functional food red yeast rice (RYR) for metabolic syndrome amelioration: a review on pros and cons. *World J. Microbiol. Biotechnol.* 32:2. doi: 10.1007/s11274-016-2035-2

Shao, Y. C., Lei, M., Mao, Z., Zhou, Y. X., and Chen, F. S. (2014). Insights into *Monascus* biology at the genetic level. *Appl. Microbiol. Biotechnol.* 98, 3911–3922. doi: 10.1007/s00253-014-5608-8

Shao, Y. C., Yang, S., Zhang, Z. W., Zhou, Y. X., and Chen, F. S. (2016). *mrskn7*, a putative response regulator gene of *Monascus ruber* M7, is involved in oxidative stress response, development, and mycotoxin production. *Mycologia* 108, 851–859. doi: 10.3852/15-200

Silveira, S. T., Daroit, D. J., Sant'Anna, V., and Brandelli, A. (2013). Stability modeling of red pigments produced by *Monascus purpureus* in submerged cultivations with ugarcane Bagasse. *Food Bioprocess Technol.* 6, 1007–1014. doi: 10.1007/s11947-011-0710-8

Sun, T., and Wang, F. (2019). Application of *Monascus*pigment in food. *Farm Product. Process.* 9, 70–72. doi: 10.16693.j.cnki.1671-9646(X).2019.09.055

Tieghem, V. (1884). *Monascus*, genre nouveau de l'ordre des Ascomycetes. *Bull. Soc. Bot. Fr.* 31, 226–231. doi: 10.1080/00378941.1884.10828230

Wang, L., Xu, G. R., and Wang, W. (2012). Problems and analysis of the development of *Monascus* pigment industry. *Sci. Technol. Food Industry* 33, 401–403. doi: 10.13386/j.issn1002-0306.2012.01.093

Xu, Y., Wang, X., Liu, X., Li, X., Zhang, C., Li, W., et al. (2021). Discovery and development of a novel short-chain fatty acid ester synthetic biocatalyst under aqueous phase from *Monascus purpureus* isolated from Baijiu. *Food Chem.* 338:128025. doi: 10.1016/j.foodchem.2020.128025

Yang, Y., Liu, B., Du, X. J., Li, P., Liang, B., Cheng, X. Z., et al. (2015). Complete genome sequence and transcriptomics analyses reveal pigment biosynthesis and regulatory mechanisms in an industrial strain, *Monascus purpureus* YY-1. *Sci. Rep.* 5:9. doi: 10.1038/srep08331

Yang, Y. S., Li, L., Li, X., Shao, Y. C., and Chen, F. S. (2012). MrflbA, encoding a putative FlbA, is involved in aerial hyphal development and secondary metabolite production in *Monascus ruber* M-7. *Fungal Biol.* 116, 225–233. doi: 10.1016/j.funbio.2011.11.005

Zhang, Y. R., Chen, Z. T., Wen, Q. Y., Xiong, Z. X., Cao, X. H., Zheng, Z. H., et al. (2020). An overview on the biosynthesis and metabolic regulation of monacolin K/lovastatin. *Food Function* 11, 5738–5748. doi: 10.1039/D0FO00691B

Conflict of Interest: The authors declare that the research was conducted in the absence of any commercial or financial relationships that could be construed as a potential conflict of interest.

frontiers in Microbiology

ORIGINAL RESEARCH
published: 29 April 2021
doi: 10.3389/fmicb.2021.673670

Characteristics of the Microbial Community in the Production of Chinese Rice-Flavor Baijiu and Comparisons With the Microflora of Other Flavors of Baijiu

*Yuanliang Hu[1,2,3], Xinyi Lei[1], Xiaomin Zhang[2,4], Tongwei Guan[5], Luyao Wang[1], Zongjie Zhang[1], Xiang Yu[1], Junming Tu[1], Nan Peng[2], Yunxiang Liang[2] and Shumiao Zhao[2]**

[1] Hubei Key Laboratory of Edible Wild Plants Conservation and Utilization, College of Life Sciences, Hubei Normal University, Huangshi, China, [2] State Key Laboratory of Agricultural Microbiology, College of Life Science and Technology, Huazhong Agricultural University, Wuhan, China, [3] Hubei Engineering Research Center of Typical Wild Vegetable Breeding and Comprehensive Utilization Technology, Huangshi, China, [4] Guangdong Deqing Incomparable Health Wine Co., Ltd., Zhaoqing, China, [5] College of Food and Biological Engineering, Xihua University, Chengdu, China

OPEN ACCESS

Edited by:
Wanping Chen,
Georg-August-Universität Göttingen, Germany

Reviewed by:
Zhuang Guo,
Hubei University of Arts and Science, China
Miao Lihong,
Wuhan Polytechnic University, China

***Correspondence:**
Shumiao Zhao
shumiaozhao@mail.hzau.edu.cn

Specialty section:
This article was submitted to Food Microbiology, a section of the journal Frontiers in Microbiology

Received: *28 February 2021*
Accepted: *06 April 2021*
Published: *29 April 2021*

Citation:
Hu Y, Lei X, Zhang X, Guan T, Wang L, Zhang Z, Yu X, Tu J, Peng N, Liang Y and Zhao S (2021) Characteristics of the Microbial Community in the Production of Chinese Rice-Flavor Baijiu and Comparisons With the Microflora of Other Flavors of Baijiu. Front. Microbiol. 12:673670. doi: 10.3389/fmicb.2021.673670

Rice-flavor baijiu is one of the four basic flavor types of Chinese baijiu. Microbial composition plays a key role in the classification of baijiu flavor types and the formation of flavor substances. In this study, we used high-throughput sequencing technology to study the changes of microbial community in the production of rice-flavor baijiu, and compared the microbial community characteristics during production of rice-, light-, and strong-flavor baijiu. The results showed that the species diversity of bacteria was much higher than that of fungi during the brewing of rice-flavor baijiu. The bacterial diversity index first increased and then decreased, while the diversity of fungi showed an increasing trend. A variety of major microorganisms came from the environment and raw rice materials; the core bacteria were *Lactobacillus*, *Weissella*, *Pediococcus*, *Lactococcus*, *Acetobacter*, etc., among which *Lactobacillus* was dominant (62.88–99.23%). The core fungi were *Saccharomyces* (7.06–83.50%) and *Rhizopus* (15.21–90.89%). Temperature and total acid content were the main physicochemical factors affecting the microbial composition. Non-metric multidimensional scaling analysis showed that during the fermentation of rice-, light-, and strong-flavor baijiu, their microbial communities formed their own distinct systems, with considerable differences among different flavor types. Compared with the other two flavor types of baijiu, in the brewing process of rice-flavor baijiu, microbial species were fewer and dominant microorganisms were prominent, which may be the main reason for the small variety of flavor substances in rice-flavor baijiu. This study provides a theoretical basis for the production of rice-flavor baijiu, and lays a foundation for studying the link between baijiu flavor formation and microorganisms.

Keywords: baijiu, fungal community, bacterial community, high-throughput sequencing, baijiu flavor

INTRODUCTION

Chinese baijiu is a traditional alcoholic beverage and one of the six major distilled spirits in the world (Wu J. et al., 2017; He et al., 2019). Compared with other distilled spirits, such as whisky and brandy, baijiu is generally produced by natural solid-state fermentation with a mixture of microbial species (yeasts, bacteria, and molds), with saccharification and fermentation taking place at the same time, and the base liquor being obtained by solid-state distillation. In contrast, other distilled spirits undergo saccharification and fermentation separately, enzyme preparation is added for saccharification, one or more yeasts are inoculated for liquid fermentation, and the base liquor is obtained by liquid distillation (Jin et al., 2017; Wanikawa, 2020). Due to the differences in the selection of raw materials, types of distillers, and production processes, etc., 12 types of baijiu have been developed in China, with four main flavor types; sauce, strong, light, and rice flavors (Yin et al., 2020a; Gao et al., 2021).

Rice-flavor baijiu is a rare type of baijiu in China that is brewed from rice (Yin et al., 2020a). The production process mainly includes raw material pretreatment, inoculation, saccharification, fermentation, distillation, aging, blending, and bottling (**Figure 1**). The microbial starter of rice-flavor baijiu is Xiaoqu, which provides various functional microorganisms, hydrolases, volatile substances, and other components for baijiu brewing, forming the unique flavor of baijiu (Arbab et al., 2020; Wang et al., 2021). During saccharification, the microorganisms and enzymes in Xiaoqu degrade the starch in rice into sugar (Wang J. et al., 2018). At the end of saccharification, water for brewing is added, semi-solid fermentation is carried out for approximately 13 days, and the base liquor is finally obtained by distillation (Li et al., 2019).

The essence of baijiu-making is the process of microbial growth and accumulation of metabolites, and the synergistic effect among populations is closely related to the flavor and quality of baijiu (He et al., 2019). *Saccharomyces* can ferment sugars to produce alcohol, and most of them can survive under high-sugar and relatively acidic conditions and enable alcoholization and esterification during the fermentation of baijiu (Liu and Miao, 2020). Among them, *Saccharomyces cerevisiae* mainly plays an alcohol-producing role and has a strong alcohol-producing capacity (Wang et al., 2020). Most of the other yeasts are ester-producing yeasts, and although their alcohol production volume is relatively small, they can convert production materials into aldehydes, esters, higher alcohols, etc., during baijiu fermentation. Molds can produce hydrolases, such as amylase, protease, and lipase, for the saccharification of starch and breakdown of macromolecules, and these enzymes provide important compounds that contribute to the formation of flavor (Wang B. et al., 2018). Bacteria are mainly used to produce flavor components and precursors of flavor components, which are important sources of the unique flavor of baijiu (Dai et al., 2020). The synergistic action of many microorganisms completes the baijiu brewing process and creates the unique style of baijiu.

Rice-flavor baijiu is very different from the other three major flavor types of baijiu; light-, strong-, and sauce-flavor (Yin et al., 2020a). These three flavor types are all spicy, while the rice-flavor type has a sweet taste, a honey aroma, a quietly elegant, and a soft mouth feel. The "rice-brewing aroma" and "Xiaoqu baijiu aroma" comprise the elegant and soft aroma composed of three substances, namely, ethyl lactate, ethyl acetate, and β-phenylethanol. Microorganisms play a decisive role in the formation of flavor substances and flavor types of baijiu (Wang et al., 2019; Huang et al., 2020). Lactic acid and acetic acid are the precursors of ethyl lactate and ethyl acetate, respectively. Lactic acid is mainly derived from *Lactobacillus* spp., while acetic acid is mainly produced by the oxidation of ethanol by *Acetobacter* spp. In addition, *Rhizopus* produces glucoamylase and proteases as well as important flavor substances, such as lactic acid, other organic acids, and aromatic series. Yeasts can produce aldehyde esters, β-phenylethanol, and other higher alcohols during fermentation, and form flavor substances with ethyl acetate as the main ester (Guan et al., 2020). Among the many microbial groups, only the core microorganisms can drive the fermentation process, and they not only produce various flavor substances, but more importantly, they can maintain the interactions among microorganisms, which together determine the quality of baijiu (Song et al., 2017). Therefore, the study of microbial composition and diversity is of great significance for gaining insight into the style characteristics and brewing mechanisms of Chinese baijiu.

Both rice-flavor baijiu and Xiaoqu light-flavor baijiu use Xiaoqu as the microbial starter and have very similar brewing cycles, yet they are different flavor types of baijiu with their own styles. It is currently unclear whether there are differences in the composition of the microbial communities in the production of these two flavor types of baijiu. In addition, there have been more studies of the brewing microorganisms of light- (Dong et al., 2020; Hu et al., 2021b), strong- (Guan et al., 2020), and sauce-flavor baijiu (Dai et al., 2020), but less of rice-flavor baijiu, and its brewing microbial composition has yet to be resolved. Therefore, in this study, high-throughput sequencing technology was used to analyze the microbial communities in the starters and production processes of rice-flavor baijiu to identify the core microbiota and study their effects on the microbial communities by combining with changes in physicochemical factors, such as flavor components. In addition, high-throughput sequencing and bioinformatics analysis were used to compare the microbial community composition of rice-, light-, and strong-flavor baijiu brewing, laying a foundation for an in-depth study of the nature of baijiu flavor formation and the linkage among microorganisms.

MATERIALS AND METHODS

Brewing Process and Sampling

The production process of rice-flavor baijiu is shown in **Figure 1**. Fermentation occurred in clay vats sealed for 13 days after 20 h of saccharification. Both saccharification and fermentation took place at room temperature. Samples were taken at the end of saccharification (d0) and at the end of fermentation on days 2 (d2), 5 (d5), 10 (d10), and 13 (d13). Three replicates were sampled each time, i.e., from three different vats. A five-point sampling

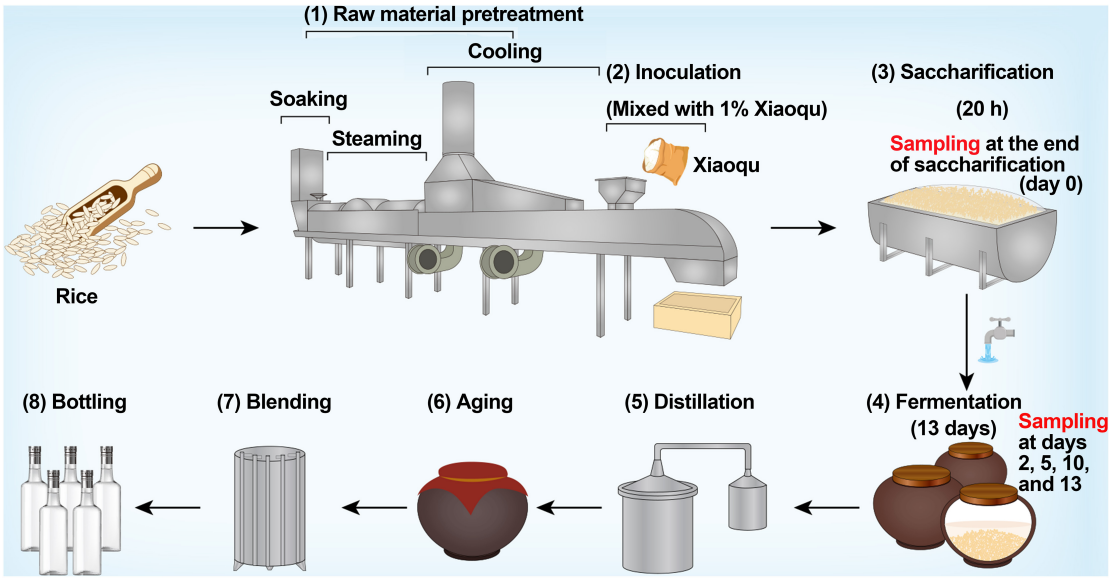

FIGURE 1 | Production process of rice-flavor baijiu and sampling design in this study.

method was used to reduce sampling errors, i.e., five sub-samples were mixed into one test sample with the sampling point being 30 cm below the surface of the fermented rice, and the sampling volume each time was approximately 600 g. After mixing well, 50 g of samples were snap frozen in liquid nitrogen and stored at −80°C for DNA extraction. Then, 500 g of samples were stored in a refrigerator at 4°C for the determination of physicochemical parameters. Three replicates of the Xiaoqu sample were crushed and stored in the same manner as the fermented rice sample.

Physicochemical Factors Determination

The temperature of fermented rice in clay vats was determined by a temperature sensor in real-time. The pH value and acidity were determined by the samples collected from the clay vats. The pH value was measured at room temperature with a pH meter (PHSJ-4F, Leici, Shanghai, China). The acidity was determined as follows: 10 g of the sample was weighed and placed in a mortar and ground thoroughly. Next, 100 mL of distilled water was added, and the mixture was stirred well, allowed to stand for 30 min, filtered through qualitative filter paper, and titrated with NaOH solution (Hu et al., 2021b).

The flavor components were determined by gas chromatography. A 50 mL centrifuge tube was filled with 30 mL of thawed fermented grain sample, sonicated at a low temperature for 10 min, and centrifuged at 10,000 r/min, 4°C for 10 min. Then, 10 mL of the supernatant was pipetted, added to 0.2 mL of n-butyl acetate internal standard, and mixed well. Finally, the mixture was filtered through a 0.22 μM filter membrane to obtain the sample to be tested, which was detected on a GC-2014C Shimadzu gas chromatograph with a mixed standard of baijiu as the reference standard. The detection conditions were as follows: packed column; carrier gas (high-purity nitrogen) flow rate, 180 mL/min; hydrogen flow rate, 40 mL/min; air flow rate, 400 mL/min; detector temperature, 180°C; injector temperature, 180°C; column temperature, 90°C; isothermal.

DNA Extraction

The samples were weighed (5 g of Xiaoqu; 15 g of fermented rice) and subjected to the following pretreatment: suspension with 30 mL of sterilized 0.1 mol/L PBS buffer, addition of three glass beads, vortex shaken for 5 min, centrifuged at 300 r/min for 5 min to obtain the supernatant; washing of the precipitate with PBS buffer three times, and centrifugation to collect the supernatant. The supernatant was centrifuged at 9,000 r/min for 3 min, the resulting supernatant was discarded, and the cell precipitate was collected. The precipitate was washed three more times with 5 mL of PBS, centrifuged at 9,000 r/min for 3 min each time, and finally resuspended in 2 mL of PBS solution, after which DNA was extracted using the Omega EZNA^{TM} Soil Genome Extraction Kit (Omega, GA, United States) according to the manufacturer's instructions. The collected DNA sample was quantified, and the mass of the extracted DNA was measured. The sample criteria for sequencing analysis were concentration >50 ng/L and clear bands on the electropherogram.

High Throughput Sequencing

The purified genomic DNA was sequenced by Shanghai Personal Biotechnology Co., Ltd. (China) using Illumina Miseq PE300. Sequencing was performed on the 16S rRNA gene V3 and V4 regions for bacteria as well as the ITS1 region for fungi (Dorn-In et al., 2013; Los et al., 2020). Bacteria were amplified with primers F338 and R806 (5′-ACTCCTACGGGAGGCAGCAG-3′; 5′-GGACTACHVGGGTWTCTAAT-3′) for 16S rRNA gene library construction. Fungi were amplified with primers ITS5-1737F

and ITS2-2043R (5′- GGAAGTAAAAGTCGTAACAAGG-3′; 5′-GCTGCGTTCTTCATCGATGC-3′) for ITS1 gene library construction. The PCR products were purified using the QIAquick PCR Purification Kit (Qiagen, Valencia, CA, United States) validated on a 2% agarose gel and diluted to equal concentrations. Finally, paired-end sequencing was performed on a MiSeq sequencer followed by splicing (Hong et al., 2016). The raw sequencing data were submitted to NCBI under sequence number PRJNA699433.

Bioinformatics and Statistical Analysis

Raw data obtained from high-throughput sequencing were processed with QIIME2 (2019.4) and subjected to quality control at 99% accuracy to remove duplicate sequences, sequences with short read length, low-abundance sequences, and chimeras. Sequences that remained well above the number in the species after quality screening and de-redundancy were subjected to OTU clustering at 97% similarity to obtain representative sequences and generate a table of OTUs (Li et al., 2011). OTUs were optimized by random sampling and processed by subsampling (sequence number of bacteria: 18,022; sequence number of fungi: 26,084). The OTUs of bacteria and fungi were classified and annotated based on the Silva database (Release 132[1]) and the UNITE database (Release 8.0[2]), respectively. Based on the OTU table, analysis of species composition and diversity indices was performed. Alpha diversity was characterized by Chao1 and observed species indices for richness, Shannon and Simpson indices for diversity, Faith's PD index for evolutionary-based diversity, and Pielou's evenness index for evenness. Beta diversity was characterized by non-metric multidimensional scaling (NMDS) and the NMDS model was evaluated by stress values. The R package VennDiagram was used to plot Venn diagrams based on the OTU table, and the number of members in each set was counted separately according to the presence or absence of OTUs among the groups. Redundancy analysis (RDA) was performed on the OTU table of samples after Hellinger pre-transformation, variance inflation factor was used to test for multicollinearity of the explanatory variables, and the reliability of RDA model was assessed by permutation test ($P < 0.05$). NMDS and RDA analyses as well as plotting were performed using the R package vegan (2.5–6).

To compare the microbial communities in the production process of rice-, light-, and strong-flavor baijiu, high-throughput sequencing data from the production process of light-flavor baijiu (PRJNA699760) and strong-flavor baijiu (PRJNA622890) were downloaded from the NCBI database. The sequencing data of the rice-flavor baijiu in this study, and the other two kinds of baijiu were combined and analyzed using NMDS. These sequencing data targeted the same gene regions; V3–V4, for bacteria and ITS1 for fungi.

Alpha diversity values were analyzed using IBM SPSS Statistics 25.0 software. Tukey's HSD test was performed to identify the statistical significance of differences between treatments, with $P < 0.05$ indicating a significant difference.

[1]http://www.arb-silva.de

[2]https://unite.ut.ee/

RESULTS

Changes in Physicochemical Factors

Fermentation began at pH 3.4, which dropped to pH 2.4 after 10 days and rose to pH 3.4 at the end of fermentation (**Figure 2A**). The trend in total acid did not correspond exactly to the changes in pH, decreasing slightly from day 0 to day 2, then increasing rapidly and stabilizing from day 5 to day 10, and increasing rapidly after 10 days. The acetic acid content showed an increasing trend, eventually reaching 0.58 g/L, and the propionic acid content decreased during the first 2 days of fermentation and then increased to 0.37 g/L at the end. The accumulation rates of acetic and propionic acids accelerated during the final 3 days of fermentation (**Figure 2B**). The levels of ethyl acetate and ethyl lactate increased as fermentation proceeded (**Figures 2C,D**). Ethyl lactate was undetectable during the first 2 days and then rapidly increased to 1.49 g/L after 13 days, which was 60 times the amount of ethyl acetate present (**Figure 2D**). Five alcoholic flavor substances; namely, isoamyl alcohol, isobutanol, β-phenylethanol, n-propanol, and methanol, were detected in the fermented rice samples. The levels of these substances, with relatively high starting concentrations, showed a decreasing trend in the first 2 days of fermentation then increased and stabilized. For example, the initial level of β-phenylethanol, a characteristic component of rice-flavor, was 0.12 g/L, which rapidly decreased to 0.04 g/L in the first 2 days of fermentation and then slowly increased to 0.067 g/L at the end of fermentation (**Figure 2E**). This indicates that visible β-phenylethanol is mainly produced during the saccharification stage and is partially decomposed during the fermentation stage. The furfural content remained stable and the acetaldehyde content showed a decreasing trend (**Figure 2F**). The analysis of the volatile components in the fermented grains during fermentation showed that, except for ethyl lactate, which accumulated rapidly and in large quantities during the fermentation process, and acetic acid and ethyl acetate, whose levels increased slowly, the other substances were already produced in the saccharification stage, and the contents did not change substantially before and after fermentation.

Changes in the Microbial Community

Figure 3 demonstrated the microbial abundance of bacteria and fungi at the phylum and genus levels. At the phylum level, bacteria mainly consisted of Firmicutes and Proteobacteria, with Firmicutes dominating. The top 10 genera of bacteria obtained according to the average relative abundance of all samples were shown in **Figure 3B** and **Supplementary Table 1**, including *Lactobacillus*, *Weissella*, *Pediococcus*, *Lactococcus*, and *Acetobacter*, etc., and the proportion of these five genera in the brewing process was above 97%. The genus *Bacillus* although in the top 10 genera, were present in extremely low proportions. In Xiaoqu, the order of proportions from high to low was *Weissella* (59.53%), *Pediococcus* (29.18%), *Acetobacter* (3.65%), and *Lactobacillus* (1.35%). The species of *Lactobacillus* were dominant during production (62.88–99.23%), with a proportion of 94.25% at the end of saccharification and a significant decrease followed by a significant increase during fermentation.

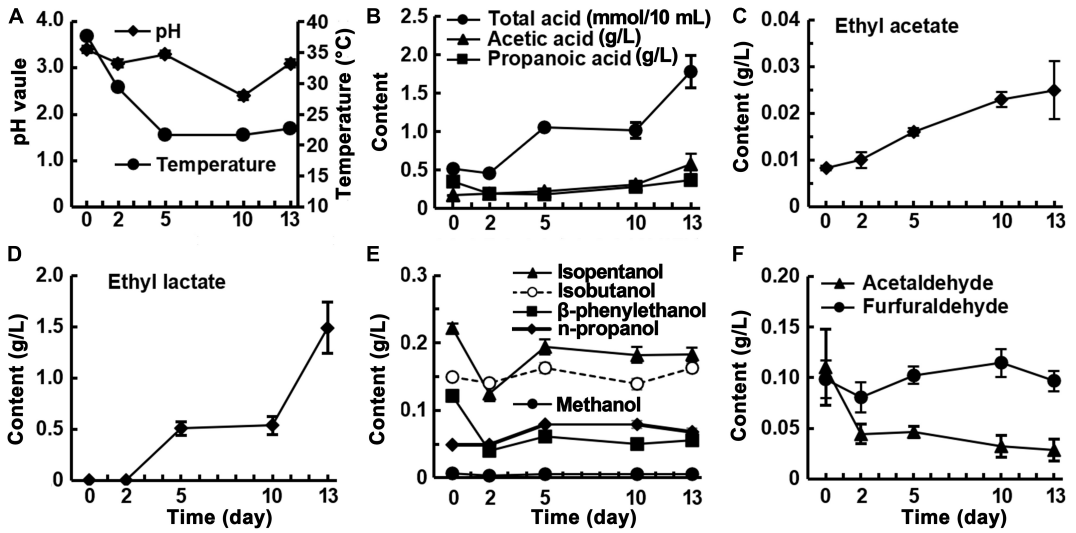

FIGURE 2 | Changes of physicochemical factors in fermented rice during the fermentation of rice-flavor baijiu.

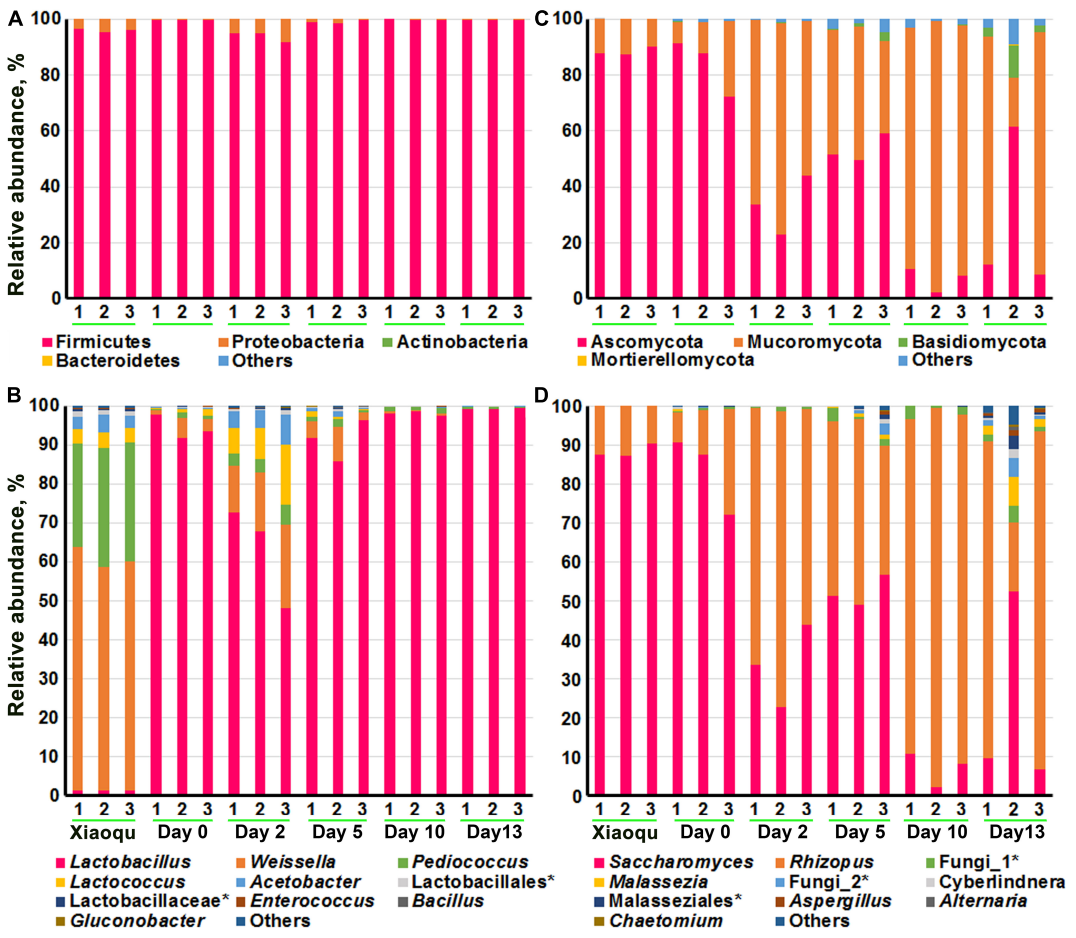

FIGURE 3 | The composition of microbial community in fermented rice in the production of rice-flavor baijiu. Bacteria at phylum **(A)**, and genus **(B)** levels. Fungi at phylum **(C)**, and genus **(D)** levels. 1, 2, and 3 represent three repeats. The rank in genera (top 10) was obtained according to the average relative abundance of all samples.

Among the microorganisms that could be identified at the species level, *Lactobacillus helveticus*, *Lactobacillus fermentum*, and *Weissella paramesenteroides* had the highest abundance. The highest abundance of *L. helveticus* was probably from the environment or raw rice material rather than from Xiaoqu (**Supplementary Table 2**).

At the phylum level, fungi included Ascomycota, Mucoromycota, Basidiomycota, etc., of which the first two were dominant. The top 10 genera of fungi were shown in **Figure 3C** and **Supplementary Table 3**, with *Saccharomyces* (7.06–83.50%) and *Rhizopus* (15.21–90.89%) being dominant. For example, *Saccharomyces* constituted 88.41% of fungi genera in Xiaoqu, with a significant decrease in abundance during fermentation. *Rhizopus* was present at 15.21% at the beginning of fermentation and increased significantly during fermentation, reaching up to 90.89% by day 10. In third place was an unclassified fungus, indicating that non-culturable fungi may be involved in the brewing process of rice-flavor baijiu. At the species level, *S. cerevisiae, Rhizopus arrhizus*, and *Rhizopus microsporus* were dominant, and the proportions of all these three microorganisms changed significantly ($P < 0.5$) during the fermentation process, with the overall trend being that *S. cerevisiae* significantly ($P < 0.5$) decreased, *R. arrhizus* and *R. microsporus* significantly increased, and the proportions were 53.53 and 8.21% at the end of fermentation, respectively (**Supplementary Table 4**).

Alpha Diversity Analysis

Alpha-diversity was calculated at the OTU level to evaluate the changes in microbial diversity during the production of rice-flavor baijiu (**Table 1**). During fermentation, the number of bacterial species first increased significantly, was highest on day 2, then decreased significantly. The trends of the Simpson and Shannon indices of bacteria as well as the number of species were the same, and at the end of the process, the species number and diversity indices were the lowest. There were only five fungal species in Xiaoqu, which was far fewer than the number of bacterial species. The number of fungal species did not change significantly from day 0 to day 10 during fermentation and increased significantly at the end. The Simpson and Shannon indices of fungi showed an increasing trend.

Beta Diversity Analysis

The NMDS analysis based on the Bray–Curtis distance was used to demonstrate beta diversity (**Figure 4**). In the analysis of bacteria, the three replicates were close to each other and the samples were easily distinguishable among groups, indicating that the bacterial communities were more different among groups. In the analysis of fungi, one sample on day 13 was more variable and similar to the samples on day 5, while the three replicates in the other groups were close to each other. The samples from two groups; Xiaoqu and samples at the end of saccharification, were close to each other, while during fermentation, d0, d2 d5, and d10 were well-distinguished, indicating that the fungal communities differed more among these four groups; the differences in fungal community composition in the fermented grains at the late stage of fermentation (days 10 and 13) were relatively small and the community structure was gradually stabilized.

Shared Species Analysis

The four groups of samples; Xiaoqu, day 0 (d0), day 2 (d2), and day 13 (d13), were used to construct the Venn diagram (**Figure 5**). In the bacterial community, 383 species of bacteria were detected in Xiaoqu, of which only 48 species were shared with the d0 sample and 10 with the end of fermentation, indicating that more species of bacteria in the saccharification and fermentation process came from the environment and raw materials, such as rice. As for the fungal community, there were only six species of fungi in Xiaoqu. These six fungal species were shared with d0, d2, and d13 samples. According to **Supplementary Table 4**, four of these were *S. cerevisiae*,

TABLE 1 | Alpha diversity of bacteria and fungi based on high throughput sequencing.

Sample	Xiaoqu	Day 0	Day 2	Day 5	Day 10	Day 13	SEM	P-value
Bacteria								
Chao1	262.0^{b}	180.6^{cd}	345.9^{a}	242.3^{bc}	150.8^{de}	102.8^{e}	20.3	<0.001
Observed_species	245.5^{b}	169.4^{cd}	303.1^{a}	224.8^{bc}	143.6^{de}	96.9^{e}	17.5	<0.001
Simpson	0.90^{a}	0.82^{ab}	0.91^{a}	0.79^{b}	0.60^{c}	0.68^{c}	0.03	<0.001
Shannon	4.66^{ab}	4.05^{b}	4.99^{a}	4.21^{ab}	3.02^{c}	2.77^{c}	0.21	<0.001
Faith_pd	3.87^{b}	3.04^{cd}	4.88^{a}	3.58^{bc}	2.55^{d}	2.69^{d}	0.21	<0.001
Pielou_e	0.59^{a}	0.55^{a}	0.61^{a}	0.54^{a}	0.42^{b}	0.42^{b}	0.02	<0.001
Fungi								
Chao1	5.0^{c}	19.4^{bc}	11.3^{bc}	30.4^{b}	14.7^{bc}	81.1^{a}	27.9	<0.001
Observed_species	5.0^{c}	19.3^{bc}	11.3^{bc}	30.3^{b}	14.6^{bc}	80.6^{a}	27.8	<0.001
Simpson	0.20^{c}	0.27^{c}	0.47^{b}	0.61^{b}	0.48^{b}	0.55^{b}	0.17	0.00
Shannon	0.52^{d}	0.74^{d}	1.10^{cd}	1.84^{b}	1.52^{bc}	2.21^{b}	0.69	0.00
Faith_pd	2.22^{d}	7.16^{bc}	5.41^{cd}	9.34^{b}	5.10^{cd}	19.58^{a}	5.91	<0.001
Pielou_e	0.21^{bc}	0.18^{c}	0.32^{ab}	0.38^{a}	0.40^{a}	0.35^{a}	0.10	0.00

SEM (standard error of the mean); n = 3; ^{a,b,c,d,e}*Mean values in the same row with different superscripts differ significantly (P < 0.05).*

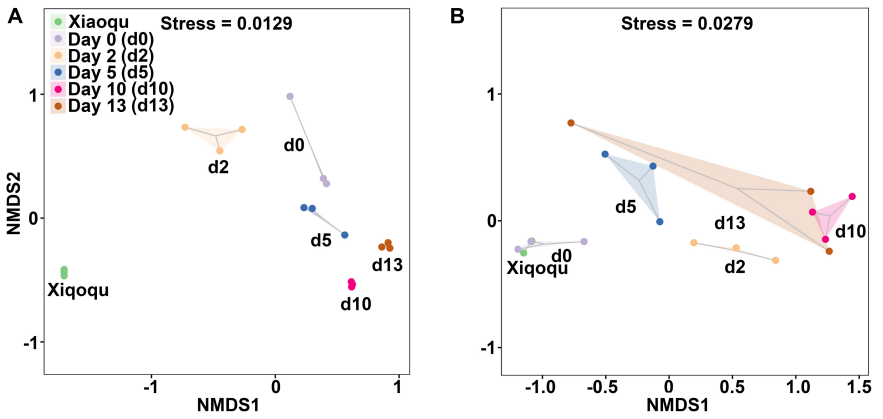

FIGURE 4 | Non-metric multidimensional scaling (NMDS) ranking of microbial community in the production of rice-flavor baijiu. Bacteria **(A)**, and fungi **(B)**. A closer distance between points indicates higher similarity; $n = 3$.

R. arrhizus, *R. microsporus*, and *Cyberlindnera fabianii*. These four species of fungi, especially *S. cerevisiae* and *R. arrhizus*, played a dominant role in the brewing process. Moreover, at the end of fermentation, 156 of the detected fungi were not present in Xiaoqu, d0, or d2, indicating that fungi tended to grow in the fermented grains with time.

Association Between Microbial Community and Physicochemical Factors

Redundancy analysis was performed to reveal the relationships between the microbial community and physicochemical factors based on OTUs (**Figure 6**). In the analysis of bacteria, axis 1 and axis 2 explained 48.57 and 10.09% of the total variance, respectively, and in the analysis of fungi, axis 1 and axis 2 explained 52.70 and 10.98% of the total variance, respectively. Among fungi and bacteria, the angles among ethyl lactate, ethyl acetate, total acid, and acetic acid were all acute, indicating a positive correlation among these four variables. Total acid was the main variable affecting the composition of d10 and d13 species; temperature was always negatively correlated with total acid, i.e., total acid always decreased with increasing temperature. As the fermentation time progressed, the species composition of the community gradually changed from being controlled by temperature to being controlled by total acid. Furthermore, in the analysis of bacteria, d0, d2, and d5 species composition were mainly influenced by pH and temperature. In the fungi, ethyl acetate was positively correlated with acetic acid, pH was positively correlated with β-phenylethanol, and temperature was negatively correlated with ethyl acetate, with temperature being the main variable affecting d0 and d2 species composition.

Comparison of the Microbial Community in Three Different Flavors of Baijiu

The bacterial and fungal communities in the fermentation process of the three flavor types of baijiu were well distinguished (**Figure 7**). As shown in **Figure 7A**, in the analysis of bacteria, the samples were close to each other in the fermentation process of the light-flavor and rice-flavor types, but the two groups could be distinguished from each other; the samples in the fermentation process of the strong-flavor type of baijiu were close to each other and were well-distinguished from the light-flavor and rice-flavor types; the samples of the two starters were easy to reproduce and each was separated from the other groups. In the analysis of fungi, for the fermentation process samples of light-, rice-, and strong-flavor baijiu, each of the three groups clustered together separately (**Figure 7B**). These results indicate that different flavor types of baijiu possess unique microbial communities.

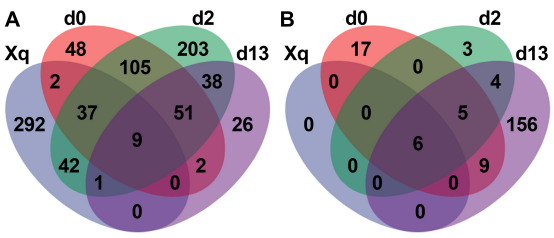

FIGURE 5 | Venn diagram showed the microbial species in Xiaoqu and fermented rice based OTUs obtained by sequencing. Bacteria **(A)**, and fungi **(B)**.

DISCUSSION

The flavor components of baijiu are complex, with nearly 100 types in strong- and sauce-flavor baijiu, and more than 50 types in light-flavor baijiu (Dai et al., 2020; Huang et al., 2020). In comparison, the rice-flavor baijiu has fewer flavor components. Only 11 major flavor components were identified in this study, which might be the main reason for the weak aroma of rice-flavor baijiu. Ethyl lactate, ethyl acetate, and β-phenylethanol are the characteristic components of rice-flavor baijiu that establish the style characteristics (Arbab et al., 2020). In this study, the content of ethyl lactate was much higher than that of ethyl acetate and

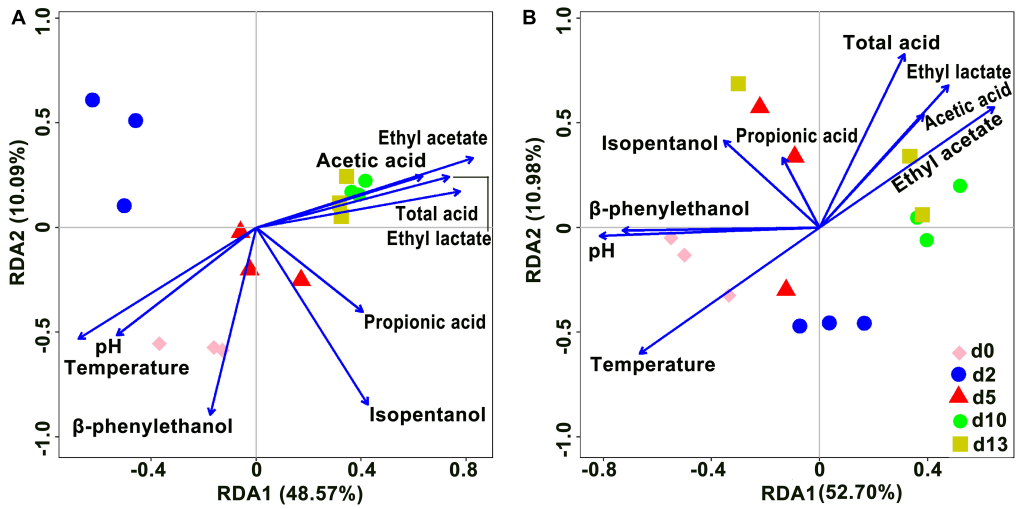

FIGURE 6 | Redundancy analysis (RDA) showed the relationship of microbial community and physicochemical factors in the brewing process of rice-flavor baijiu. Bacteria **(A)**, and fungi **(B)**.

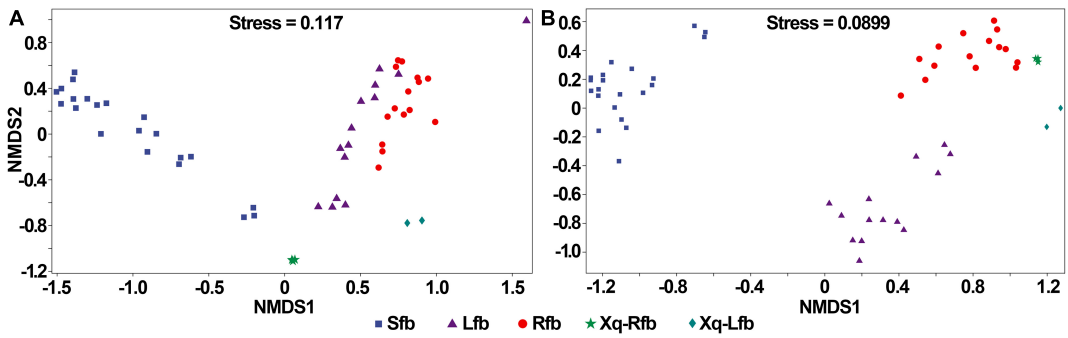

FIGURE 7 | Non-metric multidimensional scaling (NMDS) ranking of microbial community in production of rice-flavor baijiu, light-flavor baijiu, and strong-flavor baijiu. Bacteria **(A)**, and fungi **(B)**. Sfb, strong-flavor baijiu, fermented grains samples were separately collected on days 0, 7, 15, 25, 45, 70, and 95, $n = 3$; Lfb, light-flavor baijiu, fermented grains were separately collected on days 0, 1, 3, 5, 7,10, and 15, $n = 2$; Rfb, rice-flavor baijiu, samples collected in this study. Xq-Rfb, Xiaoqu used in rice-flavor baijiu, $n = 3$; Xq-Lfb, Xiaoqu used in light-flavor baijiu, $n = 2$. Sample information used for bacterial and fungal analyses were shown in **Supplementary Tables 5, 6**, respectively.

β-phenylethanol, with the former being more than 10 times that of the latter, which is in line with the typical characteristics of rice-flavor baijiu. Ethyl lactate was produced during the fermentation of rice-flavor baijiu, while the other 10 components were already produced at the saccharification stage, and other components, such as β-phenylethanol, had mostly completed accumulation at the saccharification stage.

The participation of multiple microorganisms in the fermentation process is a major feature of baijiu production and an important basis for the complexity of the flavor substances (Zou et al., 2018). In this study, the species diversity of bacteria was much higher than that of fungi, and the bacterial diversity index increased then decreased as fermentation progressed, while the fungal diversity tended to increase. As the production of baijiu moves from the saccharification stage to the fermentation stage, the intact rice grains gradually become crushed as the starch in them is digested, and the water held by the starch is gradually released. Some water is also produced while the sugar is broken down. These actions jointly cause the water content in the fermentation materials to increase, and the fermentation state changes from solid to semi-solid and further to liquid state. The changes in material form lead to changes in the composition and diversity of the microbial community. At the early stage of fermentation, the fermented rice is rich in nutrients and gradually change from an aerobic to an anaerobic environment. After the microorganisms adapt to the environment, those from the raw materials and the environment grow rapidly; thus, diversity increases. At the late stage of fermentation, the anaerobic environment is dominant, the nutrient content decreases, and the acidity and alcoholic content increases, which inhibit the growth of some microorganisms and lead to a decrease in species diversity. The changing pattern of microbial diversity is consistent with that in the brewing of strong- (Tan et al., 2019; Guan et al.,

2020), mixed- (Liu and Miao, 2020), and light-flavor baijiu (Dong et al., 2020).

Bacteria are involved in the brewing process of baijiu and influence the production of flavor substances (Arbab et al., 2020). In this study, during the brewing process, *Lactobacillus* (62.88–99.23%) was the dominant genus, followed by *Weissella*, *Pediococcus*, *Lactococcus*, and *Acetobacter*. Among them, the former four are lactic acid bacteria and are the main lactic acid source, while *Acetobacte*r is a strong producer of acetic acid (Wu X. et al., 2017). *Weissella* was the dominant genus in the starter Xiaoqu, and *Lactobacillus* rapidly became the dominant genus during the fermentation stage, with its abundance at the end of fermentation being 99.23%. *Lactobacillus* sp. are more likely to undergo homolactic fermentation, which is the main reason for the rapid increase in ethyl lactate content and only a small increase in acetic acid and ethyl acetate content at the late stage of fermentation. The main bacterial genera in the Xiaoqu light-flavor baijiu were *Lactobacillus*, *Acetobacter*, *Weissella*, *Lactococcus*, and *Bacillus* (Dong et al., 2020; Hu et al., 2021a,b). In strong-flavor baijiu, the main bacteria genera were *Kosakonia*, *Lactobacillus*, *Weissella*, *Pediococcus*, *Pantoea*, and *Bacillus*, which accounted for more than 86% of the bacterial abundance (Guan et al., 2020).

Fungi play a key role in the brewing of baijiu. In this study, the dominant fungi at the genus level were *Saccharomyces* (7.06–83.50%) and *Rhizopus* (15.21–90.89%). From Xiaoqu, at the beginning of fermentation and to the end of fermentation, *Rhizopus* was the dominant flora and the main fungi involved in the brewing of rice-flavor baijiu. Yeast draws sugar substances into the cells and decomposes monosaccharides into carbon dioxide and alcohol under anaerobic conditions (Lin et al., 2017; Wu Q. et al., 2017; Wang J. et al., 2018; Duan et al., 2020). *Rhizopus* and other molds mainly act at the early fermentation stage, providing amylase and glycolase for the fermentation process (Liu et al., 2018), degrading large molecules, such as starch and protein in raw materials, producing small molecules, such as reducing sugars and amino acids for use by yeast, etc., and producing organic acids, aromatic series, etc., which have an important impact on the quality of the liquor (Wang et al., 2008). Generally, *Rhizopus* plays major roles in the saccharification stage, and gradually decline in the fermentation stage due to the decrease in oxygen content, while the abundance of other acid-tolerant and alcoholic anaerobic fungi, such as yeast, gradually increases (Wu H. et al., 2017; Yin et al., 2020a). However, in this study, *Rhizopus* maintained high abundance from the beginning to the end of fermentation, which was very different to the microorganisms in the brewing of light- and strong-flavor baijiu (Guan et al., 2020; Hu et al., 2021b). The main fungi in light-flavor baijiu brewing are *Saccharomyces*, *Aspergillus*, *Rhizopus*, *Pichia*, *Candida*, and *Wickerhamomyces* (Hu et al., 2021b). In the brewing of strong-flavor baijiu, the main fungi are *Kazachstania*, *Thermoascus*, *Aspergillus*, *Saccharomyces*, *Thermomyces*, etc. (Guan et al., 2020).

The NMDS analysis showed that the microbial communities of the three flavor types of baijiu formed their own distinct systems during the fermentation of rice-, light-, and strong-flavor baijiu, and varied greatly among the different flavor types. Compared with the microorganisms of light- and strong-flavor baijiu brewing, the microbial composition of light-flavor baijiu was simple, with few major microbial groups, and with bacteria dominated by *Lactobacillus* and fungi dominated by *Saccharomyces* and *Rhizopus*. In contrast, the other two flavor types of baijiu had many major microbial groups, and in addition to these three microorganisms, *Lactococcus*, *Bacillus*, etc., in bacteria, and a variety of non-*Saccharomyces* yeasts among fungi had high abundance. The small number of microbial species and the prominence of dominant microorganisms may be the main reason for the thin aroma and few flavor substances in rice-flavor baijiu. As a traditional type of baijiu, the production process of rice-flavor baijiu has been passed down between generations (Yin et al., 2020b). The brewing microbial community has been naturally formed through years of domestication, and its simple microbial composition and small number of species means that process improvements can easily be achieved, for example, synthesizing microbial communities by artificial means to replace the traditional Xiaoqu, improving the fermentation method to reduce the interference from undesired microbes, etc.

CONCLUSION

In conclusion, this study revealed the microbial composition and diversity in the production of rice-flavor baijiu. The results showed that the species diversity of bacteria was much higher than that of fungi in the brewing process of rice-flavor baijiu, and the bacterial diversity index first increased and then decreased, while the fungal diversity showed an increasing trend. A variety of major microorganisms originated from the environment and raw rice materials. The main bacteria were *Lactobacillus*, and the main fungi were *Saccharomyces* and *Rhizopus*. Temperature and total acid content were the main physicochemical factors affecting the microbial composition. In addition, this study for the first time, to our knowledge, compared the high-throughput sequencing data of microbial communities of three basic types of baijiu; namely, rice-, light-, and strong-flavor types, and showed that the microbial communities differed significantly among the different flavor types of baijiu. Further study is needed to demonstrate what causes the differences in microbial composition. This study provides a basis for the production and process improvement of rice-flavor baijiu, and lays the foundation for studying the nature of baijiu flavor formation and the connection among microorganisms.

DATA AVAILABILITY STATEMENT

The datasets presented in this study can be found in online repositories. The names of the repository/repositories and accession number(s) can be found below: https://www.ncbi.nlm.nih.gov/, PRJNA699433.

AUTHOR CONTRIBUTIONS

YH, XL, XZ, LW, and ZZ analyzed the data and wrote the manuscript. YL and XZ performed the experiments. TG, XY, JT, NP, YL, and SZ contributed to manuscript preparation and

experimental design. All authors contributed to manuscript revision and approved the submitted version.

FUNDING

This work was supported by the grant 2662018JC016 of the Fundamental Research Funds for the Central Universities, the grant 2020CFB527 of the Natural Science Foundation of Hubei Province, the grant 2020BAB095 of the Key Research and Development Program of Hubei Province, and the grant EWPL201915 of the Hubei Key Laboratory of Edible Wild Plants Conservation and Utilization.

SUPPLEMENTARY MATERIAL

The Supplementary Material for this article can be found online at: https://www.frontiersin.org/articles/10.3389/fmicb.2021.673670/full#supplementary-material

REFERENCES

Arbab, S. H., Raza, H., Qaiser, F. K., and Heping, Z. (2020). Functional microbiota in Chinese traditional Baijiu and Mijiu Qu (starters): a review. *Food Res. Int.* 138:109830. doi: 10.1016/j.foodres.2020.109830

Dai, Y., Tian, Z., Meng, W., and Li, Z. (2020). Microbial diversity and physicochemical characteristics of the Maotai-flavored liquor fermentation process. *J. Nanosci. Nanotechnol.* 20, 4097–4109. doi: 10.1166/jnn.2020.17522

Dong, W., Yang, Q., Liao, Y., Liu, Y., Hu, Y., Peng, N., et al. (2020). Characterisation and comparison of the microflora of traditional and pure culture xiaoqu during the baijiu liquor brewing process. *J. Inst. Brew.* 126, 213–220. doi: 10.1002/jib.597

Dorn-In, S., Hölzel, C. S., Janke, T., Schwaiger, K., Balsliemke, J., and Bauer, J. (2013). PCR-SSCP-based reconstruction of the original fungal flora of heat-processed meat products. *Int. J. Food Microbiol.* 162, 71–81. doi: 10.1016/j.ijfoodmicro.2012.12.022

Duan, G., Liu, Y., Lv, H., Wu, F., and Wang, R. (2020). Optimization of "Zaoheibao" wine fermentation process and analysis of aroma substances. *Biotechnol. Biotec. Equ.* 34, 1056–1064. doi: 10.1080/13102818.2020.1818621

Gao, J., Liu, G., Li, A., Liang, C., Cong, R., and Xu, Y. (2021). Domination of pit mud microbes in the formation of diverse flavour compounds during Chinese strong aroma-type Baijiu fermentation. *LWT Food Sci. Technol.* 137:110442. doi: 10.1016/j.lwt.2020.110442

Guan, T., Lin, Y., Chen, K., Ou, M., and Zhang, J. (2020). Physicochemical factors affecting microbiota dynamics during traditional solid-state fermentation of Chinese strong-flavor baijiu. *Front. Microbiol.* 11:2090. doi: 10.3389/fmicb.2020.02090

He, G., Dong, Y., Huang, J., Wang, X., Zhang, S., Wu, C., et al. (2019). Alteration of microbial community for improving flavor character of Daqu by inoculation with *Bacillus velezensis* and *Bacillus subtilis*. *LWT Food Sci. Technol.* 111, 1–8. doi: 10.1016/j.lwt.2019.04.098

Hong, X., Chen, J., Liu, L., Wu, H., Tan, H., Xie, G., et al. (2016). Metagenomic sequencing reveals the relationship between microbiota composition and quality of Chinese rice wine. *Sci. Rep.* 6, 1–11.

Hu, Y., Wang, L., Zongjie, Z., Yang, Q., Chen, S., Zhang, L., et al. (2021a). Microbial community changes during the mechanized production of light aroma Xiaoqu Baijiu. *Biotechnol. Biotech. Equ.* 35, 487–495. doi: 10.1080/13102818.2021.1892525

Hu, Y., Yang, Q., Chen, D., Fu, B., Zhang, Y., Zhang, Y., et al. (2021b). Study on microbial communities and higher alcohol formations in the fermentation of Chinese Xiaoqu Baijiu produced by traditional and new mechanical technologies. *Food Res. Int.* 140:109876. doi: 10.1016/j.foodres.2020.109876

Huang, X., Fan, Y., Lu, T., Kang, J., Pang, X., Han, B., et al. (2020). Composition and metabolic functions of the microbiome in fermented grain during light-flavor baijiu fermentation. *Microorganisms* 8:1281. doi: 10.3390/microorganisms8091281

Jin, G., Zhu, Y., and Xu, Y. (2017). Mystery behind Chinese liquor fermentation. *Trends Food Sci. Technol.* 63, 18–28. doi: 10.1016/j.tifs.2017.02.016

Li, H., Qin, D., Wu, Z., Sun, B., Sun, X., Huang, M., et al. (2019). Characterization of key aroma compounds in Chinese Guojing sesame-flavor baijiu by means of molecular sensory science. *Food Chem.* 284, 100–107. doi: 10.1016/j.foodchem.2019.01.102

Li, X. R., Ma, E. B., Yan, L. Z., Meng, H., Du, X. W., Zhang, S. W., et al. (2011). Bacterial and fungal diversity in the traditional Chinese liquor fermentation process. *Int. J. Food Microbiol.* 146, 31–37. doi: 10.1016/j.ijfoodmicro.2011.01.030

Lin, J., Wu, Q., and Xu, Y. (2017). Dynamic profile of yeast community associated with urea metabolism in Chinese light-aroma liquor fermentation. *Microbiol. China* 44, 2522–2529.

Liu, J., Chen, J., Fan, Y., Huang, X., and Han, B. (2018). Biochemical characterisation and dominance of different hydrolases in different types of Daqu–a Chinese industrial fermentation starter. *J. Sci. Food Agric.* 98, 113–121. doi: 10.1002/jsfa.8445

Liu, P., and Miao, L. (2020). Multiple batches of fermentation promote the formation of functional microbiota in Chinese miscellaneous-flavor baijiu fermentation. *Front. Microbiol.* 11:75. doi: 10.3389/fmicb.2020.00075

Los, A., Ziuzina, D., Boehm, D., and Bourke, P. (2020). Effects of cold plasma on wheat grain microbiome and antimicrobial efficacy against challenge pathogens and their resistance. *Int. J. Food Microbiol.* 335:108889. doi: 10.1016/j.ijfoodmicro.2020.108889

Song, Z., Du, H., Zhang, Y., and Xu, Y. (2017). Unraveling core functional microbiota in traditional solid-state fermentation by high-throughput amplicons and metatranscriptomics sequencing. *Front. Microbiol.* 8:1294. doi: 10.3389/fmicb.2017.01294

Tan, Y., Zhong, H., Zhao, D., Du, H., and Xu, Y. (2019). Succession rate of microbial community causes flavor difference in strong-aroma baijiu making process. *Int. J. Food Microbiol.* 311, 108350–108350. doi: 10.1016/j.ijfoodmicro.2019.108350

Wang, B., Wu, Q., Xu, Y., and Sun, B. (2018). Specific volumetric weight-driven shift in microbiota compositions with saccharifying activity change in starter for Chinese baijiu fermentation. *Front. Microbiol.* 9:2349. doi: 10.3389/fmicb.2018.02349

Wang, J., Zhong, Q., Yang, Y., Li, H., Wang, L., Tong, Y., et al. (2018). Comparison of bacterial diversity between two traditional starters and the round-koji-maker starter for traditional Cantonese chi-flavor liquor brewing. *Front. Microbiol.* 9:1053. doi: 10.3389/fmicb.2018.01053

Wang, B., Wu, Q., Xu, Y., and Sun, B. (2021). Multiple sugars promote microbial interactions in Chinese baijiu fermentation. *LWT Food Sci. Technol.* 138:110631. doi: 10.1016/j.lwt.2020.110631

Wang, C., Shi, D., and Gong, G. (2008). Microorganisms in Daqu: a starter culture of Chinese Maotai-flavor liquor. *World J. Microb. Biotech.* 24, 2183–2190. doi: 10.1007/s11274-008-9728-0

Wang, C., Tang, J., and Qiu, S. (2020). Profiling of fungal diversity and fermentative yeasts in traditional Chinese Xiaoqu. *Front. Microbiol.* 11:2103. doi: 10.3389/fmicb.2020.02103

Wang, S., Wu, Q., Nie, Y., Wu, J., and Xu, Y. (2019). Construction of synthetic microbiota for reproducible flavor compound metabolism in Chinese light-aroma-type liquor produced by solid-state fermentation. *Appl. Environ. Microb.* 85:e03090-18.

Wanikawa, A. (2020). Flavors in malt whisky: a review. *J. Am. Soc. Brew. Chem.* 78, 260–278. doi: 10.1080/03610470.2020.1795795

Wu, H., Zhang, S., Ma, Y., Zhou, J., Luo, H., and Yang, J. (2017). Comparison of microbial communities in the fermentation starter used to brew Xiaoqu liquor. *J. Inst. Brew.* 123, 113–120. doi: 10.1002/jib.388

Wu, J., Huo, J., Huang, M., Zhao, M., Luo, X., and Sun, B. (2017). Structural characterization of a tetrapeptide from sesame flavor-type baijiu and its

preventive effects against AAPH-induced oxidative stress in HepG2 cells. *J. Agr. Food Chem.* 65, 10495–10504. doi: 10.1021/acs.jafc.7b04815

Wu, Q., Cao, S., and Xu, Y. (2017). Effects of glutinous and nonglutinous sorghums on *Saccharomyces cerevisiae* fermentation for Chinese liquor making. *Int. J. Food Sci. Tech.* 52, 1348–1357. doi: 10.1111/ijfs.13330

Wu, X., Li, Z., and Zhou, S. (2017). Interaction of *Saccharomyces cerevisiae* and *Acetobacter pasteurianus* in liquor fermentation. *Modern Food Sci. Technol.* 33, 61–67.

Yin, X., Yoshizaki, Y., Ikenaga, M., Han, X.-L., Okutsu, K., Futagami, T., et al. (2020a). Manufactural impact of the solid-state saccharification process in rice-flavor baijiu production. *J. Biosci. Bioeng.* 129, 315–321. doi: 10.1016/j.jbiosc.2019.09.017

Yin, X., Yoshizaki, Y., Kurazono, S., Sugimachi, M., Takeuchi, H., Han, X.-L., et al. (2020b). Characterization of flavor compounds in rice-flavor baijiu, a traditional Chinese distilled liquor, compared with Japanese distilled liquors, awamori and Kome-shochu. *Food Sci. Technol. Res.* 26, 411–422. doi: 10.3136/fstr.26.411

Zou, W., Zhao, C., and Luo, H. (2018). Diversity and function of microbial community in Chinese strong-flavor baijiu ecosystem: a review. *Front. Microbiol.* 9:671. doi: 10.3389/fmicb.2018.00671

Conflict of Interest: XZ was employed by Guangdong Deqing Incomparable Health Wine Co., Ltd.

The remaining authors declare that the research was conducted in the absence of any commercial or financial relationships that could be construed as a potential conflict of interest.

frontiers in Microbiology

ORIGINAL RESEARCH
published: 06 May 2021
doi: 10.3389/fmicb.2021.669201

Microbial Community Succession and Its Environment Driving Factors During Initial Fermentation of Maotai-Flavor Baijiu

Fei Hao[1], Yuwei Tan[2], Xibin Lv[1], Liangqiang Chen[1], Fan Yang[1], Heyu Wang[1], Hai Du[1], Li Wang[3] and Yan Xu[2]*

[1]Kweichow Moutai Distillery Co., Ltd., Guizhou, China, [2]Key Laboratory of Industrial Biotechnology, Center for Brewing Science and Enzyme Technology, Ministry of Education, Jiangnan University, Wuxi, China, [3]Kweichow Moutai Group, Guizhou, China

OPEN ACCESS

Edited by:
Xucong Lv,
Fuzhou University, China

Reviewed by:
Beizhong Han,
China Agricultural University, China
Sheng Yin,
Beijing Technology and Business University, China
Jinyuan Sun,
Beijing Technology and Business University, China

***Correspondence:**
Li Wang
zmx1019@163.com

Specialty section:
This article was submitted to Food Microbiology, a section of the journal Frontiers in Microbiology

Received: 18 February 2021
Accepted: 01 April 2021
Published: 06 May 2021

Citation:
Hao F, Tan Y, Lv X, Chen L, Yang F, Wang H, Du H, Wang L and Xu Y (2021) Microbial Community Succession and Its Environment Driving Factors During Initial Fermentation of Maotai-Flavor Baijiu. Front. Microbiol. 12:669201. doi: 10.3389/fmicb.2021.669201

The microbial composition and environmental factors can take a great influence on community succession during the solid-state fermentation (SSF) of Maotai-flavor Baijiu. In this paper, high-throughput sequencing was used to reveal the dominant microorganisms and the evolution process of microbial community structure in the initial fermentation of Maotai-flavor Baijiu. The correlation analysis was carried out for the relationship between physicochemical factors and fermented microbes. The results showed that microorganisms were obviously enriched and the diversity of bacteria and fungi showed a downward trend during the heap fermentation process of Maotai-flavor Baijiu. However, the diversity of fungi in the pit fermentation process increased. Generally, *Lactobacillus*, *Pichia*, and *Saccharomyces* were the dominant microorganisms in the initial fermentation of Maotai-flavor Baijiu. According to the redundancy analysis, we found that reducing sugar was the key driving factor for microbial succession in the heap fermentation, while acidity, alcohol, and temperature were the main driving forces in pit fermentation. This study revealed the microbial succession and its related environmental factors in the initial fermentation of Maotai-flavor Baijiu, which will enrich our knowledge of the mechanism of solid-state liquor fermentation.

Keywords: Maotai-flavor Baijiu, high throughput sequencing, microbiol community succession, solid-state fermentation, environmental driving forces

INTRODUCTION

Baijiu is produced by the solid-state fermentation (SSF) process which involves complex microbiota (Wang et al., 2018a; Guo et al., 2019). Complex microbial succession during SSF plays an important role in yield and quality of liquor production (Li et al., 2016a; Liu et al., 2017; Zhang et al., 2020). The multiple environmental factors drive microbial community changes at large spatial scales, including pH, temperature, moisture, and salinity (Zheng et al., 2014a; Xu et al., 2018). Understanding the relationship between microbial community and environment factors in fermentation process is helpful to provide controllable management strategies.

Recently, the research of Baijiu technology mainly focused on the screening of functional microorganisms, analysis of microbial community structure succession, and the correlation between volatile profiles and microbial communities (Zou et al., 2018; Jin et al., 2019; Song et al., 2019; Wang et al., 2020). These studies revealed the changes of microbial succession in the process of liquor making, the core functional strains for liquor brewing, and their contribution to liquor flavor compounds. That is a great significance for the analysis of microbial brewing mechanism. However, little is known about the relationship between environmental factors and microbial structure succession, which makes it difficult to control and manage the fermentation process. In addition, the production process of liquor is accompanied by special extreme environments, such as high temperature, high acidity, and high ethanol (Xu et al., 2017; Wang et al., 2019a). That deepens the difficulties to study the microbial community diversity and temporal succession in microbial ecology of Maotai-flavor Baijiu fermentation.

Maotai is a world-famous traditional Baijiu with complex taste and aroma, which are considered to be strongly influenced by the quality of fermentation technology (Xu and Ji, 2012). Maotai production is carried out in nine batches over the course of a year. Two batches of sorghum are added to the liquor brewing process during the first two batches, which is called the initial fermentation of Maotai flavor Baijiu. Sorghum is gelatinized after absorbing water, and then produced various flavor substances and their precursors, which laid a foundation for the smooth progress of subsequent liquor-making process. However, the core microorganisms and the environmental driving factors of community succession are not clear.

In this paper, the microbial composition during the initial fermentation of Maotai-flavor Baijiu was analyzed by high-throughput sequencing technology. The correlation between the microbial composition and the changes of physicochemical indexes was analyzed using redundancy analysis. This work aimed to explore the environmental driving force of microbial succession.

MATERIALS AND METHODS

Sample Collection

All samples were collected in a well-known sauce-flavor *Baijiu* distillery (Guizhou Province, China). The fermentation process was carried out in two distinct phases: heap fermentation and pit fermentation. Heap fermentation samples were collected on days 0, 1, 2, and 3, marked as D0, D1, D2, and D3, respectively (**Supplementary Figure S1**). For pit fermentation, samples were collected at 5-day intervals until the end of fermentation and marked as F0, F5, F10, F15, and F30 (**Supplementary Figure S1**, point C and D for heap fermentation samples, point A and B for pit fermentation samples). Samples were taken from two layers for replicate samples, and different points in the same layer were mixed to form one sample to reduce the heterogeneity of samples before extraction and analysis (Song et al., 2017). Hence, we totally collected eight samples of heap fermented grains and 10 samples of pit fermented grains.

Fermentation Parameters Detection and Analysis

To understand the fermentation processes, seven fermentation parameters, including temperature, moisture, acidity, reducing sugar, alcohol, acetic acid, and lactic acid were detected. The temperatures of the sampling locations were measured and recorded by electron probe thermometer before sample collection. Moisture of fermented grains was determined by a gravimetric method by drying samples to a constant weight at 125°C. The acidity was measured based on the methods described by others (Tan et al., 2019). Alcohol, reducing sugar, and organic acids were analyzed *via* high-performance liquid chromatography (HPLC; Waters 2,695, Milford, United States) equipped with refractive index detector (RID, 2414) and photodiode array detector (PDA, 2998), based on the method described elsewhere (Zheng et al., 2014b; Wang et al., 2017; Jiang et al., 2019).

DNA Extraction, Amplicon Sequencing, and Analysis

Sample pretreatment and DNA extraction were using a previously reported method (Du et al., 2019). Bacterial V3-V4 and the fungal ITS1 of the rRNA were amplified using forward primers (5'-GTACTCCTACGGGAGGCAGCA-3', 5'-CTTGGT CATTT AGAGGAAGTAA-3') and the reverse primer (5'-GT GGACTA CHVGGGTWTCTAAT-3', 5'-TGCGTTCTTCATCGATGC-3'), respectively (Soergel et al., 2012; Hertz et al., 2016). The barcoded PCR products were sequenced on a MiSeq benchtop sequencer for 250-bp paired-end sequencing (2 × 250 bp; Illumina, San Diego, CA, United States) at Beijing Auwigene Tech. Ltd (Beijing, China). All the raw sequences generated were processed *via* QIIME v.1.9.1 (Caporaso et al., 2010) and R (v.2.3–5). The representative bacterial OTU sequences were annotated using the Silva 132_16 S rRNA database with a QIIME-based wrapper of RDP-classifier (v.2.2). The representative fungal OTU sequences were compared using BLAST search against the UNITE fungal ITS database.[1] All sequences generated were submitted to the NCBI database under accession number: PRJNA702253.

Statistical Analysis

The dynamics of fermentation parameters and microbial diversity were fitted *via* Excel2019 (Microsoft Corporation, United States). To analyze the community driving factors, distance-based redundancy analysis (db-RDA) was conducted *via* Canoco software. The Mantel test was conducted in R (version 3.2.4) *via* the vegan package (version 2.3–4). All possible Spearman's rank correlations among the genera and fermentation parameters using R (v.2.3–5) and the significant correlations (FDR < 0.05) were retained. The network was created by Gephi (v 0.9.2) to

[1]https://unite.ut.ee/

sort through and visualize the correlations between microbiota and fermentation parameters (Kauffman et al., 2014).

RESULTS

Dynamic Changes of Fermentation Parameters During Initial Fermentation of Maotai-Flavor Baijiu

The seven fermentation parameters, including temperature, moisture, acidity, reducing sugar, alcohol, acetic acid, and lactic acid were detected and analyzed during Baijiu fermentation (**Figure 1**). In the stage of heap fermentation, alcohol increased to 0.58 ± 0.12% at the 3rd day. Reducing sugar increased significantly from day 0 to 3, with an average range from 0.64 ± 0.16% to 1.06 ± 0.01%, while the temperature increased from 21.2 ± 1.0°C to 36.2 ± 1.8°C. The acidity, lactic acid, acetic acid, and moisture also showed an upward trend. In the pit fermentation, reducing sugar and temperature decreased from 1.11 ± 0.04%, 35.4 ± 2.0°C to 0.20 ± 0.03%, 28.9 ± 3.1°C, respectively. The values of alcohol, acidity, lactic acid, and acetic acid increased significantly, from 0.64 ± 0.03%, 0.80 ± 0.01%, 0.45 ± 0.01%, and 0.16 ± 0.004% to 1.44 ± 0.01%, 3.42 ± 0.01%, 1.09 ± 0.07%, and 0.21 ± 0.01%, respectively.

Microbial Community Composition and Diversity During Initial Fermentation of Maotai-Flavor Baijiu

The high-throughput sequencing was applied to reveal the microbial community structure of samples. After quality control, 553,936 high quality reads from V3 to V4 region of 16S rRNA gene sequences, and 487,046 high quality reads from ITS region were obtained from 18 samples. For bacteria, there was an average of 30,774 reads per sample, with a range from 20,066 to 69,274 reads. For fungi, there was an average of 27,058 reads per sample, with a range from 20,036 to 53,039 reads. Bacterial and fungal OTUs were clustered at a 97% similarity level of sequences. Measures of α-diversity revealed the different trends between bacterial and fungal at different fermentation stages (**Figure 2**). The diversity of bacterial community increased in the early stage of heap fermentation, and decreased continuously from the late stage of heap fermentation to the early stage of pit fermentation. And then it was increased slightly and kept stable in the late stage of pit fermentation. However, the diversity of fungal community decreased in the early stage of heap fermentation and increased continuously from the late stage of heap fermentation to the early stage of pit fermentation. And then it was decreased slightly and kept stable in the process of pit fermentation.

A total of 210 genera of bacteria and 75 genera of fungi were detected in fermented grains of Maotai-flavor Baijiu. The genera with an average relative abundance over 0.1% across all the samples were selected. In particular, *Lactobacillus* (59.6%), *Virgibacillus* (8.2%), unidentified (7.4%), *Kroppenstedtia* (6.8%), *Bacillus* (5.7%), *Oceanobacillus* (5.4%), and *Pediococcus* (3.1%) were the dominant genera. In the process of heap fermentation, the relative abundance of *Lactobacillus*, *Kroppenstedtia*, and *Pediococcus* increased gradually, while *Virgibacillus*, *Bacillus*, and *Oceanobacillus* decreased. And in pit fermentation, *Lactobacillus* increased continuously and became the absolute dominant bacteria (**Figure 3A**).

The main fungal genera (with an average abundance above 1%) in fermented system were *Pichia* (71.1%), *Saccharomyces* (18.2%), unidentified (4.2%), *Aspergillus* (1.6%), *Thermoascus* (1.3%), and *Monascus* (1.2%). In heap fermentation, the proportion of *Pichia* was increasing and became the dominant bacterial genus (**Figure 3B**), while the other major fungal genera continues to decrease. In pit fermentation, although the abundance of *Pichia* has decreased, it was still the major fungal genus with the highest proportion. In addition,

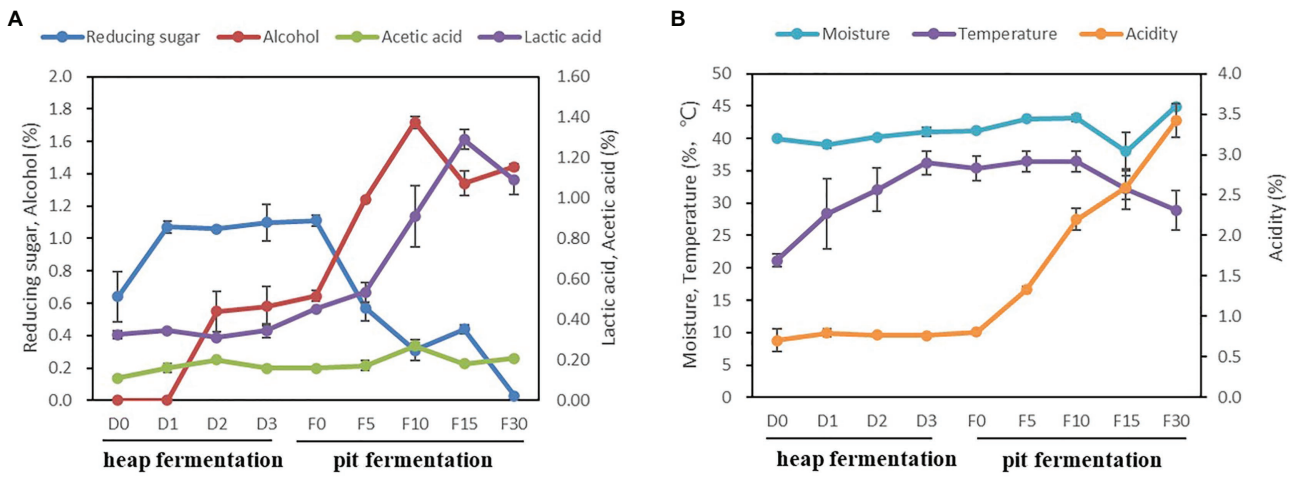

FIGURE 1 | Changes of physicochemical parameters in fermented grains during fermentation. **(A)** The trend of reducing sugar, alcohol, acetic acid, and lactic acid. **(B)** The trend of moisture, temperature, and acidity.

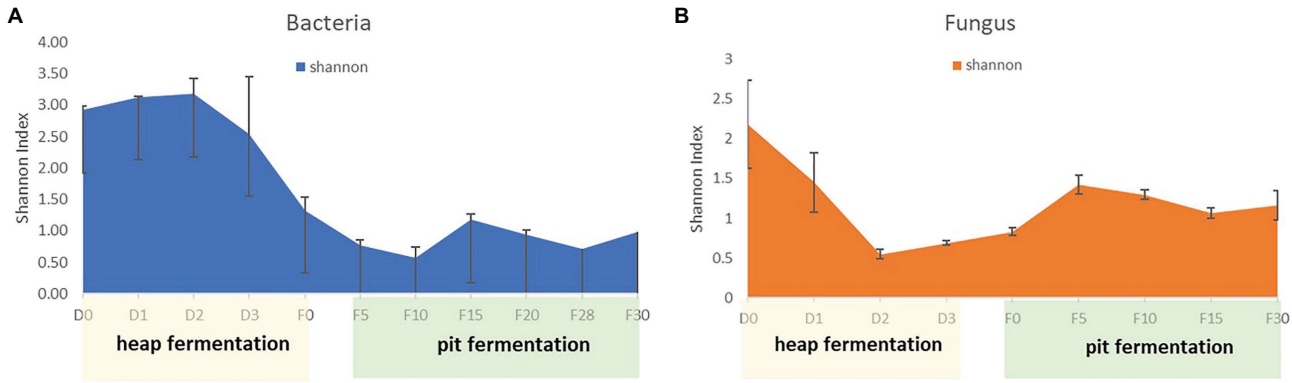

FIGURE 2 | Diversity of microbiol community in fermented grains during fermentation. **(A)** Diversity of bacterial community in fermented grains during fermentation. **(B)** Diversity of fungal community in fermented grains during fermentation.

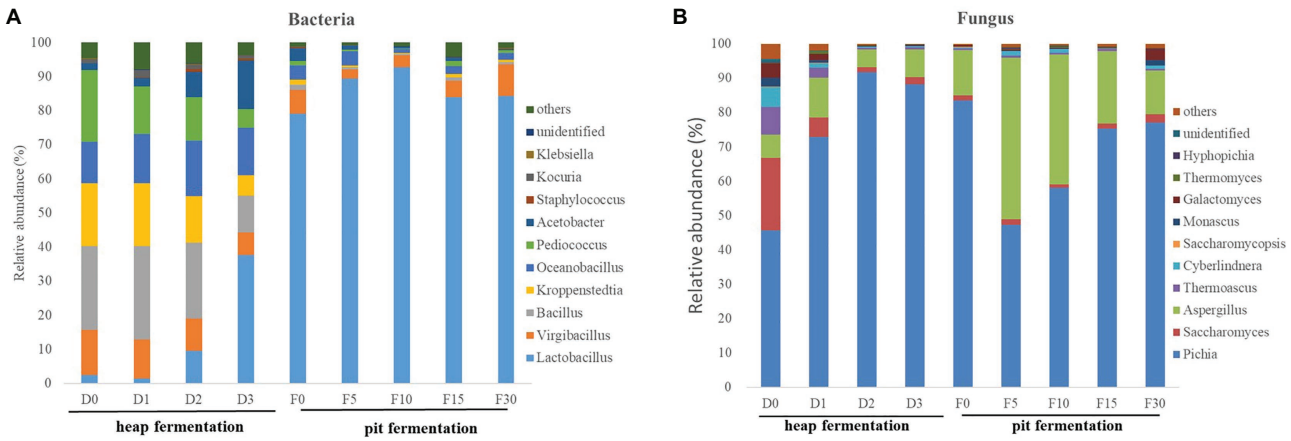

FIGURE 3 | Relative abundance of microbiol community in fermenting grains sampled from different fermentation stages. **(A)** Average bacterial distribution at the genus-level of microbiota. **(B)** Average fungal distribution at the genus-level of microbiota.

the abundance of *Saccharomyces* has been increasing and also becoming one of the main fungal microorganisms.

Driving Factors of Heap Fermentation and Pit Fermentation Process

The physicochemical parameters in fermentation can affect the growth and metabolism of microorganisms. It is helpful to understand the mechanism of fermentation process by analyzing the correlation between microorganisms and environmental factors. To clarify the main drivers in different fermentation process, distance-based redundancy analysis (db-RDA) and correlation network between microbiota and driving factors were performed as shown in **Figure 4A**. Results of db-RDA analyses showed that the explanatory rate of physicochemical indices of samples on the distribution of microbial communities was 72.4%. That indicated that physicochemical indices had an important impact on microbial succession change. Besides, reducing sugar, temperature, alcohol, and acidity had strong correlation with microbial community. Among them reducing sugar in heap fermentation was positively correlated with microbial community. Reducing sugar had higher content in this stage. Adequate sugar supply is benefited for microbial growth and metabolism (Chen et al., 2014). Sugar content was the main driving factor for microbial succession in this stage. Ethanol, acidity, temperature, and other indicators were positively correlated with the microbial community during pit fermentation process. In the pit fermentation period, microorganisms metabolize to produce alcohol and lactic acid (Yi et al., 2019). Ethanol, acidity, and temperature were the main driving factors for microbial succession in the process of pit fermentation.

To clarify the relationships among specific genera and driving forces, we analyzed their correlation *via* Spearman coefficient ($p < 0.05$; **Figure 4B**). From a network perspective, **Figure 4B** shows that the genera *Virgibacillus*, *Kroppenstedtia*, and *Pediococcus* were positively correlated with sugar content. The result indicated that there was a certain correlation between

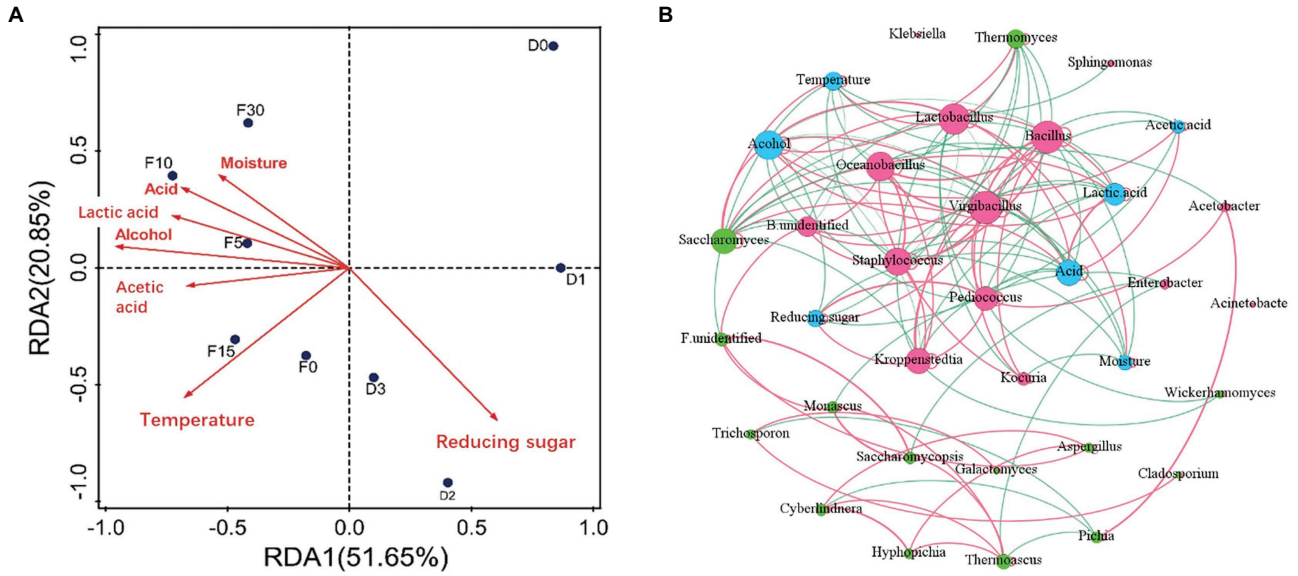

FIGURE 4 | Correlations between fermentation parameters and community composition during heap fermentation and pit fermentation stages. **(A)** Distance-based-redundancy analysis (RDA)-forwsel analysis of microbial community composition and physicochemical characteristics. The last capital letter D and F represents heap fermentation and pit fermentation, respectively. The numbers after the letters represent the fermentation days of 0, 1, 2, 3, 5, 10, 15, and 30. The significance of variables was assessed with the permutation test (n = 1,000). **(B)** Co-occurrence network of physicochemical properties and microbes based on the spearman correlation. Red, green, and blue circles represent bacteria, fungi, and physicochemical properties, respectively. Red gray and green gray represent positive and negative interactions, respectively.

sugar content and the dominant bacteria in the process of heap fermentation. Ethanol, acidity, lactic acid, and temperature were positively correlated with *Lactobacillus* and *Saccharomyces*. This indicated that the above physicochemical parameters had an important impact on the dominant microorganism succession in pit fermentation. We also found that acetic acid was negatively correlated with *Virgibacillus* and *Bacillus*, and water was negatively correlated with *Virgibacillus*, *Bacillus*, *Oceanobacillus*, *Staphylococcus*, and *Kocuria*.

DISCUSSION

Baijiu fermentation is an open SSF process, in which microorganisms are derived from the environment, and the environmental factors affect the succession of microbial community structure (Guan et al., 2020; Wang et al., 2020). However, there are few studies on the interactions of microbial and environmental factors in Maotai-flavor Baijiu fermentation process; the lack of knowledge makes it difficult to control the fermentation process. Therefore, it is important to determine the mechanisms underlying the assembly and succession of the heap fermentation and pit fermentation microbial community.

The traditional Maotai-flavor Baijiu fermentation is processed by typical two-stage fermentation, including heap fermentation and pit fermentation. Heap fermentation is a special brewing process of Maotai-flavor Baijiu, which is different from other distilled liquors in the world (Tsakiris et al., 2014; Wiśniewska et al., 2017). Due to the growth and metabolism of microorganisms, the temperature of fermented grains in the process of heap fermentation can reach above 50°C. Heap fermentation enriches and selects appropriate microorganisms for liquor fermentation. And these selected microbiota produce various flavors and flavor precursors, which are the key to the Maotai flavor (Wang et al., 2018b; Dai et al., 2020). In this study, the microbial succession in the heap fermentation was investigated, and the results showed that the main genera were *Virgibacillus*, *Kroppenstedtia*, *Bacillus*, *Lactobacillus*, *Pichia*, *Saccharomyces*, and *Thermoascus* (**Figure 3**). The dominant microorganisms in heap fermentation process are heat-resistant species, which is consistent with the previous research results (Wu and Xu, 2012).

During the heap fermentation process, the diversity of bacteria and fungi showed the opposite trend. In the beginning of heap fermentation, the stater of Baijiu fermentation, which was called daqu, was added to the fermented grains. Bacteria were the dominant microorganisms in daqu (Gan et al., 2019), which led to the growth of bacteria community in the early stage of heap fermentation. However, in the late stage of heap fermentation, the amount of fungal community increased (Wu et al., 2012), and the diversity of fungi showed an increasing trend. It is noteworthy that the reducing sugar content kept stable in the late stage of heap fermentation; however, the reducing sugar in heap fermentation was positively correlated with microbial community. Baijiu production process is solid state fermentation, saccharification and fermentation were carried out simultaneously. Therefore, the content of reducing sugar in fermented grains is a dynamic parameter, and the content

of reducing sugar remains stable in the process of heap fermentation, indicating that the production and consumption of reducing sugar reach a balance. Microorganisms decomposed the fermented grains to produce reducing sugars, so the reducing sugars could be used as nutrients for their growth and metabolization. Our results show that the heap fermentation enriched the necessary microflora for the production of Maotai-flavor Baijiu.

The pit fermentation is the main stage of alcohol accumulation in Maotai-flavor liquor production. During the pit fermentation process, *Lactobacillus* became the dominant bacteria. Meanwhile, the abundance of *Saccharomyces* increased significantly, and together with *Pichia* it has become the dominant fungi in the fermentation system. Compared with previous studies (Song et al., 2017), we found that the content of ethanol and lactic acid increased significantly during the pit fermentation process, while the temperature gradually decreased in the later stage of pit fermentation (**Figure 1**). It implied the flourishing growth of the microbial community with specific functional metabolites produced (Li et al., 2016b; Kong et al., 2017). With the content of ethanol and lactic acid increased, the extreme environmental factors inhibited the growth of most bacteria, and consequently, the diversity of bacteria decreased. However, some fungi (such as *Saccharomyces* and *Saccharomycopsis*) still maintained a good growth trend, which led to the increasing of fungal diversity in the early stage of pit fermentation process. At the end of pit fermentation, the fermented grains were got out from the pit for the spirit distillation, which led to the anaerobic fermentation environment is interrupted. Part of the alcohol and lactate could be converted into esters and other flavor substances in the late stage of pit fermentation (Jia et al., 2020), so it showed a decreasing trend of the alcohol and lactate content. These results showed that the key functional fermentation microorganisms could be enriched in pit fermentation process, which provided the basis for the continuous fermentation of Maotai-flavor Baijiu.

With the successive changes of microbial communities in the Maotai-flavor Baijiu fermentation process, *Lactobacillus*, *Saccharomyces*, and *Pichia* became the dominant microorganisms in the fermentation system (**Figure 3**). These microorganisms are common to different flavor liquor brewing processes. However, they show different succession trends in different brewing systems due to differences in raw materials, environment, and process operation (Tan et al., 2019; Wang et al., 2019b; Pang et al., 2020). *Lactobacillus* can regulate the acidity of fermented grains by lactic acid metabolism and inhibit the growth of contaminating bacteria (Du et al., 2020). *Lactobacillus*, as the core functional microorganism for the increasing acidity, has ability to produce lactic acid, ethanol, and acetic acid by heterolactic fermentation (Song et al., 2017). *Saccharomyces* has acid resistance and mainly metabolizes ethanol during fermentation in pits (Lu et al., 2015; Meng et al., 2015). It plays an important role in diversity of tastes and flavors with established qualities (Abe et al., 2019). *Pichia* was considered as non-alcoholic yeast during the liquor making process, mainly used to produce volatile compounds in liquor (Mónaco et al., 2016; Hu et al., 2018). The previous research found that *Pichia* could degrade lactic acid and upregulate the microbial metabolic activity of ethanol in *S. cerevisiae* under lactic acid stress (Mónaco et al., 2014; Yamamoto et al., 2019; Deng et al., 2020). It indicated that *Pichia* could be an important acidity-regulating microorganism for the production of liquor-making. Accordingly, the process of heap and pit fermentation significantly contributed to the enrichment of microorganisms, thus, forming the unique flavor of Maotai-flavor Baijiu. The brewing process of Maotai-flavor Baijiu is a complex microecological fermentation system, and the dynamic changes of microbial succession in this process need to be further studied.

In conclusion, we unveiled the microbial diversity and composition during the initial fermentation of Maotai-flavor Baijiu by high-throughput sequencing technologies. Both heap fermentation and pit fermentation play an important role in the screening and enrichment of microbial community for Maotai-flavor Baijiu production. In addition, reducing sugar was the key driving factor for microbial succession in the heap fermentation, while acidity, alcohol, and temperature were the main driving forces in pit fermentation. According to the best of our knowledge, this is the first report to analyze the dynamic changes of microorganism in the initial fermentation of Maotai-flavor Baijiu. Exploring the microbial succession and its relative environmental factors could provide valuable information for understanding the complete ecology of Maotai-flavor Baijiu fermentation systems.

DATA AVAILABILITY STATEMENT

The datasets presented in this study can be found in online repositories. The names of the repository/repositories and accession number(s) can be found in the article/**Supplementary Material**.

AUTHOR CONTRIBUTIONS

FH and YT are responsible for sample collection, gene extraction, and data analysis. XL and LC are responsible for sample collection and gene extraction. FY, HW, and HD are responsible for the design of specific ideas and technical guidance of this study. LW and YX are responsible for the overall design, organization, and implementation of this study. All authors contributed to the article and approved the submitted version.

ACKNOWLEDGMENTS

We would like to thank Zhang Hongxia and Wei Junlin for the samples for statistical methods and sample collection.

SUPPLEMENTARY MATERIAL

The Supplementary Material for this article can be found online at: https://www.frontiersin.org/articles/10.3389/fmicb.2021.669201/full#supplementary-material

REFERENCES

Abe, T., Toyokawa, Y., Sugimoto, Y., Azuma, H., Tsukahara, K., Nasuno, R., et al. (2019). Characterization of a new *Saccharomyces cerevisiae* isolated from hibiscus flower and its mutant with L-leucine accumulation for awamori brewing. *Front. Genet.* 10:490. doi: 10.3389/fgene.2019.00490

Caporaso, J. G., Kuczynski, J., Stombaugh, J., Bittinger, K., Bushman, F. D., Costello, E. K., et al. (2010). QIIME allows analysis of high-throughput community sequencing data. *Nat. Methods* 7, 335–336. doi: 10.1038/nmeth.f.303

Chen, B., Wu, Q., and Xu, Y. (2014). Filamentous fungal diversity and community structure associated with the solid state fermentation of Chinese Maotai-flavor liquor. *Int. J. Food Microbiol.* 179, 80–84. doi: 10.1016/j.ijfoodmicro.2014.03.011

Dai, Y., Tian, Z., Meng, W., and Li, Z. (2020). Microbial diversity and physicochemical characteristics of the Maotai-flavored liquor fermentation process. *J. Nanosci. Nanotechnol.* 20, 4097–4109. doi: 10.1166/jnn.2020.17522

Deng, N., Du, H., and Xu, Y. (2020). Cooperative response of *Pichia kudriavzevii* and *Saccharomyces cerevisiae* to lactic acid stress in Baijiu fermentation. *J. Agric. Food Chem.* 68, 4903–4911. doi: 10.1021/acs.jafc.9b08052

Du, H., Wang, X., Zhang, Y., and Xu, Y. (2019). Exploring the impacts of raw materials and environments on the microbiota in Chinese Daqu starter. *Int. J. Food Microbiol.* 297, 32–40. doi: 10.1016/j.ijfoodmicro.2019.02.020

Du, R., Wu, Q., and Xu, Y. (2020). Chinese liquor fermentation: identification of key flavor-producing *Lactobacillus spp*. by quantitative profiling with indigenous internal standards. *Appl. Environ. Microbiol.* 86:e00456–20. doi: 10.1128/AEM.00456-20

Gan, S. H., Yang, F., Sahu, S. K., Luo, R. Y., Liao, S. L., Wang, H. Y., et al. (2019). Deciphering the composition and functional profile of the microbial communities in Chinese Moutai liquor starters. *Front. Microbiol.* 10:1540. doi: 10.3389/fmicb.2019.01540

Guan, T., Lin, Y., Chen, K., Ou, M., and Zhang, J. (2020). Physicochemical factors affecting microbiota dynamics during traditional solid-state fermentation of Chinese strong-flavor Baijiu. *Front. Microbiol.* 11:2090. doi: 10.3389/fmicb.2020.02090

Guo, M. Y., Hou, C. J., Bian, M. H., Shen, C. H., Zhang, S. Y., Huo, D. Q., et al. (2019). Characterization of microbial community profiles associated with quality of Chinese strong-aromatic liquor through metagenomics. *J. Appl. Microbiol.* 127, 750–762. doi: 10.1111/jam.14279

Hertz, M., Jensen, I. R., Jensen, L. Ø., Thomsen, S. N., Winde, J., Dueholm, M. S., et al. (2016). The fungal community changes over time in developing wheat heads. *Int. J. Food Microbiol.* 222, 30–39. doi: 10.1016/j.ijfoodmicro.2016.01.018

Hu, L., Wang, J., Ji, X., Liu, R., Chen, F., and Zhang, X. (2018). Selection of non- *Saccharomyces* yeasts for orange wine fermentation based on their enological traits and volatile compounds formation. *J. Food Sci. Technol.* 55, 4001–4012. doi: 10.1007/s13197-018-3325-5

Jia, W., Fan, Z., Du, A., Li, Y., and Chu, X. (2020). Recent advances in Baijiu analysis by chromatography based technology—a review. *Food Chem.* 324:126899. doi: 10.1016/j.foodchem.2020.126899

Jiang, J., Liu, Y., Li, H., Yang, Q., Wu, Q., Chen, S., et al. (2019). Modeling and regulation of higher alcohol production through the combined effects of the C/N ratio and microbial interaction. *J. Agric. Food Chem.* 67, 10694–10701. doi: 10.1021/acs.jafc.9b04545

Jin, Y., Li, D., Ai, M., Tang, Q., Huang, J., Ding, X., et al. (2019). Correlation between volatile profiles and microbial communities: a metabonomic approach to study Jiang-flavor liquor Daqu. *Food Res. Int.* 121, 422–432. doi: 10.1016/j.foodres.2019.03.021

Kauffman, J., Kittas, A., Bennett, L., and Tsoka, S. (2014). DyCoNet: a Gephi plugin for community detection in dynamic complex networks. *PLoS One* 9:e101357. doi: 10.1371/journal.pone.0101357

Kong, Y., Wu, Q., and Xu, Y. (2017). Comparative studies on the fermentation performance of autochthonous *Saccharomyces cerevisiae* strains in Chinese light-fragrant liquor during solid-state or submerged fermentation. *J. Appl. Microbiol.* 122, 964–973. doi: 10.1111/jam.13377

Li, P., Lin, W., Liu, X., Wang, X., and Luo, L. (2016a). Environmental factors affecting microbiota dynamics during traditional solid-state fermentation of Chinese Daqu starter. *Front. Microbiol.* 7:1237. doi: 10.3389/fmicb.2016.01237

Li, X., Xu, W., Yang, J., Zhao, H., Pan, C., Ding, X., et al. (2016b). Effects of applying lactic acid bacteria to the fermentation on a mixture of corn steep liquor and air-dried rice straw. *Anim Nutr.* 2, 229–233. doi: 10.1016/j.aninu.2016.04.003

Liu, J., Wu, Q., Wang, P., Lin, J., Huang, H., and Xu, Y. (2017). Synergistic effect in core microbiota associated with sulfur metabolism in spontaneous Chinese liquor fermentation. *Appl. Environ. Microbiol.* 83:e01475–17. doi: 10.1128/AEM.01475-17

Lu, X., Wu, Q., Zhang, Y., and Xu, Y. (2015). Genomic and transcriptomic analyses of the Chinese Maotai-flavored liquor yeast MT1 revealed its unique multi-carbon co-utilization. *BMC Genomics* 16:1064. doi: 10.1186/s12864-015-2263-0

Meng, X., Wu, Q., Wang, L., Wang, D., Chen, L., and Xu, Y. (2015). Improving flavor metabolism of *Saccharomyces cerevisiae* by mixed culture with *Bacillus licheniformis* for Chinese Maotai-flavor liquor making. *J. Ind. Microbiol. Biotechnol.* 42, 1601–1608. doi: 10.1007/s10295-015-1647-0

Mónaco, S. M. D., Barda, N. B., Rubio, N. C., and Caballero, A. C. (2014). Selection and characterization of a patagonian *Pichia kudriavzevii* for wine deacidification. *J. Appl. Microbiol.* 117, 451–464. doi: 10.1111/jam.12547

Mónaco, S. M. D., Rodríguez, M. E., and Lopes, C. A. (2016). *Pichia kudriavzevii* as a representative yeast of north Patagonian winemaking terroir. *Int. J. Food Microbiol.* 230, 31–39. doi: 10.1016/j.ijfoodmicro.2016.04.017

Pang, X. N., Huang, X. N., Chen, J. Y., Yu, H. X., Wang, X. Y., and Han, B. Z. (2020). Exploring the diversity and role of microbiota during material pretreatment of light-flavor Baijiu. *Food Microbiol.* 91:103514. doi: 10.1016/j.fm.2020.103514

Soergel, D. A. W., Dey, N., Knight, R., and Brenner, S. E. (2012). Selection of primers for optimal taxonomic classification of environmental 16S rRNA gene sequences. *ISME J.* 6:1440. doi: 10.1038/ismej.2011.208

Song, Z., Du, H., Zhang, M., Nie, Y., and Xu, Y. (2019). *Schizosaccharomyces pombe* can reduce acetic acid produced by Baijiu spontaneous fermentation microbiota. *Microorganisms* 7:606. doi: 10.3390/microorganisms7120606

Song, Z., Du, H., Zhang, Y., and Xu, Y. (2017). Unraveling core functional microbiota in traditional solid-state fermentation by high-throughput amplicons and metatranscriptomics sequencing. *Front. Microbiol.* 8:1294. doi: 10.3389/fmicb.2017.01294

Tan, Y., Zhong, H., Zhao, D., Du, H., and Xu, Y. (2019). Succession rate of microbial community causes flavor difference in strong-aroma Baijiu making process. *Int. J. Food Microbiol.* 311:108350. doi: 10.1016/j.ijfoodmicro.2019.108350

Tsakiris, A., Kallithraka, S., and Kourkoutas, Y. (2014). Grape brandy production, composition and sensory evaluation. *J. Sci. Food Agric.* 94, 404–414. doi: 10.1002/jsfa.6377

Wang, X., Du, H., and Xu, Y. (2017). Source tracking of prokaryotic communities in fermented grain of Chinese strong-flavor liquor. *Int. J. Food Microbiol.* 244, 27–35. doi: 10.1016/j.ijfoodmicro.2016.12.018

Wang, X., Du, H., Zhang, Y., and Xu, Y. (2018a). Environmental microbiota drives microbial succession and metabolic profiles during Chinese liquor fermentation. *Appl. Environ. Microbiol.* 84, e02369–e02417. doi: 10.1128/AEM.02369-17

Wang, W., Liu, R., Shen, Y., and Lian, B. (2018b). The potential correlation between bacterial sporulation and the characteristic flavor of Chinese Maotai liquor. *Front. Microbiol.* 9:1435. doi: 10.3389/fmicb.2018.01435

Wang, S., Wu, Q., Nie, Y., Wu, J., and Xu, Y. (2019a). Construction of synthetic microbiota for reproducible flavor compound metabolism in Chinese light-aroma-type liquor produced by solid-state fermentation. *Appl. Environ. Microbiol.* 85, e03090–e03118. doi: 10.1128/AEM.03090-18

Wang, M. Y., Yang, J. G., Zhao, Q. S., Zhang, K. Z., and Su, C. (2019b). Research progress on flavor compounds and microorganisms of Maotai flavor Baijiu. *J. Food Sci.* 84, 6–18. doi: 10.1111/1750-3841.14409

Wang, X. J., Zhu, H. M., Ren, Z. Q., Huang, Z. G., Wei, C. H., and Deng, J. (2020). Characterization of microbial diversity and community structure in fermentation pit mud of different ages for production of strong-aroma Baijiu. *Pol. J. Microbiol.* 69, 1–14. doi: 10.33073/pjm-2020-018

Wiśniewska, P., Boqué, R., Borràs, E., Busto, O., Wardencki, W., Namieśnik, J., et al. (2017). Authentication of whisky due to its botanical origin and way of production by instrumental analysis and multivariate classification methods.

Spectrochim. Acta A Mol. Biomol. Spectrosc. 173, 849–853. doi: 10.1016/j.saa.2016.10.042

Wu, Q., Chen, L., and Xu, Y. (2012). Yeast community associated with the solid state fermentation of traditional Chinese Maotai-flavor liquor. *Int. J. Food Microbiol.* 166, 323–330. doi: 10.1016/j.ijfoodmicro.2008.09.019

Wu, Q., and Xu, Y. (2012). Transcriptome profiling of heat-resistant strain *Bacillus licheniformis* CGMCC3962 producing Maotai flavor. *J. Agric. Food Chem.* 60, 2033–2038. doi: 10.1021/jf204270h

Xu, Y., and Ji, K. (2012). "Moutai (Maotai): production and sensory properties," in *The Alcoholic Beverages: Sensory Evaluation and Consumer Research*. ed. J. Piggott (Sawston: Woodhead Publishing), 315–330.

Xu, S., Zhang, J., Luo, S., Zhou, X., Shi, S., and Tian, C. (2018). Similar soil microbial community structure across different environments after long-term succession: evidence from volcanoes of different ages. *J. Basic Microbiol.* 58, 704–711. doi: 10.1002/jobm.201800016

Xu, Y., Zhi, Y., Wu, Q., Du, R., and Xu, Y. (2017). *Zygosaccharomyces bailii* is a potential producer of various flavor compounds in Chinese Maotai-flavor liquor fermentation. *Front. Microbiol.* 8:2609. doi: 10.3389/fmicb.2017.02609

Yamamoto, M., Horie, M., Fukushima, M., and Toyotome, T. (2019). Culture-based analysis of fungi in leaves after the primary and secondary fermentation processes during Ishizuchi-kurocha production and lactate assimilation of *P. kudriavzevii*. *Int. J. Food Microbiol.* 306:108263. doi: 10.1016/j.ijfoodmicro.2019.108263

Yi, Z., Jin, Y., Xiao, Y., Chen, L., Tan, L., Du, A., et al. (2019). Unraveling the contribution of high temperature stage to Jiang-flavor Daqu, a liquor starter for production of Chinese Jiang-flavor Baijiu, with special reference to metatranscriptomics. *Front. Microbiol.* 10:472. doi: 10.3389/fmicb.2019.00472

Zhang, H., Meng, Y., Wang, Y., Zhou, Q., Li, A., Liu, G., et al. (2020). Prokaryotic communities in multidimensional bottom-pit-mud from old and young pits used for the production of Chinese strong-flavor Baijiu. *Food Chem.* 312:126084. doi: 10.1016/j.foodchem.2019.126084

Zheng, J., Wu, C., Huang, J., Zhou, R., and Liao, X. (2014a). Spatial distribution of bacterial communities and related biochemical properties in Luzhou-flavor liquor-fermented grains. *J. Food Sci.* 79, M2491–M2498. doi: 10.1111/1750-3841.12697

Zheng, X. W., Yan, Z., Nout, M. J. R., Smid, E. J., Zwietering, M. H., Boekhout, T., et al. (2014b). Microbiota dynamics related to environmental conditions during the fermentative production of fen-Daqu, a Chinese industrial fermentation starter. *Int. J. Food Microbiol.* 182-183, 57–62. doi: 10.1016/j.ijfoodmicro.2014.05.008

Zou, W., Ye, G., and Zhang, K. (2018). Diversity, function, and application of *Clostridium* in Chinese strong flavor Baijiu ecosystem: a review. *J. Food Sci.* 83, 1193–1199. doi: 10.1111/1750-3841.14134

Conflict of Interest: LW was employed by Kweichow Moutai Group. FH, XL, LC, FY, and HW were all employed by Kweichow Moutai Distillery Co., Ltd.

The remaining authors declare that the research was conducted in the absence of any commercial or financial relationships that could be construed as a potential conflict of interest.

frontiers in Microbiology

ORIGINAL RESEARCH
published: 20 May 2021
doi: 10.3389/fmicb.2021.678903

The Potential of *Flos sophorae immaturus* as a Pigment-Stabilizer to Improve the *Monascus* Pigments Preservation, Flavor Profiles, and Sensory Characteristic of *Hong Qu* Huangjiu

*Yijin Yang[1,2], Yongjun Xia[1], Xin Song[1], Zhiyong Mu[1], Huazhen Qiu[1], Leren Tao[2] and Lianzhong Ai[1]**

[1] Shanghai Engineering Research Center of Food Microbiology, School of Medical Instrument and Food Engineering, University of Shanghai for Science and Technology, Shanghai, China, [2] School of Energy and Power Engineering, University of Shanghai for Science and Technology, Shanghai, China

OPEN ACCESS

Edited by:
Xucong Lv,
Fuzhou University, China

Reviewed by:
Huaixiang Tian,
Shanghai Institute of Technology, China
Yanchun Shao,
Huazhong Agricultural University, China

***Correspondence:**
Lianzhong Ai
ailianzhong1@126.com;
ailianzhong@hotmail.com

Specialty section:
This article was submitted to Food Microbiology, a section of the journal Frontiers in Microbiology

Received: *10 March 2021*
Accepted: *12 April 2021*
Published: *20 May 2021*

Citation:
Yang Y, Xia Y, Song X, Mu Z, Qiu H, Tao L and Ai L (2021) The Potential of Flos sophorae immaturus as a Pigment-Stabilizer to Improve the Monascus Pigments Preservation, Flavor Profiles, and Sensory Characteristic of Hong Qu Huangjiu. Front. Microbiol. 12:678903. doi: 10.3389/fmicb.2021.678903

Hong Qu Huangjiu (HQW) is distinguished by its inclusion of *Monascus* pigments, meaning that photosensitivity strongly affects the sensory quality of the wine. In this study, the effects of *Flos sophorae immaturus* (*FSI*) on the stability of *Monascus* pigments, the flavor profiles, and the sensory characteristics of HQW were investigated. After sterilization, the addition of *FSI* increased the preservation rate of *Monascus* pigments in HQW by up to 93.20%, which could be accounted for by the synergy of rutin and quercetin in *FSI*. The total content of the volatile flavor compounds in HQW increased significantly as the added amounts of *FSI* were increased, especially 3-methyl-1-butanol, 2-methyl-1-propanol, and short-chain fatty acid ethyl esters (SCFAEE). Sensory evaluation and partial least-squares regression revealed that the concentration of *FSI* significantly affected the aroma characteristics of HQW but had little effect on the mouthfeel. The addition of 0.9 mg/mL *FSI* yielded a satisfactory HQW with high scores in terms of mouthfeel and aroma. The strong correlation between fruit-aroma, full-body, and SCFAEE suggests that *FSI* might alter the aroma of HQW by enhancing the synthesis of SCFAEE. Summarily, treatment with *FSI* represents a new strategy for improving the stability of photosensitive pigments and thus adjusting the aroma of HQW or similar beverages.

Keywords: Hong Qu Huangjiu, *Flos sophorae immaturus*, *Monascus* pigments, flavor profiles, sensory characteristic

Abbreviations: PLSR, partial least squares regression; SCFAEE, short-chain fatty acid ethyl esters; MCFAEE, medium-chain fatty acids ethyl esters; LCFAEE, long-chain fatty acids ethyl esters.

INTRODUCTION

Hong Qu Huangjiu (HQW), a typical form of Huangjiu (Chinese rice wine), has become increasingly popular in the rice wine market in recent years (Huang et al., 2019; Wang et al., 2020). Consumers favor HQW because of its bright red color, fine flavor, and health-promoting aspects (Park et al., 2016). The active ingredients of HQW have been proven to reduce blood pressure and blood lipid and cholesterol concentrations, and to influence metabolism and immune regulation in the human body (Lin et al., 2017; Mondal et al., 2019). Accordingly, HQW is referred to as a "ruby" Huangjiu wine.

Hong Qu Huangjiu is unique because its production involves Hong Qu (saccharification starter), which is inoculated with *Monascus* spp., introducing numerous pigments and enzymes (Feng et al., 2012; Patakova, 2013; Vendruscolo et al., 2016; Keekan et al., 2020). *Monascus* pigments contribute to the unique color and physiological effects of HQW. However, as a natural pigment, *Monascus* pigments undergo substantial photodegradation during storage, which negatively affects the appearance, sensory profile, and commercial value of HQW (Mapari et al., 2009; Wang et al., 2016; Sen et al., 2019). Although storage in brown bottles can reduce the degradation of *Monascus* pigments, these do not fully prevent the color fading of HQW during storage. To resolve this problem, manufacturers prefer the use of caramel coloring to mask the photodegradation of *Monascus* pigments. However, caramel coloring alters the original color of HQW and may have negative effects on food safety and human health (Vollmuth, 2018; Mateo-Fernández et al., 2019). Thus, the effective and inert stabilizers of *Monascus* pigments are needed to reduce the photodegradation of HQW during storage, and thus maintain and improve its sensory profile.

Numerous studies have reported that antioxidants effectively prevent the photodegradation of *Monascus* pigments (Dhale et al., 2018; Liu C. et al., 2020). Therefore, antioxidants may improve the final sensory profiles of HQW. However, the application of traditional food-industry antioxidants (e.g., Vitamin C, quercetin, and β-carotene) is limited by high cost or poor water-solubility (Qian et al., 2012; Horuz et al., 2017). Therefore, inexpensive natural herbs that contain abundant antioxidant compounds may be effective alternatives for reducing the photodegradation of *Monascus* pigments in HQW.

Flos sophorae immaturus (*FSI*) is the dried flower bud of *Sophora japonic*a L. This herb has a high flavonoid content and is considered a healthy food because of its high antioxidant activity (Abdelhady et al., 2015; Li and Fan, 2020). *FSI* has been widely used for 2,000 years in China as an important traditional Chinese medicine, due to its antitumor, anti-inflammatory, and antibacterial activities (Liu T. et al., 2019; Huang et al., 2020). Many studies have reported that the antioxidant compounds of *FSI* are responsible for its efficacy (Yao et al., 2011; Zhang et al., 2011; Hu et al., 2016; Wang et al., 2019). Therefore, *FSI* may prevent the photodegradation of *Monascus* pigments in HQW during storage.

In our previous study (submitted for publication), we observed that *FSI* preserved *Monascus* pigments to a greater extent than honeysuckle (a natural herb with high antioxidant activity) and some traditional antioxidants (e.g., Vc, EDTA, β-cyclodextrin, and quercetin). Thus, this study aimed to analyze the ability of *FSI* to preserve *Monascus* pigments in HQW during different brewing stages. Specifically, we evaluated the effects of *FSI* on the oenological properties, flavor profiles, and sensory characteristics in the resulting HQW. This study provides a basis for improving the pigment stability and sensory quality of HQW and broadens the applications for *FSI* as a novel stabilizer in beverages containing photosensitive pigments.

MATERIALS AND METHODS

Materials

Hong Qu (Saccharification starter) made using *Monascus* spp. was purchased from a commercial production facility in Gutian, Fujian province, China. *FSI* was picked from Linyi, Shandong province, China. Chlorogenic acid, rutin, and quercetin were purchased from Shanghai Yuanye Bio-Technology Co., Ltd. (Shanghai, China). All reagents and standards were purchased at Sigma Aldrich (Shanghai, China). n-Alkane (C_7-C_{40}; Supelco, Bellefonte, PA, United States) standards were used to determine the retention index.

Ten grams of Hong Qu was added in 1 L of 15% ethanol, ultrasonicated for 20 min at room temperature, and filtrated to obtain the *Monascus* pigments-solution. To obtain an extract, fresh *FSI* was dehydrated and dried in an oven at 40°C to a constant level of moisture. The dry *FSI* was then thoroughly milled using a grinder to produce powder, which was passed through a 60-mesh sieve. Two grams of the sieved powder were mixed with 40 mL of 40% ethanol at 70°C, ultrasonicated for 20 min, and filtered immediately. The filtrate was pooled and concentrated using a rotary evaporator at 55°C. Finally, a dry powder was obtained by freeze drying and stored in a desiccator in the dark at 4°C.

The Preservation Rate of *Monascus* Pigments

Ultraviolet (UV) was used to accelerate the degradation of *Monascus* pigments-solution. Chlorogenic acid, rutin, quercetin, and *FSI* were, respectively, mixed with *Monascus* pigments-solution to prepare solutions at a concentration of 0.5 mg/mL. A volume of 50 mL mixed solution was placed in a UV-transparent quartz dish with a radius of 8 cm for UV irradiation, while the pure *Monascus* pigments-solution was set as the control. The maximum absorbance (A_{max}) of *Monascus* pigments-solution and HQW were determined using a SpectraMax M5e spectrofluorometer (Molecular Devices Ltd., San Jose, CA, United States). The *Monascus* pigments-preservation rate was calculated using the following formula:

$$\text{Preservation rate of pigment } (\%) = A_x/A_o \times 100\%$$

where A_x and A_0 are the A_{max} values of pigments treated and untreated with *FSI*, respectively.

Antioxidant Constituent of *FSI*

The possibly antioxidant constituent of *FSI* was analyzed using a Waters high-performance liquid chromatograph (HPLC) system (e2695-Empower system, MA, United States). An equivalent of 5.0 mg of *FSI* was solubilized in 25 mL methanol, filtered through a 0.22 μm filter membrane, and separated on a Sepax HP-C18 column (4.6 mm × 250 mm, 5 μm) at 25°C. The mobile phase was composed of 100% acetonitrile/0.01 mol/L ammonium acetate (0 min, 10:90 and 30 min, 30:70). The flow rate was 1.0 mL/min, the injection volume was 10 μL, and the UV detection wavelength was set at 350 nm.

Brewing of HQW

Hong Qu Huangjiu was brewed according to the method described by Yang et al. (2017). *FSI* was correspondingly added during Hong Qu soaking, on day 5 of fermentation (representative of the fermentation stage), and cooled after sterilization. The *FSI* concentration in the wine was adjusted to 0, 0.1, 0.3, 0.5, 0.7, and 0.9 mg/mL. As the photodegradation of *Monascus* pigments in HQW generally occurs during storage, the young wine was stored in the dark at 4°C for 160 days, and changes were monitored. The aged wine was regularly sampled, and samples were stored at −80°C for further analysis.

Oenological Properties of HQW

Reducing sugar was detected using the method described by Miller (1959). Total acidity was determined according to Code of China Standard No. GB/T 5517-2010 (GB/T 5517-2010), and ethanol was determined using the HPLC method reported by Di Egidio et al. (2010), with the following conditions: a Carbomix H-NP (300 mm × 7.8 mm) column at a temperature of 55°C, a mobile phase of 2.5 mM sulfuric acid at a flow rate of 0.6 mL/min and using a differential detector. The amino acid nitrogen content in a 5-mL aliquot of HQW digested at 420 °C for 150 min was determined using an automatic Kjeldahl apparatus (Kjeltec 8400, FOSS Co., Sweden).

Analysis of Volatile Flavor Compounds

Volatile flavor components were extracted from HQW by solid-phase microextraction and analyzed by gas chromatography–mass spectrometry (GC-MS), according to the method reported by Yang et al. (2019). A 5-mL aliquot of each sample [diluted to 6% (v/v) ethanol] was placed in a 20-mL headspace glass vials with 2 g of sodium chloride and 10 μL internal standard of 4-methyl-2-pentanol (250 μg/mL). The volatile compounds were extracted for 30 min at 50°C using a 50 μm DVB/CAR/PDMS fiber. Then, the extracted fiber head was desorbed at the GC injection port at 250°C for 7 min for GC-MS analysis. The chromatographic conditions of GC-MS system (Thermo Fisher Inc., United States) equipped with a DB-WAX column (60 m × 0.25 mm × 0.25 μm, Agilent Technologies, United States) were as follows: programmed at an initial temperature of 40°C for 3 min, increased to 210°C at 6°C/min, and then, at 8°C/min to 230°C that is maintained for 15 min. Helium was delivered at a flow rate of 1 mL/min as the carrier gas. The conditions of the mass detector and identification of volatile compounds were operated as the method described by Yang et al. (2019). The quantity of volatile compounds was determined by the internal standard method.

Sensory Evaluation

The sensory evaluation team comprised 10 judges (five men and five women) who had been trained to evaluate the sensory attributes of HQW samples using a series of reference substances, according to the ISO Standard No. 8586-1 (ISO, 1993; **Supplementary Table 1**). After the judges reached a consensus on the sensory characteristics of all substances, they were given a sensory assessment card that listed all attributes with their definitions and 10-point scales (from 0 to 9). The scoring criteria were as follows: 0 meant very weak, 1–2 means weak, 3–4 meant average, 6 meant medium, 7–8 means high, and 9 meant extremely high. The evaluation was conducted in a room with a uniform light source and without noise or other distracting stimuli. The HQW samples were presented to the judges in a random order, in marked tulip-shaped glasses.

Statistical Analysis

Each sample was analyzed in triplicate, and the results were expressed as mean values ± standard deviations (SD). Duncan's test was used to analyze the significant differences between data using SPSS 19.0 software (SPSS Inc., Chicago, IL, United States). Partial least squares regression (PLSR) was used to explore the relationship among volatile flavor compounds, sensory attributes, and HQW samples containing different concentrations of *FSI* using UNSCRAMBLER ver. 9.7 (CAMO ASA, Oslo, Norway). TBtools (Chen et al., 2020) were used to visualize the differentiation of flavor compounds in different wines.

RESULTS

Effect of Adding *FSI* During Different Brewing Stages on the Preservation of *Monascus* Pigments in HQW

Photosensitive *Monascus* pigments may be degraded during the Hong Qu soaking stage of the brewing processes. Therefore, we investigated the preservation rates of *Monascus* pigments in HQW samples treated with different concentrations of *FSI* during different brewing stages (soaking, fermentation, and sterilization) (**Figure 1**). We found that the pigment-preservation rate increased with *FSI* concentration. Specifically, when 0.1–0.9 mg/mL *FSI* was added during Hong Qu soaking, the *Monascus* pigment-preservation rates increased by 20.68, 34.01, 39.33, 44.75, and 40.82% relative to the control (**Figure 1A**). When *FSI* was added during HQW fermentation, the pigment-preservation rate increased by 25.74, 36.25, 43.16, 58.46, and 53.02% relative to the control (**Figure 1B**). When *FSI* was added after sterilization, the rate increased by 34.89, 52.88, 66.87, 86.13, and 93.20% relative to the control (**Figure 1C**). After sterilization, the addition of 0.9 mg/mL *FSI* resulted in

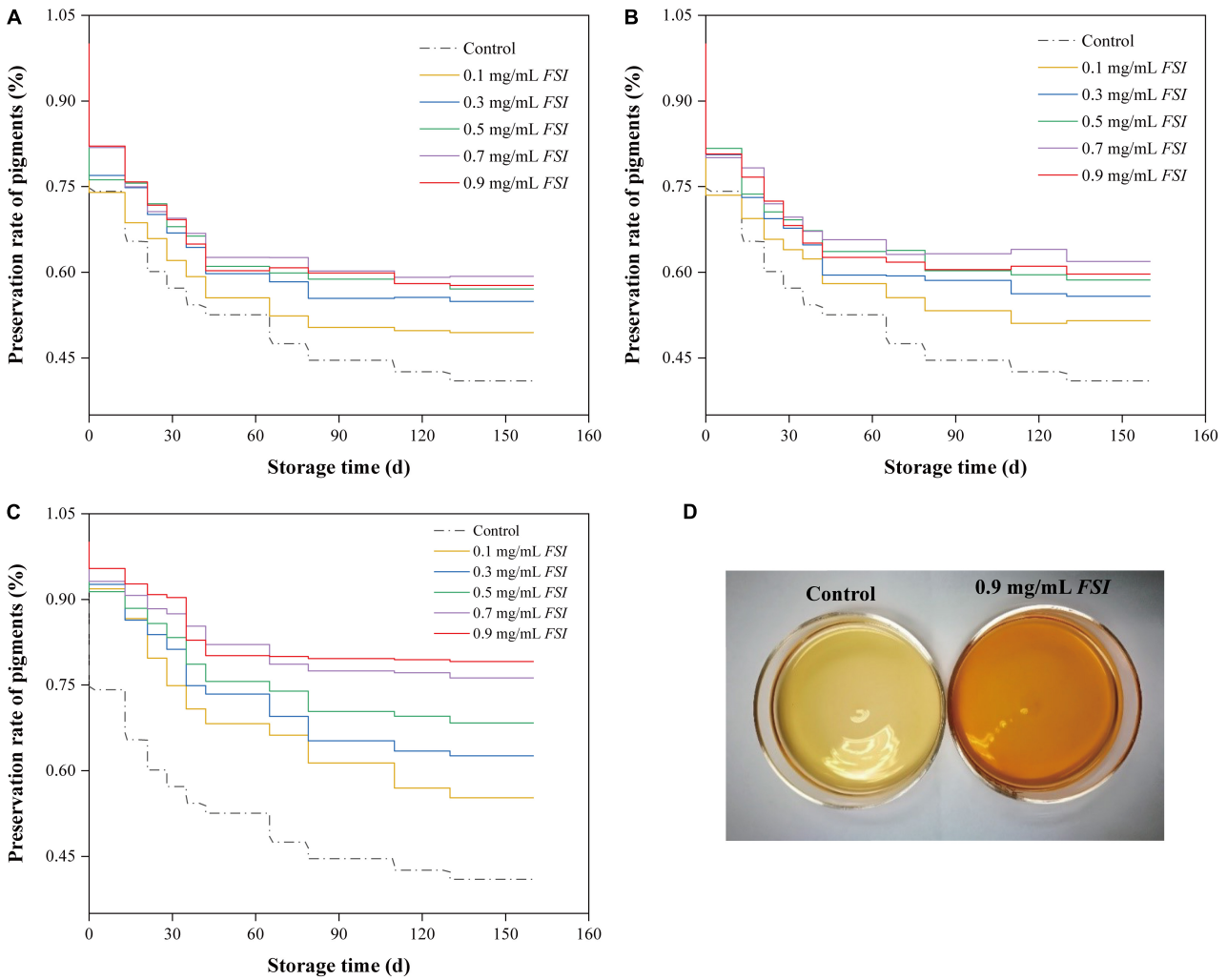

FIGURE 1 | The preservation rate of *Monascus* pigments in HQW treated with different concentrations of *FSI* during Hong Qu soaking **(A)**, wine fermentation **(B)**, and after sterilization **(C)** during 160-days storage. Appearance comparison between HQW containing 0.9 mg/mL *FSI* and the control HQW **(D)**.

the greatest preservation rate of *Monascus* pigments. A similar pattern was observed for the appearance of HQW (**Figure 1D**). After natural aging for 160 d, the color of the control HQW had faded distinctly, whereas that of *FSI*-treated HQW remained satisfactory.

Major Antioxidant Constituents in *FSI*

The effective antioxidant compositions in *FSI* were analyzed using HPLC, with rutin, chlorogenic acid, and quercetin were used as references (**Figure 2A**). The result showed that *FSI* contained abundant rutin and quercetin and their contents were 68.64 and 23.75 mg/g, respectively (**Figure 2B**). Furthermore, the effects of rutin, quercetin, and *FSI* on the preservation rate of *Monascus* pigments under UV were compared (**Figure 2C**). After irradiation by UV for 10 h, the preservation rate of *Monascus* pigments in the control, solutions containing *FSI*, rutin, and quercetin correspondingly decreased from 100 to 33.2, 80.58, 68.05, and 70.53%. *FSI* exhibited better ability in the preservation of *Monascus* pigments than rutin or quercetin.

Effect of Adding *FSI* During Different Brewing Stages on the Oenological Properties of HQW

We next evaluated the oenological properties of HQW treated with *FSI* during different brewing stages (**Figure 3**). When *FSI* was added during Hong Qu soaking or fermentation, the reducing sugar content in the resultant HQW increased significantly. In contrast, adding *FSI* after sterilization had little effect on this parameter (**Figure 3A**). Otherwise, the addition of *FSI* during different brewing stages had little effect on the ethanol, total acidity, and amino-acid nitrogen contents in the final wine samples (**Figures 3B–D**). Because the addition of *FSI* after sterilization had little effect on the oenological properties and yielding the best protection against *Monascus* pigments loss,

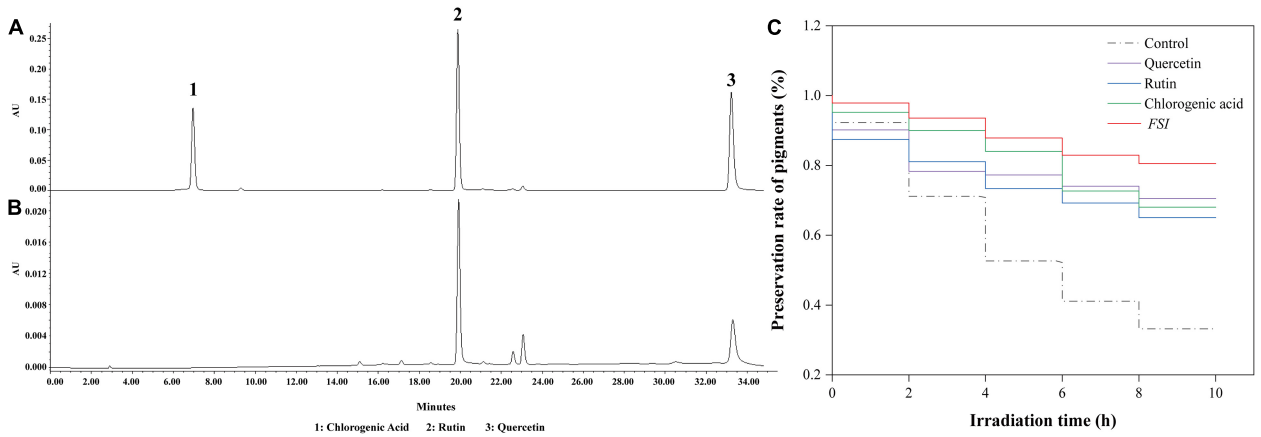

FIGURE 2 | Effective constituent of *FSI* in the preservation of *Monascus* pigments. HPLC results of reference substances **(A)** and *FSI* **(B)**. Effect of quercetin, rutin, and *FSI* on the preservation rate of *Monascus* pigments **(C)**. Component 1: chlorogenic acid; Component 2: rutin; Component 3: quercetin.

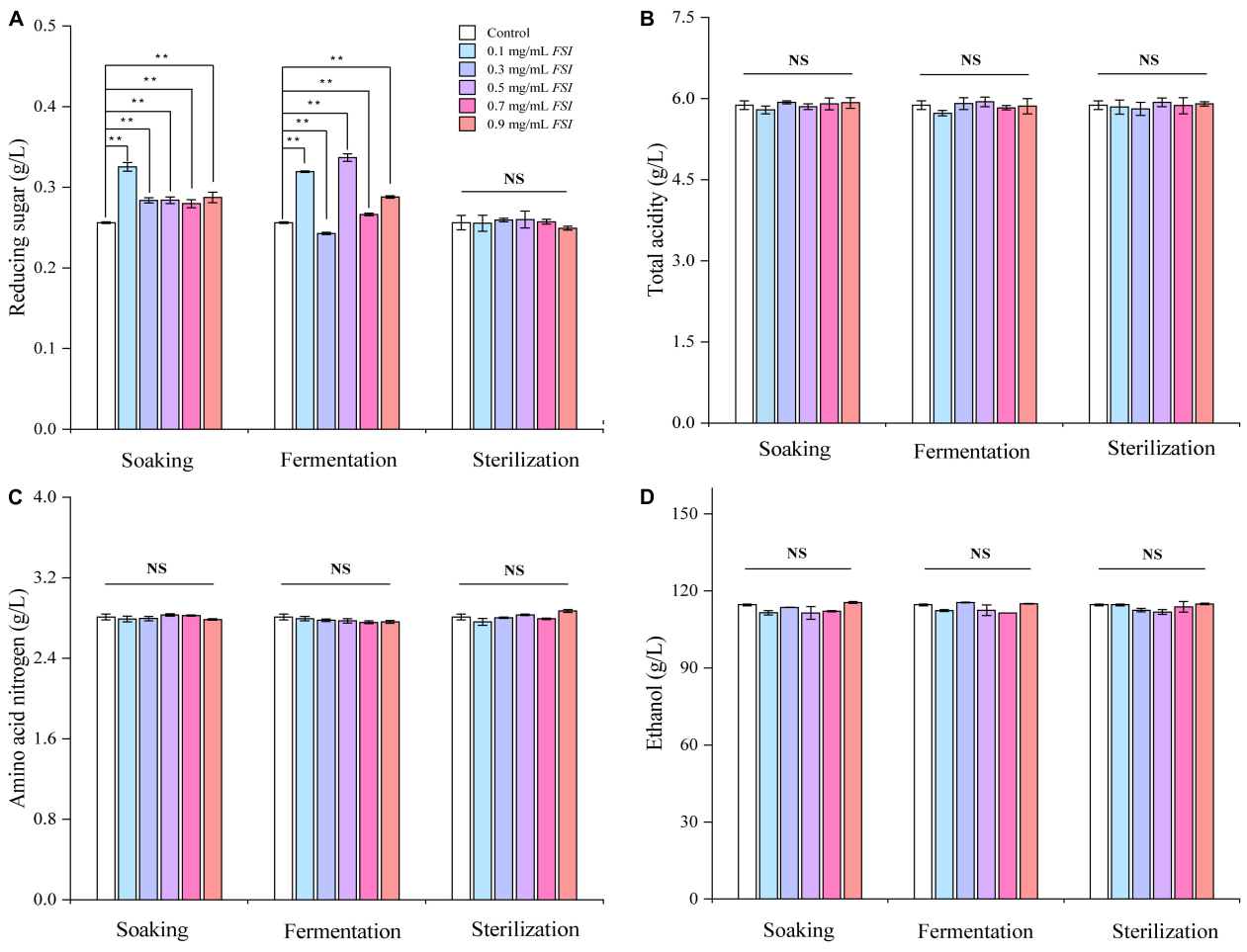

FIGURE 3 | The oenological properties of HQW treated with various concentrations of *FSI* during different brewing stages, comprising reducing sugar content **(A)**, total acidity **(B)**, amino acid nitrogen content **(C)**, and ethanol content **(D)**. **Indicates significant differences ($p < 0.01$, Duncan's tests) between different HQW. NS indicates no significant difference between the wine samples.

only wine samples to which *FSI* had been added after sterilization were further analyzed.

Effect of Adding *FSI* After Sterilization on the Flavor Profiles of HQW

The volatile flavor compounds of aged HQW treated with *FSI* after sterilization were analyzed (**Table 1**). A total of 47 compounds were detected, comprising 10 alcohols, 22 esters, six aldehydes, three phenols, two ketones, and four acids. The *FSI* had little effect on the detected number of flavor compounds, whereas the relative contents of flavor compounds were different in HQW samples containing different concentrations of *FSI* (**Figure 4**). In particular, the total content of volatile flavor compounds in HQW increased significantly as the added amounts of *FSI* were increased. HQW containing 0.9 mg/mL *FSI* exhibited the highest flavor-compound content (98.72 mg/L), followed by HQW containing 0.7 mg/mL *FSI* (95.61 mg/L), which were 10.64 and 7.15% higher than the control HQW, respectively (**Table 1**).

As shown in **Figure 4**, esters were the most abundant aroma compounds, followed by alcohols and aldehydes. However, the total content of alcohols was the greatest, and thus responsible for the differentiation of total flavor compounds in different HQW. The addition of *FSI* significantly increased the total alcohol content in HQW. The highest alcohol content (62.36 mg/L) was observed in HQW containing 0.9 mg/L *FSI*, and this represented a 15.48% relative to the control. Among the detected alcohols, 3-methyl-1-butanol, 2-methyl-1-propanol, and 2-phenylethanol accounted for more than 95% of the total alcohols. Furthermore, the 3-methyl-1-butanol content gradually increased with the amount of *FSI* and was highest in HQW containing 0.9 mg/L *FSI*. The content of 2-phenylethanol in HQW containing *FSI* was significantly higher than that in the control, although the concentration of *FSI* had little effect on this parameter. Most of the detected esters in HQW were fatty-acid ethyl-esters (FAEE) (**Figure 4** and **Table 1**)., comprising short-chain (SC, C_2-C_5), medium-chain (MC, C_6-C_{12}), and long-chain (LC, C_{13}-C_{18}) FAEE according to the chain length (Gao et al., 2018). As the *FSI* concentration was increased, the relative contents of SCFAEE and long-chain fatty acids ethyl esters (LCFAEE) in HQW also gradually increased. Compared to the control wine, the addition of 0.9 mg/L *FSI* increased the SCFAEE content by 20.95% in the resultant HQW, but only increased the LCFAEE content by 3.03% (**Table 1**). Benzaldehyde, phenylacetaldehyde, and furfural were identified as the key aldehydes in HQW (Yang et al., 2017; Liu Z. et al., 2020). The content of benzaldehyde determined the total content of aldehydes in each HQW (**Table 1**). However, no significant difference was observed between the total aldehyde contents in HQW with and without *FSI*, indicating that the addition of *FSI* had little effect on the aldehyde content of HQW during aging.

Sensory Evaluation

The aged HQW samples treated with different *FSI* concentrations after sterilization were subjected to a sensory evaluation. The mouthfeel characteristic of astringency, full-body, and aftertaste-continuation varied little in HQW containing different concentrations of *FSI* (**Figure 5**). In contrast, a significant difference in the aroma of alcohol, cereal, and fruity was observed. Different wines were perceived to have similar levels of sweet taste, however, the wines received significantly different scores for the taste of sour, despite a lack of significant differences in the total acidity. In summary, although the overall mouthfeel characteristics were similar between HQW samples with and without *FSI*, the concentration of *FSI* significantly affected the aroma characteristics of the wine. HQW treated with 0.9 mg/mL *FSI* received the highest scores for the total mouthfeel and aroma.

Correlation Among Flavor Compounds, Sensory Attributes, and HQW With *FSI* Treatment

A multivariate analysis of the variance-PLSR model was performed to study the relationship between flavor compounds and sensory attributes in samples of HQW with and without *FSI*. A total of 53 identified flavor compounds were designed as the *X*-matrix, while nine sensory attributes and six wine samples were designed as *Y*-matrix (**Figure 6**). The two-factor model explained 63% of the variance in *X*-matrix and 76% of that in *Y*-matrix, indicating that this model satisfactorily explained the flavor compounds and sensory attributes. Except for nonanal, benzaldehyde, ethyl nonanoate, ethyl dodecanoate, ethyl stearate, ethyl (9E)-9-octadecenoate, acetic acid, hexanoic acid, octanoic acid, 2-octanone, 2-furanmethanol, and 2-methoxy-phenol, all of the sensory attributes and flavor compounds were located between the small and big ellipses, where the flavor compounds could be considered as correlated with sensory attributes (Xiao et al., 2014).

DISCUSSION

Monascus pigments, as the distinguished component in HQW, its photosensitivity characteristic significantly affects the sensory quality of the resulting wine. During the manufacturing processes of HQW, *Monascus* pigments may be degraded from the stage of Hong Qu soaking, wine fermentation, and sterilization. Though the pigment-preservation rate of HQW increased with *FSI* concentration, adding *FSI* after sterilization resulted in the greatest reduction of *Monascus* pigment loss in HQW, especially when added at a concentration of 0.9 mg/mL.

Typically, the ionization reaction occurs in a water solution of Monascus pigments under light, generating superoxide anions, hydroxyl radicals, and radicals originated by the side chain fracture (Feng et al., 2012). These radicals undergo an addition reaction with the double bonds in the pigment structure, which caused the disappearance of conjugated double bonds in *Monascus* pigments, and led to the loss of color (Mapari et al., 2009; Patakova, 2013). The antioxidant substances formed chemical bonds between its hydroxyl and the ketone group on the molecular structure of *Monascus* pigments, thereby stabilizing the structure of pigments (Kennedy et al., 1999). Reportedly, *FSI* is rich in antioxidant substances, such as rutin, quercetin, and chlorogenic acid, which might be related to its ability to preserve

TABLE 1 | Identification and relative contents of volatile flavor compounds in aged HQW (160 d) containing with different concentrations of *FSI*.

Code	Compounds	KI	Identification	Relative content (mg/L)					
				Control	0.1 *FSI*	0.3 *FSI*	0.5 *FSI*	0.7 *FSI*	0.9 *FSI*
Alcohols									
al1	2-Methyl-1-propanol	1,095	MS,RI	1.81 ± 0.04^{b}	1.68 ± 0.05^{a}	2.39 ± 0.02^{d}	1.94 ± 0.08^{c}	2.55 ± 0.03^{e}	2.76 ± 0.06^{f}
al2	1-Butanol	1,158	MS,RI	0.09 ± 0.001^{a}	0.07 ± 0.005^{a}	0.05 ± 0.003^{a}	0.11 ± 0.006^{b}	0.08 ± 0.009^{a}	0.12 ± 0.002^{b}
al3	3-Methyl-1-butanol	1,212	MS,RI	32.81 ± 0.47^{a}	33.86 ± 0.39^{b}	35.61 ± 0.51^{c}	35.75 ± 0.32^{c}	35.87 ± 0.36^{c}	37.4 ± 0.44^{d}
al4	1-Hexanol	1,345	MS,RI	0.04 ± 0.001^{a}	0.06 ± 0.002^{b}	0.03 ± 0.001^{a}	0.06 ± 0.002^{b}	0.03 ± 0.001^{a}	0.04 ± 0.001^{a}
al5	1-Octen-3-ol	1,456	MS,RI	0.09 ± 0.002^{a}	0.07 ± 0.001^{a}	0.09 ± 0.002^{a}	0.06 ± 0.001^{a}	0.08 ± 0.003^{a}	0.11 ± 0.003^{b}
al6	2-Furanmethanol	1,661	MS,RIL	0.19 ± 0.002^{b}	0.24 ± 0.004^{c}	0.13 ± 0.006^{a}	0.17 ± 0.004^{b}	0.15 ± 0.001^{a}	0.18 ± 0.003^{b}
al7	3-Methylthiopropanol	1,722	MS,RIL	0.91 ± 0.01^{c}	0.83 ± 0.007^{a}	0.96 ± 0.09^{d}	0.86 ± 0.03^{b}	0.81 ± 0.004^{a}	0.98 ± 0.02^{d}
al8	Citronellol	1,772	MS,RIL	0.02 ± 0.001^{a}	0.03 ± 0.001^{a}	0.01 ± 0.001^{a}	0.04 ± 0.001^{a}	0.02 ± 0.001^{a}	0.02 ± 0.001^{a}
al9	2-Phenylethanol	1,876	MS,RI	29.85 ± 0.67^{a}	33.12 ± 0.83^{b}	33.51 ± 0.91^{b}	33.27 ± 0.75^{b}	33.38 ± 0.66^{b}	33.55 ± 0.72^{b}
al10	Cedrol	2,105	MS,RIL	0.09 ± 0.001^{b}	0.08 ± 0.003^{b}	0.1 ± 0.002^{b}	0.05 ± 0.002^{a}	0.06 ± 0.001^{a}	0.08 ± 0.001^{b}
Total				54.00	59.29	60.44	60.26	60.4	62.36
Esters									
et1	Ethyl acetate	837	MS,RI	2.34 ± 0.05^{c}	1.99 ± 0.06^{a}	2.12 ± 0.09^{b}	2.48 ± 0.04^{d}	2.69 ± 0.05^{e}	2.95 ± 0.06^{f}
et2	Ethyl butanoate	1,049	MS,RI	0.72 ± 0.007^{b}	0.76 ± 0.008^{b}	0.66 ± 0.008^{a}	0.69 ± 0.01^{a}	0.73 ± 0.005^{b}	0.75 ± 0.008^{b}
et3	Isoamyl acetate	1,135	MS,RI	1.08 ± 0.01^{b}	0.91 ± 0.007^{a}	1.11 ± 0.01^{b}	0.92 ± 0.004^{a}	1.17 ± 0.04^{c}	1.13 ± 0.03^{c}
et4	Ethyl hexanoate	1,242	MS,RI	0.03 ± 0.001^{a}	0.04 ± 0.001^{a}	0.08 ± 0.003^{b}	0.06 ± 0.002^{a}	0.09 ± 0.001^{b}	0.06 ± 0.002^{a}
et5	Ethyl heptanoate	1,318	MS,RI	0.01 ± 0.001^{a}	0.02 ± 0.003^{a}	0.02 ± 0.002^{a}	0.03 ± 0.001^{a}	0.02 ± 0.001^{a}	0.04 ± 0.001^{a}
et6	Ethyl-2-hydroxypropanoate	1,346	MS,RI	1.69 ± 0.08^{d}	1.51 ± 0.02^{c}	1.44 ± 0.05^{a}	1.62 ± 0.04^{c}	1.75 ± 0.06^{d}	1.63 ± 0.04^{c}
et7	Ethyl octanoate	1,440	MS,RI	1.35 ± 0.02^{d}	1.26 ± 0.06^{c}	1.01 ± 0.01^{a}	1.06 ± 0.03^{a}	1.19 ± 0.05^{b}	1.33 ± 0.02^{d}
et8	Ethyl nonanoate	1,528	MS,RI	0.12 ± 0.003^{b}	0.09 ± 0.006^{a}	0.11 ± 0.001^{b}	0.1 ± 0.005^{b}	0.08 ± 0.008^{a}	0.09 ± 0.002^{a}
et9	Ethyl 2-hydroxy-4-methylvalerate	1,578	MS,RIL	0.02 ± 0.001^{a}	0.05 ± 0.003^{b}	0.03 ± 0.001^{a}	0.04 ± 0.002^{a}	0.07 ± 0.001^{b}	0.06 ± 0.001^{b}
et10	Ethyl decanoate	1,640	MS,RI	1.59 ± 0.07^{c}	1.22 ± 0.09^{b}	1.63 ± 0.03^{d}	1.17 ± 0.006^{a}	1.15 ± 0.04^{a}	1.68 ± 0.06^{d}
et11	Ethyl benzoate	1,675	MS,RI	0.95 ± 0.007^{a}	0.96 ± 0.008^{a}	0.98 ± 0.01^{a}	0.94 ± 0.02^{a}	0.95 ± 0.007^{a}	0.98 ± 0.02^{a}
et12	Diethyl succinate	1,688	MS,RI	0.53 ± 0.003^{b}	0.42 ± 0.007^{a}	0.66 ± 0.005^{c}	0.45 ± 0.006^{a}	0.57 ± 0.003^{b}	0.71 ± 0.008^{d}
et13	2-Phenethyl acetate	1,821	MS,RI	0.58 ± 0.005^{b}	0.49 ± 0.004^{a}	0.62 ± 0.007^{b}	0.42 ± 0.004^{a}	0.5 ± 0.008^{a}	0.46 ± 0.005^{a}
et14	Ethyl dodecanoate	1,837	MS,RI	0.58 ± 0.006^{c}	0.55 ± 0.004^{b}	0.48 ± 0.009^{a}	0.61 ± 0.004^{d}	0.53 ± 0.003^{b}	0.57 ± 0.006^{c}
et15	γ-Nonanolactone	2,011	MS, RI	0.02 ± 0.001^{a}	0.03 ± 0.002^{a}	0.05 ± 0.002^{a}	0.12 ± 0.005^{c}	0.09 ± 0.003^{b}	0.17 ± 0.006^{d}
et16	Ethyl tetradecanoate	2,036	MS,RI	1.95 ± 0.09^{b}	1.84 ± 0.07^{a}	2.05 ± 0.1^{c}	1.91 ± 0.04^{b}	2.09 ± 0.09^{c}	1.98 ± 0.06^{b}
et17	Isopropyl myristate	2,041	MS,RI	0.08 ± 0.002^{b}	0.09 ± 0.003^{b}	0.05 ± 0.002^{a}	0.07 ± 0.001^{a}	0.07 ± 0.001^{a}	0.08 ± 0.003^{b}
et18	Ethyl hexadecanoate	2,258	MS,RI	7.31 ± 0.21^{b}	7.1 ± 0.16^{a}	7.38 ± 0.27^{b}	7.45 ± 0.13^{c}	7.56 ± 0.18^{d}	7.74 ± 0.15^{e}
et19	Ethyl 9-hexadecenoate	2,270	MS,RIL	0.11 ± 0.007^{a}	0.13 ± 0.005^{b}	0.09 ± 0.004^{a}	0.16 ± 0.008^{c}	0.12 ± 0.009b	0.09 ± 0.004^{a}
et20	Ethyl stearate	2,454	MS,RI	0.42 ± 0.005^{c}	0.33 ± 0.008^{a}	0.37 ± 0.008^{b}	0.39 ± 0.004^{b}	0.47 ± 0.006^{d}	0.36 ± 0.005^{a}
et21	Ethyl (9E)-9-octadecenoate	2,475	MS,RIL	0.95 ± 0.02^{c}	0.84 ± 0.01^{b}	0.75 ± 0.009^{a}	0.79 ± 0.01^{a}	0.86 ± 0.007^{b}	0.87 ± 0.005^{b}
et22	Linoleic acid ethyl ester	2,513	MS,RIL	1.38 ± 0.02^{c}	1.31 ± 0.01^{b}	1.27 ± 0.04^{b}	1.19 ± 0.03^{a}	1.35 ± 0.05^{b}	1.46 ± 0.07^{d}
Total				23.81	21.94	22.96	22.67	24.10	24.99
Aldehydes									
ad1	Nonanal	1,390	MS,RI	0.03 ± 0.001^{a}	0.05 ± 0.002a	0.04 ± 0.002^{a}	0.02 ± 0.001^{a}	0.05 ± 0.001^{a}	0.04 ± 0.001^{a}
ad2	Furfural	1,442	MS,RI	0.39 ± 0.01^{a}	0.39 ± 0.009^{a}	0.37 ± 0.007^{a}	0.38 ± 0.005^{a}	0.4 ± 0.008^{a}	0.38 ± 0.009^{a}
ad3	Decanal	1,503	MS,RIL	0.06 ± 0.002^{b}	0.04 ± 0.001^{a}	0.02 ± 0.001^{a}	0.03 ± 0.001^{a}	0.08 ± 0.003^{b}	0.09 ± 0.003^{b}
ad4	Benzaldehyde	1,518	MS,RI	3.56 ± 0.17^{c}	3.38 ± 0.15^{a}	3.49 ± 0.20^{b}	3.55 ± 0.12^{c}	3.41 ± 0.16^{a}	3.49 ± 0.14^{b}
ad5	4-Methyl-benzaldehyde	1,644	MS,RI	0.28 ± 0.03^{a}	0.31 ± 0.01^{a}	0.35 ± 0.009^{b}	0.3 ± 0.005^{a}	0.32 ± 0.009^{b}	0.33 ± 0.01^{b}
ad6	Benzeneacetaldehyde	1,654	MS,RI	0.39 ± 0.006^{a}	0.36 ± 0.005^{a}	0.45 ± 0.02^{b}	0.39 ± 0.007^{a}	0.51 ± 0.005^{c}	0.48 ± 0.008^{b}
Total				4.71	4.53	4.72	4.67	4.77	4.81
Phenols									
ph1	2-Methoxy-phenol	1,866	MS,RI	0.26 ± 0.01^{b}	0.24 ± 0.04^{a}	0.31 ± 0.03^{c}	0.25 ± 0.009^{b}	0.22 ± 0.02^{a}	0.29 ± 0.01^{c}
ph2	4H-Pyran-4-one, 3-hydroxy-2-methyl	1,970	MS,RIL	0.06 ± 0.003^{b}	0.04 ± 0.001^{a}	0.08 ± 0.002^{b}	0.03 ± 0.001^{a}	0.08 ± 0.003^{b}	0.05 ± 0.002^{a}

(Continued)

TABLE 1 | Continued

Code	Compounds	KI	Identification	Relative content (mg/L)					
				Control	0.1 *FSI*	0.3 *FSI*	0.5 *FSI*	0.7 *FSI*	0.9 *FSI*
ph3	2-Methoxy-4-vinylphenol	2,215	MS,RIL	0.19 ± 0.008^{b}	0.16 ± 0.005^{a}	0.21 ± 0.007^{b}	0.14 ± 0.009^{a}	0.17 ± 0.006^{b}	0.15 ± 0.004^{a}
Total				0.51	0.44	0.60	0.42	0.47	0.49
Ketones									
kt1	2-Octanone	1,312	MS,RI	0.07 ± 0.003^{a}	0.08 ± 0.002^{a}	0.06 ± 0.002^{a}	0.09 ± 0.001^{a}	0.09 ± 0.003^{a}	0.10 ± 0.003^{a}
kt2	2-Nonanone	1,390	MS,RI	1.96 ± 0.05^{d}	1.77 ± 0.08^{a}	1.83 ± 0.03^{b}	1.91 ± 0.04^{c}	1.90 ± 0.07^{c}	1.96 ± 0.03^{d}
Total				2.03	1.85	1.89	2.00	1.99	2.06
Acids									
ac1	Acetic acid	1,428	MS,RI	3.78 ± 0.19^{d}	3.61 ± 0.21^{b}	3.52 ± 0.12^{a}	3.69 ± 0.11^{c}	3.57 ± 0.17^{a}	3.64 ± 0.12^{b}
ac2	Butanoic acid	1,626	MS,RI	0.19 ± 0.01^{b}	0.21 ± 0.04^{c}	0.18 ± 0.008^{a}	0.17 ± 0.03^{a}	0.19 ± 0.009^{b}	0.16 ± 0.01^{a}
ac3	Hexanoic acid	1,855	MS,RI	0.08 ± 0.004^{b}	0.09 ± 0.002^{b}	0.06 ± 0.001^{a}	0.08 ± 0.002^{b}	0.04 ± 0.002^{a}	0.07 ± 0.001^{b}
ac4	Octanoic acid	2,070	MS,RI	0.12 ± 0.005^{b}	0.13 ± 0.004^{b}	0.09 ± 0.007^{a}	0.11 ± 0.004^{b}	0.08 ± 0.002^{a}	0.14 ± 0.005^{b}
Total				4.17	4.04	3.85	4.05	3.88	4.01
Sum				89.23	92.09	94.46	94.07	95.61	98.72

Different letters in each row indicate significant differences ($p < 0.05$, Duncan's tests) between different HQW. MS, compounds were identified by MS spectra. KI is the retention index calculated by the Kovats method. RI, compounds were identified by comparison to pure standard. RIL, compounds were identified by comparison with RI from http://webbook.nist.gov/. "Control" represents HQW without FSI; 0.1 FSI, 0.3 FSI, 0.5 FSI, 0.7 FSI, and 0.9 FSI represent HQW containing 0.1, 0.3. 0.5, 0.7, and 0.9 mg/mL FSI, respectively.

pigment under light (Hu et al., 2016). According to the HPLC analysis, the major antioxidant constituents of *FSI* were rutin and quercetin, and the content of rutin was significantly higher than quercetin (**Figure 2**). After UV irradiation, *FSI* exhibited better ability in the preservation of *Monascus* pigments than rutin or quercetin, suggesting that the combination of antioxidants enhanced the protective effect on *Monascus* pigments. However, the combination of multiple antioxidants greatly increases the cost. As a natural extraction product, *FSI* can replace the conventional antioxidants to protect natural pigments from light irradiation.

While adding *FSI* after HQW sterilization, it had little effect on the oenological properties, indicating that there was no need to change the production parameters due to the *FSI* treatment (**Figure 3**). However, *FSI* treatment contributed greatly to the flavor profiles of HQW. During the fermentation of HQW, the antioxidant constituents in *FSI* can prevent the growth and reproduction of microorganisms that contributed greatly to the stability of *Monascus* pigments (Tang et al., 2019). This may responsible for the reason that adding *FSI* after sterilization exhibited the best inhibitory effect on the *Monascus* pigment photodegradation. In addition, adding *FSI* during the Hong Qu soaking process or fermentation process will inhibit the metabolism of yeast, which generates a range of volatile flavor compounds and results in the specific flavor characteristic of HQW (Chen and Xu, 2012; Cai et al., 2018). This phenomenon affects its utilization as it reduces the sugar by microorganisms (including yeast), contributing to the formation of flavor compounds in HQW. After sterilization, the fresh HQW had an insufficient aroma and a rough taste, and a variety of chemical reactions such as oxidation, esterification, and hydrolysis reactions gradually occur (Jones et al., 2008; Tao et al., 2014). The added *FSI* may promote the chemical reactions among some flavor compounds, thereby affecting the flavor profiles of HQW. Generally, the flavor of Huangjiu is attributed to the combination of alcohols, esters, and aldehydes that make up the structural components of HQW aroma (Liu Z. et al., 2020). With *FSI* treatment, a significant difference in the total content of alcohols was observed in HQW samples containing different *FSI* concentrations, and *FSI* strongly enhanced the formation of 3-methyl-1-butanol and 2-methyl-1-propanol. In contrast, the total content of esters in HQW with *FSI* was generally lower than that in the control wine, except for HQW containing 0.7 and 0.9 mg/L *FSI* (**Figure 4** and **Table 1**). At nearly all concentrations of *FSI*, the content of MCFAEE was significantly lower in treated HQW samples relative to the control; however, treatment with 0.9 mg/L *FSI* led to a higher content of MCFAEE relative to the control. These data suggested that the addition of *FSI* significantly promoted the accumulation of SCFAEE during HQW aging. As for aldehydes, the addition of FSI had little effect on the aldehyde content of HQW during aging. Thus, the *FSI* treatment improves the flavor profiles of HQW by affecting the production of alcohols and esters, especially 3-methyl-1-butanol, 2-methyl-1-propanol, and SCFAEE. Combining with the sensory evaluation (**Figure 5**), the treatment of 0.9 mg/mL *FSI* considerably highlighted the alcohol-aroma, cereal-aroma, and fruit-aroma in the aged HQW, consistent with the content of high alcohols and esters shown in **Figure 4**. The similar score of sweet taste in different HQW samples corresponded well with oenological properties, as the sweet attribute is partly related to the content of reducing sugar (**Figure 3**). The sour taste, which is generally related to the presence of organic acids (Dysvik et al., 2020), scored different levels suggesting that the *FSI* might have significantly affected the flavor-active organic acids in HQW.

As shown in **Figure 6**, the HQW samples treated with different *FSI* concentrations were located in different quadrants,

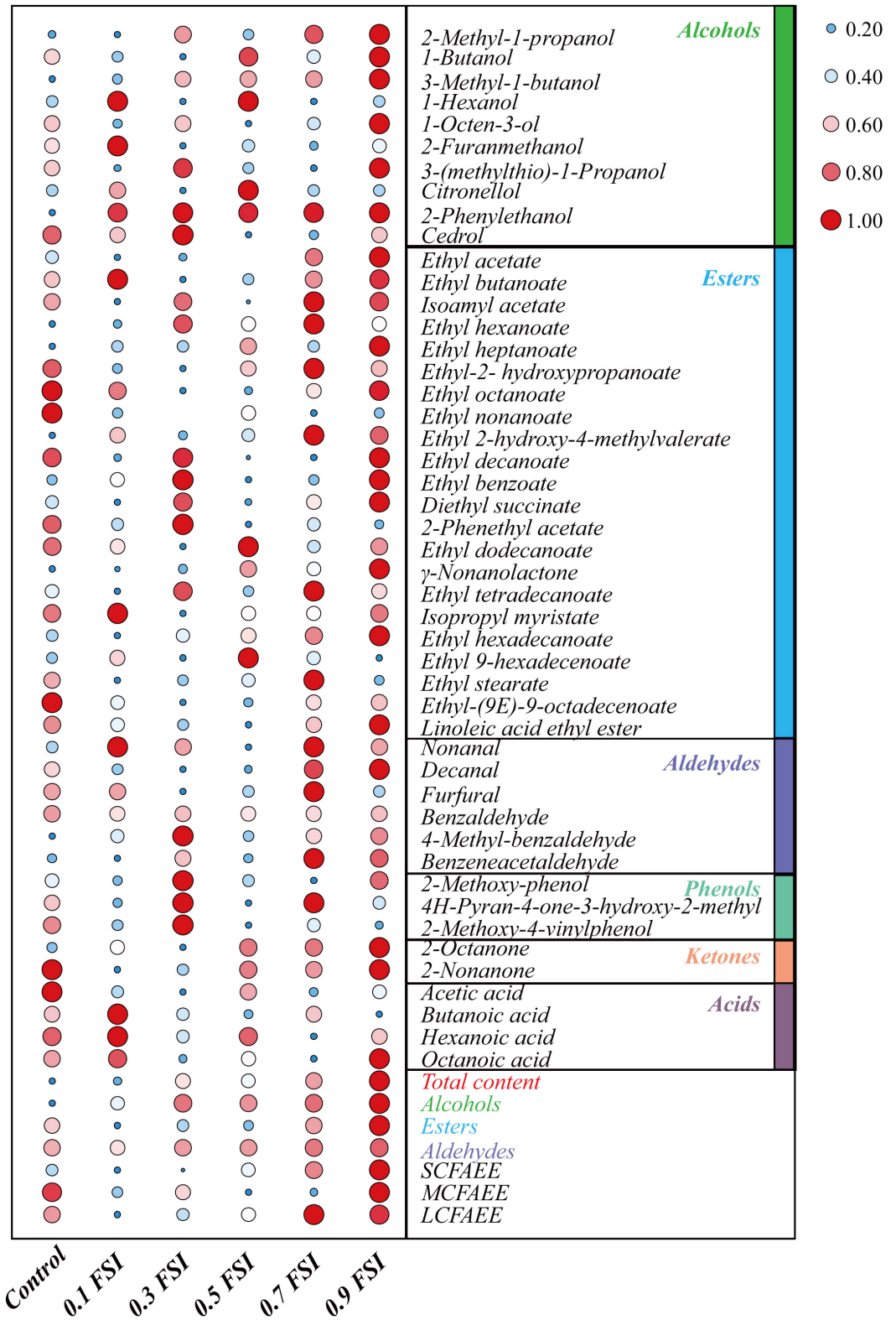

FIGURE 4 | Differentiation of volatile flavor compounds in HQW containing different concentrations of *FSI*. The 0.1 *FSI*, 0.3 *FSI*, 0.5 *FSI*, 0.7 *FSI*, and 0.9 *FSI* represented HQW containing 0.1, 0.3. 0.5, 0.7, and 0.9 mg/mL *FSI*, respectively. The color and size of the circle represent the relative content of the flavor compound (the data has been standardized). The redder (the bigger) the circle, the higher the content of the flavor compound, and the bluer (the smaller) the circle, the lower content of the flavor compound.

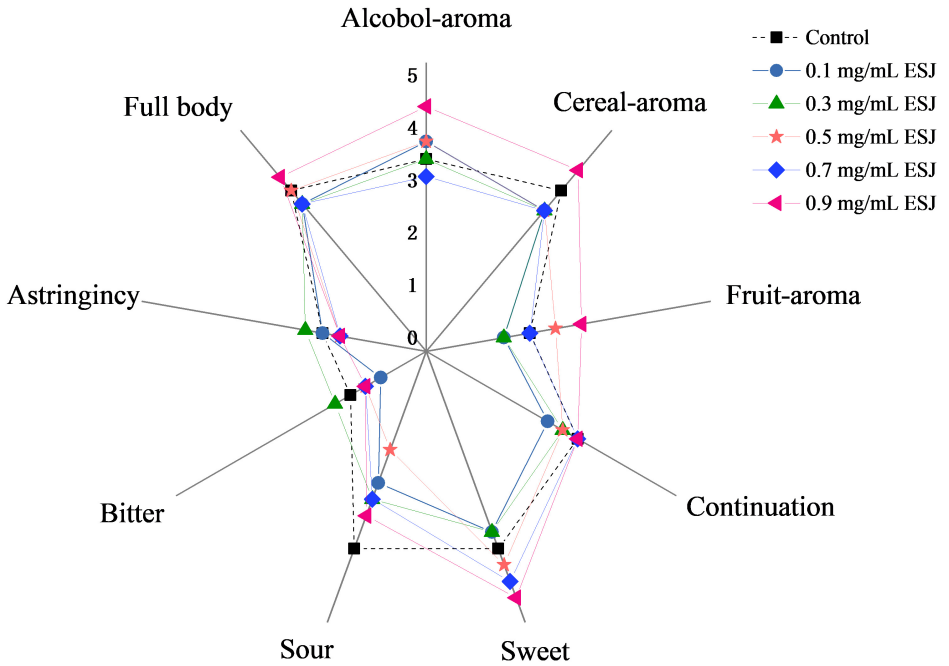

FIGURE 5 | Scores of sensorial attributes for HQW treated with different concentrations of *FSI* after sterilization and aged for 160 days.

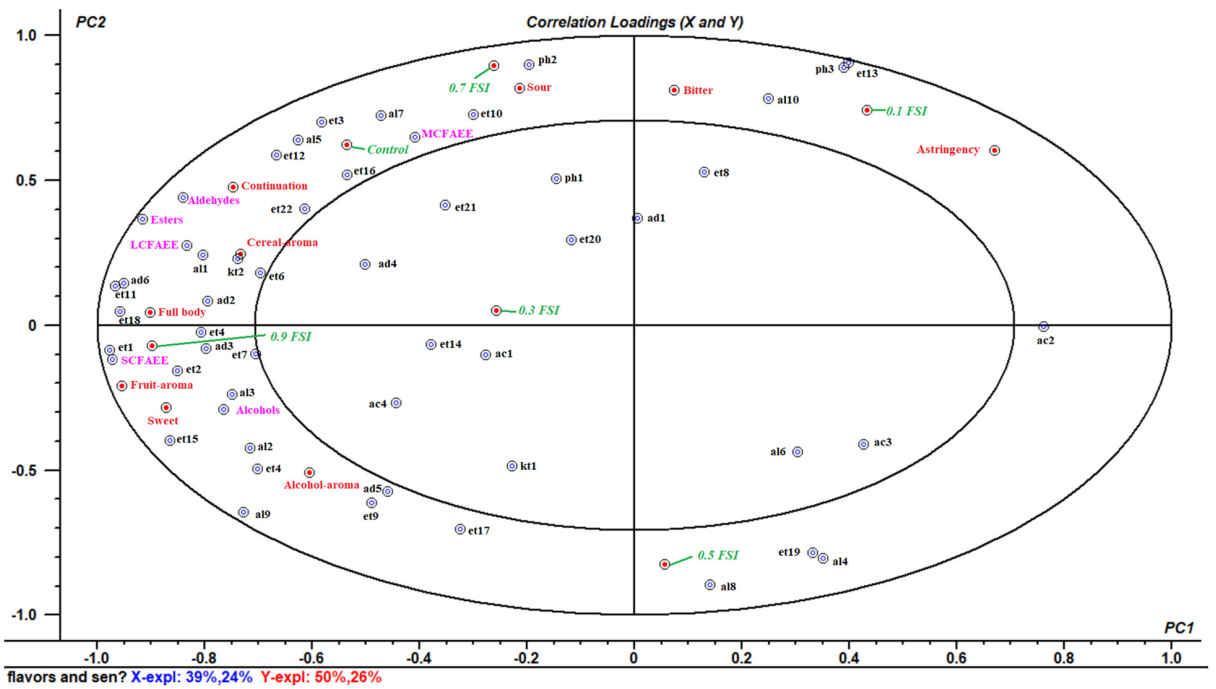

FIGURE 6 | Correlataion loadings plot between the fifty-three volatile flavor compounds and nine sensory attributes in HQW containing different concentrations of *FSI* (The codes were defined in **Table 1**).

suggesting that the concentration of *FSI* had a significant effect on the sensory characteristic of the resultant HQW. HQW treated with 0.7 mg/mL *FSI* exhibited a similar sensory profile as the control wine, and this profile was closely related to the presence of MCFAEE, 1-octen-3-ol, 3-methylthiopropanol, isoamyl acetate, diethyl succinate, ethyl tetradecanoate, and continuation. However, treatment with 0.7 mg/mL *FSI* was strongly correlated with a sour taste. Treatment with 0.1 mg/mL

FSI was correlated to astringency mouthfeel, indicating that different *FSI* concentrations increased certain sensory attributes. Treatment with 0.9 mg/mL *FSI* correlated strongly with a full body and fruit aroma, and was favored by consumers. The sensory characteristic of the resultant HQW depended greatly on the concentration of *FSI*. The addition of 0.9 mg/mL *FSI* yielded a satisfactory result, consistent with the sensory evaluation (**Figure 5**). The key attributes of the fruit and alcohol aroma were closely related to the presence of SCFAEE and to that of 1-butanol and 2-phenylethanol, respectively. The high odor activity values of ethyl acetate, ethyl butanoate, ethyl hexanoate, and 2-phenylethanol might be responsible for the fruit aroma (Yang et al., 2018). Cereal-aroma was strongly correlated with the presence of LCFAEE, 2-nonanone, ethyl-2-hydroxypropanoate and 2-methyl-1-propanol, and different types of flavor compounds (esters, alcohols, aldehydes, and ketones) suggested a complex origin for this aroma attribute (Mo et al., 2010; Liu S. et al., 2019). Both a full body and fruit aroma were strongly correlated with the presence of SCFAEE. Combining with the result of flavor compounds that the SCAFEE content was significantly accumulated by adding *FSI* (**Figure 4**), it suggested that *FSI* may alter the aroma of HQW by enhancing the synthesis of SCFAEE. Thus, the addition of *FSI* to HQW after sterilization may be a novel alternative strategy for obtaining HQW with a high-quality flavor profile.

In this study, we demonstrated that the photodegradation of *Monascus* pigments in HQW could be reduced significantly by adding *FSI* to wine after sterilization. Specifically, *FSI* considerably enhanced the accumulation of alcohols and esters as the added amounts were increased, especially 3-methyl-1-butanol, 2-methyl-1-propanol, and SCFAEE, in HQW. Furthermore, *FSI* enhanced the alcohol, cereal, and fruit aromas in HQW. HQW treated with 0.9 mg/mL *FSI* received the highest scores for the mouthfeel and aroma. A PLSR analysis of the HQW samples revealed that a pleasing aroma was strongly related to the presence of SCFAEE, the accumulation of which was significantly enhanced by *FSI*. Therefore, we inferred that *FSI* might alter the aroma of HQW by enhancing the synthesis of SCFAEE. Taken together, our results suggest the considerable potential of *FSI* treatment as a strategy for reducing the photodegradation of *Monascus* pigments, thus improving the color stability, flavor profile, and sensory characteristics of the resulting HQW. Our work provides a new strategy for improving the pigment stability and sensory quality of HQW and other beverages containing photosensitive pigments. However, further studies are needed to explore the bioactive constituents of *FSI* in detail and the mechanisms by which *FSI* enhances the formation of SCFAEE.

DATA AVAILABILITY STATEMENT

The raw data supporting the conclusions of this article will be made available by the authors, without undue reservation.

ETHICS STATEMENT

We obtained informed consent from participants in the sensory evaluation in accordance with the Code of Ethics of the World Medical Association (Declaration of Helsinki).

AUTHOR CONTRIBUTIONS

YY: experiment, investigation, software, data curation, and writing—original draft. YX: conceptualization, methodology, project administration, and writing—review and editing. XS: methodology, project administration, writing—review and editing. ZM: experiment, resources, and methodology. HQ: experiment, resources, methodology, and visualization. LT: conceptualization, software, and investigation. LA: supervision, writing—original draft, and writing—review and editing. All authors contributed to the article and approved the submitted version.

FUNDING

This work was financially supported by the National Natural Science Foundation of China (No. 32001674), the Shanghai Agriculture Applied Technology Development Program, China (2019-02-08-00-07-F01152); the Shanghai Technical Standard Program, China (18DZ2200200); and the Shanghai Engineering Research Center of food microbiology program (19DZ2281100).

SUPPLEMENTARY MATERIAL

The Supplementary Material for this article can be found online at: https://www.frontiersin.org/articles/10.3389/fmicb.2021.678903/full#supplementary-material

REFERENCES

Abdelhady, M., Kamal, A., Othman, S., Mubarak, M., and Hadda, T. (2015). Total polyphenolic content, antioxidant, cytotoxic, antidiabetic activities, and polyphenolic compounds of *Sophora japonica* grown in Egypt. *Med. Chem. Res.* 24, 482–495. doi: 10.1007/s00044-014-1101-2

Cai, H., Zhang, T., Zhang, Q., Luo, J., Cai, C., and Mao, J. (2018). Microbial diversity and chemical analysis of the starters used in traditional Chinese sweet rice wine. *Food Microbiol.* 73, 319–326. doi: 10.1016/j.fm.2018.02.002

Chen, C., Chen, H., Zhang, Y., Thomas, H. R., Frank, M. H., He, Y., et al. (2020). TBtools-an integrative toolkit developed for interactive analyses of big biological data. *Mol. Plant* 13, 1194–1202. doi: 10.1016/j.molp.2020.06.009

Chen, S., and Xu, Y. (2012). The influence of yeast strains on the volatile flavour compounds of Chinese rice wine. *J. Instit. Brewing* 116, 190–196. doi: 10.1002/j.2050-0416.2010.tb00417.x

Dhale, M., Javagal, M., and Puttananjaiah, M. (2018). Protective and antioxidative effect of rubropunctatin against oxidative protein damage induced by metal

catalyzed reaction. *Int. J. Biol. Macromol.* 116, 409–416. doi: 10.1016/j.ijbiomac.2018.04.170

Di Egidio, V., Sinelli, N., Giovanelli, G., Moles, A., and Casiraghi, E. (2010). NIR and MIR spectroscopy as rapid methods to monitor red wine fermentation. *Eur. Food Res. Technol.* 230, 947–955. doi: 10.1007/s00217-010-1227-5

Dysvik, A., La Rosa, S., Liland, K., Myhrer, K., Østlie, H., De Rouck, G., et al. (2020). Co-fermentation involving Saccharomyces cerevisiae and Lactobacillus Species tolerant to brewing-related stress factors for controlled and rapid production of sour beer. *Front. Microbiol.* 11:279. doi: 10.3389/fmicb.2020.00279

Feng, Y., Shao, Y., and Chen, F. (2012). Monascus pigments. *Appl. Microbiol. Biotechnol.* 96, 1421–1440. doi: 10.1007/s00253-012-4504-3

Gao, Q., Cao, X., Huang, Y., Yang, J., Chen, J., Wei, L., et al. (2018). Overproduction of fatty acid ethyl esters by the oleaginous yeast Yarrowia lipolytica through metabolic engineering and process optimization. *ACS Synthetic Biol.* 7, 1371–1380. doi: 10.1021/acssynbio.7b00453

GB/T 5517-2010. *Official Methods of Analysis*. China: Determination of total acidity.

Horuz, E., Bozkurt, H., Karataş, H., and Maskan, M. (2017). Effects of hybrid (microwave-convectional) and convectional drying on drying kinetics, total phenolics, antioxidant capacity, vitamin C, color and rehydration capacity of sour cherries. *Food Chem.* 230, 295–305. doi: 10.1016/j.foodchem.2017.03.046

Hu, Z., Li, S., Li, C., and Li, Z. (2016). Chitosan-assisted isolation and antioxidant evaluation of flavonoids from Sophora japonica L. *BMC Plant Biology* 16:10–24. doi: 10.1186/s12870-016-0904-3

Huang, R., Zhang, Y., Zhang, Y., Zhang, L., Pei, L., Shu, G., et al. (2020). Evaluation of the synergetic effect of Yupingfeng san and Flos Sophorae Immaturus based on free radical scavenging capacity. *Biomed. Pharmacother.* 128, 110265. doi: 10.1016/j.biopha.2020.110265

Huang, Z., Guo, W., Zhou, W., Li, L., Xu, J., Hong, J., et al. (2019). Microbial communities and volatile metabolites in different traditional fermentation starters used for Hong Qu glutinous rice wine. *Food Res. Int.* 121, 593–603. doi: 10.1016/j.foodres.2018.12.024

ISO (1993). *Sensory Analysis—General Guidance for Selection, Training and Monitoring of Assessors*. Switzerland: International Organization for Standardization Geneva.

Jones, P. R., Gawel, R., Francis, I. L., Francis, I. L., and Waters, E. J. (2008). The influence of interactions between major white wine components on the aroma, flavour and texture of model white wine. *Food Q. Pref.* 19, 596–607. doi: 10.1016/j.foodqual.2008.03.005

Keekan, K., Hallur, S., Modi, P., and Shastry, R. (2020). Antioxidant activity and role of culture condition in the optimization of red pigment production by Talaromyces purpureogenus KKP through response surface methodology. *Curr. Microbiol.* 77, 1780–1789. doi: 10.1007/s00284-020-01995-4

Kennedy, J., Auclair, K., Kendrew, S., Park, C., Vederas, J., and Hutchinson, C. (1999). Modulation of polyketide synthase activity by accessory proteins during lovastatin biosynthesis. *Science* 284, 1368–1372. doi: 10.1126/science.284.5418.1368

Li, Y., and Fan, L. (2020). Comparative studies on the stabilization of flos sophorae immaturus beverages by various hydrocolloids. *LWT* 123:109117. doi: 10.1016/j.lwt.2020.109117

Lin, C., Lin, T., and Pan, T. (2017). Alleviation of metabolic syndrome by monascin and ankaflavin: the perspective of *Monascus functional* foods. *Food Funct.* 8, 2102–2109. doi: 10.1039/C7FO00406K

Liu, C., Yan, Y., Zhang, X., Mao, Y., Ren, X., Hu, C., et al. (2020). Regulating the pro-and antioxidant capabilities of bimetallic nanozymes for the detection of Fe 2+ and protection of Monascus pigments. *Nanoscale.* 12, 3068–3075. doi: 10.1039/C9NR10135G

Liu, S., Yang, L., Zhou, Y., He, S., Li, J., Sun, H., et al. (2019). Effect of mixed moulds starters on volatile flavor compounds in rice wine. *LWT* 112:108215. doi: 10.1016/j.lwt.2019.05.113

Liu, T., Wang, S., Ma, H., Jin, H., Li, J., Yang, X., et al. (2019). Microwave-assisted extraction combined with in-capillary [Fe (ferrozine) 3] 2+-CE-DAD to screen active components with the ability to chelate ferrous ions from Flos Sophorae Immaturus (Flos Sophorae). *Molecules* 24:3052. doi: 10.3390/molecules24173052

Liu, Z., Wang, Z., Sun, J., and Ni, L. (2020). The dynamics of volatile compounds and their correlation with the microbial succession during the traditional solid-state fermentation of gutian hong qu glutinous rice wine. *Food Microbiol.* 86:103347. doi: 10.1016/j.fm.2019.103347

Mapari, S. A., Meyer, A. S., and Thrane, U. (2009). Photostability of natural orange-red and yellow fungal pigments in liquid food model systems. *J. Agric. Food Chem.* 57, 6253–6261. doi: 10.1021/jf900113q

Mateo-Fernández, M., Alves-Martínez, P., Río-Celestino, D., Font, R., Merinas-Amo, T., and Alonso-Moraga, Á (2019). Food safety and nutraceutical potential of caramel colour class IV using in vivo and in vitro assays. *Foods* 8:392. doi: 10.3390/foods8090392

Miller, G. (1959). Use of dinitrosalicylic acid reagent for determination of reducing sugar. *Anal. Chem.* 31, 426–428. doi: 10.1021/ac60147a030

Mo, X., Xu, Y., and Fan, W. (2010). Characterization of aroma compounds in Chinese rice wine Qu by solvent-assisted flavor evaporation and headspace solid-phase microextraction. *J. Agric. Food Chem.* 58, 2462–2469. doi: 10.1021/jf903631w

Mondal, S., Pandit, S. G., Puttananjaiah, M. H., Harohally, N. V., and Dhale, M. A. (2019). Structural and functional characterization of new pigment molecule monashin from monascus purpureus CFR410-11. *Proc. Biochem.* 82, 173–178. doi: 10.1016/j.procbio.2019.04.004

Park, K., Liu, Z., Park, C., and Ni, L. (2016). Microbiota associated with the starter cultures and brewing process of traditional Hong Qu glutinous rice wine. *Food Sci. Biotechnol.* 25, 649–658. doi: 10.1007/s10068-016-0115-6

Patakova, P. (2013). Monascus secondary metabolites: production and biological activity. *J. Indust. Microbiol. Biotechnol.* 40, 169–181. doi: 10.1007/s10295-012-1216-8

Qian, C., Decker, E., Xiao, H., and McClements, D. (2012). Nanoemulsion delivery systems: influence of carrier oil on β-carotene bioaccessibility. *Food Chem.* 135, 1440–1447. doi: 10.1016/j.foodchem.2012.06.047

Sen, T., Barrow, C., and Deshmukh, S. (2019). Microbial pigments in the food industrychallenges and the way forward. *Front. Nut.* 6:7. doi: 10.3389/fnut.2019.00007

Tang, R., Luo, J., Wang, W., Liu, D., Wang, G., and Guo, X. (2019). Rutin's natural source flos sophorae as potential antioxidant and improver of fungal community in Chinese sausages. *LWT* 101, 435–443. doi: 10.1016/j.lwt.2018.11.064

Tao, Y., García, J. F., and Sun, D. W. (2014). Advances in wine aging technologies for enhancing wine quality and accelerating wine aging process. *Crit. Rev. Food Sci. Nut.* 54, 817–835. doi: 10.1080/10408398.2011.609949

Vendruscolo, F., Bühler, R., de Carvalho, J., de Oliveira, D., Moritz, D., Schmidell, W., et al. (2016). Monascus: a reality on the production and application of microbial pigments. *Appl. Biochem. Biotechnol.* 178, 211–223. doi: 10.1007/s12010-015-1880-z

Vollmuth, T. (2018). Caramel color safety–an update. *Food Chem. Toxicol.* 111, 578–596. doi: 10.1016/j.fct.2017.12.004

Wang, J., Li, L., Tan, J., Song, X., Chen, D., Xu, J., et al. (2019). Variations in the components and antioxidant and tyrosinase inhibitory activities of *Styphnolobium japonicum* (L.) schott extract during flower maturity stages. *Chem. Biodiversity* 16:e1800504. doi: 10.1002/cbdv.201800504

Wang, J., Yuan, C., Gao, X., Kang, Y., Huang, M., Wu, J., et al. (2020). Characterization of key aroma compounds in Huangjiu from northern China by sensory-directed flavor analysis. *Food Res. Int.* 134:109238. doi: 10.1016/j.foodres.2020.109238

Wang, L., Dai, Y., Chen, W., Shao, Y., and Chen, F. (2016). Effects of light intensity and color on the biomass, extracellular red pigment, and citrinin production of Monascus ruber. *J. Agric. Food Chem.* 64, 9506–9514. doi: 10.1021/acs.jafc.6b04056

Xiao, Z., Yu, D., Niu, Y., Chen, F., Song, S., Zhu, J., et al. (2014). Characterization of aroma compounds of Chinese famous liquors by gas chromatography–mass spectrometry and flash GC electronic-nose. *J. Chromatography B* 945, 92–100. doi: 10.1016/j.jchromb.2013.11.032

Yang, Y., Xia, Y., Lin, X., Wang, G., Zhang, H., Xiong, Z., et al. (2018). Improvement of flavor profiles in Chinese rice wine by creating fermenting yeast with superior

ethanol tolerance and fermentation activity. *Food Res. Int.* 108, 83–92. doi: 10.1016/j.foodres.2018.03.036

Yang, Y., Xia, Y., Wang, G., Tao, L., Yu, J., and Ai, L. (2019). Effects of boiling, ultra-high temperature and high hydrostatic pressure on free amino acids, flavor characteristics and sensory profiles in Chinese rice wine. *Food Chem.* 275, 407–416. doi: 10.1016/j.foodchem.2018.09.128

Yang, Y., Xia, Y., Wang, G., Zhang, H., Xiong, Z., Yu, J., et al. (2017). Comparison of oenological property, volatile profile, and sensory characteristic of Chinese rice wine fermented by different starters during brewing. *Int. J. Food Propert.* 20, S3195–S3211. doi: 10.1080/10942912.2017.1325900

Yao, W., Wang, S., Chen, Y., and Wang, H. (2011). Composition and antibacterial activity of essential oils of Flos sophorae immaturus. *Int. J. Food Propert.* 14, 903–913. doi: 10.1080/10942910903474419

Zhang, L., Ravipati, A., Koyyalamudi, S., Jeong, S., Reddy, N., Smith, P., et al. (2011). Antioxidant and anti-inflammatory activities of selected medicinal plants containing phenolic and flavonoid compounds. *J. Agric. Food Chem.* 59, 12361–12367. doi: 10.1021/jf203146e

Conflict of Interest: The authors declare that the research was conducted in the absence of any commercial or financial relationships that could be construed as a potential conflict of interest.

frontiers in Microbiology

ORIGINAL RESEARCH
published: 24 May 2021
doi: 10.3389/fmicb.2021.686100

Effect of a *Monascus* sp. Red Yeast Rice Extract on Germination of Bacterial Spores

*Marketa Husakova, Michaela Plechata, Barbora Branska and Petra Patakova**

Department of Biotechnology, University of Chemistry and Technology Prague, Prague, Czechia

The pink-red color of traditional sausages (cured meat) is the result of nitrite addition and the formation of nitrosomyoglobin. However, the pleasant color of processed meat products is a side effect of nitrite addition while the main anticipated goal is to suppress the germination of clostridial spores. The fungus *Monascus* is known as a producer of oligoketide pigments, which are used in Asian countries, especially in China, for coloring foods, including meat products. Although, different biological activities of *Monascus* pigments have been tested and confirmed in many studies, their effect on germination of bacterial spores has never been investigated. This study is focused on testing the activity of red yeast rice (RYR) extract, containing monascin, rubropunctatin, rubropunctamine complexes and monascuspiloin as the main pigments, on germination of *Clostridium* and *Bacillus* spores. It was found that addition of nitrite alone, at the permitted concentration, had no effect on spore germination. However, the combined effects of nitrite with NaCl, tested after addition of pickling salt, was efficient in inhibiting the germination of *C. beijerinckii* spores but had no effect on *B. subtilis* spores. In contrast, total suppression of *C. beijerinckii* spore germination was reached after addition of RYR extract to the medium at a concentration of 2% v/v. For *B. subtilis*, total inhibition of spore germination was observed only after addition of 4% v/v RYR extract to the medium containing 1.3% w/w NaCl.

Keywords: ***Monascus*, red yeast rice, bacterial spores germination, nitrite, *Clostridium beijerinckii*, *Bacillus subtilis***

OPEN ACCESS

Edited by:
Wanping Chen,
Georg-August-University Goettingen, Germany

Reviewed by:
Yanli Feng,
Hubei Normal University, China
Yanchun Shao,
Huazhong Agricultural University, China

****Correspondence:***
Petra Patakova
petra.patakova@vscht.cz

Specialty section:
This article was submitted to Food Microbiology, a section of the journal Frontiers in Microbiology

Received: *26 March 2021*
Accepted: *27 April 2021*
Published: *24 May 2021*

Citation:
Husakova M, Plechata M, Branska B and Patakova P (2021) Effect of a Monascus sp. Red Yeast Rice Extract on Germination of Bacterial Spores. Front. Microbiol. 12:686100. doi: 10.3389/fmicb.2021.686100

INTRODUCTION

Red yeast rice (RYR) is rice fermented by the fungus *Monascus*, which is prepared for different applications using different *Monascus* species (for a recent review see Zhu et al., 2019). RYR has various synonyms such as hong-qu, beni-koji or ang-kak in languages of Asian countries, where the product is popular. In Europe, RYR is only permitted as a food supplement on the condition that it is prepared using *Monascus purpureus* and the preparation (food supplement) should contain 10 mg of monacolin K, administered daily, in order to guarantee the effect as described in the health claim "Monacolin K from red yeast rice contributes to the maintenance of normal blood cholesterol levels" (Commission Regulation (EU) No 432/2012, 2012). As a dose of 10 mg of monacolin K corresponds to the lowest therapeutically effective dose of statins in prescription drugs, the required amount of monacolin K in RYR food supplements was reconsidered by the EFSA Panel on Food Additives and Nutrient Sources added to Food (ANS) in

2018 (EFSA Panel on Food Additives and Nutrient Sources added to Food [ANS] et al., 2018) but with no clear conclusion. Nevertheless, the main concern associated with the use of RYR is its potential contamination with citrinin, a mycotoxin whose toxicological effects on people have not been fully elucidated (de Oliveira Filho et al., 2017). By the Commission Regulation (EU) 2019/1901, 2019, the maximum tolerated citrinin concentration in RYR was set to 100 μg/kg.

The fungus *Monascus* is especially known for its production of red pigments, which are used in certain Asian countries, such as China, Japan or Philippines, for food coloring. As the color red is associated with many different fruits, vegetables and meat products, *Monascus* pigments are mostly used for coloring cakes or other sweet products, fruit yogurts or other fermented milk products and processed meat. The suitability of *Monascus* pigments for coloring meat products, particularly with regard to color, texture, smell and other sensory parameters of the products, has already been proven in the scientific literature (Leistner et al., 1991; Fabre et al., 1993; Yu et al., 2015; Seong et al., 2017). In addition, inhibitory effects of *Monascus* pigments or *Monascus* extracts on vegetative bacterial cells, e.g., *Staphylococcus aureus, Escherichia coli, Bacillus subtilis* (Kim et al., 2006; Vendruscolo et al., 2014; Zhao et al., 2016) have been demonstrated. In addition, the safety of *Monascus* pigments for human consumption has been confirmed in several studies (Bianchi, 2005; Yu et al., 2008; Mohan Kumari et al., 2009).

The aim of the study was to test whether an ethanol extract of RYR, having a red color and containing a mixture of *Monascus* pigments but without citrinin and monacolin K, might suppress germination of bacterial spores. In traditional food processing, nitrite salts have been added to meat products in order to achieve total inhibition of germination of *Clostridium botulinum* spores. Nitrite salts are also responsible for the pleasing red color of processed meat products, caused by the formation of nitrosomyoglobin. In the work described for the first time here, *Clostridium beijerinckii* and *Bacillus subtilis* spores were used as models of anaerobic and aerobic bacterial spore formers, respectively.

MATERIALS AND METHODS

RYR Preparation

Monascus sp. DBM 4361, isolated from a non-sterile dried red fermented rice sample, was maintained on Potato-Dextrose agar (VWR Chemicals) slants at 4°C. The strain was deposited at the Department of Biochemistry and Microbiology (DBM), University of Chemistry and Technology Prague.

An amount of rice (Giana, Thailand) (150 g) was washed with hot water, then boiled for 1 min. The rice was evenly divided into three autoclavable plastic bags, which were closed with a metal ring and a cotton plug. The use of plastic bags instead of glass vessels enabled manual separation of rice kernels after sterilization without opening of the bags. The cultivation was inspired by soy koji preparation (Lotong and Suwanarit, 1983). The bags were placed in a beaker sealed with aluminum foil and sterilized at 121°C for 20 min. Sterilization was repeated after 24 h to eliminate contamination by spore-forming bacteria. Spores from the *Monascus* culture (mixture of ascospores and conidia, because the strain formed both asexual and sexual spores, see **Figure 1**) were transferred to sterile water using a sterile loop. The sterile rice in the bags was inoculated with 5 mL of the spore suspension. Cultivation of the fungus on rice was performed for 10 days at 30°C. The rice was mixed by hand daily.

Extraction of Pigments, pH Estimation

The RYR (**Figure 2**) (5 g) was extracted with 25 mL of 70% ethanol and distilled water in 250 mL Erlenmeyer flasks for 1 h, at 30°C, with shaking (laboratory shaker Infors, 100 rpm). The mixture was then filtered through Whatman 1 filter paper. Pooled ethanol extracts from 3 flasks were concentrated using a rotary vacuum evaporator (Boeck) (max. temperature 55°C), so that all ethanol was evaporated. The remaining water extract contained insoluble pigmented particles, which were collected by filtration and dissolved in 96% ethanol. The resulting ethanol extract, having dry matter concentration 9.4 mg/mL, was used for all microbiological assays and was analyzed by HPLC. The pH of pooled water extracts from 3 flasks was measured and shown to be 4.9.

RYR Extract Analysis

Spectrophotometric Analysis of the RYR Extract

The RYR extract was diluted 200-fold with 96% ethanol to adjust the absorbance to 0.1–1.0 at 330–600 nm. The absorbance of the sample was detected using a spectrophotometer (Varian Cary 50 Bio). The results were represented as an absorbance spectrum or as an absorbance value at a selected wavelength, the dilution factor being taken into consideration. As a blank, 96% ethanol was used.

UHPLC Analysis of Pigments, Citrinin, and Monacolin K

UHPLC (Agilent Technologies 1260 Infinity II) was used to determine *Monascus* pigments, citrinin and monacolin K. The

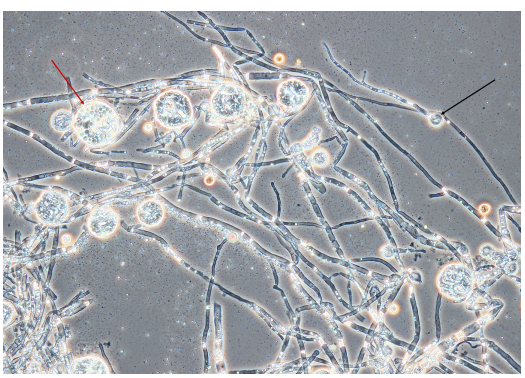

FIGURE 1 | Mycelium, conidia and cleistothecia of *Monascus* sp. DBM 4361. An example of a conidium is marked with a black arrow, the red arrow shows a cleistothecium with ascospores. The specimen was prepared from the fungus grown on a PDA agar slant for 5 days at 30°C; magnification was 400×.

FIGURE 2 | Red yeast rice fermented with *Monascus* sp. DBM 4361 for 10 days at 30°C.

following conditions were used: Kinetex Polar C18, 100A, 150 × 4.6 mm column; the mobile phase: 0.025% H_3PO_4 in water:acetonitrile at a ratio of 60:40; isocratic elution at a flow rate 1.5 mL/min; injection volume 5 μL. For determination of yellow, orange and red pigments, a photodiode detector set at 390, 470, and 500 nm resp. was used. The presence of monacolin K was detected at 237 nm. For the determination of the mycotoxin citrinin, the fluorescence detector setting was 331 nm for excitation and 500 nm for emission. For analysis, the extract sample was diluted 10-fold with 96% ethanol.

The standards of mycotoxin citrinin (Sigma-Aldrich), yellow pigment monascin (Sigma-Aldrich), and orange pigment rubropuctatin (1717 CheMall Corporation) were used as reference samples. A rubropunctamine laboratory standard was prepared from the rubropunctatin standard by reaction with NH_4OH (Penta). Unknown yellow, orange and red pigments were identified based on their absorption spectra and quantified as equivalents to their respective standards, i.e. monascin, rubropunctatin and rubropunctamine. For identification of individual compounds in the chromatogram, previous results (Patrovsky et al., 2019) were used.

HPLC-MS Analysis

HPLC-HRMS (Accella 600 Thermo Fisher Scientific) was used to determine molecular weights of the *Monascus* pigments. The following conditions were used: Luna Omega Polar 1.6 μm, 50 × 2.1 mm Phenomenex column; mobile phase: 0.1% HCOOH in water:methanol; gradient elution (A:B in ratio from 90:10 to 5:95) at a flow rate of 300 μL/min; injection volume 5 μL; ESI-positive mode; LTQ Orbitrap Velos mass analyzer (Thermo Scientific). For the analysis, the extract sample was diluted 200-fold with a solution of 90% water 10% methanol.

Spore Germination Assays

Preparation of Spore Suspensions

Clostridium beijerinckii NCIMB 8052 and *Bacillus subtilis* DBM 3006 were stored in the form of spore suspensions in sterile distilled water at 4°C. Spores of *C. beijerinckii* NCIMB 8052 were obtained after 48 h incubation of the culture in 250 mL Erlenmeyer flasks containing 100 mL of TYA medium in an anaerobic chamber (Concept 400, Ruskinn Technology, United Kingdom) at 37°C. TYA medium contained in g/L: glucose 40, yeast extract (Merck) 2, tryptone (Sigma-Aldrich) 6, potassium dihydrogenphosphate 0.5, ammonium acetate 3, magnesium sulfate heptahydrate, 0.3, ferrous sulfate heptahydrate 0.01; the pH of the medium was adjusted prior to sterilization in the autoclave (20 min, 121°C, 0.1 MPa) to 6.8. Spores of *B. subtilis* DBM 3006 were obtained after 48 h incubation of the culture in 250 mL Erlenmeyer flasks containing 50 mL of MP broth shaken on a rotary shaker (New Brunswick Scientific) at 300 rpm and 30°C. MP broth contained in g/L: meat extract (Roth) 3, peptone (Roth) 5; the pH of the medium was adjusted prior to sterilization in the autoclave (20 min, 121°C) to 7.0. Salts, HCl and NaOH for medium preparation and pH adjustment were purchased from Penta, Czech Republic. After cultivation, spores of both bacterial cultures were harvested by centrifugation (Hettich MIKRO 220R) for 5 min, 5,000 rpm, at 4°C. Spores were washed with sterile water, centrifuged under the same conditions and re-suspended in 20 mL of sterile water. Finally, the spore suspension was pipetted in 1 mL portions into Eppendorf tubes, which were stored at 4°C. All spore handling was performed under aseptic conditions using sterile tools and materials. Spore concentrations were estimated by flow cytometry (Branska et al., 2018) to be $2*10^8$ spores/mL and $8*10^8$ spores/mL for *C. beijerinckii* and *B. subtilis*, respectively. Prior to inoculation of medium for germination assays, spore suspensions were heat shocked (80°C for 30 s followed by cooling on ice for 2 min) to accelerate germination.

C. beijerinckii Germination Assay

The cultivation tests were performed in 20 mL test tubes containing 9.8 mL of medium inoculated with 0.2 mL heat shocked spore suspension of *C. beijerinckii*. Unmodified TYA medium was used as a positive control. The cultivation tests were performed in triplicate, in the anaerobic chamber, at 37°C for 48 h. Different combinations of agents were added to the TYA medium to test their effect on spore germination (see **Table 1**).

B. subtilis Germination Assay

The cultivation tests were performed on microcultivation plates using the Bioscreen C device (LabSystem) with intermittent shaking (30 s every 3 min) at 30°C for 24 h. Each well of the plate was filled with 196 μL of medium and 4 μL of *B. subtilis* heat shocked spore suspension. In each well, optical density was measured at 600 nm, every 30 min. Unmodified MP medium was used as a positive control. Each cultivation test was performed in

TABLE 1 | Design of *C. beijerinckii* germination assays in individual test tubes.

	Assay component	**TYA (μL)**	**96% ethanol (μL)**	**RYR extract (μL)**	**Citrinin (μL)**	**Inoculum Heat-shocked spores (μL)**
Code	**Type of experiment**					
TYA	Positive control	9,800	–	–	–	200
TYA	Negative control	10,000	–	–	–	–
TYA + et	Control	9,600	200	–	–	200
TYA + RYR	Test	9,600	–	200	–	200
TYA + cit	Test	9,780	–	–	20	200
TYA + RYR + cit	Test	9,580	–	200	20	200
		TYAS1 (μL)	**96% ethanol (μL)**	**RYR extract (μL)**		**Inoculum Heat-shocked spores (μL)**
TYS1	Test	9,800	–	–	–	200
TYAS1 + et	Control	9,600	200	–	–	200
TYAS1 + RYR	Test	9,600	–	200	–	200
		TYAS2 (μL)				**Inoculum Heat-shocked spores (μL)**
TYAS2	Test	9,800	–	–	–	200
		TYAN1 (μL)				**Inoculum Heat-shocked spores (μL)**
TYAN1	Test	9,800	–	–	–	200
		TYAN2 (μL)				**Inoculum Heat-shocked spores (μL)**
TYAN2	Test	9,800	–	–	–	200
		TYA + $NaNO_2$ (μL)				**Inoculum Heat-shocked spores (μL)**
TYA + $NaNO_2$	Test	9,800	–	–	–	200
		TYA + $NaNO_3$ (μL)				**Inoculum Heat-shocked spores (μL)**
TYA + $NaNO_3$	Test	9,800	–	–	–	200

TYA, unmodified TYA medium with 20 g/L glucose; TYAS1, TYAS2, TYA medium with the addition of 1.3 and 2.0% w/w NaCl, respectively, TYAN1, TYAN2, TYA medium with the addition of 1.3 and 2.0% w/w Praganda butcher's nitrite pickling mixture (K + S company, Czech Republic); TYA + $NaNO_2$ and TYA + $NaNO_3$, TYA media with the addition of 300 mg/L $NaNO_2$ or $NaNO_3$; citrinin was added from stock solution, of concentration 100 mg/L in dimethylsulfoxide; et, ethanol; cit, citrinin.

6 wells. Different combinations of agents were added to the MP medium to test their effect on spore germination (see **Table 2**).

RESULTS

C. beijerinckii Germination

Clostridium beijerinckii spores were chosen as a model substituting for *Clostridium botulinum* spores because both species belong to the same Cluster I (*sensu stricto*) of the *Clostridium* genus (Cruz-Morales et al., 2019). Heat-shocked spores of *C. beijerinckii* were inoculated to 2% by volume to the medium in test tubes and were allowed to germinate under anaerobic conditions. The TYA medium and the inoculation ratio were chosen to guarantee reliable spore germination based on previous experience with the strain (Kolek et al., 2016). The compositions of different media were designed (see **Table 1**) to be able to compare any effect of nitrite salts with the potential effect of the RYR extract, not containing citrinin and monacolin K. Nitrites are only allowed to be added to meat products in a mixture with sodium chloride in the form of $NaNO_2$ (E249 food additive) or KNO_2 (E250 food additive), in an amount not exceeding 150 mg of nitrite per 1 kg of a standard meat product (only in some national specialities produced in different EU countries can the amount of nitrite be higher, up to 300 mg/kg, for certain salamis and bacons and up to 500 mg/kg for herrings and sprouts); for a survey of rules valid in the EU for the addition of nitrite/nitrate to meat products (see Honikel, 2008).

Nitrite, in the form of $NaNO_2$, was added to the culture, either independently or as a component of Praganda nitrite pickling salt. In addition, $NaNO_3$ (E251 food additive) was tested because its addition is permitted and applied in cheeses to a maximum concentration of 150 mg/kg, with the aim of suppressing germination of *Clostridium butyricum* spores. While even the addition of $NaNO_2$ or $NaNO_3$ alone at a concentration of 300 mg/kg had no effect on the germination of *C. beijerinckii* spores, addition of nitrite pickling salt to the recommended concentration for various products, i.e., 2% (w/w) of the pickling salt or 1.3% (w/w) as recommended for products with low salt content, resulted in total inhibition of spore germination (see **Table 3**, experiment

TABLE 2 | Design of *B. subtilis* germination assays in individual wells of a microcultivation plate.

	Assay component	**MP (μL)**	**96% ethanol (μL)**	**RYR extract (μL)**	**Citrinin (μL)**	**Inoculum Heat-shocked spores (μL)**
Code	**Type of experiment**					
MP	Positive control	196	–	–	–	4
MP	Negative control	200	–	–	–	–
MP + et1	Control	192	4	–	–	4
MP + et2	Control	188	8			4
MP + RYR1	Test	192	–	4	–	4
MP + RYR2	Test	188	–	8	–	4
MP + cit	Test	196	–	–	0.8	4
MP + RYR1 + cit	Test	192	–	4	0.8	4
		MPS1 (μL)	**96% ethanol (μL)**	**RYR extract (μL)**		**Inoculum Heat-shocked spores (μL)**
MPS1	Test	196	–	–	–	4
MPS1 + et1	Control	192	4	–	–	4
MPS1 + et2	Control	188	8	–	–	4
MPS1 + RYR1	Test	192	–	4	–	4
MPS1 + RYR2	Test	188	–	8	–	4
		MPN2 (μL)				**Inoculum Heat-shocked spores (μL)**
MPN2	Test	196	–	–	–	4

MP, unmodified MP medium; MPS1, MP medium with addition of 1.3% w/w NaCl; MPN2, MP medium with addition of 2.0% w/w Praganda butcher's nitrite pickling mixture (K + S company, Czech Republic); citrinin was added from a stock solution, of concentration 100 mg/L in dimethylsulfoxide.

TABLE 3 | Results of *C. beijerinckii* germination assays.

Code	**Type of experiment**	**Experiment description**	**Result**
TYA	Positive control	–	+++
TYA	Negative control	–	—
TYA + et	Control	Control ethanol addition	+++
TYA + RYR	**Test**	**Addition of RYR extract in concentration 2% v/v**	**—**
TYA + cit	Test	Addition of citrinin in concentration 2,000 μg/kg	+++
TYA + RYR + cit	Test	Combined addition of citrinin in concentration 2,000 μg/kg and RYR in concentration 2% v/v	—
TYS1	Test	Addition of NaCl in concentration 1.3% w/w	++-*
TYAS1 + et	Control	Combined addition of NaCl in concentration 1.3% w/w and ethanol in concentration 2% v/v	—
TYAS1 + RYR	**Test**	**Combined addition of NaCl in concentration 1.3% w/w and RYR in concentration 2% v/v**	**—**
TYAS2	Test	Addition of NaCl in concentration 2% w/w	—
TYAN1	Test	Addition of nitrite pickling salt in concentration 1.3% w/w	+–*
TYAN2	Test	Addition of nitrite pickling salt in concentration 2% w/w	—
TYA + $NaNO_2$	Test	Addition of alone $NaNO_2$ in concentration 300 mg/L	+++
TYA + $NaNO_3$	Test	Addition of alone $NaNO_2$ in concentration 300 mg/L	+++

*The experimental code correlates with the experimental design given in **Table 1**. All experiments were performed in triplicate, spore outgrowth observed in all 3 test tubes is marked as +++, no growth as —. *In case of dubious results, the cultivation test was repeated but if the result was the same, i.e., ++— or +— this means unreliable suppression of germination. The most significant results are highlighted.*

codes TYA + $NaNO_2$; TYA + $NaNO_3$; TYAN2 and TYAN1). As *Clostridium beijerinckii* is sensitive to high concentrations of NaCl (Branska et al., 2020), the independent effect of NaCl addition was also tested. While addition of NaCl to 2% w/w suppressed spore germination, 1.3% w/w did not reliably suppress germination in all cases (see **Table 3**, code TYAS2 and TYAS1).

Addition of 2% v/v RYR extract was tested with standard TYA medium and with medium containing 1.3% w/w NaCl; addition of ethanol to the same concentration (2% v/v) was tested as a control (**Table 3**, codes TYA + RYR, TYA + Et, TYAS1 + RYR, TYAS1 + Et). While addition of the RYR extract suppressed spore germination, ethanol did not. The RYR extract did not contain citrinin but, because it is known that

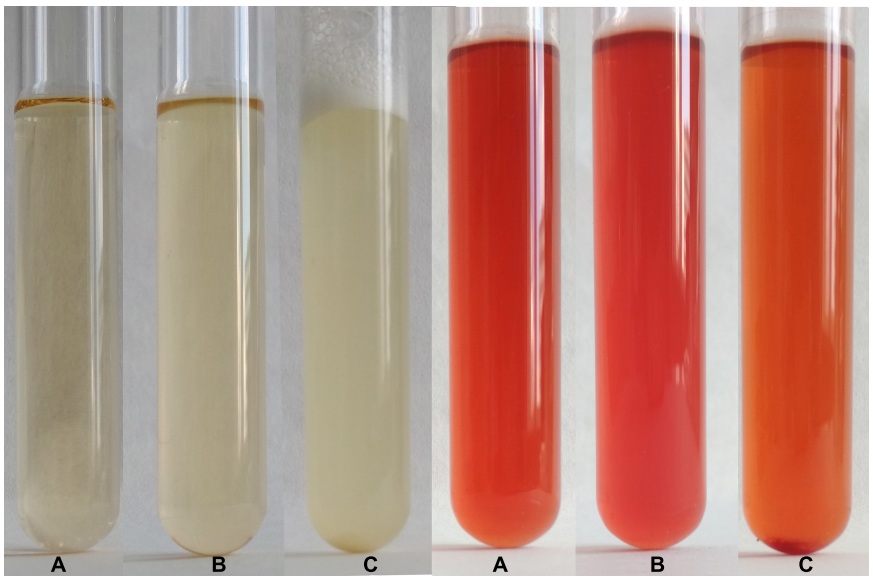

FIGURE 3 | Demonstration of growth in test tubes. Positive control, i.e., outgrowth of *C. beijerinckii* spores in TYA medium is shown on the left while suppression of spore germination after addition of RYR extract to 2% v/v is shown on the right. A test tube with medium was photographed **(A)** prior to inoculation, **(B)** after inoculation, and **(C)** after 48 h cultivation.

citrinin has certain antimicrobial properties, the citrinin effect was tested at a concentration of 2,000 μg/kg. This concentration of citrinin reflects the amount that was EU-permitted in an RYR food supplement until 2019, after which the limit was reconsidered and adjusted to 100 μg/kg. Citrinin was tested alone or in combination with RYR (**Table 3**, codes TYA + cit, TYA + RYR + cit).

Typical test tube growth characteristics of *C. beijerinckii* exhibiting high turbidity, foam and development of bubbles of fermentation gas (mixture of CO_2 and hydrogen) as well as color of the medium after addition of the RYR extract are shown in **Figure 3**. Only the ability to grow (indicated as + or −) was tested in the *C. beijerinckii* germination assay. Determination of optical density was not performed in order to not disturb the anaerobic atmosphere. Changed morphology from vegetative cells to spores influences OD values, so comparisons between tests might be misleading. Spores in TYA medium (positive control experiment) started to germinate 16–18 h after inoculation, and in other cases, germination started with different delays.

B. subtilis Germination

To follow the growth of spore formers after germination, *Bacillus subtilis* germination assays were performed, even if these spores do not normally occur in meat products (**Figure 4**). Nevertheless, *B. subtilis* spores are more resistant to adverse environmental effects in comparison with the *C. beijerinckii* spores, therefore the design of experiments had to be different (**Table 2**) in order to inhibit germination. Total suppression of spore germination was achieved only after addition of the RYR extract to 4% v/v in medium containing 1.3% w/w NaCl (**Figure 4D**, MPS1 + RYR2). In other cases, growth was always detected, even if, in some cases, germination was delayed by up to 10 h (**Figures 4B,C**, MP + RYR2; MP + RYR1 + Cit). Surprisingly, addition of nitrite pickling salt to the recommended 2% w/w did not inhibit germination of the spores (**Figure 4A**, MPN2).

RYR Extract Analysis

The absorption spectrum of the RYR extract is shown in **Figure 5**. Values of absorption found by spectrophotometric analysis at 390, 470, and 500 nm, corresponding to assumed absorption maxima of yellow, orange and red pigments, were 98, 58, and 70, respectively. Monascin (yellow), rubropunctatin (orange) and rubropunctamine (red) were identified in the RYR extract by UHPLC analysis (**Figure 6**), while their analogs with seven carbon side chains, i.e., ankaflavin (yellow), monascorubrin (orange) and monascorubramine (red) were not detected; neither was citrinin or monacolin K. The detected yellow pigments were quantified as monascin equivalents (1m220 mg/L), orange pigments as rubropunctatin equivalents (336 mg/L) and red pigments as rubropunctamine equivalents (408 mg/L). However, other compounds labeled as yellow I and red I-VI were found and for their putative identification, HPLC-MS analysis and already published m/z data on different *Monascus* metabolites were used (for survey of the *Monascus* pigments data see Chen et al., 2019). While red I-red VI are probably rubropunctamine derivatives that were formed by the reaction of rubropunctatin with available amino group containing compounds, yellow I was identified as monascuspiloin (m/z 360.4).

The RYR extract was added to TYA and MP medium to concentrations of 2 and 4% v/v, respectively, and the concentrations of pigments added to the medium are shown in **Table 4**. The water extract of the RYR had a pH 4.9 but the pH of TYA or MP medium was 6.8 or 7.0. To determine whether the pigment profile was the same as the original RYR extract in

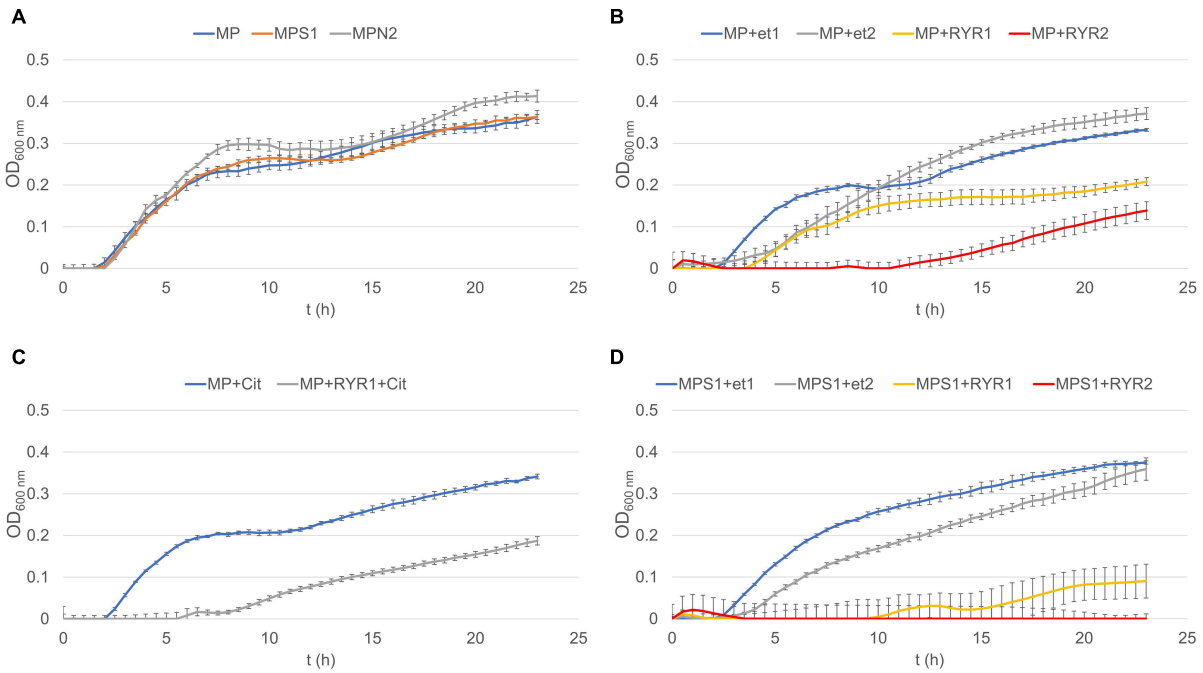

FIGURE 4 | Growth curves of *B. subtilis* using different compositions of culture medium (for the experiment design see **Table 2**). **(A)** Shows control experiment in MP medium and demonstrates the influence of NaCl to 1.3% w/w (MPS1) and pickling nitrite salt to 2.0% w/w (MPN2). **(B)** Shows the effect of ethanol at concentrations of 1.92 and 3.84% v/v to MP medium (MP + Et1, MP + Et2) and addition of RYR ethanol extract to 1.92 and 3.84% v/v (MP + RYR1, MP + RYR2). **(C)** Shows the citrinin effect independently (MP + cit) or in combination with RYR extract (MP + RYR1 + cit). **(D)** Shows the combined influence of NaCl (1.3% w/w) and ethanol (1.92 and 3.84% v/v); (MPS1 + Et1, MPS1 + Et2) or RYR ethanol extract (2 and 4% v/v); (MPS1 + RYR1, MPS1 + RYR2).

the culture medium, samples of medium containing RYR mixed in a 1:1 volume ratio were analyzed by UHPLC. As expected, rubropunctatin was absent in the samples while monascin and monascuspiloin remained (data not shown).

DISCUSSION

Nitrite and nitrate addition to meat products, together with NaCl, is traditional in European countries and is considered to be of low impact on human health even if cancerogenic nitrosamines can be formed in the acidic environment of the human stomach after ingestion of nitrite/nitrate containing food (Honikel, 2008; EFSA Panel on Food Additives Nutrient Sources added to Food [ANS] et al., 2017). It is believed that the benefits of stable red color, antioxidant and antimicrobial effects of nitrite/nitrate outweigh potential risks. Nevertheless, within this study it was found that addition of nitrite or nitrate alone, to the permitted concentration, did not suppress spore germination. Similar observations were documented in other studies for the germination of *Clostridium perfringens* (Labbe and Duncan, 1970), *Clostridium botulinum* (Sofos et al., 1979) or cheese associated clostridia including *C. beijerinckii* (Ávila et al., 2014) spores. However, combined effect of nitrite with NaCl tested after addition of the pickling salt both at the standard concentration of pickling salt (2% w/w) and at the level recommended for low salt products (1.3% w/w) was efficient in inhibiting the germination of *C. beijerinckii* spores but had no effect on germination of *B. subtilis* spores. However, total suppression of germination of *C. beijerinckii* spores was also achieved after addition of RYR extract to TYA medium, to a concentration of 2% v/v while total suppression of germination of *B. subtilis* spores was only achieved after addition of 4% v/v RYR extract to MP containing 1.3% w/w NaCl. These results suggest that the RYR extract might substitute for nitrite salts in inhibiting germination of *Clostridium* spores.

Within the study, the ethanol effect on bacterial spore germination was confirmed (Setlow et al., 2002) as well as the effect of NaCl (Nagler et al., 2014) and the synergistic effect of

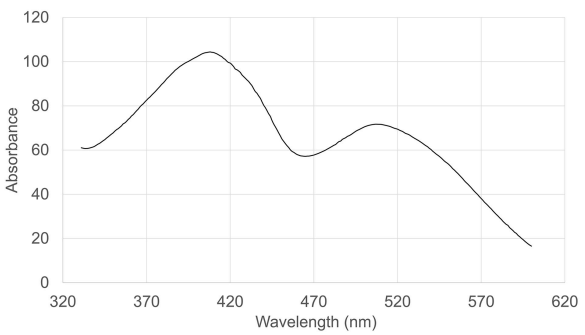

FIGURE 5 | Absorption spectrum of the RYR extract.

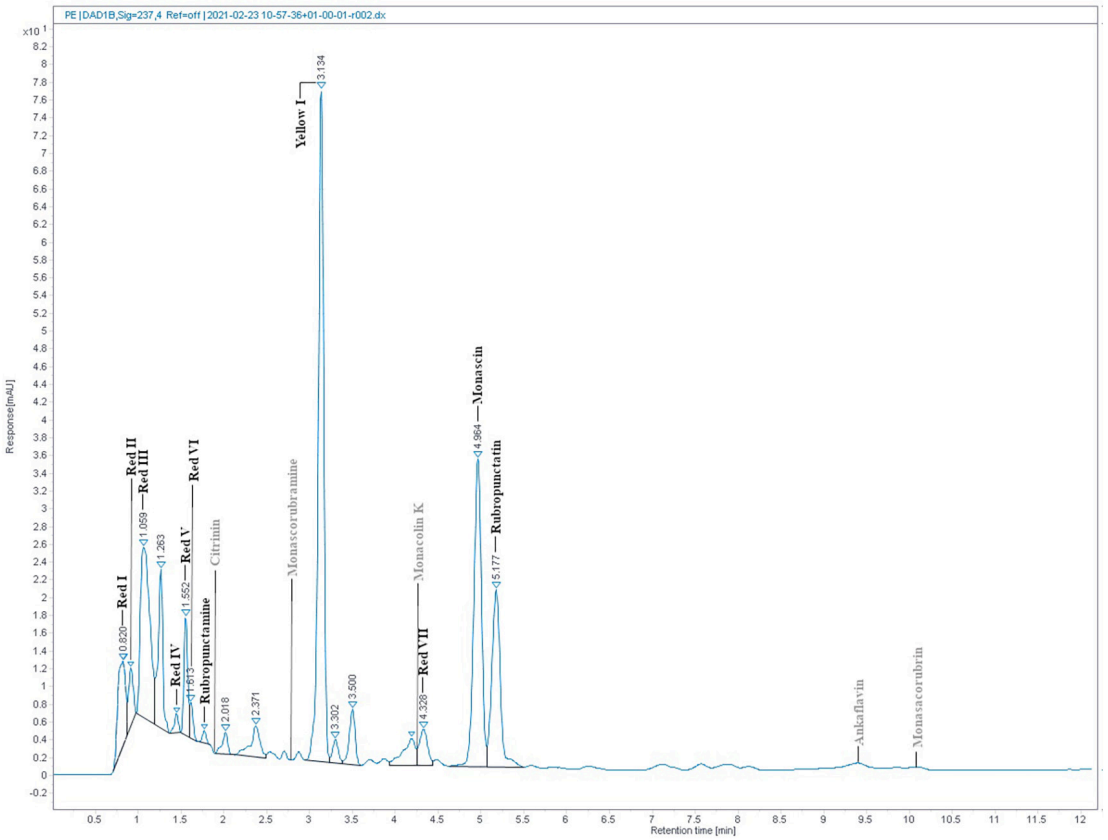

FIGURE 6 | RYR extract chromatogram from UHPLC analysis. Detected compounds are given in black while expected but undetected compounds are given in gray color. Conditions of UHPLC analysis are given in section "RYR Extract Analysis."

different agents (Nerandzic et al., 2015). Even if the RYR extract did not contain citrinin, its effect at 2,000 μg/L (the permitted concentration of citrinin in RYR food supplements in the EU until 2019) was tested, but if applied independently, had no effect on spore germination.

Monascus sp. DBM 4361, used for the preparation of RYR, was not classified on the species level but it might be *M. pilosus* because its characteristics, i.e., no citrinin production and formation of both conidia and ascospores, corresponds with an already described strain, *M. pilosus* MS-1, also isolated from the RYR (Feng et al., 2016). The absence of citrinin production was also found in *M. pilosus* NBRC4520 (Higa et al., 2020). In the RYR extract, there were found three of six iconic *Monascus* pigments; in particular monascin, rubropunctatin and rubropunctamine, together with rubropunctamine complexes with different amino group-containing compounds and monascuspiloin, a yellow pigment with a structure similar to monascin that has already been described as the metabolite of *M. pilosus* M93 (Chen et al., 2012). Interestingly, only monascin and rubropunctatin, i.e., pigments with a shorter five carbon side chain, but not their analogs (ankaflavin and monascorubrin with seven carbon side chains) were found. During the biosynthesis of pigments by *M. ruber* M7 (Chen et al., 2017), MrPigJ and MrPigK subunits of fatty acid synthase were found as the proteins responsible for the integration of β-ketooctanoic or β-ketodecanoic acid moieties into the structure of the pigments. However, the selection of the particular fatty acid moiety was considered to be random or not yet understood. Homologous genes to *MrPigJ*, *MrPigK* were described in *M. purpureus* (*MpFasA2, MpFasB2*) (Balakrishnan et al., 2013) and other *Monascus* strains (Guo et al., 2019) but not in *M. pilosus*. Even in the newest review of azaphilone

TABLE 4 | Concentration of pigments quantified as monascin, rubropunctatin, and rubropunctamine equivalents added to TYA and MP media.

Medium code*	Yellow pigments (concentration equivalent to Monascin in mg/L)	Orange pigments (concentration equivalent to Rubropunctatin in mg/L)	Red pigments (concentration equivalent to Rubropunctamine in mg/L)
TYA + RYR TYAS1 + RYR	24.4	6.7	8.2
MP + RYR1 MPS1 + RYR1	24.4	6.7	8.2
MP + RYR2 MPS1 + RYR2	48.8	13.4	16.4

Medium codes are the same as used in **Tables 1, 2.*

biosynthesis (Pavesi et al., 2021), factors that determine the selection of particular fatty acid moieties are not described.

For the detection of substances in *Monascus* extracts, it is not sufficient to use the absorption spectrum or to determine absorbance values of the extract at the absorption maxima of individual pigments, typically at 390, 470, and 500 nm. It is really necessary to analyze extracts by HPLC or other analytical method (cf. **Figures 5**, **6**). Notwithstanding, the determination of individual compounds in *Monascus* extracts is difficult because it depends *inter alia* on the pH of the extract (Shi et al., 2016).

After the addition of the RYR extract to medium, the original pH of the RYR extract changed from 4.9 to 6.8 or 7.0, resulting in the reaction of rubropunctatin with available amino group containing compounds, such as amino acids. It is possible that this reaction might contribute to the suppression of spore germination in the medium. Amino acids such as L-alanine or glycine are known germinants (factors stimulating germination) of bacterial spores (Setlow, 2014; Bhattacharjee et al., 2016) and if their amount was decreased it might affect germination. In addition, it was reported that *Monascus* red pigment derivatives had pronounced effects on the growth of Gram positive bacteria, including *B. subtilis* (Kim et al., 2006). The assumed cause of inhibition was adsorption of pigment derivatives onto the surface of cells, limiting oxygen uptake, where their MIC values were found to be 4–8 μg/L. In our assay, rubropunctatin and a mixture of red pigment derivatives, to concentrations of 13.4 mg/L and 16.4 mg/L, respectively, were added to MP culture medium used for outgrowth of *B. subtilis* spores (see **Table 4**) and *B. subtilis* was cultured under aerobic conditions; the above aerobic effect (Kim et al., 2006) might also apply here. Orange and red *Monascus* pigments, at concentrations of 10–20 mg/L, inhibited growth of Gram negative bacteria (Vendruscolo et al., 2014), which corresponds with our findings. Yellow pigments monascin and monascuspiloin, detected in the RYR, were found to have anticancerogenic effects (Akihisa et al., 2005; Chen et al., 2012; Chiu et al., 2012) but their antibacterial effect was never tested.

DATA AVAILABILITY STATEMENT

The raw data supporting the conclusions of this article will be made available by the authors, without undue reservation.

AUTHOR CONTRIBUTIONS

MH performed cultivation experiments, prepared samples for analyses, participated in analysis, performed data evaluation, and revised the manuscript. MP assisted with cultivation experiments, preparation of samples for analyses, participated in analysis, and revised the manuscript. BB developed the UHPLC method for the pigments analysis and revised the manuscript. PP conceived the study, designed and coordinated it, analyzed the data, and wrote the manuscript. All authors read and approved the final manuscript version.

FUNDING

Financial support from specific University of Chemistry and Technology in Prague research, Project No. MEYS No 8-SVV/2021.

REFERENCES

Akihisa, T., Tokuda, H., Ukiya, M., Kiyota, A., Yasukawa, K., Sakamoto, N., et al. (2005). Anti-tumor-initiating effects of monascin, an azaphilonoid pigment from the extract of *Monascus pilosus* fermented rice (red-mold rice). *Chem. Biodivers* 2, 1305–1309. doi: 10.1002/cbdv.200590101

EFSA Panel on Food Additives and Nutrient Sources added to Food [ANS], Younes, M., Aggett, P., Aguilar, F., Crebelli, R., Dusemund, B. (2018). Scientific opinion on the safety of monacolins in red yeast rice. *EFSA J.* 16:e05368.

Ávila, M., Gómez-Torres, N., Hernández, M., and Garde, S. (2014). Inhibitory activity of reuterin, nisin, lysozyme and nitrite against vegetative cells and spores of dairy-related *Clostridium* species. *Int. J. Food Microbiol.* 172, 70–75. doi: 10.1016/j.ijfoodmicro.2013.12.002

Balakrishnan, B., Karki, S., Chiu, S.-H., Kim, H.-J., Suh, J.-W., Nam, B., et al. (2013). Genetic localization and in vivo characterization of a *Monascus* azaphilone pigment biosynthetic gene cluster. *Appl. Microbiol. Biotechnol.* 97, 6337–6345. doi: 10.1007/s00253-013-4745-9

Bhattacharjee, D., McAllister, K. N., and Sorg, J. A. (2016). Germinants and their receptors in *Clostridia*. *J. Bacteriol.* 198, 2767–2775. doi: 10.1128/JB.00405-16

Bianchi, A. (2005). Extracts of *Monascusus purpureus* beyond statins —Profile of efficacy and safety of the use of extracts of *Monascus purpureus*. *Chin. J. Integr. Med.* 11, 309–313. doi: 10.1007/BF02835797

Branska, B., Fořtová, L., Dvořáková, M., Liu, H., Patakova, P., Zhang, J., et al. (2020). Chicken feather and wheat straw hydrolysate for direct utilization in biobutanol production. *Renewable Energy* 145, 1941–1948. doi: 10.1016/j.renene.2019.07.094

Branska, B., Pechacova, Z., Kolek, J., Vasylkivska, M., and Patakova, P. (2018). Flow cytometry analysis of *Clostridium beijerinckii* NRRL B-598 populations exhibiting different phenotypes induced by changes in cultivation conditions. *Biotechnol. Biofuels* 11:99. doi: 10.1186/s13068-018-1096-x

Chen, R.-J., Hung, C.-M., Chen, Y.-L., Wu, M.-D., Yuan, G.-F., and Wang, Y.-J. (2012). Monascuspiloin induces apoptosis and autophagic cell death in human prostate cancer cells via the Akt and AMPK signaling pathways. *J. Agric. Food. Chem.* 60, 7185–7193. doi: 10.1021/jf3016927

Chen, W., Chen, R., Liu, Q., He, Y., He, K., Ding, X., et al. (2017). Orange, red, yellow: biosynthesis of azaphilone pigments in *Monascus* fungi. *Chem. Sci.* 8, 4917–4925. doi: 10.1039/c7sc00475c

Chen, W., Feng, Y., Molnár, I., and Chen, F. (2019). Nature and nurture: confluence of pathway determinism with metabolic and chemical serendipity diversifies *Monascus* azaphilone pigments. *Nat. Product Rep.* 36, 561–572. doi: 10.1039/C8NP00060C

Chiu, H.-W., Fang, W.-H., Chen, Y.-L., Wu, M.-D., Yuan, G.-F., Ho, S.-Y., et al. (2012). Monascuspiloin enhances the radiation sensitivity of human prostate cancer cells by stimulating endoplasmic reticulum stress and inducing autophagy. *PLoS One* 7:e40462. doi: 10.1371/journal.pone.0040462

Commission Regulation (EU) 2019/1901, (2019). Commission Regulation (EU) 2019/1901 of 7 November 2019 Amending Regulation (EC) No 1881/2006 as Regards Maximum Levels of Citrinin in Food Supplements Based on Rice Fermented with Red Yeast Monascus Purpureus. Available online at: https://eur-lex.europa.eu/legal-content/EN/TXT/PDF/?uri=OJ:L:2019:293:FULL&from=EN

Commission Regulation (EU) No 432/2012, (2012). Commission Regulation (EU) No 432/2012 of 16May 2012 Establishing a List of Permitted Health ClaimsMade on Foods, Other Than Those Referring to the Reduction of Disease Risk and to Children's Development and Health. Available

online at: https://eur-lex.europa.eu/legal-content/EN/TXT/PDF/?uri=CELEX:32012R0432&from=CS

Cruz-Morales, P., Orellana, C. A., Moutafis, G., Moonen, G., Rincon, G., Nielsen, L. K., et al. (2019). Revisiting the evolution and taxonomy of *Clostridia*, a phylogenomic update. *Genome Biol. Evol.* 11, 2035–2044. doi: 10.1093/gbe/evz096

de Oliveira Filho, J. W. G., Islam, M. T., Ali, E. S., Uddin, S. J., Santos, J. V. D. O., de Alencar, M. V. O. B., et al. (2017). A comprehensive review on biological properties of citrinin. *Food Chem. Toxicol.* 110, 130–141. doi: 10.1016/j.fct.2017.10.002

EFSA Panel on Food Additives Nutrient Sources added to Food [ANS], Aguilar, F., Crebelli, R., Di Domenico, A., Dusemund, B., Frutos, M. J. (2017). Re-evaluation of potassium nitrite (E 249) and sodium nitrite (E 250) as food additives. *EFSA J* 15:e04786. doi: 10.2903/j.efsa.2017.4786

Fabre, C. E., Santerre, A. L., Loret, M. O., Baberian, R., Pareilleux, A., Goma, G., et al. (1993). Production and food applications of the red pigments of *Monascus ruber*. *J. Food Sci.* 58, 1099–1102. doi: 10.1111/j.1365-2621.1993.tb06123.x

Feng, Y., Chen, W., and Chen, F. (2016). A *Monascus pilosus* MS-1 strain with high-yield monacolin K but no citrinin. *Food Sci. Biotechnol.* 25, 1115–1122. doi: 10.1007/s10068-016-0179-3

Guo, X., Li, Y., Zhang, R., Yu, J., Ma, X., Chen, M., et al. (2019). Transcriptional regulation contributes more to *Monascus* pigments diversity in different strains than to DNA sequence variation. *World J. Microbiol. Biotechnol.* 35, 1–13. doi: 10.1007/s11274-019-2711-0

Higa, Y., Kim, Y.-S., Altaf-Ul-Amin, M., Huang, M., Ono, N., and Kanaya, S. (2020). Divergence of metabolites in three phylogenetically close *Monascus* species (*M. pilosus, M. ruber*, and *M. purpureus*) based on secondary metabolite biosynthetic gene clusters. *BMC Genomics* 21:679. doi: 10.1186/s12864-020-06864-9

Honikel, K.-O. (2008). The use and control of nitrate and nitrite for the processing of meat products. *Meat Sci.* 78, 68–76. doi: 10.1016/j.meatsci.2007.05.030

Kim, C., Jung, H., Kim, Y. O., and Shin, C. S. (2006). Antimicrobial activities of amino acid derivatives of monascus pigments. *FEMS Microbiol. Lett.* 264, 117–124. doi: 10.1111/j.1574-6968.2006.00451.x

Kolek, J., Branska, B., Drahokoupil, M., Patakova, P., and Melzoch, K. (2016). Evaluation of viability, metabolic activity and spore quantity in clostridial cultures during ABE fermentation. *FEMS Microbiol. Lett.* 363:fnw031. doi: 10.1093/femsle/fnw031

Labbe, R. G., and Duncan, C. L. (1970). Growth from spores of *Clostridium perfringens* in the presence of sodium nitrite. *Appl. Microbiol.* 19, 353–359.

Leistner, L., Fink-Gremmels, J., and Dresel, J. (1991). "*Monascus* extract–A possible alternative to nitrite in meats," in *Proceedings of 37th International Congress of Meat Science and Technology*, (Kulmbach: Federal Centre for Meat Research), 1252–1256.

Lotong, N., and Suwanarit, P. (1983). Production of soy sauce koji mold spore inoculum in plastic bags. *Appl. Environ. Microbiol.* 46, 1224–1226. doi: 10.1128/AEM.46.5.1224-1226.1983

Mohan Kumari, H. P., Akhilender Naidu, K., Vishwanatha, S., Narasimhamurthy, K., and Vijayalakshmi, G. (2009). Safety evaluation of *Monascus purpureus* red mould rice in albino rats. *Food Chem. Toxicol.* 47, 1739–1746. doi: 10.1016/j.fct.2009.04.038

Nagler, K., Setlow, P., Li, Y.-Q., and Moeller, R. (2014). High salinity alters the germination behavior of *Bacillus subtilis* spores with nutrient and nonnutrient germinants. *Appl. Environ. Microbiol.* 80, 1314–1321. doi: 10.1128/AEM.03293-13

Nerandzic, M. M., Sankar, C. T., Setlow, P., and Donskey, C. J. (2015). A cumulative spore killing approach: synergistic sporicidal activity of dilute peracetic acid and ethanol at low pH against *Clostridium difficile* and *Bacillus subtilis* spores. *Open Forum Infect. Dis.* 3:ofv206. doi: 10.1093/ofid/ofv206

Patrovsky, M., Sinovska, K., Branska, B., and Patakova, P. (2019). Effect of initial pH, different nitrogen sources, and cultivation time on the production of yellow or orange *Monascus purpureus* pigments and the mycotoxin citrinin. *Food Sci. Nutr.* 7, 3494–3500. doi: 10.1002/fsn3.1197

Pavesi, C., Flon, V., Mann, S., Leleu, S., Prado, S., and Franck, X. (2021). Biosynthesis of azaphilones: a review. *Nat. Prod. Rep.* doi: 10.1039/D0NP00080A

Seong, P. N., Ba, H. V., Kim, Y. S., Kang, S. M., Cho, S. H., Kim, J. H., et al. (2017). Effects of additions of *Monascus* and laccaic acid on the color and quality properties of nitrite-free emulsion sausage during refrigerated storage. *Korean J. Food Sci. Anim. Resour.* 37, 10–17. doi: 10.5851/kosfa.2017.37.1.10

Setlow, B., Loshon, C. A., Genest, P. C., Cowan, A. E., Setlow, C., and Setlow, P. (2002). Mechanisms of killing spores of *Bacillus subtilis* by acid, alkali and ethanol. *J. Appl. Microbiol.* 92, 362–375. doi: 10.1046/j.1365-2672.2002.01540.x

Setlow, P. (2014). Germination of spores of *Bacillus* species: what we know and do not know. *J. Bacteriol.* 196, 1297–1305. doi: 10.1128/JB.01455-13

Shi, K., Chen, G., Pistolozzi, M., Xia, F., and Wu, Z. (2016). Improved analysis of *Monascus* pigments based on their pH-sensitive UV-Vis absorption and reactivity properties. *Food Addit Contam. Part A* 33, 1396–1401. doi: 10.1080/19440049.2016.1214289

Sofos, J., Busta, F., and Allen, C. (1979). Sodium nitrite and sorbic acid effects on *Clostridium botulinum* spore germination and total microbial growth in chicken frankfurter emulsions during temperature abuse. *Appl. Environ. Microbiol.* 37, 1103–1109. doi: 10.1128/AEM.37.6.1103-1109.1979

Vendruscolo, F., Tosin, I., Giachini, A. J., Schmidell, W., and Ninow, J. L. (2014). Antimicrobial activity of *Monascus* pigments produced in submerged fermentation. *J. Food Process. Preserv.* 38, 1860–1865. doi: 10.1111/jfpp.12157

Yu, C.-C., Wang, J.-J., Lee, C.-L., Lee, S.-H., and Pan, T.-M. (2008). Safety and mutagenicity evaluation of nanoparticulate red mold rice. *J. Agric. Food Chem.* 56, 11038–11048. doi: 10.1021/jf801335u

Yu, X., Wu, H., and Zhang, J. (2015). Effect of *Monascus* as a nitrite substitute on color, lipid oxidation, and proteolysis of fermented meat mince. *Food Sci. Biotechnol.* 24, 575–581. doi: 10.1007/s10068-015-0075-2

Zhao, G.-P., Li, Y.-Q., Yang, J., and Cui, K.-Y. (2016). Antibacterial characteristics of orange pigment extracted from *Monascus* pigments against *Escherichia coli*. *Czech J. Food Sci.* 34, 197–203. doi: 10.17221/430/2015-CJFS

Zhu, B., Qi, F., Wu, J., Yin, G., Hua, J., Zhang, Q., et al. (2019). Red yeast rice: a systematic review of the traditional uses, chemistry, pharmacology, and quality control of an important chinese folk medicine. *Front. Pharmacol.* 10:1449. doi: 10.3389/fphar.2019.01449

Conflict of Interest: The authors declare that the research was conducted in the absence of any commercial or financial relationships that could be construed as a potential conflict of interest.

frontiers in Microbiology

REVIEW
published: 24 May 2021
doi: 10.3389/fmicb.2021.677603

Induction and Repression of Hydrolase Genes in *Aspergillus oryzae*

Mizuki Tanaka[1]* *and Katsuya Gomi*[2]*

[1]*Biomolecular Engineering Laboratory, School of Food and Nutritional Science, University of Shizuoka, Shizuoka, Japan,*
[2]*Laboratory of Fermentation Microbiology, Graduate School of Agricultural Science, Tohoku University, Sendai, Japan*

The filamentous fungus *Aspergillus oryzae*, also known as yellow *koji* mold, produces high levels of hydrolases such as amylolytic and proteolytic enzymes. This property of producing large amounts of hydrolases is one of the reasons why *A. oryzae* has been used in the production of traditional Japanese fermented foods and beverages. A wide variety of hydrolases produced by *A. oryzae* have been used in the food industry. The expression of hydrolase genes is induced by the presence of certain substrates, and various transcription factors that regulate such expression have been identified. In contrast, in the presence of glucose, the expression of the glycosyl hydrolase gene is generally repressed by carbon catabolite repression (CCR), which is mediated by the transcription factor CreA and ubiquitination/deubiquitination factors. In this review, we present the current knowledge on the regulation of hydrolase gene expression, including CCR, in *A. oryzae*.

Keywords: *Aspergillus oryzae*, hydrolase, carbon catabolite repression, transcription factor, ubiquitination, endocytosis

OPEN ACCESS

Edited by:
Kap-Hoon Han,
Woosuk University, South Korea

Reviewed by:
István Pócsi,
University of Debrecen, Hungary
Shuji Tani,
Osaka Prefecture University, Japan

***Correspondence:**
Mizuki Tanaka
mizuki.tanaka@u-shizuoka-ken.ac.jp
Katsuya Gomi
katsuya.gomi.a6@tohoku.ac.jp

Specialty section:
This article was submitted to Food Microbiology, a section of the journal Frontiers in Microbiology

Received: *08 March 2021*
Accepted: *26 April 2021*
Published: *24 May 2021*

Citation:
Tanaka M and Gomi K (2021) Induction and Repression of Hydrolase Genes in Aspergillus oryzae. Front. Microbiol. 12:677603. doi: 10.3389/fmicb.2021.677603

INTRODUCTION

The *koji* mold *Aspergillus oryzae* is a filamentous fungus that has been used for over a thousand years to manufacture Japanese fermented foods and beverages, such as shoyu (soy sauce), miso (soybean paste), and sake (rice wine) (Machida et al., 2008). The most industrially important characteristic of *A. oryzae* is the ability to produce large amounts of hydrolytic enzymes such as amylolytic and proteolytic enzymes. This is one of the reasons why *A. oryzae* has been used in the production of traditional Japanese fermented foods and beverages. Genome sequencing of *A. oryzae* has revealed that this fungus has more hydrolytic enzyme genes than other related filamentous fungi such as *Aspergillus nidulans* and *Aspergillus fumigatus* (Machida et al., 2005; Kobayashi et al., 2007). A wide variety of hydrolases produced by *A. oryzae* have been used in the food processing and pharmaceutical industries, in addition to the fermentation industry (Gomi, 2014). Moreover, promoters of hydrolytic enzyme genes, especially those of amylolytic genes, are widely used for high expression of homologous and heterologous genes in *A. oryzae*

to produce useful proteins and secondary metabolites (Tanaka and Gomi, 2014; Oikawa, 2020; Jin et al., 2021). Therefore, understanding the regulation of hydrolytic enzyme gene expression in *A. oryzae* is both scientifically and industrially important. The expression of most hydrolase genes is induced by the presence of certain substrates. For instance, it has long been known that amylolytic gene expression is induced by starch and malto-oligosaccharides (Tonomura et al., 1961; Yabuki et al., 1977). Such substrate-specific gene expression is often regulated by fungal-specific $Zn(II)_2Cys_6$-type transcription factors. Several transcription factors that control the expression of hydrolytic enzyme genes in *A. oryzae* have been identified (**Table 1**), and the regulatory mechanisms of their activation have recently been elucidated. On the other hand, in the presence of glucose, the expression of hydrolytic enzyme genes is strongly repressed even when inducing substrates are present. This phenomenon is known as carbon catabolite repression (CCR). CCR-regulating factors have been identified, and their function has been analyzed in the model filamentous fungus *A. nidulans*; however, details on the control mechanism of CCR remain unclear. Recent studies have revealed a part of the molecular mechanism of CCR regulation in *A. oryzae*.

In this review, we introduce transcription factors that induce the expression of hydrolytic enzyme genes in *A. oryzae*. In addition, we describe the molecular mechanism of CCR, which was revealed by recent studies on *A. oryzae* and other filamentous fungi.

TABLE 1 | Transcription factors involved in induction of hydrolytic gene expression in *Aspergillus oryzae*.

Transcription factor	DNA-binding motif	Major regulated genes
AmyR	$Zn(II)_2Cys_6$-type	Amylolytic genes (*amyA*, *amyB*, *amyC*, *glaA*, *glaB*, and *agdA*)
MalR	$Zn(II)_2Cys_6$-type	Maltose transporter gene (*malP*), maltase gene (*malT*)
FlbC	C_2H_2-type	Solid-state culture-specific expression genes (*glaB* and *pepA*), neutral protease gene (*nptB*)
XlnR	$Zn(II)_2Cys_6$-type	Xylolytic genes (*xynF1*, *xynG1*, *xynG2*, and *xylA*), cellulolytic genes (*celC*, *celD*, *cbhD*, and *bgl5*), pentose catabolic enzyme genes (*xyrA*, *ladA*, and *xdhA*), and putative xylose transporter genes
AraR	$Zn(II)_2Cys_6$-type	Pentose catabolic enzyme genes (*larA*, *xyrA*, *ladA*, and *xdhA*)
ManR	$Zn(II)_2Cys_6$-type	Mannanolytic genes (*manD*, *manG*, *mndB*, and *mndD*), cellulolytic genes (*celC*, *celD*, *cbhD*, and *bgl5*)
PrtR	$Zn(II)_2Cys_6$-type	Proteolytic genes (*alpA*, *pepA*, *nptA*, *nptB*, and *tppA*), di/tripeptide transporter genes (*potA*, *potB*)
FarA	$Zn(II)_2Cys_6$-type	Cutinase-like lipase gene (*cutL1*), hydrophobin genes (*rolA* and *hsbA*)

TRANSCRIPTION FACTORS THAT INDUCE GENE EXPRESSION OF HYDROLYTIC ENZYMES IN *A. ORYZAE*

AmyR and MalR

The regulation of amylolytic gene expression in *A. oryzae* has been studied for many years, because amylolytic enzymes are the major hydrolytic enzymes produced by *A. oryzae*, and are essential for sake production (Gomi, 2019). The expression of amylolytic genes is directly regulated by the transcription factor AmyR (Petersen et al., 1999; Gomi et al., 2000). This $Zn(II)_2Cys_6$-type transcription factor binds to the $CGGN_8(C/A)GG$ sequence in the promoter of amylolytic genes, such as the α-amylase (*amyA/B/C*), glucoamylase (*glaA* and *glaB*), and α-glucosidase (*agdA*) genes (Petersen et al., 1999; Ito et al., 2004). Expression of these genes is induced by maltose and isomaltose, and also by glucose when CCR is released (Suzuki et al., 2015). The *amyR* gene is constitutively expressed regardless of the presence of inducing or non-inducing sugars, and under conditions where amylolytic genes are not expressed; AmyR is localized in the cytoplasm (Suzuki et al., 2015). AmyR is rapidly transferred into the nucleus when isomaltose is added to the medium (Suzuki et al., 2015). Glucose and maltose also induce nuclear transfer of AmyR, but these sugars require higher concentrations and longer time periods than isomaltose to induce AmyR nuclear transfer and amylolytic gene expression (Suzuki et al., 2015). This dynamic of AmyR nuclear transfer is similar to that in the model filamentous fungus *A. nidulans* (Murakoshi et al., 2012). The nuclear transfer of AmyR depends on nuclear localization signals located within its DNA-binding domain (Suzuki et al., 2015). In contrast, C-terminal truncated AmyR is constitutively localized in the nucleus in both *A. nidulans* and *A. oryzae* (Makita et al., 2009; Suzuki et al., 2015). This suggests that the C-terminal region of AmyR is required to keep AmyR in the cytoplasm. C-terminal truncated *A. nidulans* AmyR retains its transcriptional activation function (Makita et al., 2009), but C-terminal truncation of *A. oryzae* AmyR leads to the loss of such function (Suzuki et al., 2015). This suggests that the function of the C-terminal region of AmyR differs among *Aspergillus* species. Therefore, the function of the C-terminal region of AmyR in other *Aspergillus* species that produce large amounts of amylolytic enzymes, such as *Aspergillus niger* and *Aspergillus luchuensis*, should be investigated.

In *A. nidulans*, maltose utilization is dependent on AmyR (Tani et al., 2001). However, a disruption mutant of *A. oryzae amyR* was able to assimilate maltose because maltose utilization in *A. oryzae* is regulated by another $Zn(II)_2Cys_6$-type transcription factor, MalR (Hasegawa et al., 2010). MalR is a homolog of

the yeast *MAL* activator, a transcriptional activator of genes encoding maltose transporter and maltase (Needleman, 1991). In contrast to AmyR, MalR is constitutively localized in the nucleus (Suzuki et al., 2015). Similar to the yeast *MAL* activator gene, *malR* comprises a gene cluster with the maltase gene (*malT*) and maltose transporter gene (*malP*), and the expression of both these genes is regulated by MalR (Hasegawa et al., 2010). The expression of *malP* and *malT* is not induced by the addition of isomaltose, but is preceded by amylolytic gene expression upon the addition of maltose (Suzuki et al., 2015). Therefore, MalR is activated prior to AmyR to convert maltose into a physiologically active inducing substrate for AmyR, i.e., isomaltose. This conversion of maltose to isomaltose is probably caused by the glycosyltransferase activity of MalT. In budding yeast, activation of the *MAL* activator is regulated by the dissociation of its chaperone proteins Hsp70 and Hsp90 (Ran et al., 2008). Although *A. oryzae* MalR interacts with orthologs of Hsp70 and Hsp90 (Konno et al., 2018), details on the activation mechanism and binding sequence are not known.

Importantly, the α-amylase (*amyB*) gene promoter is commonly used for high-level expression of heterologous genes in *A. oryzae* (Jin et al., 2021). Improved promoters *PglaA142* (Minetoki et al., 2003) and *PenoA142* (Tsuboi et al., 2005), have been constructed by tandem insertion of AmyR-binding sequences (Region III) within the glucoamylase and enolase gene promoters. These improved promoters are now utilized in homologous and heterologous protein production.

FlbC

Aspergillus oryzae has two glucoamylase genes, *glaA* and *glaB*, the expression patterns of which are quite different (Hata et al., 1991, 1998). Similar to other amylolytic enzymes, GlaA is produced in both submerged and solid-state cultures (Oda et al., 2006). On the other hand, GlaB is secreted exclusively in solid-state culture and is not produced in submerged culture. Although the expression of both *glaA* and *glaB* is regulated by AmyR (Watanabe et al., 2011), a transcription factor that binds to the promoter region of *glaB* and regulates the expression of specific genes in solid-state culture was expected to be present (Ishida et al., 2000; Hisada et al., 2013). A screening of the *A. oryzae* disruption mutant library for transcriptional regulators indicated that FlbC is a transcription factor that regulates the expression of *glaB* (Tanaka et al., 2016). In addition to that of *glaB*, the expression level of *pepA*, an aspartic protease gene that is predominantly expressed in solid-state culture, was also significantly reduced by *flbC* disruption (Tanaka et al., 2016). Therefore, FlbC is presumed to be a transcription factor that regulates the specific expression of hydrolytic enzyme genes in solid-state culture. The expression of the neutral protease gene (*nptB*) is also regulated by FlbC (Tanaka et al., 2016). FlbC is a C_2H_2-type transcription factor that was originally identified as one of the regulators of conidiospore development (Wieser et al., 1994; Kwon et al., 2010; Ogawa et al., 2010). Disruption of other transcription factors that control conidiospore development has no effect on the production of GlaB, suggesting that FlbC regulates *glaB* expression independently of the regulatory mechanism of conidiospore development (Tanaka et al., 2016). Moreover, FlbC probably binds directly to the promoter region of *glaB* and regulates its expression (Gomi, 2019). Although the FlbC-binding sequence has not been empirically identified, the sequence containing GATC would be a candidate based on recent studies of the FlbC orthologs of *Neurospora crassa* (Boni et al., 2018) and *Magnaporthe oryzae* (Matheis et al., 2017). Furthermore, the regulatory mechanism of specific gene expression in solid-state culture should be elucidated. Expression from the *glaB* promoter is induced by low water activity, high temperature, and physical barriers to hyphal extension (Ishida et al., 1998). Since these inducing factors cause environmental stress in *A. oryzae* cells, the involvement of stress response pathways, including that of mitogen-activated protein kinase (MAPK) signaling pathways, in FlbC activation should be considered.

XlnR and AraR

XlnR is a $Zn(II)_2Cys_6$-type transcription factor that regulates the expression of xylanolytic and cellulolytic genes (Marui et al., 2002). This transcription factor is also involved in the regulation of putative xylose transporter genes and pentose metabolic enzyme genes (Noguchi et al., 2009). In *Aspergillus* species, the expression of pentose catabolic pathway genes is also regulated by AraR, a paralog of XlnR (Battaglia et al., 2011). Electrophoretic mobility shift assays revealed that XlnR and AraR bind competitively to the CGGNTAAW sequence in the promoter region of pentose catabolic genes such as the xylose dehydrogenase-encoding gene (*xdhA*) (Ishikawa et al., 2018). Notably, XlnR binds to the CGGNTAAW sequence solely found in the promoter region of pentose catabolic genes as a monomer, whereas it binds to the TTAGSCTAA and TAGSCTA sequences in the promoter region of the xylanase genes (*xynF1* and *xynG2*) as a dimer (Ishikawa et al., 2018).

XlnR is constitutively located in the nucleus, similar to MalR. When xylose is added, XlnR is rapidly phosphorylated. In contrast, XlnR is rapidly dephosphorylated when xylose is removed from the culture medium (Noguchi et al., 2011). This reversible phosphorylation probably regulates the activation of XlnR. Identification of the phosphorylation site of XlnR is important for elucidating the activation mechanism of this transcription factor.

ManR

ManR is a $Zn(II)_2Cys_6$-type transcription factor that regulates the expression of mannanolytic enzyme genes. This transcription factor was identified by screening for mutants exhibiting reduced β-mannanase activity from a gene disruptant library of transcriptional regulators (Ogawa et al., 2012). ManR also regulates cellulolytic enzyme genes, such as the cellobiohydrolase, endoglucanase, and β-glucosidase genes (Ogawa et al., 2013). Most of these genes are also regulated by XlnR. Therefore, ManR and XlnR probably regulate the expression of these genes in a coordinated manner (Tani et al., 2014). ManR is an ortholog of *N. crassa* CLR-2 and *A. nidulans* ClrB, both of which regulate the expression of cellulase genes. However, the physiological roles of these transcription factors are slightly different (Kunitake and Kobayashi, 2017). ManR binds to the

promoter regions of the β-mannanase gene (*manG*), which contains the CAGAAT sequence that is conserved in the promoter regions of mannanolytic enzyme genes (Ogawa et al., 2012). However, this conserved sequence is quite different from consensus sequences for the binding of CLR-2 and ClrB (Kunitake and Kobayashi, 2017).

PrtR

PrtR is a $Zn(II)_2Cys_6$-type transcription factor; the deletion of this transcription factor results in a significant decrease in extracellular protease activity (Mizutani et al., 2008), indicating that it is essential for extracellular proteolytic gene expression. Interestingly, the *prtR* gene is located adjacent to the amylolytic gene cluster consisting of *amyR*, *agdA*, and *amyA* (Gomi, 2019). Orthologs of PrtR in other *Aspergillus* species are named PrtT (Punt et al., 2008). Duplication or triplication of the chromosomal region containing the *prtR* gene by forced translocation of the 1.4 Mb chromosome 2 resulted in a significant increase in alkaline protease and acid carboxypeptidase activity in a solid-state culture of *A. oryzae* (Takahashi et al., 2018). Over 20 proteolytic genes were upregulated in the duplicated strain. Furthermore, the expression level of an alkaline protease gene (*alpA*) increased more than 5-fold when *prtR* was highly expressed from the promoter of the α-amylase gene (Takahashi et al., 2018). In addition, the expression levels of two of the three di/tripeptide transporter genes (*potA* and *potB*) also increased upon *prtR* overexpression and decreased upon *prtR* disruption (Tanaka et al., 2021). These results suggest that PrtR plays a central role in the regulation of gene expression for the acquisition of nutrients in the presence of protein. In fact, a disruption mutant of *prtR* showed poor growth in solid-state culture using wheat bran as a substrate. In *A. niger* and *A. fumigatus*, PrtT regulates the expression of multiple protease genes and tri/tetrapeptide transporter genes (Sharon et al., 2009; Hartmann et al., 2011; Huang et al., 2020); PrtT orthologs are absent in *A. nidulans* (Punt et al., 2008). Although the expression of proteolytic genes is induced by proteins or peptides, the direct substrate that induces the activation of PrtR/PrtT is not clear for any *Aspergillus* species; hence, further studies are required to ascertain this. Disruption of multiple protease genes has resulted in highly effective heterologous protein production in *A. oryzae* (Jin et al., 2021). Considering that many extracellular protease genes are thought to be regulated by PrtR, the effect of *prtR* disruption on heterologous protein production is strongly expected.

FarA

Aspergillus oryzae can degrade polyester poly(butylene succinate-*co*-adipate) (PBSA), a biodegradable plastic. The cutinase-like lipase CutL1 is the major enzyme that degrades PBSA in *A. oryzae*, and two hydrophobic surface binding proteins (RolA and HsbA) assist in the binding of CutL1 to PBSA (Maeda et al., 2005; Takahashi et al., 2005; Ohtaki et al., 2006). FarA is a $Zn(II)_2Cys_6$-type transcription factor that regulates the expression of fatty acid metabolism genes in *A. nidulans*; its ortholog, CTF1α of *Fusarium solani*, regulates cutinase gene expression (Li and Kolattukudy, 1997; Hynes et al., 2006). The expression of the *cutL1* gene is regulated by FarA, and a disruption mutant of *farA* abolished PBSA degradation activity in *A. oryzae* (Garrido et al., 2012). In addition to that of the *cutL1* gene, the expression of *rolA* and *hsbA* is also repressed by the disruption of *farA* (Garrido et al., 2012). Although details on the mechanism of FarA regulation of the cutinase gene are unknown for all *Aspergillus* species, a recent study on *A. nidulans* showed that FarA-dependent expression of the cutinase genes is affected by CCR (Bermúdez-García et al., 2019).

CARBON CATABOLITE REPRESSION OF HYDROLYTIC ENZYME GENES

Regulating Factors of CCR

The study of CCR in filamentous fungi began with the identification of regulatory factors in *A. nidulans*. Four factors involved in the regulation of CCR in filamentous fungi were identified in the 1970s by genetic analysis of *A. nidulans* (Arst and Cove, 1973; Hynes and Kelly, 1977; Kelly and Hynes, 1977). These four factors were denoted as CreA, CreB, CreC, and CreD. Firstly, the *creA* gene was identified in an *A. nidulans* CCR-deficient mutant. This gene encodes a C_2H_2-type transcription factor that directly regulates CCR (Dowzer and Kelly, 1991). Similar to *A. nidulans* CreA, *A. oryzae* CreA binds to the SYGGRG sequence in the promoter region of the α-amylase gene (Kato et al., 1996). The amino acid sequence of the CreA DNA-binding domain is highly homologous to that of Mig1, a CCR-regulating transcription factor in the budding yeast *Saccharomyces cerevisiae*. However, the homology between CreA and Mig1 in the regions other than the DNA-binding domain is not high. In addition, recent studies have revealed that the functional control mechanisms of Mig1 and CreA are quite different (see Nuclear export-dependent degradation of CreA).

Similar to *creA* (described above), *creB* and *creC* were identified in CCR-deficient mutants as well. CreB is a deubiquitinating enzyme homolog with a particularly high homology to Ubp9 of the fission yeast *Schizosaccharomyces pombe* (Lockington and Kelly, 2001). Many deubiquitinating enzymes interact with WD40-repeat proteins that regulate the activity and function of such enzymes (Villamil et al., 2013). The *creC* gene encodes a WD40-repeat protein that shows high homology to fission yeast Bun62 (Lockington and Kelly, 2002) but has no counterpart in budding yeast. In *A. nidulans*, CreB and CreC form complexes *in vivo* (Lockington and Kelly, 2002). In fission yeast, Ubp9 interacts with Bun62 and another WD40-repeat protein, Bun107, and is involved in endocytosis, actin dynamics, and cell polarity (Kouranti et al., 2010). However, the function of the CreB and CreC complex in filamentous fungi has not been clarified.

The gene responsible for suppressing the phenotype of *creB* and *creC* mutants was identified and named *creD* (Kelly and Hynes, 1977). CreD contains two arrestin domains and three or four PxY motifs that are involved in protein-protein interactions (Boase and Kelly, 2004). There is a high homology

between CreD and yeast Rod1/Art4, an arrestin-related trafficking adaptor (ART) protein that acts as an adaptor for ubiquitin ligase and its target protein. In budding yeast, ART proteins recruit the HECT E3 ubiquitin ligase Rsp5 to cell membrane proteins (Lin et al., 2008; Nikko and Pelham, 2009). *Aspergillus oryzae* CreD also physically interacts with HulA, an ortholog of yeast Rsp5 (Tanaka et al., 2017). CreD and HulA are involved in the degradation of the maltose transporter MalP in *A. oryzae* (see Glucose-induced endocytosis of maltose transporter).

Based on the putative function of CreB and CreD, a model was proposed wherein CCR is regulated by the stabilization and degradation of CreA protein mediated by these factors (Lockington and Kelly, 2002; Boase and Kelly, 2004). However, this hypothesis was not supported by several recent studies (see Nuclear export-dependent degradation of CreA).

Improved Production of Hydrolytic Enzymes by Disruption and Mutation of CCR Regulators

The release of CCR is highly effective in improving hydrolytic enzyme production in filamentous fungi. For instance, disruption and mutation of the *creA* ortholog in *Trichoderma reesei* significantly increase the production of cellulase (Nakari-Setälä et al., 2009). α-Amylase production in *A. oryzae* also increases upon the disruption of *creA* (Ichinose et al., 2014). Disruption of *creB* also increases the production of α-amylase in *A. oryzae* (Hunter et al., 2013; Ichinose et al., 2014). Moreover, double disruption of *creA* and *creB* further increases amylase production, which is more than 10 times higher than that in the wild-type strain (Ichinose et al., 2014). The transcript level of the α-amylase gene markedly increased in the *creA* disruption strain, whereas it only slightly increased upon *creB* disruption (Ichinose et al., 2014). This suggests that the destruction of *creA* and *creB* has different effects on α-amylase production. In addition to those of α-amylase, the production levels of xylanase and β-glucosidase significantly increased upon the double disruption of *creA* and *creB* (Ichinose et al., 2018). In contrast, *creA* and *creB* disruption had no effect on cellulase (endo-β-glucanase) production. In *A. nidulans*, *creA* disruption did not result in de-repression of cellulose production; it was de-repressed by the disruption of protein kinase A gene (*pkaA*) (Kunitake et al., 2019), suggesting that CreA is not relevant to CCR regulation of cellulase production in *A. oryzae*.

In *A. oryzae* CreD, two serine residues at positions 402 and 515 were identified as phosphorylation sites (Tanaka et al., 2017). Mutation of these phosphorylation sites to glutamic acid for the phosphorylation mimic repressed the amylolytic enzyme production of the *creB* disruption mutant in the presence of glucose (Tanaka et al., 2017). In contrast, dephosphorylation mutations of CreD promoted CCR release by *creB* disruption and increased the production levels of α-amylase (Tanaka et al., 2017). This finding provides a novel approach, the combination of the dephosphorylation mutation of CreD and *creB* disruption, to improve the production of secretory glycoside hydrolases in filamentous fungi. In addition, these results suggest that CreB targets unknown factor(s) that are recognized by dephosphorylated CreD for ubiquitination. However, CreA is unlikely to be a target factor for CreB and CreD (see Nuclear export-dependent degradation of CreA).

Nuclear Export-Dependent Degradation of CreA

In budding yeast, Mig1 shuttles between the nucleus and cytoplasm in response to the glucose concentration. When green fluorescent protein (GFP) is fused to CreA in *A. oryzae*, almost all GFP fluorescence is observed in the nucleus in the presence of CCR-inducing sugars such as glucose and mannose. However, when sugars such as maltose and xylose, which induce the expression of glycosyl hydrolase genes, are used as carbon sources, CreA is exported to the cytoplasm. This nuclear export depends on a leucine-rich nuclear export signal (NES) near the C-terminus of CreA. CreA with a 3 × FLAG tag fused to its N-terminus is rapidly degraded when maltose or xylose is used as a carbon source. However, mutations in the NES significantly inhibit the degradation of CreA (Tanaka et al., 2018). These results indicate that CreA is rapidly degraded in the cytoplasm after export from the nucleus under conditions that induce the production of secretory hydrolytic enzymes. The deletion of a 20 amino acid region near the C-terminus significantly stabilizes CreA (Tanaka et al., 2018). This 20 amino acid region is highly conserved in the CreA orthologs of other filamentous fungi.

In *A. oryzae*, disruption of *creB* and *creC* significantly reduces the amount of CreA in the presence of glucose (Tanaka et al., 2018). Similarly, CreA-GFP protein levels also reduced in an *A. nidulans creC* mutant strain (Ries et al., 2016). In addition, *creA* transcript levels reduced in the presence of glucose in an *A. nidulans creB* mutant strain (Strauss et al., 1999). This reduced CreA protein level may have contributed to the release of CCR by the disruption of *creB* or *creC*. However, as mentioned above, the increase in transcript levels of the α-amylase gene by disruption of *creB* was slight, and double disruption of *creA* and *creB* resulted in a significant increase in α-amylase production (Ichinose et al., 2014), suggesting that the main reason for CCR release due to *creB* disruption is independent of the decrease in CreA abundance. In addition, CreA stability was not significantly affected by the disruption of *creD* (Tanaka et al., 2018). Therefore, there are likely to be other factor(s) involved in the regulation of CreA-independent CCR, the stability of which is controlled by CreB and CreD. Identification of such CreB and CreD target factors would lead to an understanding of CCR regulation in filamentous fungi.

In *A. nidulans*, the amount of CreA-GFP protein under repressing conditions significantly increased upon the deletion of *fbx23*, an F-box protein that constitutes the Skp-Cullin-F-box (SCF) ubiquitin ligase complex (de Assis et al., 2018). Therefore, CreA is possibly degraded in an SCF ubiquitin ligase complex-dependent manner in filamentous fungi. However, there is no direct experimental evidence for CreA ubiquitination, although the polyubiquitin precursor Ubi4 was identified as an interacting partner for both CreA and Fbx23 (de Assis et al., 2018). Further investigation of CreA degradation is required for a better understanding of the CCR regulation mechanism in filamentous fungi.

In budding yeast, Mig1 is phosphorylated by the cyclic AMP (cAMP) kinase Snf1 under low-glucose conditions, and exported from the nucleus to the cytoplasm (DeVit and Johnston, 1999). However, the subcellular localization and stability of *A. oryzae* CreA are not affected by disruption of the *SNF1* ortholog (Tanaka et al., 2018). This indicates that the regulatory mechanisms for the subcellular localization of yeast Mig1 and *A. oryzae* CreA are different. In agreement with this, the purified recombinant protein of a *T. reesei* Snf1 ortholog phosphorylates yeast Mig1 but not *T. reesei* Cre1, an ortholog of CreA (Cziferszky et al., 2003). In budding yeast, hexokinase Hxk2 is also phosphorylated by Snf1 and is involved in the regulation of Mig1 nuclear export (Ahuatzi et al., 2007). *Aspergillus* species have two functional glucose kinases, hexokinase HxkA and glucokinase GlkA (Fleck and Brock, 2010). It would be interesting to investigate the involvement of these glucose kinases in the nuclear export and degradation of CreA in *A. oryzae*.

Several recent studies have examined the phosphorylation of CreA in *A. nidulans*. Six serine residues (S262, S277, S288, S289, S312, and S319) in *A. nidulans* CreA were identified as phosphorylation sites by LC-MS analysis, and three of them (S289, S312, and S319) were phosphorylated only under conditions of growth in a glucose medium (Alam et al., 2017). Another recent study revealed six additional phosphorylation sites in *A. nidulans* CreA (S176, S268, S281, S284, T308, and S406; de Assis et al., 2021). The replacement of T308 with alanine significantly inhibited the nuclear accumulation of CreA-GFP. In contrast, the replacement of S262 or S268 with alanine increased the nuclear localization of CreA-GFP under de-repressing conditions, although these CreA-GFP mutants were not detectable by western blotting under such conditions (de Assis et al., 2021). Phosphorylation at S319 is lost upon the deletion of *pkaA*, which encodes a cAMP-dependent protein kinase, whereas CreA is not a direct target of this protein kinase (Ribeiro et al., 2019). Although the replacement of S319 with alanine has no significant effect on CreA subcellular localization, this mutation and the T308A mutation significantly increased CreA-GFP protein levels under repressing conditions (de Assis et al., 2021). However, none of the substitutions of these phosphorylation sites with alanine had a significant effect on CreA degradation under de-repressing conditions (de Assis et al., 2021). A recent study showed that replacement of S388 at the *T. reesei* Cre1 C-terminus with valine releases CCR (Han et al., 2020). This serine residue is conserved in the *Aspergillus* CreA proteins. However, deletion of 20 amino acids in the C-terminus, including this conserved serine residue, has no effect on the stability of *A. oryzae* CreA (Tanaka et al., 2018).

Identification of the protein kinase that phosphorylates CreA is an important issue that remains to be addressed. In *T. reesei*, S241 within Cre1 (corresponding to S262 in *A. nidulans* CreA) has been identified as a phosphorylation site, and the phosphorylation of this serine residue positively regulates DNA binding (Cziferszky et al., 2002). In addition, casein kinase II is a strong candidate kinase that phosphorylates Cre1 (Cziferszky et al., 2002). In *A. nidulans*, casein kinase CkiA has been identified as an interacting partner of Fbx23 (de Assis et al., 2018). Therefore, it is important to elucidate the role of casein kinase in the regulation of CreA function.

Glucose-Induced Endocytosis of Maltose Transporter

The amount of membrane proteins, including transporters involved in nutrient uptake, is tightly controlled. When the extracellular environment changes, unnecessary membrane proteins are internalized into the cell by endocytosis and transported to the vacuole for degradation (Polo and Di Fiore, 2008). This endocytosis is caused by ubiquitination of cell membrane proteins. MalP is the major maltose transporter required for amylolytic enzyme production in *A. oryzae* (Hasegawa et al., 2010; Hiramoto et al., 2015). When glucose is added, MalP is translocated from the cell membrane to the vacuole *via* endocytosis (Hiramoto et al., 2015). The addition of mannose, which induces the CCR of amylolytic genes, as well as glucose, also induces MalP endocytosis (Hiramoto et al., 2015). These results suggest that MalP is degraded to inhibit the uptake of maltose, which induces the expression of amylolytic genes. CreD and HulA are essential for this glucose-induced endocytosis of MalP (Tanaka et al., 2017). Therefore, in the presence of glucose, CreD probably induces endocytosis by recruiting HulA to MalP. Although CreD is rapidly dephosphorylated upon the addition of glucose, the phosphorylation state of CreD is not associated with the interaction with HulA and the endocytosis of MalP (Tanaka et al., 2017). The regulatory mechanism by which CreD induces glucose-specific MalP ubiquitination is unknown. In budding yeast, ART proteins, including Rod1/Art4, are also ubiquitinated by Rsp5. This ubiquitination is required for adaptor activation or degradation (Ho et al., 2017; MacDonald et al., 2020). It is important to examine whether CreD is ubiquitinated in *A. oryzae*.

The inhibition of glucose-induced endocytosis is expected to enhance substrate uptake. In fact, cellobiose consumption and ethanol production were enhanced by stabilizing heterologously expressed cellobiose transporters in budding yeast lacking four ARTs, including Rod1/Art4 (Sen et al., 2016). However, disruption of *creD* in *A. oryzae* counteracts the release of CCR by *creB* disruption and reduces α-amylase production (Tanaka et al., 2017). Therefore, stabilizing MalP without *creD* disruption, e.g., by introducing mutations in the ubiquitination sites of MalP, is necessary to increase amylase production.

DISCUSSION

As mentioned above, details on the regulatory mechanism of the induction and repression of hydrolytic gene expression in *A. oryzae* are becoming clearer, particularly for amylolytic genes (**Figure 1**). The release of CCR is significantly effective in improving the productivity of hydrolytic enzymes. In addition, constitutive activation of transcription factors leads to a reduction in the cost of producing hydrolytic enzymes (Alazi and Ram, 2018). However, the molecular mechanism of transcriptional regulation of hydrolytic enzyme genes in *A. oryzae* has not been

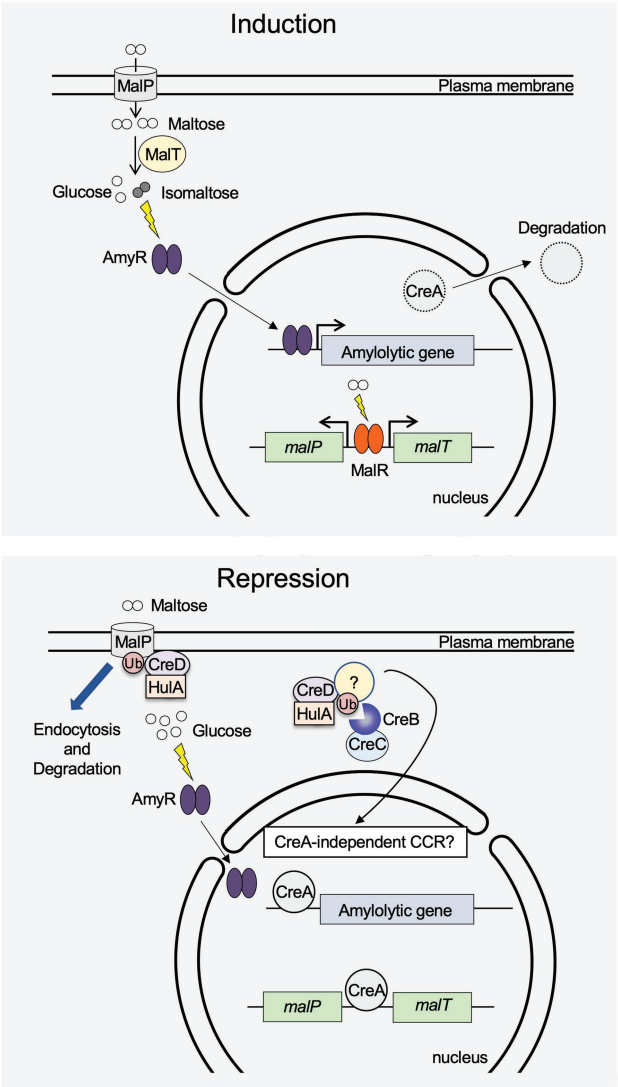

FIGURE 1 | Schematic model for induction and repression of amylolytic gene expression in *A. oryzae*. When maltose is added to the culture medium, MalR induces *malP* and *malT* expression. After the uptake of maltose into the cell by MalP, AmyR nuclear transfer is triggered by isomaltose, which is presumably generated by the glycosyltransferase activity of MalT. CreA is exported from the nucleus to the cytoplasm, where it is degraded, and amylolytic gene expression is induced by activated AmyR. In the presence of glucose, the expression of *malP* and *malT* is repressed by CreA. Moreover, MalP protein is brought into the cell by endocytosis mediated by HulA and CreD, and is degraded at the vacuole. Although a high concentration of glucose induces AmyR nuclear transfer, expression of amylolytic genes is strongly repressed by CreA. The unknown protein stabilized by the CreB-CreC complex presumably regulates CreA-independent carbon catabolite repression (CCR).

elucidated, even for amylolytic genes. For example, *glaB* gene expression in solid-state culture requires at least AmyR and FlbC, but another unidentified transcription factor(s) seems to be needed because promoter deletion analysis shows that a GC-rich sequence is important for *glaB* expression (Ishida et al., 2000; Hisada et al., 2013). The AmyR-binding sequence and putative FlbC-binding sequence are different from this GC-rich sequence, to which a certain transcription factor may bind. Moreover, because recent studies have revealed that the regulatory mechanism of hydrolytic gene expression differs among *Aspergillus* species; further research on the regulatory mechanism of hydrolytic gene expression in *A. oryzae* should be accelerated.

Autolysis of the *A. oryzae* mycelium is important for its production of volatile compounds that contribute to soy sauce flavor (Xu et al., 2016). Cell wall degrading enzymes including chitinase and β-1,3-glucanase degrade fungal cell walls, and intracellular proteases and nucleases then degrade proteins and DNA/RNA, respectively, during autolysis. In *A. nidulans*, two transcription factors, RlmA and XprG, which regulate glucanase and chitinase genes, are involved in autolysis (Katz et al., 2013; Kovács et al., 2013). Given that no intracellular protease or nuclease gene expression regulatory mechanisms have been reported thus far, identification of transcription factors involved in *A. oryzae* autolyis will aid in development of industrial applications for *A. oryzae*. In addition, chitin in the *A. oryzae* cell wall adsorbs secreted α-amylase. This adsorption is inhibited when chitin is masked by α-1,3-glucan (Sato et al., 2011; Zhang et al., 2017). In this regard, regulatory mechanisms for genes encoding cell wall remodeling enzymes are also of interest.

The analysis of gene expression mechanisms in *A. oryzae* has progressed significantly after the completion of *A. oryzae* whole genome sequencing. In particular, similar to that for *A. fumigatus* (Furukawa et al., 2020), a disruption library for transcriptional regulatory genes, including transcription factors and transcription-related machinery, has been constructed by the Japanese *A. oryzae* research community. This disruption library as well as the overexpression library which covers a part of transcription factor genes has greatly contributed to the identification of novel transcription factors responsible for hydrolytic gene expression, such as FlbC, ManR, and PrtR. Such libraries have also been effectively utilized to mine novel transcription factors, such as AtrR (azole drug resistance and ABC transporter gene regulation; Hagiwara et al., 2017), EcdR (conidiophore development; Jin et al., 2011), and KpeA (kojic acid production and conidiation; Arakawa et al., 2019), that are involved in the regulatory expression of genes other than hydrolytic genes. Since the library of disruption mutant strains contains over 500 genes putatively involved in transcriptional regulation, further identification of novel transcription factors that regulate the expression of hydrolytic genes in *A. oryzae* is highly expected.

AUTHOR CONTRIBUTIONS

MT and KG wrote the manuscript. All authors contributed to the article and approved the submitted version.

FUNDING

This study was partly supported by Grants-in-Aid for Scientific Research (JSPS KAKENHI, 22248007, 25292044, and 16H04894),

the Program for Promotion of Basic and Applied Researches for Innovations in Bio-oriented Industry, and the Science and Technology Research Promotion Program for Agriculture, Forestry, Fisheries, and Food Industry.

ACKNOWLEDGMENTS

The authors would like to thank Editage (www.editage.com) for English language editing.

REFERENCES

Ahuatzi, D., Riera, A., Peláez, R., Herrero, P., and Moreno, F. (2007). Hxk2 regulates the phosphorylation state of Mig1 and therefore its nucleocytoplasmic distribution. *J. Biol. Chem.* 282, 4485–4493. doi: 10.1074/jbc.M606854200

Alam, M. A., Kamlangdee, N., and Kelly, J. M. (2017). The CreB deubiquitinating enzyme does not directly target the CreA repressor protein in *Aspergillus nidulans*. *Curr. Genet.* 63, 647–667. doi: 10.1007/s00294-016-0666-3

Alazi, E., and Ram, A. (2018). Modulating transcriptional regulation of plant biomass degrading enzyme networks for rational design of industrial fungal strains. *Front. Bioeng. Biotechnol.* 6:133. doi: 10.3389/fbioe.2018.00133

Arakawa, G. Y., Kudo, H., Yanase, A., Eguchi, Y., Kodama, H., Ogawa, M., et al. (2019). A unique $Zn(II)_2$-Cys_6-type protein, KpeA, is involved in secondary metabolism and conidiation in *Aspergillus oryzae*. *Fungal Genet. Biol.* 127, 35–44. doi: 10.1016/j.fgb.2019.02.004

Arst, H. N., and Cove, D. J. (1973). Nitrogen metabolite repression in *Aspergillus nidulans*. *Mol. Gen. Genet.* 126, 111–141. doi: 10.1007/BF00330988

de Assis, L. J., Silva, L. P., Bayram, O., Dowling, P., Kniemeyer, O., Krüger, T., et al. (2021). Carbon catabolite repression in filamentous fungi is regulated by phosphorylation of the transcription factor CreA. *MBio* 12:e03146–20. doi: 10.1128/mBio.03146-20

de Assis, L. J., Ulas, M., Ries, L., El Ramli, N., Sarikaya-Bayram, O., Braus, G. H., et al. (2018). Regulation of *Aspergillus nidulans* CreA-mediated catabolite repression by the F-box proteins Fbx23 and Fbx47. *MBio* 9:e00840–18. doi: 10.1128/mBio.00840-18

Battaglia, E., Visser, L., Nijssen, A., van Veluw, G. J., Wösten, H. A., and de Vries, R. P. (2011). Analysis of regulation of pentose utilisation in *Aspergillus niger* reveals evolutionary adaptations in Eurotiales. *Stud. Mycol.* 69, 31–38. doi: 10.3114/sim.2011.69.03

Bermúdez-García, E., Peña-Montes, C., Martins, I., Pais, J., Pereira, C. S., Sánchez, S., et al. (2019). Regulation of the cutinases expressed by *Aspergillus nidulans* and evaluation of their role in cutin degradation. *Appl. Microbiol. Biotechnol.* 103, 3863–3874. doi: 10.1007/s00253-019-09712-3

Boase, N. A., and Kelly, J. M. (2004). A role for *creD*, a carbon catabolite repression gene from *Aspergillus nidulans*, in ubiquitination. *Mol. Microbiol.* 53, 929–940. doi: 10.1111/j.1365-2958.2004.04172.x

Boni, A. C., Ambrósio, D. L., Cupertino, F. B., Montenegro-Montero, A., Virgilio, S., Freitas, F. Z., et al. (2018). *Neurospora crassa* developmental control mediated by the *FLB-3* transcription factor. *Fungal Biol.* 122, 570–582. doi: 10.1016/j.funbio.2018.01.004

Cziferszky, A., Mach, R. L., and Kubicek, C. P. (2002). Phosphorylation positively regulates DNA binding of the carbon catabolite repressor Cre1 of *Hypocrea jecorina* (*Trichoderma reesei*). *J. Biol. Chem.* 277, 14688–14694. doi: 10.1074/jbc.M200744200

Cziferszky, A., Seiboth, B., and Kubicek, C. P. (2003). The Snf1 kinase of the filamentous fungus *Hypocrea jecorina* phosphorylates regulation-relevant serine residues in the yeast carbon catabolite repressor Mig1 but not in the filamentous fungal counterpart Cre1. *Fungal Genet. Biol.* 40, 166–175. doi: 10.1016/S1087-1845(03)00082-3

DeVit, M. J., and Johnston, M. (1999). The nuclear exportin Msn5 is required for nuclear export of the Mig1 glucose repressor of *Saccharomyces cerevisiae*. *Curr. Biol.* 9, 1231–1241. doi: 10.1016/S0960-9822(99)80503-X

Dowzer, C. E., and Kelly, J. M. (1991). Analysis of the *creA* gene, a regulator of carbon catabolite repression in *Aspergillus nidulans*. *Mol. Cell. Biol.* 11, 5701–5709. doi: 10.1128/MCB.11.11.5701

Fleck, C. B., and Brock, M. (2010). *Aspergillus fumigatus* catalytic glucokinase and hexokinase: expression analysis and importance for germination, growth, and conidiation. *Eukaryot. Cell* 9, 1120–1135. doi: 10.1128/EC.00362-09

Furukawa, T., van Rhijn, N., Fraczek, M., Gsaller, F., Davies, E., Carr, P., et al. (2020). The negative cofactor 2 complex is a key regulator of drug resistance in *Aspergillus fumigatus*. *Nat. Commun.* 11:427. doi: 10.1038/s41467-019-14191-1

Garrido, S. M., Kitamoto, N., Watanabe, A., Shintani, T., and Gomi, K. (2012). Functional analysis of FarA transcription factor in the regulation of the genes encoding lipolytic enzymes and hydrophobic surface binding protein for the degradation of biodegradable plastics in *Aspergillus oryzae*. *J. Biosci. Bioeng.* 113, 549–555. doi: 10.1016/j.jbiosc.2011.12.014

Gomi, K. (2014). "ASPERGILLUS | *Aspergillus oryzae,*" in *Encyclopedia of food microbiology. 2nd Edn*. eds. C. A. Batt and M. L. Tortorello (London, UK: Academic Press), 92–96.

Gomi, K. (2019). Regulatory mechanisms for amylolytic gene expression in the *koji* mold *Aspergillus oryzae*. *Biosci. Biotechnol. Biochem.* 83, 1385–1401. doi: 10.1080/09168451.2019.1625265

Gomi, K., Akeno, T., Minetoki, T., Ozeki, K., Kumagai, C., Okazaki, N., et al. (2000). Molecular cloning and characterization of a transcriptional activator gene, *amyR*, involved in the amylolytic gene expression in *Aspergillus oryzae*. *Biosci. Biotechnol. Biochem.* 64, 816–827. doi: 10.1271/bbb.64.816

Hagiwara, D., Miura, D., Shimizu, K., Paul, S., Ohba, A., Gonoi, T., et al. (2017). A novel Zn_2-Cys_6 transcription factor AtrR plays a key role in an azole resistance mechanism of *Aspergillus fumigatus* by coregulating *cyp51A* and *cdr1B* expressions. *PLoS Pathog.* 13:e1006096. doi: 10.1371/journal.ppat.1006096

Han, L., Tan, Y., Ma, W., Niu, K., Hou, S., Guo, W., et al. (2020). Precision engineering of the transcription factor Cre1 in *Hypocrea jecorina* (*Trichoderma reesei*) for efficient cellulase production in the presence of glucose. *Front. Bioeng. Biotechnol.* 8:852. doi: 10.3389/fbioe.2020.00852

Hartmann, T., Cairns, T. C., Olbermann, P., Morschhäuser, J., Bignell, E. M., and Krappmann, S. (2011). Oligopeptide transport and regulation of extracellular proteolysis are required for growth of *Aspergillus fumigatus* on complex substrates but not for virulence. *Mol. Microbiol.* 82, 917–935. doi: 10.1111/j.1365-2958.2011.07868.x

Hasegawa, S., Takizawa, M., Suyama, H., Shintani, T., and Gomi, K. (2010). Characterization and expression analysis of a maltose-utilizing (*MAL*) cluster in *Aspergillus oryzae*. *Fungal Genet. Biol.* 47, 1–9. doi: 10.1016/j.fgb.2009.10.005

Hata, Y., Ishida, H., Ichikawa, E., Kawato, A., Suginami, K., and Imayasu, S. (1998). Nucleotide sequence of an alternative glucoamylase-encoding gene (*glaB*) expressed in solid-state culture of *Aspergillus oryzae*. *Gene* 207, 127–134. doi: 10.1016/S0378-1119(97)00612-4

Hata, Y., Tsuchiya, K., Kitamoto, K., Gomi, K., Kumagai, C., Tamura, G., et al. (1991). Nucleotide sequence and expression of the glucoamylase-encoding gene (*glaA*) from *Aspergillus oryzae*. *Gene* 108, 145–150. doi: 10.1016/0378-1119(91)90500-b

Hiramoto, T., Tanaka, M., Ichikawa, T., Matsuura, Y., Hasegawa-Shiro, S., Shintani, T., et al. (2015). Endocytosis of a maltose permease is induced when amylolytic enzyme production is repressed in *Aspergillus oryzae*. *Fungal Genet. Biol.* 82, 136–144. doi: 10.1016/j.fgb.2015.05.015

Hisada, H., Sano, M., Ishida, H., Hata, Y., and Machida, M. (2013). Identification of regulatory elements in the glucoamylase-encoding gene (*glaB*) promoter from *Aspergillus oryzae*. *Appl. Microbiol. Biotechnol.* 97, 4951–4956. doi: 10.1007/s00253-012-4622-y

Ho, H. C., MacGurn, J. A., and Emr, S. D. (2017). Deubiquitinating enzymes Ubp2 and Ubp15 regulate endocytosis by limiting ubiquitination and degradation of ARTs. *Mol. Biol. Cell* 28, 1271–1283. doi: 10.1091/mbc.E17-01-0008

Huang, L., Dong, L., Wang, B., and Pan, L. (2020). The transcription factor PrtT and its target protease profiles in *Aspergillus niger* are negatively regulated by carbon sources. *Biotechnol. Lett.* 42, 613–624. doi: 10.1007/s10529-020-02806-3

Hunter, A. J., Morris, T. A., Jin, B., Saint, C. P., and Kelly, J. M. (2013). Deletion of *creB* in *Aspergillus oryzae* increases secreted hydrolytic enzyme activity. *Appl. Environ. Microbiol.* 79, 5480–5487. doi: 10.1128/AEM.01406-13

Hynes, M. J., and Kelly, J. M. (1977). Pleiotropic mutants of *Aspergillus nidulans* altered in carbon metabolism. *Mol. Gen. Genet.* 150, 193–204. doi: 10.1007/BF00695399

Hynes, M. J., Murray, S. L., Duncan, A., Khew, G. S., and Davis, M. A. (2006). Regulatory genes controlling fatty acid catabolism and peroxisomal functions in the filamentous fungus *Aspergillus nidulans*. *Eukaryot. Cell* 5, 794–805. doi: 10.1128/EC.5.5.794-805.2006

Ichinose, S., Tanaka, M., Shintani, T., and Gomi, K. (2014). Improved α-amylase production by *Aspergillus oryzae* after a double deletion of genes involved in carbon catabolite repression. *Appl. Microbiol. Biotechnol.* 98, 335–343. doi: 10.1007/s00253-013-5353-4

Ichinose, S., Tanaka, M., Shintani, T., and Gomi, K. (2018). Increased production of biomass-degrading enzymes by double deletion of *creA* and *creB* genes involved in carbon catabolite repression in *Aspergillus oryzae*. *J. Biosci. Bioeng.* 125, 141–147. doi: 10.1016/j.jbiosc.2017.08.019

Ishida, H., Hata, Y., Ichikawa, E., Kawato, A., Suginami, K., and Imayasu, S. (1998). Regulation of the glucoamylase-encoding gene (*glaB*), expressed in solid-state culture (*koji*) of *Aspergillus oryzae*. *J. Ferment. Bioeng.* 86, 301–307. doi: 10.1016/S0922-338X(98)80134-7

Ishida, H., Hata, Y., Kawato, A., Abe, Y., Suginami, K., and Imayasu, S. (2000). Identification of functional elements that regulate the glucoamylase-encoding gene (*glaB*) expressed in solid-state culture of *Aspergillus oryzae*. *Curr. Genet.* 37, 373–379. doi: 10.1007/s002940000118

Ishikawa, K., Kunitake, E., Kawase, T., Atsumi, M., Noguchi, Y., Ishikawa, S., et al. (2018). Comparison of the paralogous transcription factors AraR and XlnR in *Aspergillus oryzae*. *Curr. Genet.* 64, 1245–1260. doi: 10.1007/s00294-018-0837-5

Ito, T., Tani, S., Itoh, T., Tsukagoshi, N., Kato, M., and Kobayashi, T. (2004). Mode of AmyR binding to the CGGN8AGG sequence in the *Aspergillus oryzae taaG2* promoter. *Biosci. Biotechnol. Biochem.* 68, 1906–1911. doi: 10.1271/bbb.68.1906

Jin, F., Hu, S., Wang, B., and Jin, L. (2021). Advances in genetic engineering technology and its application in the industrial fungus *Aspergillus oryzae*. *Front. Microbiol.* 12:644404. doi: 10.3389/fmicb.2021.644404

Jin, F., Nishida, M., Hara, S., and Koyama, Y. (2011). Identification and characterization of a putative basic helix-loop-helix transcription factor involved in the early stage of conidiophore development in *Aspergillus oryzae*. *Fungal Genet. Biol.* 48, 1108–1115. doi: 10.1016/j.fgb.2011.10.001

Kato, M., Sekine, K., and Tsukagoshi, N. (1996). Sequence-specific binding sites in the Taka-amylase A G2 promoter for the CreA repressor mediating carbon catabolite repression. *Biosci. Biotechnol. Biochem.* 60, 1776–1779. doi: 10.1271/bbb.60.1776

Katz, M. E., Braunberger, K., Yi, G., Cooper, S., Nonhebel, H. M., and Gondro, C. (2013). A p53-like transcription factor similar to Ndt80 controls the response to nutrient stress in the filamentous fungus, *Aspergillus nidulans*. *F1000Res* 2:72. doi: 10.12688/f1000research.2-72.v1

Kelly, J. M., and Hynes, M. J. (1977). Increased and decreased sensitivity to carbon catabolite repression of enzymes of acetate metabolism in mutants of *Aspergillus nidulans*. *Mol. Gen. Genet.* 156, 87–92. doi: 10.1007/BF00272256

Kobayashi, T., Abe, K., Asai, K., Gomi, K., Juvvadi, P. R., Kato, M., et al. (2007). Genomics of *Aspergillus oryzae*. *Biosci. Biotechnol. Biochem.* 71, 646–670. doi: 10.1271/bbb.60550

Konno, Y., Suzuki, K., Tanaka, M., Shintani, T., and Gomi, K. (2018). Chaperone complex formation of the transcription factor MalR involved in maltose utilization and amylolytic enzyme production in *Aspergillus oryzae*. *Biosci. Biotechnol. Biochem.* 82, 827–835. doi: 10.1080/09168451.2018.1447359

Kouranti, I., McLean, J. R., Feoktistova, A., Liang, P., Johnson, A. E., Roberts-Galbraith, R. H., et al. (2010). A global census of fission yeast deubiquitinating enzyme localization and interaction networks reveals distinct compartmentalization profiles and overlapping functions in endocytosis and polarity. *PLoS Biol.* 8:e1000471. doi: 10.1371/journal.pbio.1000471

Kovács, Z., Szarka, M., Kovács, S., Boczonádi, I., Emri, T., Abe, K., et al. (2013). Effect of cell wall integrity stress and RlmA transcription factor on asexual development and autolysis in *Aspergillus nidulans*. *Fungal Genet. Biol.* 54, 1–14. doi: 10.1016/j.fgb.2013.02.004

Kunitake, E., and Kobayashi, T. (2017). Conservation and diversity of the regulators of cellulolytic enzyme genes in Ascomycete fungi. *Curr. Genet.* 63, 951–958. doi: 10.1007/s00294-017-0695-6

Kunitake, E., Li, Y., Uchida, R., Nohara, T., Asano, K., Hattori, A., et al. (2019). CreA-independent carbon catabolite repression of cellulase genes by trimeric G-protein and protein kinase A in *Aspergillus nidulans*. *Curr. Genet.* 65, 941–952. doi: 10.1007/s00294-019-00944-4

Kwon, N. J., Garzia, A., Espeso, E. A., Ugalde, U., and Yu, J. H. (2010). FlbC is a putative nuclear C_2H_2 transcription factor regulating development in *Aspergillus nidulans*. *Mol. Microbiol.* 77, 1203–1219. doi: 10.1111/j.1365-2958.2010.07282.x

Li, D., and Kolattukudy, P. E. (1997). Cloning of cutinase transcription factor 1, a transactivating protein containing Cys_6Zn_2 binuclear cluster DNA-binding motif. *J. Biol. Chem.* 272, 12462–12467. doi: 10.1074/jbc.272.19.12462

Lin, C. H., MacGurn, J. A., Chu, T., Stefan, C. J., and Emr, S. D. (2008). Arrestin-related ubiquitin-ligase adaptors regulate endocytosis and protein turnover at the cell surface. *Cell* 135, 714–725. doi: 10.1016/j.cell.2008.09.025

Lockington, R. A., and Kelly, J. M. (2001). Carbon catabolite repression in *Aspergillus nidulans* involves deubiquitination. *Mol. Microbiol.* 40, 1311–1321. doi: 10.1046/j.1365-2958.2001.02474.x

Lockington, R. A., and Kelly, J. M. (2002). The WD40-repeat protein CreC interacts with and stabilizes the deubiquitinating enzyme CreB in vivo in *Aspergillus nidulans*. *Mol. Microbiol.* 43, 1173–1182. doi: 10.1046/j.1365-2958.2002.02811.x

Machida, M., Asai, K., Sano, M., Tanaka, T., Kumagai, T., Terai, G., et al. (2005). Genome sequencing and analysis of *Aspergillus oryzae*. *Nature* 438, 1157–1161. doi: 10.1038/nature04300

Machida, M., Yamada, O., and Gomi, K. (2008). Genomics of *Aspergillus oryzae*: learning from the history of *Koji* mold and exploration of its future. *DNA Res.* 15, 173–183. doi: 10.1093/dnares/dsn020

MacDonald, C., Shields, S. B., Williams, C. A., Winistorfer, S., and Piper, R. C. (2020). A cycle of Ubiquitination regulates adaptor function of the Nedd4-family ubiquitin ligase Rsp5. *Curr. Biol.* 30, 465–479. doi: 10.1016/j.cub.2019.11.086

Maeda, H., Yamagata, Y., Abe, K., Hasegawa, F., Machida, M., Ishioka, R., et al. (2005). Purification and characterization of a biodegradable plastic-degrading enzyme from *Aspergillus oryzae*. *Appl. Microbiol. Biotechnol.* 67, 778–788. doi: 10.1007/s00253-004-1853-6

Makita, T., Katsuyama, Y., Tani, S., Suzuki, H., Kato, N., Todd, R. B., et al. (2009). Inducer-dependent nuclear localization of a Zn(II)(2)Cys(6) transcriptional activator, AmyR, in *Aspergillus nidulans*. *Biosci. Biotechnol. Biochem.* 73, 391–399. doi: 10.1271/bbb.80654

Marui, J., Kitamoto, N., Kato, M., Kobayashi, T., and Tsukagoshi, N. (2002). Transcriptional activator, AoXlnR, mediates cellulose-inductive expression of the xylanolytic and cellulolytic genes in *Aspergillus oryzae*. *FEBS Lett.* 528, 279–282. doi: 10.1016/S0014-5793(02)03328-8

Matheis, S., Yemelin, A., Scheps, D., Andresen, K., Jacob, S., Thines, E., et al. (2017). Functions of the *Magnaporthe oryzae* Flb3p and Flb4p transcription factors in the regulation of conidiation. *Microbiol. Res.* 196, 106–117. doi: 10.1016/j.micres.2016.12.010

Minetoki, T., Tsuboi, H., Koda, A., and Ozeki, K. (2003). Development of high expression system with the improved promoter using the *cis*-acting element in *Aspergillus* species. *J. Biol. Macromol.* 3, 89–96.

Mizutani, O., Kudo, Y., Saito, A., Matsuura, T., Inoue, H., Abe, K., et al. (2008). A defect of LigD (human Lig4 homolog) for nonhomologous end joining significantly improves efficiency of gene-targeting in *Aspergillus oryzae*. *Fungal Genet. Biol.* 45, 878–889. doi: 10.1016/j.fgb.2007.12.010

Murakoshi, Y., Makita, T., Kato, M., and Kobayashi, T. (2012). Comparison and characterization of α-amylase inducers in *Aspergillus nidulans* based on nuclear localization of AmyR. *Appl. Microbiol. Biotechnol.* 94, 1629–1635. doi: 10.1007/s00253-012-3874-x

Nakari-Setälä, T., Paloheimo, M., Kallio, J., Vehmaanperä, J., Penttilä, M., and Saloheimo, M. (2009). Genetic modification of carbon catabolite repression in *Trichoderma reesei* for improved protein production. *Appl. Environ. Microbiol.* 75, 4853–4860. doi: 10.1128/AEM.00282-09

Needleman, R. (1991). Control of maltase synthesis in yeast. *Mol. Microbiol.* 5, 2079–2084. doi: 10.1111/j.1365-2958

Nikko, E., and Pelham, H. R. (2009). Arrestin-mediated endocytosis of yeast plasma membrane transporters. *Traffic* 10, 1856–1867. doi: 10.1111/j.1600-0854.2009.00990.x

Noguchi, Y., Sano, M., Kanamaru, K., Ko, T., Takeuchi, M., Kato, M., et al. (2009). Genes regulated by AoXlnR, the xylanolytic and cellulolytic transcriptional regulator, in *Aspergillus oryzae*. *Appl. Microbiol. Biotechnol.* 85, 141–154. doi: 10.1007/s00253-009-2236-9

Noguchi, Y., Tanaka, H., Kanamaru, K., Kato, M., and Kobayashi, T. (2011). Xylose triggers reversible phosphorylation of XlnR, the fungal transcriptional activator of xylanolytic and cellulolytic genes in *Aspergillus oryzae*. *Biosci. Biotechnol. Biochem.* 75, 953–959. doi: 10.1271/bbb.100923

Oda, K., Kakizono, D., Yamada, O., Iefuji, H., Akita, O., and Iwashita, K. (2006). Proteomic analysis of extracellular proteins from *Aspergillus oryzae* grown under submerged and solid-state culture conditions. *Appl. Environ. Microbiol.* 72, 3448–3457. doi: 10.1128/AEM.72.5.3448-3457.2006

Ogawa, M., Kobayashi, T., and Koyama, Y. (2012). ManR, a novel $Zn(II)_2Cys_6$ transcriptional activator, controls the β-mannan utilization system in *Aspergillus oryzae*. *Fungal Genet. Biol.* 49, 987–995. doi: 10.1016/j.fgb.2012.09.006

Ogawa, M., Kobayashi, T., and Koyama, Y. (2013). ManR, a transcriptional regulator of the β-mannan utilization system, controls the cellulose utilization system in *Aspergillus oryzae*. *Biosci. Biotechnol. Biochem.* 77, 426–429. doi: 10.1271/bbb.120795

Ogawa, M., Tokuoka, M., Jin, F. J., Takahashi, T., and Koyama, Y. (2010). Genetic analysis of conidiation regulatory pathways in *koji*-mold *Aspergillus oryzae*. *Fungal Genet. Biol.* 47, 10–18. doi: 10.1016/j.fgb.2009.10.004

Ohtaki, S., Maeda, H., Takahashi, T., Yamagata, Y., Hasegawa, F., Gomi, K., et al. (2006). Novel hydrophobic surface binding protein, HsbA, produced by *Aspergillus oryzae*. *Appl. Environ. Microbiol.* 72, 2407–2413. doi: 10.1128/AEM.72.4.2407-2413.2006

Oikawa, H. (2020). Reconstitution of biosynthetic machinery of fungal natural products in heterologous hosts. *Biosci. Biotechnol. Biochem.* 84, 433–444. doi: 10.1080/09168451.2019.1690976

Petersen, K. L., Lehmbeck, J., and Christensen, T. (1999). A new transcriptional activator for amylase genes in *Aspergillus*. *Mol. Gen. Genet.* 262, 668–676. doi: 10.1007/s004380051129

Polo, S., and Di Fiore, P. P. (2008). Finding the right partner: science or ART? *Cell* 135, 590–592. doi: 10.1016/j.cell.2008.10.032

Punt, P. J., Schuren, F. H., Lehmbeck, J., Christensen, T., Hjort, C., and van den Hondel, C. A. (2008). Characterization of the *Aspergillus niger prtT*, a unique regulator of extracellular protease encoding genes. *Fungal Genet. Biol.* 45, 1591–1599. doi: 10.1016/j.fgb.2008.09.007

Ran, F., Bali, M., and Michels, C. A. (2008). Hsp90/Hsp70 chaperone machine regulation of the *Saccharomyces MAL*-activator as determined in vivo using noninducible and constitutive mutant alleles. *Genetics* 179, 331–343. doi: 10.1534/genetics.107.084921

Ribeiro, L., Chelius, C., Boppidi, K. R., Naik, N. S., Hossain, S., Ramsey, J., et al. (2019). Comprehensive analysis of *Aspergillus nidulans* PKA phosphorylome identifies a novel mode of CreA regulation. *MBio* 10:e02825–18. doi: 10.1128/mBio.02825-18

Ries, L. N., Beattie, S. R., Espeso, E. A., Cramer, R. A., and Goldman, G. H. (2016). Diverse regulation of the CreA carbon catabolite repressor in *Aspergillus nidulans*. *Genetics* 203, 335–352. doi: 10.1534/genetics.116.187872

Sato, H., Toyoshima, Y., Shintani, T., and Gomi, K. (2011). Identification of potential cell wall component that allows Taka-amylase A adsorption in submerged cultures of *Aspergillus oryzae*. *Appl. Microbiol. Biotechnol.* 92, 961–969. doi: 10.1007/s00253-011-3422-0

Sen, A., Acosta-Sampson, L., Alvaro, C. G., Ahn, J. S., Cate, J. H., and Thorner, J. (2016). Internalization of heterologous sugar transporters by endogenous α-arrestins in the yeast *Saccharomyces cerevisiae*. *Appl. Environ. Microbiol.* 82, 7074–7085. doi: 10.1128/AEM.02148-16

Sharon, H., Hagag, S., and Osherov, N. (2009). Transcription factor PrtT controls expression of multiple secreted proteases in the human pathogenic mold *Aspergillus fumigatus*. *Infect. Immun.* 77, 4051–4060. doi: 10.1128/IAI.00426-09

Strauss, J., Horvath, H. K., Abdallah, B. M., Kindermann, J., Mach, R. L., and Kubicek, C. P. (1999). The function of CreA, the carbon catabolite repressor of *Aspergillus nidulans*, is regulated at the transcriptional and post-transcriptional level. *Mol. Microbiol.* 32, 169–178. doi: 10.1046/j.1365-2958.1999.01341.x

Suzuki, K., Tanaka, M., Konno, Y., Ichikawa, T., Ichinose, S., Hasegawa-Shiro, S., et al. (2015). Distinct mechanism of activation of two transcription factors, AmyR and MalR, involved in amylolytic enzyme production in *Aspergillus oryzae*. *Appl. Microbiol. Biotechnol.* 99, 1805–1815. doi: 10.1007/s00253-014-6264-8

Takahashi, T., Maeda, H., Yoneda, S., Ohtaki, S., Yamagata, Y., Hasegawa, F., et al. (2005). The fungal hydrophobin RolA recruits polyesterase and laterally moves on hydrophobic surfaces. *Mol. Microbiol.* 57, 1780–1796. doi: 10.1111/j.1365-2958.2005.04803.x

Takahashi, T., Ogawa, M., Sato, A., and Koyama, Y. (2018). Translocated duplication of a targeted chromosomal segment enhances gene expression at the duplicated site and results in phenotypic changes in *Aspergillus oryzae*. *Fungal Biol. Biotechnol.* 5:17. doi: 10.1186/s40694-018-0061-6

Tanaka, M., and Gomi, K. (2014). "Strategies for increasing the production level of heterologous proteins in *Aspergillus oryzae*," in *Microbial Production*. eds. H. Anazawa and S. Shimizu (Tokyo: Springer), 149–164.

Tanaka, M., Hiramoto, T., Tada, H., Shintani, T., and Gomi, K. (2017). Improved α-amylase production by dephosphorylation mutation of CreD, an arrestin-like protein required for glucose-induced endocytosis of maltose permease and carbon catabolite derepression in *Aspergillus oryzae*. *Appl. Environ. Microbiol.* 83:e00592–17. doi: 10.1128/AEM.00592-17

Tanaka, M., Ichinose, S., Shintani, T., and Gomi, K. (2018). Nuclear export-dependent degradation of the carbon catabolite repressor CreA is regulated by a region located near the C-terminus in *Aspergillus oryzae*. *Mol. Microbiol.* 110, 176–190. doi: 10.1111/mmi.14072

Tanaka, M., Ito, K., Matsuura, T., Kawarasaki, Y., and Gomi, K. (2021). Identification and distinct regulation of three di/tripeptide transporters in *Aspergillus oryzae*. *Biosci. Biotechnol. Biochem.* 85, 452–463. doi: 10.1093/bbb/zbaa030

Tanaka, M., Yoshimura, M., Ogawa, M., Koyama, Y., Shintani, T., and Gomi, K. (2016). The C_2H_2-type transcription factor, FlbC, is involved in the transcriptional regulation of *Aspergillus oryzae* glucoamylase and protease genes specifically expressed in solid-state culture. *Appl. Microbiol. Biotechnol.* 100, 5859–5868. doi: 10.1007/s00253-016-7419-6

Tani, S., Katsuyama, Y., Hayashi, T., Suzuki, H., Kato, M., Gomi, K., et al. (2001). Characterization of the *amyR* gene encoding a transcriptional activator for the amylase genes in *Aspergillus nidulans*. *Curr. Genet.* 39, 10–15. doi: 10.1007/s002940000175

Tani, S., Kawaguchi, T., and Kobayashi, T. (2014). Complex regulation of hydrolytic enzyme genes for cellulosic biomass degradation in filamentous fungi. *Appl. Microbiol. Biotechnol.* 98, 4829–4837. doi: 10.1007/s00253-014-5707-6

Tonomura, K., Suzuki, H., Nakamura, N., Kuraya, K., and Tanabe, O. (1961). On the inducers of α-amylase formation in *Aspergillus oryzae*. *Agric. Biol. Chem.* 25, 1–6.

Tsuboi, H., Koda, A., Toda, T., Minetoki, T., Hirotsune, M., and Machida, M. (2005). Improvement of the *Aspergillus oryzae* enolase promoter (P-*enoA*) by the introduction of *cis*-element repeats. *Biosci. Biotechnol. Biochem.* 69, 206–208. doi: 10.1271/bbb.69.206

Villamil, M. A., Liang, Q., and Zhuang, Z. (2013). The WD40-repeat protein-containing deubiquitinase complex: catalysis, regulation, and potential for therapeutic intervention. *Cell Biochem. Biophy* 67, 111–126. doi: 10.1007/s12013-013-9637-1

Watanabe, J., Tanaka, H., Mogi, Y., Yamazaki, T., Suzuki, K., Watanabe, T., et al. (2011). Loss of *Aspergillus oryzae amyR* function indirectly affects hemicellulolytic and cellulolytic enzyme production. *J. Biosci. Bioeng.* 111, 408–413. doi: 10.1016/j.jbiosc.2010.12.006

Wieser, J., Lee, B. N., Fondon, J. w., and 3rd, Adams, T. H., (1994). Genetic requirements for initiating asexual development in *Aspergillus nidulans*. *Curr. Genet.* 27, 62–69. doi: 10.1007/BF00326580

Xu, N., Liu, Y., Hu, Y., Zhou, M., Wang, C., and Li, D. (2016). Autolysis of *Aspergillus oryzae* mycelium and effect on volatile flavor compounds of soy sauce. *J. Food Sci.* 81, C1883–C1890. doi: 10.1111/1750-3841.13396

Yabuki, M., Ono, N., Hoshino, K., and Fukui, S. (1977). Rapid induction of alpha-amylase by nongrowing mycelia of *Aspergillus oryzae*. *Appl. Environ. Microbiol.* 34, 1–6. doi: 10.1128/AEM.34.1.1-6.1977

Zhang, S., Sato, H., Ichinose, S., Tanaka, M., Miyazawa, K., Yoshimi, A., et al. (2017). Cell wall α-1,3-glucan prevents α-amylase adsorption onto fungal cell in submerged culture of *Aspergillus oryzae*. *J. Biosci. Bioeng.* 124, 47–53. doi: 10.1016/j.jbiosc.2017.02.013

Conflict of Interest: The authors declare that the research was conducted in the absence of any commercial or financial relationships that could be construed as a potential conflict of interest.

frontiers in Microbiology

ORIGINAL RESEARCH
published: 31 May 2021
doi: 10.3389/fmicb.2021.663744

Isolation and Identification of a High-Yield Ethyl Caproate-Producing Yeast From *Daqu* and Optimization of Its Fermentation

*Guangsen Fan[1,2], Pengxiao Liu[1,2], Xu Chang[3], Huan Yin[1,2], Liujie Cheng[1,2], Chao Teng[1,2], Yi Gong[1,2] and Xiuting Li[1,2]**

[1] Beijing Advanced Innovation Center for Food Nutrition and Human Health, Beijing Technology and Business University (BTBU), Beijing, China, [2] School of Food and Health, Beijing Technology and Business University (BTBU), Beijing, China, [3] Institute of Brewing and Bioenergy, Angel Yeast Co., Ltd., Hubei, China

Baijiu is an important fermented product in China. A yeast named YX3307 that is capable of producing a large amount of ethyl caproate (EC) was isolated from *Daqu*, a crude fermentation starter for *Baijiu*. This yeast was identified as *Clavispora lusitaniae* on the basis of its morphological properties, physiological and biochemical characteristics, and 26S rDNA sequence. Single-factor experiments were conducted to obtain the optimum fermentation conditions for EC production by YX3307. The highest EC yield (62.0 mg/L) from YX3307 was obtained with the following culture conditions: inoculum size 7.5% (v/v), seed cell age 30 h, sorghum hydrolysate medium (SHM) with a sugar content of 10 Brix and an initial pH of 6.0; incubation at 28°C with shaking at 180 rpm for 32 h; addition of 10% (v/v) anhydrous ethanol and 0.04% (v/v) caproic acid at 32 and 40 h, respectively, static culture at 20°C until 72 h. YX3307 synthesized more EC than ethyl acetate, ethyl lactate, ethyl butyrate, and ethyl octanoate. An intracellular enzyme or cell membrane enzyme was responsible for EC synthesis. YX3307 can produce many flavor compounds that are important for high-quality *Baijiu*. Thus, it has potential applications in improving the flavor and quality of *Baijiu*.

Keywords: *Baijiu*, ethyl caproate, identification, fermentation optimization, *Clavispora lusitaniae*

OPEN ACCESS

Edited by:
Xucong Lv,
Fuzhou University, China

Reviewed by:
Guo Xuewu,
Tianjin University of Science and Technology, China
Qun Wu,
Jiangnan University, China
Beizhong Han,
China Agricultural University, China

***Correspondence:**
Xiuting Li
lixt@btbu.edu.cn

Specialty section:
This article was submitted to Food Microbiology, a section of the journal Frontiers in Microbiology

Received: *03 February 2021*
Accepted: *30 April 2021*
Published: *31 May 2021*

Citation:
Fan G, Liu P, Chang X, Yin H, Cheng L, Teng C, Gong Y and Li X (2021) Isolation and Identification of a High-Yield Ethyl Caproate-Producing Yeast From Daqu and Optimization of Its Fermentation. Front. Microbiol. 12:663744. doi: 10.3389/fmicb.2021.663744

INTRODUCTION

Baijiu, a typical Chinese traditional fermented food, is made from sorghum, wheat, and/or rice by a complex fermentation process using natural mixed-culture starters (named *Daqu*) (Fan et al., 2020a). One of those starters is *Daqu*, which harbors many microorganisms for *Baijiu* brewing, and is used as a saccharifying and fermenting agent for *Baijiu* production. *Daqu* is made from cereals such as wheat, barley, and peas by spontaneous solid-state fermentation in an open environment (Fan et al., 2020a). During *Daqu* production, the raw materials are colonized by networks of microorganisms from the environment. Thus, *Daqu* used is a natural microbial library of bacteria,

Abbreviations: EC, ethyl caproate; GC-MS, gas chromatography-mass spectrometry; HS-SPME, headspace solid-phase microextraction; OD, optical density; SHM, sorghum hydrolysate medium; WL medium, Wallerstein laboratory medium; YPD medium, yeast extract peptone dextrose medium; NYGA medium, nutrient yeast glycerol agar medium.

fungi, and yeasts that play important roles during the *Baijiu* fermentation (Hu et al., 2020). Because *Daqu* is produced using a range of different preparation methods and in different environments, the microbial composition of *Daqu* produced in different places can be quite different (Zuo et al., 2020). Therefore, it is important to screen and identify microorganisms from different kinds of *Daqu*, especially the functional microorganisms that could improve *Baijiu* quality (Fan et al., 2018b).

Strong-flavor *Baijiu* accounts for more than 70% of total *Baijiu* consumed in China because of its fragrant flavor, soft mouthfeel, and long aftertaste (Liu and Sun, 2018). Although the unique taste of strong-flavor *Baijiu* is the result of the interaction of many flavor substances, ethyl caproate (EC) with its apple-like flavor is the characteristic flavor substance. This compound determines the quality and aroma profile of strong-flavor *Baijiu* (Chen et al., 2014, 2016; Tan et al., 2016; Song et al., 2020). There is a clear requirement for a certain content of EC (0.40–2.80 g/L for different grades of strong-flavor *Baijiu*) in the standard of strong-flavor *Baijiu* (China Light Industry Press, and People's Republic of China Professional Standard, 2006). As the main flavor substance, EC is the main factor that restricts the yield of excellent-grade strong-flavor *Baijiu* (Fan and Qian, 2006).

Like other esters, EC in *Baijiu* is mainly derived from microbial metabolism (Fan et al., 2020b). There are two ways that EC can be produced: synthesis from caproic acid and ethanol catalyzed by lipase or esterase; and catalysis of ethanol and caproyl-coenzyme A by ethanol hexanoyl transferase (Liu et al., 2004; Chen et al., 2014, 2016; Takahashi et al., 2017). Previous studies have shown that EC is mainly produced during the later stage of *Baijiu* brewing (Chen et al., 2014). Therefore, to increase the content of EC in strong-flavor raw *Baijiu* (without blending), the period of *Baijiu* brewing is often extended. This practice not only leads to high grain consumption and low production efficiency, but also results in the production of unpleasant flavor compounds (Chen et al., 2014, 2016). A similar problem has been encountered in sake, but it was solved by isolating a strain of sake yeast with a high yield of EC (Ichikawa et al., 1991; Arikawa et al., 2000; Aritomi et al., 2004; Takahashi et al., 2017). This provides a reference to solve the problem of the low EC content in strong-flavor *Baijiu*. That is, there is the potential to improve quality and strengthen the EC content by using functional microorganism(s) with high yields of EC in the fermentation process. In the future, strong-flavor *Baijiu* may be produced by combining and regulating the growth of a limited number of functional microorganisms, just like sake.

Among diverse microorganisms such as yeasts, molds, and bacteria, some yeasts are known to harbor the above two EC synthesis pathways (Chen et al., 2016). Therefore, screening for a yeast strain with a high yield of EC is of great significance to increase the EC content in strong-flavor *Baijiu*, as has been achieved for sake. Although some researchers have attempted to isolate yeasts with high yields of EC from the *Baijiu* brewing environment, there has been limited success in isolating a suitable strain (Wang et al., 2013). In view of these considerations, we focused on *Daqu* to isolate and characterize a yeast capable of producing a large amount of EC. In this study, a yeast with high-yields of EC was isolated and purified from *Daqu* using a traditional screening method. The yeast was identified and the fermentation conditions were optimized for EC production.

MATERIALS AND METHODS

Materials and Reagents

Daqu samples were collected from different *Baijiu* brewing enterprises in China (detailed information is provided in **Supplementary Table 1**). The EC (HPLC grade) was obtained from Roche. The EC and tetraoctanol standards were purchased from Sigma (St. Louis, MO, United States). All other chemicals were of analytical grade and commercially available unless otherwise stated.

Media Preparation

Yeast extract peptone dextrose (YPD) medium, Wallerstein laboratory nutrient agar (WL) medium, and sorghum hydrolysate medium (SHM) were prepared as described in our previous report (Fan et al., 2018b). The media for physiological and biochemical tests were prepared according to standard methods (Kurtzman et al., 2011).

Screening for Yeast With a High-Yield of EC

A mixture of 25 g *Daqu* sample and 225 mL sterilized ddH_2O was diluted into three gradients, from 10^{-4} to 10^{-6}. After serial dilution, 100-μL aliquots from each gradient suspension were spread onto YPD plates. The plates were incubated at 30°C and monitored daily for 5 days until yeast colonies developed. Single colonies showing different morphologies were picked and purified from the plates and microscopic examination was performed after lawn growth. Then, each isolated colony was inoculated into a YPD medium slant tube and stored at −80°C. Each yeast strain (1×10^6 cells/mL) was inoculated into 30 mL SHM and cultured at 28°C with shaking at 180 r/min for 24 h. After adding precursors [4% (v/v) ethanol and 0.02% (v/v) caproic acid], the cultures were incubated for a further 36 h. The cultures were centrifuged at 13,000 × *g* for 10 min, the supernatant was filtered, and then the EC content was determined by gas chromatography–mass spectrometry (GC-MS). Each yeast strain in the experiments was analyzed in parallel three times. The yeast producing the largest amount of EC was selected for further study.

Identification of Yeast

The screened strain was identified on the basis of its colony morphology, cell morphology, physiological and biochemical characteristics, and 26S rDNA sequence, as described by Kurtzman et al. (2011) and Fan et al. (2018b). Phenotypic characterization was also carried out with Biolog GEN III MicroPlates (Biolog) according to the manufacturer's instructions. Each selected strain was first grown on nutrient yeast glycerol agar medium (NYGA, 5 g/L peptone, 3 g/L yeast extract, 20 g/L glycerol, and 15 g/L agar) for 48 h at 28°C, then on solid Biolog Dehydrated Growth agar for 24 h at 28°C. Using

a cotton-tipped swab, fresh colonies were transferred into vials containing Inoculating Fluid A. After the density of the inoculum was adjusted to a transmittance of 95–98% (as measured using a turbidimeter), 100 μL prepared inoculum was dispensed into each well of the Biolog MicroPlate. The plate was incubated at 28°C and assayed using a MicroStation 2 Reader (Biolog) at various times.

Tolerance Features of YX3307

In experiments testing the temperature and pH range for growth, and tolerance to glucose, NaCl, ethanol, caproic acid, and EC, the cell density of YX3307 was monitored by measuring optical density at 560 nm (OD_{560}), as described in a previous report (Fan et al., 2018b). The levels of each factor in the growth and tolerance tests are shown in **Supplementary Table 2**.

Optimization of Culture Conditions

Various culture conditions (**Supplementary Table 3**), including pH, shaking speed, temperature, ethanol content, caproic acid content, inoculum age, sugar content, time of ethanol addition, inoculum size, time of caproic acid addition, and culture time, were optimized for EC production under submerged fermentation in SHM. For these analyses, we used the classical approach of altering only one variable per test, whereby a single factor was adjusted while others were kept constant. After optimization, the optimal conditions were used in subsequent fermentations. Before the yeast was inoculated into the fermentation medium, the yeast cells were activated in 30 mL YPD at 28°C for 24 h. After preculture, 0.1 mL yeast suspension (OD_{560} is about 45–50) was used to inoculate 30 mL SHM as described above. Thereafter, the EC content was determined by GC-MS.

Preliminary Study on EC Synthesis

To explore the primary mechanism of EC synthesis by the selected yeast, four groups of experiments were designed. In group A, SHM was adjusted to pH 4.3 (the lowest pH in the fermentation experiments), and ethanol and caproic acid were added at optimal times and concentrations as determined in the optimization experiments. In group B, fermentation was carried out according to the optimal conditions. In group C, fermentation was carried out according to the optimal conditions. In addition, the yeast was removed by centrifugation before adding the earlier precursor, and then fermentation proceeded according to the optimal conditions. In group D, opposite to group C, before adding the earliest precursor, the yeast was obtained and washed with saline solution, then transferred to fresh SHM for fermentation under optimal conditions. In group D, the EC content in the first fermentation broth before adding the precursor was also determined.

Characteristics of Ester Production

To systematically study the ester production characteristics of the screened yeast, ethanol and different acids (acetic acid, lactic acid, butyric acid, caproic acid, and octanoic acid) were added to the SHM as precursors. Each acid was added with ethanol separately. The selected acids were precursors of important ester compounds in *Baijiu*. The fermentation method was the same as that used to screen for yeasts with a high yield of EC. The esters in different samples were detected by GC-MS.

Aroma Production

To explore the functional characteristics of yeasts, the aroma-producing characteristics of the selected yeasts were analyzed as reported elsewhere (Fan et al., 2019). After preculture as described above, yeast cells (initial density, 1×10^6 cells/mL) were inoculated into 30 mL SHM and cultured at 28°C with shaking at 180 r/min for 72 h. Then, the sample was centrifuged at 13,000 × *g* for 10 min at 4°C. The aroma compounds in the supernatant were analyzed by headspace solid-phase microextraction-GC-MS (HS-SPME-GC-MS). Uninoculated SHM served as the control.

Analytical Methods

The OD of cells was detected at 560 nm with an ultraviolet spectrophotometer (TU-1901; Purkinje General Instrument Co., Ltd., Pinggu, Beijing, China). After pretreatment, the EC content in the fermentation medium was determined by GC-MS as reported previously (Fan et al., 2018b). Briefly, 2 mL of each sample was centrifuged, then mixed with an equal volume of heptane and incubated for 5 min. The organic phase was transferred to a centrifuge tube containing anhydrous sodium sulphite, and was kept at −20°C overnight to remove water from the sample. After filtering through a 0.45-μm nylon filter, the sample was analyzed by GC-MS. The GC-MS conditions were as follows: initial temperature, 50°C for 2 min, increased to 180°C for 2 min, then to 230°C for 2 min. The vaporization chamber temperature and the inlet temperature were 250°C, the carrier gas was high-purity helium, and a DB-WAX capillary column was used. The injection mode was split (split ratio of 37:1) and the injection volume was 1 μL. An electron impact ionization ion source with a 70 eV of electron energy was used, the scanning range was 30–550 amu, and the ion source temperature was 230°C (Fan et al., 2018b). The EC content was calculated by comparison with a calibration curve obtained by serial dilution of an EC standard solution. The aroma compounds were analyzed by HS-SPME-GC-MS according to Fan et al. (2018a) with minor changes. The aroma compounds in the fermentation mixture were extracted by 50/30-μm divinylbenzene/carboxen on polydimethylsiloxane (DVB/CAR on PDMS)-coated fibers. The 15-mL headspace vial contained (Supelco, Inc., Bellefonte, PA, United States) 5 mL supernatant, 2 g NaCl, and 10 μL of 0.5 g/L tetraoctanol solution. The vial was covered with a cap and kept in a water bath at 50°C for 10 min. Then, a SPME needle was inserted to extract aroma compounds for 30 min at 50°C. The extraction head was inserted into the GC-MS inlet for desorption at 250°C for 5 min. The GC-MS conditions were as follows: initial temperature, 40°C for 3 min, increased to 100°C for 5 min, then to 150°C for 3 min, and then to 280°C for 6 min. These analyses were conducted in the splitless mode. The mass spectra of aroma compounds with positive and negative matches higher than 800 with those from National Institute of Standards and Technology library (NIST) are reported. For each identified compound, the

amount was calculated as the ratio of the mass concentration of tetraoctanol to the mass concentration of the compound.

Statistical Analysis

Statistical differences among treatment groups were detected by one-way ANOVA ($P < 0.05$) followed by Tukey test. Assays were conducted at least in triplicate, and the reported values correspond to the mean value and its standard deviation. Data were processed and analyzed using SPSS 24.0 (IBM Corp., New York, NY, United States), OriginPro 9.1 (OriginLab, Northampton, MA, United States), and Excel 2016 (Microsoft, United States).

RESULTS AND DISCUSSION

Screening for Yeast Capable of Producing EC

A total of 147 yeasts were isolated from strong-flavor *Daqu*. Each yeast was inoculated into SHM to test its ability to produce EC. Although most yeasts were able to synthesize EC, the yield was relatively low, consistent with other reports (Wang et al., 2013). Previous studies have shown that most yeasts isolated from the *Baijiu*-producing environment can produce EC, but most of them have a low EC production capacity (Wu et al., 2013). This may explain the low EC content in strong-flavor raw *Baijiu*, and why it is necessary to prolong the fermentation period to increase the EC content. Only 19 yeasts produced EC at concentrations exceeding 0.5 g/L (**Supplementary Table 4**). Among those yeasts, strain YX3307 was chosen as the target strain for further experiments because it produced significantly more EC than did the other strains.

Identification of Yeast YX3307

After growth for 72 h at 28°C on WL agar, the colonies of strain YX3307 were milky white, flat with a little protuberance in the center, wet and smooth with an entire margin, and diameter of 2–3 mm (**Figure 1A**). Meanwhile, the WL agar changed from blue to light yellow where this strain grew (**Figure 1A**). The cells of YX3307 were fusiform to ovoid, occurring as a single cell or parental bud pairs. Asexual budding reproduction was observed at the ends of the cells as shown in **Figure 1B**.

As shown in **Table 1**, when YX3307 was fermented in the presence of glucose, D-galactose, maltose, saccharose, cellobiose, or raffinose, aerogenesis, and acid production occurred. In the presence of inulin or trehalose, only acid was produced by YX3307. The yeast YX3307 was unable to ferment lactose, melibiose, D-xylose, soluble starch, or arabinose, as indicated by the lack of acid or gas production. YX3307 readily utilized glucose, galactose, L-sorbose, cellobiose, maltose, saccharose, trehalose, melezitose, raffinose, D-ribose, L-rhamnose, D-sorbitol, glycerol, D-mannitol, ethyl alcohol, ribitol, DL-lactic acid, or D-glucosamine. It grew more slowly when lactose, inulin, L-arabinose, D-xylose, citric acid, succinic acid, D-glucuronic acid, or myricetrin was supplied as the sole carbon source. YX3307 was unable to assimilate melibiose, soluble starch, D-arabinose, erythritol, galactitol, inositol, methyl alcohol, α-methyl-glucoside, or hexadecane.

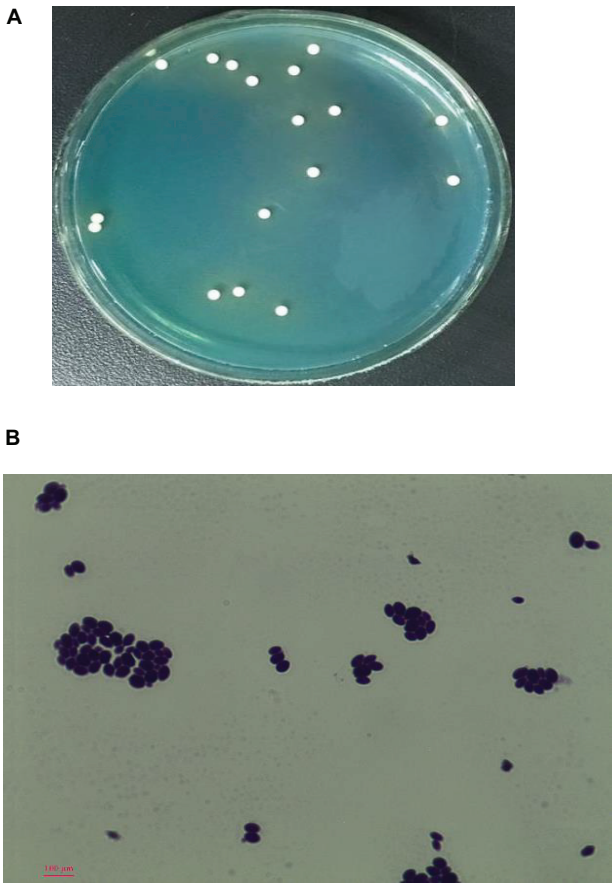

FIGURE 1 | Colony morphology on WL **(A)** and cell morphology **(B)** of strain YX3307 captured by microscopy (10 × 40). Cell was stained by the crystal violet method. The asexual budding reproduction occurred at the ends of the cells was highlighted in the blue circle.

When cadaverine dihydrochloride, ethylamine hydrochloride, L-lysine, or urea was used as the sole nitrogen source, YX3307 grew very well. It was also able to grow when potassium nitrate, L-phenylalanine, or ammonium sulfate was supplied as the sole nitrogen source. However, it could not grow in the presence of sodium nitrite or ammonium nitrite. YX3307 also grew well when supplied with test vitamins, especially thiamine (VB_1) and niacin (VB_3).

The starch hydrolysis test, methyl red test, Voges-Proskauer test, hydrogen sulfide test, tetrazolium indicator medium (TTC medium) test, citrate test, litmus milk test, gelatin liquification test, lipase activity test, canavanine-glycine-bromothymol blue (CGB) agar test, formation of extracellular amyloid compounds test, diazonium blue B color reaction and tolerance to 1% acetic acid test were negative. The indole test, urea test, melanin synthesis on L-dihydroxyphenylalanine (DOPA) medium test, and splitting of arbutin test were positive. The physiological and biochemical characteristics of YX3307 resembled those of *C. lusitaniae*, consistent with the Biolog results

TABLE 1 | Physiological and biochemical characteristics tests.

Sugar fermentation test					
Sugars	Characteristics of YX3307	Sugars	Characteristics of YX3307	Sugars	Characteristics of YX3307
D-glucose	Acid and gas production	D-galactose	Acid and gas production	D-maltose	Acid and gas production
D-saccharose	Acid and gas production	D-lactose	No acid, no gas	Inulin	Acid production, no gas
Melibiose	No acid, no gas	Cellobiose	Acid and gas production	D-xylose	No acid, no gas
D-raffinose	Acid and gas production	D-trehalose	Acid production, no gas	Soluble starch	No acid, no gas
D-arabinose	No acid, no gas				
Carbon source assimilation test					
Carbon sources	Characteristics of YX3307	Carbon sources	Characteristics of YX3307	Carbon sources	Characteristics of YX3307
D-glucose	+++	D-galactose	+++	L-sorbose	++
Cellobiose	++	D-lactose	+	D-maltose	+++
Melibiose	–	D-saccharose	++	D-trehalose	+++
Melezitose	++	D-raffinose	++	Inulin	+
Soluble starch	–	D-arabinose	–	L-arabinose	+
D-ribose	++	L-rhamnose	++	D-xylose	+
Erythritol	–	Galactitol	–	D-sorbitol	+++
Glycerol	++	Inositol	–	D-mannitol	+++
Ethyl alcohol	++	Ribitol	++	Methyl alcohol	–
Citric acid	+	DL-lactic acid	++	Succinic acid	+
D-glucuronic acid	+	α-methyl-glucoside	–	Myricetrin	+
D-glucosamine	++	Hexadecane	–		
Nitrogen source assimilation test					
Nitrogen sources	Characteristics of YX3307	Nitrogen sources	Characteristics of YX3307	Nitrogen sources	Characteristics of YX3307
Potassium nitrate	+	Cadaverine dihydrochloride	+++	Ethylamine hydrochloride	++
Sodium nitrite	–	L-phenylalanine	+	L-lysine	+++
Urea	++	Ammonium sulfate	+	Ammonium nitrite	–
Vitamin requirement test					
Riboflavin	++	Folic acid	++	Pyridoxine hydrochloride	++
Myo-inositol	++	Calcium pantothenate	++	Thiamine	+++
Niacin	+++	*p*-aminobenzoic acid	++	Biotin	++

(Continued)

TABLE 1 | Continued

Sugar fermentation test					
Other tests					
Starch hydrolysis test	–	Methyl red test	–	Indole test	+
Voges-Proskauer test	–	Hydrogen sulfide test	–	Urea test	+
TTC medium test	–	Citrate test	–	Litmus milk test	–
Gelatin liquidized test	–	Lipase activity test	–	CGB agar test	–
Formation of extracellular amyloid compounds test	–	Diazonium blue B color reaction	–	Tolerance of 1% of acetic acid test	–
DOPA medium test	+	Splitting of arbutin test	+	Actinomycin tolerance test	0–25 μg/mL
Sodium chloride osmolarity test	0–15% (w/v)	Glucose osmolarity test	0–80% (w/v)	Caproic acid tolerance test	0.06% (v/v)
Ethanol tolerance test	0–6% (v/v)	Growth temperature range	15–50°C (optimum 25°C)	Growth pH range	1.0–11.0 (optimum pH 6.0)
Ethyl caproate tolerance test	0–1200 mg/L				

"+," positive response, the more the plus sign indicated the more positive it is; "–," negative response.

(**Supplementary Figure 1**). These analyses of the physiological and biochemical characteristics of YX3307 provided information about its metabolic spectrum, and consequently, its potential functions.

After amplification and sequencing a 26S rDNA fragment from YX3307, the sequence was submitted to NCBI database[1] under the accession number MW440554, and searches were conducted to find the closest homolog. The fragment showed 100% sequence similarity with the partial 26S rDNA sequence from *C. lusitaniae* ACE6 (EF063129.1). As shown in the phylogenetic tree, YX3307, *C. lusitaniae* MB141 (KF830171.1) and *C. lusitaniae* GSWW10 (EF536910.1) clustered into a branch, indicating that they were very closely related (**Supplementary Figure 2**).

According to its morphological, physiological, and biochemical characteristics, and based on the results of the Biolog and molecular analyses, YX3307 was identified as *C. lusitaniae*. Previous studies have shown that *C. lusitaniae* occurs in a broad of substrates of plant and animal origin, as well as in wastes and clinical specimens (Zhang et al., 2010). Although *C. lusitaniae* was first reported by Pappagianis et al. (1979), few studies have focused on this yeast (1979). *C. lusitaniae* in strong-flavor *Baijiu* was first reported by Wei et al. (2013), but has subsequently been isolated from other flavors of *Baijiu*. Although some analyses of microbial diversity in *Baijiu* have noted the presence and importance of *C. lusitaniae* (Wen and Li, 2018; Cui X. L. et al., 2019; Du et al., 2019; Zhou et al., 2020), few studies have explored its function in *Baijiu*, especially its role in EC production.

Tolerance Features of YX3307

The *Baijiu* brewing environment is complex, and the pH, temperature, water activity, and contents of ethanol and other compounds change during the fermentation time. These factors affect the growth and reproduction of microorganisms in this environment. The microorganisms that can survive in this environment have certain adaptive characteristics. Therefore, we analyzed the tolerance of yeast YX3307 to provide a reference for its application in *Baijiu* brewing. As shown in **Table 1**, YX3307 showed good environmental adaptability because of its tolerance features. YX3307 was able to grow in the presence of a certain amount of actinomycin; the maximum tolerable concentration was 25 μg/mL. This indicated that YX3307 has some ability to adapt to the presence of other microorganisms, especially actinomycetes, in the *Baijiu* brewing environment. YX3307 was also tolerant to high temperature (growth was observed at 50°C) and was able to grow over a wide pH range (pH 1–11), indicating that this strain can adapt to the changing conditions during the *Baijiu* brewing process. YX3307 also showed strong tolerance to osmotic pressure, and was able to grow in media containing 80% (w/v) glucose and 15% (w/v) NaCl. To explore its ability to synthesize EC, the tolerance of the strain to the precursors, ethanol and caproic acid, and the product, EC, was analyzed. YX3307 was able to tolerate EC at 1,200 mg/L, indicating that it had the potential for high EC production. However, its tolerance

[1] https://www.ncbi.nlm.nih.gov/

to ethanol and caproic acid was relatively low [6% (v/v) and 0.06% (v/v), respectively]. Therefore, to improve EC production, YX3307 could be co-fermented with *Saccharomyces cerevisiae* and caproic acid-producing bacteria, as the yield of EC would increase by the rapid and continuous conversion of ethanol and caproic acid produced by these microorganisms.

Characteristics of Ester Production

Esters are important flavor compounds in *Baijiu*, and 506 of them have been detected in *Baijiu* to date (Liu and Sun, 2018). Among these esters, ethyl acetate, ethyl lactate, ethyl butyrate, and EC are the main four ethyl esters, and ethyl octanoate is the most important (Fan et al., 2018b; Ma et al., 2020). Although these five ester compounds are present at varying proportions in strong-flavor *Baijiu*, the EC content is low, while those of ethyl lactate and ethyl acetate are generally higher than the standard requirements for strong-flavor *Baijiu*. As a result, the proportion of ester compounds in the raw *Baijiu* is inconsistent, so that it does not meet the standard requirements of strong-flavor *Baijiu*. Now, producers of strong flavor *Baijiu* have dual goals to increase the EC content and decrease the ethyl acetate/ethyl lactate contents (Li J. H. et al., 2019; Song et al., 2019). To explore the ester production characteristics of YX3307, it was inoculated into media containing different precursors (five different acids and ethanol). The results showed that YX3307 mainly synthesized EC and produced a small amount of ethyl acetate, while the other three ester compounds were not detected (**Supplementary Table 5**). Therefore, YX3307 specifically produces EC. Even when YX3307 produced a large amount of EC, there was no increase ethyl lactate synthesis and very little ethyl acetate was produced. This feature is conducive to solving the current problem of producing strong-flavor *Baijiu* with a low EC content and high content of ethyl acetate/ethyl lactate.

Optimization of Culture Conditions

In strong-flavor *Baijiu*, EC is the important flavor compound. Sorghum is the main raw material of *Baijiu* brewing. Therefore, SHM was used as the initial fermentation medium to optimize the conditions for YX3307 to produce EC in submerged fermentation.

Effect of pH on EC Production

The pH can affect the permeability of yeast cell membranes and the activity of metabolic enzymes. Yeasts employ different metabolic reactions to adapt to the environmental pH. The growth of yeast cells and the type and yield of metabolites vary under different pH conditions (Mattey, 1992). The synthesis of fermentation products can be regulated by adjusting the pH value during fermentation. Therefore, the effect of the initial pH of SHM on the production of EC by yeast YX3307 was investigated. As shown in **Supplementary Figure 3**, the yield of EC increased first and then decreased as the initial pH of SHM increased. The highest yield of EC was at pH 6, consistent with the optimum pH for YX3307 (**Table 1**). The yield of EC from YX3307 was slightly higher when the initial pH was alkaline than when the initial pH was acid, because alkaline conditions favored the growth of YX3307. In general, the initial pH of SHM that favored yeast growth also favored EC synthesis; that is, there was a positive correlation between yeast cell growth and EC synthesis as mentioned previously (Dufour et al., 2003). In previous studies, EC was mainly synthesized by a chemical reaction between caproic acid and ethanol when the initial pH of the medium was less than 3 (Zhang et al., 2017). Therefore, if the EC produced at pH 2 or 3 was attributed to chemical synthesis, then less EC was yielded from chemical synthesis than from yeast-catalyzed synthesis (comparing yields between pH 2–3 and 4–9). When the initial pH of SHM was 6.0, the pH value of the fermentation broth was 4.3 at the end of fermentation, consistent with previous report that pH 4.0–4.5 is optimum for EC synthesis via esterification in *Daqu* (Zhang et al., 2017). The initial pH of 6.0 favored the growth of YX3307, and its metabolic activity modified the pH of the growth environment so that it was conducive to EC synthesis. Therefore, the best initial pH of SHM for EC synthesis by YX3307 was 6.0. These results indicate that EC is mainly synthesized by the metabolic processes of YX3307.

Effect of Shaking Speed on EC Production

Yeasts are facultative anaerobic microorganisms, and their metabolic pathways differ between aerobic and anaerobic conditions (Panozzo et al., 2002). Previous reports have shown that the types and amounts of metabolites are affected by the amount of dissolved oxygen (Barberel and Walker, 2000). The dissolved oxygen level was regulated by changing the shaking speed to explore its effect on the synthesis of EC by YX3307. As shown in **Supplementary Figure 4**, EC was produced by YX3307 in the static or shaking state, with higher production levels in the static state than in the shaking state, regardless of the amount of shaking. This differs from the synthesis of ethyl acetate by *Wickerhamomyces anomalus* described in our previous study, where the yield of ethyl acetate was larger in the shaking state than in the static state, and larger with a higher shaking rate than with a low shaking rate (Fan et al., 2018b). These different responses to dissolved oxygen levels are because of the different synthesis mechanisms of ethyl acetate and EC in *W. anomalus* and *C. lusitaniae*. The high yield of ethyl acetate from *W. anomalus* under high dissolved oxygen levels is due to the increased amount of acetyl coenzyme A, the precursor that is converted into ethyl acetate by acyltransferase (Fu et al., 2018). However, in *C. lusitaniae*, low dissolved oxygen levels result in the accumulation of long-chain saturated fatty acids and the inhibition of acetyl CoA carboxylase. Subsequently, acyl CoAs are released from fatty acid synthase, leading to the accumulation of medium-chain fatty acyl CoAs, which increases EC synthesis under low dissolved oxygen levels (Dufour et al., 2003). The biomass of YX3307 was lower in the static state than in the shaking state, and it was higher at high shaking speed (**Supplementary Figure 5**). Considering the difference in biomass, the dissolved oxygen level more strongly affected EC synthesis by YX3307 than did pH (**Supplementary Figure 5**). Lower dissolved oxygen levels were conducive to EC synthesis, indicating that this yeast is well-suited for producing EC in the anoxic solid-state fermentation environment of *Baijiu*.

Effect of Temperature on EC Production

A previous experimental study showed that temperature affects the number of esters profile (Dufour et al., 2003). As shown in **Supplementary Figure 6**, the yield of EC first increased and then decreased as the temperature increased. The highest yield of EC was 6.8 mg/L at 20°C. Similar to the effect of dissolved oxygen on EC production, the optimal temperature for EC production was not the optimal temperature for growth of YX3307, nor was it the optimal temperature reported for ethyl acetate synthesis in *W. anomalus* (Fan et al., 2018b). The number of acetate esters increased with increasing temperature, but the number of medium-chain fatty acid esters was not affected, consistent with the results of a previous report (Engan and Aubert, 1977). This provided further evidence that the biosynthesis pathways of the two esters in the two yeasts are different. It is likely that the increased level of acetate esters at higher temperatures is related to the increase in higher alcohols synthesis and alcohol acetyltransferase activity with increased yeast growth, while stimulation of yeast growth prevents acyl CoA accumulation and does not result in increased MCFA esters contents (Dufour et al., 2003). Although a lower temperature was not conducive to the growth of YX3307, it was beneficial for EC biosynthesis.

Effect of Ethanol Content on EC Production

Ethanol is one of the precursors of EC, which is synthesized by an esterifying enzyme. Although YX3307 could produce a little ethanol in SHM, it was insufficient to meet the needs of EC synthesis. Therefore, ethanol was added into SHM to increase EC production. The results showed that the yield of EC first increased and then decreased as the ethanol content in the medium increased (**Figure 2**). The highest yield of EC was 7.8 mg/L when the ethanol content in the medium was 10%. When less ethanol or no ethanol was added, substantially less EC was produced. This indicated that YX3307 needed ethanol to produce EC. During the *Baijiu* brewing process, YX3307 can produce EC because ethanol is produced by some other microorganisms, such as *S. cerevisiae*. However, a high ethanol content can reduce the synthesis of EC by inhibiting cell growth and enzyme activity. Interestingly, EC synthesis was highest when the ethanol content was slightly higher than the level tolerated by YX3307 (**Figure 2** and **Table 1**). This may be because sufficient biomass of YX3307 accumulated at the early stage before ethanol was added. More importantly, low temperature and dissolved oxygen conditions favored the metabolic pathway of EC synthesis, so that ethanol and caproic acid could be quickly converted into EC before having toxic effects on YX3307 (**Table 1**). High temperature or aerobic conditions affected YX3307's tolerance to ethanol (Piper, 1995). YX3307 could tolerate a higher ethanol concentration after optimization of temperature and dissolved oxygen content. That is, the toxicity of ethanol to YX3307 was reduced under low temperature and dissolved oxygen content.

Effect of Caproic Acid Content on EC Production

Because a rate-limiting step in EC synthesis is the abundance of caproic acid, it is an important precursor for EC synthesis by YX3307 (Takahashi et al., 2017). The effect of caproic acid on EC production by YX3307 was similar to that of ethanol,

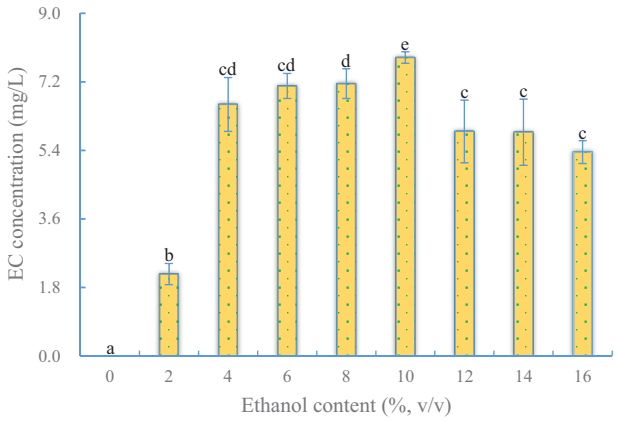

FIGURE 2 | Effect of ethanol content on EC production by YX3307. Same letters in the column indicates that the data do not differ significantly at 5% probability by the Tukey test.

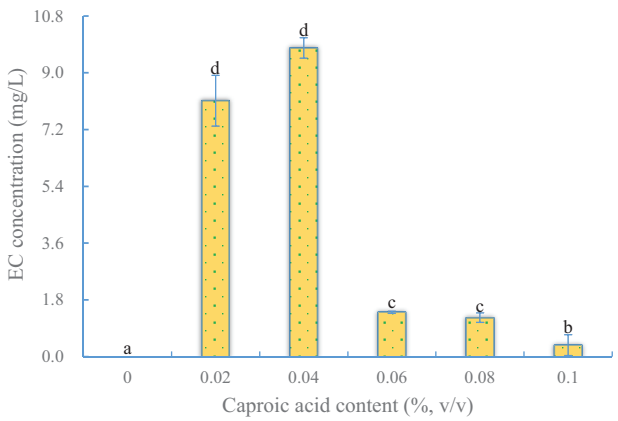

FIGURE 3 | Effect of caproic acid content on EC production by YX3307. Same letters in the column indicates that the data do not differ significantly at 5% probability by the Tukey test.

in that the yield of EC increased first and then decreased as the caproic acid content in the medium increased (**Figure 3**). The optimal caproic acid content for EC production by YX3307 was 0.04% (v/v). This is less than that in another study, and this may reflect differences in caproic acid tolerance between *S. cerevisiae* Y-E and YX3307 (Yuan et al., 2015). In addition, less EC was produced when the caproic acid content was too low or too high because of the lack of precursor or the inhibition of yeast cells, respectively. No EC was produced when no caproic acid was added, different from the case of ethyl acetate production by aroma-producing yeast. This provided further evidence that the pathways of EC synthesis and ethyl acetate synthesis are different in aroma-producing yeast (Fan et al., 2018b).

Effect of Inoculum Age on EC Production

Physiological activity differs among cells of different ages, and this affects the types and amounts of metabolites produced.

As shown in **Supplementary Figure 7**, the yield of EC from XY3307 first increased and then decreased as the inoculum age increased. The cells were mainly in the delayed phase before 6 h, during which cells were accumulating enzymes and intermediate metabolites for growth. In addition, the cell density was lower at this stage (**Supplementary Figure 8**). When cells in this phase were inoculated into SHM, there was a smaller number of cells and their vitality was low. Therefore, after 24 h of culture, there were fewer cells to produce EC. The cells were in the early and middle stages of the logarithmic period during 6–18 h. Although their metabolism was vigorous, the total number of cells was insufficient. Therefore, the yield of EC was still low when cells at these stages were used as the inoculum. During 18–30 h, the cells were in middle and late stages of the logarithmic growth period. At this stage, their metabolism was vigorous and the number of cells was sufficient. When cells at this stage were inoculated into SHM, the highest EC yield was obtained. The cells were in the stable growth phase and declining growth period at 30–42 and 42–54 h, respectively. At these stages, their metabolic activity was lower than that of cells at metaphase of logarithmic growth and the number of cells was insufficient, leading to decreased EC yields.

Effect of Sugar Content on EC Production

Glucose, maltose, and a small amount of dextrin are produced from sorghum materials after treatment with amylase and glucosidase. These carbon sources provide energy not only for growth, but also for metabolic processes that produce esters and other compounds. The Brix value is an index of the soluble sugars content of sorghum after enzymatic hydrolysis. The higher the Brix value, the higher the soluble sugars content in SHM. The yield of EC by YX3307 was low when the sugar content was low (data not shown), because the synthesis of intermediate metabolites and the expression of enzymes related to ester synthesis was limited, and there was limited growth and reproduction of yeast cells. As the sugar content increased, the cell biomass, concentration of metabolic intermediates, and expression of enzymes related to ester synthesis increased, leading to higher yields of EC. When the sugar content was 10 Brix, the highest yield of EC was 17.0 mg/L. As the sugar content increased beyond 10 Brix, the EC yield did not change significantly. Therefore, a sugar content of 10 Brix was used in subsequent experiments.

Effect of Time of Ethanol Addition on EC Production

To determine the effect of the timing of ethanol addition on EC production by YX3307, caproic acid was added at 24 h of culture, and ethanol was added at different time points as shown in **Supplementary Table 3**. Once any kind of precursor was added, the culture was kept in static and low-temperature conditions (20°C) to reduce the toxic effect of precursors on cells. After both the precursors were added, the fermentation was continued for 36 h. The results are shown in **Figure 4**. No EC was produced when ethanol was added before 16 h. This is not only because of the short fermentation period, but also because yeast cells were in the lag phase and logarithmic prophase (**Supplementary Figure 5**). During this period, EC could not be synthesized by YX3307 because of the toxicity of ethanol to cells (**Figure 4**). When yeast cells were in metaphase of logarithmic growth, the later phase of logarithmic growth, and the stable growth phase, they could tolerate a certain amount of ethanol. Therefore, they could convert the precursors (ethanol and caproic acid) into EC. The yield of EC was high when ethanol was added at metaphase and the later phase of logarithmic growth. A high yield of EC (27.0 mg/L) was obtained when ethanol was added at 32 h.

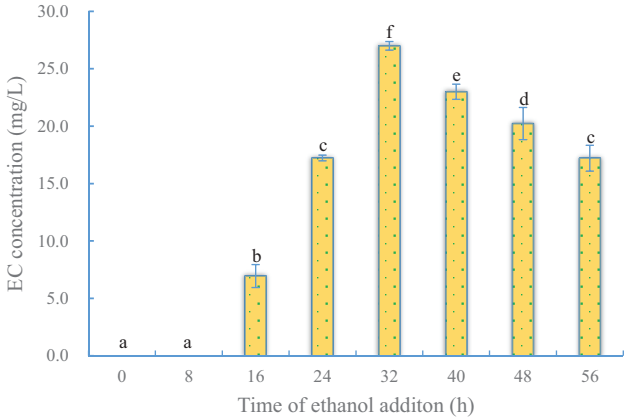

FIGURE 4 | Effect of time of ethanol addition on EC production by YX3307. Same letters in the column indicates that the data do not differ significantly at 5% probability by the Tukey test.

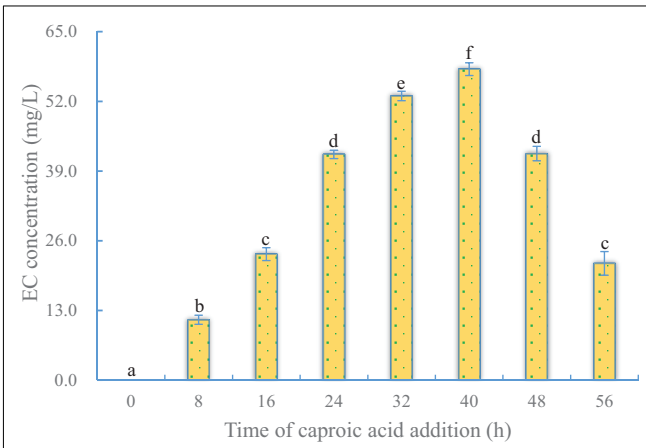

FIGURE 5 | Effect of time of caproic acid addition on EC production by YX3307. Same letters in the column indicates that the data do not differ significantly at 5% probability by the Tukey test.

Effect of Inoculum Size on EC Production

Although there is little information available about the influence of inoculum size on ester synthesis, the results of a previous experimental study indicated that EC synthesis by

YX3307 requires a sufficient biomass of cells in the optimal growth phase (Dufour et al., 2003). Therefore, the effect of inoculum size on the synthesis of EC by YX3307 was determined. There was no significant change in the yield of EC when the inoculum size was between 0.1 and 0.33% of the total volume (data not shown). As the inoculum size increased, the synthesis of EC also increased, and the highest production of EC (42.7 mg/L) was achieved with an inoculum size of 7.5%. With this inoculum size, the cell biomass was sufficient, the amount of harmful substances produced by YX3307 was small, and cells were metabolically active. In addition, the nutrient composition in the SHM was relatively rich. Cells can resist the toxic effect of precursors, such as caproic acid, and convert them into EC. However, as the inoculum size increases, the nutrients in SHM would be consumed too early because of the large biomass, and some harmful metabolites would be produced. This would reduce the ability of cells to resist precursors, leading to a decrease in the yield of EC. A larger inoculum would allow the yeast to resist the toxic effects of higher concentrations of precursors, which explains why the optimum inoculation size in this study was larger than that in most previous reports.

Effect of Timing of Caproic Acid Addition on EC Production

Just as the time point of ethanol addition was important for EC production, so was the time point of caproic acid addition. To test the effect of the timing of caproic acid addition on EC production, ethanol was added to the fermentation system at 32 h, while caproic acid was added at different times (**Supplementary Table 3**). Like in the case of ethanol addition, when caproic acid was added at the beginning, no EC was detected by 36 h after addition, indicating that the cells were sensitive to caproic acid at the early stage of fermentation. Higher yields of EC were obtained when caproic acid was added to cells at the middle and late logarithmic growth stage and the stable phase. The optimum time of caproic acid addition (40 h) was later than the optimum time for ethanol addition, because caproic acid was more toxic to cells than was ethanol (**Figure 5** and **Table 1**).

Effect of Culture Time on EC Production

The time course of EC synthesis by YX3307 is shown in **Figure 6**. No EC was detected during 0–32 h, during which no precursors were added. That is, YX3307 could not synthesize EC without precursors. No EC was detected between 32–40 h when ethanol, but not caproic acid, was present, consistent with the results of previous studies (**Figure 3**). These results showed that the synthesis of EC by YX3307 differs from the synthesis of ethyl acetate by *W. anomalus* (Fan et al., 2018b). After adding caproic acid, EC production increased and then decreased over time. The production of EC was highest between 56 and 88 h, during which the highest yield was 62.0 mg/L at 72 h. Thus, compared with other reported EC-producing

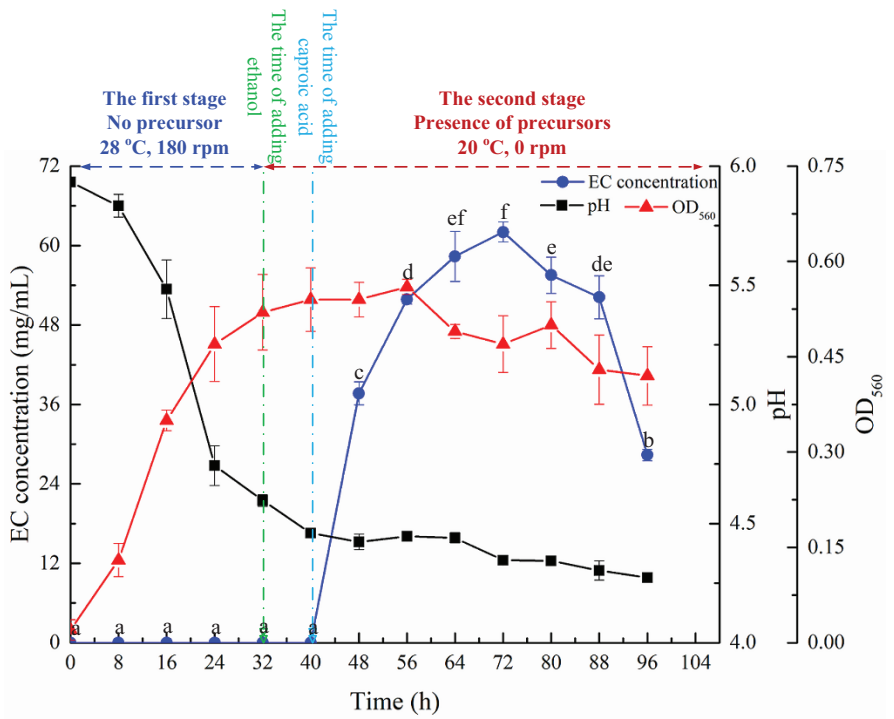

FIGURE 6 | Effect of culture time on EC production by YX3307. Same letters in the column indicates that the data do not differ significantly at 5% probability by the Tukey test.

yeast strains, YX3307 has obvious advantages in terms of yield (**Table 2**).

Preliminary Study on EC Synthesis

Four groups of tests were designed to preliminarily analyze the mechanism of EC synthesis by YX3307. The results are shown in **Supplementary Figure 9**. The pH value of SHM decreased when YX3307 consumed the soluble sugars. The lower pH conditions may have favored the formation of EC by the chemical reaction (esterification) between ethanol and caproic acid. However, no EC was detected in group A, indicating that EC was not produced by ethanol and caproic acid during fermentation with YX3307. The highest yield (61.7 mg/L) of EC was obtained in group B. By comparing the results from groups A and B, it can be concluded that EC is synthesized via a metabolic process, that is, the result of enzymatic catalysis, as was also confirmed in the previous optimization results. Compared with group B, group C produced little EC (0.1 mg/L), indicating that YX3307 produced almost no extracellular enzyme to convert ethanol and caproic acid to EC without precursors. In other words, the enzyme that catalyzes the synthesis of EC from ethanol and caproate acid by YX3307 was induced after addition of precursors, and/or was located inside the cell or on the cell membrane. In group D, some EC (3.8 mg/L) was detected in the presence of precursors after cells were added to new SHM. The higher yield in group D than in group C suggested that an extracellular enzyme for EC synthesis was induced by ethanol and caproic acid, or that the catalytic enzyme was located intracellularly or on the cell membrane. The EC yield was lower in group D than in group B, which may be due to the interference of cell treatments. These findings, combined with the results of the optimization of fermentation conditions, suggest that the enzyme that synthesizes EC is located intracellularly or on the cell membrane. A previous study demonstrated the importance of ethanol hexanoyl transferase in EC production (Lilly et al., 2006; Saerens et al., 2006; Chen et al., 2014). Precious studies have indicated that the alcohol acyltransferases EEB and EHT are the two most important enzymes for EC synthesis (Saerens et al., 2006; Takahashi et al., 2017). Although only two alcohol acyltransferases have been identified to synthesize EC so far, there may be other enzymes that synthesize EC in yeasts, and the key enzymes for EC synthesis may differ among different in different strains (Saerens et al., 2006). Thus, further studies are needed to clarify the intrinsic mechanism of EC synthesis by YX3307. The results of the present

TABLE 2 | Summary of yeasts reported for EC yield.

Strain	Origin	EC Yield (mg/L)	Year	References
Hanseniaspora uvarum Yun268	Grapery	0.021	2018	Hu et al., 2018
*Saccharomyces cerevisiae*α5	–	0.5	2016	Chen et al., 2016
Saccharomyces cerevisiae 102SC	*Ziziphus mauritiana* fruits	110	2013	Nyanga et al., 2013
Saccharomyces cerevisiae 131SC		28.7		
Saccharomyces cerevisiae 153SC		92.0		
Saccharomyces cerevisiae 143SC		28.6		
Saccharomyces cerevisiae 135SC		21.3		
Saccharomyces cerevisiae 38SC		23.2		
Pichia kudriavzevii 125PK		1.4		
Pichia kudriavzevii 129PK		2.5		
Pichia kudriavzevii 166PK		2.5		
Pichia fabianii 65PF		1.3		
Saccharomycopsis fibuligera 66SF		1.8		
Issatchenkia orientalis W8Y-21	*Baijiu*-making workshop air	2.94 (g/L, after distilled of fermented grain)	2013	Wang et al., 2013
Debaryomyces hansenii G8M-28		3.10 (g/L, after distilled of fermented grain)		
Debaryomyces hansenii S532Y-20	Fermented grain	4.86 (g/L, after distilled of fermented grain)		
Debaryomyces hansenii S442Y-44		4.87 (g/L, after distilled of fermented grain)		
Debaryomyces hansenii Z8Y-13	*Baijiu*-making workshop air	7.50 (g/L, after distilled of fermented grain)		
Zygosaccharomyces bailii H1Y-24	Pit mud	2.53 (g/L, after distilled of fermented grain)		
Issatchenkia orientalis S433Y-17	Fermented grain	2.54 (g/L, after distilled of fermented grain)		
Trichosporon coremiiforme Z8Y-32	*Baijiu*-making workshop air	2.56 (g/L, after distilled of fermented grain)		
Saccharomyces cerevisiae	*Baijiu* distillery	0.21	2013	Wu et al., 2013
Galactomyces geotrichum		0.005		
Kazachstania exigua		0.13		
Schizosaccharomyces pombe		0.38		
Saccharomyces cerevisiae Kyokai no. 7	–	1.0	2004	Aritomi et al., 2004
Hansenula mrakii IFO 0895	–	0.03 mg/kg	1994	
Clavispora lusitaniae YX3307	*Daqu*	62.0	2020	This study

"–," no details.

study provide an important experimental basis for studying EC biosynthesis.

Aroma Production

A total of 30 flavor compounds were detected by SPME-GC-MS in SHM after fermentation of YX3307 for 72 h. These flavor compounds included 12 alcohols, nine esters, two aldehydes, one phenol, one acid, one furan, three alkanes, and one ketone. Only 10 flavor compounds were detected in SHM, namely, one alcohol, four esters, one aldehyde, one furan, one ketone, and two other compounds (**Supplementary Table 6**). After comparing the flavor compounds between SHM and SHM fermented by YX3307, we concluded that: (i) the types and amounts differed between the two groups, with only four flavor compounds in both of them; (ii) six flavor compounds in SHM were not detected after culture with YX3307, indicating that they were metabolized and transformed into other flavor compounds; (iii) the 26 new flavor compounds in SHM were produced by activities of YX3307 using sugars or other nutrients as substrates; (iv) the contents of the four flavor compounds found in both groups were higher after fermentation with YX3307 because of its activity. Therefore, YX3307 can produce many volatile flavor compounds in SHM. Like other aroma-producing yeasts, YX3307 can also produce some higher alcohols, esters, aldehydes, and other flavor compounds, which can give alcoholic drinks unique characteristics (Bruner and Fox, 2020). Isobutanol, isoamyl alcohol, and furfuralcohol are important higher alcohols in *Baijiu*. When their content is less than 30 mg/L, they can impart sweetness and enhance the fragrance of other flavor compounds (Luo et al., 2015). They are also important precursors of other flavor compounds (Fan et al., 2019). There are few reports about linalool in *Baijiu*, but it is an important flavor compound in wine, conferring bergamot, lavender, and rose floral notes due to it relatively low odor perception thresholds (15 μg/L) (Li Z. H. et al., 2019; Lukic et al., 2020; Zhang X. Y. et al., 2020). Other yeasts and fungi also can produce linalool, which imparts a tea-flavor to *Baijiu* (Cui X. X. et al., 2019; Fan et al., 2019). 3-Methylthiopropanol, which has onion and meat odors, is an important contributor to the sesame aroma of *Baijiu* (Hong et al., 2020). Although YX3307 produced only small amounts of 3-methylthiopropanol, its olfactory threshold is very low. Thus, YX3307 can contribute to several characteristic flavors of *Baijiu*. (R)-(+)-β-Citronellol, geraniol bisabolol, and *trans*-nerolidol are important monoterpenols in wines and beer, and they are also present in *Baijiu* (Fan and Xu, 2013; Quan et al., 2013; Lukic et al., 2020). These terpenes can not only endow *Baijiu* with unique floral and fruit aromas, but also reduce the harm of ethanol (Sun et al., 2016; Li Z. H. et al., 2019). Some microorganisms can synthesize terpenes in the *Baijiu* fermentation environment, such as *S. cerevisiae* YF1914, *Eurotium chevalieri* CICC 41584, and YX3307 (as demonstrated in this study) (Cui X. X. et al., 2019; Fan et al., 2019). These microorganisms have potential applications in technologies to improve the health properties, flavor, and quality of *Baijiu* (Cui X. X. et al., 2019; Zhang Y. J. et al., 2020). Phenethyl alcohol with honey, spice, rose, and lilac flavors is an important flavor compound in many fermented products (Lin et al., 2020). The tastes of consumers change over time, and modern consumers tend to prefer slightly sweet, low-alcohol *Baijiu* (Han et al., 2013). YX3307 has potential applications in the development of sweet *Baijiu* because it has a high yield of phenethyl alcohol. From the aspect of ester production, YX3307 did not produce EC in the absence of caproic acid, but it produced only a small amount of ethyl acetate when acetic acid was not added. In addition, it produced phenylethyl acetate, which has a floral aroma, and 2-methyl butyric acid-2-ethyl phenyl ester, which has a tea aroma (Chen et al., 2018; Wei et al., 2020). YX3307 also produced benzaldehyde, 2, 4-dimethylbenzaldehyde, and 2, 3-dihydrobenzofuran in SHM. Previous studies have reported that benzaldehyde with almond and burnt-sugar flavors and a high odor intensity makes a major contribution to the caramel aroma of *Baijiu* (Yu et al., 2019). Similar to phenethyl alcohol, benzaldehyde is related to the sweet attributes of alcoholic drinks (Yu et al., 2019). The style of *Baijiu* is also affected by 2, 4-dimethylbenzaldehyde, which imparts an almond flavor, and 2, 3-dihydrobenzofuran, which imparts an oily incense flavor (Wu, 2008; Gao et al., 2014). In summary, the advantages of YX3307 are that it can synthesize EC and improve the flavor and quality of *Baijiu*.

CONCLUSION

A yeast with high yield of EC was isolated from *Daqu*, and was identified as *C. lusitaniae*. The strain showed high tolerance to sodium chloride, glucose, and EC, and showed outstanding advantages in terms of EC synthesis. The highest yield of EC (62.0 mg/L) was obtained under the following conditions: culture of YX3307 for 32 h in SHM at 28°C with shaking at 180 rpm, followed by addition of 10% anhydrous ethanol, fermentation at 20°C in the static state, addition of 0.04% caproic acid at 40 h of culture, then fermentation until 72 h. The brix value of the medium was 10° and the initial pH was 6.0, the inoculum age was 30 h, and the inoculum size was 7.5%. YX3307 can also produce many other flavor compounds, such as β-phenethyl alcohol and terpenes, which are considered to be important for *Baijiu* quality. *C. lusitaniae* YX3307 has potential applications to improve the quality of *Baijiu*. For example, *Daqu* rich in *C. lusitaniae* YX3307 could be preparation for *Baijiu* production, and the fermentation process could be modified to favor the growth of *C. lusitaniae* YX3307 to obtain raw *Baijiu* with a high EC content.

DATA AVAILABILITY STATEMENT

The original contributions generated for this study are included in the article/**Supplementary Material**, further inquiries can be directed to the corresponding author.

AUTHOR CONTRIBUTIONS

GF and PL performed the experiments, analyzed the data, and wrote the manuscript. XC, HY, and YG helped to modify the graphs. LC and CT assisted the manuscript checking. XL provided assistance and guidance throughout the research. All authors contributed to the article and approved the submitted version.

FUNDING

This research was supported by the National Natural Science Foundation of China (Nos. 31830069, 31701592, and 31671798), Beijing Municipal Natural Science Foundation and Beijing Municipal Education Commission (No. KZ202010011018), and Quality Construction of Talent Training-First Class Specialty Construction-Food Science and Engineering (at the beginning of year) (No. 19002020119).

ACKNOWLEDGMENTS

We thank Jennifer Smith, for editing the English text of a draft of this manuscript.

SUPPLEMENTARY MATERIAL

The Supplementary Material for this article can be found online at: https://www.frontiersin.org/articles/10.3389/fmicb.2021.663744/full#supplementary-material

REFERENCES

Arikawa, Y., Yamada, M., Shimosaka, M., Okazaki, M., and Fukuzawa, M. (2000). Isolation of sake yeast mutants producing a high level of ethyl caproate and/or isoamyl acetate. *J. Biosci. Bioeng.* 90, 675–677. doi: 10.1263/jbb.90.675

Aritomi, K., Hirosawa, I., Hoshida, H., Shiigi, M., Nishizawa, Y., Kashiwagi, S., et al. (2004). Self-cloning yeast strains containing novel FAS2 mutations produce a higher amount of ethyl caproate in Japanese sake. *Biosci. Biotech. Bioch.* 68, 206–214. doi: 10.1271/bbb.68.206

Barberel, S. I., and Walker, J. (2000). The effect of aeration upon the secondary metabolism of microorganisms. *Biotechnol. Genet. Eng. Rev.* 17, 281–323. doi: 10.1080/02648725.2000.10647996

Bruner, J., and Fox, G. (2020). Novel non-*Cerevisiae saccharomyces* yeast species used in beer and alcoholic beverage fermentations. *Fermentation* 6:116. doi: 10.3390/fermentation6040116

Chen, L., Lin, Q. X., Zhang, Y. G., Chen, J., Wang, L. L., Yu, W. Q., et al. (2018). Aroma profiling of tieguanyin oolong tea with different flavor characteristics based on chemical pattern recognition. *J. Tea Sci.* 38, 253–262. doi: 10.13305/j.cnki.jts.2018.03.005

Chen, Y. F., Li, F., Guo, J., Liu, G. X., Guo, X. W., and Xiao, D. G. (2014). Enhanced ethyl caproate production of Chinese liquor yeast by overexpressing EHT1 with deleted FAA1. *J. Ind. Microbiol. Biot.* 41, 563–572. doi: 10.1007/s10295-013-1390-3

Chen, Y. F., Luo, W. W., Gong, R., Xue, X. X., Guan, X. Y., Song, L. L., et al. (2016). Improved ethyl caproate production of Chinese liquor yeast by overexpressing fatty acid synthesis genes with OPI1 deletion. *J. Ind. Microbiol. Biot.* 43, 1261–1270. doi: 10.1007/s10295-016-1795-x

China Light Industry Press, and People's Republic of China Professional Standard (2006). *Strong flavour Chinese spirits (GB/T 10781.1-2006), General Administration of Quality Supervision, Inspection and Quarantine of the People's Republic of China and Standardization Administration of the People's Republic of China*. Beijing: China Light Industry Press, 1–5.

Cui, X. L., Shao, X. B., Zhong, H. P., Ge, Y., Yang, Y., and Zhang, H. (2019). Diversity analysis of cultivatable yeasts and screening of high-quality functional yeasts during the production of multi-grain strong-flavor Baijiu. *China Brew.* 38, 105–110. doi: 10.11882/j.issn.0254-5071.2019.07.021

Cui, X. X., Bai, F. R., Yu, X. J., Bai, X. B., Xu, L., Yu, P. P., et al. (2019). Aroma characteristics of Eurotium chevalieri CICC 41584 and its application in aroma Baijiu Daqu production. *Food Ferment. Ind.* 45, 60–67. doi: 10.13995/j.cnki.11-1802/ts.021012

Du, G., Lu, X. K., Zhan, M. T., Lou, S. Z., Chen, J., and Yang, H. Y. (2019). Isolation and identification of yeasts from Koji and the primary study on fruit wine fermentation. *Food Res. Dev.* 40, 8–13. doi: 10.12161/j.issn.1005-6521.2019.15.002

Dufour, J. P., Malcorps, P., and Silcock, P. (2003). *Control of Ester Synthesis During Brewery Fermentation, In Brewing Yeast Fermentation Performance*. Hoboken, NJ: Blackwell Publishing, 213–233.

Engan, S., and Aubert, O. (1977). Relations between fermentation temperature and the formation of some flavour components. *Proc. Cong. Eur. Brew. Conv.* 16, 591–607.

Fan, G. S., Fu, Z. L., Teng, C., Liu, P. X., Wu, Q. H., Rahman, M. K. R., et al. (2020a). Effects of aging on the quality of roasted sesame-like flavor Daqu. *BMC Microbiol.* 20:67. doi: 10.1186/s12866-020-01745-3

Fan, G. S., Liu, P. X., Wu, Q. H., Fu, Z. L., Cheng, L. J., Zhu, Y. T., et al. (2019). Optimization of cultural conditions for ethyl alcohol production by Saccharomyces cerevisiae YF1914 in aerobic conditions and its aroma-producing characteristics. *Sci. Technol. Food Ind.* 40, 52–58. doi: 10.13386/j.issn1002-0306.2019.13.009

Fan, G. S., Sun, B. G., Fu, Z. L., Xia, Y. Q., Huang, M. Q., Xu, C. Y., et al. (2018a). Analysis of physicochemical indices, volatile flavor components, and microbial community of a light-flavor Daqu. *J. Am. Soc. Brew. Chem.* 76, 209–218. doi: 10.1080/03610470.2018.1424402\qr{Citethereference‘‘Fanetal.,2018a’’insidethetext.}

Fan, G. S., Sun, B. G., Xu, D., Teng, C., Fu, Z. L., Du, Y. H., et al. (2018b). Isolation and identification of high-yield ethyl acetate-producing yeast from Gujinggong Daqu and its fermentation characteristics. *J. Am. Soc. Brew. Chem.* 76, 117–124. doi: 10.1080/03610470.2017.1396849

Fan, G. S., Wang, Y. Z., Liu, P. X., Wu, Q. H., Fu, Z. L., Zhu, Y. T., et al. (2020b). Research progress in catalytic synthesis of ethyl acetate in Baijiu by alcohol acyltransferase. *J. Chinese Instit. Food Sci. Technol.* 20, 294–304. doi: 10.16429/j.1009-7848.2020.11.034

Fan, W. L., and Qian, M. C. (2006). Identification of aroma compounds in Chinese "Yanghe Daqu" liquor by normal phase chromatography fractionation followed by gas chromatography-olfactometry. *Flavour Frag. J.* 21, 333–342. doi: 10.1002/ffj.1621

Fan, W. L., and Xu, Y. (2013). Review of important functional compounds terpenes in baijiu (Chinese liquor). *Liquor Making* 40, 11–16. doi: 10.3969/j.issn.1002-8110.2013.06.008

Fu, Z. L., Sun, B. G., Li, X. T., Fan, G. S., Teng, C., Alaa, A., et al. (2018). Isolation and characterization of a high ethyl acetate-producing yeast from Laobaigan Daqu and its fermentation conditions for producing high-quality Baijiu. *Biotechnol. Biotec. Eq.* 32, 1218–1227. doi: 10.1080/13102818.2018.1492355

Gao, Y., Jin, H. X., Wei, H. Z., Yang, S. L., Lv, S., Feng, Y. L., et al. (2014). GC determination oxidation nerolidol i, oxidation nerolidol ii, trans nerolidol of content in Dalbergiae odoriferae oil. *Chin. J. Exp. Tradit. Med. Form.* 20, 78–80. doi: 10.13422/j.cnki.syfjx.2014240078

Han, X. L., Wang, Y., Wei, J. W., Wang, D. L., Tang, K. T., and Zhao, C. Y. (2013). Analysis of polyhydric alcohols in Qing-flavor liquor. *Liquor Making Sci. Technol.* 52, 44–46. doi: 10.13746/j.njkj.2013.08.052

Hong, J., Tian, W., and Zhao, D. (2020). Research progress of trace components in sesame-aroma type of baijiu. *Food Res. Int.* 137:109695. doi: 10.1016/j.foodres.2020.109695

Hu, K., Jin, G. J., Mei, W. C., Li, T., and Tao, Y. S. (2018). Increase of medium-chain fatty acid ethyl ester content in mixed H. uvarum/S. Cerevisiae fermentation leads to wine fruity aroma enhancement. *Food Chem.* 239, 495–501. doi: 10.1016/j.foodchem.2017.06.151

Hu, X. Q., Fan, G. S., Liao, H., Fu, Z. L., Ma, C., Ni, H., et al. (2020). Optimized soluble expression of a novel endoglucanase from Burkholderia pyrrocinia in *Escherichia coli*. *3 Biotech* 10:387. doi: 10.1007/s13205-020-02327-w

Ichikawa, E., Hosokawa, N., Hata, Y., Abe, Y., Suginami, K., and Imayasu, S. (1991). Breeding sake yeasts with improved ethyl caproate productivity. *Agric. Biol. Chem.* 55, 2153–2154. doi: 10.1080/00021369.1991.10870932

Kurtzman, C. P., Fell, J. W., Boekhout, T., and Robert, V. (2011). *Methods for Isolation, Phenotypic Characterization and Maintenance of Yeasts, In The Yeasts, A Taxonomic Study*, 5th Edn. Amsterdam: Elsevier Science, 87–110.

Li, J. H., Liu, Y. J., Sui, L. N., Yang, P. P., and Wang, Y. (2019). Research progress on ethyl hexanoate-increasing and ethyl lactate-decreasing of strong-flavor Baijiu. *China Brew.* 38, 1–4. doi: 10.11882/j.issn.0254-5071.2019.01.001

Li, Z. H., Dong, L., Jeon, J., Kwon, S. Y., Zhao, C., and Baek, H. (2019). Characterization and evaluation of aroma quality in doubanjiang, a Chinese traditional fermented red pepper paste, using aroma extract dilution analysis and a sensory profile. *Molecules* 24:3107. doi: 10.3390/molecules24173107

Lilly, M., Bauer, F. F., Lambrechts, M. G., Swiegers, J. H., Cozzolino, D., and Pretorius, I. S. (2006). The effect of increased yeast alcohol acetyltransferase and esterase activity on the flavour profiles of wine and distillates. *Yeast* 23, 641–659. doi: 10.1002/yea.1382

Lin, X., Hu, X. P., Wang, Q. K., and Li, C. F. (2020). Improved flavor profiles of red pitaya (Hylocereus lemairei) wine by controlling the inoculations of Saccharomyces bayanus and Metschnikowia agaves and the fermentation temperature. *J. Food Sci. Tech. Mys.* 57, 4469–4480. doi: 10.1007/s13197-020-04484-5

Liu, H. L., and Sun, B. G. (2018). Effect of fermentation processing on the flavor of Baijiu. *J. Agr. Food Chem.* 66, 5425–5432. doi: 10.1021/acs.jafc.8b00692

Liu, S. Q., Holland, R., and Crow, V. L. (2004). Esters and their biosynthesis in fermented dairy products: a review. *Int. Dairy J.* 14, 923–945. doi: 10.1016/j.idairyj.2004.02.010

Lukic, I., Carlin, S., and Vrhovsek, U. (2020). Comprehensive 2D gas chromatography with TOF-MS detection confirms the matchless discriminatory power of monoterpenes and provides in-depth volatile profile information for highly efficient white wine varietal differentiation. *Foods* 9:1787. doi: 10.3390/foods9121787

Luo, J., Ao, Z. H., Wang, S. T., Qin, H., Cai, X. B., and Sun, X. (2015). The correlations of fusel oil in different varieties of base Nongxiang baijiu (liquor). *Liquor Mak. Sci. Technol.* 3, 43–44. doi: 10.13746/j.njkj.2014093

Ma, N., Yi, F. P., and Zhu, J. C. (2020). Characterization of aroma-active compounds and perceptual interaction between esters and sulfur compounds in Xi baijiu. *Eur. Food Res. Technol.* 246, 2517–2535. doi: 10.1007/s00217-020-03594-w

Mattey, M. (1992). The production of organic acids. *Crit. Rev. Biotechnol.* 12, 87–132. doi: 10.3109/07388559209069189

Nyanga, L. K., Nout, M. J. R., Smid, E. J., Boekhout, T., and Zwietering, M. H. (2013). Fermentation characteristics of yeasts isolated from traditionally fermented masau (*Ziziphus mauritiana*) fruits. *Int. J. Food Microbiol.* 166, 426–432. doi: 10.1016/j.ijfoodmicro.2013.08.003

Panozzo, C., Nawara, M., Suski, C., Kucharczyk, R., Skoneczny, M., Becam, A. M., et al. (2002). Aerobic and anaerobic NAD(+) metabolism in *Saccharomyes cerevisiae*. *FEBS Lett.* 517, 97–102. doi: 10.1016/S0014-5793(02)02585-1

Pappagianis, D., Collins, M. S., Hector, R., and Remington, J. (1979). Development of resistance to amphotericin B in *Candida lusitaniae* infecting a human. *Antimicrob. Agents Ch.* 16, 123–126. doi: 10.1128/AAC.16.2.123

Piper, P. W. (1995). The heat shock and ethanol stress responses of yeast exhibit extensive similarity and functional overlap. *FEMS Microbiol. Lett.* 134, 121–127. doi: 10.1111/j.1574-6968.1995.tb07925.x

Quan, Q. L., Jiang, W., Wang, D. L., Sun, Z. W., and Song, T. (2013). The change of monoterpenoids during fermentation and their contribution to hop aroma of beer. *Food Ferment. Ind.* 39, 170–175. doi: 10.13995/j.cnki.11-1802/ts.2013.05.043

Saerens, S., Verstrepen, K. J., Van Laere, S., Voet, A., Van Dijck, P., Delvaux, F. R., et al. (2006). The Saccharomyces cerevisiae EHT1 and EEB1 genes encode novel enzymes with medium-chain fatty acid ethyl ester synthesis and hydrolysis capacity. *J. Biol. Chem.* 281, 4446–4456. doi: 10.1074/jbc.M512028200

Song, R. B., Shao, Z. L., and Song, J. (2019). Analysis of the reasons and control measures for high ethyl acetate in Luzhou-flavor liquor production. *Liquor Mak.* 46, 55–60. doi: 10.3969/j.issn.1002-8110.2019.03.021

Song, X. B., Jing, S., Zhu, L., Ma, C. F., Song, T., Wu, J. H., et al. (2020). Untargeted and targeted metabolomics strategy for the classification of strong aroma-type baijiu (liquor) according to geographical origin using comprehensive two-dimensional gas chromatography-time-of-flight mass spectrometry. *Food Chem.* 314:126098. doi: 10.1016/j.foodchem.2019.126098

Sun, B. G., Li, H. H., Hu, X. M., Sun, J. Y., and Dong, W. (2016). The development trend of healthy baijiu. *J. Chin. Inst. Food Sci. Techn.* 16, 1–6. doi: 10.16429/j.1009-7848.2016.08.001

Takahashi, T., Ohara, Y., and Sueno, K. (2017). Breeding of a sake yeast mutant with enhanced ethyl caproate productivity in sake brewing using rice milled at a high polishing ratio. *J. Biosci. Bioeng.* 123, 707–713. doi: 10.1016/j.jbiosc.2017.01.014

Tan, L., Yuan, H. W., Wang, Y. F., Chen, H., Sun, Z. Y., Tang, Y. Q., et al. (2016). Behaviour of ethyl caproate during the production and distillation of ethyl caproate-rich rice Shochu. *J. Inst. Brewing* 122, 486–492. doi: 10.1002/jib.348

Wang, T., Yao, T., Li, T., You, L., Zhou, R. P., Wang, S., et al. (2013). The role of Luzhou-flavor liquor correlated yeasts in promoting caproic acid ethyl ester generating in fermentative grain. *Food Ferment. Ind.* 39, 41–45. doi: 10.13995/j.cnki.11-1802/ts.2013.01.038

Wei, C. H., Yang, X. D., Huang, Z. G., Ye, G. B., Luo, H. B., and Wang, Y. (2013). Isolation and biolog identification of two yeast strains from Nong-flavor daqu. *Liquor Mak. Sci. Technol.* 30–32. doi: 10.13746/j.njkj.2013.04.018

Wei, J. P., Zhang, Y. X., Wang, Y. W., Ju, H. M., Niu, C., Song, Z. H., et al. (2020). Assessment of chemical composition and sensorial properties of ciders fermented with different non-Saccharomyces yeasts in pure and mixed fermentations. *Int. J. Food Microbiol.* 318:108471. doi: 10.1016/j.ijfoodmicro.2019.108471

Wen, S. T., and Li, Y. (2018). Yeast diversity analysis of Laobaigan liquor Daqu. *Food Sci.* 39, 175–182. doi: 10.7506/spkx1002-6630-201824027

Wu, Q., Chen, L. Q., and Xu, Y. (2013). Yeast community associated with the solid state fermentation of traditional Chinese Maotai-flavor liquor. *Int. J. Food Microbiol.* 166, 323–330. doi: 10.1016/j.ijfoodmicro.2013.07.003

Wu, Y. L. (2008). Study on the synthesizing of 2,4- dimethylbenzaldehyde. *Mod. Chem. Res.* 1–3. doi: 10.3969/j.issn.1672-8114.2008.02.001

Yu, H. Y., Xie, T., Xie, J. R., Ai, L. Z., and Tian, H. X. (2019). Characterization of key aroma compounds in Chinese rice wine using gas chromatography-mass spectrometry and gas chromatography-olfactometry. *Food Chem.* 293, 8–14. doi: 10.1016/j.foodchem.2019.03.071

Yuan, H. W., Tan, L., Luo, S., Chen, H., Yi, X., Sun, Z. Y., et al. (2015). Development of a process for producing ethyl caproate- and ethyl lactate-rich rice shochu. *J. Inst. Brewing* 121, 432–439. doi: 10.1002/jib.240

Zhang, H., Hu, Z. H., Xing, S., Li, Z. J., Xie, B., and Xiao, D. G. (2017). Effect of acid concentration and pH on esterifying enzyme catalytic activity of Luzhou-flavor Daqu. *China Brew.* 36, 41–45. doi: 10.11882/j.issn.0254-5071.2017.05.009

Zhang, H., Ran, Y. P., Li, D. M., Liu, Y. F., Xiang, Y., Zhang, R. F., et al. (2010). Clavispora lusitaniae and Chaetomium atrobrunneum as rare agents of cutaneous infection. *Mycopathologia* 169, 373–380. doi: 10.1007/s11046-009-9266-9

Zhang, X. Y., Kontoudakis, N., Suklje, K., Antalick, G., Blackman, J. W., Rutledge, D. N., et al. (2020). Changes in red wine composition during bottle aging: impacts of grape variety, vineyard location, maturity, and oxygen availability

during aging. *J. Agr. Food Chem.* 68, 13331–13343. doi: 10.1021/acs.jafc.9b07164

Zhang, Y. J., Tang, S. Y., Zhang, W., Pan, M., and Ge, Y. (2020). Research progress in healthy baijiu based on functional microorganism regulation. *Liquor Mak. Sci. Technol.* 104–108. doi: 10.13746/j.njkj.2020120

Zhou, X., Yu, H. W., Guo, R. F., Ma, H. F., and Zhu, L. N. (2020). Temporal and spatial dynamic changes and phylogenetic analysis of fungus community in Ni Keng-flavor daqu. *Food Sci. Tech. Brazil* 45, 1–7. doi: 10.13684/j.cnki.spkj.2020.01.001

Zuo, Q. C., Huang, Y. G., and Min, G. (2020). Evaluation of bacterial diversity during fermentation process: a comparison between handmade and machine-made high-temperature Daqu of Maotai-flavor liquor. *Ann. Microbiol.* 70:57. doi: 10.1186/s13213-020-01598-1

Conflict of Interest: XC was employed by the company Angel Yeast Co., Ltd.

The remaining authors declare that the research was conducted in the absence of any commercial or financial relationships that could be construed as a potential conflict of interest.

frontiers in Microbiology

ORIGINAL RESEARCH
published: 01 June 2021
doi: 10.3389/fmicb.2021.665261

Role of Elm1, Tos3, and Sak1 Protein Kinases in the Maltose Metabolism of Baker's Yeast

Xu Yang[1], Lu Meng[1], Xue Lin[1,2,3], Huan-Yuan Jiang[1], Xiao-Ping Hu[1,2,3] and Cong-Fa Li[1,2,3]**

[1] College of Food Science and Engineering, Hainan University, Haikou, China, [2] Engineering Research Center of Utilization of Tropical Polysaccharide Resources, Ministry of Education, Haikou, China, [3] Hainan Key Laboratory of Food Nutrition and Functional Food, Haikou, China

Glucose repression is a key regulatory system controlling the metabolism of non-glucose carbon source in yeast. Glucose represses the utilization of maltose, the most abundant fermentable sugar in lean dough and wort, thereby negatively affecting the fermentation efficiency and product quality of pasta products and beer. In this study, the focus was on the role of three kinases, Elm1, Tos3, and Sak1, in the maltose metabolism of baker's yeast in lean dough. The results suggested that the three kinases played different roles in the regulation of the maltose metabolism of baker's yeast with differential regulations on *MAL* genes. Elm1 was necessary for the maltose metabolism of baker's yeast in maltose and maltose-glucose, and the overexpression of *ELM1* could enhance the maltose metabolism and lean dough fermentation ability by upregulating the transcription of *MALx1* (*x* is the locus) in maltose and maltose-glucose and *MALx2* in maltose. The native level of *TOS3* and *SAK1* was essential for yeast cells to adapt glucose repression, but the overexpression of *TOS3* and *SAK1* alone repressed the expression of *MALx1* in maltose-glucose and *MALx2* in maltose. Moreover, the three kinases might regulate the maltose metabolism via the Snf1-parallel pathways with a carbon source-dependent manner. These results, for the first time, suggested that Elm1, rather than Tos3 and Sak1, might be the dominant regulator in the maltose metabolism of baker's yeast. These findings provided knowledge about the glucose repression of maltose and gave a new perspective for breeding industrial yeasts with rapid maltose metabolism.

Keywords: Elm1, Tos3, Sak1, maltose metabolism, glucose repression, *Saccharomyces cerevisiae*

OPEN ACCESS

Edited by:
Wanping Chen,
Georg August University of Göttingen, Germany

Reviewed by:
Jun Dai,
Hubei University of Technology, China
Choowong Auesukaree,
Mahidol University, Thailand
Estéfani García Ríos,
Instituto de Salud Carlos III (ISCIII), Spain

****Correspondence:***
Xue Lin
linxiaoxuelx@163.com
Cong-Fa Li
licongfalcf@163.com;
congfa@vip.163.com

Specialty section:
This article was submitted to Food Microbiology, a section of the journal Frontiers in Microbiology

Received: *07 February 2021*
Accepted: *23 April 2021*
Published: *01 June 2021*

Citation:
Yang X, Meng L, Lin X, Jiang H-Y, Hu X-P and Li C-F (2021) Role of Elm1, Tos3, and Sak1 Protein Kinases in the Maltose Metabolism of Baker's Yeast. Front. Microbiol. 12:665261. doi: 10.3389/fmicb.2021.665261

INTRODUCTION

Glucose repression is a key regulatory system controlling the synthesis of a series of enzymes involved in the carbohydrate metabolism in yeast (Trumbly, 1992; Klein et al., 1998; Carlson, 1999; Kim et al., 2019). In the presence of glucose, the expression of genes involved in the metabolism of alternate fermentable carbon sources (such as maltose, galactose, and sucrose), non-fermentable ones (such as glycerol, ethanol, and acetate), and respiratory metabolism is repressed (Srđan et al., 2004; Martinez-Ortiz et al., 2019; Lin, 2021). This disadvantage could be substantial in biotechnological production processes, in which glucose is sometimes not the primary carbon source or respiratory metabolism is demanded (Verstrepen et al., 2004). For example, maltose is the

most abundant fermentable sugar in lean dough (Hazell and Attfield, 1999; Bell et al., 2001; Jiang et al., 2008). The ability to utilize the maltose in baker's yeast determines the fermentation efficiency and quality of pasta products (Bell et al., 2001; Jiang et al., 2008). However, glucose represses the expression of genes encoding for maltose permease and maltase, and inhibits the activity of these enzymes in baker's yeast, thereby, negatively affecting the maltose metabolism and lean dough fermentation of baker's yeast (Srđan et al., 2004; Hatanaka et al., 2009; Sun et al., 2012; Zhang et al., 2015b,c). Thus, alleviating glucose repression is essential to improve the utilization efficiency of non-glucose carbon sources.

The Snf1 protein kinase is a member of the remarkably conserved AMP-activated protein kinase (AMPK) family in eukaryotes (Meng et al., 2021). The Snf1 kinase is crucial to the glucose derepression of *Saccharomyces cerevisiae*, ensuring the availability of non-preferred carbon sources (Coccetti et al., 2018; Persson et al., 2020). Snf1 regulates the expression of glucose-repressed genes by regulating the phosphorylation status and nuclear localization of the repressor Mig1 (Östling and Ronne, 1998). In glucose limitation, Snf1 is activated, and phosphorylates repressor Mig1, thereby preventing the interaction of Mig1 with the corepressors Ssn6-Tup1 and promoting the transcription of downstream glucose-repressed genes (Östling and Ronne, 1998; Papamichos-Chronakis et al., 2004). Unphosphorylated Mig1 is retained in the nucleus, and interacts with Ssn6-Tup1 when Snf1 is inactive in high glucose (Östling and Ronne, 1998; Papamichos-Chronakis et al., 2004).

The Snf1 protein kinase is a complex that consists of an alpha catalytic subunit Snf1, a gamma regulatory subunit Snf4, and one of the three alternative beta regulatory subunits, namely, Sip1, Sip2, and Gal83 (Daniel and Carling, 2002; García-Salcedo et al., 2014; Meng et al., 2020). Snf1 activation requires at least two steps: First, Snf4 binds to the C-terminal regulatory domain of the catalytic subunit Snf1 to counteract the autoinhibition of Snf1, in which β regulatory subunits participate in the linkage of Snf1 and Snf4, and direct the subcellular localization of Snf1 (McCartney and Schmidt, 2001). Second, the phosphorylation of the Thr210 site of the catalytic subunit Snf1 is initiated by three upstream protein kinases, namely, Elm1, Tos3, and Sak1 (Hong et al., 2003; García-Salcedo et al., 2014). The three kinases exhibit a stress-dependent demand for the activation of different isoforms of Snf1, and contribute differently to cellular regulation in various carbon sources (McCartney et al., 2005). Although Sak1 appears to be the major one in the Snf1-dependent regulation of the metabolism of non-preferred carbon sources such as raffinose, ethanol, and glycerol, any of the three kinases is sufficient to activate Snf1 (Hedbacker et al., 2004; Liu et al., 2011). The *sak1*Δ mutants of *Candida albicans* fail to grow on many alternative carbon sources (Ramírez-Zavala et al., 2017). Tos3 is more important in the activation of Snf1 in non-fermentable carbon sources than in an abrupt glucose stress (Kim et al., 2005). The single mutation of *ELM1* does not display an Snf1 phenotype in raffinose, but *SAK1*, *TOS3*, and *ELM1* triple deletions do (Sutherland et al., 2003). However, the role of the three upstream kinases in maltose metabolism is unclear.

In the current study, the genes *ELM1*, *TOS3*, and *SAK1* were overexpressed and deleted in baker's yeast ABY3α alone to explore the role of the kinases Elm1, Tos3, and Sak1 in the maltose metabolism of baker's yeast. The growth characteristic, maltose utilization, lean dough leavening ability, and mRNA level of genes related to the maltose metabolism of the strains were analyzed.

MATERIALS AND METHODS

Strains and Plasmids

The strains and plasmids used in the current work were listed in **Table 1**.

Media and Culture Conditions

The *E. coli* strains were cultured in the Luria-Bertani medium (10 g/L of tryptone, 10 g/L of NaCl, and 5 g/L of yeast extract) at 37°C, and 100 mg/L of ampicillin was used for selecting the positive *E. coli* transformants. The yeast strains were cultured in the yeast extract peptone dextrose (YEPD) medium that contains

TABLE 1 | Characteristics of strains and plasmids used in the current study.

Strains or plasmids	Relevant characteristic	Reference or source
Strains		
Escherichia coli DH5α	Φ80 *lacZ*Δ*M15* Δ*lacU169 recA1 endA1 hsdR17 supE44 thi-1 gyrA relA1*	This lab
S. cerevisiae ABY3α	Industrial baker's yeast haploid strain	This lab
A+YP	Yep-PK	This study
A+E	Yep-PEK	This study
A+T	Yep-PTK	This study
A+S	Yep-PSK	This study
A-E	*MAT* α, Δ*elm1*:: *loxP*	This study
A-T	*MAT* α, Δ*tos3*:: *loxP*	This study
A-S	*MAT* α, Δ*sak1*:: *loxP*	This study
A-SNF1	*MAT* α, Δ*snf1*:: *loxP*	This study
A+PK-SNF1	*MAT* α, Yep-PK, Δ*snf1*:: *loxP*	This study
A-REG1	*MAT* α, Δ*reg1*:: *loxP*	This study
A+PK-REG1	*MAT* α, Yep-PK, Δ*reg1*:: *loxP*	This study
A+E-SNF1	*MAT* α, Yep-PEK, Δ*snf1*:: *loxP*	This study
A+E-REG1	*MAT* α, Yep-PEK, Δ*reg1*:: *loxP*	This study
A+T-REG1	*MAT* α, Yep-PTK, Δ*reg1*:: *loxP*	This study
A+S-REG1	*MAT* α, Yep-PSK, Δ*reg1*:: *loxP*	This study
Plasmids		
pUG6	*E. coli/S. cerevisiae shuttle vector*, *containing* Amp^+, *loxP-KanMX-loxP* disruption cassette	This lab
pSH-Zeocin	Zeo^r, Cre expression vector	This lab
Yep-P	$URA3^+$, Amp^R *ori* control vector, $PGK1_P$-$PGK1_T$	Gifted by Zhang et al. (2015a)
Yep-PK	*KanMX*, $PGK1_P$-$PGK1_T$	This study
Yep-PEK	*KanMX*, $PGK1_P$-*ELM1*-$PGK1_T$	This study
Yep-PTK	*KanMX*, $PGK1_P$-*TOS3*-$PGK1_T$	This study
Yep-PSK	*KanMX*, $PGK1_P$-*SAK1*-$PGK1_T$	This study

20 g/L of glucose, 20 g/L of peptone, and 10 g/L of yeast extract. Maltose fermentation was conducted in the low sugar model liquid dough (LSMLD) medium, in which 33.25 g/L of maltose mixed with 5 g/L of glucose or 38 g/L of maltose was used as the carbon source, according to the previous study (Lin et al., 2018).

The yeast strains, which were preserved on slopes at the exponential phase, were inoculated into the YEPD medium by an inoculating loop to the stationary stage at 30°C. Then, 10% of the cultures were inoculated to the YEPD medium at 30°C with 180 rpm rotary shaking for 24 h. The second-cultures were centrifugated at 4°C with 1,500 × *g* for 5 min. The cells were collected after washing with distilled water twice.

Construction of Plasmids and Transformants

Yeast genomic DNA was obtained using the yeast DNA kit (D1900, Solarbio, Beijing, China). Plasmids were obtained using the Plasmid Mini Kit II (DC201-01, Vazyme, Jiangsu, China). The gene fragments were cloned to the plasmids using the ClonExpressIIOne Step Cloning Kit (C112, Vazyme, Jiangsu, China). Primers used in this work were listed in **Table 2**.

To construct the episomal plasmid Yep-PEK, firstly, the gene *ELM1* was amplified using the primers ELM1-F/ELM1-R with the genome of ABY3α as a template. Secondly, the fragment of *ELM1* was inserted into the *Xho*I site of the promoter and terminator of *PGK1* in the plasmid Yep-P, yielding the plasmid Yep-PE. Finally, the selectable marker fragment *KanMX*, which was amplified using the primers Kan-F/Kan-R with the vector pUG6 as a template, was inserted into the *Sph*I site of the plasmid Yep-PE. The episomal plasmids Yep-PTK and Yep-PSK were constructed using the abovementioned strategy with the primers TOS3-F/TOS3-R and SAK1-F/SAK1-R, respectively.

To obtain the *ELM1*-deleted mutant, the method 'DNA assembler' was used to rapidly assemble the fragments on the chromosome (Shao et al., 2008; Li et al., 2018). The upstream and downstream sequences of *ELM1* were amplified using the primers ELM1-BA-F/ELM1-BA-R, and ELM1-BB-F/ELM1-BB-R, respectively, with the genome of ABY3α as a template. The selectable marker gene *KanMX* was amplified using the primers ELM1-Kan-F/ELM1-Kan-R with the vector pUG6 as a template. The three fragments were transformed into the strain ABY3α, and *KanMX* was integrated to the *ELM1* site of ABY3α by homologous recombination. The *TOS3*-deleted and *SAK1*-deleted mutants were constructed using the same strategy with the primers TOS3-BA-F/TOS3-BA-R, TOS3-BB-F/TOS3-BB-R, and TOS3-Kan-F/TOS3-Kan-R and SAK1-BA-F/SAK1-BA-R, SAK1-BB-F/SAK1-BB-R, and SAK1-Kan-F/SAK1-Kan-R, respectively.

To obtain the *SNF1*-deleted mutant, firstly, the selectable marker gene *KanMX* was amplified using the primers SNF1-Kan-F/SNF1-Kan-R with the vector pUG6 as a template. Secondly, the fragment SNF1F-Kan-SNF1R was integrated to the *SNF1* fragment site of ABY3α. Finally, the gene *KanMX* was knocked out by the Cre/*Lox* system. The *REG1*-deleted mutant was constructed using the same strategy with the primers REG1-Kan-F/REG1-Kan-R.

TABLE 2 | Primers used in the present study.

Primer	Sequence (5′ → 3′)
For genes overexpression	
ELM1-F	CAAGATCGGAATTCCAGATCTATGTCACCTCGACA GCTTATACCG
ELM1-R	ATCTATCGCAGATCCCTCGAGCTATATTTGACCATTA TCTGCAAAGTTC
TOS3-F	CAAGATCGGAATTCCAGATCTATGGTACTACTTAAAG AACCTGTTCAGC
TOS3-R	ATCTATCGCAGATCCCTCGAGCTAAAGCTTATAAAG AGACATTCTTCTTCTC
SAK1-F	CAAGATCGGAATTCCAGATCTATGGATAGGAGTGAT AAAAAAGTTAACG
SAK1-R	ATCTATCGCAGATCCCTCGAGTCATGGAAGTGCACT CCTTCTCT
Kan-F	AGAGTCGACCTGCATGCCAGCTGAAGCTTCGTACG CTG
Kan-R	GCCAGTGCCAAGCTTGCATGCGCATAGGCCACTAG TGGATCTGA
For genes deletion	
ELM1-BA-F	ACGCTGCCTTATCCATTGACCGAG
ELM1-BA-R	TCCTGCAGCGTACGAAGCTTCAGCTGTTCATGCTAA GTAATTATTGTTAAC
ELM1-Kan-F	GTTAACAATAATTACTTAGCATGAACAGCTGAAGCTT CGTACGCTGCAGG
ELM1-Kan-R	GACAGATATCATCCTGTAGTTTCATGCATAGGCCAC TAGTGGATCTGATA
ELM1-BB-F	TATCAGATCCACTAGTGGCCTATGCATGAAACTACA GGATGATATCTGTC
ELM1-BB-R	ATGAGTTCGCACTGGTGCAGGTAC
TOS3-BA-F	AGGTCAAGACGAAAACCATAAATA
TOS3-BA-R	CCTGCAGCGTACGAAGCTTCAGCTGATTCTTCAAA GCTTCCTTTTTATAT
TOS3-Kan-F	ATATAAAAAGGAAGCTTTGAAGAATCAGCTGAAGCT TCGTACGCTGCAGG
TOS3-Kan-R	ATTAAAATAATTTACATATATCATGGCATAGGCCACT AGTGGATCTGATA
TOS3-BB-F	TATCAGATCCACTAGTGGCCTATGCCATGATATATGT AAATTATTTTAAT
TOS3-BB-R	GATTTTACGAATGCCTATGGTGAC
SAK1-BA-F	CGAACGATACCTCAAGGAGCAAGA
SAK1-BA-R	CCTGCAGCGTACGAAGCTTCAGCTGGTTCAAAACT CCTTATTAATATGCT
SAK1-Kan-F	AGCATATTAATAAGGAGTTTTGAACCAGCTGAAGCTT CGTACGCTGCAGG
SAK1-Kan-R	ATGGAAATTACTTTGAATTTTACACGCATAGGCCACT AGTGGATCTGATA
SAK1-BB-F	TATCAGATCCACTAGTGGCCTATGCGTGTAAAATTCA AAGTAATTTCCA
SAK1-BB-R	AAGCTGGTGGGAAATAACAAGGAT
SNF1-K-F	GAAGTTTTTTTTTGTAACAAGTTTTGCTACACTCCCT TAATAAAGTCAACCAGCTGAAGCTTCGTACGC
SNF1-K-R	CCCAGCCGTCAAATTTGAAATCCACCAAATAATTATT GGTTGCATAGGCCACTAGTGGATCTG
REG1-K-F	TGACGAAGACGAGATAAGAAAAATCCAAAACAGCT GAAGCTTCGTACGC
REG1-K-R	TTCATGTTGACTTCAAAATTCTTTCTTGCATAGGCCA CTAGTGGATCTG

(Continued)

TABLE 2 | Continued

Primer	Sequence (5′ → 3′)
For verification	
PGK-F	TCTAACTGATCTATCCAAAACTGA
PGK-R	TAACGAACGCAGAATTTTC
Kan-FV	CAGCTGAAGCTTCGTACGC
Kan-RV	GCATAGGCCACTAGTGGATCTG
ELM1-U1	CTGGTCGTAGCCACATAACCGTTCC
ELM1-D1	TCGTCATCAAAATCACTCGCATCA
ELM1-U2	GCGTTGCCAATGATGTTACAGATG
ELM1-D2	ATCCTACCAGATACGCTTCGCTTG
TOS3-U1	TTTAGTTAGTTTCTTCATCGTTCG
TOS3-D1	CAGCCAGTTTAGTCTGACCATCTCAT
TOS3-U2	ATGCTGGTCGCTATACTGCTGTCG
TOS3-D2	AGAAGAACAAGACTCAGACGATGC
SAK1-U1	ACTGATACATCTCCACAGGCTAAG
SAK1-D1	GATAAAATGCTTGATGGTCGGAAG
SAK1-U2	GCTGGTCGCTATACTGCTGTCGAT
SAK1-D2	CTCTTTTACCACTGTGCCCCAATC
S-F	GGCTGTTTCAATAATCATAGCGAAAGAAATA
S-R	CCGTCAAATTTGAAATCCACCAAATAATTATTG
R-F	GGCTGTTATACGTATAACCACACAC
R-R	CTTCGCTGTCTACATTTGTCCTTGA
K-F	CTTGCTAGGATACAGTTCTCACATCA
K-R	CGCATCAACCAAACCGTTATTCATTC
Z-F	CCCACACACCATAGCTTCA
Z-R	AGCTTGCAAATTAAAGCCTT
For RT-PCR	
ACT1-F	ATTGATAACGGTTCTGGT
ACT1-R	AATTGGGTAACGTAAAGTC
MAL61-F	TACCTCCGTTTGTTTGCG
MAL61-R	AGGACCATTGTGAGACCC
MAL62-F	AGTTTCCTGGCAAATCGG
MAL62-R	GTCCCACGGCAATCATAC
MAL31-F	TCCCAGAACAAATATGCCAACT
MAL31-R	TCTCGGGTCCTTTACCACTTAA
MAL32-F	TCCAGAAACAGAACCAAAGTGG
MAL32-R	AGTCATAAAACGGACAAACCCA

Yeast transformations were obtained using the lithium acetate/PEG method (Gietz, 2015). A total of 800 mg/L of G418 (Promega, Madison, WI, United States) was used to select the positive *S. cerevisiae* transformants. The YEPG medium (20 g/L of galactose, 20 g/L of peptone, and 10 g/L of yeast extract) was used for the Cre expression in the yeast transformants. A total of 500 mg/L of Zeocin (R25001, Invitrogen, Carlsbad, CA, United States) was used to select the yeast strains carrying the plasmid pSH-Zeocin. The plasmids Yep-PK, Yep-PEK, Yep-PTK, and Yep-PSK were transformed into the parental strain to obtain the transformants A+YP, A+E, A+T, and A+S, respectively. The plasmid Yep-PEK was transformed into the *SNF1*-deleted mutant to get the transformant A+E-SNF1. The plasmids Yep-PEK, Yep-PTK, and Yep-PSK were transformed into the *REG1*-deleted mutant to get the transformants A+E-REG1, A+T-REG1, and A+S-REG1, respectively. The primers used in the verification of the strains were listed in **Table 2**. The fragment containing *PGK1* and the overexpressed gene was verified by PCR to confirm the transformation of an episomal plasmid. The fixed-point verification method, which used the primers that were intercepted from the outside of the upstream/downstream homologous of the target gene and from the inside of the *KanMX* gene, was used to verify the gene-deleted mutants. The amplification of *Zeocin* was used to verify the transformation of the plasmid pSH-Zeocin.

Measurement of Growth Curve

Yeast cells were inoculated in the 2% glucose and 2% maltose conditions at 30°C. Then, the 3% (vol/vol) inoculations (equivalent to 3×10^8 cells) were transferred to the same condition, and the cell density OD_{600} was monitored at 30°C using a UV spectrophotometer (T6, Persee, Beijing, China). The specific growth rate was calculated by the change in the OD_{600} Napierian logarithm versus time during exponential growth. A total of 10 mL of the cell culture was filtered in the stationary phase, washed twice with 10 mL of distilled water, and then dried at 105°C for 24 h to measure the cell dry weight. The biomass yield was expressed as the gram (dry weight) of yeast cells per liter of medium. Experiments were conducted thrice.

Measurement of Extracellular Sugar

A total of 2 g of fresh yeast was cultured in the LSMLD media at 30°C. The cultures were sampled at different fermentation time points. The measurement of extracellular sugars and the calculation of maltose utilization efficiency and time span value were conducted using the previous method (Lin et al., 2018). The samples were filtered through 0.45 μm pore size cellulose acetate filters (Millipore Corp, Danvers, MA, United States) and analyzed by high-performance liquid chromatography with a refractive index detector and a SilGreen R GH0830078H column (300*7.8 mm*8 um, SilGreen, Beijing, China) at 65°C. 5 mM H_2SO_4 was used as the mobile phase at a flow rate of 0.6 mL/min.

The maltose utilization efficiency in the maltose LSMLD medium was determined by the ratio of the consumed maltose in the whole process to the total maltose. The maltose utilization efficiency in the maltose-glucose LSMLD medium was determined by the ratio of the consumed maltose when glucose was exhausted to the total maltose. The time span refers to the difference between the time points at which half of the maltose and half of the glucose was consumed in the maltose-glucose LSMLD medium. Three independent experiments were performed.

Test of CO_2 Production

The leavening ability of yeast cells in lean dough was tested according to the previous study (Zhang et al., 2015b), based on the Chinese National Standards for yeast used in food processing with the following modification. First, 140 g of standard flour, 72.5 mL of water, 4.5 g of fresh yeast, and 2 g of salt were evenly and quickly mixed at 30 ± 0.2°C of the dough center temperature in 5 min. Then, 50 g of mixed lean dough was transferred to a 250 mL graduated cylinder and

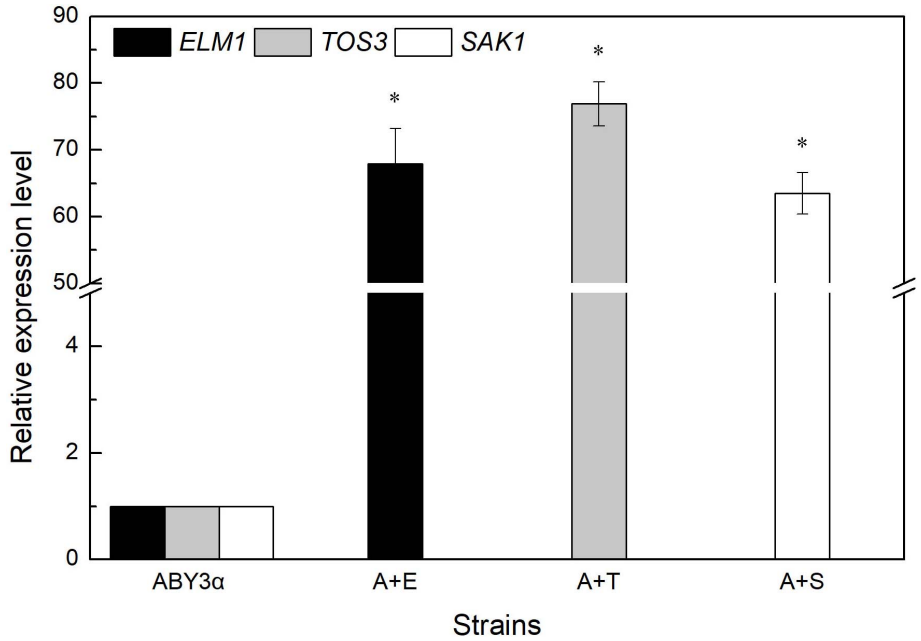

FIGURE 1 | mRNA level of the overexpressed genes. The expression level of *ELM1* in the strain A+E, *TOS3* in the strain A+T, and *SAK1* in the strain A+S was tested using qRT-PCR. The cells were sampled from YEPD medium at 16 h. ABY3α: the parental strain; A+E: the transformant carrying *ELM1* overexpression; A+T: the transformant carrying *TOS3* overexpression; A+S: the transformant carrying *SAK1* overexpression. Significant differences of the transformants to the parental strain were confirmed at $^*p < 0.05$.

fermented at 30°C. CO_2 amounts were measured by the change of dough height in 120 min. Three independent experiments were carried out.

Real-Time Quantitative PCR (RT-qPCR)

Two grams (2 g) of fresh yeast was cultured in the LSMLD media, and 1 mL cultures (equivalent to 5×10^6 cells) were sampled at 30 min. The expression levels of the genes *MAL61*/*MAL31* encoding maltose permease and *MAL62*/*MAL32* encoding maltase were tested according to the previous study (Lin et al., 2018). The total cellular RNA was extracted using an RNA-eazy isolation reagent (R701, Vazyme, Jiangsu, China). Using mRNA as a template, cDNA was synthesized using a HIScript III RT SuperMix for qPCR (+gDNA wiper) (R323-01, Vazyme, Jiangsu, China). Changes in the expression levels of *MAL* genes were assessed through qRT-PCR with a ChamQ Universal SYBR qPCR Master Mix (Q711-02, Vazyme, Jiangsu, China). Actin was used as the loading control. The primers used for amplifying the target genes and the reference gene *ACT1* were shown in **Table 2**. The expression level of the target genes in the parental strain ABY3α was normalized to the reference gene. Experiments were conducted thrice.

Statistical Analysis

Student's *t*-test was performed to analyze the differences of the transformants and the parental strain. Differences at $P < 0.05$ were considered as statistically significant differences.

RESULTS

Growth Property

Under the control of the constitutive yeast phosphoglycerate kinase gene (*PGK1*) promoter ($PGK1_P$) and terminator ($PGK1_T$), the mRNA expression level of *ELM1*, *TOS3*, and *SAK1* were upregulated by 68-, 77-, and 64-fold in the transformants A+E, A+T, and A+S, respectively, compared with the parental strain (**Figure 1**). To test the influence of *ELM1*/*TOS3*/*SAK1* overexpression on the growth characteristic of baker's yeast, the growth curves of the strains were monitored in 2% glucose and maltose (**Figure 2**). Moreover, the specific growth rate and biomass yield of the strains were calculated (**Table 3**). Transformant A+YP, a blank control to reflect any possible influence of an empty vector, displayed growth similar to that of the parental strain. *ELM1*-overexpressed transformant A+E, *TOS3*-overexpressed transformant A+T, and *SAK1*-overexpressed transformant A+S improved cell proliferation to varying degrees in glucose. In maltose, compared with parental strain ABY3α, the specific growth rate of the transformant A+E decreased from 0.460 to 0.423 h^{-1} in maltose, but the final biomass yield showed a slight change. Only the transformant A+S exhibited an enhanced specific growth rate and biomass yield in maltose. Compared with the parental strain, although obvious changes of the specific growth rate were observed in the gene-deleted mutants (**Supplementary Table 1**, **Supplementary Figure 1**), the deletion of any of the three genes did not influence the final biomass yield in glucose; the deletions of *ELM1* and *SAK1* inhibited the biomass yield in maltose instead.

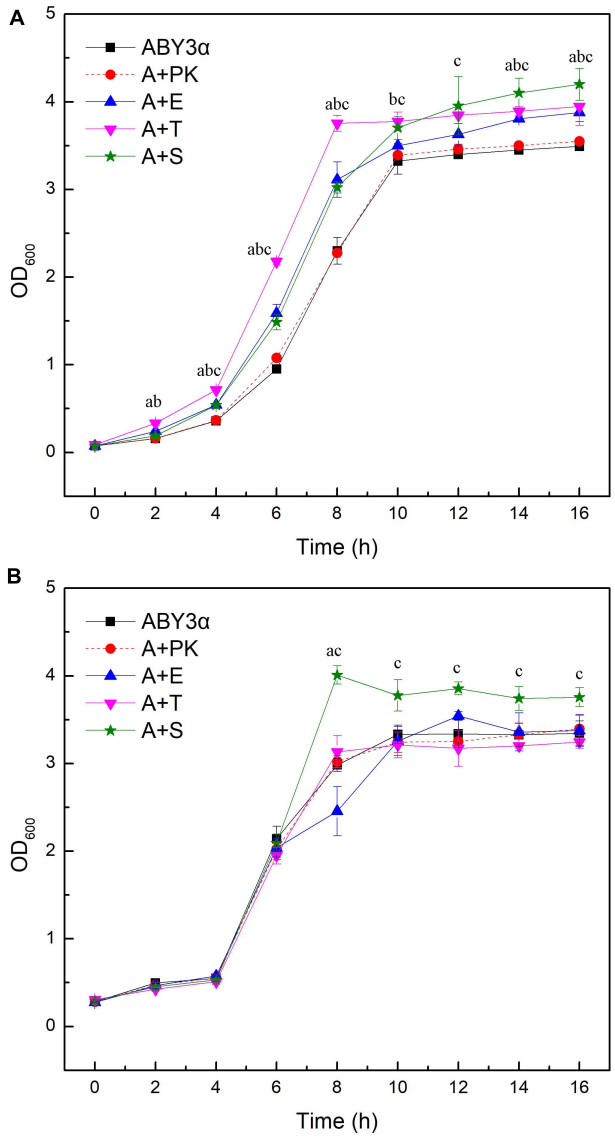

FIGURE 2 | Growth curves of the strains carrying genes overexpression. Growth curves were monitored in **(A)** 2% glucose (YEPD medium) and **(B)** 2% maltose (YEPM medium consisted of 20 g/L maltose, 20 g/L peptone, and 10 g/L yeast extract) conditions at appropriate time intervals at 30°C. ABY3α, the parental strain; A+PK, the strain carrying the vector Yep-PK used as a blank control to demonstrate any possible effect of the empty vector; A+E, the transformant carrying *ELM1* overexpression; A+T, the transformant carrying *TOS3* overexpression; A+S, the transformant carrying *SAK1* overexpression. Significant differences of the transformants A+E, A+T, and A+S to the parental strain were confirmed at $^{a}p < 0.05$, $^{b}p < 0.05$, and $^{c}p < 0.05$, respectively.

These results demonstrated that the three kinases had a redundancy function in the cell growth of baker's yeast in glucose. However, increasing each gene dosage was sufficient to enhance cell growth in glucose, and only an increased *SAK1* level could promote cell growth in maltose. Therefore, the three kinases, Elm1, Tos3, and Sak1, performed a different regulation of the baker's yeast growth via a carbon source-dependent pathway.

TABLE 3 | Specific growth rate (h^{-1}) and biomass yield (g/L) of the strains carrying genes overexpression.

Strains	Glucose		Maltose	
	Specific growth rate	Biomass yield	Specific growth rate	Biomass yield
ABY3α	0.512 ± 0.002	8.24 ± 0.12	0.460 ± 0.002	8.08 ± 0.09
A+PK	0.514 ± 0.003	8.27 ± 0.11	0.454 ± 0.003	8.11 ± 0.08
A+E	0.520 ± 0.002	9.04 ± 0.08*	0.423 ± 0.005*	8.30 ± 0.11
A+T	0.539 ± 0.003*	8.88 ± 0.09*	0.465 ± 0.003	8.14 ± 0.09
A+S	0.551 ± 0.004*	9.36 ± 0.10*	0.583 ± 0.003*	8.94 ± 0.09*

ABY3α, the parental strain; A+PK, the strain carrying the vector Yep-PK used as a blank control to demonstrate any possible effect of the empty vector; A+E, the transformant carrying ELM1 overexpression; A+T, the transformant carrying TOS3 overexpression; A+S, the transformant carrying SAK1 overexpression.
*Significant differences of the transformants to the parental strain were confirmed at *$p < 0.05$.*

Sugar Consumption in the LSMLD Media

To investigate the influence of *ELM1*/*TOS3*/*SAK1* overexpression on the maltose metabolism of baker's yeast, the utilization of maltose and glucose was tested in the LSMLD media (**Figure 3**). Blank control strain A+YP exhibited sugar consumption similar to that of the parental strain ABY3α. Compared with the parental strain ABY3α, *ELM1* overexpression strain A+E increased the maltose utilization efficiency by 15 and 11% in the maltose-glucose and maltose LSMLD media, respectively, and no evident changes of glucose utilization were observed in the maltose-glucose condition. Simultaneously, the deletion of *ELM1* repressed the maltose consumption in maltose-glucose and maltose (**Supplementary Figure 2**). Time span value, a parameter that judges the degree of glucose repression, was calculated from **Figure 3B**. An 18% decrease (1.65 h in the parental strain and 1.35 h in the strain A+E) of the time span was obtained in the transformant A+E compared with the parental strain. Unexpectedly, *TOS3* overexpression strain A+T and *SAK1* overexpression strain A+S showed a much lower maltose utilization than the parental strain in the maltose-glucose and maltose conditions, with no noticeable difference in glucose consumption. The single deletion of *TOS3* and *SAK1* did not affect maltose consumption in maltose, whereas, a negative effect was observed in maltose-glucose (**Supplementary Figure 2**).

These findings reflected that Elm1 might be the positive regulator of the maltose metabolism in baker's yeast used in this work in the analyzed conditions. Tos3 and Sak1 were not necessary for maltose metabolism in maltose, and even negatively regulated the maltose metabolism at a high expression level. Nevertheless, native expression levels of *TOS3* and *SAK1* were essential for the baker's yeast cell to resist glucose repression to utilize maltose in the maltose-glucose condition.

Fermentation Property in Lean Dough

The fermentation capacity of the transformants and the parental strain was measured in lean dough to further test the influence of *ELM1*/*TOS3*/*SAK1* overexpression on the maltose metabolism of baker's yeast (**Figure 4**). Blank control strain A+YP exhibited

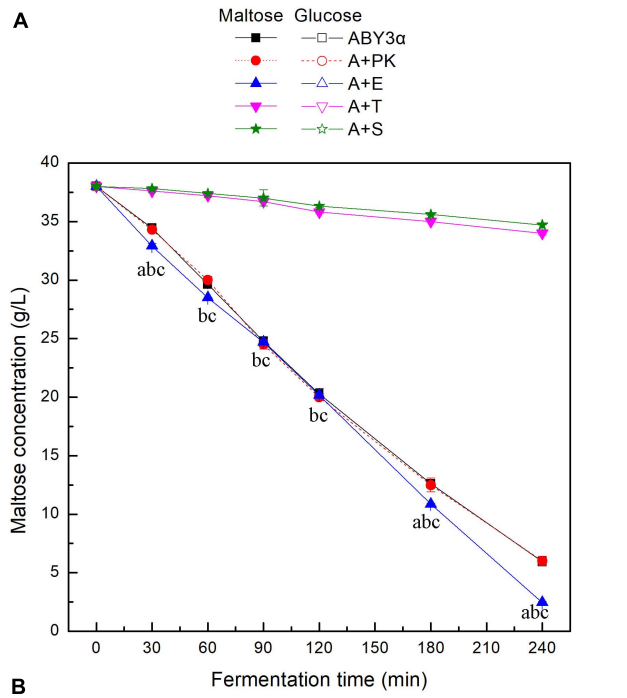

FIGURE 3 | Sugar consumption of the strains carrying genes overexpression in LSMLD media. 2 g fresh yeast was cultured in the **(A)** maltose and **(B)** maltose-glucose LSMLD media at 30°C and 1 mL cultures were sampled at a certain interval. ABY3α, the parental strain; A+PK, the strain carrying the vector Yep-PK used as a blank control to demonstrate any possible effect of the empty vector; A+E, the transformant carrying *ELM1* overexpression; A+T, the transformant carrying *TOS3* overexpression; A+S, the transformant carrying *SAK1* overexpression. Significant differences of the transformants A+E, A+T, and A+S to the parental strain were confirmed at $^{a}p < 0.05$, $^{b}p < 0.05$, and $^{c}p < 0.05$, respectively.

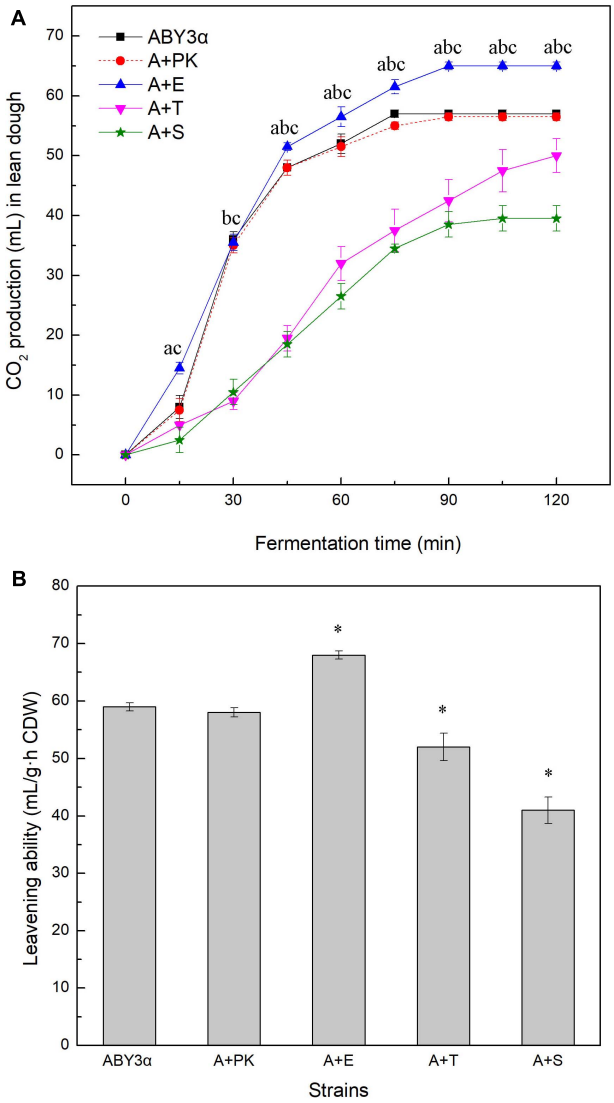

FIGURE 4 | CO_2 production of the strains carrying genes overexpression in lean dough. **(A)** Mixed dough was placed into a graduated cylinder, and CO_2 amounts were recorded at 30°C for 120 min. Significant differences of the transformants A+E, A+T, and A+S to the parental strain were confirmed at $^{a}p < 0.05$, $^{b}p < 0.05$, and $^{c}p < 0.05$, respectively. **(B)** Leavening ability was determined by CO_2 production per hour per gram (dry weight) of yeast cells. Significant differences of the transformants to the parental strain were confirmed at $^{*}P < 0.05$. ABY3α, the parental strain; A+PK, the strain carrying the vector Yep-PK used as a blank control to demonstrate any possible effect of the empty vector; A+E, the transformant carrying *ELM1* overexpression; A+T, the transformant carrying *TOS3* overexpression; A+S, the transformant carrying *SAK1* overexpression.

a fermentation performance similar to that of the parental strain ABY3α. *ELM1* overexpression strain A+E exhibited a stronger CO_2-releasing ability than the parental strain. Compared with the parental strain ABY3α, the transformant A+E increased the total amounts of CO_2 within 120 min and leavening ability by 12 and 15%, respectively; decreases of 21 and 26% were observed in the *ELM1* deletion (**Supplementary Figure 3**). On the contrary, the total amounts of CO_2 within 120 min and the leavening power of *TOS3* overexpression strain A+T were 12 and 23% lower than those of the parental strain, respectively; those for *SAK1* overexpression strain A+S were 30 and 21% lower, respectively.

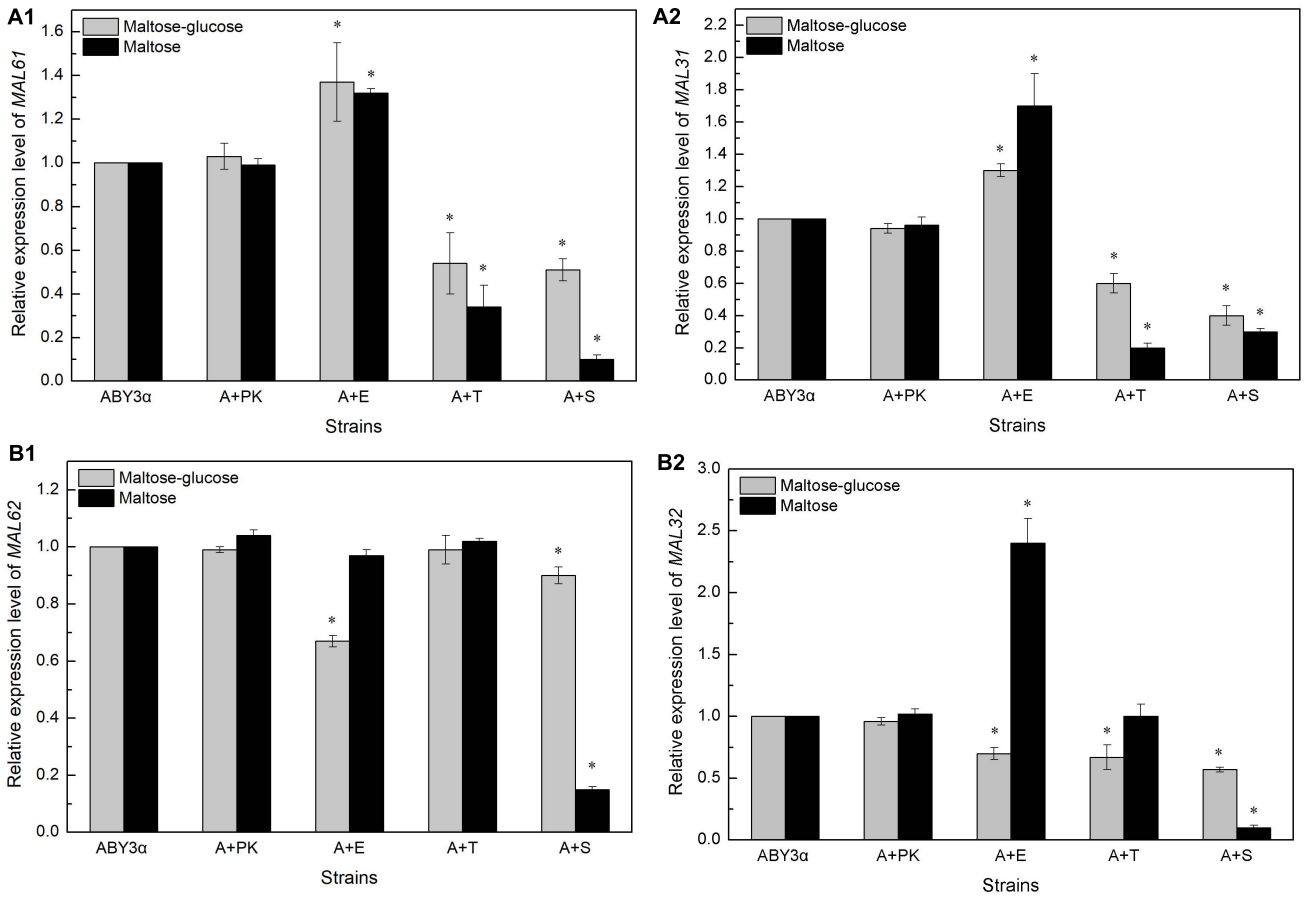

FIGURE 5 | Expression levels of **(A)** *MALx1* and **(B)** *MALx2* in the single-kinase gene overexpression. 2 g fresh yeast was cultured in the LSMLD media and cultures were sampled at 30 min. The expression levels of genes **(A1)** *MAL61*, **(A2)** *MAL31* and **(B1)** *MAL62*, **(B2)** *MAL32* were tested using qRT-PCR. ABY3α, the parental strain; A+PK, the strain carrying the vector Yep-PK used as a blank control to demonstrate any possible effect of the empty vector; A+E, the transformant carrying *ELM1* overexpression; A+T, the transformant carrying *TOS3* overexpression; A+S, the transformant carrying *SAK1* overexpression. Significant differences of the transformants to the parental strain were confirmed at * $P < 0.05$.

The single deletion of *TOS3* and *SAK1* delayed the release of CO_2 in the early stage of fermentation, but this inhibition effect might be relieved with the release of glucose repression in lean dough.

These results confirmed the positive effect of *ELM1* overexpression on maltose metabolism of baker's yeast and suggested the importance of the normal transcription of *TOS3* and *SAK1* in the lean dough fermentation.

Expression Level of *MAL* Genes

The transcription of genes *MAL61*/*MAL31* and *MAL62*/*MAL32* was analyzed in the maltose-glucose and maltose conditions (**Figure 5**, **Supplementary Figure 4**). In general, Elm1 positively regulated the transcription of *MAL61* and *MAL31* in maltose and maltose-glucose and the transcription of *MAL62* and *MAL32* in maltose. By contrast, Tos3 and Sak1 negatively regulated the expression of *MAL61*/*MAL31* in maltose-glucose and the expression of *MAL32* in maltose.

The *MAL61* mRNA level was tested in the overexpression of *ELM1* combined with the deleted *SNF1* to investigate whether Elm1 regulated the expression of *MALx1* via the Snf1 pathway. Compared with the parental strain, the expression of *MAL61* considerably decreased in strain A+E-SNF1 (**Figure 6A**), suggesting the possibility of the Elm1-Snf1-Malx1 pathway in the maltose metabolism of baker's yeast. The downregulated transcription of *MAL* in the overexpression strains suggested the Snf1-independent regulatory pathways by the kinases. Liu et al. (2011) showed that Sak1 interacted with the other protein (mainly referred to Reg1) without relying on Snf1 in glucose. Reg1 is one of the regulatory subunits of the type 1 protein phosphatase of baker's yeast and regulates glucose repression by targeting the catalytic subunit Glc7 to the corresponding substrates (Tabba et al., 2010). The deletion of *REG1* can increase the expression of *MAL61* and *MAL62*, and enhance the activities of maltose permease and maltase of industrial baker's yeast (Lin et al., 2015, 2018). Therefore, the expression levels of *MAL61* and *MAL62* were tested in the *REG1*-deleted genetic background. The expression levels of *MAL61* and *MAL62* in strain A+S-REG1 were lower than those of the parental strain in maltose-glucose and maltose (**Figure 6**). These results suggested the possibility of a Reg1-independent form

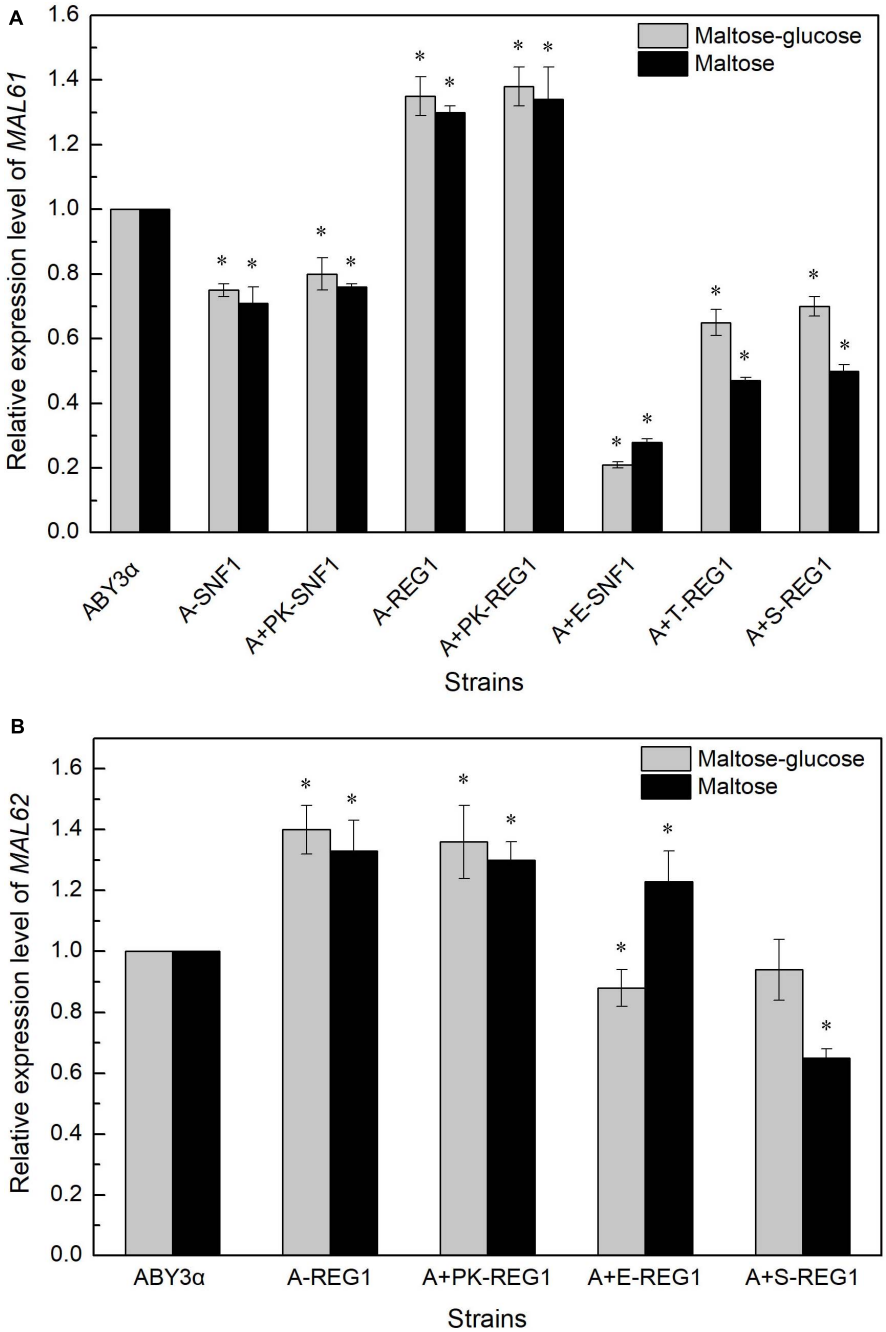

FIGURE 6 | Expression levels of **(A)** *MALx1* and **(B)** *MALx2* in the gene-combination mutants. 2 g fresh yeast was cultured in the LSMLD media and cultures were sampled at 30 min. The expression levels of genes **(A)** *MAL61* and **(B)** *MAL62* were tested using qRT-PCR. ABY3α, the parental strain; A-SNF1, the *SNF1*-deleted mutant; A+PK-SNF1, the *SNF1*-deleted mutant carrying the vector Yep-PK; A-REG1, the *REG1*-deleted mutant; A+PK-REG1, the *REG1*-deleted mutant carrying the vector Yep-PK; A+E-SNF1, the *SNF1*-deleted mutant carrying *ELM1* overexpression; A+E-REG1, the *REG1*-deleted mutant carrying *ELM1* overexpression; A+T-REG1, the *REG1*-deleted mutant carrying *TOS3* overexpression; A+S-REG1, the *REG1*-deleted mutant carrying *SAK1* overexpression. Significant differences of the transformants to the parental strain were confirmed at $^*P < 0.05$.

in the regulation of genes involved in maltose metabolism by Sak1. Similarly, Tos3 regulated the expression of *MAL61* via pathways unrelated to Reg1 under the maltose-glucose and maltose conditions as well as the regulation of *MAL62* by Elm1 (**Figure 6**). These results indicated that the three kinases differentially regulated the transcription of *MAL* genes via unknown, complex pathways but in a carbon source- and *MAL*-dependent manner.

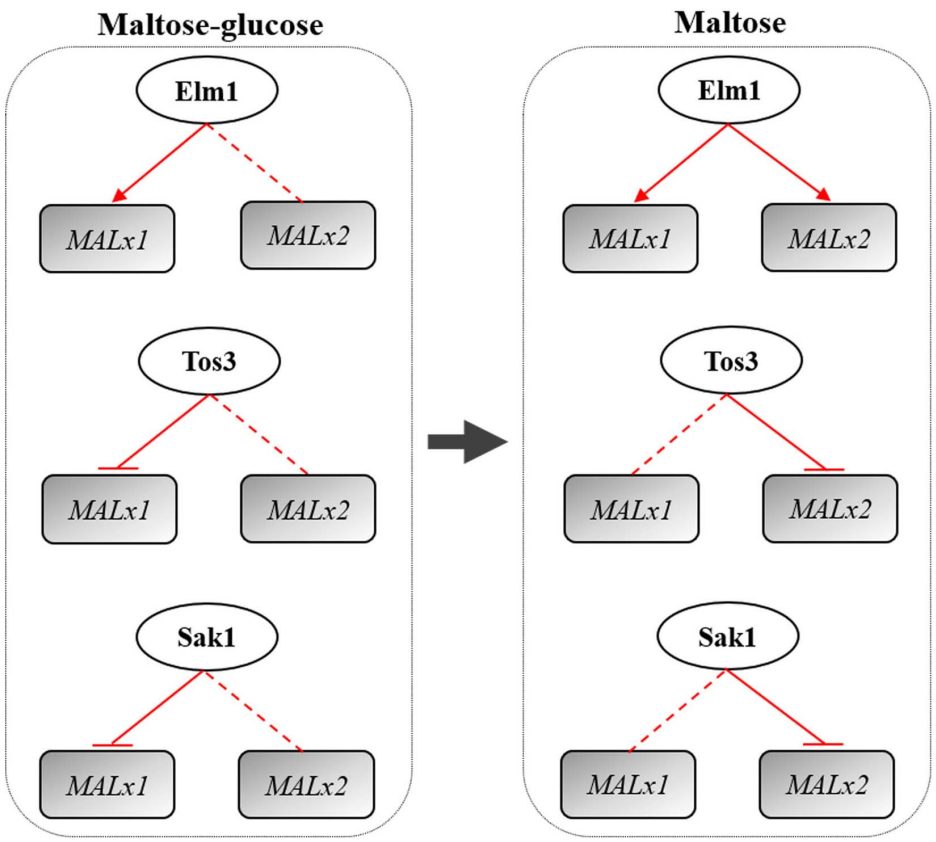

FIGURE 7 | Regulation of the kinases Elm1, Tos3, and Sak1 on *MALx1* and *MALx2* in maltose-glucose and maltose. *x* was the locus and *MAL3* and *MAL6* were analyzed in this study. Red arrow line: positive regulation. Red straight line: native level of the kinase needed. Red flat end line: negative regulation. *MALx2* in the regulation of Tos3 in maltose mainly was *MAL32*. *MALx1* in the regulation of Sak1 in maltose-glucose mainly was *MAL31*. *MALx2* in the regulation of Sak1 in maltose mainly was *MAL32*.

DISCUSSION

Saccharomyces cerevisiae Elm1, Tos3, and Sak1 kinases are known as the upstream regulators of the Snf1-Mig1 pathway in glucose repression (Hedbacker and Carlson, 2008). In this study, the focus was on the role of the three upstream kinases in the maltose metabolism of baker's yeast. The results suggested that Elm1, Tos3, and Sak1 played different roles in the regulation of the maltose metabolism of baker's yeast. Elm1 was necessary for the maltose metabolism of baker's yeast in maltose and maltose-glucose, and the overexpression of *ELM1* could promote the utilization of maltose. Native Tos3 and Sak1 were essential for yeast cells to adapt glucose inhibition, but high levels of *TOS3* and *SAK1* negatively affected the maltose metabolism.

In this study, the overexpression of *ELM1* alleviated glucose repression and upregulated the expression of *MAL61* and *MAL31* in glucose repression and maltose induction. The increase in maltose uptake by *MAL61* overexpression could facilitate the maltose metabolism and fermentation ability of baker's yeast in lean dough (Zhang et al., 2015b). The existence of the Elm1-Snf1-Mal61 pathway demonstrated that Elm1 might be one of the dominant upstream regulators in the glucose repression of maltose. The inferior transcription of *MAL62* and *MAL32* could affect maltose hydrolysis and delay the release of CO_2 in the initial lean dough fermentation in *ELM1* overexpression, and then, high CO_2 was produced with an upregulated *MAL32* in a glucose derepression condition. These findings demonstrated the differential regulation on *MAL* genes by Elm1. Snf1 is a positive regulator of maltose metabolism in baker's yeast. Elm1 functions in many cellular activities of yeast in addition to glucose repression, and multiple pathways intersect in response to signals (Souid et al., 2006; Ye et al., 2008; Casamayor et al., 2012). Therefore, Elm1 might regulate the expression of *MALx2,* even *MALx1,* via other unknown pathways rather than relying on Snf1.

The overexpression of *TOS3* and *SAK1* repressed the uptake of maltose with a downregulated transcription of *MAL61/MAL31* in maltose-glucose, thereby inhibiting maltose metabolism and lean dough fermentation. However, native Tos3 and Sak1 were necessary to adapt the glucose repression because the deletion of *TOS3* and *SAK1* decreased maltose metabolism in maltose-glucose and the initial lean dough fermentation. The increased expression of *MAL32* without glucose repression could contribute to the release of CO_2 in the late lean dough fermentation in *TOS3* and *SAK1* deletions. These findings did

not contradict the view that Sak1 is the central upstream kinase involved in the regulation of Snf1 in glucose repression (Hedbacker et al., 2004) and suggested Snf1-independent pathways other than the Reg1-dependent form by the kinases. The regulation of the kinases on maltose metabolism differed from that of invertase in glucose limitation (McCartney et al., 2005). Therefore, the three protein kinases regulated carbon sources metabolism in a signal-dependent manner, and different responses were produced in the same signal (Hong et al., 2003). The specific regulation pathway of Elm1, Tos3, and Sak1 in the maltose metabolism of baker's yeast needs to be studied further.

The function of the three protein kinases in the regulation of cell growth differed from that in the regulation of maltose metabolism. The overexpression of *ELM1* improved the growth of baker's yeast in glucose, confirming the role of Elm1 in the coordination of cell growth in budding yeast (Bouquin et al., 2000; Sreenivasan et al., 2003). A similar effect was caused by *TOS3* overexpression in the same condition. This result showed a discrepancy to the findings of Kim et al. (2005), who reported that the mutation of *TOS3* negatively affects the growth of a laboratory *S. cerevisiae* strain in a non-fermentable carbon source with no effect on glucose and raffinose. This finding may be attributed to the discrepancy of yeast strains and the test method used. The overexpression of *SAK1* enhanced the growth of baker's yeast in glucose and maltose. This finding was consistent with the results of Raab et al. (2011), who analyzed in glucose and non-fermentable carbon source conditions, and suggested the dominant role of Sak1 in the regulation of cell growth in maltose. The increase in growth cannot compensate for the reduction in maltose metabolism caused by downregulated *MAL* in *TOS3* and *SAK1* mutants.

Overall, Elm1, Tos3, and Sak1 played different roles in the regulation of maltose metabolism of baker's yeast with differential regulations on *MAL* genes (**Figure 7**). Elm1 was necessary for the maltose metabolism of baker's yeast in maltose and maltose-glucose, and the overexpression of *ELM1* could enhance the maltose metabolism and lean dough fermentation ability of baker's yeast by upregulating the transcription of *MAL61* and *MAL31* in maltose and maltose-glucose and the transcription of *MAL62* and *MAL32* in maltose. The native level of *TOS3* and *SAK1* was essential for yeast cells to adapt glucose repression, but the overexpression of *TOS3* and *SAK1* alone negatively affected maltose metabolism largely by repressing the expression of *MAL61*/*MAL31* in maltose-glucose and the expression of *MAL32* in maltose. Moreover, the three upstream kinases might regulate maltose metabolism via the Snf1-parallel pathways with a carbon source-dependent manner. These findings provided a new perspective for breeding industrial yeasts with rapid maltose metabolism and insights into the study of glucose repression in other carbon sources.

DATA AVAILABILITY STATEMENT

The original contributions presented in the study are included in the article/**Supplementary Material**, further inquiries can be directed to the corresponding author.

AUTHOR CONTRIBUTIONS

XL conceived and designed the research, and drafted the manuscript. XY and LM preformed the experiments. H-YJ participated in the data analysis. X-PH and C-FL revised the manuscript. All authors read and approved the manuscript.

FUNDING

This study was financially supported by the Hainan Provincial Natural Science Foundation of China (grant number 2019RC083), the Scientific Research Foundation of Hainan University (grant number KYQD1660), and the Foundation (No. 2018KF001) of Key Laboratory of Industrial Fermentation Microbiology of Ministry of Education and Tianjin Key Lab of Industrial Microbiology (Tianjin University of Science & Technology).

SUPPLEMENTARY MATERIAL

The Supplementary Material for this article can be found online at: https://www.frontiersin.org/articles/10.3389/fmicb.2021.665261/full#supplementary-material

REFERENCES

Bell, P., Higgins, V. J., and Attfield, P. V. (2001). Comparison of fermentative capacities of industrial baking and wild-type yeasts of the species *Saccharomyces cerevisiae* in different sugar media. *Lett. Appl. Microbiol.* 32, 224–229. doi: 10.1046/j.1472-765X.2001.00894.x

Bouquin, N., Barral, Y., Courbeyrette, R., Blondel, M., Snyder, M., and Mann, C. (2000). Regulation of cytokinesis by the Elm1 protein kinase in *Saccharomyces cerevisiae*. *J. Cell Sci.* 113, 1435–1445. doi: 10.1023/A:1005568132027

Carlson, M. (1999). Glucose repression in yeast. *Curr. Opin. Microbiol.* 2, 202–207. doi: 10.1016/S1369-5274(99)80035-6

Casamayor, A., Serrano, R., Platara, M., Casado, C., Ruiz, A., and Ariño, J. (2012). The role of the Snf1 kinase in the adaptive response of *Saccharomyces cerevisiae* to alkaline pH stress. *Biochem. J.* 444, 39–49. doi: 10.1042/BJ20112099

Coccetti, P., Nicastro, R., and Tripodi, F. (2018). Conventional and emerging roles of the energy sensor Snf1/AMPK in *Saccharomyces cerevisiae*. *Microb. Cell* 5, 482–494. doi: 10.15698/mic2018.11.655

Daniel, T., and Carling, D. (2002). Expression and regulation of the AMP-activated protein kinase-SNF1 (sucrose non-fermenting 1) kinase complexes in yeast and mammalian cells: studies using chimaeric catalytic subunits. *Biochem. J.* 365, 629–638. doi: 10.1042/BJ20020124

García-Salcedo, R., Lubitz, T., Beltran, G., Elbing, K., Tian, Y., Frey, S., et al. (2014). Glucose de-repression by yeast AMP-activated protein kinase SNF1 is controlled via at least two independent steps. *FEBS. J.* 281, 1901–1917. doi: 10.1111/febs.12753

Gietz, R. D. (2015). "High efficiency DNA transformation of *Saccharomyces cerevisiae* with the LiAc/SS-DNA/PEG method," in *Genetic Transformation Systems in Fungi. Fungal Biology*, Vol. 1, eds M. Van den Berg and K. Maruthachalam (Cham: Springer), 177–186. doi: 10.1007/978-3-319-10142-2_17

Hatanaka, H., Omura, F., Kodama, Y., and Ashikari, T. (2009). Gly-46 and His-50 of yeast maltose transporter Mal21p are essential for its resistance against glucose-induced degradation. *J. Biol. Chem.* 284, 15448–15457. doi: 10.1074/jbc.M808151200

Hazell, B., and Attfield, P. (1999). Enhancement of maltose utilisation by *Saccharomyces cerevisiae* in medium containing fermentable hexoses. *J. Ind. Microbiol. Biot.* 22, 627–632. doi: 10.1038/sj.jim.2900672

Hedbacker, K., and Carlson, M. (2008). SNF1/AMPK pathways in yeast. *Front. Biosci.* 13:2408–2420. doi: 10.2741/2854

Hedbacker, K., Hong, S. P., and Carlson, M. (2004). Pak1 protein kinase regulates activation and nuclear localization of Snf1-Gal83 protein kinase. *Mol. Cell. Biol.* 24, 8255–8263. doi: 10.1128/MCB.24.18.8255-8263.2004

Hong, S. P., Leiper, F. C., Woods, A., Carling, D., and Carlson, M. (2003). Activation of yeast Snf1 and mammalian AMP-activated protein kinase by upstream kinases. *Proc. Natl. Acad. Sci. U.S.A.* 100, 8839–8843. doi: 10.1073/pnas.1533136100

Jiang, T. X., Xiao, D. G., and Gao, Q. (2008). Characterisation of maltose metabolism in lean dough by lagging and non-lagging baker's yeast strains. *Ann. Microbiol.* 58, 655–660. doi: 10.1007/BF03175571

Kim, M. D., Hong, S. P., and Carlson, M. (2005). Role of Tos3, a Snf1 protein kinase, during growth of *Saccharomyces cerevisiae* on nonfermentable carbon sources. *Eukaryot. Cell* 4, 861–866. doi: 10.1128/EC.4.5.861-866.2005

Kim, S. B., Kwon, D. H., Park, J. B., and Ha, S. J. (2019). Alleviation of catabolite repression in *Kluyveromyces marxianus*: the thermotolerant SBK1 mutant simultaneously coferments glucose and xylose. *Biotechnol. Biofuels* 12:90. doi: 10.1186/s13068-019-1431-x

Klein, C. J., Olsson, L., and Nielsen, J. (1998). Glucose control in *Saccharomyces cerevisiae*: the role of Mig1 in metabolic functions. *Microbiology* 144, 13–24. doi: 10.1099/00221287-144-1-13

Li, P., Gao, Y. Y., Wang, C. L., Zhang, C. Y., Guo, X. W., and Xiao, D. G. (2018). Effect of ILV6 deletion and expression of aldB from *Lactobacillus plantarum* in *Saccharomyces uvarum* on diacetyl production and wine flavor. *J. Agr. Food Chem.* 66, 8556–8565. doi: 10.1021/acs.jafc.8b02356

Lin, X. (2021). The regulation of *Saccharomyces cerevisiae* Snf1 protein kinase on glucose utilization is in a glucose-dependent manner. *Curr. Genet.* 67, 245–248. doi: 10.1007/s00294-020-01137-0

Lin, X., Zhang, C. Y., Bai, X. W., and Xiao, D. G. (2015). Effects of *GLC7* and *REG1* deletion on maltose metabolism and leavening ability of baker's yeast in lean dough. *J. Biotechnol.* 209, 1–6.

Lin, X., Zhang, C. Y., Meng, L., Bai, X. W., and Xiao, D. G. (2018). Overexpression of *SNF4* and deletions of *REG1*- and *REG2*-enhanced maltose metabolism and leavening ability of baker's yeast in lean dough. *J. Ind. Microbiol. Biotechnol.* 45, 827–838. doi: 10.1007/s10295-018-2058-9

Liu, Y., Xu, X., and Carlson, M. (2011). Interaction of SNF1 protein kinase with its activating kinase Sak1. *Eukaryot. Cell* 10, 313–319. doi: 10.1128/EC.00291-10

Martinez-Ortiz, C., Carrillo-Garmendia, A., Correa-Romero, B. F., Canizal-García, M., González-Hernández, J. C., Regalado-Gonzalez, C., et al. (2019). SNF1 controls the glycolytic flux and mitochondrial respiration. *Yeast* 36, 487–494. doi: 10.1002/yea.3399

McCartney, R. R., and Schmidt, M. C. (2001). Regulation of Snf1 kinase Activation requires phosphorylation of threonine 210 by an upstream kinase as well as a distinct step mediated by the Snf4 subunit. *J. Biol. Chem.* 276, 36460–36466. doi: 10.1074/jbc.M104418200

McCartney, R. R., Rubenstein, E. M., and Schmidt, M. C. (2005). Snf1 kinase complexes with different beta subunits display stress-dependent preferences for the three Snf1-activating kinases. *Curr. Genet.* 47, 335–344. doi: 10.1007/s00294-005-0576-2

Meng, L., Liu, H. L., Lin, X., Hu, X. P., and Liu, S. X. (2020). Enhanced multi-stress tolerance and glucose utilization of *Saccharomyces cerevisiae* by overexpression of the *SNF1* gene and varied beta isoform of Snf1 dominates in stresses. *Microb. Cell Fact.* 19:134. doi: 10.1186/s12934-020-01391-4

Meng, L., Yang, X., Lin, X., Jiang, H. Y., and Liu, S. X. (2021). Effect of overexpression of *SNF1* on the transcriptional and metabolic landscape of baker's yeast under freezing stress. *Microb. Cell Fact.* 20:10. doi: 10.1186/s12934-020-01503-0

Östling, J., and Ronne, H. (1998). Negative control of the MIG1p repressor by Snf1p-dependant phosphorylation in the absence of glucose. *Eur. J. Biochem.* 252, 162–168. doi: 10.1046/j.1432-1327.1998.2520162.x

Papamichos-Chronakis, M., Gligoris, T., and Tzamarias, D. (2004). The Snf1 kinase controls glucose repression in yeast by modulating interactions between the Mig1 repressor and the Cyc8-Tup1 co-repressor. *EMBO Rep.* 5, 368–372. doi: 10.1038/sj.embor.7400120

Persson, S., Welkenhuysen, N., Shashkova, S., and Cvijovic, M. (2020). Fine-tuning of energy levels regulates *SUC2* via a SNF1-dependent feedback loop. *Front. Physiol.* 11:954. doi: 10.3389/fphys.2020.00954

Raab, A. M., Hlavacek, V., Bolotina, N., and Lang, C. (2011). Shifting the fermentative/oxidative balance in *Saccharomyces cerevisiae* by transcriptional deregulation of Snf1 via overexpression of the upstream activating kinase Sak1p. *Appl. Environ. Microbiol.* 77, 1981–1989. doi: 10.1128/AEM.02219-10

Ramírez-Zavala, B., Mottola, A., Haubenreißer, J., Schneider, S., Allert, S., Brunke, S., et al. (2017). The Snf1-activating kinase Sak1 is a key regulator of metabolic adaptation and in vivo fitness of *Candida albicans*. *Mol. Microbiol.* 104, 989–1007. doi: 10.1111/mmi.13674

Shao, Z. Y., Zhao, H., and Zhao, H. M. (2008). DNA assembler, an in vivo genetic method for rapid construction of biochemical pathways. *Nucleic Acids Res.* 37:e16. doi: 10.1093/nar/gkn991

Souid, A. K., Gao, C., Wang, L. M., Milgrom, E., and Shen, W.-C. W. (2006). *ELM1* is required for multidrug resistance in *Saccharomyces cerevisiae*. *Genetics* 173, 1919–1937. doi: 10.1534/genetics.106.057596

Srđan, N., Vesna, Z. K., and Vladimir, M. (2004). Regulation of maltose transport and metabolism in *Saccharomyces cerevisiae*. *Food Technol. Biotech.* 42, 213–218. doi: 10.1016/S0950-3293(03)00100-9

Sreenivasan, A., Bishop, A. C., Shokat, K. M., and Kellogg, D. R. (2003). Specific inhibition of Elm1 kinase activity reveals functions required for early G1 events. *Mol. Cell Biol.* 23, 6327–6337. doi: 10.1128/mcb.23.17.6327-6337.2003

Sun, X., Zhang, C., Dong, J., Wu, M., Zhang, Y., and Xiao, D. (2012). Enhanced leavening properties of baker's yeast overexpressing *MAL62* with deletion of *MIG1* in lean dough. *J. Ind. Microbiol. Biotechnol.* 39, 1533–1539. doi: 10.1007/s10295-012-1144-7

Sutherland, C. M., Hawley, S. A., Mccartney, R. R., Leech, A., Stark, M. J. R., Schmidt, M. C., et al. (2003). Elm1p is one of three upstream kinases for the *Saccharomyces cerevisiae* SNF1 complex. *Curr. Biol.* 13, 1299–1305. doi: 10.1016/s0960-9822(03)00459-7

Tabba, S., Mangat, S., McCartney, R., and Schmidt, M. C. (2010). PP1 phosphatase-binding motif in Reg1 protein of *Saccharomyces cerevisiae* is required for interaction with both the PP1 phosphatase Glc7 and the Snf1 protein kinase. *Cell Signal.* 22, 1013–1021. doi: 10.1016/j.cellsig.2010.02.003

Trumbly, R. J. (1992). Glucose repression in the yeast *Saccharomyces cerevisiae*. *Mol. Microbiol.* 6, 15–21. doi: 10.1111/j.1365-2958.1992.tb00832.x

Verstrepen, K. J., Iserentant, D., Malcorps, P., Derdelinckx, G., Van Dijck, P., Winderickx, J., et al. (2004). Glucose and sucrose: hazardous fast-food for industrial yeast? *Trends Biotechnol.* 22, 531–537. doi: 10.1016/j.tibtech.2004.08.001

Ye, T., Elbing, K., and Hohmann, S. (2008). The pathway by which the yeast protein kinase Snf1p controls acquisition of sodium tolerance is different from that mediating glucose regulation. *Microbiology* 154, 2814–2826. doi: 10.1099/mic.0.2008/020149-0

Zhang, C. Y., Bai, X. W., Lin, X., Liu, X. E., and Xiao, D. G. (2015a). Effects of *SNF1* on maltose metabolism and leavening ability of baker's yeast in lean dough. *J. Food Sci.* 80, M2879–M2885. doi: 10.1111/1750-3841.13137

Zhang, C. Y., Lin, X., Song, H. Y., and Xiao, D. G. (2015b). Effects of *MAL61* and *MAL62* overexpression on maltose fermentation of baker's yeast in lean dough. *World J. Microbiol. Biotechnol.* 31, 1241–1249. doi: 10.1007/s11274-015-1874-6

Zhang, C. Y., Song, H. Y., Lin, X., Bai, X. W., and Xiao, D. G. (2015c). "Expression, purification and characterization of maltase from "Quick" baker's yeast," in *Advances in Applied Biotechnology. Lecture Notes in Electrical Engineering*, Vol. 333, eds T. C. Zhang and M. Nakajima (Berlin: Springer), doi: 10.1007/978-3-662-46318-5_29

Conflict of Interest: The authors declare that the research was conducted in the absence of any commercial or financial relationships that could be construed as a potential conflict of interest.

frontiers in Microbiology

REVIEW
published: 07 June 2021
doi: 10.3389/fmicb.2021.645435

A Review: Microbial Diversity and Function of Fermented Meat Products in China

Zhengli Wang, Zhengxi Wang, Lili Ji, Jiamin Zhang, Zhiping Zhao, Rui Zhang, Ting Bai, Bo Hou, Yin Zhang, Dayu Liu, Wei Wang and Lin Chen**

Key Laboratory for Meat Processing of Sichuan Province, Chengdu University, Chengdu, China

OPEN ACCESS

Edited by:
Wanping Chen,
Georg August University of Göttingen, Germany

Reviewed by:
Dengyong Liu,
Bohai University, China
Lixin Luo,
South China University of Technology, China
Xianchao Feng,
Northwest A & F University Apple Research Center, China

***Correspondence:**
Wei Wang
wangwei8619@163.com
Lin Chen
chenlin@edu.edu.cn

Specialty section:
This article was submitted to Food Microbiology, a section of the journal Frontiers in Microbiology

Received: *23 December 2020*
Accepted: *30 April 2021*
Published: *07 June 2021*

Citation:
Wang Z, Wang Z, Ji L, Zhang J, Zhao Z, Zhang R, Bai T, Hou B, Zhang Y, Liu D, Wang W and Chen L (2021) A Review: Microbial Diversity and Function of Fermented Meat Products in China. Front. Microbiol. 12:645435. doi: 10.3389/fmicb.2021.645435

Fermented meat products have a long history in China. These products exhibit a characteristic unique flavor, compact meat quality, clear color, long shelf life and wide variety and are easy to transport. During the processing and storage of fermented meat products, microorganisms are present and exhibit diverse characteristics. Microorganisms can accelerate the degradation of proteins and fats to produce flavor compounds, inhibit the growth and reproduction of heterozygous bacteria, and reduce the content of chemical pollutants. This paper reviews the microbial diversity of Chinese ham, sausage, preserved meat, pressed salted duck, preserved fish and air-dried meat and provides analyses of the microbial compositions of various products. Due to the differences in raw materials, technology, auxiliary materials, and fermentation technology, the microbial species found in various fermented meat products in China are different. However, most fermented meat products in China are subjected to pickling and fermentation, so their microbial compositions also have similarities. Microorganisms in fermented meat products mainly include staphylococci, lactobacilli, micrococci, yeasts, and molds. The study of microbial diversity is of great significance for the formation of quality flavor and the safety control of fermented meat products, and it provides some theoretical reference for the study of fermented meat products in China.

Keywords: fermented meat products, microbial diversity, bacteria, fungi, function of microorganisms

INTRODUCTION

Fermented meat products are meat products with longer shelf lives and special flavors, textures and colors that are made of raw meat under specific temperature and humidity conditions by fermentation via microorganisms or enzymes (Liu Y. L. et al., 2020). Fermentation methods include natural fermentation and the artificial addition of a starter to regulate fermentation (Sivamaruthi et al., 2020). The microorganisms involved in the natural fermentation process are primarily derived from raw materials and the environment. Under specific curing and maturing process conditions, typical local microbial communities are formed through competition, thus significantly affecting the product quality and safety (Frédéric et al., 2006). In the 1990s, with the transformation of Chinese people's demand for meat from quantity to quality, fermented meat

products with artificially added microbial starters were gradually introduced into the Chinese market (Yu et al., 2010).

Many traditional meat products, such as Sichuan preserved meat, Hunan preserved meat, Nanjing pressed salted duck, Cantonese sausage, Sichuan sausage, Jinhua ham, Xuanwei ham, and Rugao ham, are all fermented. In recent years, with the improvement of production technology and equipment, research on the flavor, sensory perception, nutritional characteristics and safety of fermented meat products has become a hot topic (Douglas et al., 2020). Microorganisms play an important role during the fermentation of meat products. Flavor formation in fermented meat products is a complex biochemical process that has not been completely understood to date. The microbial diversity of the primary fermented meat products in China is summarized in this paper, and the characteristics of their microbial compositions were analyzed to provide a theoretical basis for further study on fermented meat products.

THE FUNCTION OF MICROORGANISMS IN FERMENTED MEAT PRODUCTS

Food fermentation is not only an effective method of food preservation but also an economical method of food processing (He et al., 2017). Microorganisms play an important role in fermented meat products, and their functions are as follows:

Promotion of the production of special flavors in meat products (PaPamanoli et al., 2002; Polka et al., 2015). Studies have shown that *Staphylococcus carnosus* (*S. carnosus*) and *Staphylococcus xylosus* (*S. xylosus*) can significantly promote the hydrolysis of fat and protein in preserved meat, improve the color and promote the rapid formation of flavor (Zhou et al., 2018). The esterases, proteases and catalases produced by microorganisms have synergistic effects with endogenous enzymes, causing biochemical changes in the proteins and fats in raw meat and forming small molecules, such as amino acids, esters, peptides and short-chain volatile fatty acids. The digestive function is greatly improved, and the contents of essential amino acids, vitamins and bifidobacterium are increased, enhancing the effects on nutrition and health (Liang et al., 2010). Chen et al. (2017) inoculated Harbin dried sausage with a mixed starter, and the free fatty acid (FFA) content in the inoculated group was significantly higher than that in the uninoculated group. The peroxide value and thiobarbituric acid contents in the inoculated group were significantly reduced compared with those in the uninoculated group, and the contents of aldehydes, ketones and hydrocarbons, which are related to lipid oxidation, were significantly reduced compared with those in the uninoculated group. The mixed starter promoted the hydrolysis of fat, inhibited lipid peroxidation and improved the fermentation flavor of Harbin dried sausage. Wang et al. (2014) added complex microbial starters to traditional preserved meat, and the contents of free amino acids and the types of volatile flavor substances in the preserved meat increased, which improved its nutritional value, flavor and safety.

Inhibition of the growth and reproduction of heterozygous bacteria (Swetwiwathana and Visessanguan, 2015). Microorganisms primarily inhibit the growth and reproduction of harmful bacteria through bacterial competition, acid production and bacteriocin production. Studies have shown that *S. xylosus* can inhibit the growth of *Listeria monocytogenes (L. monocytogenes*) in sausage (PaPamanoli et al., 2002). Wang et al. (2013) inoculated *Latilactobacillus sakei subsp. sakei* (*L. sakei*) as a starter culture into Sichuan sausage, and the results showed that the lactic acid bacteria rapidly controlled the growth of the total bacterial colonies during sausage fermentation and inhibited the growth of foodborne pathogenic bacteria, such as *Escherichia coli* (*E. coli*) and enterobacteriaceae. Lactic acid bacteria can decompose carbohydrates in sausages to produce a large number of lactic acid and a small number of acetic acid as well as propionic acid, formic acid, 3-methyl-butyric acid, butyric acid and other organic acids, thus extending the shelf life of sausages (Li et al., 2015). Lactic acid bacteria can reportedly inhibit or kill spoilage microorganisms and pathogenic microorganisms in food (Zhang et al., 2017). Zhao et al. (2017) isolated and screened a strain of lactic acid bacteria with obvious antibacterial activity against *E. coli* and *Staphylococcus aureus* (*S. aureus*) from five kinds of fermented meat products, which was identified as *Weissella hellenica* (*W. hellenica*). Studies have shown that *L. sakei* C2 can produce broad-spectrum antibacterial bacteriocins and inhibit the growth of harmful microorganisms (Gao et al., 2014).

Reducing the content of biogenic amines (BAs). Sun et al. (2016) found that six types of BAs (cadaverine, putrescine, tryptamine, 2-phenylethylamine, histamine, and tyramine) were inhibited by the presence of *L. plantarum* and *S. xylosus*, and a mixture of these bacteria had the highest inhibitory effect. Niu et al. (2019) selected *L. plantarum* PL-ZL001 from four types of fermented meat products and added it to sausage. PL-ZL001 inhibited the accumulation of six BAs, and its inhibitory effect on the most toxic histamine was significantly greater than that of commercial *S. xylosus*.

Reducing the nitrite content. Wang et al. (2013) inoculated *L. sakei* as a starter culture into Sichuan sausage. The results showed that the nitrite content in the sausage containing added *L. sakei* decreased rapidly from 100 to 9.6 ppm, whereas the nitrite content in the naturally fermented sausage decreased slowly from 100 to 32.1 ppm. You et al. (2015) inoculated lactic acid bacteria into dried salted fish as a starter, and the results showed that the mass fraction of nitrite in the dried salted fish with added lactic acid bacteria was (0.1 ± 0.04) mg·kg^{-1}, which was significantly lower than that in the group without the addition of lactic acid bacteria at (0.8 ± 0.04) mg/kg^{-1}. Lactic acid bacteria had an inhibitory effect on the formation of nitrosamines. Gao et al. (2014) inoculated 5 log CFU/g and 7 log CFU/g *L. sakei* C2 into sausage, and the results showed that the nitrite content decreased with increasing inoculation concentrations.

Microorganisms can improve the quality of fermented meat products to a certain extent. They can not only promote the degradation of protein and fat and accelerate the formation of flavor substances but can also improve the nutritional value of fermented meat products. At the same time, they can inhibit the growth and reproduction of harmful bacteria, reduce the use of salt in fermented meat products, improve the taste,

reduce the content of nitrite and BAs, and improve the safety of fermented meat products.

MICROBIAL DIVERSITY IN FERMENTED MEAT PRODUCTS

Ham

Ham is a non-ready-to-eat meat product made from fresh (frozen) pig hind legs as the primary raw material with other auxiliary materials add after finishing, curing, washing, desalting, air-drying and fermentation, and other processes. The most famous Chinese-style hams are Jinhua, Rugao, and Xuanwei hams. Alcohols, ketones, aldehydes, esters, alkanes, and acids are considered the primary volatile compounds in hams (Radovčić et al., 2016; Liu D. Y. et al., 2020; Wu et al., 2020). There is a close relationship between the staphylococci and the aldehyde compounds produced as hexanal, nonanal, benzaldehyde, and phenylacetaldehyde, indicating their contributions to the formation of characteristic flavor substances in Jinhua dry-cured ham (Wang Y. B. et al., 2021). Yeasts and molds were primarily present on the surface of Anfu ham, and cocci and yeasts were primarily present inside the ham (Huang et al., 2003). During the dehydration of Jinhua ham, the number of microorganisms inside the ham reached 1.39×10^6 CFU/g, and during the maturation stage, the number of microorganisms inside decreased to 2.0×10^3 CFU/g. Lactic acid bacteria and staphylococci are the dominant bacteria in Jinhua ham. The lactic acid bacteria have primarily been identified as *Pediococcus urinaeequi* (*P. urinaeequi*), *Pediococcus pentosaceus* (*P. pentosaceus*), and *Lactiplantibacillus pentosus* (*L. pentosus*). The staphylococci species primarily include *S. xylosus*, S*taphylococcus equus* (*S. equus*) and *Staphylococcus gallinarum* (*S. gallinarum*) (He et al., 2007). The dominant microorganisms in Xuanwei ham were micrococci, staphylococci and molds, the number of which reached greater than 10^6 CFU/g on the surface and greater than 10^2 CFU/g inside (Li et al., 2003). Twenty-seven fungi were detected in Xuanwei ham using PCR-DGGE technology. The primary species were *Aspergillus pseudoglaucus* (*A. pseudoglaucus*), *Phialosimplex caninus* (*P. caninus*), *Aspergillus penicillioides* (*A. penicillioides*), *Yamadazyma triangularis* (*Y. triangularis*), *Wallemia sebi* (*W. sebi*), and *Candida glucosophila* (*C. glucosophila*), among which the dominant fungus was *A. pseudoglaucus* (Zou et al., 2020). The diversity and abundance of bacteria in Panxian ham were higher than those of fungi. Ten bacterial phyla were detected at the phylum level, of which Firmicutes and Proteobacteria were dominant. Firmicutes and Proteobacteria were the dominant phyla in the curing process, while Proteobacteria was the dominant phylum in the maturing process. A total of 154 bacterial genera was detected at the genus level, and the dominant genera were *Psychrobacter*, *Acinetobacter*, *Ochrobactrum*, *Staphylococcus*, and *Micrococcus*. Four fungal phyla were detected at the phylum level, and the dominant fungus was Ascomycota. Fifty-one fungal genera were detected at the genus level, and the dominant fungi were *Debaryomyces*, *Aspergillus*, *Yamadazyma*, *Candida*, and *Penicillium* (Mu et al., 2019). After isolation and purification of the dominant microorganisms in Weining ham, a total of 10 strains was obtained, including 4 strains of *Staphylococcus equinosus* (*S. equinosus*), 2 strains of *S. xylosus*, 2 strains of *Lactococcus lactis*, 1 strain of *Candida metapsilosis* (*C. metapsilosis*), and 1 strain of *Candida parapsilosis (C. parapsilosis)* (Zhang et al., 2019). Among the different processing procedures of Nuodeng ham, the bacterial diversity at the salting stage was the highest, and the dominant bacteria at the phylum level were Firmicutes, Proteobacteria, Actinobacteria, and Bacteroidetes. At the genus level, the dominant bacteria included *Psychrobacter, Aeromonas, Shewanella, Pseudomonas*, and *Acinetobacter* (Wang X. R. et al., 2021). The primary species of microorganisms in different hams are presented in **Table 1**.

Sausage

Sausage is a type of non-ready-to-eat meat product made from fresh (frozen) livestock and poultry meat and other auxiliary materials by cutting (or mincing), stirring, curing, filling (or shaping), drying by baking (or drying in the sun, air-drying in the shade), smoking (or not smoking) and other processes. Sausage is primarily produced in Sichuan, Guangdong, Guangxi, Hunan, and Shanghai. The most famous sausages are Cantonese- and Sichuan-style sausages. Sichuan-style sausage is spicy and hot, whereas Cantonese-style sausage is salty and sweet. Among the different styles, Sichuan sausage is distinguished by its high processing and consumption, multiflavored nature and excellent flavor. The flavor components of mature sausage primarily include acetic acid, 3-hydroxy-2-butanone, 2-butanone, esters, volatile phenols, aldehydes and small amounts of alkene, and nitrogen compounds (Hu et al., 2020). Firmicutes, Proteobacteria, Actinobacteria, and Bacteroidetes were detected at the phylum level in Sichuan sausage. Firmicutes

TABLE 1 | Primary microorganisms in different hams.

Type of ham	Primary microorganisms	References
Anfu ham[1]	Skin coat: yeasts, molds Interior: cocci, yeasts	Huang et al., 2003
Jinhua ham[1]	*P. urinaeequi*, *P. pentosaceus*, *L. pentosus*, *S. xylosus*, *S. equus*, *S. gallinarum*	He et al., 2007
Xuanwei ham[2]	*A. pseudoglaucus*, *P. caninus*, *A. penicillioides*, *Y. triangularis*, *W. sebi*, *C. glucosophila*	Zou et al., 2020
Panxian ham[2]	*Psychrobacter*, *Acinetobacter*, *Ochrobactrum*, *Staphylococcus*, *Micrococcus*, *Debaryomyces*, *Aspergillus*, *Yamadazyma*, *Candida*, *Penicilliums*	Mu et al., 2019
Weining ham[2]	*S. equorum*, *S. xylosus*, *P. acidilactici*, *C. metapsilosis*, *C. parapsilosis*	Zhang et al., 2019
Nuodeng ham[2]	*Psychrobacter*, *Aeromonas*, *Shewanella*, *Pseudomonas*, *Acinetobacter*	Wang X. R. et al., 2021

[1] Represents the identification of microorganisms by pure culture, and [2] represents the identification of microorganisms by molecular biological methods (same below).

(85.65∼93.96%) and Proteobacteria (5.59∼13.95%) were the dominant phyla. *Lactobacillus*, *Weissella*, *Brochothrix*, *Pediococcus*, and *Staphylococcus* were detected at the genus level. Among them, *Weissella* (26.74%) and *Lactobacillus* (63.14%) were the dominant genera. Ninety percent of the fungi in Sichuan sausage were unclassified, and only Bangiales and Ascomycota exceeded 0.1% at the phylum level. *Porphyra* (10.75%) was dominant at the genus level, and *Debaryomyces* and *Saccharomyces* accounted for less than 0.1% (Wang et al., 2019). Nineteen strains of staphylococci and 12 strains of lactic acid bacteria were isolated from Cantonese sausage. According to PCR-DGGE identification, the primary dominant bacteria were *Staphylococcus saprophyticus* (*S. saprophyticus*), *S. xylosus* and *Lactobacillus*, whereas the secondary dominant bacteria were *S. epidermidis*, *Staphylococcus cohnii* (*S. cohnii*), *Lactococcus garvieae* (*L. garvieae*), and *Bacillus* spp. (Xie et al., 2013). At the phylum level, Firmicutes (57.01%), Proteobacteria (30.43%), Cyanobacteria (7.67%), Bacteroidetes (2.63%), and Actinobacteria (2.01%) were present in Hubei Enshi sausage, among which Firmicutes and Proteobacteria were the dominant phyla. At the genus level, *Brochothrix* (38.34%), *Staphylococcus* (9.79%), *Psychrobacter* (7.55%), *Photobacterium* (5.90%), *Pseudomonas* (4.82%), *Lactobacillus* (2.80%), *Leuconostoc* (2.29%), and *Acinetobacter* (2.19%) were identified, among which *Brochothrix* was the dominant genus (Deng et al., 2018). Scholars have studied 16 types of traditional Chinese sausages and found that Firmicutes is the dominant phylum in most sausages. In addition, *Lactobacillus*, *Micrococcus*, *Psychrobacter*, *Tetragenococcus*, and *Pseudomonas* were the dominant genera. The dominant fungal phylum was Ascomycota (Li et al., 2019). Studies have shown that the dominant phyla in five types of northeast sausage are Firmicutes and Proteobacteria, whereas *Lactobacillus*, *Staphylococcus*, *Leuconostoc*, *Lactococcus*, and *Weissella* are the dominant genera. The dominant species are *S. xylosus*, *L. sakei*, *W. hellenica*, *Leuconostoc citreum* (*L. citreum*), *Lactococcus raffinolactis* (*L. raffinolactis*), and *L. plantarum* (Hu et al., 2020). The primary species of microorganisms in different sausages are presented in **Table 2**.

TABLE 2 | Primary microorganisms in different sausages.

Type of sausage	Primary microorganisms	References
Sichuan-style sausage[2]	*Lactobacillus*, *Weissella*, *Brochothrix*, *Pediococcus*, *Staphylococcus*, *Porphyra*, *Debaryomyces*, *Saccharomyces*	Wang et al., 2019
Cantonese-style sausage[2]	*S. saprophyticus*, *S. xylosus*, *S. epidermidis*, *S. cohnii*, *L. garvieae*, *Bacillus* spp.	Xie et al., 2013
Enshi sausage[2]	*Brochothrix*, *Staphylococcus*, *Psychrobacter*, *Photobacterium*, *Pseudomonas*, *Lactobacillus*, *Leuconostoc*, *Acinetobacter*	Deng et al., 2018
16 types of traditional sausage[2]	*Micrococcus*, *Psychrobacter*, *Tetragenococcus*, *Pseudomonas*, *Debaryomyces*, *Wallemia*, *Aspergillus*	Li et al., 2019
Sausages from Northeast China[2]	*S. xylosus*, *L. sakei*, *W. hellenica*, *L. citreum*, *L. raffinolactis*, *L. plantarum*	Hu et al., 2020

[2] *Represents the identification of microorganisms by molecular biologica methods.*

Preserved Meat

Preserved meat is a type of non-ready-to-eat meat product made from fresh (frozen) livestock meat as the primary raw material, along with other auxiliary materials by curing, drying by baking (or drying in the sun, air-drying in the shade), smoking (or not smoking), and other processes. Preserved meat is primarily popular in Sichuan, Hunan, and Guangdong. Hexanal, 3-methyl butyraldehyde, 3-methyl valeraldehyde, (E)-2-octenal, octanal, linalool, nonanal, hexanoic acid, ethyl hexanoate, anisole, and acetone were the primary flavor contributors in preserved meat (Guo et al., 2020; Mao et al., 2021). The bacteria at the phylum level in Sichuan traditional preserved meat include Firmicutes, Proteobacteria, Actinobacteria, Cyanobacteria, and Bacteroidetes, and the dominant phylum is Firmicutes. At the genus level, the bacteria included *Staphylococcus*, *Micrococcus*, *Acinetobacter*, *Psychrobacter*, *Pseudomonas*, *Brochothrix*, *Cupriavidus*, *Citrobacter*, and *Enterobacter*, and the dominant genus was *Staphylococcus*. The fungi at the phylum level in Sichuan traditional preserved meat include Ascomycota, Basidiomycota, Glomeromycota, and Rozellomycota, and the dominant phylum was Ascomycota. At the genus level, *Aspergillus*, *Debaryomyces*, *Candida*, *Wallemia*, *Penicillium*, *Malassezia*, and *Didymella* were dominant, and the dominant fungus was *Aspergillus* (Wen et al., 2020). The dominant microorganisms during the shelf life of Sichuan preserved meat were *Staphylococcus* and *Micrococcus* followed by *Lactobacillus* (Quan et al., 2017). At the phylum level, the microorganisms in Hubei Enshi preserved meat primarily included Firmicutes (54.05%) and Proteobacteria (44.28%), while at the genus level, the microorganisms were primarily *Staphylococcus* (40.18%), *Psychrobacter* (24.02%), *Pseudoalteromonas* (9.37%), *Brochothrix* (8.53%), *Cobetia* (4.71%), and *Acinetobacter* (2.31%) (Deng et al., 2018). The number of yeasts and molds in Xiangxi preserved meat in Hunan Province reached 2.6×10^7 CFU/g. The number of staphylococci and micrococci reached 3.7×10^6 CFU/g. The number of lactic acid bacteria reached 2.4×10^6 CFU/g, and the number of heat-resistant microorganisms reached 3.5×10^3 CFU/g (Dong et al., 2018). A study on the microbial diversity of preserved meats in Hunan Province found that the microorganisms included approximately 20 phyla, among which Firmicutes, Proteobacteria, Cyanobacteria, and Actinobacteria were the dominant phyla. In addition, there were more than 10 microbial genera, among which *Staphylococcus*, *Sphingomonas*, *Pseudomonas*, *Enterobacter*, and *Leuconostoc* were the dominant genera (Yi et al., 2017). The lactic acid bacteria in Longxi preserved meat included *L. plantarum*, *Latilactobacillus curvatus* (*L. curvatus*), *L. sakei*, *Companilactobacillus alimentarius* (*C. alimentarius*), *P. pentosaceus*, and *Leuconostoc mesenteroides* (*L. mesenteroides*), of which *L. plantarum* has strong acid production capacity and is quite tolerant to sodium chloride and sodium nitrite (Deng et al., 2019). The total microbial number in Jilin Changchun preserved meat was 2.863×10^7 CFU/g. At the genus level, before

air drying, the dominant microorganisms included *Bacillus*, *Acinetobacter*, and *Halospirulina*. After air drying for 1 week, the dominant microorganisms were *Pseudomonas*, *Acinetobacter*, *Psychrobacter*, and *Halospirulina*. After air drying for 2 weeks, the dominant microorganisms were *Erwinia*, *Halospirulina*, *Enterobacter*, and *Acinetobacter*. After air drying for 3 weeks, the dominant microorganisms included *Bacillus*, *Halospirulina*, *Enterobacter*, and *Erwinia*. After air drying for 4 weeks, the dominant microorganisms were *Halospirulina*, *Acinetobacter*, *Enterobacter*, and *Microbacteriaceae* (Li et al., 2020). The primary microorganisms species in different preserved meats are presented in **Table 3**.

Pressed Salted Duck

Pressed salted duck is a non-ready-to-eat meat product made from duck as the raw material processed by slaughter, hair removal, evisceration, cleaning and curing, shaping, and air drying. Pressed salted duck is a specialty of the southwest region, and famous products include Chongqing Baishiyi pressed salted duck, Nanan pressed salted duck, and Jianchang pressed salted duck. Benzaldehyde and (E, E)-2,4-nonadienal are the key flavor compounds of pressed salted duck. Hexanal, nonanal, naphthalene, (Z)-2-heptenal, (E)-2-octenal, (E)-2-kunienal, 1-octene-3-ol, 2-n-pentylfuran and linalool were the primary compounds affecting the flavor differences in pressed salted ducks from different regions (Tong et al., 2018). The total number of microbial colonies in Sichuan air-dried ducks was 4.692×10^3 CFU/g, and *Neisseria*, *Micrococcus*, and *Staphylococcus* were the primary dominant genera (Liu et al., 2007). The beneficial microorganisms in Jianchang pressed salted duck primarily include staphylococci, lactic acid bacteria, micrococci, yeasts, and molds. The staphylococci include *S. carnosus*, *Staphylococcus simulans* (*S. simulans*), and *S. xylosus*. The lactic acid bacteria include *Lactobacillus* [*L. plantarum*, *L. sakei*, *Lactobacillus acidophilus* (*L. acidophilus*), *L. lactis*, *Lacticaseibacillus casei* (*L. casei*), *L. curvatus*, *Limosilactobacillus fermentum* (*L. fermentum*), *Loigolactobacillus bifermentans* (*L. bifermentans*), *Levilactobacillus brevis* (*L. brevis*), *Lentilactobacillus buchneri subsp. buchneri* (*L. buchneri*), *Lactobacillus helveticus* (*L. helveticus*), and *Lactobacillus delbrueckii subsp. bulgaricus* (*L. delbrueckii*)], *Streptococcus* [*Streptococcus lactis* (*S. lactis*), *Streptococcus acidilactis* (*S. acidilactis*), *Streptococcus diacetilactis* (*S. diacetilactis*)] and *Pediococcus* [*Pediococcus acidilactici* (*P. acidilactici*), *P. pentosaceus*, and *Pediococcus cerevisiae* (*P. cerevisiae*)]. The micrococci include *Micrococcus auterisiae* (*M. auterisiae*), *Micrococcus candidus* (*M. candidus*), *Micrococcus varians* (*M. varians*), *Micrococcus roseus* (*M. roseus*), *Micrococcus epidermidis* (*M. epidermidis*), and *M. luteus* (Lin, 2017). The predominant spoilage bacteria in water-cooked salted duck at the end of the shelf life were *Brochothrix thermosphacta* (*B. thermosphacta*) and lactic acid bacteria, and minor components were enterobacteriaceae, micrococci, yeasts and molds (Li et al., 2010). The primary species of microorganisms in different pressed salted ducks are presented in **Table 4**.

Preserved Fish

Preserved fish are made from fresh fish that are processed by slaughter and scale removal, evisceration, curing, and drying by baking (or drying in the sun, air-drying in the shade). Preserved fish are characterized by their unique flavor and storage stability (Hu and Wang, 2018). The volatile flavor compounds in traditional preserved fish are primarily aldehydes, alcohols and heterocyclic compounds.

TABLE 3 | Primary microorganisms in different preserved meats.

Type of preserved meat	Primary microorganisms	References
Sichuan preserved meat[2]	*Staphylococcus*, *Micrococcus*, *Acinetobacter*, *Psychrobacter*, *Pseudomonas*, *Brochothrix*, *Cupriavidus*, *Citrobacter*, *Enterobacter*, *Aspergillus*, *Debaryomyces*, *Candida*, *Wallemia*, *Penicillium*, *Malassezia*, *Didymella*	Wen et al., 2020; Quan et al., 2017
Enshi preserved meat[2]	*Staphylococcus*, *Psychrobacter*, *Pseudoalteromonas*, *Brochothrix*, *Cobetia*, *Acinetobacter*	Deng et al., 2018
Hunan preserved meat[1]	*Staphylococcus*, *Sphingomonas*, *Pseudomonas*, *Enterobacter*, *Leuconostoc*	Yi et al., 2017
Longxi preserved meat[1]	*L. plantarum*, *L. curvatus*, *L. sakei*, *C. alimentarius*, *P. pentosaceus*, *L. mesenteroides*	Deng et al., 2019

[1] Represents the identification of microorganisms by pure culture, and [2] represents the identification of microorganisms by molecular biological methods.

TABLE 4 | Primary microorganisms in different pressed salted ducks.

Type of pressed salted duck	Primary microorganisms	References
Sichuan air-dried duck[1]	*Neisseria*, *Micrococcus*, *Staphylococcus*	Liu et al., 2007
JianChang pressed salted duck[2]	*S. carnosus*, *S. simulans*, *S. xylosus*, *L. plantarum*, *L. sakei*, *L. acidophilus*, *L. lactis*, *L. casei*, *L. curvatus*, *L. fermentum*, *L. bifermentans*, *L. brevis*, *L. buchneri*, *L. helveticus*, *L. delbrueckii.*, *S. lactis*, *S. acidilactis*, *S. diacetilactis*, *P. acidilactici*, *P. pentosaceus*, *P. cerevisiae*, *M. auterisiae*, *M. candidus*, *M. varians*, *M. roseus*, *M. epidermidis*, *M. luteus*, yeasts, molds	Lin, 2017
Water-cooked salted duck[1]	*B. thermosphacta*, lactic acid bacteria, enterobacteriaceae, micrococci, yeasts, molds	Li et al., 2010

[1] Represents the identification of microorganisms by pure culture, and [2] represents the identification of microorganisms by molecular biological methods.

Among them, hexanal, caprylic aldehyde, nonyl aldehyde, 2-non-ene aldehyde, decanal, 3-methyl butyraldehyde, (z)-4-heptylaldehyde, benzaldehyde, 1-octene-3-ol, 1-pentene-3-ol, 3-methyl butanol, heptanol, trimethylamine, and 3-methyl-1H-indole are the primary active substances (Gu et al., 2019; Xu et al., 2020; Zhang et al., 2020). Microbes at the phylum level in Enshi-preserved fish from Hubei included Proteobacteria (61.29%), Firmicutes (30.21%), Bacteroidetes (5.34%), and Actinobacteria (1.74%). At the genus level, the primary genera included *Psychrobacter* (35.70%), *Brochothrix* (19.74%), *Pseudomonas* (7.13%), *Staphylococcus* (7.12%), *Acinetobacter* (4.19%), *Vibrio* (3.90%), *Pseudoalteromonas* (3.09%), and *Chryseobacterium* (1.98%) (Wang et al., 2018). Zeng et al. (2009) found that the dominant microorganisms during the processing of preserved fish were lactic acid bacteria, micrococci, staphylococci, and yeasts. The dominant microorganisms at the phylum level during the processing of dried preserved fish included Bacteroidetes, Firmicutes and Proteobacteria. At the family level, the dominant microorganisms largely included Xanthomonadaceae, Comamonadaceae, Campylobacteraceae, Clostridiaceae, Lacto bacteriaceae, Vibrionaceae, Streptococcaceae, Aeromonadaceae, Moraxellaceae, Planococcaceae, Shewanellaceae, Entero coccaceae, Pseudomonadaceae, Staphylococcaceae, Bacillaceae, and Enterobacteriaceae (Wu et al., 2017). The primary species of microorganisms in different preserved fish are presented in **Table 5**.

TABLE 5 | Primary microorganisms in different preserved fish.

Type of preserved fish	Primary microorganisms	References
Enshi preserved fish[2]	*Psychrobacter*, *Brochothrix*, *Pseudomonas*, *Staphylococcus*, *Acinetobacter*, *Vibrio*, *Pseudoalteromonas*, *Chryseobacterium*	Wang et al., 2018
Preserved fish[2]	Lactic acid bacteria, micrococci, staphylococci, yeasts	Zeng et al., 2009
Salted dried fish[2]	Xanthomonadaceae, Comamonadaceae, Campylobacteraceae, Clostridiaceae, Lactobacteriaceae, Vibrionaceae, Streptococcaceae, Aeromonadaceae, Moraxellaceae, Planococcaceae, Shewanellaceae, Enterococcaceae, Pseudomonadaceae, Staphylococcaceae, Bacillaceae, Enterobacteriaceae	Wu et al., 2017

[2] Represents the identification of microorganisms by molecular biologica methods.

Air-Dried Meat

Air-dried meat is stored at temperatures below zero. The meat is cut into small strips and treated with spices, pickled and hung in the shade, and it is naturally air-dried for approximately 3 months to form a directly edible product. After drying, the meat is crispy, and this product is commonly found in Xizang and northwestern Inner Mongolia. The volatile flavor compounds in air-dried meat include acids, aldehydes, ketones, alcohols, alkenes, sulfur-containing compounds and heterocyclic compounds, among which heptanal, 1-octene-3-ol, cyclopentanol, 3-hydroxy-2-heptanone, and 6-methyl-5-heptene-2-ketone are the primary contributors (Ma et al., 2021). The dominant microorganisms during the air-drying process of Xinjiang air-dried beef were lactic acid bacteria, staphylococci and micrococci. The total number of microorganisms was 8.0×10^8 CFU/g, the number of lactic acid bacteria was 1.48×10^7 CFU/g, the number of staphylococci and micrococci was approximately 4.40×10^8 CFU/g, the number of enterobacteria was approximately 10^2 CFU/g, the number of enterococci was less than 10^5 CFU/g, and the number of yeasts and molds was approximately 1.50×10^4 CFU/g (Wang et al., 2016). Lei et al. (2017) found 36% enterobacteria, 33% yeasts, 16% pseudomonades, 10% cocci, and 5% lactic acid bacteria in Xinjiang air-dried beef. In naturally fermented air-dried meat, 21 microbial phyla and 241 microbial genera were detected, and the dominant phyla included Firmicutes (39%), Proteobacteria (40%), and Bacteroidetes (14%) (Tian et al., 2019). The primary species of microorganisms in different air-dried meat samples are presented in **Table 6**.

TABLE 6 | Primary microorganisms in different air-dried meat.

Type of air-dried meat	Primary microorganisms	References
Xinjiang air-dried beef[1]	Lactic acid bacteria, staphylococci, micrococci, enterobacteria, pseudomonades, enterococci, molds, yeasts, cocci	Wang et al., 2016; Lei et al., 2017
Naturally fermented air-dried meat[2]	Firmicutes, Proteobacteria, Bacteroidetes	Tian et al., 2019

[1] Represents the identification of microorganisms by pure culture, and [2] represents the identification of microorganisms by molecular biological methods.

CONCLUSION AND PROSPECT

Due to differences in raw materials, technology, auxiliary materials and fermentation time, the microbial species in fermented meat products in China are different. However, most fermented meat products in China are subjected to salting and fermentation, so the microbial compositions share some similarities. Microorganisms in fermented meat products mainly include staphylococci, lactobacilli, micrococci, yeasts, and molds.

At present, research on fermented meat products largely focuses on the microbial diversity of fermented meat products, the mechanisms by which specific microbes influence the quality of fermented meat products, the characteristic flavor of fermented meat products and their production pathway. A large number of studies have shown that microorganisms can promote the formation flavor of fermented meat products and inhibit the

generation of BAs, nitrosamines and other harmful chemicals in fermented meat products, but the specific mechanisms have not been fully reported. In the future, research on these mechanisms will provide effective theoretical support for improving the production process and the modernization and standardization of production of fermented meat products.

AUTHOR CONTRIBUTIONS

ZLW and ZXW conducted the literature collection and literature research. ZLW drafted the original manuscript. ZLW, ZXW, and LC modified the manuscript. All authors critically reviewed, contributed to, and approved the final manuscript.

FUNDING

This work was supported by the Key Research and Development Program of Sichuan Province (2020YFN0147), the National Modern Agriculture Industry Technology System (SCSZTD-3-007), the Key Research and Development Program of Sichuan Province (2019YFN0172), and the Department of Science and Technology of Sichuan Province (2020ZYD067).

ACKNOWLEDGMENTS

We would like to thank AJE (www.aje.cn) for english language editing. We would also like to appreciate the reviewers for their constructive comments.

REFERENCES

Chen, Q., Kong, B. H., Han, Q., Xia, X. F., and Xu, L. (2017). The role of bacterial fermentation in lipolysis and lipid oxidation in Harbin dry sausages and its flavour development. *LWT Food Sci. Technol.* 77, 389–396. doi: 10.1016/j.lwt.2016.11.075

Deng, F., Wang, Y. R., Shang, X. J., She, M. N., Ge, D. Y., Zhao, H. J., et al. (2018). Bacterial diversity of sausages in Enshi of Hubei province. *Meat Res.* 32, 18–22. doi: 10.7506/rlyj1001-8123-201809004

Deng, Z. R., Yun, J. M., Guo, J., Niu, Y. X., and Li, Y. H. (2019). Study on isolation and fermentation performance of dominant lactic acid bacteria during the processing of Longxi Bacon. *Curr. Biotechnol.* 9, 200–209. doi: 10.19586/j.2095-2341.2018.0098

Dong, Y., Wang, Y. R., Wang, Y., Liao, H., Zhao, H. J., and Guo, Z. (2018). Evaluation of bacterial diversity in Chinese bacon from enshi by denatured gradient gel electrophoresis and MiSeq high-throughput sequencing. *Meat Res.* 32, 37–42. doi: 10.7506/rlyj1001-8123-201810007

Douglas, P., Erick, S., Manuel, L. J., Mirian, P., Ruben, D., Alves, D. S. B., et al. (2020). Low-sodium dry-cured rabbit leg: a novel meat product with healthier properties. *Meat Sci.* 173:108372. doi: 10.1016/j.meatsci.2020.108372

Frédéric, L., Jurgen, V., and Luc, D. V. (2006). Functional meat starter cultures for improved sausage fermentation. *Intern. J. Food Microbiol.* 106, 270–285.

Gao, Y. R., Li, D. P., and Liu, X. Y. (2014). Bacteriocin-producing *Lactobacillus sakei* C2 as starter culture in fermented sausages. *Food Control* 35, 1–6. doi: 10.1016/j.foodcont.2013.06.055

Gu, S. Q., Tang, J. J., Zhou, X. X., Zheng, H. M., Zhou, H. X., and Ding, Y. T. (2019). Quality change and aroma formation in cured fish during traditional sun drying processing. *Food Sci.* 40, 36–44. doi: 10.7506/spkx1002-6630-20180716-201

Guo, J., Wang, Q., Chen, C. G., Yu, H., and Xu, B. (2020). Effects of different smoking methods on sensory properties, free amino acids and volatile compounds in bacon. *J. Sci. Food Agric.* 101, 2984–2993. doi: 10.1002/jsfa.10931

He, G. Q., Liu, T. J., Sadiq, F. A., Gu, J. S., and Zhang, G. H. (2017). Insights into the microbial diversity and community dynamics of Chinese traditional fermented foods from using high-throughput sequencing approaches. *J. Zhejiang Univ. Sci. B* 18, 289–302. doi: 10.1631/jzus.B1600148

He, Z. F., Li, H. Y., Yu, X., Zhou, R. H., and Zhang, M. (2007). Study on the changes in microbial flora of jinhua ham in modern fermentation technology. *J. Southwest Univ* . 29, 142–150. doi: 10.3969/j.issn.1673-9868.2007.03.030

Hu, D., and Wang, M. (2018). Research on processing technology of Chinese traditional preserved fish. *Technol. Econ. Guide* 26:61.

Hu, Y. Y., Zhang, L., Liu, Q., Wang, Y., Chen, Q., and Kong, B. H. (2020). The potential correlation between bacterial diversity and the characteristic volatile flavour of traditional dry sausages from Northeast China. *Food Microbiol.* 91:103505. doi: 10.1016/j.fm.2020.103505

Huang, Z. W., Xu, M. S., Tang, K. J., Jiang, Y., and Wu, S. F. (2003). Separation of fermentation microorganism in Aufu Ham and its fermentation technology. *Acta Agric. Univ. Jiangxien.* 25, 635–638. doi: 10.3969/j.issn.1000-2286.2003.04.037

Lei, Y. H., Guo, J. N., Sun, B. Z., Xie, P., Zhang, Y., Li, H. B., et al. (2017). Characteristics of microbial changes in the processing of dried beef in Xinjiang. *J. Food Saf. Q.* 8, 2914–2921. doi: 10.3969/j.issn.2095-0381.2017.08.013

Li, J. X., Wang, W., Wang, X. H., and Bai, T. (2015). The source and formation of flavor substances in fermented sausage. *Food Sci. Technol.* 40, 160–165. doi: 10.13684/j.cnki.spkj.2015.05.032

Li, L., Zou, D., Ruan, L. Y., Wen, Z. Y., Chen, S. W., Xu, L., et al. (2019). Evaluation of the biogenic amines and microbial contribution in traditional Chinese sausages. *Front. Microbiol.* 10:872. doi: 10.3389/fmicb.2019.00872

Li, P. L., Shen, Q. W., Lv, Y. N., Jiang, Z. J., and Ma, C. W. (2003). Analysis of main of microorganisms in Xuanwei Ham. *Chin. J. Microecol.* 15, 12–13. doi: 10.3969/j.issn.1005-376X.2003.05.007

Li, X. R., Liu, L. Y., Yang, Y., Hou, P. P., Zhao, Y. T., Zhang, T. H., et al. (2020). Physicochemical, microbial and flavor profiles of traditional Chinese cured meat. *Meat Res.* 34, 22–26. doi: 10.7506/rlyj1001-8123-20190821-187

Li, Y. L., Yao, D. R., Wang, D. Y., Xu, W. M., Zhu, Y. Z., and Jin, B. Q. (2010). Sensory, physicochemical and microbiological changes in water-cooked salted duck during storage at 4°C. *Asian Austr. J. Anim. Sci.* 23, 960–964. doi: 10.5713/ajas.2010.90550

Liang, J., Zhao, J. R., Ji, Y. G., Sun, S. L., and Zhan, J. F. (2010). Microbiological safety analysis of several fermented meat products. *Heilongjiang Anim. Sci. Vet. Med.* 52, 34–35. doi: 10.13881/j.cnki.hljxmsy.2010.22.002

Lin, Q. (2017). Jianchang Duck in the fermentation process of microorganism. *Modern Food* 33, 66–69. doi: 10.16736/j.cnki.cn41-1434/ts.2017.06.027

Liu, D. Y., Bai, L., Feng, X., Chen, Y. P., Zhang, D. N., Yao, W. S., et al. (2020). Characterization of Jinhua ham aroma profiles in specific to aging time by gas chromatography-ion mobility spectrometry (GC-IMS). *Meat Sci.* 168:108178. doi: 10.1016/J.MEATSCI.2020.108178

Liu, X., Zhang, W. X., Yue, Y. Y., Wang, W., and Yu, H. (2007). A preliminary study on the microflora of Wind-blown duck from Sichuan. *Sci. Technol. Food Indust.* 28, 82–87. doi: 10.3969/j.issn.1002-0306.2007.07.022

Liu, Y. L., Yu, Q. L., Wan, Z., Li, H. Y., Liu, J., and Wang, J. (2020). Research progress of antioxidant activity of starter culture on the quality of fermented meat products. *Food Sci.* 82, 1–17. doi: 10.7506/spkx1002-6630-20200704-052

Ma, G. L., Tang, S. H., Li, S. N., Liu, H. L., and Ren, R. (2021). Changes of physicochemical properties and volatile flavor substances in tibetan air-dried yak meat jerky during the simulated processing. *Sci. Technol. Food Industr.* 42, 19–25. doi: 10.13386/j.issn1002-0306.20200301018

Mao, Y. Q., Li, Y. H., Yun, J. M., He, K., Wang, R., and Wu, S. J. (2021). Volatile flavor compounds in traditional Longxi bacon production. *Food Fermentat. Industr.* 47, 144–152. doi: 10.13995/j.cnki.11-1802/ts.025248

Mu, Y., Su, W., Mu, Y. C., and Jiang, L. (2019). Combined application of high-throughput sequencing and metabolomics reveals metabolically active microorganisms during Panxian Ham processing. *Front. Microbiol.* 10:3012. doi: 10.3389/fmicb.2019.03012

Niu, T. J., Chen, L. S., Kong, H. G., Guo, Y. J., and Ma, Y. (2019). Screening, identification and application of biogenic amine degrading strains derived from

traditional fermented meat products. *China Brew.* 38, 43–48. doi: 10.11882/j.issn.0254-5071.2019.09.009

PaPamanoli, E., Kotzekidou, P., Tzanetakis, N., and Litopoulou-Tzanetaki, E. (2002). Characterization of Mieroeoccaeeae isolated from dry fermented sausage. *Food Microbiol.* 19, 441–449. doi: 10.1006/fmic.2002.0503

Polka, J., Rebecchi, A., Pisacane, V., Morelli, L., and Puglisi, E. (2015). Bacterial diversity in typical Italian salami at different ripening stages as revealed by high-throughput sequencing of 16S rRNA Amplicons. *Food Microbiol.* 46, 342–356. doi: 10.1016/j.fm.2014.08.023

Quan, T., Deng, D. C., Li, H. J., He, Z. F., Zhang, Y. H., and Zhang, J. X. (2017). Study on the main microorganisms of traditional Sichuan bacon during its shelf life. *J. Southwest Univ.* 39, 14–21. doi: 10.13718/j.cnki.xdzk.2017.02.003

Radovčić, N. M., Vidaček, S., Janči, T., and Medić, H. (2016). Characterization of volatile compounds, physico-chemical and sensory characteristics of smoked dry-cured ham. *J. Food Sci. Technol.* 53, 4093–4105. doi: 10.1007/s13197-016-2418-2

Sivamaruthi, B. S., Kesika, P., and Chaiyasut, C. (2020). A narrative review on biogenic amines in fermented fish and meat products. *J. Food Sci. Technol.* 58, 1623–1639. doi: 10.1007/s13197-020-04686-x

Sun, Q. X., Chen, Q., Li, F. F., Zheng, D. M., and Kong, B. H. (2016). Biogenic amine inhibition and quality protection of Harbin dry sausages by inoculation with *Staphylococcus xylosus* and *Lactobacillus plantarum*. *Food Control* 68, 358–366. doi: 10.1016/j.foodcont.2016.04.021

Swetwiwathana, A., and Visessanguan, W. (2015). Potential of bacteriocin-producing lactic acid bacteria for safety improvements of traditional Thai fermented meat and human health. *Meat Sci.* 109, 101–105. doi: 10.1016/j.meatsci.2015.05.030

Tian, J. J., Zhang, K. P., Yang, M. Y., Jing, Z. B., Li, Q. W., Zhao, L. H., et al. (2019). Comparative bacterial diversity analysis and microbial safety assessment of air-dried meat products by Illumina MiSeq Sequencing technology. *Food Sci.* 40, 33–40. doi: 10.7506/spkx1002-6630-20180504-043

Tong, H. G., Wang, W., Zhang, H. F., Li, P. J., Chen, C. G., and Chen, J. (2018). Comparative analysis flavor components of dry-cured ducks from different regions by HPLC, GC-MS combined with multivariate statistical analysis. *Modern Food Sci. Technol.* 34, 228–238. doi: 10.13982/j.mfst.1673-9078.2018.12.034

Wang, J. G., Li, Y. H., Guo, A. M., Han, D. Y., and Liu, C. J. (2016). Physico-chemical and microbial properties of Xinjiang dry-cured beef during the ripening process. *Food Fermentat. Industr.* 42, 129–133. doi: 10.13995/j.cnki.11-1802/ts.201610022

Wang, W., Liu, Y., Wang, X. H., and Zhang, J. M. (2014). Effects of microbial fermentation agents on the storable nature and flavor characteristics of Sichuan bacon. *Food Sci. Technol.* 39, 159–164. doi: 10.13684/j.cnki.spkj.2014.09.035

Wang, X. H., Ren, H. Y., Liu, D. Y., Zhu, W. Y., and Wang, W. (2013). Effects of inoculating *Lactobacillus sakei* starter cultures on the microbiological quality and nitrite depletion of Chinese fermented sausages. *Food Control* 32, 591–596. doi: 10.1016/j.foodcont.2013.01.050

Wang, X. H., Wang, S. H., and Zhao, H. (2019). Unraveling microbial community diversity and succession of Chinese Sichuan sausages during spontaneous fermentation by high-throughput sequencing. *J. Food Sci. Technol.* 56, 3254–3263. doi: 10.1007/s13197-019-03781-y

Wang, X. R., Shi, Q., Liu, B. Q., Lei, Y. D., Tang, H. H., Zhang, S. Z., et al. (2021). Bacterial dynamics during the processing of nuodeng Dry-cured Ham. *Sci. Technol. Food Industry* 42, 83–89. doi: 10.13386/j.issn1002-0306.2020030129

Wang, Y. B., Li, F., Chen, J., Sun, Z. H., Wang, F. F., Wang, C., et al. (2021). High-throughput sequencing-based characterization of the predominant microbial community associated with characteristic flavor formation in Jinhua Ham. *Food Microbiol.* 94:103643. doi: 10.1016/J.FM.2020.103643

Wang, Y. R., Liao, H., Zhao, H. J., Zhang, Z. D., and Guo, Z. (2018). Evaluation of the bacterial diversity in cured fish samples collected from Enshi by PCR-DGGE and MiSeq high-throughput sequencing. *Modern Food Sci. Technol.* 34, 208–213. doi: 10.13982/j.mfst.1673-9078.2018.11.031

Wen, K. Y., Wang, Y., Wen, P. C., Zhu, Y., Yang, M., Zhang, Z. M., et al. (2020). Study on microbial community structure in Sichuan traditional bacon. *Food Fermentat. Industr.* 46, 36–42. doi: 10.13995/j.cnki.11-1802/ts.022133

Wu, W. H., Zhou, Y., Wang, G. Y., Zhu, R. J., Ge, C. R., and Liao, G. Z. (2020). Changes in the physicochemical properties and volatile flavor compounds of dry-cured Chinese Laowo ham during processing. *J. Food Process. Preserv.* 44:e14593. doi: 10.1111/jfpp.14593

Wu, Y. Y., Qian, X. X., Li, L. H., Chen, S. J., Deng, J. C., and Li, C. S. (2017). Microbial community diversity in dried-salted fish during processing revealed by Illumina MiSeq sequencing. *Food Sci.* 38, 1–8. doi: 10.7506/spkx1002-6630-201712001

Xie, K., Yu, X. F., Zheng, H. S., Zong, K., Lian, Y. Q., and Liu, G. Q. (2013). Analysis of dominant microbial species in cantonese sausage by independent culture and PCR-DGGE technology. *Food Sci.* 34, 157–160.

Xu, Y. S., Zang, J. H., Regenstein, J. M., and Xia, W. S. (2020). Technological roles of microorganisms in fish fermentation: a review. *Critic. Rev. Food Sci. Nutr.* 61, 1000–1012. doi: 10.1080/10408398.2020.1750342

Yi, L. B., Su, G. R., Hu, G., and Peng, Q. Z. (2017). Diversity study of microbial community in bacon using metagenomic analysis. *J. Food Saf.* 37:e12334. doi: 10.1111/jfs.12334

You, G., Wu, Y. Y., Li, L. H., Yang, X. Q., Qi, B., and Chen, S. J. (2015). Effect of inoculating compound lactic acid bacteria on microbial,nitrites and nitrosamines of salted fish. *South China Fish. Sci.* 11, 109–115. doi: 10.3969/j.issn.2095-0780.2015.04.016

Yu, C. Q., Yao, D., Man, Y. G., and Wang, C. Y. (2010). Harm and control on biogenic amines of fermented meat products. *Meat Res.* 31, 41–45. doi: 10.3969/j.issn.1001-8123.2010.01.013

Zeng, L. B., Xiong, S. B., and Wang, L. (2009). Changes in microbe quantity and physico-chemical properties during processing of cured silver carp. *Food Sci.* 30, 54–57. doi: 10.3321/j.issn:1002-6630.2009.03.011

Zhang, C. X., He, Z. F., and Li, H. J. (2017). Research of bacteriocins from lactic acid bacteria and their applications in preservation of meat products. *Food Fermentat. Industr.* 43, 271–277. doi: 10.13995/j.cnki.11-1802/ts.013971

Zhang, Q., Ding, Y. C., Gu, S. Q., Zhu, S. C., Zhou, X. X., and Ding, Y. T. (2020). Identification of changes in volatile compounds in dry-cured fish during storage using HS-GC-IMS. *Food Res. Intern.* 137:109339. doi: 10.1016/J.FOODRES.2020.109339

Zhang, S. Y., Tang, N., Huang, P., Zhou, Y., Xu, B. C., and Li, P. J. (2019). Isolation, identification and tolerance characteristics of microorganisms from Weining Ham. *Meat Res.* 33, 12–17. doi: 10.7506/rlyj1001-8123-20190625-147

Zhao, D. B., Wang, L. Y., Fu, Y., Wang, J. H., Tan, C. X., Wang, M. M., et al. (2017). Study on strain screening, identification and physical and chemical properties characteristics of bacteriocin- producing lactic acid bacteria in Nanjing dry-cured duck. *Meat Industry* 37, 19–23. doi: 10.3969/j.issn.1008-5467.2017.01.007

Zhou, H. M., Zhang, S. L., Zhao, B., Li, S., Pan, X. Q., Ren, S., et al. (2018). Effect of starter culture mixture of *Staphylococcus xylosus* and *S. carnosus* on the quality of dry-cured meat. *Food Sci.* 39, 32–38. doi: 10.7506/spkx1002-6630-201822006

Zou, Y. L., Liu, S. Y., Wang, G. Y., Pu, Y. H., Ge, C. G., and Liao, G. Z. (2020). Analysis of fungal community structure in Xuanwei ham by PCR-DGGE. *Food Fermentat. Industr.* 46, 269–274. doi: 10.13995/j.cnki.11-1802/ts.022394

Conflict of Interest: The authors declare that the research was conducted in the absence of any commercial or financial relationships that could be construed as a potential conflict of interest.

frontiers in Microbiology

ORIGINAL RESEARCH
published: 09 June 2021
doi: 10.3389/fmicb.2021.670684

Cocultivation Study of *Monascus* spp. and *Aspergillus niger* Inspired From Black-Skin-Red-Koji by a Double-Sided Petri Dish

Xi Yuan[1,2] *and Fusheng Chen*[1,2]*

[1] Hubei International Scientific and Technological Cooperation Base of Traditional Fermented Foods, Huazhong Agricultural University, Wuhan, China, [2] College of Food Science and Technology, Huazhong Agricultural University, Wuhan, China

Cocultivation is an emerging and potential way to investigate microbial interaction in the laboratory. Extensive researches has been carried out over the years, but some microorganism cocultivation are not easy to implement in the laboratory, especially the fungus-fungus (FF) cocultivation, owing to the obstacles such as fungal different growth rate, limited growing space, hyphae intertwining, and difficulty of sample separation, etc. In this research, a double-sided petri dish (DSPD) was designed and carried out as a tool to study FF cocultivation in the laboratory. A natural FF cocultivation of *Monascus* spp. and *Aspergillus niger* inspired from black-skin-red-koji (BSRK), were studied. By using DSPD, the aforementioned obstacles in the FF cocultivation study were overcome through co-culturing *Monascus* spp. and *A. niger* on each side of DSPD. The characteristics of monocultured and co-cultured *Monascus* spp. and *A. niger* were compared and analyzed, including colonial and microscopic morphologies, and main secondary metabolites (SMs) of *Monascus* spp. analyzed by high performance liquid chromatography. And a novel SM was found to be produced by *Monascus ruber* M7 when co-cultured with *A. niger* CBS 513.88. Since the above mentioned obstacles, were overcome, we obtained good quality of transcriptome data for further analysis. These results indicate that DSPD might be an efficient tool for investigation of microbial interaction, in particular, for FF interaction.

Keywords: *Aspergillus niger*, cocultivation, HPLC, transcriptome, *Monascus* spp., double-sided petri dish

OPEN ACCESS

Edited by:
Van-Tuan Tran,
Vietnam National University, Vietnam

Reviewed by:
Laurent Dufossé,
Université de la Réunion, France
Zhilong Wang,
Shanghai Jiao Tong University, China
Lourdes Morales-Oyervides,
Universidad Autónoma de Coahuila, Mexico

***Correspondence:**
Fusheng Chen
chenfs@mail.hzau.edu.cn

Specialty section:
This article was submitted to Food Microbiology, a section of the journal Frontiers in Microbiology

Received: *22 February 2021*
Accepted: *12 April 2021*
Published: *09 June 2021*

Citation:
Yuan X and Chen F (2021) Cocultivation Study of Monascus spp. and Aspergillus niger Inspired From Black-Skin-Red-Koji by a Double-Sided Petri Dish. Front. Microbiol. 12:670684. doi: 10.3389/fmicb.2021.670684

INTRODUCTION

Black-skin-red-koji (BSRK), also known as *Wuyihongqu* (烏衣紅曲) in Chinese, is a special traditional Chinese mixed starter which has been utilized for brewing rice wine and cereal vinegar for more than 1,000 years mainly in Fujian and Zhejiang provinces (Fang et al., 2011; Huang et al., 2018). As a representative model of fungus-fungus (FF) cocultivation, the main filamentous fungi in BSRK are *Monascus* spp. and *Aspergillus niger* (Huang et al., 2019). Usually, *A. niger* strains grow on the surface of the steamed rice, and *Monascus* spp. strains grow in the center of the steamed rice, so BSRK has a "red heart" and black "coat" (**Figure 1**).

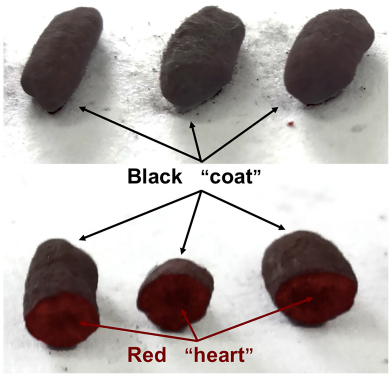

FIGURE 1 | Appearance and cross-sections of black-skin-red-koji (BSRK).

Monascus spp. belong to the family Monascaceae and were first screened from red yeast rice and characterized by van Tieghem (1884). *Monascus* spp. have been used to produce the food and health products due to their functional secondary metabolites (SMs) such as *Monascus* pigments (MPs), monacolin K (MK), dimerumic acid, and γ-aminobutyric acid (Chen et al., 2015; Feng et al., 2016). However, nephrotoxin citrinin (CIT) can also be produced by a few of *Monascus* spp. strains, which can lead to the food safety concerns of *Monascus* related products (He and Cox, 2016). *A. niger* is most widely used industrially for citric acid production and is also a tool for the production of enzymes such as α-amylase, cellulose, and pectinase (Nielsen et al., 2009; Andersen et al., 2011; Show et al., 2015). However, to date, as a natural FF cocultivation model, the reason why both of *Monascus* spp. and *A. niger* can harmoniously grow in BSRK and the mechanisms relating to how they affect each other are still undiscovered.

Cocultivation is regarded as an experimental imitation of the competition within natural microbe communities in laboratory conditions, microbial cocultivation has been studied for various uses, such as improving SMs production (Wakefield et al., 2017), accelerating the fermentation process (Yan et al., 2008), increasing bioenergy production (Camacho-Zaragoza et al., 2016), speeding up organic pollutants degradation (Kumari and Naraian, 2016), and especially mining novel SMs (Marmann et al., 2014; Yu M. et al., 2019). To date, microbial cocultivation research can be generally classified into three models including bacteria-bacteria (Zhang et al., 2015; Gao et al., 2021), bacteria-fungus (Moussa et al., 2019), and FF (Jimenez-Barrera et al., 2018). Since fungi are one of the biggest sources of natural products and enzymes (Meyer et al., 2016), research on the FF cocultivation has contributed to enhancing SMs production and discovering novel SMs (Shang et al., 2017; Vinale et al., 2017; Yu G. et al., 2019). However, compared to the other models, FF cocultivation is lesser studied, probably due to technical difficulties under laboratory conditions such as fungal different growth rates, limited growth spaces, hyphae intertwining, and difficulty in sample separation, etc.

Genome sequencing technology has revealed that there are a large number of gene clusters regulating SMs synthesis in fungi. However, when fungi are under laboratory culture conditions, most of fungal SMs gene clusters remaines silent (Pettit, 2009). Cocultivation is one of the most efficient methods to activate the silent fungal SMs gene clusters through interspecific communications by co-culture of two or more kinds of fungi in a specific culture environment (Nett et al., 2009; Chiang et al., 2011; Xu et al., 2015).

Since *A. niger* and *Monascus* spp. can be well symbiotic in BSRK, both of them may be an ideal research model of cocultivation. However, usually *A. niger* grows much faster than *Monascus* spp., which has become an obstacle to observing and analyzing the variation between monoculture and co-culture (Favela-Torres et al., 1998). The preliminary results also showed (data not shown) that *Monascus* spp. and *A. niger* could grow together which led to a difficulty in sample separations for further analysis. Furthermore, BSRK and its major fermentation products are all based on rice (Chen et al., 2009; Li et al., 2009), sugars and proteins from rice can cause serious interference to transcriptome sequencing.

In current study, a double-sided petri dish (DSPD, **Figure 2**) was designed to study the cocultivation of *M. ruber* M7 which can produce high yields of MPs and CIT but no MK, *M. pilosus* MS-1which can produce high yields of MK but no CIT (Feng et al., 2016; Wang et al., 2016), *A. niger* CBS 513.88 which is often used for enzyme production, and *A. niger* CBS 113.46 which is usually applied for citric acid production (Andersen et al., 2011), respectively. The colonial and microscopic morphologies were observed and compared, main SMs were analyzed, novel SMs were mined, and transcriptomes were elucidated, when the aforementioned fungal strains were monocultured and co-cultured on DSPD. The results are proven that DSPD is an efficient tool for FF cocultivation research.

MATERIALS AND METHODS

Strains and Chemicals

The strains *M. ruber* M7 (CCAM 070120, Culture Collection of State Key Laboratory of Agricultural Microbiology, which is part of China Center for Type Culture Collection, Wuhan, China), *M. pilosus* MS-1 (CCTCC M 2013295, China Center for Type Culture Collection, Wuhan, China) and *A. niger* CBS 513.88, *A. niger* ATCC 1015 (Both were purchased from The Westerdijk Fungal Biodiversity Institute) were used in this study. The potato dextrose agar (PDA), potato dextrose broth (PDB), Czapek yeast extract agar (CYA), malt extract agar (MEA), and 25% glycerol nitrate agar (G25N) were taken as culture media. PDB: Potato (200 g/L), sugar (20 g/L), agar power (2 g/L); PDA: PDB with agar power (2 g/L); CYA: $NaNO_3$ (3 g/L), K_2HPO_4 (1 g/L), KCl (0.5 g/L), $MgSO_4 \cdot 7H_2O$ (0.5 g/L), $FeSO_4$ (0.01 g/L), sucrose (30 g/L), yeast extracts power (1 g/L), agar power (2 g/L); MEA: Malt extract power (30 g/L); G25N: CYA with 25% glycerol. Rice powders agar (RA): rice power (50 g/L), agar power (2 g/L). MK and CIT standard substances were purchased from Sigma Co.

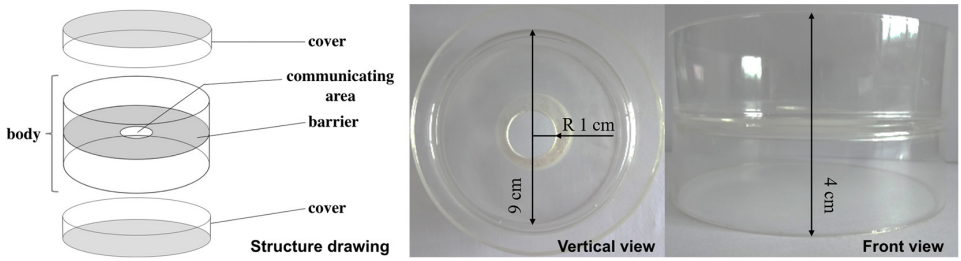

FIGURE 2 | Structure drawing, vertical view, and front view of the double-sided petri dish (DSPD).

Other chemicals were bought from China National Medicines Corporation Ltd.

Design of a Double-Sided Petri Dish

A double-sided petri dish (DSPD, **Figure 2**) was produced by two resin petri dishes (ϕ = 9.0 cm). Firstly, the bottoms of two petri dishes were sticked together by glue, then a hole (ϕ = 2.0 cm) in the middle of the petri dishes was drilled. Each DSPD consists of one body part and two covers. When DSPD is used, the metabolites, signal factors, ect. that are produced by the tested microbial strains grown on each side of DSPD can pass and interact through the hole (Xu et al., 2018; Yan et al., 2008). Prior to pouring the media in to DSPD, a round piece of sterile cellophane ($\phi \approx$ 9.0 cm) is pasted on any side of the DSPD to cover the hole (communicating area) and prevent the media from leaking. After the media solidification on one side, the media are poured on another side.

Cocultivation Experiments

Two *Monascus* spp. strains were co-cultured with two *A. niger* strains by the following combinations: *M. ruber* M7 and *A. niger* CBS 513.88, *M. ruber* M7 and *A. niger* CBS 113.46, *M. pilosus* MS-1 and. *niger* CBS 513.88, and *M. pilosus* MS-1 and *A. niger* CBS 113.46. All the combinations were investigated by the conventional cocultivation and the cocultivation using DSPD.

Conventional Cocultivation

The conventional cocultivation, means co-culturing two fungal strains in the same petri dish directly (Zuck et al., 2011; Bertrand et al., 2013; Nonaka et al., 2015). Firstly, the strains were cultured on PDA slants at 30 ± 1°C for 7 days and then sterile water was added into the slants and spores were scraped using an inoculating loop. After the mycelia were filtered by sterile filter paper, the spore solution of *Monascus* spp. and *A. niger* were obtained, respectively (Feng et al., 2014). After that, two inoculation methods were used for cocultivation. Coating inoculation: 1 mL *Monascu* spp. and *A. niger* spore solutions were evenly spread on half of the same petri dish, respectively. Point inoculation: 1 μL *Monascus* spp. and *A. niger* spore solutions were inoculated on two points of the same petri dish, respectively, and the distance of the two points was about 2 cm (Shang et al., 2017; **Figures 3**, **4**). After inoculation, all the petri dishes were incubated at 30 ± 1°C for 9 days.

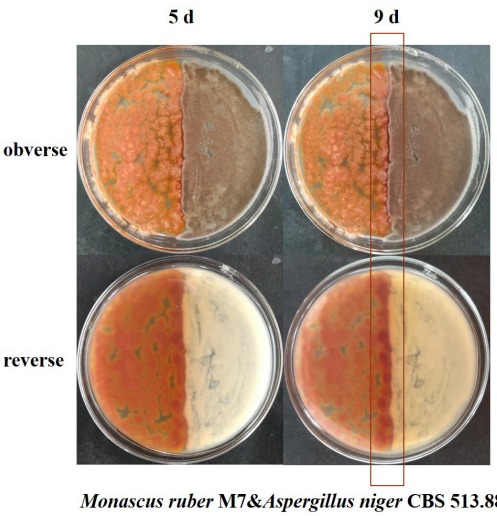

FIGURE 3 | Cocultivation of *Monascus ruber* M7 and *Aspergillus niger* CBS 513.88 by coating inoculation method at 5 and 9 days &-co-cultured with.

Cocultivation in DSPD

After the media solidification in two sides, the tested *Monascus* spp. and *A. niger* strains were inoculated on each side of DSPD, respectively. The cocultivation conditions were the same as the conventional cocultivation.

Observation of Colonial and Microscopic Morphologies

The colonial morphologies of *M. ruber* M7, *M. pilosus* MS-1, *A. niger* CBS 513.88, and *A. niger* CBS 113.46 were observed by the naked eye, and photos were taken by camera at 3, 5, 7, and 9 days (**Figures 3**–**5**). The micromorphologies were observed and photos were taken by the microscope (Leica, DM300, Wetzlar, Germany), focusing on mycelia, conidia, and cleistothecia (**Figure 6**).

Determination of Color Value of MPs

MPs can be divided into *Monascus* yellow pigment (MYP, 330–450 nm), *M*onascus orange pigment (MOP, 460–480 nm), and *Monascus* red pigment (MRP, 490–530 nm) according to MPs maximum absorption wavelength (Feng et al., 2012; Chen et al.,

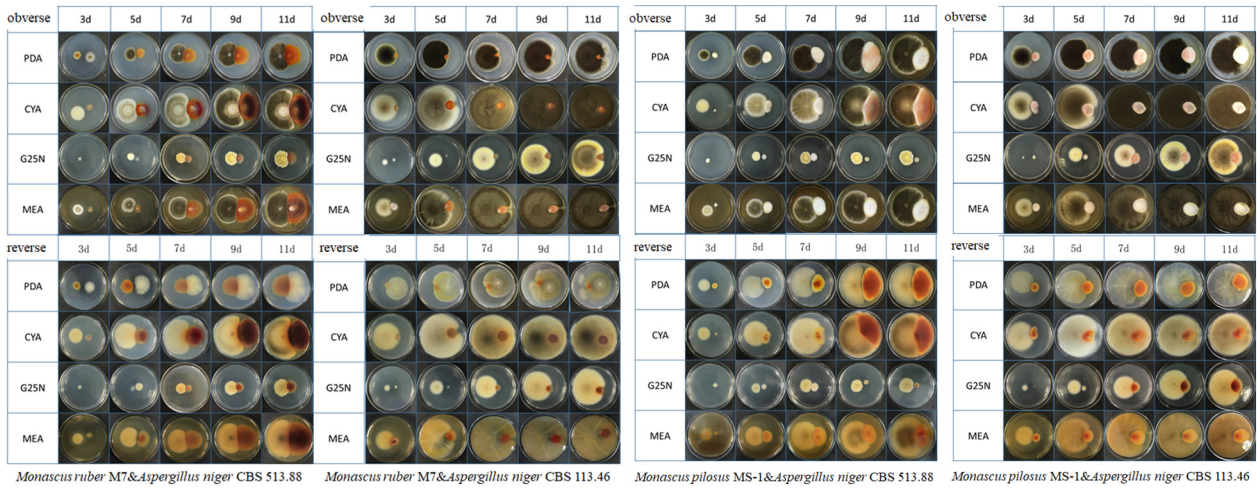

FIGURE 4 | Colonial morphologies of *Monascus ruber* M7, *Monascus pilosus* MS-1 when co-cultured with *Aspergillus niger* CBS 513.88 and *A. niger* CBS 113.46 by conventional (direct) cocultivation at 3, 5,7,9, and 11 days &-co-cultured with.

2017). The color values, which can represent the MPs contents, are defined as optical density values at the given wavelength per milliliter or gram (Feng et al., 2012). Samples were dried by vacuum freeze drying and then weighed (about 1 mg), dissolved by 70% ethanol, and subject to ultrasonic extraction. The extracted solutions were filtrated by filter paper and diluted by 70% ethanol. Diluted solutions were detected by UV–vis UV-1700 Spectrophotometer (Shimadzu, Tokyo, Japan). One unit of optical density at a given wavelength corresponded to one unite (U) of color value (Li et al., 2019):

$$\text{Color value (U/g)} = \frac{\text{A} \times \text{dillution ratio} \times \text{V}}{\text{m}}$$

where *A* is the absorbance of the pigment extract at a given wavelength, *V* is the total volume of extracted solutions, and *m* is the dry weight of the samples used for pigment extraction. The given wavelengths used to detect MYP, MOP, and MRP were 380, 470, and 520 nm, respectively. In addition, 505 nm was taken as the given wavelength to measure total MPs (Ding et al., 2008; Wang et al., 2016).

Determination of SMs

MK, CIT and MPs varieties were detected by high performance liquid chromatography (HPLC; Feng et al., 2014, 2016; Li et al., 2019). Samples for MK and MPs detection were ultrasonically extracted for 1 h, then centrifugated at 12000 rpm (Heal Force Neofuge 15R, Shanghai, China) for 10 min. Samples for CIT detection were dried and ultrasonically extracted with 80% methanol solvent, then centrifugated at 12000 rpm for 40 min. The supernatants were filtered through a 0.22 μm membrane before HPLC detection. Then MK, CIT and MPs were assessed by HPLC, which were performed on a chromatographic system (Shimadzu, model LC-20A Prominence, Tokyo, Japan), equipped with a diode-array detector (Shimadzu, Tokyo, Japan). The column of inertsil ODS-3 (4.6 mm×250 mm, id, 5 μm) was employed. For MK detection, the mobile phases were acetonitrile (ACN) and water (contains 0.1% phosphoric acid) (60%:40%, v/v) by isocratic elution, the column temperature was set at 25°C, the flow rate was maintained at 1.0 mL/min and the injection volume was 20 μL. Both acid and lactone forms of MK were calculated as MK yield (Feng et al., 2014). For MPs detection, the mobile phases were ACN and water (contains 0.1% formic acid). Gradient elution was performed as follows: step gradient for ACN was 55% (v/v) to 65% (v/v) in 3 min; 65% (v/v) to 90% (v/v) in 22 min; 90% (v/v) for 5 min; 90% (v/v) to 55% in 1 min; 55% (v/v) for 9 min. The column temperature was kept at 30°C. The detection wavelength was 210 nm to 600 nm. For CIT detection, the mobile phases were ACN and water (contains 0.1% formic acid) (70%:30%, v/v) by isocratic elution, and the flow rate was 1 mL/min. The observation wavelength was 331 nm (Liu et al., 2016). The column temperature was set at 30°C, and the injection volume was 10 μL. When co-cultured with *A. niger*, MK producing strain *M. pilosus* MS-1 was selected to study MK variation while *M. ruber* M7 was selected to study CIT and MPs variation.

Mining Novel SMs

Our preliminary results (data not shown) found two new SMs from the cocultivation of *M. ruber* M7 and *A. niger* CBS 513.88 in the steamed rice. In this study, DSPD was applied for further research and rice agar was employed to simulated steamed rice. By using DSPD, the mycelia of *M. ruber* M7 were harvested and extracted by ethyl acetate, rotary evaporated, redissolved by 70% ethyl alcohol, then detected by HPLC. The mobile phase condition was ACN and water (contains 0.1% phosphoric acid) (70%:30%, v/v). The observation wavelength was 420 nm according to the maximum absorption wavelength.

Mycelia Preparation for Transcriptome

DSPD was utilized to separate the tested strains, and cellophane was covered on the surfaces of rice agar. After 5 days of cocultivation, both fungi grew well and the mycelia of co-cultured *M. ruber* M7 and *A. niger* CBS 513.88 were scraped down and collected from the cellophane, respectively. After liquid nitrogen freezing, the mycelia were stored at −80°C and sent to Shanghai Majorbio Bio-pharm Technology Co., Ltd. for transcriptome sequencing.

RNA Isolation, Library Preparation, and Sequencing

Total RNA was extracted from mycelia using the TRIzol method (Invitrogen, Carlsbad, CA, United States), and the concentration and purity of the extracted RNA were detected by Nanodrop2000. RNA integrity was detected by agarose gel electrophoresis, and the RNA integrity number (RIN) value was determined by Agilent2100. The libraries were constructed after the RNA samples were qualified by using magnetic beads with Oligo(dT) and polyA to pair A-T bases to enrich mRNA. The fragmentation buffer solution was added to randomly break the mRNA into small fragments of about 300 bp. Double-stranded cDNA was synthesized using a SuperScript double-stranded cDNA synthesis kit (Invitrogen, Carlsbad, CA, United States) with random hexamer primers (Illumina). Then the synthesized cDNA was subjected to end-repair, phosphorylation, and "A" base addition according to Illumina's library construction protocol. The cDNA library was constructed with an Illumina Paired End Sample Prep kit (Illumina, San Diego, CA, United States), quantified by TBS380 (Picogreen, Invitrogen, Carlsbad, CA, United States), and was then sequenced on the Illumina HiSeqTM2500 (2 × 150 bp read length) platform. The transcriptomeic data were analyzed online platform of Majorbio Cloud Platform (www.majorbio.com).

Statistical Analysis

All experiments were carried out in triplicate. Analysis of variance (ANOVA) was computed for testing the significance of the experiment. Data were analyzed in Microsoft Excel.

RESULTS

Comparison of Colonial Morphologies of the Strains on DSPD

Conventional cocultivation of *Monascus* spp. and *A. niger* was carried out at first. Taking *M. ruber* M7 and *A. niger* CBS 513.88 as an example of coating inoculation method (**Figure 3**), no antagonistic zone can be observed between *M. ruber* M 7 and *A. niger* CBS 513.88. The area color of the *Monascus* spp. colony, which had contacted with *A. niger* CBS 513.88, became redder. By point inoculation method of a different combination of *Monascus* spp. and *A. niger*, there was still no antagonistic zone and the contacted area color was also redder (**Figure 4**). No significant change in the *A. niger* colony was observed but *A. niger* CBS 113.46 can inhibit the growth of *Monascus* spp. As it was also limited by the growth space, the shape of the colony was irregular. **Figure 5** showed that by using DSPD, besides the results observed by conventional cocultivation, all the colonies kept the original shape and the color of the communicating area of *A. niger*, which seemed redder than other areas in the colonies of *Monascus* strains. On the PDA media, the color of co-cultured *M. ruber* M7 was redder than those of the monocultured examples. Especially on CYA media, the colony color of *M. ruber* M7 changed from red to orange when co-cultured with *A. niger* CBS 513.88.

Comparison of Micromorphologies of the Strains on DSPD

The micromorphologies of monocultured and co-cultured *Monascus* spp. and *A. niger* could hardly compared by conventional cocultivation due to the difficulty in separation and distinguishing of the tested strains. The DSPD solved the problem. The results showed that at the 3rd day, on CYA media, cleistothecia could not be observed in monocultured *M. ruber* M7 but could be observed in co-cultured *M. ruber* M7 (with *A. niger* CBS 513.88) (**Figure 6A**). At the 7th days, on CYA and G25N media, the mycelia of *M. pilosus* MS-1 changed significantly from

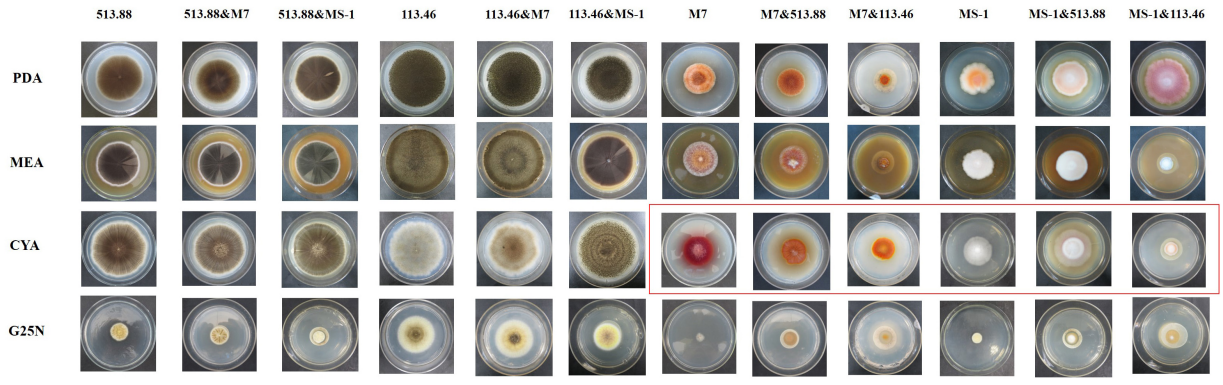

FIGURE 5 | Colonial morphologies of *Monascus ruber* M7, *Monascus pilosus* MS-1 when co-cultured with *Aspergillus niger* CBS 513.88 and *A. niger* CBS 113.46 by using DSPD at 9 days. M7-*M. ruber* M7; MS-1-*M. pilosus* MS-1; 513.88-*A. niger* CBS 513.88; 113.46-*A. niger* CBS 113.46; &-co-cultured with.

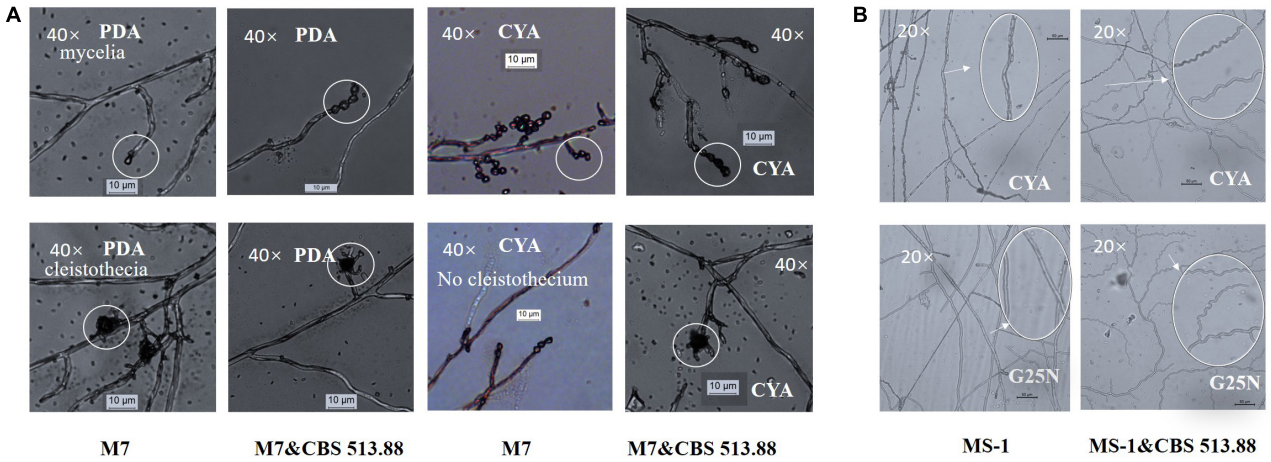

FIGURE 6 | Cocultivation micromorphologies: **(A)** comparison of monocultured and co-cultured (with *Aspergillus niger* CBS 513.88) *M. ruber* M7 on PDA and CYA media; **(B)** mycelia shape variation of *M. pilosus* MS-1 when co-cultured with *A. niger* CBS 513.88. Abbreviations: M7-*M. ruber* M7; M7&CBS 513.88-*M. ruber* M7 co-cultured with *A. niger* CBS 513.88; MS-1-*M. pilosus* MS-1; MS-1&CBS 513.88-*M. pilosus* MS-1 co-cultured with *A. niger* CBS 513.88.

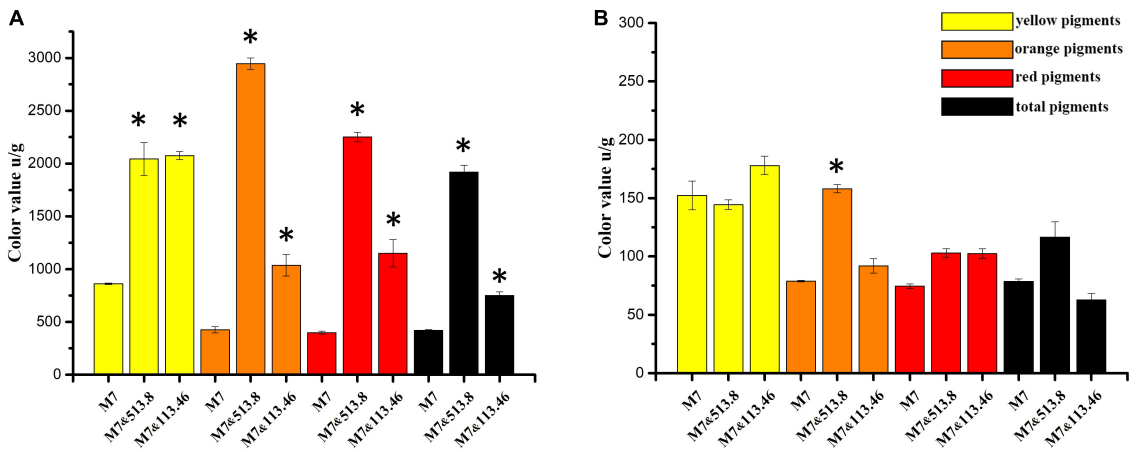

FIGURE 7 | Color value variation of *Monascus* spp. and *Aspergillus niger* cocultivation: **(A)** comparison of *Monascus ruber* M7 intracellular (mycelia) color value among monoculture, co-cultured with *A. niger* CBS 513.88 and co-cultured with *A. niger* CBS 113.46; **(B)** comparison of *M. ruber* M7 extracellular (media) color value among monoculture, co-cultured with *A. niger* CBS 513.88 and co-cultured with *A. niger* CBS 113.46. Abbreviations: M7-monocultured *M. ruber* M7; M7&513.88-*M. ruber* M7 co-cultured with *A. niger* CBS 513.88; M7&113.46-*M. ruber* M7 co-cultured with *A. niger* CBS 113.46. *Represents significant difference compared with control ($P < 0.05$).

straight to curve (**Figure 6B**). For the micromorphologies of tested *A. niger* strains, no significant change was observed.

Analysis of SMs From *Monascus* spp. Strains on DSPD

Color Value Variation by Cocultivation

As a MP producing strain, *M. ruber* M7 was selected to investigate the changes of color value and MPs (Chen et al., 2017). The results demonstrated a significant change in color value, which reflected the MPs variation of *M. ruber* M7 when co-cultured with *A. niger* strains, respectively. As illustrated in **Figure 7**, it was clear that both *A. niger* CBS 513.88 and *A. niger* CBS 113.46 could induce *M. ruber* M7 to produce more intracellular (mycelia) MPs (**Figure 7A**), among which *A. niger* CBS 513.88 acted better than *A. niger* CBS 113.46 in increasing MPs yields. The color value of orange pigments, red pigments, and total pigments increased nearly 6-fold, 4-fold, and 3-fold, respectively. Compared to *A. niger* CBS 513.88, *A. niger* CBS 113.46 was less efficient in the increase of orange and red pigments but was equivalent to an increase of yellow pigments. However, both selected *A. niger* strains had little effect on extracellular (media) MPs of *M. ruber* M7 (**Figure 7B**).

MK and CIT Variation by Cocultivation

MK and CIT are both crucial SMs of *Monascus* spp. As detailed in **Table 1**, MK was only produced by monocultured *M. pilosus* MS-1 on PDA media. When *M. pilosus* MS-1 was co-cultured with *A. niger* CBS 513.88 and *A. niger* CBS 113.46, respectively

TABLE 1 | Monacolin K and citrinin variation when *Monascus* spp. were co-cultured with *Aspergillus niger* on PDA media.

Monascus spp.	Cultivation type	Monacolin K (μg/mg)		Citrinin (μg/mg)	
		Intracellular	Extracellular	Intracellular	Extracellular
MS-1	Mono	4.0828	0.4855	Nd	Nd
	Co with CBS 513.88	Nd*	Nd*	Nd	Nd
	Co with CBS 113.46	Nd*	Nd*	Nd	Nd
M7	Mono	Nd	Nd	0.2975	0.0829
	Co with CBS 513.88	Nd	Nd	0.2391*	0.1888*
	Co with CBS 113.46	Nd	Nd	0.2326	0.1231

*Nd: not detected; mono: monocultured; co: co-cultured; *co-culture group compared to monoculture group, p-value ≤ 0.05.*

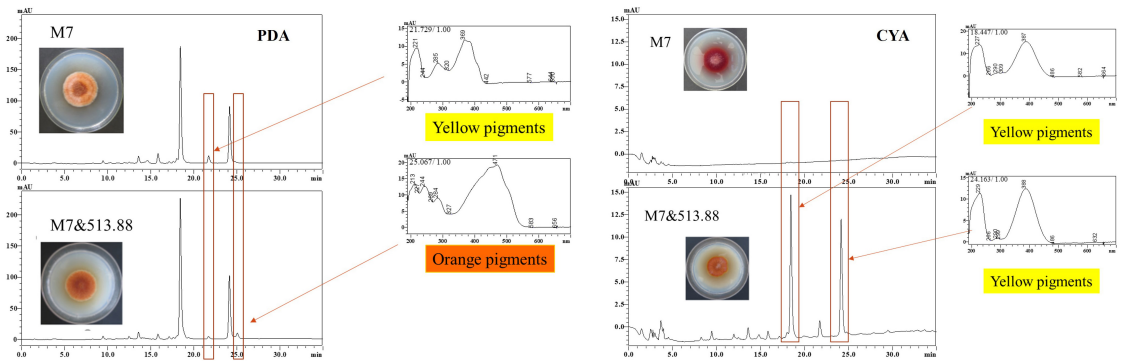

FIGURE 8 | High performance liquid chromatography results of MPs of monocultured *Monascus ruber* M7 and co-cultured *M. ruber* M7 with *Aspergillus niger* CBS 513.88.

MK was undetectable. As a non-CIT producing strain, CIT was undetected in *M. pilosus* MS-1 samples as reported (Feng et al., 2016). According to the CIT content of monocultured and co-cultured *M. ruber* M7, both *A. niger* strains could decrease the intracellular CIT content while increasing the extracellular CIT content of *M. ruber* M7.

MPs Variation by Cocultivation

As mentioned in the colonial morphologies results (**Figure 5**), on DSPD we observed that on PDA and CYA media, the colony color of *M. ruber* M7 changed significantly. The HPLC results in **Figure 8** could support the above conclusion. The MPs peaks of *M. ruber* M7 can be identified by retention time and UV spectrum according to our previous work (Chen et al., 2017). Under the observing wavelength of 380 nm (Chen et al., 2017), one yellow pigment decreased while one orange pigment increased when *M. ruber* M7 was co-cultured with *A. niger* CBS 513.88 on PDA media. On the CYA media, the colony color changed from red to orange due to the production of more yellow pigments when *M. ruber* M7 was stimulated by *A. niger* CBS 513.88.

Mining and Primary Localization of Novel SMs by DSPD

Two novel SMs, namely substance A and B, were discovered by cocultivation of *M. ruber* M7 and *A. niger* CBS 513.88 on the steamed rice in our preliminary experiments (Data not shown). However, the rice-based mixture was not easily analyzed further on account of sample separation. As we saw from **Figure 9**, when DSPD was applied, substance A can only be detected in the mycelia of co-cultured *M. ruber* M7. Substance B with low yield was detected in culture media and *A. niger* CBS 513.88 mycelia. Compared to monocultured *A. niger* CBS 513.88, a new peak appeared in co-cultured *A. niger* CBS 513.88 mycelia. According to the retention time and UV spectrum, this new peak was similar to peak C that appeared in *M. ruber* M7 mycelia. According to the previous work of our lab (Chen et al., 2017), peak C was identified as a yellow *Monascus* pigment.

Transcriptomic Analysis of the Strains on DSPD

Considering that novel SMs can only be detected in the combination of *M. ruber* M7 and *A. niger* CBS 513.88, and that the genomes of these two fungi have been sequenced or published on NCBI (Andersen et al., 2011). the combination of *M. ruber* M7 and *A. niger* CBS 513.88 was selected for transcriptome analysis. The samples of co-cultured *M. ruber* M7. and co-cultured *A. niger* CBS 513.88 on DSPD were used for total RNA isolation, respectively. Taken samples on the fifth day as an example, in this case monocultured *M. ruber* M7, co-cultured *M. ruber* M7, monocultured *A. niger* CBS 513.88, and co-cultured *A. niger* CBS 513.88, total four samples were chosen as samples to study transcriptome variation during cocultivation. The results of agarose gel electrophoresis (**Figure 10**) showed that all samples had clear 28S and 18S bands, no significant contamination of

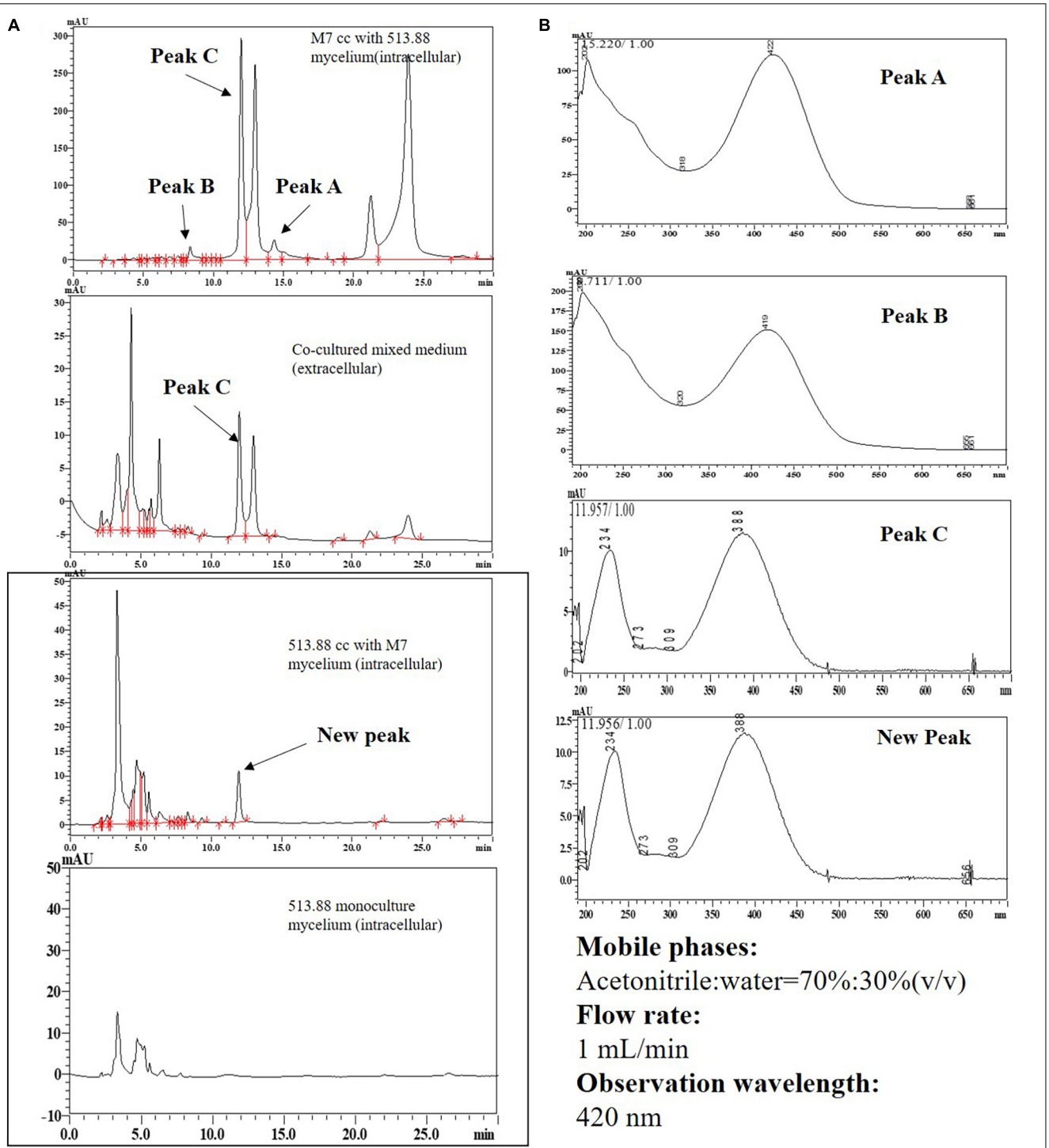

FIGURE 9 | High performance liquid chromatography results of substance A and B in different cocultivation samples: **(A)** HPLC results; **(B)** UV-spectrum results. Abbreviations: CC-cocultured; M7-*Monascus ruber* M7; 513.88- *A. niger* CBS 513.88.

proteins, sugars, and other impurities were observed and good RNA integrity was achieved. All samples were in line with sequencing requirements and met the requirements for library construction (**Table 2**).

For *M. ruber* M7 samples, after quality control processing, a total of 46.14 Gb of clean data were obtained. The clean data of each sample reached more than 6.76 Gb. A total of 9,165 genes were detected in this analysis, including 8,671 known genes

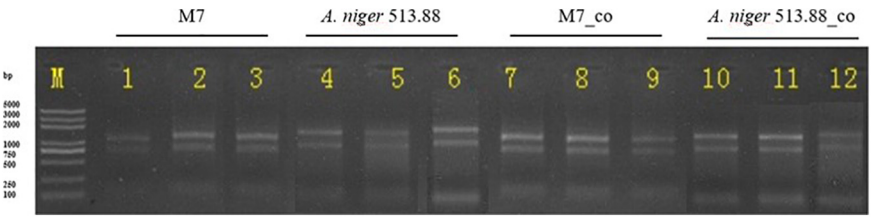

FIGURE 10 | Total RNA of 12 samples for RNA-Seq in 1% agarose gel electrophoresis.

TABLE 2 | The quality results of the total RNA of 12 samples.

Sample	Con (ng/μL)	OD260/280	OD260/230	RIN value
M7_1	112.80	1.96	1.27	9.40
M7_2	180.00	2.05	1.24	9.50
M7_3	245.00	2.05	1.29	10.00
M7_co_1	51.20	2.03	1.12	9.00
M7_co_2	115.60	1.98	1.03	8.20
M7_co_3	130.30	1.90	1.06	9.30
AN5_2	159.60	2.00	1.24	8.60
AN5_3	83.50	2.03	1.73	7.00
AN5_1	73.10	2.05	1.26	8.60
AN5_co_2	285.00	2.02	2.01	8.50
AN5_co_3	301.10	2.02	20.04	8.60
AN5_co_1	715.60	2.25	2.24	6.60

RIN (RNA integrity number) value represents the integrity of the RNA sample, and the higher the value is, the better the integrity of RNA will be. Abbreviations: Con-Concentration; M7-monocultured M. ruber M7; M7_co-M. ruber M7 co-cultured with A. niger CBS 513.88; AN5-A. niger CBS 513.88; AN5_co-A. niger CBS 513.88 co-cultured with M. ruber M7.

and 494 new genes. There were 15,985 expressed transcripts, including 8,262 known transcripts and 7,723 new transcripts. The quality values of base Q20 and Q30 were higher than 98% and 95%, respectively, and GC content was higher than 52%, indicating that the data quantity was rich and reliable, which could be used for subsequent analysis in this study. The obtained clean reads were compared with the reported *M. purpureus* genome[1], and there were six libraries (as listed in **Table 3**), and more than 95.13% of clean reads in each library could be compared with the reference genome.

For *A. niger* CBS 513.88 samples, after quality control processing, a total of 46.33 Gb clean data were obtained, and the clean data of each sample reached more than 7.39 Gb. A total of 12,635 expressed genes were detected in this analysis, including 12,428 known genes and 207 new genes. There were 17,068 expressed transcripts, including 11,653 known transcripts and 5,415 new transcripts. The quality values of base Q20 and Q30 were higher than 98% and 95%, respectively, and GC content was higher than 54%, indicating that the data quantity was rich and reliable, which could be used for subsequent analysis in this study. The obtained clean reads were compared with the reported *A. niger CBS 513.88* genome[2], and there were six libraries (as listed in **Table 4**), and more than 93.37% of clean reads in each library that could be compared with the reference genome.

DISCUSSION

Black-skin-red-koji, as a natural FF cocultivation model, has been applied for wine and vinegar production for over 1,000 years but has been seldom studied (Fang et al., 2011; Mao et al., 2011). In this work, a DSPD was developed and applied to explore BSRK, started from the cocultivation of *Monascus* spp. and *A. niger*. In conventional cultivation of *Monascus* spp. and *A. niger,* we found no antagonism but a symbiosis between *Monascus* spp. and *A. niger* (**Figures 3**, **4**). Moreover, *Monascus* spp. may be stimulated to produce more MPs (**Figure 7**). Although *Monascus* spp. and *A. niger* can grow together, *A. niger*, especially *A. niger* CBS 113.46 can inhibit the growth of *Monascus* spp. strains. It became more meaningful to lucubrate the reason why *Monascus* spp. and *A. niger* can grow together and has been applied to fermented food for over 1,000 years. Further molecular mechanisms should be studied to reveal the meaning of this cocultivation mode in the biological and food industry. According to the micromorphologic results, at the third day, *A. niger* CBS 513.88 affected *M. ruber* M7 to produce cleistothecia on CYA media. Since cleistothecia are the sexual reproductive organ of *M. ruber* M7 (Ojeda-Lopez et al., 2018), it is speculated that *A. niger* CBS 513.88 might change the proliferation of *M. ruber* M7 under nutrient deficiency conditions. When using PDA as a culture media, there was no significant differences between monocultured *M. ruber* M7 and *M. pilosus* MS-1 on micromorphologic characterics. However, by using CYA and G25N as culture media, *A. niger* can affect the mycelia of *M. pilosus* MS-1 significantly, from straight to curved. The recent research shows that *A. niger* might be stimulated by carbon starving and produce a variety of pectinases which can break cell walls (van Munster et al., 2014). Therefore, considering CYA and G25N are all carbon-starved culture media, it is likely that *A. niger* can be forced to produce pectinase to achieve more carbon resources, meanwhile, the cell wall of *M. pilosus* MS-1 was broken by pectinase and caused a change of mycelia shape (**Figure 6B**). No significant change was observed by conventional cocultivation of *A. niger*, while on DSPD, the color of the

[1]https://genome.jgi.doe.gov/portal/pages/dynamicOrganismDownload.jsf?organism=Monpu1

[2]http://www.aspergillusgenome.org/cache/A_niger_CBS_513_88_genomeSnapshot.html

TABLE 3 | RNA-Seq clean reads and the counts, percentage of reads mapping statistics to *Monascus purpureus* genome.

	Sample	Raw reads	Clean reads	Clean bases	Q20 (%)	Q30 (%)	Total mapped	Uniquely mapped
Control	M7_1	48.97 Mb	48.00 Mb	7.17 Gb	98.27	95.03	46.22 Mb (96.31%)	46.04 Mb (95.92%)
	M7_2	58.01 Mb	57.19 Mb	8.54 Gb	98.43	95.36	55.33 Mb (96.75%)	55.10 Mb (96.34%)
	M7_3	51.15 Mb	50.38 Mb	7.55 Gb	98.29	95.00	48.88 Mb (97.02%)	48.67 Mb (96.60%)
Cocultured	M7_co_1	52.72 Mb	51.99 Mb	7.75 Gb	98.47	95.49	49.69 Mb (95.58%)	49.50 Mb (95.22%)
M. ruber M7	M7_co_2	57.00 Mb	56.08 Mb	8.37 Gb	98.44	95.42	53.85 Mb (96.02%)	53.65 Mb(95.65%)
transcriptome	M7_co_3	45.76 Mb	44.99 Mb	6.76 Gb	98.41	95.34	42.80 Mb (95.13%)	42.59 Mb (94.66%)

M7-monocultured M. ruber M7; M7_co-M. ruber M7 co-cultured with A. niger CBS 513.88.

TABLE 4 | RNA-Seq clean reads and the counts, percentage of reads mapping statistics to *Aspergillus niger* CBS 513.88 genome.

	Sample	Raw reads	Clean reads	Clean bases	Q20 (%)	Q30 (%)	Total mapped	Uniquely mapped
Control	AN5_1	54.46 Mb	53.76 Mb	7.99 Gb	98.30	95.02	50.86 Mb (94.62%)	45.47 Mb (84.59%)
	AN5_2	54.60 Mb	53.90 Mb	8.00 Gb	98.17	94.69	51.22 Mb (95.02%)	45.42 Mb (84.27%)
	AN5_3	51.42 Mb	50.76 Mb	7.52 Gb	98.23	94.87	48.37 Mb (95.29%)	41.94 Mb (82.63%)
Cocultured	AN5_co_1	51.09 Mb	50.46 Mb	7.39 Gb	98.37	95.24	47.12 Mb (93.37%)	42.54 Mb (84.30%)
A.niger CBS 513.88	AN5_co_2	52.09 Mb	51.42 Mb	7.67Gb	98.16	94.69	48.79 Mb (94.89%)	46.16 Mb (89.77%)
transcriptome	AN5_co_3	52.74 Mb	52.12 Mb	7.74 Gb	98.30	95.02	49.53 Mb (95.03%)	45.61 Mb (87.51%)

AN5-A. niger CBS 513.88; AN5_co-A. niger CBS 513.88 co-cultured with M. ruber M7.

communicating area of *A. niger* was darker than other areas in the colony. Research shows that the black color (melanin) of *A. niger* originated from spores (Kumaran et al., 2017). *Monascus* spp. strains may promote the production of the spores of *A. niger*. The molecular mechanisms about this phenomenon are still being studied.

By conventional cocultivation of fungi, the mycelia are very hard to separate and harvest if there is no antagonism phenomenon between the tested strains, which is an obstacle for SM analysis in this study. DSPD overcame this obstacle efficiently. From MK and CIT results (**Table 1**), we speculated that *A. niger* may affect the biosynthesis of MK and CIT produced by *Monascus* spp. These results can guide us on transcriptome analysis. With the help of DSPD, more intuitive and completed *Monascus* spp. colony pictures demonstrated the effects of *A. niger* on the MPs production. The above conclusions were further illustrated by the detection of color value and the HPLC analysis of MPs. Both tested *A. niger* can increase the MPs production of *M. ruber* M7, especially the orange pigments. Among them, on increasing MPs of *M. ruber* M7, *A. niger* CBS 513.88 was more efficient (**Figure 7**). The ultraviolet spectrograms and retention time of MPs peaks from HPLC results were compared to the published research about MPs (Chen et al., 2017), which have demonstrated that *A. niger* can cause variation of several known MPs contents. It was reported that the cocultivation of yeast and *Monascus* spp. and MPs production increased significantly (Shin et al., 1998). This may provide a reference to study the molecular mechanisms about MPs variation. Research has shown that CIT synthesis is related to MPs synthesis (He and Cox, 2016), which may explain the effects of *A. niger* CBS 513.88 on changing the intracellular and extracellular CIT content of *M. ruber* M7.

Research on SMs determination has shown that by using PDA, MEA, CYA, and G25N, no new peak can be observed by HPLC which represents a new compound. This study thus mined novel SMs by other attempts, changing culture temperatures, culture media, and extraction methods. When the rice was taken as a culture media, at 420 nm, two new compounds, namely substance A and B. The chemical structure of A and B are still being identified by LCMS-MS and NMR and will be brought out in the future. DSPD offered an effective method for sample preparation, which is necessary for the preparation and purification of substances A and B. In addition, with the help of DSPD, substance A was almost verified to be produced by *M. ruber* M7 when co-cultured with *A. niger* CBS 513.88. Surprisingly, a peak whose retention time and UV-spectrum were a similar yellow MP, identified by our previous work (Chen et al., 2017), was detected in *A. niger* CBS 513.88 mycelia, indicating that *M. ruber* M7 may stimulate *A. niger* CBS 513.88 to produce MP. These results offer important information for follow-up research. The related experiments on the identification of these new compounds and transcriptome analysis are still ongoing and will be presented in future studies.

To study the most natural co-cultured method of *Monascus* spp. and *A. niger*, which is growing on rice together in a way similar to BSRK, sample preparation represented a huge challenge for transcriptome analyses, due to the separation problems. *Monascus* spp. can grow together with *A. niger* on rice, the mycelia and spores of both sides are intertwined, and difficult to separate from each other. The tested strains were rooted in rice, which made it difficult to separate strains from rice. Rice contains proteins and saccharides which would interfere with the transcriptome sequencing results. The DSPD presented a breakthrough for overcoming this problem. Out of the tested strains, *M. ruber* M7 and *A. niger* CBS 513.88 were chosen as the advisable research subjects for further transcriptome analysis after comprehensive consideration according to the sequenced genome, based on similar growth rate and SMs richness.

DSPD broke down the first barrier of transcriptome analysis. All the separation problems about strain-strains and strain-media were solved and good quality transcriptome data were obtained (**Tables 4**, **5**).

]This article reveals some promising superficial results relating to *Monascus* spp. and *A. niger* cocultivation that are worth further exploration. Although we choose *M. ruber* M7 and *A. niger* CBS 513.88 as the main research subjects for some reasonable causes, the results achieved by the DSPD showed that the different pairs of *A. niger* and *Monascus* spp. strains had different interactions, which indicates that it is important to choose appropriate strains for cocultivation to increase beneficial metabolites, decrease detrimental ones, or even find new substances. Beyond the two new substances found by the SMs profiles of *M. ruber* M7 when co-cultured with *A. niger* CBS 513.88, there still may be more undiscovered compounds that were in this case limited by the culture conditions, extraction methods, and instrumental methods. The MPs only changed on yields and not in terms of kind, and the reasons for this on a molecular level are also worth studying in the future. For transcriptome analyses, the present study overcomes the barrier of sample preparation, opening further avenues for the study of the molecular mechanisms of *M. ruber* M7 and *A. niger* CBS 513.88, and obtaining good quality transcriptome results. The DSPD developed in the present study presents an excellent stepping-stone to success. All the above conclusions obtained by DSPD provide the theoretical foundations for further study of the molecular mechanisms between *Monascus* spp. and *A. niger*.

DATA AVAILABILITY STATEMENT

The datasets presented in this study can be found in online repositories. The names of the repository/repositories and accession number(s) can be found below: NCBI Sequence Read Archive (SRA) with BioProject number PRJNA721011.

AUTHOR CONTRIBUTIONS

XY and FC conceived the study and designed the experiments. XY carried out the experiments, analyzed the data, wrote the manuscript, undertook investigation, methodology, writing, reviewing, editing, and supervision. FC reviewed the manuscript and the experiments, oversaw conceptualization, and project administration. Both authors contributed to the article and approved the submitted manuscript.

FUNDING

This work was supported by the Major Program of the National Natural Science Foundation of China (Nos. 31730068 and 31330059 to FC), the National Key Research and Development Program of China (No. 2018YFD0400404 to FC), the Shandong Province Taishan Industry Leading Talents High-Efficiency Agriculture Innovation Project (No. tscy20180120 to FC), and Project supported by the Fundamental Research Funds for the Central Universities of China (No. 2662018JC013).

REFERENCES

Andersen, M. R., Salazar, M. P., Schaap, P. J., Van De Vondervoort, P. J., Culley, D., Thykaer, J., et al. (2011). Comparative genomics of citric-acid-producing *Aspergillus niger* ATCC 1015 versus enzyme-producing CBS 513.88. *Genome Res.* 21, 885–897. doi: 10.1101/gr.112169.110

Bertrand, S., Schumpp, O., Bohni, N., Monod, M., Gindro, K., and Wolfender, J. L. (2013). De novo production of metabolites by fungal co-culture of *Trichophyton rubrum* and *Bionectria ochroleuca*. *J. Nat. Prod.* 76, 1157–1165. doi: 10.1021/np400258f

Camacho-Zaragoza, J. M., Hernandez-Chavez, G., Moreno-Avitia, F., Ramirez-Iniguez, R., Martinez, A., Bolivar, F., et al. (2016). Engineering of a microbial coculture of *Escherichia coli* strains for the biosynthesis of resveratrol. *Microb. Cell Fact.* 15:163. doi: 10.1186/s12934-016-0562-z

Chen, F., Li, L., Qu, J., and Chen, C. (2009). "Cereal vinegars made by solid-state fermentation in China," in *Vinegars of the world*, eds L. Solieri and P. Giudici (Milano: Springer), 243–259.

Chen, W., Chen, R., Liu, Q., He, Y., He, K., Ding, X., et al. (2017). Orange, red, yellow: biosynthesis of azaphilone pigments in *Monascus* fungi. *Chem. Sci.* 8, 4917–4925. doi: 10.1039/c7sc00475c

Chen, W., He, Y., Zhou, Y., Shao, Y., Feng, Y., Li, M., et al. (2015). Edible filamentous fungi from the species *Monascus*: early traditional fermentations, modern molecular biology, and future genomics. *Compr. Rev. Food Sci. Food Saf.* 14, 555–567.

Chiang, Y., Chang, S., Oakley, B. R., and Wang, C. C. (2011). Recent advances in awakening silent biosynthetic gene clusters and linking orphan clusters to natural products in microorganisms. *Curr. Opin. Chem. Biol.* 15, 137–143. doi: 10.1016/j.cbpa.2010.10.011

Ding, G., Zhao, J., Zhang, W., Yao, J. C., Xu, H., Ding, Y. Z., et al. (2008). *National Standard GB4926-2008: Food Additive-Red Kojic Rice (Powder) AQSIQ*. China. 1–5.

Fang, S., Yang, Y., Zhen, D., and Chen, M. (2011). Production of koji by black-skin-red-koji. *Adv. Mater. Res.* 236-238, 2748–2752.

Favela-Torres, E., Cordova-López, J., Garda-Rivero, M., and Gutirrrez-Rojas, M. (1998). Kinetics of growth of *Aspergillus niger* during submerged, agar surface and solid state fermentations. *Process Biochem.* 33, 103–107.

Feng, Y., Chen, W., and Chen, F. (2016). A *Monascus pilosus* MS-1 strain with high-yield monacolin K but no citrinin. *Food Sci. Biotechnol.* 25, 1115–1122. doi: 10.1007/s10068-016-0179-3

Feng, Y., Shao, Y., and Chen, F. (2012). *Monascus* pigments. *Appl. Microbiol. Biotechnol.* 96, 1421–1440.

Feng, Y., Shao, Y., Zhou, Y., and Chen, F. (2014). Monacolin K production by citrinin-free *Monascus pilosus* MS-1 and fermentation process monitoring. *Eng. Life Sci.* 14, 538–545.

Gao, G., Fan, H., Zhang, Y., Cao, Y., Li, T., Qiao, W., et al. (2021). Production of nisin-containing bacterial cellulose nanomaterials with antimicrobial properties through co-culturing *Enterobacter* sp. FY-07 and *Lactococcus lactis* N8. *Carbohydr. Polym.* 251:117131. doi: 10.1016/j.carbpol.2020.117131

He, Y., and Cox, R. J. (2016). The molecular steps of citrinin biosynthesis in fungi. *Chem. Sci.* 7, 2119–2127.

Huang, L., Chen, K., Zhang, M., Wang, J., Ren, X., Yang, H., et al. (2019). Comparative analysis of physicochemical components and volatile components in rice wines brewed by *Aspergillus niger* and *Monascus purpureus* in Chinese. *J. Food Saf. Qual.* 10, 4896–4904.

Huang, Z., Hong, J., Xu, J., Li, L., Guo, W., Pan, Y., et al. (2018). Exploring core functional microbiota responsible for the production of volatile flavour during the traditional brewing of Wuyi Hong Qu glutinous rice wine. *Food Microbiol.* 76, 487–496. doi: 10.1016/j.fm.2018.07.014

Jimenez-Barrera, D., Chan-Cupul, W., Fan, Z., and Osuna-Castro, J. A. (2018). Fungal co-culture increases ligninolytic enzyme activities: statistical optimization using response surface methodology. *Prep. Biochem. Biotechnol.* 48, 787–798. doi: 10.1080/10826068.2018.1509084

Kumaran, S., Abdelhamid, H. N., and Wu, H. (2017). Quantification analysis of protein and mycelium contents upon inhibition of melanin for *Aspergillus niger*: a study of matrix assisted laser desorption/ionization mass spectrometry (MALDI-MS). *RSC Adv.* 7, 30289–30294.

Kumari, S., and Naraian, R. (2016). Decolorization of synthetic brilliant green carpet industry dye through fungal co-culture technology. *J. Environ. Manag.* 180, 172–179. doi: 10.1016/j.jenvman.2016.04.060

Li, K., Chen, M., and Zhu, Z. (2009). Production of koji by black-skin-red-koji. *China Brewing* 4, 124–126.

Li, L., Chen, S., Gao, M., Ding, B., Zhang, J., Zhou, Y., et al. (2019). Acidic conditions induce the accumulation of orange *Monascus* pigments during liquid-state fermentation of *Monascus ruber* M7. *Appl. Microbiol. Biotechnol.* 103, 8393–8402. doi: 10.1007/s00253-019-10114-8

Liu, Q., Cai, L., Shao, Y., Zhou, Y., Li, M., Wang, X., et al. (2016). Inactivation of the global regulator *LaeA* in *Monascus ruber* results in a species-dependent response in sporulation and secondary metabolism. *Fungal Biol.* 120, 297–305. doi: 10.1016/j.funbio.2015.10.008

Mao, Q., Tu, X., Jia, X., and Zhou, L. (2011). The fermentation technology of black-skin-red-koji and the brewing of indica rice wine. *Jiangsu Condiment Subsidiary Food* 28, 28–31.

Marmann, A., Aly, A. H., Lin, W., Wang, B., and Proksch, P. (2014). Co-cultivation–a powerful emerging tool for enhancing the chemical diversity of microorganisms. *Mar. Drugs* 12, 1043–1065. doi: 10.3390/md12021043

Meyer, V., Andersen, M. R., Brakhage, A. A., Braus, G. H., Caddick, M. X., Cairns, T. C., et al. (2016). Current challenges of research on filamentous fungi in relation to human welfare and a sustainable bio-economy: a white paper. *Fungal Biol. Biotechnol.* 3:6. doi: 10.1186/s40694-016-0024-8

Moussa, M., Ebrahim, W., Bonus, M., Gohlke, H., M'Andi, A., Kurt'An, T., et al. (2019). Co-culture of the fungus *Fusarium tricinctum* with *Streptomyces lividans* induces production of cryptic naphthoquinone dimers. *RSC Adv.* 9, 1491-1500.

Nett, M., Ikeda, H., and Moore, B. S. (2009). Genomic basis for natural product biosynthetic diversity in the actinomycetes. *Nat. Prod. Rep.* 26, 1362–1384.

Nielsen, K. F., Mogensen, J. M., Johansen, M., Larsen, T. O., and Frisvad, J. C. (2009). Review of secondary metabolites and mycotoxins from the *Aspergillus niger* group. *Anal. Bioanal. Chem.* 395, 1225–1242. doi: 10.1007/s00216-009-3081-5

Nonaka, K., Iwatsuki, M., Horiuchi, S., Shiomi, K., Ômura, S., and Masuma, R. (2015). Induced production of BE-31405 by co-culturing of *Talaromyces siamensis* FKA-61 with a variety of fungal strains. *J. Antibiot.* 68, 573–578.

Ojeda-Lopez, M., Chen, W., Eagle, C. E., Gutierrez, G., Jia, W. L., Swilaiman, S. S., et al. (2018). Evolution of asexual and sexual reproduction in the aspergilli. *Stud. Mycol.* 91, 37–59.

Pettit, R. K. (2009). Mixed fermentation for natural product drug discovery. *Appl. Microbiol. Biotechnol.* 83, 19–25.

Shang, Z., Salim, A. A., and Capon, R. J. (2017). Chaunopyran A: co-Cultivation of marine mollusk-derived fungi activates a rare class of 2-alkenyl-tetrahydropyran. *J. Natural Prod.* 80, 1167–1172. doi: 10.1021/acs.jnatprod.7b00144

Shin, C. S., Kim, H. J., Kim, M. J., and Ju, J. Y. (1998). Morphological change and enhanced pigment production of *Monascus* when cocultured with *Saccharomyces cerevisiae* or *Aspergillus oryzae*. *Biotechnol. Bioeng.* 59, 576–581. doi: 10.1002/(sici)1097-0290(19980905)59:5<576::aid-bit7>3.0.co;2-7

Show, P. L., Oladele, K. O., Siew, Q. Y., Aziz Zakry, F. A., Lan, J. C.-W., and Ling, T. C. (2015). Overview of citric acid production from *Aspergillus niger*. *Front. Life Sci.* 8:271–283. doi: 10.1080/21553769.2015.1033653

van Munster, J. M., Daly, P., Delmas, S., Pullan, S. T., Blythe, M. J., Malla, S., et al. (2014). The role of carbon starvation in the induction of enzymes that degrade plant-derived carbohydrates in *Aspergillus niger*. *Fungal Genet. Biol.* 72, 34–47. doi: 10.1016/j.fgb.2014.04.006

Vinale, F., Nicoletti, R., Borrelli, F., Mangoni, A., Parisi, O. A., Marra, R., et al. (2017). Co-culture of plant beneficial microbes as source of bioactive metabolites. *Sci. Rep.* 7:14330. doi: 10.1038/s41598-017-14569-5

Wakefield, J., Hassan, H. M., Jaspars, M., Ebel, R., and Rateb, M. E. (2017). Dual induction of new microbial secondary metabolites by fungal bacterial co-cultivation. *Front. Microbiol.* 8:1284. doi: 10.3389/fmicb.2017.01284

Wang, L. W., Dai, Y., Chen, W., Shao, Y., and Chen, F. (2016). Effects of light intensity and color on the biomass, extracellular red pigment, and citrinin production of *Monascus ruber*. *J. Agric. Food Chem.* 64, 9506–9514. doi: 10.1021/acs.jafc.6b04056

Xu, D., Wang, L., and Du, C. (2015). Progress in microbial co-culture -A review. *Acta Microbiol. Sin.* 55, 1089–1096.

Xu, M., Bai, H. Y., Fu, W. Q., Sun, K., Wang, H. W., Xu, D. L., et al. (2021). Endophytic bacteria promote the quality of *Lyophyllum decastes* by improving non-volatile taste components of mycelia. *Food Chem.* 336, 127672. doi: 10.1016/j.foodchem.2020.127672

Xu, T., Li, J., Yu, B., Liu, L., Zhang, X., Liu, J., et al. (2018). Transcription factor SsSte12 was involved in mycelium growth and development in *Sclerotinia sclerotiorum*. *Front. Microbiol.* 9:2476. doi: 10.3389/fmicb.2018.02476

Yan, P., Xue, W., Tan, S., Zhang, H., and Chang, X. (2008). Effect of inoculating lactic acid bacteria starter cultures on the nitrite concentration of fermenting Chinese paocai. *Food Control* 19, 50–55.

Yu, G., Sun, Z., Peng, J., Zhu, M., Che, Q., Zhang, G., et al. (2019). Secondary metabolites produced by combined culture of *Penicillium crustosum* and a *Xylaria* sp. *J. Natural Prod.* 82, 2013–2017. doi: 10.1021/acs.jnatprod.9b00345

Yu, M., Li, Y., Banakar, S. P., Liu, L., Shao, C., Li, Z., et al. (2019). New metabolites from the co-culture of marine-derived actinomycete *Streptomyces rochei* MB037 and Fungus *Rhinocladiella similis* 35. *Front. Microbiol.* 10:915. doi: 10.3389/fmicb.2019.00915

Zhang, H., Li, Z., Pereira, B., and Stephanopoulos, G. (2015). Engineering *E. coli-E. coli* cocultures for production of muconic acid from glycerol. *Microb. Cell Fact.* 14:134. doi: 10.1186/s12934-015-0319-0

Zuck, K. M., Shipley, S., and Newman, D. J. (2011). Induced production of N-formyl alkaloids from *Aspergillus fumigatus* by co-culture with *Streptomyces peucetius*. *J. Nat. Prod.* 74, 1653–1657. doi: 10.1021/np200255f

Conflict of Interest: The authors declare that the research was conducted in the absence of any commercial or financial relationships that could be construed as a potential conflict of interest.

frontiers in Microbiology

ORIGINAL RESEARCH
published: 16 June 2021
doi: 10.3389/fmicb.2021.680629

An Integrated Approach to Determine the Boundaries of the Azaphilone Pigment Biosynthetic Gene Cluster of *Monascus ruber* M7 Grown on Potato Dextrose Agar

Qingpei Liu[1,2], Siyu Zhong[1], Xinrui Wang[1], Shuaibiao Gao[1], Xiaolong Yang[1], Fusheng Chen[3,4]* and István Molnár[2]**

[1] The Modernization Engineering Technology Research Center of Ethnic Minority Medicine of Hubei Province, School of Pharmaceutical Sciences, South-Central University for Nationalities, Wuhan, China, [2] Southwest Center for Natural Products Research, The University of Arizona, Tucson, AZ, United States, [3] Hubei International Scientific and Technological Cooperation Base of Traditional Fermented Foods, Huazhong Agricultural University, Wuhan, China, [4] College of Food Science and Technology, Huazhong Agricultural University, Wuhan, China

Monascus-type azaphilone pigments (MonAzPs) are produced in multi-thousand ton quantities each year and used as food colorants and nutraceuticals in East Asia. Several groups, including ours, described MonAzPs biosynthesis as a highly complex pathway with many branch points, affording more than 110 MonAzP congeners in a small group of fungi in the Eurotiales order. MonAzPs biosynthetic gene clusters (BGCs) are also very complex and mosaic-like, with some genes involved in more than one pathway, while other genes playing no apparent role in MonAzPs production. Due to this complexity, MonAzPs BGCs have been delimited differently in various fungi. Since most of these predictions rely primarily on bioinformatic analyses, it is possible that genes immediately outside the currently predicted BGC borders are also involved, especially those whose function cannot be predicted from sequence similarities alone. Conversely, some peripheral genes presumed to be part of the BGC may in fact lay outside the boundaries. This study uses a combination of computational and transcriptional analyses to predict the extent of the MonAzPs BGC in *Monascus ruber* M7. Gene knockouts and analysis of MonAzPs production of the mutants are then used to validate the prediction, revealing that the BGC consists of 16 genes, extending from *mrpigA* to *mrpigP*. We further predict that two strains of *Talaromyces marneffei*, ATCC 18224 and PM1, encode an orthologous but non-syntenic MonAzPs BGC with 14 genes. This work highlights the need to use comprehensive, integrated approaches for the more precise determination of secondary metabolite BGC boundaries.

Keywords: *Monascus* azaphilone pigment, gene cluster boundary, comparative genomics, transcription analysis, gene knockout

OPEN ACCESS

Edited by:
Xucong Lv,
Fuzhou University, China

Reviewed by:
Fernando Guzman Chavez,
University of Cambridge, United Kingdom
Sameer Ahmed Shamsuddin Mapari,
University of Mumbai, India
Sheng Yin,
Beijing Technology and Business University, China
Chan Zhang,
Beijing Technology and Business University, China

****Correspondence:***
Xiaolong Yang
yxl19830915@163.com
Fusheng Chen
chenfs@mail.hzau.edu.cn
István Molnár
imolnar@email.arizona.edu

Specialty section:
This article was submitted to Food Microbiology, a section of the journal Frontiers in Microbiology

Received: *15 March 2021*
Accepted: *21 May 2021*
Published: *16 June 2021*

Citation:
Liu Q, Zhong S, Wang X, Gao S, Yang X, Chen F and Molnár I (2021) An Integrated Approach to Determine the Boundaries of the Azaphilone Pigment Biosynthetic Gene Cluster of Monascus ruber M7 Grown on Potato Dextrose Agar. Front. Microbiol. 12:680629. doi: 10.3389/fmicb.2021.680629

INTRODUCTION

Monascus-type azaphilone pigments (MonAzPs) are a complex mixture of secondary metabolites (SMs) with a tricyclic azaphilone scaffold, produced by a few fungal genera in the Eurotiales order such as *Monascus* and *Talaromyces* spp. MonAzPs are traditionally classified as red, orange, and yellow pigments based on their absorbance maxima (Feng et al., 2012). To the best of our knowledge, more than 110 MonAzPs components have been identified from various fungi (Chen et al., 2019). As colorants, MonAzPs have been widely used in various food products for centuries, especially in Southeast Asian countries (Chen et al., 2015). Moreover, MonAzPs also possess wide-ranging biological activities such as preventing hypertension (Lee and Pan, 2012a), lowering cholesterol levels (Lee et al., 2010), causing hypolipidemic effects (Lee and Pan, 2012b), and displaying anti-obesity (Choe et al., 2012) and anti-tumor activities (Akihisa et al., 2005).

Investigations of the MonAzPs biosynthetic pathway started in the 1960s (Birch et al., 1962; Kurono et al., 1963; Hadfield et al., 1967). With the advent of fungal genome sequencing, several groups, including ours, proposed a unified MonAzPs biosynthetic process active in various *Monascus* species and strains that differ in their azaphilone pigment and citrinin productivities (He and Cox, 2016; Chen et al., 2019). This pathway was found to consist of a trunk pathway with many biosynthetic branches that use enzymes with substrate- and product flexibility. It was also seen to utilize adventitious biochemical or chemical transformations, and to incorporate some still not well characterized biosynthetic steps (Chen et al., 2019). Functional studies on the biosynthesis of MonAzPs utilized a combination of targeted gene knockouts, heterologous gene expression, and *in vitro* chemical and enzymatic reactions (Balakrishnan et al., 2013, 2014a,b,c, 2015, 2017a,b,c; Xie et al., 2013; Liu et al., 2014; Liu J. et al., 2016; Chen et al., 2017; Liang et al., 2018; Li et al., 2020). These studies also revealed that the MonAzPs biosynthetic gene cluster (BGC) in *Monascus ruber* M7 also encodes the biosynthesis of monasones, anthraquinone-type SMs with antibacterial activities (Li et al., 2020).

The functional and structural complexities of MonAzPs BGCs and biosynthetic processes, and their variability among different fungi make it difficult to predict the extent of these BGCs, especially when relying only on routine sequence similarity searches to draw cluster boundaries. It remains possible that genes outside the currently predicted boundaries of the BGC are also involved in MonAzPs production, especially when their functions cannot be easily predicted from the similarities of their encoded proteins alone. Conversely, it is also possible that bioinformatic methods over-estimate the extent of MonAzPs BGCs, and include genes in the predicted clusters that have in fact no role in pigment biosynthesis. Such prediction mistakes may undermine biosynthetic proposals by omitting important genes or including spurious ones, thus highlighting the need for more comprehensive prediction workflows to delimit BGC boundaries.

The carbon skeletons of SMs are often synthesized by "core" enzymes such as polyketide synthases (PKSs) and non-ribosomal peptide synthetases (NRPSs). Several widely used software tools that predict fungal SM BGCs, including SMURF[1] and antiSMASH[2] detect the genes encoding such core enzymes, and anchor the predicted BGCs around these genes (Khaldi et al., 2010; Blin et al., 2019). However, these very useful software tools are not particularly well suited to define BGC boundaries. To address this need, Takeda et al. (2014) devised a novel comparative genomics method to predict the extent of SM BGCs by searching for gene similarities in genome sequence assemblies, and by evaluating the presence of similar genes even in non-syntenic blocks. This method made it possible to better identify known SM BGCs featuring core genes, and some even without such anchors, in the genome sequences of 10 filamentous fungi (Takeda et al., 2014).

The biosynthesis of fungal SMs is governed by a hierarchical regulatory network that often involves pathway-specific regulators (Lyu et al., 2020). Some pathway-specific regulators control the transcription of all the genes involved in the production of a given SM, while others regulate only a key subset of the structural genes. For example, the transcription factor Sol4 governs all six biosynthetic genes in the BGC of solanapyrone, a polyketide-derived phytotoxic SM from the fungus *Ascochyta rabiei* (Kim et al., 2015). Such pathway-specific regulators may also be exploited for cluster boundary predictions. Thus, the boundaries of the BGC for azanigerone A, an azaphilone pigment from *Aspergillus niger*, were predicted using RT-PCR analysis in a strain with an activated pathway-specific positive regulator (Zabala et al., 2012). In contrast, the expression of only some key structural genes is modulated by the pathway-specific regulators for apicidin, a histone deacetylase inhibitor, fusaric acid, a mycotoxin produced by fusaria, and sterigmatocystin, a carcinogenic mycotoxin produced by aspergilli (Jeon et al., 2011; Studt et al., 2016; Wiemann et al., 2018). Finally, pathway-specific regulators may also modulate the expression of genes with no obvious function in SM biosynthesis, resistance or export, as is the case with the fusarin C BGC in *Fusarium fujikuroi* (Niehaus et al., 2013). Therefore, transcription analysis that relies solely on the differential expression of genes governed by a pathway-specific regulator to predict SM BGC boundaries may also omit important genes, or overestimate BGC size due to pleiotropic effects, or the extent of euchromatic regions.

In the current study, we determined the boundaries of the MonAzPs BGC of *Monascus ruber* M7 by an integrated approach. We compared a 100 kb stretch of the *M. ruber* M7 genome flanking the MonAzPs PKS gene *mrpigA*, to the genome sequences of eight other species of filamentous fungi. Next, we conducted a differential transcriptomic analysis of the MonAzPs BGC in *M. ruber* M7 and its knockout mutant deficient in the pathway-specific regulator MrPigB. Finally, we knocked out genes at the predicted BGC boundaries, and compared the MonAzPs metabolic profiles of the resulting strains to that of the wild-type strain. This work provides a more accurate prediction of the extent of the MonAzPs BGC in *M. ruber* M7, and by extension in other *Monascus*-type azaphilone pigment producer fungi. It also exemplifies a workflow to predict, with

[1] www.jcvi.org/smurf/

[2] http://antismash.secondarymetabolites.org

higher confidence, the boundaries of similarly complex SM BGCs in other fungi.

MATERIALS AND METHODS

Fungal Strains, Culture Conditions, and DNA Extraction

The wild-type strain *Monascus ruber* M7 (CCAM 070120, Culture Collection of the State Key Laboratory of Agricultural Microbiology, China Center for Type Culture Collection, Wuhan, China) (Chen and Hu, 2005; Liu et al., 2014; Liu J. et al., 2016; Chen et al., 2017, 2019; Li et al., 2020) and its derivatives used in this study are listed in **Table 1**. For the generation of the Δ*mrpigAup1*, Δ*mrpigAup2*, Δ*mrpigPdown1,* and Δ*mrpigPdown2* strains, initial transformants were selected on potato dextrose agar (PDA) medium containing 30 μg/mL hygromycin B (Sigma-Aldrich, Shanghai, China) at 28°C. For phenotypic characterization, all the tested strains were cultivated in triplicates on PDA plates at 28°C for 10 d. Fungal genomic DNA was isolated from mycelia grown on cellophane membranes covering PDA plates, using the cetyltrimethylammonium bromide (CTAB) method (Shao et al., 2009).

Bioinformatic Methods

The nucleotide and deduced amino acid sequences of the genomes of nine strains of filamentous fungi, including *M. ruber* M7, were retrieved from the Broad Institute[3] and GenBank[4], as shown in **Supplementary Table 1**. To predict the MonAzPs gene cluster boundaries, the predicted proteomes encoded by these genome sequences were subjected to comprehensive pairwise comparisons (Takeda et al., 2014). Briefly, pairwise similarities among the deduced proteome of *M. ruber* M7 and the other species were determined first, to detect orthologous, co-located genes that may form a BGC "seed" region ($e < 1.0e^{-10}$; gap penalty: −0.2; and mismatch penalty: −0.2; **Figures 1A,B**). In the second step, the seed region was extended and the boundaries of the extended BGC were trimmed (extension length: 35 genes; negative penalty: −0.3; **Figures 1C,D**), as previously described (Takeda et al., 2014).

[3]http://www.broadinstitute.org/scientific-community/data

[4]http://www.ncbi.nlm.nih.gov/genome/

TABLE 1 | *Monascus ruber* strains used in this study.

Strain	Parent	Genotype	References
M. ruber M7	–	Wild-type	Chen and Hu, 2005
Δ*mrpigAup2*	*M. ruber* M7	Δ*mrpigAup2*::*hph*	This study
Δ*mrpigAup1*	*M. ruber* M7	Δ*mrpigAup1*::*hph*	This study
Δ*mrpigA*	*M. ruber* M7	Δ*mrpigA*::*hph*	Xie et al., 2015
Δ*mrpigB* (Δ*pigR*)	*M. ruber* M7	Δ*mrpigB*:*hph*	Xie et al., 2013
Δ*mrpigO*	*M. ruber* M7	Δ*mrpigO*::*hph*	Chen et al., 2017
Δ*mrpigP*	*M. ruber* M7	Δ*mrpigP*::*hph*	Chen et al., 2017
Δ*mrpigPdown1*	*M. ruber* M7	Δ*mrpigPdown1*::*hph*	This study
Δ*mrpigPdown2*	*M. ruber* M7	Δ*mrpigPdown2*::*hph*	This study

100–kb sequences flanking the MonAzPs polyketide synthase MrPigA (Xie et al., 2015) in the genome of *M. ruber* M7 were submitted to antiSMASH 5.0 (Blin et al., 2019), and PRISM (Skinnider et al., 2020) for SM gene cluster characterization. The MIBiG 2.0 curated repository for SM BGCs was also considered (Kautsar et al., 2020). The SMURF[5] and CASSIS servers[6] could not be accessed, or returned uncharacterized errors. The amino acid sequences encoded by the genes were deduced using FGENESH[7], and analyzed using Pfam 27.0[8]. Similarities of the deduced amino acid sequence were analyzed using BLASTP[9].

Quantitative Reverse Transcription PCR (RT-qPCR) Analysis

The wild-type *M. ruber* M7 and the pathway-specific regulator knockout strain Δ*mrpigB* were cultured in PDB medium with shaking at 180 rpm for 6 days at 28°C (start of the active production phase for MonAzPs). RT-qPCR was performed by Wuhan Goodbio Technology Co., Ltd. (Wuhan, Hubei, China) as described by Liu et al. (2014). For both the wild-type and Δ*mrpigB* strains, three biological replicates were analyzed, and for each sample, three technical replicates for each targeted gene were performed. GADPH was used as the reference gene, and the relative expression fold-change was calculated using the comparative CT method. Significance analysis was performed using the one-way ANOVA test and significance level was set as 0.05. The used primers are listed in **Supplementary Table 2**.

Gene Knockouts

M. ruber M7 knockout strains Δ*mrpigA*, Δ*mrpigO,* and Δ*mrpigP* have been described (Xie et al., 2013, 2015; Chen et al., 2017; Li et al., 2020). For the deletion of the *mrpigAup1* gene, a gene disruption cassette carrying the hygromycin B resistance gene (*hph*) flanked by targeting arms (TA) derived from the 5′ or 3′regions of *mrpigAup1*, respectively, was prepared using the double-joint PCR method (Yu et al., 2004). Briefly, the 5′ and 3′flanking regions (910 and 893 bp, respectively) of the *mrpigAup1* gene were amplified with the primer pairs P1–P2 and P3–P4, respectively. The 2.1 kb *hph* cassette was amplified from plasmid pSKH (He et al., 2013) with the primer pair P7–P8. The PCR products were purified with a TransGen gel purification kit (TransGen, Beijing, China), the three amplicons were mixed at a 1:1:2 molar ratio, then fused by PCR using primer pair P1–P4. The fused PCR product was purified, cloned into pMD19–T (Takara, Dalian, Japan), and confirmed by sequencing. The disruption cassette was then transferred from the resulting plasmid into the *Kpn*I and *Xba*I sites of pCAMBIA3300 (He et al., 2013) to generate plasmid pCPIGAUP1. Analogous strategies were used to generate the pCPIGAUP2, pCPIGPDOWN1, and pCPIGPDOWN2 plasmids for the deletion of *mrpigAup2*, *mrpigPdown1,* and *mrpigPdown2*, respectively, using primers listed in **Supplementary Table 3**.

[5]http://smurf.jcvi.org

[6]https://sbi.hki-jena.de/cassis/

[7]http://linux1.softberry.com/berry.phtml

[8]http://pfam.sanger.ac.uk/

[9]http://blast.ncbi.nlm.nih.gov/Blast.cgi

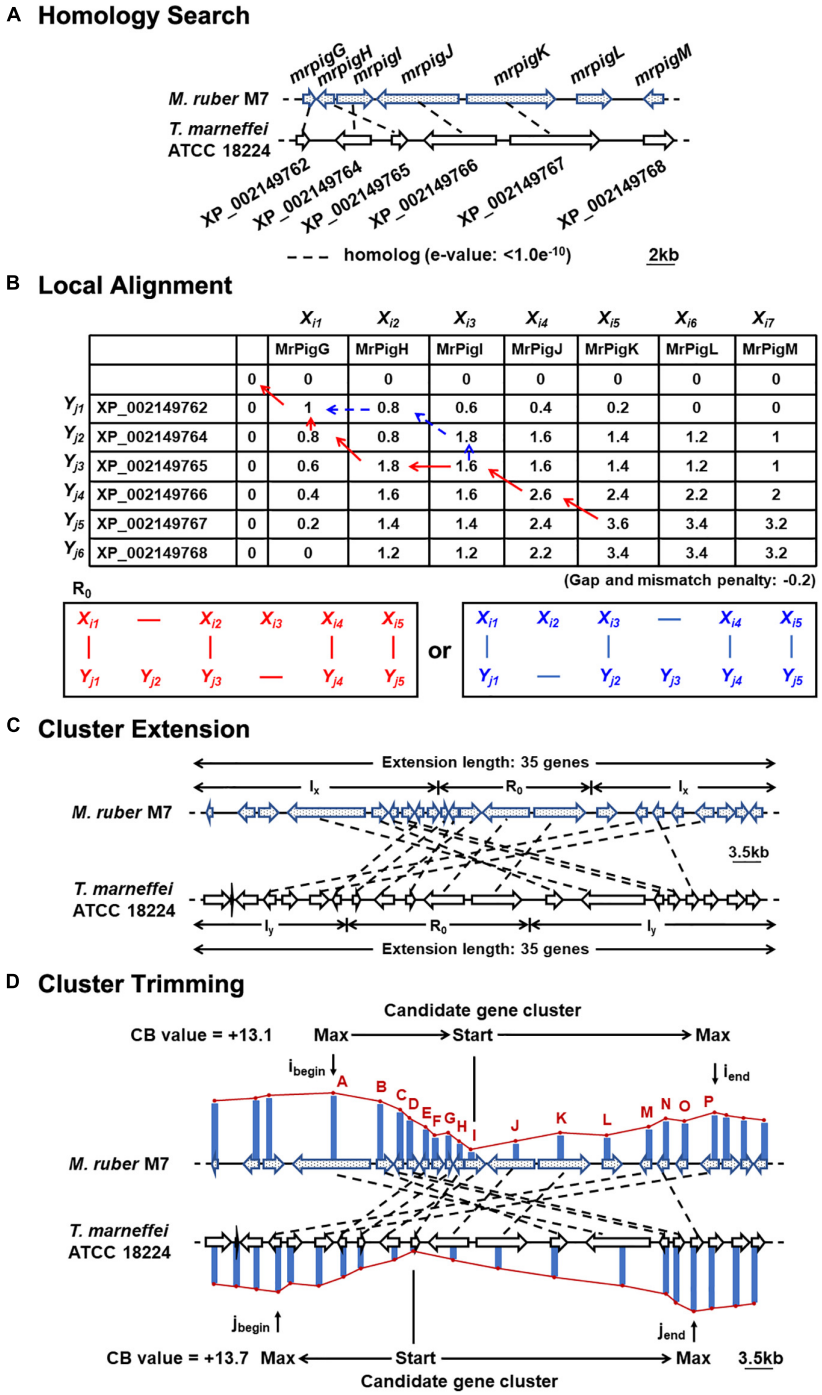

			X_{i1} MrPigG	X_{i2} MrPigH	X_{i3} MrPigI	X_{i4} MrPigJ	X_{i5} MrPigK	X_{i6} MrPigL	X_{i7} MrPigM
		0	0	0	0	0	0	0	0
Y_{j1}	XP_002149762	0	1	0.8	0.6	0.4	0.2	0	0
Y_{j2}	XP_002149764	0	0.8	0.8	1.8	1.6	1.4	1.2	1
Y_{j3}	XP_002149765	0	0.6	1.8	1.6	1.6	1.4	1.2	1
Y_{j4}	XP_002149766	0	0.4	1.6	1.6	2.6	2.4	2.2	2
Y_{j5}	XP_002149767	0	0.2	1.4	1.4	2.4	3.6	3.4	3.2
Y_{j6}	XP_002149768	0	0	1.2	1.2	2.2	3.4	3.4	3.2

FIGURE 1 | Motif-independent comparative genomic prediction of the MonAzPs BGC boundaries. **(A)** Homology search against the deduced proteome of *T. marneffei* ATCC 18224 using the MonAzPs biosynthesis-related proteins of *M. ruber* M7 as the bait. *Dashed lines*, gene pairs encoding homologous proteins ($e < 1.0e^{-10}$ for the encoded proteins). Due to mis-annotation, XP_002149763 is described in NCBI as a separate gene; however, this nucleotide sequence is in fact part of the XP_002149764 gene. **(B)** Local protein sequence alignment using the Smith-Waterman algorithm. Pairs of contiguous genes encoding MrPigG to MrPigK in *M. ruber* M7 and from XP_002149762 to XP_002149767 in *T. marneffei* ATCC 18224 form the seed region (R_0) for predicting the MonAzPs BGC. SW scores shown were calculated as described (Takeda et al., 2014). **(C)** Extension of the gene cluster. The seed region (R_0) was extended to include a total of 35 genes (Takeda et al., 2014). The symbols l_x and l_y represent the stretches of genes added to the seed region in the *M. ruber* M7 and the *T. marneffei* ATCC 18224 genomes, respectively. **(D)** Trimming of the BGC boundaries. i_{begin} and i_{end}, the locations of the genes at the beginning and end, respectively, of the MonAzPs gene cluster in *M. ruber* M7; j_{begin} and j_{end}, the corresponding gene locations in *T. marneffei* ATCC 18224. *CB values* are the maximum cumulative SW scores of the predicted BGCs with the upstream and the downstream boundaries indicated (Takeda et al., 2014).

The gene disruption plasmids were individually transformed into *Agrobacterium tumefaciens* EHA105 (Hood et al., 1993) using the freeze-thaw method (Yu et al., 2003), and used for the transformation of *M. ruber* M7 to yield the gene knockout strains Δ*mrpigAup1*, Δ*mrpigAup2*, Δ*mrpigPdown1,* and Δ*mrpigPdown2*, using methods described previously (Shao et al., 2009; Wang et al., 2011). Gene knockouts and the absence of the wild-type allele in the mutants were confirmed by PCR and end sequencing of the resulting amplicons.

MonAzPs Analysis

Freshly harvested spores (5×10^4) of representative isolates of the gene knockout strains, Δ*mrpigAup1*, Δ*mrpigAup2*, Δ*mrpigA*, Δ*mrpigO*, Δ*mrpigP*, Δ*mrpigPdown1*, Δ*mrpigPdown2*, and the wild-type strain *M. ruber* M7 were spread on cellophane membranes on PDA plates, and cultivated at 28°C for 10 days. The mycelia were harvested by scraping from the membranes, freeze-dried, and ground in a mortar with a pestle under liquid nitrogen. The mycelia powder (0.05 g) was suspended in 1.5 mL methanol, incubated at 65°C for 1 h, then centrifuged at 10,000 × g for 10 min to collect the supernatant for analysis. HPLC was performed following the method described by Liu Q. et al. (2016) on a Waters system fitted with an Inertsil ODS–3 C18 column (250 × 4.6 mm, 5.0 μm, GL Sciences). The mobile phases consisted of water (A), acetonitrile (B), and 0.5% phosphoric acid in water (C). The flow rate was kept at 0.8 mL/min. The system was run with the following gradient program: from 40 to 30% A for 3 min, from 30 to 5% A for 22 min, 5% A for 5 min, from 5 to 40% A for 1 min, and 40% A for 5 min. C was kept constant at 5% throughout the program. Absorbance was monitored with a 2487 UV/Vis Detector (Waters) at 190- to 700-nm wavelength. Metabolites were identified based on comparison to authentic standards (Chen et al., 2017, 2019).

Accession Numbers

The genes *mrpigAup1*, *mrpigAup2*, *mrpigPdown1,* and *mrpigPdown2* of *M. ruber* M7 have been assigned GenBank accessions MH729876, MW557663, KC561931, and MW557664, respectively.

RESULTS

Bioinformatic Prediction of the MonAzPs BGC Boundaries

MonAzPs BGCs display two characteristically different architectures in the sequenced genomes of *Monascus* spp. (Chen et al., 2017). In *M. ruber* M7 and *M. purpureus* strains NRRL 1596 and YY–1, the MonAzPs cluster is interrupted by the *pigL* gene that encodes an ankyrin repeat protein with no discernible function in MonAzPs biosynthesis (**Figure 2A**; Chen et al., 2017). In *M. ruber* NRLL 1597 and *M. pilosus*, the *pigL* gene is replaced by a six-gene sub-cluster encoding proteins with putative transport or regulatory functions, but none of these proteins are predicted to be necessary for MonAzPs biosynthesis (Balakrishnan et al., 2014a; Chen et al., 2017). Since the insertion of this six-gene sub-cluster would easily confuse bioinformatic methods for BGC boundary prediction, we concentrated on the near-identical genomic loci of the *M. ruber* M7 and the *M. purpureus* strains.

The MonAzPs BGC in *M. purpureus* was originally delineated by Balakrishnan et al. (2014a) by manually comparing *Monascus* spp. genomic loci, and described to include 21 genes over 60 kb, extending from *mpp–1* (ortholog of *mrpigAup1* in *M. ruber* M7) to *mpp–14* (ortholog of *mrpigPdown4* in M7) (**Figure 2A**). The MIBiG (Minimum Information about a Biosynthetic Gene Cluster, Kautsar et al., 2020), a curated repository of BGCs, describes the *M. pilosus* MonAzPs cluster to extend from AGN71602 to AGN71625, corresponding to *mrpigAup2* to *mrpigP* on the *M. ruber* M7 genome, but inclusive of the six-gene sub-cluster with no role in MonAzPs biosynthesis (**Figure 2A**). In contrast, antiSMASH (Blin et al., 2019), the computational method most frequently used to define SM BGCs, delineated the cluster to include only 11 genes (*mrpigAup2* to *mrpigI*), spanning approximately 30 kb in the *M. ruber* M7 or the two *M. purpureus* genomes (**Figure 2A**). PRISM (Skinnider et al., 2020), another SM BGC prediction tool[10], identified only *mrpigA* as the sole constituent of the cluster. Unfortunately, neither SMURF (Khaldi et al., 2010) nor CASSIS (Wolf et al., 2016) provided useful output for our comparisons, due to persistent problems with the webservers. Considering these radically different cluster boundary predictions, we sought a more definite workflow to delimit the complex MonAzPs BGC.

To do this, we first considered the motif-independent comparative genomics method described by Takeda et al. (2014). In a preliminary step, we compared a 100-kb stretch bracketing the MonAzPs polyketide synthase *mrpigA* (Xie et al., 2015) on the *M. ruber* M7 genome with the genome sequences of eight other species of filamentous fungi from the Eurotiales order (**Supplementary Table 1**). We have not included the genomes of other *Monascus* spp. in this comparison, considering that the extended MonAzPs loci in these genomes are syntenic apart from the presence of *pigL* vs. the six-gene sub-cluster, and that the encoded protein sequences are near-identical (95–100% identity) (Chen et al., 2017). Thus, these loci would have furnished no useful information for our analysis. The preliminary comparison of the *M. ruber* M7 genes identified the highest similarities to the genome of *Talaromyces (Penicillium) marneffei* ATCC 18224, a thermally dimorphic opportunistic fungal pathogen endemic in Southeast Asia and associated with immunocompromised individuals. Thus, we used the genome sequence of this fungus as the comparator for our subsequent analysis. Using the optimized parameters (Takeda et al., 2014), we assigned the seed region (R_0) of the MonAzPs cluster to include *mrpigG* to *mrpigK* (XP_002149762 to XP_002149767 in the *T. marneffei* ATCC 18224 genome, **Figures 1A,B**). To extend the seed region, 15 genes bracketing R_0 were added to each end (regions I_x, **Figure 1C**), yielding a 35–gene candidate BGC (Takeda et al., 2014). Finally, the boundaries of the candidate cluster were trimmed at both ends, based on the local maxima of the combined scores for the member genes (**Figure 1D**). This analysis predicted

[10]https://prism.adapsyn.com/

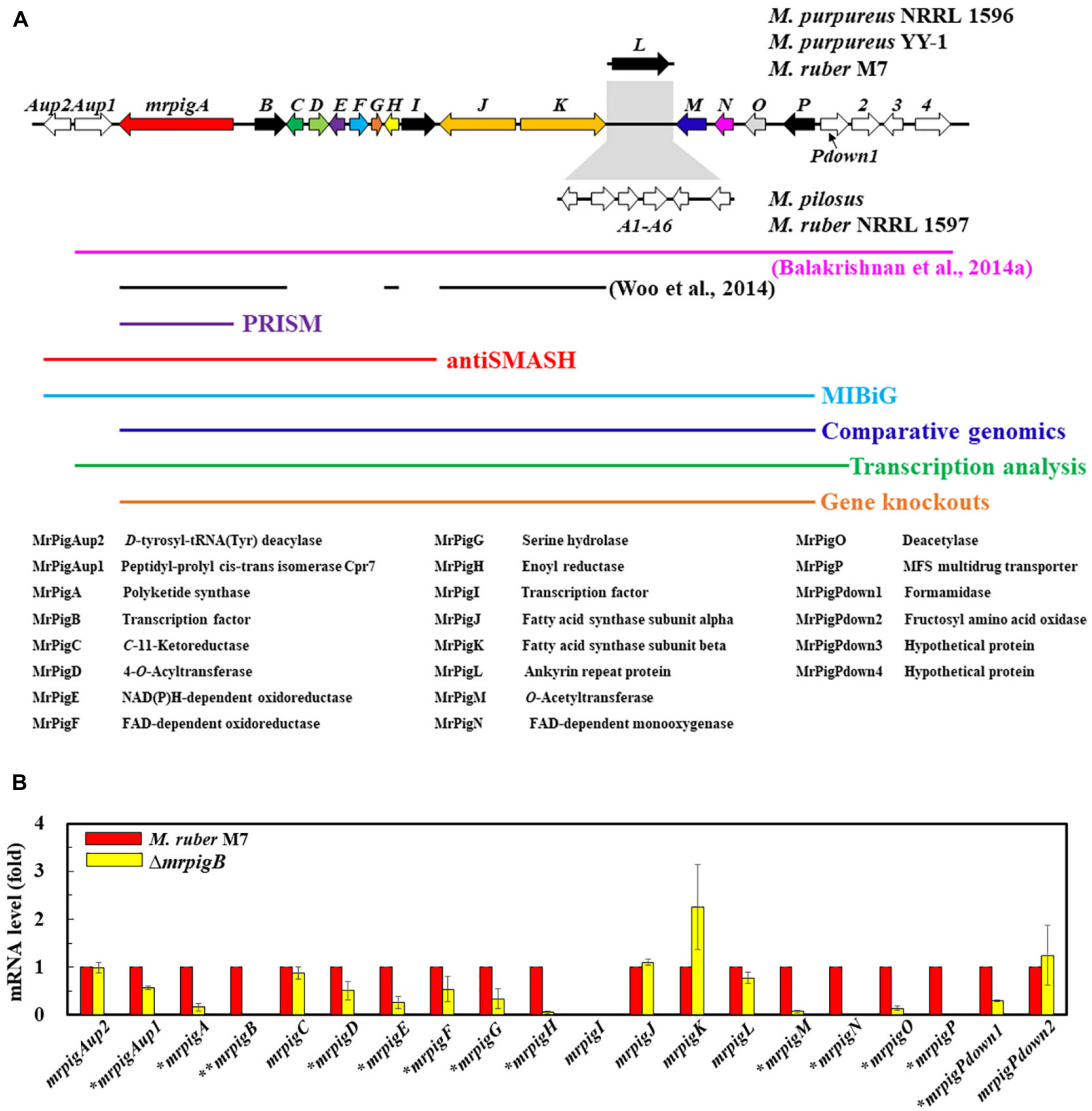

FIGURE 2 | Bioinformatic and transcriptomic analysis of the MonAzPs BGC. **(A)** Gene map of the MonAzPs locus and the extent of the MonAzPs BGC in different fungi according to different authors and different bioinformatic or experimental assignment methods. The predicted functions of the proteins encoded in the MonAzPs locus are also listed. **(B)** RT-qPCR analysis of the genes in the MonAzPs locus of the wild-type *M. ruber* M7 strain and its Δ*mrpigB* derivative, measured under identical cultication conditions. Gene expression levels in the wild-type M7 strain are taken as the basis of comparison, with the means and standard deviation calculated from measurements in three biological replicates for each strain. Statistically significant differences ($p < 0.05$) in expression levels are indicated by *stars*.

that the MonAzPs BGC extends from *mrpigA* to *mrpigP* in the *M. ruber* M7 genome (**Figure 2A**).

Transcriptional Analysis of the MonAzPs Locus in *M. ruber* M7

Analysis of mutants of the pathway-specific $Zn(II)_2Cys_6$ regulators has proven to be useful in demarcating the ends of SM BGCs (Zabala et al., 2012; Wiemann et al., 2013a). In *M. ruber* M7, MonAzPs biosynthesis is governed by the pathway-specific regulator MrPigB (PigR1 in *M. pilosus*) (Balakrishnan et al., 2013; Xie et al., 2013). To substantiate the bioinformatic prediction of the boundaries of the MonAzPs BGC, we used quantitative reverse transcription PCR (RT-qPCR) to compare the transcription levels of the 20 genes flanking *mrpigA* (i.e., *mrpigAup2* to *mrpigPdown2*) at the start of MonAzPs accumulation in the wild-type *M. ruber* M7 with those of the same genes in the Δ*mrpigB* mutant. As shown in **Figure 2B**, all these genes were expressed in the wild-type strain, apart from *mrpigI* that encodes a transcription factor with no apparent role in MonAzPs biosynthesis (Chen et al., 2017). The expression of *mrpigAup2* and *mrpigPdown2*, the two genes at the edges of the MonAzPs locus were not affected by the deletion of *mrpigB*, indicating that these genes may lay outside the boundaries of the BGC, as expected from the comparative genomic analysis (**Figure 1**). The expression of six MonAzPs genes (*mrpigA*,

mrpigH, and *mrpigM-mrpigP*) was almost completely abolished in the Δ*mrpigB* strain, as observed earlier (Li et al., 2020). The transcription of a further six genes was also moderately downregulated ($p < 0.05$). These included *mrpigD-mrpigE*, all with established roles in MonAzPs biosynthesis. However, the expression of *mrpigAup1* and *mrpigPdown1* were also significantly reduced in the Δ*mrpigB* strain, indicating that the transcription of these genes with no known roles in MonAzPs biosynthesis is, nevertheless, activated by MrPigB (**Figure 2B**). These two genes were predicted to lay outside the MonAzPs BGC by comparative genomic analysis (**Figure 1**).

The transcriptional analysis is further complicated by the fact that the expression of four genes well inside the MonAzPs locus (*mrpigC*, *mrpigJ*, *mrpigK,* and *mrpigL*) were not affected by the deletion of *mrpigB*. Among these, the putative ankyrin repeat protein MrPigL plays no role in the production of MonAzPs (Chen et al., 2017). However, *mrpigC* encodes the C11–ketoreductase, *mrpigJ,* and *mrpigK* encode the two subunits of the fatty acid synthase that are all necessary for MonAzPs biosynthesis (Chen et al., 2017). Thus, while *mrpigC*, *mrpigJ,* and *mrpigK* must be part of the MonAzPs BGC, their expression is not directly controlled by MrPigB—a consequence of the complex, mosaic-like structure of this BGC (Li et al., 2020).

Combining the comparative genomic prediction with the transcriptomic analysis, *mrpigAup2,* and *mrpigPdown2* are not likely to be part of the MonAzPs BGC, while the cluster can be confidently predicted to extend at least from *mrpigA* to *mrpigP*. However, the status of *mrpigAup1* and *mrpigPdown1* remains ambiguous in light of the disagreement of the bioinformatic prediction and the transcription data (**Figure 1** vs. **Figure 2**).

Knockout of the Genes at the Predicted Boundaries of the MonAzPs BGC

Since the comparative genomic and transcriptomic analyses still did not provide a definitive answer to the extent of the MonAzPs BGC, we sought additional functional proof for the roles of the genes at the proposed BGC boundaries. Thus, we created four new gene knockout strains, affecting the genes that lay at/beyond the border of the MonAzPs BGC in *M. ruber* M7. Five hygromycin B resistant, putative *mrpigPdown2* knockout isolates were obtained by ATMT (*Agrobacterium tumefaciens*-mediated transformation). The putative disruptants and the wild-type control were characterized by PCR analysis, using primer pairs specific for the *hygR* transgene (P7–P8); the *mrpigPdown2* target gene (P25–P26); the gene replacement cassette (P21–P24); and the gene replacement locus (P33–P8 and P7–P34, **Figure 3**). All five putative disruptants yielded amplicons whose sizes and nucleotide sequences were consistent with the integration of the *hygR* gene into the targeted locus. At the same time, these isolates failed to provide amplicons specific for the target gene, consistent with the loss of *mrpigPdown2* from the genome. The gene knockouts were validated using analogous procedures for the *mrpigAup1* (six verified isolates; **Supplementary Figure 1**), *mrpigAup2* (two verified isolates; **Supplementary Figure 2**), and the *mrpigPdown1* genes (three verified isolates; **Supplementary Figure 3**).

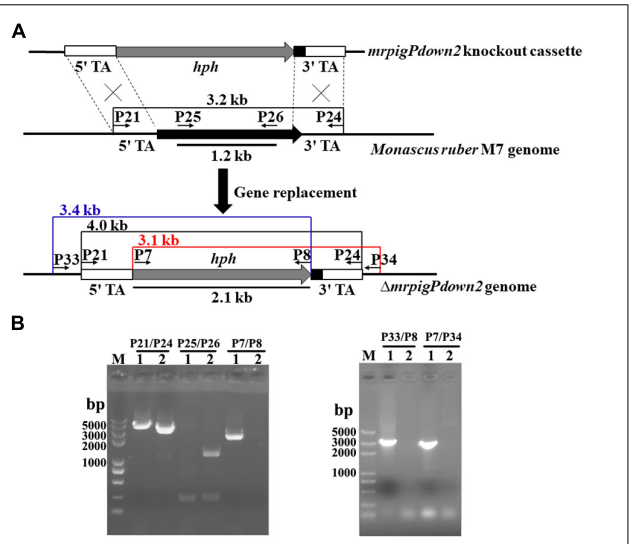

FIGURE 3 | Knockout of the *mrpigPdown2* gene in *M. ruber* M7. **(A)** Schematic representation of the gene knockout strategy yielding the Δ*mrpigPdown2* strain. The primers, and the sizes of the corresponding PCR amplicons used to verify the gene knockout event are indicated. **(B)** Confirmation of the gene deletion event using PCR. *Lane 1*, a representative isolate of the Δ*mrpigPdown2* strain; *Lane 2*, the wild-type strain *M. ruber* M7.

Phenotypic and MonAzPs Production Analysis Confirms the BGC Boundaries

We cultivated the wild-type strain *M. ruber* M7 and representative isolates of the knockout strains Δ*mrpigAup1*, Δ*mrpigAup2*, Δ*mrpigPdown1*, and Δ*mrpigPdown2* together with the previously isolated disruptant strains Δ*mrpigA*, Δ*mrpigO*, Δ*mrpigP*, and analyzed their colony phenotypes and MonAzPs production (**Figure 4**). The wild-type *M. ruber* M7 strain is able to produce several major MonAzPs congeners (Chen et al., 2017). Its product spectrum is determined by the culture conditions, including the ingredients of the culture media and the cultivation time. The growth of strain M7 on PDA plates at 28°C for 10 days afforded colonies of an intense orange color, corresponding to the production of four well-known MonAzPs: two yellow pigments (monascin **1** and ankaflavin **3**) and two orange pigments (rubropunctatin **2** and monascorubrin **4**, **Figure 4**). Compared to the wild-type strain, no gross differences in colony growth, morphology, or coloration were observed upon the deletion of the *mrpigAup1* and *mrpigAup2* genes at the "left" border, and with the knockout of the *mrpigPdown1* and *mrpigPdown2* genes at the "right" border. The production of MonAzPs was also unchanged with these strains, with the yields and mutual ratios of compounds **1**, **2**, **3,** and **4** indistinguishable from those of the wild-type strain (**Figure 4**). These results confirm that *mrpigAup2* and *mrpigPdown2* are not part of the MonAzPs BGC, in agreement with the comparative genomic and transcriptional analyses (**Figures 1**, **2**). However, these results also show that *mrpigAup1* and *mrpigPdown1* do not play discernible roles in MonAzPs biosynthesis and thus should not

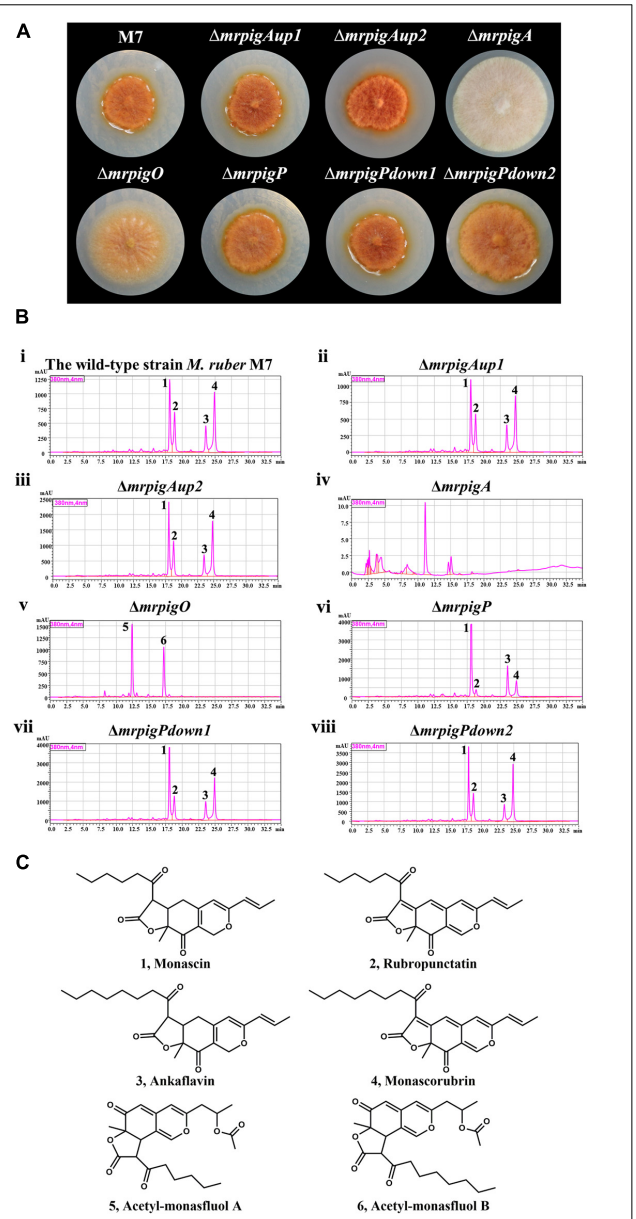

FIGURE 4 | Colony morphology and MonAzPs production of *M. ruber* strains. **(A)** Representative colonies of the indicated *M. ruber* strains, grown at 28°C for 10 d on PDA plates. **(B)** HPLC traces (PDA, 380 nm) of crude extracts of the cultures of the indicated strains. Unlabeled peaks are unidentified *M. ruber* metabolites not related to MonAzPs. **(C)** Structures of MonAzPs.

be considered to be part of the MonAzPs BGC, in spite of the contrary prediction from the transcriptional analysis (**Figure 2**).

In contrast, the Δ*mrpigA* and Δ*mrpigO* strains exhibited significantly different phenotypes and MonAzPs production profiles, compared to that of *M. ruber* M7. The colonies of Δ*mrpigA*, with the deletion affecting this gene at the "left" border of the cluster, were off-white with the production of all MonAzPs completely abolished. This is in agreement with the crucial role of the MrPigA PKS in the formation of the polyketide core of all MoAzPs in this fungus. The colonies of the Δ*mrpigO* strain, with the knockout eliminating the second gene from the "right" border of the predicted BGC, were yellow to pale orange. This strain produced two known MonAzPs derailment products, the yellow pigments acetyl-monasfluol A and B (compounds **5** and **6**; Chen et al., 2019, **Figure 4C**). This is consistent with MrPigO being a deacetylase, and emphasizes the central role of this enzyme in favoring the appropriate intramolecular Knoevenagel cyclization that yields MonAzPs congeners with the characteristic linear tricyclic ring system, instead of the angular system seen in shunt products **5** and **6** (Chen et al., 2019). The phenotype of the Δ*mrpigP* strain, with the deletion affecting this gene at the "right" border of the cluster, was similar to that of *M. ruber* M7. The Δ*mrpigP* strain produced large amounts of MonAzPs, although with a shift in the product ratios toward monascin **1** and ankaflavin **3**. MrPigP is an MFS transporter with a role in the export of monasones, the naphthoquinone co-metabolites of this supercluster (Li et al., 2020). However, deletion of this gene was seen earlier not to influence MonAzPs production in liquid media (Li et al., 2020), so this transporter plays, at best, a supplementary part in azaphilone pigment production.

Taken together, our comparative genomic, differential transcriptomic, and gene knockout data predict that the MonAzPs BGC of *M. ruber* M7 extends from *mrpigA* to *mrpigP*, with *mrpigAup1*, *mrpigAup2*, *mrpigPdown1,* and *mrpigPdown2* laying just outside the borders of the cluster.

Bioinformatic Analysis of the Azaphilone Gene Cluster in *T. marneffei*

The gene cluster in *T. marneffei* ATCC 18224 that we took advantage of to predict the boundaries of the MonAzPs BGC in *M. ruber* M7 is nearly identical to a genomic locus in *T. marneffei* PM1. This locus in strain PM1 was described to contain a 5–gene BGC responsible for the production of a variety of soluble red-colored *Monascus*-type azaphilone pigments (Woo et al., 2014). These compounds are γ-vinylogous pyridines that are produced when the orange azaphilone pigments, rubropunctatin **2,** and monascorubrin **4** form adducts to effect an *O*-to-*N* substitution with various amines, including amino acids from the cell or the media. The same BGC was also described to be responsible for the biosynthesis of yellow azaphilone pigments such as ankaflavin **3** in strain PM1, as expected (Woo et al., 2014).

Comparison of the *M. ruber* M7 MonAzPs BGC with the genome sequences of *T. marneffei* ATCC 18224 and PM1 showed that most MonAzPs biosynthetic genes are conserved and localized in a single locus in the two *Talaromyces* genomes (**Supplementary Table 4**), although these pigment BGCs in *Monascus* vs. the two *T. marneffei* strains are not syntenic. Genes similar to *mrpigF* and *mrpigO* of *M. ruber* M7 are encoded outside of the *T. marneffei* BGCs, while orthologs of the ankyrin repeat protein-encoding *mrpigL* are not immediately obvious, nor are they necessary for azaphilone pigment biosynthesis.

We propose that the apparent *Monascus*-type azaphilone BGC in *T. marneffei* ATCC 18224 includes the genes XP_002149758 to XP_002149772 (corresponding to KFX40792 to KFX45538 in strain PM1, **Supplementary Table 4**). Together with the

additional MonAzPs gene homologs that are outside the BGCs in the *Talaromyces* genomes, this cluster is the functional equivalent of the MonAzPs BGC of *M. ruber* M7 (**Supplementary Table 4**, Woo et al., 2014; Chen et al., 2019). Importantly, our model for the *Talaromyces* BGCs includes a much more extensive genomic region than the originally delineated five-gene cluster (Woo et al., 2014), again highlighting the difficulties of boundary predictions for complex BGCs in fungi. Functional verification of this more extensive BGC using transcriptomic and gene knockout studies is still necessary to clarify the biosynthesis of *Monascus*-type azaphilone pigments in the two *Talaromyces* strains.

DISCUSSION

A significant aspect of fungal development is the production of SMs that serve as allelochemicals, pigments, intra- and interspecies signaling compounds and modulators of metabolic processes. Many of these molecules display a broad range of antibiotic, antitumor, enzyme modulatory, and immunosuppressive activities that can be exploited for drug discovery and development (Hyde et al., 2019). Advances in genomics revealed that the genes necessary for the production of a given SM are typically (although not always) clustered on the fungal genome (Weber et al., 2009). Such BGCs encode core enzymes for SM scaffold biosynthesis; modifying enzymes for scaffold editing, complexity generation, and SM maturation; and transcription factors, self-resistance, and SM export mediators (Keller, 2019).

Traditionally, SM BGCs are detected in genome sequence assemblies by identifying the core genes (such as PKSs, NRPSs, or terpene synthases), based on their conserved sequence motifs. Next, the putative BGCs are extended by recruiting flanking genes that are similar to genes frequently found in known SM BGCs, including those that encode hydroxylases, oxidases, methyltransferases, transcription factors, and transporters (Keller, 2019). This process is often facilitated by specialized software tools, such as SMURF, antiSMASH, CASSIS, or Prism, and may utilize curated repositories such as MIBiG (Khaldi et al., 2010; Wolf et al., 2016; Blin et al., 2019; Kautsar et al., 2020; Skinnider et al., 2020). While this workflow met with spectacular success in the last two decades (Khaldi and Wolfe, 2011; Wiemann et al., 2013b; Leadmon et al., 2020), SM BGCs without core genes remain difficult to detect, and cluster boundaries usually remain provisional or even arbitrary. The MonAzPs BGC is a prime example for the latter problem: different prediction methods and different authors delimited this cluster with widely different boundaries (**Figure 2A**), despite the availability of multiple genome sequences from several MonAzPs-producing fungi, mostly *Monascus* spp.

We decided to investigate this problem by cross-referencing a motif-independent, comparative genomics-based BGC prediction method (Takeda et al., 2014) with differential transcriptional analysis in a cluster-specific regulator mutant, and gene knockouts followed by the analysis of MonAzPs production by the resulting strains. These approaches collectively defined the MonAzPs BGC of *M. ruber* M7 to extend from *mrpigA* to *mrpigP*, encompassing 16 genes. This assignment, supported by multiple lines of experimental evidence, offers a more secure basis for the retrobiosynthetic analysis of MonAzPs production, and provides a better focus for engineering approaches toward designer *Monascus*-type azaphilone pigments that may be useful to produce nutraceuticals, food and feed products, and specialty chemicals (Tolborg et al., 2020). Additional transcriptional studies utilizing different cultivation conditions may further refine BGC border assignments.

The BGC responsible for MonAzPs production in *Talaromyces (Penicillium) marneffei* ATCC 18224 was also provisionally delimited during our comparative genomics process (**Figure 1**). *T. marneffei* was reported to produce MonAzPs-type soluble red pigments (Ogihara et al., 2000, 2001; Frisvad et al., 2013; Arai et al., 2015; Jin et al., 2018; Morales-Oyervides et al., 2020; Tolborg et al., 2020), and accordingly, orthologs of most of the *M. ruber* M7 MonAzPs biosynthetic genes were found to be encoded in the *T. marneffei* ATCC 18224 BGC, albeit in a non-syntenic arrangement (Chen et al., 2017, 2019; Pavesi et al., 2021). While the genes corresponding to *mrpigF*, *mrpigO,* and *mrpigL* were absent from the *T. marneffei* BGC, similar genes to *mrpigF* and *mrpigO* are encoded elsewhere in the genome of this fungus (**Supplementary Table 4**), and a *mrpigL* equivalent is not necessary for azaphilone pigment biosynthesis. Functional studies with a near-identical genomic locus in *T. marneffei* strain PM1 have been reported by Woo et al. (2014). Surprisingly, the knockdown of only five genes of this locus was shown to lead to the loss of *Monascus*-type azaphilone pigment production. Correspondingly, only *pks3* (66% identity to *mrpigA*), *rp1* (46% identity to *mrpigB*), *rp2* (58% identity to *mrpigK*), *rp3* (58% identity to *mrpigJ*), and *rp4* (65% identity to *mrpigH*) were annotated as constituents of the *Monascus*-type azaphilone BGC in *T. marneffei* PM1. Further research is necessary to reveal why the knockdown of genes *orf3* (65% identity to *mrpigN*), *orf4* (63% identity to *mrpigD*), *orf5* (70% identity to *mrpigC*), *orf7* (71% identity to *mrpigG*), *orf8* (70% identity to *mrpigE*), or *orf9* (57% identity to *mrpigP*) were seen to be neutral for pigment biosynthesis in *T. marneffei* PM1 when the knockout of the orthologous genes in *M. ruber* M7 eliminates or at least severely reduces the production of the classical MonAzPs **1–4** (Liu et al., 2014; Woo et al., 2014; Chen et al., 2017). In addition, gene knockdown experiments in *T. marneffei* PM1, targeting *pks3* (XP_002149769 in strain ATCC 18224, the ortholog of the *mrpigA* PKS), and *rp1* (XP_002149768 in strain ATCC 18224, the ortholog of *mrpigB*, encoding a transcriptional regulator) seem to also connect the BGC in strain PM1 to the production of citrinin, a mycotoxin with a similar but not identical chromophore to that of MonAzPs (Woo et al., 2014). Importantly, citrinin biosynthesis is governed in *Monascus* spp. by a BGC different from the one for MonAzPs (He and Cox, 2016), necessitating the further evaluation of the proposed connection of the *T. marneffei* PM1 BGC (and its equivalent in strain ATCC 18224) to citrinin biosynthesis. Integration of further bioinformatic, transcriptomic, gene knockdown/gene knockout, gene overexpression, and metabolite analyses, as described here for the MonAzPs BGC of *M. ruber* M7, is expected to answer such outstanding questions.

The MonAzPs BGC represents an especially tough challenge for cluster boundary prediction. This is because of the composite, mosaic-like nature of this BGC. First, it is a supercluster with genes necessary to produce two structurally different SM groups: MonAzPs-type azaphilones and monasone-type naphthoquinones (Li et al., 2020). Some genes are involved solely in the biosynthesis of one or the other SM group, while others are necessary for both. Next, MonAzPs production itself is highly complex, with many metabolic branch points opening up shunt pathways, and integrating fortuitous enzymatic and chemical reactions that afford a huge variety of pigment products (Chen et al., 2019). Last, this BGC also straddles genes or even sub-clusters (such as the six-gene sub-cluster in *M. pilosus* and *M. ruber* NRRL 1597) with no relationship to the production of MonAzPs or monasones (Balakrishnan et al., 2013; Chen et al., 2017). Any and all of these characteristics could easily confuse BGC border prediction methods that rely on one type of dataset. Thus, during the trimming step of the comparative genomics-based prediction (Takeda et al., 2014), the calculated scores at *mrpigG*, *mrpigK,* and *mrpigN* all showed inflection points (**Figure 1D**), potentially misleading a user to call the end of the MonAzPs BGC at any of these genes. When analyzing differential trascriptomic data by comparing the wild-type and the Δ*mrpigB* strains, the expression levels of the *mrpigC*, *mrpigJ*, *mrpigK,* or *mrpigL* genes were not significantly downregulated in the strain that is deficient in the cluster-specific regulator (**Figure 2B**). This could have been taken as a sure sign that the end of the BGC was already reached. Conversely, although both the *mrpigAup1* (at the left border) and the *mrpigPdown1* gene (at the right border) were found to be downregulated in Δ*mrpigB* strains (**Figure 2B**), neither comparative genomics nor gene knockouts support the inclusion of these genes in the MonAzPs BGC (**Figures 1**, **4**). Finally, gene disruption of *mrpigL*, a gene well within the BGC boundaries, does not affect the production of MonAzPs (Chen et al., 2017), again giving a false signal for reaching the end of the BGC. Based on these and similar examples, we believe that only the integration of all three methods used in this study (comparative genomics, differential transcriptomics, and gene deletion with subsequent metabolite analysis) could adequately identify BGC borders in fungi, at least in the case of highly complex clusters such as the one for MonAzPs production.

DATA AVAILABILITY STATEMENT

The datasets presented in this study can be found in online repositories. The names of the repository/repositories and accession number(s) can be found in the article/ **Supplementary Material**.

AUTHOR CONTRIBUTIONS

QL designed and performed the experiment, contributed to data analysis, and wrote the draft manuscript. SZ, XW, and SG contributed to bioinformatic analysis. XY and FC contributed to manuscript editing. IM designed the project, analyzed the data, and wrote and edited the manuscript. All authors have read and approved the manuscript prior to submission.

FUNDING

This research was supported by the National Natural Science Foundation of China (22007102 to QL), the Hubei Provincial Natural Science Foundation of China (2020CFB157 to QL), the Fundamental Research Funds for the Central Universities, South-Central University for Nationalities (YZZ19007 to QL), the USDA National Institute of Food and Agriculture Hatch project (1020652 to IM), the Higher Education Institutional Excellence Program of the Ministry of Human Capacities in Hungary (NKFIH-1150-6/2019 to IM), the U.S. National Institutes of Health (NIGMS 5R01GM114418 to IM), the National Key Research and Development Program of China (2018YFD0400404 to FC), the Major Program of the National Natural Science Foundation of China (31730068 and 31330059 to FC), and the Shandong Province Taishan Industry Leading Talents High-Efficiency Agriculture Innovation Project (tscy20180120 to FC).

SUPPLEMENTARY MATERIAL

The Supplementary Material for this article can be found online at: https://www.frontiersin.org/articles/10.3389/fmicb.2021.680629/full#supplementary-material

REFERENCES

Akihisa, T., Tokuda, H., Ukiya, M., Kiyota, A., Yasukawa, K., Sakamoto, N., et al. (2005). Anti-tumor-initiating effects of monascin, an azaphilonoid pigment from the extract of *Monascus pilosus* fermented rice (red-mold rice). *Chem. Biodivers.* 2, 1305–1309. doi: 10.1002/cbdv.200590101

Arai, T., Kojima, R., Motegi, Y., Kato, J., Kasumi, T., and Ogihara, J. (2015). PP-O and PP-V, *Monascus* pigment homologues, production, and phylogenetic analysis in *Penicillium purpurogenum*. *Fungal Biol.* 119, 1226–1236. doi: 10.1016/j.funbio.2015.08.020

Balakrishnan, B., Chandran, R., Park, S.-H., and Kwon, H.-J. (2015). A new protein factor in the product formation of non-reducing fungal polyketide synthase with a C-terminus reductive domain. *J. Microbiol. Biotechnol.* 25, 1648–1652. doi: 10.4014/jmb.1504.04086

Balakrishnan, B., Chen, C.-C., Pan, T.-M., and Kwon, H.-J. (2014a). Mpp7 controls regioselective Knoevenagel condensation during the biosynthesis of *Monascus* azaphilone pigments. *Tetrahedron Lett.* 55, 1640–1643. doi: 10.1016/j.tetlet.2014.01.090

Balakrishnan, B., Karki, S., Chiu, S.-H., Kim, H.-J., Suh, J.-W., Nam, B., et al. (2013). Genetic localization and in vivo characterization of a *Monascus* azaphilone pigment biosynthetic gene cluster. *Appl. Microbiol. Biotechnol.* 97, 6337–6345. doi: 10.1007/s00253-013-4745-9

Balakrishnan, B., Kim, H.-J., Suh, J.-W., Chen, C.-C., Liu, K.-H., Park, S.-H., et al. (2014b). *Monascus* azaphilone pigment biosynthesis employs a dedicated fatty acid synthase for short chain fatty acyl moieties. *J. Korean Soc. Appl. Biol. Chem.* 57, 191–196. doi: 10.1007/s13765-014-4017-0

Balakrishnan, B., Lim, Y. J., Hwang, S. H., Lee, D. W., Park, S.-H., and Kwon, H.-J. (2017a). Selective production of red azaphilone pigments in a *Monascus*

purpureus mppDEG deletion mutant. *J. Appl. Biol. Chem.* 60, 249–256. doi: 10.3839/jabc.2017.040

Balakrishnan, B., Park, S.-H., and Kwon, H.-J. (2017b). A reductase gene *mppE* controls yellow component production in azaphilone polyketide pathway of *Monascus*. *Biotechnol. Lett.* 39, 163–169. doi: 10.1007/s10529-016-2232-y

Balakrishnan, B., Park, S.-H., and Kwon, H.-J. (2017c). Inactivation of the oxidase gene *mppG* results in the selective loss of orange azaphilone pigments in *Monascus purpureus*. *Appl. Biol. Chem.* 60, 437–446. doi: 10.1007/s13765-017-0296-6

Balakrishnan, B., Suh, J.-W., Park, S.-H., and Kwon, H.-J. (2014c). Delineating *Monascus* azaphilone pigment biosynthesis: oxidoreductive modifications determine the ring cyclization pattern in azaphilone biosynthesis. *RSC Adv.* 4, 59405–59408. doi: 10.1039/C4RA11713A

Birch, A., Cassera, A., Fitton, P., Holker, J., Smith, H., Thompson, G., et al. (1962). Studies in relation to biosynthesis. Part XXX. Rotiorin, monascin, and rubropunctatin. *J. Chem. Soc.* 3583–3586. doi: 10.1039/jr9620003583

Blin, K., Shaw, S., Steinke, K., Villebro, R., Ziemert, N., Lee, S. Y., et al. (2019). antiSMASH 5.0: updates to the secondary metabolite genome mining pipeline. *Nucleic Acids Res.* 47, W81–W87. doi: 10.1093/nar/gkz310

Chen, F., and Hu, X. (2005). Study on red fermented rice with high concentration of monacolin K and low concentration of citrinin. *Int. J. Food Microbiol.* 103, 331–337. doi: 10.1016/j.ijfoodmicro.2005.03.002

Chen, W., Chen, R., Liu, Q., He, Y., He, K., Ding, X., et al. (2017). Orange, red, yellow: biosynthesis of azaphilone pigments in *Monascus* fungi. *Chem. Sci.* 8, 4917–4925. doi: 10.1039/c7sc00475c

Chen, W., Feng, Y., Molnár, I., and Chen, F. (2019). Nature and nurture: confluence of pathway determinism with metabolic and chemical serendipity diversifies *Monascus* azaphilone pigments. *Nat. Prod. Rep.* 36, 561–572. doi: 10.1039/c8np00060c

Chen, W., He, Y., Zhou, Y., Shao, Y., Feng, Y., Li, M., et al. (2015). Edible filamentous fungi from the species *Monascus*: early traditional fermentations, modern molecular biology, and future genomics. *Compr. Rev. Food Saf.* 14, 555–567. doi: 10.1111/1541-4337.12145

Choe, D., Lee, J., Woo, S., and Shin, C. S. (2012). Evaluation of the amine derivatives of *Monascus* pigment with anti-obesity activities. *Food Chem.* 134, 315–323. doi: 10.1016/j.foodchem.2012.02.149

Feng, Y., Shao, Y., and Chen, F. (2012). *Monascus* pigments. *Appl. Microbiol. Biotechnol.* 96, 1421–1440. doi: 10.1007/s00253-012-4504-3

Frisvad, J. C., Yilmaz, N., Thrane, U., Rasmussen, K. B., Houbraken, J., and Samson, R. A. (2013). *Talaromyces atroroseus*, a new species efficiently producing industrially relevant red pigments. *PLoS One* 8:e84102. doi: 10.1371/journal.pone.0084102

Hadfield, J., Holker, J., and Stanway, D. (1967). The biosynthesis of fungal metabolites. Part II. the β-oxo-lactone equivalents in rubropunctatin and monascorubrin. *J. Chem. Soc.* 751–755. doi: 10.1039/J39670000751

He, Y., and Cox, R. J. (2016). The molecular steps of citrinin biosynthesis in fungi. *Chem. Sci.* 7, 2119–2127. doi: 10.1039/c5sc04027b

He, Y., Liu, Q., Shao, Y., and Chen, F. (2013). *ku70* and *ku80* null mutants improve the gene targeting frequency in *Monascus ruber* M7. *Appl. Microbiol. Biotechnol.* 97, 4965–4976. doi: 10.1007/s00253-013-4851-8

Hood, E., Gelvin, S., Melchers, L., and Hoekema, A. (1993). New *Agrobacterium* helper plasmids for gene transfer to plants. *Transgenic Res.* 2, 208–218. doi: 10.1007/bf01977351

Hyde, K. D., Xu, J., Rapior, S., Jeewon, R., Lumyong, S., Niego, A. G. T., et al. (2019). The amazing potential of fungi: 50 ways we can exploit fungi industrially. *Fungal Divers.* 97, 1–136. doi: 10.1007/s13225-019-00430-9

Jeon, H. G., Seo, J., Lee, M. J., Han, K., and Kim, E. S. (2011). Analysis and functional expression of NPP pathway-specific regulatory genes in *Pseudonocardia autotrophica*. *J. Ind. Microbiol. Biotechnol.* 38, 573–579. doi: 10.1007/s10295-011-0939-2

Jin, H. J., Zhang, X., Cao, H., Niu, Y. J., Li, C., and Liu, H. (2018). Chemical composition, security and bioactivity of the red pigment from *Penicillium purpurogenum* Li-3. *Chem. Biodivers.* 15:e1800300. doi: 10.1002/cbdv.201800300

Kautsar, S. A., Blin, K., Shaw, S., Navarro-Muñoz, J. C., Terlouw, B. R., van der Hooft, J. J. J., et al. (2020). MIBiG 2.0: a repository for biosynthetic gene clusters of known function. *Nucleic Acids Res.* 48, D454–D458. doi: 10.1093/nar/gkz882

Keller, N. P. (2019). Fungal secondary metabolism: regulation, function and drug discovery. *Nat. Rev. Microbiol.* 17, 167–180. doi: 10.1038/s41579-018-0121-1

Khaldi, N., and Wolfe, K. H. (2011). Evolutionary origins of the fumonisin secondary metabolite gene cluster in *Fusarium verticillioides* and *Aspergillus niger*. *Int. J. Evol. Biol.* 2011:423821. doi: 10.4061/2011/423821

Khaldi, N., Seifuddin, F. T., Turner, G., Haft, D., Nierman, W. C., Wolfe, K. H., et al. (2010). SMURF: genomic mapping of fungal secondary metabolite clusters. *Fungal Genet. Biol.* 47, 736–741. doi: 10.1016/j.fgb.2010.06.003

Kim, W., Park, J. J., Gang, D. R., Peever, T. L., and Chen, W. (2015). A novel type pathway-specific regulator and dynamic genome environments of a solanapyrone biosynthesis gene cluster in the fungus *Ascochyta rabiei*. *Eukaryot. Cell* 14, 1102–1113. doi: 10.1128/EC.00084-15

Kurono, M., Nakanishi, K., Shindo, K., and Tada, M. (1963). Biosyntheses of monascorubrin and monascoflavin. *Chem. Pharm. Bull.* 11, 359–362. doi: 10.1248/cpb.11.359

Leadmon, C. E., Sampson, J. K., Maust, M. D., Macias, A. M., Rehner, S. A., Kasson, M. T., et al. (2020). Several *Metarhizium* species produce ergot alkaloids in a condition-specific manner. *Appl. Environ. Microbiol.* 86, e00373–20. doi: 10.1128/AEM.00373-20

Lee, B.-H., and Pan, T.-M. (2012a). Benefit of *Monascus*-fermented products for hypertension prevention: a review. *Appl. Microbiol. Biotechnol.* 94, 1151–1161. doi: 10.1007/s00253-012-4076-2

Lee, C.-L., and Pan, T.-M. (2012b). Development of *Monascus* fermentation technology for high hypolipidemic effect. *Appl. Microbiol. Biotechnol.* 94, 1449–1459. doi: 10.1007/s00253-012-4083-3

Lee, C.-L., Kung, Y.-H., Wu, C.-L., Hsu, Y.-W., and Pan, T.-M. (2010). Monascin and ankaflavin act as novel hypolipidemic and high-density lipoprotein cholesterol-raising agents in red mold *Dioscorea*. *J. Agric. Food Chem.* 58, 9013–9019. doi: 10.1021/jf101982v

Li, M., Kang, L., Ding, X., Liu, J., Liu, Q., Shao, Y., et al. (2020). Monasone naphthoquinone biosynthesis and resistance in *Monascus* fungi. *mBio* 11:e02676–19. doi: 10.1128/mBio.02676-19

Liang, B., Du, X., Li, P., Sun, C., and Wang, S. (2018). *MptriA*, an acetyltransferase gene involved in pigment biosynthesis in *M. purpureus* YY-1. *J. Agric. Food Chem.* 66, 4129–4138. doi: 10.1021/acs.jafc.8b00661

Liu, J., Zhou, Y., Yi, T., Zhao, M., Xie, N., Lei, M., et al. (2016). Identification and role analysis of an intermediate produced by a polygenic mutant of *Monascus* pigments cluster in *Monascus ruber* M7. *Appl. Microbiol. Biotechnol.* 100, 7037–7049. doi: 10.1007/s00253-016-7397-8

Liu, Q., Cai, L., Shao, Y., Zhou, Y., Li, M., Wang, X., et al. (2016). Inactivation of the global regulator LaeA in *Monascus ruber* results in a species-dependent response in sporulation and secondary metabolism. *Fungal Biol.* 120, 297–305. doi: 10.1016/j.funbio.2015.10.008

Liu, Q., Xie, N., He, Y., Wang, L., Shao, Y., Zhao, H., et al. (2014). *MpigE*, a gene involved in pigment biosynthesis in *Monascus ruber* M7. *Appl. Microbiol. Biotechnol.* 98, 285–296. doi: 10.1007/s00253-013-5289-8

Lyu, H.-N., Liu, H.-W., Keller, N. P., and Yin, W.-B. (2020). Harnessing diverse transcriptional regulators for natural product discovery in fungi. *Nat. Prod. Rep.* 37, 6–16. doi: 10.1039/c8np00027a

Morales-Oyervides, L., Ruiz-Sánchez, J. P., Oliveira, J. C., Sousa-Gallagher, M. J., Méndez-Zavala, A., Giuffrida, D., et al. (2020). Biotechnological approaches for the production of natural colorants by *Talaromyces*/*Penicillium*: a review. *Biotechnol. Adv.* 43:107601. doi: 10.1016/j.biotechadv.2020.107601

Niehaus, E. M., Kleigrewe, K., Wiemann, P., Studt, L., Sieber, C. M., Connolly, L. R., et al. (2013). Genetic manipulation of the *Fusarium fujikuroi* fusarin gene cluster yields insight into the complex regulation and fusarin biosynthetic pathway. *Chem. Biol.* 20, 1055–1066. doi: 10.1016/j.chembiol.2013.07.004

Ogihara, J., Kato, J., Oishi, K., and Fujimoto, Y. (2001). PP-R, 7-(2-hydroxyethyl)-monascorubramine, a red pigment produced in the mycelia of *Penicillium* sp. AZ. *J. Biosci. Bioeng.* 91, 44–47. doi: 10.1016/S1389-1723(01)80109-2

Ogihara, J., Kato, J., Oishi, K., Fujimoto, Y., and Eguchi, T. (2000). Production and structural analysis of PP-V, a homologue of monascorubramine, produced by a new isolate of *Penicillium* sp. *J. Biosci. Bioeng.* 90, 549–554. doi: 10.1016/S1389-1723(01)80039-6

Pavesi, C., Flon, V., Mann, S., Leleu, S., Prado, S., and Franck, X. (2021). Biosynthesis of azaphilones: a review. *Nat. Prod. Rep.* doi: 10.1039/d0np00080a [Epub ahead of print].

Shao, Y., Ding, Y., Zhao, Y., Yang, S., Xie, B., and Chen, F. (2009). Characteristic analysis of transformants in T-DNA mutation library of *Monascus ruber*. *World J. Microbiol. Biotechnol.* 25, 989–995. doi: 10.1007/s11274-009-9977-6

Skinnider, M. A., Johnston, C. W., Gunabalasingam, M., Merwin, N. J., Kieliszek, A. M., MacLellan, R. J., et al. (2020). Comprehensive prediction of secondary metabolite structure and biological activity from microbial genome sequences. *Nat. Commun.* 11:6058. doi: 10.1038/s41467-020-19986-1

Studt, L., Janevska, S., Niehaus, E. M., Burkhardt, I., Arndt, B., Sieber, C. M., et al. (2016). Two separate key enzymes and two pathway-specific transcription factors are involved in fusaric acid biosynthesis in *Fusarium fujikuroi*. *Environ. Microbiol.* 18, 936–956. doi: 10.1111/1462-2920.13150

Takeda, I., Umemura, M., Koike, H., Asai, K., and Machida, M. (2014). Motif-independent prediction of a secondary metabolism gene cluster using comparative genomics: application to sequenced genomes of *Aspergillus* and ten other filamentous fungal species. *DNA Res.* 21, 447–457. doi: 10.1093/dnares/dsu010

Tolborg, G., Ødum, A. S. R., Isbrandt, T., Larsen, T. O., and Workman, M. (2020). Unique processes yielding pure azaphilones in *Talaromyces atroroseus*. *Appl. Microbiol. Biotechnol.* 104, 603–613. doi: 10.1007/s00253-019-10112-w

Wang, L., Wang, W., and Xu, G. (2011). Promotion of monacolin K production by *Agrobacterium tumefaciens*-mediated transformation in *Monascus albidus* 9901. *Curr. Microbiol.* 62, 501–507. doi: 10.1007/s00284-010-9735-x

Weber, T., Rausch, C., Lopez, P., Hoof, I., Gaykova, V., Huson, D., et al. (2009). CLUSEAN: a computer-based framework for the automated analysis of bacterial secondary metabolite biosynthetic gene clusters. *J. Biotechnol.* 140, 13–17. doi: 10.1016/j.jbiotec.2009.01.007

Wiemann, P., Guo, C.-J., Palmer, J. M., Sekonyela, R., Wang, C. C., and Keller, N. P. (2013a). Prototype of an intertwined secondary-metabolite supercluster. *Proc. Natl. Acad. Sci. U.S.A.* 110, 17065–17070. doi: 10.1073/pnas.1313258110

Wiemann, P., Sieber, C. M., von Bargen, K. W., Studt, L., Niehaus, E. M., Espino, J. J., et al. (2013b). Deciphering the cryptic genome: genome-wide analyses of the rice pathogen *Fusarium fujikuroi* reveal complex regulation of secondary metabolism and novel metabolites. *PLoS Pathog.* 9:e1003475. doi: 10.1371/journal.ppat.1003475

Wiemann, P., Soukup, A. A., Folz, J. S., Wang, P. M., Noack, A., and Keller, N. P. (2018). CoIN: co-inducible nitrate expression system for secondary metabolites in *Aspergillus nidulans*. *Fungal Biol. Biotechnol.* 5:6. doi: 10.1186/s40694-018-0049-2

Wolf, T., Shelest, V., Nath, N., and Shelest, E. (2016). CASSIS and SMIPS: promoter-based prediction of secondary metabolite gene clusters in eukaryotic genomes. *Bioinformatics.* 32, 1138–1143. doi: 10.1093/bioinformatics/btv713

Woo, P. C., Lam, C.-W., Tam, E. W., Lee, K.-C., Yung, K. K., Leung, C. K., et al. (2014). The biosynthetic pathway for a thousand-year-old natural food colorant and citrinin in *Penicillium marneffei*. *Sci. Rep.* 4:6728. doi: 10.1038/srep06728

Xie, N., Liu, Q., and Chen, F. (2013). Deletion of *pigR* gene in *Monascus ruber* leads to loss of pigment production. *Biotechnol. Lett.* 35, 1425–1432. doi: 10.1007/s10529-013-1219-1

Xie, N., Zhang, Y., and Chen, F. (2015). Identification of a pigment-polyketide synthase gene deleted mutant of *Monascus ruber* M7. *Wei Sheng Wu Xue Bao* 55, 863–872.

Yu, J.-H., Hamari, Z., Han, K.-H., Seo, J.-A., Reyes-Domínguez, Y., and Scazzocchio, C. (2004). Double-joint PCR: a PCR-based molecular tool for gene manipulations in filamentous fungi. *Fungal Genet. Biol.* 41, 973–981. doi: 10.1016/j.fgb.2004.08.001

Yu, Y., Du, J., Wang, G., and Ji, J. (2003). Studies on the freeze-thaw method of transforming recombinant plasmid DNA into *Agrobacterium tumefaciens*. *J. Jilin Agric. Univ.* 25, 257–259.

Zabala, A. O., Xu, W., Chooi, Y.-H., and Tang, Y. (2012). Characterization of a silent azaphilone gene cluster from *Aspergillus niger* ATCC 1015 reveals a hydroxylation-mediated pyran-ring formation. *Chem. Biol.* 19, 1049–1059. doi: 10.1016/j.chembiol.2012.07.004

Conflict of Interest: IM has disclosed financial interests in Teva Pharmaceutical Works Ltd., Hungary and the University of Debrecen, Hungary that are unrelated to the subject of the research presented here.

The remaining authors declare that the research was conducted in the absence of any commercial or financial relationships that could be construed as a potential conflict of interest.

frontiers in Microbiology

ORIGINAL RESEARCH
published: 21 June 2021
doi: 10.3389/fmicb.2021.702951

Development of a Novel Restrictive Medium for *Monascus* Enrichment From Hongqu Based on the Synergistic Stress of Lactic Acid and Ethanol

Kangxi Zhou[1,2], Li Wu[2], Guimei Chen[2], Zhibin Liu[2], Xinze Zhao[2], Chen Zhang[2], Xucong Lv[2], Wen Zhang[2], Pingfan Rao[2] and Li Ni[1,2]**

[1] College of Chemical Engineering, Fuzhou University, Fuzhou, China, [2] Fujian Center of Excellence for Food Biotechnology, Institute of Food Science and Technology, Fuzhou University, Fuzhou, China

OPEN ACCESS

Edited by:
Van-Tuan Tran,
Vietnam National University, Hanoi, Vietnam

Reviewed by:
Zhilong Wang,
Shanghai Jiao Tong University, China
Chan Zhang,
Beijing Technology and Business University, China
Yanping Li,
Nanchang University, China

***Correspondence:**
Li Ni
nili@fzu.edu.cn
Xucong Lv
xucong1154@163.com

Specialty section:
This article was submitted to Food Microbiology, a section of the journal Frontiers in Microbiology

Received: 30 April 2021
Accepted: 25 May 2021
Published: 21 June 2021

Citation:
Zhou K, Wu L, Chen G, Liu Z, Zhao X, Zhang C, Lv X, Zhang W, Rao P and Ni L (2021) Development of a Novel Restrictive Medium for Monascus Enrichment From Hongqu Based on the Synergistic Stress of Lactic Acid and Ethanol. Front. Microbiol. 12:702951. doi: 10.3389/fmicb.2021.702951

Hongqu is a famous fermented food produced by *Monascus* and has been used as food coloring, wine starters and food additives for thousands of years in China. Excellent *Monascus* strain is an important prerequisite for producing high-quality Hongqu. However, the isolation of *Monascus* pure culture from Hongqu samples is time-consuming and laborious because it is easily interfered by other microorganisms (especially filamentous fungi). Therefore, the development of restrictive medium for *Monascus* enrichment from Hongqu is of great significance for the preparation and screening of excellent *Monascus* strains. Results of this study showed that *Monascus* has good tolerance to lactic acid and ethanol. Under the conditions of tolerance limits [7.5% lactic acid (v/v) and 12.0% ethanol (v/v)], *Monascus* could not grow but it still retained the vitality of spore germination, and the spore activity gradually decreased with the increasing concentrations of lactic acid and ethanol. More interestingly, the addition of lactic acid and ethanol significantly changed the microbial community structure in rice milk inoculated with Hongqu. After response surface optimization, *Monascus* could be successfully enriched without the interference of other microorganisms when 3.98% (v/v) lactic acid and 6.24% (v/v) ethanol were added to rice milk simultaneously. The optimal enrichment duration of *Monascus* by the restrictive medium based on the synergistic stress of lactic acid and ethanol is 8∼24 h. The synergistic stress of lactic acid and ethanol had no obvious effects on the accumulation of major metabolites in the progeny of *Monascus*, and was suitable for the enrichment of *Monascus* from different types of Hongqu. Finally, the possible mechanisms on the tolerance of *Monascus* to the synergistic stress of lactic acid and ethanol were preliminarily studied. Under the synergistic stress of lactic acid and ethanol, the cell membrane of *Monascus* defends against lactic acid and ethanol into cells to some extent, and the superoxide dismutase (SOD), catalase (CAT) and glutathione peroxidase (GSH-Px) activities of *Monascus* were higher than those of other fungi, which significantly reduced the degree of lipid peroxidation of cell membrane, while secreting more amylase to make reducing sugars to provide the cells with enough energy to resist environmental stress. This work has great application value for the construction of *Monascus* strain library and the better development of its germplasm resources.

Keywords: *Monascus* enrichment, restrictive medium, Hongqu, lactic acid, ethanol

INTRODUCTION

Hongqu, also called red fermented rice, red yeast rice and *Anka*, is produced from steamed rice inoculated with *Monascus* seed culture through solid-state fermentation (Liu et al., 2018). It has been used for thousands of years in Asian countries and is currently used worldwide as a food coloring, fermentation starter and food additives (Tian et al., 2016; Lei et al., 2019). *Monascus*, an essential microorganism for the production of Hongqu, can metabolize a variety of useful enzymes and secondary metabolites (Zhou et al., 2019). For example, liquefying enzymes and saccharifying enzymes contribute to the degradation of starch in grains and the formation of reducing sugars (Shin et al., 2017; Ai et al., 2019); *Monascus* pigment can be used for food coloring and antisepsis (Agboyibor et al., 2018); and lovastatin and γ-aminobutyric acid are beneficial to the development of lipid-lowering and blood pressure-reducing drugs, respectively (Eren et al., 2015; Zhang et al., 2018; Xiong et al., 2019). To fully understand the production and application values of *Monascus*, it is necessary to isolate and purify the original strain from Hongqu to obtain high-quality *Monascus*.

Most Hongqu production follows the manual fermentation techniques of ancient China, so the production process of Hongqu is not strictly controlled (Park et al., 2016; Huang et al., 2019). In addition to *Monascus*, bacteria such as *Lactobacillus* and *Bacillus* and fungi such as yeast, *Aspergillus niger*, and *Aspergillus oryzae* may be present in Hongqu (Lv et al., 2015, 2016). The presence of these microorganisms can cause serious disturbance during the preparation of *Monascus* pure culture from Hongqu. Most of the purification of *Monascus* does not involve exclusive pretreatment and involves direct coating or streaking on mold medium. The media used in these methods include conventional mold media such as potato dextrose agar (Lv et al., 2016), Rose Bengal medium (Huang et al., 2014), malt extract agar (Barbosa et al., 2017) and mold media supplemented with antibiotics or sodium deoxycholate (Zhang et al., 2015). Although these methods are convenient to operate, they cannot exclude the interference of fungi other than *Monascus*. The spores of various microorganisms often diffuse in the culture dish, and repeated operations are required to obtain *Monascus*. Therefore, it is necessary to invent a novel restrictive medium for the enrichment of *Monascus*.

To enrich all kinds of *Monascus* as much as possible, the type and concentration of regulatory factors for purification should meet the following requirements: other microorganisms are eliminated without inactivation of *Monascus*. Thus, *Monascus* must be well tolerated with these regulatory factors. *Monascus* has been reported to have good tolerance characteristics toward lactic acid and ethanol. For example, *Monascus ruber* CBS 127564 can tolerate 14.5% (v/v) lactic acid (Weusthuis et al., 2017), and *Monascus purpureus* FJMR24 can tolerate 18% (v/v) ethanol (Ren et al., 2021). However, although it is not uncommon for microorganisms to tolerate lactic acid or ethanol, just as *Terrilactibacillus laevilacticus* SK5-6 can tolerate approximately 12% (v/v) lactic acid (Prasirtsak et al., 2017) and *Candida tropicalis* can tolerate approximately 30% (v/v) ethanol (Balia et al., 2018), there are very few reports on non-genetically modified microorganisms that can tolerate high concentrations of lactic acid and ethanol simultaneously. *Monascus* has the potential to tolerate lactic acid and ethanol simultaneously, so it is expected to be enriched from Hongqu through a restrictive medium based on the synergistic stress of lactic acid and ethanol.

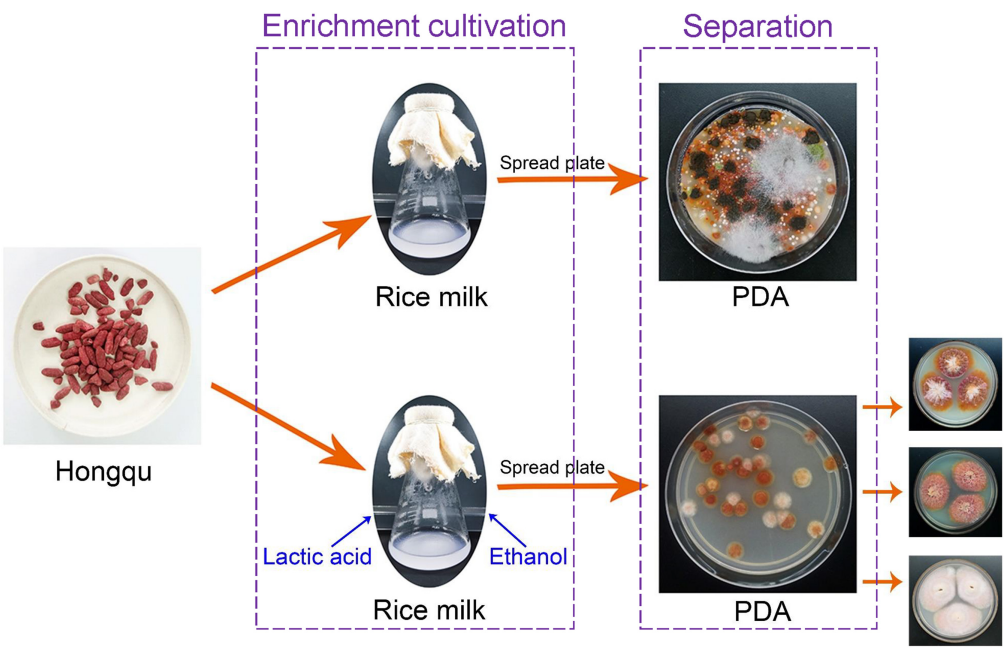

GRAPHICAL ABSTRACT | The restrictive medium containing lactic acid and ethanol enabled the enrichment of *Monascus* sp.

In this study, we explored the possibility of lactic acid and ethanol as regulatory factors of a restrictive medium for *Monascus* enrichment from Hongqu, and also preliminarily speculated the possible mechanisms on the tolerance of *Monascus* to the synergistic stress of lactic acid and ethanol. These results would help to improve the efficiency of *Monascus* enrichment from Hongqu and provides a reference for better mining of *Monascus* germplasm resources.

MATERIALS AND METHODS

Sources of *Monascus* and Hongqu

M. serorubescens A1, *M. lunisporas* A4, *M. sanguineus* B1, *M. kaoliang* B6, *M. argentinensis* B7, *M. purpureus* C1 was isolated from Hongqu by our laboratory (Lv et al., 2012; Cai et al., 2019). Nucleotide sequences for ITS-5.8S rDNA region of these Monascus were deposited in the NCBI database under accession numbers MZ297243-MZ297247 and MZ297277 respectively. Hongqu samples used in this study were collected from different cities in Fujian Province, China: BHQ26 (Hongqu for rice wine brewing, from Ningde city), BHQ33 (Hongqu for rice wine brewing, from Quanzhou city), PHQ30 (Hongqu for pigment production, from Ningde city), WHQ38 (Wuyi Hongqu, a special Hongqu for rice wine brewing that contains more *Aspergillus niger* than other Hongqu, from Fuzhou city).

Mediums for Microbial Culture and Fermentation

Potato dextrose agar (PDA) (Guangdong Huankai Microbial Sci. & Tech. Co., Ltd., Guangzhou, China) was configured according to the product manual. The modified PDA medium was prepared by adding 0.1 g/L chloramphenicol and 0.5 g/L sodium deoxycholate to the original PDA. The modified potato dextrose water (PD) medium is based on PD medium (Guangdong Huankai Microbial Sci. & Tech. Co., Ltd., Guangzhou, China) with 15 g/L indica rice flour, 10 g/L sodium glutamate, and 5 g/L glycerol. The rice milk containing 15 g/L indica rice flow, 5 g/L glucose and 0.1 g/L chloramphenicol was used as the basic medium, and different contents of hydrochloric acid (HCl), lactic acid and ethanol were added to this rice milk as the restrictive medium according to the experimental requirements.

Tolerance Test of *Monascus* Against Lactic Acid and Ethanol

All the *Monascus* strains were activated on PDA plates and incubated at 30°C for 7 days under aerobic conditions. Spores were harvested by flooding the surface of the agar with normal saline. The spore suspension was adjusted with sterile saline solution to 10^6 CFU/mL with a hemocytometer. The *Monascus* spore suspension was connected to different restrictive medium at 1% (v/v) inoculum size and cultured for 7 days. After the fermentation, samples were taken to determine the viable number and biomass increment of *Monascus*.

Separation of *Monascus* Pure Culture From Hongqu

Hongqu was ground into Hongqu powder by using a sterile mortar. Direct dilution coating method: 0.1500 ± 0.0010 g Hongqu powder was accurately weighed and put into 30 mL sterile saline solution and shake for 90 s. The insoluble particles were filtered out with four layers of gauze and the remaining liquid containing microbial spores diluted and coated on the modified PDA medium. Fermentation-coating method: 0.1500 ± 0.0010 g Hongqu powder was accurately weighed and fermented in a 250 mL shake flask containing 30 mL restrictive medium at 30℃ and 200 r/min. After the fermentation, the fermentation broth was diluted and coated on the modified PDA medium for 4 days at 30℃.

Effects of Lactic Acid and Ethanol on Morphology and Metabolism of Purified *Monascus* Progeny

The spore suspension of *Monascus* A1, A4, B1, B6, B7, C1 were respectively inoculated into the restrictive medium containing 3.98% (v/v) lactic acid and 6.24% (v/v) ethanol for 7 days at 30℃ and 200 r/min. The fermentation broth of the restrictive medium was used as the treatment group, and the spore suspension harvested from the PDA plate was used as the control group. Each group contained 6 *Monascus* species. The two groups of *Monascus* have activated to PDA plates again and then spotted on the modified PDA for 7 days at 30°C to observe the colony morphology, at the same time, fermented in a 250 mL shake flask containing 30 mL modified PD medium at 30℃ and 200 r/min for 7 days to detect metabolites.

Metabolic Behaviors of Fungus Isolated From BHQ33 Against Lactic and Ethanol Stress

All the fungus isolated from BHQ33 were activated to PDA plates and incubated at 30°C for 7 days under aerobic conditions. Spores were harvested by flooding the surface of the agar with sterile saline solution and were adjusted with normal saline to 10^6 CFU/mL with a hemocytometer. The above fungal spore suspensions were first respectively inoculated at 1% (v/v) inoculum size into basal medium (rice milk, containing 15 g/L indica rice flour, 5 g/L glucose, and 0.1 g/L chloramphenicol) for adaptive growth at 30°C and 200 r/min for 7 days, followed by centrifugation at 3,000 r/min for 15 min to collect the cells, which were then washed 3 times with sterile saline solution. The washed cells were resuspended to 10 mg/mL with sterile saline solution and were connected to different selective media at 10% (v/v) inoculum size and cultured for 24 h. There are four kinds of selective media in this part experiment: basal medium without lactate and ethanol (control), basal medium supplemented with 3.98% (v/v) lactic acid (experimental group 1), basal medium supplemented with 6.24% (v/v) ethanol (experimental group 2) and basal medium supplemented with both 3.98% (v/v) lactic acid and 6.24% (v/v) ethanol (experimental group 3).

Analysis of Fungi Quantity

In the tolerance test of *Monascus*, the plate count and glucosamine content of biomass were used to analyze the biomass increment of *Monascus* in different selective media, and the plate count method was used to determine the number of viable fungi in the samples in other experiments. Glucosamine is the main component of chitin in *Monascus* cell wall, and its content is often used to predict the biomass of *Monascus* in samples containing indica rice. With the dry cell of *Monascus* as a standard reference, the standard curve between the absorbance value and the dry weight of the cell was drawn after four steps of acidolysis, neutralization, Elson-Morgan reaction and colorimetric determination (Sakural et al., 1977; Chysirichote et al., 2013). The sample was converted into biomass based on the standard curve.

Identification of Isolated Fungal Strains

The fungi isolated and purified from the modified PDA medium were identified by DNA analysis: ITS-5.8S rDNA region was partially amplified and sequenced using primers ITS1/ITS4 as described by Park et al. (2004). Each 25 μL PCR reaction mixture consisted of 1 μL DNA template, 12.5 μL 2 × Power Taq PCR MasterMix (containing $MgCl_2$) (Sangon Biotech Co., Ltd. Shanghai, China), 1 μL primer, and ddH_2O was added to a final volume of 25 μL. The PCR was conducted under the following conditions: initial denaturation at 95°C for 5 min, 35 cycles of denaturation at 94°C for 45 s, annealing at 55°C for 45 s, extension at 72°C for 120 s, followed by a final extension cycle at 72°C for 10 min prior to maintaining the mixture at 4°C. Products were analyzed on 1.5% agarose gel containing 0.1 μL/mL of 4S Red Plus nucleic acid stain (Sangon Biotech Co., Ltd. Shanghai, China) and visualized under UV light (UV source GelDoc 1000, Bio-Rad). PCR products were gel-purified with GFX^{TM} PCR DNA and Gel Band Purification Kit (Amersham Biosciences AB, Uppsala), according to the manufacturer's instructions. Purified PCR products were directly sequenced using the ABI prism 3730 DNA analyzer (Applied Biosystems, Foster). Sequences were analyzed using Blast at NCBI.[1] Nucleotide sequences for ITS-5.8S rDNA region of isolates represent *Monascus purpureus* BHQ33.M01, *Monascus purpureus* BHQ33.M02, *Monascus purpureus* BHQ33.M03, *Saccharomyces cerevisiae* BHQ33.S01, *Aspergillus niger* BHQ33.AN01, *Lichtheimia ramosa* BHQ33.L01, *Trichoderma* BHQ33.T01, and *Aspergillus flavus* BHQ33.AF01 were deposited in the NCBI database under accession numbers MW581230–MW581237.

Analysis of Metabolites in the Regenerated Progenies of *Monascus*

The analytical method of γ-aminobutyric acid was referenced to the agricultural industry-standard NY/T 2890-2016 of the people's Republic of China, unit: μg/mL. The pigment, lovastatin and citrinin were extracted with 70% (v/v) ethanol at 60℃ for 2 h. The mycelium of the sample was removed by centrifugation at 5,000 r/min for 10 min, and the supernatant was diluted and filtered through a 0.22 μm filter membrane to be tested. The content of *Monascus* pigment was predicted by the absorbance value using a spectrophotometer (U1900, Hitachi, Japan) at 505 nm referred to the national standards of the people's Republic of China GB 1886.19-2015, unit: U/mL; The HPLC (L2000, Hitachi, Japan) analysis method of lovastatin referred to the light industry standard of the people's Republic of China GB/T 2847-2007, unit: μg/mL; The HPLC analysis method of citrinin refers to the national standard of the people's Republic of China GB 5009.222-2016, unit: ng/mL.

The amylase activity was measured using an α-amylase assay kit (all kits used in the current study were purchased from Nanjing Jiancheng Bioengineering Institute, Nanjing, China, unless otherwise indicated) based on QB/T 4257-2011. One unit of amylase activity was defined as the quantity of enzyme metabolized by 1 g mycelium that was required to hydrolyze 1 mg soluble starch per hour, at 35°C and pH 4.6. The glucoamylase activity was measured according to the Light Industry Standard of the People's Republic of China QB/T 4257-2011 with slight modifications. One unit of glucoamylase was defined as the amount of enzyme metabolized by 1 g mycelia that was required to release 1 mg glucose per hour from soluble starch, at 35°C and pH 4.6.

Metabolic Behaviors of Fungus Isolated From BHQ33 Against Lactic Acid and Ethanol Stress

The fermented medium was diluted to 10 mg/mL with sterile saline solution. 20 mL aliquot of the sample was centrifuged at 3,000 r/min for 15 min, and the supernatant, which had been filtered through a 0.45 μm filter, was used as a sample to be tested for extracellular metabolites. The centrifuged cells were washed 3 times with sterile saline solution and resuspended to 15 mL, followed by ultrasonic disruption (FS-200T, SXSONIC, China) at 200 W for 30 min under ice bath conditions. The ultrasonic fragmentation cycle times were as follows: 5 s working, 5 s stagnating, and 20 kHz frequency. After disruption, cell debris was removed by centrifugation at 4,500 r/min for 20 min, and the supernatant was used as the sample to be tested for intracellular metabolites.

The analytical methods for lactic acid and ethanol were referred to previous studies by Jiang et al. (2019), and Cai et al. (2019), respectively. The reducing sugars were determined by 3, 5-dinitrosalicylicacid method (Xu et al., 2014). Protein concentrations were measured using a coomassie (Bradford) protein assay kit. Soluble starch content and amylase activity were measured using an α-amylase assay kit with some modifications. In detail, soluble starch content is measured by the chromogenic reaction of the iodide solution with the extracellular solution, and the definition of one unit of amylase activity in this system was modified as the quantity of enzyme metabolized by 1 mL extracellular solution that was required to hydrolyze 1 mg soluble starch per hour, at 35°C and pH 4.6. Total superoxide dismutase (SOD), malondialdehyde (MDA), catalase (CAT), and total glutathione peroxidase (GSH-Px) levels of intracellular

[1] http://www.ncbi.nlm.nih.gov/

metabolism were measured with the assay kits according to the manufacturer's instructions (Nanjing Jiancheng Institute of Biotechnology, China).

Statistical Analysis

The experiments were conducted in triplicate, and the results were presented as the mean ± standard deviation (SD). One-way analysis of variance (ANOVA) was performed across multiple groups to test significance ($p < 0.05$) using SPSS 23.0 software (SPSS Inc., Chicago, United States). A histogram was generated using Origin 2018 software (OriginLab, Northampton, MA, United States). Response surface design (RSD) was carried out by Design-Expert V8.0.6.1software (Stat-Ease, Inc., Minneapolis, MN, United States).

RESULTS

Tolerance of *Monascus* to Lactic Acid and Ethanol

The range of common tolerance of *Monascus* to growth regulatory factors can be roughly determined by tolerance tests with multiple species *Monascus*, which facilitates selection of the type and concentrations of growth regulatory factors added to the restrictive medium. *Monascus* can grow in the medium containing low concentrations of lactic acid and ethanol with a certain number of live spores (**Figure 1**) and mycelium (**Figure 1** and **Supplementary Figure 1**). Specific concentrations of lactic acid [7.5% (v/v)] inhibited but did not eliminate the growth of *Monascus* because the number of viable spores in the fermentation broth did not change much compared with the initial amount, and a similar result was observed when ethanol was added to 12.0% (v/v). The inhibition of spore activity of *Monascus* by 7.5% (v/v) lactic acid did not depend exclusively on H^+ concentration because the pH of this medium was 2.1 (**Supplementary Figure 2**), and *Monascus* was found to tolerate $10^{-1.5}$ mol/L HCl (pH = 1.5).

BHQ33 Hongqu powder was added to the medium containing different growth regulatory factors for 7 days (**Figure 2**). After fermentation, the fermentation broth was diluted and coated in modified PDA for observation. Coating results showed that adding HCl or ethanol alone did not help to obtain *Monascus*, while adding 4.5% (v/v) lactic acid caused *Monascus* to appear in the plate. However, lactic acid alone did not inhibit *Aspergillus niger*, which grows significantly faster than *Monascus*, a situation that was unfavorable for obtaining as many different kinds of *Monascus* as possible. Combined with the results of **Figures 2B3,C3**, 9% (v/v) ethanol was able to eliminate *Aspergillus niger*, while 4.5% (v/v) lactic acid could eliminate yeast, and adding lactic acid and ethanol simultaneously was able to enrich *Monascus* (**Figures 2D2,D3**).

Optimization of Lactic Acid and Ethanol Addition in the Restrictive Medium

To eliminate fungi other than *Monascus* from BHQ33 Hongqu powder and to enrich as much *Monascus* as possible, response surface optimization was applied to optimize the amount of lactic acid and ethanol added to the restrictive medium. According to the tolerance test of *Monascus* in **Figure 1**, the concentration ranges of lactic acid and ethanol in the restrictive medium were selected to be 0∼6% (v/v) and 0∼12% (v/v), respectively. The response surface methodology uses a 2-factor 3-level model of Design-Expert software. The test scheme and results are listed in **Table 1** and **Figure 3**. The test results in **Table 1** confirm the conclusion in **Figures 2C,D** that it is difficult to grow *Monascus* only in culture dishes by using single lactic acid or ethanol. The fitting equation of the response surface model is as follows:

$$Y_1 = 4.64507 + 0.32330A + 0.01023B - 0.00458AB - 0.08453A^2 - 0.00317B^2 \quad (1)$$

$$Y_2 = 36.74284 + 24.53848A + 3.50424B - 0.38486AB - 2.42989A^2 - 0.086916B^2 \quad (2)$$

where Y_1 is the number of *Monascus* colonies, unit: Log10 CFU/mL; Y_2 is the proportion of *Monascus*, unit: %; A is the amount of lactic acid added, unit: % (v/v); and B is the amount of ethanol added, unit: % (v/v). The constraints of equations (1) and (2) are $f(A) = \min\{A\}$, $f(B) = \min\{B\}$, $f(Y_1) = \max\{Y_1\}$, $f(Y_2) = \max\{Y_2\}$, $0 \leq A \leq 6.0$, $0 \leq B \leq 12.0$ and $Y_2 \geq 100$. The optimal solution is $A = 3.98$, $B = 6.24$, $Y_1 = 4.420$, and $Y_2 = 104.8$ (according to the actual situation, $Y_2 = 100$).

Therefore, when the amount of lactic acid and ethanol reached 3.98% (v/v) and 6.24% (v/v), respectively, the amount of *Monascus* was 4.420 Log10 CFU/mL, and the proportion of *Monascus* was 100%. The actual plate coating verification shows that the number of viable *Monascus* under this condition is 4.49 ± 0.12 Log10 CFU/mL, accounting for 100% (3 strains of fungi could be obtained from the plate (**Supplementary Figure 3**), and all were *Monascus purpureus* after ITS gene sequencing).

Dynamics of *Monascus* in Restrictive Medium During the Fermentation Process

After the optimal addition of lactic acid and ethanol in the restrictive medium, the number and proportion of *Monascus* in the fermentation broth containing BHQ33 powder rapidly increased and gradually decreased from the first day to the 7th day of fermentation (**Figure 4A**). However, the samples fermented to the 7th day did not affect the enrichment of *Monascus*, and the amount of *Monascus* still exceeded 1.0×10^4 CFU/mL, accounting for 100%. To study the changing pattern of flora changes in this culture system more meticulously and determine the optimal enrichment duration, the enrichment process from 0 to 24 h was followed up by sampling and spread analysis (**Figure 4B**). The dominant fungi in the fermentation broth were *Monascus*, *Saccharomyces cerevisiae*, *Aspergillus niger* and *Aspergillus flavus*, while *Lichtheimia ramos* and *Trichoderma* were observed sporadically. From the initial state to 8 h of enrichment culture, the proportion of fungi except for *Monascus* gradually decreased until they disappeared. To obtain *Monascus* quickly and conveniently, sampling and coating are were carried

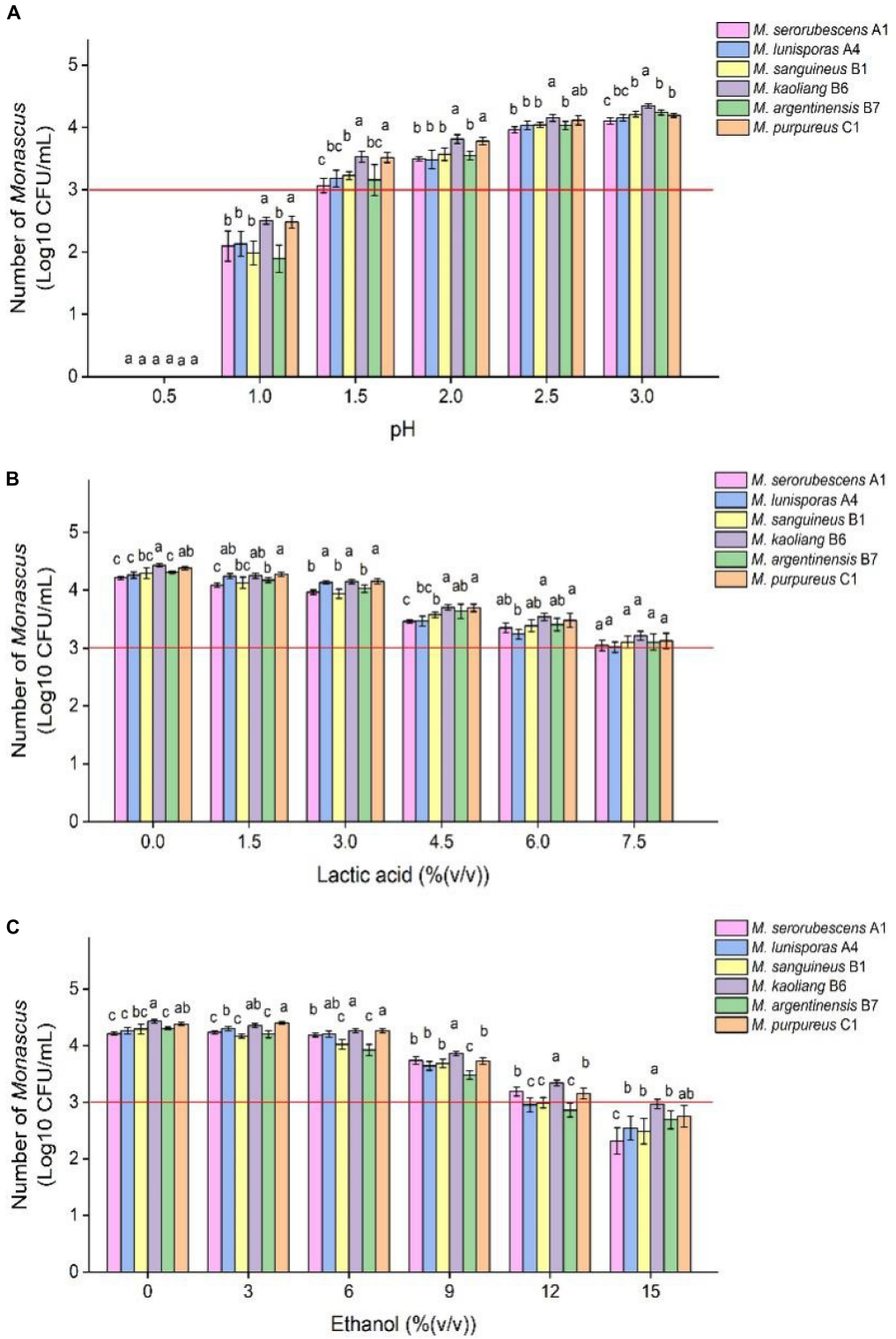

FIGURE 1 | Tolerance test of different species of *Monascus* to different growth inhibitors. The six *Monascus* species were cultured in restrictive medium containing different concentrations of HCl **(A)**, lactic acid **(B)** and ethanol **(C)** at 30°C and 200 r/min for 7 days, and the number of viable spores of *Monascus* was determined by plate coating after fermentation. Error bars indicate the standard deviation (SD) of the means ($n = 3$), and different lowercase letters represent significant differences in the number of viable cells of different *Monascus* strains under the same treatment condition ($p < 0.05$). The red auxiliary line indicates that the initial amount of *Monascus* is 1.0×10^3 CFU/mL.

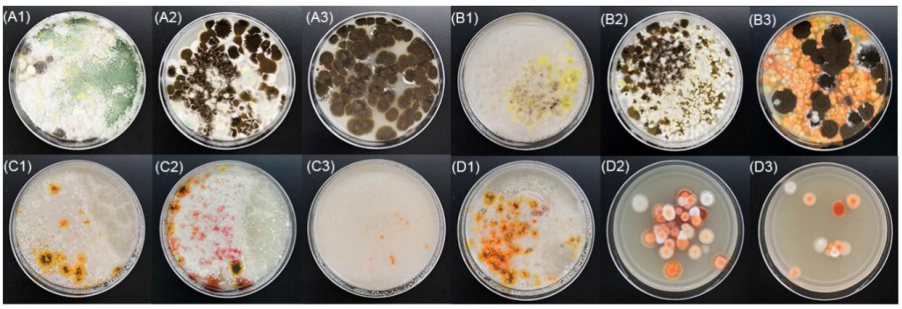

FIGURE 2 | Effect of different growth inhibitors on the enrichment of *Monascus* from Hongqu BHQ33. Hongqu BHQ33 was added to ferment respectively with different fermentation media containing $10^{-2.5}$mol/L HCl **(A1)**, 10^{-2}mol/L HCl **(A2)**, $10^{-1.5}$mol/L HCl **(A3)**, 1.5% (v/v) lactic acid **(B1)**, 3% (v/v) lactic acid **(B2)**, 4.5% (v/v) lactic acid **(B3)**, 3% (v/v) ethanol **(C1)**, 6% (v/v) ethanol **(C2)**, 9% (v/v) ethanol **(C3)**, 1.5% (v/v) lactic acid & 3% (v/v) ethanol **(D1)**, 3% (v/v) lactic acid & 6% (v/v) ethanol **(D2)**, 4.5% (v/v) lactic acid & 9% (v/v) ethanol **(D3)** at 30°C and 200 r/min for 7 days, and then coated on the modified PDA medium with the fermentation broth to culture for 4 days at 30°C.

out between 8 and 24 h after enrichment culture, which can save time and eliminate the interference of other fungi.

Metabolic Behaviors of *Monascus* Against Lactic Acid and Ethanol Stress

The fungi isolated from BHQ33 were inoculated into the restrictive medium containing different concentrations of lactic acid and ethanol for 24 h and sampled for analysis. Compared with experimental groups 1 and 2, the decreases in extracellular lactate and ethanol in experimental group 3 were significantly increased (**Figures 5A,B**), indicating that the cell membrane permeability could be changed by the synergistic effect of lactate and ethanol. Under the simultaneous stress of lactic acid and ethanol, *Monascus* reduced the amount of lactic acid in the cell, and the intracellular scavenging ability of lactic acid and ethanol was better than that of other fungi (**Figures 5C,D**).

Extracellular metabolites were analyzed (**Figure 6**). For the experimental groups supplemented with lactic acid (groups 1 and 3), the amylase activity and extracellular reducing sugar concentration of *Monascus* were higher than those of other fungi, and their extracellular soluble starch contents and those of other filamentous fungi were not significantly different. Extracellular amylase can peel soluble starch from rice flour granules and then degrade soluble starch into reducing sugars, so it can be speculated that the liquefaction capacity and saccharification capacity of *Monascus* under lactic acid stress are better than those of other fungi, while higher contents of reducing sugars can provide more energy sources for cells.

Intracellular metabolites were analyzed (**Figure 7**). Lactic acid and ethanol can cause lipid peroxidation damage of cell membrane, so the content of MDA in experimental group 1 and experimental group 2 is higher than that in the control group. Lipid peroxidative damage to the cell membrane was more intense when lactic acid and ethanol were present simultaneously (**Figure 7A**). Under the synergistic stress of lactate and ethanol, the accumulated amount of MDA in *Monascus* cells was significantly lower than that in other fungi, which might be related to the higher activities of intracellular antioxidant enzymes (SOD, GSH and CAT). This antioxidant enzyme is able to scavenge oxygen free radicals and reduce the oxidative damage of polyunsaturated fatty acids in biofilms, which has a positive effect on maintaining the structure and function of biofilms.

TABLE 1 | Response surface test scheme and results for optimizing the addition of lactic acid and ethanol.

Number	Lactic acid(%(v/v))	Ethanol (%(v/v))	The viable count of *Monascus* (Log10 CFU/mL)	The proportion of *Monascus* (%)
1	3	6	4.758	100
2	0	12	4.271	68.77
3	3	12	4.448	100
4	0	0	4.668	36.42
5	3	6	4.771	100
6	6	12	2.824	100
7	6	0	3.551	95.36
8	3	6	4.678	100
9	0	6	4.609	52.47
10	3	0	4.822	89.95
11	3	6	4.655	100
12	3	6	4.671	100
13	6	6	3.368	100

Three parallel experiments were conducted in each group. For the convenience of software operation, only the mean value is input.

DISCUSSION

In addition to a large number of *Monascus*, Hongqu also contains lactic acid bacteria, yeasts, and others (Liu et al., 2018; Hong et al., 2020). In the process of applying Hongqu to brew rice wine, it was found that *Monascus* has a certain resistance to lactic acid and alcohol (He et al., 2016; Cai et al., 2019; Liang et al., 2020), while the resistance of other microorganisms in the system is different from it (Lv et al., 2015;

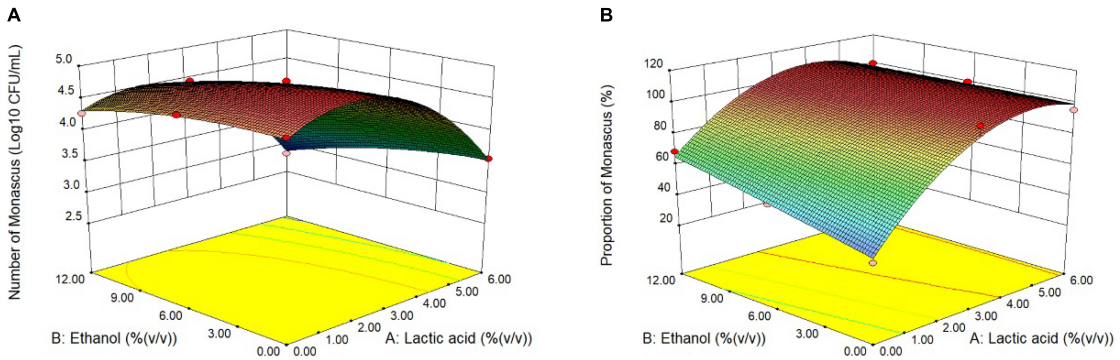

FIGURE 3 | Response surface optimization of lactic acid and ethanol addition in restrictive medium. Hongqu BHQ33 was added to the restrictive medium containing different concentrations of lactic acid and ethanol for fermentation at 30℃ and 200 r/min for 7 days, the number of viable *Monascus* spores **(A)** and the proportion of the number of *Monascus* **(B)** were calculated after the fermentation broth was diluted and spread on the modified PDA medium to culture for 4 days at 30℃.

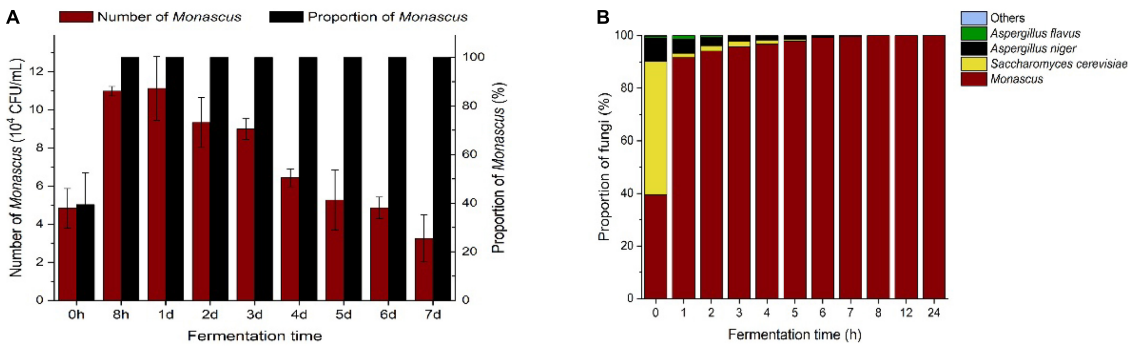

FIGURE 4 | Trends of *Monascus* and other culturable dominant fungi in the optimized restrictive medium supplemented with Hongqu BHQ33 during the fermentation process. Hongqu BHQ33 was added to the optimized restrictive medium containing 3.98% (v/v) lactic acid and 6.24%(v/v) ethanol for fermentation at 30℃ and 200 r/min for 7 days, the number of *Monascus* and its proportion over time **(A)** and proportion of culturable dominant fungi over time **(B)** were calculated after the fermentation broth was diluted and spread on the modified PDA medium to culture for 4 days at 30℃. Error bars indicate the standard deviation (SD) of the means (n = 3).

Huang et al., 2018). We speculate that it's a potential way to screen *Manascus* using the synergistic effect of lactic acid and ethanol, so finding the right ratio and concentration of both is the key point. In this study, when 4.5% (v/v) lactic acid was added alone, *Monascus* and *Aspergillus niger* coexisted; while 9% (v/v) ethanol was added alone, *Monascus* and *Saccharomyces cerevisiae* coexisted. After further optimization by response surface method, *Monascus* could be successfully enriched only when 3.98% (v/v) lactic acid and 6.24% (v/v) ethanol were added to the enrichment medium simultaneously. Traditionally, growth regulatory factors have been used to screen microbial strains, but they also may lead to the targeted domestication of the target strain, resulting in the loss of some metabolic functions (Yang et al., 2018). Fortunately, the novel restrictive medium for *Monascus* enrichment based on the synergistic stress of lactic acid and ethanol can shorten the pretreatment time without repeated operations, avoiding the abnormal changes in the metabolic characteristics of *Monascus* progeny to some extent. The morphological characteristics and metabolic function of *Monascus* progeny were not significantly changed after the treatment with the developed restrictive medium based on the synergistic stress of lactic acid and ethanol (**Supplementary Figure 4** and **Supplementary Table 1**).

When cells are stimulated or stressed, the metabolic activities related to environmental adaptation become active, especially those related to substance transport, substance transformation, and energy metabolism processes. According to previous studies, lactic acid bacteria can resist the damage of acid to cells through neutralization process, biofilm and cell density, proton pump, protection of macromolecules, preadaptation and cross-protection, and effect of solutes (Wang et al., 2018); yeast can resist the damage of ethanol to cells through modification of the membrane, amino acids, trehalose and vacuolar proton-translocating ATPase functions (Saini et al., 2018). However, the tolerance mechanism of *Monascus* to the synergistic stress of lactic acid and ethanol has not been reported. The cell membrane is the key site to defend against environmental growth inhibitors, while the protection mechanism of the cell membrane is related to the kind and proportion of unsaturated fatty acids on the membrane because these fatty acids directly affect the fluidity of the phospholipid bilayer and the running capacity of carrier proteins on the membrane (Li et al., 2011;

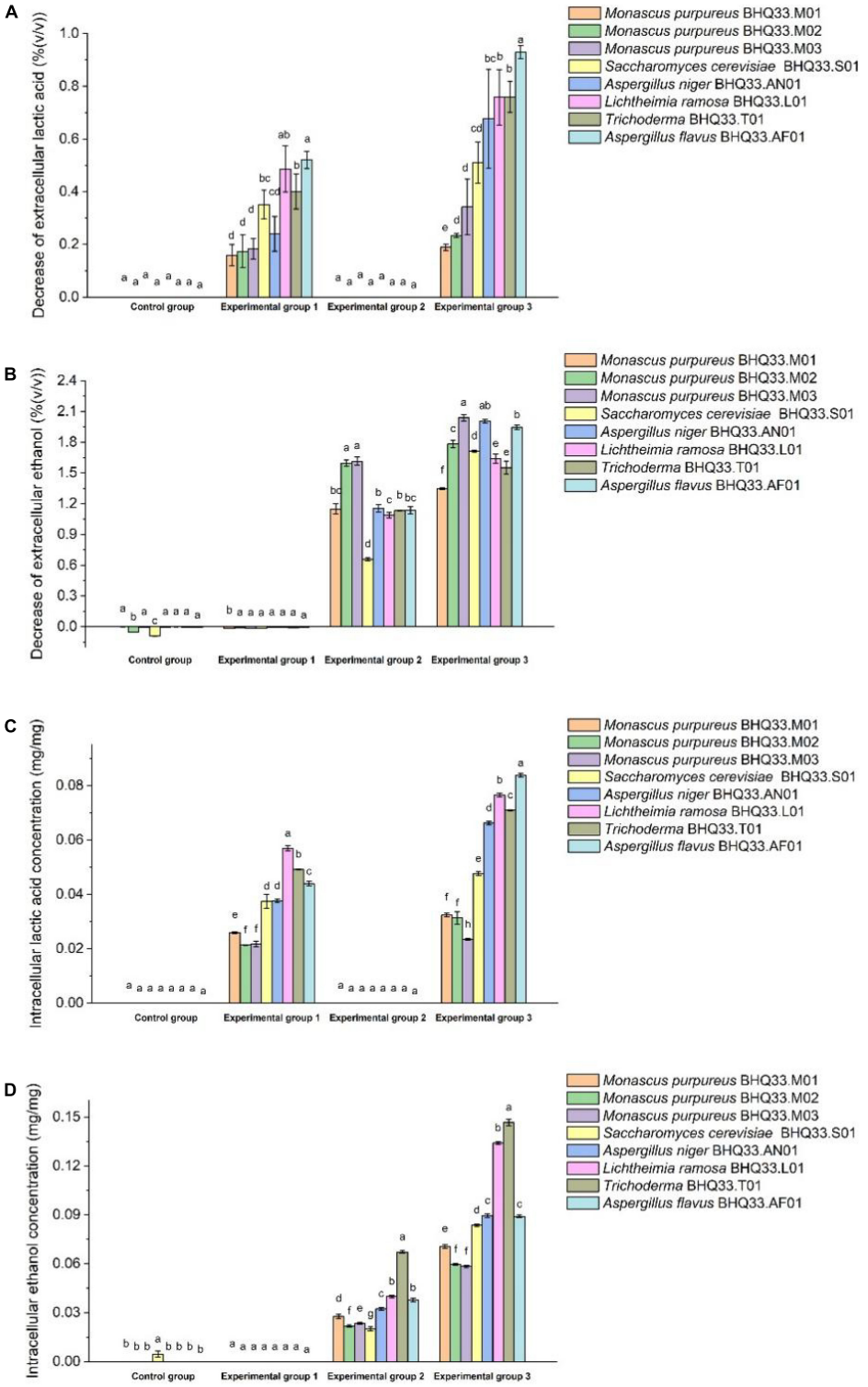

FIGURE 5 | Changes in intracellular and extracellular lactic acid and ethanol contents before and after fermentation by different fungi isolated from Hongqu BHQ33. Different fungi isolated from Hongqu BHQ33 were cultured in medium containing different concentrations of lactic acid and ethanol at 30°C and 200 r/min for 24 h, and the decrease of extracellular lactic acid **(A)**, the decrease of extracellular ethanol **(B)**, the accumulation of intracellular lactic acid **(C)** and the accumulation of intracellular ethanol **(D)** were detected. In the initial medium, control group was basal medium without lactate and ethanol, experimental group 1 was supplemented with 3.98% (v/v) lactic acid in basal medium, experimental group 2 with 6.24% (v/v) ethanol, and experimental group 3 with both 3.98% (v/v) lactic acid and 6.24% (v/v) ethanol. Error bars indicate the standard deviation (SD) of the means ($n = 3$), and different lowercase letters represent significant differences in the detection indexes of fungi isolated from Hongqu BHQ33 under the same treatment conditions ($p < 0.05$).

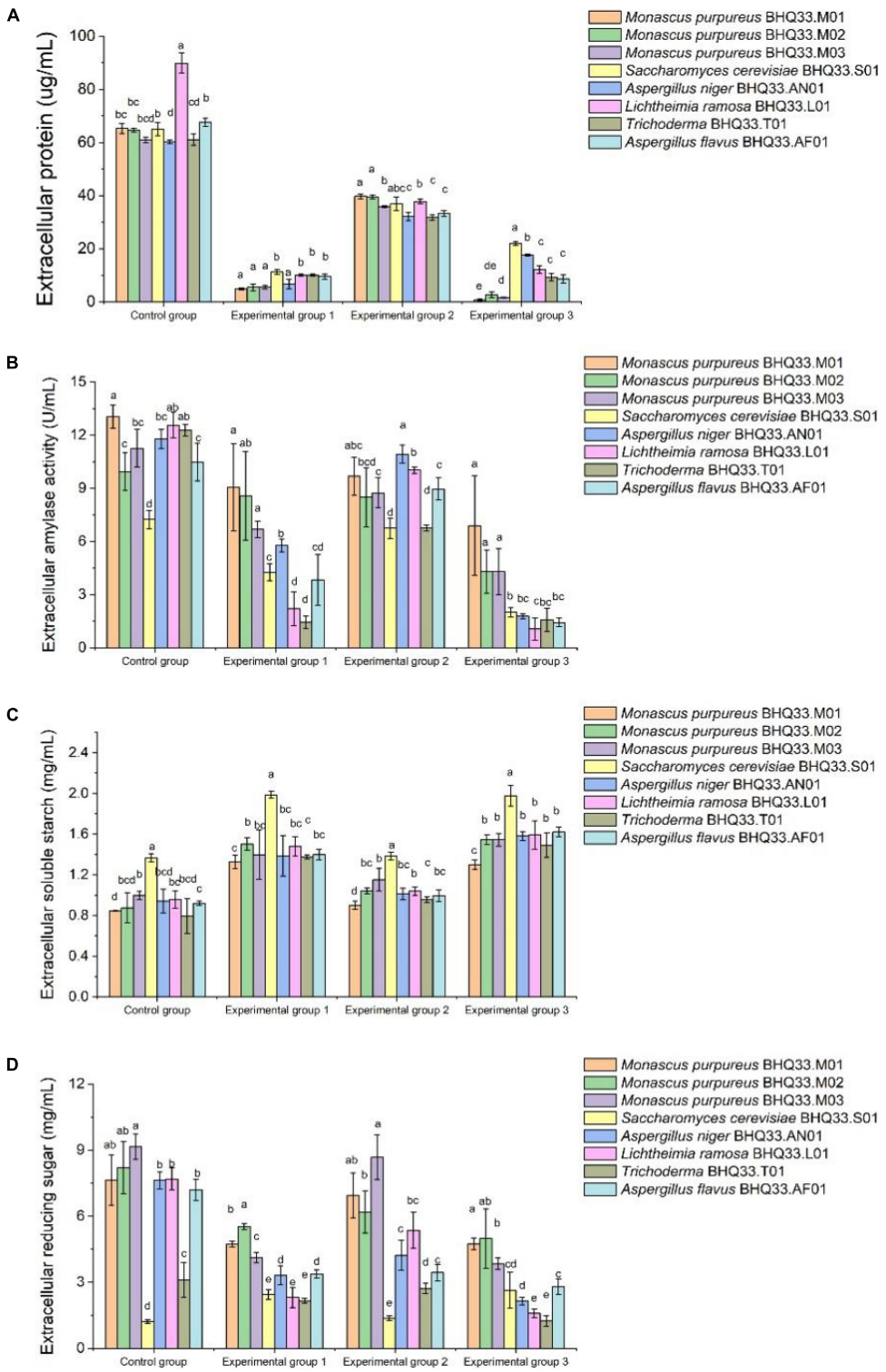

FIGURE 6 | Degradation and utilization of substrates by different fungi isolated from Hongqu BHQ33. Different fungi isolated from Hongqu BHQ33 were cultured in medium containing different concentrations of lactic acid and ethanol at 30°C and 200 r/min for 24 h, and extracellular protein concentration **(A)**, extracellular amylase activity **(B)**, extracellular soluble starch concentration **(C)**, and extracellular reducing sugar concentration **(D)** were detected. In the initial medium, control group was basal medium without lactate and ethanol, experimental group 1 was supplemented with 3.98% (v/v) lactic acid in basal medium, experimental group 2 with 6.24% (v/v) ethanol, and experimental group 3 with both 3.98% (v/v) lactic acid and 6.24% (v/v) ethanol. Error bars indicate the standard deviation (SD) of the means ($n = 3$), and different lowercase letters represent significant differences in the detection indexes of fungi isolated from Hongqu BHQ33 under the same treatment conditions ($p < 0.05$).

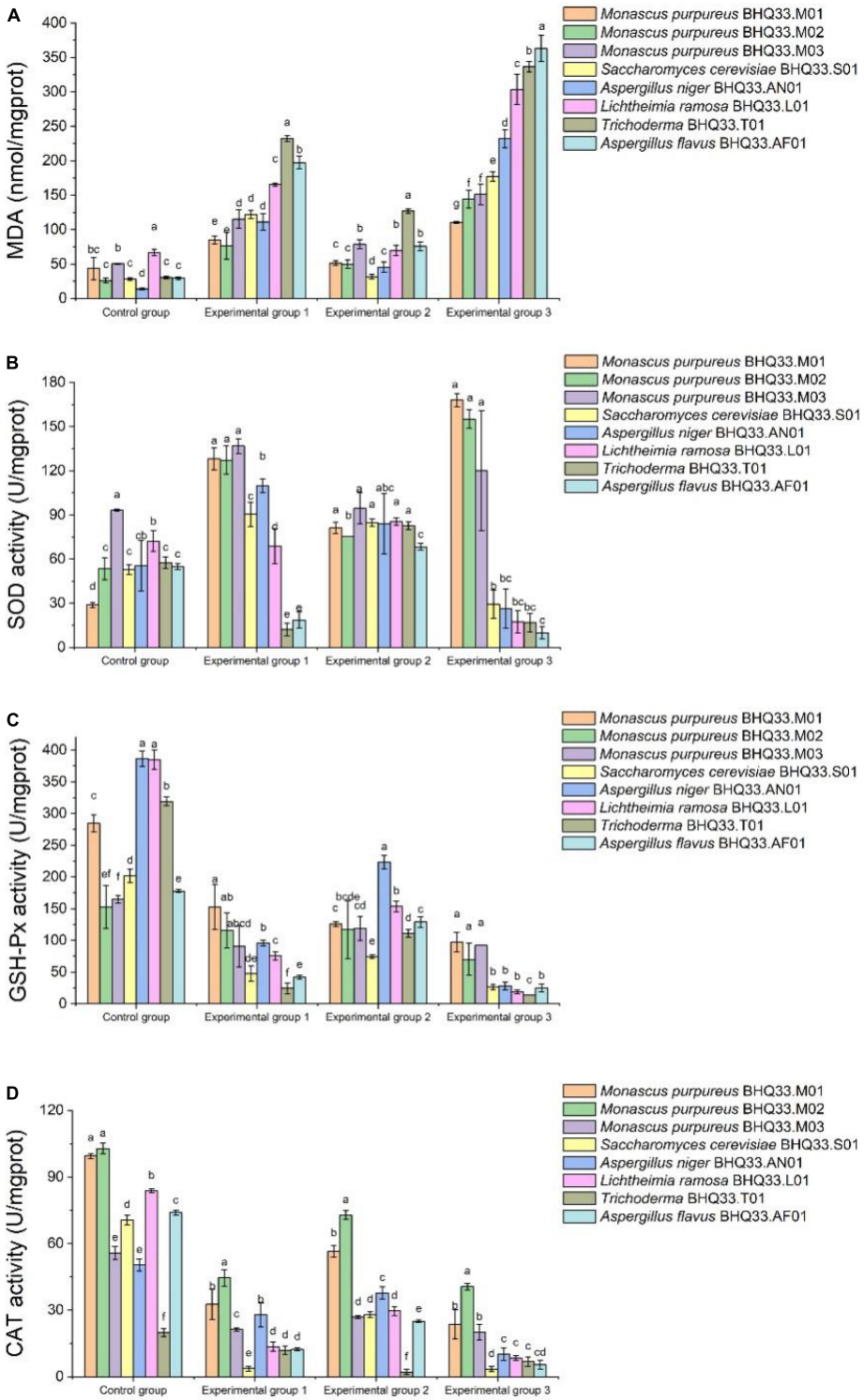

FIGURE 7 | Intracellular antioxidant capacity of different fungi isolated from Hongqu BHQ33 under lactic and ethanol stress. Different fungi isolated from Hongqu BHQ33 were cultured in medium containing different concentrations of lactic acid and ethanol at 30°C and 200 r/min for 24 h, and intracellular metabolites malondialdehyde (MDA) **(A)**, total superoxide dismutase (SOD) **(B)**, total glutathione peroxidase (GSH-Px) **(C)**, and catalase (CAT), **(D)** were detected. In the initial medium, control group was basal medium without lactate and ethanol, experimental group 1 was supplemented with 3.98% (v/v) lactic acid in basal medium, experimental group 2 with 6.24% (v/v) ethanol, and experimental group 3 with both 3.98% (v/v) lactic acid and 6.24% (v/v) ethanol. Error bars indicate the standard deviation (SD) of the means ($n = 3$), and different lowercase letters represent significant differences in the detection indexes of fungi isolated from Hongqu BHQ33 under the same treatment conditions ($p < 0.05$).

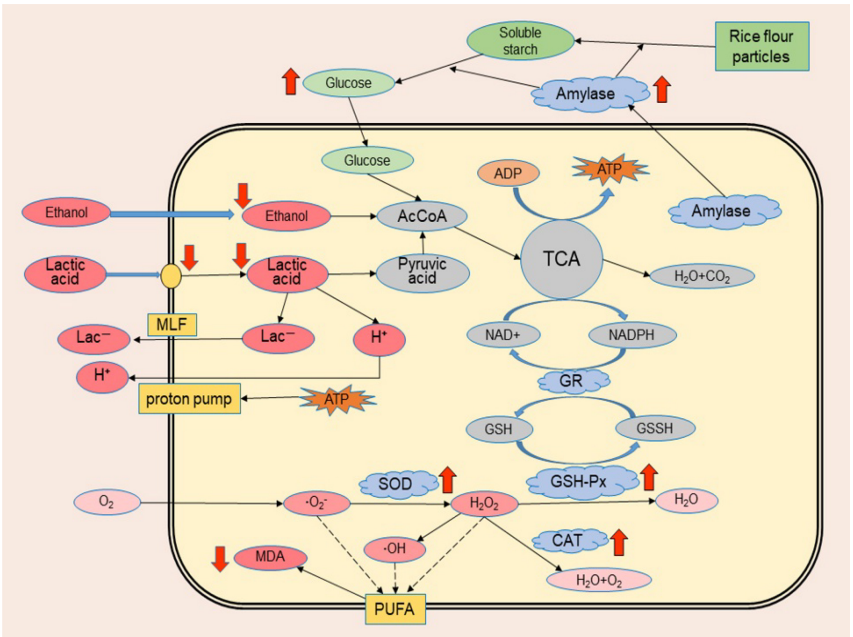

FIGURE 8 | Schematic illustration of the possible tolerance mechanism of *Monascus* to synergistic stress of lactic acid and ethanol. Red arrows indicate significant metabolic differences between *Monascus* and other fungi isolated from BHQ33 in the optimized restrictive medium containing both lactic acid and ethanol, with arrows up-regulated and arrows down-regulated.

Fonseca et al., 2019; Liu et al., 2020). For example, the addition of oleic acid to lipid-poor media significantly reduced oxidative damage to *Saccharomyces cerevisiae* cell membranes and resulted in improved resistance to oxidative stress (Landolfo et al., 2010). In addition, lactic acid and ethanol can cause oxidative damage to cells. Excessive reactive oxygen species will attack unsaturated fatty acids on the cell membrane, resulting in increased intracellular MDA, which may cause cross-linking polymerization of life macromolecules such as proteins and nucleic acids and have a toxic effect on cells (Talbi et al., 2019; Požgajová et al., 2020). The oxidative damage of unsaturated fatty acids also affects the resistance of the cell membrane to external growth inhibitors (Fonseca et al., 2019; Liu et al., 2020). *Monascus* has an active system of fatty acid metabolism (Peters et al., 1993; Moharram et al., 2012). The polyketide synthesis (pigment, lovastatin and citrinin) of *Monascus* are associated with fatty acid metabolism which also provides unsaturated long-chain fatty acids to serve as synthetic feedstocks for phospholipids on biological membranes (Wang, 2006; Panda and Ali, 2012; Balakrishnan et al., 2014; Thomanek et al., 2018). Therefore, it can be speculated that the simultaneous tolerance of *Monascus* to lactic acid and ethanol may be associated with the protective function of cell membranes, and this series of metabolic processes is involved in maintaining the structure and function of cell membranes. In the presence of higher concentrations of lactic acid and ethanol simultaneously, *Monascus* is more resistant to cell invasion by lactic acid than other fungi and alleviates the interference of lactic acid and ethanol on the normal metabolism of cells; intracellular antioxidant enzymes are able to reduce the oxidative damage of unsaturated fatty acids on the cell membrane; and higher activity of extracellular amylase and higher concentrations of extracellular reducing sugars are able to provide energy for the cell to defend against stress (**Figure 8**).

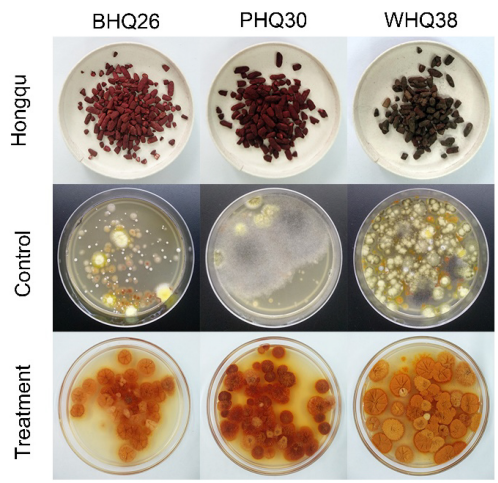

FIGURE 9 | Application of the optimized restricted medium for enrichment of *Monascus* from different Hongqu. The direct dilution coating method (control group) and the fermentation-coating method (treatment group) were used to separate *Monascus* from three Hongqu, respectively. Among them, BHQ26 is a Hongqu for rice wine brewing, PHQ33 is a Hongqu for pigment production, WHQ38 is a special Hongqu for rice wine brewing that contains more *Aspergillus niger* than other Hongqu.

It is worth mentioning that an attempt to prejudge by high-throughput sequencing how many kinds of *Monascus* species are present in the Hongqu BHQ33 revealed only *Monascus purpureus* in this sample (**Supplementary Figure 5**), but it is not clear how many different types of *Monascus* exist. This study obtained 3 strains of *Monascus purpureus* with different morphological types by using optimized restricted medium supplemented with lactic acid and ethanol (**Supplementary Figure 3**), which illustrated that a suitable culture method was able to increase the discrimination ability of *Monascus* species and subspecies levels and could also assist in analyzing the species distribution of *Monascus* in Hongqu at the species level.

Finally, this method was applied to *Monascus* enrichment from different types of Hongqu (**Figure 9**). Although the fungi in these Hongqu are very complex and diverse, *Monascus* pure culture can still be enriched and obtained by the restrictive medium based on the synergistic stress of lactic acid and ethanol. The feasibility of lactic acid and ethanol as regulators for directional enrichment of *Monascus* was verified. The possible mechanisms on the tolerance of *Monascus* to the synergistic stress of lactic acid and ethanol can be further explored by transcriptomics and metabolomics, which has important practical significance for the application of *Monascus* in fermentation.

CONCLUSION

The preparation of *Monascus* pure culture from Hongqu is easily interfered by other microorganisms. Therefore, the development of restrictive medium for *Monascus* enrichment from Hongqu is of great significance for the screening of excellent *Monascus* strains. This study showed that *Monascus* has good tolerance to lactic acid and ethanol, and retains the vitality of spore germination at high concentrations of lactic acid and ethanol. Under the synergistic stress of lactic acid and ethanol, *Monascus* pure culture can be directionally enriched from Hongqu at appropriate concentrations without affecting the morphological characteristics and metabolic function in *Monascus* progeny. *Monascus* can maintain the barrier function of of its cell membrane and help it defend against the synergistic stress of lactic acid and ethanol. The novel restrictive medium developed for *Monascus* enrichment from Hongqu based on the synergistic stress of lactic acid and ethanol is of great value for the construction of *Monascus* strain libraries and better development of their germplasm resources.

DATA AVAILABILITY STATEMENT

The datasets presented in this study can be found in online repositories. The names of the repository/repositories and accession number(s) can be found in the article/ **Supplementary Material**.

AUTHOR CONTRIBUTIONS

KZ, XL, and LN designed the experiments. KZ, LW, GC, and XZ carried out the experiments. KZ, WZ, and CZ analyzed the experimental results. KZ, XL, LN, ZL, and PR wrote the manuscript. All authors contributed to the article and approved the submitted version.

FUNDING

This work was supported by National Keypoint Research and Invention Program of the Thirteenth (No. 2018YFC1604106), University-Industry Cooperation Project of the Science and Technology Department of Fujian Province (No. 2019N5002).

SUPPLEMENTARY MATERIAL

The Supplementary Material for this article can be found online at: https://www.frontiersin.org/articles/10.3389/fmicb.2021.702951/full#supplementary-material

REFERENCES

Agboyibor, C., Kong, W., Chen, D., Zhang, A., and Niu, S. (2018). *Monascus* pigments production, composition, bioactivity and its application: a review. *Biocatal. Agric. Biotechnol.* 16, 433–447. doi: 10.1016/j.bcab.2018.09.012

Ai, M., Qiu, X., Huang, J., Wu, C., Jin, Y., and Zhou, R. (2019). Characterizing the microbial diversity and major metabolites of Sichuan bran vinegar augmented by *Monascus purpureus*. *Int. J. Food Microbiol.* 292, 83–90. doi: 10.1016/j.ijfoodmicro.2018.12.008

Balakrishnan, B., Kim, H. J., Suh, J. W., Chen, C. C., Liu, K. H., Park, S. H., et al. (2014). *Monascus azaphilone* pigment biosynthesis employs a dedicated fatty acid synthase for short chain fatty acyl moieties. *J. Korean Soc. Appl. Biol. Chem.* 57, 191–196. doi: 10.1007/s13765-014-4017-0

Balia, R. L., Kurnani, T. B. A., and Utama, G. L. (2018). Selection of mozzarella cheese whey native yeasts with ethanol and glucose tolerance ability. *Int. J. Adv. Sci. Eng. Inf. Technol.* 8, 1091–1097. doi: 10.18517/ijaseit.8.4.5869

Barbosa, R. N., Leong, S. L., Vinnere-Pettersson, O., Chen, A. J., Souza-Motta, C. M., Frisvad, J. C., et al. (2017). Phylogenetic analysis of *Monascus* and new species from honey, pollen and nests of stingless bees. *Stud. Mycol.* 86, 29–51. doi: 10.1016/j.simyco.2017.04.001

Cai, Q., Zhou, K., Liu, Z., Zhang, C., Zhang, W., and Ni, L. (2019). Studies on growth inhibitory factors of *Monascus* in the brewing process of Hongqu rice wine. *J. Chin. Inst. Food Sci. Technol.* 19, 143–149. doi: 10.16429/j.1009-7848.2019.10.017

Chysirichote, T., Takahashi, R., Asami, K., and Ohtaguchi, K. (2013). Effects of starch and protein on glucosamine content in the biomass of *Monascus ruber*. *J. Chem. Eng. Japan* 46, 695–698. doi: 10.1252/jcej.13we026

Eren, T., Atar, N., Yola, M. L., and Karimi-Maleh, H. (2015). A sensitive molecularly imprinted polymer based quartz crystal microbalance nanosensor for selective determination of lovastatin in red yeast rice. *Food Chem.* 185, 430–436. doi: 10.1016/j.foodchem.2015.03.153

Fonseca, F., Pénicaud, C., Tymczyszyn, E. E., Gómez-Zavaglia, A., and Passot, S. (2019). Factors influencing the membrane fluidity and the impact on production of lactic acid bacteria starters. *Appl. Microbiol. Biotechnol.* 103, 6867–6883. doi: 10.1007/s00253-019-10002-1

He, D., Liang, S., Liu, Z., Zhang, W., and Ni, L. (2016). Application of liquid-state Hong Qu to the brewing of Fujian Hong Qu glutinous rice wine. *J. Chin. Inst. Food Sci. Technol.* 16, 133–140. doi: 10.16429/j.1009-7848.2016.12.018

Hong, J., Chen, M., Zhou, W., Guo, W., Li, L., Huang, Z., et al. (2020). Effects of lactic acid bacteria on the growth of yeast and the formation of flavor

compounds in the fermentation of Hongqu glutinous rice wine. *J. Chin. Inst. Food Sci. Technol.* 20, 91–100. doi: 10.16429/j.1009-7848.2020.01.012

Huang, C., Wu, L., Lu, L., Zhang, Z., and Liu, Z. (2014). Isolation and identification of *Monascus* sp. strain with monacolin K producing ability from Guangxi red yeast rice. *China Condiment* 39, 36–40. doi: 10.3969/j.issn.1000-9973.2014.05.010

Huang, Z., Guo, W., Zhou, W., Li, L., Xu, J., Hong, J., et al. (2019). Microbial communities and volatile metabolites in different traditional fermentation starters used for Hong Qu glutinous rice wine. *Food Res. Int.* 121, 593–603. doi: 10.1016/j.foodres.2018.12.024

Huang, Z., Hong, J., Xu, J., Li, L., Guo, W., Pan, Y., et al. (2018). Exploring core functional microbiota responsible for the production of volatile flavour during the traditional brewing of Wuyi Hong Qu glutinous rice wine. *Food Microbiol.* 76, 487–496. doi: 10.1016/j.fm.2018.07.014

Jiang, Y., Lv, X., Zhang, C., Zheng, Y., Zheng, B., Duan, X., et al. (2019). Microbial dynamics and flavor formation during the traditional brewing of *Monascus* vinegar. *Food Res. Int.* 125:108531. doi: 10.1016/j.foodres.2019.108531

Landolfo, S., Zara, G., Zara, S., Budroni, M., Ciani, M., and Mannazzu, I. (2010). Oleic acid and ergosterol supplementation mitigates oxidative stress in wine strains of *Saccharomyces cerevisiae*. *Int. J. Food Microbiol.* 141, 229–235. doi: 10.1016/j.ijfoodmicro.2010.05.020

Lei, M., Liu, J., Fang, Y., Shao, Y., Li, L., Yu, J. H., et al. (2019). Effects of different g-protein α-subunits on growth, development and secondary metabolism of *Monascus ruber* M7. *Front. Microbiol.* 10:1555. doi: 10.3389/fmicb.2019.01555

Li, X., Wang, J., Bu, D., Wei, H., Hu, H., and Zhou, L. (2011). Advanced research of effect of polyunsaturated fatty acids on cell membrane function. *Biotechnol. Bull.* 12, 22–26.

Liang, Z., Lin, X., He, Z., Li, W., Ren, X., and Lin, X. (2020). Dynamic changes of total acid and bacterial communities during the traditional fermentation of Hong Qu glutinous rice wine. *Electron. J. Biotechnol.* 43, 23–31. doi: 10.1016/j.ejbt.2019.12.002

Liu, P., Zheng, X., Duan, C., Chen, B., and Yan, G. (2020). A review of the effect of unsaturated fatty acids on the cell growth and aroma production of *Saccharomyces cerevisiae* during fermentation. *Food Sci.* 41, 314–322. doi: 10.7506/spkx1002-6630-20190729-397

Liu, Z., Wang, Z., Lv, X., Zhu, X., Chen, L., and Ni, L. (2018). Comparison study of the volatile profiles and microbial communities of Wuyi Qu and Gutian Qu, two major types of traditional fermentation starters of Hong Qu glutinous rice wine. *Food Microbiol.* 69, 105–115. doi: 10.1016/j.fm.2017.07.019

Lv, X., Chen, Z., Jia, R., Liu, Z., Wen, Z., Shaojun, C., et al. (2015). Microbial community structure and dynamics during the traditional brewing of Fuzhou Hong Qu glutinous rice wine as determined by culture-dependent and culture-independent techniques. *Food Control* 57, 216–224. doi: 10.1016/j.foodcont.2015.03.054

Lv, X., Jia, R., Li, Y., Chen, F., Chen, Z., Liu, B., et al. (2016). Characterization of the dominant bacterial communities of traditional fermentation starters for Hong Qu glutinous rice wine by means of MALDI-TOF mass spectrometry fingerprinting, 16S rRNA gene sequencing and species-specific PCRs. *Food Control* 67, 292–302. doi: 10.1016/j.foodcont.2016.03.005

Lv, X., Weng, X., Han, M., Zhang, W., Rao, P., and Ni, L. (2012). Identification and characterization of *Monascus sp.* from Fujian Hongqu. *J. Chin. Inst. Food Sci. Technol.* 12, 88–97. doi: 10.16429/j.1009-7848.2012.02.019

Moharram, A. M., Mostafa, M. E., and Ismail, M. A. (2012). Chemical profile of *Monascus ruber* strains. *Food Technol. Biotechnol.* 50, 490–499. doi: 10.1016/j.ifset.2012.09.007

Panda, B. P., and Ali, M. (2012). Reduction of citrinin biosynthesis by fatty acids in *Monascus* fermented food. *World Mycotoxin J.* 5, 163–167. doi: 10.3920/wmj2011.1335

Park, H. G., Stamenova, E. K., and Jong, S. C. (2004). Phylogenetic relationships of *Monascus* species inferred from the ITS and the partial b-tubulin gene. *Bot. Bull. Acad. Sin.* 47, 325–330. doi: 10.7016/BBAS.200410.0325

Park, K. H., Liu, Z., Park, C. S., and Ni, L. (2016). Microbiota associated with the starter cultures and brewing process of traditional Hong Qu glutinous rice wine. *Food Sci. Biotechnol.* 25, 649–658. doi: 10.1007/s10068-016-0115-6

Peters, N., Panitz, C., and Kunz, B. (1993). The influence of carbohydrate dissimilation on the fatty acid metabolism of *Monascus purpureus*. *Appl. Microbiol. Biotechnol.* 39, 589–592. doi: 10.1007/bf00205057

Požgajová, M., Navrátilová, A., Šebová, E., Kovár, M., and Kačániová, M. (2020). Cadmium-induced cell homeostasis impairment is suppressed by the tor1 deficiency in fission yeast. *Int. J. Mol. Sci.* 21:7847. doi: 10.3390/ijms21217847

Prasirtsak, B., Thitiprasert, S., Tolieng, V., Assabumrungrat, S., Tanasupawat, S., and Thongchul, N. (2017). Characterization of D-lactic acid, spore-forming bacteria and *Terrilactibacillus laevilacticus* SK5-6 as potential industrial strains. *Ann. Microbiol.* 67, 763–778. doi: 10.1007/s13213-017-1306-y

Ren, X., He, Z., Lin, X., Lin, X., Liang, Z., Liu, D., et al. (2021). Screening and evaluation of *Monascus purpureus* FJMR24 for enhancing the raw material utilization rate in rice wine brewing. *J. Sci. Food Agric.* 101, 185–193. doi: 10.1002/jsfa.10630

Saini, P., Beniwal, A., Kokkiligadda, A., and Vij, S. (2018). Response and tolerance of yeast to changing environmental stress during ethanol fermentation. *Process Biochem.* 72, 1–12. doi: 10.1016/j.procbio.2018.07.001

Sakural, Y., Lee, H. G., and Shiota, H. (1977). On the convenient method for glucosamine estimation in koji. *Agric. Biol. Chem.* 41, 619–624. doi: 10.1080/00021369.1977.10862552

Shin, H. M., Lim, J. W., Shin, C. G., and Shin, C. S. (2017). Comparative characteristics of rice wine fermentations using *Monascus* koji and rice nuruk. *Food Sci. Biotechnol.* 26, 1349–1355. doi: 10.1007/s10068-017-0187-y

Talbi, W., Ghazouani, T., Braconi, D., Ben Abdallah, R., Raboudi, F., Santucci, A., et al. (2019). Effects of selenium on oxidative damage and antioxidant enzymes of eukaryotic cells: wine *Saccharomyces cerevisiae*. *J. Appl. Microbiol.* 126, 555–566. doi: 10.1111/jam.14150

Thomanek, N., Arends, J., Lindemann, C., Barkovits, K., Meyer, H. E., Marcus, K., et al. (2018). Intricate crosstalk between lipopolysaccharide, phospholipid and fatty acid metabolism in *Escherichia coli* modulates proteolysis of LpxC. *Front. Microbiol.* 9:3285. doi: 10.3389/fmicb.2018.03285

Tian, Y., Huang, J., Xie, T., Huang, L., Zhuang, W., Zheng, Y., et al. (2016). Oenological characteristics, amino acids and volatile profiles of Hongqu rice wines during pottery storage: effects of high hydrostatic pressure processing. *Food Chem.* 203, 456–464. doi: 10.1016/j.foodchem.2016.02.116

Wang, C., Cui, Y., and Qu, X. (2018). Mechanisms and improvement of acid resistance in lactic acid bacteria. *Arch. Microbiol.* 200, 195–201. doi: 10.1007/s00203-017-1446-2

Wang, P. (2006). *Cloning and Analysis of the Monacolin K cDNA Encoding Biosynthesis Related Genes in Monascus purpureus BCRC 31615*. Master's thesis. Taibei: National Taiwan University.

Weusthuis, R. A., Mars, A. E., Springer, J., Wolbert, E. J., Wal, H. V. D., Vrije, T. G. D., et al. (2017). *Monascus ruber* as cell factory for lactic acid production at low pH. *Metab. Eng.* 42, 66–73. doi: 10.1016/j.ymben.2017.05.005

Xiong, Z., Cao, X., Wen, Q., Chen, Z., Cheng, Z., Huang, X., et al. (2019). An overview of the bioactivity of monacolin K / lovastatin. *Food Chem. Toxicol.* 131:110585. doi: 10.1016/j.fct.2019.110585

Xu, M., Lv, X., Liu, Z., Zhang, W., and Ni, L. (2014). Identification and characterization of *Rhizopus sp.* from Fujian White Koji. *J. Chin. Inst. Food Sci. Technol.* 14, 205–210. doi: 10.16429/j.1009-7848.2014.03.049

Yang, Y., Xia, Y., Lin, X., Wang, G., Zhang, H., Xiong, Z., et al. (2018). Improvement of flavor profiles in Chinese rice wine by creating fermenting yeast with superior ethanol tolerance and fermentation activity. *Food Res. Int.* 108, 83–92. doi: 10.1016/j.foodres.2018.03.036

Zhang, R., Li, Q., Zhu, L., Liu, C., and Li, Y.-X. (2018). Study on the γ-aminobutyric acid (GABA) in highland barley *Monascus* beer. *J. Food Sci. Biotechnol.* 37, 1148–1152. doi: 10.3969/j.issn.1673-1689.2018.11.005

Zhang, W., Cai, Q., Rao, T., Zhou, K., Huang, Y., Liu, Z., et al. (2015). Analysis of dominate fungal community and characteristics of Gutian Hong Qu. *J. Chin. Inst. Food Sci. Technol.* 15, 180–185. doi: 10.16429/j.1009-7848.2015.12.025

Zhou, W., Guo, R., Guo, W., Hong, J., Li, L., Ni, L., et al. (2019). *Monascus* yellow, red and orange pigments from red yeast rice ameliorate lipid metabolic disorders and gut microbiota dysbiosis in Wistar rats fed on a high-fat diet. *Food Funct.* 10, 1073–1084. doi: 10.1039/c8fo02192a

Conflict of Interest: The authors declare that the research was conducted in the absence of any commercial or financial relationships that could be construed as a potential conflict of interest.

frontiers in Microbiology

ORIGINAL RESEARCH
published: 24 June 2021
doi: 10.3389/fmicb.2021.672661

pH Changes Have a Profound Effect on Gene Expression, Hydrolytic Enzyme Production, and Dimorphism in *Saccharomycopsis fibuligera*

*Mohamed El-Agamy Farh, Najib Abdellaoui and Jeong-Ah Seo**

School of Systems Biomedical Science, Soongsil University, Seoul, South Korea

Saccharomycopsis fibuligera is an amylolytic yeast that plays an important role within *nuruk* (a traditional Korean fermentation starter) used for the production of *makgeolli* (Korean rice wine), which is characterized by high acidity. However, the effect of pH change (neutral to acidic) on the yeast cell to hyphal transition and carbohydrate-hydrolyzing enzyme activities for *S. fibuligera* has not been investigated yet. In this study, *S. fibuligera* strains were cultured under the different pH conditions, and the effect on the enzyme production and gene expression were investigated. An acidic pH induced a hyphal transition from yeast cell of *S. fibuligera* KPH12 and the hybrid strain KJJ81. In addition, both strains showed a gradual decrease in the ability to degrade starch and cellulose as the pH went down. Furthermore, a transcriptome analysis demonstrated that the pH decline caused global expression changes in genes, which were classified into five clusters. Among the differentially expressed genes (DEGs) under acidic pH, the downregulated genes were involved in protein synthesis, carbon metabolism, and *RIM101* and cAMP-PKA signaling transduction pathways for the yeast-hyphal transition. A decrease in pH induced a dimorphic lifestyle switch from yeast cell formation to hyphal growth in *S. fibuligera* and caused a decrease in carbohydrate hydrolyzing enzyme production, as well as marked changes in the expression of genes related to enzyme production and pH adaptation. This study will help to elucidate the mechanism of adaptation of *S. fibuligera* to acidification that occur during the fermentation process of *makgeolli* using *nuruk*.

Keywords: *Saccharomycopsis fibuligera*, *nuruk*, transcriptome analysis, yeast cell-hyphae transition, pH effect, starch and cellulose hydrolysis

OPEN ACCESS

Edited by:
Xucong Lv,
Fuzhou University, China

Reviewed by:
Du Zhu,
Jiangxi Science and Technology Normal University, China
Giacomo Zara,
University of Sassari, Italy

****Correspondence:***
Jeong-Ah Seo
sja815@ssu.ac.kr

Specialty section:
This article was submitted to Food Microbiology, a section of the journal Frontiers in Microbiology

Received: *26 February 2021*
Accepted: *25 May 2021*
Published: *24 June 2021*

Citation:
Farh ME-A, Abdellaoui N and Seo J-A (2021) pH Changes Have a Profound Effect on Gene Expression, Hydrolytic Enzyme Production, and Dimorphism in Saccharomycopsis fibuligera. Front. Microbiol. 12:672661. doi: 10.3389/fmicb.2021.672661

INTRODUCTION

The Korean traditional wine *makgeolli* is made by fermenting the starch materials of rice (Jang, 1989; Yeo and Jeong, 2010). High-quality *makgeolli* is characterized by high acidity and alcohol content (Song et al., 2015). Over 100 traditional *makgeolli* brands are available, and they are worth millions of dollars on the market (Jang, 1989; Yeo and Jeong, 2010). To produce *makgeolli*, the fermentation starter *nuruk* needs to be prepared from several kinds of grains, especially rice grains, using airborne microorganisms. These microorganisms provide a source of several hydrolytic enzymes that are required for starch degradation during saccharification to produce glucose and

other organic acids (Song, 2013; Yang et al., 2013; Bal et al., 2014, 2015; Kim et al., 2014; Park et al., 2016). Then, glucose is fermented by *Saccharomyces cerevisiae* to produce alcohol. Thus, the quality of alcohol in *makgeolli* critically depends on the characteristics of the *nuruk* used for fermentation. The saccharification capability is an essential index used to estimate the quality of the *nuruk* (Lee et al., 2017), and it is based on microorganisms that occupy the *nucleus* and produce hydrolytic enzymes (Lee et al., 2017). Currently, several *nuruk*-inhabiting fungi, yeasts, and bacteria have been isolated from traditional *nuruk* and used to make commercial *nuruk* products (Jo and Lee, 1997; Seo et al., 2007; Carroll et al., 2017).

Since *nuruk* ingredients are mainly composed of polysaccharides, predominant microorganisms capable of degrading polysaccharides in *nuruk* include filamentous fungi, such as *Rhizopus oryzae* and *Aspergillus oryzae* (Kim et al., 2014). Because of the temperature increase during fermentation, the heat-resistant strain *A. oryzae* has an advantage over the heat-labile strain *R. oryzae* (Yang et al., 2011). *A. oryzae* secretes amylases at high levels (Norihiro et al., 1989; Liu et al., 2014) and is thus an important fungus for the saccharification step (Yang et al., 2011, 2013; Song, 2013). There have also been attempts to use alternative and more beneficial and risk-free yeasts, such as *Monascus* (Shin et al., 2017) and *Saccharomycopsis fibuligera* (Park et al., 2014). Of the microorganisms involved in *nuruk* fermentation, another important microorganism is *S. fibuligera*, a member of Saccharomycotina, which is a subphylum of Ascomycota. *S. fibuligera* is characterized by a morphology-switching lifestyle known as dimorphism and can propagate by branched hyphal growth or yeast cell-like growth (Kurtzman and Smith, 2011). *S. fibuligera* is considered the best producer of amylolytic enzymes among all ascomycetous yeasts (de Mot et al., 1984). It was found to be a predominant yeast in various Asian fermentation starters, including *nuruk* in Korea (Bal et al., 2014; Carroll et al., 2017; Farh et al., 2017). It produces cellulose-degrading enzymes that play a key role in the saccharification process of lignocellulosic compounds (Ma et al., 2015; Van Zyl et al., 2016). Ethanol can be produced from carbohydrate-type substrates by cocultivation of *S. fibuligera* with ethanol producers such as *S. cerevisiae* and *Zymomonas mobiliz* (Abouzied and Reddy, 1987; Reddy and Basappa, 1996; Park et al., 2014).

Saccharification by *nuruk* mostly produces simple sugars. Glucose is mainly fermented by *S. cerevisiae,* while other sugars can be converted by other microorganisms into organic acids, resulting in a decline in pH from neutral to acidic. The pH is weakly basic to neutral at the starting point, suddenly becomes strongly acidic (pH 3.31–2.96), and slightly increases to 3.34 at the end of the fermentation process (Song et al., 2015). The dynamic pH change during fermentation could affect the growth, morphology and physiology of microorganisms involved in fermentation. Some microorganisms, such as *Sclerotinia sclerotiorum*, a plant necrotrophic pathogen, and *Ustilago maydis*, a filamentous and pathogenic form of the dimorphic biotrophic pathogen, grow well under acidic pH (Cotton et al., 2003), whereas other microorganisms, such as *Candida albicans* and *Cryptococcus neoformans,* show better growth under alkaline pH conditions (Davis, 2003; O'Meara and Alspaugh, 2012). In addition, certain environmental microorganisms, such as *Yarrowia lipolytica,* favor dimorphic growth under ambient pH conditions but secrete protein-degrading enzymes under both acidic and alkaline pH conditions (Gonzalez-Lopez et al., 2002; Ruiz-Herrera and Sentandreu, 2002). Thus, environmental pH greatly influences the growth and activity of microorganisms. Microorganisms should sense the environmental pH and adapt to the conditions. To understand such adaptation, signaling cascades have been elucidated in various types of yeast and filamentous fungi at the molecular level, and they consist of MAPK, cAMP-PKA, and PacC/Rim101. MAPK and cAMP-PKA have also been shown to regulate dimorphic growth and morphology-dependent pathogenesis (Leberer et al., 2001; Martínez-Espinoza et al., 2004; Kozubowski et al., 2009), whereas PacC/Rim101 is involved in the regulation of adhesins, secretion of hydrolytic enzymes, and resistance to sodium and lithium (Cotton et al., 2003; Cornet and Gaillardin, 2014).

The pH change occurs during fermentation in the process of rice wine production. However, little is known about the effect of pH change on the growth and activity of microorganisms that grow in *nuruk*, such as *S. fibuligera*. In this study, we examined the effect of dynamic pH changes on the growth and physiology of *S. fibuligera* strain KPH12 and its newly discovered interspecies hybrid KJJ81 (Choo et al., 2016) by focusing on hydrolytic enzyme production, dimorphism, and gene expression. We provided evidence that KPH12 and the hybrid strain KJJ81 of *S. fibuligera* showed a morphological switch from the yeast-like form to hyphae-like elongated form in response to pH reduction. In addition, we identified the gene classes that were dramatically upregulated and downregulated due to the pH change occurring during fermentation.

MATERIALS AND METHODS

Strains, Medium, and Growth Conditions

Saccharomycopsis fibuligera KJJ81 and KPH12 strains were obtained from the original authors and used in this study. Here, the strains were routinely cultured on yeast extract peptone glucose (YPG) agar medium [2% (w/v) glucose, 1% (w/v) yeast extract, 1% (w/v) peptone, 2% (w/v) agar, pH 6.0] which was modified with YEPD described as the previous report (Zhu et al., 2017). To test the pH effect on hydrolytic enzyme secretion, yeast cells of each strain (10^7 CFU/ml) were spotted on YPG agar buffered with phosphate buffer (0.2 M disodium hydrogen phosphate, and 0.2 M sodium dihydrogen phosphate) for pH 7.0 and citrate buffer (0.1 M citric acid, and 0.1 M sodium citrate) for pH 6.0, 5.0, 4.0, and 3.0. Three sets of buffered medium were inoculated with each strain; the first set was supplemented with 0.2% (w/v) starch to assess starch degradation, the second set was supplemented with 0.2% (w/v) carboxymethylcellulose (CMC) to estimate cellulose degradation, and the third set was supplemented with 2% (w/v) skim milk to estimate protein degradation. The inoculated plates were incubated at 25°C. Starch degradation was examined 3 days after incubation, and cellulose and protein degradation was examined

5 days after incubation. To test the pH effect on dimorphic growth, yeast cells of both strains (10^6 CFU/ml) were cultured in YPG broth buffered as described above. The inoculated broths were incubated at 25°C with shaking (200 rpm), and the cell morphology was examined 20 h after incubation; the proportion of yeast and hyphal cells was measured under a light microscope as described for *Y. lipolytica* (Ruiz-Herrera and Sentandreu, 2002). To test whether the pH or glucose concentration plays a role in hydrolytic enzyme production, particularly those for starch and cellulose degradation, the yeast cells of both strains were spotted on YPG agar [2% (w/v)] plates supplemented with 0.1, 0.5, 2, or 10% (w/v) glucose. For each concentration, one type of substrate was added to estimate the degradation under three different buffered conditions: non-buffered, pH 7-buffered (using phosphate buffer), and pH 3-buffered (using citrate buffer) conditions. To test the effect of glucose or pH on dimorphism regulation, yeast cells of both strains were grown on YPG broth supplemented with the glucose concentrations set mentioned above under the same three buffered conditions. To confirm the involvement of cAMP-PKA in hyphal growth induction, the yeast cells of both strains were grown in pH 4-buffered YPG broth and agar supplemented with 600 μM clozapine, a cAMP-PKA blocker. Clozapine was filter-sterilized and added to autoclaved medium after cooling. Cells were cultured on clozapine-free broths and plates as controls. The inoculated plates were incubated at 25°C for 5 days, while inoculated broths were incubated at 25°C with shaking (200 rpm) for 20 h. Hyphae development was examined using a light microscope.

Scanning Electron Microscopy (SEM)

Cells grown in YPG at different pH values starting from pH 7.0 to pH 3.0 were collected by filtration and prepared for SEM examination as described previously (Staniszewska et al., 2013) with some modifications. Cells were suspended in fixation buffer [2.5% (w/v) glutaraldehyde in 0.2 M cacodylate buffer, pH 7.2–7.4] for 19 h at 4°C. Samples were washed three times with 0.05 M sodium cacodylate buffer and subsequently suspended in 2% (w/v) osmium tetroxide and 0.1 M cacodylate buffer (1:1, v/v) for further fixation. Afterward, initial dehydration of cells was carried out by placing them in serial concentrations of 50 and 70% ethanol two times for 10 min each; 95% ethanol two times for 5 min each; and 100% ethanol two times for 1 min each. The final dehydration step was carried out by placing the samples in liquid CO_2 for 90 min following the critical drying point method. Subsequently, the samples were subjected to silver coating under vacuum evaporation and examined by SEM.

RNA-Seq Analysis

To examine the whole transcriptional responses at each pH point, yeast cells were grown in YPG broth buffered at different pH values starting from 7.0 to 3.0 as described above. Cells were collected 18 h after incubation using vacuum filtration and rapidly stored at –80°C. Total RNA was prepared using an easy-spin total RNA extraction kit (iNtRON, South Korea), and sequencing of the total RNA was performed using an Illumina HiSeq 2500 instrument (Illumina, United States). Complementary DNA (cDNA) libraries were constructed at Theragen Etex Bioinstitute (Seoul, South Korea). Pair-end RNA sequencing was performed by the company as reported previously (Mardis, 2008). Clean reads with high nucleotide accuracy were aligned with the genomes of either KPH12 or KJJ81 using Burrows-Wheeler Aligner (BWA) (Li and Durbin, 2009), and the total counting, expressed as RPKM (reads per kilobase of transcript, per million mapped reads), of the aligned fragments with the exon parts of the genes was determined using HTSeq (Anders et al., 2015). Counts were normalized to be expressed as RPKHM (reads per kilobase of transcript per hundred million mapped reads). The predicted protein was blasted against the NCBI database of non-redundant protein sequences (nr), Uniprot, and relative fungi RefSeq (i.e., *S. cerevisiae*, *C. glabrata*, *A. oryzae*, and *S. pombe*) databases with a E-value cutoff of 10^{-10}. The raw data were filtered to remove the genes with zero reads among all samples and then transformed. Filtration and transformation were performed using the R package EdgeR (Robinson et al., 2010). A multidimensional scaling (MDS) plot was generated to show the variation in the expression of genes in the samples using the R package *mixOmics* (Rohart et al., 2017). Differentially expressed genes (DEGs) were determined by EdgeR, and *P*-values were controlled using the false discovery rate (FDR) (Benjamini and Hochberg, 1995) with a threshold lower than 0.05.

For the clustering analysis, the average RPKM of the DEG lists of KPH12 and KJJ81 was clustered using the R package *Mfuzz*. Five clusters were identified, and the fuzzifier coefficient was set to optimal. Following the clustering analysis, genes in each cluster with memberships lower than 0.5 were excluded and the remaining genes were subjected to a Gene Ontology (GO) enrichment analysis. GO enrichments of chosen clusters were filtered using the online public website REVIGO, and the resulting GO terms were visualized on Cytoscape.

Reverse Transcription, PCR, and Quantitative Reverse Transcription-PCR (qRT-PCR)

Prior to sending the RNA samples for RNA sequencing, aliquots were obtained for qRT-PCR validation of the gene of interest. Samples were kept at –80°C until cDNA synthesis. Only samples at pH 7 and pH 3 were considered for the qRT-PCR validation for the gene of interest. cDNAs were synthesized using SuperScript III First-Strand (Invitrogen, United States) according to protocols provided by the manufacturer. Two micrograms of total RNA was mixed with the synthesis mixture at a volume of 20 μl, and the total volume was further diluted to 50 μl for qRT-PCR. Primer pairs of target genes were designed manually after aligning the gene sequences of the KPH12 and A and B genomes of KJJ81 using ClustalX2 (Larkin et al., 2007) and chemically synthesized (Macrogen Inc., Seoul, South Korea). The primers used in this study are listed in **Supplementary Table 7**. Quantitative real-time PCR (qRT-PCR) was carried out in a 10 μl reaction volume consisting of 1 μl cDNA, 10 pmol each of forward and reverse primers, 5 μl 2X iQ™ SYBR® Green Supermix (BioRad, United States), and water to the final volume. Reactions were carried out using a CFX Connect™

Real-Time System (Bio-Rad, United States) in a Hard-Shell® 96-Well PCR Plate (Bio-Rad, United States). Among the well-known housekeeping genes, *Y*-tubulin (*TUB4*) was selected as a control since it showed the most stable expression throughout all pH values. The following thermal cycler conditions were based on the manufacturer's recommendations: 3 min at 95°C; 39 cycles at 95°C for 10 s and the proper annealing temperature for 30 s; and one more cycle starting from 65 to 95°C for 5 s in 0.5°C increments for the melt curve analysis. The fluorescent product was detected during the annealing step of each cycle. Amplification, detection, and data analysis were performed on a CFX Manager™ Maestro version 1.0 (Bio-Rad, United States). The relative fold differences in template abundance for each sample were determined by deducting the C_T value of each gene expression from the C_T value of *TUB4*.

Statistical Analysis

All data were analyzed using SPSS v. 26.0 software (SPSS Inc., Chicago, IL, United States). The statistical analysis includes comparison of group mean values with one-way ANOVA, and multiple comparisons among the groups with Scheffe *post-hoc* test at a significance level of $p < 0.05$.

Accession Numbers

The RNA-seq raw data were deposited in the BioSample database of NCBI. The accession numbers are serial numbers from SRX10182890 to SRX10182919.

RESULTS

Acidic pH but Not Glucose Causes Dimorphic Growth of *S. fibuligera*

The effect of the pH change occurring during fermentation on the growth of *S. fibuligera* was investigated by growing *S. fibuligera* on YPG medium with different pH values, and we examined the morphology. Various pH values were used to mimic the pH change occurring during fermentation. Both the KPH12 and KJJ81 strains of *S. fibuligera* were grown on these plates and observed for morphological changes. For both the KPH12 and KJJ81 strains, when the pH of the medium was decreased from pH 7 to pH 3, the number of yeast-type cells gradually decreased, and concomitantly, the number of cells with hyphae increased (**Figures 1A,C**), indicating that a decline in the pH value induced the dimorphic growth of *S. fibuligera*. The single cells started to elongate at pH 6 for both strains, indicating that hyphal growth is induced at pH 6. The interspecies hybrid strain KJJ81 was more responsive to the change in pH in terms of hyphal growth than KPH12 (**Figures 1B,D**).

Previously, we showed that the glucose concentration controls the dimorphic growth and hydrolytic enzyme production of *S. fibuligera* KPH12 and KJJ81 (Choo et al., 2016). During fermentation, the glucose concentration also changes because of starch or carbohydrate degradation in *nuruk*. Thus, to obtain a better understanding of the underlying cause of the dimorphic switch in the growth of *S. fibuligera* during fermentation, we examined the effect of glucose concentration on dimorphic changes. Under non-buffered conditions, both strains showed that the yeast-to-hyphae switch was induced when the glucose concentration changed from 0.1 to 10% (**Figure 2** and **Supplementary Figure 1**). Yeast cells were dominant at the lowest glucose concentration, whereas hyphal cells were dominant at the highest glucose concentration (**Figures 2A,D** and **Supplementary Figures 1A,C**). Since *S. fibuligera* was grown under non-buffered conditions, the pH may have changed during the incubation and subsequently affected the yeast-to-hyphae switch. Thus, to assess the pH effect on the yeast-to-hyphae switch, we measured the pH at each glucose concentration 20 h after incubation with both strains and found that the pH was changed from neutral to weakly basic in 0.1% glucose, whereas the pH was acidic in 2–10% glucose (**Supplementary Figures 1B,D**). Both strains developed complete hyphal growth under buffered conditions at pH 3 (**Figures 2B,E** and **Supplementary Figures 1A,C**) and yeast growth (**Figures 2C,F** and **Supplementary Figures 1A,C**) regardless of the glucose concentration. These results suggest that both carbohydrate degradation and dimorphism are regulated by pH change and not by glucose concentration.

pH Change (Not Glucose Concentration) Has a Suppressive Effect on the Secretion of Hydrolytic Enzymes From *S. fibuligera*

The effect of pH change on fermentation was examined by investigating the degradation of carbohydrates (e.g., starch and cellulose) and proteins by *S. fibuligera*. Both strains of *S. fibuligera* were grown on plates with different pH values ranging from 7 to 3. The pH of the plate was maintained using specific buffers. *S. fibuligera* showed a significant difference in the ability to degrade starch and carbohydrates depending on pH. The KPH12 strain showed the highest activity for hydrolysis of starch and cellulose at pH 7. The hydrolytic activity gradually decreased with decreasing pH and reached its lowest level at pH 3 (**Figure 3A**). Similarly, the hybrid strain KJJ81 also showed a linear decline in carbohydrate degradation (**Figure 3B**). Next, we examined the effect of acidic pH values on protein degradation by both strains and found that protein degradation was low at acidic pH values for both strains (**Figures 3A,B**), indicating that acidic pH conditions suppress the ability of *S. fibuligera* to degrade proteins.

Next, we examined the effect of glucose concentration on carbohydrate hydrolyzing activity. Both the KPH12 and KJJ81 strains were grown on YPG medium plates supplemented with different glucose concentrations. First, we examined the production of carbohydrate hydrolyzing enzymes. pH had a higher influence on the production of carbohydrate hydrolyzing enzymes than glucose concentration. Starch and cellulose were hydrolyzed at high levels in non-buffered medium supplemented with a low glucose concentration. However, hydrolysis was remarkably reduced in both strains when the glucose concentration was increased, particularly to 10% glucose (**Figure 4** and **Supplementary Figure 2**).

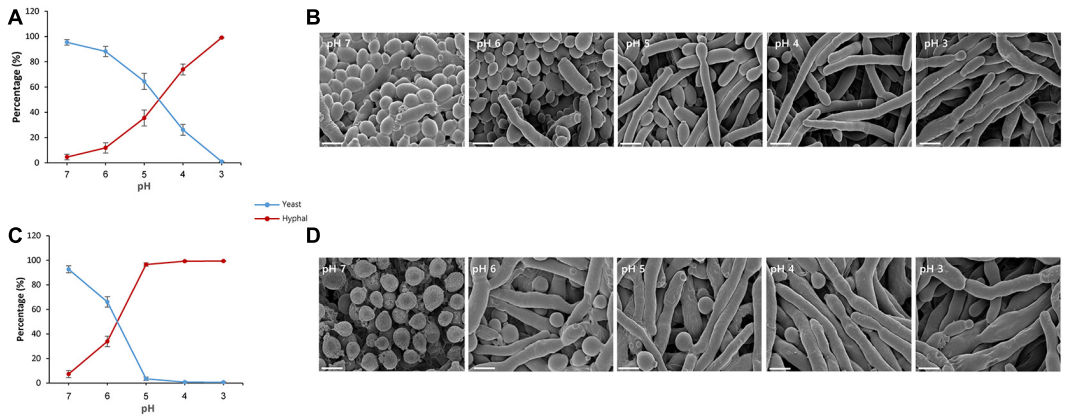

FIGURE 1 | Yeast-to-hyphae transition of *Saccharomycopsis fibuligera* at acidic pH values. KPH12 strain **(A,B)** and KJJ81 interspecies hybrid strain **(C,D)** were grown at the indicated pH values. **(A,C)** Percentage of yeast and mycelium in *S. fibuligera* grown in YPG broth buffered at pH 7, 6, 5, 4, 3 and incubated at 25°C for 20 h with shaking at 200 rpm. *Blue,* yeast percentage; *Red,* hyphae percentage. **(B,D)** Morphology and size of the cells at each pH value; scale bar = 4 μm.

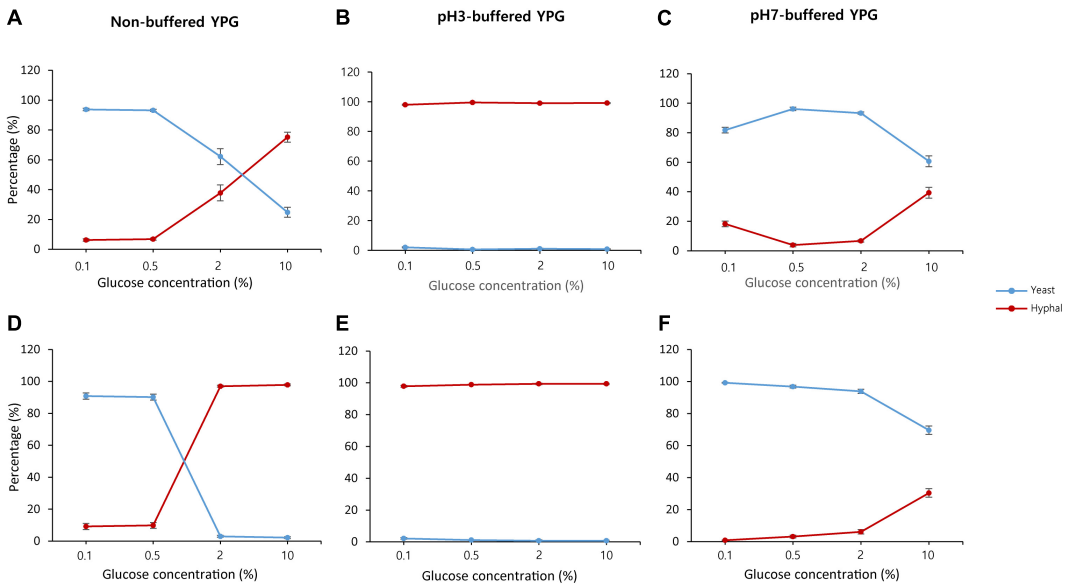

FIGURE 2 | Percentage of yeast and mycelium in *Saccharomycopsis fibuligera*. KPH12 strain **(A–C)** and KJJ81 interspecies hybrid strain **(D–F)** were grown in YPG broth supplemented with 0.1, 0.5, 2, and 10% glucose in non-buffered conditions **(A,D)**, pH 3-buffered conditions **(B,E)**, and pH 7-buffered conditions **(C,F)**. *Blue,* yeast percentage; and *red,* hyphae percentage.

Next, we examined the effect of pH on the hydrolysis activity. We examined the hydrolysis activity at pH 3 or pH 7 and found that the hydrolysis activity of starch and cellulose was inhibited at pH 3 and stimulated at pH 7, regardless of the glucose concentration (**Figure 4** and **Supplementary Figure 2**), thus indicating that pH has a stronger influence than glucose in determining the levels of hydrolyzing activity.

pH Change Greatly Affects Gene Expression in *S. fibuligera*

Based on previous results, we showed that the morphological and enzymatic alterations occurring during fermentation in *S. fibuligera* are caused by the change in pH. To investigate the effect of the changes in pH that occur during fermentation on the physiology of *S. fibuligera*, we analyzed the transcriptome of *S. fibuligera* at 5 different pH values (pH 3 to pH 7). Total RNA samples were prepared from the cultures, and poly (A)-enriched RNA samples were subjected to high-throughput Illumina HiSeq 2500 sequencing. We obtained 18–40 million reads with Q30 percentages ranging from 88 to over 92%. After alignment with reference genomes of KPH12 and KJJ8, the transcripts were annotated, and out of 6,231 and 12,341 genes annotated in the *S. fibuligera* KPH12 and KJJ81 strains, 6,075 (**Supplementary Table 1**) and 12,026 (**Supplementary Table 2**) were expressed, respectively.

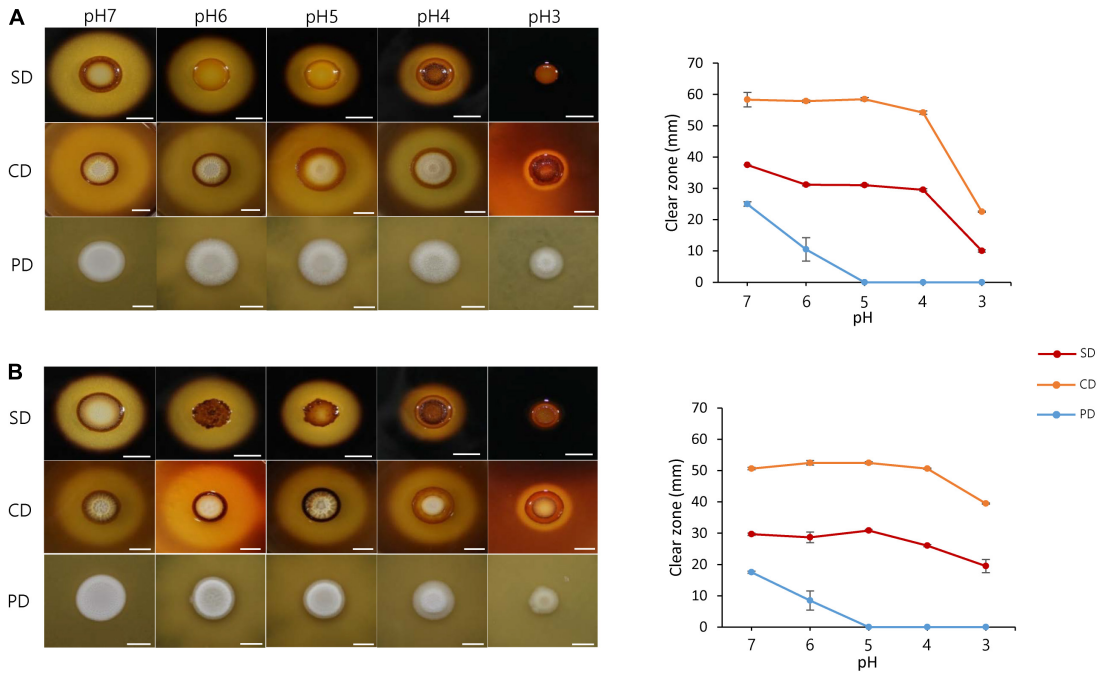

FIGURE 3 | Starch, cellulose, and protein degradation by *Saccharomycopsis fibuligera*. KPH12 strain **(A)** and KJJ81 interspecies hybrid strain **(B)** grown on YPG agar buffered at pH 7, pH 6, pH 5, pH 4, and pH 3 at 25°C. Degradation assays for starch, cellulose, and proteins were performed by adding 0.2% starch, 0.2% carboxymethylcellulose, and 2% skim milk. The results for starch degradation were obtained 3 days after incubation, and the results for cellulose and protein degradation were obtained 5 days after incubation. SD, starch degradation; CD, cellulose degradation; PD, protein degradation; scale bar = 10 mm.

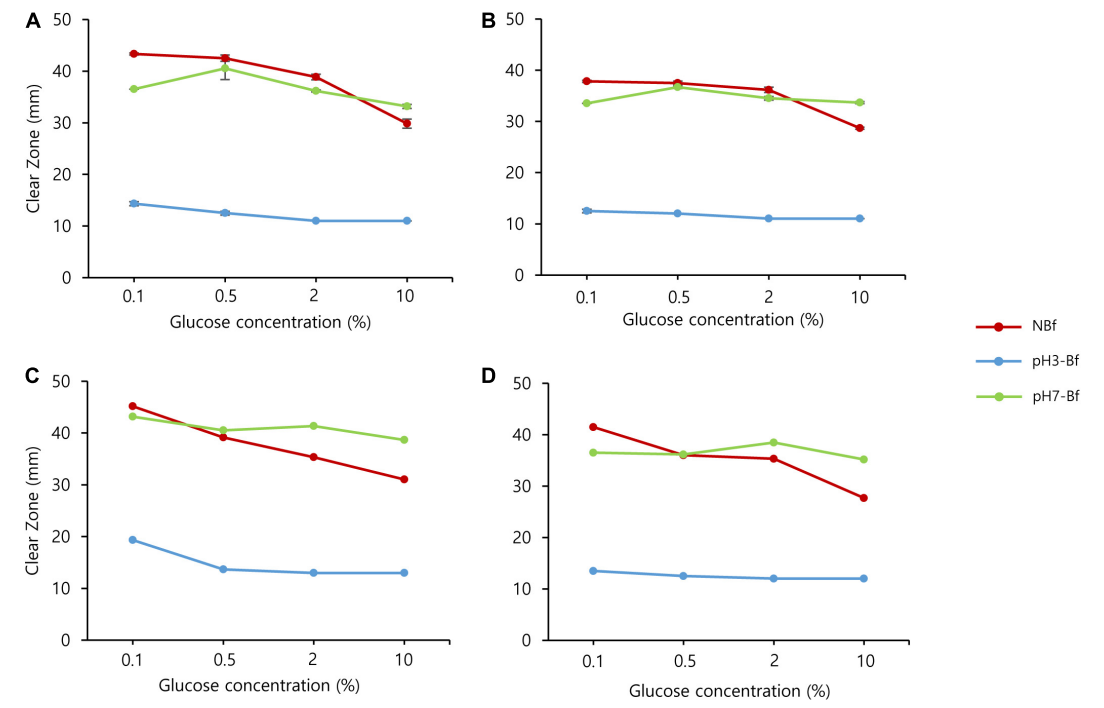

FIGURE 4 | *Saccharomycopsis fibuligera* shows reduced starch and cellulose degradation as pH decreases. Starch **(A,C)** and cellulose degradation **(B,D)** by *Saccharomycopsis fibuligera.* KPH12 **(A,B)** strain and KJJ81 interspecies hybrid strain **(C,D)** were grown on YPG agar plates supplemented with 0.1, 0.5, 2, and 10% glucose in non-buffered (NBf), pH 3-buffered (pH 3-Bf), and pH 7-buffered (pH 7-Bf) conditions. *Red,* non-buffered; *blue,* pH 3-buffered; and *green,* pH 7-buffered.

Multidimensional scaling (MDS) analysis was performed with the RNA samples of each strain to estimate the variability among the samples. We found that the samples aggregated on the PCs based on the pH point. The three replicates at each pH point were clustered together (**Figure 5**). PC1 accounted for 56–61% of the total variation among the samples, and PC2 accounted for limited variations (20–29%). This result indicates high variation between different pH conditions as well as relatively low variation among replicates.

Detection of Differentially Expressed Genes (DEGs)

At the beginning and end of fermentation, the pH values were 7 and 3, respectively. At these two pH values, *S. fibuligera* showed the clearest difference in hydrolytic enzyme production and morphology. Thus, we determined the genes differentially expressed at the two pH values (pH 7 and pH 3). The EdgeR package in R was used for differentially expressed gene (DEG) determination based on a FDR less than 0.05. Accordingly, 3,867 out of 6,075 genes (**Figure 6A** and **Supplementary Table 3**) and 9,176 out of 12,026 genes (**Figure 6B** and **Supplementary Table 4**) were detected as DEGs in the transcriptomes of the KPH12 and KJJ81 strains, respectively. To identify the DEGs that were extremely up- and downregulated between pH 7 and pH 6, we employed fuzzy c-means clustering for all DEGs of each strain and investigated the enrichment of the biological processes (BPs) of each cluster. We grouped 3,867 DEGs and 9,176 DEGs of KPH12 and KJJ81 into five clusters (**Supplementary Figure 3**), respectively. For the KPH12 (**Supplementary Table 5**) and KJJ81 (**Supplementary Table 6**) strains, each cluster displayed a unique expression pattern and had significant BPs. Among them, we selected the clustered genes whose expression was highly increased and decreased between pH 7 and pH 6; cluster 2 and cluster 5 of KPH12 and cluster 4 and cluster 2 of KJJ81 contained highly upregulated and highly downregulated genes, respectively (**Figure 7A**).

Expression Pattern and Biological Processes of the Selected Clusters

The expression patterns of cluster 5 of KPH12 and cluster 2 of KJJ81 were similar to each other and represented the DEGCs (**Figure 7A**). The expression of the genes in these clusters was highest at pH 7 and then rapidly declined at pH 6 by more than twofold. The BPs enriched in these clusters were investigated using the R package topGO, filtered and visualized using REVIGO (Supek et al., 2011). The BPs related to transporting cellular components, signaling, protein modification, and metabolism were predominant in the DEGCs of both strains (**Figures 7B,C** and **Supplementary Figure 4A**). The BP of carbohydrate metabolism was also found in these clusters, indicating that both strains share many common features in gene regulation and that carbohydrate metabolism is highly influenced by pH. In addition, among the BPs identified by the clusters, a few differences were found between the two strains. For example, the regulation of GTPase activity was higher in KPH12 than in KJJ81.

Unlike DEGCs, the expression patterns of clusters 2 and 4, which represented the increasingly expressed gene clusters (IEGCs) of KPH12 and KJJ81, respectively, were different from each other. The expression of the genes in cluster 2 of the KPH12 strain was extremely low at pH 7 and then increased rapidly to reach the highest level at pH 4, whereas the expression of the genes in cluster 4 of KJJ81 was at the highest level at pH 4 (**Figure 7A**). BPs that were predominant in these clusters of both strains were related to protein synthesis and RNA metabolism. The gene number of ribosome biogenesis-related BP was higher in KJJ81 than KPH12 (**Figures 7B,C**, **Supplementary Figure 4A**, and **Supplementary Tables 5,6**). These results suggest that adaptation to acidic pH involves a change in metabolism.

The KEGG pathway enrichment analysis revealed that the DEGs were enriched in arginine biosynthesis, aminoacyl-tRNA biosynthesis, starch and sucrose metabolism in both strains (**Supplementary Figure 4B**). In strain KJJ81, the upregulated genes were clustered in the fatty acid biosynthesis and N-glycan biosynthesis pathways and the downregulated genes were enriched in starch and sucrose metabolism. In strain KPH12, the upregulated genes were enriched in the lipopolysaccharide biosynthesis pathway and the downregulated genes were clustered in amino acid biosynthesis pathways (**Supplementary Figure 4B**).

Expression of the Genes Involved in Carbohydrate Degradation

In *S. fibuligera*, we investigated the expression of genes previously known to be involved in starch degradation, such as *a*-amylase (*ALP1*) and glucoamylases (*GAM1* and *GLU*), and those involved in cellulose degradation, such as β-glucosidases (*BGL*), polysaccharide monooxygenase (*Cel61a*) and alpha-L-arabinofuranosidase C (*abfC*). Most of the genes involved in starch degradation were downregulated (**Figure 8A**). Three of these genes, *GAM1* (KPH12A7G027400, KJJ81A4G036700, KJJ81B7G026300), *GLU1* (KPH12A1G148700, KJJ81A6G044500, KJJ81B1G146400) and *GLU2* (KPH12A6G044000, KJJ81A6G044500, KJJ81B 6G043300), are among the DEGs of KPH12 and KJJ81. We confirmed the downregulation of most of these genes at pH 3 by qRT-PCR (**Figure 8B**). All these genes were present in clusters 1 and 5 except *GLU2,* which was present in clusters 2 and 3 in KPH12 (**Supplementary Figure 3A**). On the other hand, most of these genes were present in cluster 2 of the DEGCs and in cluster 5 in both the A and B genomes of hybrid strain KJJ81 (**Figure 7A**). Only *GAM1* was located in different clusters, and it was in cluster 5 of genome A and cluster 2 of genome B (**Supplementary Figure 3A**).

Among the genes related to cellulose degradation, five out of the 8 genes in genome A and 6 out of 9 in genome B were downregulated in the two strains (**Figure 8A**). All the downregulated genes of KPH12 were located in DEGs. Among them, *BGL3* and *Cel61a1* were in cluster 5 of the DEGCs, whereas the remaining 3 genes, *BGL1* (KPH12A2G002200, KJJ81A2G002300, KJJ81B2G002200), *Cel61a3* (KPH12A2G080500, KJJ81A2G080600, KJJ81B2

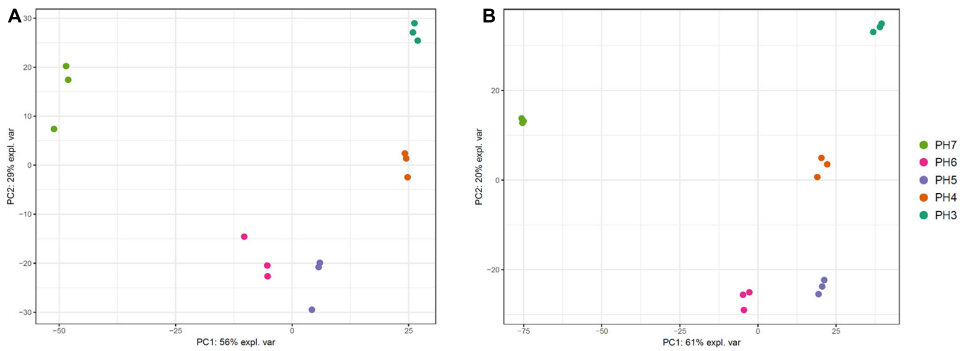

FIGURE 5 | Multidimensional scaling (MDS) plot of 15 RNA samples of *Saccharomycopsis fibuligera*. KPH12 strain **(A)** and KJJ81 interspecies hybrid strain **(B)** were grown at five different pH values for 18 h after inoculation, and total mRNA was prepared and sequenced. *Dot colors*: each dot color indicates the samples at the same pH point.

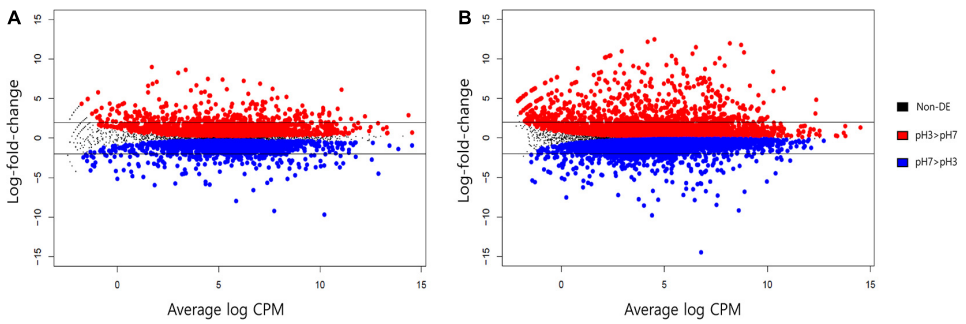

FIGURE 6 | MD plot analysis for the average expression level of all genes of *Saccharomycopsis fibuligera*. KPH12 strain **(A)** and KJJ81 interspecies hybrid strain **(B)** at pH 3 and the $\log_2$ fold-change of each gene from pH 3 to pH 7. *Blue*: genes with a significant decrease in expression at an FDR of 5%; and *red*: genes with a significant increase in expression at an FDR of 5%. Non-significant genes are in black. Horizontal black bars indicate genes that exhibited at least a fourfold change in expression ($\log_2$FC = 2).

G078400), and *abfC* (KPH12A3G089600, KJJ81A3G090700, KJJ81B5G075900), were in cluster 1 (**Supplementary Figure 3A**). On the other hand, these genes were downregulated in the hybrid strains and were present in the DEGs except *Cel61a3* of genome B. Two of these DEGs, *BGL1* and *Cel61a1,* were found in cluster 2, and *BGL3* was in cluster 5 (**Supplementary Figure 3A**). *abfC* of genome A was found in cluster 2 of the DEGCs (**Figure 7A**), while that of genome B was not found in any cluster. The reduced expression of most of these genes was confirmed by qRT-PCR (**Figure 8B**). *RIM101* (KPH12A2G072500, KJJ81A2G072500, KJJ81B2G070400), a pH-response transcription factor, was associated with the expression of starch and cellulose degradation-related genes (**Figure 8A**). Thus, we examined its expression in both strains under different pH conditions. *RIM101* was found in clusters 5 and 2 of the DEGCs in KPH12 and KJJ81, respectively. We confirmed the low expression of *RIM101* at pH 3 by qRT-PCR, which was consistent with the RNA-Seq data (**Figure 8B**).

Expression of the Genes Involved in the Dimorphism

cAMP-PKA and MAPK cascades are well-known signaling pathways involved in the induction of pseudohyphal growth of the model yeast *S. cerevisiae* (Pan et al., 2000) and the hyphal or yeast form in other dimorphic fungal models (Leberer et al., 2001; Martínez-Espinoza et al., 2004). We examined the expression of homologous genes in *S. fibuligera* that are involved in these cascades, such as transcriptional activator *FLO8* (KPH12A6G0101800, KJJ81A6G018300), enhanced filamentous growth *EFG1* (KPH12A1G008700, KJJ81A1G009000, KJJ81B1G008600), and transcription factor *TEC1* (KPH12A7G016700, KJJ81A7G016700, KJJ81B7G015800), for cAMP-PKA and transcription factor *CPH1* (KPH12A3G005900, KJJ81A3G005800, KJJ81B3G006100) for MAPK. These transcriptional activators were among the DEGs except for *FLO8* and *TEC1*. The expression of *CPH1* was slightly downregulated in KPH12 and the two genomes of the hybrid strain KJJ81 (**Figure 9A**), and at least one of the cAMP-PKA transcriptional activators *FLO8*, *EFG1*, or *TEC1* was upregulated (**Figure 9A**). These results suggest that the cAMP-PKA pathway is involved in the hyphal growth of *S. fibuligera*. To confirm this supposition, KPH12 and KJJ81 cells were grown in YPG broth media buffered at pH 4 in the presence or absence of clozapine, which blocks the cAMP-PKA signaling pathway (Midkiff et al., 2011), and the morphology was examined. In the liquid cultures, hyphal growth was suppressed in both strains by up to 60.4 and 26.2% for KPH12 and KJJ81, respectively,

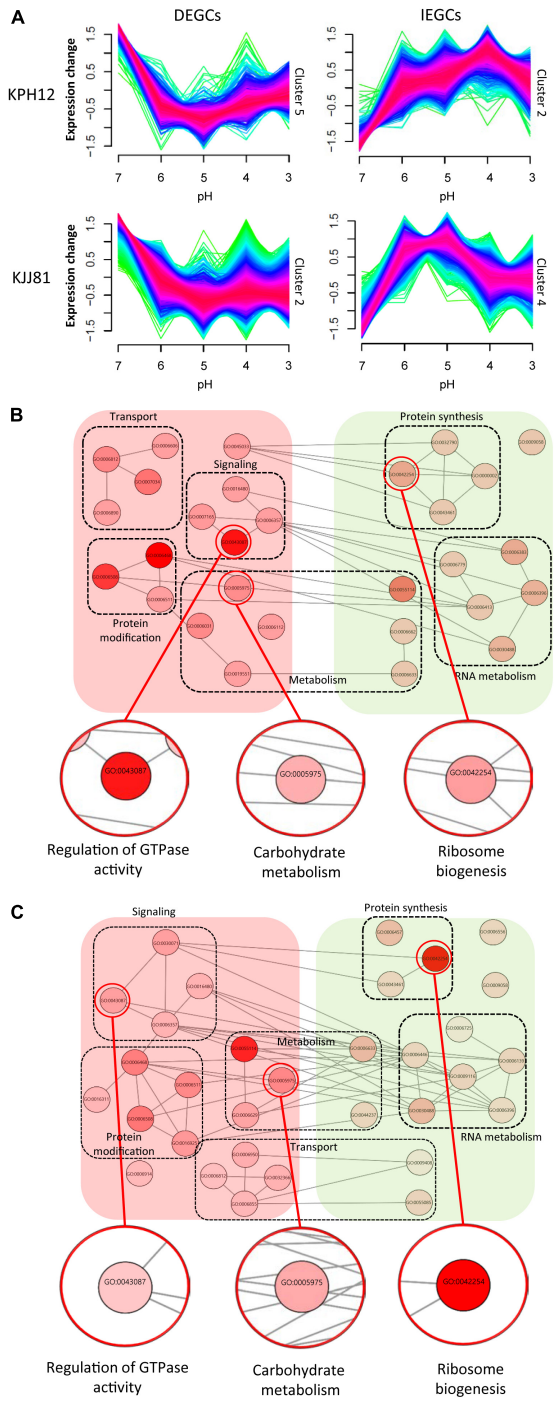

FIGURE 7 | Fuzzy c-means clustering identifies general gene expression patterns of *Saccharomycopsis fibuligera*. **(A)** Clusters of DEGCs and IEGCs of KPH12 and KJJ81 strains at pH values from 7 to 3. Among the five gene clusters classified by fuzzy c-means, two clusters that showed extreme upregulation and downregulation at pH 6 were selected. The membership of a given gene within a cluster is represented by color, with red indicating high association. **(B,C)** For each cluster, enriched biological processes were identified, and only those belonging to the chosen clusters were visualized based on REVIGO. Nodes represent the terms, and edges represent the strength of the terms pairwise similarity. Significance is represented by node color. DEGCs, decreasingly expressed gene clusters; IEGCs, increasingly expressed gene clusters.

in the presence of clozapine (**Figure 9B**), indicating that the cAMP-PKA pathway plays a pivotal role in hyphal induction in both strains, KPH12 and KJJ81.

DISCUSSION

In this study, we investigated the growth of *S. fibuligera* and production of hydrolytic enzymes during fermentation. During *makgeolli* production, the microorganisms originating from *nuruk* affect the environmental conditions of fermentation and vice versa. We focused on *S. fibuligera* because this microorganism is one of the most predominant amylolytic and cellulose-degrading yeasts in *nuruk* (Carroll et al., 2017). We found that *S. fibuligera* undergoes several phenotypic changes, such as the dimorphic transition as the pH goes down. Additionally, we showed that acidic conditions (pH 5–3) induce the yeast-to-hyphal transition of *S. fibuligera*, whereas neutral conditions (pH 7) induce yeast growth. Thus, the morphological change of *S. fibuligera* is consistent with the pH decline that is observed on the second day of *makgeolli* fermentation (Song et al., 2015). The morphological change of *S. fibuligera* was similar to that of *U. maydis*, which grows as mycelium at pH 3 and as yeast at pH 7 (Ruiz-Herrera et al., 1995), but differs from that of *Y. lipolytica* and *C. ablicans,* which grow as yeast at acidic pH and as hyphae under neutral pH conditions (Ruiz-Herrera and Sentandreu, 2002; Davis, 2003). Compared with the parental strains, we observed that the hybrid strain underwent hyperfilamentation, which might be another kind of adaptation to acidic pH. However, Choo and coworkers (Choo et al., 2016) found that a high concentration of glucose also induced the hyphal growth of the two strains of *S. fibuligera*, KPH12 and KJJ81.

The yeast to hyphal transition of *S. fibuligera* during fermentation was further examined at the level of gene expression. The expression patterns of genes involved in the dimorphic transition in *S. fibuligera* were investigated through transcriptome analysis. The Rim101/Pac signaling pathway plays an essential role during the dimorphic transition in response to alkaline pH (Davis, 2009). As shown in **Figure 8**, the *RIM101* gene was upregulated at neutral pH and downregulated at acidic pH. Wang et al. (2020) found that in *Trichosporon cutaneum*, neutral and acidic pH induces and inhibit the expression of *RIM101*, respectively, which correlates with our findings. Under alkaline conditions, *C. albicans* senses pH signals through the membrane receptor *RIM21*, which activates the arresting protein *RIM8*. *RIM8* interacts with the endosomal sorting complexes required for transport (ESCRT) complex and stimulates the expression of *RIM20* (zinc finger transcription factor) and *RIM13* (calpain protease) (Henne et al., 2011). *RIM20* and RIM13 form a complex that hydrolyzes the long form of RIM101 into a short form (Garnaud et al., 2018). The short form of *RIM101* induces the expression of pH-responsive protein 1 (*PHR1*), which plays an important role in growth at alkaline pH (Saporito-Irwin et al., 1995), and suppresses the expression of *PHR2* (pH-responsive protein 2) (Baek et al., 2006). PHR2 is induced at acidic pH and required for infection by *C. albicans*. In our study, the meiotic activator *RIM4* (KPH12A1G023400) and

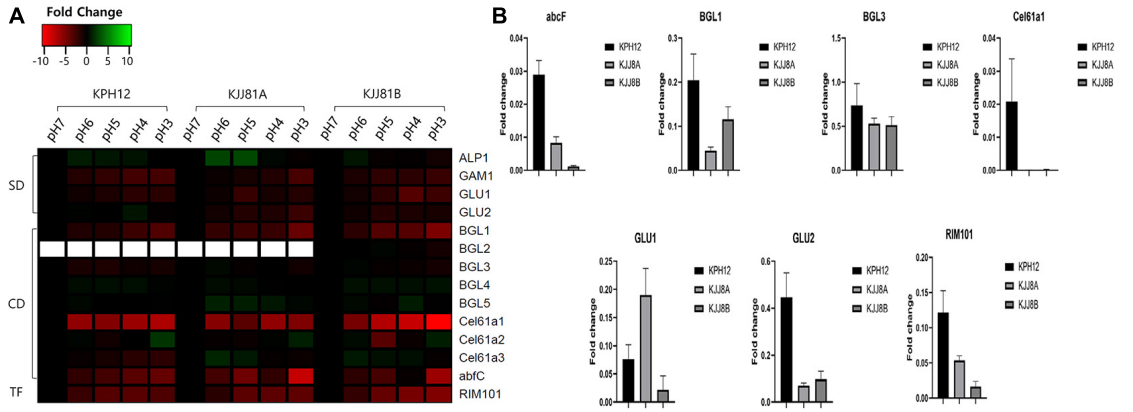

FIGURE 8 | Expression profiles of *Saccharomycopsis fibuligera* genes associated with starch and cellulose degradation as well as the transcription factor RIM101. **(A)** Genes encoding the hydrolytic enzymes were analyzed using the data from RNA-Seq for their expression at the five pH values and presented as a heat map. pH 7 was considered the starting point (log_2 FC = 0), and the expression change at each pH was calculated based on pH 7. SD, starch degradation; CD, cellulose degradation; TF, transcription factor. **(B)** qRT-PCR analysis. To confirm the results obtained from the RNA-seq data, a qRT-PCR assay was performed for the indicated genes using specific primers. Error bar, standard deviation (n = 3).

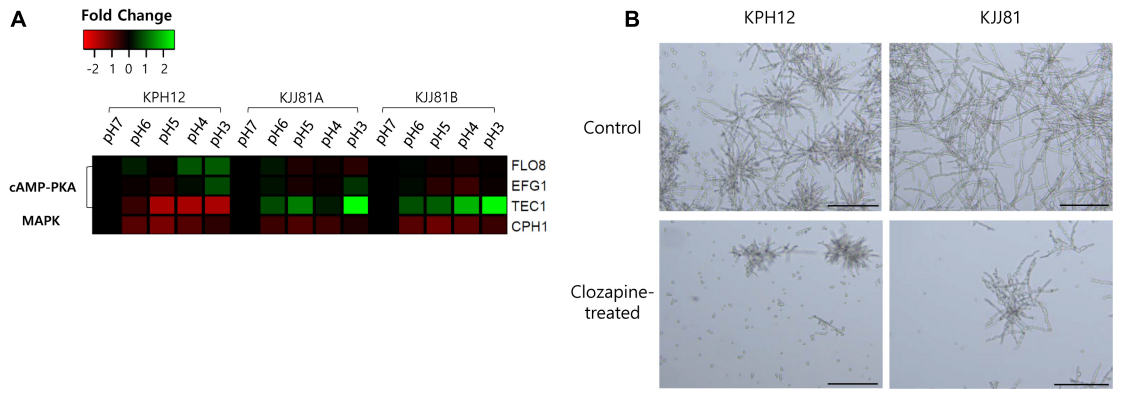

FIGURE 9 | Expression profiles of *Saccharomycopsis fibuligera* transcriptional activators of cAMP-PKA and MAPK, the two signaling pathways associated with the dimorphic growth of several model yeasts and fungi, at each pH point. pH 7 was considered the starting point (log_2 FC = 0), and the expression at each pH was calculated based on pH 7. **(A)** shows the RNA-Seq data and **(B)** shows the cell morphology of *S. fibuligera* strains in the presence or absence of the cAMP-PKA blocker clozapine. SD, starch degradation; CD, cellulose degradation; TF, transcription factor; scale bar = 100 μm.

pH-response regulator protein *RIM20* (KPH12A4G038700) were downregulated under acidic pH conditions along with the key regulator *RIM101* (KPH12A2G072500) in *S. fibuligera* KPH12 (**Supplementary Table 8**). In addition, the expression patterns of *RIM101* (KJJ81A2G072500), *RIM4* (KJJ81A1G023900) and *RIM20* (KJJ81B4G038300) in the hybrid strain KJJ81 were similar to those in *S. fibuligera* KPH12. These results may indicate conservation of the RIM101 pathway in *S. fibuligera*. Furthermore, the transcriptional repressor of filamentous growth *TUP1* (KPH12A4G054300), which is under the control of the RIM101 pathway, was downregulated at acidic pH (**Supplementary Table 8**). *TUP1* forms with the general transcriptional corepressor *SNN6* a complex repressor (TUP1-SSN6), which is conserved in eukaryotes. The TUP1-SSN6 complex plays a key role in growth regulation in several dimorphic fungi (Smith and Johnson, 2000) by modulating sequence-specific DNA-binding proteins (DBPs). Among the DPBs, *MIG1* (regulator protein MIG1 involved in glucose repression), *NRG1* (transcriptional repressor involved in regulation of glucose repression) and *RFG1* (repressor of filamentous growth 1) inhibit filament-inducing genes by binding to the TUP1-SSN6 complex in *C. albicans* (Kebaara et al., 2008; Sánchez-Arreguin et al., 2021). Compared with the results of previous studies, the current study found that *NRG1* (KPH12A4G012800, KPH12A2G036800, KJJ81A3G036900, KJJ81B3G035800) and *RFG1* (KPH12A2G100300, KJJ81B2G097900) were upregulated in *S. fibuligera* under acidic pH conditions (**Supplementary Tables 8, 9**). These results suggest that *NRG1* and *RFG1* could play different roles during changes in environmental pH.

In addition to transcription factors, we found that some DEGs involved in the cAMP/PKA pathway were differentially expressed (**Figure 9** and **Supplementary Figure 4**). Cyclic AMP-protein kinase (cAMP/PKA) and MAPK are two signaling pathways

that play a central role in the regulation of morphogenesis in several fungi, including *S. cerevisiae* (Conrad et al., 2014), *C. albicans* (Lin and Chen, 2018), and *T. cutaneum* (Wang et al., 2020). However, the two signaling pathways are not functionally conserved among various fungi. For instance, both signaling pathways are involved in the induction of the pseudohyphal and hyphal growth of *S. cerevisiae* and *C. albicans*, respectively (Sudbery, 2011), whereas in *Y. lipolytica,* only MAPK is involved in the induction of hyphal growth while cAMP/PKA induces yeast growth (Ruiz-Herrera and Sentandreu, 2002; Cervantes-Chávez and Ruiz-Herrera, 2006; Martínez-Soto and Ruiz-Herrera, 2015). In *U. maydis,* hyphal growth is induced only by cAMP/PKA and yeast growth is induced by MAPK (Martínez-Espinoza et al., 2004). Alkaline pH signals induce the activation of adenylate cyclase (*CYR1*) and *PKA* through *RAS2* and *GPA2,* which leads to the activation of transcription factors, such *RGT1*, *EFG1* and *TEC1*, in *C. albicans* (Zhang et al., 2016). These transcription factors play a key role in hyphal growth, and their activation leads to translation from yeast to hyphal form (Han et al., 2011; Cornet and Gaillardin, 2014). In this study, the expression of G-protein alpha-subunit (*GPA2*, KJJ81B5G067700), Ras-like protein 1 (*RAS1*, KJJ81B2G095300), and G protein-coupled receptor 1 (*GPR1*, KJJ81B4G062500) involved in the cAMP/PKA pathway was upregulated at acidic pH in hybrid strain KJJ81 (**Supplementary Table 9**). Furthermore, the transcription factors *TEC1* (KJJ81A7G016700, KJJ81B7G015800) and *EFG1* (KPH12A1G008700) were upregulated under acidic conditions (**Supplementary Tables 8, 9**), which is consistent with previous studies in *T. cutaneum* (Wang et al., 2020). Thus, these results suggest that the cAMP/PKA pathway is involved in the regulation of hyphal growth at acidic pH in the hybrid strain *S. fibuligera* KJJ81 (**Figure 9** and **Supplementary Table 9**).

During fermentation, the most crucial process is the degradation of carbohydrates in *nuruk* to produce substrates of alcohol. Thus, the production of hydrolyzing enzymes should be crucial for successful fermentation. However, as fermentation progresses, the pH drops, which in turn leads to a decrease in the production of hydrolytic enzymes for starch, cellulose and proteins in *S. fibuligera* (**Figure 3**), and these conditions are not favorable for fermentation. In addition, a high concentration of glucose suppresses the production of hydrolytic enzymes for starch, protein, and cellulose in *S. fibuligera* (Chi et al., 2009). Choo et al. (2016) showed that the reduced production of these enzymes under high concentrations of glucose is caused by the downregulation of the genes encoding hydrolytic enzymes. A previous study showed that a high concentration of glucose changed the environmental pH to alkaline conditions in *C. albicans* (Carman, 2008). Thus, it is not clear whether a high glucose concentration directly affects the production of hydrolytic enzymes. However, in this work, we showed that the pH change resulting from glucose utilization but not glucose itself plays a critical role in the dimorphic transition and the reduced production of hydrolytic enzymes in *S. fibuligera* (**Supplementary Figure 2**). The transcriptome analysis revealed that genes encoding enzymes involved in starch, cellulose and protein degradation were downregulated at acidic pH (**Figure 8**). *ALP1* (KPH12A6G028500, KJJ81A6G028500, KJJ81B6G028100), *GAM1* (KPH12A7G027400, KJJ81A7G027600, KJJ81B7G026300), *GLU1* (KPH12A1G148700, KJJ81A1G148800, KJJ81B1G146400) and *GLU2* (KPH12A6G044000, KJJ81A6G044500, KJJ81B6G043300), which encode enzymes involved in starch degradation, were downregulated at acidic pH compared to alkaline pH (**Supplementary Tables 8, 9**). In addition, the expression of *RIM101* was decreased at acidic pH. In the model filamentous organism *Aspergillus nidulans*, the deletion of *RIM101* resulted in a lower expression of carbohydrate degradation-related genes (Peñalva et al., 2008). Thus, it is possible that *RIM101* could be involved in the regulation of carbohydrate degradation-related genes in *S. fibuligera*.

We investigated the expression of genes involved in protein synthesis and RNA metabolism. Through an analysis of BPs, the genes linked to RNA metabolism and protein synthesis, such as *CTK2* (CTD kinase subunit beta, KPH12A5G020700, KJJ81B5G020000), *DBP3* (ATP-dependent RNA helicase DBP3, KPH12A7G005900, KJJ81A7G005800, KJJ81B7G005500) and *CBP6* (KPH12A2G119900, KJJ81A2G119600, KJJ81B2G116300), were upregulated under hyphal induction conditions (**Supplementary Tables 8, 9**). A transcriptome analysis of *C. albicans* under the condition of transition from yeast to hyphae showed an upregulation of genes involved in RNA metabolism and protein synthesis (Carlisle and Kadosh, 2013). Similar results were observed with *U. maydis* during the transition from yeast to hyphal forms (Larraya et al., 2005). However, contrasting cases are observed as well, and genes linked with protein synthesis and RNA metabolism were involved in the transition to the yeast form in *Paracoccidioides brasiliensis* (Nunes et al., 2005; Parente et al., 2008), *Penicillium marneffei* (a human pathogen) (Yang et al., 2014) and *Ophiostoma novo-ulmi* (a plant pathogen) (Nigg and Bernier, 2016). *C. albicans* and *U. maydis* exist in yeast form as saprotrophs in the environment (Vollmeister et al., 2011; Carlisle and Kadosh, 2013; Ruiz-Herrera et al., 2020), and they turn into filamentous forms to infect their hosts. In contrast, the opposite is true for *P. brasiliensis*, *P. marneffei* and *O. novo-ulmi* (Rooney and Klein, 2002; Naruzawa and Bernier, 2014). Therefore, the high-level expression of genes involved in protein synthesis and RNA metabolism may not be a direct indicator of the transition from yeast to hyphae but rather an indication of adaptation to changing environmental conditions. Accordingly, the transition of *S. fibuligera* from yeast to hyphae is an adaptation to acidic pH supported by the high-level expression of genes related to protein synthesis and RNA metabolism. In addition, cell wall synthesis is tightly regulated under hyphal formation conditions. *BCR1* (biofilm and cell wall regulator 1) is a transcription factor that plays a key role in the regulation of cell wall formation and regulates the expression of genes involved in cell wall synthesis (*HWP1*, *ALS1*, *ALS3*, and *HYR1*) (Nobile et al., 2006; Sosinska et al., 2011). The deletion of *BCR1* in *C. albicans* induced a decrease in the expression of the cell wall chitinase *Cht2* (Sherrington et al., 2017). Under acidic conditions, the *S. fibuligera* hybrid strain KJJ81 showed an upregulation of *BCR1*

(**Supplementary Table 9**, KJJ81B4G072900), indicating that the function of *BCR1* is conserved and may play an important role in yeast-hyphal transition through regulation of cell wall synthesis and regulation of the wall proteome during adaptation.

CONCLUSION

In conclusion, the study provides evidence that the acidic pH conditions that occur during fermentation of *nuruk* underlie the phenotypes of *S. fibuligera,* such as the lower-level starch and cellulose degradation and hyphal growth. Here, we also provide the first detailed analysis of transcriptome changes in *S. fibuligera* upon pH decline. During the first phase of fermentation of *nuruk*, *S. fibuligera* contributes to the degradation of starch through secretion of carbohydrate-hydrolyzing enzymes. As fermentation progresses, the environmental pH drops to an acidic level (pH 3). Under these conditions, *S. fibuligera* undergoes a morphological transition to give rise to the hyphal form and metabolic modifications, such as inhibition of carbohydrate metabolism, to survive under acidic pH conditions as a means of adapting to fermentation environments. In addition, our transcriptome analysis contributes to elucidating some aspects of the dimorphism transition of *S. fibuligera* under low pH conditions that occur when fermenting *makgeolli* using *nuruk*.

DATA AVAILABILITY STATEMENT

The datasets presented in this study can be found in online repositories. The names of the repository/repositories and accession number(s) can be found below: https://www.ncbi.nlm.nih.gov/, PRJNA705233.

AUTHOR CONTRIBUTIONS

J-AS conceived the conceptualization, funding acquisition, project administration, supervision, writing the original draft, responding to revision, and editing the whole manuscript. MF performed the experiment and the RNA-sequence analysis, and drafted the first manuscript. NA participated in the RNA-seq analysis and drafted the manuscript. All authors contributed to the article and approved the submitted version.

FUNDING

This work was supported by the Korea Institute of Planning and Evaluation for Technology in Food, Agriculture and Forestry (IPET) through Agricultural Microbiome R&D Program, funded by the Ministry of Agriculture, Food and Rural Affairs (MAFRA-918010-4).

ACKNOWLEDGMENTS

We thank I. H. Hwang and Y. W. Lee for their valuable comments and discussions. We thank Ghazal Ayoub for providing the algorism used for extracting the DEGs list.

SUPPLEMENTARY MATERIAL

The Supplementary Material for this article can be found online at: https://www.frontiersin.org/articles/10.3389/fmicb.2021.672661/full#supplementary-material

REFERENCES

Abouzied, M. M., and Reddy, C. A. (1987). Fermentation of starch to ethanol by a complementary mixture of an amylolytic yeast and Saccharomyces cerevisiae. *Biotechnol. Lett.* 9, 59–62. doi: 10.1007/bf01043395

Anders, S., Pyl, P. T., and Huber, W. (2015). HTSeq–a Python framework to work with high-throughput sequencing data. *Bioinformatics* 31, 166–169. doi: 10.1093/bioinformatics/btu638

Baek, Y. U., Martin, S. J., and Davis, D. A. (2006). Evidence for novel pH-dependent regulation of Candida albicans Rim101, a direct transcriptional repressor of the cell wall beta-glycosidase Phr2. *Eukaryot. Cell* 5, 1550–1559. doi: 10.1128/EC.00088-06

Bal, J., Yun, S. H., Choi, M. S., Yeo, S. H., Kim, J. M., and Kim, D. H. (2015). Pyrosequencing reveals bacterial diversity in Korean traditional wheat-based nuruk. *J. Microbiol.* 53, 812–819. doi: 10.1007/s12275-015-5516-3

Bal, J., Yun, S. H., Song, H. Y., Yeo, S. H., Kim, J. H., Kim, J. M., et al. (2014). Mycoflora dynamics analysis of Korean traditional wheat-based nuruk. *J. Microbiol.* 52, 1025–1029. doi: 10.1007/s12275-014-4620-0

Benjamini, Y., and Hochberg, Y. (1995). Controlling the false discovery rate: a practical and powerful approach to multiple testing. *J. R. Stat. Soc. B (Methodol.)* 57, 289–300. doi: 10.1111/j.2517-6161.1995.tb02031.x

Carlisle, P. L., and Kadosh, D. (2013). A genome-wide transcriptional analysis of morphology determination in Candida albicans. *Mol. Biol. Cell* 24, 246–260. doi: 10.1091/mbc.E12-01-0065

Carman, A. J. (2008). *Acetate Metabolism and the Control of Environmental pH in Candida Albicans and Saccharomyces cerevisiae*. Ph.D dissertation. Houston, TX: The University of Texas Graduate School of Biomedical Sciences at Houston.

Carroll, E., Trinh, T. N., Son, H., Lee, Y.-W., and Seo, J.-A. (2017). Comprehensive analysis of fungal diversity and enzyme activity in nuruk, a Korean fermenting starter, for acquiring useful fungi. *J. Microbiol.* 55, 357–365.

Cervantes-Chávez, J. A., and Ruiz-Herrera, J. (2006). STE11disruption reveals the central role of a MAPK pathway in dimorphism and mating in *Yarrowia lipolytica*. *FEMS Yeast Res.* 6, 801–815. doi: 10.1111/j.1567-1364.2006.00084.x

Chi, Z., Chi, Z., Liu, G., Wang, F., Ju, L., and Zhang, T. (2009). *Saccharomycopsis fibuligera* and its applications in biotechnology. *Biotechnol. Adv.* 27, 423–431. doi: 10.1016/j.biotechadv.2009.03.003

Choo, J. H., Hong, C. P., Lim, J. Y., Seo, J. A., Kim, Y. S., Lee, D. W., et al. (2016). Whole-genome de novo sequencing, combined with RNA-Seq analysis, reveals unique genome and physiological features of the amylolytic yeast Saccharomycopsis fibuligera and its interspecies hybrid. *Biotechnol. Biofuels* 9:246. doi: 10.1186/s13068-016-0653-4

Conrad, M., Schothorst, J., Kankipati, H. N., Van Zeebroeck, G., Rubio-Texeira, M., and Thevelein, J. M. (2014). Nutrient sensing and signaling in the yeast *Saccharomyces cerevisiae*. *FEMS Microbiol. Rev.* 38, 254–299. doi: 10.1111/1574-6976.12065

Cornet, M., and Gaillardin, C. (2014). pH signaling in human fungal pathogens: a new target for antifungal strategies. *Eukaryot. Cell* 13, 342–352. doi: 10.1128/EC.00313-13

Cotton, P., Kasza, Z., Bruel, C., Rascle, C., and Fèvre, M. (2003). Ambient pH controls the expression of endopolygalacturonase genes in the necrotrophic fungus Sclerotinia sclerotiorum. *FEMS Microbiol. Lett.* 227, 163–169. doi: 10.1016/s0378-1097(03)00582-2

Davis, D. (2003). Adaptation to environmental pH in Candida albicans and its relation to pathogenesis. *Curr. Genet.* 44, 1–7. doi: 10.1007/s00294-003-0431-2

Davis, D. A. (2009). How human pathogenic fungi sense and adapt to pH: the link to virulence. *Curr. Opin. Microbiol.* 12, 365–370. doi: 10.1016/j.mib.2009.05.006

de Mot, R., Andries, K., and Verachtert, H. (1984). Comparative study of starch degradation and amylase production by Ascomycetous yeast species. *Syst. Appl. Microbiol.* 5, 106–118. doi: 10.1016/s0723-2020(84)80055-7

Farh, M. E. A., Cho, Y., Lim, J. Y., and Seo, J. A. (2017). A diversity study of Saccharomycopsis fibuligera in rice wine starter nuruk, reveals the evolutionary process associated with its interspecies hybrid. *J. Microbiol.* 55, 337–343. doi: 10.1007/s12275-017-7115-y

Garnaud, C., García-Oliver, E., Wang, Y., Maubon, D., Bailly, S., Despinasse, Q., et al. (2018). The rim pathway mediates antifungal tolerance in Candida albicans through newly identified Rim101 transcriptional targets, including Hsp90 and Ipt1. *Antimicrob. Agents Chemother.* 62:e01785-17. doi: 10.1128/AAC.01785-17

Gonzalez-Lopez, C. I., Szabo, R., Blanchin-Roland, S., and Gaillardin, C. (2002). Genetic control of extracellular protease synthesis in the yeast *Yarrowia lipolytica*. *Genetics* 160, 417–427.

Han, T. L., Cannon, R. D., and Villas-Bôas, S. G. (2011). The metabolic basis of Candida albicans morphogenesis and quorum sensing. *Fungal Genet. Biol.* 48, 747–763. doi: 10.1016/j.fgb.2011.04.002

Henne, W. M., Buchkovich, N. J., and Emr, S. D. (2011). The ESCRT pathway. *Dev. Cell* 21, 77–91. doi: 10.1016/j.devcel.2011.05.015

Jang, J. (1989). History of Korean traditional rice wine. *Korean Diet. Cult.* 4, 271–274.

Jo, G., and Lee, C. (1997). Isolation and identification of the fungi from nuruk. *J. Korean. Soc. Food. Sci. Nutr.* 26, 759–766.

Kebaara, B. W., Langford, M. L., Navarathna, D. H. M. L. P., Dumitru, R., Nickerson, K. W., and Atkin, A. L. (2008). *Candida albicans* Tup1 is involved in farnesol-mediated inhibition of filamentous-growth induction. *Eukaryot. Cell* 7, 980–987. doi: 10.1128/EC.00357-07

Kim, M. S., Kim, S., Ha, B. S., Park, H. Y., Baek, S. Y., Yeo, S. H., et al. (2014). Diversity, saccharification capacity, and toxigenicity analyses of fungal isolates in Nuruk. *Korean J. Mycol.* 42, 191–200. doi: 10.4489/kjm.2014.42.3.191

Kozubowski, L., Lee, S. C., and Heitman, J. (2009). Signalling pathways in the pathogenesis of *Cryptococcus*. *Cell. Microbiol.* 11, 370–380. doi: 10.1111/j.1462-5822.2008.01273.x

Kurtzman, C. P., and Smith, M. T. (2011). *Saccharomycopsis Schiönning (1903)*. Amsterdam: Elsevier Science BV.

Larkin, M. A., Blackshields, G., Brown, N. P., Chenna, R., McGettigan, P. A., McWilliam, H., et al. (2007). Clustal W and Clustal X version 2.0. *Bioinformatics* 23, 2947–2948. doi: 10.1093/bioinformatics/btm404

Larraya, L. M., Boyce, K. J., So, A., Steen, B. R., Jones, S., Marra, M., et al. (2005). Serial analysis of gene expression reveals conserved links between protein kinase A, ribosome biogenesis, and phosphate metabolism in Ustilago maydis. *Eukaryot. Cell* 4, 2029–2043. doi: 10.1128/EC.4.12.2029-2043.2005

Leberer, E., Harcus, D., Dignard, D., Johnson, L., Ushinsky, S., Thomas, D. Y., et al. (2001). Ras links cellular morphogenesis to virulence by regulation of the MAP kinase and cAMP signalling pathways in the pathogenic fungus *Candida albicans*. *Mol. Microbiol.* 42, 673–687. doi: 10.1046/j.1365-2958.2001.02672.x

Lee, J. E., Lee, A. R., Kim, H., Lee, E., Kim, T. W., Shin, W. C., et al. (2017). Restoration of traditional Korean Nuruk and analysis of the brewing characteristics. *J. Microbiol. Biotechnol.* 27, 896–908. doi: 10.4014/jmb.1610.10039

Li, H., and Durbin, R. (2009). Fast and accurate short read alignment with Burrows-Wheeler transform. *Bioinformatics* 25, 1754–1760. doi: 10.1093/bioinformatics/btp324

Lin, C. J., and Chen, Y. L. (2018). Conserved and divergent functions of the cAMP/PKA signaling pathway in *Candida albicans* and *Candida tropicalis*. *J. Fungi* 4:68. doi: 10.3390/jof4020068

Liu, L., Feizi, A., Österlund, T., Hjort, C., and Nielsen, J. (2014). Genome-scale analysis of the high-efficient protein secretion system of *Aspergillus oryzae*. *BMC Syst. Biol.* 8:73. doi: 10.1186/1752-0509-8-73

Ma, Y., Liu, X., Yin, Y., Zou, C., Wang, W., Zou, S., et al. (2015). Expression optimization and biochemical properties of two glycosyl hydrolase family 3 beta-glucosidases. *J. Biotechnol.* 206, 79–88. doi: 10.1016/j.jbiotec.2015.04.016

Mardis, E. R. (2008). Next-generation DNA sequencing methods. *Annu. Rev. Genom. Hum. Genet.* 9, 387–402. doi: 10.1146/annurev.genom.9.081307.164359

Martínez-Espinoza, A. D., Ruiz-Herrera, J., León-Ramírez, C. G., and Gold, S. E. (2004). MAP kinase and cAMP signaling pathways modulate the pH-induced yeast-to-mycelium dimorphic transition in the corn smut fungus *Ustilago maydis*. *Curr. Microbiol.* 49, 274–281. doi: 10.1007/s00284-004-4315-6

Martínez-Soto, D., and Ruiz-Herrera, J. (2015). Regulation of the expression of the whole genome of *Ustilago maydis* by a MAPK pathway. *Arch. Microbiol* 197, 575–588. doi: 10.1007/s00203-015-1087-2

Midkiff, J., Borochoff-Porte, N., White, D., and Johnson, D. I. (2011). Small molecule inhibitors of the *Candida albicans* budded-to-hyphal transition act through multiple signaling pathways. *PLoS One* 6:e25395. doi: 10.1371/journal.pone.0025395

Naruzawa, E. S., and Bernier, L. (2014). Control of yeast-mycelium dimorphism in vitro in Dutch elm disease fungi by manipulation of specific external stimuli. *Fungal Biol.* 118, 872–884. doi: 10.1016/j.funbio.2014.07.006

Nigg, M., and Bernier, L. (2016). From yeast to hypha: defining transcriptomic signatures of the morphological switch in the dimorphic fungal pathogen *Ophiostoma* novo-ulmi. *BMC Genom.* 17:920. doi: 10.1186/s12864-016-3251-8

Nobile, C. J., Andes, D. R., Nett, J. E., Smith, F. J., Yue, F., Phan, Q. T., et al. (2006). Critical role of Bcr1-dependent adhesins in *C. albicans* biofilm formation in vitro and in vivo. *PLoS Pathog.* 2:e63. doi: 10.1371/journal.ppat.0020063

Norihiro, T., Makoto, F., Hiroki, N., Norie, K., Akio, T., and Shigezo, U. (1989). Isolation of a cDNA encoding Aspergillus oryzae Taka-amylase A: evidence for multiple related genes. *Gene* 84, 319–327. doi: 10.1016/0378-1119(89)90506-4

Nunes, L. R., Costa de Oliveira, R., Leite, D. B., da Silva, V. S., dos Reis Marques, E., da Silva Ferreira, M. E., et al. (2005). Transcriptome analysis of *Paracoccidioides brasiliensis* cells undergoing mycelium-to-yeast transition. *Eukaryot. Cell* 4, 2115–2128. doi: 10.1128/EC.4.12.2115-2128.2005

O'Meara, T. R., and Alspaugh, J. A. (2012). The Cryptococcus neoformans capsule: a sword and a shield. *Clin. Microbiol. Rev.* 25, 387–408. doi: 10.1128/CMR.00001-12

Pan, X., Harashima, T., and Heitman, J. (2000). Signal transduction cascades regulating pseudohyphal differentiation of *Saccharomyces cerevisiae*. *Curr. Opin. Microbiol.* 3, 567–572. doi: 10.1016/s1369-5274(00)00142-9

Parente, J. A., Borges, C. L., Bailão, A. M., Felipe, M. S. S., Pereira, M., and de Almeida Soares, C. M. (2008). Comparison of transcription of multiple genes during mycelia transition to yeast cells of Paracoccidioides brasiliensis reveals insights to fungal differentiation and pathogenesis. *Mycopathologia* 165, 259–273. doi: 10.1007/s11046-007-9078-8

Park, J. S., Song, S. H., Choi, J. B., Kim, Y. S., Kwon, S. H., and Park, Y. S. (2014). Physicochemical properties of Korean rice wine (Makgeolli) fermented using yeasts isolated from Korean traditional nuruk, a starter culture. *Food Sci. Biotechnol.* 23, 1577–1585. doi: 10.1007/s10068-014-0214-1

Park, K. H., Liu, Z., Park, C. S., and Ni, L. (2016). Microbiota associated with the starter cultures and brewing process of traditional Hong Qu glutinous rice wine. *Food Sci. Biotechnol.* 25, 649–658. doi: 10.1007/s10068-016-0115-6

Peñalva, M. A., Tilburn, J., Bignell, E., and Arst, H. N. (2008). Ambient pH gene regulation in fungi: making connections. *Trends Microbiol.* 16, 291–300. doi: 10.1016/j.tim.2008.03.006

Reddy, O. V. S., and Basappa, S. C. (1996). Direct fermentation of cassava starch to ethanol by mixed cultures of *Endomycopsis fibuligera* and *Zymomonas mobilis*: synergism and limitations. *Biotechnol. Lett.* 18, 1315–1318. doi: 10.1007/bf00129962

Robinson, M. D., McCarthy, D. J., and Smyth, G. K. (2010). edgeR: a Bioconductor package for differential expression analysis of digital gene expression data. *Bioinformatics* 26, 139–140. doi: 10.1093/bioinformatics/btp616

Rohart, F., Gautier, B., Singh, A., and Lê Cao, K. A. (2017). mixOmics: an R package for 'omics feature selection and multiple data integration. *PLoS Comput. Biol.* 13:e1005752. doi: 10.1371/journal.pcbi.1005752

Rooney, P. J., and Klein, B. S. (2002). Linking fungal morphogenesis with virulence. *Cell. Microbiol.* 4, 127–137. doi: 10.1046/j.1462-5822.2002.00179.x

Ruiz-Herrera, J., Leon, C. G., Guevara-Olvera, L., and Carabez-Trejo, A. (1995). Yeast-mycelial dimorphism of haploid and diploid strains of *Ustilago maydis*. *Microbiology* 141, 695–703. doi: 10.1099/13500872-141-3-695

Ruiz-Herrera, J., Pérez-Rodríguez, F., and Velez-Haro, J. (2020). The signaling mechanisms involved in the dimorphic phenomenon of the Basidiomycota

fungus *Ustilago maydis*. *Int. Microbiol.* 23, 121–126. doi: 10.1007/s10123-019-00100-5

Ruiz-Herrera, J., and Sentandreu, R. (2002). Different effectors of dimorphism in *Yarrowia lipolytica*. *Arch. Microbiol.* 178, 477–483. doi: 10.1007/s00203-002-0478-3

Sánchez-Arreguin, J. A., Ruiz-Herrera, J., Mares-Rodriguez, FdJ, León-Ramírez, C. G., Sánchez-Segura, L., Zapata-Morín, P. A., et al. (2021). Acid pH strategy adaptation through NRG1 in *Ustilago maydis*. *J. Fungi.* 7:91. doi: 10.3390/jof7020091

Saporito-Irwin, S. M., Birse, C. E., Sypherd, P. S., and Fonzi, W. A. (1995). PHR1, a pH-regulated gene of *Candida albicans*, is required for morphogenesis. *Mol. Cell. Biol.* 15, 601–613. doi: 10.1128/mcb.15.2.601

Seo, D. H., Jung, J. H., Kim, H. Y., Kim, Y. R., Ha, S. J., Kim, Y. C., et al. (2007). Identification of lactic acid bacteria involved in traditional Korean rice wine fermentation. *Food Sci. Biotechnol.* 16, 994–998.

Sherrington, S. L., Sorsby, E., Mahtey, N., Kumwenda, P., Lenardon, M. D., Brown, I., et al. (2017). Adaptation of *Candida albicans* to environmental pH induces cell wall remodelling and enhances innate immune recognition. *PLoS Pathog.* 13:e1006403. doi: 10.1371/journal.ppat.1006403

Shin, H. M., Lim, J. W., Shin, C. G., and Shin, C. S. (2017). Comparative characteristics of rice wine fermentations using *Monascus koji* and rice nuruk. *Food Sci. Biotechnol.* 26, 1349–1355. doi: 10.1007/s10068-017-0187-y

Smith, R. L., and Johnson, A. D. (2000). Turning genes off by Ssn6–Tup1: a conserved system of transcriptional repression in eukaryotes. *Trends Biochem. Sci.* 25, 325–330. doi: 10.1016/s0968-0004(00)01592-9

Song, H., Choi, J., Park, C. W., Shin, D. B., Kang, S. S., Oh, S. H., et al. (2015). Study of quality control of traditional wine using IT sensing technology. *J. Korean Soc. Food Sci. Nutr.* 44, 904–911. doi: 10.3746/jkfn.2015.44.6.904

Song, S. H. (2013). Analysis of microflora profile in Korean traditional Nuruk. *J. Microbiol. Biotechnol.* 23, 40–46. doi: 10.4014/jmb.1210.10001

Sosinska, G. J., de Koning, L. J., de Groot, P. W. J., Manders, E. M. M., Dekker, H. L., Hellingwerf, K. J., et al. (2011). Mass spectrometric quantification of the adaptations in the wall proteome of *Candida albicans* in response to ambient pH. *Microbiology* 157, 136–146. doi: 10.1099/mic.0.044206-0

Staniszewska, M., Bondaryk, M., Swoboda-Kopec, E., Siennicka, K., Sygitowicz, G., and Kurzatkowski, W. (2013). Candida albicans morphologies revealed by scanning electron microscopy analysis. *Braz. J. Microbiol.* 44, 813–821. doi: 10.1590/S1517-83822013005000056

Sudbery, P. E. (2011). Growth of *Candida albicans* hyphae. *Nat. Rev. Microbiol.* 9, 737–748. doi: 10.1038/nrmicro2636

Supek, F., Bošnjak, M., Škunca, N., and Šmuc, T. (2011). REVIGO summarizes and visualizes long lists of gene ontology terms. *PLoS One* 6:e21800. doi: 10.1371/journal.pone.0021800

Van Zyl, J. H. D., Den Haan, R., and Van Zyl, W. H. (2016). Overexpression of native Saccharomyces cerevisiae ER-to-Golgi SNARE genes increased heterologous cellulase secretion. *Appl. Microbiol. Biotechnol.* 100, 505–518. doi: 10.1007/s00253-015-7022-2

Vollmeister, E., Schipper, K., Baumann, S., Haag, C., Pohlmann, T., Stock, J., et al. (2011). Fungal development of the plant pathogen *Ustilago maydis*. *FEMS Microbiol. Rev.* 36, 59–77. doi: 10.1111/j.1574-6976.2011.00296.x

Wang, Y., Tang, L. J., Peng, X., Zhang, Z. B., Yang, H. L., Yan, R. M., et al. (2020). Transcriptome analysis of the dimorphic transition induced by pH change and lipid biosynthesis in *Trichosporon cutaneum*. *J. Ind. Microbiol. Biotechnol.* 47, 49–61. doi: 10.1007/s10295-019-02244-9

Yang, E., Chow, W. N., Wang, G., Woo, P. C. Y., Lau, S. K. P., Yuen, K. Y., et al. (2014). Signature gene expression reveals novel clues to the molecular mechanisms of dimorphic transition in *Penicillium marneffei*. *PLoS Genet.* 10:e1004662. doi: 10.1371/journal.pgen.1004662

Yang, S., Choi, S. J., Kwak, J., Kim, K., Seo, M., Moon, T. W., et al. (2013). *Aspergillus oryzae* strains isolated from traditional Korean Nuruk: fermentation properties and influence on rice wine quality. *Food Sci. Biotechnol.* 22, 425–432. doi: 10.1007/s10068-013-0097-6

Yang, S., Lee, J., Kwak, J., Kim, K., Seo, M., and Lee, Y. W. (2011). Fungi associated with the traditional starter cultures used for rice wine in Korea. *J. Korean Soc. Appl. Biol. Chem.* 54, 933–943. doi: 10.1007/bf03253183

Yeo, S. H., and Jeong, Y. J. (2010). Current trends and development a plan in the Korean Makgeolli industry. *Food Sci. Ind.* 43, 55–64.

Zhang, Q., Tao, L., Guan, G., Yue, H., Liang, W., Cao, C., et al. (2016). Regulation of filamentation in the human fungal pathogen *Candida tropicalis*. *Mol. Microbiol.* 99, 528–545. doi: 10.1111/mmi.13247

Zhu, L. B., Wang, Y., Zhang, Z. B., Yang, H. L., Yan, R. M., and Zhu, D. (2017). Influence of environmental and nutritional conditions on yeast–mycelial dimorphic transition in *Trichosporon cutaneum*. *Biotechnol. Biotechnol. Equip.* 31, 516–526. doi: 10.1080/13102818.2017.1292149

Conflict of Interest: The authors declare that the research was conducted in the absence of any commercial or financial relationships that could be construed as a potential conflict of interest.

frontiers in Microbiology

ORIGINAL RESEARCH
published: 12 July 2021
doi: 10.3389/fmicb.2021.714726

Understanding the Shifts of Microbial Community and Metabolite Profile From Wheat to Mature *Daqu*

*Yuandi Zhang[1], Yi Shen[2], Wei Cheng[2], Xi Wang[2], Yansong Xue[1], Xiaoxue Chen[1] and Bei-Zhong Han[1]**

[1] Beijing Laboratory for Food Quality and Safety, College of Food Science and Nutritional Engineering, China Agricultural University, Beijing, China, [2] Sichuan Langjiu Co., Ltd., Luzhou, China

Wheat-originated microbes play an important role in shaping the quality of high-temperature *Daqu* which is commonly used as a starter for producing sauce-flavor *Baijiu*. However, the shifts of microbiota from raw material to fresh *Daqu* and then to mature *Daqu* remain unclear. Hence, in the present study, the inner and outer of fresh and mature *Daqu* were collected to explore the correlation between microbiota and metabolites as well as the source of the microbiota in *Daqu*. Results indicated that the activities of amylase and protease between the inner and outer of fresh *Daqu* varied significantly while both parts became similar after maturation. The predominant bacteria shifted from *Saccharopolyspora* (outer) and *Staphylococcus* (inner) to *Kroppenstedtia* (both outer and inner), while the predominant fungi shifted from *Thermoascus* (both outer and inner) to *Byssochlamys* (outer) and *Fusarium* (inner). A combining analysis of headspace solid-phase micro extraction-gas chromatography-mass spectrometry, headspace gas chromatography-ion mobility spectrometry, and nuclear magnetic resonance was employed to detect the metabolites. The network analysis was conducted to perform the relationships between microbes and metabolites. The results showed that the bacteria, especially *Saccharopolyspora*, *Bacillus*, and *Acinetobacter*, had a strong correlation with the productions of esters, amino acids and their derivatives, and sugars and their derivatives, while most fungi such as *Thermoascus*, were negatively correlated with the phenylalanine, trimethylamine n-oxide, and isovalerate. SourceTracker analysis indicated that wheat was the important source of the *Daqu* microbiota, especially, the microorganisms in the inner of *Daqu* might be the drivers of the microbial succession during maturation. This study provided a comprehensive exploration to understand the microbial sources and shifts in high-temperature *Daqu* during maturation.

Keywords: *Daqu*, maturation, microbiota, metabolites, wheat

OPEN ACCESS

Edited by:
Wanping Chen,
Georg-August-University Goettingen, Germany

Reviewed by:
Yuanliang Hu,
Hubei Normal University, China
Guiming Fu,
Nanchang University, China

***Correspondence:**
Bei-Zhong Han
hbz@cau.edu.cn

Specialty section:
This article was submitted to Food Microbiology, a section of the journal Frontiers in Microbiology

Received: *25 May 2021*
Accepted: *14 June 2021*
Published: *12 July 2021*

Citation:
Zhang Y, Shen Y, Cheng W, Wang X, Xue Y, Chen X and Han B-Z (2021) Understanding the Shifts of Microbial Community and Metabolite Profile From Wheat to Mature Daqu. Front. Microbiol. 12:714726. doi: 10.3389/fmicb.2021.714726

INTRODUCTION

Baijiu is a fermented alcoholic beverage and plays an important role in the history of Chinese food culture for 3000 years (Jin et al., 2017). The popularity of *Baijiu* to a great extent is due to its rich tastes and characterized flavors, both of which are produced in the complex production processes, including solid-state fermentation, distillation, storage, and blending (Xu et al., 2010).

Particularly, fermentation plays an important role in the production of volatile flavors and critical secondary metabolites (Zheng et al., 2011). *Daqu*, made of wheat, barley, pea, and/or corn, is the most common starter and adopted in all the famous *Baijiu* in China (Wang et al., 2021). *Daqu* production needs a series of steps, including moistening, breaking, mixing shaping, spreading, incubating, and maturation (Zheng et al., 2011). Among them, maturation is the vital step that involves microbial enrichment, primary and secondary metabolic processes, and changes in diverse microbes and metabolites (Fan et al., 2019).

Daqu production still mainly relies on the experience of the operators to evaluate the quality of the raw materials and the maturation degree of the *Daqu*, which might not be objective all the time (Deng et al., 2020). The development of the new detection methods, like gas chromatography-mass spectrometry (GC-MS), high performance liquid chromatography-mass spectrometry (HPLC-MS), leads to the discrimination of *Daqu* maturation easier and more accurate to some extent (Pang et al., 2020). However, the microbiota is the original driver of the maturation. Maturation can promote enriched microbes to interact further, thereby leading to the mixed microbial communities and various metabolites to form balanced and stable *Daqu* (Gou et al., 2015). Culture-dependent and Illumina MiSeq sequencing methods were used to determine the microbial community during the maturation. A comprehensive understanding of the source and succession of the microbiota and the metabolites is very useful and urgent for the stable production of the high-quality *Daqu*.

Sauce-flavor *Baijiu*, one of the most popular *Baijiu* in China, is famous for its flavor resembling soy sauce, full-body, and long-lasting aroma (Zheng and Han, 2016). Its production relies on the high-temperature *Daqu* and the traditional production steps as shown in **Supplementary Figure 1**. Recently, microbiological and physicochemical methods were combined to explore the distribution of microbiota and various metabolites in *Daqu*. Jin et al. (2019) revealed the dominant microbes in *Daqu* and their distribution characteristics and detected the volatile flavors by headspace solid-phase micro extraction-gas chromatography-mass spectrometry (HS-SPME-GC-MS). Their results showed that the dominant bacteria of sauce-flavor *Daqu* were *Bacillales*, *Enterobacteriales*, and *Lactobacillales*, while the dominant fungi were *Trichoderma*, *Candida*, *Aspergillus*, *Thermomyces*, and *Trichosporon*. In Jin et al. (2019) study, the results showed that bacterial diversity was higher than fungal diversity in *Daqu*, and had the significant differences in microbial composition, distribution and physicochemical indices between the inner and outer parts of *Daqu*. These studies were all conducted on the mature *Daqu* and not associated with the changes during the maturation.

In the present study, Illumina MiSeq sequencing was used to investigate the microbiota succession from wheat, to fresh *Daqu* and mature *Daqu*. HS-SPME-GC-MS, headspace gas chromatography-ion mobility spectrometry (HS-GC-IMS), and nuclear magnetic resonance (^{1}H NMR) were combined to comprehensively evaluate the metabolites in the different parts of *Daqu*, and different steps of *Daqu* production. Besides, SourceTracker analysis was employed to evaluate the contribution of wheat to *Daqu* in microbiota (Jin et al., 2019; Chen et al., 2021). It is the first comprehensive study on shifts in microbiota and metabolites for maturation of the sauce-flavor *Daqu* and will shed light on the improvement of *Daqu* production and the quality of the sauce-flavor *Baijiu*.

MATERIALS AND METHODS

Sampling

The samples were collected from a sauce-flavor *Baijiu* manufacturer in Sichuan, China in 2020. Samples were collected in two different points: fresh *Daqu* and mature *Daqu*. Fresh *Daqu* (F-*Daqu*) refers to the newly made *Daqu* that needs 6 months of maturation. Mature *Daqu* (M-*Daqu*) refers to *Daqu* that is ready for *Baijiu* fermentation. To get reliable samples, *Daqu* bricks from each step were randomly selected from upper, middle, and lower locations in triplicate. Then each *Daqu* block was separated into two parts, the surface layer of 2.0∼3.0 cm thick was named the outer part of *Daqu* (O-*Daqu*), and the remaining central part was named the inner part of *Daqu* (I-*Daqu*). Raw material (wheat) samples (3.0 kg) were collected randomly from the storage. All samples were made in triplicate. *Daqu* samples were stored at 4°C for microbial counts and −20°C for metabolite analysis and Illumina MiSeq sequencing analysis.

Microbiological Analysis

Total aerobic bacteria and thermophilic bacteria were enumerated on Plate Count Agar (PCA) (Aobox, Beijing, China), and were cultured at 37 and 55°C, respectively. Lactic acid bacteria (LAB) were enumerated on LAB culture medium (MRS; Aobox, Beijing, China) with natamycin 500 μg/ml. The plates were incubated at 30°C for 48–72 h (Pradhan and Tamang, 2019). Fungi were enumerated on two different media named Malt Extract Agar (MEA) (Aobox, Beijing, China) and Rose Bengal Chloramphenicol Agar (RBCA) (Aobox, Beijing, China), respectively, to which 100 mg/L chloramphenicol (Oxoid, SR0078E) was added. Colony Forming Units (CFU) were calculated and converted to the value of base 10 Logarithm and recorded as $\log_{10}$ (CFU/g) (Zheng et al., 2012).

Analyses of Physicochemical Properties and Enzymology Properties

Moisture in *Daqu* samples was determined with a gravimetric method by drying 5.0 g samples at 105°C for 3 h (Pang et al., 2020). *Daqu* powder (5.0 g) was soaked in 50 mL of distilled water for 30 min, and water extracts were collected after filtration. The pH was measured using a pH meter positioned in the slurry (Zheng et al., 2012). The activity of glucoamylase and protease were determined according to the 3,5-dinitrosalicylic acid (DNS) method and Folin-phenol method, respectively (Fan G. S. et al., 2020). One unit of glucoamylase activity was defined as the amount of *Daqu* required for the liberation of 1 μmol glucose per minute in PBS buffer (50 mM, pH 6.5) at 40°C. One unit of protease activity was defined as the amount of *Daqu* required for the liberation of 1 mg tyrosine per minute in PBS buffer (50 mM, pH 7.0) at 40°C (Li et al., 2017).

Analysis of Volatile Flavors by HS-SPME-GC-MS

The volatile flavors were analyzed by HS-SPME-GC-MS. The pre-treatment of HS-SPME-GC-MS was carried out as described below: 2.0 g sample was mixed with 8.0 mL Milli-Q water and subjected to ultrasonic treatment for 30 min (Liu et al., 2019; Pang et al., 2020). This was carried out in triplicates. Following this, the sample solutions were centrifuged at 6000 × *g* at 4°C for 15 min. Subsequently, 8 mL supernatant from the samples, and 2.0 g sodium chloride were placed into a 20 ml vial. This process was repeated with all three (triplicate) samples (Fan Y. et al., 2020). The volatile compounds were extracted with SPME fiber at 50°C for 50 min. The contents of volatile compounds were detected by GC-MS (Zhang et al., 2020).

Analysis of Volatile Flavors by HS-GC-IMS

To investigate the spectrum changes of metabolites in *Daqu* samples, an untargeted analysis of volatile fingerprints was performed on a GC-IMS system (FlavourSpec®, Gesellschaft für Analytische Sensorsysteme mbH, Dortmund, Germany) equipped with an automatic headspace sampler unit (CTC-PAL, CTC Analytics AG, Zwingen, Switzerland). Extraction of volatile flavors from *Daqu* by SPME refers to the method of Yang et al. (2020) with minor modifications. In brief, 2.5 g of *Daqu* was weighed and placed into 20 mL headspace glass sampling vial. Subsequently, samples were incubated at 60°C for 15 min. After incubation, 200 μL of headspace was automatically injected into the injector. The volatile flavors from the *Daqu* were analyzed by GC-IMS referring to the method of Li et al. (2019) with minor modifications. The volatile flavors were separated and analyzed using a GC-IMS instrument, equipped with a quartz capillary column (FS-SE-54-CB-1, 15 m × 0.53 mm, 0.5 μm). The GC condition is as following: column temperature, 60°C; carrier gas: ultrapure nitrogen (purity ≥ 99.999%); carrier gas flow rate, 2 mL/min (0–2 min), 2–10 mL/min (2–10 min), 10–100 mL/min (10–20 min), 100–150 mL/min (20–30 min); detection time, 25 min (Yang et al., 2020). The following conditions were maintained in the automatic headspace sampler condition: incubation temperature, 60°C; incubation time, 15 min; injection method, headspace injection; injection volume, 200 μL; injection needle temperature, 85°C; heating method, shaking heating; shaking speed, 500 r/min; splitless injection (Márquez-Sillero et al., 2011). IMS detection condition is as follows: length of the drift tube, 98 mm; linear voltage in the tube, 500 V/cm; the temperature of drift tube, 45°C; drift gas, ultrapure nitrogen (purity ≥ 99.999%); the volume of drift gas, 150 mL/min; radioactive source, β-rays (tritium, 3H); ionization mode, positive ion (Yang et al., 2020).

Analysis of Polar Metabolites by NMR

The aqueous extracts for NMR measurements were prepared as reported previously. A 600 μl aliquot of each sample was transferred into a 5-mm NMR tube. All ^{1}H NMR spectra were measured at 300 K using an AVANCE NMR spectrometer (proton frequency 1/4 600.13 MHz, 14.1 T; Bruker, Billerica, Germany) with a cryogenic NMR probe (Wu et al., 2009). The ^{1}H NMR experiments were performed using the following conditions: NOESYGPPRR1D pulse sequence; relaxation delay, 4.00 s; mixing time (for NOESY), 1.00 s; acquisition time, 2.28 s; number of steady states transients (dummy scans), 4; gradient pulse time, 1.00 ms; solvent suppression, pre-saturation with spoil gradient; spectral width, 7184 Hz; and time domain size, 32 k (Li et al., 2018). The compounds were identified and quantified with Chenomx software (version 7.6; Chenomx, Edmonton, Canada) with reference to the internal standard TSP. Each ^{1}H NMR spectrum was equally divided into 242 fragments with width of 0.04 ppm. Spectra both with a range of 0.00∼10.00 ppm and exception of residual water resonance (4.50∼4.80 ppm), were divided into 0.04 ppm wide bins, followed by importing the achieved integral values into Microsoft® Excel (Microsoft Corporation, Redmond, WA, United States) (Wu et al., 2009).

DNA Extraction and Illumina MiSeq Sequencing Analysis

DNA extraction was carried out with E.Z.N.A.® Soil DNA kits (Omega, Norcross, GA, United States) as per the manufacturer's instructions. For bacteria, the V3-V4 domains of the 16 S rRNA genes were amplified using primers 338F and 806R. For fungi, the internal transcribed spacer (ITS) ITS1 regions were amplified with primers ZIT_F and ZITS_R (He et al., 2019). Reaction conditions consisted of an initial 95°C for 3 min followed by 35 cycles of 95°C for 30 s, 55°C for 30 s, and 72°C for 45 s, and a final extension of 72°C for 10 min. The purified amplicons were paired-end sequenced on an Illumina MiSeq PE300 system (Illumina, San Diego, CA, United States). Trimmomatic software (version 0.36) was used for mass filtering of the merged sequence (Bolger et al., 2014). Then Uchime software (version 8.1) was used to identify and remove chimeric sequences. Bioinformatics analysis of high-quality sequences was performed on a quantitative insight in microbial ecology (QIIME 1.8.0) platform. Clustering operation taxonomic units (OTUs) from clean tags with 97% similarity was done using the Uparse software (version 9.6). Then the taxonomic information was assigned to all bacterial OTUs via searching against Silva database (Release 132)[1] and all fungal OTUs via searching against Unite (Release 7.2)[2] by using RDP classifier (version 2.2).

Statistical Analysis

Statistical analysis was carried out using IBM-SPSS V22.0 (IBM, United States). A one-way ANOVA with Duncan's test was used to determine the significance of physicochemical properties and microbial counts (Li et al., 2020). Principal component analysis (PCA) was performed to analyze the metabolites data by SIMCA-14.1. Paired *t*-test and wilcoxon tests were performed to test the difference in the alpha and beta diversity indices within the stats R package (Version 2.15.3) (Dai et al., 2020).

[1] http://www.arb-silva.de

[2] http://unite.ut.ee/index.php

The relationship between microbiota structure and metabolites was analyzed by Two-way Orthogonal Partial Least Squares (O2PLS) and visualized via Cytoscape (v.3.4.0) (Langille et al., 2013). We calculated the Pearson correlation coefficient among the different *Daqu* samples and raw materials to analyze the relationships among them. SourceTracker (version 0.9.8) was used to analyze the sources of microbial communities in *Daqu* (Knights et al., 2011).

RESULTS

Physicochemical Properties

The physicochemical properties of inner of fresh *Daqu* (F-I-D), outer of fresh *Daqu* (F-O-D), inner of mature *Daqu* (M-I-D), and outer of mature *Daqu* (M-O-D) were shown in **Table 1**. The moisture changed with the maturation. Obviously, the moisture in F-*Daqu* was significantly higher ($P < 0.05$) than M-*Daqu*, and the moisture in I-*Daqu* was significantly higher ($P < 0.05$) than O-*Daqu*. The pH of I-*Daqu* decreased slightly while that of O-*Daqu* increased. After the 6 months maturation, both activities of amylase and protease decreased in the I-*Daqu*, while their activities show a opposite trend.

Microbiological Analysis

The microbial counts of bacteria and fungi in *Daqu* samples were shown in **Table 2**. The microbial counts in the F-I-D were significantly higher than that in F-O-D ($P < 0.05$) while the microbial counts of M-I-D was close to that of M-O-D. The difference in microbial counts between I-*Daqu* and O-*Daqu* reduced during maturation. The microbial counts in I-*Daqu* decreased while those in O-*Daqu* increased. The changes of the environment during maturation drove the microbiota inner and outer of *Daqu* to become similar and eventually to form a stable system.

Illumina MiSeq sequencing was utilized to characterize the microbiota structures in F-I-D, F-O-D, M-I-D, and M-O-D. A total of 983,228 high quality reads from V3-V4 region of 16S rRNA gene sequences, and 1,684,859 high quality reads from ITS region were obtained from all samples. For bacteria, there was an average of 49,161 reads per sample, with a range from 29,943 to 73,680 reads. For fungi, there was an average of 84,243 reads per sample, with a range from 32,867 to 144,177 reads. OTUs in samples were defined with a ≥97% sequence identity cutoff, and all samples had high Good's coverage (1.00). Chao1 richness and other information were shown in **Supplementary Table 1**. The rarefaction curves of both bacterial and fungal communities approached the saturation plateau, which indicated that the microbial communities were well represented at the sequencing depth (**Supplementary Figure 2**).

Taxonomic classification of sequences from bacterial communities (a) and fungal communities (b) was showed in **Supplementary Figure 3**. As for bacterial communities, several types of microbial abundance of *Daqu* such as *Lactobacillus*, *Sphingobacterium*, and *Staphylococcus* decreased after maturation while the abundance of *Kroppenstedtia* and *Lentibacillus* increased, indicating that maturation-related changes had occurred at the genus level (**Supplementary Figure 3A**). As for fungal communities, the results showed that *Thermoascus*, as the absolute dominant flora, significantly decreased in abundance during the maturation (**Supplementary Figure 3B**).

The distribution of microbiota at the genus level was shown in **Figure 1**. For bacterial communities, *Staphylococcus* predominated in the F-I-D with an average abundance of 70.14%, followed by *Kroppenstedtia* (24.46%). After maturation, *Kroppenstedtia* (84.88%) became the predominant bacterial genus, followed by *Staphylococcus* (1.68%). Besides, *Saccharopolyspora* and *Kroppenstedtia* predominated at the F-O-D with an average abundance of 35.71 and 31.58%, respectively. In M-O-D, *Kroppenstedtia* (82.60%) became the predominant bacterial genus, followed by *Saccharopolyspora* (3.40%). After maturation, the bacterial compositions in both M-I-D and M-O-D became similar (**Figure 1A**). As for fungal communities (**Figure 1B**), *Thermoascus* possessed an absolutely dominant position in both F-I-D and F-O-D. After maturation, the proportion of *Fusarium* was increased both in the M-I-D and M-O-D from the fresh *Daqu*. The relative abundance of *Byssochlamys* in M-O-D increased significantly (from 0.27 to 24.46%). Besides, it was mainly the rise of *Microascus*

TABLE 1 | Physicochemical properties of *Daqu* samples.

Sample	Moisture (%)	pH	Amylase Activity (U/g)	Protease Activity (U/g)
F-I-D	17.28 ± 1.39^{d}	6.38 ± 0.05^{c}	7.40 ± 0.14^{d}	14.80 ± 2.18^{b}
F-O-D	12.60 ± 0.35^{c}	4.74 ± 0.13^{a}	0.73 ± 0.02^{a}	1.28 ± 0.34^{a}
M-I-D	9.24 ± 0.26^{b}	6.29 ± 0.07^{c}	4.35 ± 0.03^{c}	12.67 ± 1.59^{b}
M-O-D	7.63 ± 0.27^{a}	5.77 ± 0.08^{b}	2.16 ± 0.03^{b}	2.87 ± 1.59^{a}

Values represent means ± SD (n = 3).
Means with different superscripts are significantly different (One-Way ANOVA; P < 0.05).

TABLE 2 | Microbial counts in *Daqu* samples.

Log_{10} CFU/g	F-*Daqu*		M-*Daqu*	
Microbial groups	F-I-D	F-O-D	M-I-D	M-O-D
Mesophilic aerobic bacteria	8.36 ± 0.11^{d}	4.73 ± 0.07^{a}	5.64 ± 0.07^{c}	5.00 ± 0.04^{b}
Thermophilic bacteria	6.96 ± 0.07^{d}	4.63 ± 0.11^{a}	5.73 ± 0.13^{c}	5.10 ± 0.06^{b}
Lactic acid bacteria	8.28 ± 0.02^{d}	3.64 ± 0.07^{a}	4.94 ± 0.03^{b}	5.06 ± 0.07^{c}
Fungi on RBCA	8.22 ± 0.04^{d}	2.48 ± 0.01^{a}	5.17 ± 0.02^{c}	4.47 ± 0.04^{b}
Fungi on MEA	8.21 ± 0.02^{d}	2.49 ± 0.01^{a}	5.29 ± 0.03^{c}	4.68 ± 0.03^{b}

Values represent means ± SD (n = 3).
F-I-D: Inner of fresh Daqu; F-O-D: Outer of fresh Daqu; M-I-D: Inner of mature Daqu; M-O-D: Outer of mature Daqu.
Cluster analysis was based on Unweighted UniFrac distance matrix and the UPGMA method. Means with different superscripts are significantly different (One-Way ANOVA; P < 0.05).

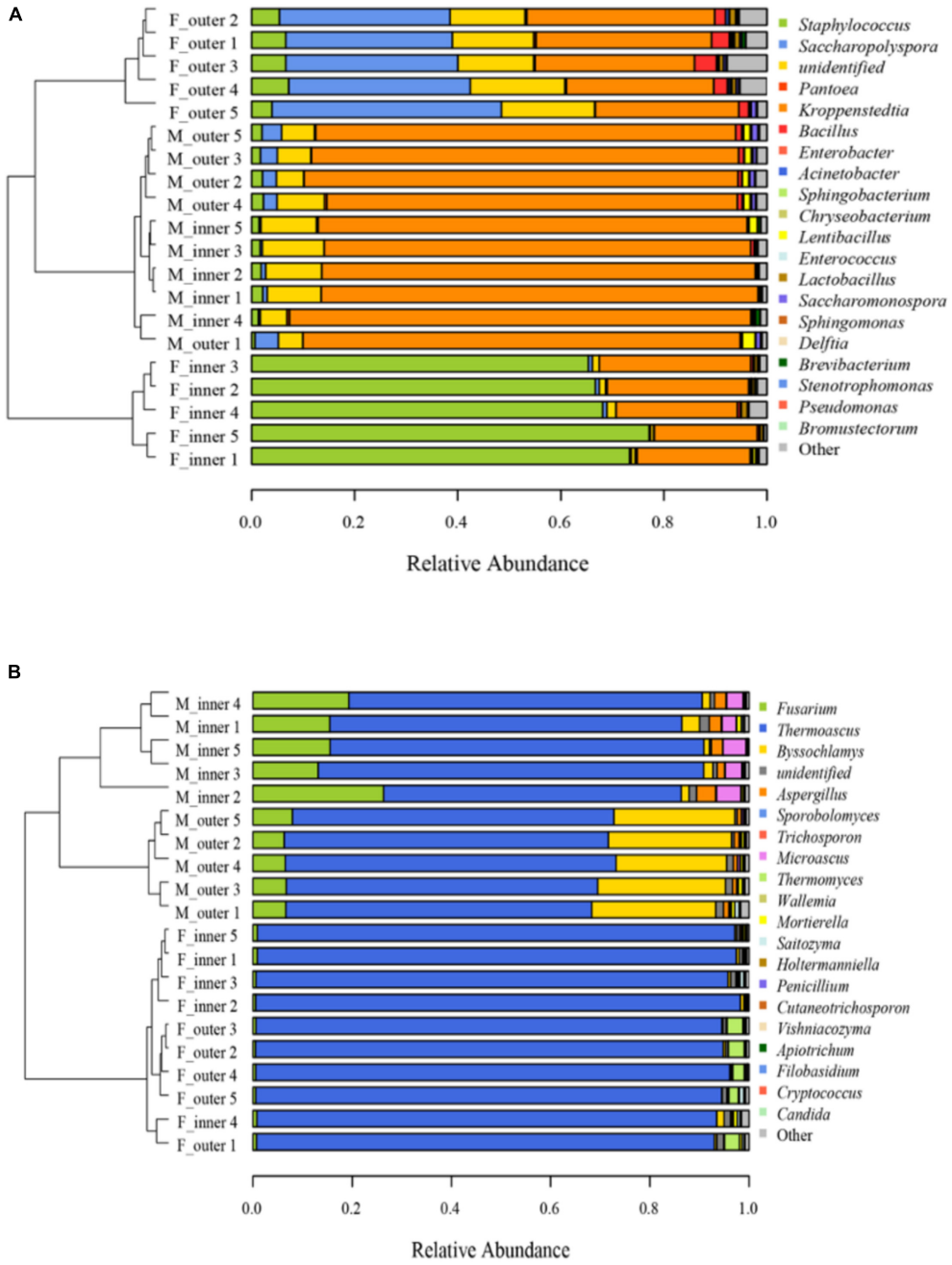

FIGURE 1 | Microbial communities of *Daqu* samples **(A)** Bacterial community. **(B)** Fungal community. F-inner: Inner of fresh *Daqu*; F-outer: Outer of fresh *Daqu*; M-inner: Inner of mature *Daqu*; M-outer: Outer of mature *Daqu*. Cluster analysis was based on Unweighted UniFrac distance matrix and the UPGMA method. Genus level ($n = 5$).

and *Aspergillus* (from 0.03 to 3.80% and from 0.24 to 2.48%, respectively) in M-I-D.

Multivariate Analysis of Volatile Flavors of *Daqu*

A total of 76 volatile flavors were detected from both F-*Daqu* and M-*Daqu* by HS-SPME-GC-MS, including 11 esters, 15 alcohols, 2 organic acids, 11 ketones, 8 aldehydes, 6 phenols, 5 pyrazine, and 18 others (**Supplementary Table 2**). Partial least squares discriminant analysis (PLS-DA) was used to analyze the volatile flavor, and the substances with lower variable importance in the projection (VIP) value were eliminated. As shown in **Figure 2**, the results explained 47.5% of the total variance with R2X (30.7%) and R2Y (16.8%).

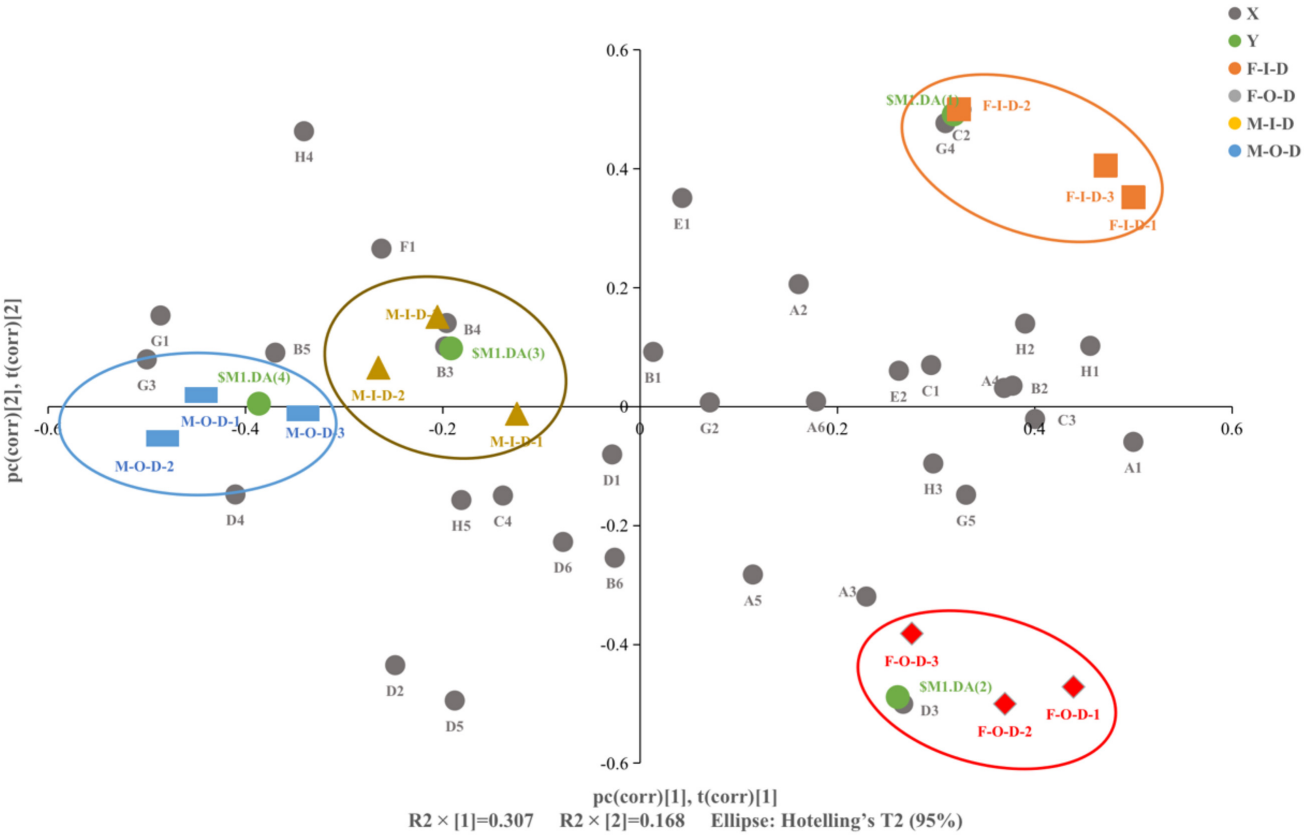

A1	3-octanol
A2	2-ethylhexan-1-ol
A3	Nonan-1-ol
A4	2-propylheptan-1-ol
A5	Dl-1-phenethylalcohol
A6	2-butoxyethanol
B1	Butyl acrylate
B2	Propanoic acid, 2-methyl-, 2,2-dimethyl-1-(1-methylethyl)-1,3-propanediyl ester
B3	Benzene, 1-isocyano-3-methyl
B4	Methyl 3-methylbenzoate
B5	Ethyl pentadecanoate
B6	Ethyl palmitate
C1	2,5-hexanedione
C2	2-methylundecan-4-one
C3	2-cyclohexen-1-1,2,4,4-trimethyl-3-(3-methylbutyl)
C4	1-phenyl-5-methyl-1-hexanone

D1	Acrolein
D2	Pyrrole-2-carboxaldehyde
D3	2-phenyl-5-methyl-2-hexenal
D4	Benzaldehyde
D5	2,4-dimethylbenzaldehyde
D6	Mesitaldehyde
E1	5-isopropyl-2-methylphenol
E2	2,4-di-tert-butylphenol
F1	Dl-phenylsuccinic acid
G1	Tetramethylpyrazine
G2	2,5-dimethyl-3-butylpyrazine
G3	2,3,5-trimethylpyrazine
G4	2,5-dimethyl-3-pentylpyrazine
G5	Pyrazine,3,5-dimethyl-2-(3-methylbutyl)- (9cl)
H1	Toluene
H2	1,2,4-trimethylbenzene
H3	Styrene
H4	Undecan-6-ylbenzene
H5	Pentane,2,2,3,4-tetramethyl

FIGURE 2 | Partial least squares discriminant analysis (PLS-DA) analysis of flavor compounds in *Daqu* samples. F-I-D: Inner of fresh *Daqu*; F-O-D: Outer of fresh *Daqu*; M-I-D: Inner of mature *Daqu*; M-O-D: Outer of mature *Daqu*. X: "•" means flavor compounds. Y: "•" defines the different classes membership of *Daqu* samples in PLS-DA model. Biplot superimposed the scores and loadings of PLS-DA. The middle number in the sample code represents different plants.

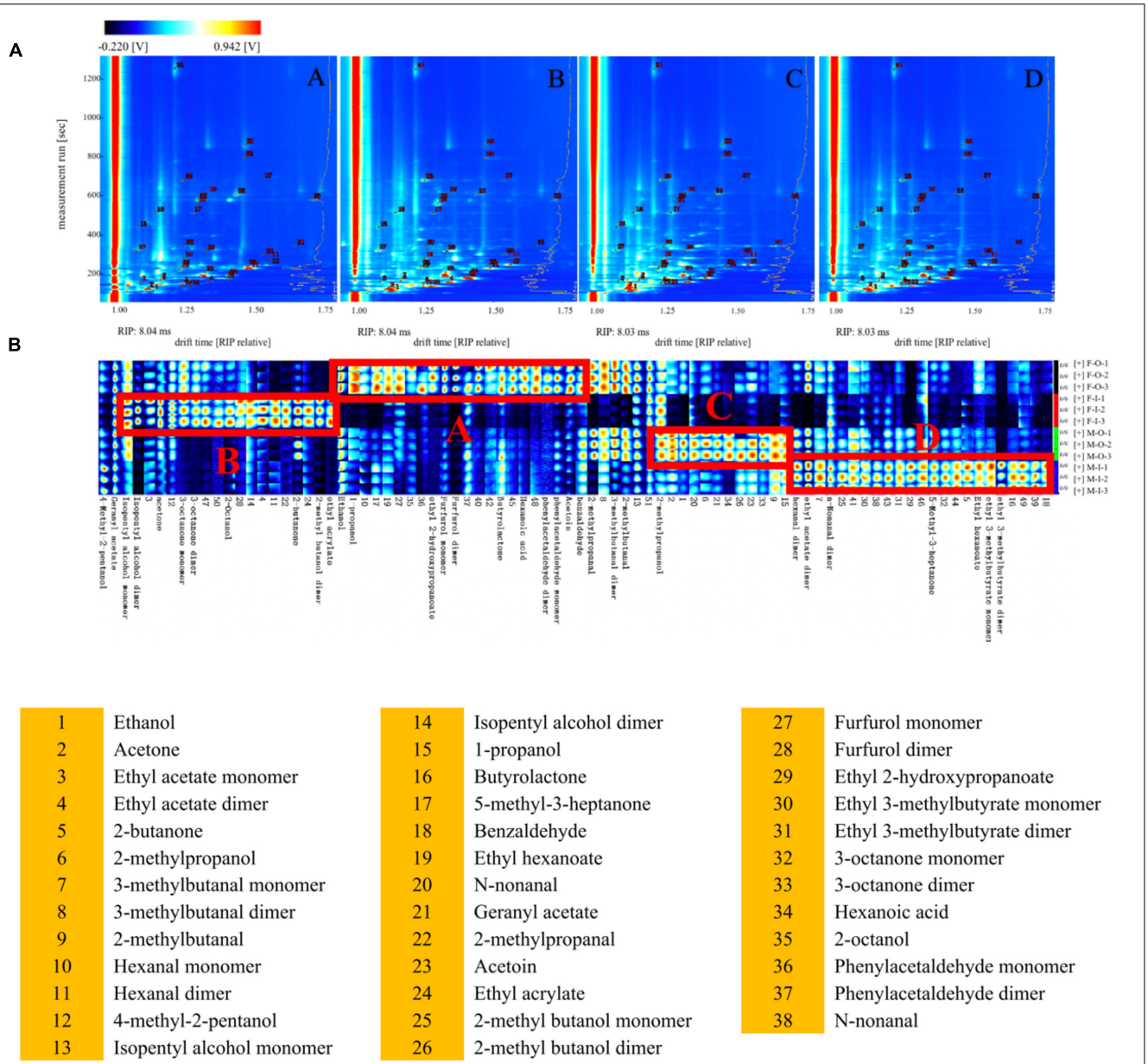

FIGURE 3 | Comparison **(A)** and fingerprints **(B)** of volatile flavors via HS-GC-IMS. A: Inner of fresh *Daqu*; B: Outer of fresh *Daqu*. C: Inner of mature *Daqu*; D: Outer of mature *Daqu*.

The detailed distinctions of volatile flavors profiles in different samples were revealed by the loading plot of PLS-DA. Terms with large VIP were the most relevant for explaining Y. The VIP of benzene, 1-isocyano-3-methyl, 2-phenyl-5-methyl-2-hexenal, 2,4-dimethylbenzaldehyde, 2-methylundecan-4-one, undecan-6-ylbenzene, pyrrole-2-carboxaldehy, 2,5-dimethyl-3-pentylpyrazine, mesitaldehyde, ethyl pentadecanoate, 5-isopropyl-2-methylphenol, dl-1-phenethylalcohol, 2,3,5-trimethylpyrazine, tetramethylpyrazine, toluene, and 3-octanol (VIP > 1.0) contributed to the specificity of *Daqu* samples. Detailed VIP value was provided in the **Supplementary Table 3**. The categories and the content of volatile flavors decreased after maturation. The main differences between F-I-D and F-O-D were shown in the categories and the content of aldehydes and organic acids (**Supplementary Table 2**). After maturation, the total number of volatile flavors categories of I-*Daqu* had little change. However, the categories of alcohols, esters and aldehydes increased, while the types of aldehydes and alkanes decreased. It is worth noting that the direct contact between the O-*Daqu* and air resulting in the volatization of some volatile flavors and the decreased abundance of flavor-producing microorganisms (e.g., *Saccharopolyspora*) in O-*Daqu* during the maturation, contributing to the sharp decrease in categories of volatile flavors in O-*Daqu* (Yang et al., 2020).

As a new flavor detection technology, GC-IMS is widely used for analyzing volatile flavors under the normal atmospheric pressure and highly sensitive to compounds with high electronegativity, which can be used as a supplementary tool for GC-MS to conduct a more comprehensive and systematic detection of the volatile flavors of *Daqu*. The two-dimensional imaging of GC-IMS consisted of drift time, retention time, and the intensity of the ion signals. A total of 88 peaks were detected in *Daqu* samples, and 37 compounds, including 14 aldehydes, 7 alcohols, 6 ketones, 1 organic acid, and 9 esters, were identified by the NIST 2014 and IMS database (**Supplementary Table 4**). Many volatile flavors present in different degree of polymerization, such as monomers and dimers depending upon their concentrations. **Figure 3A** displayed that these products pass through the drift region and multiple signals can be observed as a single compound due to the formation of adducts between the ions and neutral molecules (such as dimers and trimers), including 2-methyl butanol, 2-methylbutanal, 3-methylbutanal, 3-octanone, ethyl 2-hydroxypropanoate, ethyl acrylate, furfurol dimer, hexanal, isopentyl alcohol, n-non-anal, and phenylacetaldehyde. These products exhibited similar retention times, but different drift time (Fan et al., 2021). **Figure 3B** displays that all compounds, identified via GC-IMS, have been selected to compare the differences of four types of *Daqu* samples. Each column represented the signal peak of one volatile compound. The brighter spot indicated the higher concentration of the volatile compound. The monomers and dimers of the same compound were indicated by different columns with the same compound name. However, due to the proton affinity and higher concentration, the drift time of dimers increased and showed distinct spots in the fingerprint (Yang et al., 2020). The total volatile flavors of F-O-D and M-O-D were relatively similar, and the same condition was shown in M-O-D and M-I-D based on the spot color. Compounds of regional A in **Figure 3B** (ethanol, ethyl 2-hydroxy propyl alcohol, propionic acid, furfural, butyrolactone, caproic acid, benzene acetaldehyde, ethyl benzoin, benzene, and formaldehyde, etc.), regional B (isoamyl alcohol, acetone, ketone, octanol, butanone, 2-methyl ethyl acrylate, and butyl alcohol), regional C (2-methyl propyl alcohol, etc.), and regional D (hexanal, ethyl acetate, nonyl aldehyde and 3-methyl ethyl caproate, ethyl butyrate, etc.) represented the characteristics of volatile flavors in F-O-D, F-I-D, M-O-D, and M-I-D.

Polar Metabolites of *Daqu*

Nuclear magnetic resonance (^{1}H NMR spectroscopy) coupled with multivariate statistical analysis was used to investigate the differences of the *Daqu* samples in the polar metabolic changes to better characterize *Daqu* maturation. As shown in **Supplementary Table 5**, a total of 76 polar metabolites including 17 esters, 19 amino acids and their derivatives, 6 alkalamides, 4 alcohols, 30 sugars and their derivatives, and salt of organic acid were detected in *Daqu* samples. Due to a series of complicated metabolism like the Maillard reaction and enzymatic reaction, the polar metabolites in *Daqu* increased with the maturation. For example, in terms of the type and content of esters, F-I-D and F-O-D differed greatly, while M-I-D and M-O-D became closer at the end of maturation. These trends were caused by the shifts of microbiota during maturation. Of all the polar metabolites, the most abundant compounds were alcohols, especially ethanol and glycerol. They were the substrates or precursors for a series of subsequent reactions (Zheng et al., 2011). The polar metabolites' contents especially esters, amino acids and sugars in F-I-D were significantly lower than those in F-O-D.

Network Analysis of the Interactions Among Microbiota, Polar Metabolites and Volatile Flavors in *Daqu*

We analyzed the correlations among microbiota, polar metabolites, and volatile flavors in *Daqu* via Pearson correlation analysis (**Figure 4**) and the detailed value of Pearson correlation coefficients (Pearson correlation $> |0.7|$) was shown in **Supplementary Table 6**. Correlation analysis between microbiota and polar metabolites was shown in **Figure 4A**. Bacteria such as *Saccharopolyspora*, *Bacillus*, and *Acinetobacter* showed a strong correlation with polar metabolites. *Saccharopolyspora* had the highest abundance in F-O-D, which produced more polar metabolites such as esters, amino acids and their derivatives, and sugars and their derivatives in the production process of *Daqu*. For fungi, the correlation network showed that *Thermoascus* was negatively correlated with phenylalanine, trimethylamine n-oxide, and isovalerate. In previous studies, *Thermoascus* could produce some thermostable enzyme and epipolythiodioxopiperazine metabolite derived from the amino acid pathway, and these metabolites exhibited antibacterial and antiviral properties (Leite et al., 2008; Siddiquee, 2018). The abundances of *Fusarium*, *Byssochlamys*, *Aspergillus*, and *Microascus* in M-*Daqu* were significantly higher than those in F-*Daqu* and they showed a strong correlation with 23 polar metabolites including amino acids and their derivatives and esters such as 3-hydroxyisovalerate, propionate, fumarate, acetoacetate, and methionine. These fungi were closely related to the synthesis of most esters and some amino acids during maturation.

Correlation analysis between microbiota and volatile flavors showed that the abundance of *Kroppenstedtia* was positively correlated with tetramethylpyrazine, 2,3,5-trimethyl pyrazine, 2,4-dimethyl benzaldehyde, hexanal monomer, and ethyl pentadecanoate (**Figure 5B**). The abundance of *Kroppenstedtia* increased significantly after *Daqu* maturation, and the content of associated pyrazines such as tetramethylpyrazine and 2,3,5-trimethyl pyrazine were also significantly higher in mature *Daqu* than those in fresh *Daqu*. Interestingly, *Kroppenstedtia*'s abundance was negatively correlated with 3-octanone and 3-octanol, while *Thermoascus*'s abundance was positively correlated with these substances. From the point of view of the microbiota succession, *Kroppenstedtia* and *Thermoascus* showed the rule of ebb and flow because *Kroppenstedtia* had a higher tolerance to ethanol which was accumulated in the later step of *Daqu* maturation. *Bacillus* has a positive correlation with esters, sugars and derivatives, organic acids, aldehydes and ketones due to its high-temperature resistance and strong secretion enzyme function (Siddiquee, 2018). *Fusarium* and *Aspergillus*

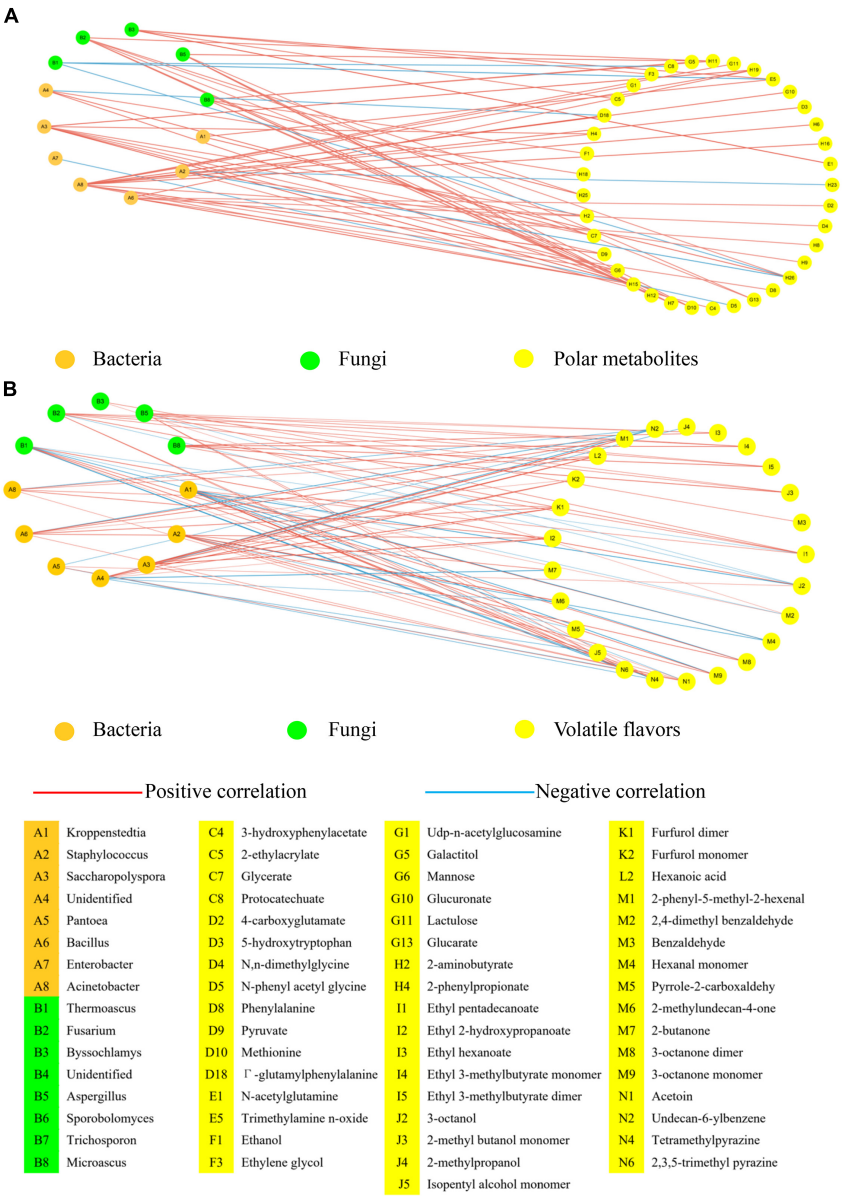

FIGURE 4 | Network analysis of the interactions among microbiota, polar metabolites (^{1}H NMR) and volatile flavors (HS-SPME-GC-MS and HS-GC-IMS). **(A)** The correlated network between microbiota and polar metabolites. **(B)** The correlated network between microbiota and volatile flavors. Population data was considered at the OTU level and statistically significant Pearson correlations were calculated among *Daqu* samples. A connection stands for a significant ($P < 0.05$) and positive (Pearson correlation > |0.7|) correlation.

had a similar correlation with volatile flavors, and both had a strong positive correlation with esters and alcohols. Studies have pointed out that *Fusarium* could decompose cellulose and other organic compounds and could degrade phenolic compounds and polycyclic aromatic hydrocarbons at the same time (Leite et al., 2008). *Aspergillus* could decompose proteins to produce volatile flavors and also produce organic acids (Yu et al., 2021).

Kroppenstedtia was positively correlated with some pyrazines such as tetramethylpyrazine and 2,3,5-trimethyl pyrazine. Other bacteria such as *Saccharopolyspora*, *Bacillus*, and *Acinetobacter* were positively correlated with organic acid, amino acids and their derivatives, and sugars and their derivatives. Besides, *Fusarium* and *Aspergillus* had a strong positive correlation with esters, alcohols, organic acid while *Thermoascus* showed a negative correlation with phenylalanine, trimethylamine n-oxide, and isovalerate.

SourceTracker Analysis of Raw Materials and *Daqu*

SourceTracker has been widely used as an important tool of tracking microbial source in many fields, including food

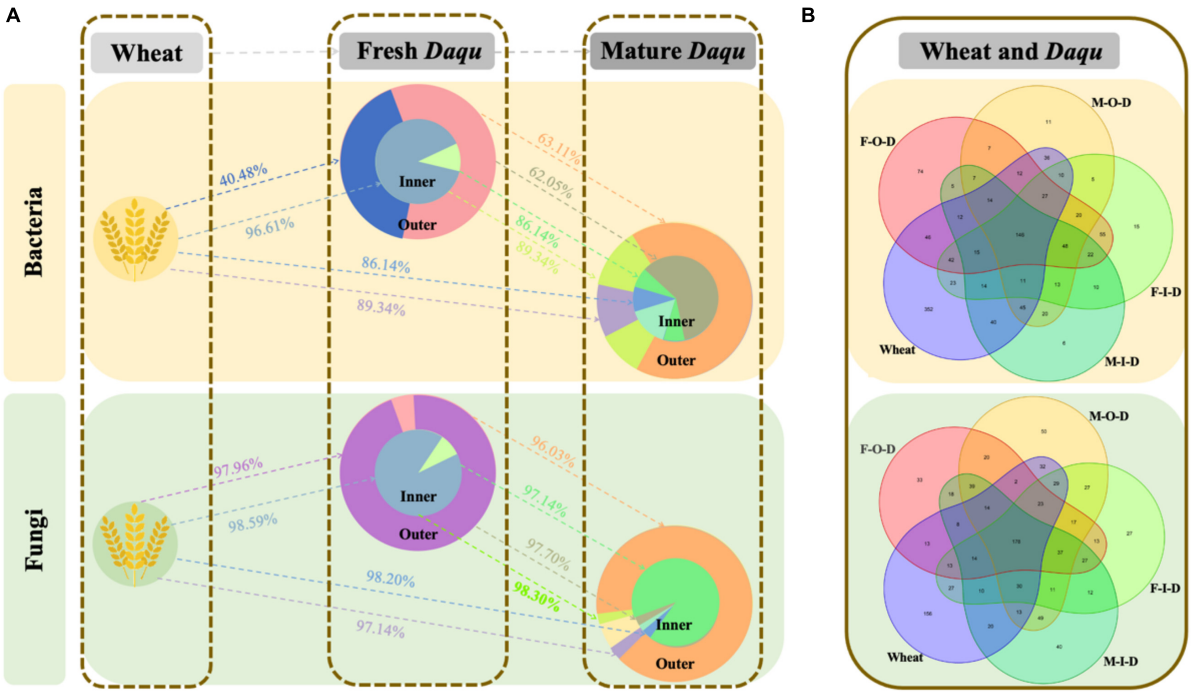

FIGURE 5 | SourceTracker results for the wheat and *Daqu* sample via SourceTracker. **(A)** Estimation of shift pathway and proportion. **(B)** Specific numbers of OTUs. The "→" represent microbiota shift direction. F-I-D: Inner of fresh *Daqu*; F-O-D: Outer of fresh *Daqu*; M-I-D: Inner of mature *Daqu*; M-O-D: Outer of mature *Daqu*.

fermentation and meat processing (Du et al., 2019). Thus, we exploited SourceTracker to estimate the source and succession of microbiota in *Daqu*. In addition to the microbiota in *Daqu*, we also analyzed the microbiota on the surface of wheat, the raw material for *Daqu*-making (**Supplementary Table 7**). The traceability of microbiota in high-temperature *Daqu* were shown in **Figure 5**. Schematic diagram showed that the microbiota shifted from wheat to fresh *Daqu* and finally to mature *Daqu*. In particular, the proportion of microbiota shifted as shown in **Figure 5A** and the specific number of OTUs were shown in **Figure 5B**. The bacterial community of F-I-D mainly came from wheat (96.61%), while only about 40.48% of F-O-D came from wheat. In detail, *Staphylococcus*, *Saccharopolyspora*, and *Kroppenstedtia* might shifted to *Daqu* from wheat and became dominant bacteria in *Daqu*. Besides, most of the wheat-based microbiota were shown in the I-*Daqu* (Du et al., 2019). Compared with F-*Daqu*, M-*Daqu* were more from the F-I-D rather than the F-O-D. Approximately 89.34% of bacterial community in M-O-D was shifted from F-I-D, slightly higher than that in M-I-D (86.14).

Combined with the results of Illumina MiSeq sequencing, the fungal traceability of I-*Duqu* and O-*Daqu* was similar. However, the difference of fungal community (**Figure 1B**) in M-I-D and M-O-D after maturation became larger than that of the maturation at the beginning. *Thermoascus*, the dominant fungus with the highest abundance in the *Daqu* maturation, was also detected on the surface of wheat. It could be inferred that part of *Thermoascus* shifted from wheat to the F-*Daqu* and then its abundance reduced due to the growth of thermophilic bacteria and *Byssochlamys* (Du et al., 2019). There were also some fungi such as *Fusarium* and *Aspergillus* in wheat and M-*Daqu* with high abundance, but low abundance in F-*Daqu*.

DISCUSSION

This study explored the microbiota from wheat and the contribution of the inner and outer of *Daqu* microbiota during maturation. Physicochemical properties, including moisture, pH, amylase activity, and protease activity reflect the maturity and quality of *Daqu* (Deng et al., 2020). The moisture in F-*Daqu* was higher than that in M-*Daqu*, and the moisture in I-*Daqu* was higher than that of O-*Daqu*. It is due to the open and well-ventilated storage condition and the dry and cool air in the environment, which lead more moisture loss in O-*Daqu* (Chen et al., 2021). The difference in pH is related to the difference in composition of organic acids and the changes in the diversity of slightly acidic bacteria like the *Acetobacter* and *Lactobacillus* (Fan et al., 2019). The changes in the microbiota that produced amylase and protease might be the mainly reason for the changes in enzyme activities (Guan et al., 2020).

During the maturation, the microbiota in different parts of *Daqu* underwent great changes. The bacterial communities of F-I-D and F-O-D were quite different because microbes from the environment had a great influence on F-O-D exposed to the air during the whole production process, while most of the microbiome in F-I-D came from raw materials (He et al., 2019). Besides, the bacterial community of M-I-D and M-O-D became similar after maturation. Compared

with medium-temperature and low-temperature *Daqu*, high-temperature *Daqu* had relatively fewer bacterial species due to high fermentation temperature (Zheng et al., 2011). The abundance of *Saccharopolyspora* was high in F-O-D, and the microbiota came from the environment or the raw materials that provided the initial microbiota for enzymatic reactions to produce metabolites. In the mature step of *Daqu*, the microbial abundance in *Daqu* decreased after high temperature fermentation, mainly including some thermotolerant and thermophilic bacteria. *Kroppenstedtia* became the absolute dominant strain in the M-*Daqu*. It was isolated recently and was identified in several types of *Daqu* (Fan et al., 2019). However, its role in *Daqu* manufacture is not clear. Studies had shown that *Lactobacillus* could inhibit *Kroppenstedtia* to a certain extent, which explained that the decline of *Lactobacillus* abundance promoted the growth of *Kroppenstedtia* after maturation (Yan et al., 2016). For *Staphylococcus*, the absolute dominant bacterial genera in F-I-D, Stevens et al. (2015) discovered that *Staphylococcus* were dominant across different foot sites and comprised almost the entire bacterial population on the plantar surface (Stevens et al., 2015). Du et al. (2019) proved that both the raw materials and the environments acted as important sources for *Daqu* microbiota (Du et al., 2019). Because of the relatively open processing environment and the barefoot stepping process by women, there might be some microbiota such as *Staphylococcus* originating from the environment or women' feet in *Daqu* (Wang et al., 2021). During maturation, it was gradually inhibited by *Kroppenstedtia* (He et al., 2019). For fungal communities, few fungi can stand the temperature in the high-temperature *Daqu* making process because they prefer the low temperature environment for reproduction. However, the microflora showed a tendency of enrichment after maturation. Specifically, the abundance of *Fusarium*, *Byssochlamys*, *Aspergillus*, and *Microascus* in mature *Daqu* was significantly higher than that in fresh *Daqu*. *Fusarium* was widely found in nature especially in crops such as wheat and is beneficial to agriculture such as gibberellin (Franco et al., 2021). *Fusarium* in fresh *Daqu* was mainly derived from wheat and had a certain inhibitory effect on *Thermoascus* in the maturation process and became one of the dominant strains in mature *Daqu* (He et al., 2019). As the absolute dominant fungus in fresh *Daqu*, *Thermoascus* was negatively correlated with ethanol, and the accumulation of ethanol in the maturation process had a certain inhibitory effect on it (Wei et al., 2021).

The maturation of *Daqu* involves the changes of temperature, and the competition between bacteria and fungi lead to the change of volatile flavors produced by their metabolisms, which is also the reason for the production of the abundant volatile flavors in *Daqu* (Chen et al., 2021). From all volatile flavors detected by HS-SPME-GC-MS and HS-GC-IMS, there were obvious differences among the four *Daqu* samples. The incubation temperature of sauce-flavor *Daqu* is usually very high (reaching up to 70°C), and the Maillard reaction causes color changes and produces a series of volatile flavors like ketones, aldehydes, and heterocyclic compounds (Zheng et al., 2011). Besides, Sauce-flavor *Daqu* bricks are big and heavy (above 4.8 kg), which results in the different temperatures of the I-*Daqu* and O-*Daqu* and color gradients from brown inside to yellow outside (Huang et al., 2020). According to the detected results, F-I-D and F-O-D show great differences in compound compositions because of the metabolic reactions at different temperatures before maturation. At the end of maturation, the compositions of M-I-D and M-O-D became similar. It is probably because microbial succession, and compounds exchange took place in the inner and outer *Daqu*, leading to the formation of a relatively uniform system during maturation. Longitudinally, microbiota succession had been in progress in the whole maturation period. The bacterial community structures of F-*Daqu* and M-*Daqu* were very different, mainly reflected in the abundance of *Kroppenstedtia*, *Saccharopolyspora*, *Staphylococcus*, and *Bacillus*. High-intensity *Staphylococcus* produced volatile flavors such as 3-methyl-1-butanol, 2-butanone, and acetoin, which might play important roles in *Baijiu* production (Guan et al., 2020). *Bacillus* could convert starch and proteins into glucose and amino acids by secreting amylase, protease, cellulases, glucanases, and other enzymes, thereby contributing to the development of volatile flavors (Fan G. S. et al., 2020). At the same time, F-*Daqu* and M-*Daqu* showed significant differences in fungal community structure. After maturation, the abundance of *Fusarium* and *Byssochlamys* increased significantly, and the interaction between microorganisms became more complex. This played a decisive role in the change of metabolites between F-*Daqu* and M-*Daqu*. Besides, ^{1}H NMR spectroscopy was used to investigate the differences of the *Daqu* samples in the polar metabolic changes. The results show that esters, amino acids and sugars in F-I-D were significantly lower than those in F-O-D. This was probably because the abundance of *Thermomyces* in F-O-D was significantly higher than that in F-I-D. *Thermomyces* secreted cellulase, amylase, and protease, which converted starch, cellulose, and other raw substances into small molecules such as glucose and amino acids. These small molecules supplied nutrition and energy for the growth and metabolism of the microbial community (Ali et al., 2019). The contents of esters in M-I-D and M-O-D were similar because of the similar ester producing bacterial community structure between M-I-D and M-O-D, while the higher abundance of *Aspergillus* in M-I-D contributed to the significantly higher contents of amino acids and derivatives, sugars and their derivatives in M-I-D than M-O-D due to *Aspergillus*'s ability to decompose the large molecules such as starch into small polar metabolites (e.g., glucose) (Ali et al., 2019).

Some studies in medium temperature *Daqu* had shown that fungal communities were mainly originated from *Daqu* making environments (especially tools and indoor ground) while most of bacterial communities were from raw materials (Du et al., 2019). During the maturation, the bacterial community of wheat participated in microbiota succession and showed a migration phenomenon from inner to outer of *Daqu*. In other words, I-*Daqu* was an important channel for wheat microorganisms to act on *Daqu* (from wheat to F-I-D to the whole *Daqu*). Some bacteria migrated to the O-*Daqu* from I-*Daqu*, mainly *Kroppenstedtia*, *Saccharopolyspora*, and *Staphylococcus*, etc., which resulted in a similar and stable community structure in M-I-D and M-O-D.

In short, the core bacterial community in the F-I-D was the most important driving force for the maturation of *Daqu*. Wheat might be the source of these fungi whose growth was inhibited during the *Daqu* making (Yu et al., 2021). Another important reason was that these fungi in the environment transferred to the outer of *Daqu* and enriched in the maturation process and reproduced during maturation under suitable moisture and temperature, and finally increased its abundance in mature *Daqu* (Du et al., 2019). On this basis, the mechanism of raw material microbiota in *Daqu* still needs to be further studied.

CONCLUSION

Taken together, wheat-originated microbes were an important source for the microbial community formation of *Daqu*, especially the inner of *Daqu*. The bacterial community in the inner of *Daqu* was an important driving force of maturation. During the maturation, the difference in the bacterial community between the inner and outer of *Daqu* decreased and the predominant microbes shifted from *Saccharopolyspora* (outer) and *Staphylococcus* (inner) of fresh *Daqu* to *Kroppenstedtia* (both outer and inner) of mature *Daqu*, in which was indicated by the difference in metabolites. For fungal community, the predominant fungi shifted from *Thermoascus* (both outer and inner) in fresh *Daqu* to *Byssochlamys* (outer) and *Fusarium* (inner) in mature *Daqu*. Bacteria such as *Saccharopolyspora*, *Bacillus*, and *Acinetobacter* had a strong correlation with the contents of esters, amino acids and their derivatives, and sugars and their derivatives, which confirmed the important role of bacterial community in the inner of *Daqu*. Our study provided a deeper understanding of the role of microbiota during *Daqu* maturation and improvement of the quality and stability of *Daqu*.

DATA AVAILABILITY STATEMENT

The data presented in the study are deposited in the NCBI Sequence Read Archive (SRA) repository, accession number (PRJNA727444).

AUTHOR CONTRIBUTIONS

YZ designed and conducted the experimental work assisted by XC, performed the data analysis, and wrote the first draft of the manuscript. YX contributed to the manuscript revision. B-ZH contributed to the supervision, manuscript revision, and overall support of this study. All authors read and approved the final version of the manuscript.

FUNDING

This work was supported by the National Natural Science Foundation of China (No. 31972975) and China Alcoholic Drinks Association (Migration of Wheat-originated Microorganisms in the Process of High-Temperature *Daqu*).

SUPPLEMENTARY MATERIAL

The Supplementary Material for this article can be found online at: https://www.frontiersin.org/articles/10.3389/fmicb.2021.714726/full#supplementary-material

REFERENCES

Ali, B., Yi, Z. L., Fang, Y., Chen, L. C., He, K. Z., Liu, D. Y., et al. (2019). Characterization of a fungal thermostable endoglucanase from Chinese Nong-flavor *Daqu* by metatranscriptomic method. *Int. J. Biol. Macromol.* 121, 183–190. doi: 10.1016/j.ijbiomac.2018.09.173

Bolger, A. M., Lohse, M., and Usadel, B. (2014). Trimmomatic: a flexible trimmer for Illumina sequence data. *Bioinformatics* 30, 2114–2120. doi: 10.1093/bioinformatics/btu170

Chen, Y. R., Li, K. M., Liu, T., Li, R. Y., Fu, G. M., Wan, Y., et al. (2021). Analysis of difference in microbial community and physicochemical indices between surface and central parts of Chinese special-flavor *Baijiu Daqu*. *Front. Microbiol.* 11:1–12. doi: 10.3389/fmicb.2020.592421

Dai, Y. J., Tian, Z. G., Meng, W. N., and Li, Z. J. (2020). Microbial diversity and physicochemical characteristics of the maotai-flavored liquor fermentation process. *J. Nanosci. Nanotechnol.* 20, 4097–4109. doi: 10.1166/jnn.2020.17522

Deng, L., Mao, X., Liu, D., Ning, X. Q., Shen, Y., Chen, B., et al. (2020). Comparative analysis of physicochemical properties and microbial composition in high-temperature *Daqu* with different colors. *Front. Microbiol.* 11:1–13. doi: 10.3389/fmicb.2020.588117

Du, H., Wang, X. S., Zhang, Y. H., and Xu, Y. (2019). Exploring the impacts of raw materials and environments on the microbiota in Chinese *Daqu* starter. *Int. J. Food Microbiol.* 297, 32–40. doi: 10.1016/j.ijfoodmicro.2019.02.020

Fan, G. S., Fu, Z. L., Sun, B. G., Zhang, Y. H., Wang, X. L., Xia, Y. Q., et al. (2019). Roles of aging in the production of light-flavored *Daqu*. *J. Biosci. Bioeng.* 127, 309–317. doi: 10.1016/j.jbiosc.2018.08.005

Fan, G. S., Fu, Z. L., Teng, C., Liu, P. X., Wu, Q. H., Rahman, M. K. R., et al. (2020). Effects of aging on the quality of roasted sesame-like flavor *Daqu*. *BMC Microbiol.* 20:1–16. doi: 10.1186/s12866-020-01745-3

Fan, X. J., Jiao, X., Liu, J. G., Jia, M., Blanchard, C., and Zhou, Z. K. (2021). Characterizing the volatile compounds of different sorghum cultivars by both GC-MS and HS-GC-IMS. *Food Res. Int.* 140:109975. doi: 10.1016/j.foodres.2020.109975

Fan, Y., Huang, X. N., Chen, J. Y., and Han, B. Z. (2020). Formation of a mixed-species biofilm is a survival strategy for unculturable lactic acid bacteria and saccharomyces cerevisiae in *Daqu*, a Chinese traditional fermentation starter. *Front. Microbiol.* 11:1–13. doi: 10.3389/fmicb.2020.00138

Franco, M. F., Lori, G. A., Cendoya, M. G., Panelo, J. S., Alonso, M. P., Mirabella, N. E., et al. (2021). Using anthesis date as a covariate to accurately assessing type II resistance to Fusarium head blight in field-grown bread wheat. *Crop Prot.* 142:105504. doi: 10.1016/j.cropro.2020.105504

Gou, M., Wang, H. Z., Yuan, H. W., Zhang, W. X., Tang, Y. Q., and Kida, K. (2015). Characterization of the microbial community in three types of fermentation starters used for Chinese liquor production. *J. Inst. Brew.* 121, 620–627. doi: 10.1002/jib.272

Guan, T. W., Lin, Y. J., Chen, K. B., Ou, M. Y., and Zhang, J. X. (2020). Physicochemical factors affecting microbiota dynamics during traditional solid-state fermentation of Chinese strong-flavor *Baijiu*. *Front. Microbiol.* 11:2090. doi: 10.3389/fmicb.2020.02090

He, Z. L., Fan, W. L., Xu, Y., He, S. G., and Liu, X. Y. (2019). Aroma profile of folium isatidis leaf as a raw material of making bingqu for chixiang aroma- and flavor-type *Baijiu*. *ACS Symp. Ser.* 1321, 263–275. doi: 10.1021/bk-2019-1321.ch016

Huang, X. N., Fan, Y., Lu, T., Kang, J. M., Pang, X. N., Han, B. Z., et al. (2020). Composition and metabolic functions of the microbiome in fermented grain during light-flavor *Baijiu* fermentation. *Microorg* 8:1281. doi: 10.3390/microorganisms8091281

Jin, G. Y., Zhu, Y., and Xu, Y. (2017). Mystery behind Chinese liquor fermentation. *Trends Food Sci. Technol.* 63, 18–28. doi: 10.1016/j.tifs.2017.02.016

Jin, Y., Li, D. Y., Ai, M., Tang, Q. X., Huang, J., Ding, X. F., et al. (2019). Correlation between volatile profiles and microbial communities: a metabonomic approach to study Jiang-flavor liquor *Daqu*. *Food Res. Int.* 121, 422–432. doi: 10.1016/j.foodres.2019.03.021

Knights, D., Kuczynski, J., Charlson, E. S., Zaneveld, J., Mozer, M. C., Collman, R. G., et al. (2011). Bayesian community-wide culture-independent microbial source tracking. *Nat. Methods* 8, 761–765. doi: 10.1038/nmeth.1650

Langille, M. G. I., Zaneveld, J., Caporaso, J. G., McDonald, D., Knights, D., Reyes, J. A., et al. (2013). Predictive functional profiling of microbial communities using 16s rRNA marker gene sequences. *Nat. Biotechnol.* 31, 814–821. doi: 10.1038/nbt.2676

Leite, R. S. R., Alves-Prado, H. F., Cabral, H., Pagnocca, F. C., Gomes, E., and Da-Silva, R. (2008). Production and characteristics comparison of crude β-glucosidases produced by microorganisms *Thermoascus aurantiacus e Aureobasidium* pullulans in agricultural wastes. *Enzyme Microb. Technol.* 43, 391–395. doi: 10.1016/j.enzmictec.2008.07.006

Li, M. Q., Yang, R. W., Zhang, H., Wang, S. L., Chen, D., and Lin, S. Y. (2019). Development of a flavor fingerprint by HS-GC-IMS with PCA for volatile compounds of tricholoma matsutake singer. *Food Chem.* 29, 32–39. doi: 10.1016/j.foodchem.2019.03.124

Li, P., Lin, W. F., Liu, X., Wang, X. W., Gan, X., Luo, L. X., et al. (2017). Effect of bioaugmented inoculation on microbiota dynamics during solid-state fermentation of *Daqu* starter using autochthonous of bacillus, *Pediococcus, Wickerhamomyces* and *Saccharomycopsis*. *Food Microbiol.* 61, 83–92. doi: 10.1016/j.fm.2016.09.004

Li, R. Y., Zheng, X. W., Zhang, X., Yan, Z., Wang, X. Y., and Han, B. Z. (2018). Characterization of bacteria and yeasts isolated from traditional fermentation starter (Fen-*Daqu*) through a ^{1}H NMR-based metabolomics approach. *Food Microbiol.* 76, 11–20. doi: 10.1016/j.fm.2018.03.015

Li, W. W., Fan, G. S., Fu, Z. L., Wang, W. H., Xu, Y. Q., Teng, C., et al. (2020). Effects of fortification of *Daqu* with various yeasts on microbial community structure and flavor metabolism. *Food Res. Int.* 129:108837. doi: 10.1016/j.foodres.2019.108837

Liu, C. C., Feng, S. B., Wu, Q., Huang, H. Q., Chen, Z. X., Li, S. W., et al. (2019). Raw material regulates flavor formation via driving microbiota in Chinese liquor fermentation. *Front. Microbiol.* 10:1–13. doi: 10.3389/fmicb.2019.01520

Márquez-Sillero, I., Aguilera-Herrador, E., Cárdenas, S., and Valcárcel, M. (2011). Ion-mobility spectrometry for environmental analysis. *TrAC-Trends Anal. Chem.* 30, 677–690. doi: 10.1016/j.trac.2010.12.007

Pang, X. N., Huang, X. N., Chen, J. Y., Yu, H. X., Wang, X. Y., and Han, B. Z. (2020). Exploring the diversity and role of microbiota during material pretreatment of light-flavor *Baijiu*. *Food Microbiol.* 91:103514. doi: 10.1016/j.fm.2020.103514

Pradhan, P., and Tamang, J. P. (2019). Phenotypic and genotypic identification of bacteria isolated from traditionally prepared dry starters of the Eastern Himalayas. *Front. Microbiol.* 10:2526. doi: 10.3389/fmicb.2019.02526

Siddiquee, S. (2018). Recent advancements on the role of biologically active secondary metabolites from *Aspergillus*. *N. Futur. Dev. Microb. Biotechnol. Bioeng.* 69–94. doi: 10.1016/B978-0-444-63501-3.00004-1

Stevens, D., Cornmell, R., Taylor, D., Grimshaw, S. G., Riazanskaia, S., Arnold, D. S., et al. (2015). Spatial variations in the microbial community structure and diversity of the human foot is associated with the production of odorous volatiles. *FEMS Microbiol. Ecol.* 91, 1–11. doi: 10.1093/femsec/fiu018

Wang, Y. R., Cai, W. C., Wang, W. P., Shu, N., Zhang, Z. D., Hou, Q. C., et al. (2021). Analysis of microbial diversity and functional differences in different types of high-temperature *Daqu*. *Food Sci. Nutr.* 9, 1003–1016. doi: 10.1002/fsn3.2068

Wei, J. L., Du, H., Zhang, H. X., Nie, Y., and Xu, Y. (2021). Mannitol and erythritol reduce the ethanol yield during Chinese *Baijiu* production. *Int. J. Food Microbiol.* 337:108933. doi: 10.1016/j.ijfoodmicro.2020.108933

Wu, X. H., Zheng, X. W., Han, B. Z., Vervoort, J., and Robert Nout, M. J. (2009). Characterization of Chinese liquor starter, "*Daqu*" by flavor type with^{1}H NMR-based nontargeted analysis. *J. Agric. Food Chem.* 57, 11354–11359. doi: 10.1021/jf902881p

Xu, Y., Wang, D., Fan, W. L., Mu, X. Q., and Chen, J. (2010). Traditional Chinese biotechnology. *Adv. Biochem. Eng. Biotechnol.* 122, 189–233. doi: 10.1007/10_2008_36

Yan, Z. K., Meng, Q. Y., Wang, X. Z., and Du, J. (2016). Analysis on physicochemical indexes and cultivation technology of traditional Xifeng *Daqu* sensory evaluation. *Liquor Making* 43, 51–55.

Yang, F., Liu, Y., Wang, B., Song, H. L., and Zou, T. T. (2020). Screening of the volatile compounds in fresh and thermally treated watermelon juice via headspace-gas chromatography-ion mobility spectrometry and comprehensive two-dimensional gas chromatography-olfactory-mass spectrometry analysis. *LWT* 137:110478. doi: 10.1016/j.lwt.2020.110478

Yu, R. L., Li, M. Z., Wang, Y., Bai, X. L., Chen, J. W., Li, X. N., et al. (2021). Chemical investigation of a co-culture of aspergillus fumigatus d and fusarium oxysporum r1. *Rec. Nat. Prod.* 15, 130–135. doi: 10.25135/rnp.199.20.07.1728

Zhang, X. Y., Wang, C. C., Wang, L. L., Chen, S., and Xu, Y. (2020). Optimization and validation of a head space solid-phase microextraction-arrow gas chromatography-mass spectrometry method using central composite design for determination of aroma compounds in Chinese liquor (*Baijiu*). *J. Chromatogr. A* 1610:460584. doi: 10.1016/j.chroma.2019.460584

Zheng, X. W., and Han, B. Z. (2016). *Baijiu* (白酒), Chinese liquor: History, classification and manufacture. *J. Ethn. Foods* 3, 19–25. doi: 10.1016/j.jef.2016.03.001

Zheng, X. W., Tabrizi, M. R., Robert Nout, M. J., and Han, B. Z. (2011). *Daqu*-a traditional Chinese liquor fermentation starter. *J. Inst. Brew.* 117, 82–90. doi: 10.1002/j.2050-0416.2011.tb00447.x

Zheng, X. W., Yan, Z., Han, B. Z., Zwietering, M. H., Samson, R. A., Boekhout, T., et al. (2012). Complex microbiota of a Chinese "Fen" liquor fermentation starter (Fen-*Daqu*), revealed by culture-dependent and culture-independent methods. *Food Microbiol.* 31, 293–300. doi: 10.1016/j.fm.2012.03.008

Conflict of Interest: YS, WC, and XW were all employed by Sichuan Langjiu Co., Ltd.

The remaining authors declare that the research was conducted in the absence of any commercial or financial relationships that could be construed as a potential conflict of interest.

frontiers in Microbiology

ORIGINAL RESEARCH
published: 13 July 2021
doi: 10.3389/fmicb.2021.691296

Comparison of Two *Aspergillus oryzae* Genomes From Different Clades Reveals Independent Evolution of Alpha-Amylase Duplication, Variation in Secondary Metabolism Genes, and Differences in Primary Metabolism

*Katherine Chacón-Vargas[1,2], Colin O. McCarthy[2], Dasol Choi[3,4], Long Wang[5], Jae-Hyuk Yu[4,6] and John G. Gibbons[1,2,7]**

[1] Molecular and Cellular Biology Graduate Program, University of Massachusetts, Amherst, MA, United States, [2] Department of Food Science, University of Massachusetts, Amherst, MA, United States, [3] Deapertment of Food Science, University of Wisconsin-Madison, Madison, WI, United States, [4] Department of Bacteriology, and Food Research Institute, University of Wisconsin-Madison, Madison, WI, United States, [5] State Key Laboratory of Mycology, Institute of Microbiology, Chinese Academy of Sciences, Beijing, China, [6] Department of Systems Biotechnology, Konkuk University, Seoul, South Korea, [7] Organismic & Evolutionary Biology Graduate Program, University of Massachusetts, Amherst, MA, United States

OPEN ACCESS

Edited by:
Kwangcheol Casey Jeong, University of Florida, United States

Reviewed by:
Lin Teng, Zhejiang University, China
Kap-Hoon Han, Woosuk University, South Korea

***Correspondence:**
John G. Gibbons
jggibbons@umass.edu

Specialty section:
This article was submitted to Food Microbiology, a section of the journal Frontiers in Microbiology

Received: 06 April 2021
Accepted: 22 June 2021
Published: 13 July 2021

Citation:
Chacón-Vargas K, McCarthy CO, Choi D, Wang L, Yu J-H and Gibbons JG (2021) Comparison of Two Aspergillus oryzae Genomes From Different Clades Reveals Independent Evolution of Alpha-Amylase Duplication, Variation in Secondary Metabolism Genes, and Differences in Primary Metabolism. Front. Microbiol. 12:691296. doi: 10.3389/fmicb.2021.691296

Microbes (bacteria, yeasts, molds), in addition to plants and animals, were domesticated for their roles in food preservation, nutrition and flavor. *Aspergillus oryzae* is a domesticated filamentous fungal species traditionally used during fermentation of Asian foods and beverage, such as sake, soy sauce, and miso. To date, little is known about the extent of genome and phenotypic variation of *A. oryzae* isolates from different clades. Here, we used long-read Oxford Nanopore and short-read Illumina sequencing to produce a highly accurate and contiguous genome assemble of *A. oryzae* 14160, an industrial strain from China. To understand the relationship of this isolate, we performed phylogenetic analysis with 90 *A. oryzae* isolates and 1 isolate of the *A. oryzae* progenitor, *Aspergillus flavus*. This analysis showed that *A. oryzae* 14160 is a member of clade A, in comparison to the RIB 40 type strain, which is a member of clade F. To explore genome variation between isolates from distinct *A. oryzae* clades, we compared the *A. oryzae* 14160 genome with the complete RIB 40 genome. Our results provide evidence of independent evolution of the alpha-amylase gene duplication, which is one of the major adaptive mutations resulting from domestication. Synteny analysis revealed that both genomes have three copies of the alpha-amylase gene, but only one copy on chromosome 2 was conserved. While the RIB 40 genome had additional copies of the alpha-amylase gene on chromosomes III, and V, 14160 had a second copy on chromosome II and an third copy on chromosome VI. Additionally, we identified hundreds of lineage specific genes, and putative high impact mutations in genes involved in secondary metabolism, including several of the core biosynthetic

genes. Finally, to examine the functional effects of genome variation between strains, we measured amylase activity, proteolytic activity, and growth rate on several different substrates. RIB 40 produced significantly higher levels of amylase compared to 14160 when grown on rice and starch. Accordingly, RIB 40 grew faster on rice, while 14160 grew faster on soy. Taken together, our analyses reveal substantial genome and phenotypic variation within *A. oryzae*.

Keywords: *Aspergillus oryzae*, comparative genomics, Oxford Nanopore sequencing, fermentation, amylase, Koji

INTRODUCTION

Domestication is an evolutionary process that involves the genetic modification of a species by breeding it in isolation from its ancestral population in an effort to enhance its utility to humans (Larson et al., 2014). Early farmers used selective breeding to continuously cross individuals with desired traits, eventually yielding crops with more food (i.e., larger/more seeds and fruits) that were easier to harvest (i.e., loss of seed shattering in grains), and livestock that were less aggressive and more fertile (Purugganan and Fuller, 2009; Abbo et al., 2014; Larson and Fuller, 2014; Larson et al., 2014). Domestication can also lead to sub specialization and genetic divergence of lineages within a given domesticated species as observed in chickens, which were independently bred for meat and for eggs (Rubin et al., 2010).

In parallel with plants and animals, microbes (bacteria, yeasts, and molds) were also domesticated, most likely because of their role in food preservation (Gibbons and Rinker, 2015; Steensels et al., 2019). Archeological chemistry evidence of ruminant dairy fat from ∼8,000 year old pottery shards in Northern Europe suggest that humans were employing microbial fermentation to produce cheese (Salque et al., 2013). Similarly, the chemical signatures of a "proto rice wine" were discovered embedded in ∼9,000 year old pottery shards from China (McGovern et al., 2004). Further, the long-term relationship between humans and fungi used for food fermentation is evident through the analysis of archeological remains using (i) ancient DNA sequencing (Cavalieri et al., 2003), (ii) microscopy paired with morphological characterization (Liu et al., 2019) and, (iii) direct isolation of characterization of microbial specimens (Aouizerat et al., 2019, 2020).

Saccharomyces yeasts are the most thoroughly studied domesticated fungi. In particular, there are a number of domesticated lineages of *Saccharomyces cerevisiae* that have been shaped by artificial selection for particular fermentation applications. For example, lineages of beer yeasts have an increased capacity to metabolize maltotriose (a highly abundant sugar in wort) while also producing fewer off-flavor compounds like 4-vinyl guaiacol (Gallone et al., 2016). In addition to yeasts, several filamentous fungi have been domesticated. For instance, the white mold *Penicillium camemberti* was domesticated for its role in the maturation of soft cheeses (Ropars et al., 2020). Artificial selection in *P. camemberti* resulted in white color, increased aerial growth, reduced toxin production, and increased inhibition of fungal competitors compared to its progenitor (Ropars et al., 2020). Additionally, *Penicillium roqueforti* was domesticated for the production of blue cheeses like Roquefort (Dumas et al., 2020). Two distinct lineages of *P. roqueforti* exist that are associated with pre-industrial and industrial cheese production, and possess beneficial traits for these usages.

Aspergillus oryzae is a domesticated filamentous fungal species used in the production of traditionally fermented Asian foods and beverages, such as shoyu, miso, sake, and meju (Machida et al., 2005, 2008; Gibbons et al., 2012; Alshannaq et al., 2018; Watarai et al., 2019). *A. oryzae* was domesticated from *Aspergillus flavus* (Geiser et al., 1998; Machida et al., 2005; Gibbons et al., 2012), or perhaps the closely related species *Aspergillus aflatoxiformans* or *Aspergillus minisclerotigenes* (Kjaerbolling et al., 2020). As a result of domestication and specialization to the fermented food environment, *A. oryzae* has reduced capacity to produce many secondary metabolites like aflatoxin and cyclopiazonic acid, and increased carbohydrate metabolism, in part due to the duplication of the alpha-amylase encoding gene (Machida et al., 2005; Hunter et al., 2011; Gibbons et al., 2012; Nemoto et al., 2012). Recently, Watarai et al. (2019) sequenced and analyzed the genomes of 82 *A. oryzae* strains, and identified eight distinct clades. However, little is known about the genome and functional divergence between these *A. oryzae* groups.

In this study, we used a combination of short-read and long-read DNA sequencing to assemble a highly contiguous genome of the clade A isolate *A. oryzae* 14160, originally isolated from China. To gain insight into *A. oryzae* genome variation, we compared the *A. oryzae* 14160 genome to the *A. oryzae* RIB 40 (clade F) reference genome. We also examined phenotypic differences between the two isolates by measuring amylase activity and growth rate on several culture medias. Our results show that *A. oryzae* 14160 and RIB 40 differ substantially in terms of their genomes and phenotypes.

MATERIALS AND METHODS

Isolates, Fungal Culturing, and DNA Extraction

A. oryzae 14160 was originally isolated from Xinyang City, Henan Province, China. Spores were cultured in potato dextrose agar (PDA) at 30°C for 48 h. DNA was extracted directly from spores following the protocol from Lee et al. (2017). Qubit and Nanodrop were used to quantify DNA.

Illumina and Oxford Nanopore Sequencing

PCR-free Illumina libraries were constructed and sequenced by Novogene. Illumina sequencing was conducted in paired-end 150 bp format. Raw reads were deduplicated by Tally using "with-quality" and "pair-by-offset" parameters to remove exact paired-end duplicates (Davis et al., 2013). Deduplicated reads were then trimmed with Trim Galore[1] using "stringency 1," "quality 30," and "length 50" parameters to remove any adaptor sequences and low quality positions. Error correction was performed using the default settings in SPAdes (Bankevich et al., 2012). Data quality was assessed using FASTQC[2].

Oxford Nanopore (ONT) libraries were prepared using 400 ng of gDNA following the manufacturer's instructions with the 1D Rapid Sequencing Kit (SQK-NSK007). ONT sequencing was performed on a MinION following the manufacturer's instructions. The *A. oryzae* 14160 library was run for 12 h. ONT reads were mapped against the *A. oryzae* 14160 genome assembly to assess quality of reads using minimap2 (Li, 2018). Raw Illumina and ONT data for *A. oryzae* 14160 are available through the NCBI SRA under BioProject accession number PRJNA717291.

Phylogenetic Analysis of *A. oryzae* 14160

To reconstruct the evolutionary history of *A. oryzae* 14160 we analyzed the phylogenetic relationship of 89 *A. oryzae* strains from Gibbons et al. (2012) and Watarai et al. (2019) as well as the *A. oryzae* RIB 40 and *A. flavus* 3357 reference genomes (Machida et al., 2005; Nierman et al., 2015). BioProject accession numbers for samples are as follows: PRJDB7763 for TK-10, TK-11, TK-12, TK-13, TK-14, TK-15, TK-16, TK-17, TK-18, TK-19, TK-1, TK-20, TK-21, TK-22, TK-23, TK-24, TK-25, TK-26, TK-27, TK-28, TK-29, TK-2, TK-30, TK-31, TK-32, TK-33, TK-34, TK-35, TK-36, TK-37, TK-38, TK-39, TK-3, TK-40, TK-41, TK-42, TK-43, TK-44, TK-45, TK-46, TK-47, TK-48, TK-49, TK-4, TK-50, TK-51, TK-52, TK-53, TK-54, TK-55, TK-56, TK-57, TK-58, TK-59, TK-5, TK-60, TK-61, TK-62, TK-63, TK-64, TK-65, TK-66, TK-67, TK-68, TK-69, TK-6, TK-70, TK-71, TK-72, TK-73, TK-74, TK-75, TK-76, TK-77, TK-78, TK-79, TK-7, TK-80, TK-81, TK-82, TK-8, and TK-9, and PRJNA164603 for AO_302 (SRRC 302), AO_331 (RIB 331), AO_333 (RIB 333), AO_537 (RIB 537), AO_632 (RIB 632), AO_642 (RIB 642), and AO_949 (RIB 949). First, Illumina whole-genome data was de-duplicated, and adapter and quality trimmed as described above. Next, sequence reads from each isolate were mapped to the *A. oryzae* RIB40 reference genome with BWA-MEM v0.7.15 (Li and Durbin, 2009, 2010). SAM files were converted into sorted BAM format using the samtools v1.4.1 "view" and "sort" option (Li et al., 2009). Variant calling was performed with GATK using the "Germline short variant discovery" best practices pipeline (McKenna et al., 2010). The GATK "Haplotype Caller" option was used to call SNPs. Genotype calls for the 92 samples were combined using the "GenotypeVCFs" option. SNPs were extracted and filtered using the "SelectVariants" and "VariantFiltration" options. SNP filtering was performed using "hard filtering" with the parameters: "QD < 21.0 || FS > 0.5 || MQ < 60.0 || MQRankSum < −0.2 || ReadPosRankSum < −4.0 || SOR > 1.0." Phylogenetic analysis was performed with RAxML (Stamatakis, 2014) with the GTRGAMMA model and 100 bootstrap replicates. The phylogenetic tree was visualized with ggtree (Yu, 2020) and ggplot2 (Wickham, 2009). Phylogenetic analysis was conducted independently with alignments of 243,486, 7,641, and 3,340 SNPs. Phylogenetic trees generated from reduced SNP marker alignments were performed to investigate the impact of linkage on the inferred phylogenetic relationship. SNPs were separated by a minimum of 4 and 10 Kb for the 7,641, and 3,340 SNP marker sets, respectively.

Genome Assembly and Annotation

The *A. oryzae* 14160 genome was assembled using a hybrid approach that combined the short-read Illumina and long-read ONT data. Error correction and genome assembly was performed with the MaSuRCa assembler with the default parameters (Zimin et al., 2013). The quality of the *A. oryzae* 14160 genome assembly was assessed with QUAST (Gurevich et al., 2013) and genome completeness was evaluated with BUSCO (Simao et al., 2015).

Gene prediction and annotation of *A. oryzae* 14160 strain were performed using the Funannotate pipeline[3]. Gene model prediction was evaluated with BUSCO (Simao et al., 2015). Functional annotation was performed with Interproscan 5 (Jones et al., 2014) using the default settings and complemented with Phobius (Kall et al., 2004, 2007) for transmembrane topology and signal peptide prediction. Finally, secondary metabolism associated gene clusters were predicted using antiSMASH using the "strict" detection strictness setting (Medema et al., 2011). The *A. oryzae* 14160 genome assembly is available through the BioProject accession number PRJNA717291.

Whole Genome Alignment

MUMer was used to align the *A. oryzae* 14160 assembly to the RIB 40 reference genome using the parameters "-mum," "-b," and "-c" (Delcher et al., 1999). The Nucmer alignment tool was used to identify conserved synteny between the *A. oryzae* 14160 and RIB 40 genomes using the "-maxmatch" and "-c 1000" parameters. Nucmer output was filtered using the Delta-Filter tool from with the parameter "-I 4000." Alignment coordinates were extracted by the "show-coords" function from MUMmer using the "-r", "-c," and "−l" parameters. Whole genome synteny was visualized using Circos (Krzywinski et al., 2009).

Alpha-Amylase Locus Synteny Analysis

A. oryzae isolates possess between 1 and 4 copies of the alpha-amylase encoding gene (Watarai et al., 2019). We compared the alpha-amylase encoding genes and their flanking regions between *A. oryzae* RIB 40 and *A. oryzae* 14160 to determine whether the duplication events shared an evolutionary history, or evolved independently. To identify the alpha-amylase encoding genes in *A. oryzae* 14160 we used BLASTN with the *A. oryzae* RIB 40

[1] http://www.bioinformatics.babraham.ac.uk/projects/trim_galore/

[2] https://www.bioinformatics.babraham.ac.uk/projects/fastqc/

[3] https://github.com/nextgenusfs/funannotate

amy1 gene (*AO090023000944*) as the query and *A. oryzae* 14160 predicted transcripts as the subject, with an *e*-value cutoff of 1e-30 (Altschul et al., 1997). We also conducted this BLASTN search with the *A. oryzae* 14160 genome assembly. These searches yielded three independent loci containing the alpha-amylase encoding gene in the *A. oryzae* 14160 genome. Finally, the Funannotate annotation was used for validation (each of the three alpha-amylase copies in the *A. oryzae* 14160 genome were annotated as "AMY1").

Next, we used SimpleSynteny to visualize the synteny between *A. oryzae* RIB40 and the *A. oryzae* 14160 alpha-amylase loci, using the default settings (Veltri et al., 2016). To increase confidence that our results were not the byproduct of assembly errors, we also assembled the *A. oryzae* 14160 genome with Canu (ONT data only) and SPAdes (ONT and Illumina data), using the default settings (Bankevich et al., 2012; Koren et al., 2017). We reasoned that independent misassembles of identical loci would be exceedingly rare. Synteny analysis of each of the three *A. oryzae* 14160 alpha-amylase loci (including five genes upstream and five genes downstream of the alpha-amylase encoding genes) were visualized between the MaSuRCA (primary assembly), Canu, and SPAdes assemblies and the *A. oryzae* RIB 40 reference genome. Additionally, because some alpha-amylase loci in *A. oryzae* contain the a transposable element likely responsible for duplications, we used BLASTN to search for the presence of the Tc1/Mariner class putative transposable element (NCBI accession AB072434.1) in the *A. oryzae* 14160 genome using an *e*-value cutoff of 1e-30. Finally, to provide further evidence for accurate assembly of the alpha-amylase loci, we used BLASTN searches to identify long ONT reads that spanned the alpha-amylase gene and flanking genes that differentiated each *A. oryzae* 14160 alpha-amylase loci using an *e*-value cutoff of 1e-30 and a query coverage cutoff of 80%.

Alpha-Amylase Upstream Sequence Analysis

We aligned the 1 Kb upstream region of each of the six alpha-amylase genes to explore whether divergence between gene copies or strains correlated with amylase activity. Bedtools was used to extract the 1 Kb upstream region from each alpha-amylase locus (Quinlan and Hall, 2010). The alignment was performed with MAFFT with the following parameters: "–kimura 1," "–op 3.0," and "–ep 0.5" (Katoh and Standley, 2013).

Single Nucleotide Polymorphism Analysis

We predicted single nucleotide polymorphisms (SNPs) in *A. oryzae* 14160 vs. the *A. oryzae* RIB 40 reference genome (Machida et al., 2005). *A. oryzae* 14160 quality and adapter trimmed and error corrected Illumina reads were mapped against the *A. oryzae* RIB 40 reference genome using BWA-MEM v0.7.15 (Li and Durbin, 2009, 2010). SNPs were called using freebayes v1.3.1 with the default settings with the exception of setting ploidy to haploid (–ploidy = 1) (Garrison and Marth, 2012). Next, we used vcftools v0.1.14 to filter variants with the following parameters "–remove-indels," "–remove-filtered-all," "–min-meanDP 25," "–minQ 20," "—recode," and "–recode-INFO-all" (Danecek et al., 2011). SNPs from this filtered VCF file were annotated with SnpEff v4.3t using "Aspergillus_oryzae" as the genome database (Cingolani et al., 2012). Using the SnpEff output, we calculated missense variant rate for each gene to identify genes with relatively elevated occurrences of missense variants. Per gene missense variant rate was calculated as:

$$Missense\ Variant\ Rate = \frac{number\ of\ missense\ variants}{length\ of\ all\ exons} \quad (1)$$

Gene Ontology Enrichment of gene sets with SNP profiles of interest was conducted through the FungiFun2 server[4], using the default settings (Priebe et al., 2015).

Identification of Lineage Specific Genes

To identify gene absences specific to the *A. oryzae* 14160 and RIB40 genomes, we used control-FREEC to estimate the copy number of each 1 kb window with a 200 bp step size (Boeva et al., 2012). The following parameters were used: window = 10, telocentromeric = 0, minExpectedGC = 0.33, and maxExpectedGC = 0.63. To estimate CNV for each gene, we used a custom perl script that takes gene coordinates and the control-FREEC output as input (CNV_gene-overlap.pl script is available here: https://github.com/DaRinker/PolarBearCNV) (Rinker et al., 2019). Entire genes (a minimum of start codon to stop codon) with copy numbers of zero when mapped against the non-self genome assembly (i.e., *A. oryzae* RIB 40 vs. *A. oryzae* 14160 reference, or *A. oryzae* 14160 vs. *A. oryzae* RIB 40 reference) were considered lineage specific genes in the reference genome.

Amylase Activity Assays

We used a quantitative method to measure amylase activity *via* the Megazyme (Bray, Ireland) alpha-amylase Assay Kit (Ceralpha Method). Short grain sushi rice was sterilized and cooked in distilled water at a ratio of 1:1.7 at 121°C for 15 min. Fifteen grams of cooked rice was inoculated with ∼100,000 conidia suspended in 20 μL H_2O and incubated for 48 h at 32°C. The entire sample was transferred into a 50 ml centrifuge tube, washed with 10 ml distilled H_2O and vortexed for 1 min. A 2 ml aliquot of wash water was transferred to a 5 ml tube and centrifuged at 1,000 RPM for 10 min. A one mL aliquot of the supernatant was diluted with 49 mL alpha-amylase buffer. Buffered enzyme extract was preheated at 40°C for 5 min after which a 0.1 mL aliquot was added to an equal amount of Megazyme Ceralpha Amylase HR Reagent in triplicate and maintained at 40°C for 10 min. Next, 1.5 mL 1% sodium triphosphate solution was added to halt the reaction. Control samples were prepared by immediately adding the sodium triphosphate solution to the enzyme-substrate solution. The samples and controls were transferred into a 24 well microplate and absorbance was measured at 405 nm.

We also used an iodine-based qualitative assay to examine amylase activity (Fuwa, 1954) while isolates grew on starch agar

[4]https://elbe.hki-jena.de/fungifun/

(per 1 L: 3 g beef extract, 10 g soluble starch and 12 g agar at pH 7.5). In this assay, iodine forms a black/dark blue complex with starch, but does not stain sugars, resulting in a yellowish zone surrounding the colony where starches have been metabolized. ∼10,000 conidia suspended in 20 μL H_2O were pipetted onto the center of the starch plates. Plates were incubated at 32°C for 39 h then flooded with iodine. This experiment was performed in triplicate. Plates were imaged with the Interscience Scan1200.

Proteolytic Assay

To examine the proteolytic activity of isolates, we performed an established zone of clearance assay (Rajamani and Hilda, 1987). Briefly, ∼100,000 conidia suspended in 20 μL H_2O were inoculated onto media consisting of 2.5 g agar, 2.5 g powdered skim milk and 125 mL distilled H_2O. Ten biological replicates of each strain were grown at 32°C for 72 h, at which time the zone of clearance was measured at two independent locations using digital calipers. The size of the zone is positively associated with higher proteolytic activity (Rajamani and Hilda, 1987). A 2-talied *t*-test was conducted to compare zone of clearance size between isolates.

Growth Rate of *A. oryzae* 14160 and *A. oryzae* RIB 40

We compared the growth rate of *A. oryzae* 14160 and RIB 40 on starch agar (as defined above), PDA, rice agar and soy agar. PDA (Fisher Scientific DF0013) was prepared according to manufacturer instructions. Rice agar was prepared using 75 g of short grain sushi rice which was powered in a dry blender, and 15 g agar in 1 L distilled H_2O. For the soybean agar, dried soybeans were soaked in H_2O for 24 h, then 30 g soybean and 15 g agar were pureed together in 1 L distilled H_2O. All media was sterilized and cooked *via* autoclaving, and 30 mL of media was plated into petri dishes. 20 μL of 500,000 conidia/mL spore solutions were pipetted onto the center of each plate. All growth rate experiments were performed in 10 replicates. Plates were incubated at 32°C for 39 h. Because colony morphology is not always uniformly circular, colony diameter was measured at two independent points for each colony using digital calipers. The average colony diameter for each plate value was used for the statistical analysis. One-way ANOVA was used to test the null hypothesis that growth rate did not differ between culture media for each isolate. *T*-tests were performed on each culture media to test the null hypothesis that *A. oryzae* 14160 and RIB 40 growth rates did not differ.

RESULTS

DNA Sequencing Data

We generate 830,485 ONT reads totaling ∼5 billion bp with an average and median read length of 6,065 and 4,092 bp, respectively, and an N50 value of 10,289 bp (**Supplementary Figure 1**). 96.69% of ONT reads mapped to the *A. oryzae* 14160 assembly. For Illumina data, a total of 17,286,313 paired-end reads were retained after adapter trimming, quality trimming, and error correction.

Phylogenetic Analysis

We performed phylogenetic analysis to investigate the relationship of *A. oryzae* 14160 in relation to the eight major clades of *A. oryzae* (Watarai et al., 2019). Specifically, we identified 243,486 SNPs from publicly available Illumina whole-genome sequencing data from 91 *A. oryzae* isolates and *A. flavus* NRRL 3357 (Gibbons et al., 2012; Nierman et al., 2015; Watarai et al., 2019) (see Methods for NCBI BioProject accession numbers). A phylogenetic tree was inferred from the alignment of SNPs with RAxML (Stamatakis, 2014) and the tree was rooted by *A. flavus* NRRL 3357. Our results were identical with Watarai et al. (2019) in showing that *A. oryzae* isolates group into eight major clades (A-H) (**Figure 1**). *A. oryzae* 14160 was nested within clade A, which contained 26 other *A. oryzae* isolates from Japan (Watarai et al., 2019), and *A. oryzae* RIB 40 was nested within clade F (**Figure 1**). To explore the impact of SNP marker linkage on inferred evolutionary relationship of isolates, we also conducted phylogenetic analysis using smaller subsets of SNP markers separated by a minimum physical distance of 4 and 10 Kb. For all analyses, the clade compositions were identical (**Figure 1** and **Supplementary Figures 2**, **3**).

A. oryzae 14160 Genome Assembly and Annotation

De novo hybrid genome assembly of *A. oryzae* 14160 was performed with the MaSuRCA assembler (Zimin et al., 2013). The *A. oryzae* 14160 genome was assembled into 24 scaffolds with a cumulative length of 36.5 Mb, largest scaffold length of 4.15 Mb, an N50 of 2.21 Mb and an N90 of 937 Kb. Genome assessment was performed with Quast (Gurevich et al., 2013) and showed a 95% genome fraction compare to the reference *A. oryzae* RIB40 genome. Genome completeness was evaluated with BUSCO (Simao et al., 2015) and showed 99% recovery of complete BUSCO genes with (0.1% fragmented BUSCO genes and 0.9% missing BUSCO genes). Both analyses indicate that the *A. oryzae* 14160 genome assembly is of high quality in terms of contiguity and accuracy.

Genome prediction and annotation of *A. oryzae* 14160 was performed using the Funannotate pipeline which relies on Augustus for gene prediction (Stanke and Waack, 2003). Using this pipeline, we predicted 11,852 protein-coding genes in *A. oryzae* 14160, which is similar to the RIB 40 genome (12,074 protein-coding genes). The gene set was assessed for completeness using BUSCO, resulting in 93% completeness with only 5% fragmented genes and 1.7% missing genes.

A. oryzae 14160 and RIB40 Chromosomal Alignment

We used Mummer to investigate the synteny between the 24 *A. oryzae* 14160 scaffolds and the eight *A. oryzae* RIB 40 chromosomes. contig_8, contig_10, contig_20, contig_15, contig_16, and contig_7 mapped to chromosome 1, contig_14 and part of contig_5 mapped to chromosome 2, contig_1 and contig_13 mapped to chromosome 3, contig_2, contig_22, contig_23, and contig_24 mapped to chromosome 4, contig_12, contig_11, contig_19, and contig_25 mapped to chromosome

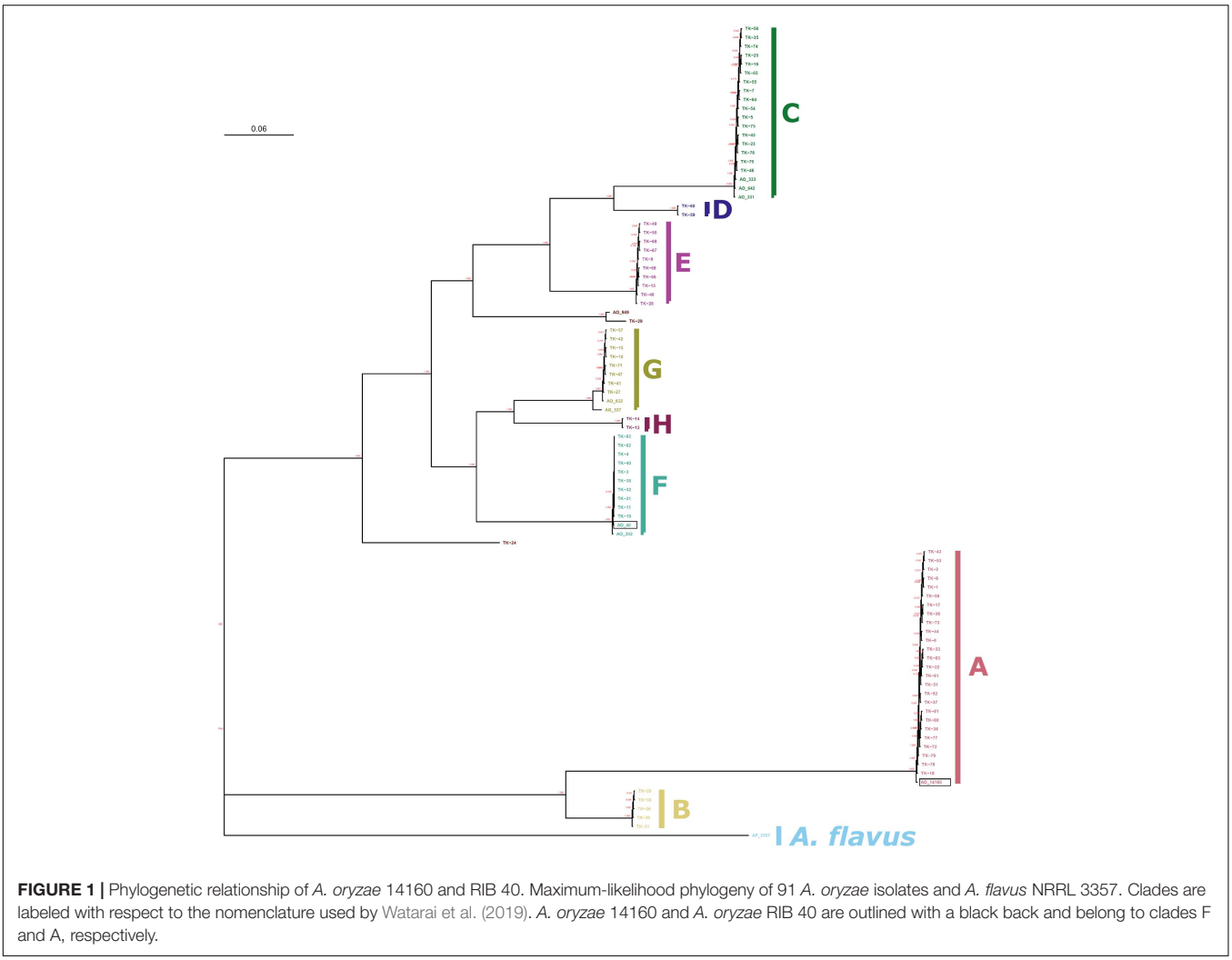

FIGURE 1 | Phylogenetic relationship of *A. oryzae* 14160 and RIB 40. Maximum-likelihood phylogeny of 91 *A. oryzae* isolates and *A. flavus* NRRL 3357. Clades are labeled with respect to the nomenclature used by Watarai et al. (2019). *A. oryzae* 14160 and *A. oryzae* RIB 40 are outlined with a black back and belong to clades F and A, respectively.

5, contig_7 mapped to chromosome 6, contig_6 and contig_18 mapped to chromosome 7, and contig_4 and contig_3 mapped to chromosome 8 (**Figure 2**). Nearly all contigs from *A. oryzae* 14160 mapped uniquely to their respective RIB40 chromosome with exception of contig_5 and contig_9, which aligned to multiple chromosomes (**Figure 2**).

Alpha-Amylase Synteny

We identified three distinct loci containing the alpha-amylase encoding gene in the *A. oryzae* 14160 genome (**Figure 3**) (alpha-amylase gene IDs = contig_14: *FUN_004371*, contig_5: *FUN_008670*, and contig_7 = *FUN_010081*). The alpha-amylase locus on *A. oryzae* 14160 contig_14 displayed conserved synteny with the *A. oryzae* RIB 40 chromosome 2 alpha-amylase locus (**Figure 3A**). In addition to the chromosome 2 locus, *A. oryzae* RIB 40 harbors alpha-amylase loci on chromosomes 3 and 5, however, we did not observe shared synteny between these loci in *A. oryzae* 14160 (**Figures 3B,C**).

The *A. oryzae* 14160 genome contained alpha-amylase loci on contig_5 and contig_7, which map to *A. oryzae* RIB40 chromosomes 2 and 6, respectively (**Figure 2**). The contig_5 locus contains 9 predicted genes not present on the *A. oryzae* RIB 40 genome nested within two syntenic genes (*FUN_008665* and *FUN_008675*) (**Figure 3B**). Importantly, this locus was assembled identically in the *A. oryzae* 14160 MaSuRCA and Canu assemblies, while the SPAdes assembly was also identical with the exception of an assembly break that did not include an additional copy of the genes *FUN_008673* and *FUN_008668* (**Figure 3B**). Additionally, we identified several long ONT reads (>30 Kb) that spanned the alpha-amylase gene as well as up-stream and/or down-stream flanking region genes. Specifically, one ONT read (ONT read ID 07fba920-71fc-460e-ba46-46ebda40194a) spanned *FUN_008668–FUN_008672* (contig_5:1,224,311–1,258,020) while another (ONT read ID a63546c6-6767-4fcf-9051-9393777f6572) spanned *FUN_008669–FUN_008673* (contig_5: 1,231,983–1,265,735). We also identified a ∼9 Kb region nearly identical to the Tc1/mariner class transposable element directly upstream of *FUN_008671* (contig_5: 1,240,697–1,245,364), which has been previously observed in the some alpha-amylase loci in *A. oryzae* strains (Hunter et al., 2011).

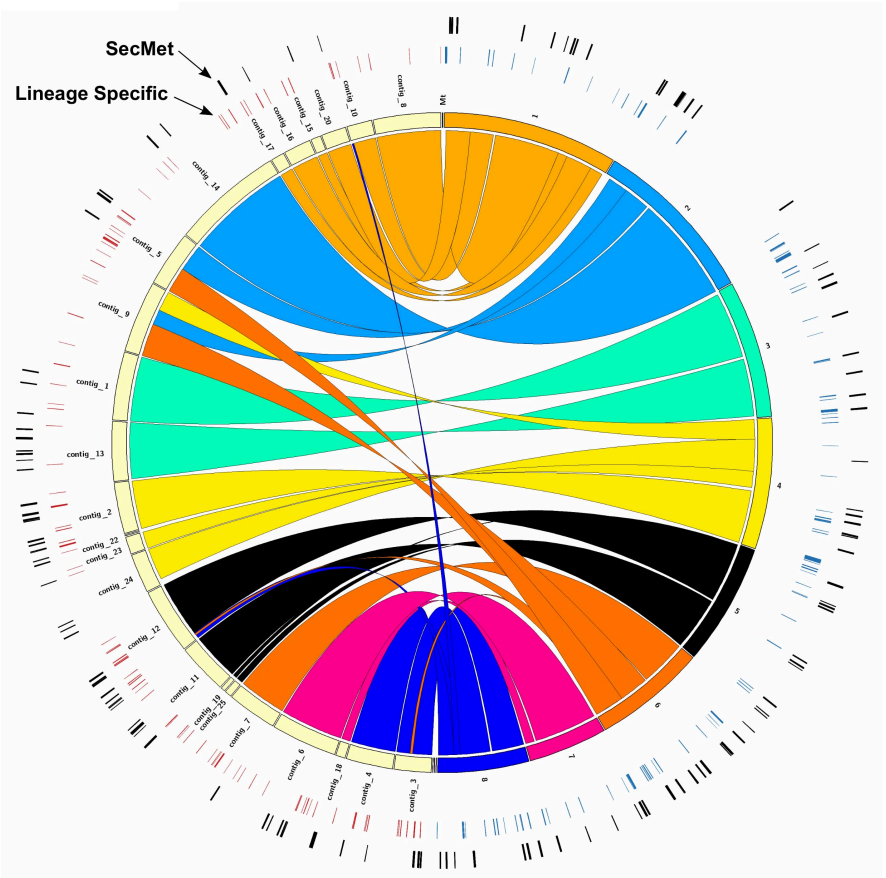

FIGURE 2 | Genome architecture between *A. oryzae* 14160 and RIB 40. Circos plot displaying similarity between the *A. oryzae* 14160 (left half of circle) and RIB 40 (right half of circle) genomes. The innermost ring represents *A. oryzae* 14160 scaffold ID or *A. oryzae* RIB 40 chromosome ID, and colored regions connecting the two represent regions with high sequence similarity (≥95%, length ≥ 10 Kb). The outer circles represent lineage specific genes and genes located within putative secondary metabolite encoding gene clusters (SecMet). The three small contigs to the left of *A. oryzae* RIB 40 chromosome 8 are AP007160, AP007177, and AP007156 (from left to right).

The *A. oryzae* 14160 alpha-amylase locus on contig_7 mapped to *A. oryzae* RIB 40 chromosome 6, and displayed conserved synteny for the majority of the locus albeit without the alpha-amylase encoding gene (*FUN_010081*) and the upstream flanking gene (*FUN_010082*) in *A. oryzae* RIB 40 (**Figure 3C**). We identified two long ONT reads that spanned the genomic regions harboring *FUN_010076–FUN_010082* and *FUN_010076–FUN_010083*, respectively (ONT read ID 05e9d1bc-f5c1-4a64-85a2-6d5df71f58db = contig_7: 977,243–1,011,315 and ONT read ID f5434ebf-bbda-48dd-8f74-28ed565a5c6b = contig_7: 977,137–1,018,308). Again, we identified the Tc1/mariner class transposable element directly upstream of *FUN_010082* (contig_7: 1,013,761–1,018,433). These results suggest convergent evolution of alpha-amylase duplication in the *A. oryzae* 14160 and RIB 40 genomes.

Alpha-Amylase Upstream Region Conservation

To investigate if differences in the regulatory region of the alpha-amylase genes corresponded to differences in amylase activity or starch metabolism, we aligned the 1 Kb upstream region of the six alpha-amylase genes. We observed only two polymorphic sites (**Supplementary Figure 4**). Specifically, we observed a transversion from A to C at one position in the *A. oryzae* 14160 alpha-amylase gene on chromosome 6 (contig_7). In another position, we observed a transversion from T to A in the *A. oryzae* RIB 40 chromosome 2 copy. These results suggest that it is unlikely that differences in the regulatory regions of the alpha-amylase genes contribute to differences in amylase activity or starch metabolism.

Single Nucleotide Polymorphism Analysis

We used freebayes and vcftools to identify high quality SNPs in *A. oryzae* 14160 relative to the *A. oryzae* RIB 40 reference genome. We identified 130,311 SNPs in *A. oryzae* 14160 (∼1 SNPs per 290 bp) and used SnpEff to annotate and predict the putative impact of these SNPs (Cingolani et al., 2012). ∼35% of SNPs were located within the coding region of genes. Of this subset, 55.64% were silent variants,

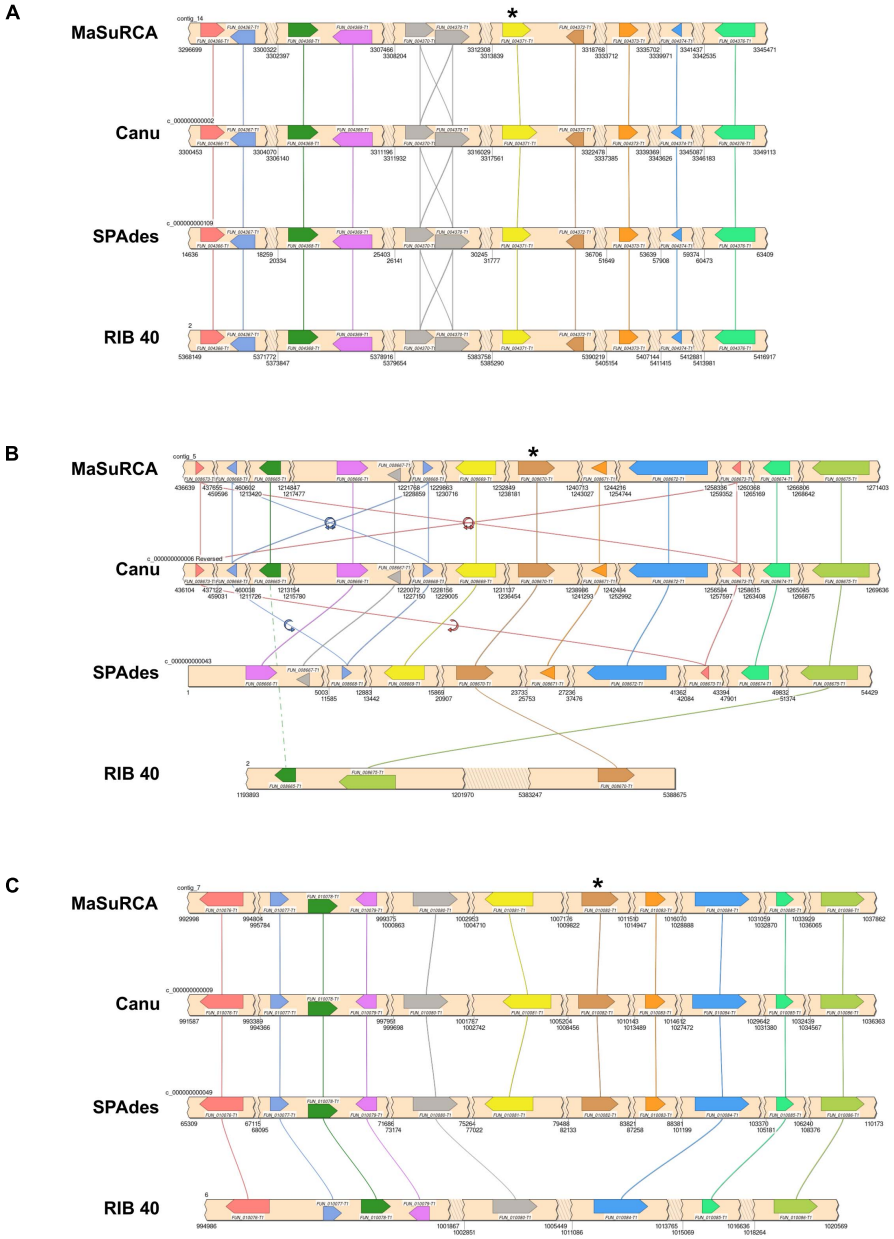

FIGURE 3 | Independent evolution of alpha-amylase duplication in *A. oryzae* 14160. Synteny analysis of the conserved *A. oryzae* 14160 alpha-amylase locus on chromosome 2 **(A)**, the non-syntenic alpha-amylase locus on chromosome 2 **(B)**, and the non-syntenic alpha-amylase locus on chromosome 6 **(C)** from three independent genome assemblies of *A. oryzae* 14160 (MaSuRCA, Canu, and SPAdes) and the reference RIB 40 genome. For each locus, gene direction is indicated by pointed ends, jagged edges indicate a genomic region without protein-coding genes that is skipped for figure clarity. Gene names are with respect to the primary *A. oryzae* 14160 annotation [generated from the MaSuRCA assembly (Zimin et al., 2013) and annotated with the Funannotate pipeline]. Scaffold ID or chromosome number and coordinates are labeled. "*" represents the alpha-amylase encoding genes. Lines connecting genes indicated conservation, and flip arrows represent a change in gene direction **(B)**. Locus schematics were generated with SimpleSynteny (Veltri et al., 2016).

43.78% were missense variants, and 0.58% were nonsense variants. We quantified the missense variant rate in each gene which ranged from 0 (no missense variants) to 0.039 (mean = 0.0014, median = 0.00047). We considered the upper 0.05% of per-gene missense variant rates as significant (≥0.0152), which included 60 genes (**Supplementary Figure 5**). This subset of genes showed no significant enrichment for GO terms. A variety of PFAM protein domains were identified in this subset of genes including transporter, protein kinase, glycosyl hydrolase, endonuclease, transposase, and transcription factor domains (**Supplementary Table 1**). Additionally, five genes with elevated missense variant rates were part of secondary metabolite encoding gene clusters (*AO090026000589*, *AO090102000459*, *AO090103000221*, *AO090103000351*,

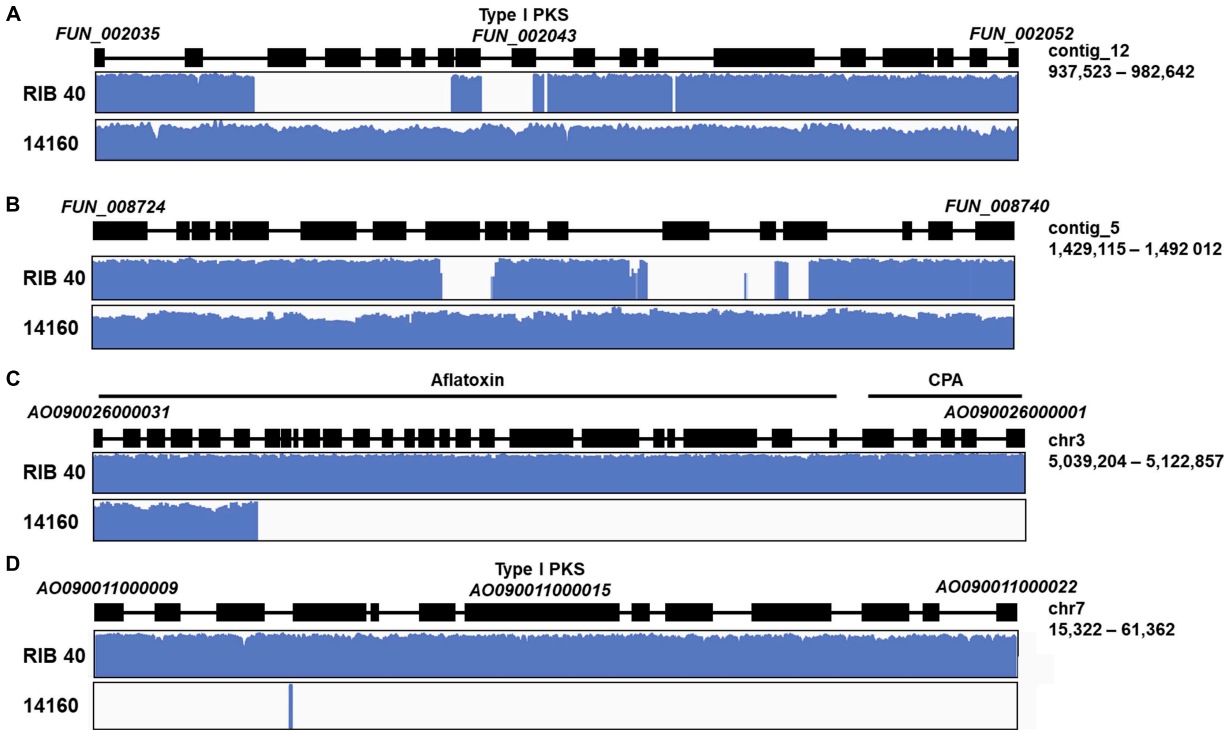

FIGURE 4 | Examples of lineage specific genes in secondary metabolite encoding gene clusters. Lineage specific genes with functional involvement in secondary metabolite production, regulation, and transport in *A. oryzae* 14160 **(A,B)**, and RIB 40 **(C,D)**. For each example, a schematic of the secondary metabolite encoding gene cluster is shown where black boxes represent genes. The first and last gene, scaffold/chromosome ID and scaffold/chromosome coordinates are labeled for each example. Graphs below the gene cluster schematic display the log10 read depth across the gene cluster for each isolate.

and *AO090701000565*), although we did not observe an overrepresentation of genes in secondary metabolite encoding gene clusters compared to the background (Fisher's Exact Test, p = 0.60). Two of the genes with elevated missense variant rates neighbored one another (*AO090003001358* and *AO090003001359*) and both genes encode proteins with predicted glycosyl hydrolases family 18 PFAM domains. Interestingly, the set of genes with elevated missense variant rates had significantly shorter coding sequences compared with the background genes ($mean_{elevatedmissensevariantrategenes}$ = 785 bp, $mean_{backgroundgenes}$ = 1,352 bp; Wilcoxon Signed-Rank Test, p = 1.1e-9).

Additionally, we examined gene enrichment analysis for the 480 genes that had one or more predicted *HIGH* impact mutations, as defined by SnpEff (i.e., loss of stop codon, gain of stop codon, loss of start codon, splice donor variant, and splice acceptor variant) (**Supplementary Table 2**). We identified 10 biological process GO terms that were enriched in the genes containing *HIGH* impact mutations [GO:1900557 (emericellamide biosynthetic process), p = 0.0003; GO:0050763 (depsipeptide biosynthetic process), p = 0.0006; GO:1900555 (emericellamide metabolic process), p = 0.0006; GO:0032774 (RNA biosynthetic process), p = 0.0013; GO:1901336 (lactone biosynthetic process), p = 0.0013; GO:1900560 (austinol biosynthetic process), p = 0.0028; GO:1900558 (austinol metabolic process), p = 0.0028; GO:1900561 (dehydroaustinol metabolic process), p = 0.0036; GO:1900563 (dehydroaustinol biosynthetic process), p = 0.0036; GO:0008610 (lipid biosynthetic process), p = 0.0062]. In support of the functional enrichment results, we identified *HIGH* impact mutations in 9 of the 75 secondary metabolite biosynthetic "backbone" genes [i.e., polyketide synthase (PKS), non-ribosomal peptide synthetase (NRPS), polyketide synthase/non-ribosomal peptide synthetase hybrid (PKS-NRPS), dimethylallyl tryptophan synthase (DMATS), and diterpene synthase (DTS)]. Of these genes, eight contained nonsense variants (*AO090009000052, AO090009000131, AO090010000404, AO090011000328, AO090038000098, AO090038000543, AO090103000224*, and *AO090103000355*) and one gene contained a nonstop variant (*AO090001000009*). *AO090009000131* and *AO090010000404* contained two nonsense variants, and *AO090011000328* contained a nonsense variant and a splice acceptor variant. Gene length (combined exon length) was not significantly different between genes with *HIGH* impact mutations and genes lacking *HIGH* impact mutations ($mean_{highimpactvariantgenes}$ = 1,418 bp, $mean_{backgroundgenes}$ = 1,346 bp; Wilcoxon Signed-Rank Test, p = 0.46).

Lineage Specific Genes

We used control-FREEC to predict gene deletions each gene in the *A. oryzae* RIB 40 and *A. oryzae* 14160 reference genomes. Genes that were absent (copy number = 0) in the mapped genome

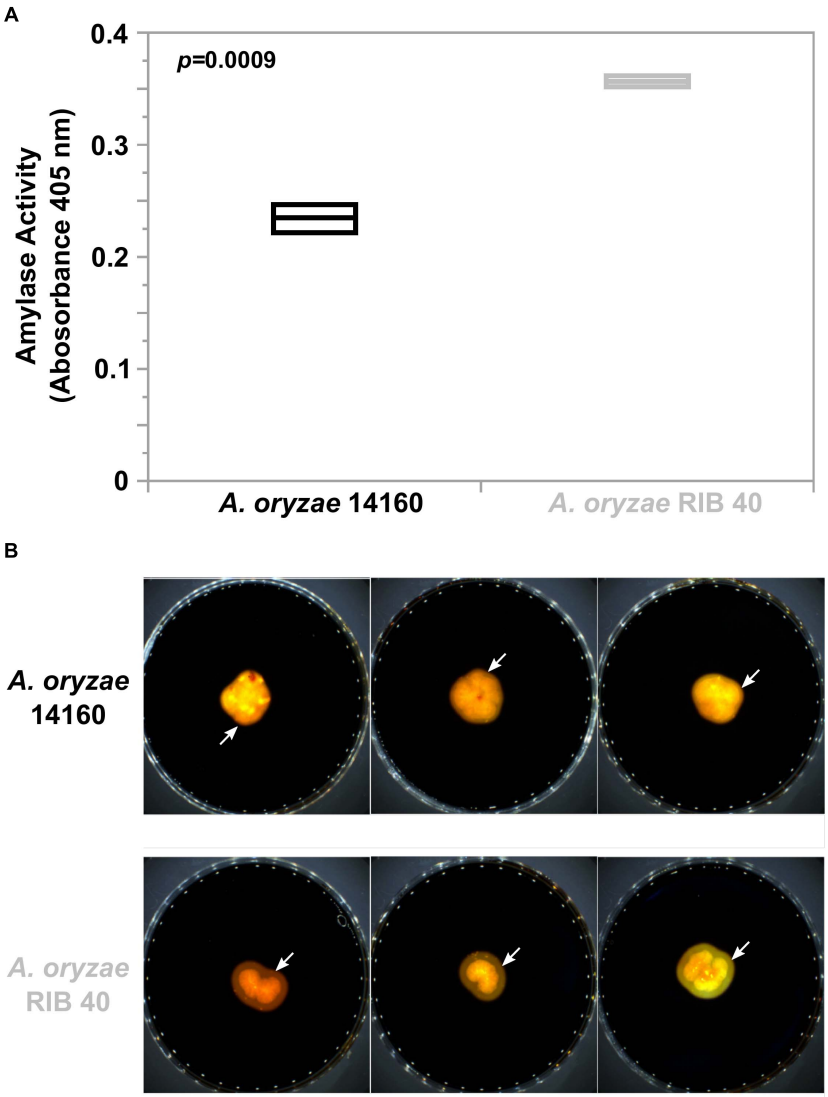

FIGURE 5 | Alpha-amylase activity in *A. oryzae* 14160 and RIB 40. **(A)** Quantitative analysis of amylase activity during solid state rice fermentation. Amylase activity was measured in triplicate using the Megazyme alpha-amylase Assay Kit. Black and Gray box plots and text represent the *A. oryzae* 14160 and RIB 40 isolates, respectively. **(B)** Qualitative iodine based amylase activity assay. Isolates were grown on starch agar and media was stained with iodine. Yellow zones surrounding the fungal colonies (white arrows) indicate amylase activity.

were considered lineage specific genes in the reference genome. Using this approach, we identified 447 and 251 genes in the *A. oryzae* RIB 40 and *A. oryzae* 14160 genomes, respectively (**Figure 2** and **Supplementary Tables 3**, **4**). Lineage specific genes were often found in clusters of neighboring genes, likely because of deletion, duplication or insertion events spanning multiple genes. For instance, *A. oryzae* RIB 40 lineage specific genes were found in 87 loci, with only 18 loci containing one gene (average = 5.1, median = 3, max = 34). The largest cluster of lineage specific genes in *A. oryzae* RIB 40 contained 34 genes and overlapped the aflatoxin and cyclopiazonic acid encoding gene clusters (**Figure 4C**). *A. oryzae* 14160 lineage specific genes were found in 101 loci, with 41 loci containing one gene (average = 2.5, median = 2, max = 14). The largest lineage specific gene cluster in *A. oryzae* 14160 contained 14 genes (*FUN_008412–FUN_008425*).

A. oryzae RIB 40 lineage specific genes were functionally enriched for the biological process GO terms "secondary metabolite biosynthetic process" (p = 7.87e-10), and "sterigmatocystin biosynthetic process" (p = 1.35e-5), and the molecular function GO terms "oxidoreductase activity, acting on paired donors, with incorporation or reduction of molecular oxygen" (p = 1e-6), "heme binding" (p = 1.24e-5), "iron ion binding" (p = 1.91e-5), and "electron carrier activity" (p = 2.21e-5). Because we observed an overrepresentation of lineage specific genes involved in secondary metabolism in *A. oryzae* RIB 40, we also tested whether this trend was present in *A. oryzae* 14160 lineage specific genes. For this analysis, we

tested whether genes annotated within secondary metabolite encoding gene clusters (as annotated by antiSMASH; Medema et al., 2011) were overrepresented in the lineage specific genes vs. the non-lineage specific genes. Indeed, we observed an overrepresentation of genes involved in secondary metabolism in the *A. oryzae* 14160 lineage specific genes (Fisher's exact test, $p = 0.0013$). Specifically, 11.5% of *A. oryzae* 14160 lineage specific genes were annotated within secondary metabolite encoding gene clusters compared to 5.6% in the background, and these genes fell within 11 independent secondary metabolite encoding gene clusters. Using the same approach, we again identified an enrichment of genes in secondary metabolite encoding gene clusters in *A. oryzae* RIB 40 (Fisher's exact test, $p = 2e\text{-}11$).

A. oryzae 14160 and *A. oryzae* RIB 40 Amylase Activity, Proteolytic Activity, and Growth Rate

Because we observed widespread genomic variation between *A. oryzae* 14160 and RIB 40, we were interested in how this variation may affect phenotype. Thus, we measured and compared amylase activity and growth rate of both strains. We hypothesized that alpha-amylase activity would be similar between *A. oryzae* 14160 and RIB 40 because both strains possess three copies of the alpha-amylase encoding gene (**Figure 3**). Interestingly, quantitative analysis of amylase activity during solid-state rice fermentation, and qualitative amylase activity on starch agar showed that *A. oryzae* RIB 40 produces higher levels of amylase (**Figure 5**). However, *A. oryzae* 14160 and RIB 40 did not significantly differ in their proteolytic activity (**Supplementary Figure 6**).

Both strains showed significantly different growth rates between media types (*A. oryzae* 14160: Oneway Anova, *d.f.* = 3, F-ratio = 31.4, $p = 1.73e\text{-}10$ and *A. oryzae* RIB 40: Oneway Anova, *d.f.* = 3, F-ratio = 22.8, $p = 1.07e\text{-}8$) (**Supplementary Figure 7**). *A. oryzae* 14160 grew fastest on PDA and starch, while growing significantly slower on soy, followed by rice (**Supplementary Figure 7A**). *A. oryzae* RIB 40 grew fastest on PDA, while growth on starch, rice and soy were not significantly different from one another (**Supplementary Figure 7B**). We also compared the growth rate of *A. oryzae* 14160 vs. RIB 40 for each media type. *A. oryzae* 14160 grew significantly faster on soy (*t*-test, t-ratio = −2.3, $p = 0.03$) and starch (*t*-test, t-ratio = −5.1, $p = 0.00003$) while *A. oryzae* RIB 40 grew significantly faster on PDA (*t*-test, t-ratio = 2.3, $p = 0.017$) and rice (*t*-test, t-ratio = 2.8, $p = 0.006$) (**Figure 6**).

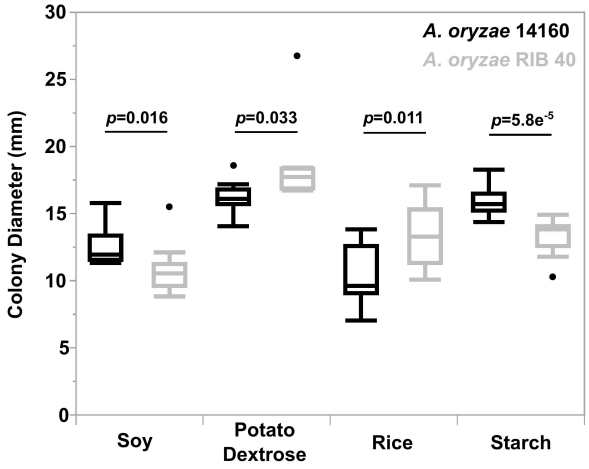

FIGURE 6 | Growth characteristics of *A. oryzae* 14160 and RIB 40 in various media. The Y-axis represents colony growth, while the X-axis represents culture media. Points outside of the boxplots represent outliers. Black and gray boxes represent *A. oryzae* 14160 and RIB 40, respectively. *T*-test *p*-values are provided for each culture media.

DISCUSSION

Here, we used long-read ONT and short-read Illumina sequencing data to assemble an accurate and highly contiguous genome of *A. oryzae* 14160. To date, only four *A. oryzae* isolates have genome assemblies comprised of fewer than 30 scaffolds (RIB40, BP2-1, BCC7051, and TK-29) (Thammarongtham et al., 2018; Watarai et al., 2019; Jeon et al., 2020). These isolates belong to clade F (RIB 40), clade E (BCC7051), clade BP2-1 (BP2-1), and a smaller clade closely related the BP2-1 clade (TK-29) (Watarai et al., 2019). Our phylogenetic analysis revealed that *A. oryzae* 14160 is part of clade A, and thus represents the first highly contiguous genome assembly from this group. Importantly, high quality genome assemblies from representative isolates across clades will enable comparative genomic analysis of structural variants, as we have demonstrated here with our synteny analysis of the alpha-amylase loci (**Figure 3**).

The assembly and annotation of the *A. oryzae* 14160 genome enabled in depth comparative genomic analysis with the complete chromosome assembly of the *A. oryzae* RIB 40 reference genome. We conducted several analyses to identify genes with divergent patterns (i.e., relative abundance of missense variants, putative impact of variants, and gene presence/absence) in the *A. oryzae* 14160 and RIB 40 genomes. Collectively, these analyses revealed that genes with involvement in secondary metabolism were highly variable (**Figures 2**, **4**). For instance, we observed a large-scale deletion event of the aflatoxin biosynthetic gene cluster that includes more than half of the cluster and the neighboring cyclopiazonic acid encoding gene cluster (**Figure 4C**). Large-scale chromosomal deletions of the aflatoxin encoding gene cluster have been previously characterized in *A. oryzae* isolates (Lee et al., 2006; Tominaga et al., 2006; Chang and Ehrlich, 2010; Alshannaq et al., 2018). Interestingly, a number of independent loss of function variants have also been observed in *A. oryzae* strains resulting in their inability to produce aflatoxin. This observation indicates the loss of aflatoxin has independently evolved in different *A. oryzae* clades, perhaps to reallocate the high energy demands required to produce this secondary metabolite into primary metabolism (Gibbons, 2019).

In addition we observed a number of high impact variants and gene presence polymorphisms in several putative secondary metabolite backbone encoding genes whose products are not as well-characterized as aflatoxin and cyclopiazonic acid (**Figure 4**). For example, *FUN_002043* encodes a type I iterative polyketide

synthetase and is absent in the *A. oryzae* RIB 40 genome, and a large secondary metabolite encoding gene cluster on *A. oryzae* chromosome 7 is entirely absent from the *A. oryzae* 14160 genome (**Figure 4A**). These results are consistent with observations in *Aspergillus* species that show secondary metabolite encoding gene clusters are highly variable both between and within species (Gibbons et al., 2012; Ehrlich and Mack, 2014; Lind et al., 2017; Alshannaq et al., 2018; Zhao and Gibbons, 2018; Drott et al., 2020; Kjaerbolling et al., 2020; Steenwyk et al., 2020). For example, genomic analysis of three *Aspergillus nidulans* genomes revealed more than 70 secondary metabolite encoding gene clusters in each genome while nine of these clusters displayed presence/absence polymorphisms (Drott et al., 2020). Similarly, we previously observed a polymorphic locus with two distinct secondary metabolite gene clusters in *A. oryzae* and *A. flavus* (Gibbons et al., 2012).

Alpha-amylase is an enzyme that hydrolyzes the alpha-D-glyosidic bond in starch to produce dextrin, and the high production of this carbohydrate metabolizing enzyme is, perhaps, *A. oryzae*'s most important industrial characteristic. Alpha-amylase copy number varies from one to four in *A. oryzae* isolates and these gene duplication events likely derive from the Tc1/mariner like transposable element that flanks this locus (Hunter et al., 2011; Watarai et al., 2019). Hunter et al. (2011) provided evidence for at least three independent duplication events of the alpha-amylase locus from the ancestral chromosome 2 copy. Interestingly, we also observed conservation of the alpha-amylase locus on chromosome 2 in *A. oryzae* 14160 (**Figure 3**), which is also conserved in the *A. flavus* NRRL 3357 genome (Nierman et al., 2015). However, we did not observe alpha-amylase copies on chromosomes 3 and 5 as in the *A. oryzae* RIB 40 genome. Instead, we identified an additional copy of the alpha-amylase locus on chromosome 2 and chromosome 6, providing further evidence for convergent evolution of alpha-amylase duplication in *A. oryzae*. The independent duplication of alpha-amylase indicates that artificial selection for increased amylase production was very strong during the domestication of *A. oryzae*.

Because we observed extensive genome variation between *A. oryzae* 14160 and RIB 40 we investigated how these strains differed phenotypically. First, we measure amylase activity using two independent assays. Both assays showed that *A. oryzae* RIB 40 produces greater levels of alpha-amylase (**Figure 5**). This observation was somewhat surprising considering the genomes of both strains contain three copies of the alpha-amylase encoding gene, and the upstream regions of these genes are nearly identical (**Supplementary Figure 4**). However, a study that generated single, double, and triple disruptant mutants of the three alpha-amylase encoding genes in RIB 40 revealed that the contribution of amylase gene and protein expression was not equal between the three copies (Nemoto et al., 2012). More specifically, *amyA* (the conserved alpha-amylase copy on chromosome 2) contributed least to amylase production. Consequently, the newly duplicated copies of alpha-amylase may also dominate amylase expression in other *A. oryzae* isolates, and chromosomal location of alpha-amylase paralogs may influence their gene expression. For instance, position effect variegation was observed in *A. nidulans* where a translocation of the developmental regulator *brlA* resulted a conidiophore that remained as a stiff hyphae and did not develop a vesicle, sterigmata, and conidia (Clutterbuck, 1970). Similarly, the chromosomal position of the alpha-amylase loci in *A. oryzae* could potentially influence expression.

Finally, we observed differential growth preferences between *A. oryzae* 14160 and RIB 40. Interestingly, *A. oryzae* 14160 grew significantly faster on soy and starch agar, while RIB 40 grew significantly faster on PDA and rice agar. Though *A. oryzae* RIB 40 did not grow faster on starch agar, amylase activity was visibly greater, suggesting that growth rate may have increased during a longer incubation period. Additionally, the starch agar contained beef extract which provides a source of proteins and peptides. Thus, *A. oryzae* 14160 grew faster where protein content was higher (soy and starch), and RIB 40 grew faster when carbohydrates were the major available energy source (potato dextrose and rice). This observation suggests that *A. oryzae* 14160 is better suited for soy fermentation, while RIB 40 is better suited for rice fermentation.

DATA AVAILABILITY STATEMENT

The datasets presented in this study can be found in online repositories. The names of the repository/repositories and accession number(s) can be found below: https://www.ncbi.nlm.nih.gov/, PRJNA717291.

AUTHOR CONTRIBUTIONS

KC-V and JG conducted genomic and statistical analysis. CM performed growth rate and amylase experiments. J-HY and DC maintained the cultures and extracted DNA for Illumina sequencing. LW provided the *A. oryzae* 14160. All authors contributed to manuscript revision and approved the submitted version.

FUNDING

This work was funded through NSF Grant 1942681 to JG which also supports KC-V.

ACKNOWLEDGMENTS

Computational analysis was conducted on the Massachusetts Green High Performance Computing Center (MGHPCC).

SUPPLEMENTARY MATERIAL

The Supplementary Material for this article can be found online at: https://www.frontiersin.org/articles/10.3389/fmicb.2021.691296/full#supplementary-material

REFERENCES

Abbo, S., Pinhasi van-Oss, R., Gopher, A., Saranga, Y., Ofner, I., and Peleg, Z. (2014). Plant domestication versus crop evolution: a conceptual framework for cereals and grain legumes. *Trends Plant Sci.* 19, 351–360. doi: 10.1016/j.tplants.2013.12.002

Alshannaq, A. F., Gibbons, J. G., Lee, M. K., Han, K. H., Hong, S. B., and Yu, J. H. (2018). Controlling aflatoxin contamination and propagation of *Aspergillus flavus* by a soy-fermenting *Aspergillus oryzae* strain. *Sci. Rep*. 8:16871. doi: 10.1038/s41598-018-35246-1

Altschul, S. F., Madden, T. L., Schaffer, A. A., Zhang, J., Zhang, Z., Miller, W., et al. (1997). Gapped BLAST and PSI-BLAST: a new generation of protein database search programs. *Nucleic Acids Res.* 25, 3389–3402. doi: 10.1093/nar/25.17.3389

Aouizerat, T., Gutman, I., Paz, Y., Maeir, A. M., Gadot, Y., Gelman, D., et al. (2019). Isolation and characterization of live yeast cells from ancient vessels as a tool in bio-archaeology. *Mbio* 10:e00388–19. doi: 10.1128/mBio.00388-19

Aouizerat, T., Maeir, A. M., Paz, Y., Gadot, Y., Szitenberg, A., Alkalay-Oren, S., et al. (2020). Isolation and characterization of live yeast cells from ancient clay vessels. *Bio Protoc.* 10:e3473. doi: 10.21769/BioProtoc.3473

Bankevich, A., Nurk, S., Antipov, D., Gurevich, A. A., Dvorkin, M., Kulikov, A. S., et al. (2012). SPAdes: a new genome assembly algorithm and its applications to single-cell sequencing. *J. Comput. Biol.* 19, 455–477. doi: 10.1089/cmb.2012.0021

Boeva, V., Popova, T., Bleakley, K., Chiche, P., Cappo, J., Schleiermacher, G., et al. (2012). Control-FREEC: a tool for assessing copy number and allelic content using next-generation sequencing data. *Bioinformatics* 28, 423–425. doi: 10.1093/bioinformatics/btr670

Cavalieri, D., McGovern, P. E., Hartl, D. L., Mortimer, R., and Polsinelli, M. (2003). Evidence for S. cerevisiae fermentation in ancient wine. *J. Mol. Evol.* 57 Suppl 1, S226–S232. doi: 10.1007/s00239-003-0031-2

Chang, P. K., and Ehrlich, K. C. (2010). What does genetic diversity of *Aspergillus flavus* tell us about *Aspergillus oryzae*? *Int. J. Food Microbiol.* 138, 189–199. doi: 10.1016/j.ijfoodmicro.2010.01.033

Cingolani, P., Platts, A., Wang, L. L., Coon, M., Nguyen, T., Wang, L., et al. (2012). A program for annotating and predicting the effects of single nucleotide polymorphisms, SnpEff: SNPs in the genome of Drosophila melanogaster strain w(1118); iso-2; iso-3. *Fly* 6, 80–92. doi: 10.4161/fly.19695

Clutterbuck, A. J. (1970). A variegated position effect in *Aspergillus nidulans*. *Genet. Res.* 16, 303–316. doi: 10.1017/s0016672300002561

Danecek, P., Auton, A., Abecasis, G., Albers, C. A., Banks, E., DePristo, M. A., et al. (2011). Genomes project analysis, the variant call format and VCFtools. *Bioinformatics* 27, 2156–2158. doi: 10.1093/bioinformatics/btr330

Davis, M. P., van Dongen, S., Abreu-Goodger, C., Bartonicek, N., and Enright, A. J. (2013). Kraken: a set of tools for quality control and analysis of high-throughput sequence data. *Methods* 63, 41–49. doi: 10.1016/j.ymeth.2013.06.027

Delcher, A. L., Kasif, S., Fleischmann, R. D., Peterson, J., White, O., and Salzberg, S. L. (1999). Alignment of whole genomes. *Nucleic Acids Res.* 27, 2369–2376. doi: 10.1093/nar/27.11.2369

Drott, M. T., Bastos, R. W., Rokas, A., Ries, L. N. A., Gabaldon, T., Goldman, G. H., et al. (2020). Diversity of secondary metabolism in aspergillus nidulans clinical isolates. *mSphere* 5:e00156–20. doi: 10.1128/mSphere.00156-20

Dumas, E., Feurtey, A., Rodriguez de la Vega, R. C., Prieur, S. Le, Snirc, A., Coton, M., et al. (2020). Independent domestication events in the blue-cheese fungus *Penicillium roqueforti*. *Mol. Ecol.* 29, 2639–2660. doi: 10.1111/mec.15359

Ehrlich, K. C., and Mack, B. M. (2014). Comparison of expression of secondary metabolite biosynthesis cluster genes in *Aspergillus flavus*, *A. parasiticus*, and *A. oryzae*. *Toxins (Basel)* 6, 1916–1928. doi: 10.3390/toxins6061916

Fuwa, H. (1954). A new method for microdetermination CF amylase activity by the use of amylose as the substrate. *J. Biochem.* 41, 583–603. doi: 10.1093/oxfordjournals.jbchem.a126476

Gallone, B., Steensels, J., Prahl, T., Soriaga, L., Saels, V., Herrera-Malaver, B., et al. (2016). Domestication and divergence of *Saccharomyces cerevisiae* beer yeasts. *Cell* 166, 1397–1410.e16.

Garrison, E., and Marth, G. (2012). Haplotype-based variant detection from short-read sequencing. *arXiv* [Preprint] arXiv: 1207.3907v2,

Geiser, D. M., Pitt, J. I., and Taylor, J. W. (1998). Cryptic speciation and recombination in the aflatoxin-producing fungus *Aspergillus flavus*. *Proc. Natl. Acad. Sci. U.S.A.* 95, 388–393. doi: 10.1073/pnas.95.1.388

Gibbons, J. G. (2019). How to train your fungus. *Mbio* 10:e003031–19. doi: 10.1128/mBio.03031-19

Gibbons, J. G., and Rinker, D. C. (2015). The genomics of microbial domestication in the fermented food environment. *Curr. Opin. Genet. Dev.* 35, 1–8. doi: 10.1016/j.gde.2015.07.003

Gibbons, J. G., Salichos, L., Slot, J. C., Rinker, D. C., McGary, K. L., King, J. G., et al. (2012). The evolutionary imprint of domestication on genome variation and function of the filamentous fungus *Aspergillus oryzae*. *Curr. Biol.* 22, 1403–1409. doi: 10.1016/j.cub.2012.05.033

Gurevich, A., Saveliev, V., Vyahhi, N., and Tesler, G. (2013). QUAST: quality assessment tool for genome assemblies. *Bioinformatics* 29, 1072–1075. doi: 10.1093/bioinformatics/btt086

Hunter, A. J., Jin, B., and Kelly, J. M. (2011). Independent duplications of alpha-amylase in different strains of *Aspergillus oryzae*. *Fungal Genet. Biol.* 48, 438–444. doi: 10.1016/j.fgb.2011.01.006

Jeon, J., Kim, J. A., Park, S. Y., Kim, G. W., Park, C. S., Kim, C., et al. (2020). Draft genome sequence of *Aspergillus oryzae* BP2-1, isolated from traditional malted rice in South Korea. *Microbiol. Resour. Announc.* 9, e1405–e1419. doi: 10.1128/MRA.01405-19

Jones, P., Binns, D., Chang, H. Y., Fraser, M., Li, W., McAnulla, C., et al. (2014). InterProScan 5: genome-scale protein function classification. *Bioinformatics* 30, 1236–1240. doi: 10.1093/bioinformatics/btu031

Kall, L., Krogh, A., and Sonnhammer, E. L. (2004). A combined transmembrane topology and signal peptide prediction method. *J. Mol. Biol.* 338, 1027–1036. doi: 10.1016/j.jmb.2004.03.016

Kall, L., Krogh, A., and Sonnhammer, E. L. (2007). Advantages of combined transmembrane topology and signal peptide prediction–the Phobius web server. *Nucleic Acids Res.* 35, W429–W432.

Katoh, K., and Standley, D. M. (2013). MAFFT multiple sequence alignment software version 7: improvements in performance and usability. *Mol. Biol. Evol.* 30, 772–780. doi: 10.1093/molbev/mst010

Kjaerbolling, I., Vesth, T., Frisvad, J. C., Nybo, J. L., Theobald, S., Kildgaard, S., et al. (2020). A comparative genomics study of 23 Aspergillus species from section Flavi. *Nat. Commun.* 11:1106. doi: omparativegenomicsstud

Koren, S., Walenz, B. P., Berlin, K., Miller, J. R., Bergman, N. H., and Phillippy, A. M. (2017). Canu: scalable and accurate long-read assembly via adaptive k-mer weighting and repeat separation. *Genome Res.* 27, 722–736. doi: 10.1101/gr.215087.116

Krzywinski, M., Schein, J., Birol, I., Connors, J., Gascoyne, R., Horsman, D., et al. (2009). Circos: an information aesthetic for comparative genomics. *Genome Res.* 19, 1639–1645. doi: 10.1101/gr.092759.109

Larson, G., and Fuller, D. Q. (2014). The evolution of animal domestication. *Annu. Rev. Ecol. Evol Syst.* 45, 115–136.

Larson, G., Piperno, D. R., Allaby, R. G., Purugganan, M. D., Andersson, L., Arroyo-Kalin, M., et al. (2014). Current perspectives and the future of domestication studies. *Proc. Natl. Acad. Sci. U.S.A.* 111, 6139–6146. doi: 10.1073/pnas.1323964111

Lee, M. K., Park, H. S., Han, K. H., Hong, S. B., and Yu, J. H. (2017). High molecular weight genomic DNA mini-prep for filamentous fungi. *Fungal Genet. Biol.* 104, 1–5. doi: 10.1016/j.fgb.2017.04.003

Lee, Y. H., Tominaga, M., Hayashi, R., Sakamoto, K., Yamada, O., and Akita, O. (2006). Aspergillus oryzae strains with a large deletion of the aflatoxin biosynthetic homologous gene cluster differentiated by chromosomal breakage. *Appl. Microbiol. Biotechnol.* 72, 339–345. doi: 10.1007/s00253-005-0282-5

Li, H. (2018). Minimap2: pairwise alignment for nucleotide sequences. *Bioinformatics* 34, 3094–3100. doi: 10.1093/bioinformatics/bty191

Li, H., and Durbin, R. (2009). Fast and accurate short read alignment with Burrows-Wheeler transform. *Bioinformatics* 25, 1754–1760. doi: 10.1093/bioinformatics/btp324

Li, H., and Durbin, R. (2010). Fast and accurate long-read alignment with Burrows-Wheeler transform. *Bioinformatics* 26, 589–595. doi: 10.1093/bioinformatics/btp698

Li, H., Handsaker, B., Wysoker, A., Fennell, T., Ruan, J., Homer, N., et al. (2009). Genome project data processing. The sequence alignment/map format and SAMtools. *Bioinformatics* 25, 2078–2079. doi: 10.1093/bioinformatics/btp352

Lind, A. L., Wisecaver, J. H., Lameiras, C., Wiemann, P., Palmer, J. M., Keller, N. P., et al. (2017). Drivers of genetic diversity in secondary metabolic gene

clusters within a fungal species. *PLoS Biol.* 15:e2003583. doi: 10.1371/journal.pbio.2003583

Liu, L., Wang, J., Levin, M. J., Sinnott-Armstrong, N., Zhao, H., Zhao, Y., et al. (2019). The origins of specialized pottery and diverse alcohol fermentation techniques in Early Neolithic China. *Proc. Natl. Acad. Sci. U.S.A.* 116, 12767–12774. doi: 10.1073/pnas.1902668116

Machida, M., Asai, K., Sano, M., Tanaka, T., Kumagai, T., Terai, G., et al. (2005). Genome sequencing and analysis of *Aspergillus oryzae*. *Nature* 438, 1157–1161. doi: 10.1038/nature04300

Machida, M., Yamada, O., and Gomi, K. (2008). Genomics of *Aspergillus oryzae*: learning from the history of Koji mold and exploration of its future. *DNA Res.* 15, 173–183. doi: 10.1093/dnares/dsn020

McGovern, P. E., Zhang, J., Tang, J., Zhang, Z., Hall, G. R., Moreau, R. A., et al. (2004). Fermented beverages of pre- and proto-historic China. *Proc. Natl. Acad. Sci. U.S.A* 101, 17593–17598. doi: 10.1073/pnas.0407921102

McKenna, A., Hanna, M., Banks, E., Sivachenko, A., Cibulskis, K., Kernytsky, A., et al. (2010). The genome analysis toolkit: a MapReduce framework for analyzing next-generation DNA sequencing data. *Genome Res.* 20, 1297–1303. doi: 10.1101/gr.107524.110

Medema, M. H., Blin, K., Cimermancic, P., de Jager, V., Zakrzewski, P., Fischbach, M. A., et al. (2011). antiSMASH: rapid identification, annotation and analysis of secondary metabolite biosynthesis gene clusters in bacterial and fungal genome sequences. *Nucleic Acids Res.* 39, W339–W346. doi: 10.1093/nar/gkr466

Nemoto, T., Maruyama, J., and Kitamoto, K. (2012). Contribution ratios of amyA, amyB, amyC genes to high-level alpha-amylase expression in *Aspergillus oryzae*. *Biosci. Biotechnol. Biochem.* 76, 1477–1483. doi: 10.1271/bbb.120142

Nierman, W. C., Yu, J., Fedorova-Abrams, N. D., Losada, L., Cleveland, T. E., Bhatnagar, D., et al. (2015). Genome Sequence of *Aspergillus flavus* NRRL 3357, a strain that causes aflatoxin contamination of food and feed. *Genome Announc.* 3:e00168–15. doi: 10.1128/genomeA.00168-15

Priebe, S., Kreisel, C., Horn, F., Guthke, R., and Linde, J. (2015). FungiFun2: a comprehensive online resource for systematic analysis of gene lists from fungal species. *Bioinformatics* 31, 445–446. doi: 10.1093/bioinformatics/btu627

Purugganan, M. D., and Fuller, D. Q. (2009). The nature of selection during plant domestication. *Nature* 457, 843–848. doi: 10.1038/nature07895

Quinlan, A. R., and Hall, I. M. (2010). BEDTools: a flexible suite of utilities for comparing genomic features. *Bioinformatics* 26, 841–842. doi: 10.1093/bioinformatics/btq033

Rajamani, S., and Hilda, A. (1987). Plate assay to screen fungi for proteoltyic activity. *Curr. Sci.* 56, 1179–1181.

Rinker, D. C., Specian, N. K., Zhao, S., and Gibbons, J. G. (2019). Polar bear evolution is marked by rapid changes in gene copy number in response to dietary shift. *Proc. Natl. Acad. Sci. U.S.A.* 116, 13446–13451. doi: 10.1073/pnas.1901093116

Ropars, J., Didiot, E., Rodriguez de la Vega, R. C., Bennetot, B., Coton, M., Poirier, E., et al. (2020). Domestication of the emblematic white cheese-making fungus penicillium camemberti and its diversification into two varieties. *Curr. Biol.* 30, 4441–4453.e4. doi: 10.1016/j.cub.2020.08.082

Rubin, C. J., Zody, M. C., Eriksson, J., Meadows, J. R., Sherwood, E., Webster, M. T., et al. (2010). Whole-genome resequencing reveals loci under selection during chicken domestication. *Nature* 464, 587–591. doi: 10.1038/nature08832

Salque, M., Bogucki, P. I., Pyzel, J., Sobkowiak-Tabaka, I., Grygiel, R., Szmyt, M., et al. (2013). Earliest evidence for cheese making in the sixth millennium BC in northern Europe. *Nature* 493, 522–525. doi: 10.1038/nature11698

Simao, F. A., Waterhouse, R. M., Ioannidis, P., Kriventseva, E. V., and Zdobnov, E. M. (2015). BUSCO: assessing genome assembly and annotation completeness with single-copy orthologs. *Bioinformatics* 31, 3210–3212. doi: 10.1093/bioinformatics/btv351

Stamatakis, A. (2014). RAxML version 8: a tool for phylogenetic analysis and post-analysis of large phylogenies. *Bioinformatics* 30, 1312–1313. doi: 10.1093/bioinformatics/btu033

Stanke, M., and Waack, S. (2003). Gene prediction with a hidden Markov model and a new intron submodel. *Bioinformatics* 19 Suppl 2, ii215–ii225. doi: 10.1093/bioinformatics/btg1080

Steensels, J., Gallone, B., Voordeckers, K., and Verstrepen, K. J. (2019). Domestication of industrial microbes. *Curr. Biol.* 29, R381–R393. doi: 10.1016/j.cub.2019.04.025

Steenwyk, J. L., Mead, M. E., Knowles, S. L., Raja, H. A., Roberts, C. D., Bader, O., et al. (2020). Variation among biosynthetic gene clusters, secondary metabolite profiles, and cards of virulence across aspergillus species. *Genetics* 216, 481–497. doi: 10.1534/genetics.120.303549

Thammarongtham, C., Nookaew, I., Vorapreeda, T., Srisuk, T., Land, M. L., Jeennor, S., et al. (2018). Genome characterization of oleaginous aspergillus oryzae bcc7051: a potential fungal-based platform for lipid production. *Curr. Microbiol.* 75, 57–70. doi: 10.1007/s00284-017-1350-7

Tominaga, M., Lee, Y. H., Hayashi, R., Suzuki, Y., Yamada, O., Sakamoto, K., et al. (2006). Molecular analysis of an inactive aflatoxin biosynthesis gene cluster in Aspergillus oryzae RIB strains. *Appl. Environ. Microb.* 72, 484–490. doi: 10.1128/aem.72.1.484-490.2006

Veltri, D., Wight, M. M., and Crouch, J. A. (2016). Simple Synteny: a web-based tool for visualization of microsynteny across multiple species. *Nucleic Acids Res.* 44, W41–W45.

Watarai, N., Yamamoto, N., Sawada, K., and Yamada, T. (2019). Evolution of *Aspergillus oryzae* before and after domestication inferred by large-scale comparative genomic analysis. *DNA Res.* 26, 465–472. doi: 10.1093/dnares/dsz024

Wickham, H. (2009). *ggplot2: Elegant Graphics for Data Analysis*. New York, NY: Springer-Verlag.

Yu, G. (2020). Using ggtree to visualize data on tree-like structures. *Curr. Protoc. Bioinformatics* 69:e96.

Zhao, S., and Gibbons, J. G. (2018). A population genomic characterization of copy number variation in the opportunistic fungal pathogen *Aspergillus fumigatus*. *PLoS One* 13:e0201611. doi: 10.1371/journal.pone.0201611

Zimin, A. V., Marcais, G., Puiu, D., Roberts, M., Salzberg, S. L., and Yorke, J. A. (2013). The MaSuRCA genome assembler. *Bioinformatics* 29, 2669–2677. doi: 10.1093/bioinformatics/btt476

Conflict of Interest: The authors declare that the research was conducted in the absence of any commercial or financial relationships that could be construed as a potential conflict of interest.

frontiers in Microbiology

REVIEW
published: 22 July 2021
doi: 10.3389/fmicb.2021.690211

Glycosphingolipids in Filamentous Fungi: Biological Roles and Potential Applications in Cosmetics and Health Foods

Chunmiao Jiang[1†], Jinxin Ge[1†], Bin He[1] and Bin Zeng[1,2*]*

[1] *Jiangxi Key Laboratory of Bioprocess Engineering and Co-Innovation Center for In-Vitro Diagnostic Reagents and Devices of Jiangxi Province, College of Life Sciences, Jiangxi Science and Technology Normal University, Nanchang, China,* [2] *College of Pharmacy, Shenzhen Technology University, Shenzhen, China*

OPEN ACCESS

Edited by:
Wanping Chen, Georg-August-University Göettingen, Germany

Reviewed by:
Leonardo Freire-de-Lima, Federal University of Rio de Janeiro, Brazil
Aly Farag El Sheikha, Jiangxi Agricultural University, China

***Correspondence:**
Bin He
hebin.li@foxmail.com
Bin Zeng
zengtx001@aliyun.com

† These authors have contributed equally to this work and share first authorship

Specialty section:
This article was submitted to Food Microbiology, a section of the journal Frontiers in Microbiology

Received: *02 April 2021*
Accepted: *28 June 2021*
Published: *22 July 2021*

Citation:
Jiang C, Ge J, He B and Zeng B (2021) Glycosphingolipids in Filamentous Fungi: Biological Roles and Potential Applications in Cosmetics and Health Foods. Front. Microbiol. 12:690211. doi: 10.3389/fmicb.2021.690211

Filamentous fungi are a group of economically important fungi used in the production of fermented foods, industrial enzymes, and secondary metabolites. Glycosphingolipids (GSLs) as constituents of lipid rafts are involved in growth, differentiation, and response to environment stress in filamentous fungi. In addition to these key roles, GSLs are also important in the barrier function of skin to retain moisture as a moisturizing ingredient in cosmetics or health products for their strong biological activity as a functional component. GSLs found in filamentous fungi are divided in two major classes: neutral GSLs (glycosylceramides), glucosylceramides (GlcCers), and/or galactosylceramides (GalCers) and acidic GSLs, mannosylinositol phosphorylceramide (MIPC) and mannosyldiinositol phosphorylceramide [$M(IP)_2C$]. Glycosylceramides are one of the abundant GSLs in *Aspergillus* and known to improve skin-barrier function and prevent intestinal impairment as a prebiotic. Some filamentous fungi of *Aspergillus* spp., synthesizing both GlcCer and GalCer, would be an amenable source to exploit glycosylceramides that wildly adding in cosmetics as moisturizing ingredients or health food as dietary supplements. In this minireview, the types, structures, and biosynthetic pathways of GSLs in filamentous fungi, and the relevance of GSLs in fungal growth, spore formation, and environmental stress response are explained. Furthermore, the advantage, potential development, and application of GlcCer and GalCer from filamentous fungi *Aspergillus* spp. are also investigate based on the use of plant GlcCer in health foods and cosmetics.

Keywords: filamentous fungi, *Aspergillus*, glycosphingolipids, biosynthetic pathway, glucosylceramide and galactosylceramide, application of glycosylceramide

INTRODUCTION

Filamentous fungi, particularly *Aspergillus* spp., *Trichoderma reesei*, and *Neurospora crassa*, are a group of economically important fungi used in the production of fermented foods, industrial enzymes, antibiotic substances, and organic acids (Brunt, 1986; Cherry and Fidantsef, 2003; Allgaier et al., 2009; Karaffa and Kubicek, 2019). For more than a century, filamentous fungi have been known to produce and secrete different types of enzymes in large quantities, which has resulted in

an increased interest in studying them and using them in industrial applications. The production of more than 60% of total industrial enzymes is done by *Aspergillus* genus of filamentous fungi. In addition, filamentous fungi are well-known producers of secondary metabolites with various biological activities. Many of these compounds such as penicillin, cyclosporine or lovastatin are of great importance to human health (Nützmann et al., 2012). For example, two important antibiotics cephalosporin and penicillin are produced by *Cephalosporium acremonium* and *Penicillium chrysogenum*, respectively (Nash and Huber, 1971; Nielsen and Jorgensen, 1995). Furthermore, filamentous fungi are also widely used in the production of organic acids in industrial fermentation, such as citric acid, itaconic acid, fumaric acid, and malic acid (Papagianni, 2007; Knuf et al., 2013; Hu et al., 2014; Karaffa and Kubicek, 2019). *Aspergillus niger* and *Aspergillus oryzae* have a long history of use in the fermentation industry and are generally recognized as safe (GRAS) in accordance with the Food and Drug Administration (FDA). Amylase, a well-known enzyme is produced from *A. niger* and *A. oryzae* and applicated in diverse processes, ranging from food and beverage to medical (Wirsel et al., 2010; Silano et al., 2018). Soy sauce, a traditional fermented condiment widely consumed in China, Japan, Korea, and other Asian countries, is fermented from soybean by *A. oryzae* (Liang et al., 2009). Therefore, due to the economic importance of filamentous fungi, the secondary metabolite pathways, organic compound, and fermentation processes in these filamentous fungi have attracted attention of the scientists.

In the industrial application of filamentous fungi, the conditions of the fermentation play a vital role in the growth and metabolism of a microbial population. Filamentous fungi have the potential to grow or ferment under diverse environmental conditions by utilizing a wide variety of substrates as nutrients (Chen et al., 2011). The ability of microorganisms to adapt to different environmental factors has attracted considerable attention, with many studies investigating the molecular mechanisms of microorganism in response to environmental stress. Fungi adapt to environmental changes using a range of molecular mechanisms. One mechanism is *via* change in the composition of cellular lipids, such as phospholipids, neutral lipids, or unique glycosphingolipids (GSLs) (Suutari, 1995; Řezanka et al., 2016, 2018). Fungal GSLs, including neutral and acidic GSLs, are the main lipid components of microdomains in fungal membranes and are clustered along with sterols to form lipid rafts, which play crucial roles in cell polarization, hyphal growth, fungal fitness, and adaptation to most diverse environments as a signaling molecules (Sonnino et al., 2007; Guimarães et al., 2014; Řezanka et al., 2016, 2018). Although GSLs have been studied extensively, the details of their function are difficult to understand owing to complex and dynamic changing synthetic pathways of interconversion and utilization. Nonetheless, the role of yeast GSLs in response to heat stress has been investigated thoroughly (Chen et al., 2013; Řezanka et al., 2016, 2018). However, the GSL pathways and related genes that contribute to fungal growth, differentiation, morphogenesis, particularly those involved in response to environmental stress in filamentous fungi, are less appreciated.

In addition to fungal growth and response to environmental stress, neutral GSLs (also call glycosylceramides) are also known to have nutritive functions such as preventing intestinal impairment and enhancing the moisture content of skin (Ono et al., 2010; Duan et al., 2012; Hamajima et al., 2016). For example, neutral GSLs can be added to food as a "functional components" for their strong biological activity in health food products such as nutritional supplements, infant foods, and beverages that help in reduction of blood pressure, activation of immunity and inhibition of cancer cell proliferation. Previous studies reported that *A. oryzae* glycosylceramides functions as a prebiotic, can alter the intestinal microbial flora and increase *Blautia coccoides* (Hamajima et al., 2019). Since there are many reports of the effects of *B. coccoides* on health, an increase in intestinal *B. coccoides* by *koji* glycosylceramide might be the connection between intestinal microbial flora and healthy. Besides, neutral GSLs are also important due to their barrier function as a moisturizing ingredient in cosmetics that help of skin retain its moisture (Alessandrini et al., 2004; Tessema et al., 2017; Miyagawa et al., 2019). However, plant cell membrane contents such as neutral GSLs, are difficult to extract due to the thick cell wall and GSLs from neural tissues of animals are not acceptable for cosmetic or other human use due to the underlying risk of prion diseases. Therefore, filamentous fungi *koji*, which are safe for humans and contain abundant (0.5–2 mg/g dry weight koji) neutral GSLs, would be important resources for exploiting neutral GSLs in the future.

In this review, we discuss the relevance of GSLs in fungal growth, spore formation and environmental stress response, which are key to the production of fermented foods, commercial enzymes, and secondary metabolites in industrial fermentation, and the potential development and application of filamentous fungi GSLs in cosmetics and health foods.

THE KINDS AND STRUCTURES OF GSLs IN FILAMENTOUS FUNGI

Glycosphingolipids are ubiquitous membrane components and are involved in many biological processes crucial for filamentous fungi, such as growth, signal transduction, morphological transition, and pathogenesis (Heung et al., 2006; Huber et al., 2019). Our knowledge of GSL biosynthesis in filamentous fungi is mainly based on investigations of yeasts, the human pathogenic *Candida albicans* (Oura and Kajiwara, 2010), the model organisms *N. crassa* (Park et al., 2005) and *Aspergillus nidulans* (Levery et al., 2002; Fernandes et al., 2016), and the plant pathogen *Fusarium graminearum* (Duarte et al., 1998; Ramamoorthy et al., 2007, 2009; Zaüner et al., 2008). The basic structure of GSL consists of an 18-carbon-alcohol chain called long chain base (LCB) that is linked to a C_{16-26} fatty acid (FA) chain through an amide bond to form ceramide (**Figure 1A**), which in turn is linked to a polar head group (**Figures 1B,C**) (Barreto-Bergter et al., 2004, 2011; Del Poeta et al., 2014). GSLs have been isolated and identified from various filamentous fungi, such as *C. albicans*, *F. graminearum*, *N. crassa*, and *Aspergillus* spp., and divided in two major classes of neutral and acidic GSLs

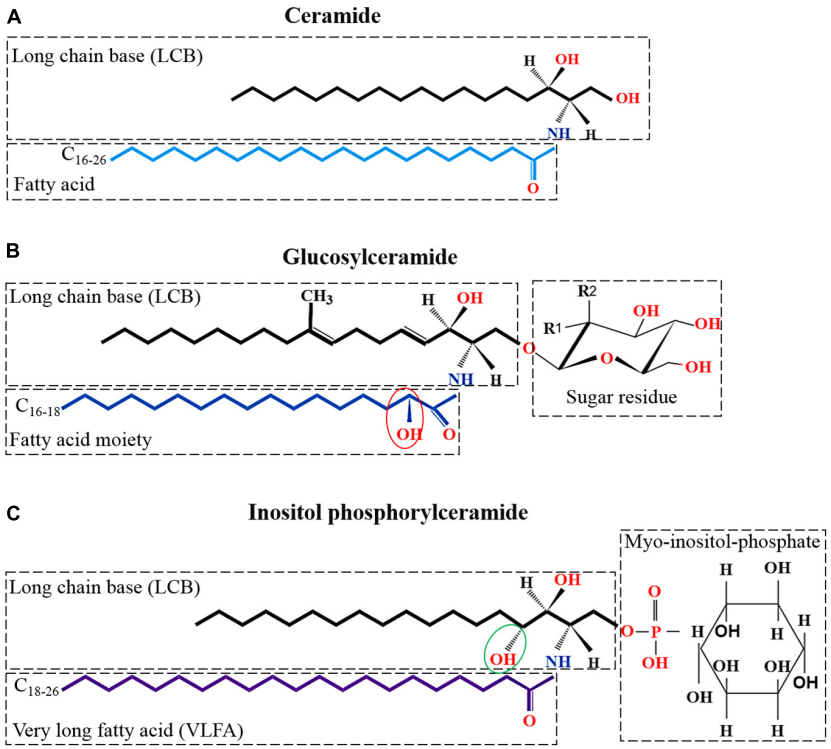

FIGURE 1 | Kinds and structures of glycosphingolipid in filamentous fungi. **(A)** Structure of ceramide; the basic unit of neutral and acidic glycosphingolipids; made up of a LCBs and a FA moiety. **(B)** Structure of neutral glycosphingolipid which is linked to a sugar residue on the base of ceramide. Neutral glycosphingolipid contains an-OH moiety at C_2 in the FA chain (showed with red ellipse); a double bond between C_{4-5} and C_{8-9}; and a methyl C_9 of the LCB. Monosaccharide may be either glucosyl (Glc) (R1 = OH, R2 = H) or galactosyl (Gal) residues (R1 = H, R2 = OH). **(C)** The basic structure of acidic glycosphingolipid, inositol phosphorylceramide, is shown. Inositol phosphorylceramide is different from neutral glycosphingolipids in that it contains an additional hydroxy at C_4 of the LCB (showed with green ellipse) and lacks double bonds between C_{4-5} and C_{8-9}, and the C_9 methyl of the LCB. In addition, acidic glycosphingolipids are composed of a very long FA chain (C_{18-26}) instead of the C_{16-18} chain that found in neutral glycosphingolipids.

(Totani et al., 2001; Park et al., 2005; Zhang et al., 2007; Zaüner et al., 2008; Takahashi et al., 2009; Hirata et al., 2012; Guimarães et al., 2014; Tani et al., 2014; Fernandes et al., 2016).

In filamentous fungi, neutral GSLs (also call glycosylceramides) include glucosylceramide (GlcCer) and galactosylceramide (GalCer), while acidic GSLs consist of two forms of glycosyl inositol phosphoryl ceramides (GIPCs), mannosylinositol phosphorylceramide (MIPC) and mannosyldiinositol phosphorylceramide [$M(IP)_2C$] (Barreto-Bergter et al., 2004, 2011; Buré et al., 2014). Neutral GSLs contain 9-methyl-Δ4,Δ8-sphingadienine as the LCB linked to a C_{16-18} N-2-hydroxy or unsaturated N-2-hydroxy-Δ3 FA chain and a glucose or galactose moiety to form GlcCer or GalCer. In contrast, the ceramide moiety of acidic GSLs is composed of a 4-hydroxysphinganine (phytosphingosine) as the LCB attached to a very long fatty acid (VLFA) chain (C_{18-26}) and complex glycan groups *via* an inositol phosphate linker. All filamentous fungi investigated so far contain GlcCer or GalCer, with most mold species, such as *Aspergillus fumigatus* (Boas et al., 1994; Toledo et al., 1999; Fontaine, 2017), *A. niger* (Wagner and Fiegert, 1969; Levery et al., 2000), *A. oryzae*, *Aspergillus sojae*, and *Aspergillus awamori* (Tani et al., 2014), containing both GlcCer and GalCer (**Table 1**). Interestingly, *Sporothrix schenckii* mycelia synthesize only GlcCer, while the yeast forms are found to contain both GlcCer and GalCer (**Table 1**; Dickson and Lester, 1999; Toledo et al., 2000). In fungi, GlcCer and GalCer are considered the final step of the pathway, whereas in mammalian cells GlcCer and GalCer are then used to make hundreds of complex GSLs. In fungi and plants, acidic GSLs include inositol phosphorylceramides (IPCs), which are used as building blocks for more complex molecules, such as MIPC and $M(IP)_2C$. In summary, GlcCer is the only GSLs found in all organisms studied, especially eukaryotic cell, such as fungi, plants as well as invertebrates and vertebrates (**Table 2**). In contrast, GIPCs occur only in fungi and plants, whereas GalCer is restricted to fungi, vertebrates, and invertebrates (**Table 2**).

Neutral and acidic GSLs have specific differences in the structures of their ceramide backbones. In filamentous fungi, the differences in hydroxylation, saturation levels and methylation levels result in different LCBs of both GSLs (Warnecke and Heinz, 2003; Gault et al., 2010). Neutral GSLs normally contain the monosaccharide, glucose or galactose, in glycosidic linkage with the 9-methyl-Δ4, Δ8-sphingoid (ceramide) (Takahashi et al., 2009). The structure of 9-methyl-Δ4, Δ8-sphingadienine, which contains two double bonds in C_{4-5} and C_{8-9} and a methylation at C_9 (Fujino and Ohnishi, 1977;

TABLE 1 | The type and structure of neutral GSLs in filamentous fungi.

Organism	GlcCer	GalCer	Structural features of FA	Structural features of LCB	References
Aspergillus fumigatus	+	+	2-hydroxyoctadec-Δ3-unsaturation	Δ4, Δ8-unsaturation; 9-methyl	Boas et al., 1994; Toledo et al., 1999; Fontaine, 2017
Aspergillus niger	+	+	2-hydroxyoctadec-Δ3-unsaturation	Δ4, Δ8-unsaturation; 9-methyl	Wagner and Fiegert, 1969; Levery et al., 2000
Aspergillus nidulans	+	–	2-hydroxyoctadec	Δ4, Δ8-unsaturation; 9-methyl	Levery et al., 2002
Aspergillus oryzae	+	+	2-hydroxyoctadec	Δ4, Δ8-unsaturation; 9-methyl	Fujino and Ohnishi, 2003; Tani et al., 2014
Aspergillus versicolor	+	–	2-hydroxyoctadec	Δ4, Δ8-unsaturation; 9-methyl	Boas et al., 1994
Aspergillus sojae	+	+	2-hydroxyoctadec	Δ4, Δ8-unsaturation; 9-methyl	Tani et al., 2014
Aspergillus awamori	+	+	2-hydroxyoctadec	Δ4, Δ8-unsaturation; 9-methyl	Tani et al., 2014
Aspergillus kawachii	+	–	2-hydroxyoctadec	Δ4, Δ8-unsaturation; 9-methyl	Hirata et al., 2012
Sporothrix schenckii (mycelia forms)	+	–	2-hydroxyoctadec-Δ3-unsaturation	Δ4, Δ8-unsaturation; 9-methyl	Dickson and Lester, 1999; Toledo et al., 2000
Sporothrix schenckii (yeast forms)	+	+	2-hydroxyoctadec-Δ3-unsaturation	Δ4, Δ8-unsaturation; 9-methyl	Dickson and Lester, 1999; Toledo et al., 2000

GlcCer, glucosylceramide; GalCer, galactosylceramide; FA, fatty acid; LCB, long chain base. +,presence; –, absence.

TABLE 2 | Relative presence of glycosphingolipids (GSLs) in filamentous fungi, plants, invertebrates, and vertebrates.

Kinds of GSLs	Filamentous fungi	Plants	Invertebrates and vertebrates
GlcCer	+	+	+
GalCer	+	–	+
MIPC	+	+	–
$M(IP)_2C$	+	+	–

+, presence; –, absence; GlcCer, glucosylceramide; GalCer, galactosylceramide; MIPC, mannosylinositol phosphorylceramide; $M(IP)_2C$, mannosyldiinositol phosphorylceramide.

Barreto-Bergter et al., 2004, 2011; Takahashi et al., 2009; Del Poeta et al., 2014), is unique to neutral GSLs of filamentous fungi and distinguishes them from plant and mammalian sphingosines (**Figure 1B**). While Δ4-sphingenine with a double bond in C_{4-5} is predominantly found as LCB in mammals and is rare in fungi and plants, Δ4,Δ8-sphingadienine with two double bonds in C_{4-5} and C_{8-9} is found in plants (Sperling and Heinz, 2003; Barreto-Bergter et al., 2004; Takahashi et al., 2009). In contrast, acidic GSLs are different from neutral GSLs in that they contain an additional hydroxyl group at C_4 of their LCB (4-hydroxyshinganine) (**Figure 1C** showed with green ellipse) and lack Δ4,Δ8-unsaturations and C_9-methylation found in the LCBs of neutral GSLs in filamentous fungi (**Figure 1C**). In addition, the FA lengths of neutral and acidic GSLs is also different. In filamentous fungi, C_{16-18} FA chains are observed in neutral GSLs, and C_{24-26} chains are observed in acidic GSLs (Marques et al., 2018), while the mammalian FA length is predominantly a C_{16} or C_{18} FA chain. In plants, the lengths of FA chains range from C_{14} to C_{26} (Sperling and Heinz, 2003). Interestingly, some filamentous fungal GSLs contain a Δ3-desaturated in FA chain, which is a unique modification of fungal GSLs and has been reported in *A. fumigatus* (Boas et al., 1994; Toledo et al., 1999), *A. niger* (Wagner and Fiegert, 1969; Levery et al., 2000), and *S. schenckii* (Toledo et al., 2001; **Table 1**).

In summary, filamentous fungal GlcCer or GalCer mainly consists of a β-D-glucose or galactose attached to C_1 of 9-methyl-Δ4,Δ8-sphingadienine which is N-acylated with a C_{16-18} N-2-hydroxy or N-2-hydroxy-Δ3 FA chain. In contrast, the ceramide moiety of acidic GSLs is usually formed by 4-hydroxysphinganine (phytosphingosine) as the LCB, bound to a VFFA chain (C_{18-26}), linked to a polar head group. IPC is further modified upon addition of mannose and a second inositol phosphate group to generate MIPC (with a mannose sugar unit) and $M(IP)_2C$ (with two inositol groups).

KEY GENES AND IMPORTANT PRODUCTS INVOLVED IN BIOSYNTHESIS OF GSLs IN FILAMENTOUS FUNGI

Raw ceramide for the synthesis of GSLs is derived from three pathways, de novo GSL synthesis, sphingomyelin degradation and GSL recycling. Here we focus on the de novo synthesis pathway of GSLs that is conserved among filamentous fungi (Gault et al., 2010). The whole process of GSL synthesis pathway was divided into three modules for better understanding, the synthesis of dihydrosphingosine, synthesis of neutral GSLs, and synthesis of acidic GSLs (**Figure 2**). In this section, the productions of GSLs *via* the *de novo* biosynthetic pathway and the key genes involved are discussed.

The Role of Dihydrosphingosine

The biosynthesis of dihydrosphingosine (DhSph), involves two key enzyme-catalyzed reactions and is the starting point in the biosynthesis of all GSLs (**Figure 2I**). The first and rate-determining step is the condensation of palmitoyl coenzyme A (palmitoyl-CoA) and L-serine, catalyzed by serine palmitoyltransferase (SPT), to produce 3-keto dihydrosphingosine (3-keto DhSph), which is then reduced to DhSph by 3-keto DhSph reductase (KDSR)

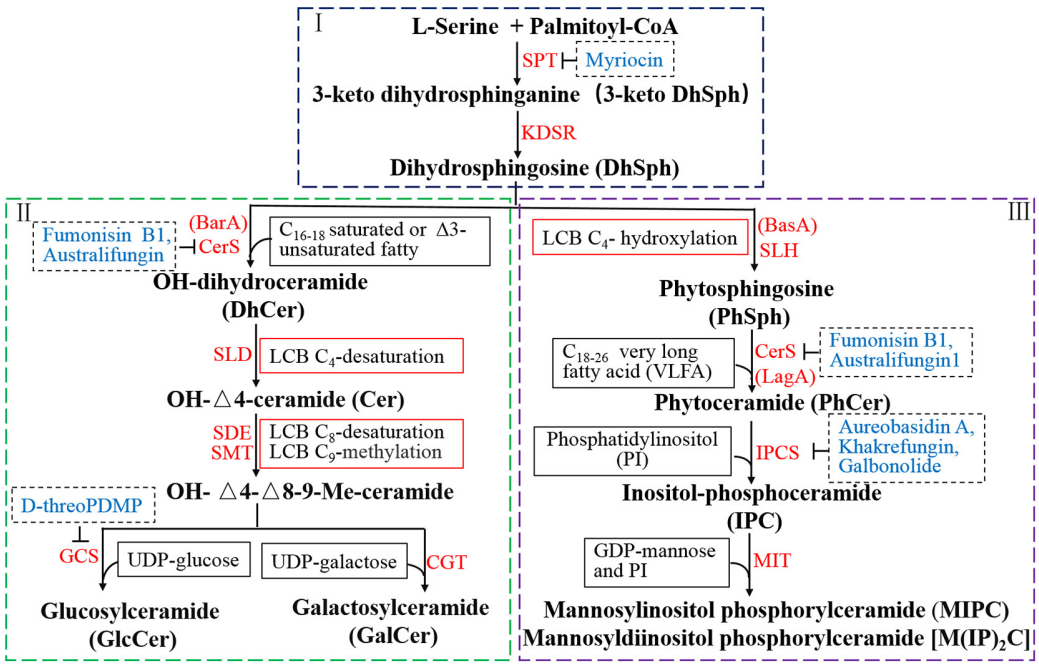

FIGURE 2 | Reorganized biosynthetic pathway of glycosphingolipid in filamentous fungi. The first part (I) involves two key enzyme-catalyzed reactions and is the starting point and common to neutral and acidic GSL synthesis. The second part (II) represents the biosynthetic pathway of neutral GSLs (GlcCer and GalCer) from DhSph including four enzyme-catalyzed reactions. GlcCer and GalCer are the final products of neutral GSL pathway in filamentous fungi. The third part (III) is the biosynthetic process of acidic GSLs, including the production of IPC, MIPC, and $M(IP)_2C$, which also starts from DhSph and includes three enzyme-catalyzed reactions. IPCs, used as building blocks for more complex molecules, are further modified upon addition of mannose and a second inositol phosphate group to generate MIPC and $M(IP)_2C$. Red texts represent genes or relative enzymes involved in the GSL pathway. Blue texts indicate the inhibitors of the specific enzyme in the biosynthetic steps.

(Barreto-Bergter et al., 2004). The genes encoding SPT and KDSR are conserved among all organisms and have been identified from various species of fungi. Two genes, *LCB1* and *LCB2*, which are necessary for SPT activity, have been identified in *Saccharomyces cerevisiae* (Buede et al., 1991; Nagiec et al., 1994). Deletion of either *LCB1* or *LCB2* was found to abolish GSL production in yeast (Mukherjee and Dekker, 1990; Zhao et al., 1994; Dickson, 2008). In *A. nidulans*, the gene encoding SPT was identified and named *lcbA* owing to its homology to the *S. cerevisiae LCB1*. The *lcbA* is essential for polarity and growth in *A. nidulans* and under the control of the *alcA* promoter, which is alcohol inducible and glucose repressible (Waring et al., 1989; Cheng et al., 2001). An important third subunit of SPT is Tsc3p, which coimmunoprecipitates with LCB1 or/and LCB2, and is required for optimal and high level SPT activity during maximal GSL biosynthesis in *S. cerevisiae* (Gable et al., 2000).

The role of 3-keto DhSph reductase remains poorly investigated in filamentous fungi. In *A. fumigatus*, KDSR is encoded by the *ksrA* gene, but the biological role of *ksrA* in *Aspergillus* remains to be elucidated (Fornarotto et al., 2006). Deletion of *C. albicans ksr1* shows compromised filamentation, suggesting that the expression of *ksr1* may be important for polarized growth (Fornarotto et al., 2006).

Although poorly studied, the production of DhSph is a critical and common pathway in the biosynthesis of neutral and acidic GSLs. This compound can generate two distinct ceramide pools of dihydroceramide and phytoceramide, which are utilized for the formation of neutral and acidic GSLs, respectively. Two genes, *BarA* and *BasA*, are involved in this step in filamentous fungi (Li et al., 2006; Rittenour et al., 2011; Cheon et al., 2012; Fontaine, 2017). The ceramide pool involved in the neutral GSL synthesis (dihydroceramide) is generated by *BarA*, while acidic GSL synthesis (phytoceramide) is catalyzed by *BasA* (also called *Sur2* in *S. cerevisiae*). Therefore, filamentous fungi possess two distinct ceramide pools that make independent contributions to polarized hyphal growth, through the formation of specialized lipid microdomains that regulate the organization of the cytoskeleton (Li et al., 2006).

Biosynthetic Process of Neutral GSLs

Synthesis of the neutral GlcCer and GalCer from DhSph includes four enzyme-catalyzed reactions (**Figure 2II**).

OH-Dihydroceramide

Dihydrosphingosine is first N-acylated with saturated or Δ3-unsaturated C_{16-18} FA chain catalyzed by ceramide synthase (CerS) to produce dihydroceramide (DhCer). A hydroxyl group is then inserted at C_2 in the FA chain of DhCer generating OH-DhCer. The ceramide pool involved in the DhCer synthesis is unique to filamentous fungi and catalyzed by ceramide synthase encoded by *BarA* (or *Cer1*, *Bar1*) (Li et al., 2006; Rittenour et al., 2011). *BarA* is specifically necessary to produce

neutral GSLs in fungi and contributes differentially to polarized hyphal growth. The Δ*BarA* or Δ*Cer1* or Δ*Bar1*mutant can produce normal IPC but completely lacks GlcCer, fails to display the distinct sterol-rich domain at the hyphal tip and is incapable of producing perithecia (Rittenour et al., 2011; Cheon et al., 2012; Munshi et al., 2018).

OH-Δ4-Ceramide

The LCB of OH-DhCer is reduced by sphingolipid Δ4-desaturase (SLD) to generate OH-Δ4-ceramide in the cytosolic face of the endoplasmic reticulum (ER) (Michel and van Echten-Deckert, 1997; Ternes et al., 2002). Sphingolipid Δ4-desaturase, encoded by the *DEGS1*, is involved in the double bond formation at C_{4-5} of DhCer (Michel et al., 1997; Rodriguez-Cuenca et al., 2015).

9-Methyl-Δ4, Δ8-Ceramide

Then, a double bond at C_{8-9} and a methyl group at C_9 are introduced into the LCB by sphingolipid Δ8-desaturase (SDE) and sphingolipid C_9-methyltransferase (SMT), respectively, resulting in the formation of OH-Δ4,Δ8-9-methyl-ceramide (Ternes et al., 2006; Rhome et al., 2007). Sphingolipid Δ8-desaturase is encoded by *SdeA* in *A. nidulans*. There are two genes encoding C_9-methyltransferases in *A. nidulans* (*smtA* and *smtB*) and *F. graminearum* (*FgMT1* and *FgMT2*), but only one candidate has been identified in *N. crassa* (Ternes et al., 2006). OH-Δ4,Δ8-9-methyl-ceramide is produced in the ER and transported to the Golgi apparatus for synthesis of GalCer and GlcCer.

GlcCer and GalCer

The final step of the neutral GSL biosynthetic pathway is the transfer of a sugar residue from UDP-glucose or UDP-galactose to the OH-Δ4,Δ8-9-methyl-ceramide catalyzed by glucosylceramide synthase (GCS) or ceramide galactosyltransferase (CGT), respectively in the Golgi apparatus (Leipelt et al., 2001; Warnecke and Heinz, 2003; Ternes et al., 2011). GCS is encoded by *GCSA* or *GCS1* that is essential for mycelial growth and filamentation in filamentous fungi (Ramamoorthy et al., 2007; Fernandes et al., 2016). Although most of the genes responsible for GlcCer biosynthesis have been identified and cloned, the gene encoding ceramide galactosyltransferase has been detected only in *N. crassa* and *Magnaporthe grisea* (Lester et al., 1974; Maciel et al., 2002). Limited information is available on the occurrence of GalCer in fungi and information on their function or on the galactosyltransferase responsible for their formation is lacking.

Synthetic Process of Acidic GSLs

The synthesis of acidic GSLs, including the productions of IPCs, MIPCs, and $M(IP)_2Cs$, also starts from DhSph and includes three enzyme-catalyzed reactions (**Figure 2III**).

Phytosphingosine

The LCB at C_4 of DhSph is hydroxylated by the sphingolipid C_4-hydroxylase (SLH) that is present only in fungi and plants. This reaction generates phytosphingosine (PhSph) that is essential for filamentous fungal growth and viability (Li et al., 2006). In *S. cerevisiae*, *Sur2* encoding sphingolipid C_4-hydroxylase is essential for sphingolipid C_4-hydroxylation activity but is not essential for normal growth (Cliften et al., 1996; Haak et al., 1997). In *A. nidulans*, deletion of *basA* leads to a reduced growth with an hyperbranching of hyphae, an aberrant cell wall thickening and a strong defect in conidiation (Li et al., 2006, 2007).

Phytoceramide

A C_{18-26} FA chain is linked to PhSph *via* an amide by ceramide synthase (CerS) to form phytoceramide (PhCer) that seems to be relevant for fungal viability and hyphal morphogenesis. In *A. nidulans*, ceramide synthase is encoded by the *lagA* and is required for the apical growth and morphology (Li et al., 2006). PhCer is transported from the ER to the outer leaflet of the Golgi membrane for the synthesis of IPC in the next step (Dickson et al., 2006).

IPC, MIPC, and $M(IP)_2C$

The myo-inositol-1-phosphate group is transferred from phosphatidylinositol (PI) to the C_1 hydroxyl of PhCer to produce IPC, catalyzed by the IPC synthase (Cheng et al., 2001; Dickson et al., 2006). IPC synthase is also a rate-limiting enzyme encoded by the *IPC1* or *AUR1*, found in *S. cerevisiae*, *Schizosaccharomyces pombe*, *Candida* spp., and *Aspergillus* spp. (Hashida-Okado et al., 1996; Nagiec et al., 1997; Kuroda et al., 1999; Georgopapadakou, 2000; Cheng et al., 2001). The *aurA* is required for polarized cell growth in *A. nidulans*; repression of *aurA* in *A. nidulans alcA*::*aurA* causes a terminal phenotype of germinating spores and lacks polarized hyphal growth (Cheng et al., 2001). In filamentous fungi, IPC is further modified by addition of mannose and a second inositol phosphate group in a reaction catalyzed by MIPC transferase (MIT, encoded by *mitA*) to generate two products, MIPC that has a mannose sugar unit and $M(IP)_2C$ that has a mannose unit as well as two inositol groups (Leber et al., 1997). The *mitA* gene is essential for the addition of the first mannose residue to the inositol ring. Although *A. fumigatus* Δ*mitA* abolishes the production of MIPCs and MIPC-derived GSLs, leading to accumulation of the precursor IPC, the Δ*mitA* mutant shows normally growth and no defects in cell wall or membrane organization, suggesting that MIPC is not critical for fungal differentiation (Kotz et al., 2010). MIPC and $M(IP)_2C$ are two forms of GIPCs found in several fungi that are particularly regulated during morphogenesis (Takahashi et al., 2009; Guimarães et al., 2014; Buré et al., 2014).

Enzyme Inhibitors in Key Steps of GSL Biosynthesis

Blocking GSL biosynthesis has become a target for developing antifungal therapies and understanding fungal biology. Thus, enzyme inhibitors of synthetic GSLs for a variety of biological processes have already been demonstrated. There are five key steps in which enzymes can be blocked by inhibitors in the GSL biosynthetic pathway (**Figure 2** the blue fonts). As the first rate-limiting enzyme of the GSL biosynthetic pathway, SPT has been the subject of many studies to identify inhibitors. One of the earliest SPT inhibitors identified is the mechanism-based inhibitor L-cysteine (Zheng et al., 1994, 1998). The most

widely used and studied natural product SPT inhibitors are myriocin and sphingofungin that have been shown to block biofilm formation and polarized growth of fungal hyphae in *Candida* and *Aspergillus* species (Cheng et al., 2001; Lattif et al., 2011; Perdoni et al., 2015; Harrison et al., 2018). In addition, β-chloroalanine, β-fluoroalanine, and halide can also be used to inhibit SPT (Lev and Milford, 1981; Medlock and Merrill, 1988; Smith and Merrill, 1995). Fumonisin B1 and australifungin are inhibitors of ceramide synthase that alter GSL metabolism by inhibiting ceramide synthesis, and act as antifungal agents in *Cryptococcus*, *Candida*, and *Aspergillus* species (Mandala et al., 1995; Merrill et al., 2001). Glucosylceramide synthase is involved in the final step of GlcCer synthesis and can be blocked by D-threo-1-phenyl-2-decanoylamino-3-morpholino-1-propanol (D-threoPDMP) that cause a reduction in hyphal germination and colony growth in *A. nidulans*, *A. fumigatus*, and *Aspergillus terreus* (Levery et al., 2002).

Inositol phosphorylceramides synthases are unique structures in fungi involved in many cellular processes, including growth, differentiation, and morphogenesis, but are not found in mammals (Barr and Lester, 1984; Levery et al., 1998, 2002; Loureiro y Penha et al., 2001). Therefore, IPC synthases constitute potential targets for the development of new antifungal drugs, as inhibiting it will lead to the accumulation of PhSph and PhCer and, ultimately fungal death. Aureobasidin A, khakrefungin, and galbonolide inhibitors of IPC synthase can block transfer of myo-inositol-1-phosphate from PI to ceramide, resulting in accumulation of PhSph and PhCer, and complete inhibition of IPC production, along with cell cycle arrest in *C. albicans*, *Cryptococcus neoformans*, *S. cerevisiae*, and *A. nidulans* (Cheng et al., 2001; Cerantola et al., 2009; Tan and Tay, 2013). Therefore, IPC inhibitors, with low toxicity in mammals due to the lack of a mammalian IPC synthase, might be possible candidates as ideal antifungal drugs (Takesako et al., 1993; Mandala et al., 1997, 1998; Georgopapadakou, 2000; Rollin-Pinheiro et al., 2016).

BIOLOGICAL ROLES OF GSLs IN FILAMENTOUS FUNGI

Role of GSLs in Filamentous Fungal Growth

Glycosphingolipids are the main lipid components of microdomains and are clustered along with sterols in specialized membrane microdomains to form lipid rafts in filamentous fungi (Sonnino et al., 2007). These regions play crucial roles in cell polarization and hyphal growth, mediated by the cytoskeleton and accumulation of lipid raft components at the growing tip of hyphal cells (Cheng et al., 2001; Barreto-Bergter et al., 2004; Pearson et al., 2004; Nimrichter and Rodrigues, 2011; Guimarães et al., 2014). Biological functions of GSLs have been studied through gene deletion and inhibitory approaches in filamentous fungi (Rittershaus et al., 2006; Oura and Kajiwara, 2008, 2010; Ramamoorthy et al., 2009; Zhu et al., 2014; Fernandes et al., 2016). Several studies have demonstrated that impairment of any steps of GlcCer biosynthetic pathway leads to compromised mycelium growth, hyphal elongation, and lipid raft mislocalization. For example, disruption of the initial step of GlcCer synthesis by deletion of *barA* or by inhibition in presence of HSAF strongly reduces polarized growth and leads to the formation of enlarged and hyperbranched hyphae, with altered cell wall (Li et al., 2006, Li et al., 2009). Similarly, disruption of the final step of GlcCer synthesis by deletion of *GCS* or by glucosylceramide synthase inhibitors also impairs hyphal extension in *A. nidulans* and inhibits morphological transitions such as budding and germ tube formation in *A. fumigatus* (Levery et al., 2002; Ramamoorthy et al., 2007; Fernandes et al., 2016). These results suggest that GlcCer synthase is essential for the establishment and maintenance of the polarity axis, fungal growth, and differentiation in filamentous fungi (**Figure 3**).

In filamentous fungi, not only is growth and differentiation reduced upon impairment of neutral GSL synthesis, but growth also relies on the production of IPC (**Figure 3**). Inhibition of IPC synthase is followed by an accumulation of PhSph and PhCer intermediates that lead to fungal cell cycle arrest and apoptosis (Cheng et al., 2001). Integrity of the IPC synthesis pathway is relevant for filamentous fungal viability, not only due to the role of IPC in fungal differentiation but also due to the need for highly regulation of DhSph, PhSph, and PhCer levels, as DhSph and PhSph are highly toxic to fungal cells. Thus, changes in their levels may have uncontrolled effects on signaling events, resulting in fungal cell death which indicate that PhCer synthase and IPC synthase can be potential targets for development of new antifungal drugs, as inhibiting these enzymes will lead to the accumulation of PhSph and PhCer, and, ultimately, fungal death.

Role of GSLs in Response to Environmental Stress in Filamentous Fungi

In addition to fungal polarization and hyphal growth, GSLs also play important role in filamentous fungal fitness and adaptation to diverse environments as a signaling molecules (Grimm et al., 2006; Lingwood and Simons, 2010; **Figure 3**). The fungal heat shock response is characterized by the production of heat shock proteins that function as chaperonins, and in the processes of protein degradation. GSLs possess the capacity to serve as bioactive signaling molecules in early heat stress response. This signaling function influences the regulation of the cell cycle and the synthesis of heat shock proteins, which have important secondary effects, especially if heat shock proteins are not available to serve as protectors of other proteins (Jenkins, 2003). For example, *C. albicans* treatment with inhibitor of SPT, leads to the decrease in lipid domain accumulation, resulting in less recruitment of heat-shock proteins (Insenser et al., 2006). In addition, environmental stresses directly affect the representation of fungal GSL classes (Řezanka et al., 2018). Thermophilic microorganisms can change the contents of IPC, MIPC, or $M(IP)_2C$ to mediate fungal apoptosis in response to high temperature stress (Řezanka et al., 2016, 2018). *N. crassa* synthesizes PhCer as signal molecules to mediate fungal apoptosis in response to heat stress (Plesofsky et al., 2008). In

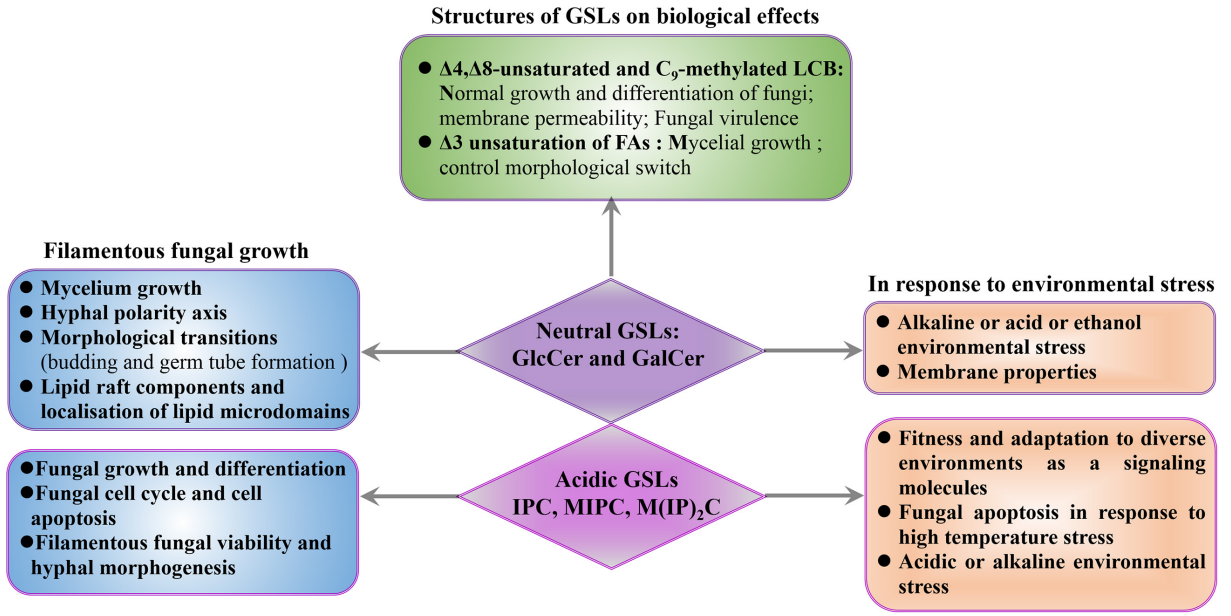

FIGURE 3 | Biological roles of GSLs in filamentous fungi. The effects of GSLs on filamentous fungi were discussed from three aspects, mainly including fungal growth and environmental stress. Meanwhile, the functions of the Δ3-unsaturated FAs, and Δ4, Δ8-unsaturated, and C9-methylated structures of GlcCer and GalCer were also summarized.

S. cerevisiae, the accumulation of IPC is detrimental to yeast under low pH conditions, and downregulation of IPC levels is one of the adaptation mechanisms for low pH conditions (Otsu et al., 2020). In contrast, reduction of the IPC level increases the sensitivity of *C. neoformans* to low pH and impairs the growth and the pathogenicity of *C. neoformans* (Luberto, 2001). Besides, blocking the pathway of GSL synthesis or adding exogenous GSLs can significantly affect fungal tolerance to acidic or alkaline environmental stress. For example, in *C. neoformans*, the Δ*cer1* mutant cannot survive in acid or alkaline environments due to its inability to synthesize GlcCer (Ishibashi et al., 2012; Munshi et al., 2018). Besides, the *C. neoformans*Δ*sld8* mutant that only synthesizes saturated GlcCer is more susceptible to membrane stressors and shows increased membrane permeability, resulting in decreased stress resistance (Raj et al., 2017). Similarly, *S. cerevisiae*, which is incapable of synthesizing GlcCer, can adapt to alkaline and ethanol stress after exposure to *Aspergillus kawachii*-derived GlcCer *via* altering the yeast membrane properties by exogenous GlcCer (Sawada et al., 2015). These results demonstrate that GSLs play important roles in response to environmental stress in fungi (**Figure 3**).

Structures of GSLs on Biological Effects in Filamentous Fungi

Impairment of polarized hyphal growth and mislocalization of lipid microdomains were observed when the biosynthetic steps of sphingolipid desaturase and sphingolipid C_9-methyltransferase were interrupted, demonstrating that unsaturation and C_9-methylation of the neutral GSLs are essential for growth and differentiation in filamentous fungi. The structures of Δ4,Δ8-unsaturated and C_9-methylated LCB, distinguishing filamentous fungi from plant and mammalian sphingosines, are unique to fungal neutral GSLs (Barreto-Bergter et al., 2004, 2011; Del Poeta et al., 2014). Disruption of the *A. nidulans sdeA* leads to increase accumulation of saturated and unmethylated GlcCer and reduce mycelium growth (Fernandes et al., 2016). Previous studies in *C. neoformans* showed that Δ*sld8* mutant synthesizing only saturated GlcCer is more susceptible to membrane stressors follow by increasing membrane permeability, even though saturated GlcCer produced more lipid rafts than unsaturated GlcCer species (Raj et al., 2017). The C_9-methylated found in LCB is required for normal growth and differentiation in filamentous fungi (Ramamoorthy et al., 2009; Fernandes et al., 2016). *A. nidulans smtA* deletion combined with conditional repression of *smtB* significantly increases unmethylated GlcCer levels and compromises filamentous growth (Fernandes et al., 2016). The Δ*Fgmt2* mutant produces 65–75% unmethylated GlcCer shows severe growth defects when compared to the wild-type strain (Ramamoorthy et al., 2009). In pathogenic yeasts, deletion of the gene encoding C_9-methyltransferase results in a mutant with attenuated virulence (Noble et al., 2010; Singh et al., 2012). Interestingly, certain plant defensins require the C_9-methylation for fungal GSL recognition (Oguro et al., 2014; Fernandes et al., 2016), which suggest that plant defensins may have a therapeutic potential for treatment of fungal infections for fungus specific C_9-methylation (**Figure 3**).

The unsaturated FAs of neutral GSLs are also important for the mycelial growth in filamentous fungi. The Δ3-unsaturated FA is a unique modification of fungal GSLs,

which has been reported in neutral GSLs of *A. oryzae* (Yasuhiko and Masao, 1997), *A. fumigatus* (Toledo et al., 1999), and *S. schenckii* (Toledo et al., 2001), and is involved in signaling pathways that control morphological switch (**Figure 3**). In fact, the ratio of saturated and Δ3-unsaturated 2-hydroxy FAs vary among the GSLs from different fungal morphotypes. For example, only 15% of GlcCer extracted from the *Paracoccidioides brasiliensis* yeasts is composed of Δ3-unsaturated FAs, while 50% of GlcCer contains the Δ3-unsaturation in *P. brasiliensis* mycelium (Toledo et al., 1999). Similarly, GlcCer from *Histoplasma capsulatum* yeast contains a higher proportion of saturated FAs, while the GlcCer from mycelium is almost exclusively constituted by the Δ3-unsaturated FAs (Toledo et al., 2001). The higher contents of Δ3-unsaturated GlcCer in mycelial forms of *P. brasiliensis* and *H. capsulatum* may be ascribed to the activation of desaturase activity during the yeast-to-hypha transition, suggesting that Δ3-unsaturation of GlcCer may be involved in signaling pathways that control morphological switch.

In contrast to GlcCer, most studies of GalCer have been performed in mammals and its biological function in filamentous fungi remains unknown. It has been previously shown that sphingolipids regulate the activity of protein kinases, such as protein kinase C and protein phosphatases, involved in signaling cascades that ultimately modulate cell growth, differentiation, and proliferation (Hannun and Obeid, 2008). *S. schenckii* mycelia synthesize only GlcCer, while yeast forms are found to contain both GlcCer and GalCer, suggesting that the ceramide galactosyltransferase may be activated during the *S. schenckii* mycelium-yeast switch or inhibited during the yeast-to-hypha transition (Dickson and Lester, 1999; Toledo et al., 2000). Structural analyses of neutral GSLs between *A. fumigatus* and *S. schenckii* show that GalCer and GlcCer possess identical ceramide backbones, except that GalCer contains a higher proportion of Δ3-unsaturated FA (Toledo et al., 1999, 2000). Similarly, the GalCer production and differential Δ3-unsaturation of FAs may constitute a molecular mechanism of GSL control over fungal morphogenesis through the activation/inactivation of signal transduction pathways (Fernandes et al., 2018).

THE POTENTIAL EXPLOITATION AND PERSPECTIVE OF FILAMENTOUS FUNGAL GlcCer AND GalCer

Acidic GSLs in plants and fungi are more structurally diverse and difficult to analyze due to unavailability of commercial standards required by mass spectrometry. Therefore, neutral GSLs are mainly exploited and applicated in the cosmetics and health food products. Neutral GSLs are a common natural component in plants, animals, and fungi. Experiments show that neutral GSLs are not toxic, and no adverse reactions in humans. Therefore, neutral GSLs, mainly GlcCers obtained from plants, are now widely added in cosmetics as moisturizing ingredients and health foods as functional component (Alessandrini et al., 2004; Tessema et al., 2017).

GlcCers Are Important for the Barrier Function of Skin as Moisturizing Ingredients or Dietary Supplements

Ceramide is thought to be a critical molecule in the maintenance and formation of the epidermal permeability barrier and an important component in water-retention of skin (Hamanaka et al., 2005). GlcCer can be hydrolyzed to ceramide by β-glucocerebrosidase in keratinocytes, and the resultant ceramide is stored in stratum corneum (**Figure 4**). Levels of GlcCer significantly increase during epidermal differentiation, and then GlcCer is enzymatically hydrolyzed to ceramides to regulate permeability barrier function. The level of epidermal ceramide is regulated by a balance between β-glucocerebrosidase, sphingomyelinase, and ceramidase (Holleran et al., 2006). A deficiency or inhibition of β-glucocerebrosidase in the epidermis can alter the distribution of ceramide and GlcCer, resulting in decreased the epidermal permeability barrier function (Alessandrini et al., 2004; Carneiro et al., 2011). Low levels of GluCer and ceramide in atherosclerosis-prone mice led to skin inflammation and hair discoloration and loss (Bedja et al., 2018). Prior studies demonstrated that all molecular species of stratum corneum ceramides are derived from GlcCer (Uchida et al., 2000; Hamanaka et al., 2002). In addition, GlcCer also prevents dehydration of the stratum corneum and repaired the barrier function of skin. Therefore, the GlcCers play critical role in enhancing the epidermal permeability barrier function.

Furthermore, the beneficial effects of oral intake of plant GlcCer for skin hydration and skin barrier reinforcement have also been established in several studies involving animal models (Tsuji et al., 2006; Uchiyama et al., 2008; Yeom et al., 2012; Kawano and Umemura, 2013) as well as human subjects (Miyanishi et al., 2005; Kimata, 2006; Uchiyama et al., 2008; Guillou et al., 2011; **Figure 4**). The present studies suggest that the lipophilic fraction of GlcCer, present in plants has protective effects against intestinal impairment, but it requires extraction since digestion alone is not enough to elicit its complete protective action. Therefore, purified GlcCers are usually added in health food as a function complement. Some studies report that an intake of 0.6–1.8 mg/day of GlcCer from supplements is enough to improve human skin health (Uchiyama et al., 2008; Hirakawa et al., 2013). Shimoda et al. (2012) established the effects of GlcCer on the changes in epidermal ceramide and GlcCer in mice after oral intake of rice-derived GlcCer, as well as in a human epidermal equivalent. These findings demonstrated an increase in the level of epidermal ceramide follow by a decrease in the amounts of GlcCer (accompanied with enhanced β-glucocerebrosidase and GlcCer synthase expressions), suggesting epidermal GlcCer metabolism enhancing effect by oral intake of GlcCers. Oral administration of GluCer from maize significantly reduced UVA-induced wrinkle formation in the skin as well as epidermal hypertrophy of hairless mice (Shimada et al., 2011). Oral intake of konjac GlcCer has been reported to decrease the transepidermal water loss (TEWL) in atopic dermatitis (AD) patients (Miyanishi et al., 2005), and improve skin symptoms (including TEWL reduction) and reduce skin allergic responses in children with moderate AD

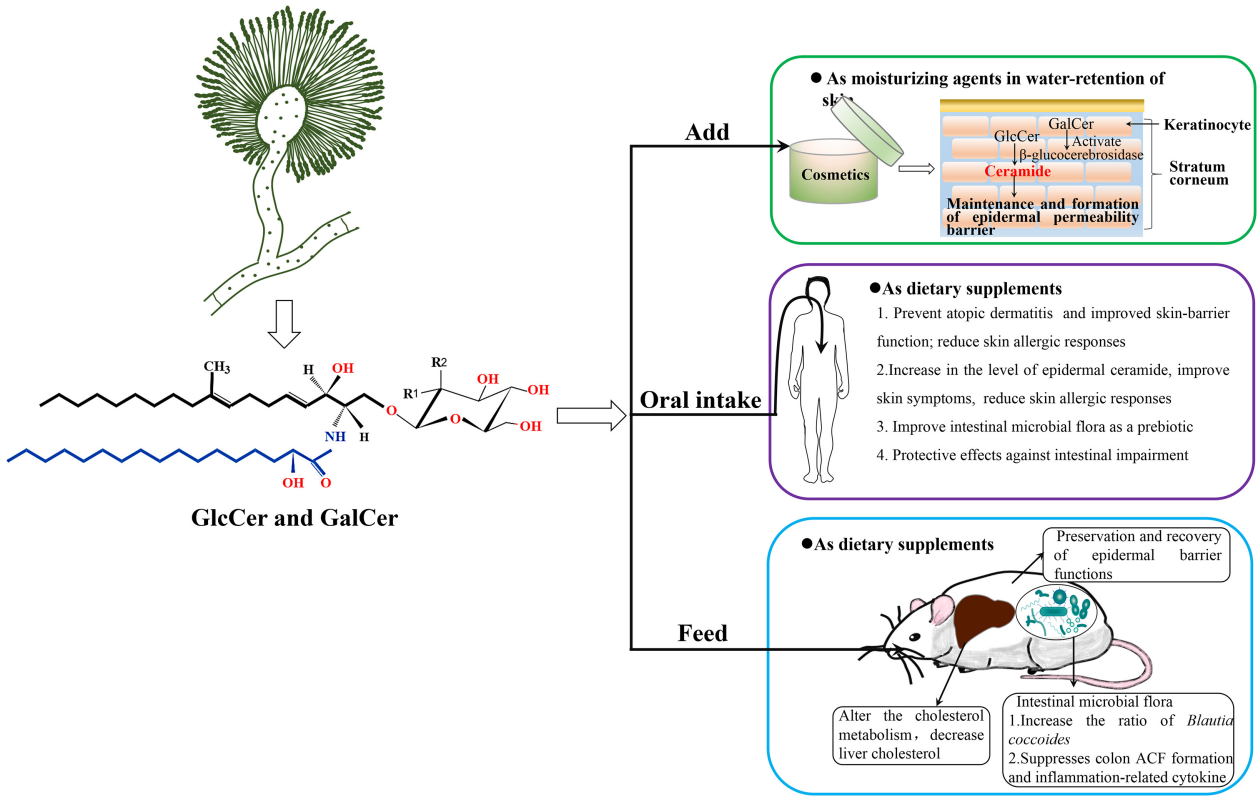

FIGURE 4 | The potential application diagram of filamentous fungal glycosylceramides, taking *A. oryzae* as an example. *A. oryzae* produces GlcCers and GalCers of glycosylceramides which might be safe to add in cosmetics as moisturizing ingredient or health food products as nutritional supplements. *A. oryzae* glycosylceramides, which function as a prebiotic, have been confirmed to increase ratio of *Blautia coccoides* and significantly decrease liver cholesterol in obese mice fed with koji glycosylceramide. Monosaccharide may be either glucosyl (Glc) (R1 = OH, R2 = H) or galactosyl (Gal) residues (R1 = H, R2 = OH) in the chemical structure.

(Kimata, 2006). These studies support the beneficial effects of oral intake of plant GlcCer and their potential complementary and alternative therapeutic applications in the restoration and maintenance of skin barrier function. Therefore, GlcCers exhibit a wide potential for development and application as an important biological resource in improving epidermal barrier function.

GlcCers Are Important in Repairing Intestinal Impairments as Functional Components

In addition to prevent AD and improved skin-barrier function, plant GlcCer also prevent intestinal impairment as dietary supplements (**Figure 4**). Recently, the incidence rate of intestinal impairments, such as colon cancer and inflammatory bowel disease (IBD), has increased in East Asian countries and Western countries (Molodecky et al., 2012). It is difficult to recover completely from IBD and these patients have an increased risk of developing colon cancer (Triantafillidis et al., 2009). There are many studies on the effect of GlcCer contained in food on intestinal impairment. *In vitro* experiments indicate the possibility that GlcCer protects the colon surface from the harmful effects of various drugs (Yamashita et al., 2017). In addition, GlcCer has been shown to have an apoptosis-inducing effect on colon cancer cells *in vitro* (Aida et al., 2004). Previous studies demonstrate that uptake of dietary GlcCer may improve the microenvironment of intestinal tract *via* modulating the intestinal microbiota (Schmelz et al., 2015). Yamashita et al. (2019) had confirmed that dietary GlcCer can significantly suppress aberrant crypt foci (ACF) formation and the production of inflammation-related cytokines in mice fed with rice-derived extracted GlcCer, which suggest GlcCer extracted from polished rice has protective effects against intestinal impairment. Collectively, dietary GlcCers can be digested by the intestinal microbial flora and display preventive and chemotherapeutic effects on colon cancer in animal models; however, clinical trials are urgently needed to investigate the response of colon carcinogenesis to dietary GlcCer in the future.

The Application of Fungal GlcCer and GalCer in Cosmetics or Health Foods

Although there are few studies on the applications of fungal glycosylceramides, we summarized several applications of them in cosmetics or foods. Interestingly, Takahashi confirmed that GlcCer produced by *A. oryzae* constituted the most abundant species (43% of the total GlcCer) in the sake lees, which

is brewed with *A. oryzae* and *S. cerevisiae*, and has long been recognized for its moisture-holding activity in cosmetics in Japan (Takahashi et al., 2014). Torula yeast (*Candida utilis*)-derived GlcCer has been reported to increase dermal fibroblast proliferation and collagen production to maintain dermal elasticity (Fukunaga et al., 2019). Miyagawa et al. (2019) investigated the effects of glycosylceramides on gene expression in normal human epidermal keratinocytes, which reveal that *koji* and *Aspergillus luchuensis* and *A. oryzae* glycosylceramides increased the expression of occludin (OCLN, an epidermal tight junction protein) and ATP-binding cassette sub-family A member 12 (ABCA12, a cellular membrane transporter) to increase ceramide in the keratinocytes. These results indicated that glycosylceramides have an effect of increasing genes expression which involved in skin barrier function and the transport of lipids in the keratinocytes, and suggest that *koji* exerts its cosmetic effect by increasing ceramide and tight junctions *via* glycosylceramides. In addition to function in cosmetics, fungal neutral GSLs also play an important role in foods. For example, Ferdouse et al. (2018) have proved that addition of *A. oryzae* glycosylceramide can affect the flavor and metabolic profiles of sake yeast in the manufacture of sake. They also demonstrate that addition of *A. oryzae*, *Glycine max*, and *Grifola frondosa* GlcCers confer a similar effect on the flavor profiles of sake yeast (Ferdouse et al., 2018), which indicate that the effects of plant GlcCer and *A. oryzae* GlcCer on flavor profiles are similar. In addition, *A. oryzae* glycosylceramide, used as a prebiotic in obese mice, can be digested by the intestinal microbial flora and increased ratio of *B. coccoides*, which is a potentially beneficial species in the intestine (Hamajima et al., 2019). Besides, feeding of *A. oryzae* glycosylceramide to obese mice can alter the cholesterol metabolism that liver cholesterol is significantly decreased in obese mice fed with *A. oryzae* glycosylceramide (**Figure 4**). These results will be of value in the utilization of fungal GlcCer and GalCer for cosmetics and functional foods.

The Limitations of Plant GlcCer and Animal GalCer in Application

Although neutral GSLs are originally derived from soybean and bovine sources, currently almost all the GlcCers used in cosmetics or health foods are extracted from plants. GlcCers from wheat flour (Ohnishi et al., 1985), potatoes (Bartke et al., 2006), maize, rice (Sugawara et al., 2010), and konjac (Uchiyama et al., 2008; Usuki et al., 2015) are now widely added in cosmetics as moisturizing agents or in health foods as "functional components." The most abundant classes of GSLs in plant tissue are mono-GlcCers. In contrast, the GalCer of glycosylceramides is rarely detected or reported in plants (Sullards et al., 2000; Spassieva and Hille, 2003). In cosmetics, GlcCer must be hydrolyzed to ceramide that is then deposited in stratum corneum to form the epidermal barrier. The more selective and efficient approach of transforming GlcCer to ceramide is enzymatic hydrolysis of β-glucocerebrosidase. Interestingly, GalCer, restricted to mainly in neural tissues in mammals, can activate β-glucocerebrosidase to hydrolyze GlcCer in keratinocytes and increase ceramide content to improve dry skin and AD (Alessandrini et al., 2004). However, GalCer is mainly extracted from neural tissues of animals such as cows and has been for the subject of several studies until the discovery of bovine spongiform encephalopathy. Although the animal glycosylceramides obtained from bovine brain and biotechnological sources have been investigated, the safety profile for cosmetic and food applications has not yet been established (Adam, 2001; Ono et al., 2010). Thus, GalCer from neural tissues of animals is not acceptable for cosmetic or other human use due to the underlying risk for prion diseases. As an alternative, glycosylceramides isolated from edible plants are highly safe and preferable for cosmetic and therapeutic applications. Unfortunately, plant glycosylceramides only contain GlcCer and are totally devoid of GalCer. Therefore, it is important to seek new biological resources that can synthesize both GlcCer and GalCer, along with attempts to improve their contents by modifying the biosynthetic pathway of neutral GSLs using genetic engineering technology in known resources.

The Advantage of Exploiting GlcCer and GalCer From Filamentous Fungi Aspergillus

Glycosylceramides, which have now been commercialized as moisturizing agents or dietary supplements for dry skin, are mainly sourced from edible plants that only contain GlcCer and are completely without GalCer. Surprisingly, there are many reports that filamentous fungi *Aspergillus* species, such as *A. oryzae*, *A. awamori*, and *A. sojae* that are used in various Japanese fermented foods and drinks, can produce both GlcCer and GalCer (Fujino and Ohnishi, 1977; Zhang et al., 2007; Hirata et al., 2012; Tani et al., 2014). Therefore, glycosylceramides from *Aspergillus* that include both GlcCer and GalCer can make up for the lack of GalCer in plants and would be more effective for their barrier function of skin in cosmetics as compared to plant GlcCer, due to the GalCer can activate β-glucocerebrosidase to promote the hydrolysis of GlcCer to ceramide (**Figure 4**; Alessandrini et al., 2004; Tani et al., 2014). Furthermore, previous studies have elucidated that koji (*A. oryzae*, *A. awamori*, and *A. sojae*) contains abundant glycosylceramides (0.5–2 mg/g dry weight koji), which are comprised of GalCer (30.3%) and GlcCer (69.7%), and are one of the highest amounts found in any cuisine (Hirata et al., 2012; Hamajima et al., 2016). Therefore, since filamentous fungi *Aspergillus* are economically important in the industrial production and can synthesize both GlcCer and GalCer, they would be new sources for exploiting neutral glycosylceramides in future.

Another advantage of filamentous fungi in the production of GlcCer and GalCer is that the cell growth cycle of fungi is much shorter than that of plants, which can provide a large amount of mycelium for extraction of GlcCer and GalCer. In addition, most filamentous fungi used in the production of fermented foods are safe for humans, especially *A. oryzae*, which is generally regarded as safe according to the FDA and has been used for making fermented foods such as saké, shoyu (soy sauce), and miso (soybean paste) for thousands of years. Therefore, the *A.*

oryzae would be a suitable source for production of GlcCer and GalCer due to their food safety. Furthermore, the availability of genome sequences of *A. oryzae* and the availability of DNA arrays, GeneChips, and RNA sequence have provided an unprecedented resource for studying and modifying the biosynthetic pathways of GlcCer and GalCer. In summary, we believe that filamentous fungi would be important resources for exploiting neutral glycosylceramides in the future, especially GalCer.

CONCLUSION AND FUTURE TRENDS

There is no doubt that exogenous or endogenous GSLs as moisturizing ingredients or dietary supplements continue to surprise us today and there are exciting times for the field. GSLs are a chemically complex group of substances, widely existing in fungi, plant, and animals. In this review, we summarized the kinds and structures of filamentous fungi GSLs. The synthetic pathway and biological roles of GSLs in filamentous fungi were also discussed. Importantly, we particularly focused on the important role of neutral GSLs adding in cosmetics as moisturizing ingredients and dietary supplements as functional components. Meanwhile we also drawn attention to the limitation of GSLs from plants and animals and the advantage of GSLs from filamentous fungi. Collectively, neutral GSLs from filamentous fungi *Aspergillus* will play important roles in the barrier function of skin and intestinal impairment of human health, which greatly increase the demand for neutral GSL. Nowadays, the market demand of GSLs as a new raw ingredient in beauty products is increasing rapidly at an annual growth rate of about 15%.

Since neutral GSLs are benefit to human health, a broader assessment of the types of GSLs adding in cosmetics and health foods is needed because they may have beneficial effects on human health. Not only are endogenous GSLs involved in obesity-related pathologies, prevention or treatment of obesity, and reducing skin allergic responses, but exogenous GSLs may be beneficial in the barrier function of skin (Walls et al., 2013; Miyagawa et al., 2019; Le Barz et al., 2020). Nowadays neutral GSLs, mainly GlcCers obtained from plants, are now widely included in cosmetics or health food. Previous studies done on improving AD and skin moisture suggest that oral intake of GlcCer activates enteric canal immunity and ceramide metabolism in the skin, rather than the direct reutilization of dietary GlcCer (Ono et al., 2010; Duan et al., 2012), which conclude that the maintenance of intestinal homeostasis by dietary GlcCer might be indirectly related to these mechanisms. In addition, GlcCers mast be hydrolyzed by β-glucocerebrosidase to ceramide in keratinocytes or mucosal cells of the small intestine and colon; and then ceramide is taken up directly by intestinal cells in human intestinal epithelial cell models (Nicolas et al., 2005). GalCer was reported to activate β-glucocerebrosidase in keratinocytes and increase ceramide content to improve dry skin and prevent AD (Alessandrini et al., 2004; Carneiro et al., 2011). Unfortunately, neutral GSLs derive from plants without any GalCer; while GalCer extracted from neural tissue of animals such as bovine has been applied for several research until the finding of bovine spongiform encephalopathy. What is more, the production of GalCer from neural tissues of animals would not be acceptable for cosmetic or other human uses. Also, GalCer from pathogenic fungi is not suitable for oral intake. Since neutral GSLs from plants do not contain GalCer, and GalCer from animals is at risk of viral infection, those from filamentous fungi *Aspergillus* that include both GlcCer and GalCer would be highly effective for barrier function of skin and safe for health food as dietary supplements. Therefore, the filamentous fungi *Aspergillus*, synthesizing both GlcCer and GalCer, could be an amenable source to produce glycosylceramides, because they are food safe. We believe that the development of GlcCer and GalCer, especially GalCer, from *Aspergillus* would become a trend and major source in the future.

AUTHOR CONTRIBUTIONS

JG: conceptualization and writing—original draft preparation. CJ: writing—review and editing, conceptualization, and funding acquisition. BZ: supervision and funding acquisition. BH: project administration. All authors contributed to the article and approved the submitted version.

FUNDING

This research was funded by the National Natural Science Foundation of China (NSFC), grant number 31900063, the Science and Technology Research Project of Jiangxi Provincial Department of Education, grant number GJJ180630, and Natural Science Foundation of Jiangxi Province, grant number 20192ACBL20012.

ACKNOWLEDGMENTS

We Thank to those who made critical review on this manuscript.

REFERENCES

Adam, D. (2001). Review blames BSE outbreak on calffeed. *Nature* 412:467. doi: 10.1038/35087720

Aida, K., Kinoshita, M., Sugawara, T., Ono, J., Miyazawa, T., and Ohnishi, M. (2004). Apoptosis inducement by plant and fungus sphingoid bases in human colon cancer cells. *J. Oleo Sci.* 53, 503–510. doi: 10.5650/jos.53.503

Alessandrini, F., Pfister, S., Kremmer, E., Gerber, J. K., Ring, J., and Behrendt, H. (2004). Alterations of glucosylceramide-beta-glucosidase levels in the skin of patients with psoriasis vulgaris. *J. Invest. Dermatol.* 123, 1030–1036. doi: 10.1111/j.0022-202x.2004.23469.x

Allgaier, S., Taylor, R. D., Brudnaya, Y., Jacobson, D. J., Cambareri, E., and Stuart, W. D. (2009). Vaccine production in Neurospora crassa. *Biological* 37, 128–132. doi: 10.1016/j.biologicals.2009.02.006

Barr, K., and Lester, R. L. (1984). Occurrence of novel antigenic phosphoinositol-containing sphingolipids in the pathogenic yeast Histoplasma capsulatum. *Biochemistry* 23, 5581–5588. doi: 10.1021/bi00318a031

Barreto-Bergter, E., Pinto, M. R., and Rodrigues, M. L. (2004). Structure and biological functions of fungal cerebrosides. *An. Acad. Bras. Cienc.* 76, 67–84. doi: 10.1590/s0001-37652004000100007

Barreto-Bergter, E., Sassaki, G. L., and De Souza, L. M. (2011). Structural analysis of fungal cerebrosides. *Front. Microbiol.* 2:239. doi: 10.3389/fmicb.2011.00239

Bartke, N., Fischbeck, A., and Humpf, H. U. (2006). Analysis of sphingolipids in potatoes (Solanum tuberosum L.) and sweet potatoes (Ipomoea batatas (L.) lam.) by reversed phase high-performance liquid chromatography electrospray ionization tandem mass spectrometry (HPLC-ESI-MS/MS). *Mol. Nutr. Food Res.* 50, 1201–1211. doi: 10.1002/mnfr.200600140

Bedja, D., Yan, W., Lad, V., Iocco, D., Sivakumar, N., Bandaru, V. V. R., et al. (2018). Inhibition of glycosphingolipid synthesis reverses skin inflammation and hair loss in apoe-/- mice fed western diet. *Sci. Rep.* 8:11463.

Boas, M. H., Egge, H., Pohlentz, G., Hartmann, R., and Bergter, E. B. (1994). Structural determination of N-20-hydroxyoctadecenoyl-1O-b-D-glucopyranosyl-9-methyl-4,8-sphingadieninefrom species of *Aspergillus*. *Chem. Phys. Lipids* 70, 11–19.

Brunt, J. V. (1986). Fungi: the perfect hosts? *Nat. Biotechnol.* 4, 1057–1062. doi: 10.1038/nbt1286-1057

Buede, R., Rinker-schaffer, C., Pinto, W. J., Lester, R. L., and Dickson, R. C. (1991). Cloning and characterization of LCB1, a Saccharomyces gene required for biosynthesis of the long-chain base component of sphingolipids. *J. Bacteriol.* 173, 4325–4332. doi: 10.1128/jb.173.14.4325-4332.1991

Buré, C., Cacas, J. L., Mongrand, S., and Schmitter, J. M. (2014). Characterization of glycosyl inositol phosphoryl ceramides from plants and fungi by mass spectrometry. *Anal. Bioanal. Chem.* 406, 995–1010. doi: 10.1007/s00216-013-7130-8

Carneiro, R., Salgado, A., Raposo, S., Marto, J., Simoes, S., Urbano, M., et al. (2011). Topical emulsions containing ceramides: effects on the skin barrier function and anti-inflammatory properties. *Eur. J. Lipid Sci. Tech.* 113, 961–966. doi: 10.1002/ejlt.201000495

Cerantola, V., Guillas, I., Roubaty, C., Vionnet, C., Uldry, D., Knudsen, J., et al. (2009). Aureobasidin A arrests growth of yeast cells through both ceramide intoxication and deprivation of essential inositolphosphorylceramides. *Mol. Microbiol.* 71, 1523–1537. doi: 10.1111/j.1365-2958.2009.06628.x

Chen, P. W., Fonseca, L. L., Hannun, Y. A., and Voit, E. O. (2013). Coordination of rapid sphingolipid responses to heat stress in yeast. *PLoS Comput. Biol.* 9:e1003078. doi: 10.1371/journal.pcbi.1003078

Chen, T., Xiong, S., Jiang, S., Wang, M., Wu, Q., and Wei, H. (2011). Molecular identification of microbial community in Chinese douchi during post-fermentation process. *Food Sci. Biotechnol.* 20, 1633–1638. doi: 10.1007/s10068-011-0225-0

Cheng, J., Park, T. S., Fischl, A. S., and Ye, X. S. (2001). Cell cycle progression and cell polarity require sphingolipid biosynthesis in *Aspergillus nidulans*. *Mol. Cell. Biol.* 21, 6198–6209. doi: 10.1128/mcb.21.18.6198-6209.2001

Cheon, S. A., Bal, J., Song, Y., Hwang, H. M., Kim, A. R., Kang, W. K., et al. (2012). Distinct roles of two ceramide synthases, CaLag1p and CaLac1p, in the morphogenesis of *Candida albicans*. *Mol. Microbiol.* 83, 728–745. doi: 10.1111/j.1365-2958.2011.07961.x

Cherry, J. R., and Fidantsef, A. L. (2003). Directed evolution of industrial enzymes: an update. *Curr. Opin. Biotechnol.* 14, 438–443. doi: 10.1016/s0958-1669(03)00099-5

Cliften, P., Wang, Y., Mochizuki, D., Miyakawa, T., Wangspa, R., Hughes, J., et al. (1996). SYR2, a gene necessary for syringomycin growth inhibition of *Saccharomyces cerevisiae*. *Microbiology* 142, 477–484. doi: 10.1099/13500872-142-3-477

Dickson, R. C. (2008). Thematic review series: sphingolipids. New insights into sphingolipid metabolism and function in budding yeast. *J. Lipid Res.* 49, 909–921. doi: 10.1194/jlr.r800003-jlr200

Dickson, R. C., and Lester, R. L. (1999). Yeast sphingolipids. *Biochim. Biophys. Acta* 1426, 347–357.

Dickson, R. C., Sumanasekera, C., and Lester, R. L. (2006). Functions and metabolism of sphingolipids in Saccharomyces cerevisiae. *Prog. Lipid Res.* 45, 447–465. doi: 10.1016/j.plipres.2006.03.004

Duan, J., Sugawara, T., Hirose, M., Aida, K., Sakai, S., Fujii, A., et al. (2012). Dietary sphingolipids improve skin barrier functions via the upregulation of ceramide synthases in the epidermis. *Exp. Dermatol.* 21, 448–452. doi: 10.1111/j.1600-0625.2012.01501.x

Duarte, R. S., Polycarpo, C. R., Wait, R., Hartmann, R., and Bergter, E. B. (1998). Structural characterization of neutral glycosphingolipids from *Fusarium* species. *Biochim. Biophys. Acta* 1390, 186–196. doi: 10.1016/s0005-2760(97)00179-3

Ferdouse, J., Yamamoto, Y., Taguchi, S., Yoshizaki, Y., Takamine, K., and Kitagaki, H. (2018). Glycosylceramide modifies the flavor and metabolic characteristics of sake yeast. *Peer J.* 6:e4768. doi: 10.7717/peerj.4768

Fernandes, C. M., de Castro, P. A., Singh, A., Fonseca, F. L., Pereira, M. D., Vila, T. V., et al. (2016). Functional characterization of the *Aspergillus nidulans* glucosylceramide pathway reveals that LCB Δ8-desaturation and C9-methylation are relevant to filamentous growth, lipid raft localization and Psd1 defensin activity. *Mol. Microbiol.* 102, 488–505. doi: 10.1111/mmi.13474

Fernandes, C. M., Goldman, G. H., Poeta, M. D., and Garsin, D. A. (2018). Biological roles played by sphingolipids in dimorphic and filamentous fungi. *Mbio* 9:2472555217719372.

Fontaine, T. (2017). Sphingolipids from the human fungal pathogen *Aspergillus fumigatus*. *Biochimie* 141, 9–15. doi: 10.1016/j.biochi.2017.06.012

Fornarotto, M., Xiao, L., Hou, Y., Koch, K. A., Chang, E., O'Malley, R. M., et al. (2006). Sphingolipid biosynthesis in pathogenic fungi: identification and characterization of the 3-ketosphinganine reductase activity of *Candida albicans* and *Aspergillus fumigatus*. *Biochim. Biophys. Acta* 1761, 52–63. doi: 10.1016/j.bbalip.2005.11.013

Fujino, Y., and Ohnishi, M. (1977). Structure of cerebroside in *Aspergillus oryzae*. *Biochim. Biophys. Acta 486*, 161–171.

Fujino, Y., and Ohnishi, M. (2003). Structure of cerebroside in *Aspergillus oryzae*. *Biochim. Biophys. Acta* 486, 161–171.

Fukunaga, S., Wada, S., Yamashita, M., Morita, M., Aoi, W., Naito, Y., et al. (2019). Torula yeast (Candida utilis)-derived glucosylceramide contributes to dermal elasticity in vitro. *J. Food Biochem.* 43:e12847.

Gable, K., Slife, H., Bacikova, D., Monaghan, E., and Dunn, T. M. (2000). Tsc3p Is an 80-amino acid protein associated with serine Palmitoyltransferase and required for optimal Enzyme activity. *J. Biol. Chem.* 275, 7597–7603. doi: 10.1074/jbc.275.11.7597

Gault, C. R., Obeid, L. M., and Hannun, Y. A. (2010). An overview of sphingolipid metabolism: from synthesis to breakdown. *Adv. Exp. Med. Biol.* 688, 1–23. doi: 10.1007/978-1-4419-6741-1_1

Georgopapadakou, N. H. (2000). Antifungals targeted to sphingolipid synthesis: Focus on inositol phosphorylceramide synthase. *Expert Opin. Investig. Drugs* 9, 1787–1796. doi: 10.1517/13543784.9.8.1787

Grimm, M. O. W., Tschpe, J. A., Grimm, H. S., Zinser, E. G., and Hartmann, T. (2006). Altered membrane fluidity and lipid raft composition in presenilin-deficient cells. *Acta Neurol. Scandinavica* 114, 27–32. doi: 10.1111/j.1600-0404.2006.00682.x

Guillou, S., Ghabri, S., Jannot, C., Gaillard, E., Lamour, I., and Boisnic, S. (2011). The moisturizing effect of a wheat extract food supplement on women's skin: a randomized, double-blind placebo-controlled trial. *Int. J. Cosmet. Sci.* 33, 138–143. doi: 10.1111/j.1468-2494.2010.00600.x

Guimarães, L. L., Toledo, M. S., Ferreira, F. A., Straus, A. H., and Takahashi, H. K. (2014). Structural diversity and biological significance of glycosphingolipids in pathogenic and opportunistic fungi. *Front. Cell Infect. Microbiol.* 4:138. doi: 10.3389/fcimb.2014.00138

Haak, D., Gable, K., Beeler, T., and Dunn, T. (1997). Hydroxylation of *Saccharomyces* cerevisiae ceramides requires Sur2p and Scs7p. *J. Biol. Chem.* 272, 29704–29710. doi: 10.1074/jbc.272.47.29704

Hamajima, H., Fujikawa, A., Yamashiro, M., Ogami, T., Kitamura, S., Tsubata, M., et al. (2016). Chemical analysis of the sugar moiety of monohexosylceramide contained in koji, Japanese traditional rice fermented with *Aspergillus*. *Fermentation* 2:2. doi: 10.3390/fermentation2010002

Hamajima, H., Tanaka, M., Miyagawa, M., Sakamoto, M., Nakamura, T., Yanagita, T., et al. (2019). Koji glycosylceramide commonly contained in Japanese traditional fermented foods alters cholesterol metabolism in obese mice. *Biosci. Biotechnol. Biochem.* 83, 1514–1522. doi: 10.1080/09168451.2018.1562877

Hamanaka, S., Hara, M., Nishio, H., Otsuka, F., and Uchida, Y. (2002). Human epidermal glucosylceramides are major precursors of stratum corneum ceramides. *J. Invest. Dermatol.* 119, 416–423. doi: 10.1046/j.1523-1747.2002.01836.x

Hamanaka, S., Nakazawa, S., Yamanaka, M., Uchida, Y., and Otsuka, F. (2005). Glucosylceramide accumulates preferentially in lamellar bodies in

differentiated keratinocytes. *Br. J. Dermatol.* 152, 426–434. doi: 10.1111/j.1365-2133.2004.06333.x

Hannun, Y. A., and Obeid, L. M. (2008). Principles of bioactive lipid signalling: lessons from sphingolipids. *Nat. Rev. Mol. Cell. Biol.* 9, 139–150. doi: 10.1038/nrm2329

Harrison, P. J., Dunn, T. M., and Campopiano, D. J. (2018). Sphingolipid biosynthesis in man and microbes. *Nat. Prod. Rep.* 35, 921–954. doi: 10.1039/c8np00019k

Hashida-Okado, T., Ogawa, A., Endo, M., Yasumoto, R., Takesako, K., and Kato, I. (1996). AUR1, a novel gene conferring aureobasidin resistance on *Saccharomyces* cerevisiae: a study of defective morphologies in Aur1p-depleted cells. *Mol. Gen. Genet.* 251, 236–244. doi: 10.1007/bf02172923

Heung, L. J., Luberto, C., and Del Poeta, M. (2006). Role of sphingolipids in microbial pathogenesis. *Infect. Immun.* 74, 28–39. doi: 10.1128/iai.74.1.28-39.2006

Hirakawa, S., Sato, A., Hattori, Y., Matsumoto, T., Yokoyama, K., and Kanai, A. (2013). Dietary rice bran extract improves TEWL of whole body. *Jpn. Pharmacol. Ther.* 41, 1051–1059.

Hirata, M., Tsuge, K., Jayakody, L., Urano, Y., Sawada, K., Inaba, S., et al. (2012). Structural determination of glucosylceramides in the distillation remnants of shochu, the Japanese traditional liquor, and its production by *Aspergillus kawachii*. *J. Agric. Food Chem.* 60, 11473–11482. doi: 10.1021/jf303117e

Holleran, W. M., Takagi, Y., and Uchida, Y. (2006). Epidermal sphingolipids: metabolism, function, and roles in skin disorders. *FEBS Lett.* 580, 5456–5466. doi: 10.1016/j.febslet.2006.08.039

Hu, W., Liu, J., Chen, J. H., Wang, S. Y., Lu, D., Wu, Q. H., et al. (2014). A mutation of *Aspergillus niger* for hyper-production of citric acid from corn meal hydrolysate in a bioreactor. *J. Zhejiang Univ. Sci. B* 15, 1006–1010. doi: 10.1631/jzus.b1400132

Huber, A., Oemer, G., Malanovic, N., Lohner, K., Kovács, L., Salvenmoser, W., et al. (2019). Membrane sphingolipids regulate the fitness and antifungal protein susceptibility of *Neurospora crassa*. *Front. Microbiol.* 10:605. doi: 10.3389/fmicb.2019.00605

Insenser, M., Nombela, C., Molero, G., and Gil, C. (2006). Proteomic analysis of detergentresistant membranes from *Candida albicans*. *Proteomics* 6, S74–S81.

Ishibashi, Y., Ikeda, K., Sakaguchi, K., Okino, N., Taguchi, R., and Ito, M. (2012). Quality control of fungus-specific glucosylceramide in *Cryptococcus* neoformans by endoglycoceramidase-related protein 1 (EGCrP1). *J. Biol. Chem.* 287, 368–381. doi: 10.1074/jbc.m111.311340

Jenkins, G. M. (2003). The emerging role for sphingolipids in the eukaryotic heat shock response. *Cell Mol. Life Sci.* 60, 701–710. doi: 10.1007/s00018-003-2239-0

Karaffa, L., and Kubicek, C. P. (2019). Citric acid and itaconic acid accumulation: variations of the same story? *Appl. Microbiol. Biotechnol.* 103, 2889–2902. doi: 10.1007/s00253-018-09607-9

Kawano, K., and Umemura, K. (2013). Oral intake of beet extract provides protection against skin barrier impairment in hairless mice. *Phytother Res.* 27, 775–783. doi: 10.1002/ptr.4792

Kimata, H. (2006). Improvement of atopic dermatitis and reduction of skin allergic responses by oral intake of konjac ceramide. *Pediatr. Dermatol.* 23, 386–389. doi: 10.1111/j.1525-1470.2006.00268.x

Knuf, C., Nookaew, I., Brown, S. H., McCulloch, M., Berry, A., and Nielsen, J. (2013). Investigation of malic acid production in *Aspergillus oryzae* under nitrogen starvation conditions. *Appl. Environ. Microbiol.* 79, 6050–6058. doi: 10.1128/aem.01445-13

Kotz, A., Wagener, J., Engel, J., Routier, F., Echtenacher, B., Pich, A., et al. (2010). The mitA gene of Aspergillus fumigatus is required for mannosylation of inositol-phosphorylceramide, but is dispensable for pathogenicity. *Fungal Genet. Biol.* 47, 169–178. doi: 10.1016/j.fgb.2009.10.001

Kuroda, M., Hashida-Okado, T., Yasumoto, R., Gomi, K., Kato, I., and Takesako, K. (1999). An aureobasidin a resistance gene isolated from *Aspergillus* is a homolog of yeast AUR1, a gene responsible for inositol phosphorylceramide (IPC) synthase activity. *Mol. Gen. Genet.* 261, 290–296. doi: 10.1007/s004380050969

Lattif, A. A., Mukherjee, P. K., Chandra, J., Roth, M. R., Welti, R., Rouabhia, M., et al. (2011). Lipidomics of *Candida albicans* biofilms reveals phase-dependent production of phospholipid molecular classes and role for lipid rafts in biofilm formation. *Microbiology* 157, 3232–3242. doi: 10.1099/mic.0.051086-0

Le Barz, M., Boulet, M. M., Calzada, C., Cheillan, D., and Michalski, M. C. (2020). Alterations of endogenous sphingolipid metabolism in cardiometabolic diseases: Towards novel therapeutic approaches. *Biochimie* 169, 133–143. doi: 10.1016/j.biochi.2019.10.003

Leber, A., Fischer, P., Schneiter, R., Kohlwein, S. D., and Daum, G. (1997). The yeast mic2 mutant is defective in the formation of mannosyldiinositolphosphorylceramide. *FEBS Lett.* 411, 211–214.

Leipelt, M., Warnecke, D., Zähringer, U., Ott, C., Müller, F., Hube, B., et al. (2001). Glucosylceramide synthases, a gene family responsible for the biosynthesis of glucosphingolipids in animals, plants, and fungi. *J. Biol. Chem.* 276, 33621–33629. doi: 10.1074/jbc.m104952200

Lester, R. L., Smith, S. W., Wells, G. B., Rees, D. C., and Angus, W. W. (1974). The isolation and partial characterization of two novel sphingolipids from Neurospora crassa: di(inositolphosphoryl)ceramide and ((gal)3glu) ceramide. *J. Biol. Chem.* 249, 3388–3394. doi: 10.1016/s0021-9258(19)42584-2

Lev, M., and Milford, A. F. (1981). The 3-ketodihydrosphingosine synthetase of *Bacteroides* melaninogenicus: Partial purification and properties. *Arch. Biochem. Biophys.* 212, 424–431. doi: 10.1016/0003-9861(81)90384-2

Levery, S. B., Momany, M., Lindsey, R., Toledo, M. S., Shayman, J. A., Fuller, M., et al. (2002). Disruption of the glucosylceramide biosynthetic pathway in *Aspergillus nidulans* and *Aspergillus fumigatus* by inhibitors of UDP-Glc:ceramide glucosyltransferase strongly affects spore germination, cell cycle, and hyphal growth. *FEBS Lett.* 525, 59–64. doi: 10.1016/s0014-5793(02)03067-3

Levery, S. B., Toledo, M. S., Doong, R. L., Straus, A. H., and Takahashi, H. K. (2000). Comparative analysis of ceramide structural modification found in fungal cerebrosides by electrospray tandem mass spectrometry with low energy collision-induced dissociation of Li+ adduct ions. *Rapid. Commun. Mass Spectrom* 14, 551–563. doi: 10.1002/(sici)1097-0231(20000415)14:7<551::aid-rcm909>3.0.co;2-l

Levery, S. B., Toledo, M. S., Straus, A. H., and Takahashi, H. K. (1998). Structure elucidation of sphingolipids from the mycopathogen *Paracoccidioides brasiliensis*: an immunodominant beta-galactofuranose residue is carried by a novel glycosylinositol phosphorylceramide antigen. *Biochemistry* 37, 8764–8775. doi: 10.1021/bi9730083

Li, S., Bao, D., Yuen, G., Harris, S. D., and Calvo, A. M. (2007). basA regulates cell wall organization and asexual/sexual sporulation ratio in *Aspergillus nidulans*. *Genetics* 176, 243–253. doi: 10.1534/genetics.106.068239

Li, S., Du, L., Yuen, G., and Harris, S. D. (2006). Distinct ceramide synthases regulate polarized growth in the filamentous fungus *Aspergillus nidulans*. *Mol. Biol. Cell* 17, 1218–1227. doi: 10.1091/mbc.e05-06-0533

Li, S., Calvo, A. M., Yuen, G. Y., Du, L., and Harris, S. D. (2009). Induction of cell wall thickening by the antifungal compound dihydromaltophilin disrupts fungal growth and is mediated by sphingolipid biosynthesis. *J. Eukaryot. Microbiol.* 56, 182–187.

Liang, Y., Pan, L., and Lin, Y. (2009). Analysis of extracellular proteins of *Aspergillus oryzae* grown on Soy Sauce Koji. *Biosci. Biotechnol. Biochem.* 73, 192–195. doi: 10.1271/bbb.80500

Lingwood, D., and Simons, K. (2010). Lipid rafts as a membrane-organizing principle. *Science* 327, 46–50. doi: 10.1126/science.1174621

Loureiro y Penha, C. V., Todeschini, A. R., Lopes-Bezerra, L. M., Wait, R., Jones, C., Mattos, K. A., et al. (2001). Characterization of novel structures of mannosylinositolphosphorylceramides from the yeast forms of Sporothrix schenckii. *Eur. J. Biochem.* 268, 4243–4250. doi: 10.1046/j.1432-1327.2001.02339.x

Luberto, C. (2001). Roles for inositol-phosphoryl ceramide synthase 1 (IPC1) in pathogenesis of C. neoformans. *Genes Dev.* 15, 201–212. doi: 10.1101/gad.856001

Maciel, D. M., Rodrigues, M. L., Wait, R., Villas Boas, M. H., Tischer, C. A., and Barreto-Bergter, E. (2002). Glycosphingolipids from Magnaporthe grisea cells: expression of a ceramide dihexoside presenting phytosphingosine as the long-chain base. *Arch. Biochem. Biophys.* 405, 205–213. doi: 10.1016/s0003-9861(02)00365-x

Mandala, S. M., Thornton, R. A., Frommer, B. R., Curotto, J. E., Rozdilsky, W., Kurtz, M. B., et al. (1995). The discovery of australifungin, a novel inhibitor of sphinganine N-acyltransferase from *Sporormiella australis*. Producing organism, fermentation, isolation, and biological activity. *J. Antibiot.* 48, 349–356. doi: 10.7164/antibiotics.48.349

Mandala, S. M., Thornton, R. A., Milligan, J., Rosenbach, M., Garcia-Calvo, M., Bull, H. G., et al. (1998). Rustmicin, a potent antifungal agent, inhibits sphingolipid synthesis at the inositol phosphoceramide synthase. *J. Biol. Chem.* 273, 14942–14949. doi: 10.1074/jbc.273.24.14942

Mandala, S. M., Thornton, R. A., Rosenbach, M., Milligan, J., Garcia-Calvo, M., Bull, H. G., et al. (1997). Khafrefungin, a novel inhibitor of sphingolipid synthesis. *J. Biol. Chem.* 272, 32709–32714. doi: 10.1074/jbc.272.51.32709

Marques, J. T., Marinho, H. S., and De Almeida, R. F. M. (2018). Sphingolipid hydroxylation in mammals, yeast and plants-an integrated view. *Prog. Lipid Res.* 71, 18–42. doi: 10.1016/j.plipres.2018.05.001

Medlock, K. A., and Merrill, A. H. (1988). Inhibition of serine palmitoyltransferase in vitro and long-chain base biosynthesis in intact Chinese hamster ovary cells by β-chloroalanine. *Biochemistry* 27, 7079–7084. doi: 10.1021/bi00418a061

Merrill, A. H. J., Sullards, M. C., Wang, E., Voss, K. A., and Riley, R. T. (2001). Sphingolipid metabolism: roles in signal transduction and disruption by fumonisins. *Environ. Health Perspect.* 109, 283–289. doi: 10.2307/3435020

Michel, C., and van Echten-Deckert, G. (1997). Conversion of dihydroceramide to ceramide occurs at the cytosolic face of the endoplasmic reticulum. *FEBS Lett.* 416, 153–155. doi: 10.1016/s0014-5793(97)01187-3

Michel, C., van Echten-Deckert, G., Rother, J., Sandhoff, K., Wang, E., and Merrill, A. H. (1997). Characterization of ceramide synthesis. A dihydroceramide desaturase introduces the 4,5-trans-double bond of sphingosine at the level of dihydroceramide. *J. Biol. Chem.* 272, 22432–22437.

Miyagawa, M., Fujikawa, A., Nagadome, M., Kohama, K., Ogami, T., Kitamura, S., et al. (2019). Glycosylceramides purified from the Japanese traditional Non-Pathogenic Fungus *Aspergillus* and *Koji* increase the expression of genes involved in tight junctions and ceramide delivery in normal human epidermal Keratinocytes. *Fermentation* 5:43. doi: 10.3390/fermentation5020043

Miyanishi, K., Shiono, N., Shirai, H., Dombo, M., and Kimata, H. (2005). Reduction of transepidermal water loss by oral intake of glucosylceramides in patients with atopic eczema. *Allergy* 60, 1454–1455. doi: 10.1111/j.1398-9995.2005.00915.x

Molodecky, N. A., Soon, I. S., Rabi, D. M., Ghali, W. A., Ferris, M., Chernoff, G., et al. (2012). Increasing incidence and prevalence of the inflammatory bowel diseases with time, based on systematic review. *Gastroenterology* 142, 46–54. doi: 10.1053/j.gastro.2011.10.001

Mukherjee, J. J., and Dekker, E. E. (1990). 2-Amino-3-ketobutyrate CoA ligase of *Escherichia coli*: stoichiometry of pyridoxal phosphate binding and location of the pyridoxyllysine peptide in the primary structure of the enzyme. *Biochim. Biophys. Acta* 1037, 24–29. doi: 10.1016/0167-4838(90)90097-y

Munshi, M. A., Gardin, J. M., Singh, A., Luberto, C., Rieger, R., Bouklas, T., et al. (2018). The role of ceramide synthases in the pathogenicity of *Cryptococcus neoformans*. *Cell Rep.* 22, 1392–1400. doi: 10.1016/j.celrep.2018.01.035

Nagiec, M. M., Baltisberger, J. A., Wells, G. B., Lester, R. L., and Dickson, R. C. (1994). The LCB2 gene of *Saccharomyces* and the related LCB1 gene encode subunits of serine palmitoyltransferase, the initial enzyme in sphingolipid synthesis. *Proc. Natl. Acad. Sci. USA* 91, 7899–7902. doi: 10.1073/pnas.91.17.7899

Nagiec, M. M., Nagiec, E. E., Baltisberger, J. A., Wells, G. B., Lester, R. L., and Dickson, R. C. (1997). Sphingolipid synthesis as a target for antifungal drugs. Complementation of the inositol phosphorylceramide synthase defect in a mutant strain of *Saccharomyces cerevisiae* by the AUR1 gene. *J. Biol. Chem.* 272, 9809–9817.

Nash, C. H., and Huber, F. M. (1971). Antibiotic synthesis and morphological differentiation of cephalosporium acremonium. *Appl. Microbiol.* 22, 6–10. doi: 10.1128/aem.22.1.6-10.1971

Nicolas, G., Nadira, T. E., Nouara, Y., and Jacques, F. (2005). Apical uptake and transepithelial transport of sphingosine monomers through intact human intestinal epithelial cells: Physicochemical and molecular modeling studies. *Arch. Biochem. Biophys.* 440, 91–100. doi: 10.1016/j.abb.2005.06.001

Nielsen, J., and Jorgensen, H. S. (1995). Metabolic control analysis of the penicillin biosynthetic pathway in a high-yielding strain of *Penicillium chrysogenum*. *Biotechnol. Prog.* 11, 299–305. doi: 10.1021/bp00033a010

Nimrichter, L., and Rodrigues, M. L. (2011). Fungal glucosylceramides: from structural components to biologically active targets of new antimicrobials. *Front. Microbiol.* 2:212. doi: 10.3389/fmicb.2011.00212

Noble, S. M., French, S., Kohn, L. A., Chen, V., and Johnson, A. D. (2010). Systematic screens of a *Candida albicans* homozygous deletion library decouple morphogenetic switching and pathogenicity. *Nat. Genet.* 42, 590–598. doi: 10.1038/ng.605

Nützmann, H. W., Schroeckh, V., and Brakhage, A. A. (2012). Regulatory cross talk and microbial induction of fungal secondary metabolite gene clusters. *Methods Enzymol.* 517, 325–341. doi: 10.1016/b978-0-12-404634-4.00016-4

Oguro, Y., Yamazaki, H., Takagi, M., and Takaku, H. (2014). Antifungal activity of plant defensin AFP1 in Brassica juncea involves the recognition of the methyl residue in glucosylceramide of target pathogen *Candida albicans*. *Curr. Genet.* 60, 89–97. doi: 10.1007/s00294-013-0416-8

Ohnishi, M., Ito, S., and Fujino, Y. (1985). Sphingolipid classes and their molecular species in wheat flour. *Agric. Biol. Chem. Tokyo* 49, 3609–3611. doi: 10.1271/bbb1961.49.3609

Ono, J., Kinoshita, M., Aida, K., Tamura, M., and Ohnishi, M. (2010). Effects of dietary glucosylceramide on dermatitis in atopic dermatitis model mice. *Eur. J. Lipid Sci. Technol.* 112, 708–711. doi: 10.1002/ejlt.200900268

Otsu, M., Toume, M., Yamaguchi, Y., and Tani, M. (2020). Proper regulation of inositolphosphorylceramide levels is required for acquirement of low pH resistance in budding yeast. *Sci. Rep.* 10:10792.

Oura, T., and Kajiwara, S. (2008). Disruption of the sphingolipid Delta8-desaturase gene causes a delay in morphological changes in *Candida albicans*. *Microbiology* 154, 3795–3803. doi: 10.1099/mic.0.2008/018788-0

Oura, T., and Kajiwara, S. (2010). Candida albicans sphingolipid C9-methyltransferase is involved in hyphal elongation. *Microbiology* 156, 1234–1243. doi: 10.1099/mic.0.033985-0

Papagianni, M. (2007). Advances in citric acid fermentation by *Aspergillus niger*: biochemical aspects, membrane transport and modeling. *Biotechnol. Adv.* 25, 244–263. doi: 10.1016/j.biotechadv.2007.01.002

Park, C., Bennion, B., Francois, I. E., Ferket, K. K., Cammue, B. P., Thevissen, K., et al. (2005). Neutral glycolipids of the filamentous fungus *Neurospora crassa*: altered expression in plant defensin-resistant mutants. *J. Lipid Res.* 46, 759–768. doi: 10.1194/jlr.m400457-jlr200

Pearson, C. L., Xu, K., Sharpless, K. E., and Harris, S. D. (2004). MesA, a novel fungal protein required for the stabilization of polarity axes in *Aspergillus nidulans*. *Mol. Biol. Cell* 15, 3658–3672. doi: 10.1091/mbc.e03-11-0803

Perdoni, F., Signorelli, P., Cirasola, D., Caretti, A., Galimberti, V., Biggiogera, M., et al. (2015). Antifungal activity of Myriocin on clinically relevant *Aspergillus fumigatus* strains producing biofilm. *BMC Microbiol.* 15:248. doi: 10.1186/s12866-015-0588-0

Plesofsky, N. S., Levery, S. B., Castle, S. A., and Brambl, R. (2008). Stress-induced cell death is mediated by ceramide synthesis in *Neurospora crassa*. *Eukaryot Cell* 7, 2147–2159. doi: 10.1128/ec.00147-08

Del Poeta, M, Nimrichter, L., Rodrigues, M. L., and Luberto, C. (2014). Synthesis and biological properties of fungal glucosylceramide. *PLoS Pathog.* 10:e1003832. doi: 10.1371/journal.ppat.1003832

Raj, S., Nazemidashtarjandi, S., Kim, J., Joffe, L., Zhang, X., Singh, A., et al. (2017). Changes in glucosylceramide structure affect virulence and membrane biophysical properties of *Cryptococcus neoformans*. *Biochim. Biophys. Acta Biomembr.* 1859, 2224–2233. doi: 10.1016/j.bbamem.2017.08.017

Ramamoorthy, V., Cahoon, E. B., Li, J., Thokala, M., Minto, R. E., and Shah, D. M. (2007). Glucosylceramide synthase is essential for alfalfa defensin-mediated growth inhibition but not for pathogenicity of *Fusarium* graminearum. *Mol. Microbiol.* 66, 771–786. doi: 10.1111/j.1365-2958.2007.05955.x

Ramamoorthy, V., Cahoon, E. B., Thokala, M., Kaur, J., Li, J., and Shah, D. M. (2009). Sphingolipid C-9 methyltransferases are important for growth and virulence but not for sensitivity to antifungal plant defensins in Fusarium graminearum. *Eukaryot Cell* 8, 217–229. doi: 10.1128/ec.00255-08

Řezanka, T., Kolouchová, I., Gharwalová, L., Doležalová, J., Nedbalová, L., and Sigle, K. (2018). Sphingolipidomics of thermotolerant yeasts. *Lipids* 53, 627–639. doi: 10.1002/lipd.12076

Řezanka, T., Kolouchová, I., and Sigle, K. (2016). Lipidomic analysis of *psychrophilic* yeasts cultivated at different temperatures. *Biochim. Biophys. Acta* 1861, 1634–1642. doi: 10.1016/j.bbalip.2016.07.005

Rhome, R., McQuiston, T., Kechichian, T., Bielawska, A., Hennig, M., Drago, M., et al. (2007). Biosynthesis and immunogenicity of glucosylceramide in *Cryptococcus neoformans* and other human pathogens. *Eukaryot Cell* 6, 1715–1726. doi: 10.1128/ec.00208-07

Rittenour, W. R., Chen, M., Cahoon, E. B., and Harris, S. D. (2011). Control of glucosylceramide production and morphogenesis by the Bar1 ceramide

synthase in Fusarium graminearum. *PLoS One* 6:e19385. doi: 10.1371/journal.pone.0019385

Rittershaus, P. C., Kechichian, T. B., Allegood, J. C., Merrill, A. H. J., Hennig, M., Luberto, C., et al. (2006). Glucosylceramide synthase is an essential regulator of pathogenicity of *Cryptococcus neoformans*. *J. Clin. Invest* 116, 1651–1659. doi: 10.1172/jci27890

Rodriguez-Cuenca, S., Barbarroja, N., and Vidal-Puig, A. (2015). Dihydroceramide desaturase 1, the gatekeeper of ceramide induced lipotoxicity. *Biochim. Biophys. Acta Mol. Cell Biol. Lipids* 1851, 40–50. doi: 10.1016/j.bbalip.2014.09.021

Rollin-Pinheiro, R., Singh, A., Barreto-Bergter, E., and Del Poeta, M. (2016). Sphingolipids as targets for treatment of fungal infections. *Future Med. Chem.* 8, 1469–1484. doi: 10.4155/fmc-2016-0053

Sawada, K., Sato, T., Hamajima, H., Jayakody, L. N., Hirata, M., Yamashiro, M., et al. (2015). Glucosylceramide contained in koji mold-cultured cereal confers membrane and flavor modification and stress tolerance to Saccharomyces cerevisiae during coculture fermentation. *Appl. Environ. Microbiol.* 81, 3688–3698. doi: 10.1128/aem.00454-15

Schmelz, E. M., Zhou, H., and Roberts, P. C. (2015). *Dietary sphingolipids in colon cancer prevention*. Cham: Springer International Publishing.

Shimada, E., Aida, K., Sugawara, T., and Hirata, T. (2011). Inhibitory effect of topical maize glucosylceramide on skin photoaging in UVA-irradiated hairless mice. *J. Oleo Sci.* 60, 321–325. doi: 10.5650/jos.60.321

Shimoda, H., Terazawa, S., Hitoe, S., Tanaka, J., Nakamura, S., Matsuda, H., et al. (2012). Changes in ceramides and glucosylceramides in mouse skin and human epidermal equivalents by rice-derived glucosylceramide. *J. Med. Food* 15, 1064–1072. doi: 10.1089/jmf.2011.2137

Silano, V., Bolognesi, C., Castle, L., and Chipman, K. (2018). Safety evaluation of the food enzyme α-amylase from a genetically modified *Aspergillus niger* (strain NZYM-MC). *EFSA J.* 16:e05451.

Singh, A., Wang, H., Silva, L. C., Na, C., Prieto, M., Futerman, A. H., et al. (2012). Methylation of glycosylated sphingolipid modulates membrane lipid topography and pathogenicity of *Cryptococcus neoformans*. *Cell Microbiol.* 14, 500–516. doi: 10.1111/j.1462-5822.2011.01735.x

Smith, E. R., and Merrill, A. H. J. (1995). Differential roles of de novo sphingolipid biosynthesis and turnover in the "burst" of free sphingosine and sphinganine, and their 1-phosphates and N-acyl-derivatives, that occurs upon changing the medium of cells in culture. *J. Biol. Chem.* 270, 18749–18758. doi: 10.1074/jbc.270.32.18749

Sonnino, S., Mauri, L., Chigorno, V., and Prinetti, A. (2007). Gangliosides as components of lipid membrane domains. *Glycobiology* 17, 1R–13R.

Spassieva, S., and Hille, J. (2003). Plant sphingolipids today-are they still enigmatic? *Plant Biol.* 5, 125–136. doi: 10.1055/s-2003-40726

Sperling, P., and Heinz, E. (2003). Plant sphingolipids: structural diversity, biosynthesis, first genes and functions. *Biochim. Biophys. Acta* 1632, 1–15. doi: 10.1016/s1388-1981(03)00033-7

Sugawara, T., Duan, J., Aida, K., Tsuduki, T., and Hirata, T. (2010). Identification of glucosylceramides containing sphingatrienine in maize and rice using ion trap mass spectrometry. *Lipids* 45, 451–455. doi: 10.1007/s11745-010-3417-0

Sullards, M. C., Lynch, D. V., Merrill, A. H. J., and Adams, J. (2000). Structure determination of soybean and wheat glucosylceramides by tandem mass spectrometry. *J. Mass Spectr.* 35, 347–353. doi: 10.1002/(sici)1096-9888(200003)35:3<347::aid-jms941>3.0.co;2-3

Suutari, M. (1995). Effect of growth temperature on lipid fatty acids of four fungi (*Aspergillus niger*, *Neurospora crassa*, *Penicillium chrysogenum*, *andTrichoderma reesei*). *Arch. Microbiol.* 164, 212–216. doi: 10.1007/bf02529973

Takahashi, H. K., Toledo, M. S., Suzuki, E., Tagliari, L., and Straus, A. H. (2009). Current relevance of fungal and trypanosomatid glycolipids and sphingolipids: studies defining structures conspicuously absent in mammals. *An. Acad. Bras. Cienc.* 81, 477–488. doi: 10.1590/s0001-37652009000300012

Takahashi, K., Izumi, K., Nakahata, E., Hirata, M., Sawada, K., Tsuge, K., et al. (2014). Quantitation and structural determination of glucosylceramides contained in sake lees. *J. Oleo. Sci.* 63, 15–23. doi: 10.5650/jos.ess13086

Takesako, K., Kuroda, H., Inoue, T., Haruna, F., Yoshikawa, Y., Kato, I., et al. (1993). Biological properties of Aureobasidin A, a cyclic depsipeptide antifungal antibiotic. *J. Antibiot.* 46, 1414–1420. doi: 10.7164/antibiotics.46.1414

Tan, H. W., and Tay, S. T. (2013). The inhibitory effects of aureobasidin A on Candida planktonic and biofilm cells. *Mycoses* 56, 150–156. doi: 10.1111/j.1439-0507.2012.02225.x

Tani, Y., Amaishi, Y., Funatsu, T., Ito, M., Itonori, S., Yamamoto, K., et al. (2014). Structural analysis of cerebrosides from *Aspergillus* fungi: the existence of galactosylceramide in A. oryzae. *Biotechnol. Lett.* 36, 2507–2513. doi: 10.1007/s10529-014-1631-1

Ternes, P., Franke, S., Zähringer, U., Sperling, P., and Heinz, E. (2002). Identification and characterization of a sphingolipid Δ4-desaturase family. *J. Biol. Chem.* 277, 25512–25518. doi: 10.1074/jbc.m202947200

Ternes, P., Sperling, P., Albrecht, S., Franke, S., Cregg, J. M., Warnecke, D., et al. (2006). Identification of fungal sphingolipid C9-methyltransferases by phylogenetic profiling. *J. Biol. Chem.* 281, 5582–5592. doi: 10.1074/jbc.m512864200

Ternes, P., Wobbe, T., Schwarz, M., Albrecht, S., Feussner, K., Riezman, I., et al. (2011). Two pathways of sphingolipid biosynthesis are separated in the yeast *Pichia* pastoris. *J. Biol. Chem.* 286, 11401–11414. doi: 10.1074/jbc.m110.193094

Tessema, E. N., Gebre-Mariam, T., Neubert, R. H. H., and Wohlrab, J. (2017). Potential applications of phyto-derived ceramides in improving epidermal barrier function. *Skin Pharmacol. Physiol.* 30, 115–138. doi: 10.1159/000464337

Toledo, M. S., Levery, S. B., Straus, A. H., Suzuki, E., Momany, M., Glushka, J., et al. (1999). Characterization of sphingolipids from mycopathogens: factors correlating with expression of 2-hydroxy fatty acyl (E)-Delta 3-unsaturation in cerebrosides of *Paracoccidioides brasiliensis* and *Aspergillus fumigatus*. *Biochemistry* 38, 7294–7306. doi: 10.1021/bi982898z

Toledo, M. S., Levery, S. B., Straus, A. H., and Takahashi, H. K. (2000). Dimorphic expression of cerebrosides in the mycopathogen Sporothrix schenckii. *J. Lipid Res.* 41, 797–806. doi: 10.1016/s0022-2275(20)32388-9

Toledo, M. S., Levery, S. B., Suzuki, E., Straus, A. H., and Takahashi, H. K. (2001). Characterization of cerebrosides from the thermally dimorphic mycopathogen Histoplasma capsulatum: expression of 2-hydroxy fatty N-acyl (E)-Δ3-unsaturation correlates with the yeast-mycelium phase transition. *Glycobiology* 11, 113–124. doi: 10.1093/glycob/11.2.113

Totani, K., Yasutake, N., Ohi, H., Murata, T., and Usui, T. (2001). Enzymatic synthesis of aliphatic beta-lactosides as mimic units of glycosphingolipids by use of *Trichoderma reesei* cellulase. *Arch. Biochem. Biophys.* 385, 70–77. doi: 10.1006/abbi.2000.2133

Triantafillidis, J. K., Nasioulas, G., and Kosmidis, P. A. (2009). Colorectal cancer and inflammatory bowel disease: epidemiology, risk factors, mechanisms of carcinogenesis and prevention strategies. *Anticancer Res.* 29, 2727–2737.

Tsuji, K., Mitsutake, S., Ishikawa, J., Takagi, Y., Akiyama, M., Shimizu, H., et al. (2006). Dietary glucosylceramide improves skin barrier function in hairless mice. *J. Dermatol. Sci.* 44, 101–107. doi: 10.1016/j.jdermsci.2006.08.005

Uchida, Y., Hara, M., Nishio, H., Sidransky, E., Inoue, S., Otsuka, F., et al. (2000). Epidermal sphingomyelins are precursors for selected stratum corneum ceramides. *J. Lipid Res.* 41, 2071–2082. doi: 10.1016/s0022-2275(20)32369-5

Uchiyama, T., Nakano, Y., Ueda, O., Mori, H., Nakashima, M., Noda, A., et al. (2008). Oral intake of glucosylceramide improves relatively higher level of transepidermal water loss in mice and healthy human subjects. *J. Health Sci.* 54, 559–566. doi: 10.1248/jhs.54.559

Usuki, S., Tamura, N., Sakai, S., Tamura, T., Mukai, K., and Igarashi, Y. (2015). Chemoenzymatically prepared konjac ceramide inhibits NGF-induced neurite outgrowth by a semaphorin 3A-like action. *Biochem. Biophys. Rep.* 5, 160–167. doi: 10.1016/j.bbrep.2015.11.016

Wagner, H., and Fiegert, E. (1969). Sphingolipids and glycolipids of fungi and higher plants. 3. Isolation of a cerebroside from *Aspergillus niger* (in German). *Z Naturforsch B* 24:359.

Walls, S. M., Attle, S. J., Brulte, G. B., Walls, M. L., Finley, K. D., Chatfield, D. A., et al. (2013). Identification of sphingolipid metabolites that induce obesity via mis-regulation of appetite, caloric intake and fat storage in drosophila. *PLoS Genet.* 9:e1003970. doi: 10.1371/journal.pgen.1003970

Waring, R. B., May, G. S., and Morris, N. R. (1989). Characterization of an inducible expression system in *Aspergillus nidulans* using alcA and tubulin coding genes. *Gene* 79, 119–130. doi: 10.1016/0378-1119(89)90097-8

Warnecke, D., and Heinz, E. (2003). Recently discovered functions of glucosyl ceramides in plants and fungi. *Cell Mol. Life Sci.* 60, 919–941. doi: 10.1007/s00018-003-2243-4

Wirsel, S., Lachmund, A., Wildhardt, G., and Ruttkowski, E. (2010). Three alpha-amylase genes of *Aspergillus oryzae* exhibit identical intron-exon organization. *Mol. Microbiol.* 3, 3–14. doi: 10.1111/j.1365-2958.1989.tb00097.x

Yamashita, S., Seino, T., Aida, K., and Kinoshita, M. (2017). Effects of plant sphingolipids on inflammatory stress in differentiated Caco-2 cells. *J. Oleo. Sci.* 66, 1337–1342. doi: 10.5650/jos.ess17171

Yamashita, S., Yamamoto, M., Hirakawa, K., Kikuchi, N., Kinoshita, M., and Miyazawa, T. (2019). Extraction of lipophilic fraction from polished rice improves its ameliorative effect on intestinal impairment. *J. Oleo. Sci.* 68, 463–470. doi: 10.5650/jos.ess19013

Yasuhiko, F., and Masao, O. (1997). Structure of cerebroside in *Aspergillus oryzae*. *Biochim. Biophys. Acta* 486, 161–171. doi: 10.1016/0005-2760(77)90080-7

Yeom, M., Kim, S. H., Lee, B., Han, J. J., Chung, G. H., Choi, H. D., et al. (2012). Oral administration of glucosylceramide ameliorates inflammatory dry-skin condition in chronic oxazolone-induced irritant contact dermatitis in the mouse ear. *J. Dermatol. Sci.* 67, 101–110. doi: 10.1016/j.jdermsci.2012.05.009

Zaüner, S., Zähringer, U., Lindner, B., Warnecke, D., and Sperling, P. (2008). Identification and functional characterization of the 2-hydroxy fatty N-acyl-Delta3(E)-desaturase from Fusarium graminearum. *J. Biol. Chem.* 283, 36734–36742. doi: 10.1074/jbc.m807264200

Zhang, Y., Wang, S., Li, X. M., Cui, C. M., Feng, C., and Wang, B. G. (2007). New sphingolipids with a previously unreported 9-methyl C20-sphingosine moiety from a marine algous endophytic fungus *Aspergillus niger* EN-13. *Lipids* 42, 759–764.

Zhao, C., Beeler, T., and Dunn, T. (1994). Suppressors of the Ca(2+)-sensitive yeast mutant (csg2) identify genes involved in sphingolipid biosynthesis. Cloning and characterization of SCS1, a gene required for serine palmitoyltransferase activity. *Biol. Chem.* 269, 21480–21488.

Zheng, L., Cash, V. L., Flint, D. H., and Dean, D. R. (1998). Assembly of iron-sulfur clusters-identification of an iscSUA-hscBA-fdx gene cluster from Azotobacter vinelandii. *J. Biol. Chem.* 273, 13264–13272.

Zheng, L., White, R. H., Cash, V. L., and Dean, D. R. (1994). Mechanism for the desulfurization of l-cysteine catalyzed by the nifS gene product. *Biochemistry* 33, 4714–4720.

Zhu, C., Wang, M., Wang, W., Ruan, R., Ma, H., Mao, C., et al. (2014). Glucosylceramides are required for mycelial growth and full virulence in *Penicillium* digitatum. *Biochem. Biophys. Res. Commun.* 455, 165–171.

Conflict of Interest: The authors declare that the research was conducted in the absence of any commercial or financial relationships that could be construed as a potential conflict of interest.

frontiers in Microbiology

MINI REVIEW
published: 22 July 2021
doi: 10.3389/fmicb.2021.703391

Origin, Succession, and Control of Biotoxin in Wine

Xiaoyu Xu, Tian Li, Yanyu Ji, Xia Jiang, Xuewei Shi and Bin Wang**

School of Food Science and Technology, Shihezi University, Shihezi, China

Wine is a worldwide alcoholic beverage with antioxidant active substances and complex flavors. Moderate drinking of wine has been proven to be beneficial to health. However, wine has some negative components, such as residual pesticides, heavy metals, and biotoxins. Of these, biotoxins from microorganisms were characterized as the most important toxins in wine. Wine fermentation mainly involves alcoholic fermentation, malolactic fermentation, and aging, which endue wine with complex flavors and even produce some undesirable metabolites. These metabolites cause potential safety risks that are not thoroughly understood. This review aimed to investigate the origin, evolution, and control technology of undesirable metabolites (e.g., ochratoxin A, ethyl carbamate, and biogenic amines) in wine. It also highlighted current wine industry practices of minimizing the number of biotoxins in wine.

Keywords: biogenic amines, biotoxin, ethyl carbamate, ochratoxin A, wine

OPEN ACCESS

Edited by:
Van-Tuan Tran,
Vietnam National University, Hanoi, Vietnam

Reviewed by:
Pasquale Russo,
University of Foggia, Italy
Francisco Salinas,
Universidad Austral de Chile, Chile

****Correspondence:***
Xuewei Shi
shixuewei@shzu.edu.cn
Bin Wang
binwang0228@shzu.edu.cn

Specialty section:
This article was submitted to Food Microbiology, a section of the journal Frontiers in Microbiology

Received: *30 April 2021*
Accepted: *22 June 2021*
Published: *22 July 2021*

Citation:
Xu X, Li T, Ji Y, Jiang X, Shi X and Wang B (2021) Origin, Succession, and Control of Biotoxin in Wine. Front. Microbiol. 12:703391. doi: 10.3389/fmicb.2021.703391

INTRODUCTION

Wine is an alcoholic beverage made from fresh grapes or grape juice that undergoes complex biochemical changes in the presence of microorganisms. The wine originated in ancient Egypt or ancient Greece or the Greek island of Crete (Alebaki and Koutsouris, 2019). The wine industry has progressed globally since its development to date (Thorpe, 2009). Based on the geography, winemaking history, and winemaking tradition, some winemaking countries with a long history of production (mostly Europe and the Mediterranean region) are classified as "Old World," while the rising stars in the international market are classified as "New World" (emerging wine-producing countries outside of Europe, such as the United States, China, etc.) (Banks and Overton, 2010; Li et al., 2018). The three leading wine-producing countries worldwide are France, Italy, and Spain, which produce almost half of the world's wine (Schamel, 2006). According to the latest data from the International Organization of Vine and Wine (OIV), global wine production is estimated at 26 billion liters, and the wine trade continues to trend toward internationalization (OIV, 2020).

Nowadays, wine is attracting an increasing amount of attention due to its taste, aroma, and health benefits (Ditano-Vázquez et al., 2019; Rivera et al., 2019). While exploiting the various benefits of wine, its quality is often easily overlooked. Similar to other fermented foods, the fermentation process of wine creates a complex system of grape flavors and may also present some quality risks, such as heavy metals, pesticide residues, and biotoxins (Weng and Neethirajan, 2017). Among these, ethyl carbamate (EC) from yeast and lactic acid bacteria (LAB) (Uthurry et al., 2006; Du et al., 2018), biogenic amines (BAs) from LAB (García-Ruiz et al., 2011), and ochratoxin A (OTA) from mold (Iacumin et al., 2009) have gradually received attention in recent years. EC was shown to be a carcinogen as early as 1943 (Nettleship et al., 1943), and alcohol contributes to the

carcinogenic effects of EC (Beland et al., 2005). BAs are also precursors to carcinogens (Guo et al., 2015), and hence their excessive intake can pose a threat to human health.

The production of high-quality wine has stringent requirements for grape raw materials (Morata et al., 2019), ferments, and grape processes, but their potential safety risks cannot be ignored. The risk factors of OTA, EC, and BAs have been identified in wine one after another; however, the sources of these risk factors and their evolution patterns are still unclear. This review focused on the dynamic changes in risk factors in wine fermentation, traced the risk factors, and proposed corresponding prevention and control to provide a theoretical basis for wine risk control.

SAFETY RISKS AND COUNTERMEASURES IN WINE

Moderate drinking of wine has been proven to be beneficial to health because wine comprises antioxidant active substances, minerals, and vitamins (Guilford and Pezzuto, 2011). However, wine can also have some negative components, such as residual pesticides (Guo T. et al., 2016), heavy metals (Bora et al., 2015), and some biotoxins. Of these, biotoxins from microorganisms were the most important toxins in wine (Vitali Čepo et al., 2018). These biotoxins can affect the drinking quality and food safety of wine and lead to a range of diseases if consumed in excess over a long period (**Figure 1**; Welke, 2019). The biotoxins of microbial origin in wine mainly comprise OTA, EC, and BAs. The process from grapes to wines is long and complex, including transportation, pretreatment, maceration, and alcoholic fermentation (Ruiz et al., 2019). During wine fermentation, OTA, EC, and BAs undergo continuous evolution (Christaki and Tzia, 2002; Fernández-Segovia et al., 2014). Grape harvesting, maceration, alcoholic fermentation, and malolactic fermentation (MLF) involve the production of OTA. EC is always produced in alcoholic fermentation, MLF, and aging. Furthermore, various BAs are formed during MLF and aging (**Figure 2**).

Ochratoxin A

Ochratoxin is a mycotoxin composed of seven structurally similar compounds, including OTA, OTB, and OTC (**Supplementary Figure 1**). Among these, OTA is an IIB carcinogen, which has teratogenicity, nephrotoxicity, hepatotoxicity, neurotoxicity, and immunotoxicity to several kinds of animals (Silva et al., 2019). The OTA biosynthesis and the two possible key pathways involved are shown in **Supplementary Figure 2** (Karlovsky, 1999; Gallo et al., 2017). OTA has attracted much attention because of its strong biological toxicity and potential pathogenicity in various cereal crops and fermented foods (Agriopoulou et al., 2020). As far as 1996, OTA was first identified in wine and then classified as the key mycotoxin in wine (Zimmerli and Dick, 1996). The European Commission set the maximum limit for OTA content in wine at 2 μg/kg (European Food Safety Authority (EFSA), 2006).

OTA is produced by various mycetes, including *Aspergillus ochraceus*, *Penicillium verrucosum*, *Aspergillus niger*, and *Aspergillus carbonarius*. However, the main fungal sources of OTA in grapes are *A. carbonarius* and *A. niger* (Oliveri et al., 2017). *A. carbonarius* has been considered as the most important ochratoxin-producing species in grapes because it is widespread on grapes and produces a high concentration of OTA (Varga and Kozakiewicz, 2006). Like other mycetes, *Aspergillus* spp. can produce spores, which are blown to the surrounding grape racks by wind and flying animals (Jiang et al., 2013). During the ripening of grapes, humid weather and high relative humidity can easily cause the rotting of grapes by providing favorable conditions for the growth of *Aspergillus* spp. (Cañas et al., 2008). Obviously, the environmental conditions of a vineyard play a key role in the contamination of ochratoxin-producing species in wine grapes, further leading to the accumulation of OTA in wine (Gil-Serna et al., 2018; Abarca et al., 2019). Before wine fermentation, the grape skin and pulp are crushed and macerated together, which is conducive to the release of OTA into the grape juice (Visconti et al., 2008). The OTA content changes greatly in the whole winemaking process (Anli and Bayram, 2009; Freire et al., 2020). Due to the different winemaking processes, red wines generally have higher OTA levels compared with white wines (Lasram et al., 2008; Dachery et al., 2017).

Some methods, such as avoiding mycete infection, degrading OTA, and adsorbing OTA, have been developed to decrease the contamination of OTA (Chen et al., 2018). Applying biological control methods to avoid mold infection during the storage of grapes after harvest and removing moldy grape clusters before fermentation can greatly reduce the possibility of toxin-producing fungal growth and production of OTA (Hocking et al., 2007; Gil-Serna et al., 2018). Inorganic adsorbents (such as zeolite and activated carbon) (Piotrowska et al., 2013; Abrunhosa et al., 2014) and microbial adsorbents (such as *Saccharomyces* spp., *Rhodotorula* spp., *Lactobacillus* spp., and *Cryptococcus* spp.) (Abrunhosa et al., 2010; Russo et al., 2016) reduce the OTA content through adsorbing or converting OTA into less toxic phenylalanine (Phe) and ochratoxin alpha (OTα). However, the application of these adsorbents in OTA control in wine is limited because they can adsorb phenolic compounds and pigments of wine to varying degrees, resulting in wine discoloration, besides adsorbing the risky OTA (Caridi, 2013; Petruzzi et al., 2015). Moreover, microbial-derived enzymes with carboxypeptidase A activity also affect the degradation of OTA (Amézqueta et al., 2009).

Ethyl Carbamate

As early as 1943, EC was classified as a Class 2A carcinogen by the International Agency for Research on Cancer of the World Health Organization (2007) (Conacher and Page, 1986; Zimmerli and Schlatter, 1991). EC is a carcinogenic compound involved, among others, in lung cancer, lymphoma, liver cancer, and skin cancer (Gowd et al., 2018). However, it is believed that EC widely occurs in traditional fermented foods (Li and Bardají, 2017). EC has been recognized as one of the biggest challenges facing the alcoholic beverage industry since EC was

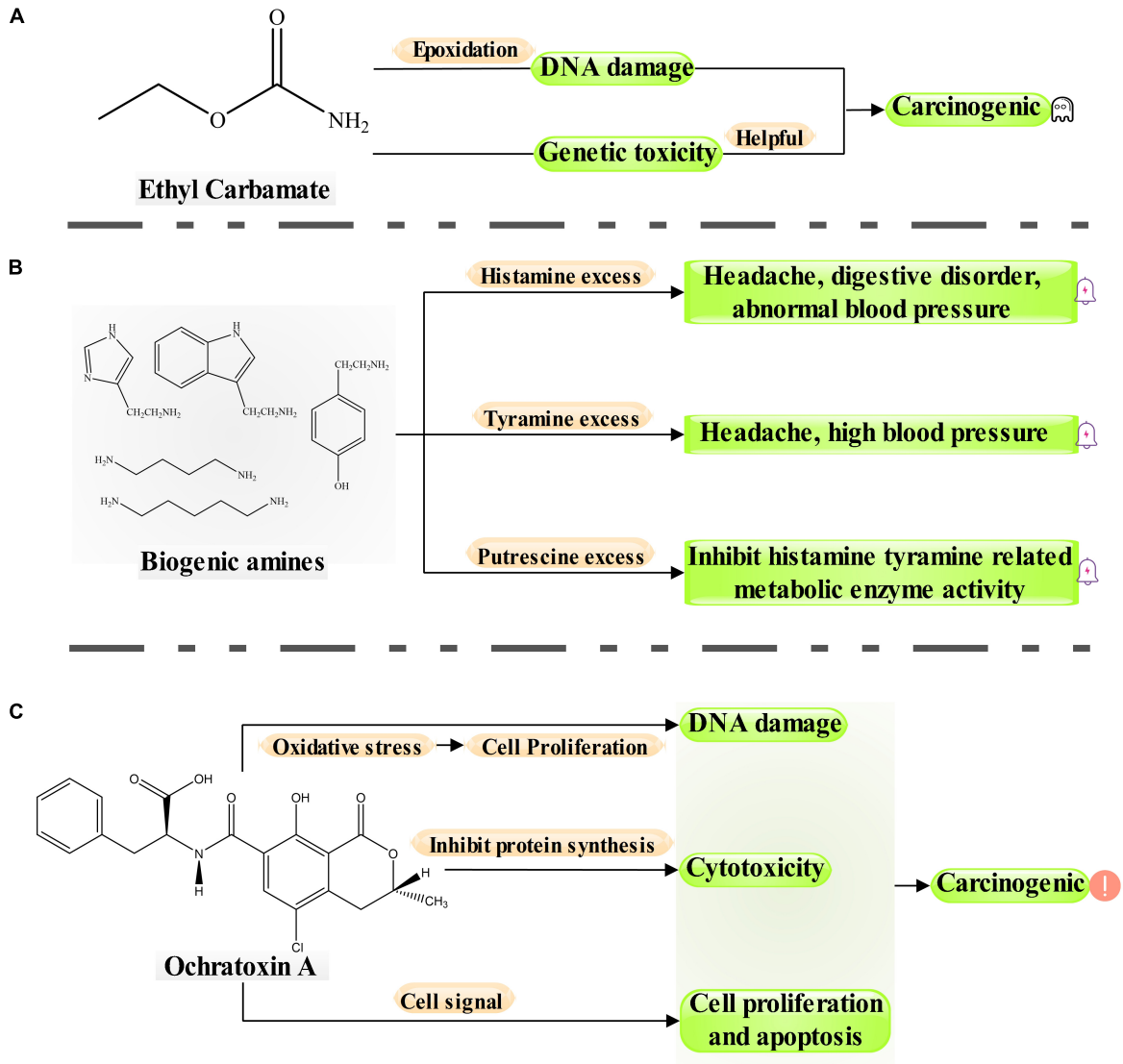

FIGURE 1 | Hazard process of biologically harmful products (ethyl carbamate, biogenic amines and ochratoxin A) in wine.

detected in alcoholic beverages in 1976 (Ough, 1976; Zhao et al., 2013a). **Supplementary Figure 3** shows the possible pathways of the formation of EC and the mechanism of carcinogenesis (Zhao et al., 2013a). Different countries and organizations around the world have different standards for the concentration of EC in alcoholic beverages (**Supplementary Table 1**). Also, no unified maximum EC limit exists in the EU. However, the concentration of EC in 30.6% of wines exceeds 20 μg/L (standard of the Food and Agriculture Organization of the United Nations), which is a threat to the health of consumers and the sustainable development of the wine industry (Gowd et al., 2018).

EC is generally produced by the spontaneous reaction of ethanol and compounds containing carbamoyl groups (such as urea, citrulline, carbamoyl phosphate, and so on) (Jiao et al., 2014). Among these reactions, the urea formation pathway is believed to be the main formation pathway of EC (Zimmerli and Schlatter, 1991; Cerreti et al., 2016). Wine environments (such as temperature and acidity) and microorganisms can affect the production of EC during fermentation (Zhao et al., 2013a). During grape plantation, the application of nitrogen fertilizer increased the urea content, providing EC precursors in grapes (Garde-Cerdán et al., 2015). Furthermore, yeast and LAB produced a large amount of citrulline through the urea cycle pathway and the arginine deiminase metabolism pathway, respectively (Azevedo et al., 2002; Vrancken et al., 2009). During wine fermentation, some EC precursors have been released, increasing the urea content in wine (Mira de Orduña et al., 2000). The EC content in wine varied with grape varieties (Ubeda et al., 2020), grape maturity (Lago et al., 2017), pH value (Araque et al., 2013), EC precursor concentration (Zhao et al., 2013b), the volume fraction of ethanol (Araque et al., 2013), and ecological

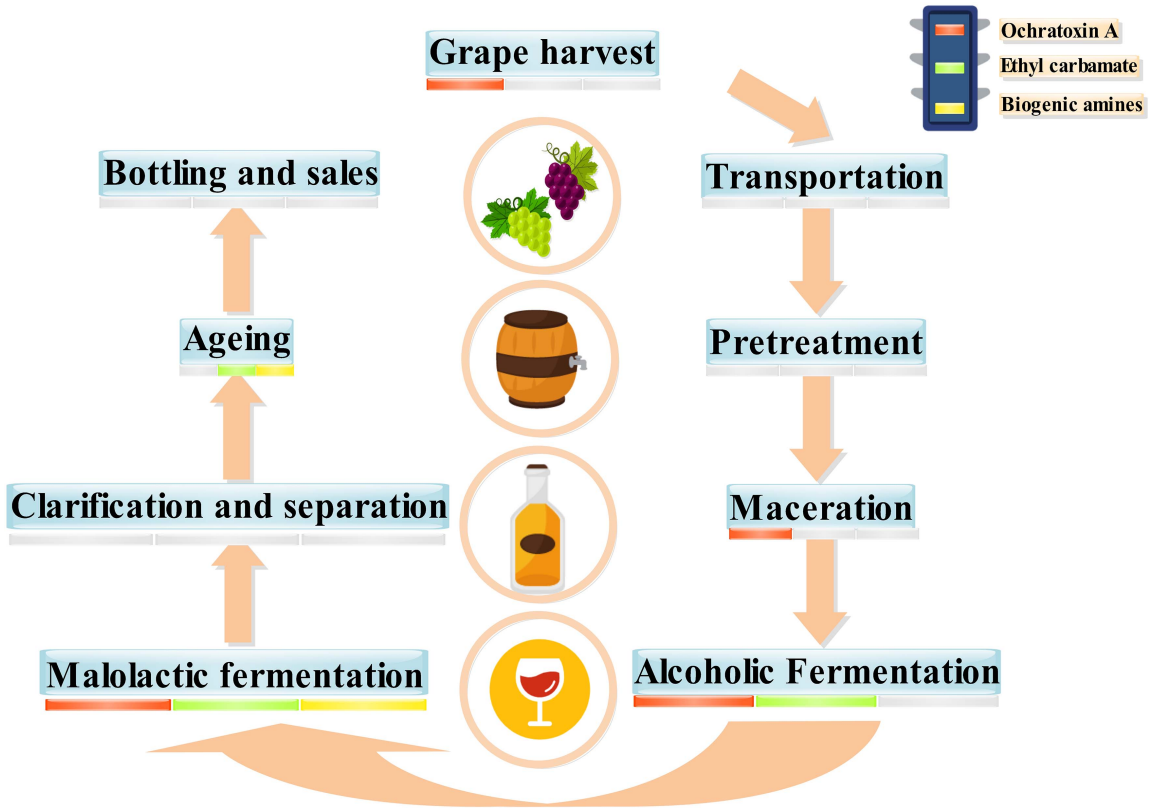

FIGURE 2 | Winemaking process and possible safety hazards.

conditions (such as temperature, precipitation, and extreme climate) (Diamantidou et al., 2018).

Controlling the EC content in wine mainly focuses on yeast strains (Araque et al., 2013; Guo T. et al., 2016), grapes (Bell and Henschke, 2005), excipients (Bell and Henschke, 2005), and fermentation conditions (Stevens and Ough, 1993; Xue et al., 2015). The enhancement of genes encoding for enzymes involved in urea degradation and transport or the knockout of genes encoding for arginase allowed the selection of yeast strains with low urea production capacity and arginase activity (Araque et al., 2013; Guo X. W. et al., 2016). Properly adjusted vineyard management practices, such as fertilization, pruning, irrigation, and ground cover, can also control the EC content in wine to some extent (Soufleros et al., 2003). Without affecting the flavor of the wine, an appropriate reduction in temperature also helps reduce the EC content in the wine, which is a key adjustment point for EC control from a process perspective (Hasnip et al., 2004). Some studies showed that acid urease catalyzed the decomposition of urea to ammonia and carbon dioxide, decreasing the content of an important precursor of EC in wine (Cerreti et al., 2016; Liu et al., 2018; Yang et al., 2021). Since 1999, Europe has approved the use of acid urease extracted from fermented LAB in wine (Cerreti et al., 2016). However, urease is a metalloenzyme with nickel as a prosthetic group, which can lead to nickel residues in wine (Follmer et al., 2004). Furthermore, urea adsorbents, EC degrading enzymes, EC adsorbents, and so forth have been used as effective and potential agents to controlling the EC content in wine under the premise of ensuring the flavor characteristics of the original wine (Wu et al., 2014; Zhou et al., 2017).

Biogenic Amines

BAs are a class of low-molecular-weight nitrogen-containing organic compounds (Manetta et al., 2016). A physiological concentration of BAs is involved in important biological reactions in the human body (Cinquina et al., 2004). However, the excessive intake of exogenous BAs can lead to allergic reactions, such as headache, nausea, blood pressure changes, and respiratory disorders, and is even life-threatening (Spano et al., 2010). BAs include mainly tryptamine, cadaverine, tyramine, histamine, putrescine, spermidine, and spermine (**Supplementary Table 2**), which are usually produced after decarboxylation of the corresponding amino acids by different decarboxylases (**Supplementary Figure 4**; Wolken et al., 2006). As the most toxic BAs, histamine is regarded as a key indicator of the hygienic value during wine fermentation (Cunha et al., 2017). It can be broken down by two different oxidase enzymes (monoamine oxidase and diamine oxidase) (Seiler, 2004). However, ethanol is an inhibitor of diamine oxidase (histamine-degrading) at the gut level (García-Ruiz et al., 2011). Putrescine has been found to be one of the most abundant BAs in wine (Henríquez-Aedo et al., 2012; Cunha et al., 2017).

Therefore, the BA content is more stringent in alcoholic foods compared with other fermented foods (Rollan et al., 1995; García-Ruiz et al., 2011). The European countries have set limits for histamine below 10 mg/L in wine, with Germany being the strictest (not higher than 2 mg/L) (Smit et al., 2008; Costantini et al., 2019).

BAs are produced by microorganisms with amino acid decarboxylase activity in the presence of sufficient free amino acids at any stage of winemaking (Santos, 1996). The presence of precursors (amino acids) and microorganisms with decarboxylase activity are the main factors affecting the BA content (Landete et al., 2011; Russo et al., 2016). During winemaking, yeast strains weakly contribute to BA accumulation (Smit et al., 2013), but LAB responsible for MLF has been identified as the main producer of BAs in wine (Spano et al., 2010). For example, *Oenococcus oeni*, *Lactobacillus hilgardii*, and *Pediococcus parvulus* increased the BA content in wine through histamine accumulation (Özogul and Hamed, 2018). As one of the main catabolites from arginine degradation, putrescine has been identified as one of the most abundant BAs in wine, because arginine is the main amino acids in grapes (Henríquez-Aedo et al., 2012; Ortega-Heras et al., 2014; Cunha et al., 2017). *O. oeni* also contributes to putrescine accumulation after sequential degradation of arginine and ornithine (Pessione and Cirrincione, 2016). On the other hand, increasing pH can increase the number and variety of microorganisms, further enhancing the risk (Guo et al., 2015). The BA content in white wines is less than that in red wines because of a lower pH and the different winemaking processes (García-Marino et al., 2010).

The production of BAs is a strategy to obtain metabolic advantages to face certain stress conditions. Therefore, conditions encouraging the expression of decarboxylase genes should be avoided and controlled (Mohedano et al., 2015). Moreover, commercial starters with negative decarboxylase activity are also recommended (Gardini et al., 2016). Several authors have proposed that yeast can convert amino acids into fused alcohols through the well-known Ehrlich pathway during alcoholic fermentation, plausibly leading to a decrease in the BA content (Mas et al., 2014). In a sense, the presence of putrescine in wine seems inevitable, because the ornithine decarboxylation occurs simultaneously with MLF at a high speed (Martínez-Pinilla et al., 2013; Battistelli et al., 2020). Due to the presence of the indigenous strains capable of degrading arginine to ornithine, the use of the malolactic starters that are unable to degrade ornithine or arginine cannot completely avoid accumulation of putrescine (Pramateftaki et al., 2012). It is plausible that removing or inhibiting the activity of LAB immediately after MLF to avoid arginine degradation may be an effective method to reduce potential risk from putrescine in wine (Wunderlichová et al., 2014). Therefore, controlling microbiota is a good strategy to reduce BA production. García-Ruiz et al. (2011) found that nine strains belonging to the *Lactobacillus* and *Pediococcus* groups showed the greatest BA degradation capacity, the best being for *L. casei* IFI-CA52. Capozzi et al. (2012) have investigated that *Lactobacillus plantarum* NDT 09 and NDT 16 could enhance the overall aroma of wine and degrade putrescine and tyramine. Some yeasts were also capable of degrading BAs. Bäumlisberger et al. (2015) observed that some strains of *Debaryomyces hansenii* and *Yarrowia lipolytica* could degrade BAs. The degradation of BAs by the most efficient strain, *D. hanseniii* H525, could be attributed to a peroxisomal amine oxidase activity. Callejón et al. (2016) reported the employment of laccase to degrade BAs, which provides a new perspective on the use of microorganisms or purified microbial enzymes. Further research should be conducted to find new strains capable of degrading BAs. Also, histamine, putrescine, cadaverine, spermine, and spermidine in wine can be adsorbed and removed by phosphonic acid and sulfonic acid bifunctional mesoporous silica materials, which may also be an effective way to reduce the BA content in wine in the future (Rodríguez-Bencomo et al., 2020).

CONCLUSION AND FUTURE PERSPECTIVES

The quality and safety risks of wine involve many links. To ensure food safety and improve the quality of wine, we need to control the contamination of raw materials, strictly select winemaking microorganisms, and control the fermentation and post-management processes. The study of the origin, evolution, and control techniques of undesirable metabolites in wine (OTA, EC, and BAs) can reduce not only the quality hazards of wine but also the economic losses due to microbial spoilage. In the future, we should pay attention to various potentially harmful substances that have pathogenic effects on human beings during the grape growth and winemaking process, and implement effective prevention and control through testing. In summary, only by clarifying the factors that affect the quality of winemaking can we ensure a clear direction for quality management and ultimately a quality wine production.

AUTHOR CONTRIBUTIONS

XX wrote the main manuscript. TL and YJ conceived the framework of the manuscript. XJ contributed to the pictures in the manuscript. XS and BW coordinated contributions and provided the final draft of the manuscript. All authors commented on the manuscript at all stages.

FUNDING

This study was supported by the Xinjiang Production and Construction Corps (Nos. 2019AB025 and 2020AB014), the Shihezi Science and Technology Bureau (No. 2020GY07), the Shuanghe Science and Technology Bureau (No. 20GY01), and the National Natural Science Foundation of China (No. 31960465).

SUPPLEMENTARY MATERIAL

The Supplementary Material for this article can be found online at: https://www.frontiersin.org/articles/10.3389/fmicb.2021.703391/full#supplementary-material

REFERENCES

Abarca, M. L., Bragulat, M. R., Castellá, G., and Cabañes, F. J. (2019). Impact of some environmental factors on growth and ochratoxin A production by *Aspergillus niger* and *Aspergillus welwitschiae*. *Int. J. Food Microbiol.* 291, 10–16. doi: 10.1016/j.ijfoodmicro.2018.11.001

Abrunhosa, L., Inês, A., Rodrigues, A. I., Guimarães, A., Pereira, V. L., Parpot, P., et al. (2014). Biodegradation of ochratoxin A by *Pediococcus parvulus* isolated from Douro wines. *Int. J. Food Microbiol.* 188, 45–52. doi: 10.1016/j.ijfoodmicro.2014.07.019

Abrunhosa, L., Paterson, R. R., and Venâncio, A. (2010). Biodegradation of ochratoxin A for food and feed decontamination. *Toxins* 2, 1078–1099. doi: 10.3390/toxins2051078

Agriopoulou, S., Stamatelopoulou, E., and Varzakas, T. (2020). Advances in occurrence, importance, and mycotoxin control strategies: prevention and detoxification in foods. *Foods* 9:137. doi: 10.3390/foods9020137

Alebaki, M., and Koutsouris, A. (2019). "Wine tourism destinations across the life-cycle: a comparison of Northern Greece, Peloponnese and Crete," in *Wine Tourism Destination Management and Marketing: Theory and Cases*, eds M. Sigala and R. N. S. Robinson (Cham: Springer International Publishing), 463–482. doi: 10.1007/978-3-030-00437-8_29

Amézqueta, S., González-Peñas, E., Murillo-Arbizu, M., and de Cerain, A. L. (2009). Ochratoxin A decontamination: a review. *Food Control* 20, 326–333. doi: 10.1016/j.foodcont.2008.05.017

Anli, E., and Bayram, M. (2009). Ochratoxin A in wines. *Food Rev. Int.* 25, 214–232. doi: 10.1080/87559120902956182

Araque, I., Bordons, A., and Reguant, C. (2013). Effect of ethanol and low pH on citrulline and ornithine excretion and arc gene expression by strains of *Lactobacillus brevis* and *Pediococcus pentosaceus*. *Food Microbiol.* 33, 107–113. doi: 10.1016/j.fm.2012.09.005

Azevedo, Z., Couto, J. A., and Hogg, T. (2002). Citrulline as the main precursor of ethyl carbamate in model fortified wines inoculated with *Lactobacillus hilgardii*: a marker of the levels in a spoiled fortified wine. *Lett. Appl. Microbiol.* 34, 32–36. doi: 10.1046/j.1472-765x.2002.01045.x

Banks, G., and Overton, J. (2010). Old world, new world, third world? Reconceptualising the worlds of wine. *J. Wine Res.* 21, 57–75. doi: 10.1080/09571264.2010.495854

Battistelli, N., Perpetuini, G., Perla, C., Arfelli, G., Zulli, C., Rossetti, A. P., et al. (2020). Characterization of natural *Oenococcus oeni* strains for Montepulciano d'Abruzzo organic wine production. *Eur. Food Res. Technol.* 246, 1031–1039. doi: 10.1007/s00217-020-03466-3

Bäumlisberger, M., Moellecken, U., König, H., and Claus, H. (2015). The potential of the yeast *Debaryomyces hansenii* H525 to degrade biogenic amines in food. *Microorganisms* 3, 839–850. doi: 10.3390/microorganisms3040839

Beland, F. A., Benson, R. W., Mellick, P. W., Kovatch, R. M., Roberts, D. W., Fang, J.-L., et al. (2005). Effect of ethanol on the tumorigenicity of urethane (ethyl carbamate) in B6C3F1 mice. *Food Chem. Toxicol.* 43, 1–19. doi: 10.1016/j.fct.2004.07.018

Bell, S. J., and Henschke, P. A. (2005). Implications of nitrogen nutrition for grapes, fermentation and wine. *Aust. J. Grape Wine Res.* 11, 242–295. doi: 10.1111/j.1755-0238.2005.tb00028.x

Bora, F. D., Bunea, C. I., Rusu, T., and Pop, N. (2015). Vertical distribution and analysis of micro-, macroelements and heavy metals in the system soil-grapevine-wine in vineyard from North-West Romania. *Chem. Cent. J.* 9:19. doi: 10.1186/s13065-015-0095-2

Callejón, S., Sendra, R., Ferrer, S., and Pardo, I. (2016). Cloning and characterization of a new laccase from *Lactobacillus plantarum* J16 CECT 8944 catalyzing biogenic amines degradation. *Appl. Microbiol. Biotechnol.* 100, 3113–3124.

Cañas, P. I., Romero, E. G., Alonso, S. G., González, M. F., and Herreros, M. P. (2008). Amino acids and biogenic amines during spontaneous malolactic fermentation in Tempranillo red wines. *J. Food Compos. Anal.* 21, 731–735. doi: 10.1016/j.jfca.2007.11.002

Capozzi, V., Russo, P., Ladero, V., Fernández, M., Fiocco, D., Alvarez, M. A., et al. (2012). Biogenic amines degradation by *Lactobacillus plantarum*: toward a potential application in wine. *Front. Microbiol.* 3:122. doi: 10.3389/fmicb.2012.00122

Caridi, A. (2013). Improved screening method for the selection of wine yeasts based on their pigment adsorption activity. *Food Technol. Biotech.* 51, 137–144. doi: 10.1155/2013/578781

Cerreti, M., Fidaleo, M., Benucci, I., Liburdi, K., Tamborra, P., and Moresi, M. (2016). Assessing the potential content of ethyl carbamate in white, red, and rosé wines as a key factor for pursuing urea degradation by purified acid urease. *Afr. J. Food Sci.* 81, C1603–C1612. doi: 10.1111/1750-3841.13344

Chen, W., Li, C., Zhang, B., Zhou, Z., Shen, Y., Liao, X., et al. (2018). Advances in biodetoxification of ochratoxin A-a review of the past five decades. *Front. Microbiol.* 9:1386. doi: 10.3389/fmicb.2018.01386

Christaki, T., and Tzia, C. (2002). Quality and safety assurance in winemaking. *Food Control* 13, 503–517. doi: 10.1016/S0956-7135(02)00030-0

Cinquina, A. L., Calı, A., Longo, F., De Santis, L., Severoni, A., and Abballe, F. (2004). Determination of biogenic amines in fish tissues by ion-exchange chromatography with conductivity detection. *J. Chromatogr. A* 1032, 73–77. doi: 10.1016/j.chroma.2004.01.013

Conacher, H. B. S., and Page, B. D. (1986). Ethyl carbamate in alcoholic beverages, a canadian case history; proceedings of the euro food toxicity, interdisciplinary conference on natural toxicants in food. *Eur. Soc. Toxicol.* 1, 237–242.

Costantini, A., Vaudano, E., Pulcini, L., Carafa, T., and Garcia-Moruno, E. (2019). An overview on biogenic amines in wine. *Beverages* 5:19. doi: 10.3390/beverages5010019

Cunha, S. C., Lopes, R., and Fernandes, J. O. (2017). Biogenic amines in liqueurs: influence of processing and composition. *J. Food Compos. Anal.* 56, 147–155. doi: 10.1016/j.jfca.2016.11.016

Dachery, B., Veras, F. F., Dal Magro, L., Manfroi, V., and Welke, J. E. (2017). Exposure risk assessment to ochratoxin A through consumption of juice and wine considering the effect of steam extraction time and vinification stages. *Food Chem. Toxicol.* 109, 237–244. doi: 10.1016/j.fct.2017.09.013

Diamantidou, D., Zotou, A., and Theodoridis, G. (2018). Wine and grape marc spirits metabolomics. *Metabolomics* 14:159. doi: 10.1007/s11306-018-1458-1

Ditano-Vázquez, P., Torres-Peña, J. D., Galeano-Valle, F., Pérez-Caballero, A. I., Demelo-Rodríguez, P., Lopez-Miranda, J., et al. (2019). The fluid aspect of the mediterranean diet in the prevention and management of cardiovascular disease and diabetes: the role of polyphenol content in moderate consumption of wine and olive oil. *Nutrients* 11:2833. doi: 10.3390/nu11112833

Du, H., Song, Z., and Xu, Y. (2018). Ethyl carbamate formation regulated by lactic acid bacteria and nonconventional yeasts in solid-state fermentation of Chinese Moutai-flavor liquor. *J. Agric. Food Chem.* 66, 387–392. doi: 10.1021/acs.jafc.7b05034

European Food Safety Authority (EFSA) (2006). Opinion of the scientific panel on contaminants in the food chain on a request (from) commission related to Ochratoxin A in food. *EFSA J.* 365, 1–56.

Fernández-Segovia, I., Pérez-Llácer, A., Peidro, B., and Fuentes, A. (2014). Implementation of a food safety management system according to ISO 22000 in the food supplement industry: a case study. *Food Control* 43, 28–34. doi: 10.1016/j.foodcont.2014.02.042

Follmer, C., Pereira, F. V., Da Silveira, N. P., and Carlini, C. R. (2004). Jack bean urease (EC 3.5. 1.5) aggregation monitored by dynamic and static light scattering. *Biophys. Chem.* 111, 79–87. doi: 10.1016/j.bpc.2004.03.009

Freire, L., Braga, P. A., Furtado, M. M., Delafiori, J., Dias-Audibert, F. L., Pereira, G. E., et al. (2020). From grape to wine: fate of ochratoxin A during red, rose, and white winemaking process and the presence of ochratoxin derivatives in the final products. *Food Control* 113:107167. doi: 10.1016/j.foodcont.2020.107167

Gallo, A., Ferrara, M., and Perrone, G. (2017). Recent advances on the molecular aspects of ochratoxin A biosynthesis. *Curr. Opin. Food Sci.* 17, 49–56. doi: 10.1016/j.cofs.2017.09.011

García-Marino, M., Trigueros, Á, and Escribano-Bailón, T. (2010). Influence of oenological practices on the formation of biogenic amines in quality red wines. *J. Food Compos. Anal.* 23, 455–462. doi: 10.1016/j.jfca.2010.02.003

García-Ruiz, A., González-Rompinelli, E. M., Bartolomé, B., and Moreno-Arribas, M. V. (2011). Potential of wine-associated lactic acid bacteria to degrade biogenic amines. *Int. J. Food Microbiol.* 148, 115–120. doi: 10.1016/j.ijfoodmicro.2011.05.009

Garde-Cerdán, T., Santamaría, P., Rubio-Bretón, P., González-Arenzana, L., López-Alfaro, I., and López, R. (2015). Foliar application of proline, phenylalanine, and urea to Tempranillo vines: effect on grape volatile

composition and comparison with the use of commercial nitrogen fertilizers. *LWT Food Sci. Technol.* 60, 684–689. doi: 10.1016/j.lwt.2014.10.028

Gardini, F., Özogul, Y., Suzzi, G., Tabanelli, G., and Özogul, F. (2016). Technological factors affecting biogenic amine content in foods: a review. *Front. Microbiol.* 7:1218. doi: 10.3389/fmicb.2016.01218

Gil-Serna, J., Vázquez, C., González-Jaén, M. T., and Patiño, B. (2018). Wine contamination with ochratoxins: a review. *Beverages* 4:6. doi: 10.3390/beverages4010006

Gowd, V., Su, H., Karlovsky, P., and Chen, W. (2018). Ethyl carbamate: an emerging food and environmental toxicant. *Food Chem.* 248, 312–321. doi: 10.1016/j.foodchem.2017.12.072

Guilford, J. M., and Pezzuto, J. M. (2011). Wine and health: a review. *Am. J. Enol. Viticult.* 62:471. doi: 10.5344/ajev.2011.11013

Guo, T., Fang, P., Jiang, J., Zhang, F., Yong, W., Liu, J., et al. (2016). Rapid screening and quantification of residual pesticides and illegal adulterants in red wine by direct analysis in real time mass spectrometry. *J. Chromatogr. A* 1471, 27–33. doi: 10.1016/j.chroma.2016.09.073

Guo, X. W., Li, Y. Z., Guo, J., Wang, Q., Huang, S. Y., Chen, Y. F., et al. (2016). Reduced production of ethyl carbamate for wine fermentation by deleting CAR1 in *Saccharomyces cerevisiae*. *J. Ind. Microbiol. Biotechnol.* 43, 671–679. doi: 10.1007/s10295-016-1737-7

Guo, Y. Y., Yang, Y. P., Peng, Q., and Han, Y. (2015). Biogenic amines in wine: a review. *Int. J. Food Sci. Technol.* 50, 1523–1532. doi: 10.1111/ijfs.12833

Hasnip, S., Caputi, A., Crews, C., and Brereton, P. (2004). Effects of storage time and temperature on the concentration of ethyl carbamate and its precursors in wine. *Food Addit. Contam.* 21, 1155–1161. doi: 10.1080/02652030400019851

Henríquez-Aedo, K., Vega, M., Prieto-Rodríguez, S., and Aranda, M. (2012). Evaluation of biogenic amines content in Chilean reserve varietal wines. *Food Chem. Toxicol.* 50, 2742–2750. doi: 10.1016/j.fct.2012.05.034

Hocking, A. D., Leong, S. L., Kazi, B. A., Emmett, R. W., and Scott, E. S. (2007). Fungi and mycotoxins in vineyards and grape products. *Int. J. Food Microbiol.* 119, 84–88. doi: 10.1016/j.ijfoodmicro.2007.07.031

Iacumin, L., Chiesa, L., Boscolo, D., Manzano, M., Cantoni, C., Orlic, S., et al. (2009). Moulds and ochratoxin A on surfaces of artisanal and industrial dry sausages. *Food Microbiol.* 26, 65–70. doi: 10.1016/j.fm.2008.07.006

Jiang, C., Shi, J., and Zhu, C. (2013). Fruit spoilage and ochratoxin a production by *Aspergillus carbonarius* in the berries of different grape cultivars. *Food Control* 30, 93–100. doi: 10.1016/j.foodcont.2012.07.039

Jiao, Z., Dong, Y., and Chen, Q. (2014). Ethyl carbamate in fermented beverages: presence, analytical chemistry, formation mechanism, and mitigation proposals. *Compr. Rev. Food Sci. Food Saf.* 13, 611–626. doi: 10.1111/1541-4337.12084

Karlovsky, P. (1999). Biological detoxification of fungal toxins and its use in plant breeding, feed and food production. *Nat. Toxins* 7, 1–23. doi: 10.1002/(SICI)1522-7189(199902)7:1<1::AID-NT37<3.0.CO;2-9

Lago, L. O., Nicolli, K. P., Marques, A. B., Zini, C. A., and Welke, J. E. (2017). Influence of ripeness and maceration of the grapes on levels of furan and carbonyl compounds in wine–simultaneous quantitative determination and assessment of the exposure risk to these compounds. *Food Chem.* 230, 594–603. doi: 10.1016/j.foodchem.2017.03.090

Landete, J. M., de las Rivas, B., Marcobal, A., and Muñoz, R. (2011). PCR methods for the detection of biogenic amine-producing bacteria on wine. *Ann. Microbiol.* 61, 159–166. doi: 10.1007/s13213-010-0068-6

Lasram, S., Mani, A., Zaied, C., Chebil, S., Abid, S., Bacha, H., et al. (2008). Evolution of ochratoxin A content during red and rose vinification. *J. Sci. Food Agric.* 88, 1696–1703. doi: 10.1002/jsfa.3266

Li, H., Wang, H., Li, H., Goodman, S., van der Lee, P., Xu, Z., et al. (2018). The worlds of wine: old, new and ancient. *Wine Econ. Policy* 7, 178–182. doi: 10.1016/j.wep.2018.10.002

Li, Y., and Bardají, I. (2017). A new wine superpower? An analysis of the Chinese wine industry. *Cah. Agric.* 26:65002. doi: 10.1051/cagri/2017051

Liu, Q., Yao, X., Liang, Q., Li, J., Fang, F., Du, G., et al. (2018). Molecular engineering of *Bacillus paralicheniformis* acid urease to degrade urea and ethyl carbamate in model Chinese rice wine. *J. Agric. Food Chem.* 66, 13011–13019. doi: 10.1021/acs.jafc.8b04566

Manetta, A. C., Di Giuseppe, L., Tofalo, R., Martuscelli, M., Schirone, M., Giammarco, M., et al. (2016). Evaluation of biogenic amines in wine: determination by an improved HPLC-PDA method. *Food Control* 62, 351–356. doi: 10.1016/j.foodcont.2015.11.009

Martínez-Pinilla, O., Guadalupe, Z., Hernández, Z., and Ayestarán, B. (2013). Amino acids and biogenic amines in red varietal wines: the role of grape variety, malolactic fermentation and vintage. *Eur. Food Res. Technol.* 237, 887–895. doi: 10.1007/s00217-013-2059-x

Mas, A., Guillamon, J. M., Torija, M. J., Beltran, G., Cerezo, A. B., Troncoso, A. M., et al. (2014). Bioactive compounds derived from the yeast metabolism of aromatic amino acids during alcoholic fermentation. *BioMed. Res. Int.* 2014:898045. doi: 10.1155/2014/898045

Mira de Orduña, R., Liu, S. Q., Patchett, M. L., and Pilone, G. J. (2000). Ethyl carbamate precursor citrulline formation from arginine degradation by malolactic wine lactic acid bacteria. *FEMS Microbiol. Lett.* 183, 31–35. doi: 10.1111/j.1574-6968.2000.tb08929.x

Mohedano, M. L., López, P., Spano, G., and Russo, P. (2015). "Controlling the formation of biogenic amines in fermented foods," in *Advances in Fermented Foods and Beverages*, ed. W. Holzapfel (Sawston: Woodhead Publishing), 273–310.

Morata, A., Bañuelos, M. A., Vaquero, C., Loira, I., Cuerda, R., Palomero, F., et al. (2019). *Lachancea thermotolerans* as a tool to improve pH in red wines from warm regions. *Eur. Food Res. Technol.* 245, 885–894. doi: 10.1007/s00217-019-03229-9

Nettleship, A., Henshaw, P. S., and Meyer, H. L. (1943). Induction of pulmonary tumors in mice with ethyl carbamate (urethane). *J. Natl. Cancer Inst.* 4, 309–319. doi: 10.1093/jnci/4.3.309

OIV (2020). *State of the World Vitivinicultural Sector in 2020*. Available online at: https://www.oiv.int/en/oiv-life/2020-a-year-of-resilience (accessed April 20, 2021)

Oliveri, C., Bella, P., Tessitori, M., Catara, V., and La Rosa, R. (2017). Grape and environmental mycoflora monitoring in old, traditionally cultivated vineyards on Mount Etna, southern Italy. *J. Sci. Food Agric.* 97, 65–73. doi: 10.1002/jsfa.7683

Ortega-Heras, M., Pérez-Magariño, S., Del-Villar-Garrachón, V., González-Huerta, C., Moro Gonzalez, L. C., Guadarrama Rodríguez, A., et al. (2014). Study of the effect of vintage, maturity degree, and irrigation on the amino acid and biogenic amine content of a white wine from the *Verdejo* variety. *J. Sci. Food Agric.* 94, 2073–2082. doi: 10.1002/jsfa.6526

Ough, C. S. (1976). Ethyl carbamate in fermented beverages and foods. I. Naturally occurring ethylcarbamate. *J. Agric. Food. Chem.* 24, 323–328. doi: 10.1021/jf60204a033

Özogul, F., and Hamed, I. (2018). The importance of lactic acid bacteria for the prevention of bacterial growth and their biogenic amines formation: a review. *Crit. Rev. Food Sci. Nutr.* 58, 1660–1670. doi: 10.1080/10408398.2016.1277972

Pessione, E., and Cirrincione, S. (2016). Bioactive molecules released in food by lactic acid bacteria: encrypted peptides and biogenic amines. *Front. Microbiol.* 7:876. doi: 10.3389/fmicb.2016.00876

Petruzzi, L., Baiano, A., De Gianni, A., Sinigaglia, M., Corbo, M. R., and Bevilacqua, A. (2015). Differential adsorption of ochratoxin A and anthocyanins by inactivated yeasts and yeast cell walls during simulation of wine aging. *Toxins* 7, 4350–4365. doi: 10.3390/toxins7104350

Piotrowska, M., Nowak, A., and Czyzowska, A. (2013). Removal of ochratoxin A by wine *Saccharomyces cerevisiae* strains. *Eur. Food Res. Technol.* 236, 441–447. doi: 10.1007/s00217-012-1908-3

Prameteftaki, P. V., Metafa, M., Karapetrou, G., and Marmaras, G. (2012). Assessment of the genetic polymorphism and biogenic amine production of indigenous *Oenococcus oeni* strains isolated from Greek red wines. *Food Microbiol.* 29, 113–120. doi: 10.1016/j.fm.2011.09.007

Rivera, K., Salas-Pérez, F., Echeverría, G., Urquiaga, I., Dicenta, S., Pérez, D., et al. (2019). Red wine grape pomace attenuates atherosclerosis and myocardial damage and increases survival in association with improved plasma antioxidant activity in a murine model of lethal ischemic heart disease. *Nutrients* 11:2135. doi: 10.3390/nu11092135

Rodríguez-Bencomo, J. J., Rigou, P., Mattivi, F., López, F., and Mehdi, A. (2020). Removal of biogenic amines from wines by chemisorption on functionalized silica and effects on other wine components. *Sci. Rep.* 10:17279. doi: 10.1038/s41598-020-74287-3

Rollan, G. C., Coton, E., and Lonvaud-Funel, A. (1995). Histidine decarboxylase activity of *Leuconostoc oenos* 9204. *Food Microbiol.* 12, 455–461. doi: 10.1016/S0740-0020(95)80130-8

Ruiz, J., Kiene, F., Belda, I., Fracassetti, D., Marquina, D., Navascués, E., et al. (2019). Effects on varietal aromas during wine making: a review of the impact of varietal aromas on the flavor of wine. *Appl. Microbiol. Biotechnol.* 103, 7425–7450. doi: 10.1007/s00253-019-10008-9

Russo, P., Capozzi, V., Spano, G., Corbo, M. R., Sinigaglia, M., and Bevilacqua, A. (2016). Metabolites of microbial origin with an impact on health: ochratoxin A and biogenic amines. *Front. Microbiol.* 7:482. doi: 10.3389/fmicb.2016.00482

Santos, M. S. (1996). Biogenic amines: their importance in foods. *Int. J. Food Microbiol.* 29, 213–231. doi: 10.1016/0168-1605(95)00032-1

Schamel, G. (2006). Geography versus brands in a global wine market. *Agribusiness* 22, 363–374. doi: 10.1002/agr.20091

Seiler, N. (2004). Catabolism of polyamines. *Amino Acids* 26, 217–233. doi: 10.1007/s00726-004-0070-z

Silva, L. J. G., Rodrigues, A. P., Pereira, A. M. P. T., Lino, C. M., and Pena, A. (2019). Ochratoxin A in the Portuguese wine market, occurrence and risk assessment. *Food Addit. Contam. B* 12, 145–149. doi: 10.1080/19393210.2019.1595169

Smit, A. Y., du Toit, W. J., Stander, M., and du Toit, M. (2013). Evaluating the influence of maceration practices on biogenic amine formation in wine. *LWT Food Sci. Technol.* 53, 297–307. doi: 10.1016/j.lwt.2013.01.006

Smit, A., du Toit, W., and Du Toit, M. (2008). Biogenic amines in wine: understanding the headache. *S. Afr. J. Enol. Vitic.* 29, 109–127. doi: 10.21548/29-2-1444

Soufleros, E. H., Bouloumpasi, E., Tsarchopoulos, C., and Biliaderis, C. G. (2003). Primary amino acid profiles of Greek white wines and their use in classification according to variety, origin and vintage. *Food Chem.* 80, 261–273. doi: 10.1016/S0308-8146(02)00271-6

Spano, G., Russo, P., Lonvaud-Funel, A., Lucas, P., Alexandre, H., Grandvalet, C., et al. (2010). Biogenic amines in fermented foods. *Eur. J. Clin. Nutr.* 64, S95–S100. doi: 10.1038/ejcn.2010.218

Stevens, D. F., and Ough, C. S. (1993). Ethyl carbamate formation: reaction of urea and citrulline with ethanol in wine under low to normal temperature conditions. *Am. J. Enol. Viticult.* 44, 309–312. doi: 10.1016/S0065-2164(08)70598-7

Thorpe, M. (2009). The globalisation of the wine industry: new world, old world and China. *China Agr. Econ. Rev.* 1, 301–313. doi: 10.1108/17561370910958873

Ubeda, C., Hornedo-Ortega, R., Cerezo, A. B., Garcia-Parrilla, M. C., and Troncoso, A. M. (2020). Chemical hazards in grapes and wine, climate change and challenges to face. *Food Chem.* 314:126222. doi: 10.1016/j.foodchem.2020.126222

Uthurry, C. A., Lepe, J. A. S., Lombardero, J., and García Del Hierro, J. R. (2006). Ethyl carbamate production by selected yeasts and lactic acid bacteria in red wine. *Food Chem.* 94, 262–270. doi: 10.1016/j.foodchem.2004.11.017

Varga, J., and Kozakiewicz, Z. (2006). Ochratoxin A in grapes and grape-derived products. *Trends Food Sci. Technol.* 17, 72–81. doi: 10.1016/j.tifs.2005.10.007

Visconti, A., Perrone, G., Cozzi, G., and Solfrizzo, M. (2008). Managing ochratoxin A risk in the grape-wine food chain. *Food Addit. Contam. A* 25, 193–202. doi: 10.1080/02652030701744546

Vitali Čepo, D., Pelajić, M., Vinković Vrček, I., Krivohlavek, A., Žuntar, I., and Karoglan, M. (2018). Differences in the levels of pesticides, metals, sulphites and ochratoxin A between organically and conventionally produced wines. *Food Chem.* 246, 394–403. doi: 10.1016/j.foodchem.2017.10.133

Vrancken, G., Rimaux, T., Weckx, S., De Vuyst, L., and Leroy, F. (2009). Environmental pH determines citrulline and ornithine release through the arginine deiminase pathway in *Lactobacillus fermentum* IMDO 130101. *Int. J. Food Microbiol.* 135, 216–222. doi: 10.1002/bit.260480111

Welke, J. E. (2019). Fungal and mycotoxin problems in grape juice and wine industries. *Curr. Opin. Food Sci.* 29, 7–13. doi: 10.1016/j.cofs.2019.06.009

Weng, X., and Neethirajan, S. (2017). Ensuring food safety: quality monitoring using microfluidics. *Trends Food Sci. Technol.* 65, 10–22. doi: 10.1016/j.tifs.2017.04.015

Wolken, W. A., Lucas, P. M., Lonvaud-Funel, A., and Lolkema, J. S. (2006). The mechanism of the tyrosine transporter TyrP supports a proton motive tyrosine decarboxylation pathway in *Lactobacillus brevis*. *J. Bacteriol.* 188, 2198–2206. doi: 10.1128/JB.188.6.2198-2206.2006

Wu, P., Cai, C., Shen, X., Wang, L., Zhang, J., Tan, Y., et al. (2014). Formation of ethyl carbamate and changes during fermentation and storage of yellow rice wine. *Food Chem.* 152, 108–112. doi: 10.1016/j.foodchem.2013.11.135

Wunderlichová, L., Buňková, L., Koutný, M., Jančová, P., and Buňka, F. (2014). Formation, degradation, and detoxification of putrescine by foodborne bacteria: a review. *Compr. Rev Food Sci. Food Saf.* 13, 1012–1030. doi: 10.1111/1541-4337.12099

Xue, J., Fu, F., Liang, M., Zhao, C., Wang, D., and Wu, Y. (2015). Ethyl carbamate production kinetics during wine storage. *S. Afr. J. Enol. Vitic.* 36, 277–284.

Yang, H., Cai, G., Lu, J., and Gómez Plaza, E. (2021). The production and application of enzymes related to the quality of fruit wine. *Crit. Rev. Food Sci. Nutr.* 61, 1605–1615. doi: 10.1080/10408398.2020.1763251

Zhao, X., Du, G., Zou, H., Fu, J., Zhou, J., and Chen, J. (2013a). Progress in preventing the accumulation of ethyl carbamate in alcoholic beverages. *Trends Food Sci. Technol.* 32, 97–107. doi: 10.1016/j.tifs.2013.05.009

Zhao, X., Zou, H., Fu, J., Chen, J., Zhou, J., and Du, G. J. Y. (2013b). Nitrogen regulation involved in the accumulation of urea in *Saccharomyces cerevisiae*. *Yeast* 30, 437–447. doi: 10.1002/yea.2980

Zhou, W., Fang, R., and Chen, Q. (2017). Effect of gallic and protocatechuic acids on the metabolism of ethyl carbamate in Chinese yellow rice wine brewing. *Food Chem.* 233, 174–181. doi: 10.1016/j.foodchem.2017.04.113

Zimmerli, B., and Dick, R. (1996). Ochratoxin A in table wine and grape-juice: occurrence and risk assessment. *Food Addit. Contam.* 13, 655–668. doi: 10.1080/02652039609374451

Zimmerli, B., and Schlatter, J. (1991). Ethyl carbamate: analytical methodology, occurrence, formation, biological activity and risk assessment. *Mutat. Res.* 259, 325–350. doi: 10.1016/0165-1218(91)90126-7

Conflict of Interest: The authors declare that the research was conducted in the absence of any commercial or financial relationships that could be construed as a potential conflict of interest.

frontiers in Microbiology

MINI REVIEW
published: 29 July 2021
doi: 10.3389/fmicb.2021.703284

A Review on the General Cheese Processing Technology, Flavor Biochemical Pathways and the Influence of Yeasts in Cheese

Xiaochun Zheng, Xuewei Shi and Bin Wang**

Food College, Shihezi University, Shihezi, China

Cheese has a long history and this naturally fermented dairy product contains a range of distinctive flavors. Microorganisms in variety cheeses are an essential component and play important roles during both cheese production and ripening. However, cheeses from different countries are still handmade, the processing technology is diverse, the microbial community structure is complex and the cheese flavor fluctuates greatly. Therefore, studying the general processing technology and relationship between microbial structure and flavor formation in cheese is the key to solving the unstable quality and standardized production of cheese flavor on basis of maintaining the flavor of cheese. This paper reviews the research progress on the general processing technology and key control points of natural cheese, the biochemical pathways for production of flavor compounds in cheeses, the diversity and the role of yeasts in cheese. Combined with the development of modern detection technology, the evolution of microbial structure, population evolution and flavor correlation in cheese from different countries was analyzed, which is of great significance for the search for core functional yeast microorganisms and the industrialization prospect of traditional fermented cheese.

Keywords: cheese, flavor compounds, general craftsmanship, yeast, biochemical pathways

OPEN ACCESS

Edited by:
Xucong Lv,
Fuzhou University, China

Reviewed by:
Yongqiang Zhao,
Chinese Academy of Fishery Sciences (CAFS), China
Aly Farag El Sheikha,
Jiangxi Agricultural University, China

****Correspondence:***
Bin Wang
binwang0228@shzu.edu.cn
Xuewei Shi
shixuewei@shzu.edu.cn

Specialty section:
This article was submitted to Food Microbiology, a section of the journal Frontiers in Microbiology

Received: *30 April 2021*
Accepted: *12 July 2021*
Published: *29 July 2021*

Citation:
Zheng X, Shi X and Wang B (2021) A Review on the General Cheese Processing Technology, Flavor Biochemical Pathways and the Influence of Yeasts in Cheese. Front. Microbiol. 12:703284. doi: 10.3389/fmicb.2021.703284

INTRODUCTION

Cheese is an ancient traditional fresh or fermented dairy product with a long history of production. Cheese making originated in various West Asian countries about 8,000 years ago (Sandine and Elliker, 1970); it is traditionally called "milk pimples" by Mongolian, Kazak, and other nomadic people in northwestern China (Zheng et al., 2021). Cheese is made by curdling milk, cream, or partially skimmed buttermilk from cow or goat or a mixture of these products and then separating the whey. In general, it is prepared by adding an appropriate amount of lactic acid bacteria (LAB) starter along with rennet to milk, the fermentation by which transforms the milk proteins (mainly casein), carbohydrates, and fats. Next, the whey is removed and the remaining product is ripened for a certain period. LAB may not be added for making some cheeses.

Fermented dairy products with high nutritional value are considered "the pearls in the crown of the dairy industry" (Kourkoutas et al., 2006). With the improvement of the quality of life, the people's dietary needs and demands have been changing in terms of quantity and quality.

Furthermore, the lactose content in cheese is low, and its consumption is thus highly suitable for people with lactose intolerance (Monti et al., 2017). Currently, nearly 130 countries and regions produce various cheese, and the total global cheese production measures nearly 2,000 × 10^4 tons, with the European Union countries (e.g., Netherlands and Germany) being the largest cheese exporters worldwide. From the development perspective of the global dairy industry, cheese is a very important dairy product, but it has not yet become an independent industry in China. At present, cheese production in developing countries remains in its infancy, with the most individuals from these countries being unfamiliar with cheese. Simultaneously, dairy processing companies face funds and technologies limitations. Thus far, no cheese has been widely accepted. Therefore, the study of cheese is particularly urgent (Kourkoutas et al., 2006; El Sheikha, 2018). With the development of dairy industry in various countries, the vigorous development of the cheese industry has become the focus of attention in recent years.

Globally, there is a lack of an authoritative cheese-making process, which can be used for cheese production followed in any country – China or abroad. This is due to differences in regions, production methods, and available raw materials. The earliest method of producing cheese in the world was to carry the milk to the animal's internal and the milk was fermented into cheese by constant oscillation during the migration. Cheese is made differently in different regions. For instance, for making cheddar cheese in southwest England, the raw material is sterilized and cooled; then, the fermenting agent, calcium chloride, and rennet are added to ferment the curd (Lawrence et al., 2004). After 30–40 min, the formed clot is cut into 5-mm sized pieces, which are then allowed to stand for 15 min and stirred for another 5–10 min. The clot is then turned over and stacked, broken, salted, molded, and pressed. The pressed cheese is put into a fermentation room for fermenting and ripening after the cloth is changed (Banks et al., 1989; Azarnia et al., 2006). In contrast, the milk used to make Parmesan cheese is collected in two separate steps, where the overnight milk and the fresh milk (collected the next morning) are mixed in a copper cheese tank. When the temperature reaches 52°C, the cheese is wrapped with gauze for cutting, molding, pressing, and then, soaking in brine for 3 weeks (D'Incecco et al., 2020). Approximately 5 kg of water is evaporated during maturity. On the other hand, soft and semi-hard cheeses, such as feta cheese, are soaked in brine for a short period (Marino et al., 2017). For Kazak cheese making, the milk collection process is similar to that of Parmesan cheese, with few differences: In a goatskin bag, old yogurt may or may not be added as a starter, followed by fermentation into yogurt (Zheng et al., 2021). Next, this yogurt is boiled with stirring to evaporate water. The remaining curds are placed in a canvas bag, which is then hung outdoors to remove moisture further and solidify into fresh cheese. This fresh cheese is then cut into small pieces or made into a pie shape and finally placed on a bamboo board for 30–90 days of spontaneous ripening (Zheng et al., 2018b).

The acceptability of cheese to the final consumer largely depends on specific sensory characteristics, including flavor and aroma. The unique characteristics and special quality of cheese all depend on the various compounds and molecules that constitute it, including fatty acids, amines, ketones, free amino acids, alcohols, aldehydes, lactones, and sulfur compounds (Califano and Bevilacqua, 2000). Nevertheless, the presence of these molecules is associated with cheese-making factors, including climate, regional conditions, geographical position, technology used, the cheese-associated microbiota, and ripening conditions (Buffa et al., 2004; Soggiu et al., 2016; Pino et al., 2018). Four pathways, namely glycolysis, citrate utilization, proteolysis, and lipolysis, are involved in cheese flavor formation (Vlieg and Hugenholtz, 2007; Landaud et al., 2008). In addition to bacteria and mold in cheese, studies have indicated that *Geotrichum candidum* has expression characteristics associated with carbohydrate, lipid, and amino acid metabolism; whereas *Debaromyces hansenii* is involved in the metabolism of other amino acids (Ray et al., 2014; Monnet et al., 2016). Yeast also deaminates amino acids to the corresponding ketoacids and NH_3, increasing the pH of the cheese (Beresford et al., 2001; El Sheikha and Montet, 2014). Flavor compound production relies on the milk-degrading enzymes of each fermenting strain and on the complementation of metabolic pathways between strains; the produced flavor compounds may enhance the cheese flavor quality and variety. Therefore, functional diversity – which is closely related to the complexity of the cheese microbiota – is crucial in the flavor compounds multiplicity produced during ripening (Irlinger and Mounier, 2009).

Traditionally fermented cheeses have complex microbial communities, multi-strain co-fermentation, complex metabolic mechanisms, and different flavor profiles. Therefore, microbes play a pivotal role in cheese flavor formation. The current review aims to provide a comprehensive overview of dynamics of the cheese microbiota in various cheese-making processes and technologies as well as understand the main biochemical pathways of cheese flavor formation, with a specific focus on the role of yeasts in cheese. Furthermore, this review provides important advances in understanding the effects of different cheese-making techniques and microbial diversity on cheese flavor and quality.

GENERAL PROCESS OF CHEESE FERMENTATION AND KEY CONTROL POINTS

Characteristics of Various Cheeses

More than 2,000 different cheese varieties exist in the world, of which more than 400 are more famous (Fox, 1993). Depending on the moisture content, cheese preservation and ripening methods can vary greatly (**Table 1**). Extra-hard cheeses, such as Parmesan and Romano, are produced from very hard curds. These cheeses are low in moisture, produced from partially skimmed milk, and matured slowly (over 1–2 years) by bacteria. For hard cheeses, such as cheddar and Kazak, the curd is acidified before salting and pressing, and their ripening period is 3–12 months, whereas for semi-hard cheese, this period is 2–3 months. Semi-soft cheeses (e.g., Limburger and blue cheese)

TABLE 1 | Classification and main varieties of cheese.

Form facture	Moisture content/%	Mature microorganisms	Main cheese variety	Cheese flavor	Country of origin
Extra hard cheese	**25–35**	Bacterial	Parmesan	Fruit flavor and salt	Italy (Woo and Lindsay, 1984)
			Romano	Strong flavor	
Hard cheese	**35–45**	Bacterial: atmospheric hole	Emmanuel	Fruity aroma and taste stimulation	Switzerland (Anifantakis et al., 2009)
			Gruyere	Aromatic, rich, and smooth smell	
		Bacterial: no air holes	Cheddar	Walnut flavor	United Kingdom (Zerfiridis et al., 1984; Fox, 1993)
Semi-hard cheese	**45–50**	Bacterial: small air hole	Gouda	Caramel and creamy candy	Netherlands (Aishima and Nakai, 2010)
		Bacterial: no air holes	Edam	Sweet and nutty	
Semi-soft cheese	**42–55**	Bacterial	Brick	Spicy	German (Brackett et al., 1982)
			Limburg	Spicy	
		Mold	Roquefort	Strong salt aroma	France, Denmark (Woo et al., 1984)
			Blue	Strong spicy	
Soft cheese	**55–80**	Mold	Camembert	Mild	France (Kubíčková and Grosch, 1997)
		Not mature	Cottage	Mild	America (Goel et al., 1971)
			Cream	Slightly sour	

Bold values indicate the values of the header and moisture content.

are ripened using bacteria (*Brevibacterium*) and/or mold (*Penicillium*). During ripening, mold is primarily grown on the surface of some cheeses (e.g., Camembert) but under the surface of other such cheeses (e.g., blue cheese).

Milk high in bacterial numbers may contain lactose-fermenting bacteria, which may interfere with milk acidification during cheese making. A cheese maker would not have strict control over the rate and extent of acidification during cheese making, which is one of the key components of successful cheese making. Pasteurization kills most bacteria capable of fermenting lactose, so it is sometimes necessary to use added starter for proper fermentation. Pasteurization kills most lactose fermenters and enables more stringent acidification control during the cheese-making process more stringent, in turn facilitating cheese quality control. Therefore, adding a starter is necessary for proper fermentation here. For some cheese varieties, especially cheddar, Parmesan, and aged Gouda, it is a common practice to add adjunct bacteria (mostly *Lactobacillus* species) in milk to produce unique, characteristic flavors. The added adjuncts may include bacterial species that inhibit undesirable bacteria in the cheese and possibly have probiotic effects. Mold-ripened cheeses (e.g., Camembert) and soft, surface-ripened cheeses (e.g., Limburger) do not offer sufficient protection against pathogen growth of because they do not meet the required criteria. These cheeses have high water activity and lose their acidity during ripening, both of which facilitate the growth of contaminants. The cheese uniformity, hardness, and shape are related to certain basic factors, crucial to ensure that cheese has the suitable ripening conditions and develops the ideal basic characteristics. Softness is associated with higher water content, higher fat content, and stronger protein breakdown ability. In contrast, hard cheeses have a firm shape. The variety of cheese that may be obtained is determined by raw milk characteristics, fresh curd preparation method, and microorganisms in the milk or curds (associated with the unique flavor and characteristics produced during cheese production and ripening). The types of microbes involved in cheese production or ripening are decided by the inoculated microbes, cheese production conditions, and environmental factors.

Cheese Fermentation Processes

For centuries, the milk used to make many cheese varieties in the world has not pretreated in anyway before curdling. That is, raw milk, especially artisanal cheese, is conventionally used for making these cheeses (Kelly et al., 2008). Cheeses are traditionally manufactured by converting fluid milk to a semisolid mass by using a coagulating agent – such as rennet, acid, heat plus acid, or a combination of these. Cheeses can vary widely in their characteristics, including color, aroma, texture, flavor, and firmness, all of which are generally attributable to their production technology, milk source, moisture content, and aging length in addition to the presence of specific molds, yeast, and bacteria (Santiago-López et al., 2018). When milk is converted to cheese, some of the milk components are retained, whereas the others convert to unique components of the cheese. For instance, the microbial fermentation that milk undergoes during its transformation into cheese can modulate cheese composition directly *via* vitamin B synthesis (Reif et al., 1976). Microbial fermentation also indirectly regulates the composition of cheese by dissolving certain minerals and lactates lost in the whey after milk coagulation (Lucey and Fox, 1993). In addition, the composition of cheese changes according to the cheese-making process used (Mucchetti et al., 2008). Some of the major processes of natural cheese production are universal (**Figure 1**).

Cheese is generally produced from cow's milk, but several cheeses, such as Roquefort, feta, and Manchego, are produced using the sheep or goat milk (Branciari et al., 2000). In general, raw milk has to be used for cheese production as soon as possible after it is expressed. However, delivering raw milk to a cheese factory in time can often be difficult in remote areas. Moreover, such factories may need to place the collected milk for 1 day before processing it. If the storage period ranges between 24 and 72 h, the bacterial numbers can increase to 10^6 colony forming units/ml. The fat content in raw milk is

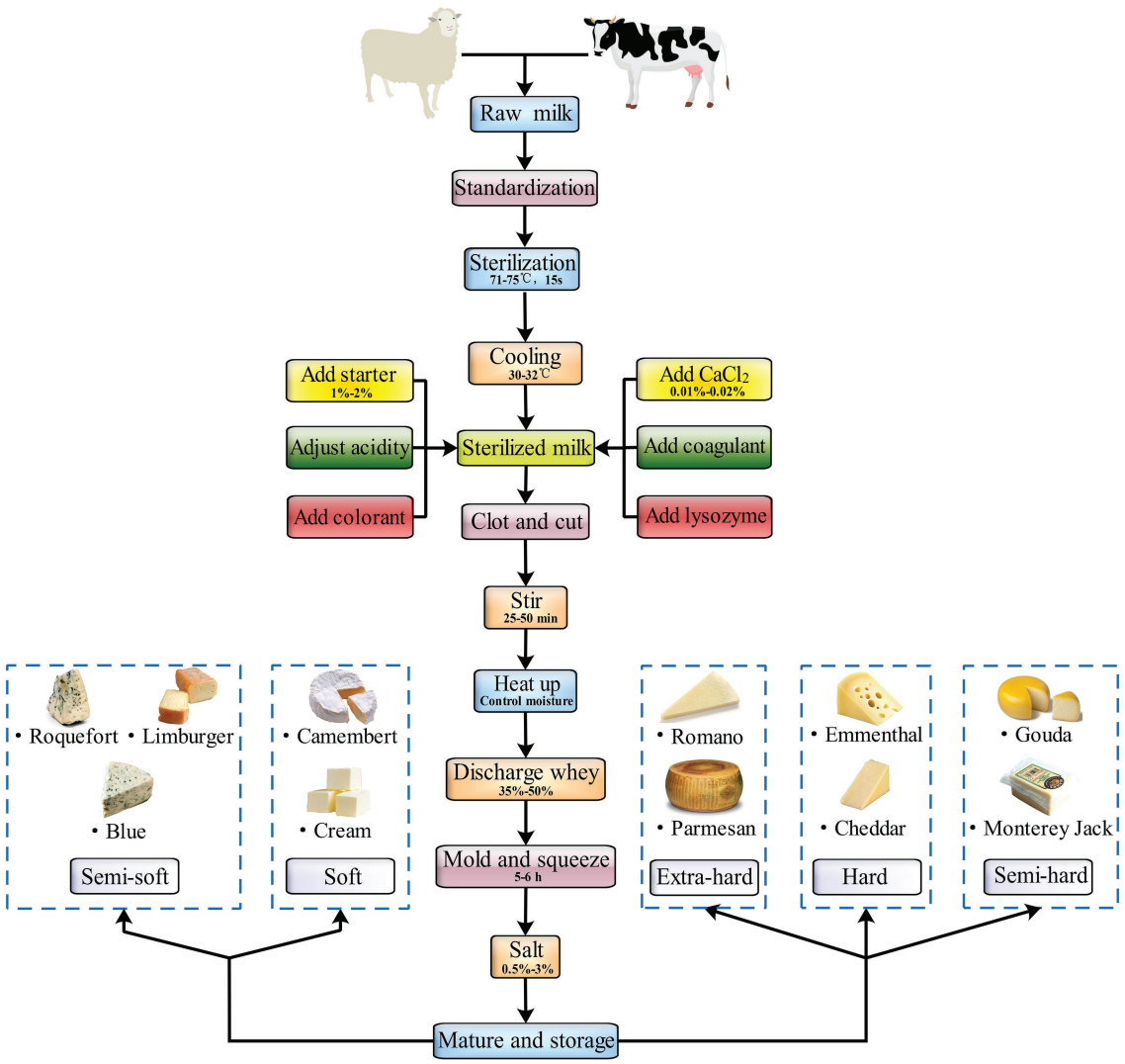

FIGURE 1 | The general processing process of natural cheeses.

determined by the fat content required in cheese, which in turn has a proportional relationship with the casein content of whole milk. Milk standardization can be done by adding cream, separating part of the fat, and adding skimmed milk or non–milk fat solids to achieve a uniform weight and reduce any deviation. To eliminate harmful and pathogenic bacteria, ensure uniform quality, and increase the stability of cheese quality, sterilized raw milk is used to produce most cheese varieties. The sterilization is performed at 63°C for 30 min or at 71–75°C for 15 s. Before cheese production, contaminating bacteria, mainly *Lactobacillus* spp., from the environment may ferment lactose; therefore, milk must be screened for acid and flavor compound–producing microbiota strains before the starter agents are added so as to maintain a stable acid production rate during clot formation and ensure cheese stability and quality. In addition to the starter, other agents can be added based on whether the cheese variety and production condition requires them; for instance, calcium chloride and colorants can be added to produce a curd with suitable hardness and consistent color. A clot can be only cut after it reaches appropriate hardness. Cutting allows for the conversion of large clots to smaller clots, thus speeding up the discharge of whey. It also increases the clot's surface area, allowing for shrinkage *via* dehydration. As the firmness of the clot increases, its water-holding capacity decreases. Clot shrinkage and whey precipitation cause the clot to lose more water and become firmer. Generally, whey removal is performed to remove whey at a volume equal to 35–50% of the milk volume. The higher the temperatures during the whey discharge process, the higher is the clot moisture content. This is because clot particles deform quickly at high temperatures; as a result, the holes in the cheese particles close together rapidly, preventing water emission. Adding the proper content of salt during the cheese-making process can ensure proper acidity of the cheese, improve its texture properties and flavor, control the number of holes, adjust the moisture, and inhibit contaminating microbes (Upreti and Metzger, 2006).

Regarding ripening and storage, fresh cheeses, such as cottage and cream cheese, do not need to be matured, whereas hard cheeses, such as cheddar and Swiss, do. Matured cheeses are generally made with a rennet curd. During ripening, unique flavors develop in a fresh clot through probiotic and enzymatic action, the intensity of which depends on the type of cheese (Moghaddas Kia et al., 2018). For ripening of extra-hard and hard cheeses such as Parmesan and cheddar, the clot is stored under conditions not conducive to the growth of surface microorganisms. This limits microbial and enzymatic activity. For instance, cheddar cheese is ripened in caves (Krishnan et al., 2019). For ripening all soft and some semi-soft cheeses – such as Limburger and Brie – the clots are stored under conditions that promote the growth of surface microorganisms. For instance, *Penicillium camemberti* is involved in the ripening of cheese such as Camembert and Brie, and *Brevibacterium linens* is involved in the ripening of spotted mature cheeses such as Limburg (Łopusiewicz et al., 2020). Interestingly, Blue cheeses such as Stilton and Roquefort are ripening in these two ways. In contrast, some traditional handmade cheeses, including Kazak and Plaisentif, do not have a specific standardized production process; they vary based on the traditional methods used by the cheese makers (Dalmasso et al., 2016; Zheng et al., 2021).

Critical Control Points of Cheese

Extra-hard cheeses have very low water and fat contents. The key components of their production include low-fat milk, thermophilic LABs, high blanching temperature, long salt water–soaking period, and long-term slow ripening (Gobbetti and Di Cagno, 2017). For Parmesan, milk is collected in two batches: first, milk is left to stand overnight (to allow the fat to rise to the surface of the milk) and then churned to remove all the butter at the next morning. The remaining buttermilk is mixed with fresh milk. The milk is then fermented in a copper cheese tank. This process is similar to that Xinjiang Kazak cheese making, with only difference being that this cheese is fermented in a goatskin bag, not a copper tank (Zheng et al., 2018b). Next, after their formation, Parmesan clots are heated to about 52°C, and some part of the whey is scooped out as a starter for the next day's cheese making; this part is essential for receiving a Parmigiano-Reggiano cheese certification (Neviani et al., 2013). Cheddar cheese, made from whole milk, contains 48% fat and 39% water and is fermented by the thermophilic *Streptococcus lactis*. It is produced at a low temperature, and it needs to reach a certain level of acidity before it is clotted and pressed. The clots are ground in the tearing or slicing mill, after which dry salt is added. Cheddar cheese is produced in way similar to Dutch cheese, with only difference being that the clot is repeatedly turned, stacked, and crushed. Since the high acidity of cheddar cheese during ripening inhibits the growth of butyric acid bacteria, nitrates are not added (Rilla et al., 2003).

The carbon dioxide produced by propionic acid bacteria (PAB) leads to formation of holes (also called "eyes") in hard cheeses, such as Swiss and Emmental (Guggisberg et al., 2015). During the production of these cheeses, producing sufficiently elastic curds is critical. The ripening of Swiss cheese involves slow protein and lipid decomposition in the clot, which produces flavor substances and promotes the growth of PAB, which fermented lactates. The raw materials and starters used for Emmental are different from those used for other cheeses: the fresh milk used for making Emmental cheese is sourced from cows that are feed only grass and/or hay, no other feed or additives (Fröhlich-Wyder et al., 2002). Moreover, its starter culture consists of thermophilic *Lactobacillus* and *Propionibacterium*. However, few common limitations of using these raw materials include crack formation, few holes, pink spots, and insufficient flavor (Bertuzzi et al., 2018).

Semi-hard cheeses have a wide range of flavor profiles and structures because of the various LABs used and their effects. For Caerphilly and Lancashire cheeses, the growth of strains is promoted during the clot production stage: the low acidity (pH 5.0–5.2) of fresh cheese produces acidic clots that cause the cheese to have a crumbly texture (Jones et al., 2005; Tedeschi et al., 2013). In cheeses such as Edam and Gouda, a portion of the whey is discharged during mixing and replaced with water to limit acid production (Ibáñez et al., 2020). Therefore, the lactose content of the cheese decreases, its pH increase, and it develops firm but elastic structure. However, Gouda is made using pasteurized whole milk, whereas Edam is made using pasteurized or partially pasteurized buttermilk (Jo et al., 2018). Cleaning and removing whey are performed simultaneously during the manufacture process of Gouda – where some whey is removed and hot water is added to clean the curd. Finally, the moisture content in the cheese is controlled, and the final pH of it is also controlled by washing off the lactose to reduce the emission of lactic acid (Fox et al., 1990). In addition, Gouda is pressed further to remove whey and form a closed crust.

Limburger is called "smelly cheese" because of its strong aroma, mainly originating from the rind, rather than the cheese itself. Limburger is first stored for 2 weeks under higher temperature and humidity and then matured for 2–3 months under refrigerated conditions. During this time, it is soaked in brine several times to stimulate the growth of bacteria and the formation of a light brown crust and a unique taste. For storage, Limburger is wrapped in packaging made of breathable material such as aluminum foil or paper to ensure that the cheese remains ripe. Blue cheeses, including Roquefort and Danish blue cheese, are produced from high-acid, semi-soft curds, involving slow acid production over a long period of whey removal. The clots are not heated during processing, and the cheese is not mechanically pressed like pasta filata cheeses. The typical process of producing blue cheese includes puncturing the cheese for aeration to promote the growth of *Penicillium roqueforti*, which produces the typical blue lines. Camembert is a typical mature cheese with mold on the surface, which is soft and sticky. Traditional Camembert is made with fresh milk from local Normandy cows. After the cheese is basically shaped, dry salt is sprinkled on the surface, followed by inoculation with *Penicillium albicans*.

Mozzarella cheese is a semi-hard, fresh pasta filata family cheese. Its most unique processing technique includes hot stretching, which gives the cheese its distinctive texture. Mozzarella requires rapid acid production, but high acidity

can also lead to low-quality cheese production. High-fat cheeses are sour curd cheeses. For these cheeses, whey is traditionally drained by hanging the clots in bags – similar to traditional Kazak cheese making (Zheng et al., 2018a). Feta cheese is made from sheep or goat milk, which is higher in short-chain fatty acids and thus produces a distinctive sour taste. However, the inherent lipase in this milk is destroy during the heat treatment process, and it is compensated for by adding lipase in the subsequent steps to ensure that the short-chain fatty acids generated *via* hydrolysis provide the unique sour taste.

Development of Industrial Processing Technologies and Its Advantages

In contrast, the main forces that drive cheese technology are economics, equipment/engineering, consumer demands, and regulatory standards. In addition, production of consistent and high-quality cheese, while maintaining high-volume throughput is a key challenge in cheese manufacture (Panikuttira et al., 2018). Adoption of process analytical technology (PAT) for continuous monitoring and control of relevant processing parameters in dairy processing mini-mises the production of low-quality product and increases productivity and profitability (Tajammal Munir et al., 2015). Alternative processes for the reduction of bacterial load include the use of specially designed centrifuges or microfiltration. Hydrogen peroxide/catalase treatment of milk and Bactofugation (a high-speed centrifuge) could be used to remove bacteria and bacterial spores from milk (Legg et al., 2017). More recently, adjusting the protein content of the milk through the use of ultrafiltration technology was to achieve the desired final composition. Advantages include a more uniform starting material, profitable use of a lactose stream, and greater throughput of milk solids through the cheese vat. The choice of equipment for the vat stage of the cheese-making process depends on many external factors, including type of cheese to be made, downstream curd processing, flexibility, cost, and throughput, to name but a few.

In recent years, new biotechnologies to promote cheese maturation and improve flavor have been explored frequently, including the inoculation of additional cultures and exogenous enzymes, and the impact of temperature and high pressure on the quality of cheese (Khattab et al., 2019). Instrumental techniques and sensory panels can be expensive and require trained personnel warranting for more innovative, rapid-detection systems for ripening monitoring and evaluation of cheese quality such as infrared (IR) spectroscopy, electronic nose, and optical techniques. In order to increase consumer acceptance of processed cheese products, manufacturers are often seeking new ways to increase their functionality. The main cheese fortification methods are through the incorporation of probiotics and prebiotics, vitamin enhancement, and fortification of the PC with other macronutrients (Talbot-Walsh et al., 2018).

The development of dairy technology has allowed for the standardization of industrial production technology for some cheeses, whereas other cheeses are still prepared using with the traditional non-standardized methods. For example, ultrafiltration and concentration technologies are more suitable for feta production, but Kazak cheese is made using the traditional non-standardized manual processes. In addition, use of edible films and coatings in cheese preservation has opportunities and challenges (Costa et al., 2018).

RESEARCH PROGRESS ON CHEESE FLAVOR-RELATED METABOLIC MECHANISMS AND DETECTIOIN TECHNOLOGIES

Cheese Flavor: Origin and Production

Cheese is a product of biochemical dynamics occurring during its production and ripening (McSweeney and Sousa, 2000). Each cheese has its unique flavor compound composition. Cheese flavor production mainly involves three main reactions: residual lactose, lactate, and citrate metabolism; proteolysis; and lipolysis (McSweeney, 2011). The enzymes involved in cheese production and ripening are mainly derived from the milk, the starter culture, rennet, and the secondary microbiota. Various changes in non–starter LAB (NSLAB) and secondary or adjunct cultures also occur depending on cheese types and processing methods. Food flavor substances are mainly volatile and nonvolatile. Volatile flavor substances include alcohols, acids, esters, aldehydes, and ketones – all of which are the source of food aroma (Marsili, 1985). In contrast, nonvolatile flavor substances mainly include organic acids, amino acids, reducing sugars, nucleotides, polypeptides, and other small molecules – all of which are the source of food taste (Delgado et al., 2010).

Cheese flavor substances include acids, alcohols, esters, ketones, and lactones – all of which are affected by raw milk quality and fermentation and/or ripening processes (Urbach, 1993; Santiago-López et al., 2018). In particular, ripening is the most important factor affecting cheese flavor. Cheese ripening process involves very complex biochemical reactions, which include primary and secondary metabolism. The basic flavor of cheese is determined by primary metabolism and mainly contains threes changes: carbohydrate decomposition, protein hydrolysis, and fat degradation. Secondary metabolism is responsible for the formation of flavor specific to a cheese variety. It mainly includes amino acid decarboxylation, transamination, deamination, de-sulfation, fatty acid beta-oxidation, and esterification (Marilley and Casey, 2004). Yeast can effectively produce many secondary metabolites crucial to the quality of cheese, including carbonyl compounds, sulfur compounds, fatty acid derivatives, phenolic compounds, and higher alcohols – which are directly related to cheese aromas (Dzialo et al., 2017).

Residual Lactose, Lactate, and Citrate Metabolism

Lactose and citrate are the main carbohydrates in all mammalian milks, but the lactose content varies widely from mammal to mammal (range, 0–100 g/L; Lai et al., 2016; **Figure 2**). The principal products of lactose metabolism are L-lactate, DL-lactate, or a racemic mixture of both, which is essential to the flavor

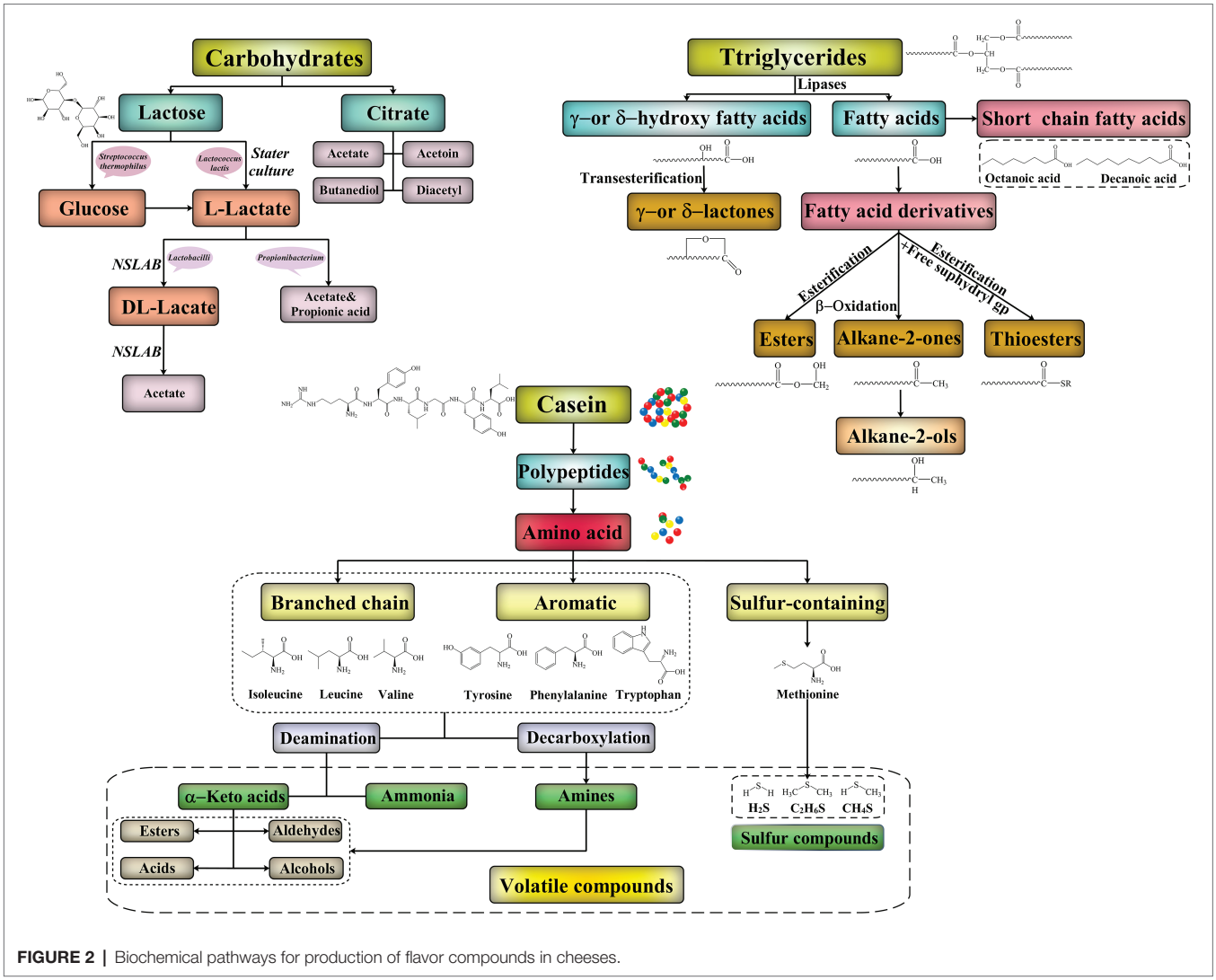

FIGURE 2 | Biochemical pathways for production of flavor compounds in cheeses.

production in all cheeses. However, some bacteria including *Leuconostoc* spp. also produce other products such as ethanol (Vedamuthu, 1994). The nonstarter microbiota of cheddar, Dutch-type, and similar cheeses isomerize the L-lactate produced by the *Lactococcus lactis* starter to DL-lactate (McSweeney et al., 2017). However, a high DL-lactate concentration can affect the sensory quality of a cheese. Certain starter bacteria (e.g., *Streptococcus thermophilus*) growing with galactose-positive microorganisms cannot metabolize the galactose moiety of lactose, leading to galactose accumulation in the curds. Pyruvate – an intermediate of lactose metabolism – is the precursor for the production of several short-chain flavor compounds, including acetate, acetoin, diacetyl, ethanol, and acetaldehyde (Melchiorsen et al., 2002). In Swiss cheese, lactate is metabolized into propionates, acetates, carbon dioxide, and water by *Propionibacterium* spp., among which carbon dioxide is the cause of the characteristic "eyes" in the cheese (Duru et al., 2018). Acetate is an important flavor compound in many cheeses. In addition to being metabolized from lactose by LAB, acetate may also form *via* lactate and citrate metabolism (McSweeney and Sousa, 2000).

In mature cheeses such as Camembert and Brie, lactate in the surface layer is metabolized and decomposed into water and oxygen by the mold and yeast on the surface, causing their pH to increase (Lucey and Fox, 1993). This is similar to the changes occurring in Dutch and Swiss cheese, but not in cheddar. Lactose concentration in the cheese can drop as a result of washing or being replaced by whey; in this case, the remaining lactose in the clot is quickly metabolized with an increase in pH value. Consequently, cheeses with low-residue lactose have a fresh and mild flavor; whereas those with high-residue lactose may have a strong and pungent flavor because of low pH value.

In milk, citrate mainly exists in the form of ionized salts at concentrations of ≤1.8 g/L, most of which is lost in the whey during cheese making. This is because nearly 94% of the citrate is in the soluble phase of the milk (McSweeney et al., 2017). Citrate is not metabolized by *S. thermophilus* or thermophilic lactobacilli but by certain mesophilic lactobacilli in the NSLAB microbiota. Citrate is not metabolized by *S. thermophilus* or by thermophilic lactobacilli, but is metabolized by certain mesophilic lactobacilli in the NSLAB microbiota.

A number of important flavors compounds, such as acetate, diacetyl, acetoin, butanediol, and carbon dioxide, are produced from citrate if some citrate-positive lactate (e.g., *L. lactis* and *Leuconostoc*) are promoted. Diacetyl is an important aroma compound converted to acetoin, 2,3-butanediol, and 2-butanone in some varieties of cheese, such as Dutch-type cheeses, quark, and cottage cheese (Dimos et al., 1996). Citrate metabolism is of particular importance in Dutch-type cheeses, where the CO_2 produced is responsible for eye formation (McSweeney and Sousa, 2000). In addition, citrate provides the primary substrate for Cit^+ starter cultures and NSLAB, and residual citrate metabolized by NSLAB may also lead to tissue laxity in some cheeses, such as cheddar (Fox et al., 2017).

Lipolysis and Fatty Acid Metabolism

Lipolysis has an important effect on cheese flavor and texture (Voigt et al., 2012). Lipases in cheese are derived from milk, rennet, starter, auxiliary starter, nonstarter bacteria, and exogenous enzymes. Of all lipases, lipoprotein lipase is important in the development of flavor in raw milk cheeses, but it has little effect on the flavor of cheese made from pasteurized milk (Sert et al., 2014). The lipolytic enzymes present in LAB can hydrolyze a substrate to generate free fatty acid esters, triacylglycerides, diacylglycerides, and monoacylglycerides. LAB esterase is active for $<C_{18}$-monoacylglycerides, with especially higher sensitivity to C_8-monoacylglyceride, but has no effect on $>C_6$-diacylglycerides (Holland et al., 2005). In addition, ethyl-butyric acid is generated by the transfer of butyl from triglycerides to ethanol *via* transferase in the cells of LAB (Tomita et al., 2018). The ability of PAB to decompose fat is 10–100 times that of LAB. In Swiss cheese, PAB play a key role in the conversion of lactate to acetate, the production of characteristic flavor *via* carbon dioxide, and the formation of free acids (Schwenninger et al., 2011).

The formation of typical flavor of cheese through lipolysis mainly reflects in the following: the ester bonds between triglycerides and fatty acids break under the action of lipase and monoglycerides, diglycerides, and free fatty acids are produced (Deeth and Touch, 2000; **Figure 2**). Fatty acids have an important influence on the flavor of cheese. During cheese fermentation and ripening, a series of fatty acids with medium and short carbon chains ($C > 4$) are formed after milk fat degradation. This leads to the formation of characteristic flavor substances in cheese, and these substances are important indicators that determine the maturity of the cheese. The oxidation of fatty acids, especially polyunsaturated fatty acids, can produce various unsaturated aldehydes with intense flavors. This can lead to an unpleasant smell associated with rancidity; it is observed in Gouda, cheddar, and Swiss cheese after they spoil (Forde and Fitzgerald, 2000). Nevertheless, lipolysis has a positive effect in most cheeses, including such as Parmesan, Emmental, blue cheeses, and Italian cheese (e.g., Romano; Thierry et al., 2017).

Fatty acids produced *via* lipolysis, especially free fatty acids such as acetic, octanoic, and decanoic acids, are cheese flavor substances. Moreover, the unique texture and hardness of cheeses result from continuous volatilization of water. Of the free fatty acids produced, acetic acid provides cheese with a sharp taste, but too much acetic acid can afford the cheese a vinegar-like odor. The flavors produced by fatty acids vary according to the differences of fatty acid types and contents in the many cheese types (Mallatou et al., 2003). Butyric acid is an important flavor compound in cheese such as Romano and cottage cheese, whereas the main characteristic flavor of Swiss cheese is propionic acid produced by PAB (Singh et al., 2003). Moreover, hexanoic acid is responsible for a sweaty, pungent, and rancid flavor (Carunchiawhetstine et al., 2003); octanoic acid imparts a goaty, waxy flavor; and decanoic acid affords a fatty, citrus odor (Gan et al., 2016).

Short-chain fatty acids provide strong characteristic flavors, some of which are precursors to flavor and are converted to other aromatic substances, including lactones and alcohols (Temizkan et al., 2015). The principal lactones in cheese are γ- and δ-lactones – which have five- and six-sided rings, respectively, and impart an intense aroma. The esters in cheese are produced by the esterification reaction between short-chain fatty acids and medium-long-chain fatty acids produced by the degradation of milk fat and primary and secondary alcohols produced by lactose fermentation or amino acid metabolism during fermentation (Fox et al., 2015). The esters in cheese are produced *via* the esterification reaction between short-chain fatty acids and medium–long-chain fatty acids produced during milk fat degradation. Moreover, primary and secondary alcohols are produced through lactose fermentation or amino acid metabolism during fermentation. The ester compounds in cheese play an important role in the formation of aromas that are sweet, fruity, and floral. However, an excessive amount of ethyl butyrate and ethyl caproate leads to an overpowering fruity flavor defect (Castada et al., 2019). In addition, thioesters (i.e., s-methyl thioacetate, thioethyl-2-methylpropanoate, and s-methyl thiobutyrate) produced through the reaction of free fatty acids with sulfhydryl groups impart a garlicky, sulfur-like, or eggy flavor (Iwasawa et al., 2014). Finally, β-oxidation and subsequent decarboxylation of free fatty acids in some cheeses (e.g., blue cheese) result in the formation of methyl ketones or alkan-2-ones, especially heptanone and nonanone (McSweeney et al., 2004).

Proteolysis and Amino Acid Metabolism

Protein hydrolysis, a main biochemical reaction, is crucial to the formation of cheese flavor and has an important influence on the release and taste of cheese flavor during cheese ripening process (Gan et al., 2016). The peptides and free amino acids, decomposed from protein by protease in cheese, are precursors of many cheese flavor substances. Milk proteins mainly include caseins (α-, β-, and κ-casein), which are lost in whey because they are not degraded significantly. Casein hydrolysis is the most important biochemical pathway for flavor formation in hard and semi-hard cheeses. Proteinases and peptidases catalyze the cleavage of the polypeptide chains to produce free amino acids, some of which act as precursors to flavor compounds during cheese production and ripening (McSweeney, 2011).

Free amino acid content and metabolism in mature cheese play essential roles in cheese flavor development. Under the

action of transaminase, deaminase, decarboxylase, and other enzymes, free amino acids in cheese are transformed into a series of volatile and nonvolatile flavor substances (e.g., ketones, aldehydes, acids, and alcohols) *via* deamination, amination, and decarboxylase (Fox and McSweeney, 1998; **Figure 2**). Methionine, leucine, and glutamic acid concentrations are typically considered the indicators of the degree of protein hydrolysis in cheese. The enzymatic removal of the amino terminus of amino acids leads to the formation of flavor and aromatic substances, such as 3-methyl-butanol, methionyl-propyl aldehyde, sulfides, and aromatic esters – which impart a malty, a baked potato-like, a pungent, and a flowery odor, respectively (Suzuki-Iwashima et al., 2020). Amino acid concentrations, especially those of glutamic acid and lysine, are significantly higher in Parmesan than in Gouda, cheddar, or Emmental. Starter LAB (SLAB), NSLB, and other bacterial strains can produce amino acid–metabolizing enzymes that specifically act on branched-chain, aromatic, or sulfur-containing amino acids (Forde and Fitzgerald, 2000).

Branched-chain amino acids – the precursors of aromatic compounds such as isobutyl ester, 3-methylbutanal, and 2-methylbutanal – are found in different cheeses (Curioni and Bosset, 2002). In addition, isoleucine, leucine, and valine can be decarboxylated into isobutyl ester, 2-methylacetaldehyde, and ketoisocaproate, all of which possess strong unpleasant aromas (McSweeney, 2011). Aromatic amino acid catabolism begins with a transamination step – where indole pyruvate, phenyl pyruvate, and p-hydroxy-phenyl pyruvate are produced from tryptophan, phenylalanine, and tyrosine, respectively. The conversion of tryptophan or phenylalanine in many hard and soft cheeses leads to the formation of benzaldehyde, which is characterized by a bitter almond flavor. Amino acids are also deaminated and decarboxylated to produce compounds such as α-keto acids, ammonia, and amines – which are further transformed into compounds such as alcohols, esters, and acids. Ammonia is also an important flavor substance in many cheeses, such as Camembert and Gruyère (Corsetti et al., 2001; Engel et al., 2001).

In cheese, methionine is converted to volatile sulfur compounds, such as methanethiol (which has a rancid flavor) as well as dimethyl sulfide and dimethyl trisulfide (which have a garlicky flavor); they represent the basic flavor substances in many cheese varieties (Smit et al., 2005). S-Compounds are the major contributors of the characteristic aroma of cheddar; they also contribute to the garlicky smell of a well-ripened Camembert (McSweeney and Sousa, 2000). In addition to producing flavor substance, proteolysis followed by oxidative decarboxylation of amino acids may produce low–molecular-weight biogenic amines (BA) – an excessive amount of which can cause adverse physiological reactions (Spano et al., 2010). Therefore, BA detection is a necessary part of cheese safety analysis.

Progress in Cheese Flavor Detection Technology Research

The various cheeses have varied aromas and complex structures, the analysis of which mainly based on volatile component extraction. At present, the main extraction methods include distillation, solvent extraction, headspace capture method (HS), and solid-phase microextraction (SPME). Distillation is a relatively simple extraction technique; however, it is time and labor intensive (Wang et al., 2008). Solvent extraction method requires a relatively high amount of solvent. HS is relatively fast and easy to operate, but the concentration of volatiles present in the headspace can be low, which may limit the results. SPME is a fast and effective sample flavor material enrichment technology, which shows effective flavor substance sampling, separation, concentration, and enrichment. SPME is often used in conjunction with methods such as gas chromatography (GC)–mass spectrometry (MS) for the detection of volatile flavor constituents in food (Kataoka et al., 2000; Bertuzzi et al., 2018).

Gas chromatography–mass spectrometry, which plays a significant role in food flavor substance analysis, has been widely used in the detection of volatile and semi-volatile samples (El Sheikha and Hu, 2020). GC–MS technology has certain advantages in the application process. At present, HS plus SPME (HS-SPME) in combination with GC–MS has applied to analyze the flavor substances of cheese, white wine, rice wine, Pu'er tea, and beer (Plutowska and Wardencki, 2007). Delgado used SPME–GC–MS to analyze the volatile constituents of four different mature stages of the soft Spanish goat milk cheese (Delgado et al., 2010). A total of 46 volatile flavor compounds were detected, including 13 acids, nine esters, four ketones, seven alcohols, three aldehydes, seven aromatic compounds and others. Frenzel et al. (2015) used GC–MS to determine the volatile constituents of Italian Fiore Sardo PDO mature sheep cheese and detected carboxylic acid compounds (68%), while esters (14%), ketone (9%), and alcohol (8%) to be the main characteristic volatile compounds. Ceruti et al. (2016) used GC to separate volatile components from the ripening process of Reggianito cheese under different temperature–time combinations and isolated 41 volatile compounds including acid, ketones, aldehydes, esters, alcohols, and hydrocarbons.

More than 600 compounds have been identified as food volatile components thus far. Only a few of these compounds have a significant effect on the sensory flavor profile of the analyzed food. Only GC–MS can analyze for a wide range of volatile compounds. However, it cannot determine the flavor active ingredients that contribute the most to the flavor in food. Gas chromatography olfactometry (GC-O) is the most effective for detecting and identifying aroma component identification; the analytical methods that can be used with this technique mainly include the time–intensity method, Charm analysis, and aroma extraction dilution analysis (Zhu et al., 2015). In a time–intensity method, the key aromas in foods are identified by a sensory appraiser to describe the specific flavor of the volatile components they can smell. They then rank the aromas according to the intensity of the smell and the degree to which they contribute to the flavor. Research has shown that a combination of solvent extraction, SPME, and GC–O can be used to identify the key aroma compounds of blue-grain mature cheeses; the identified compounds include methyl mercaptan, 2(3)-methyl-butyric acid (cheese, pungent odor), 3-methylthiopropanal, 2,3-butanedione,

dimethyl sulfide, butyric acid, 1-octene-3-ol (Z)-4-heptenal, phenylacetaldehyde, 2-ethyl-3,5-dimethylpyrazine, and acetic acid (Majcher et al., 2018).

YEAST DIVERSITY IN CHEESE AND ITS EFFECTS ON FLAVOR

Structural Diversity of Yeast Microbiota in Cheese

The traditional fermented foods, including Chinese liquor, cheese, vinegar, and bread, are enriched with various microorganisms in an open environment. Consequently, cooperative metabolism of multiple microbiotas underlies the fermentation involved in these foods (Wolfe et al., 2014). In addition, the microbial community structure and flavor of these foods are closely related. Therefore, a microbial community that inhabits in a cheese has a strong ecological adaptability and diversity. Microbial communities in traditional fermented foods also play an important role in food preservation and flavor formation (Wu et al., 2012). High-throughput metagenomics may reveal the diversity and succession of the microbial community on the surface of cheese – which is a food ecosystem with relatively simple microbiota. Moreover, metagenomics, macro-transcriptomics, and proteomics may be combined to greatly facilitate the mining of the metabolic functions of microbial communities in traditional fermented cheese (Almeida et al., 2014; Delcenserie et al., 2014; Gkatzionis et al., 2014). Combining pure cultivable and noncultivable methods (metagenomic techniques) to explore microbial communities has greatly increased out understanding of the microbiota on traditional fermented cheese (Aldrete-Tapia et al., 2014). However, few studies have focused on yeast strains in cheese, even though a diverse yeast microbiota inhabiting cheese has significant roles in cheese quality control.

The cheese ecosystem is a special habitat that supports the coexistence of yeast, bacteria, and filamentous fungi. The initial dominant yeasts are acid and salt tolerant; they can metabolize lactate produced by the SLAB and produce NH_3 from amino acids. Yeast in cheese originates from not only milk but also the processing environment and storage process during the cheese fermentation process (Gonçalves Dos Santos et al., 2017). Yeasts that exist in the environment of raw milk and dairy products can easily settle on the surface of new cheese and form a complex biofilm along with other microorganisms (Fröhlich-Wyder et al., 2019). This phenomenon is usually seen in traditional mature cheeses. Numerous yeast species have been isolated from the surface of various cheeses; however, the roles they play in cheese ripening remains poorly understood. *Yarrowia lipolytica*, *D. hansenii*, *Kluyveromyces lactis*, and *Kluyveromyces marxianus* have been mainly isolated from French artisanal cheese surface and cores (Ceugniez et al., 2015). Around 137 different cheeses from 10 countries were collected and 24 cultivatable bacteria and fungi were found to be widely distributed in on cheese surface *via* metagenomic sequencing and strain isolation (Wolfe et al., 2014). Commercial yeast cultures, such as *G. candidum*, have been used in cheese production for many years. The use of yeast as an adjunct culture has also become popular in recent years. In the German Harzer and quark, the addition of highly active yeasts (*D. hansenii* and *Candida krusei*) can promote ripening (Fröhlich-Wyder et al., 2019). However, most of the yeasts found inside cheese are strictly anaerobic; these yeasts include *K. marxianus*, which metabolizes residual lactose.

A study on the diversity of 44 types of cheese fungi found that *D. hansenii* was the most abundant yeast and *Pe. roqueforti* was the most common mold (especially in blue cheese); moreover, most of the fungi were isolated from dairy products (Banjara et al., 2015). However, the potential safety issues associated with consumption of fungi such as *Aspergillus flavus* also require attention. Nineteen filamentous fungi and five yeast strains have identified to be part of traditional Turkish cheese fermentation; these especially include *Penicillum* spp. and *D. hansenii* (Budak et al., 2016). Moreover, *Lactobacillus*, *Lactococcus*, *Enterococcus*, and some yeasts have been found in PDO Ragusano cheese; these microbes play an important role in flavor formation (Carpino et al., 2017). In terms of fungi, Slovak cheese mainly contains *Hansenula debali*, *Y. lipolytica* and *G. candidum* (Chebeňová-Turcovská et al., 2011), whereas Livarot cheese mainly includes *Y. lipolytica*, *Candida* spp., *Candida intermedia*, and *Geotrichum* (as detected *via* fluorescence *in situ* hybridization; Mounier et al., 2009). *Pichia kudriavzevii* is the predominant yeast in Kazak cheese, followed by *K. marxianus* and *K. lactis* (Zheng et al., 2018a). A broad range of yeasts has been isolated from Camembert and Brie, with *D. hansenii* and *Y. lipolytica* being the most abundant isolated species (Viljoen et al., 2003). The main metabolic end-products of lactose and galactose fermentation by yeast isolated from water-buffalo Mozzarella cheese demonstrates great variability depending on the species (Suzzi et al., 2000). In general, *K. marxianus* and *K. lactis*, with their anamorphous species *D. hansenii* and *Saccharomyces cerevisiae*, are the most common yeasts in cheese, but their role in the cheese ripening process has not been fully evaluated.

Effects of Yeast on Cheese Quality During Fermentation

Traditional fermented cheeses show complex microbial communities, multispecies cofermentation, complex metabolic mechanism, and varied flavors. The flavors in cheese are mainly produced *via* lactose and casein decomposition as well as lipid metabolism. In cheese ripening, most of the flavor substances are derived from protein hydrolysis and amino acid conversion (Engels et al., 1997). Moreover, the formation of flavor substances is inseparable from the metabolism of the microbiota and the conversion of substances during fermentation. A certain number of LAB is usually present in fresh milk and immature cheese, and some of the LABs have more highly active amino acid–converting enzymes; this increased the flavor diversity and richness in cheese (Centeno et al., 2002). Penicillium brevicompactum, Penicillium cavernicola, and Penicillium olsonii have a higher protease activity in handmade goat milk cheese, where Mucor produces more lipase. Moreover, *Y. lipolytica* has the best protease and lipase activity (Ozturkoglu-Budak et al., 2016). In addition

to LAB and mold, various yeasts participate in protein hydrolysis, lipid and lactose degradation, and lactate and citrate assimilation during cheese ripening – all of which are important in cheese flavor formation (Fox and McSweeney, 1998; McSweeney, 2010; Padilla et al., 2014). Furthermore, *Metschnikowia reukaufii*, *Y. lipolytica*, and *Pi. kudriavzevii* affect the release of proteases, which was vital for the formation of free amino acids from proteins (Akpınar et al., 2011).

Traditional fermented cheeses have a stable core microbiota; however, the yeast species present in this microbiota needs to be further analyzed based on their metamorphic genome and metabolomics. The effects of microbial interactions, environment, and production processes on the microbial community of cheese have demonstrated that the microbes distributed in cheese surfaces are highly reproducible, making cheese an easy-to-handle, constructible microecosystem model. The focus of ongoing relevant research includes the following: (1) a method for effective control of the ripening stage of cheese for ensuring the flavor and quality of the finished cheese; (2) identification of the core microbiota including various yeast species involved and their interactions during cheese production and ripening; (3) exploration of the correlation between the aforementioned interactions or dynamic changes and the flavor changes during cheese production and ripening; and (4) a method to analyze the internal relationship between the ecological and functional characteristics of the cheese microbial community.

Yeasts play an important role in the manufacture of nearly all traditional ripened cheeses, especially some smear ripened cheeses such as Gruyère, Tilsit, and Reblochon (Rea et al., 2007). Some fermenting yeasts can grow in the interior of acid curd cheeses, such as the German Harzer; they produce ethanol and carbon dioxide in the early stage of manufacture (Fröhlich-Wyder et al., 2019). However, yeasts may also be the reason of some major defects in cheese, causing early blowing, an off flavor, brown discoloration, and other visible alterations (Jakobsen and Narvhus, 1996). Yeasts can perform deacidification at the surface of the cheese, causing a pH gradient to form between the surface and the center of the cheese, followed by outward lactate diffusion. When lactate depletes, yeasts break down amino acids to produce NH_3, which diffuses inward and further increases the pH value (Gori et al., 2013; Monnet et al., 2015). The deacidification process contributes to the establishment of salt-tolerant, gram-positive, and catalase-positive bacterial communities with lower acid tolerance (Wolfe et al., 2014).

The development of yeast in cheese depends on many physicochemical conditions, such as low pH, mold content, high salt concentration, refrigerated ripening, and storage conditions (Viljoen et al., 2003). Yeasts that grow on the surface of cheese must be able to grow at low pH, low temperature, low water activity, and high salt concentrations (Monnet et al., 2015). For instance, using metagenomics, Filippis, et al. (2016) found changes in microbial communities and their functions during temperature-driven cheese ripening: increased microbial proteolysis, lipolysis, amino-acid and lipid catabolism–related gene expression, and cheese ripening rate. The distinct cheese flavors are produced according to the differences in fermentation conditions and starter cultures, which mainly contain bacterial and yeast starter cultures. Fungal starters, such as those containing *Pe. albicans* and *Pe. roqueforti*, can have proteolytic and lipolytic activities (Nielsen et al., 2005). Moreover, *Pe. albicans* produces white hyphae, whereas *Pe. roqueforti* can accelerates cheese ripening and produce a spicy flavor and a dark green color. In recent years, yeasts have also been used as assistant strains in starter cultures to produce cheese; for example, *Candida lipidotica* is used to produce blue cheese (Roostita and Fleet, 1996). As adjunct cultures, yeast species contribute to the development of flavor and texture during the production and ripening of certain cheese types. This is because their lipolytic and proteolytic activities can shorten the ripening time and thus enable economic cheese manufacture (Roostita and Fleet, 1996). In many cases, the most common yeasts in mold and bacterial surface–matured cheese include *Kluyveromyces*, *Debaryomyces*, and other species of *Saccharomyces*. Studies have found the presence of *Candida* spp., *Candida zeylanoides*, and dairy yeast in French Reblochon cheese; *D. hansenii* and *K. marxianus* yeasts in St. Nectaire cheese; and *Y. lipolytic*, *K. marxianus*, and *D. hansenii* in Tilsiter cheese (Corredor et al., 2000; Fröhlich-Wyder et al., 2019).

Most of the yeasts isolated from the surface of mature cheeses are salt tolerant, of which *D. hansenii* can tolerate high sodium chloride levels and utilize lactose, lactic, and citric acids for its proliferation (Gori et al., 2005; Breuer and Harms, 2006). Yeasts use residual lactate to deacidify the surface of cheese and produce vitamins and precursor substances, including niacin, riboflavin, and p-aminobenzoic acid, and thus promote *B. linens* growth on the cheese surface (Seiler and Busse, 1990). *Debaromyces hansenii* and *Y. lipolytica* are used to accelerate the ripening of cheddar cheese and enhance its flavor characteristics, whereas *Y. lipolytica* and *K. lactis* are employed for accelerating blue cheese ripening (Ferreira and Viljoen, 2003). *Kluyveromyces lactis* and *K. marxianus* are important components of the cheese microbiota because they can use the lactose left over from fermentation in the curd to produce carbon dioxide; this is beneficial for producing the open structure of cheeses such as Roquefort (Dias et al., 2014). *Kluyveromyces marxianus* can produce volatile aroma compounds through proteolytic and lipolytic activity in blue and bloomy rind cheeses and produce esters (fruity flavor compounds) and acetaldehyde from ethanol and carboxylic acids produced during lactose fermentation (Binetti et al., 2013). Research has shown that *Pi. kudriavzevii* N-X has the strongest extracellular proteolytic activity in skim milk agar and that it produces a range of aroma compounds (including ethanol, ethyl acetate, 3-methylbutanol, and acetic acid) in Kazak cheese (Zheng et al., 2018a). Research has also found that the texture of cheese with yeasts including *K. marxianus* and *Pi. kudriavzevii* added is relatively more brittle (Xiao et al., 2020). *Kluyveromyces marxianus* contributes to the formation of free amino acids and organic acids, especially glutamate and lactate. In addition, *K. marxianus* provides cheese with onion, oily, and floral aromas. Furthermore, *Pi. kudriavzevii* promotes a strong brandy, herbaceous and onion flavor. Both *K. lactis* and *Pichia fermentans* can ferment and constitute the typical yeast microbiota in feta (Rantsiou et al., 2008). Moreover, *Y. lipolytica* and *G. candidum*

have important influences on its flavor during cheese production and ripening (Steensels and Verstrepen, 2014).

Geotrichum candidum strains can be found in inside and on the surface of cheese; they grow rapidly at the early stages of cheese ripening in Limburger, Tilsit, and Romano cheeses (Lessard et al., 2014; Banjara et al., 2015). However, they can metabolize galactose, but not lactose. In contrast, *D. hansenii* simultaneously metabolizes lactose and lactate, both of which are present in cheese at its early ripening stages (Mansour et al., 2008). Interestingly, *Y. lipolytica* is strictly aerobic, and it metabolizes lactate. *Geotrichum candidum* is the most active species involved in casein and fat degradation, which leads to an increased release of ammonia (Dugat-Bony et al., 2015). Recent studies have shown that *D. hansenii*, *G. candidum*, and *Y. lipolytica* may produce volatile compounds that contribute to cheese flavor, such as branched-chain aldehydes and alcohols (Sørensen et al., 2011; Padilla et al., 2014). *Yarrowia lipolytica* is found in foods with high protein or fat content because of its strong lipolytic and proteolytic activities (Nicaud, 2012). High amounts of volatile compounds, such as organic acids, sulfides, furans, and short-chain ketones, are produced by *Y. lipolytica* during cheese ripening (Sørensen et al., 2011). The coexistence of *Y. lipolytica* with *G. candidum* can have a negative effect on hypha formation. Moreover, *D. hansenii* and *Y. lipolytica* can dominate the yeast biota of smear ripened cheeses (Mounier et al., 2008; Atanassova et al., 2016; Ceugniez et al., 2017). In the presence of other yeasts, such as *Y. lipolytica* and *G. candidum*, the population of *D. hansenii* significantly decreases. However, *D. hansenii* may inhibit the growth of *K. lactis* and *G. candidum* (Lessard et al., 2012). Finally, the yeasts, bacteria, and mold in cheese may have a symbiotic effect that promotes the flavor development in cheese, but the underlying complex mechanism requires further analysis.

Traditional fermented cheeses are mostly fermented naturally using multiple microbial strains. Scientific problems such as unclear mechanism underlying flavor substance formation and unstable flavor quality have become a bottleneck for developing standardized cheese production processes – severely restricting the transformation of manual production to industrial processing. In recent years, studies have screened the functional microbial strains that improve the flavor of cheese. A study reported that the contents of ethanol, esterase, and glycol acyltransferase are the main factors limiting the synthesis of ethyl acetate in French Camembert (Hong et al., 2018). The results showed that adding *L. lactis* CCFM 12 with high esterase activity and ethanol acyltransferase activity significantly increased the contents of ethyl acetate and fruit aroma. Price et al. (2014) studied the effects of the addition of the functional yeasts *Y. lipolytica* and *K. lactis* on the aroma of blue cheese. These effects were studied by using model combining *Y. lipolytica*, *K. lactis*, and *Pe. roqueforti*, and the results indicated that the low inoculum of *K. lactis* was positively correlated with the cheese flavor, especially the formation of ketone compounds when a small inoculum of *Y. lipolytica* and *K. lactis* was used, the flavor of blue cheese was enhanced. Sørensen et al. (2011) inoculated a combination of *Y. lipolytica*, *S. cerevisiae*, and *D. hansenii* into the cheese fermentation process to improve the flavor quality of the cheese. Compared with the control group, *Y. lipolytica* mainly produced sulfides, furans, and short-chain ketones and *D. hansenii* significantly increased the content of branched-chain aldehydes and alcohols. Therefore, it is important to enhance the formation of flavor by strengthening these advantageous yeasts during the process of cheese ripening. During the process of cheese ripening, the proteolysis, lipolysis, and lactose degradation ability of yeast as well as their lactate and citrate assimilation play important roles – all of which are closely related to the formation of the cheese flavor (Fox and McSweeney, 1998). Therefore, how to maintain the flavor stability of handmade traditional cheese through the strengthening of functional yeasts will provide ideas for later research.

CONCLUSION

With the advancement of science and technology, the use of various traditional methods may decrease. Thus, application and protection of microbial resources used in traditional fermented foods, such as cheese, is urgently needed. Therefore, evaluating the impact of dairy products on human health by using microbial resources in traditional fermented dairy products is essential. The microbial population inhabiting cheese has strong ecological adaptability; it also determines microbial community structural diversity and flavors of the various cheeses from different countries. The regional and climatic differences and diversification of processing technologies have induced considerable changes in the cheeses worldwide in terms of factors, such as appearance and flavor. The metabolic effects of yeast on cheese ripening and quality have long been underestimated, and the metabolic mechanisms of yeast have slowly been elucidated in the recent years. Therefore, studying the relationship of yeast community structure with the formation of yeast microbiota and flavor substances in the process of cheese fermentation is the key to producing cheese with the desired flavor and stable quality by using a cheese-specific standardized process. In summary, cheese has the potential to become a dairy product consumed on a large-scale in the future, and thus, it has very broad market prospects. The current review provided a theoretical basis for the succession and selection of functional yeast strains, and optimization of cheese processing technologies to improve flavor and quality of fermented cheese.

AUTHOR CONTRIBUTIONS

XZ wrote the main text of the manuscript. BW and XS supervised the research activities. All authors contributed to the article and approved the submitted version.

FUNDING

We are grateful for the Young Innovative Talents Cultivation Program of Shihezi University (No. CXBJ202004), the financial support from National Natural Science Foundation of China (No. 31660453 and No. 31960465), Scientific and Technological

Research Projects in Key Areas of the Corps (No. 2019AB025, No. 2020AB014), Science and Technology Research Project of the Eighth Division (No. 2020GY07), Science and Technology Research Project of the Fifth Division (No. 20GY01), and the Shihezi University High-level Talent Research Start-up Project (No. RCSX201712).

REFERENCES

Aishima, T., and Nakai, S. (2010). Pattern recognition of GC profiles for classification of cheese variety. *J. Food Sci.* 52, 939–942. doi: 10.1111/j.1365-2621.1987.tb14248.x

Akpınar, O., Uçar, F., and Yalçın, H. T. (2011). Screening and regulation of alkaline extracellular protease and ribonuclease production of *Yarrowia lipolytica* strains isolated and identified from different cheeses in Turkey. *Ann. Microbiol.* 61, 907–915. doi: 10.1007/s13213-011-0213-x

Aldrete-Tapia, A., Escobar-Ramírez, M. C., Tamplin, M. L., and Hernández-Iturriaga, M. (2014). High-throughput sequencing of microbial communities in poro cheese, an artisanal Mexican cheese. *Food Microbiol.* 44, 136–141. doi: 10.1016/j.fm.2014.05.022

Almeida, M., Hébert, A., Abraham, A. L., Rasmussen, S., Monnet, C., Pons, N., et al. (2014). Construction of a dairy microbial genome catalog opens new perspectives for the metagenomic analysis of dairy fermented products. *BMC Genomics* 15:1101. doi: 10.1186/1471-2164-15-1101

Anifantakis, E. M., Veinoglou, B. C., and Kandarakis, J. G. (2009). Manufacture of Gruyère-type cheese with 50:50 rennet/swine pepsin. *J. Dairy Res.* 48, 513–518. doi: 10.1017/s0022029900022019

Atanassova, M. R., Fernández-Otero, C., Rodríguez-Alonso, P., Fernández-No, I. C., Garabal, J. I., and Centeno, J. A. (2016). Characterization of yeasts isolated from artisanal short-ripened cows' cheeses produced in Galicia (NW Spain). *Food Microbiol.* 53, 172–181. doi: 10.1016/j.fm.2015.09.012

Azarnia, S., Robert, N., and Lee, B. (2006). Biotechnological methods to accelerate cheddar cheese ripening. *Crit. Rev. Biotechnol.* 26, 121–143. doi: 10.1080/07388550600840525

Banjara, N., Suhr, M. J., and Hallen-Adams, H. E. (2015). Diversity of yeast and mold species from a variety of cheese types. *Curr. Microbiol.* 70, 792–800. doi: 10.1007/s00284-015-0790-1

Banks, J. M., Brechany, E. Y., and Christie, W. (1989). The production of low fat cheddar-type cheese. *Int. J. Dairy Technol.* 42, 6–9. doi: 10.1111/j.1471-0307.1989.tb01699.x

Beresford, T. P., Fitzsimons, N. A., Brennan, N. L., and Cogan, T. M. (2001). Recent advances in cheese microbiology. *Int. Dairy J.* 11, 259–274. doi: 10.1016/S0958-6946(01)00056-5

Bertuzzi, A. S., McSweeney, P. L. H., Rea, M. C., and Kilcawley, K. N. (2018). Detection of volatile compounds of cheese and their contribution to the flavor profile of surface-ripened cheese. *Compr. Rev. Food Sci. Food Saf.* 17, 371–390. doi: 10.1111/1541-4337.12332

Binetti, A., Carrasco, M., Reinheimer, J., and Suárez, V. (2013). Yeasts from autochthonal cheese starters: technological and functional properties. *J. Appl. Microbiol.* 115, 434–444. doi: 10.1111/jam.12228

Brackett, R. E., Applebaum, R. S., Wiseman, D. W., and Marth, E. H. (1982). Fate of aflatoxin M1 in brick and limburger-like cheese. *J. Food Prot.* 45, 553–556. doi: 10.4315/0362-028X-45.6.553

Branciari, R., Nijman, I. J., Plas, M. E., Di Antonio, E., and Lenstra, J. A. (2000). Species origin of milk in Italian mozzarella and Greek feta cheese. *J. Food Prot.* 63, 408–411. doi: 10.4315/0362-028X-63.3.408

Breuer, U., and Harms, H. (2006). *Debaryomyces hansenii*-an extremophilic yeast with biotechnological potential. *Yeast* 23, 415–437. doi: 10.1002/yea.1374

Budak, S. O., Figge, M. J., Houbraken, J., and Vries, R. P. D. (2016). The diversity and evolution of microbiota in traditional Turkish divle cave cheese during ripening. *Int. Dairy J.* 58, 50–53. doi: 10.1016/j.idairyj.2015.09.011

Buffa, M., Guamis, B., Saldo, J., and Trujillo, A. J. (2004). Changes in organic acids during ripening of cheeses made from raw, pasteurized or high-pressure-treated goats' milk. *LWT* 37, 247–253. doi: 10.1016/j.lwt.2003.08.006

Califano, A. N., and Bevilacqua, A. E. (2000). Multivariate analysis of the organic acids content of gouda type cheese during ripening. *J. Food Compos. Anal.* 13, 949–960. doi: 10.1006/jfca.2000.0930

Carpino, S., Randazzo, C. L., Pino, A., Russo, N., Rapisarda, T., Belvedere, G., et al. (2017). Influence of PDO Ragusano cheese biofilm microbiota on flavour compounds formation. *Food Microbiol.* 61, 126–135. doi: 10.1016/j.fm.2016.09.006

Carunchiawhetstine, M. E., Karagul-Yuceer, Y., Avsar, Y. K., and Drake, M. A. (2003). Identification and quantification of character aroma components in fresh chevre-style goat cheese. *J. Food Sci.* 68, 2441–2447. doi: 10.1111/j.1365-2621.2003.tb07043.x

Castada, H. Z., Hanas, K., and Barringer, S. A. (2019). Swiss cheese flavor variability based on correlations of volatile flavor compounds, descriptive sensory attributes, and consumer preference. *Foods* 8:78. doi: 10.3390/foods8020078

Centeno, J. A., Tomillo, F. J., Fernández-García, E., Gaya, P., and Nuñez, M. (2002). Effect of wild strains of *Lactococcus lactis* on the volatile profile and the sensory characteristics of ewes' raw milk cheese. *J. Dairy Sci.* 85, 3164–3172. doi: 10.3168/jds.S0022-0302(02)74404-4

Ceruti, R. J., Zorrilla, S. E., and Sihufe, G. A. (2016). Volatile profile evolution of Reggianito cheese during ripening under different temperature–time combinations. *Eur. Food Res. Technol.* 242, 1–10. doi: 10.1007/s00217-016-2640-1

Ceugniez, A., Drider, D., Jacques, P., and Coucheney, F. (2015). Yeast diversity in a traditional French cheese "Tomme d'orchies" reveals infrequent and frequent species with associated benefits. *Food Microbiol.* 52, 177–184. doi: 10.1016/j.fm.2015.08.001

Ceugniez, A., Taminiau, B., Coucheney, F., Jacques, P., Delcenserie, V., Daube, G., et al. (2017). Fungal diversity of "Tomme d'Orchies" cheese during the ripening process as revealed by a metagenomic study. *Int. J. Food Microbiol.* 258, 89–93. doi: 10.1016/j.ijfoodmicro.2017.07.015

Chebeňová-Turcovská, V., Ženišová, K., Kuchta, T., Pangallo, D., and Brežná, B. (2011). Culture-independent detection of microorganisms in traditional Slovakian bryndza cheese. *Int. J. Food Microbiol.* 150, 73–78. doi: 10.1016/j.ijfoodmicro.2011.07.020

Corredor, M., Davila, A.-M., Gaillardin, C., and Casaregola, S. (2000). DNA probes specific for the yeast species *Debaryomyces hansenii*: useful tools for rapid identification. *FEMS Microbiol. Lett.* 193, 171–177. doi: 10.1111/j.1574-6968.2000.tb09420.x

Corsetti, A., Rossi, J., and Gobbetti, M. (2001). Interactions between yeasts and bacteria in the smear surface-ripened cheeses. *Int. J. Food Microbiol.* 69, 1–10. doi: 10.1016/S0168-1605(01)00567-0

Costa, M. J., Maciel, L. C., Teixeira, J. A., Vicente, A. A., and Cerqueira, M. A. (2018). Use of edible films and coatings in cheese preservation: opportunities and challenges. *Food Res. Int.* 107, 84–92. doi: 10.1016/j.foodres.2018.02.013

Curioni, P. M. G., and Bosset, J. O. (2002). Key odorants in various cheese types as determined by gas chromatography-olfactometry. *Int. Dairy J.* 12, 959–984. doi: 10.1016/S0958-6946(02)00124-3

Dalmasso, A., Soto Del Rio, M. L. D., Civera, T., Pattono, D., Cardazzo, B., and Bottero, M. T. (2016). Characterization of microbiota in Plaisentif cheese by high-throughput sequencing. *LWT* 69, 490–496. doi: 10.1016/j.lwt.2016.02.004

Deeth, H. C., and Touch, V. (2000). Methods for detecting lipase activity in milk and milk products. *Aust. J. Dairy Technol.* 55:153.

Delcenserie, V., Taminiau, B., Delhalle, L., Nezer, C., Doyen, P., Crevecoeur, S., et al. (2014). Microbiota characterization of a Belgian protected designation of origin cheese, Herve cheese, using metagenomic analysis. *J. Dairy Sci.* 97, 6046–6056. doi: 10.3168/jds.2014-8225

Delgado, F. J., González-Crespo, J., Cava, R., García-Parra, J., and Ramírez, R. (2010). Characterisation by SPME–GC–MS of the volatile profile of a Spanish soft cheese P.D.O. Torta del Casar during ripening. *Food Chem.* 118, 182–189. doi: 10.1016/j.foodchem.2009.04.081

Dias, O., Pereira, R., Gombert, A. K., Ferreira, E. C., and Rocha, I. (2014). iOD907, the first genome-scale metabolic model for the milk yeast *Kluyveromyces lactis*. *Biotechnol. J.* 9, 776–790. doi: 10.1002/biot.201300242

Dimos, A., Urbacha, G. E., and Miller, A. J. (1996). Changes in flavour and volatiles of full-fat and reducedfat cheddar cheeses during maturation. *Int. Dairy J.* 6, 981–995. doi: 10.1016/S0958-6946(97)84214-8

D'Incecco, P., Limbo, S., Hogenboom, J., Rosi, V., Gobbi, S., and Pellegrino, L. (2020). Impact of extending hard-cheese ripening: a multiparameter characterization of parmigiano reggiano cheese ripened up to 50 months. *Foods* 9:268. doi: 10.3390/foods9030268

Dugat-Bony, E., Straub, C., Teissandier, A., Onésime, D., Loux, V., Monnet, C., et al. (2015). Overview of a surface-ripened cheese community functioning by meta-omics analyses. *PLoS One* 10:e0124360. doi: 10.1371/journal.pone.0124360

Duru, I. C., Laine, P., Andreevskaya, M., Paulin, L., Kananen, S., Tynkkynen, S., et al. (2018). Metagenomic and metatranscriptomic analysis of the microbial community in swiss-type Maasdam cheese during ripening. *Int. J. Food Microbiol.* 281, 10–22. doi: 10.1016/j.ijfoodmicro.2018.05.017

Dzialo, M. C., Park, R., Steensels, J., Lievens, B., and Verstrepen, K. J. (2017). Physiology, ecology and industrial applications of aroma formation in yeast. *FEMS Microbiol. Rev.* 41, S95–S128. doi: 10.1093/femsre/fux031

El Sheikha, A. F. (2018). "Revolution in fermented food: from artisan household technology to era of biotechnology," in *Molecular Techniques in Food Biology: Safety, Biotechnology, Authenticity & Traceability*. eds. A. F. El Sheikha, R. Levin and J. P. Xu (Chichester, UK: John Wiley & Sons Ltd.), 241–260.

El Sheikha, A. F., and Hu, D. M. (2020). Molecular techniques reveal more secrets of fermented foods. *Crit. Rev. Food Sci. Nutr.* 60, 11–32. doi: 10.1080/10408398.2018.1506906

El Sheikha, A. F., and Montet, D. (2014). "African fermented foods: historical roots and real benefits," in *Microorganisms and Fermentation of Traditional Foods*. eds. R. C. Ray and D. Montet (Boca Raton, Florida, USA: Science Publishers Inc. and CRC Press), 248–282.

Engel, E., Septier, C., Leconte, N., Salles, C., and Le Quere, J.-L. (2001). Determination of taste-active compounds of a bitter camembert cheese by omission tests. *J. Dairy Res.* 68, 675–688. doi: 10.1017/S0022029901005209

Engels, W. J. M., Dekker, R., de Jong, C., Neeter, R., and Visser, S. (1997). A comparative study of volatile compounds in the water-soluble fraction of various types of ripened cheese. *Int. Dairy J.* 7, 255–263. doi: 10.1016/s0958-6946(97)00003-4

Ferreira, A. D., and Viljoen, B. C. (2003). Yeasts as adjunct starters in matured Cheddar cheese. *Int. J. Food Microbiol.* 86, 131–140. doi: 10.1016/S0168-1605(03)00252-6

Filippis, F. D., Genovese, A., Ferranti, P., Gilbert, J. A., and Ercolini, D. (2016). Metatranscriptomics reveals temperature-driven functional changes in microbiome impacting cheese maturation rate. *Sci. Rep.* 6:21871. doi: 10.1038/srep21871

Forde, A., and Fitzgerald, G. F. (2000). Biotechnological approaches to the understanding and improvement of mature cheese flavour. *Curr. Opin. Biotechnol.* 11, 484–489. doi: 10.1016/S0958-1669(00)00130-0

Fox, P. F. (ed.) (1993). "Cheese: an overview," in *Cheese: Chemistry, Physics and Microbiology*. Boston: Springer, 1–36.

Fox, P. F., Guinee, T. P., Cogan, T. M., and McSweeney, P. L. H. (eds.) (2017). "Starter cultures," in *Fundamentals of Cheese Science*. Boston: Springer, 121–183.

Fox, P. F., Lucey, J. A., and Cogan, T. M. (1990). Glycolysis and related reactions during cheese manufacture and ripening. *Crit. Rev. Food Sci. Nutr.* 29, 237–253. doi: 10.1080/10408399009527526

Fox, P. F., and McSweeney, P. L. H. (1998). Dairy chemistry and biochemistry. *Mol. Asp. Med.* 24, 3–9.

Fox, P. F., Uniacke-Lowe, T., McSweeney, P., and O'Mahony, J. A. (2015). "Chemistry and biochemistry of cheese," in *Dairy Chemistry and Biochemistry*. ed. P. F. Fox (New York: Springer), 499–546.

Frenzel, M., Zerge, K., Clawin-Rädecker, I., and Lorenzen, P. C. (2015). Comparison of the galacto-oligosaccharide forming activity of different β-galactosidases. *LWT Food Sci. Technol.* 60, 1068–1071. doi: 10.1016/j.lwt.2014.10.064

Fröhlich-Wyder, M.-T., Arias Roth, E., and Jakob, E. (2019). Cheese yeasts. *Yeast* 36, 129–141. doi: 10.1002/yea.3368

Fröhlich-Wyder, M.-T., Bachmann, H. P., and Casey, M. G. (2002). Interaction between propionibacteria and starter/non-starter lactic acid bacteria in swiss-type cheeses. *Lait* 82, 1–15. doi: 10.1051/lait:2001001

Gan, H. H., Yan, B., Linforth, R. S. T., and Fisk, I. D. (2016). Development and validation of an APCI-MS/GC–MS approach for the classification and prediction of cheddar cheese maturity. *Food Chem.* 190, 442–447. doi: 10.1016/j.foodchem.2015.05.096

Gkatzionis, K., Yunita, D., Linforth, R. S. T., Dickinson, M., and Dodd, C. E. R. (2014). Diversity and activities of yeasts from different parts of a stilton cheese. *Int. J. Food Microbiol.* 177, 109–116. doi: 10.1016/j.ijfoodmicro.2014.02.016

Gobbetti, M., and Di Cagno, R. (2017). "Chapter 32: Extra-hard varieties," in *Cheese. 4th Edn.* eds. P. L. H. McSweeney, P. F. Fox, P. D. Cotter and D. W. Everett (San Diego: Academic Press), 809–828.

Goel, M. C., Kulshrestha, D. C., Marth, E. H., Francis, D. W., Bradshaw, J. G., and Read, R. B. (1971). Fate on coliforms in yogurt, buttermilk, sour cream, and cottage cheese during refrigerated storage. *J. Milk Food Technol.* 34, 54–58. doi: 10.4315/0022-2747-34.1.54

Gonçalves Dos Santos, M. T. P., Benito, M. J., Córdoba, M. D. G., Alvarenga, N., and Ruiz-Moyano Seco de Herrera, S. (2017). Yeast community in traditional Portuguese Serpa cheese by culture-dependent and -independent DNA approaches. *Int. J. Food Microbiol.* 262, 63–70. doi: 10.1016/j.ijfoodmicro.2017.09.013

Gori, K., Mortensen, H. D., Arneborg, N., and Jespersen, L. (2005). Expression of the GPD1 and GPP2 orthologues and glycerol retention during growth of *Debaryomyces hansenii* at high NaCl concentrations. *Yeast* 22, 1213–1222. doi: 10.1002/yea.1306

Gori, K., Ryssel, M., Arneborg, N., and Jespersen, L. (2013). Isolation and identification of the microbiota of Danish farmhouse and industrially produced surface-ripened cheeses. *Microb. Ecol.* 65, 602–615. doi: 10.1007/s00248-012-0138-3

Guggisberg, D., Schuetz, P., Winkler, H., Amrein, R., Jakob, E., Fröhlich-Wyder, M.-T., et al. (2015). Mechanism and control of the eye formation in cheese. *Int. Dairy J.* 47, 118–127. doi: 10.1016/j.idairyj.2015.03.001

Holland, R., Liu, S. Q., Crow, V. L., Delabre, M. L., Lubbers, M., Bennett, M., et al. (2005). Esterases of lactic acid bacteria and cheese flavour: milk fat hydrolysis, alcoholysis and esterification. *Int. Dairy J.* 15, 711–718. doi: 10.1016/j.idairyj.2004.09.012

Hong, Q., Liu, X. M., Hang, F., Zhao, J. X., Zhang, H., and Chen, W. (2018). Screening of adjunct cultures and their application in ester formation in camembert-type cheese. *Food Microbiol.* 70, 33–41. doi: 10.1016/j.fm.2017.08.009

Ibáñez, R. A., Govindasamy-Lucey, S., Jaeggi, J. J., Johnson, M. E., McSweeney, P. L. H., and Lucey, J. A. (2020). Low-and reduced-fat milled curd, direct-salted gouda cheese: comparison of lactose standardization of cheesemilk and whey dilution techniques. *J. Dairy Sci.* 103, 1175–1192. doi: 10.3168/jds.2019-17292

Irlinger, F., and Mounier, J. (2009). Microbial interactions in cheese: implications for cheese quality and safety. *Curr. Opin. Biotechnol.* 20, 142–148. doi: 10.1016/j.copbio.2009.02.016

Iwasawa, A., Suzuki-Iwashima, A., Iida, F., and Shiota, M. (2014). Effects of flavor and texture on the desirability of Cheddar cheese during ripening. *Food Sci. Technol. Res.* 20, 23–29. doi: 10.3136/fstr.20.23

Jakobsen, M., and Narvhus, J. (1996). Yeasts and their possible beneficial and negative effects on the quality of dairy products. *Int. Dairy J.* 6, 755–768. doi: 10.1016/0958-6946(95)00071-2

Jo, Y., Benoist, D. M., Ameerally, A., and Drake, M. A. (2018). Sensory and chemical properties of gouda cheese. *J. Dairy Sci.* 101, 1967–1989. doi: 10.3168/jds.2017-13637

Jones, E. L., Shingfield, K. J., Kohen, C., Jones, A. K., Lupoli, B., Grandison, A. S., et al. (2005). Chemical, physical, and sensory properties of dairy products enriched with conjugated linoleic acid. *J. Dairy Sci.* 88, 2923–2937. doi: 10.3168/jds.S0022-0302(05)72973-8

Kataoka, H., Lord, H. L., and Pawliszyn, J. (2000). Applications of solid-phase microextraction in food analysis. *J. Chromatogr. A* 880, 35–62. doi: 10.1016/S0021-9673(00)00309-5

Kelly, A. L., Huppertz, T., and Sheehan, J. J. (2008). Pre-treatment of cheese milk: principles and developments. *Dairy Sci. Technol.* 88, 549–572. doi: 10.1051/dst:2008017

Khattab, A. R., Guirguis, H. A., Tawfik, S. M., and Farag, M. A. (2019). Cheese ripening: a review on modern technologies towards flavor enhancement, process acceleration and improved quality assessment. *Trends Food Sci. Technol.* 88, 343–360. doi: 10.1016/j.tifs.2019.03.009

Kourkoutas, Y., Bosnea, L., Taboukos, S., Baras, C., Lambrou, D., and Kanellaki, M. (2006). Probiotic cheese production using *lactobacillus casei* cells immobilized on fruit pieces. *J. Dairy Sci.* 89, 1439–1451. doi: 10.3168/jds.S0022-0302(06)72212-3

Krishnan, K., Campbell, Y. L., To, K. V., Lima, G., Byron, M. D., Zhang, X., et al. (2019). Effects of temperature, relative humidity, and protective netting on Tyrophagus putrescentiae (schrank) (sarcoptiformes: Acaridae) infestation, fungal growth, and product quality of cave-aged Cheddar cheese. *J. Stored Prod. Res.* 83, 44–53. doi: 10.1016/j.jspr.2019.05.014

Kubíčková, J., and Grosch, W. (1997). Evaluation of potent odorants of camembert cheese by dilution and concentration techniques. *Int. Dairy J.* 7, 65–70. doi: 10.1016/S0958-6946(96)00044-1

Lai, F. N., Zhai, H. L., Cheng, M., Ma, J. Y., Cheng, S. F., Ge, W., et al. (2016). Whole-genome scanning for the litter size trait associated genes and SNPs under selection in dairy goat (*Capra hircus*). *Sci. Rep.* 6:38096. doi: 10.1038/srep38096

Landaud, S., Helinck, S., and Bonnarme, P. (2008). Formation of volatile sulfur compounds and metabolism of methionine and other sulfur compounds in fermented food. *Appl. Microbiol. Biotechnol.* 77, 1191–1205. doi: 10.1007/s00253-007-1288-y

Lawrence, R. C., Gilles, J., Creamer, L. K., Crow, V. L., Heap, H. A., Honoré, C. G., et al. (2004). "Cheddar cheese and related dry-salted cheese varieties," in *Cheese: Chemistry, Physics and Microbiology*. eds. P. F. Fox, P. L. H. McSweeney, T. M. Cogan and T. P. Guinee (Boston, MA: Springer), 71–102.

Legg, A. K., Carr, A. J., Bennett, R. J., and Johnston, K. A. (2017). "Chapter 26: General aspects of cheese technology," in *Cheese. 4th Edn.* eds. P. L. H. McSweeney, P. F. Fox, P. D. Cotter and D. W. Everett (San Diego: Academic Press), 643–675.

Lessard, M.-H., Bélanger, G., St-Gelais, D., and Labrie, S. (2012). The composition of camembert cheese-ripening cultures modulates both mycelial growth and appearance. *Appl. Environ. Microbiol.* 78:1813. doi: 10.1128/AEM.06645-11

Lessard, M.-H., Viel, C., Boyle, B., St-Gelais, D., and Labrie, S. (2014). Metatranscriptome analysis of fungal strains Penicillium camemberti and Geotrichum candidumreveal cheese matrix breakdown and potential development of sensory properties of ripened camembert-type cheese. *BMC Genomics* 15:235. doi: 10.1186/1471-2164-15-235

Łopusiewicz, Ł., Drozłowska, E., Tarnowiecka-Kuca, A., Bartkowiak, A., Mazurkiewicz-Zapałowicz, K., and Salachna, P. (2020). Biotransformation of flaxseed oil cake into bioactive camembert-analogue using lactic acid bacteria, *Penicillium camemberti* and *Geotrichum candidum*. *Microorganisms* 8:1266. doi: 10.3390/microorganisms8091266

Lucey, J. A., and Fox, P. F. (1993). Importance of calcium and phosphate in cheese manufacture: a review. *J. Dairy Sci.* 76, 1714–1724. doi: 10.3168/jds.S0022-0302(93)77504-9

Majcher, M. A., Myszka, K., Gracka, A., Grygier, A., and Jeleń, H. H. (2018). Key odorants of Lazur, a polish mold-ripened cheese. *J. Agric. Food Chem.* 66, 2443–2448. doi: 10.1021/acs.jafc.6b04911

Mallatou, H., Pappa, E., and Massouras, T. (2003). Changes in free fatty acids during ripening of Teleme cheese made with ewes', goats', cows' or a mixture of ewes' and goats' milk. *Int. Dairy J.* 13, 211–219. doi: 10.1016/S0958-6946(02)00153-X

Mansour, S., Beckerich, J. M., and Bonnarme, P. (2008). Lactate and amino acid catabolism in the cheese-ripening yeast *Yarrowia lipolytica*. *Appl. Environ. Microbiol.* 74:6505. doi: 10.1128/AEM.01519-08

Marilley, L., and Casey, M. G. (2004). Flavours of cheese products: metabolic pathways, analytical tools and identification of producing strains. *Int. J. Food Microbiol.* 90, 139–159. doi: 10.1016/S0168-1605(03)00304-0

Marino, M., Innocente, N., Maifreni, M., Mounier, J., Cobo-Díaz, J. F., Coton, E., et al. (2017). Diversity within Italian cheesemaking brine-associated bacterial communities evidenced by massive parallel 16S rRNA gene tag sequencing. *Front. Microbiol.* 8:2119. doi: 10.3389/fmicb.2017.02119

Marsili, R. (1985). Monitoring chemical changes in Cheddar cheese during aging by high performance liquid chromatography and gas chromatography techniques. *J. Dairy Sci.* 68, 3155–3161. doi: 10.3168/jds.S0022-0302(85)81221-2

McSweeney, P. L. H. (2010). Biochemistry of cheese ripening. *Int. J. Dairy Technol.* 57, 127–144. doi: 10.1111/j.1471-0307.2004.00147.x

McSweeney, P. L. H. (2011). "Encyclopedia of dairy sciences (second edition)," in *Cheese Biochemistry of Cheese Ripening*. ed. J. W. Fuquay (San Diego: Academic Press), 667–674.

McSweeney, P. L. H., Fox, P. F., and Ciocia, F. (2017). "Chapter 16: Metabolism of residual lactose and of lactate and citrate," in *Cheese. 4th Edn.* eds. P. L. H. McSweeney, P. F. Fox, P. D. Cotter and D. W. Everett (San Diego: Academic Press), 411–421.

McSweeney, P. L. H., Ottogalli, G., and Fox, P. F. (2004). "Cheese: chemistry, physics and microbiology," in *Diversity of Cheese Varieties: An Overview*. eds. P. F. Fox, P. L. H. McSweeney, T. M. Cogan and T. P. Guinee (San Diego: Academic Press), 1–23.

McSweeney, P. L. H., and Sousa, M. J. (2000). Biochemical pathways for the production of flavour compounds in cheeses during ripening: a review. *Lait* 80, 293–324. doi: 10.1051/lait:2000127

Melchiorsen, R. C., Jokumsen, V. K., Villadsen, J., Israelsen, H., and Arnau, J. (2002). The level of pyruvate-formate lyase controls the shift from homolactic to mixed-acid product formation in *Lactococcus lactis*. *Appl. Microbiol. Biotechnol.* 58, 338–344. doi: 10.1007/s00253-001-0892-5

Moghaddas Kia, E., Alizadeh, M., and Esmaiili, M. (2018). Development and characterization of probiotic UF feta cheese containing *lactobacillus paracasei* microencapsulated by enzyme based gelation method. *J. Food Sci. Technol.* 55, 3657–3664. doi: 10.1007/s13197-018-3294-8

Monnet, C., Dugat-Bony, E., Swennen, D., Beckerich, J. M., Irlinger, F., Fraud, S., et al. (2016). Investigation of the activity of the microorganisms in a reblochon-style cheese by metatranscriptomic analysis. *Front. Microbiol.* 7:536. doi: 10.3389/fmicb.2016.00536

Monnet, C., Landaud, S., Bonnarme, P., and Swennen, D. (2015). Growth and adaptation of microorganisms on the cheese surface. *FEMS Microbiol. Lett.* 362, 1–9. doi: 10.1093/femsle/fnu025

Monti, L., Negri, S., Meucci, A., Stroppa, A., Galli, A., and Contarini, G. (2017). Lactose, galactose and glucose determination in naturally "lactose free" hard cheese: HPAEC-PAD method validation. *Food Chem.* 220, 18–24. doi: 10.1016/j.foodchem.2016.09.185

Mounier, J., Monnet, C., Jacques, N., Antoinette, A., and Irlinger, F. (2009). Assessment of the microbial diversity at the surface of Livarot cheese using culture-dependent and independent approaches. *Int. J. Food Microbiol.* 133, 31–37. doi: 10.1016/j.ijfoodmicro.2009.04.020

Mounier, J., Monnet, C., Vallaeys, T., Arditi, R., Sarthou, A. S., Hélias, A., et al. (2008). Microbial interactions within a cheese microbial community. *Appl. Environ. Microbiol.* 74:172. doi: 10.1128/AEM.01338-07

Mucchetti, G., Bonvini, B., Remagni, M. C., Ghiglietti, R., Locci, F., Barzaghi, S., et al. (2008). Influence of cheese-making technology on composition and microbiological characteristics of Vastedda cheese. *Food Control* 19, 119–125. doi: 10.1016/j.foodcont.2007.02.011

Neviani, E., Bottari, B., Lazzi, C., and Gatti, M. (2013). New developments in the study of the microbiota of raw-milk, long-ripened cheeses by molecular methods: the case of grana Padano and Parmigiano Reggiano. *Front. Microbiol.* 4:36. doi: 10.3389/fmicb.2013.00036

Nicaud, J. M. (2012). Yarrowia lipolytica. *Yeast* 29, 409–418. doi: 10.1002/yea.2921

Nielsen, K. F., Dalsgaard, P. W., Smedsgaard, J., and Larsen, T. O. (2005). Andrastins a–d, *Penicillium roqueforti* metabolites consistently produced in blue-mold-ripened cheese. *J. Agric. Food Chem.* 53, 2908–2913. doi: 10.1021/jf047983u

Ozturkoglu-Budak, S., Wiebenga, A., Bron, P. A., and Vries, R. P. D. (2016). Protease and lipase activities of fungal and bacterial strains derived from an artisanal raw ewe's milk cheese. *Int. J. Food Microbiol.* 237, 17–27. doi: 10.1016/j.ijfoodmicro.2016.08.007

Padilla, B., Belloch, C., López-Díez, J. J., Flores, M., and Manzanares, P. (2014). Potential impact of dairy yeasts on the typical flavour of traditional ewes' and goats' cheeses. *Int. Dairy J.* 35, 122–129. doi: 10.1016/j.idairyj.2013.11.002

Panikuttira, B., O'Shea, N., Tobin, J. T., Tiwari, B. K., and O'Donnell, C. P. (2018). Process analytical technology for cheese manufacture. *Int. J. Food Sci. Technol.* 53, 1803–1815. doi: 10.1111/ijfs.13806

Pino, A., Liotta, L., Randazzo, C. L., Todaro, A., Mazzaglia, A., De Nardo, F., et al. (2018). Polyphasic approach to study physico-chemical, microbiological and sensorial characteristics of artisanal Nicastrese goat's cheese. *Food Microbiol.* 70, 143–154. doi: 10.1016/j.fm.2017.09.005

Plutowska, B., and Wardencki, W. (2007). Aromagrams – aromatic profiles in the appreciation of food quality. *Food Chem.* 101, 845–872. doi: 10.1016/j.foodchem.2005.12.028

Price, E. J., Linforth, R. S. T., Dodd, C. E. R., Phillips, C. A., Hewson, L., Hort, J., et al. (2014). Study of the influence of yeast inoculum concentration

(*Yarrowia lipolytica* and *Kluyveromyces lactis*) on blue cheese aroma development using microbiological models. *Food Chem.* 145, 464–472. doi: 10.1016/j.foodchem.2013.08.081

Rantsiou, K., Urso, R., Dolci, P., Comi, G., and Cocolin, L. (2008). Microflora of feta cheese from four Greek manufacturers. *Int. J. Food Microbiol.* 126, 36–42. doi: 10.1016/j.ijfoodmicro.2008.04.031

Ray, R., El Sheikha, A. F., and Kumar, S. (2014). "Oriental fermented functional (probiotic) foods," in *Microorganisms and Fermentation of Traditional Foods*. eds. R. C. Ray and D. Montet (Boca Raton, Florida, USA: Science Publishers Inc. and CRC Press), 283–311.

Rea, M. C., Görges, S., Gelsomino, R., Brennan, N. M., Mounier, J., Vancanneyt, M., et al. (2007). Stability of the biodiversity of the surface consortia of Gubbeen, a red-smear cheese. *J. Dairy Sci.* 90, 2200–2210. doi: 10.3168/jds.2006-377

Reif, G. D., Shahani, K. M., Vakil, J. R., and Crowe, L. K. (1976). Factors affecting b-complex vitamin content of cottage cheese1, 2. *J. Dairy Sci.* 59, 410–415. doi: 10.3168/jds.S0022-0302(76)84221-X

Rilla, N., Martínez, B., Delgado, T., and Rodríguez, A. (2003). Inhibition of clostridium tyrobutyricum in Vidiago cheese by *Lactococcus lactis* ssp. lactis IPLA 729, a nisin Z producer. *Int. J. Food Microbiol.* 85, 23–33. doi: 10.1016/S0168-1605(02)00478-6

Roostita, R., and Fleet, G. H. (1996). The occurrence and growth of yeasts in camembert and blue-veined cheeses. *Int. J. Food Microbiol.* 28, 393–404. doi: 10.1016/0168-1605(95)00018-6

Sandine, W. E., and Elliker, P. R. (1970). Microbially induced flavors and fermented foods. Flavor in fermented dairy products. *J. Agric. Food Chem.* 18, 557–562. doi: 10.1021/jf60170a023

Santiago-López, L., Aguilar-Toalá, J. E., Hernández-Mendoza, A., Vallejo-Cordoba, B., Liceaga, A. M., and González-Córdova, A. F. (2018). Invited review: bioactive compounds produced during cheese ripening and health effects associated with aged cheese consumption. *J. Dairy Sci.* 101, 3742–3757. doi: 10.3168/jds.2017-13465

Schwenninger, S. M., Meile, L., and Lacroix, C. (2011). "Protective cultures, antimicrobial metabolites and bacteriophages for food and beverage biopreservation," in *2—Antifungal Lactic Acid Bacteria and Propionibacteria for Food Biopreservation*. ed. C. Lacroix (New York: Woodhead Publishing), 27–62.

Seiler, H., and Busse, M. (1990). The yeasts of cheese brines. *Int. J. Food Microbiol.* 11, 289–303. doi: 10.1016/0168-1605(90)90022-W

Sert, D., Akin, N., and Aktumsek, A. (2014). Lipolysis in Tulum cheese produced from raw and pasteurized goats' milk during ripening. *Small Rumin. Res.* 121, 351–360. doi: 10.1016/j.smallrumres.2014.06.006

Singh, T. K., Drake, M. A., and Cadwallader, K. R. (2003). Flavor of Cheddar cheese: a chemical and sensory perspective. *Compr. Rev. Food Sci. Food Saf.* 2, 166–189. doi: 10.1111/j.1541-4337.2003.tb00021.x

Smit, G., Smit, B. A., and Engels, W. J. M. (2005). Flavour formation by lactic acid bacteria and biochemical flavour profiling of cheese products. *FEMS Microbiol. Rev.* 29, 591–610. doi: 10.1016/j.fmrre.2005.04.002

Soggiu, A., Piras, C., Mortera, S. L., Alloggio, I., Urbani, A., Bonizzi, L., et al. (2016). Unravelling the effect of clostridia spores and lysozyme on microbiota dynamics in grana Padano cheese: a metaproteomics approach. *J. Proteome* 147, 21–27. doi: 10.1016/j.jprot.2016.03.035

Sørensen, L. M., Gori, K., Petersen, M. A., Jespersen, L., and Arneborg, N. (2011). Flavour compound production by *Yarrowia lipolytica*, *Saccharomyces cerevisiae* and *Debaryomyces hansenii* in a cheese-surface model. *Int. Dairy J.* 21, 970–978. doi: 10.1016/j.idairyj.2011.06.005

Spano, G., Russo, P., Lonvaud-Funel, A., Lucas, P., Alexandre, H., Grandvalet, C., et al. (2010). Biogenic amines in fermented foods. *Eur. J. Clin. Nutr.* 64, S95–S100. doi: 10.1038/ejcn.2010.218

Steensels, J., and Verstrepen, K. J. (2014). Taming wild yeast: potential of conventional and nonconventional yeasts in industrial fermentations. *Annu. Rev. Microbiol.* 68, 61–80. doi: 10.1146/annurev-micro-091213-113025

Suzuki-Iwashima, A., Matsuura, H., Iwasawa, A., and Shiota, M. (2020). Metabolomics analyses of the combined effects of lactic acid bacteria and *Penicillium camemberti* on the generation of volatile compounds in model mold-surface-ripened cheeses. *J. Biosci. Bioeng.* 129, 333–347. doi: 10.1016/j.jbiosc.2019.09.005

Suzzi, G., Lombardi, A., Lanorte, M. T., Caruso, M., Andrighetto, C., and Gardini, F. (2000). Phenotypic and genotypic diversity of yeasts isolated from water-buffalo mozzarella cheese. *J. Appl. Microbiol.* 88, 117–123. doi: 10.1046/j.1365-2672.2000.00926.x

Tajammal Munir, M., Yu, W., Young, B. R., and Wilson, D. I. (2015). The current status of process analytical technologies in the dairy industry. *Trends Food Sci. Technol.* 43, 205–218. doi: 10.1016/j.tifs.2015.02.010

Talbot-Walsh, G., Kannar, D., and Selomulya, C. (2018). A review on technological parameters and recent advances in the fortification of processed cheese. *Trends Food Sci. Technol.* 81, 193–202. doi: 10.1016/j.tifs.2018.09.023

Tedeschi, T., Galaverna, G., Dossena, A., and Sforza, S. (2013). "Chapter 19: Comprehensive analytical chemistry," in *Cheeses*. eds. M. de la Guardia and A. Gonzálvez (Italy: Elsevier), 479–509.

Temizkan, R., Yasar, K., and Hayaloglu, A. A. (2015). Changes during ripening in chemical composition, proteolysis, volatile composition and texture in Kashar cheese made using raw bovine, ovine or caprine milk. *Int. J. Food Sci. Technol.* 49, 2643–2649. doi: 10.1111/ijfs.12597

Thierry, A., Collins, Y. F., Abeijón Mukdsi, M. C., McSweeney, P. L. H., Wilkinson, M. G., and Spinnler, H. E. (2017). "Chapter 17: Lipolysis and metabolism of fatty acids in cheese," in *Cheese. 4th Edn.* eds. P. L. H. McSweeney, P. F. Fox, P. D. Cotter and D. W. Everett (San Diego: Academic Press), 423–444.

Tomita, S., Nakamura, T., and Okada, S. (2018). NMR- and GC/MS-based metabolomic characterization of sunki, an unsalted fermented pickle of turnip leaves. *Food Chem.* 258, 25–34. doi: 10.1016/j.foodchem.2018.03.038

Upreti, P., and Metzger, L. E. (2006). Influence of calcium and phosphorus, lactose, and salt-to-moisture ratio on Cheddar cheese quality: manufacture and composition. *J. Dairy Sci.* 89, 420–428. doi: 10.3168/jds.S0022-0302(06)72106-3

Urbach, G. (1993). Relations between cheese flavour and chemical composition. *Int. Dairy J.* 3, 389–422. doi: 10.1016/0958-6946(93)90025-U

Vedamuthu, E. R. (1994). The dairy *Leuconostoc*: use in dairy products. *J. Dairy Sci.* 77, 2725–2737.

Viljoen, B. C., Khoury, A. R., and Hattingh, A. (2003). Seasonal diversity of yeasts associated with white-surface mould-ripened cheeses. *Food Res. Int.* 36, 275–283. doi: 10.1016/S0963-9969(02)00169-2

Vlieg, J. V. H., and Hugenholtz, J. (2007). Mining natural diversity of lactic acid bacteria for flavour and health benefits. *Int. Dairy J.* 17, 1290–1297. doi: 10.1016/j.idairyj.2007.02.010

Voigt, D. D., Chevalier, F., Donaghy, J. A., Patterson, M. F., Qian, M. C., and Kelly, A. L. (2012). Effect of high-pressure treatment of milk for cheese manufacture on proteolysis, lipolysis, texture and functionality of Cheddar cheese during ripening. *Innovative Food Sci. Emerg. Technol.* 13, 23–30. doi: 10.1016/j.ifset.2011.10.004

Wang, C. L., Shi, D. J., and Gong, G. L. (2008). Microorganisms in Daqu: a starter culture of Chinese Maotai-flavor liquor. *World J. Microbiol. Biotechnol.* 24, 2183–2190. doi: 10.1007/s11274-008-9728-0

Wolfe, B. E., Button, J. E., Santarelli, M., and Dutton, R. J. (2014). Cheese rind communities provide tractable systems for in situ and in vitro studies of microbial diversity. *Cell* 158, 422–433. doi: 10.1016/j.cell.2014.05.041

Woo, A. H., Kollodge, S., and Lindsay, R. C. (1984). Quantification of major free fatty acids in several cheese varieties1. *J. Dairy Sci.* 67, 874–878. doi: 10.3168/jds.S0022-0302(84)81380-6

Woo, A. H., and Lindsay, R. C. (1984). Concentrations of major free fatty acids and flavor development in italian cheese varieties1. *J. Dairy Sci.* 67, 960–968. doi: 10.3168/jds.S0022-0302(84)81394-6

Wu, Q., Xu, Y., and Chen, L. (2012). Diversity of yeast species during fermentative process contributing to Chinese Maotai-flavour liquor making. *Lett. Appl. Microbiol.* 55, 301–307. doi: 10.1111/j.1472-765X.2012.03294.x

Xiao, J., Chen, Y., Li, J., Shi, X., Deng, L., and Wang, B. (2020). Evaluation of the effect of auxiliary starter yeasts with enzyme activities on Kazak cheese quality and flavor. *Front. Microbiol.* 11:614208. doi: 10.3389/fmicb.2020.614208

Zerfiridis, G. K., Vafopoulou-Mastrogiannaki, A., and Litopoulou-Tzanetaki, E. (1984). Changes during ripening of commercial Gruyère cheese. *J. Dairy Sci.* 67, 1397–1405. doi: 10.3168/jds.S0022-0302(84)81454-X

Zheng, X. C., Ge, Z., Lin, K., Zhang, D., Chen, Y., Xiao, J., et al. (2021). Dynamic changes in bacterial microbiota succession and flavour development during milk fermentation of Kazak artisanal cheese. *Int. Dairy J.* 113:104878. doi: 10.1016/j.idairyj.2020.104878

Zheng, X. J., Li, K., Shi, X., Ni, Y., Li, B., and Zhuge, B. (2018a). Potential characterization of yeasts isolated from Kazak artisanal cheese to produce flavoring compounds. *MicrobiologyOpen* 7:e00533. doi: 10.1002/mbo3.533

Zheng, X. J., Liu, F., Shi, X., Wang, B., Li, K., Li, B., et al. (2018b). Dynamic correlations between microbiota succession and flavor development involved in the ripening of Kazak artisanal cheese. *Food Res. Int.* 105, 733–742. doi: 10.1016/j.foodres.2017.12.007

Zhu, J., Chen, F., Wang, L., Niu, Y., Yu, D., Shu, C., et al. (2015). Comparison of aroma-active volatiles in oolong tea infusions using GC–olfactometry, GC–FPD, and GC–MS. *J. Agric. Food Chem.* 63, 7499–7510. doi: 10.1021/acs.jafc.5b02358

Conflict of Interest: The authors declare that the research was conducted in the absence of any commercial or financial relationships that could be construed as a potential conflict of interest.

Publisher's Note: All claims expressed in this article are solely those of the authors and do not necessarily represent those of their affiliated organizations, or those of the publisher, the editors and the reviewers. Any product that may be evaluated in this article, or claim that may be made by its manufacturer, is not guaranteed or endorsed by the publisher.

frontiers in Microbiology

ORIGINAL RESEARCH
published: 02 August 2021
doi: 10.3389/fmicb.2021.715295

Comparative Study on the Antioxidant Activity of *Monascus* Yellow Pigments From Two Different Types of *Hongqu*—Functional Qu and Coloring Qu

Li Wu[1,2,3], Kangxi Zhou[2], Feng Chen[2], Guimei Chen[2], Ying Yu[2], Xucong Lv[1,2], Wen Zhang[2], Pingfan Rao[2] and Li Ni[1,2]**

[1] College of Chemistry, Fuzhou University, Fuzhou, China, [2] Institute of Food Science and Technology, College of Biological Science and Engineering, Fuzhou University, Fuzhou, China, [3] Research Institute of Agri-Engineering and Technology, Fujian Academy of Agricultural Sciences, Fuzhou, China

OPEN ACCESS

Edited by:
Mutamed Ayyash,
United Arab Emirates University,
United Arab Emirates

Reviewed by:
Laurent Dufossé,
Université de la Réunion, France
Zhenqiang Wu,
South China University of Technology, China

***Correspondence:**
Xucong Lv
xucong1154@163.com
Li Ni
nili-fzu@qq.com

Specialty section:
This article was submitted to Food Microbiology, a section of the journal Frontiers in Microbiology

Received: 26 May 2021
Accepted: 05 July 2021
Published: 02 August 2021

Citation:
Wu L, Zhou K, Chen F, Chen G, Yu Y, Lv X, Zhang W, Rao P and Ni L (2021) Comparative Study on the Antioxidant Activity of Monascus Yellow Pigments From Two Different Types of Hongqu—Functional Qu and Coloring Qu. Front. Microbiol. 12:715295. doi: 10.3389/fmicb.2021.715295

This study is the first to investigate the difference in the composition of *Monascus* azaphilone pigments (MonAzPs) between functional Qu (FQ) and coloring Qu (CQ) and analyze their relationships with antioxidant activity. The composition of key active components and antioxidant activity of the ethanol extracts of FQ and CQ were analyzed by Uv-vis, HPLC, and chemical antioxidant tests. The composition of MonAzPs of the ethanol extracts was further analyzed by HPLC-MS. Seven *Monascus* yellow pigments (MYPs) with high abundance were successfully purified for the antioxidation evaluation *in vitro* and in the cell. Correlation analysis between the metabolites and the antioxidant activity of *Hongqu* indicated that MonAzPs might play an essential role in the antioxidant activity ($r > 0.80$). By contrast, the monacolin K (MK), polysaccharide, ergosterol, and γ-aminobutyric acid (GABA) were not significantly correlated with the antioxidant activity. Orthogonal partial least squares discriminant analysis (OPLS-DA) based on the composition of MonAzPs revealed that the abundance of MYPs is significantly different between FQ and CQ ($P < 0.05$ and $VIP > 1.0$). Seven MYPs (monasfluore A, monaphilone B, monascuspilion, monascin, monaphilone A, ankaflavin, and new yellow pigment) with high abundance were successfully purified for the antioxidation evaluation. Chemical antioxidant tests revealed that the antioxidant activities of monaphilone A, ankaflavin, and new yellow pigment only from CQ were significantly more potent than monasfluore A and monascuspilion only separated from FQ. The cellular antioxidant assay (CAA) showed that the new yellow pigment had the best antioxidant activity (quercetin equivalent 7.23 μM), followed by monasfluore A and monaphilone B, all of which were significantly better than monascin and ankaflavin, the two most frequently reported MYPs. Research on the structure–activity relationship demonstrated that alterations of the hydroxyl that occurred on C-3′ or C-11 obviously affected the

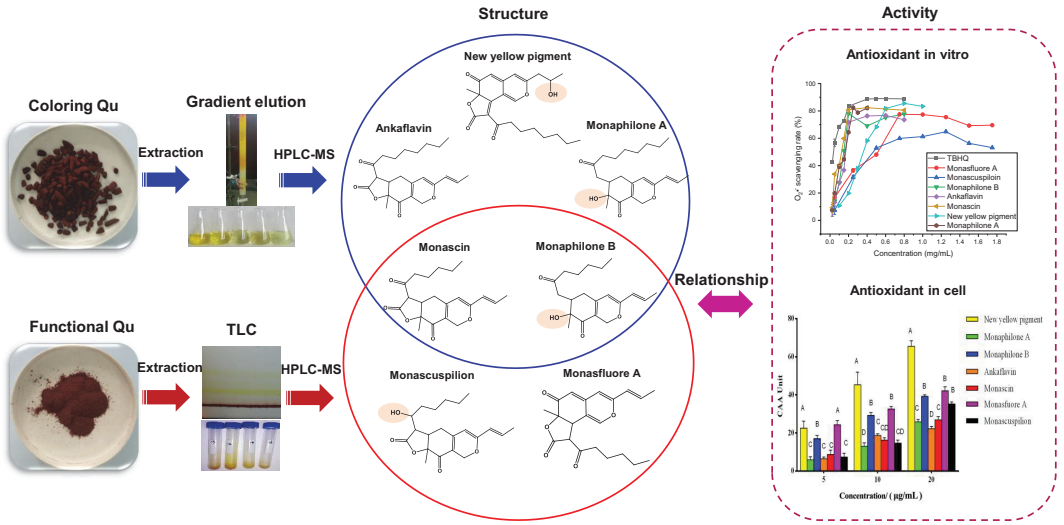

GRAPHICAL ABSTRACT | *Monascus* yellow pigments (MYPs) in functional Qu (FQ) have a higher antioxidant potential than those in coloring Qu (CQ). The difference in antioxidant activities of MYPs is due to the critical hydroxyl group on C-3′ or C-11.

antioxidant activities of MYPs. Our findings provide evidence that MYPs may be the key active components for CQ to have a more potent antioxidant capacity than FQ. The alterations of the hydroxyl that occurred on C-3′ or C-11 obviously affected the antioxidant activities of MYPs.

Keywords: *Hongqu*, *Monascus* azaphilone pigments, *Monascus* yellow pigment, antioxidant activity, cellular antioxidation

INTRODUCTION

Hongqu (rice fermented by *Monascus*) is used as medicine and food for thousands of years in Asia (Huang Z. et al., 2019). According to the different *Monascus* strains (*Monascus pilosus* for FQ and *Monascus purpureus* for CQ) and fermentation processes (**Supplementary Figure 1**), *Hongqu* is mainly divided into functional Qu (FQ) and coloring Qu (CQ). FQ is rich in Monacolin K (MK, over 4.0 mg/g)(National Development and Reform Commission of the People's Republic of China, 2007), and CQ is rich in *Monascus* Azaphilone pigments (MonAzPs, over 1000 U/g)(National Health and Family Planning Commission of the People's Republic of China, 2015). FQ and CQ are fermented with different *Monascus* strains with excellent pigment and MK production ability, respectively. Besides, CQ is generally fermented in a large pond for 5–7 days, and FQ is generally fermented in an Erlenmeyer flask (500 or 1,000 ml) for 35–42 days. Because of the differences in the fermentation strains and fermentation processes, the fermented products (FQ and CQ) have different metabolite compositions and functional characteristics. The ancient medical work "*Compendium of Materia Medica*" recorded that *Hongqu* has the beneficial effects of promoting blood circulation and removing blood stasis. Modern medical researches verified and explored multiple pharmacological activities of *Hongqu* and its metabolites, including hypolipidemia (Wang and Pan, 2003; Lee and Pan, 2012; Lee C. L. et al., 2013), hypoglycemia (Shi et al., 2012; Zhou et al., 2019), and anti-aging (Chen et al., 2015). Certain correlations between those pharmacological activities and antioxidation had been found with the in-depth study. The mechanism may be related to that special molecular structure transferring hydrogen to free radicals or accepting free radical electrons (Zhang et al., 2020), which can scavenge excessive free radicals and maintain redox balance. The study of antioxidant activity has been the basis for other activities. The antioxidant activity of *Hongqu* may be related to the key active components of *Monascus*, including MonAzPs, MK, γ-aminobutyric acid (GABA), ergosterol, and polysaccharides. However, the effects or contribution of the metabolites in *Hongqu* on the antioxidant activity needs to be further evaluated.

Among the metabolites in *Hongqu*, MonAzPs have excellent antioxidant capacity (Qu et al., 2008; Chen et al., 2017), of which MYPs have the most potent antioxidant capacity (Zhang et al., 2020). A previous study found that ANKASCIN 568 plus (monascin and ankaflavin as the main functional components) may increase the antioxidant enzyme activities and inhibit the oxidation reaction induced by amyloid Aβ, thereby significantly improving the memory and learning ability of Alzheimer's (Chen et al., 2015). Besides, monascin may inhibit the oxidative stress caused by the phosphorylation of peroxisome proliferator-activated receptor-γ (PPARγ) by attenuating the activation of protein kinase C (PKC),

thereby repairing pancreatic damage (Hsu W. H. et al., 2013). The antioxidant activity has been further confirmed to be closely related to other pharmacological activities (Lee C. L. et al., 2013). The relationship between MonAzPs (especially MYPs) and antioxidant activity needs to be further explored to promote the development and utilization of MYPs antioxidant resources.

In this study, the difference of key active components in *Hongqu* (FQ and CQ) and their relationship with antioxidant activity were compared. Besides, the composition of MonAzPs and the *in vitro* antioxidant activity (chemical antioxidant tests and cellular antioxidant assay) of MYPs isolated from two types of *Hongqu* were further investigated. Finally, the relationship between the antioxidant activities and the structure of MYPs was also analyzed, which laid the foundation for the research on the antioxidant activity of MYPs and also provided a reference for studying the antioxidative related effects of MYPs.

MATERIALS AND METHODS

Material

Hongqu samples were mainly collected from Ningde City and Fuzhou City in Fujian Province, and Jinhua City and Jiangshan City in Zhejiang Province, including five samples with MK over 4.0 mg/g (also named functional Qu, FQ1–5) and six samples with pigment over 1,000 U/g (also named coloring Qu, CQ1–6) (**Table 1**). The appearance of *Hongqu* showed that the shape of FQ was powder and CQ was rice grains, and the color of CQ was redder and darker than FQ (**Figure 1**).

Analysis of the Composition of Key Active Components

Determination of the Total Color Value

The pigments quantification was done with a UV-vis spectrophotometer (CLARIOstar, BMG LABTECH GmbH, Ortenberg, Germany). The total color value was assessed by measuring the absorbance of 75% ethanol extract of *Hongqu* at 505 nm. The result was expressed as the absorbance unit per gram at a specific wavelength (Srianta et al., 2016).

Determination of MK by HPLC

Determination of MK by HPLC was in accordance to the method in QB/T 2847-2007 and reference (Huang C. F. et al., 2019) with minor modification. Before chromatographic analysis, the supernatant was filtered through a 0.22 μm filter. The supernatant was measured by Waters e2695 with a chromatographic column (Zorbax SB-C18 column, 5 μm × 250 mm × 4.6 mm) and a UV detector at 238 nm. The mobile phase was composed of methanol:water:phosphoric

TABLE 1 | The source and region of *Hongqu*.

Hongqu	Source	Region	Remarks
FQ1	Zhejiang Sanhe Biotech Co., Ltd.	Jiangshan City, Zhejiang Province	MK 3.0%
FQ2	Zhejiang Sanhe Biotech Co., Ltd.	Jiangshan City, Zhejiang Province	MK 1.5%
FQ3	Fuzhou University	Jinhua City, Zhejiang Province	MK 0.5%
FQ4	Fujian Outlet Biotech Co., Ltd.	Fuzhou City, Fujian Province	MK0.5%
FQ5	Fujian Outlet Biotech Co., Ltd.	Fuzhou City, Fujian Province	MK 1.0%
CQ1	Fujian Pinghuhong Bio-tech Co., Ltd.	Ningde City, Fujian Province	Color value 1,000 U/g
CQ2	Fujian Chengjiu *Hongqu* Co., Ltd.	Ningde City, Fujian Province	Color value 1,300 U/g
CQ3	Fujian Pinghuhong Bio-tech Co., Ltd.	Ningde City, Fujian Province	Color value 2,000 U/g
CQ4	Fujian Pinghuhong Bio-tech Co., Ltd.	Ningde City, Fujian Province	Color value 4,000 U/g
CQ5	Fujian Chengjiu *Hongqu* Co., Ltd.	Ningde City, Fujian Province	Color value 500 U/g
CQ6	Fujian Chengjiu *Hongqu* Co., Ltd.	Ningde City, Fujian Province	Color value 3,500 U/g

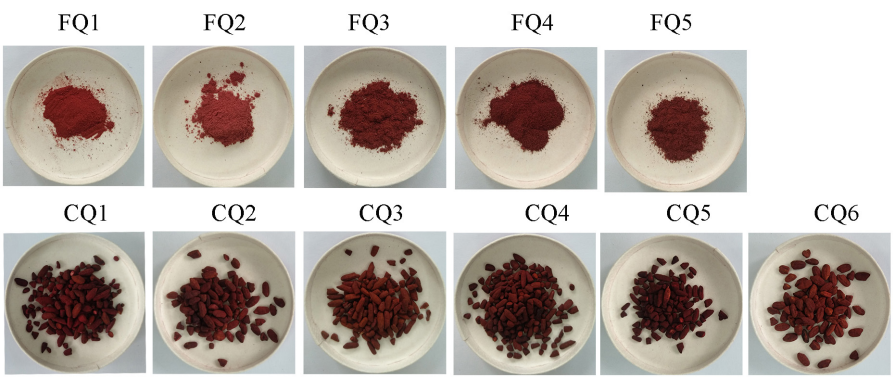

FIGURE 1 | Appearance of *Hongqu*. FQ1–FQ5 were functional Qu (FQ). CQ1–CQ6 were coloring Qu (CQ).

acid in a ratio of 385:115:0.14 (v/v), with an accompanying flow rate of 1.0 ml/min.

Determination of γ-Aminobutyric Acid by HPLC

γ-Aminobutyric acid was extracted and analyzed according to the method in QB/T 4587-2013 (Ministry of Industry and Information Technology of the People's Republic of China, 2013). The content of GABA was determined by HPLC equipped with a reversed-phase column (Novapack C18, 300 mm × 3.9 mm × 4 μm, Waters, Milford, MA, United States). Eluted GABA was detected at 280 nm and expressed as mg/100 g dry *Hongqu* (Garzón et al., 2020).

Determination of Ergosterol by HPLC

The content of ergosterol was determined by HPLC equipped with an ODS18 column (250 mm × 4.6 mm × 5 μm, Waters, Milford, MA, United States) at 280 nm. Ergosterol in *Hongqu* was identified by a combination of the retention time in HPLC chromatograms with standards (Guan et al., 2016).

Determination of Polysaccharides by HPLC

The preparation of *Hongqu* polysaccharides was under the method in the literature (Xie et al., 2012). The polysaccharide was detected by the phenol-sulfuric acid method (Dubois et al., 1956).

Composition of MonAzPs

Determination of pigment compounds was in accordance to the method (Liang et al., 2019) with some modifications. The analysis was conducted by Agilent 2000 HPLC system (Agilent Technologies, Santa Clara, CA, United States) comprised of a binary pump, an autosampler, and a thermostatically controlled column compartment. Pigments were separated on a 250 × 4.6 mm ODS18 column (5 μm, Waters, Milford, MA, United States) with a linear gradient of the mobile phase of solvent A (water, containing 0.1% formic acid, v/v) and solvent B (acetonitrile), a flow rate of 1.0 ml/min, oven temperature of 35°C, and run time for 55 min. Mass spectrometry was operated with a 6520 QTOF-MS (Agilent Technologies, Santa Clara, CA, United States) equipped with an ESI source. The parameters of the ESI source were set as follows: capillary voltage, 3,500 V; fragmentor voltage, 135 V; drying gas (N2) temperature, 350°C; drying gas (N_2) flow rate, 10.0 L/min; nebulizer gas pressure, 30 psig; OCT RF V, 750 V; skimmer voltage, 65 V. Each sample was analyzed in positive modes with a mass scan range of m/z 50–1,200 Da, and collision energy (CE) was set as 15 and 30 eV. Data acquisition and analysis were operated by Agilent LC/MS Qualitative Analysis Software (version B.04.00).

Antioxidant Activity of Hongqu and MYPs *in vitro*

DPPH Free Radical Scavenging Experiment

The DPPH radical scavenging capacity was determined according to the method described by reference (Brand Williams et al., 1995) with minor modification. Each sample with a fixed volume of 1.0 ml was mixed with 1.0 ml DPPH solution (0.2 mM in anhydrous ethanol) stored in the dark at room temperature for 30 min. Then, its absorbance A_i was measured at 517 nm using a microplate reader (CLARIOstar, BMG LABTECH GmbH, Ortenberg, Germany). At the same time, the absorbance A_c of the mixture of DPPH solution and an equal volume of anhydrous ethanol and the absorbance A_j of the mixture of the sample solution and the equal volume of anhydrous ethanol were determined at 517 nm. The DPPH radical scavenging activity was expressed as the percentage of inhibition of DPPH according to the following formula. Inhibition rate of DPPH = $[1- (A_i-A_j)/A_c] \times 100\%$.

ABTS Free Radical Scavenging Experiment

ABTS radical scavenging ability was determined according to the method with some modifications (Sridhar and Charles, 2019). The $ABTS^{\cdot+}$ working solution was produced by reacting the $ABTS^{\cdot+}$ stock solution (7.4 mM ABTS) with the $K_2S_2O_8$ stock solution (2.6 mM $K_2S_2O_8$) in equal quantities and allowed them to react for 12–16 h at room temperature in the dark and diluting with anhydrous ethanol to make its absorbance 0.70 ± 0.02 at 734 nm. $ABTS^{\cdot+}$ working solution (1.0 ml) was mixed with 0.25 ml of the ethanol extract of *Hongqu* or standard (dibutyl hydroxytoluene, BHT) at different concentrations (0.1–10 μg/ml). The mixture was incubated at room temperature for exactly 10 min in the dark and determined the absorbance at 734 nm (A). The control (A_0) was prepared by mixing 1.0 ml of $ABTS^{\cdot+}$ solution with 0.25 ml of anhydrous ethanol. The percentage results of scavenging activity were calculated as inhibition rate using the following equation. Inhibition rate of $ABTS^{\cdot+} = [(A_0 - A)/A_0] \times 100\%$.

Ferrous-Reducing Power

Ferrous-reducing power was determined as described in the literature (Eda et al., 2016) with some modifications. Sample solution (0.25 ml), phosphate buffer (0.25 ml) (pH 6.6, 0.2 mol/L), and potassium ferricyanide (0.25 ml) (10 g/L) were placed in a 1.5 ml centrifuge tube. After incubation at 50°C for 20 min and cooling to room temperature, 0.25 ml of 10% (m/v) trichloroacetic acid (TCA) solution was added and centrifuged at 4°C and 10,000 r/min for 15 min. Supernatant (0.5 ml), distilled water (0.5 ml), and 0.1% (m/v) ferric chloride solution (0.1 ml) were added and reacted for 10 min. The absorption was measured at 700 nm.

Superoxide Anion Free Radical Scavenging Experiment

The superoxide anion was produced by the AP-TEMED system and reacted with hydroxylamine hydrochloride to form NO_2^-. Then, NO_2^- was reacted with paminobenzenesulfonic acid and α-naphthylamine to form a red azo compound with a characteristic absorption peak at 530 nm (Takei et al., 2017). The scavenging ability of oxygen anions was negatively correlated with the absorbance at 530 nm. O^{2-} radical-scavenging activity was measured by a non-enzymatic method with a test kit produced by Beijing Solarbio Science and Technology Co., Ltd.

Determination of the Inhibition Rate of Yolk Lipoprotein (AOA%)

The inhibition rate of yolk lipoprotein (AOA%) was determined as described in our previous report (Wu et al., 2016). Phosphoric

acid buffer (3.0 ml) (0.1 mol/L), 1:25 yolk suspension (0.4 ml), $FeSO_4$ solution (0.2 ml) (25 mmol/L), and sample solution (0.2 ml) were placed in 10 ml tubes, respectively. The control tube (A_0) was placed with 0.2 ml of phosphoric acid buffer instead of the sample solution (A). After incubation at 37°C for 12 h, 1.0 ml of 20% trichloroacetic acid was added, centrifuging for 10 min at 3,500 r/min. Supernatant (4.0 ml) was reacted with 2.0 ml of 0.8% thiobarbituric acid solution for 15 min at 100°C. The absorbance was determined at 532 nm and calculated by the following formula, Yolk lipoprotein inhibition rate (AOA%) = $[(A_0 - A)/A_0] \times 100$.

Determination of the Cellular Antioxidant Activity of MYPs

Cellular antioxidant measurements were determined following the method (Wolfe and Liu, 2007) with modifications. Caco-2 cells in the logarithmic growth phase were inoculated into 96 well cell culture plates at the density of 6×10^4 cells/well. The growth medium was removed, and the cells were washed with HBS to remove any non-adherent and dead cells. Next, 50 μl DCFH-DA working solution (25 μM) was added to each well, followed by 50 μl of the sample solution (in triplicate wells). For positive control, 50 μl of quercetin (the final dilution concentration was 2, 4, 6, 8, and 10 μM) were applied in triplicate wells, while the blank group was treated with DCFH-DA without ABAP. Once the DCFH-DA and antioxidant treatments were added, the cells were placed in the incubator for 1.0 h at 37°C. After this period, the cells were washed with HBS, and DCFH-DA was removed. Then, each well was added with 100 μl ABAP (600 μM). The cells were immediately placed in a FlexStation3 multifunctional calcium flow detection workstation (Molecular devices, United States), where real-time fluorescence was read initially and every 5 min, then after for 1.0 h. Fluorescence was measured at an excitation wavelength of 485 nm and an emission wavelength of 538 nm (Zhou et al., 2020).

$$\text{The formula was as follows : CAA unit} = \%\text{reduction} = 100 - \left(\int \text{SA} - \int \text{CA}\right) \times 100$$

where $\int$SA was the integrated area under the sample fluorescence vs. time curve and $\int$CA was the integrated area from the control curve.

Isolation of MYPs From Crude Extracts of FQ and CQ

Coloring Qu sample was prepared according to 0.1 g/ml CQ ethanol extracts: 200–300 mesh silica gel = 2:1 (v/m), mixed and dried at 50°C for 48 h. Then, CQ sample was located on a silica gel column and eluent with the solvent of n-hexane/ethyl acetate (5:1, v/v) to yield yellow pigments. The similar fractions were combined into five main fractions according to OD 410 nm and 300–600 nm scan, and the solvent was removed under reduced pressure. The ethyl acetate phase of the FQ sample was prepared and repeated three times according to the rate of 0.1 g/ml FQ ethanol extracts:ethyl acetate:double distilled water = 1:2:3 in a 500 ml separating funnel and isolated by TLC (developing solvent was n-hexane:ethyl acetate:petroleum ether = 30:17:8), The band with the same R_f (drew under UV 365 nm light) was collected. These resultant fractions were further analyzed by HPLC, and then fractions with the same retention time were combined, and the solvent was removed under reduced pressure. The obtained seven yellow pigments, namely, monaphilone B, monascin, monascuspilion, monasfluore A, new yellow pigment, monaphilone A, and ankaflavin, were dissolved in ethanol for HPLC-QTOF-MS analysis and antioxidative activity determination. The HPLC diagram, mass spectrum, and structure diagram of MYPs were shown in **Supplementary Figures 2–8**.

Statistical Analysis

The measurement data were expressed as mean value ± standard deviation (mean ± SD). Single-factor variance analysis and spearman's correlations coefficient were calculated by using SPSS 22.0 (SPSS Inc., United States). Bioplot diagram, permutation test diagram of orthogonal partial least squares discriminant analysis (OPLS-DA), VIP diagram, and HCA diagram were drawn using the SIMCA-14.1 (UMETRICS, Sweden) based on the relative abundance of MonAzPs determined with HPLC-MS.

RESULTS AND DISCUSSION

Analysis of the Composition of Key Active Components of FQ and CQ

The Total Color Value

According to **Figure 2**, the units of absorbance at 505 nm (E_{505}) of CQ, indicating the total color value, were extremely significantly higher than those of FQ. The average value of E_{505} of CQ was approximately 2,569.60 U/g, while that of FQ was only 283.24 U/g. The E_{505} of CQ was approximately 9.0 times compared with that of FQ. For example, Huang et al. (2017) reported a higher antioxidative potential in a fermented mixture of Radix Puerariae and rice than in that fermented by only Radix Puerariae and rice due to the higher levels of pigments. The total color value of red yeast rice (RYR) and fermented Radix Puerariae and rice (FPR) was 1,300 ± 25 units/g and 6,164 ± 799 units/g, respectively. FPR increased the color value by three times compared with RYR. The result indicated that the total color value between CQ and FQ was different, so the differences in *Monascus* pigments composition needed to be further analyzed.

MK

Monacolin K is one of the well-documented metabolites of *Monascus* and is recognized as a cholesterol-lowering regent because of its competitive inhibitory effect on 3-hydroxy-3-methylglutaryl coenzyme A (HMG-CoA) reductase. The total amount of MK is composed of the lactone form and the acid form of MK. The content of MK in *Hongqu* was shown in **Table 2**. The total contents of MK of FQ 1–FQ 5 were 33.73, 20.27, 6.98, 9.02, and 10.66 mg/g, respectively. So, FQ 1–FQ 5 met the requirements of the light industry standard of the People's Republic of China that the MK of FQ should be over 4.0 mg/g.

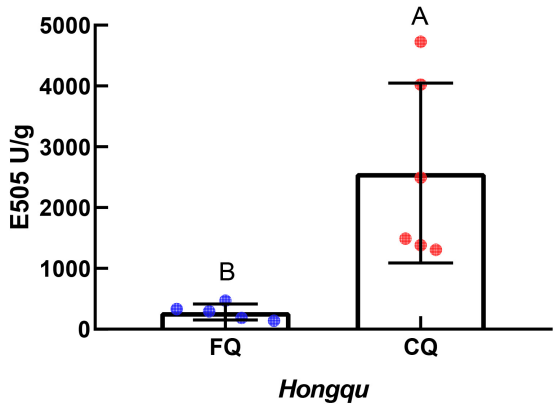

FIGURE 2 | Units of absorbance at 505 nm (E_{505}) of functional Qu (FQ) and coloring Qu (CQ), respectively.

TABLE 2 | The content of MK in *Hongqu* (mg/g).

Hongqu	Lactone forms of MK	Acid forms of MK	The total content of MK
CQ4	–	0.26 ± 0.01	0.26 ± 0.01
FQ1	29.13 ± 0.02	4.60 ± 0.01	33.73 ± 0.00
FQ2	17.66 ± 0.08	2.61 ± 0.02	20.27 ± 0.11
FQ3	5.11 ± 0.01	1.88 ± 0.02	6.98 ± 0.03
FQ4	7.38 ± 0.04	1.64 ± 0.03	9.02 ± 0.07
FQ5	7.78 ± 0.04	2.88 ± 0.01	10.66 ± 0.05

Use "–" to indicate that it cannot be detected.

The ratios of the active open-hydroxyl acid form and the prodrug lactone form of MK of FQ 1- FQ 5 were 13.64, 12.88, 26.93, 18.18, and 27.02%, respectively. The MK of CQ 4 was the highest among all CQ samples, reaching 0.26 mg/g (less than the requirements of FQ). Gum et al. (2017) reported higher antioxidant activity in *Hongqu* fermented *Bacillus subtilis* than in *Hongqu* due to the alteration in the physicochemical property of MK.

GABA, Polysaccharides, and Ergosterol

The contents of GABA, polysaccharide, and ergosterol of CQ were 0.103, 14.58, and 246.92 mg/g, while those of FQ were 0.198, 35.97, and 443.65 mg/g, representing increases of 92.23, 146.70, and 79.67%, respectively. The contents of GABA, polysaccharide, and ergosterol of FQ were higher than those of CQ. However, there was no significant difference between them (**Figure 3**). Lee et al. (2016) reported that amino acids contributed to antioxidant activity in wheat and rice gochujang. Lu et al. (2015) reported that *Huangjiu* had the highest antioxidant capacity among the three traditional fermented wines (*Baijiu*, *Huangjiu*, grape wine) because the amino acid content was 2,923 μg/ml, and GABA was 10 μg/ml. Numerous studies reported that polysaccharides from different sources and modified products had certain antioxidant activities (Mirzadeh et al., 2020). Liang et al. (2019) reported that the ergosterol in RYR could significantly reduce the levels of total cholesterol, triglycerides, and low-density lipoprotein cholesterol in C57BL/6J mice fed a high-fat diet. Therefore, GABA, polysaccharides, and ergosterol might be potential contributors to antioxidant activity.

In vitro Antioxidant Activity of Ethanol Extracts of FQ and CQ

The ferric ion reducing antioxidant power (FRAP) of 1.0 mg/ml ethanol extracts of FQ and CQ was measured (**Figure 4A**). The average FRAP of CQ was 0.645, which was significantly better than that of FQ (0.301). When the FRAP of 1.0 mg/ml vitamin C was 0.918, the FRAP of CQ 4 was the strongest among all samples, reaching 0.702. Generally, IC_{50} values were used to reflect the antioxidant capacity of various materials. The 50% inhibitory concentration (IC_{50}) was defined as the concentration of a sample that gave a 50% inhibition rate. The IC_{50} value was smaller, and the DPPH radical scavenging activity or ABTS radical scavenging activity was stronger. While the IC_{50} of DPPH radical scavenging activity of vitamin C was 0.023 mg/ml, the average IC_{50} of DPPH radical scavenging activity of CQ (0.176 mg/ml) was significantly lower than that of FQ (0.544 mg/ml) (**Figure 4B**). The IC_{50} of DPPH radical scavenging activity of CQ 3 was the smallest among all samples, reaching 0.100 mg/ml. While the IC_{50} of the ABTS radical scavenging activity of vitamin C was 4.437 μg/ml, the average IC_{50} of ABTS radical scavenging activity of CQ (28.98 μg/ml) was significantly lower than that of FQ (57.54 μg/ml) (**Figure 4C**). The IC_{50} of CQ 4 was the smallest among all samples, reaching 22.18 μg/ml. Gum et al. (2017) reported that the DPPH radical scavenging activity of 2 mg/ml RYR was approximately 20%, and that of RYR fermented

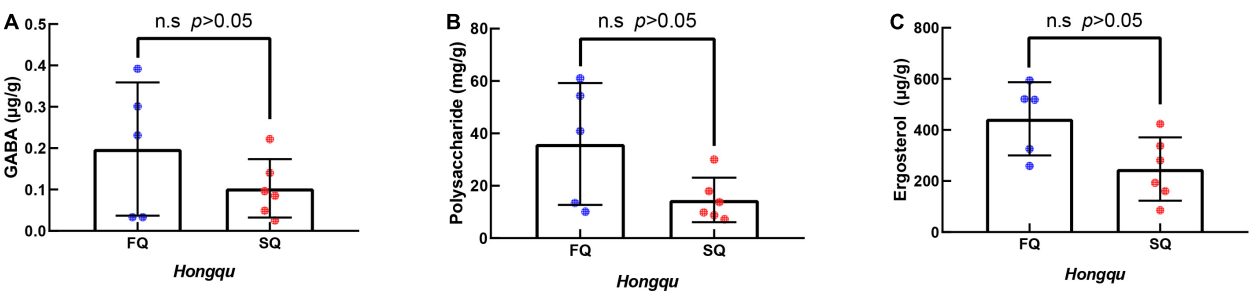

FIGURE 3 | The γ-aminobutyric acid (GABA), polysaccharides, and ergosterol of functional Qu (FQ) and coloring Qu (CQ), respectively. **(A)** The γ-aminobutyric acid. **(B)** Polysaccharides. **(C)** Ergosterol.

with *B. subtilis* was increased to 70%. The average IC_{50} of DPPH radical scavenging activity was 0.100–0.690 mg/ml, which implied that FQ and CQ had a stronger antioxidant activity than those RYR reported previously. Huang et al. (2017) reported higher antioxidant activities in a fermented mixture of Radix Puerariae and rice than RYR due to the three times higher pigment intensity. For example, the DPPH scavenging capacity was 10.58 mg AEE/g of the sample, and the FRAP was 0.11 mmol Fe^{2+}/g of the sample. Those pieces of literature were very consistent with the stronger antioxidant capacity of CQ than FQ because of the higher color value.

Correlation Analysis Among Key Active Components and Antioxidant Activities of FQ and CQ

Correlation analysis among key active components and antioxidant activities of FQ and CQ was shown in **Table 3**. There was a strong correlation between the total color value (E_{505}) and antioxidant activities. The correlation coefficients of FRAP, DPPH, ABTS, and E_{505} were 0.806, 0.818, and 0.822, respectively. However, there were negative correlations between FRAP and MK ($r = -0.700$), polysaccharide ($r = -0.091$), and ergosterol ($r = -0.182$). DPPH was negatively correlated with ergosterol ($r = -0.427$), polysaccharide ($r = -0.336$), MK ($r = -0.200$), and GABA ($r = -0.046$). There was a negative correlation between ABTS and MK ($r = -0.500$). Correlation analysis indicated that MonAzPs played an important role in the antioxidant activities of *Hongqu*. In contrast, the contents of MK, polysaccharide, ergosterol, and GABA were not significantly correlated with the antioxidant activities of *Hongqu*. The fermentation of the rice and Radix Puerariae mixture dramatically increased the yields of pigments and significantly improved the antioxidant capacity (Huang et al., 2017).

MonAzPs

HPLC-QTOF-MS was used to detect the composition of MonAzPs in FQ and CQ. As shown in **Table 4** and **Figure 5**, a total of eighteen different MonAzPs were detected, including eleven yellow pigments (monascin, monaphilone B, ankaflavin, monasfluore B, monasfluore A, FK17-P2B2, monapurfluore, monaphilone A, monascuspilion, monarubrin, and new yellow pigment), two orange pigments (rubropunctatin and monascorubrin), and five red pigments (rubropunctamine, monascorubramine, new red pigment, N-GABA-rubropunctatin, and red pigment). It is worth noting that the chemical composition and the relative abundance of yellow pigments in FQ and CQ were quite different. There were only eight different MonAzPs (five yellow pigments and three red pigments) in FQ (**Figure 5A**), and the relative abundance of yellow pigments (monascuspilion, monasfluore A, monaphilone B, and monascin) was higher than that of the others. There were seventeen different MonAzPs (eleven yellow pigments, four red pigments, and two orange pigments) in CQ (**Figure 5B**), and the relative abundance of yellow pigments (monascin, ankaflavin, and monaphilone A) was greater than that of other MonAzPs.

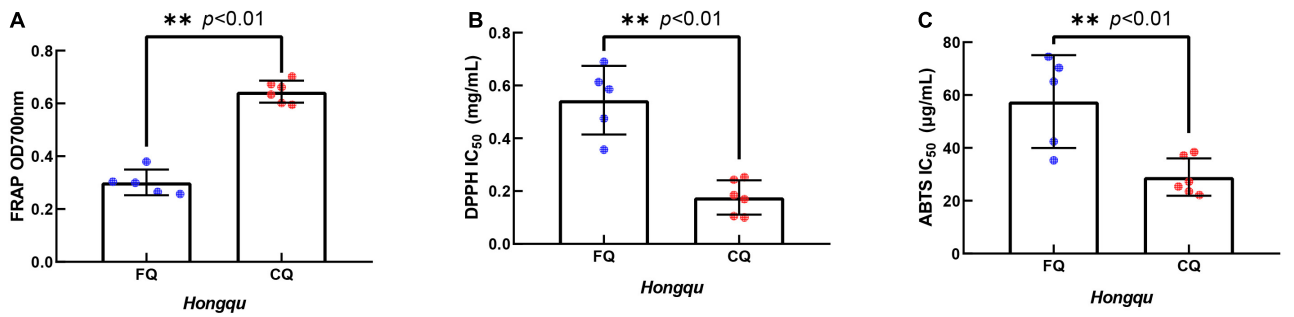

FIGURE 4 | *In vitro* antioxidant activity of extracts of functional Qu (FQ) and coloring Qu (CQ), respectively. **(A)** The ferric ion reducing antioxidant power of FQ and CQ. **(B)** The DPPH radical scavenging activity of FQ and CQ. **(C)** The ABTS radical scavenging activity of FQ and CQ.

TABLE 3 | Correlation analysis among key active components and antioxidant activities of FQ and CQ.

	E_{505}	Ergosterol	MK	GABA	Polysaccharide	FRAP	DPPH	ABTS
E_{505}	1.000	−0.184	−0.694	−0.011	−0.227	0.806**	0.818**	0.822**
Ergosterol		1.000	−0.600	0.811**	0.945**	−0.182	−0.427	0.009
MK			1.000	−0.872	−0.500	−0.700	−0.200	−0.500
GABA				1.000	0.779**	0.123	−0.046	0.241
Polysaccharide					1.000	−0.091	−0.336	0.073
FRAP						1.000	0.791**	0.918**
DPPH							1.000	0.782**
ABTS								1.000

The reciprocal of the half inhibition rate of DPPH and ABTS free radicals was used in correlation analysis.
*"**" indicated that significantly correlated at the 0.01 level.*

TABLE 4 | *Monascus* pigments composition.

No.	Tr/min	Identification	Color	Max absorbance	Formula	Proposal ions	Experimental m/z	References
1	43.81	Monascorubrin	Orange	472	$C_{23}H_{26}O_5$	$[M+H]^+$	383.1846	Manchand et al., 1973
2	36.68	Monascin	Yellow	386	$C_{21}H_{26}O_5$	$[M+H]^+$	359.1865	Chen et al., 1969; Salomon and Karrer, 1932
3	35.39	Monaphilone B	Yellow	390	$C_{20}H_{28}O_4$	$[M+H]^+$	333.2049	Hsu et al., 2010
4	31.54	Monascorubramine	Red	529	$C_{23}H_{27}NO_4$	$[M+H]^+$	382.2000	Birch et al., 1962; Sweeny et al., 2012
5	24.19	Rubropunctamine	Red	528	$C_{21}H_{23}NO_4$	$[M+H]^+$	354.1702	Birch et al., 1962; Sweeny et al., 2012
6	37.01	Rubropunctatin	Orange	473	$C_{21}H_{22}O_5$	$[M+H]^+$	355.1538	Chen et al., 1969
7	43.18	Ankaflavin	Yellow	390	$C_{23}H_{30}O_5$	$[M+H]^+$	387.2168	Manchand et al., 1973
8	40.65	Monasfluore B	Yellow	390	$C_{23}H_{28}O_5$	$[M+H]^+$	385.2017	Huang et al., 2008
9	33.47	Monasfluore A	Yellow	386	$C_{21}H_{24}O_5$	$[M+H]^+$	357.1690	Huang et al., 2008
10	14.77	FK17-P2B2	Yellow	390	$C_{13}H_{16}O_4$	$[M+H]^+$	237.1114	Jongrungruangchok et al., 2004
11	22.59	New red pigment	Red	520	$C_{23}H_{27}NO_5$	$[M+H]^+$	398.1951	Liang et al., 2019
12	45.67	Monapurfluore	Yellow	390	$C_{23}H_{32}O_4$	$[M+H]^+$	373.2372	Hsu et al., 2010
13	43.17	Monaphilone A	Yellow	390	$C_{22}H_{32}O_4$	$[M+H]^+$	361.2372	Hsu et al., 2010
14	32.04	Monascuspilion	Yellow	390	$C_{21}H_{28}O_5$	$[M+H]^+$	361.2009	Chiu et al., 2012
15	22.19	Red pigment	Red	520	$C_{21}H_{26}O_6$	$[M+H]^+$	375.1797	Liang et al., 2019
16	23.38	N-GABA-rubropunctatin	Red	520	$C_{25}H_{29}NO_6$	$[M+H]^+$	440.2072	Chen et al., 2017
17	30.15	Monarubrin	Yellow	390	$C_{20}H_{26}O_4$	$[M+H]^+$	331.1901	Loret and Morel, 2010
18	49.44	New yellow pigment	Yellow	410	$C_{23}H_{28}O_6$	$[M+H]^+$	401.2349	Chen et al., 2017

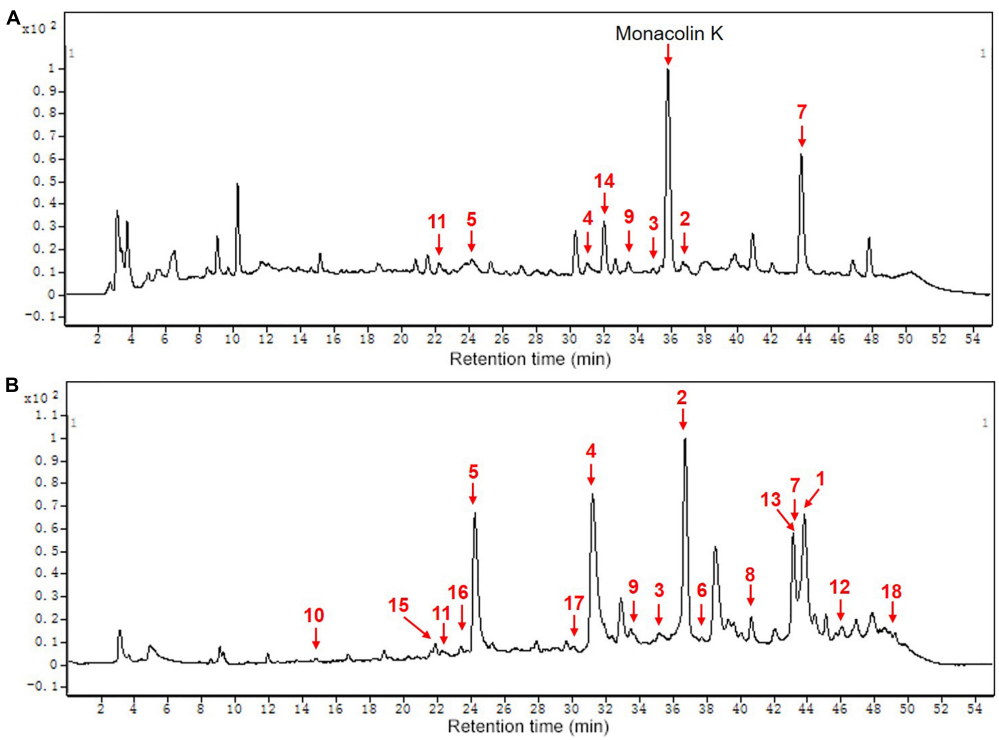

FIGURE 5 | The chemical composition of MPs of functional Qu (FQ) and coloring Qu (CQ), respectively. **(A)** functional Qu (FQ). **(B)** Coloring Qu (CQ). 1, monascorubrin; 2, monascin; 3, monaphilone B; 4, monascorubramine; 5, rubropunctamine; 6, rubropunctatin; 7, ankaflavin; 8, monasfluore B; 9, monasfluore A; 10, FK17-P2B2; 11, new red pigment; 12, monapurfluore; 13, monaphilone A; 14, monascuspilion; 15, red pigment; 16, N-GABA-rubropunctatin; 17, monarubrin; 18, new yellow pigment.

The differences of MonAzPs may be the reason for their different antioxidant activities.

From the bioplot diagram (**Figure 6A**) and the HCA diagram (**Figure 6D**), FQ (green hexagon) and CQ (blue hexagon) were located on different sides of the y-axis or divided into different clusters, which indicates that FQ and CQ had significant differences. Red, orange, and yellow dots were used to represent red, orange, and yellow pigments, respectively. The smaller distance between *Hongqu* and MPs indicated that *Hongqu* played a more important role in MPs. CQ and most of the MPs were located on the right side of the y-axis, indicating that most of the MPs came from CQ. The distance between FQ and monascuspilion was smaller than that between CQ and monascuspilion, which meant monascuspilion mainly came from FQ. This was consistent with the results in **Figure 5**. According to the permutation test diagram of the OPLS-DA model (**Figure 6B**), it can be seen that the OPLS-DA model was effective and not overfit ($R^2 > 0.4$). According to the VIP diagram (**Figure 6C**), there were nine different MPs with a significant difference between FQ and CQ (**Supplementary Table 1**, VIP > 1), including monascuspilion, ankaflavin, monaphilone A, monascin, new red pigment, monarubrin, monascorubramine, and new yellow pigment.

Antioxidant Activity of MYPs

Antioxidant Activity of MYPs *in vitro*

The antioxidant activities of seven MYPs were evaluated by antioxidant assay *in vitro*, including the DPPH free radical scavenging rate (**Figure 7A**), superoxide anion clearance rate (**Figure 7B**), and inhibition rate of peroxidation of yolk lipoprotein (**Figure 7C**). The three chemical assays reveal the different antioxidant characteristics of MYPs based on different antioxidant mechanisms. The antioxidant capacity

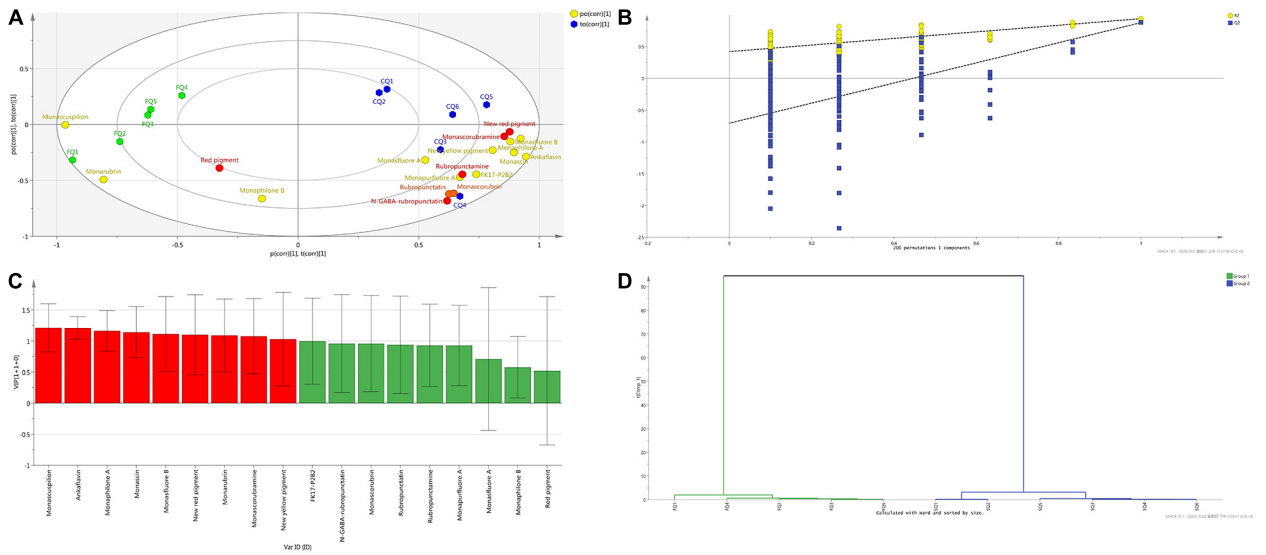

FIGURE 6 | Orthogonal projections to latent structures-discriminant analysis (OPLS-DA) of *Monascus* pigments composition of functional Qu (FQ) and coloring Qu (CQ), respectively. **(A)** Bioplot diagram of FQ (green hexagon), CQ (blue hexagon), and *Monascus* pigments (red, yellow, orange dots). **(B)** Permutation test diagram of OPLS-DA model (R^2 = 0.421, Q^2 = –0.706). **(C)** VIP diagram. **(D)** HCA diagram.

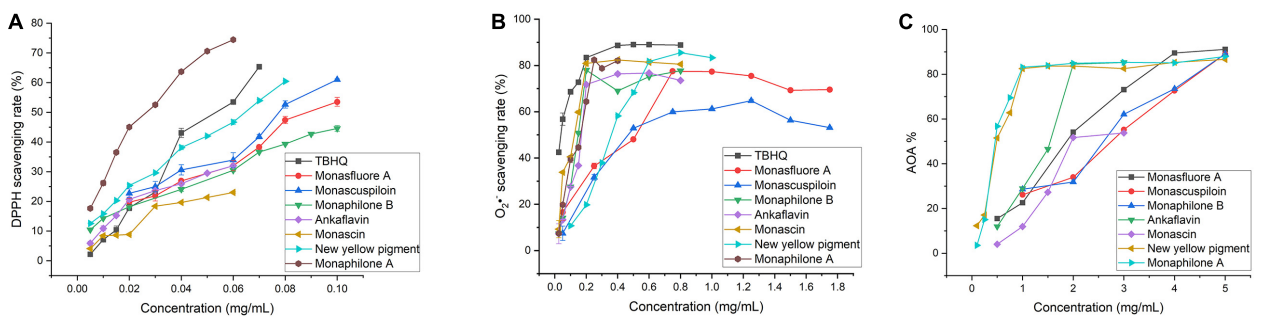

FIGURE 7 | *In vitro* antioxidant of yellow pigments purified from functional Qu (FQ) and coloring Qu (CQ). **(A)** The DPPH radical scavenging activity of yellow pigment from FQ and CQ. **(B)** The superoxide anion radical scavenging activity of yellow pigment from FQ and CQ. **(C)** The inhibition rate of yolk lipoprotein peroxidation of yellow pigment from FQ and CQ.

of MYPs increased with the increase of concentration. The antioxidant activities of MYP were similar in the three chemical antioxidant assays. Chemical antioxidant tests revealed that the antioxidant activities of monaphilone A, ankaflavin, and new yellow pigment only separated from CQ were significantly stronger than monasfluore A and monascuspilion only separated from FQ. For example, the IC_{50} of the new yellow pigment in three chemical assays (0.062, 0.376, and 0.580 mg/ml) was smaller than that of monascuspiloin (0.080, 0.548, and 2.670 mg/ml). This might be the main reason for the significantly stronger antioxidant capacity of the crude ethanol extract of CQ than FQ. MYPs have good DPPH radical scavenging ability and superoxide anion scavenging capacity, and bad vitellin inhibitory capacity. The IC_{50} of the DPPH free radical scavenging rate of MYPs from FQ (0.080–0.091 mg/ml) was smaller than the IC_{50} of crude ethanol extracts of FQ (0.544 mg/ml). The results indicated that the antioxidant activity of yellow pigments was improved significantly after purification.

Cellular Antioxidant Activity of MYPs

Compared with the antioxidant assay *in vitro* and animal experiments, the evaluation of antioxidant activity by cell model test was more economical and faster. It is widely used to quantify the cellular antioxidant activity (CAA) of phytochemicals, food extracts, and nutritional supplements. Therefore, we consider CAA assays as reliable and sensitive methods for antioxidative activity evaluation. With quercetin as a positive control, CAA of seven pigments was evaluated with an oxidative damage model of human colon adenocarcinoma Caco-2 cells induced by AAPH (Kellett et al., 2018). The CAA value of MYPs at the 20 μg/ml concentration showed that the new yellow pigment (65.46 units) had the best antioxidant activity, followed by monasfluore A (42.15 units) and monaphilone B (39.19 units), which were all significantly better than monascin (26.86 units) and ankaflavin (22.19 units), the two most frequently reported MYPs (**Figure 8A**). The antioxidant capacity of the natural product was usually converted to an equivalent concentration of quercetin based on its CAA values for making the result more

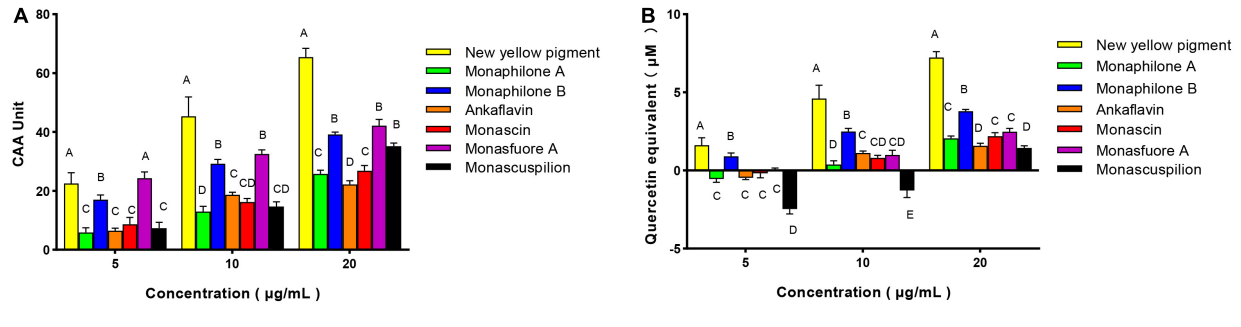

FIGURE 8 | Cellular antioxidant activity (CAA) of *Monascus* yellow pigment from functional Qu (FQ) and coloring Qu (CQ) and quercetin equivalent in Caco-2 cells. **(A)** Cellular antioxidant activity value. **(B)** Quercetin equivalent.

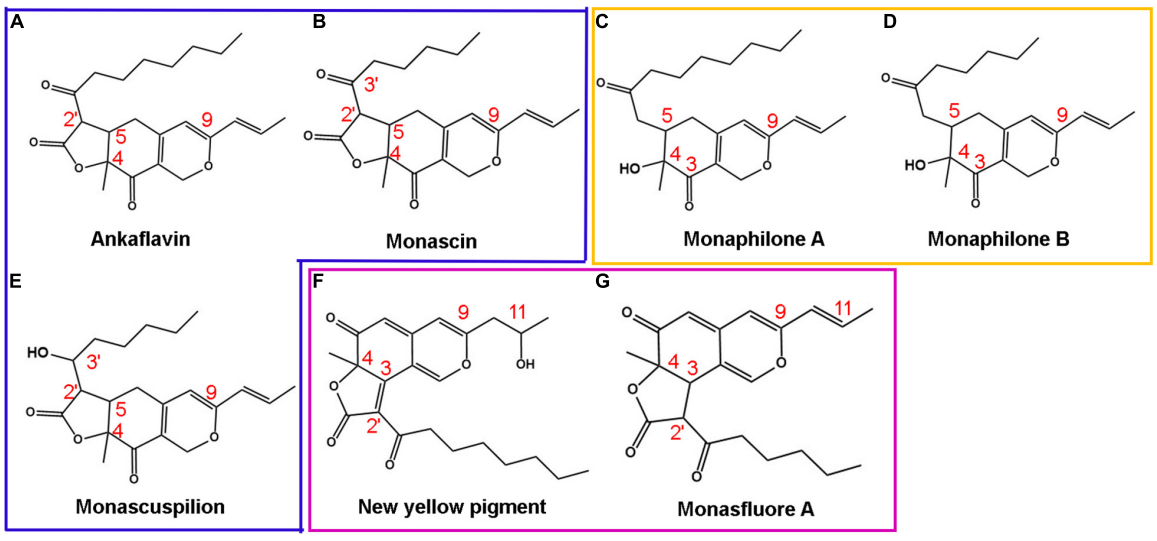

FIGURE 9 | Structures of *Monascus* yellow pigments. **(A)** ankaflavin, **(B)** monascin, **(C)** monaphilone A, **(D)** monaphilone B, **(E)** monascuspilion, **(F)** new yellow pigment, and **(G)** monasfluore A. Similar structures are represented by different colored boxes. *Monascus* yellow pigments (MYPs) in the blue box have a C5-C2′ linear tricyclic carbon skeleton, MYPs in the orange box do not have a lactone ring, and MYPs in the purple box have a C3-C2′ angular tricyclic carbon skeleton.

comparable (Zhou et al., 2020). The quercetin equivalent of MYPs was shown in **Figure 8B**. The quercetin equivalent of the new yellow pigment was 7.23 μM. In short, the new yellow pigment had outstanding antioxidant capacity *in vitro*, and its antioxidant capacity *in vivo* was worthy of in-depth study.

With the help of *in vitro* and *in vivo* antioxidant experiments, the relationship between the structure and antioxidant activity was further investigated. Based on the structure of 111 identified single pigment, the tricyclic carbon skeleton structure or the dicyclic carbon skeleton was the core structure of MonAzPs, which generally contained one to three carbonyl groups and two to five unsaturated double bonds. To date, a unitary trunk pathway had been revealed to produce four classical pigments and intermediates. All other 106 species MonAzPs were generated by various shunt pathways branching off from the trunk pathway (Chen et al., 2019). First, the alterations in the position and number of hydroxyl groups affect the antioxidant activity. The hydroxyl group of C-4 was prone to condensation reaction to form a lactone ring C5-C2′ condensation and cyclization formed a C5-C2′ linear tricyclic carbon skeleton or C3-C2′ condensation and cyclization formed a C3-C2′ angle tricyclic carbon skeleton. The seven yellow pigments could be divided into three categories according to carbon skeleton characteristics and the CAA. New yellow pigment and monasfluore A (**Figures 9F,G**) had an angular tricyclic carbon skeleton, obviously different from the linear tricyclic core of classical monascin, ankaflavin, and monascuspilion (**Figures 9A,B,E**). It is worth noting that the antioxidant activity of the new yellow pigment and monasfluore A was stronger and that of monascin, ankaflavin, and monascuspilion. Monaphilone A and monaphilone B had moderate antioxidant activity lacking the γ-lactone ring (instead of a C-4 hydroxyl group) (**Figures 9C,D**). First of all, alterations of the hydroxyl group of MYPs affect the antioxidant activities significantly. The results showed that the new yellow pigment with a hydroxyl group on C-11 possessed much higher antioxidant activities than monasfluore A and the others with a C10 (11) double bond on C-11. Monascuspilion with a hydroxyl group on C-3′ brought higher antioxidant activities than monascin with a ketone group on C-3′. In the case of MYPs, alterations of the γ-lactone ring and alkyl side chain could affect the antioxidant activities slightly. Monaphilone A and monaphilone B (lacking γ-lactone ring) possessed higher antioxidant activity than ankaflavin and monascin (linear tricyclic core), respectively. Moreover, monaphilone B and monascin (R = C_5H_{11}) had higher antioxidant activities than monaphilone A and ankaflavin (R = C_7H_{15}). In short, the alterations that occurred at C-3′, C-11, and the carbon skeleton more obviously affected the antioxidant activities.

The inhibitory effects of azaphilonoid pigments on 12-O-tetradecanoylphorbol-13-acetate (TPA)-induced ear edema were much stronger than those of non-azaphilonoid pigments (Akihisa et al., 2005). The critical structures that enhance the anti-inflammatory activity of *Monascus* yellow and orange pigments were found by Hsu (Hsu L. C. et al., 2013), and the structure–activity relationship was consistent with the results of the relationship between the structure and antioxidant activity of MYPs in this article. Because inflammation is a kind of exogenous stress, the Keap1-Nrf2/ARE antioxidant signal pathway is often activated (Lee B. H. et al., 2013). Nrf2 is an important transcription factor that regulates cell protection mechanisms such as antioxidant and anti-inflammatory activities (Pall and Levine, 2015). Therefore, anti-inflammatory activity is closely related to antioxidant activity. It is worth noting that MonAzPs with hydroxyl groups on C-3′, C-11 had significantly stronger antioxidant activity than a ketone group and C10 (11) double bond on C-3′, C-11, respectively. The previous studies had reported that the antioxidant potential of MYPs could easily transfer hydrogen to and accept electrons from free radicals through HAT and SET mechanisms. This result was consistent with the alterations of key antioxidant structures of MYPs.

CONCLUSION

This study analyzes the difference of key active components from two types of *Hongqu* (FQ and CQ). It found that MonAzPs may play an essential role in the antioxidant activity. The antioxidant activities of monaphilone A, ankaflavin, and new yellow pigment only from CQ are significantly more potent than monasfluore A and monascuspilion only from FQ. The new yellow pigment has the best antioxidant activity, whereas monascin and ankaflavin, the two most frequently reported MYPs, have the worst antioxidant activity. MYPs with hydroxyl groups on C-3′ and C-11 are proved to displace higher antioxidant activity than MYPs with a ketone group or C10 (11) double bond on C-3′ and C-11. Thus, it provides a potential antioxidant resource for functional foods. Future studies should focus on the antioxidant activities *in vivo* and the potential mechanism to better elucidate the antioxidant mechanisms *via* hydrogen atom transfer and single electron transfer.

DATA AVAILABILITY STATEMENT

The raw data supporting the conclusions of this article will be made available by the authors, without undue reservation.

AUTHOR CONTRIBUTIONS

LW performed the research and wrote the manuscript. KZ and FC participated in collecting raw materials and analyzing the metabolites. GC and YY calculated and analyzed the data. XL, WZ, PR, and LN designed the study. All authors reviewed and approved the final version of the manuscript.

FUNDING

This research project was financed by the National Key R&D Program of China (grant no. 2018YFC1604106), University-Industry Cooperation Project of the Science and Technology Department of Fujian Province (grant no. 2019N5002), and the National Natural Science Foundation of China (grant no. 32072204).

ACKNOWLEDGMENTS

We would like to thank Huiqin Wang of Zhejiang Gongshang University for testing the cellular antioxidant activity.

SUPPLEMENTARY MATERIAL

The Supplementary Material for this article can be found online at: https://www.frontiersin.org/articles/10.3389/fmicb.2021.715295/full#supplementary-material

REFERENCES

Akihisa, T., Tokuda, H., Yasukawa, K., Ukiya, M., Kiyota, A., Sakamoto, N., et al. (2005). Azaphilones, furanoisophthalides, and amino acids from the extracts of Monascus pilosus-fermented rice (red-mold rice) and their chemopreventive effects. *J. Agric. Food Chem.* 53, 562–565. doi: 10.1021/jf040199p

Birch, A. J., Cassera, A., Fitton, P., Holker, J. S. E., Smith, H., Thompson, G. A., et al. (1962). 699. Studies in relation to biosynthesis. part XXX. Rotiorin, monascin, and rubropunctatin. *J. Chem. Soc.* 3583–3586. doi: 10.1039/jr9620003583

Brand Williams, W., Cuvelier, M. E., and Berset, C. (1995). Use of a free radical method to evaluate antioxidant activity. *LWT Food Sci. Technol.* 28, 25–30. doi: 10.1016/s0023-6438(95)80008-5

Chen, C. L., Chang, K. Y., and Pan, T. M. (2015). Monascus purpureus NTU 568 fermented product improves memory and learning ability in rats with aluminium-induced Alzheimer's disease. *J. Funct. Foods* 21, 167–177. doi: 10.1016/j.jff.2015.12.017

Chen, F. C., Manchard, P. S., and Whalley, W. B. (1969). The structure of monascin. *J. Chem. Soc. D Chem. Commun.* 21, 130–131. doi: 10.1039/c29690000130

Chen, W., Chen, R., Liu, Q., He, Y., He, K., Ding, X., et al. (2017). Orange, red, yellow: biosynthesis of azaphilone pigments in *Monascus fungi*. *Chem. Sci.* 8, 4917–4925. doi: 10.1039/c7sc00475c

Chen, W., Feng, Y., Molnar, I., and Chen, F. (2019). Nature and nurture: confluence of pathway determinism with metabolic and chemical serendipity diversifies Monascus azaphilone pigments. *Nat. Prod. Rep.* 36, 561–572. doi: 10.1039/c8np00060c

Chiu, H. W., Fang, W. H., Chen, Y. L., Wu, M. D., Yuan, G. F., Ho, S. Y., et al. (2012). Monascuspiloin enhances the radiation sensitivity of human prostate cancer cells by stimulating endoplasmic reticulum stress and inducing autophagy. *PLoS One* 7:e40462. doi: 10.1371/journal.pone.0040462

Dubois, M., Gilles, K. A., Hamilton, J. K., Rebers, P. A., and Smith, F. (1956). Colorimetric method for determination of sugars and related substances. *Anal. Chem.* 28, 350–356. doi: 10.1021/ac60111a017

Eda, M., Kuda, T., Kataoka, M., Takahashi, H., and Kimura, B. (2016). Anti-glycation properties of the aqueous extract solutions of dried algae products harvested and made in the Miura Peninsula, Japan, and effect of lactic acid fermentation on the properties. *J. Appl. Phycol.* 28, 3617–3624. doi: 10.1007/s10811-016-0891-7

Garzón, A. G., Van de Velde, F., and Drago, S. R. (2020). Gastrointestinal and colonic in vitro bioaccessibility of γ-aminobutiric acid (GABA) and phenolic compounds from novel fermented sorghum food. *LWT* 130:109664. doi: 10.1016/j.lwt.2020.109664

Guan, W., Zhang, J., Yan, R., Shao, S., Zhou, T., Lei, J., et al. (2016). Effects of UV-C treatment and cold storage on ergosterol and vitamin D2 contents in different parts of white and brown mushroom (*Agaricus bisporus*). *Food Chem.* 210, 129–134. doi: 10.1016/j.foodchem.2016.04.023

Gum, S. I., Nguyen, P. A., Lee, J. R., Han, Y. H., and Cho, M. K. (2017). The physico-chemical alteration of lovastatin and enhanced antioxidant effect of *Bacillus subtilis* fermented-red yeast rice product. *Food Chem.* 232, 203–209. doi: 10.1016/j.foodchem.2017.04.023

Hsu, L. C., Liang, Y. H., Hsu, Y. W., Kuo, Y. H., and Pan, T. M. (2013). Anti-inflammatory properties of yellow and orange pigments from *Monascus purpureus* NTU 568. *J. Agric. Food Chem.* 61, 2796–2802.

Hsu, W. H., Lee, B. H., Li, C. H., Hsu, Y. W., and Pan, T. M. (2013). Monascin and AITC attenuate methylglyoxal-induced PPARγ phosphorylation and degradation through inhibition of the oxidative stress/PKC pathway depending on Nrf2 activation. *J. Agric. Food Chem.* 61, 5996–6006. doi: 10.1021/jf401197r

Hsu, Y. W., Hsu, L. C., Liang, Y. H., Kuo, Y. H., and Pan, T. M. (2010). Monaphilones A-C, three new antiproliferative azaphilone derivatives from *Monascus purpureus* NTU 568. *J. Agric. Food Chem.* 58, 8211–8216. doi: 10.1021/jf100930j

Huang, C. F., Shen, S. M., Chen, W. T., and Chen, C. C. (2019). The effects of mutation and temperature variation on monacolin K production by monascus sp. and relative statistical parameter analysis of monacolin K production. *Phytochem. Lett.* 32, 143–150. doi: 10.1016/j.phytol.2019.05.011

Huang, Q., Zhang, H., and Xue, D. (2017). Enhancement of antioxidant activity of Radix Puerariae and red yeast rice by mixed fermentation with *Monascus purpureus*. *Food Chem.* 226, 89–94. doi: 10.1016/j.foodchem.2017.01.021

Huang, Z., Guo, W., Zhou, W., Li, L., Xu, J., Hong, J. L., et al. (2019). Microbial communities and volatile metabolites in different traditional fermentation starters used for Hong Qu glutinous rice wine. *Food Res. Int.* 121, 593–603. doi: 10.1016/j.foodres.2018.12.024

Huang, Z., Xu, Y., Li, L., and Li, Y. (2008). Two new monascus metabolites with strong blue fluorescence isolated from red yeast rice. *J. Agric. Food Chem.* 56, 112–118. doi: 10.1021/jf072985a

Jongrungruangchok, S., Kittakoop, P., Yongsmith, B., Bavovada, R., Tanasupawat, S., Lartpornmatulee, N., et al. (2004). Azaphilone pigments from a yellow mutant of the fungus Monascus kaoliang. *Phytochemistry* 65, 2569–2575. doi: 10.1016/j.phytochem.2004.08.032

Kellett, M. E., Greenspan, P., and Pegg, R. B. (2018). Modification of the cellular antioxidant activity (CAA) assay to study phenolic antioxidants in a Caco-2 cell line. *Food Chem.* 244, 359–363. doi: 10.1016/j.foodchem.2017.10.035

Lee, B. H., Hsu, W. H., Huang, T., Chang, Y. Y., Hsu, Y. W., and Pan, T. M. (2013). Effects of monascin on anti-inflammation mediated by Nrf2 activation in advanced glycation end product-treated THP-1 monocytes and methylglyoxal-treated wistar rats. *J. Agric. Food Chem.* 61, 1288–1298. doi: 10.1021/jf305067n

Lee, C. L., and Pan, T. M. (2012). Development of Monascus fermentation technology for high hypolipidemic effect. *Appl. Microbiol. Biotechnol.* 94, 1449–1459. doi: 10.1007/s00253-012-4083-3

Lee, C. L., Hung, Y. P., Hsu, Y. W., and Pan, T. M. (2013). Monascin and ankaflavin have more anti-atherosclerosis effect and less side effect involving increasing creatinine phosphokinase activity than monacolin K under the same dosages. *J. Agric. Food Chem.* 61, 143–150. doi: 10.1021/jf304346r

Lee, D. E., Shin, G. R., Lee, S., Jang, E. S., Shin, H. W., Moon, B. S., et al. (2016). Metabolomics reveal that amino acids are the main contributors to antioxidant activity in wheat and rice gochujangs (Korean fermented red pepper paste). *Food Res. Int.* 87, 10–17. doi: 10.1016/j.foodres.2016.06.015

Liang, J. X., Zhang, Q. Q., Huang, Y. F., Pang, H. Q., Liu, X. G., Gao, W., et al. (2019). Comprehensive chemical profiling of monascus-fermented rice product and screening of lipid-lowering compounds other than monacolins. *J. Ethnopharmacol.* 238:111879. doi: 10.1016/j.jep.2019.111879

Loret, M. O., and Morel, S. (2010). Isolation and structural characterization of two new metabolites from monascus. *J. Agric. Food Chem.* 58, 1800–1803. doi: 10.1021/jf903231p

Lu, Q. Y., Lee, R. P., Huang, J., Yang, J., Henning, S. M., Hong, X., et al. (2015). Quantification of bioactive constituents and antioxidant activity of Chinese yellow wine. *J. Food Composit. Anal.* 44, 86–92. doi: 10.1016/j.jfca.2015.07.005

Manchand, P. S., Whalley, W. B., and Chen, F. (1973). Isolation and structure of ankaflavin: a new pigment from Monascus anka. *Phytochemistry* 12, 2531–2532. doi: 10.1016/0031-9422(73)80470-4

Ministry of Industry and Information Technology of the People's Republic of China (2013). *Light Industry Standard the People's Republic of China QB/T 4587-2013, Gamma-Aminobutyric acid*. Beijing: Ministry of Industry and Information Technology

Mirzadeh, M., Arianejad, M. R., and Khedmat, L. (2020). Antioxidant, antiradical, and antimicrobial activities of polysaccharides obtained by microwave-assisted extraction method: a review. *Carbohydr. Polym.* 229:115421. doi: 10.1016/j.carbpol.2019.115421

National Development and Reform Commission of the People's Republic of China (2007). *Light Industry Standard of the People's Republic of China QB/T 2847-2007, Functional Red Kojic Rice (Powder)*. Beijing: National Development and Reform Commission.

National Health and Family Planning Commission of the People's Republic of China (2015). *National Standard of the people's Republic of China GB 1886.19-2015. Food Safety National Standard Food Additives*. Beijing: National Health and Family Planning Commission.

Pall, M. L., and Levine, S. (2015). Nrf2, a master regulator of detoxification and also antioxidant, anti- inflammatory and other cytoprotective mechanisms, is raised by health promoting factors. *Acta Physiol. Sin.* 67, 1–18.

Qu, J., Wang, B., Wu, J. J., Xu, C., Zhu, S. M., and Chen, F. S. (2008). Study on separation of monascus pigment and their antioxidative properties. *Modern Food Sci. Technol.* 24, 527–531.

Salomon, H., and Karrer, P. (1932). Pflanzenfarbstoffe XXXVIII. Ein Farbstoff aus „rotem" Reis, Monascin. *Helvetica Chim. Acta* 15, 18–22.

Shi, Y. C., Liao, V. H.-C., and Pan, T.-M. (2012). Monascin from red mold dioscorea as a novel antidiabetic and antioxidative stress agent in rats and *Caenorhabditis elegans*. *Free Radic. Biol. Med.* 52, 109–117. doi: 10.1016/j.freeradbiomed.2011.09.034

Srianta, I., Zubaidah, E., Estiasih, T., Yamada, M., and Harijono. (2016). Comparison of *Monascus purpureus* growth, pigment production and composition on different cereal substrates with solid state fermentation. *Biocatal. Agric. Biotechnol.* 7, 181–186. doi: 10.1016/j.bcab.2016.05.011

Sridhar, K., and Charles, A. L. (2019). In vitro antioxidant activity of Kyoho grape extracts in DPPH and ABTS assays: estimation methods for EC50 using advanced statistical programs. *Food Chem.* 275, 41–49 doi: 10.1016/j.foodchem.2018.09.040

Sweeny, J. G., Estrada-Valdes, M. C., Iacobucci, G. A., Sato, H., and Sakamura, S. (2012). Photoprotection of the red pigments of Monascus anka in aqueous media by 1,4,6-trihydroxynaphthalene. *J. Agricult. Food Chem.* 29, 1189–1193. doi: 10.1021/jf00108a023

Takei, M., Kuda, T., Eda, M., Shikano, A., Takahashi, H., and Kimura, B. (2017). Antioxidant and fermentation properties of aqueous solutions of dried algal products from the Boso Peninsula, Japan. *Food Biosci.* 19, 85–91. doi: 10.1016/j.fbio.2017.06.006

Wang, J. J., and Pan, T. M. (2003). Effect of red mold rice supplements on serum and egg yolk cholesterol levels of laying hens. *J. Agric. Food Chem.* 51, 4824–4829. doi: 10.1021/jf034296e

Wolfe, K. L., and Liu, R. H. (2007). Cellular antioxidant activity (CAA) assay for assessing antioxidants, foods, and dietary supplements. *J. Agric. Food Chem.* 55, 8896–8907. doi: 10.1021/jf0715166

Wu, L., Shen, H. S., Tang, B. S., Yang, Y. L., and Chen, J. C. (2016). Effects of *Canellia oleifera* abel extraction on enhancing mycelial metabolism for compounds with *Agrocybe chaxingu* Huang and antioxidant function. *J. Chinese Institute Food Sci. Technol.* 16, 59–64.

Xie, J. H., Shen, M. Y., Xie, M. Y., Nie, S. P., Chen, Y., Li, C., et al. (2012). Ultrasonic-assisted extraction, antimicrobial and antioxidant activities of *Cyclocarya paliurus* (Batal.) *Iljinskaja polysaccharides*. *Carbohydr. Polym.* 89, 177–184. doi: 10.1016/j.carbpol.2012.02.068

Zhang, X., Liu, C., Tian, W., Zhang, H., and Li, P. (2020). Theoretical and experimental investigation of the antioxidative activity of monascin. *Food Funct.* 11, 5915–5923. doi: 10.1039/c9fo02410g

Zhou, J., Gao, G., Zhang, S., Wang, H., Ke, L., Zhou, J., et al. (2020). Influences of calcium and magnesium ions on cellular antioxidant activity (CAA) determination - ScienceDirect. *Food Chem.* 320, 1–7.

Zhou, W., Guo, R., Guo, W., Hong, J., and Li, L. (2019). Monascus yellow, red and orange pigments from red yeast rice ameliorate lipid metabolic disorders and gut microbiota dysbiosis in Wistar rats fed on a high-fat diet. *Food Funct.* 10, 1073–1084. doi: 10.1039/c8fo02192a

Conflict of Interest: The authors declare that the research was conducted in the absence of any commercial or financial relationships that could be construed as a potential conflict of interest.

frontiers in Microbiology

PERSPECTIVE
published: 04 August 2021
doi: 10.3389/fmicb.2021.702093

Hanseniaspora vineae and the Concept of Friendly Yeasts to Increase Autochthonous Wine Flavor Diversity

Francisco Carrau[1]* *and Paul A. Henschke*[2,3]

[1] Área Enología y Biotecnología de Fermentaciones, Departamento Ciencia y Tecnología de Alimentos, Universidad de la Republica, Montevideo, Uruguay, [2] The Australian Wine Research Institute, Adelaide, SA, Australia, [3] School of Agriculture, Food and Wine, The University of Adelaide, Urrbrae, SA, Australia

In this perspective, we will explain the concept of "friendly" yeasts for developing wine starters that do not suppress desirable native microbial flora at the initial steps of fermentation, as what usually happens with *Saccharomyces* strains. Some non-*Saccharomyces* strains might allow the development of yeast consortia with the native terroir microflora of grapes and its region. The positive contribution of non-*Saccharomyces* yeasts was underestimated for decades. Avoiding them as spoilage strains and off-flavor producers was the main objective in winemaking. It is understandable, as in our experience after more than 30 years of wine yeast selection, it was shown that no more than 10% of the isolated native strains were positive contributors of superior flavors. Some species that systematically gave desirable flavors during these screening processes were *Hanseniaspora vineae* and *Metschnikowia fructicola*. In contrast to the latter, *H. vineae* is an active fermentative species, and this fact helped to build an improved juice ecosystem, avoiding contaminations of aerobic bacteria and yeasts. Furthermore, this species has a complementary secondary metabolism with *S. cerevisiae*, increasing flavor complexity with benzenoid and phenylpropanoid synthetic pathways practically inexistent in conventional yeast starters. How does *H. vineae* share the fermentation niche with other yeast strains? It might be due to the friendly conditions it creates, such as ideal low temperatures and low nitrogen demand during fermentation, reduced synthesis of medium-chain fatty acids, and a rich acetylation capacity of aromatic higher alcohols, well-known inhibitors of many yeasts. We will discuss here how inoculation of *H. vineae* strains can give the winemaker an opportunity to develop ideal conditions for flavor expression of the microbial terroir without the risk of undesirable strains that can result from spontaneous yeast fermentations.

Keywords: microbial terroir, mixed cultures, yeast consortia, low-input winemaking, minimal intervention

OPEN ACCESS

Edited by:
Xucong Lv,
Fuzhou University, China

Reviewed by:
Laura Canonico,
Marche Polytechnic University, Italy
Maurzio Ugliano,
University of Verona, Italy
Yongsheng Tao,
Northwest A&F University, China

***Correspondence:**
Francisco Carrau
fcarrau@fq.edu.uy

Specialty section:
This article was submitted to Food Microbiology, a section of the journal Frontiers in Microbiology

Received: *29 April 2021*
Accepted: *18 June 2021*
Published: *04 August 2021*

Citation:
Carrau F and Henschke PA (2021) Hanseniaspora vineae and the Concept of Friendly Yeasts to Increase Autochthonous Wine Flavor Diversity. Front. Microbiol. 12:702093. doi: 10.3389/fmicb.2021.702093

INTRODUCTION

Traditionally, our ancestors produced wines by exploiting the indigenous yeast diversity present on grapes without knowledge of their winemaking capability. As wine quality was highly variable within and across different vintages, the challenge at that time was to obtain consistency and to search for vinification conditions that allowed greater standardization of their own wine styles.

After Pasteur in 1866 showed that many yeast species rather than simple chemical reactions were responsible for wine fermentation (Barnett, 2000), wine masters from the beginning of the 20th century began to search for the "pure ferment" concept (Hansen, 1895; Regenberg and Hansen, 2001), so as to increase the reliability of vintage quality. This period saw the improvement of wine quality until the 1980s which promoted the successful growth of the wine industry globally and increased the consumption of better quality wine. Thanks to a considerable expansion of knowledge on the roles of yeast and bacteria in winemaking over the past 60 years (Ribereau-Gayon et al., 1951; Rankine, 1967; Amerine and Kunkee, 1968), wines became more flavorsome, especially more fruity, and less faulty than in the past (Lambrechts and Pretorius, 2000; Fleet, 2003; Ugliano and Henschke, 2009; Steensels and Verstrepen, 2014; Pretorius, 2020). However, in the 1990s, some winemakers and consumers noticed that wines in the general wine markets were becoming more uniform in flavor in terms of lacking complexity and diversity. In particular, the flavor characteristics of wines from major producing countries, which have specific terroirs, were becoming less apparent (Bisson et al., 2002). The majority of the wine producers were using the same conventional fermentation technology based on *Saccharomyces cerevisiae* (Jolly et al., 2014), which essentially precluded the opportunity for their respective microbial terroir to participate in the vinification process. This led some artisans to suggest that wine styles needed to return to their "grape roots" and develop the concept of microbial terroir flavors based on "low-input" winemaking strategies (Ramey, 1995). The challenge was to return to traditional winemaking technologies but guided by a greater wealth of knowledge compared with earlier times (Carrau, 2006; van Wyk et al., 2020). It is now well established that increased yeast diversity can contribute to the diversity of the volatile chemical composition of wine (Romani et al., 2020), which might increase the sensory diversity of wine flavor, a still controversial concept of sensory complexity (Varela et al., 2009; Smith, 2012; Köster and Mojet, 2016; Borren and Tian, 2021). Moreover, increased diversity can also results in process stability and productivity in microbial communities (Lehman and Tilman, 2000; Briones and Raskin, 2003). Whilst complex ecological studies are needed to prove this phenomenon in several fermentation niches, there is an increasing numbers of studies showing that mixed cultures can more effciently exhaust nutrients when compared with single cultures (Medina et al., 2012; Perez et al., 2020). This effect might further allow the reduction of microbial contamination during wine maturation. However, studies in real winemaking conditions at winery scale are very scarce (Romani et al., 2020), and when scaling up this technology of increased yeast diversity, the risks of appearance of undesirable flavors might result. At industrial sized fermentations, unpredictable interactions within a complex natural microflora, as the result of increasing reductive or oxidative conditions (Fariña et al., 2012; Varela et al., 2021) will demand careful daily process control by tasting. The attraction for food and wine is all about the flavor phenotype (Cordente et al., 2012; Carrau et al., 2015). These winemaking strategies are not romantic, and understanding deeply wine microbiology management is fundamental to obtain high-quality differentiated wines which reflect the region. Our proposal for developing friendly starters is based on careful strain selection by flavor and low nitrogen demand that was developed in order to obtain consistent screenings of superior native strains (Carrau et al., 2015). In our experience these aspects combined with an active but moderate fermentation capacity at temperatures below 20°C, resulted in wines of desirable flavors with certain yeast strains. By this selection strategy, we detected *Hanseniaspora vineae* at the initial steps of fermentation. In addition, we have characterized this yeast as having very different metabolic synthetic pathways compared with *Saccharomyces* that enrich wines with several grape flavor compounds related to the three aromatic amino acids such as benzenoids (Martin et al., 2016b; Valera et al., 2020a), other phenylpropanoids, and isoprenoids (Giorello et al., 2019; Del Fresno et al., 2020; Martin et al., 2021b). In this perspective, we will discuss the concept of "friendly" yeasts for developing wine starters and how the inoculation of *H. vineae* strains compared with conventional *Saccharomyces* strains gives the winemaker new tools to manage the microbial terroir flavor expression without the risk of unreliable spontaneous fermentations (Knight et al., 2020; Griggs et al., 2021).

FRIENDLY YEASTS COOPERATE WITH THE MICROBIAL TERROIR

It is well known that the majority of commercial yeasts added to a grape juice fermentation as starter culture rapidly control the process by reaching above 90% of the total yeast flora (Fleet, 1993; Medina et al., 2013; Carrau et al., 2020). This situation is common with *Saccharomyces* starters that are highly competitive compared with the native microflora, which we can defined as "selfish" or "unfriendly" strains (Rendueles and Ghigo, 2012). This species has evolved a highly competitive strategy for removing key nutrients in a grape juice, such as amino acids and vitamins, within a few hours (Alonso-del-Real et al., 2019). Furthermore, they actively use the glycolytic and

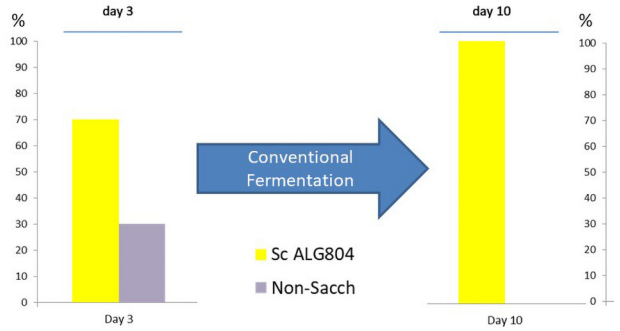

FIGURE 1 | Under conventional wine production, winemakers initiate fermentation by inoculating with a selected commercial strain. Commercial inocula of *Saccharomyces* strains are well known for efficient initiation of fermentation and typically result in the exclusion of other strains during the course of fermentation [results shown were adapted from Medina et al. (2013)].

alcohol fermentation pathways to exclude the native microflora of grape must niches, not only by producing ethanol and CO_2 but also increasing temperature and producing compounds such as short- and medium-chain fatty acids, isoacids, or higher alcohols that can inhibit other yeast species (Goddard, 2008; Valera et al., 2019). These aroma compounds can be defined as "toxic" intercellular communication mechanisms, in contrast to the reduced production of these flavors by a friendly yeast strain. During the last decade or more, many non-*Saccharomyces* starters in mixed culture fermentation with a strain of *Saccharomyces* have been studied, usually inoculated in sequential mode, so as to enhance the opportunity of the non-*Saccharomyces* to influence the winemaking process compared with co-inoculations where its impact can be limited by exclusion or competition with *Saccharomyces* (Padilla et al., 2016; Aranda, 2019; Borren and Tian, 2021). In summary, the competitive advantage of *Saccharomyces* over the majority of non-*Saccharomyces* yeasts can reside in various stress mechanisms, including nitrogen depletion, sugar transporter adaptations to high osmotic pressure of grape juice (high sugar content) and to a more active proton-pump ATPase adapted to low pH and high ethanol (Ganucci et al., 2018; Palmgren and Morsomme, 2019). These key adaptations that are strain dependent can explain why *Saccharomyces* species and their related hybrids typically dominate the fermentation niche. Interestingly, in reference to secondary fermentation compounds, that are inhibitors of cell activity, we have noted that some characteristics of *H. vineae* metabolism can explain the resulting friendlier environment from its activity. Metabolic reactions such as its extreme capacity for higher alcohol acetylation represents a well-known mechanisms for detoxifing acetates and their corresponding alcohol in the fermentation medium (Peddie, 1990). Furthermore, we have determined that *H. vineae* produces significantly lower concentrations of fatty acids and has a slower rate of ethanol and CO_2 production compared with *Saccharomyces* strains (Valera et al., 2020b). These attributes are characteristic of *H. vineae* within the apiculate group of the *Hanseniaspora* genus (Martin et al., 2018; Giorello et al., 2019; Valera et al., 2020a,b). During Chardonnay winemaking with *H. vineae* strains (Medina et al., 2013), we noted that in control-inoculated wines with *S. cerevisiae* ALG804, the native grape microflora was invariably dominated by this strain within several days. In **Figure 1**, we show a yeast profile of conventional wine fermentation inoculated with 10 g/Hl of active dry yeast, which clearly reveals numerical dominance by this species. In contrast, **Figure 2** shows that inoculation with *H. vineae* HV025 permitted the participation of eight different strains at day 10 of the fermentation process. Although we can see in **Figure 2** that two commercial strains appeared that might come from previous winemaking vintages, it is interesting to note that there were also four native *Saccharomyces* strains according to our yeast commercial data bank by DNA microsatellite profiles (Jubany et al., 2008).

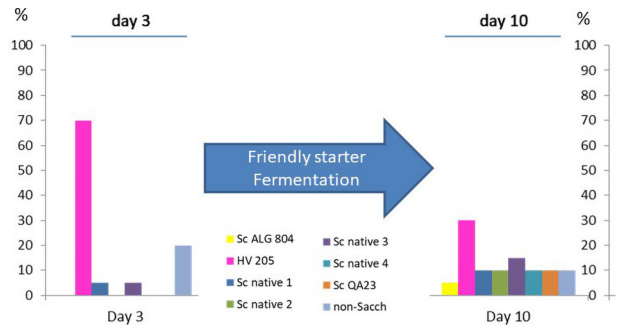

FIGURE 2 | This shows an example of the yeast profile of a Chardonnay grape must inoculated with a single strain of HV025. This treatment shows an increase in yeast diversity during fermentation, as *H. vineae* allows the native or winery microflora to participate during fermentation. We apply the concept of "friendly starters" to a yeast inoculum that allows various yeast species and strains to share the fermentation environment.

THE IMPACT OF NON-*SACCHAROMYCES* STRAINS ON SENSORY WINE DIFFERENTIATION

Few publications have focused on demonstrating increased sensory diversity associated with fermentation microflora using high-quality sensory techniques. Over the past two decades, many investigations have shown a great diversity of chemical compound analysis by GCMS of wines made with non-*Saccharomyces* and mixed species cultures compared with *Saccharomyces* yeasts. A large range of volatile compounds can be detected, but their impact on the sensory properties of wine is often lacking (Spence and Wang, 2019). The challenge today is to correlate wine chemical data with formal sensory analysis using for example a trained panel of judges or simple methods at the winery (Lesschaeve and Noble, 2010). Wines made with different yeast strains can often be consistently differentiated by sensory profiling techniques or can be judged as being sensorially more complex than others (Padilla et al., 2016; Binati et al., 2019). Many reports showing detailed chemical analyses will need to be validated with sensory analysis as they are merely showing just the chemical diversity of yeast metabolism in different winemaking conditions. Many of the reports on experimental vinification were performed with either chemically defined or natural grape fermentation media with either undefined or an excess concentration of yeast assimilable nitrogen (Carrau et al., 2017; Perli et al., 2020). Although it is clear that many of the recent non-*Saccharomyces* vinification studies have demonstrated an impact on wine quality in different grape varieties or under mixed culture conditions, there is still very limited information on the behavior of non-*Saccharomyces* strains at winery scale (Jolly et al., 2014; Comitini et al., 2017; Morata et al., 2020). Since 2007, white wines have been produced with *H. vineae* on a commercial scale (Medina et al., 2007) and could be sensorially differentiated from wines produced by conventional *Saccharomyces* fermentations (Medina et al., 2013; Lleixa et al., 2016; Martin et al., 2018; Del Fresno et al., 2020, 2021). However, although red wines made under these treatments can be differentiated by chemical techniques, the

sensory differentiation or quality conclusions of these processes in red wine vinification at winery scale were less clear. Our observation is that young red wines might be differentiated more easily than strong body red wines and even less following barrel maturation. Chemically, red wines made with *H. vineae* showed the presence of increased concentrations of benzenoids and acetate esters when compared with conventionally vinified red wines. In the meantime, metabolic footprinting techniques of these wines (Howell et al., 2006) allowed us to show that *H. vineae* had contributed to the aromatic chemical composition of wine on an industrial wine fermentation scale (Martín et al., 2021a).

INCREASED YEAST DIVERSITY INCREASES FLAVOR COMPLEXITY

It is widely known that protection of biodiversity should be a main biological focus for conserving agricultural ecosystems. As we previously mentioned, it was demonstrated that increased biodiversity in a given ecosystem niche increased community stability and productivity (Lehman and Tilman, 2000). The flavor complexity concept is still not clear and some authors believe it is more of an increase of flavor compound diversity from a chemical point of view. However, the relevant concept should include the sensory complexity when we talk about fermented beverages (Tempère et al., 2018). Increased flavor diversity has been demonstrated by the use of mixed culture inocula by which increased flavor complexity from a sensory point of view could be achieved, for example, in Chardonnay (Soden et al., 2000; Medina et al., 2013) or Sauvignon Blanc wines (Anfang et al., 2009; Knight et al., 2018). More recently, sensory studies of mixed culture fermentations in some other white and red varieties, have been reported (Varela, 2016; Padilla et al., 2017; Hranilovic et al., 2018; Benito et al., 2019; Castrillo et al., 2019; Binati et al., 2020; Del Fresno et al., 2020; Romani et al., 2020; Muñoz-Redondo et al., 2021). In our experience, a chemically defined grape must medium with low assimilable nitrogen has allowed the selection of non-*Saccharomyces* and *Saccharomyces* strains with a combination of both low nitrogen demand and intense desirable flavors production (Carrau et al., 2015). This procedure contributed to the selection of a new generation of native yeast strains adapted for low-input winemaking strategies, where the addition of DAP can be avoided. It is known that ammonium salts inhibit the synthesis of some of the main aroma compounds of particular interest for the varietal character of some grapes, such as phenylpropanoids or sulfur thiols (Martin et al., 2016a). This strategy is expected to identify yeasts that can share fermentation medium nutrients as they will have decreased nitrogen demand characteristics and will ensure the development of clean flavors. However, further studies regarding unpredictable yeast interactions at winery scale are being carried out to better understand the appearance of sluggish fermentations in some rich sugar white grape musts such as Petit Manseng and Chardonnay grapes which would yield ethanol concentrations exceeding above 13% alcohol by volume (Carrau et al., 2020).

YEAST DIVERSITY FROM NATIVE ENVIRONMENTS TO THE WINERY

The systematic use of *Saccharomyces* starter cultures in wine production has contributed to more uniform wine quality in the past 50 years. However, it is now considered by some that there is a limitation of flavor diversity due to this phenomenon affecting the development of new wine styles. This has led to a decrease in the flavor differentiation of wines from regional terroir sites which were previously described as having a "typical"

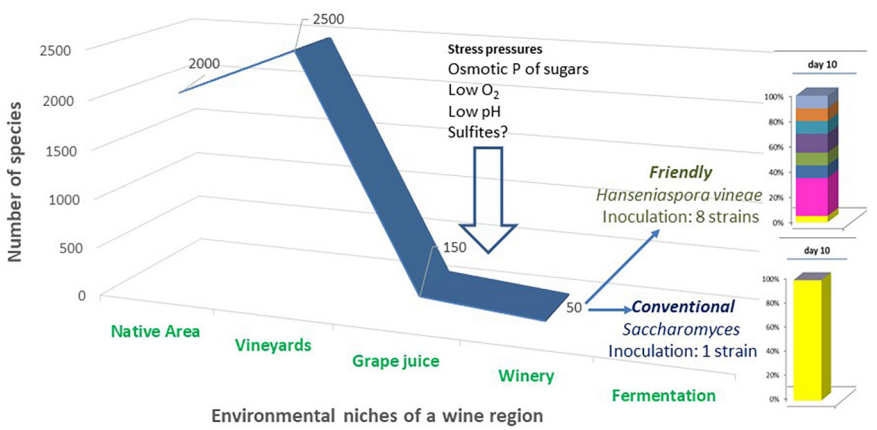

FIGURE 3 | Yeast diversity along the different environments of a wine region ecosystem. Winemakers have the alternative to increase strain diversity when working with yeast strains that might share the fermentation niche with other native strains. The number of species data of the different niches was obtained from recent studies (Morrison-Whittle and Goddard, 2018), and fermentation data with *H. vineae* were adapted from Carrau et al. (2020).

flavor profile as associated with a given region (Liu et al., 2019, 2020). In **Figure 3**, we show the interesting process of how yeast diversity in a certain wine region is reduced from the vine to the final wine. This graph clearly shows that the addition of a pure culture inoculum of *Saccharomyces* at the initial step of fermentation in the winery restricts the rich microbial terroir flora to a single culture process.

Studies concerning yeast diversity in a wine region showed that the grape plants, including the fruit and soil niche ecosystems, lodge the higher number of yeast species compared with the native and winery environments (Morrison-Whittle and Goddard, 2018). **Figure 3** shows the process from nature to the fermentation ecosystem revealing how yeast diversity undergoes a slight increase at the fruit ecosystem and, subsequently, a continuous decrease until the commencement of fermentation. Winemaker management of fermentation, that is interventions, can increase or even decrease yeast diversity to a single fermentation strain. In contrast to the rich biodiversity in a certain wine region, conventional inoculation of a pure *Saccharomyces* ferment finished with a single culture fermentation process.

DISCUSSION

The development of "friendly" yeasts can promote a sharing of the fermentation medium with some strains from natural environments so as to recover potential metabolic diversity along the process. The concept of introducing a starter with the characteristics described is based on the difficult task that would be incurred by a winery in selecting native yeasts with superior flavors from their vines, as it has been mentioned such strains might represent less than 10% of the total natural microflora. We have shown that a selection strategy for friendly yeast based on sensory analysis at low YAN concentrations and moderate fermentation capacity minimize the risk of sluggish processes or the production of undesirable flavors such as acetic acid, hydrogen sulfide, or acetaldehyde. *H. vineae* might also well fit the concept of friendly yeast owing to its low formation of higher alcohols and fatty acids compared with *Saccharomyces*, known inhibitors of many yeast strains. However, this approach to allowing the natural microflora to participate in the process should be controlled daily by tasting. However, in the wineries the fermentation increase microbial competition under such complex situations might be a small risk compared to the benefit of obtaining increased flavor complexity. The potential risks that could result from this approach are believed to be significantly smaller than the application of spontaneous fermentation processes. The future challenge for wine microbiologists and winemakers will be to understand fermentation from a holistic view point, so as to provide an alternative management of the process with the aim of minimizing the loss of strain diversity which would contribute to the loss of terroir characteristics. Strain interactions which increase strain diversity give infinite opportunities to explore flavor development. It is well known that in a complex consortia fermentation, there are many factors that can change the final flavor of a wine, such as size of the inocula, nutrient competition, metabolite–cell and cell–cell interactions, temperature, tank sizes, redox situations, and aeration. The development of friendly yeasts that share their environment with other strains is an interesting low-input winemaking strategy. This biotechnological approach might be considered a "romantic" way of producing particular or unique wines representing regionality. However, these strategies demand deep knowledge of microbiology and systematic tasting and sensory training at the winery to obtain quality and market differentiation.

DATA AVAILABILITY STATEMENT

The original contributions presented in the study are included in the article, further inquiries can be directed to the corresponding author.

AUTHOR CONTRIBUTIONS

FC wrote the article. PH wrote part of the article and reviewed the general presentation. Both authors contributed to the article and approved the submitted version.

FUNDING

We thank the CSIC Group Project numbers 802 and 983 of UdelaR, Facultad de Quimica and CSIC Offices of Universidad de la Republica, Uruguay; Agencia Nacional de Investigación e Innovación (ANII): *Hanseniaspora vineae* FMV 6956 project; and Proyecto Centros 2015 del CEINBIO-Facultad de Medicina for financial support. We also thank ANII for supporting our project Alianza on *H. vineae* metabolic characterization and application (ALI_2_2019_1_155314), and Lage y Cia Uruguay and Oenobrands France for pilot yeast starter preparations for winery-scale applications. The AWRI is supported by Australia's grape growers and winemakers through their investment body Wine Australia with matching funds from the Australian Government.

ACKNOWLEDGMENTS

We thank Carrau lab (Facultad de Quimica, Uruguay) and the Australian Wine Research Institute members for their help and critical comments during the last decade concerning this topic, and many authors that have contributed to this topic and were not cited due to the short structure of the article.

REFERENCES

Alonso-del-Real, J., Pérez-Torrado, R., Querol, A., and Barrio, E. (2019). Dominance of wine *Saccharomyces cerevisiae* strains over *S. kudriavzevii* in industrial fermentation competitions is related to an acceleration of nutrient uptake and utilization. *Environ. Microbiol.* 21, 1627–1644. doi: 10.1111/1462-2920.14536

Amerine, M., and Kunkee, R. (1968). Microbiology of winemaking. *Annu. Rev. Microbiol.* 22, 323–358.

Anfang, N., Brajkovich, M., and Goddard, M. R. (2009). Co-fermentation with *Pichia kluyveri* increases varietal thiol concentrations in Sauvignon Blanc. *Aust. J. Grape Wine Res.* 15, 1–8. doi: 10.1111/j.1755-0238.2008.00031.x

Aranda, A. (2019). Enological repercussions of Non-*Saccharomyces* Species. *Fermentation* 5:68. doi: 10.3390/fermentation5030068

Barnett, J. A. (2000). A history of research on yeasts 2: Louis Pasteur and his contemporaries, 1850–1880. *Yeast* 16, 755–771. doi: 10.1002/1097-0061(20000615)16:8<755::aid-yea587>3.0.co;2-4

Benito, S., Ruiz, J., Belda, I., Kiene, F., Beisert, B., Navascués, E., et al. (2019). "Application of non-*Saccharomyces* yeasts in wine production," in *Non-Conventional Yeasts: From Basic Research to Application*, ed. A. Sibirny (Cham: Springer), 75–89. doi: 10.1007/978-3-030-21110-3_3

Binati, R. L., Innocente, G., Gatto, V., Celebrin, A., Polo, M., Felis, G. E., et al. (2019). Exploring the diversity of a collection of native non-Saccharomyces yeasts to develop co-starter cultures for winemaking. *Food Res. Int.* 122, 432–442. doi: 10.1016/j.foodres.2019.04.043

Binati, R. L., Junior, W. J. L., Luzzini, G., Slaghenaufi, D., Ugliano, M., and Torriani, S. (2020). Contribution of non-*Saccharomyces* yeasts to wine volatile and sensory diversity: a study on *Lachancea thermotolerans*, *Metschnikowia spp*. and *Starmerella bacillaris* strains isolated in Italy. *Int. J. Food Microbiol.* 318:108470. doi: 10.1016/j.ijfoodmicro.2019.108470

Bisson, L. F., Waterhouse, A. L., Ebeler, S. E., Walker, M. A., and Lapsley, J. T. (2002). The present and future of the international wine industry. *Nature* 418, 696–699. doi: 10.1038/nature01018

Borren, E., and Tian, B. (2021). The important contribution of non-*Saccharomyces* yeasts to the aroma complexity of wine: a review. *Foods* 10:13. doi: 10.3390/foods10010013

Briones, A., and Raskin, L. (2003). Diversity and dynamics of microbial communities in engineered environments and their implications for process stability. *Curr. Opin. Biotechnol.* 14, 270–276. doi: 10.1016/S0958-1669(03)00065-X

Carrau, F. (2006). "Native yeasts for low input winemaking: searching for wine diversity and increased complexity," in *Proceedings of the International Wine Microbiology Symposium*, CSU International Wine Microbiology Symposium, (Tenaya Lodge, CA: California State University), 33–39.

Carrau, F., Boido, E., and Dellacassa, E. (2017). "Yeast diversity and flavor compounds," in *Fungal Metabolites*, eds J. M. Mérillon and K. Ramawat (Cham: Springer), 569–597. doi: 10.1007/978-3-319-19456-1_32-1

Carrau, F., Boido, E., and Ramey, D. (2020). Yeasts for low input winemaking: microbial terroir and flavor differentiation. *Adv. Appl. Microbiol.* 111, 89–121. doi: 10.1016/bs.aambs.2020.02.001

Carrau, F., Gaggero, C., and Aguilar, P. S. (2015). Yeast diversity and native vigor for flavor phenotypes. *Trends Biotechnol.* 33, 148–154. doi: 10.1016/j.tibtech.2014.12.009

Castrillo, D., Rabuñal, E., Neira, N., and Blanco, P. (2019). Oenological potential of non-*Saccharomyces* yeasts to mitigate effects of climate change in winemaking: impact on aroma and sensory profiles of Treixadura wines. *FEMS Yeast Res.* 19:foz065.

Comitini, F., Capece, A., Ciani, M., and Romano, P. (2017). New insights on the use of wine yeasts. *Curr. Opin. Food Sci.* 13, 44–49. doi: 10.1016/j.cofs.2017.02.005

Cordente, A. G., Curtin, C. D., Varela, C., and Pretorius, I. S. (2012). Flavour-active wine yeasts. *Appl. Microbiol. Biotechnol.* 96, 601–618. doi: 10.1007/s00253-012-4370-z

Del Fresno, J. M., Escott, C., Loira, I., Carrau, F., Cuerda, R., Schneider, R., et al. (2021). The impact of *Hanseniaspora vineae* fermentation and ageing on lees on the terpenic aromatic profile of white wines of the Albillo variety. *Int. J. Mol. Sci.* 22:2195. doi: 10.3390/ijms22042195

Del Fresno, J. M., Escott, C., Loira, I., Herbert-Pucheta, J. E., Schneider, R., Carrau, F., et al. (2020). Impact of *Hanseniaspora vineae* in alcoholic fermentation and ageing on lees of high-quality white wine. *Fermentation* 6:66. doi: 10.3390/FERMENTATION6030066

Fariña, L., Medina, K., Urruty, M., Boido, E., Dellacassa, E., and Carrau, F. (2012).). Redox effect on volatile compound formation in wine during fermentation by *Saccharomyces cerevisiae*. *Food Chem.* 134, 933–939. doi: 10.1016/j.foodchem.2012.02.209

Fleet, G. H. (1993). "Yeast growth during fermentation," in *Wine Microbiology and Biotechnology*, ed. G. H. Fleet (Chur: Harwood Academic Publishers), 27–54.

Fleet, G. H. (2003). Yeast interactions and wine flavour. *Int. J. Food Microbiol.* 86, 11–22. doi: 10.1016/S0168-1605(03)00245-9

Ganucci, D., Guerrini, S., Mangani, S., Vincenzini, M., and Granchi, L. (2018). Quantifying the effects of ethanol and temperature on the fitness advantage of predominant *Saccharomyces cerevisiae* strains occurring in spontaneous wine fermentations. *Front. Microbiol.* 9:1563. doi: 10.3389/fmicb.2018.01563

Giorello, F., Valera, M. J., Martin, V., Parada, A., Salzman, V., Camesasca, L., et al. (2019). Genomic and transcriptomic basis of Hanseniaspora vineae's impact on flavor diversity and wine quality. *Appl. Environ. Microbiol.* 85:e01959-18. doi: 10.1128/AEM.01959-18

Goddard, M. R. (2008). Quantifying the complexities of *Saccharomyces cerevisiae*'s ecosystem engineering via fermentation. *Ecology* 89, 2077–2082. doi: 10.1890/07-2060.1

Griggs, R. G., Steenwerth, K. L., Mills, D. A., Cantu, D., and Bokulich, N. A. (2021). Sources and assembly of microbial communities in vineyards as a functional component of winegrowing. *Front. Microbiol.* 12:836. doi: 10.3389/fmicb.2021.673810

Hansen, E. C. (1895). Experimental studies on the variation of Yeast-cells. *Ann. Bot.* 9, 549–560. doi: 10.1093/oxfordjournals.aob.a090755

Howell, K. S., Cozzolino, D., Bartowsky, E. J., Fleet, G. H., and Henschke, P. A. (2006). Metabolic profiling as a tool for revealing *Saccharomyces* interactions during wine fermentation. *FEMS Yeast Res.* 6, 91–101. doi: 10.1111/j.1567-1364.2005.00010.x

Hranilovic, A., Li, S., Boss, P. K., Bindon, K., Ristic, R., Grbin, P. R., et al. (2018). Chemical and sensory profiling of Shiraz wines co-fermented with commercial non-*Saccharomyces* inocula. *Aust. J. Grape Wine Res.* 24, 166–180. doi: 10.1111/ajgw.12320

Jolly, N. P., Varela, C., and Pretorius, I. S. (2014). Not your ordinary yeast: non-*Saccharomyces* yeasts in wine production uncovered. *FEMS Yeast Res.* 14, 215–237. doi: 10.1111/1567-1364.12111

Jubany, S., Tomasco, I., Ponce de León, I., Medina, K., Carrau, F., Arrambide, N., et al. (2008). Toward a global database for the molecular typing of Saccharomyces cerevisiae strains. *FEMS Yeast Res.* 8, 472–484. doi: 10.1111/j.1567-1364.2008.00361.x

Knight, S. J., Karon, O., and Goddard, M. R. (2020). Small scale fungal community differentiation in a vineyard system. *Food Microbiol.* 87:103358. doi: 10.1016/j.fm.2019.103358

Knight, S. J., Klaere, S., Morrison-Whittle, P., and Goddard, M. R. (2018). Fungal diversity during fermentation correlates with thiol concentration in wine. *Aust. J. Grape Wine Res.* 24, 105–112. doi: 10.1111/ajgw.12304

Köster, E. P., and Mojet, J. (2016). "Familiarity, monotony, or variety: the role of flavor complexity in food intake," in *Flavor: From Food to Behaviors, Wellbeing and Health*, eds P. Etiévant, E. Guichard, C. Salles, and A. Voilley (Sawston: Woodhead Publishing), doi: 10.1016/B978-0-08-100295-7.00013-X

Lambrechts, I. G., and Pretorius, I. S. (2000). Yeast and its importance to wine aroma-A review. *South Afr. J. Enol. Vitic.* 21, 97–129.

Lehman, C. L., and Tilman, D. (2000). Biodiversity, stability, and productivity in competitive communities. *Am. Nat.* 156, 534–552. doi: 10.1086/303402

Lesschaeve, I., and Noble, A. C. (2010). "Sensory analysis of wine," in *Managing Wine Quality Viticulture and Wine Quality, Woodhead Publishing Series in Food Science, Technology and Nutrition*, ed. A. G.

Reynolds (Amsterdam: Elsevier), 189–217. doi: 10.1533/9781845699284.2.189

Liu, D., Chen, Q., Zhang, P., Chen, D., and Howell, K. S. (2020). The fungal microbiome is an important component of vineyard ecosystems and correlates with regional distinctiveness of wine. *Msphere* 5, e00534-20.

Liu, D., Zhang, P., Chen, D., and Howell, K. S. (2019). From the vineyard to the winery: how microbial ecology drives regional distinctiveness of wine. *Front. Microbiol.* 10:2679. doi: 10.3389/fmicb.2019.02679

Lleixa, J., Martin, V., Portillo, C., Carrau, F., Beltran, G., and Mas, A. (2016). Comparison of the performances of *Hanseniaspora vineae* and *Saccharomyces cerevisiae* during winemaking. *Front. Microbiol.* 7:338. doi: 10.3389/fmicb.2016.00338

Martín, V., Boido, E., Dellacassa, E., Schneider, R., Román, T., Morata, A., et al. (2021a). "Application of *Hanseniaspora vineae* Hv025 in white and red grapes vinification on a winery scale," in *Proceedings of the National Conference American.Society. Enology and Viticulture. June 23th*, Monterrey, CA.

Martin, V., Boido, E., Giorello, F., Mas, A., Dellacassa, E., and Carrau, F. (2016a). Effect of yeast assimilable nitrogen on the synthesis of phenolic aroma compounds by *Hanseniaspora vineae* strains. *Yeast* 33, 323–328. doi: 10.1002/yea.3159

Martin, V., Giorello, F., Fariña, L., Minteguiaga, M., Salzman, V., Boido, E., et al. (2016b). De Novo synthesis of Benzenoid compounds by the yeast *Hanseniaspora vineae* increases the flavor diversity of wines. *J. Agric. Food Chem.* 64, 4574–4583. doi: 10.1021/acs.jafc.5b05442

Martin, V., Jose Valera, M., Medina, K., Boido, E., and Carrau, F. (2018). Oenological impact of the *Hanseniaspora/Kloeckera* yeast genus on wines — A review. *Fermentation* 4:76. doi: 10.3390/fermentation4030076

Martin, V., Valera, M. J., Medina, K., Schneider, R., Boido, E., and Carrau, F. (2021b). "Application of Hanseniaspora vineae to improve white wine quality," in *White Wine Technology*, Chap 9, 1st Edn, ed. A. Morata (Academic Press), 340.

Medina, K., Boido, E., Dellacassa, E., and Carrau, F. (2012). Growth of non-*Saccharomyces* yeasts affects nutrient availability for *Saccharomyces cerevisiae* during wine fermentation. *Int. J. Food Microbiol.* 157, 245–250. doi: 10.1016/j.ijfoodmicro.2012.05.012

Medina, K., Boido, E., Fariña, L., Gioia, O., Gomez, M. E., Barquet, M., et al. (2013). Increased flavour diversity of Chardonnay wines by spontaneous fermentation and co-fermentation with *Hanseniaspora vineae*. *Food Chem.* 141, 2513–2521. doi: 10.1016/j.foodchem.2013.04.056

Medina, K., Ferreri, L., Fariña, L., Boido, E., Dellacassa, E., Gaggero, C., et al. (2007). Aplicación de la levadura *Hanseniaspora vineae* en cultivos mixtos con *Saccharomyces cerevisiae* en la vinificación. *Rev. Enol.* 4, 1–6.

Morata, A., Escott, C., Bañuelos, M. A., Loira, I., Del Fresno, J. M., González, C., et al. (2020). Contribution of non-*Saccharomyces* yeasts to wine freshness. A review. *Biomolecules* 10:34. doi: 10.3390/biom10010034

Morrison-Whittle, P., and Goddard, M. R. (2018). From vineyard to winery: a source map of microbial diversity driving wine fermentation. *Environ. Microbiol.* 20, 75–84. doi: 10.1111/1462-2920.13960

Muñoz-Redondo, J. M., Puertas, B., Cantos-Villar, E., Jiménez-Hierro, M. J., Carbú, M., Garrido, C., et al. (2021). Impact of sequential inoculation with the Non-*Saccharomyces T. delbrueckii* and *M. pulcherrima* combined with *Saccharomyces cerevisiae* strains on chemicals and sensory profile of Roseì wines. *J. Agric. Food Chem.* 69, 1598–1609. doi: 10.1021/acs.jafc.0c06970

Padilla, B., Gil, J. V., and Manzanares, P. (2016). Past and future of non-*Saccharomyces* yeasts: from spoilage microorganisms to biotechnological tools for improving wine aroma complexity. *Front. Microbiol.* 7:411. doi: 10.3389/fmicb.2016.00411

Padilla, B., Zulian, L., Ferreres, À, Pastor, R., Esteve-Zarzoso, B., Beltran, G., et al. (2017). Sequential inoculation of native non-*Saccharomyces* and *Saccharomyces cerevisiae* strains for wine making. *Front. Microbiol.* 8:1293. doi: 10.3389/fmicb.2017.01293

Palmgren, M., and Morsomme, P. (2019). The plasma membrane H+-ATPase, a simple polypeptide with a long history. *Yeast* 36, 201–210. doi: 10.1002/yea.3365

Peddie, H. A. B. (1990). Ester formation in brewery fermentations. *J. Insitute Brew.* 96, 327–331. doi: 10.1002/j.2050-0416.1990.tb01039.x

Perez, G., Debernardis, F., Boido, E., and Carrau, F. (2020). Simultaneous identification to monitor consortia strain dynamics of four biofuel yeast species during fermentation. *J. Ind. Microbiol. Biotechnol.* 47, 1133–1140. doi: 10.1007/s10295-020-02310-7

Perli, T., Wronska, A. K., Ortiz-Merino, R. A., Pronk, J. T., and Daran, J. M. (2020). Vitamin requirements and biosynthesis in *Saccharomyces cerevisiae*. *Yeast* 37, 283–304.

Pretorius, I. S. (2020). Tasting the terroir of wine yeast innovation. *FEMS Yeast Res.* 20:foz084.

Ramey, D. (1995). "Low input winemaking- let nature do the work," in *Proceedings of the Australian Wine Industry Technical Conference*, eds A. N. Sas, C. S. Stockley, R. S. Johnstone, and T. H. Lee (Adelaide, SA: Winetitles), 26–29.

Rankine, B. C. (1967). Influence of yeast strain and pH on pyruvic acid content of wines. *J. Sci. Food Agric.* 18, 41–44. doi: 10.1002/jsfa.2740180201

Regenberg, B., and Hansen, J. (2001). A history of research on yeasts 3: Emil Fischer Eduard Buchner and their contemporaries, 1880-1900. *Yeast* 18, 363–388. doi: 10.1002/1097-0061(20010315)18:4<363::aid-yea677>3.0.{\break}co;2-r

Rendueles, O., and Ghigo, J.-M. (2012). Multi-species biofilms: how to avoid unfriendly neighbors. *FEMS Microbiol. Rev.* 36, 972–989. doi: 10.1111/j.1574-6976.2012.00328.x

Ribereau-Gayon, J., Peynaud, E., and Lafourcade, S. (1951). Sur L'influence de L'aeration au cours de la fermentation. *Ind. Agric. Aliment.* 68, 141–150.

Romani, C., Lencioni, L., Biondi Bartolini, A., Ciani, M., Mannazzu, I., and Domizio, P. (2020). Pilot scale fermentations of *Sangiovese*: an overview on the impact of *Saccharomyces* and Non-*Saccharomyces* Wine Yeasts. *Fermentation* 6:63. doi: 10.3390/fermentation6030063

Smith, B. (2012). Perspective: complexities of flavour. *Nature* 486:S6. doi: 10.1038/486S6a

Soden, A., Francis, I. L., Oakey, H., and Henschke, P. A. (2000). Effects of co-fermentation with *Candida stellata* and *Saccharomyces cerevisiae* on the aroma and composition of Chardonnay wine. *Aust. J. Grape Wine Res.* 6, 21–30. doi: 10.1111/j.1755-0238.2000.tb00158.x

Spence, C., and Wang, Q. J. (2019). Wine expertise: perceptual learning in the chemical senses. *Curr. Opin. Food Sci.* 27, 49–56. doi: 10.1016/j.cofs.2019.05.003

Steensels, J., and Verstrepen, K. J. (2014). Taming wild yeast: potential of conventional and nonconventional yeasts in industrial fermentations. *Annu. Rev. Microbiol.* 68, 61–80. doi: 10.1146/annurev-micro-091213-113025

Tempère, S., Marchal, A., Barbe, J. C., Bely, M., Masneuf-Pomarede, I., Marullo, P., et al. (2018). The complexity of wine: clarifying the role of microorganisms. *Appl. Microbiol. Biotechnol.* 102, 3995–4007. doi: 10.1007/s00253-018-8914-8

Ugliano, M., and Henschke, P. A. (2009). "Yeasts and wine flavour," in *Wine Chemistry and Biochemistry*, eds M. V. Moreno-Arribas and M. C. Polo (New York, NY: Springer), 313–392. doi: 10.1007/978-0-387-74118-5_17

Valera, M. J., Boido, E., Dellacassa, E., and Carrau, F. (2020b). Comparison of the glycolytic and alcoholic fermentation pathways of *Hanseniaspora vineae* with *Saccharomyces cerevisiae* wine yeasts. *Fermentation* 6:78. doi: 10.3390/fermentation6030078

Valera, M. J., Boido, E., Ramos, J. C., Manta, E., Radi, R., Dellacassa, E., et al. (2020a). The Mandelate pathway, an alternative to the phenylalanine ammonia lyase pathway for the synthesis of benzenoids in ascomycete yeasts. *Appl. Environ. Microbiol.* 86, e701–e720.

Valera, M. J., Morcillo-Parra, M. Á, Zagórska, I., Mas, A., Beltran, G., and Torija, M. J. (2019). Effects of melatonin and tryptophol addition on fermentations carried out by *Saccharomyces cerevisiae* and non-*Saccharomyces* yeast species under different nitrogen conditions. *Int. J. Food Microbiol.* 289, 174–181. doi: 10.1016/j.ijfoodmicro.2018.09.013

van Wyk, N., von Wallbrunn, C., Swiegers, J. H., and Pretorius, I. S. (2020). Biotechnology of wine yeasts. *Encycl. Mycol.* 2, 428–446. doi: 10.1016/B978-0-12-819990-9.00007-X

Varela, C. (2016). The impact of non-*Saccharomyces* yeasts in the production of alcoholic beverages. *Appl. Microbiol. Biotechnol.* 100, 9861–9874. doi: 10.1007/s00253-016-7941-6

Varela, C., Cuijvers, K., Van Den Heuvel, S., Rullo, M., Solomon, M., Borneman, A., et al. (2021). Effect of aeration on yeast community structure and volatile composition in uninoculated chardonnay wines. *Fermentation* 7:97. doi: 10.3390/fermentation7020097

Varela, C., Siebert, T., Cozzolino, D., Rose, L., Maclean, H., and Henschke, P. A. (2009). Discovering a chemical basis for differentiating wines made by fermentation with 'wild' indigenous inoculated yeasts: role of yeast volatile compounds. *Aust. J. Grape Wine Res.* 15:238. doi: 10.1111/j.1755-0238.2009.00054.x

Conflict of Interest: The authors declare that the research was conducted in the absence of any commercial or financial relationships that could be construed as a potential conflict of interest.

frontiers in Microbiology

ORIGINAL RESEARCH
published: 12 August 2021
doi: 10.3389/fmicb.2021.717387

Investigation of Volatile Compounds, Microbial Succession, and Their Relation During Spontaneous Fermentation of Petit Manseng

Yanqin Ma, Tian Li, Xiaoyu Xu, Yanyu Ji, Xia Jiang, Xuewei Shi and Bin Wang**

Food College, Shihezi University, Shihezi, China

Petit Manseng is widely used for fermenting sweet wine and is popular among younger consumers because of its sweet taste and attractive flavor. To understand the mechanisms underlying spontaneous fermentation of Petit Manseng sweet wine in Xinjiang, the dynamic changes in the microbial population and volatile compounds were investigated through high-throughput sequencing (HTS) and headspace solid-phase microextraction (HS-SPME) coupled to gas chromatography-mass spectrometry (GC-MS) technology, respectively. Moreover, the relationship between the microbial population and volatile compounds was deduced *via* multivariate data analysis. *Candida* and *Mortierella* were dominant genera in Petit Manseng wine during spontaneous fermentation. Many fermentative aroma compounds, including ethyl octanoate, isoamyl acetate, ethyl butyrate, ethyl decanoate, isoamyl alcohol, ethyl laurate, isopropyl acetate, hexanoic acid, and octanoic acid, were noted and found to be responsible for the strong fruity and fatty aroma of Petit Manseng sweet wine. Multivariate data analysis indicated that the predominant microorganisms contributed to the formation of these fermentative aroma compounds. *Hannaella* and *Neomicrosphaeropsis* displayed a significantly positive correlation with the 6-methylhept-5-en-2-one produced. The current results provide a reference for producing Petit Manseng sweet wine with desirable characteristics.

Keywords: Petit Manseng, spontaneous fermentation, fungal community, volatile composition, correlation analysis

OPEN ACCESS

Edited by:
Van-Tuan Tran,
Vietnam National University, Hanoi, Vietnam

Reviewed by:
Eduardo Dellacassa,
Universidad de la República, Uruguay
Tao Feng,
Shanghai Institute of Technology, China

****Correspondence:***
Xuewei Shi
shixuewei@shzu.edu.cn
Bin Wang
binwang0228@shzu.edu.cn

Specialty section:
This article was submitted to Food Microbiology, a section of the journal Frontiers in Microbiology

Received: *30 May 2021*
Accepted: *21 July 2021*
Published: *12 August 2021*

Citation:
Ma Y, Li T, Xu X, Ji Y, Jiang X, Shi X and Wang B (2021) Investigation of Volatile Compounds, Microbial Succession, and Their Relation During Spontaneous Fermentation of Petit Manseng. Front. Microbiol. 12:717387. doi: 10.3389/fmicb.2021.717387

INTRODUCTION

Wine is an alcoholic beverage derived from grapes, and its production involves chemistry and biology (Belda et al., 2017). Based on its sugar content, wine can be classified into dry, semi-dry, sweet, and semi-sweet wine (Brainina et al., 2004). Because of their taste and rich flavor, sweet wines are popular (Swami et al., 2014). The grape varieties used to make sweet wine mainly include Riesling, Sauvignon Blanc, and Petit Manseng (Englezos et al., 2018; Lan et al., 2021). Of these, Petit Manseng is a thick-skinned, white grape variety grown in southwest France, and it is widely used to produce high-quality sweet wines rich in a fruity, slightly spicy aroma (Gardner et al., 2017). As a late-harvest cultivar, Petit Manseng has a high sugar and acid content, and consequently, it is strongly resistant to several fungal diseases (Robinson et al., 2013).

A wine's quality is determined based on its taste (Loureiro et al., 2016), color (Zhang et al., 2018), and aroma (Sherman et al., 2020). An important component of wine, the aroma is considered to be indicative of the regional and cultivar characteristics of a wine. This is because aroma is affected by natural elements (e.g., grape cultivars and climatic condition) (Mirás-Avalos et al., 2017), wine-making techniques (e.g., oak maturation and fermentation method) (Crump et al., 2015; Shi et al., 2019), and indigenous microorganism (e.g., bacteria, yeast, and fungi) (Liu et al., 2017). Wine aroma can be divided into varietal, fermentative, and aging (Belda et al., 2017). Varietal aromas, derived from wine grapes, are responsible for most of the aromas in a wine (Waterhouse et al., 2016). For example, when homologous, *Cabernet Franc*, *Cabernet Sauvignon*, *Sauvignon Blanc*, *Merlot*, and *Carmenère* have a typical bell pepper, vegetal, and earthy aroma (Ruiz et al., 2019).

High-throughput sequencing (HTS) is useful for evaluating dynamic changes in microbial populations during fermentation (Guo et al., 2020). Therefore, HTS has enabled the identification of a variety of dominant microorganisms, especially culture-independent microorganisms, in wine (Bučková et al., 2018). Wine is fermented by various indigenous microorganisms, and these vary based on the wine grape cultivar (Francesca et al., 2016). For instance, *Hanseniaspora*, *Metschnikowia*, *Saccharomyces*, *Lactococcus*, and *Leuconostoc* are predominant in Grüner Veltliner ice wine (Alessandria et al., 2013), whereas *Leuconostoc*, *Lactococcus*, and *Saccharomyces* are dominant in "Marselan" red wine (Lu et al., 2020). Among the aforementioned indigenous microorganisms, *Saccharomyces cerevisiae* not only promotes alcoholic fermentation but also increases phenol and antioxidant content through alcoholic fermentation (Caridi et al., 2017). Non-*Saccharomyces* yeasts are gaining increasing attention because they can improve the aroma complexity or mouth-feel of wines (Padilla et al., 2016).

Based on whether or not a starter culture is used, wine fermentation can be divided into inoculated fermentation and spontaneous fermentation. Compared with inoculated fermentation, spontaneous fermentation, which is caused by complex indigenous microorganisms, can provide a more complex and richer flavor in wine (Lu et al., 2021). Spontaneous fermentation makes full use of diverse microorganisms, especially the specific autochthonous yeasts (de Celis et al., 2019). The spontaneous fermentation by non-*Saccharomyces* yeasts has been found to enhance the aroma character of Cabernet Sauvignon, Chardonnay, and Vidal wines (Lu et al., 2020).

High-throughput sequencing (HTS) combined with multivariate data analysis has been widely used to investigate microbial diversity and its impact on wine quality (Böhmer et al., 2020). An increasing number of microorganisms, contributing to potential wine flavors, including *Hanseniaspora uvarum*, *Wickerhamomyces anomalus*, and *Lachancea thermotolerans*, have been identified (Belda et al., 2016).

Petit Manseng sweet wines are popular among young consumers (Chaplin, 2011). Although the sensory characteristics of Petit Manseng wines have been investigated *via* headspace solid-phase microextraction (HS-SPME) coupled to gas chromatography-mass spectrometry (GC-MS) and by using a polymer electronic nose (Gardner et al., 2017), the relationship of volatile compounds with the microbial community in these wines during spontaneous fermentation remains unclear. To understand the mechanisms underlying the spontaneous fermentation of Petit Manseng sweet wine in Xinjiang, dynamic changes in the microbial community and volatile compounds during spontaneous fermentation were investigated through HTS and HS-SPME/GC-MS, respectively. The relationship between the microbial populations and the volatile compounds was elucidated using multivariate data analysis. The current results provide a theoretical reference for producing Petit Manseng sweet wines with typical characteristics.

MATERIALS AND METHODS

Wine Making and Sampling

Petit Manseng was harvested from Changji County, Xinjiang Province, China in October 2019. After strict screening, healthy grapes were immediately crushed. The biochemistry of these grapes was then analyzed: residual sugar content, 347.35 g/L; yeast assimilable nitrogen (YAN): 347 mg N/L; pH, 3.49; soluble solids, 32.6 °Brix; total acidity, 5.17 g/L. This was followed by the addition of 20 mg/L pectinase. The grapes were macerated at 8−10°C for 48 h; then, the separated grape supernatants were subjected to alcoholic fermentation. All fermentation was performed in 50-L fermenters at 15–17°C (factory ambient temperature) under static conditions for 14°days. The alcohol fermentation was considered to be completed when residual sugar content was <110 g/L. The fermentation liquid (250 mL) was collected on fermentation days 0, 1, 4, 7, 11, and 14. All samples were centrifuged at 1,000 × g at 4°C for 10 min. The precipitates were then collected and used for HTS analysis, whereas the supernatants were used to assess volatile compound analysis. All samples were stored at −80°C until analysis. Each sample was analyzed in triplicate.

Determination of Physicochemical Properties

During alcoholic fermentation, some fermentation parameters were measured including pH, total acidity, and residual sugar and ethanol content. The pH of wine was measured using a calibrated pH meter (PHS-3C; Shanghai Jingke, Shanghai, China). Residual sugar content was assessed using dinitrosalicylic acid (DNS) method (Miller, 1959). Total acidity and ethanol content were determined according to the national standard of China: GB/T 15038-2006, "Analytical methods of wine and fruit wine." Organic acids in the wine samples were analyzed through high-performance liquid chromatography (HPLC) using previously described methods with some modifications (Murtaza et al., 2017). Each sample was centrifuged and filtered through a 0.22-μm filter, and the organic acids were identified through HPLC equipped with a Spursil C18 column (250 mm × 4.6 mm × 5 μm; Dima Technology, Guangzhou, China). A mixture of 0.1% phosphoric acid-methanol was regarded as the mobile phase, with a flow rate of 1 mL/min. The UV detection wavelength was maintained at 210 nm, and the

column temperature was 40°C. Each sample was measured in three replicates.

Fungal Isolation and Identification

The wine sample was serially diluted from 1×10 to 1×10^5 times by using sterile water and plated on yeast extract-peptone-dextrose (YPD) agar, and all plates were cultured at 28°C for 3 days under sterile conditions. After incubation, the fungal colonies on each plate were selected and isolated as representative fungal populations present during spontaneous fermentation. All representative strains were incubated on the WL nutrient agar (Haibo, Qingdao, China) at 28°C for 5 days. Then, fungal colonies with different morphological types were selected for the next step of identification. Single colonies of fungi were purified and stored in YPD liquid medium with 40% glycerol at −20°C. Fungal strains were analyzed and identified by comparing nucleotide sequences in the GenBank database (NCBI: https://blast.ncbi.nlm.nih.gov/blast.cgi).

HTS

The total DNA of fungal colonies isolated and selected from our wine samples was extracted using the CTAB/SDS method (Lin et al., 1994; Brandfass and Karlovsky, 2008). Next, the DNA of microorganisms were sent to Novegene Company (China) for PCR amplification and HTS. The primers used were ITS5-1737F (5′-GGAAGTAAAAGTCGTAACAAGG-3′) and ITS2-2043R (5′-GCTGCGTTCTTCATCGATGC-3′). For PCR, the total reaction volume was 25 μL, comprising 15 μL of the PCR Master Mix, 2 μL of the forward and reverse primers, 10 ng of the template DNA, and water (PCR-grade) to adjust the volume. We used the following thermal cycling program: initial denaturation at 98°C for 1 min, followed by 35 cycles of denaturation at 98°C for 10 s, annealing at 50°C for 30 s, and elongation at 72°C for 30 s, and finally, extension at 72°C for 5 min. All PCR products were detected through 2% agarose gel electrophoresis and purified using the Qiagen Gel Extraction Kit (Qiagen, Germany). Next, sequencing libraries were generated using TruSeq DNA PCR-Free Sample Preparation Kit (Illumina, United States). The library was assessed on a Qubit 2.0 Fluorometer (Thermo Fisher Scientific) and Agilent Bioanalyzer 2100. The Illumina NovaSeq platform was used to sequence 250-bp paired-end reads.

Processing of Sequence Analysis

Paired-end reads were assigned to samples based on their unique barcodes and truncated by cutting off the barcodes and primer sequences. Paired-end reads were merged using FLASH (version 1.2.7). The raw reads were filtered to obtain high-quality clean reads using QIIME (version 1.9.1). Moreover, the chimeric sequences were filtered out by comparing them with those in the SILVA database (a reference database). Moreover, the same operational taxonomic units (OTUs) were clustered from sequences with 97% sequence similarity by using Uparse (version 7.0.1001). The most abundant sequence in each OTU was selected as the representative sequence. Taxonomic units were assigned to the representative sequence (i.e., to each OTU) using the SILVA database. MUSCLE (version 3.8.31) was used for multiple sequence alignment and studied the phylogenetic relationship of different OTUs. Finally, alpha diversity indexes such as Shannon, Simpson, Chao1, and ACE were calculated on QIIME (version 1.9.1).

Determination of Volatile Compounds

Headspace solid-phase microextraction (HS-SPME)/gas chromatography-mass spectrometry (GC-MS) was used to extract and analyze volatile compounds in our wine, by using Kong's et al. (2019) method with some modifications. In brief, 1 g of NaCl was added to 5 mL of sample supernatants. This mixture was then transferred to a 20-mL HS vial, followed by 1 μL of 3-octanol (165 mg/mL) as the internal standard. The vial was sealed immediately with a polytetrafluoroethene (PTFE) silicone diaphragm and balanced at 40°C for 10 min. An SPME fiber (DVB/CAR/PDMS 50/30 μm; Supelco, Bellefonte, PA, United States) was then inserted into the sealed glass vial and exposed to the HS for resolution for 40 min at 40°C. After extraction, the fiber was inserted into the GC injection port at an interface temperature of 250°C for 5 min. Each volatile compound was analyzed using an HP INNOWAX column (30 m × 0.25 mm; Agilent). Helium was the carrier gas, circulated at 1 mL/min, and the electron ionization energy was maintained at 70 eV. The scanning range of the total ion chromatographs was 35–350 m/z. The temperature program was as follows: 3 min at 50°C, followed by 2°C/min to 100°C, 4°C/min to 180°C, and 10°C/min to 230°C.

The volatile aroma compounds were identified by matching their retention indexes with those in the mass spectra library (NIST). Moreover, the retention indexes were evaluated using the Kovats system (Zenkevich, 2002). All compounds were semiquantified as 3-octanol equivalents. The semi-quantitative data of the aroma compounds were calculated as follows:

$$\mathrm{RCAC}(\mu g/L) = \frac{\mathrm{PAVC}}{\mathrm{PAIS}} \times \mathrm{CIS}(\mu g/L) \quad (1)$$

where RCAC is the relative concentration of the volatile compounds, PAVC is the peak area of volatile compounds, PAIS is the peak area of internal standard, and CIS is the final concentration of internal standard.

Sensory Analysis of Wine

In this study, the Petit Manseng grapes were used as raw materials for vinification, we also compared them with the Petit Manseng wine. Sensory analysis was performed using Belda's et al. (2015) method with some modifications. In brief, the wine was assessed by 10 trained panelists (6 female and 4 male) from Shihezi University. During the formal sensory analysis process, the team members were asked to form consistent terminology by consensus and described the sensory notes. Sensory descriptions included fruity, floral, green, acidity, sweetness, fatty, and bitterness, all scored from 0 (weak) to 10 (intense).

Statistical Analysis

For each sample group, three parallel samples were analyzed. The differences between our samples were analyzed using analysis

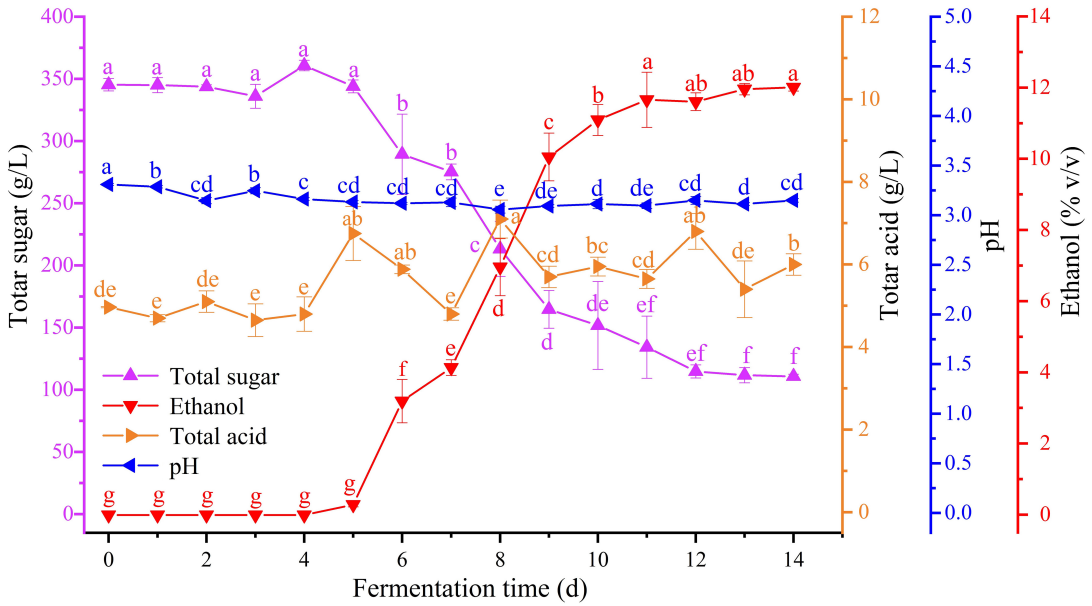

FIGURE 1 | Change of physicochemical indexes in different fermentation time: total sugar (purple), ethanol (red), total acid (orange), and pH (blue) (for interpretation of the references to color in this figure legend, the reader is referred to the Web version of this article).

TABLE 1 | Organic acid content in the wine (mg/mL).

Organic acids	A	B	C	D	E	F
Tartaric acid	0.36 ± 0.02^{a}	0.28 ± 0.01^{b}	0.31 ± 0.02^{ab}	0.20 ± 0.03^{b}	0.19 ± 0.04^{b}	0.03 ± 0.00^{c}
Lactic acid	0.03 ± 0.00^{b}	0.02 ± 0.00^{b}	0.00 ± 0.00^{c}	0.00 ± 0.00^{c}	0.04 ± 0.00^{a}	0.04 ± 0.00^{a}
Acetic acid	0.04 ± 0.00^{c}	0.05 ± 0.00^{c}	0.05 ± 0.01^{c}	0.06 ± 0.01^{b}	0.10 ± 0.00^{a}	0.09 ± 0.01^{a}
Citric acid	1.07 ± 0.03^{b}	1.13 ± 0.05^{b}	1.09 ± 0.03^{b}	1.13 ± 0.03^{b}	1.26 ± 0.02^{a}	1.22 ± 0.00^{a}
Succinic acid	0.28 ± 0.01^{a}	0.30 ± 0.02^{a}	0.28 ± 0.00^{a}	0.24 ± 0.01^{b}	0.23 ± 0.01^{b}	0.22 ± 0.00^{b}

Data are expressed as the means ± standard (n = 3). The different lowercase letters in each row indicate a significant difference between the samples ($P < 0.05$).

of variance with Duncan multiple tests, with the significance level set at 5% ($P < 0.05$) on SPSS (version 20; IBM, Chicago, United States). R (version 4.0.4) was used to produce a heat-map for the microbial populations and volatile compounds. The correlation among microorganisms and volatile compounds was determined multivariate data analysis, including bidirectional partial least squares (O2PLS), on the software program SIMCA (version 14.1). The linear correlation coefficient between the selected microbial genera and volatile compounds was visualized *via* O2PLS on Cyto-scape (version 3.6.1).

RESULTS

Physicochemical Properties During Spontaneous Fermentation

Dynamic changes in the ethanol, total sugar, and total acid content and the pH of zymotic fluid from six periods during Petit Manseng spontaneous fermentation were detected (**Figure 1**). The total sugar content of Petit Manseng juice reached up to 345.35 g/L. During Petit Manseng spontaneous fermentation, sugar in the zymotic fluid was converted to ethanol. Thus, total sugar content sharply decreased after 4 days of fermentation and remained at 110.84 ± 1.69 g/L on the 14th day. Then, ethanol concentrations increased after 4 days of fermentation and reached up to 12.01 ± 0.09% (v/v) on the 14th day. Total acid content fluctuated from 4.97 ± 0.02 to 6.00 ± 0.26 g/L. The pH remained relatively stable at 3.2 throughout the fermentation process.

The organic acid content directly affects the flavor and taste of white wine (Nie et al., 2017). In this study, the organic acids detected from Petit Manseng were tartaric acid, lactic acid, acetic acid, citric acid, and succinic acid (**Table 1**). Tartaric acid content sharply decreased throughout the fermentation process, with it almost depleted at the end of fermentation. In contrast, lactic acid content showed a slight increase, with a final value of 0.04 ± 0.00 mg/mL. Acetic acid content showed an upward trend overall, increasing sharply on the 11th day and then slowly decreasing to finally reach a concentration of 0.09 ± 0.01 mg/mL. Citric acid showed an upward trend overall. In particular, citric acid was continuously consumed and synthesized during spontaneous fermentation. Finally, succinic acid content remained relatively stable throughout the fermentation process.

TABLE 2 | Dynamic changes of flavor compound content during Petit Manseng fermentation process (μg/L).

Compounds	RI	A	B	C	D	E	F	Odor threshold (μg/L)	OAV[2]	Odors[1]
Esters										
Ethyl acetate	888	4.91 ± 0.19^{d}	3.83 ± 0.35^{d}	104.27 ± 0.09^{d}	842.00 ± 102.42^{c}	1637.48 ± 285.66^{b}	3170.56 ± 350.13^{a}	7500 [A]	0.1–1	Fruity, sweet [A]
Isobutyl acetate	1000	ND	ND	3.49 ± 0.52^{c}	16.85 ± 1.90^{b}	32.89 ± 3.27^{a}	35.92 ± 2.19^{a}	1600 [B]	<0.1	Strawberry, fruity, flowery[A]
Ethyl butyrate	1036	0.59 ± 0.11^{c}	ND	3.53 ± 0.52^{c}	122.38 ± 15.27^{b}	313.73 ± 14.04^{a}	293.68 ± 52.54^{a}	20[B]	>1	Sour fruity, fruity, strawberry [B]
Isoamyl acetate	1147	1.13 ± 0.16^{d}	2.21 ± 0.94^{d}	327.43 ± 32.69*d*	3893.87 ± 466.31^{c}	5950.84 ± 390.73^{b}	9052.43 ± 325.06^{a}	30 [B]	>1	Banana, sweet [B]
Ethyl hexanoate	1233	1.78 ± 0.07^{c}	4.28 ± 0.32^{c}	1457.11 ± 14.16^{b}	1557.17 ± 155.66^{b}	3947.08 ± 416.23^{a}	1283.17 ± 98.92^{b}	5[B]	>1	Fruity, green apple, floral, violet[B]
Hexyl acetate	1272	0.31 ± 0.23^{e}	17.10 ± 4.00^{e}	671.51 ± 40.18^{d}	1498.46 ± 257.60^{b}	2463.10 ± 155.47^{a}	1117.32 ± 29.89^{c}	670[B]	>1	fruity, pear, cherry[B]
Propyl hexanoate	1293	ND	ND	4.52 ± 0.46^{c}	7.48 ± 0.20^{a}	4.12 ± 0.03^{c}	5.64 ± 1.07^{b}	nf		nf
3-Hexen-1-yl salicylate	1315	0.32 ± 0.01^{e}	0.53 ± 0.12^{e}	11.88 ± 1.10^{d}	25.55 ± 2.38^{c}	66.25 ± 0.42^{a}	42.95 ± 2.20^{b}	320 [Q]	<0.1	nf
Ethyl octanoate	1435	0.41 ± 0.19^{d}	7.13 ± 0.33^{d}	929.25 ± 6.74^{c}	5187.56 ± 309.43^{a}	1825.99 ± 109.78^{b}	1931.56 ± 25.46^{b}	2 [B]	>1	Fruity, pineapple, pear, floral[B]
Isopropyl acetate	882	ND	1.22 ± 0.19^{c}	3.65 ± 0.30^{c}	10.93 ± 1.16^{c}	410.79 ± 1.77^{b}	830.95 ± 21.3^{a}	500[I]	>1	Fruity, unpleasant[I]
Ethyl decanoate	1638	0.37 ± 0.05^{c}	2.03 ± 0.27^{c}	552.21 ± 35.61^{c}	2488.33 ± 106.52^{b}	10138.64 ± 103.75^{a}	2723.78 ± 655.16^{b}	200[C]	>1	Fruity, pleasant [A]
3-Methylbutyl octanoate	1122	ND	ND	1.52 ± 0.50^{d}	24.16 ± 0.20^{c}	35.26 ± 2.75^{b}	41.86 ± 0.21^{a}	nf		nf
Ethyl 9-decenoate	1694	ND	ND	23.84 ± 2.35^{a}	15.46 ± 0.47^{b}	13.41 ± 1.16^{b}	4.21 ± 0.73^{c}	100[A]	<0.1	Green, fruity, fatty [A]
2-Phenylethyl acetate	1807	ND	ND	96.95 ± 0.05^{d}	1053.22 ± 15.55^{a}	627.80 ± 29.68^{c}	770.53 ± 37.87^{b}	250[D]	>1	Floral, roses[D]
Ethyl nonanoate	1531	ND	ND	3.41 ± 0.40^{c}	5.48 ± 0.14^{b}	6.27 ± 0.25^{a}	6.64 ± 0.04^{a}	1300 [B]	<0.1	Waxy, fruity [B]
Ethyl palmitate	2262	ND	ND	0.41 ± 0.04^{d}	18.30 ± 0.88^{a}	1.44 ± 0.08^{c}	4.20 ± 0.14^{b}	1000[E]	<0.1	Wax, fatty [F]
Ethyl laurate	1835	0.59 ± 0.00^{e}	1.71 ± 0.39^{e}	552.21 ± 35.61^{d}	3194.99 ± 112.38^{b}	6140.38 ± 151.79^{a}	2220.85 ± 56.09^{c}	500[E]	>1	Sweet, floral, fruity, cream[A]
Alcohols										
1-Butanol	1142	ND	2.36 ± 0.42^{c}	4.57 ± 0.47^{c}	26.03 ± 0.12^{c}	141.22 ± 1.66^{b}	261.12 ± 46.36^{a}	150000 [D]	<0.1	Sweet, medicinal [D]
1-Penten-3-ol	1159	0.71 ± 0.04^{d}	1.09 ± 0.03^{c}	4.33 ± 0.18^{a}	3.33 ± 0.27^{b}	4.19 ± 0.04^{a}	ND	400 [Q]	<0.1	nf
2-Penten-1-ol	1318	2.81 ± 0.26^{d}	1.47 ± 0.32^{e}	3.69 ± 0.06^{d}	52.90 ± 0.65^{a}	20.01 ± 0.01^{b}	5.57 ± 0.59^{c}	720 [Q]	<0.1	nf
Ethanol	932	88.30 ± 0.56^{e}	438.94 ± 5.26^{e}	7421.74 ± 349.66^{d}	27824.56 ± 2171.11^{c}	76334.58 ± 2463.02^{a}	44631.88 ± 2884.43^{b}	950 [N]	>1	nf
Isoamyl alcohol	1209	ND	341.79 ± 41.82^{d}	1328.36 ± 186.88^{d}	7238.78 ± 101.75^{c}	23298.19 ± 1181.43^{b}	36852.34 ± 4323.93^{a}	30000[B]	>1	Whiskey, malt, burnt [B]
3-Hexen-1-ol	1382	26.49 ± 1.65^{d}	33.51 ± 2.37^{c}	24.43 ± 2.10^{d}	36.44 ± 3.87^{c}	55.94 ± 4.45^{b}	68.33 ± 0.02^{a}	400[J]	0.1–1	Green grass, herb [C]
2-Hexen-1-ol	1405	201.88 ± 1.08^{a}	12.60 ± 0.26^{b}	5.47 ± 0.08^{d}	ND	6.84 ± 0.21^{c}	7.90 ± 0.46^{c}	400[D]	<0.1	Fruity, unripe banana [D]
1-Hexanol	1355	429.47 ± 13.31^{c}	790.79 ± 55.36^{b}	756.59 ± 47.07^{b}	736.84 ± 1.36^{b}	399.44 ± 13.04^{c}	1160.55 ± 83.06^{a}	8000 [C]	0.1–1	Green, herb[B]

(Continued)

TABLE 2 | Continued

Compounds	RI	A	B	C	D	E	F	Odor threshold (μg/L)	OAV[2]	Odors[1]
1-Octanol	1557	ND	ND	21.49 ± 0.05^{a}	9.70 ± 0.59^{c}	13.43 ± 0.51^{b}	ND	900 [A]	<0.1	Flesh orange, rose, sweet herb[A]
1-Octen-3-ol	1450	11.71 ± 0.78^{b}	18.35 ± 0.82^{a}	ND	ND	ND	ND	10 [K]		Mushroom [P]
1-Decanol	1752	ND	ND	ND	7.99 ± 0.21^{b}	9.00 ± 0.27^{a}	1.69 ± 0.08^{c}	400[B]	<0.1	Orange flowery, special fatty[A]
Terpinen-4-ol	1602	1.78 ± 0.25^{c}	2.74 ± 0.28^{b}	7.67 ± 0.11^{a}	7.38 ± 0.64^{a}	ND	0.84 ± 0.28^{d}	5000 [E]	<0.1	Light aroma, wood, soil [Q]
Citronellol	1765	0.42 ± 0.25^{e}	2.74 ± 0.28^{d}	9.80 ± 0.19^{a}	2.56 ± 0.27^{d}	5.69 ± 0.08^{c}	7.06 ± 0.08^{b}	100 [B]	<0.1	Green lemon [B]
Benzyl alcohol	1870	2.00 ± 0.16^{c}	3.38 ± 0.28^{b}	5.31 ± 0.13^{a}	5.24 ± 0.08^{a}	0.90 ± 0.04^{d}	ND	200000 [A]	<0.1	Almond,fatty [A]
1-Nonanol	1660	1.21 ± 0.13^{c}	3.30 ± 0.35^{c}	26.59 ± 3.37^{a}	15.72 ± 0.16^{b}	16.53 ± 0.25^{b}	ND	600[B]	<0.1	Green [B]
Phenylethyl alcohol	1906	9.47 ± 0.25^{d}	26.09 ± 0.95^{d}	244.90 ± 6.55^{c}	1321.92 ± 177.12^{a}	659.52 ± 38.09^{b}	752.06 ± 19.2^{b}	10000 [G]	<0.1	Rose, sweet[G]
Undec-2-en-1-ol	1899	0.70 ± 0.08^{c}	1.82 ± 0.09^{b}	2.29 ± 0.37^{a}	0.76 ± 0.12^{c}	ND	ND	nf		nf
1-Pentanol	1250	3.35 ± 0.37^{e}	1.70 ± 0.01^{e}	15.67 ± 2.09^{d}	19.53 ± 0.14^{c}	32.65 ± 2.7^{b}	37.67 ± 1.25^{a}	64000 [E]	<0.1	nf
2-Nonanol	1499	ND	ND	9.75 ± 0.26^{c}	21.28 ± 0.20^{b}	41.88 ± 2.68^{a}	ND	30 [O]	>1	Citric[P]
Acids										
Hexanoic acid	1846	8.09 ± 0.04^{d}	35.82 ± 0.68^{d}	364.81 ± 15.39^{c}	1833.66 ± 87.26^{b}	1807.23 ± 10.85^{b}	2126.05 ± 77.99^{a}	420 [A]	>1	Cheese, rancid[A]
2-Methylhexanoic acid	1960	0.39 ± 0.09^{e}	1.09 ± 0.20^{e}	4.17 ± 0.14^{d}	7.65 ± 0.18^{b}	11.17 ± 0.16^{a}	6.25 ± 0.31^{c}	nf		nf
2-Hexenoic acid	1967	1.34 ± 0.45^{e}	2.44 ± 0.04^{d}	8.33 ± 0.06^{a}	5.35 ± 0.06^{b}	3.15 ± 0.19^{c}	0.90 ± 0.15^{e}	3000 [Q]	0.1–1	Fatty[Q]
Octanoic acid	2060	5.77 ± 0.29^{c}	62.87 ± 2.98^{c}	1766.29 ± 28.36^{b}	5567.66 ± 448.39^{a}	1570.26 ± 277.62^{b}	1322.85 ± 270.91^{b}	500[A]	>1	Rancid, cheese, fatty acid [A]
Dodecanoic acid	2498	ND	1.10 ± 0.14^{e}	94.57 ± 3.30^{b}	256.93 ± 8.72^{a}	46.78 ± 4.03^{c}	34.92 ± 0.11^{d}	1000[B]	<0.1	Daurel oil flavor [B]
n-Decanoic acid	2276	0.48 ± 0.13^{d}	11.85 ± 1.21^{d}	733.35 ± 9.95^{b}	2135.69 ± 175.09^{a}	498.38 ± 59.90^{c}	684.66 ± 110.50^{bc}	1000[M]	0.1–1	Fatty, unpleasant [A]
3-Methylbutanoic acid	1655	ND	3.48 ± 0.23^{d}	8.82 ± 0.30^{d}	21.13 ± 0.92^{c}	38.14 ± 2.62^{a}	30.30 ± 0.21^{b}	33 [H]	0.1–1	Rancid, cheese [H]
Butanoic acid	1950	2.67 ± 0.25^{d}	5.95 ± 0.43^{c}	6.98 ± 1.19^{c}	26.29 ± 2.83^{ab}	26.64 ± 1.58^{a}	22.75 ± 1.32^{b}	2200[I]	0.1–1	Sharp, cheesy, rancid [E]
Nonanoic acid	2171	ND	1.07 ± 0.21^{bc}	1.50 ± 0.67^{b}	5.56 ± 0.20^{a}	4.63 ± 0.52^{a}	4.96 ± 0.87^{a}	500-800 [B]	<0.1	Cheese, waxy flavor [B]
Aldehydes										
Hexanal	1083	64.04 ± 2.5*a*	47.06 ± 0.65^{b}	1.57 ± 0.52^{cd}	ND	3.08 ± 0.06^{c}	ND	5-15[B]	0.1–1	Apple, green grassy [B]
Hexen-2-al	1213	5.82 ± 0.11^{d}	23.96 ± 0.90^{b}	ND	40.23 ± 4.77^{a}	14.78 ± 1.78^{c}	8.55 ± 0.46^{d}	24.2 [Q]	0.1–1	Green, fruity [Q]
Dodecanal	1711	0.81 ± 0.10^{d}	1.31 ± 0.31^{d}	2.05 ± 0.21^{cd}	3.26 ± 0.40^{b}	8.50 ± 0.52^{a}	2.84 ± 0.27^{bc}	0.13-0.29 [N]	>1	Orange [N]
Benzaldehyde	1520	1.05 ± 0.04^{d}	4.38 ± 0.46^{d}	11.89 ± 0.15^{c}	23.99 ± 1.45^{b}	13.67 ± 1.63^{c}	28.28 ± 3.56^{a}	2000 [D]	<0.1	Bitter almond, nut [B]
Ketones										
2-Octanone	1287	1.81 ± 0.26^{d}	2.58 ± 0.02^{d}	2.12 ± 0.30^{d}	6.49 ± 0.00^{c}	74.47 ± 1.58^{a}	39.07 ± 1.69^{b}	5 [N]	>1	Green, fruity [N]

(Continued)

TABLE 2 | Continued

Compounds	RI	A	B	C	D	E	F	Odor threshold (μg/L)	OAV[2]	Odors[1]
6-Methylhept-5-en-2-One	1338	5.07 ± 1.04^{a}	3.76 ± 0.27^{abc}	2.42 ± 0.42^{d}	2.49 ± 0.32^{cd}	3.53 ± 0.43^{bcd}	3.83 ± 0.01^{ab}	0.068 [N]	>1	nf
Acetoin	1284	0.53 ± 0.08^{c}	2.58 ± 0.02^{c}	320.72 ± 38.45^{b}	551.65 ± 50.23^{a}	48.36 ± 2.81^{c}	58.36 ± 5.41^{c}	150000[I]	<0.1	Buttery, fatty [I]
Acetol	1308	ND	ND	70.65 ± 4.57^{a}	16.01 ± 0.02^{b}	ND	ND	nf		nf
Others										
2,5-Dimethyl-hexane	1640	3.51 ± 0.44^{d}	1.70 ± 0.01^{d}	15.67 ± 2.09^{c}	19.50 ± 0.19^{bc}	25.14 ± 5.67^{ab}	28.56 ± 2.13^{a}	nf		nf
2,4-Di-tert-butylphenol	2318	2.14 ± 0.28^{d}	2.45 ± 0.40^{d}	14.38 ± 0.01^{c}	93.45 ± 4.43^{a}	14.12 ± 0.28^{c}	22.84 ± 0.18^{b}	200 [J]	0.1–1	Phenolic[A]
Phenol	2000	0.56 ± 0.00^{d}	0.80 ± 0.18^{cd}	1.22 ± 0.11^{c}	1.98 ± 0.11^{b}	2.98 ± 0.37^{a}	0.82 ± 0.07^{cd}	31 [Q]	<0.1	Phenolic [L]

Data are expressed as the means ± standard (n = 3). The different lowercase letters in each row indicate a significant difference between the samples (P < 0.05). ND, not detected.

[1]Odor threshold and odors were obtained from literatures: [A] (Tao and Li, 2009); [B] (Peng et al., 2013); [C] (Ferreira et al., 2000); [D] (Noguerol et al., 2009); [E] (Zea et al., 2001); [F] (Zhang et al., 2010); [G] (Niu et al., 2011); [H] (Mayr et al., 2014); [I] (Peinado et al., 2006); [J] (Gómez et al., 2007); [K] (Song Y. et al., 2017); [L] (López et al., 2004); [M] (Culleré et al., 2004); [N] (Zhao C. et al., 2020); [P] (Mihail et al., 2019); [O] (Guth, 1997); [P] (Du et al., 2011); [Q] (Gemert, 2011).

[2]OAV was calculated by dividing concentration by the odor threshold value of the compound. The scope of OAV is shown but not the specific value. The nf represented not found.

Volatile Compounds During Spontaneous Fermentation

Volatile compounds from six fermentation periods of Petit Manseng wine during spontaneous fermentation included 17 esters, 19 alcohols, 9 acids, 4 aldehydes, 4 ketones, and 3 other volatile compounds (**Table 2**).

The esters mainly included isoamyl acetate, ethyl lurate, ethyl decanoate, ethyl acetate, hexyl acetate, ethyl hexanoate, and ethyl octanoate. A large amount of acetate esters and ethyl esters were produced because a high concentration of alcohol and the related acetyl-CoA and acyltransferases interacted during spontaneous fermentation. Moreover, the produced wine contained high levels of ethanol, isoamyl alcohol, 1-hexanol, and phenylethyl alcohol. Our wine was also rich in hexanoic acid, octanoic acid, and decanoic acid. These esters, alcohols, and acids mainly conferred the overall flavor of our Petit Manseng wine. Aldehydes, ketones, and other volatiles may have also contributed to its flavors.

To better understand the dynamic changes in these volatile compounds, we analyzed the aroma components throughout the spontaneous fermentation process (**Figure 2**). The volatile compounds were divided into two classes based on the trends during the fermentation process: Class I contained 26 aromatic compounds (mainly including higher alcohols, C_6 compounds, and fatty acids) and Class II contained 30 aromatic compounds (mainly including benzene derivatives, ethyl esters, acetic esters, and other volatiles). The high content of acetic and ethyl esters is responsible for the fruity flavor in the wine, whereas excessive concentrations of higher alcohols and fatty acids lead to unpleasant green, pungent, and rancid flavor in the wine. Based on our results, the spontaneous fermentation of Petit Manseng might produce wines with a more coordinated wine aroma (Shi et al., 2019).

We next used principal component analysis (PCA) to understand the correlation and segregation of aroma compounds in different wine samples (**Figure 3**). Here, 76.2% of the variance was explained by 56 different components, with PC1 and PC2 accounted for 51.3 and 24.9% of the variance, respectively. Most volatile compounds clustered at stages D and F, which corroborated the results indicating higher concentrations of volatile compounds in the wine. The rest of the wine samples clustered with only a few volatile compounds, also consistent with their lower concentration of volatile compounds in the respective stages. The variations in the location indicated that the aroma of Petit Manseng wine differed by the fermentation stage. Notably, half of the volatile compounds at stage D (i.e., alcohols and esters) were all located in the upper right quadrant.

Sensory Analysis of Wine

The average scores of the sensory descriptions are presented in **Figure 4D**. Obvious differences were recorded in Petit Manseng grapes and wine fermented by Petit Manseng. The bitterness, green, acidity, and sweetness of the grapes scored higher than wine. The scores were almost similar of Petit Manseng grape and wine. Interestingly, the wine was noted to produce slightly stronger floral sensations than our grapes after spontaneous

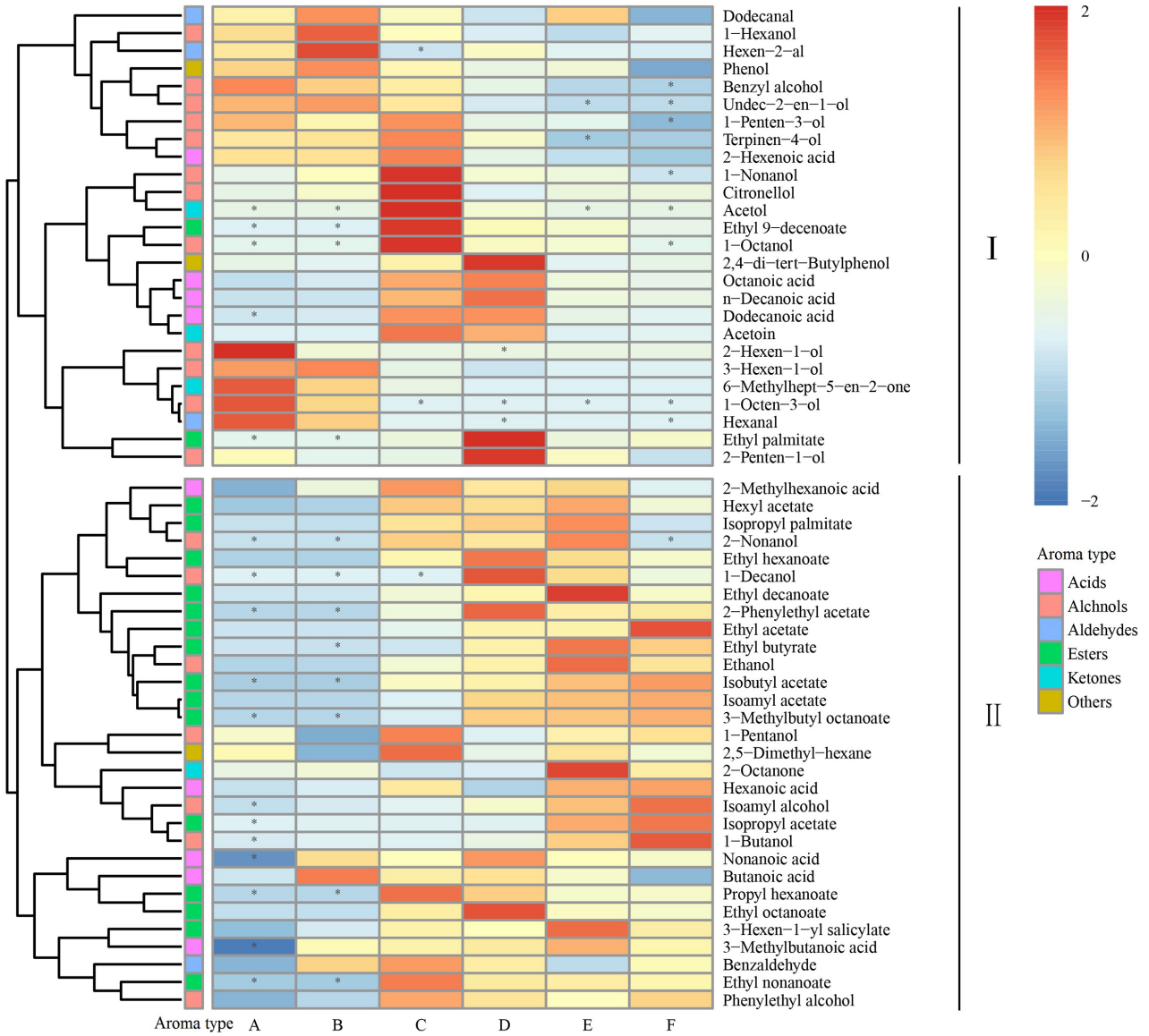

FIGURE 2 | Heatmap cluster analysis of the volatile components during the fermentation. The asterisk indicates the substance with $P < 0.05$. Samples collected on fermentation days 0, 1, 4, 7, 11, and 14, respectively (for interpretation of the references to color in this figure legend, the reader is referred to the Web version of this article).

fermentation. These results indicated that our Petit Manseng wine has great market potential.

Richness and Diversity Analysis

A total of 844,661 sequences for the fungal communities were clustered into 643 OTUs at a 97% identity threshold. The rarefaction curves of all samples tended to be flat, indicating that the amount of our sequencing data was reasonable (**Supplementary Figure 1**). For fungal communities, the richness in stage F was the highest according to the Chao1 and ACE indexes; stage F also showed the highest diversity based on the Shannon and Simpson indexes (**Supplementary Table 1**). Moreover, the values of the Chao1, ACE, Shannon, and Simpson indexes at stages E and F were higher than those at other stages, whereas Robbins index was the highest at stage C among all the stages (**Supplementary Figure 2**). Therefore, the fungal richness and diversity of the wine samples from different fermentation stages showed differences according to the alpha indexes. In addition, this study described the common and unique OTUs of the microorganisms from different fermentation stages. There were 37, 9, 11, 65, 54, and 67 fungal OTUs noted in stages A, B, C, D, E, and F, respectively, and 3 OTUs were shared among all six fermentation stages (**Figure 5A**). Therefore, the structure of the fungal communities in the sweet wine of Petit Manseng demonstrated differences based on the fermentation stage. Moreover, we investigated the dynamic

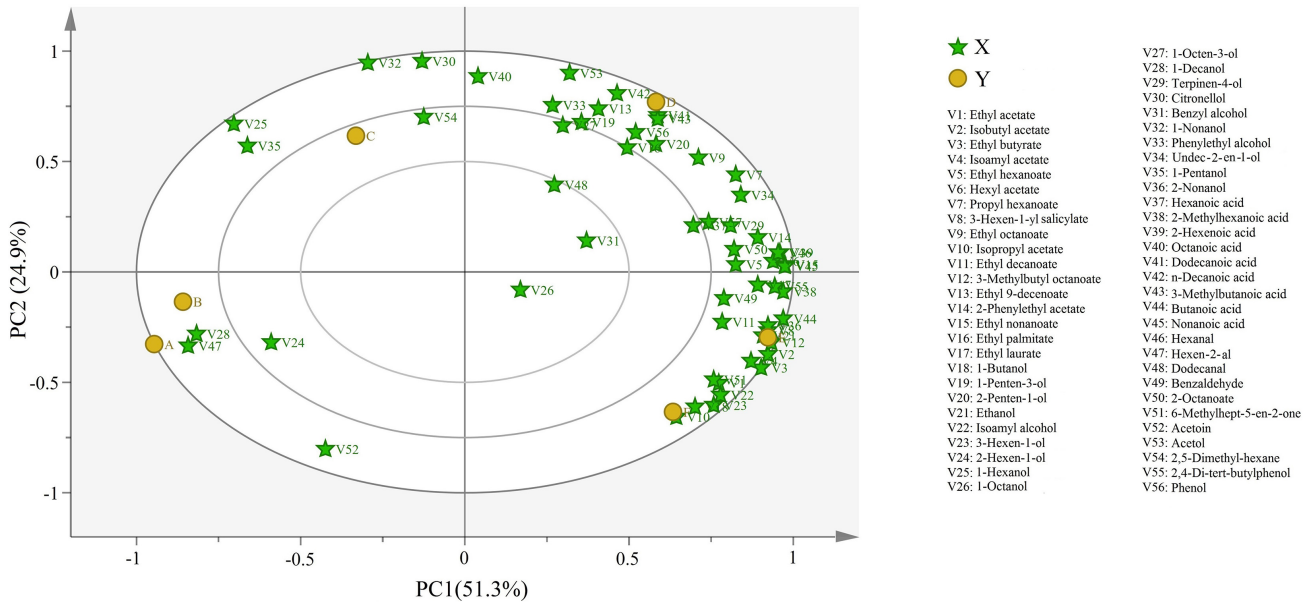

FIGURE 3 | Bioplot of PCA for volatile compound of wine samples. A, B, C, D, E, and F represented samples collected on fermentation days 0, 1, 4, 7, 11, and 14, respectively.

changes in fungal communities during different fermentation periods. Although the original OTU data showed that the total number of OTUs increased as fermentation continued, the number of cultivable fungi gradually decreased (**Supplementary Table 2**). The changes corresponding to the fermentation stages, along with changes in environmental factors, led to changes in fungal adaptability. Four colony micrographs (**Supplementary Figure 4**), five genera, and seven species of yeast were isolated in the spontaneous fermentation process based on the phylogenetic tree (**Supplementary Figure 7**).

Our beta diversity analysis of the fungal structure based on PCA during wine fermentation indicated that the contribution rate of PC1 was 48.9%, whereas that of PC2 was 5.6% (**Figure 5B**). We found that the structure of fungal composition was clustered together at stages A, B, and C and was very large at stages D, E, and F. These results contradicted the previous results, possibly because the previous study performed incomplete fermentation of Petit Manseng wine (Chen et al., 2020). We also noted some unusual dissimilarities. For example, our D1 deviated from the main clusters. In summary, our data indicated that fungal community abundance was dependent on the fermentation stage.

Microbial Abundance During Spontaneous Fermentation

By comparing the fungal communities in wine samples from different fermentation stages, we found that the main phyla appeared in all samples, but their content varied (**Figure 4A**). In particular, the top 10 relatively abundant fungal phyla included Ascomycota, Basidiomycota, Mortierellomycota, Glomeromycota, Anthophyta, Chytridiomycota, Olpidiomycota, Rozellomycota, Blastocladiomycota, and Mucoromycota (**Figure 4C**). The distinction of fungal abundance was obvious in different fermentation stages. For example, the relative abundance of Ascomycota was 78, 81, 56, 53, 50, and 72% in stages A, B, C, D, E, and F, respectively. Moreover, fungal abundance was confirmed to be affected by the fermentation stage.

The extracted high abundance of fungal OTUs as well as the distribution of six different phylum-to-species species is illustrated in **Supplementary Figure 3**. The result showed that Ascomycota had a denser species distribution than other phyla, whereas Glomeromycota showed the opposite trend. At the fungal genus level, *Candida* and *Malassezia* had the highest percent relative abundance at stage A. These results differed from those reported previously, possibly because of differences in the grape varieties and origins used (Sirén et al., 2019). Moreover, *Candida* and *Malassezia*, the abundant genera, dominated in the early and middle stages of fermentation (**Figure 4B**), whereas *Mortierella* and *Humicola* dominated the later fermentation stages. The relative abundance of *Aspergillus* demonstrated notable fluctuations, which may be the reason for the increased alcohol concentration. The relative abundance of *Penicillium* peaked at stage A and then decreased rapidly. Moreover, *Vishniacozyma*, *Hanseniaspora*, and *Pichia*, as dominant fungi present on the grapes in China's vine-growing regions, were found in our wine during spontaneous fermentation (Li et al., 2010). Regarding the fungal communities, *Hanseniaspora*, *Pichia*, *Vishniacozyma*, *Filobasidium*, *Diaporthe,* and *Candida* were the dominant taxa at stage A (**Figure 5C**). In addition, *Lecythophora*, *Inocybe*, *Alternaria*, *Meyerozyma*, and *Erysiphe* dominated stages B and C, whereas at stages E and F, the dominant taxa were *Humicola*, *Podospora*, *Archaeorhizomyces*, and *Metarhizium*. Furthermore, *Metschnikowia* and *Issatchenkia* were detected in

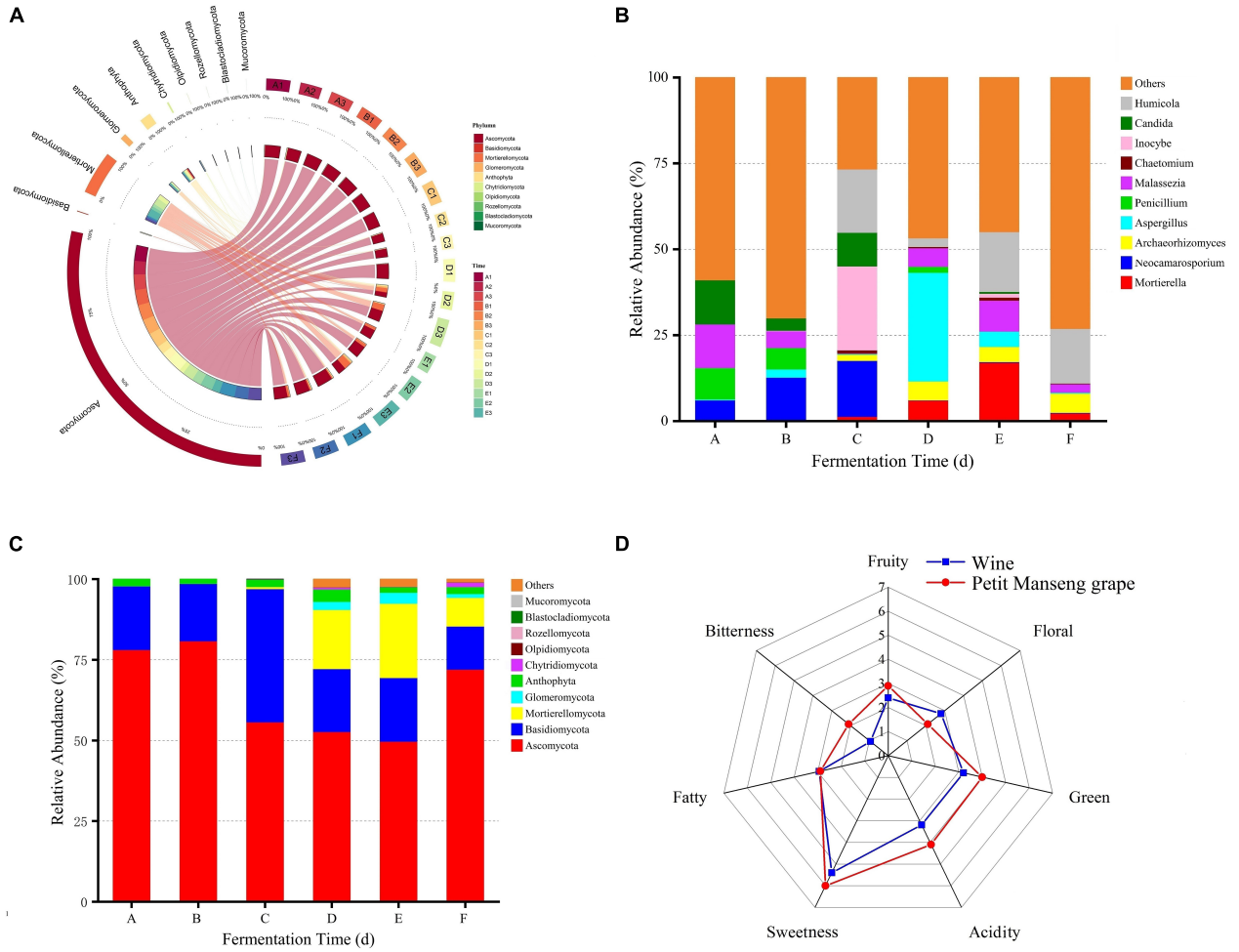

FIGURE 4 | The relative abundance between fungal groups at the phylum **(A)** level, the relative abundance of the top 10 fungi at the genus **(B)** level, the relative abundance of top 10 fungi at the phylum **(C)** level, and sensory analysis of wine samples **(D)**. A, B, C, D, E, and F represented samples collected on fermentation days 0, 1, 4, 7,11, and 14, respectively.

the fermentation process, with a strong positive correlation at stages D and E. *Metschnikowia* and *Issatchenkia* may also be responsible for the increased alcohol contents (Liu et al., 2016).

Co-occurrence and Exclusion Analysis Reveals the Relationships Among Different Microorganisms

The interaction of microorganisms is considered an important factor supporting the structure of microbial communities (Huang et al., 2018). We calculated Pearson's rank correction coefficients to represent beneficial or antagonistic relationships between the dominant microorganisms. The correlations of different fungi are displayed in **Figure 6**. *Issatchenkia* showed weak exclusion from other fungal genera except for *Hannaella*, *Naganishia*, *Fusarium*, *Aspergillus*, and *Cortinarius* ($P < 0.05$). In addition, *Dioscorea* and *Erysiphe* showed obvious exclusion toward *Talaromyces*, *Humicola*, *Podospora*, *Archaeorhizomyces*, and *Metarhizium*. In contrast, *Paraphoma*, *Clavaria*, *Mortierella*, and *Chaetomium* demonstrated strong co-occurrence with *Malassezia* and *Issatchenkia*, and *Pichia* and *Hanseniaspora* presented strong co-occurrence with *Diaporthe*, *Filobasidium*, and *Vishniacozyma* ($P < 0.05$). Thus, most genera present during spontaneous fermentation presented weak co-occurrence patterns.

Correlation Analysis Between Core Microbiota and Volatile Compounds

The correlation of core microbiota and volatile compounds were analyzed during the Petit Manseng wine fermentation process, as shown in **Figure 7**. Three criteria were used to discover the relationship between the microbiota and the aroma compounds: (1) a relatively stable abundance was maintained throughout the fermentation process, (2) the variable importance for the predictive component (VIP) values of microorganisms and volatiles were >1.0, and (3) the absolute values of linear correlation coefficient (R) between the concentration of volatile compounds and the relative abundance of microbial were >0.7

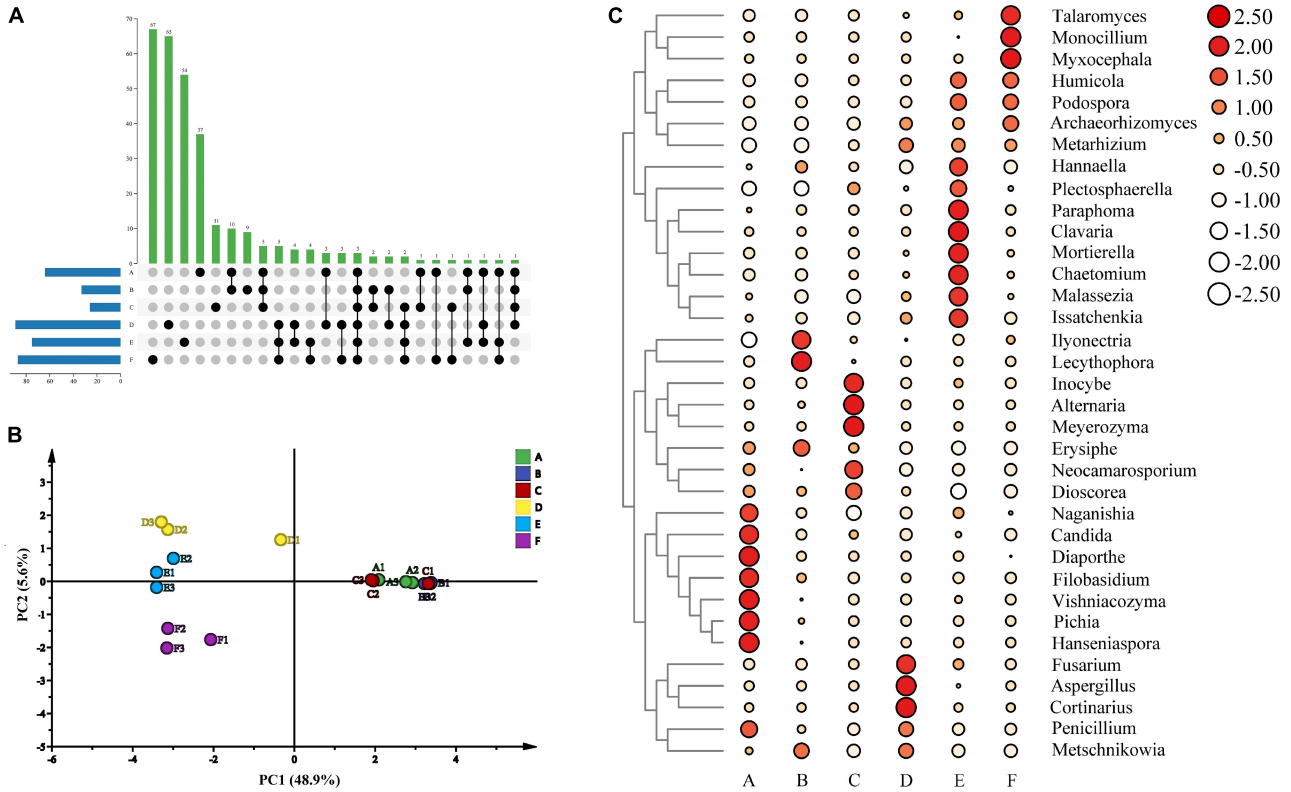

FIGURE 5 | The upset diagram of the fungi genus among samples **(A)**, PCA of wine samples **(B)**, abundance clustering heatmap of major fungi genera in zymotic fluids collected from different fermentation times **(C)**. The scale bar shows the relative abundance (log scale) of each genus within a sample. A, B, C, D, E, and F represented samples collected on fermentation days 0, 1, 4, 7,11, and 14, respectively.

(He et al., 2020). The changes in VIP values for the fungal group at the genus level and the volatile compounds are shown in **Supplementary Figures 5**, **6**, respectively.

According to the aforementioned criteria, 10 microbial genera were regarded as key microorganisms in spontaneous fermentation. *Udeniomyces*, *Hannaella*, and *Neomicrosphaeropsis* presented high correlations with alcohol and acids, such as 1-octen-3-ol and nonanoic acid. *Vishniacozyma* correlated with five core volatile compounds, of which it was positively correlated with 3-hexen-1-ol, 1-nonanol, and benzyl alcohol. *Cladosporium* negatively correlated with hexen-2-al and 3-methylbutyl octanoate. Non-*Saccharomyces cerevisiae* yeasts commonly found in wine, such as *Hanseniaspora* and *Pichia*, were positively correlated with some alcohols. *Metarhizium* presented characteristics similar to *Filobasidium* concerning 3-methylbutyl octanoate. In general, most fungal genera, except *Metarhizium* and *Filobasidium*, were negatively correlated with 3-methylbutyl octanoate. Whether the aforementioned microorganisms can produce and absorb related volatile compounds warrants further study.

Overall, the changes in the microbial community differed throughout the spontaneous fermentation process of Petit Manseng. As reported previously, wine quality is related to the metabolic activity and fermentation behaviors of the yeasts (Antonelli et al., 1999). Compared with *S. cerevisiae*, non-*Saccharomyces* yeasts have gained more attention because they produce esterase, β-glucosidase, lipase, and protease and thus increase the amount of active aroma substance (Escribano et al., 2017).

In this study, *Hanseniaspora*, *Vishniacozyma*, and *Pichia* were significantly correlated with at least one volatile compound during spontaneous fermentation. Based on our multivariate analysis results, the correlation between microorganisms and volatile compounds was evident. This requires further research using multiomics methods to verify the association between core microorganisms and specific flavors (Huang et al., 2018).

DISCUSSION

Our Petit Manseng wine was produced *via* spontaneous fermentation and had a final alcohol concentration of 12.01% (v/v), accompanied by a quick decrease in the total sugar content from 345.35 to 110.84 g/L. The gradually accumulated ethanol inhibited yeast metabolism and the ability to produce ethanol.

With regard to organic acids, *Pichia* can metabolize lactic acid to pyruvate and then to acetyl-CoA and acetaldehyde during liquor production (Song Z. et al., 2017). The microorganisms that accumulated citric acid mainly include some fungi from the genera *Aspergillus*, *Candida*, and *Penicillium* (Papagianni, 2007).

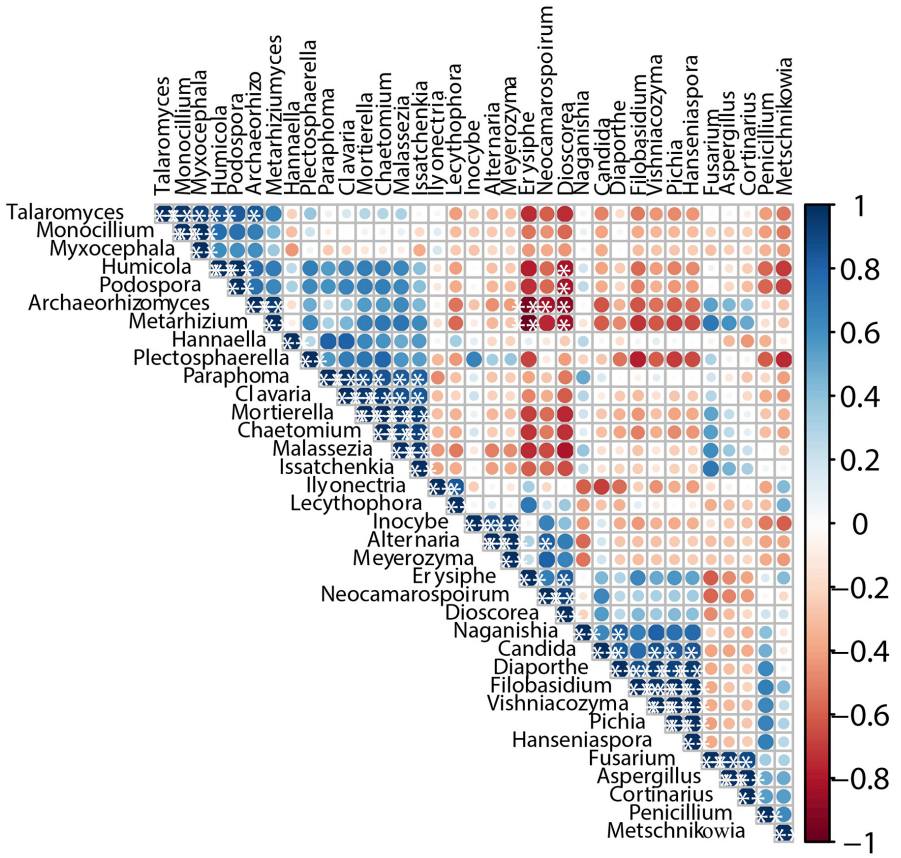

FIGURE 6 | Co-occurrence and co-exclusion relationship analysis of fungi. The figure presents a Pearson's rank correlation matrix of the top 35 fungi genera abundance. Strong correlations are indicated by large circles, whereas weak correlations are indicated by small circles. The color of the scale bar denotes the nature of the correlation, with 1 indicating a perfect positive correlation (dark blue) and -1 indicating a perfect negative correlation (dark red). Only significant correlations ($|r| > 0.7$, FDR < 0.05) are shown with *.

Tartaric acid is resistant to degradation and metabolism by wine microorganisms (Torija et al., 2003). In this study, the wine tartaric acid concentration decreased slowly because it was precipitated as potassium and calcium salts during fermentation.

In the present study, we identified 56 volatile compounds linked to spontaneous wine fermentation. Esters, which can increase the complexity of volatiles with the extension of the fermentation stage, are indispensable components of wine (Guo et al., 2020). The concentrations of fatty acid ethyl esters, ethyl butyrate, ethyl hexanoate, ethyl octanoate, ethyl decanoate, and ethyl laurate initially increased and then showed a downward trend. In contrast, the contents of the acetic esters like isoamyl acetate, isopropyl acetate, and 2-phenylethyl acetate increased during the fermentation process. The odor activity values (OAVs) of these compounds were >1 at the end of spontaneous fermentation; this observation may be related to high acyltransferase and alcohol acetyltransferase expression during spontaneous fermentation (Saerens et al., 2006; Procopio et al., 2011).

Alcohols represented one of the largest groups of volatile compounds noted during spontaneous fermentation, and they included 1-hexanol, phenylethyl alcohol, isoamyl alcohol, and ethanol. The contents of all alcohols except ethanol gradually increased during the fermentation process. However, these alcohols (1-hexanol and phenylethyl alcohol) do not positively enhance the wine flavor wines because of their relatively high odor threshold. In contrast, ethanol with a low threshold showed an OAV of >1. Moreover, citronellol's OAVs were also >1 and influenced the fruity character of the wine (Pérez et al., 2018). Acids, considered important for wine fermentation, were produced *via* yeast metabolism during spontaneous fermentation. These acids primarily comprised hexanoic acid and octanoic acid and flocked in the late stage of spontaneous fermentation, with a total content of 3448.90 μg/L.

Aldehydes, the significant source of herbaceous in wine, mainly came from fatty acid oxidation and amino acid degradation due to microbial fermentation (Zhao G. et al., 2020). Benzaldehyde was a widely used aromatic aldehyde, with an OAV of <0.1 at the end of fermentation. Fatty acid release and flavor substance catabolism *via* β-oxidation led to ketone formation (Collins et al., 2003). 2-Octanone actively contributed to the fruity of wine, with an OAV of >1.

The OAVs of the trace compounds formed during spontaneous fermentation were <1. In addition, most of

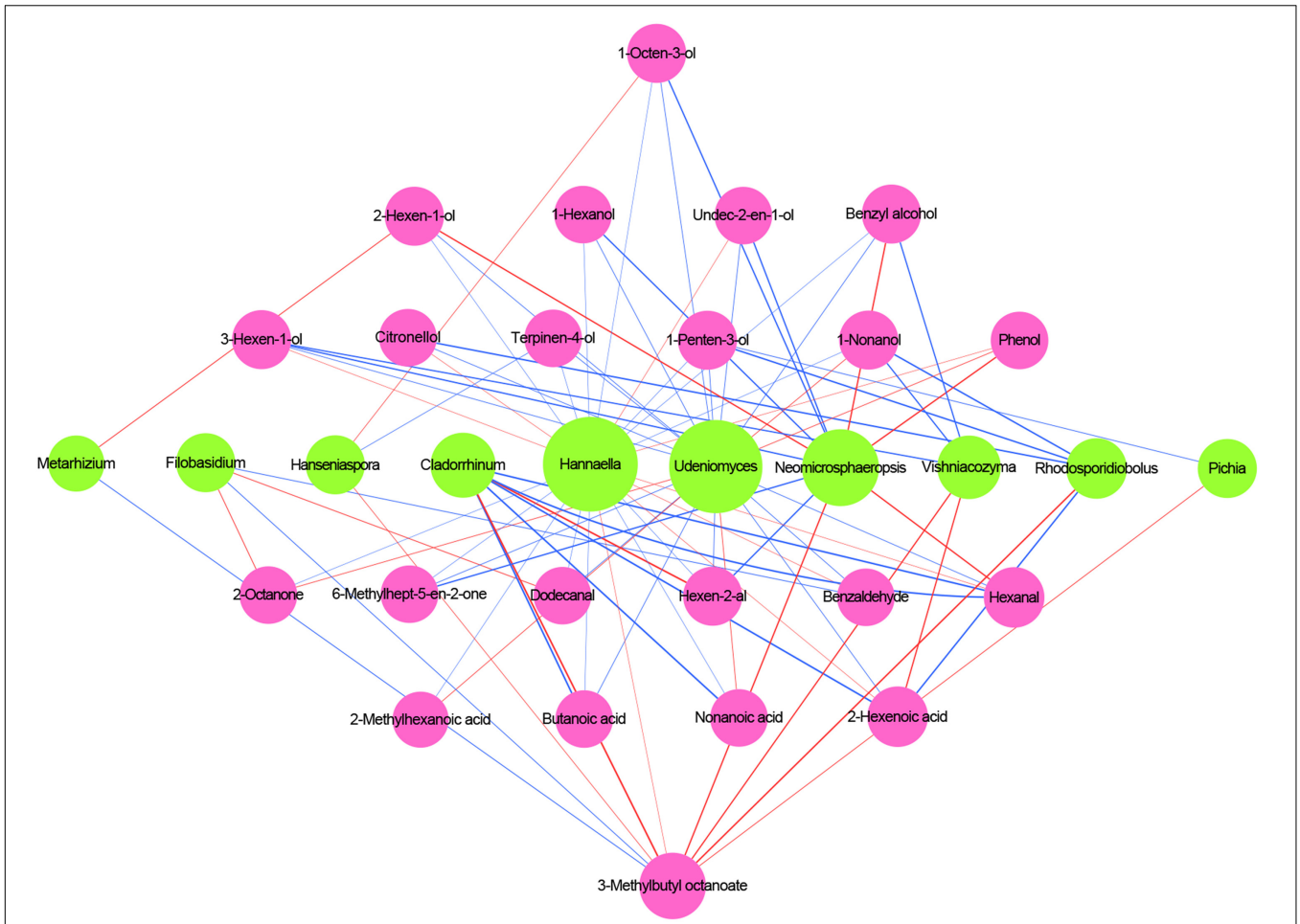

FIGURE 7 | Correlation analysis of microbiota and volatile compounds during spontaneous fermentation. Core fungal genera are shown in green and core volatile compounds are shown in purple. Blue lines indicate positive correlations, and red lines indicate negative correlations.

these volatile compounds showed a concentration increase throughout wine fermentation. Although these compounds were present at a relatively low concentration, some of them had an indirect effect on the flavor and countered the organoleptic properties of the wine (Asproudi et al., 2018).

Changes were also noted in the indigenous microorganisms during the spontaneous fermentation process. The microbial communities participating in initial spontaneous alcoholic fermentation are inherently present in Petit Manseng grapes. Nevertheless, many other microorganisms also participate in this process. Therefore, the relative abundance of fungal communities during spontaneous fermentation demonstrated obvious fluctuations, possibly also reflecting the effects of the ethanol fermentation environment. Wang and Liu (2013) reported fungal communities were inhibited by harsh conditions until they became tolerant or adapted to the harsh fermentation environments. In the current study, the abundance of *Candida* reduced during spontaneous fermentation due to its sensitivity to ethanol, similar to that described in previous studies (Heard and Fleet, 1985). Notably, *Humicola* began to appear at stage C and gradually increased in abundance at the end fermentation. This result was expected because *Humicola* was resistant to ethanol (Bassey et al., 2017). Some *Humicola* species positively contributed flavor by producing various enzymes, thus indicating many of their potential applications in various industries (Bokhari et al., 2010). *Aspergillus* was present throughout the fermentation process with different relative abundance values. Their abundance peaked in the middle stage of the fermentation. *Aspergillus* has powerful environmental adaptability, and it is resistant to acids and ethanol (Freire et al., 2017; Sheng et al., 2018). Some fungi such as *Pichia*, the important producers of various secondary metabolites, occurred in the early spontaneous fermentation period of our wine. This result indicated a potential application of these microorganisms in producing many aroma substances to improve the quality of Petit Manseng wine.

The relationship between volatile compounds and microbial succession dynamics during the spontaneous fermentation of Petit Manseng wine remains unclear. We thus investigated the key functional microorganism responsible for the generation

of aroma compounds. We found that *Hannaella*, *Udeniomyces*, and *Neomicrosphaeropsis* were the highest contributors to the generation of volatile compounds, especially during alcohol production. In addition, *Filobasidium* and *Hannaella* abundance was negatively correlated with 2-octanone production. Moreover, *Vishniacozyma* produced antibiotic compounds or enzymes to maintain their niches (Gramisci et al., 2018). This was related to the formation of aldehydes, such as hexanal, and acids, such as 2-hexanoic acid, during fermentation.

In this study, the indigenous microbial of wine grapes reflect the health of grapes and play an indispensable role in wine flavor and quality. To the best of our knowledge, this is the first study of microbial succession during the spontaneous fermentation of sweet wine fermented by Petit Manseng using HTS technology. Additional studies on the indigenous non-*Saccharomyces* species detected in this study may aid in understanding their role during spontaneous fermentation, their contribution to the sensory quality of sweet wine, and microbial safety.

CONCLUSION

Spontaneous fermentation of Petit Manseng could strengthen its aromatic profile. Fungi, as a significant part of wine, were responsible for the formation of the characteristic aroma and volatile compounds (including many esters and alcohols) in the wine. The results of this study may be used as a reference for producing Petit Manseng sweet wine with typical characteristics.

DATA AVAILABILITY STATEMENT

The data presented in the study are deposited in the National Center for Biotechnology Information (NCBI) repository, accession number PRJNA748614 (https://www.ncbi.nlm.nih.gov/bioproject/PRJNA748614). The accession numbers for dataset of our 18 samples that have been generated or analyzed in the study are: SRX11512770, SRX11513000, SRX11513001, SRX11513002, SRX11513003, SRX11513004, SRX11513005, SRX11513006, SRX11513007, SRX11513008, SRX11513009, SRX11513010, SRX11513011, SRX11513012, SRX11513013, SRX11513014, SRX11513015, and SRX11513016.

AUTHOR CONTRIBUTIONS

YM wrote the main text of the manuscript and performed the experiment. BW analyzed the fungi data. TL, XX, YJ, and XJ analyzed the volatile component data. XS supervised the research activities. All authors reviewed the manuscript.

FUNDING

We are grateful for the Science and Technology Research Project of the Xinjiang Production and Construction Corps (Nos. 2019AB025 and 2020AB014), the Science and Technology Research Project of the Eighth Division (No. 2020GY07), the Science and Technology Research Project of the Fifth Division (No. 20GY01), and the National Natural Science Foundation of China (No. 31960465).

SUPPLEMENTARY MATERIAL

The Supplementary Material for this article can be found online at: https://www.frontiersin.org/articles/10.3389/fmicb.2021.717387/full#supplementary-material

REFERENCES

Alessandria, V., Giacosa, S., Campolongo, S., Rolle, L., Rantsiou, K., and Cocolin, L. (2013). Yeast population diversity on grapes during on-vine withering and their dynamics in natural and inoculated fermentations in the production of icewines. *Food Res. Int.* 54, 139–147. doi: 10.1016/j.foodres.2013.06.018

Antonelli, A., Castellari, L., Zambonelli, C., and Carnacini, A. (1999). Yeast influence on volatile composition of wines. *J. Agr. Food Chem.* 47, 1139–1144. doi: 10.1021/jf9807317

Asproudi, A., Ferrandino, A., Bonello, F., Vaudano, E., Pollon, M., and Petrozziello, M. (2018). Key norisoprenoid compounds in wines from early-harvested grapes in view of climate change. *Food Chem.* 268, 143–152. doi: 10.1016/j.foodchem.2018.06.069

Bassey, N. S., Whong, C., and Ado, S. A. (2017). Determination of fermentative properties of yeast strains isolated from spoilt fruits and beverages. *Sci. J. Microbiol.* 6, 166–173. doi: 10.14196/sjm.v6i7.2552

Belda's, I., Navascués, E., Marquina, D., Santos, A., Calderon, F., and Benito, S. (2015). Dynamic analysis of physiological properties of *Torulaspora delbrueckii* in wine fermentations and its incidence on wine quality. *Appl. Microbiol. Biot.* 99, 1911–1922. doi: 10.1007/s00253-014-6197-2

Belda, I., Ruiz, J., Alastruey, A., Navascués, E., Marquina, D., and Santos, A. (2016). Unraveling the enzymatic basis of wine "flavorome": a phylo-functional study of wine related yeast species. *Front. Microbiol.* 7:12. doi: 10.3389/fmicb.2016.00012

Belda, I., Ruiz, J., Esteban-Fernández, A., Navascués, E., Marquina, D., Santos, A., et al. (2017). Microbial contribution to wine aroma and its intended use for wine quality improvement. *Molecules.* 22:189. doi: 10.3390/molecules22020189

Böhmer, M., Smoľak, D., Ženišová, K., Čaplová, Z., Pangallo, D., Puškárová, A., et al. (2020). Comparison of microbial diversity during two different wine fermentation processes. *FEMS Microbiol. Lett.* 367:fnaa150. doi: 10.1093/femsle/fnaa150

Bokhari, S. A. I., Latif, F., Akhtar, M. W., and Rajoka, M. I. (2010). Characterization of a β-xylosidase produced by a mutant derivative of *Humicola lanuginosa* in solid state fermentation. *Ann. Microbiol.* 60, 21–29. doi: 10.1007/s13213-010-0026-3

Brainina, K. Z., Stozhko, N. Y., Belysheva, G. M., Inzhevatova, O. V., Kolyadina, L. I., Cremisini, C., et al. (2004). Determination of heavy metals in wines by anodic stripping voltammetry with thick-film modified electrode. *Anal. Chim. Acta.* 514, 227–234. doi: 10.1016/j.aca.2004.03.047

Brandfass, C., and Karlovsky, P. (2008). Upscaled CTAB-based DNA extraction and real-time PCR assays for *Fusarium culmorum* and *F. graminearum* DNA in plant material with reduced sampling error. *Int. J. Mol Sci.* 9, 2306–2321. doi: 10.3390/ijms9112306

Bučková, M., Puškárová, A., Ženišová, K., Kraková, L., Piknová, L., Kuchta, T., et al. (2018). Novel insights into microbial community dynamics during the fermentation of central European ice wine. *Int. J. Food Microbiol.* 266, 42–51. doi: 10.1016/j.ijfoodmicro.2017.11.010

Caridi, A., De Bruno, A., De Salvo, E., Piscopo, A., Poiana, M., and Sidari, R. (2017). Selected yeasts to enhance phenolic content and quality in red wine from low pigmented grapes. *Eur. Food Res Technol.* 243, 367–378. doi: 10.1007/s00217-016-2750-9

Chaplin, B. (2011). South-west france: the wines and winemakers. *Gastronomica* 11, 119–120. doi: 10.1525/gfc.2011.11.2.119

Chen, Y., Zhang, W., Yi, H., Wang, B., Xiao, J., Zhou, X., et al. (2020). Microbial community composition and its role in volatile compound formation during the spontaneous fermentation of ice wine made from Vidal grapes. *Process Biochem.* 92, 365–377. doi: 10.1016/j.procbio.2020.01.027

Collins, Y. F., McSweeney, P. L. H., and Wilkinson, M. G. (2003). Lipolysis and free fatty acid catabolism in cheese: a review of current knowledge. *Int. Dairy J.* 13, 841–866. doi: 10.1016/S0958-6946(03)00109-2

Crump, A. M., Johnson, T. E., Wilkinson, K. L., and Bastian, S. E. P. (2015). Influence of oak maturation regimen on composition, sensory properties, quality, and consumer acceptability of Cabernet Sauvignon wines. *J. Agr. Food Chem.* 63, 1593–1600. doi: 10.1021/jf5044025

Culleré, L., Escudero, A., Cacho, J., and Ferreira, V. (2004). Gas chromatography-olfactometry and chemical quantitative study of the aroma of six premium quality Spanish aged red wines. *J. Agr. Food Chem* 52, 1653–1660. doi: 10.1021/jf0350820

de Celis, M., Ruiz, J., Martín-Santamaría, M., Alonso, A., Marquina, D., Navascués, E., et al. (2019). Diversity of *Saccharomyces cerevisiae* yeasts associated to spontaneous and inoculated fermenting grapes from Spanish vineyards. *Lett. Appl. Microbiol.* 68, 580–588. doi: 10.1111/lam.13155

Du, X., Plotto, A., Baldwin, E., and Rouseff, R. (2011). Evaluation of volatiles from two subtropical strawberry cultivars using GC–olfactometry, GC-MS odor activity values, and sensory analysis. *J. Agr. Food Chem.* 59, 12569–12577. doi: 10.1021/jf2030924

Englezos, V., Rantsiou, K., Cravero, F., Torchio, F., Pollon, M., Fracassetti, D., et al. (2018). Volatile profile of white wines fermented with sequential inoculation of *Starmerella bacillaris* and *Saccharomyces cerevisiae*. *Food Chem.* 257, 350–360. doi: 10.1016/j.foodchem.2018.03.018

Escribano, R., González, L., Garijo, P., Berlanas, C., López, I., López, R., et al. (2017). Screening of enzymatic activities within different enological non-Saccharomyces yeasts. *J. Food Sci. Tech.* 54, 1555–1564. doi: 10.1007/s13197-017-2587-7

Ferreira, V., López, R., and Cacho, J. F. (2000). Quantitative determination of the odorants of young red wines from different grape varieties. *J. Sci. Food Agr.* 80, 1659–1667. doi: 10.1002/1097-0010(20000901)80:11<1659::AID-JSFA693<3.0.CO;2-6

Francesca, N., Gaglio, R., Alfonzo, A., Settanni, L., Corona, O., Mazzei, P., et al. (2016). The wine: typicality or mere diversity? The effect of spontaneous fermentations and biotic factors on the characteristics of wine. *Agric. Sci. Proc.* 8, 769–773. doi: 10.1016/j.aaspro.2016.02.064

Freire, L., Passamani, F. R. F., Thomas, A. B., Nassur, R. D. C. M. R., Silva, L. M., Paschoal, F. N., et al. (2017). Influence of physical and chemical characteristics of wine grapes on the incidence of *Penicillium* and *Aspergillus fungi* in grapes and ochratoxin A in wines. *Int. J. Food Microbiol.* 241, 181–190. doi: 10.1016/j.ijfoodmicro.2016.10.027

Gardner, D. M., Duncan, S. E., and Zoecklein, B. W. (2017). Aroma characterization of Petit Manseng wines using sensory consensus training, SPME GC-MS, and electronic nose analysis. *Am. J. Enol. Viticul.* 68, 112–119. doi: 10.5344/ajev.2016.15099

Gemert, L. J. V. (2011). Compilations of Odour Threshold Values in Air, Water and Other Media (Second Enlarged and Revised Edition). Utrecht: Oliemans Punter & Partners BV. 1–648.

Gómez, M. J., Cacho, J. F., Ferreira, V., Vicario, I. M., and Heredia, F. J. (2007). Volatile components of Zalema white wines. *Food Chem.* 100, 1464–1473. doi: 10.1016/j.foodchem.2005.11.045

Gramisci, B. R., Lutz, M. C., Lopes, C. A., and Sangorrín, M. P. (2018). Enhancing the efficacy of yeast biocontrol agents against postharvest pathogens through nutrient profiling and the use of other additives. *Bio. Control.* 121, 151–158. doi: 10.1016/j.biocontrol.2018.03.001

Guo, L., Luo, Y., Zhou, Y., Bianba, C., Guo, H., Zhao, Y., et al. (2020). Exploring microbial dynamics associated with flavours production during highland barley wine fermentation. *Food Res. Int.* 130:108971. doi: 10.1016/j.foodres.2019.108971

Guth, H. (1997). Quantitation and sensory studies of character impact odorants of different white wine varieties. *J. Agar. Food Chem.* 45, 3027–3032. doi: 10.1021/jf970280a

He, G., Huang, J., Wu, C., Jin, Y., and Zhou, R. (2020). Bioturbation effect of fortified Daqu on microbial community and flavor metabolite in Chinese strong-flavor liquor brewing microecosystem. *Food Res. Int.* 129:108851. doi: 10.1016/j.foodres.2019.108851

Heard, G. M., and Fleet, G. H. (1985). Growth of natural yeast flora during the fermentation of inoculated wines. *Appl. Environ Microb.* 50, 727–728. doi: 10.1128/AEM.50.3.727-728.1985

Huang, Z., Hong, J., Xu, J., Li, L., Guo, W., Pan, Y., et al. (2018). Exploring core functional microbiota responsible for the production of volatile flavour during the traditional brewing of Wuyi Hong Qu glutinous rice wine. *Food Microbiol.* 76, 487–496. doi: 10.1016/j.fm.2018.07.014

Kong's, C., Li, A., Jin, G., Zhu, X., and Tao, Y. (2019). Evolution of volatile compounds treated with selected non-*Saccharomyces extracellular* extract during Pinot noir winemaking in monsoon climate. *Food Res. Int.* 119, 177–186. doi: 10.1016/j.foodres.2019.01.036

Lan, Y., Guo, J., Qian, X., Zhu, B., Shi, Y., Wu, G., et al. (2021). Characterization of key odor-active compounds in sweet petit manseng (*Vitis vinifera* L.) wine by gas chromatography-olfactometry, aroma reconstitution, and omission tests. *J. Food Sci.* 86, 1258–1272. doi: 10.1111/1750-3841.15670

Li, S., Cheng, C., Li, Z., Chen, J., Yan, B., Han, B., et al. (2010). Yeast species associated with wine grapes in China. *Int. J. Food Microbiol.* 138, 85–90. doi: 10.1016/j.ijfoodmicro.2010.01.009

Lin, Z., Cai, J. J., Scriven, L. E., and Davis, H. T. (1994). Spherical-to-wormlike micelle transition in CTAB solutions. *J. Phys. Chem.* 98, 5984–5993. doi: 10.1021/j100074a027

Liu, P., Lu, L., Duan, C., and Yan, G. (2016). The contribution of indigenous non-Saccharomyces wine yeast to improved aromatic quality of Cabernet *Sauvignon wines* by spontaneous fermentation. *Lwt Food Sci. Technol.* 71, 356–363. doi: 10.1016/j.lwt.2016.04.031

Liu, Y., Rousseaux, S., Tourdot-Maréchal, R., Sadoudi, M., Gougeon, R., Schmitt-Kopplin, P., et al. (2017). Wine microbiome: a dynamic world of microbial interactions. *Crit. Rev. Food Sci.* 57, 856–873. doi: 10.1080/10408398.2014.983591

López, R., Ezpeleta, E., Sánchez, I., Cacho, J., and Ferreira, V. (2004). Analysis of the aroma intensities of volatile compounds released from mild acid hydrolysates of odourless precursors extracted from Tempranillo and *Grenache grapes* using gas chromatography-olfactometry. *Food Chem.* 88, 95–103. doi: 10.1016/j.foodchem.2004.01.025

Loureiro, V., Brasil, R., and Malfeito-Ferreira, M. (2016). A new wine tasting approach based on emotional responses to rapidly recognize classic European wine styles. *Beverages*. 2:6. doi: 10.3390/beverages2010006

Lu, Y., Guan, X., Li, R., Wang, J., Liu, Y., Ma, Y., et al. (2021). Comparative study of microbial communities and volatile profiles during the inoculated and spontaneous fermentation of persimmon wine. *Process Biochem.* 100, 49–58. doi: 10.1016/j.procbio.2020.09.023

Lu, Y., Sun, F., Wang, W., Liu, Y., Wang, J., Sun, J., et al. (2020). Effects of spontaneous fermentation on the microorganisms diversity and volatile compounds during 'Marselan'from grape to wine. *LWT* 134:110193. doi: 10.1016/j.lwt.2020.110193

Mayr, C. M., Geue, J. P., Holt, H. E., Pearson, W. P., Jeffery, D. W., and Francis, I. L. (2014). Characterization of the key aroma compounds in *Shiraz wine* by quantitation, aroma reconstitution, and omission studies. *J. Agr. Food Chem.* 62, 4528–4536. doi: 10.1021/jf405731v

Mihail, M., Călugăr, A., Pop, N., Gal, E., and Pop, T. I. (2019). Odor activity value in red wines aroma from three wine regions in Romania. *Agricultura* 109, 29–38. doi: 10.15835/agrisp.v109i1-2.13245

Miller, G. L. (1959). Use of dinitrosalicylic acid reagent for determination of reducing sugar. *Anall Chem.* 31, 426–428. doi: 10.1021/ac60147a030

Mirás-Avalos, J. M., Fandiño, M., Trigo-Córdoba, E., Rey, B. J., Orriols, I., and Cancela, J. J. (2017). Influence of irrigation on consumer acceptability of

Albariño and *Godello wines*. *Lwt Food Sci. Technol.* 85, 345–352. doi: 10.1016/j.lwt.2017.01.076

Murtaza, M. A., Huma, N., Shabbir, M. A., Murtaza, M. S., and Anees-ur-Rehman, M. (2017). Survival of micro-organisms and organic acid profile of probiotic Cheddar cheese from buffalo milk during accelerated ripening. *Int. J. Dairy Technol.* 70, 562–571. doi: 10.1111/1471-0307.12406

Nie, Z., Zheng, Y., Xie, S., Zhang, X., Song, J., Xia, M., et al. (2017). Unraveling the correlation between microbiota succession and metabolite changes in traditional Shanxi aged vinegar. *Sci. Rep.* 7, 1–12. doi: 10.1038/s41598-017-09850-6

Niu, Y., Zhang, X., Xiao, Z., Song, S., Eric, K., Jia, C., et al. (2011). Characterization of odor-active compounds of various cherry wines by gas chromatography–mass spectrometry, gas chromatography–olfactometry and their correlation with sensory attributes. *J. Chromatogr. B.* 879, 2287–2293. doi: 10.1016/j.jchromb.2011.06.015

Noguerol, R., González, C., Cancho, B., and Simal, J. (2009). Quantitative determination and characterisation of the main odourants of Mencía monovarietal red wines. *Food Chem.* 117, 473–484. doi: 10.1016/j.foodchem.2009.04.014

Padilla, B., Gil, J. V., and Manzanares, P. (2016). Past and future of non-*Saccharomyces* yeasts: from spoilage microorganisms to biotechnological tools for improving wine aroma complexity. *Front. Microbiol.* 7:411. doi: 10.3389/fmicb.2016.00411

Papagianni, M. (2007). Advances in citric acid fermentation by *Aspergillus niger*: *Biochemical aspects*, membrane transport and modeling. *Biotechnol. Adv.* 25, 244–263. doi: 10.1016/j.biotechadv.2007.01.002

Peinado, R. A., Mauricio, J. C., and Moreno, J. (2006). Aromatic series in sherry wines with gluconic acid subjected to different biological aging conditions by *Saccharomyces cerevisiae* var. capensis. *Food Chem.* 94, 232–239. doi: 10.1016/j.foodchem.2004.11.010

Peng, C. T., Wen, Y., Tao, Y. S., and Lan, Y. Y. (2013). Modulating the formation of Meili wine aroma by prefermentative freezing process. *J. Agr. Food Chem.* 61, 1542–1553. doi: 10.1021/jf3043874

Pérez, D., Assof, M., Bolcato, E., Sari, S., and Fanzone, M. (2018). Combined effect of temperature and ammonium addition on fermentation profile and volatile aroma composition of Torrontés Riojano wines. *LWT* 87, 488–497. doi: 10.1016/j.lwt.2017.09.020

Procopio, S., Qian, F., and Becker, T. (2011). Function and regulation of yeast genes involved in higher alcohol and ester metabolism during beverage fermentation. *Eur. Food Res. Technol.* 233, 721–729. doi: 10.1007/s00217-011-1567-9

Robinson, J., Harding, J., and Vouillamoz, J. (2013). *Wine Grapes: a Complete Guide to 1,368 Vine Varieties, Including Their Origins and Flavours*. New York, NY: Penguin.

Ruiz, J., Kiene, F., Belda, I., Fracassetti, D., Marquina, D., Navascués, E., et al. (2019). Effects on varietal aromas during wine making: a review of the impact of varietal aromas on the flavor of wine. *Appl. Microbiol. Biot.* 103, 7425–7450. doi: 10.1007/s00253-019-10008-9

Saerens, S. M. G., Verstrepen, K. J., Van Laere, S. D. M., Voet, A. R. D., Van Dijck, P., Delvaux, F. R., et al. (2006). The *Saccharomyces cerevisiae* EHT1 and EEB1 genes encode novel enzymes with medium-chain fatty acid ethyl ester synthesis and hydrolysis capacity. *J. Biol. Chem.* 281, 4446–4456. doi: 10.1074/jbc.M512028200

Sheng, X. D., Zeng, X., Lin, D., and Yao, S. (2018). Ethanol tolerant endoglucanase from *Aspergillus niger* isolated from wine fermentation cellar. *Biocatal. Agric. Biotechnol.* 15, 19–24. doi: 10.1016/j.bcab.2018.04.016

Sherman, E., Coe, M., Grose, C., Martin, D., and Greenwood, D. R. (2020). Metabolomics approach to assess the relative contributions of the volatile and non-volatile composition to expert quality ratings of Pinot Noir wine quality. *J. Agr. Food Chem.* 68, 13380–13396. doi: 10.1021/acs.jafc.0c04095

Shi, W. K., Wang, J., Chen, F. S., and Zhang, X. Y. (2019). Effect of *Issatchenkia terricola* and *Pichia kudriavzevii* on wine flavor and quality through simultaneous and sequential co-fermentation with *Saccharomyces cerevisiae*. *LWT* 116:108477. doi: 10.1016/j.lwt.2019.108477

Sirén, K., Mak, S. S. T., Melkonian, C., Carøe, C., Swiegers, J. H., Molenaar, D., et al. (2019). Taxonomic and functional characterization of the microbial community during spontaneous in vitro fermentation of Riesling must. *Front. Microbiol.* 10:697. doi: 10.3389/fmicb.2019.00697

Song, Y., Zhang, Y. J., Liu, N., Ye, D., Gong, X., Qin, Y., et al. (2017). Volatile compounds in wild strawberry and their odorants of wild strawberry wines: effects of different stages of fermentation. *Int. J. Food Prop.* 20, S399–S415. doi: 10.1080/10942912.2017.1297951

Song, Z., Du, H., Zhang, Y., and Xu, Y. (2017). Unraveling core functional microbiota in traditional solid-state fermentation by high-throughput amplicons and metatranscriptomics sequencing. *Front. Microbiol.* 8:1294. doi: 10.3389/fmicb.2017.01294

Swami, S. B., Thakor, N. J., and Divate, A. D. (2014). Fruit wine production: a review. *J. Food Res. Technol.* 2, 93–100. doi: 10.17508/CJFST.2018.10.2.19

Tao, Y. S., and Li, H. (2009). Active volatiles of cabernet sauvignon wine from Changli County. *Health.* 1, 176–182. doi: 10.4236/health.2009.13028

Torija, M. J., Beltran, G., Novo, M., Poblet, M., Rozès, N., Mas, A., et al. (2003). Effect of organic acids and nitrogen source on alcoholic fermentation: study of their buffering capacity. *J. Agr. Food. Chem.* 51, 916–922. doi: 10.1021/jf020094r

Wang, C., and Liu, Y. (2013). Dynamic study of yeast species and *Saccharomyces cerevisiae* strains during the spontaneous fermentations of Muscat blanc in Jingyang. *China. Food Microbiol.* 33, 172–177. doi: 10.1016/j.fm.2012.09.014

Waterhouse, A. L., Sacks, G. L., and Jeffery, D. W. (2016). *Understanding Wine Chemistry*. Hoboken, NJ: John Wiley & Sons.

Zea, L., Moyano, L., Moreno, J., Cortes, B., and Medina, M. (2001). Discrimination of the aroma fraction of sherry wines obtained by oxidative and biological ageing. *Food Chem.* 75, 79–84. doi: 10.1016/S0308-8146(01)00190-X

Zenkevich, I. G. (2002). "Kovats retention index system," in *Encyclopedia of Chromatography*, ed. J. Cazes (New York: Marcel Dekker Inc).

Zhang, X., He, F., Zhang, B., Reeves, M. J., Liu, Y., Zhao, X., et al. (2018). The effect of prefermentative addition of gallic acid and ellagic acid on the red wine color, copigmentation and phenolic profiles during wine aging. *Food Res. Int.* 106, 568–579. doi: 10.1016/j.foodres.2017.12.054

Zhang, Y., Li, X., Lo, C. K., and Guo, S. T. (2010). Characterization of the volatile substances and aroma components from traditional soypaste. *Molecules* 15, 3421–3427. doi: 10.3390/molecules15053421

Zhao, C., Su, W., Mu, Y., Jiang, L., and Mu, Y. (2020). Correlations between microbiota with physicochemical properties and volatile flavor components in black glutinous rice wine fermentation. *Food Res. Int.* 138:109800. doi: 10.1016/j.foodres.2020.109800

Zhao, G., Kuang, G., Li, J., Hadiatullah, H., Chen, Z., Wang, X., et al. (2020). Characterization of aldehydes and hydroxy acids as the main contribution to the traditional Chinese rose vinegar by flavor and taste analyses. *Food Res. Int.* 129:108879. doi: 10.1016/j.foodres.2019.108879

Conflict of Interest: The authors declare that the research was conducted in the absence of any commercial or financial relationships that could be construed as a potential conflict of interest.

Publisher's Note: All claims expressed in this article are solely those of the authors and do not necessarily represent those of their affiliated organizations, or those of the publisher, the editors and the reviewers. Any product that may be evaluated in this article, or claim that may be made by its manufacturer, is not guaranteed or endorsed by the publisher.

frontiers in Microbiology

ORIGINAL RESEARCH
published: 20 August 2021
doi: 10.3389/fmicb.2021.705967

Deciphering the Shifts in Microbial Community Diversity From Material Pretreatment to Saccharification Process of *Fuyu*-Flavor *Baijiu*

*Jiamu Kang[1], Yunan Hu[1], Ziyuan Ding[2,3], Li Ye[4], Haoran Li[2,3], Jun Cheng[4], Lin Fan[4], Hu Zhao[4], Beizhong Han[1] and Xiaowei Zheng[2,3,4]**

[1] College of Food Science and Nutritional Engineering, China Agricultural University, Beijing, China, [2] Nutrition & Health Research Institute, COFCO Corporation, Beijing, China, [3] Beijing Key Laboratory of Nutrition, Health and Food Safety, Beijing, China, [4] Jiugui Liquor Co., Ltd., Hunan, China

The microbiota of the pretreatment phase is crucial to the assembly of the microbial community in the saccharification of *fuyu*-flavor *baijiu*. This study investigates the shifts in microbial community diversity from the pretreatment of raw materials to the end of saccharification. High-throughput sequencing reveals that *Lactobacillus*, *Weissella*, and *Bacillus* in the bacterial community and *Rhizopus*, *Candida*, *Pichia*, and *Aspergillus* in the fungal community are predominant during raw material pretreatment and saccharification processes. Also, 11 bacterial genera, including *Bacillus*, *Lactobacillus*, *Leuconostoc*, *Weissella*, *Lactococcus*, and *Acetobacter*, and eight yeast genera, including *Candida*, *Pichia*, *Saccharomyces*, and *Wickerhamomyces*, were isolated from the initial saccharification stage by culture-dependent approaches. Sourcetracker analysis indicates that the cooling grains and rice husks were the main contributors to the bacterial community composition of the saccharification process, and *Qu* was the main contributor to the shaping of the fungal community structure during the saccharification process. Abundance variation of the predictive functional profiles of microbial communities encoding for key enzymes involved in pyruvate metabolism, starch and sucrose metabolism, and glycolysis/gluconeogenesis during the pretreatment and saccharification phases were inferred by PICRUSt2 analysis. The results of this study will be utilized to produce consistently high-quality *fuyu*-flavor *baijiu* via better controlling the shaping of microbial community structures during the pretreatment and fermentation processes.

Keywords: saccharification, raw materials, pretreatment, microbiota, SourceTracker, *Fuyu*-flavor *Baijiu*

OPEN ACCESS

Edited by:
Xucong Lv,
Fuzhou University, China

Reviewed by:
Yu Zheng,
Tianjin University of Science and Technology, China
Chi Zhao,
Guizhou University, China

***Correspondence:**
Xiaowei Zheng
zhengxiaowei@cofco.com

Specialty section:
This article was submitted to Food Microbiology, a section of the journal Frontiers in Microbiology

Received: *06 May 2021*
Accepted: *26 July 2021*
Published: *20 August 2021*

Citation:
Kang J, Hu Y, Ding Z, Ye L, Li H, Cheng J, Fan L, Zhao H, Han B and Zheng X (2021) Deciphering the Shifts in Microbial Community Diversity From Material Pretreatment to Saccharification Process of Fuyu-Flavor Baijiu. Front. Microbiol. 12:705967. doi: 10.3389/fmicb.2021.705967

INTRODUCTION

Baijiu (Chinese liquor) is one of the oldest distillates globally, and it has various flavor types, most of which are produced by traditional manufacturing techniques in different regions of China (Zheng and Han, 2016; Liu and Sun, 2018). *Fuyu*-flavor *baijiu*, one of the famous mixed-flavor *baijiu* produced in the *Xiangxi* region, Hunan, China, is popular among consumers because of its fragrant aroma and sweet, mellow, and harmonious taste (Wu and Fan, 2009). The *fuyu*-flavor *baijiu* manufacturing process includes raw material pretreatment, starter preparation,

solid-state saccharification, pit fermentation, distillation, aging, and blending. Traditionally, the manufacturing method uses a mixture of sorghum, rice, glutinous rice, and maize as raw materials and performs a preliminary solid-saccharification process after a series of raw material pretreatment processes. Then, the saccharified grains are mixed with *Daqu* starter to carry out fermentation in the pit. The solid-saccharification process enriches natural microbiota, contributing to the accumulation of unique and abundant flavor compounds (Wu and Fan, 2009; Zheng and Han, 2016).

Spontaneous saccharification is a complex biochemical process involving microbiota, including bacteria, yeasts, and filamentous fungi, resulting in high-quality properties of products. Raw materials are a key factor for *baijiu* flavor profiles, and the microbial community composition is highly correlated with the accumulation of flavor substances (Liu et al., 2019). The environment is regarded as an important contributor to the shaping of microbial community diversity during *baijiu* fermentation (Wang X. et al., 2018). The raw material pretreatment process of *fuyu*-flavor *baijiu* involves the mixing, soaking, cooking, and cooling of grains and then the addition of *Xiaoqu* (a *Rhizopus xiaoqu*, *Qu*) and rice husks (RH) to the pretreated grains. The entire pretreatment process is exposed to an open operation environment, and unsterilized cold water is used in the soaking and cooking processes. *Lactobacillus* introduced into the sorghum from the environment during the cooling processing is an important source of *Lactobacillus* during light-flavor *baijiu* fermentation (Pang et al., 2020). Also, RH is an auxiliary material used in the saccharification process as a filler for fermentation to improve the contact interface between microbiota and grains in the fermentation process and accelerate microbe propagation (Fan et al., 2020). These operations gather the environmental microbiota; however, considerably less is known regarding the microbial community composition shifts from pretreatment to the saccharification process.

Generally, the culture-dependent method offers quantitative data on microorganism occurrence and is widely used to isolate pure cultures from fermented samples for experimental fermentation tests, but it underestimates microbial diversity (Zheng et al., 2012). In recent years, high-throughput sequencing has promoted tremendous advances in the microbial community structure analysis of various traditional fermented foods based on the advantages of no culture, high throughput, and fast detection speed (Pang et al., 2018; Liu et al., 2020; Rizo et al., 2020). Hence, this study aimed to explain the shifts in microbial community structures and diversity in the pretreatment to saccharification stage via Illumina MiSeq PE300 sequencing. Predictive gene functionality of the bacterial and fungal community, involving pyruvate metabolism, starch and sucrose metabolism, and glycolysis/gluconeogenesis, were also inferred via Phylogenetic Investigation of Communities by Reconstruction of Unobserved States 2 (PICRUSt2). A culture-dependent approach was used to analyze further the samples' microbial composition at initial saccharification. We identified 30 bacteria strains and 30 yeast strains randomly isolated from saccharified grains. These results create a basis for further research regarding the strains naturally occurring during saccharification having excellent fermentation and flavor-producing properties.

MATERIALS AND METHODS

Experimental Design and Sample Collection

Samples were collected in a *fuyu*-flavor *baijiu* distillery in Hunan Province, China. **Figure 1** shows the 11 detailed sampling sites whose name was marked "red." The samples were collected at the beginning of raw material pretreatment until the end of saccharification, at P1_SOS, P2_MG, P3_SOMG, P4_ST, P5_CO, *Qu*, RH, SP_0h, SP_5h, SP_10h, and SP_20h. Approximately 100 g of grains with different pretreatment levels, *Qu*, RH, and grains in different saccharification stages at each point were aseptically collected in triplicate. To reduce sample heterogeneity, three production processes of the same batch were randomly selected, and triplicate subsamples were collected from each chain. All collected samples were immediately placed in an icebox for transportation to our laboratory for further analysis.

Metagenomic DNA Extraction

For microbial metagenomic DNA extraction, one third of each of the three parallel samples was mixed. Then, DNA was extracted from 10 g of each mixed sample using the E.Z.N.A.® Soil DNA Kit (Omega, Norcross, GA) according to the manufacturer's instructions. Concentration of DNA was then quantified using a spectrometer. Then, 1% agarose gel electrophoresis was used to evaluate the integrity and purity of the extracted DNA under ultraviolet light. All extracted DNA samples were stored at −80°C before further experiments.

Amplicon Sequencing

For bacterial PCR amplification, we targeted the hypervariable regions V3-V4 of the 16S ribosomal RNA (rRNA) gene using the universal forward primer 341F (5′-CCTAYGGGRBGCASCAG-3′) and reverse primer 806R (5′-GGACTACNNGGGTATCTA AT-3′). For fungal PCR amplification, we targeted the internal transcribed spacer (ITS) region using forward primer (5′-GGAAGTAAAAGTCGTAACAAGG-3′) and reverse primer (5′-GCTGCGTTCTTCATCGATGC-3′). The PCR products were checked by electrophoresis on 1% agarose gel and a Qubit fluorescence quantifier. The amplicon library preparation procedure was performed by the Illumina TruSeq DNA Sample Preparation Guide, and the amplicon sequencing was carried out using the Illumina MiSeq PE300 system (Illumina, San Diego, CA) according to the manufacturer's standard protocols.

Sequencing Data Processing and Bioinformatics

The original paired-end reads from Miseq sequencing were merged via FLASH software (version 1.2.11) (Magoc and Salzberg, 2011). Trimmomatic software (version 0.33) was employed to carry out the quality filtering of the merged sequences (Bolger et al., 2014). Subsequently, UCHIME

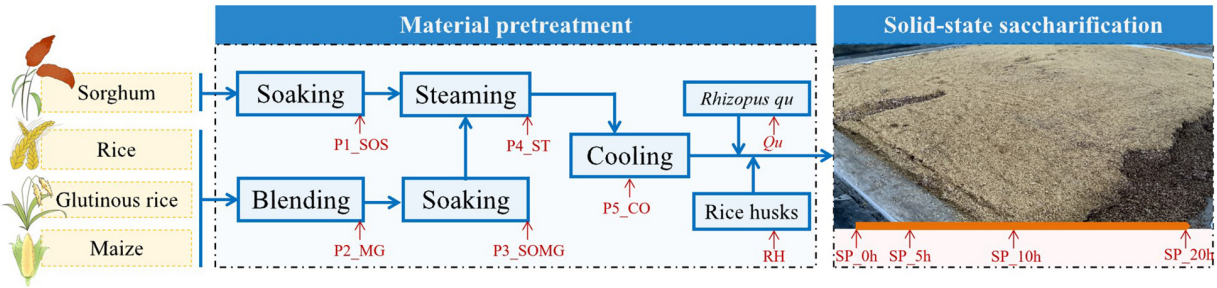

FIGURE 1 | Diagram of the raw material pretreatment and solid-state saccharification processes of *fuyu*-flavor *baijiu*.

software (version 8.1) was employed to identify and remove chimera sequences. Operational taxonomic units (OTUs) were clustered from clean tags with 97% similarity using UPARSE software (version 10.0) (Edgar, 2013). Then, to achieve the microbial taxonomic annotation, the representative bacterial OTU sequences were aligned with the Silva databases (Release132[1]), and the representative fungal OTU sequences were aligned with Unite databases (Release 8.0[2]). Sequencing data are available at NCBI with Sequence Read Archive (SRA) accession: PRJNA705302.

Per the OTU cluster information, rarefaction curves and alpha diversity indices, including observed OTU number, Chao1 richness estimator, Ace richness estimator, Shannon diversity index, Simpson diversity index, Good's coverage, and phylogenetic diversity (PD whole tree), were calculated with the QIIME2 program (Bolyen et al., 2019). The beta diversity was evaluated using the Bray–Curtis distance matrix and was further visualized via Origin Lab software (version 9.0). The SourceTracker program was used to predict the sources of microbial communities in grain samples at different saccharification stages based on the default parameters. The Interactive Tree of Life (iTol) was used to visualize and annotate phylogenetic trees. In addition, PICRUSt2 predicted functional profiling of the metagenome based on bacterial and fungal amplicon sequencing profiles (Douglas et al., 2020). The functional annotation of predicted features was carried out based on the Kyoto Encyclopedia of Genes and Genomes (KEGG) database. A raw OTU count data set was performed through the PICRUSt2 pipeline with default parameters. Then, Enzyme Commission (EC) numbers and metabolic process abundances in each given sample were imputed. The relative abundance of each individual EC term related to pyruvate metabolism, starch and sucrose metabolism, and glycolysis/gluconeogenesis was calculated and visualized.

Isolation and Identification of Bacteria and Yeasts From the Initial Saccharification

Culturable bacteria and yeasts of the initial saccharification samples were analyzed by the culture-dependent method as described by Zheng et al. (2012). A total of 10 g of sample was transferred into sterile stomacher bags and homogenized with 0.85% (w/v) sterile NaCl solution (90 mL). An appropriate serial dilution was performed, and 100 μL of the diluted suspension was dispensed on different selective agar media. Lactic acid bacteria (LAB) were grown on De Man, Rogosa, and Sharpe agar (MRSA) with 500 μg/mL natamycin at 37°C for 48 h to achieve distinct LAB colonies. Thermoduric bacteria and Enterobacteriaceae were grown on Luria–Bertani agar (LBA) and violet red bile glucose agar (VRBGA), respectively, and were incubated at 37°C for 24 h. Yeasts were grown on potato dextrose agar (PDA) and incubated at 28°C for 48 h. Then, one to three colonies with different morphologies were randomly isolated from each plate for purification and identification. Pure cultures were stored at −80°C in glycerol (30% v/v) stocks. Total DNA of bacteria and yeast were extracted using a bacterial or fungal genomic DNA extraction kit, respectively (Tiangen, Beijing, China). The 16S rRNA gene of bacterial strains and the ITS gene of yeasts were amplified using the primers 27F/1492R and ITS1/ITS4, respectively (Dong et al., 2020). The resulting PCR products were purified, cloned, and sequenced using the Sanger sequencing platform (BGI Inc., China). The sequencing results were compared with the BLAST algorithm's GenBank database (National Center for Biotechnology Information, United States). Nucleotide sequences of evaluated bacteria and yeasts have been deposited at GenBank with accession numbers MZ057699-MZ057728 and MZ089518-MZ089547, respectively.

RESULTS

Characteristics of the Sequencing Results and Alpha Diversity

Metagenomic DNA extracted from pretreated and saccharified samples was detected via an amplicon sequencing tool, generating 586,131 total raw reads for 16S rRNA gene sequences with an average of 44,569 clean reads for the bacterial community. For the fungal community, a total of 1,640,536 raw ITS gene sequences were collected; after quality control, an average of 124,217 clean reads were obtained per sample. Based on a similarity threshold of 97%, the number of OTUs clustered from

[1]http://www.arb-silva.de

[2]https://unite.ut.ee/

TABLE 1 | Observed operational taxonomic units (OTUs), richness indices (ACE and Chao1), diversity indices (Simpson and Shannon), phylogenetic diversity (PD whole tree), and Good's coverage of microbial community.

	Samples	OTU	ACE	Chao1	Simpson	Shannon	PD whole tree	Coverage
Bacterial community	P1_SOS	102	109.0323	111.4286	0.8085	3.1533	8.1128	0.9997
	P2_MG	124	130.0231	128.5833	0.7058	2.5683	9.0968	0.9998
	P3_SOMG	72	74.852	73.6667	0.5266	1.9845	6.5195	0.9999
	P4_ST	92	104.1773	113.8571	0.7167	2.3786	7.5156	0.9997
	P5_CO	101	107.5016	106.5	0.5112	2.1258	7.7153	0.9998
	Qu	115	116.3863	116	0.7189	2.9506	9.463	0.9999
	RH	92	100.1536	103.375	0.821	3.0425	7.1955	0.9996
	SP_0h	82	85.6321	84.1	0.7961	2.8368	7.5458	0.9998
	SP_5h	61	72.9297	68.8	0.5069	1.6933	5.6612	0.9997
	SP_10h	70	83.8043	80.1111	0.6263	2.0241	6.5261	0.9996
	SP_20h	98	107.5217	106.0769	0.5274	1.9752	8.3716	0.9995
Fungal community	P1_SOS	76	104.0427	86.1111	0.4792	1.7773	11.4923	0.9999
	P2_MG	101	103.6779	103.5	0.469	1.9906	16.377	1
	P3_SOMG	45	57.8549	56	0.0953	0.4364	8.7696	0.9999
	P4_ST	104	104	104	0.8763	3.9352	16.9568	1
	P5_CO	18	23.8787	19	0.2608	0.8991	5.4322	1
	Qu	16	73.2319	38.5	0.0011	0.0083	5.4795	0.9999
	RH	80	82.9827	81.6667	0.7376	2.5836	14.8141	1
	SP_0h	22	23.2597	22.125	0.0304	0.1464	7.4477	1
	SP_5h	48	53.6663	50.625	0.5134	1.4434	9.4758	0.9999
	SP_10h	31	41.3997	32.6667	0.2927	0.7387	8.8735	1
	SP_20h	15	30.7193	24.3333	0.0137	0.0622	5.0977	0.9999

these reads and their diversity index are exhibited in **Table 1**. A total of 173 bacterial and 120 fungal OTUs were identified. Microbial OTUs were annotated further at the phylum and genus levels. All bacterial OTUs were assigned into 8 different phyla, 13 classes, 25 orders, 46 families, and 100 genera. Fungal OTUs were assigned into 3 phyla, 9 classes, 16 orders, 33 families, and 50 genera.

The Shannon and Simpson indices reflect the community diversity and evenness for the alpha diversity indices, and the Chao1 and ACE estimator characterizes the community richness (Liu et al., 2020). Among these samples, the bacterial and fungal ACE and Chao1 indexes were higher in P2_MG and P1_SOS samples, indicating higher microbial community richness. Moreover, from the viewpoint of bacterial Shannon and Simpson indices, P1_SOS and RH had the higher community diversity although the samples in the saccharification stage from 5 to 20 h had lower bacterial diversity. P4_ST had the highest community diversity from the fungal diversity aspect, and both *Qu* and SP_20h had the lowest fungal diversity. The phylogenetic diversity (PD) index of the tree reflects the genetic relationship of species. The PD whole tree value of *Qu* in the bacterial community was 9.463, the biggest among all samples, indicating a complex genetic relationship. In contrast, the P4_ST had the most complex genetic relationship in the fungal community and the farthest evolutionary distance among all groups. Also, the Good's coverage estimators of all samples were near 1.00, suggesting that the sequencing depth is enough to represent the studied microbial community.

Changes in the Bacterial Community During Pretreatment and Saccharification Process

Annotation of the samples' generated bacterial OTUs is shown in **Figures 2A**, **3A**. Firmicutes and Proteobacteria were the main bacterial phyla identified in all samples. At the genus level, the evolutionary relationship of 173 bacterial OTUs from all samples was constructed. *Lactobacillus*, *Weissella*, and *Bacillus* comprised the top three genera, and *Lactobacillus* was the most abundant genus (**Figure 2A**). In detail, the most dominant bacteria in the soaked sorghum sample was *Lactobacillus* with an abundance of 58.63%. In contrast, the dominant bacteria in the rice, glutinous rice, and maize mixture were norank_f_ Mitochondria (47.78%), norank_o_Chloroplast (19.65%), *Weissella* (16.29%), and *Lactobacillus* (9.65%). After the steeping of mixed grains, *Lactobacillus* (68.25%) remained the most abundant bacterial genus, followed by *Weissella* (11.30%).

Bacillus (45.91%) became the dominant bacterial genus in the cooked soaked grains due to their excellent heat resistance, and the relative abundance of *Lactobacillus* was reduced to 0.18%. After cooling, the main bacterial genera identified in the pretreated grains were *Weissella* (69.16 %) and *Lactobacillus* (15.58 %). *Qu* and RH were used as a starter and auxiliary material in the solid-state saccharification process, respectively. *Bacillus* was detected as the dominant bacterial genus in the *Qu*, followed by *Pantoea* (7.67%), *Staphylococcus* (5.38%), and unclassified Enterobacteriaceae

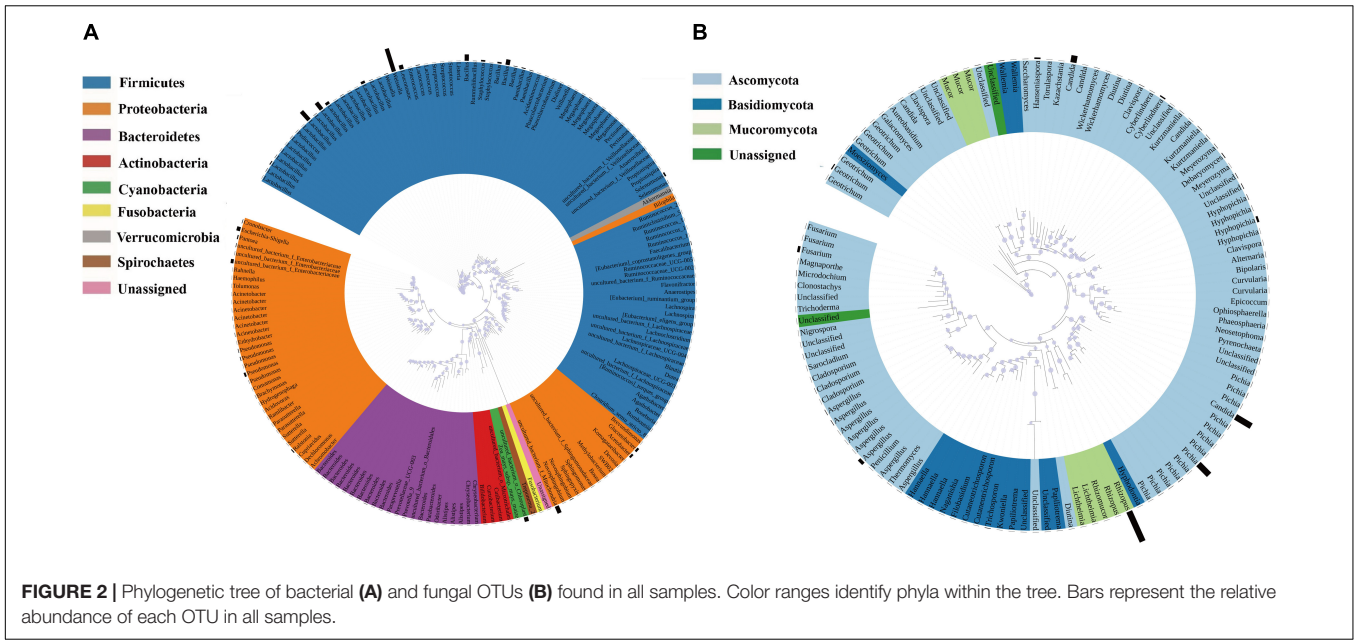

FIGURE 2 | Phylogenetic tree of bacterial **(A)** and fungal OTUs **(B)** found in all samples. Color ranges identify phyla within the tree. Bars represent the relative abundance of each OTU in all samples.

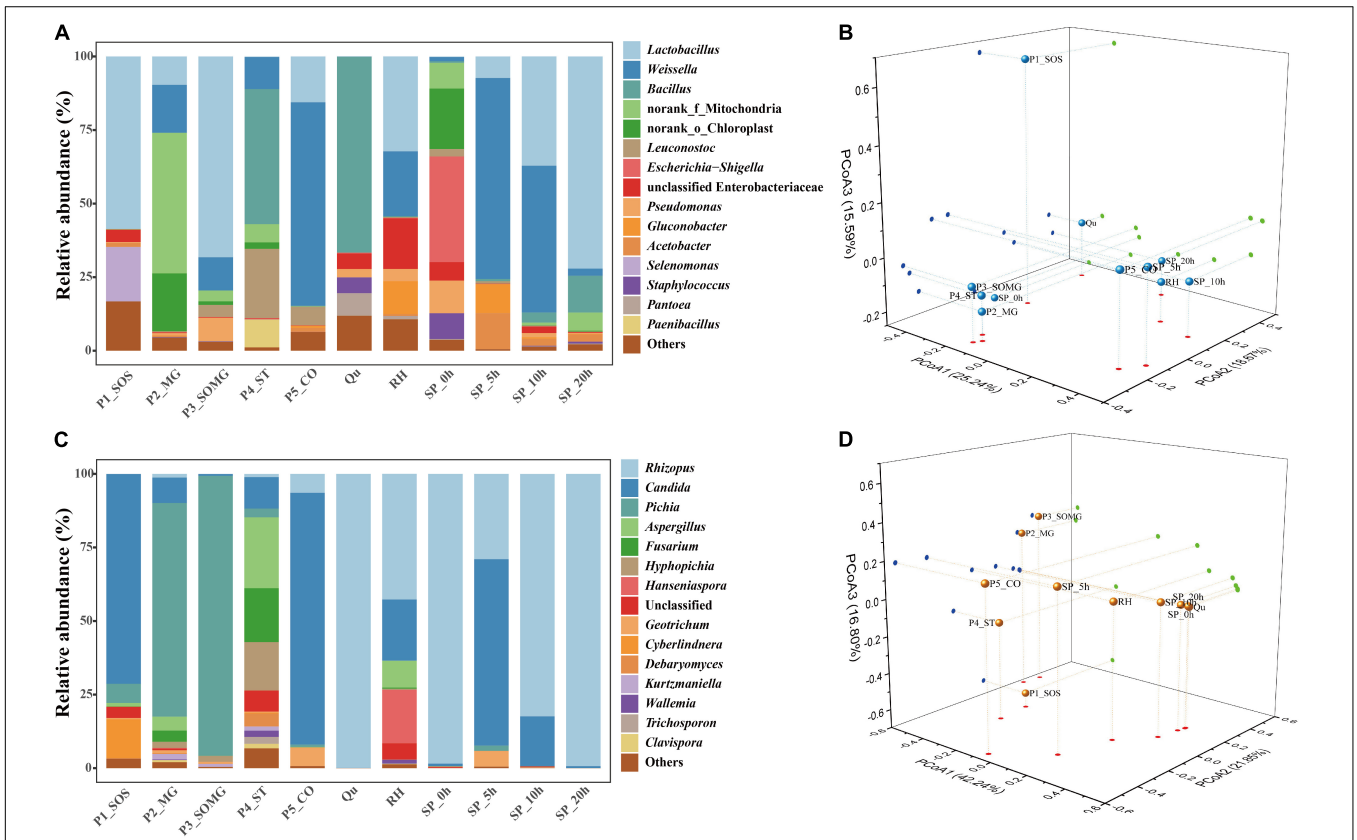

FIGURE 3 | Relative abundance of bacterial **(A)** and fungal communities **(C)** in pretreated and saccharified samples. PCoA analysis of the bacterial **(B)** and fungal communities **(D)**, based on the Bray–Curtis distance.

(5.28%). *Lactobacillus* (32.25%), *Weissella* (22.13%), unclassified Enterobacteriaceae (17.18%), and *Gluconobacter* (11.21%) were preponderant genera in RH.

The saccharification process's initial bacterial structure mainly included *Escherichia-Shigella*, norank_o_Chloroplast, *Pseudomonas*, *Staphylococcus*, norank_f_Mitochondria,

unclassified Enterobacteriaceae, *Weissella*, *Bacteroides*, and *Lactobacillus*, comprising 35.91%, 20.57%, 11.07%, 8.76%, 8.74%, 6.29%, 1.43%, 0.19%, and 0.18% of the bacterial community, respectively. As the saccharification process progressed, LAB gradually became the dominant bacterial genera; in particular, *Lactobacillus* showed a linear increase from 0 to 20 h.

To further understand the composition of natural cultivable bacteria and collect functional strains for laboratory-scale research, culture-dependent isolation coupled with the 16S rRNA gene identification method were used to isolate and identify the bacteria. A total of 30 bacterial strains were randomly isolated from the samples of the initial saccharification stage. After 16S rRNA gene sequencing, these isolated strains were matched against GenBank of NCBI, and the detailed assignments can be found in **Supplementary Table 1**. As shown in **Supplementary Table 1**, all strains were classified into 11 bacterial genera, including *Bacillus* (n = 7), *Lactobacillus* (n = 6), *Leuconostoc* (n = 4), *Weissella* (n = 3), *Lactococcus* (n = 3), *Acetobacter* (n = 2), *Staphylococcus* (n = 1), *Paraburkholderia* (n = 1), *Acinetobacter* (n = 1), *Franconibacter* (n = 1), and *Pantoea* (n = 1).

A PCoA plot assessed the beta diversity of the bacterial community structure. The first three principal components (PCoA1, PCoA2, and PCoA3) explained more than 59% of the total variance (**Figure 3B**). P1_SOS and *Qu* samples were separate from all other samples. The bacterial community structures of P2_MG, P3_SOMG, and P4_ST samples in the pretreatment stage were relatively similar to the bacterial community during initial saccharification. The P5_CO and RH samples were closer to the bacterial composition of the saccharification process. These results indicated that the bacterial community structures in the pretreatment process were closely related to the saccharification process.

Changes in the Fungal Community During Pretreatment and Saccharification Process

A phylogenetic tree of 120 fungal OTUs was constructed to perform the evolutionary relationship of fungi (**Figure 2B**), *Rhizopus*, *Candida*, *Pichia*, and *Aspergillus* comprise the top four fungal genera. The generated fungal OTU sequences were mainly ascribed to three phyla: Ascomycota, Mucoromycota, and Basidiomycota. At the genus level (**Figure 3C**), *Candida* (71.27%), *Cyberlindnera* (13.35%), and *Pichia* (6.52%) were the dominant fungal genera in the P1_SOS. In the P2_MG and P3_SOMG samples, *Pichia* was the most important fungi. *Aspergillus* (24.07%), *Fusarium* (18.32%), *Hyphopichia* (16.45%), and *Candida* (10.68%) became the dominant fungal genera after the soaked grains were cooked. After the steamed grains were cooled down, *Candida* was the main genus comprising 80% of the fungal community. *Rhizopus* was the fungal genus occupying 99.94% abundance in the *Qu* sample. The RH sample's predominant genera were *Rhizopus*, *Candida*, *Hanseniaspora*, and *Aspergillus* with 42.71%, 20.73%, 18.15%, and 9.09% respective relative abundances. Due to the fermentation starter, the fungal community at the initial stage of saccharification was similar to the *Qu* sample. In the SP_5h sample, *Candida* was the dominant fungal genus, followed by *Rhizopus*. In the subsequent saccharification process, the relative abundance of *Candida* gradually decreased, and the *Rhizopus* gradually increased. By the end of saccharification, the proportion of *Rhizopus* reached 99.31%.

To further understand the natural yeast compositions and collect pure cultures for laboratory-scale fermentation, a total of 30 yeasts were randomly isolated from the samples of the initial saccharification stage by the culture-dependent method coupled with ITS gene identification. These isolated strains were matched against GenBank using BLAST analysis as shown in **Supplementary Table 2**. Isolated strains were identified as yeast belonging to eight genera, including *Candida* (n = 6), *Pichia* (n = 9), *Saccharomyces* (n = 5), *Wickerhamomyces* (n = 5), *Issatchenkia* (n = 2), *Debaryomyces* (n = 1), *Diutina* (n = 1), and *Hyphopichia* (n = 1).

As shown in **Figure 3D**, the first three principal components were constructed in the PCoA plot, explaining 42.24%, 21.85%, and 16.80% of the variance in the data set, respectively. SP_0h, SP_10h, SP_20h, and *Qu* samples were closer on the map, suggesting that *Qu* plays an essential role in shaping the fungal community during saccharification.

The Microbial Association Between Pretreatment and the Saccharification Process

Petal plots were constructed to investigate the similarities and differences between the pretreated and saccharified samples' bacterial and fungal communities (**Figure 4**). As illustrated in **Figures 4A,B**, 10 bacterial genera and four fungal genera, which were most common to all the samples, were classified as core genera. **Figure 4C** shows the distribution of these common bacterial and fungal genera during the pretreatment and saccharification stages. Lactic acid bacteria was the dominant bacterial genus in the pretreatment stage of raw materials and the late saccharification stage. The dominance of *Rhizopus* in the fungal community mainly appeared after the adding of *Qu*. During the pretreatment processes of raw materials, the main fungal genera in all samples were mainly various yeasts. Moreover, for the bacterial community, except for the two samples P4_ST and *Qu*, the abundance of these common bacterial genera in the remaining samples accounted for most of the total 16S rRNA sequences (greater than 60% bacterial composition). The core fungal abundance in P3_SOMG, P5_CO, and *Qu* samples and the four samples collected from saccharification processes accounted for more than 95% of the total ITS sequences for the fungal community.

As shown in **Figures 4D,E**, a source tracker was employed to predict the sources of bacteria and fungi found in saccharified grains. For the bacterial community, 90.04% of the bacteria in the SP_0h sample was from an unknown source, 6.62% was P2_MG-derived, and the remaining pretreated samples' contribution was less than 1%. In the SP_5h samples, P5_CO and RH samples contributed 76.49% and 4.21% of the bacteria, respectively. The samples P5_CO, RH, and *Qu* contributed 98.3% of the bacterial community in the sample at the 10^{th} hour of saccharification.

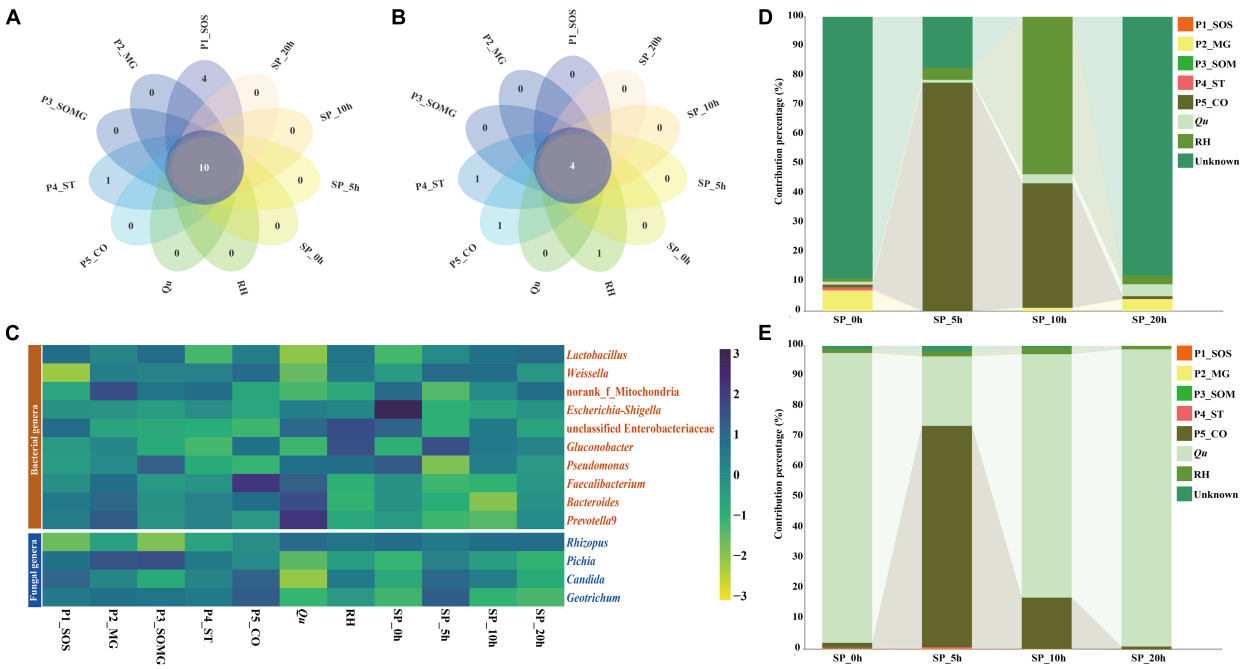

FIGURE 4 | The petal diagram shows the unique and shared bacterial **(A)** and fungal genera **(B)** among different samples. The heat map shows the relative abundance of the microbial genera shared in all samples **(C)**. Sourcetracker results highlight the contribution percentages of the source bacterial **(D)** and fungal **(E)** community in the pretreatment stage to the saccharification stage.

In the sample of SP_20h, most of the bacteria did not originate from the pretreatment stage, and only 10.44% of the bacteria came from the three pretreatment samples of P2_MG, *Qu*, and RH. For fungal communities, *Qu* was the primary fungal source of both SP_0h (95.6%), SP_10h (80.2%), and SP_20h (97.9%) samples, whereas P5_CO was the main contributor to the fungal community of sample SP_5h. P5_CO sample contributed 73.0% of the fungal community to the SP_5h sample and 16.8% to the SP_10h sample.

Changes in the Expression of Predicted Functional Enzymes During Pretreatment and the Saccharification Process

The PICRUSt2 platform contains an updated and more extensive database of gene families and reference genomes, which provides improved accuracy and flexibility for marker gene metagenome inference (Douglas et al., 2020). In this study, we used PICRUSt2 to predict the metagenome functions of the bacterial and fungal community during raw material pretreatment and saccharification processes. **Figure 5** shows the changes in the enzyme-encoding genes of bacteria and fungi as annotated using KEGG regarding the categories of pyruvate metabolism, starch and sucrose metabolism, and glycolysis/gluconeogenesis. For pyruvate metabolism of the bacterial community, the relative abundance of core enzymes in the P4_ST, *Qu*, and SP_0h samples was higher. The functional enzymes involved in starch and sugar metabolism of the bacterial community gradually decreased in the middle and late stages of saccharification (**Figure 5B**). In contrast, the relative abundance of these key enzymes in the fungal community showed different changes. The enzymes of the fungal community regarding pyruvate metabolism in the P1_SOS, P4_ST, *Qu*, SP_10h, and SP_20h were relatively high than in other samples. Meanwhile, P4_ST contributed a higher abundance of functional enzymes in the fungal communities (**Figure 5C**). For these important enzymes presented in **Figures 5A,C**, the fungal community of samples collected from saccharification stage showed a high abundance of these enzymes. These findings suggested that bacteria and fungi contributed to the rich metabolic activities of the saccharified grains.

DISCUSSION

The pretreatment of raw material is an integral part of the fermentation processing of *baijiu* as it changes the property of the material and is beneficial to the growth and metabolism of microorganisms. The microbial community associated with alcoholic fermentation is related to the fermentation starters and the environmental microbiota during material pretreatment (Pang et al., 2020). In this study, we systematically investigated the changes in microbial composition and function from the raw material pretreatment to the saccharification processes of the *fuyu*-flavor *baijiu*. We analyzed the potential contribution of each operation of the pretreatment process to the shaping of the microbial community in the saccharification process. Many functional microorganisms exhibited in the saccharification

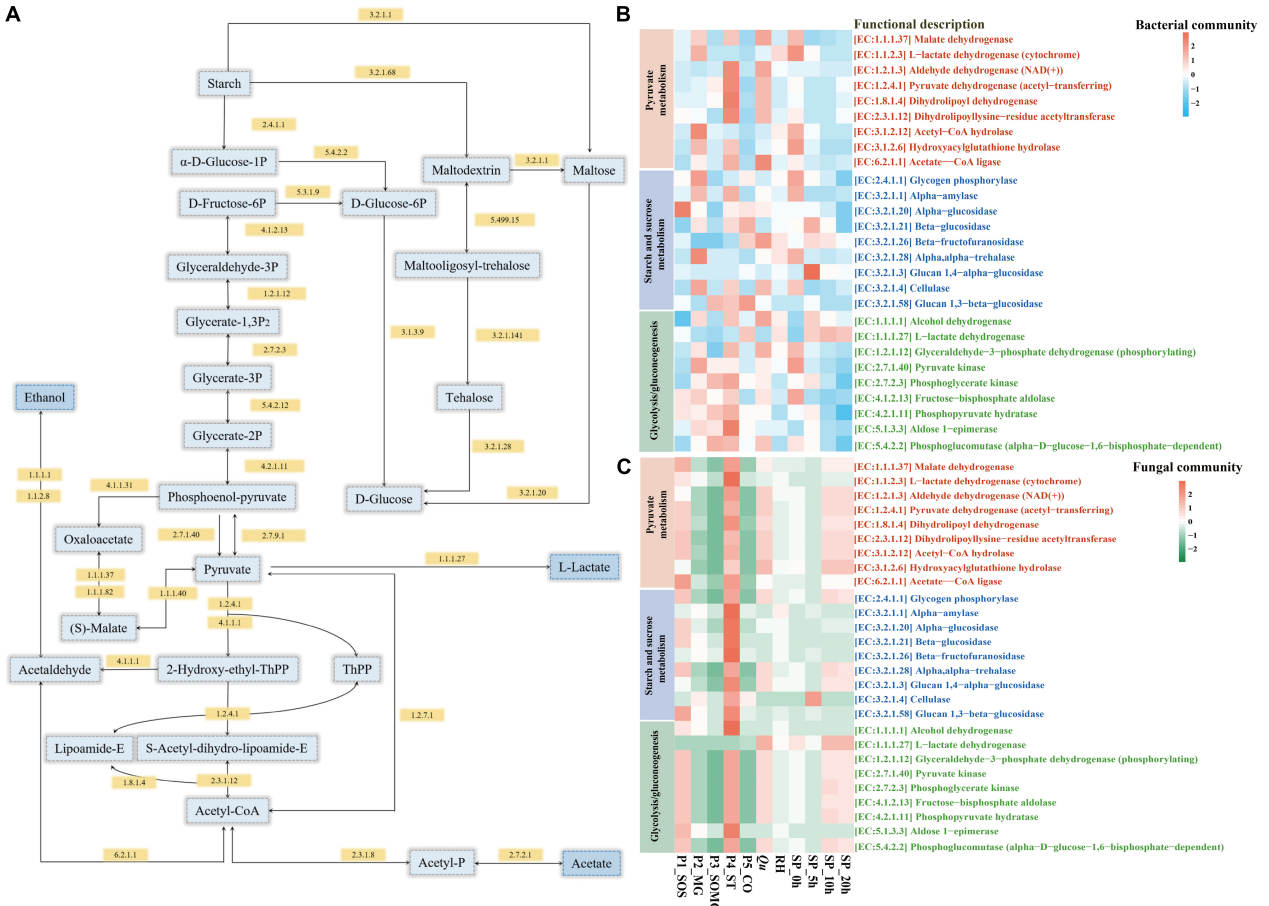

FIGURE 5 | Schematic overview of the metabolic processes involving pyruvate metabolism, starch and sucrose metabolism, and glycolysis/gluconeogenesis **(A)**. Heat map shows changes in the relative abundance of annotated functional enzymes related to saccharification and the formation of flavor compounds [**(B)** bacterial community and **(C)** fungal community].

process, such as LAB, *Bacillus,* and yeasts, might derive from environment, raw material, and unsterilized cold water. A series of pretreatment operations may display a positive impact on shaping the naturally sourced microbial communities. Thus, we used the culture-dependent method to isolate naturally sourced bacteria and yeasts from the initial saccharification samples. On the one hand, the acquisition of these strains assisted the high-throughput sequencing results to explain the microbial composition of saccharification at the species level. On the other hand, these results laid the foundation for the synthetic functional microbiota and the management of the saccharification process.

In this study, we found that the abundance of LAB in grains increased after soaking treatment. Pang et al. (2020) reported that *Lactobacillus* (84.6%) was the dominant bacterial genus after the steeping of sorghum for approximately 20 h, which is consistent with our results. Steeping of cereal-based raw materials can be practiced to increase bioactive components and reduce the content of some antinutritional components and fermentation with LAB, which can further accumulate functional bioactive components (Hassani et al., 2016). High-temperature favors thermotolerant and aerobic endospore-forming bacteria (Zheng et al., 2014). This explains why *Bacillus* members became the dominant bacteria in the P4_ST sample. Members of *Bacillus* genera were regarded as a constant factor in *baijiu* fermentation starter. They can contribute to the formation and accumulation of flavor compounds and functional enzyme activities (i.e., amylases and proteinases) needed to ferment cooked sorghum for alcoholic fermentation (Zheng et al., 2011). In the solid-state saccharification process of rice-flavor *baijiu*, LAB species are potentially responsible for the high amount of lactic acid in the sample after saccharification (Yin et al., 2020). Pang et al. (2018) reported that *Lactobacillus* was positively correlated with essential esters in *baijiu*. These may be important reasons for the accumulation of flavor compounds in the saccharification process. The results of culture-dependent analyses show 16 LAB strains, including *Lactobacillus hilgardii*, *Lactobacillus fermentum*, *Lactobacillus paracasei*, *Lactobacillus plantarum*, *Lactococcus lactis*, *Lactococcus lactis* subsp. *Hordniae*, *Lactococcus taiwanensis*, *Leuconostoc lactis*, *Leuconostoc pseudomesenteroides*, *Weissella confusa*, and *Weissella cibaria*, were found in the samples collected from the initial saccharification stage. In contrast, LAB populations were not dominant in the bacterial

diversity as shown by the high-throughput perspective of the initial saccharification sample. The reason could be that these LAB populations were not picked up by high-throughput sequencing because of their low numbers but could be enriched by culture-dependent approaches (Zhadyra et al., 2021). In addition, the low abundance of *Bacillus* during saccharification may be due to the lower oxygen concentration, and higher alcohol content prevented the growth of *Bacillus* (Ren et al., 2019).

Rhizopus is a fungal genus widely used as a bioconversion organism in solid-state fermentation. Several characteristics, including wide growth temperature interval, wide growth and survival pH range, board fermentative substrates, and the range of by-products produced, make this genus useful in industrial applications, particularly the *baijiu* industry (Zheng et al., 2011; Jin et al., 2017; Ibarruri and Hernández, 2018). In a *Huaxi Xiaoqu* collected from Sichuan, China, the fungal community was relatively simple, consisting only of a few species, in which *Rhizopus stolonifera* constituted 94.98% of the community (Wu et al., 2017). Wang B. et al. (2018) found that the *Rhizopus* was the most abundant genus (above 60.00%) represented in all six *Jiuqu* samples, where its secreted glucoamylase and played a vital role as a saccharifying agent. In *baijiu* fermentation, alpha-amylase and glucoamylase were related to starch hydrolysis and affiliated with *Rhizopus*, *Aspergillus*, and *Rhizomucor* (Wang et al., 2020). In addition, *Rhizopus* can produce lactic acid in high quantities with potential applications in the production of rice-flavor *baijiu* (Yin et al., 2020). In addition to *Rhizopus*, yeasts, including *Candida* and *Pichia*, were important non-*Saccharomyces* yeasts in the saccharification process. Yeasts are the most important fungal populations contributing to *baijiu* quality in the solid-state fermentation process (Wu et al., 2013). Traditionally, *Xiaoqu* is usually prepared by cultivating mold in rice flour and, in some cases, with yeast (Yin et al., 2020). Although the starter selected in this study is *Rhizopus xiaoqu*, we identified a rich population of yeast in the initial saccharification stage by combining the results of culture-dependent and -independent analyses. Pang et al. (2020) reported that *Pichia* and *Candida* were the main fungal genera at the end of soaking, positively correlated with most flavors. Interestingly, the lower abundances of *Pichia*, *Wickerhamomyces*, and *Aspergillus* in fermented grain might decrease flavor compounds, including volatile alcohols, aromatics, and esters (Wang X. et al., 2018). Also, members of *Pichia* are good ethanol producers identified in *baijiu* fermentation (Jin et al., 2017; Li et al., 2018). In the light-flavor *baijiu* fermentation process, the genus *Candida* was positively correlated with acetic acid (Wang X. et al., 2018). This appears to be evidence that these fungi subtly shape the flavor quality of *baijiu*.

To explore the contribution of each operation in the pretreatment stage to the microbiota formation of the saccharification process, we analyzed the shared microorganisms at all sampling points via a petal diagram and revealed the potential connections regarding microbial composition between the two processes with the help of Sourcetracker. Most microorganisms in raw materials were killed after the steaming treatment (Pang et al., 2020). Considering that cooling processing was performed in an open environment, the microbiota in cooled samples was presumably derived from the environment. Environmental microbiota is an important source of fermentation microbiota and could drive both microbial succession and metabolic profiles during *baijiu* fermentation (Wang X. et al., 2018). In this study, the microorganisms inhabiting raw materials after cooling, *Qu*, and RH were closely related to the microbiota involved in the saccharification process. Similarly, in terms of the fermentation of light-flavor *baijiu*, sorghum after cooling and *Daqu* contributed 51.4% and 23.9% to the bacterial community in fermented grains (Pang et al., 2020). *Daqu* was also considered the main source of the fungal community in fermented grains (Wang X. et al., 2018).

Furthermore, based on the KEGG pathway, PICRUSt2 analyzed the sample's potential functional characteristics to explain changes in microbial metabolic functions during two processes. Glucoamylase and alpha-1,4-glucan phosphorylase were the main enzymes attributed to the genus *Rhizopus* in *Jiuqu* (Wang B. et al., 2018). Wang et al. (2020) reported that alpha-amylase and glucoamylase are positively related to starch hydrolysis and ethanol production. They also indicated that these key saccharifying enzymes are associated with alcoholic fermentation in *baijiu* fermentation. In contrast, the bacterial community exhibited a greater contribution to alcohol dehydrogenase (EC:1.1.1.1), essential for ethanol production during the production of fermented foods. Huang et al. (2020) found that *Lactobacillus acetotolerans* strongly contributed to alcohol dehydrogenase, and it positively correlates with the content of ethanol in the fermented grains. L-lactate dehydrogenase (EC:1.1.1.27) is required for lactate and acetate production. The gene abundance for this enzyme in the P5_CO sample's bacterial community was highest and had a higher abundance in saccharification's middle and late stages. LAB, including *Lactobacillus plantarum*, *Lactobacillus acetotolerans*, and *Lactobacillus brevis* are essential contributors to L-lactate dehydrogenase (Huang et al., 2020). In addition, specific sugars can promote the interactions of the core microbial community members and ethanol production in a simulative *baijiu* fermentation under laboratory, which are associated with the saccharifying enzymes from starters (Wang et al., 2021). In general, the saccharification process's fungal community is shaped by *Qu* and exhibited higher functional enzyme activity. Moreover, the activity of these enzymes in the bacterial community could contribute to flavor compounds' metabolism.

CONCLUSION

In summary, this study enhances our understanding of the relationship of the pretreatment and saccharification phase microbiota. Mainly the cooling raw material's and RH's bacterial community and *Qu's* fungal community exhibited an important contribution in shaping the microbiota of the saccharification process. *Lactobacillus* and *Weissella* were the dominant bacteria in the P5_CO and RH samples, and the *Rhizopus* genus was the most dominant fungi in the *Qu* sample; these microbes were leading contributors of functional enzymes throughout saccharification. Further research will explore the

contribution of the microbiota inhabiting the pretreatment and saccharification phases to the formation and accumulation of *fuyu*-flavor *baijiu* flavors and provide a strategy for better management of the traditional solid-state fermentation process.

DATA AVAILABILITY STATEMENT

The datasets presented in this study can be found in online repositories. The names of the repository/repositories and accession number(s) can be found in the article/ **Supplementary Material**.

AUTHOR CONTRIBUTIONS

JK and YH analyzed the data and wrote the manuscript. JK, XZ, and HL performed the experiments. BH and XZ proofread the revised manuscript. ZD, LY, JC, LF, HZ, and XZ provided experimental samples and financial support of this study. All authors contributed to manuscript revision and approved the submitted version.

FUNDING

This work was supported by the National Natural Science Foundation of China (Grant No. 31972975) and National Key Research and Development Program of China (Grant No. 2018YFC1604101).

SUPPLEMENTARY MATERIAL

The Supplementary Material for this article can be found online at: https://www.frontiersin.org/articles/10.3389/fmicb.2021.705967/full#supplementary-material

REFERENCES

Bolger, A. M., Lohse, M., and Usadel, B. (2014). Trimmomatic: a flexible trimmer for Illumina sequence data. *Bioinformatics* 30, 2114–2120. doi: 10.1093/bioinformatics/btu170

Bolyen, E., Rideout, J. R., Dillon, M. R., Bokulich, N. A., Abnet, C. C., Al-Ghalith, G. A., et al. (2019). Reproducible, interactive, scalable and extensible microbiome data science using QIIME 2. *Nat. Biotechnol.* 37, 852–857. doi: 10.1038/s41587-019-0209-9

Dong, W., Yang, Q., Liao, Y., Liu, Y., Hu, Y., Peng, N., et al. (2020). Characterisation and comparison of the microflora of traditional and pure culture xiaoqu during the baijiu liquor brewing process. *J. Inst. Brew.* 126, 213–220. doi: 10.1002/jib.597

Douglas, G. M., Maffei, V. J., Zaneveld, J. R., Yurgel, S. N., Brown, J. R., Taylor, C. M., et al. (2020). PICRUSt2 for prediction of metagenome functions. *Nat. Biotechnol.* 38, 685–688. doi: 10.1038/s41587-020-0548-6

Edgar, R. C. (2013). UPARSE: highly accurate OTU sequences from microbial amplicon reads. *Nat. Methods* 10, 996–998. doi: 10.1038/nmeth.2604

Fan, B., Xiang, L., Yu, Y., Chen, X., Wu, Q., Zhao, K., et al. (2020). Solid-state fermentation with pretreated rice husk: green technology for the distilled spirit (Baijiu) production. *Environ. Technol. Innov.* 20:101049. doi: 10.1016/j.eti.2020.101049

Hassani, A., Procopio, S., and Becker, T. (2016). Influence of malting and lactic acid fermentation on functional bioactive components in cereal-based raw materials: a review paper. *Int. J. Food Sci. Technol.* 51, 14–22. doi: 10.1111/ijfs.12965

Huang, X., Fan, Y., Lu, T., Kang, J., Pang, X., Han, B., et al. (2020). Composition and metabolic functions of the microbiome in fermented grain during light-flavor baijiu fermentation. *Microorganisms* 8:1281. doi: 10.3390/microorganisms8091281

Ibarruri, J., and Hernández, I. (2018). Rhizopus oryzae as fermentation agent in food derived sub-products. *Waste Biomass Valor.* 9, 2107–2115. doi: 10.1007/s12649-017-0017-8

Jin, G., Zhu, Y., and Xu, Y. (2017). Mystery behind Chinese liquor fermentation. *Trends Food Sci. Technol.* 63, 18–28. doi: 10.1016/j.tifs.2017.02.016

Li, R.-Y., Zheng, X.-W., Zhang, X., Yan, Z., Wang, X.-Y., and Han, B.-Z. (2018). Characterization of bacteria and yeasts isolated from traditional fermentation starter (Fen-Daqu) through a 1H NMR-based metabolomics approach. *Food Microbiol.* 76, 11–20. doi: 10.1016/j.fm.2018.03.015

Liu, C., Feng, S., Wu, Q., Huang, H., Chen, Z., Li, S., et al. (2019). Raw material regulates flavor formation via driving microbiota in Chinese liquor fermentation. *Front. Microbiol.* 10:1520. doi: 10.3389/fmicb.2019.01520

Liu, H., and Sun, B. (2018). Effect of fermentation processing on the flavor of Baijiu. *J. Agric. Food Chem.* 66, 5425–5432. doi: 10.1021/acs.jafc.8b00692

Liu, T., Kang, J., Liu, L., Hu, X., Wang, X., Li, X., et al. (2020). Microbial community diversity of traditional dough starter (Jiaozi) from two provinces in northwest China. *Ann. Microbiol.* 70:18. doi: 10.1186/s13213-020-01544-1

Magoc, T., and Salzberg, S. L. (2011). FLASH: fast length adjustment of short reads to improve genome assemblies. *Bioinformatics* 27, 2957–2963. doi: 10.1093/bioinformatics/btr507

Pang, X. N., Han, B. Z., Huang, X. N., Zhang, X., Hou, L. F., Cao, M., et al. (2018). Effect of the environment microbiota on the flavour of light-flavour baijiu during spontaneous fermentation. *Sci. Rep.* 8:3396. doi: 10.1038/s41598-018-21814-y

Pang, X. N., Huang, X. N., Chen, J. Y., Yu, H. X., Wang, X. Y., and Han, B. Z. (2020). Exploring the diversity and role of microbiota during material pretreatment of light-flavor Baijiu. *Food Microbiol.* 91:103514. doi: 10.1016/j.fm.2020.103514

Ren, Q., Sun, L., Sun, Z., Liu, Q., Lu, X., Li, Z., et al. (2019). Bacterial succession and the dynamics of flavor compounds in the Huangjiu fermented from corn. *Arch. Microbiol.* 202, 299–308. doi: 10.1007/s00203-019-01748-3

Rizo, J., Guillen, D., Farres, A., Diaz-Ruiz, G., Sanchez, S., Wacher, C., et al. (2020). Omics in traditional vegetable fermented foods and beverages. *Crit. Rev. Food Sci. Nutr.* 60, 791–809. doi: 10.1080/10408398.2018.1551189

Wang, B., Wu, Q., Xu, Y., and Sun, B. (2018). Specific volumetric weight-driven shift in microbiota compositions with saccharifying activity change in starter for Chinese baijiu fermentation. *Front. Microbiol.* 9:2349. doi: 10.3389/fmicb.2018.02349

Wang, B., Wu, Q., Xu, Y., and Sun, B. (2020). Synergistic effect of multi-saccharifying enzymes on alcoholic fermentation for Chinese baijiu production. *Appl. Environ. Microbiol.* 86:e00013-20. doi: 10.1128/AEM

Wang, B., Wu, Q., Xu, Y., and Sun, B. (2021). Multiple sugars promote microbial interactions in Chinese baijiu fermentation. *LWT* 138:110631. doi: 10.1016/j.lwt.2020.110631

Wang, X., Du, H., Zhang, Y., and Xu, Y. (2018). Environmental microbiota drives microbial succession and metabolic profiles during Chinese liquor fermentation. *Appl. Environ. Microbiol.* 84:e02369-17. doi: 10.1128/AEM.02369-17

Wu, H., Zhang, S., Ma, Y., Zhou, J., Luo, H., and Yang, J. (2017). Comparison of microbial communities in the fermentation starter used to brew Xiaoqu liquor. *J. Inst. Brew.* 123, 113–120. doi: 10.1002/jib.388

Wu, Q., Chen, L., and Xu, Y. (2013). Yeast community associated with the solid state fermentation of traditional Chinese Maotai-flavor liquor. *Int. J. Food Microbiol.* 166, 323–330. doi: 10.1016/j.ijfoodmicro.2013.07.003

Wu, X., and Fan, L. (2009). Characteristic production techniques of heavy perfume liquor. *Liquor Mak. Sci. Technol.* 175, 74–75. doi: 10.13746/j.njkj.2009.01.018

Yin, X., Yoshizaki, Y., Ikenaga, M., Han, X. L., Okutsu, K., Futagami, T., et al. (2020). Manufactural impact of the solid-state saccharification process in rice-flavor baijiu production. *J. Biosci. Bioeng.* 129, 315–321. doi: 10.1016/j.jbiosc.2019.09.017

Zhadyra, S., Han, X., Anapiyayev, B. B., Tao, F., and Xu, P. (2021). Bacterial diversity analysis in Kazakh fermented milks shubat and ayran by combining culture-dependent and culture-independent methods. *LWT* 141:110877. doi: 10.1016/j.lwt.2021.110877

Zheng, X.-W., and Han, B.-Z. (2016). Baijiu (白 酒), Chinese liquor: history, classification and manufacture. *J. Ethn. Foods* 3, 19–25. doi: 10.1016/j.jef.2016.03.001

Zheng, X.-W., Tabrizi, M. R., Robert Nout, M. J., and Han, B.-Z. (2011). Daqu–a traditional Chinese liquor fermentation starter. *J. Inst. Brew.* 117, 82–90. doi: 10.1002/j.2050-0416.2011.tb00447.x

Zheng, X. W., Yan, Z., Han, B. Z., Zwietering, M. H., Samson, R. A., Boekhout, T., et al. (2012). Complex microbiota of a Chinese "Fen" liquor fermentation starter (Fen-Daqu), revealed by culture-dependent and culture-independent methods. *Food Microbiol.* 31, 293–300. doi: 10.1016/j.fm.2012.03.008

Zheng, X. W., Yan, Z., Nout, M. J., Smid, E. J., Zwietering, M. H., Boekhout, T., et al. (2014). Microbiota dynamics related to environmental conditions during the fermentative production of Fen-Daqu, a Chinese industrial fermentation starter. *Int. J. Food Microbiol.* 182, 57–62. doi: 10.1016/j.ijfoodmicro.2014.05.008

Conflict of Interest: ZD, HL, and XZ were employed by the company Nutrition & Health Research Institute, COFCO Corporation. LY, JC, LF, HZ, and XZ were all employed by Jiugui Liquor Co., Ltd.

The remaining authors declare that the research was conducted in the absence of any commercial or financial relationships that could be construed as a potential conflict of interest.

Publisher's Note: All claims expressed in this article are solely those of the authors and do not necessarily represent those of their affiliated organizations, or those of the publisher, the editors and the reviewers. Any product that may be evaluated in this article, or claim that may be made by its manufacturer, is not guaranteed or endorsed by the publisher.

frontiers in Microbiology

ORIGINAL RESEARCH
published: 31 August 2021
doi: 10.3389/fmicb.2021.718261

Succession of Fungal Communities at Different Developmental Stages of Cabernet Sauvignon Grapes From an Organic Vineyard in Xinjiang

Lihua Zhu, Tian Li, Xiaoyu Xu, Xuewei Shi and Bin Wang**

Food College, Shihezi University, Shihezi, China

Fungi present on grape surface considerably impact grape growth and quality. However, information of the fungal community structures and dynamics on the worldwide cash crop, the Cabernet Sauvignon grape, from the budding to ripening stages remains limited. Here, we investigated the succession of fungal communities on Cabernet Sauvignon grapes from an organic vineyard in Xinjiang, China at different developmental stages *via* high-throughput sequencing combined with multivariate data analysis. In total, 439 fungal amplicon sequence variants (ASVs) from six phyla were identified. The fungal communities differed over the budding to the berry stages. Moreover, *Aspergillus*, *Malassezia*, *Metschnikowia*, and *Udeniomyces* were predominant during the unripe stage, whereas *Erysiphe*, *Cryptococcus*, *Vishniacozyma*, and *Cladosporium* were dominant in the ripe stages. Notably, *Vishniacozyma* was the most abundant genus, conserved in all development stages. Moreover, network analysis resulted in 171 edges—96 negative and 75 positive. Moreover, fungal genera such as *Vishniacozyma*, *Sporobolomyces*, *Aspergillus*, *Alternaria*, *Erysiphe*, *Toxicodendron*, and *Metschnikowia* were present in the hubs serving as the main connecting nodes. Extensive mutualistic interactions potentially occur among the fungi on the grape surface. In conclusion, the current study expounded the characteristics of the Cabernet Sauvignon grape fungal community during the plant growth process, and the results provided essential insights into the potential impacts of fungal communities on grape growth and health.

Keywords: Cabernet Sauvignon grape, fungi community, Illumina high-throughput sequencing, ripening process, organic vineyard

OPEN ACCESS

Edited by:
Xucong Lv,
Fuzhou University, China

Reviewed by:
Di Liu,
The University of Melbourne, Australia
Yanlun Ju,
Northwest A&F University, China
Zhigang He,
Fujian Academy of Agricultural Sciences, China

****Correspondence:***
Bin Wang
binwang0228@shzu.edu.cn
Xuewei Shi
shixuewei@shzu.edu.cn

Specialty section:
This article was submitted to Food Microbiology, a section of the journal Frontiers in Microbiology

Received: *31 May 2021*
Accepted: *28 July 2021*
Published: *31 August 2021*

Citation:
Zhu L, Li T, Xu X, Shi X and Wang B (2021) Succession of Fungal Communities at Different Developmental Stages of Cabernet Sauvignon Grapes From an Organic Vineyard in Xinjiang. Front. Microbiol. 12:718261. doi: 10.3389/fmicb.2021.718261

INTRODUCTION

Wine is a traditional alcoholic beverage fermented from various fruits and vegetables, particularly grapes. According to the time of fermentation, grape varieties, and grape color, wine can be classified into red, rose, and white (Swami et al., 2014). Moreover, the classic dry red wine is the most popular wine worldwide, with the largest production and sales volumes. The grapes used to make dry red wine mainly include Cabernet Sauvignon (*Vitis vinifera* L.), Merlot, Cabernet Franc, and Syrah (Rajha et al., 2017). In particular, Cabernet Sauvignon, originating from the Bordeaux region of France (Bowers and Meredith, 1997), is currently the most famous and important red grape variety; it also is widely cultivated in China because of its strong adaptability and the premium-quality wines that it produces (Jiang and Zhang, 2012).

Yeast colonizing on grapes have been widely investigated for their impact on wine quality and flavor complexity (Capozzi et al., 2015). Research has also focused on a series of plant pathogenic fungi that affect grapes, including *Erysiphe necator*, *Botrytis cinerea*, and *Plamospara viticola*—the causative agents of grapevine powdery mildew, gray rot, and downy mildew, respectively. In addition, grapes may bear saprophytic molds such as *Aspergillus* spp., *Cladosporium* spp., and *Penicillium* spp., which are directly responsible for several grape rots and are indirectly involved in food spoilage because they produce mycotoxins (Martins et al., 2014). These fungi are unable to grow in wines, and their effect on wine quality is due to grape damage.

The grape berry surface is, nevertheless, an unstable habitat of microorganisms. Diversity and stability of the aforementioned indigenous yeasts on the surface of grape are strongly associated with numerous factors, such as vineyard geography (altitude, latitude, and longitude) (Gao et al., 2019), climatic conditions (rain, temperature, humidity, and maturity period) (Liu et al., 2019), grape variety (Zhang et al., 2019), and viticultural practice (herbicides, fertilizers, pesticides, and fungicides used) (Cadez et al., 2010). It is reported that the berry development process contributes to changes in the composition and structures of fungal populations on grapes (Carmichael et al., 2017; Kioroglou et al., 2019). In particular, microbial community, especially fermentative yeasts, significantly increased at harvest and not in the early fruit developmental stage (Renouf et al., 2005).

Xinjiang Uygur Autonomous Region of China is a world-renowned wine-producing area due to the unique climate and geographical characteristics. As the primary red grape cultivars, Cabernet Sauvignon has been widely used to ferment premium-quality red wines globally (Bowers and Meredith, 1997; Radovanović and Radovanović, 2010). Recent research has shown that indigenous microorganisms, especially fungal communities, are key in grapevine health and growth (Novello et al., 2017). Although microbial communities in the microenvironment and fermentation process have been investigated, fungal community succession during Cabernet Sauvignon grape development warrants further research.

In the present study, we investigated the dynamic changes in fungal communities during the ripening stages through high-throughput sequencing combined with multivariate data analysis. In particular, the fungal communities of Cabernet Sauvignon grapes from an organic vineyard in Xinjiang at different developmental stages were characterized. Our results lay the foundation for research on the fungal community on Cabernet Sauvignon grapes and provides insights into fungal community structures and their potential role in grape growth and health during its agricultural production.

MATERIALS AND METHODS

Grape Sampling

Cabernet Sauvignon grapes used in this study were collected from the vineyard of the professional winery Great Wall Wine in Xinjiang, China (86°03′E, 45°19′N) in 2020. Because of a dry continental climate, grapes grown in this region have few diseases originating from microorganisms or pest. The study vineyard is commercially managed under the principles of organic farming by the winery. No chemical fertilizers or insecticides are applied for pest or disease control within the grape growing season, and weeds are controlled via manually weeding every month.

To evaluate changes in the fungal communities during the grape maturation process, Cabernet Sauvignon grape berries were collected using sterile scissors at the following development stages based on the modified Eichhorn–Lorenz (E-L) system (Coombe, 1995): before flowering (A, E-L stage 19), fruit set (B, E-L stage 27), berries pea size (C, E-L stage 31), berries still hard and green (D, E-L stage 33), berries begin to color (E, E-L stage 35), berries not quite ripe (F, E-L stage 37), and completely ripe (G, E-L stage 38). Three biological replicates were sampled for each developmental berry stage, and each replicate was collected from five sample points of the vineyard. Considering the heterogeneity of the tested grapes, the berries were collected from the upper, central, and lower part of cluster at each sample point, both from the sun-exposed and shaded side. In total, 21 wine grape samples were collected. These grape samples were placed in sterilized plastic bags and then into cool boxes, immediately shipped back to the laboratory, and stored at −80°C before molecular analysis.

Genomic DNA Extraction and Amplification

After thawing for 30 min at 28°C, 20 g of healthy, undamaged berries were placed in sterile flasks with 40 ml of sterile water and subjected to orbital shaking at 150 rpm for 1 h. The suspension was separated from the berries by vacuum filtration using a 0.22-μm filter. Next, the sediment filtered were used for the extraction of total genome DNA using the CTAB/SDS method (Yu et al., 2019). The DNA concentration and purity were monitored using 1% agarose gel electrophoresis and a NanoDrop 2000 Spectrophotometer. The DNA was diluted to l μg/μl with sterile water and used as a template for polymerase chain reaction (PCR) amplification. The internal transcribed spacer (ITS) primer pair—namely ITS1f (5′-CTTGGTCATTTAGAGGAAGTAA-3′) and ITS2 (5′-GCTGCGTTCTTCATCGATGC-3′)—was used to amplify the partial fungal ITS region to assess fungal communities (Hamad et al., 2017). All PCR reaction systems were conducted in using a 30 μl volume, including 15 μl of Phusion High-Fidelity PCR Master Mix (New England Biolabs), 0.2 μM of the forward and reverse primers, and approximately 10 ng of template DNA. Thermal cycler conditions consisted of an initial denaturation at 98°C for 1 min, followed by 30 cycles of 98°C for 10 s, 50°C for 30 s, and 72°C for 30 s and a final extension at 72°C for 5 min.

PCR Product Purification and Library Preparation

The PCR products were mixed with the same volume of 1× loading buffer (containing SYB green), which were then detected *via* 2% agarose gel electrophoresis. Then, the PCR products were mixed in equimolar ratios and purified using a Qiagen Gel Extraction Kit (Qiagen, Germany) (Zetsche et al., 2017).

Sequencing libraries were generated using a TruSeq DNA PCR-Free Sample Preparation Kit (Illumina, United States) following the manufacturer's recommendations, and index codes were added (Nones et al., 2014). The library quality was evaluated on a Qubit@2.0 Fluorometer (Thermo Scientific) and an Agilent Bioanalyzer 2100 system (Kao et al., 2016). Finally, the library preparations were sequenced on an Illumina NovaSeq platform with 250-bp paired-end reads generated.

Bioinformatic Analyses

Paired-end reads were assigned to samples according to their unique barcodes and then truncated by removing barcodes and primer sequences. The paired-end reads were then merged using FLASH (Magoč and Salzberg, 2011). Quality filtering of the raw tags was performed under specific conditions to obtain the high-quality clean tags according to the QIIME quality control process (Bokulich et al., 2013). The tags were compared with a reference database using the UCHIME algorithm (Edgar et al., 2011) to detect chimera sequences, which were subsequently removed, and effective tags were obtained (Haas et al., 2011).

Sequence analyses of the clean tags were performed using Divisive Amplicon Denoising Algorithm 2 (DADA2; version 1.6.0) in R (version 3.3.4) (Callahan et al., 2016). Within DADA2, sequences were subjected to filtering, de-replication, and further filtering by using the sample inference algorithm and learned error rates within the DADA2 pipeline. The paired-end reads were merged using standard arguments, and chimeric sequences were filtered out.

Taxonomy was assigned using the Unite database (version 10.10.2017). The DADA2 method created an amplicon sequence variant [Amplicon sequence variants (ASVs); similar to operational taxonomic units, but with the ability to resolve amplicons to a single nucleotide], enabling species-level identification when 100% of the sequences matched the reference.

Statistical Analyses

Operational taxonomic unit-level alpha diversity indices, including Chao1 richness estimator, Shannon diversity index, Simpson index, and Abundance-based Coverage Estimator (ACE) metric, were measured using the ASV table in QIIME. Rarefaction curves were plotted to investigate sequencing depth. The microbial community distribution patterns among different growth stages were analyzed using principal components analysis (PCA) based on beta diversity by using Simca (version 14.1). Amplicon sequence variants aggregates and intersections between the seven grape stages were visualized graphically on R (version 2.15.3) with the UpSet package. Hierarchical cluster analysis and heatmap construction were also performed using R (version 2.15.3) with the heatmap package. The similarities and differences in the composition and structures of the different samples are shown using the corrplot package in R. A linear discriminant analysis effect size (LEfSe) was applied to estimate discriminant fungal clades using The Huttenhower Lab website[1]. In addition, based on an LDA score (log10) of >2.0, the significantly enriched fungal groups were screened via linear discriminant analysis (LDA). Furthermore, network analysis based on Pearson's correlation coefficient (r) of >0.8 or <-0.3 between two genera was performed and visualized using Gephi (version 0.9.2).

[1]http://huttenhower.org/galaxy

RESULTS

Richness and Diversity Assessment

High-throughput sequencing was used to assess fungal communities present on grape surface at different ripening stages (**Figure 1**). In total, 644,112 fungal sequences were obtained from 21 samples at seven different mature stages. Of the fungal sequences, 439 unique fungal ASVs were detected. The ASVs belonged to 6 phyla, 25 classes, 51 orders, 83 families, and 121 genera. The rarefaction curves tended to be flat, indicating that the sequencing results adopted were sufficient to reflect the whole fungal diversity (**Supplementary Figure 1**).

Alpha Diversity Analysis

The alpha diversity was analyzed using the Shannon, Simpson, ACE, Chao, and richness indices, which represent the fungal community richness and diversity (**Table 1**). Among the present diversity indices, the richness, Chao1, and ACE indices increased and then decreased after the growth process changed. Among all growth stages, the A stage had the highest Shannon index but the lowest Simpson diversity index, indicating a high diversity in a fungal community. In addition, compared with the samples from other developmental stages, D time points had higher-than-expected species community richness, based on the richness indices (e.g., richness, Chao1, and ACE), but not diversity, based on the Simpson index. The C stage had significantly greater richness than did the A and B stages, based on the richness, Chao, and ACE indices. However, the richness, Chao, and ACE index values for the A, B, F, and G stages were similar. Therefore, fungal community richness and diversity exhibited a correlation with the growth process, and differences were observed according to the alpha diversity indexes.

Beta Diversity Analysis

To compare significant differences and understand clustering of samples between the groups, beta diversity was investigated *via* PCA. PC1 and PC2 accounted for 43.2% and 19.9% of the variance, respectively (**Figure 2**). The samples from the same developmental stages tended to cluster well together. In the PCA score plot, samples from different ripening stages could be divided into three different categories. Moreover, the score plot deriving from the PCA highlighted that A, B, and C stages were located at the negative side of PC1, whereas the B stage was located in the negative side of the PC2. All the sample groups were clustered together during the A and C stages, and the distance from the B stage was scattered—indicating that the differences were obvious between the B stage and the A and C stages. The four late time points (i.e., D, E, F, and G) related samples were clustered into one group located on the positive side of the PC1.

Notably, the D stage was found to be a key stage of diversity changes in grape-associated fungi. The PCA of grape-related

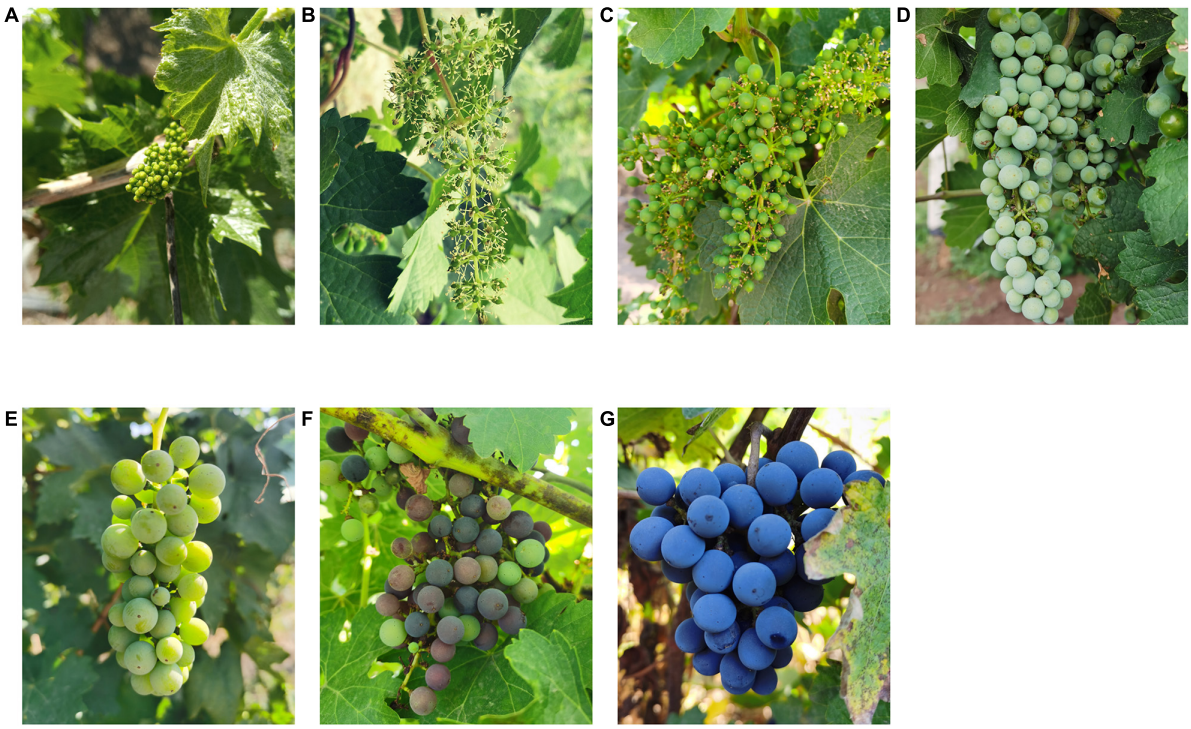

FIGURE 1 | Appearance changes of Cabernet Sauvignon grape at different growth stages. **(A)** before flowering; **(B)** fruit set; **(C)** berries pea size; **(D)** berries still hard and green; **(E)** the beginning of the berry ripening; **(F)** berries not quite ripe; **(G)** harvest ripe.

TABLE 1 | Abundance and diversity indexes of fungi communities on the surface of wine grapes at seven different growth stages.

Sample	Richness	Chao1	ACE	Shannon	Simpson
A	95.33 ± 15.50	110.69 ± 23.98	115.01 ± 27.86	2.73 ± 0.08	0.14 ± 0.01
B	117.67 ± 21.94	183.51 ± 17.75	192.24 ± 14.19	2.40 ± 0.32	0.21 ± 0.08
C	162.67 ± 17.95	199.46 ± 20.23	207.40 ± 14.55	2.64 ± 0.14	0.18 ± 0.02
D	185.33 ± 2.29	229.74 ± 32.47	215.07 ± 20.64	2.46 ± 0.10	0.18 ± 0.02
E	154.00 ± 40.04	196.15 ± 43.86	201.91 ± 53.52	2.24 ± 0.20	0.22 ± 0.03
F	110.67 ± 6.03	153.25 ± 19.10	150.12 ± 8.25	2.11 ± 1.17	0.19 ± 0.01
G	129.00 ± 5.20	161.00 ± 10.99	171.14 ± 1.75	2.32 ± 0.06	0.14 ± 0.01

The values in the table are shown as the mean ± standard deviation; the different lowercase letters express significant differences among different ripening stages in the 95% confidence interval. (A: before flowering; B: fruit set; C: berries pea size; D: berries still hard and green; E: the beginning of the berry ripening; F: berries not quite ripe; G: harvest ripe).

fungal at different growth stages showed that different growth times may contribute to the differentiation of fungal composition. Moreover, the fungal community structure of the grape epidermis was gradually established at the D stage.

ASV-Based UpSet View

To visualize unique ASVs and those shared between different developmental stages, an UpSet plot was created (**Figure 3**). In an UpSet plot, a single point represents a unique species in each natural growth stage of grapes. According to the current results, 29, 23, 40, 5, 1, and 4 ASVs were uniquely present at the A, B, C, D, E, and G stages, respectively. Most ASVs ($n = 40$) on the skin of grapes were present at the C stage. At the same time, the C stage shared 6, 4, 5, and 1 fungal ASV with the A, B, D, and E stages, respectively. In total, 10 ASVs—accounting for 2.72% of the total ASVs—were shared by the samples from the seven growth periods, indicating that whole periods had a low similar level of fungal diversity. Two fungal ASVs were shared at the early developmental stages (i.e., A, B, and C stages), and two ASVs were shared at the later developmental stages (i.e., D, E, F, and G stages). Consequently, the differences of grape epiphytic fungal community structures were found to be primarily controlled by the grape mature stage.

Dynamics of Fungal Community at Grapes Phenological Stages

To examine the similarities and differences between samples from different developmental stages, a correlation heatmap was

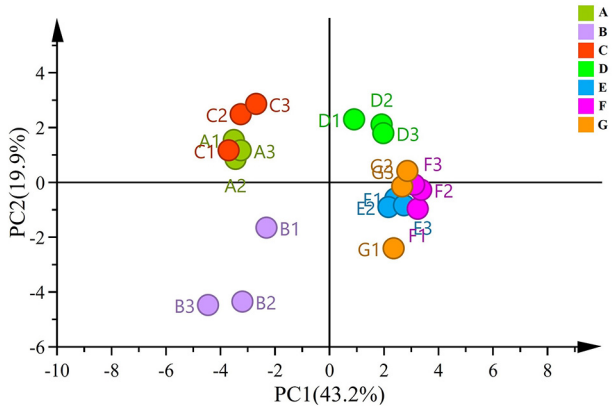

FIGURE 2 | PCA plots based on unweighted UniFrac distance metrics for fungal communities.

generated on the basis of the Bray–Curtis distance (**Figure 4**). Systematic cluster analysis illustrated that the correlation of samples collected between the three early growth stages (i.e., A, B, and C) and the four later growth stages (i.e., D, E, F, and G) was small, whereas the grape samples collected within the same or similar ripening stage had relatively strong correlations. The results showed that the correlation of the fungal community in the late developmental stage was higher than that in the early developmental stage.

Grape fungal community compositions evolved over time. At the phylum level, most significant was the massive colonization of the grapes by *Basidiomycota*, which increased as the development stage proceeded; their abundance reached 77% at the G stage. The second highest abundance was shown by *Anthophyta* (43%) in the E stage. In contrast, the low abundance was demonstrated by *Ascomycota* (41%) in the B stage (**Figure 5** and **Supplementary Figure 2**). At the genus level, the dominant taxa found included representatives of the genera *Neocamarosporium*, *Aspergillus*, *Alternaria*, *Malassezia*, *Vishniacozyma*, *Erysiphe*, *Penicillium*, *Thyrostroma*, *Metschnikowia*, and *Udeniomyces* (**Figure 6**). Of these, *Penicillium* and *Thyrostroma* mainly appeared at the early phenological stages and finally became undetectable at harvest, whereas *Vishniacozyma* remained the most abundant yeast in grape berries along with several grape spoilage fungi such as *Erysiphe* and *Aspergillus* throughout all the developmental stages. The relative abundances of *Erysiphe* reached a maximum (28%) in the E stage and a minimum (1%) in the G stage. Notably, the relative abundance of *Vishniacozyma* tended to increase and reach a maximum at harvest time. In contrast, the abundance of

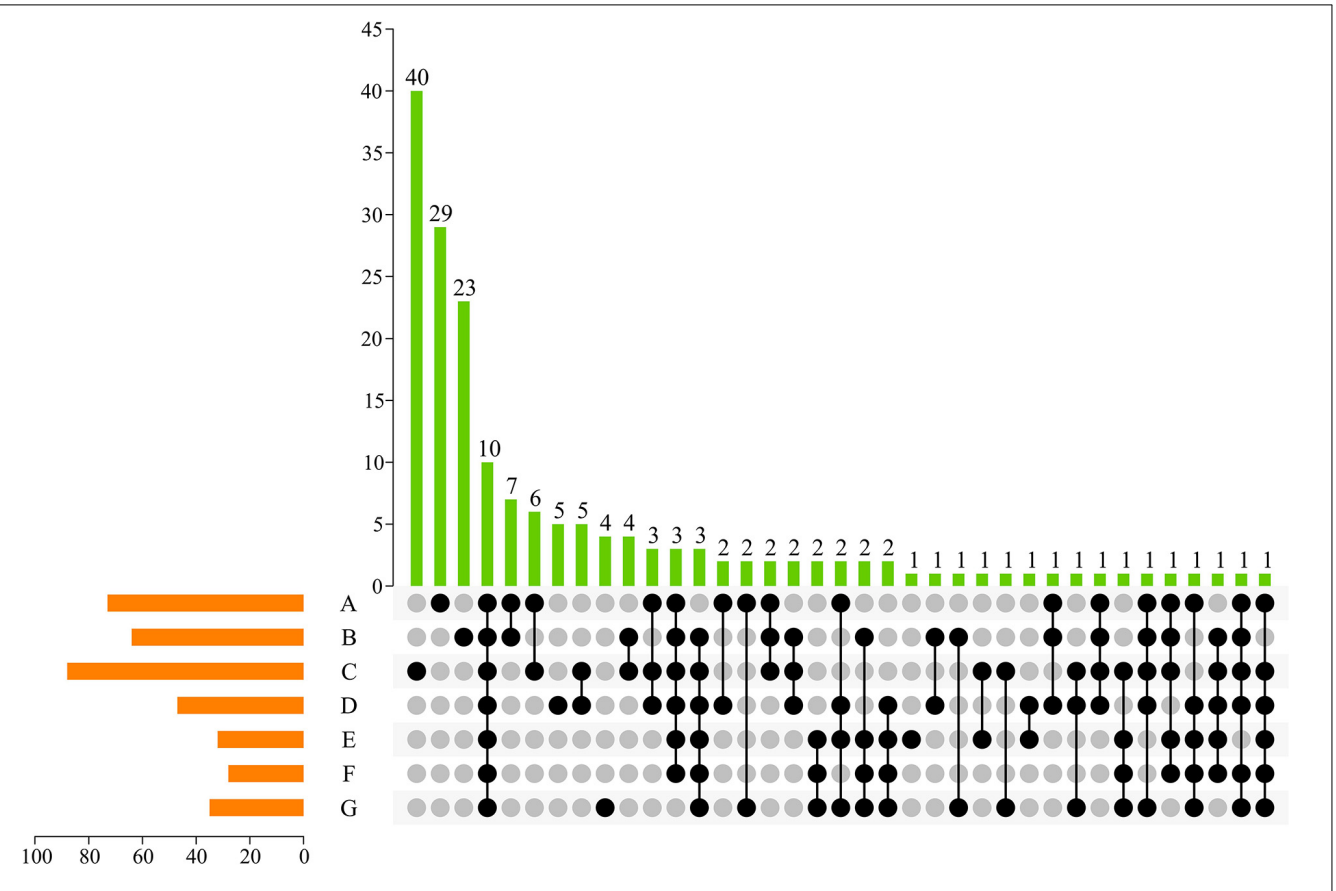

FIGURE 3 | UpSet plot of ASVs of fungal communities in different growing periods. Dark circles indicated samples with containing accessions and connecting bar indicated multiple overlapping samples.

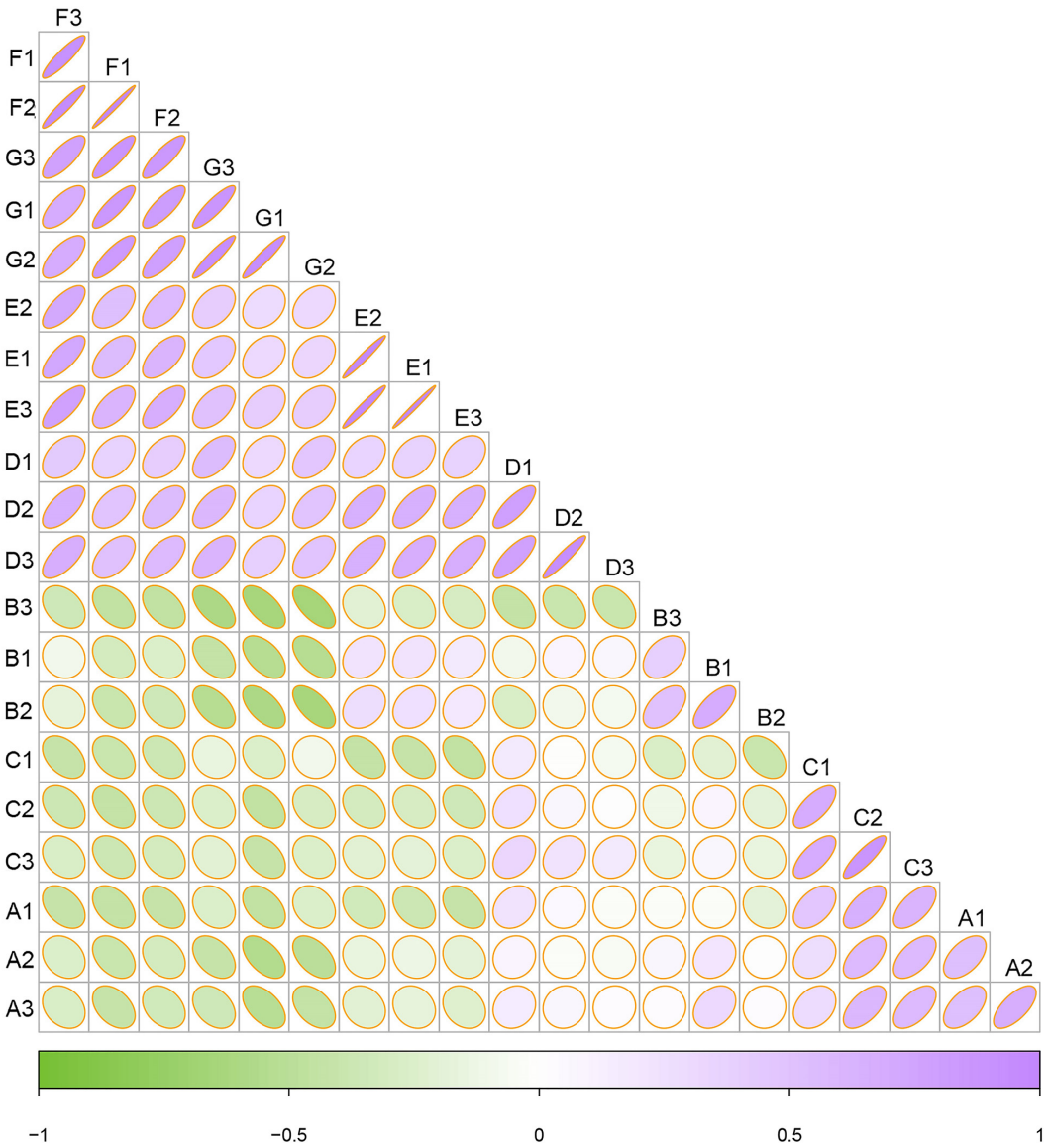

FIGURE 4 | Heatmap of fungal communities based on Bray–Curtis distance indices. Clustering of samples based on Bray–Curtis distance indices was calculated by ASVs at a distance of 3%. Color from green to purple indicated increased similarity. The radian of the fan corresponds to the correlation.

Malassezia and Aspergillus decreased during grape ripening, and these fungi were more highly abundant at the first ripening stage that at other stages.

Some of the fungi detected here—namely, *Alternaria*, *Metschnikowia*, and *Udeniomyces*—have been previously described to be present on grape surfaces; some of them are even known to be inhabitants of grapes. The results showed that the yeast diversity generally tends to be poor, and the dominant species become increasingly prominent as the berries' expansion and development progresses.

Cluster Analysis

Using the species annotation and abundance results obtained from all the samples at the genetic level, the genus with the top 35 abundance were selected; the species and samples were then clustered based on the abundance information of samples and a heatmap was generated (**Figure 7**). The use of a heatmap allows for intuitively determining changing patterns are more or less concentrated in which taxa (or group) in the samples. The composition of fungi in the samples at different sampling times differed considerably. A large gap between the C stage and the other stages was reflected by the color gradient and similarity. Moreover, most of the identified genera belonged to the phyla of *Ascomycota* and *Basidiomycota*. The D stage had the highest alpha diversity index (the richness, Chao1, and ACE index), containing mainly *Rhodotorula*, *Thyrostroma*, *Archaeorhizomyces*, *Dematiopleospora*, and *Ampelomyces*. *Malassezia*, *Aspergillus*, *Buckleyzyma*, *Chaetomium*, *Neoetophoma*, *Alternaria*, and

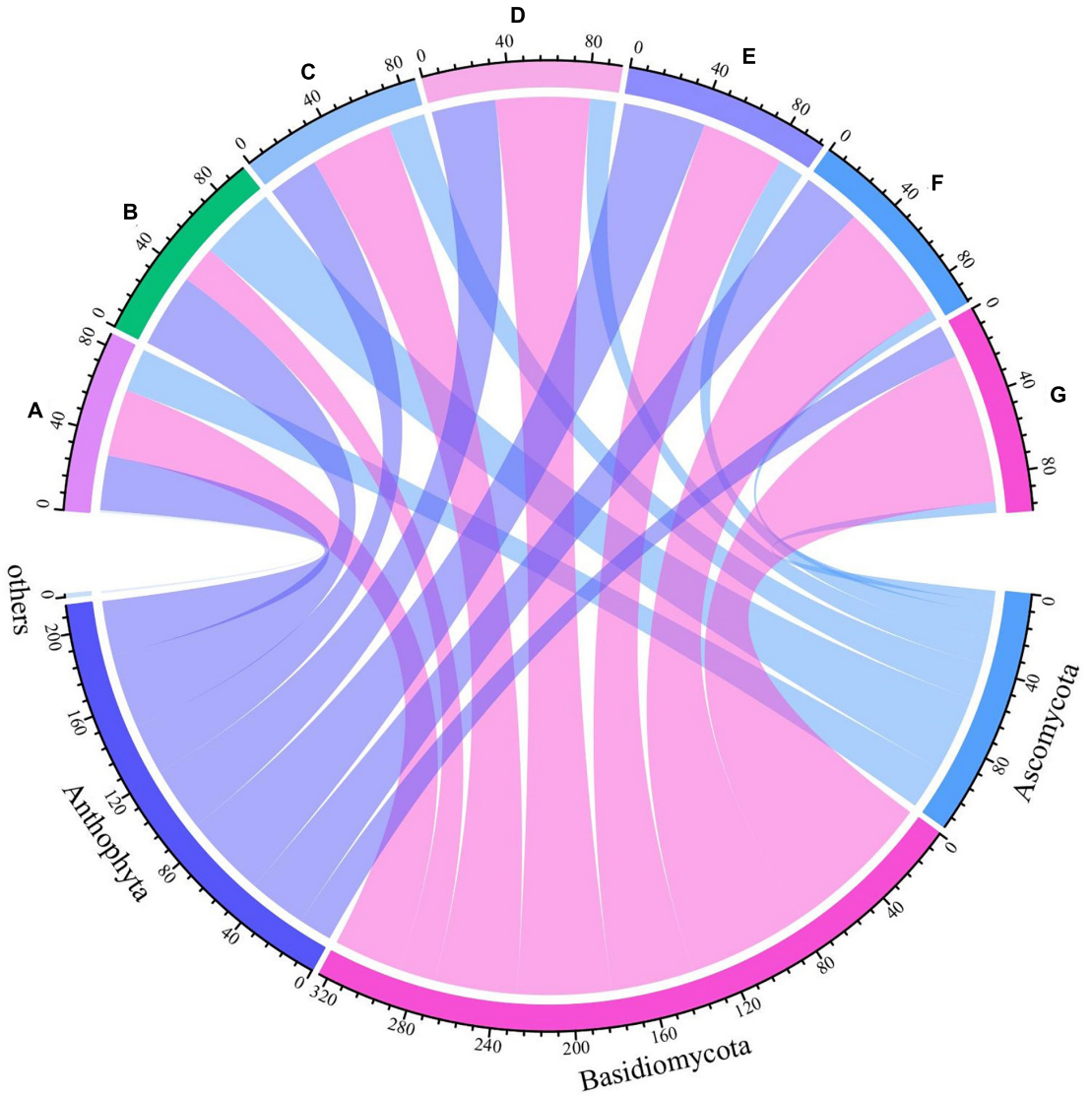

FIGURE 5 | Differences in fungal communities on Cabernet Sauvignon grapes at different growth stages at the phylum levels.

Neocamarosporium were the dominant genera at the A stage. At the C stage, *Camarosporidiella*, *Stachys*, *Phaeococcomyces*, *Cystobasidium*, *Elasticomyces*, *Cladosporium*, *Chaetomium*, *Neocamarosporium*, *Alternaria*, and *Undeniomyces* were the primary genera. At the E stage, the most abundant sequences were related to *Ampelomyces*, *Dematiopleospora*, *Archaeorhizomyces*, *Throstroma*, and *Rhodotorula*. Notably, *Cystofilobasidium*, *Vishniacozyma*, *Rhodosporidiobolu*, and *Ganoderma* were dominant in the G stage.

Biomarker Discovery

Here, we used the LDA effect size (LEfSe) to recognize the significant biomarkers among fungal taxa in different phenological stages of Cabernet Sauvignon grapes. The LEfSe of all species demonstrated 63 fungal taxa with significant differences among the different developmental stages at an LDA threshold of 2.0, namely, 3 phyla, 11 classes, 14 orders, 17 families, and 18 genera (**Figure 8**). In total, 13 fungal classes were significantly enriched in the A stage—including *Malasseziomycetes*, *Dothideomycetes*, and *Aureobasidium*. Seven fungal classes were significantly enriched at the B stage—including *Ascomycota*, *Aspergillaceae*, and *Eurotiales*. Nine fungal groups were significantly enriched at the C stage—including *Valsaceae* and *Holtermanniales*. Four fungal groups were significantly enriched at the D stage. Moreover, 14 fungal groups were significantly enriched at the E stage—including *Anthophyta*, *Dioscoreales*, and *Cystobasidiomycetes*—and 7 fungal groups were significantly enriched at the F stage. Nine fungal groups were significantly enriched at the G stage—including *Basidiomycota*, *Cystofilobasidiales*, and *Tremellomycetes*.

Thus, from the flowering begin to mature stages, wine grape microbiota can be distinguished at least at the phylum and

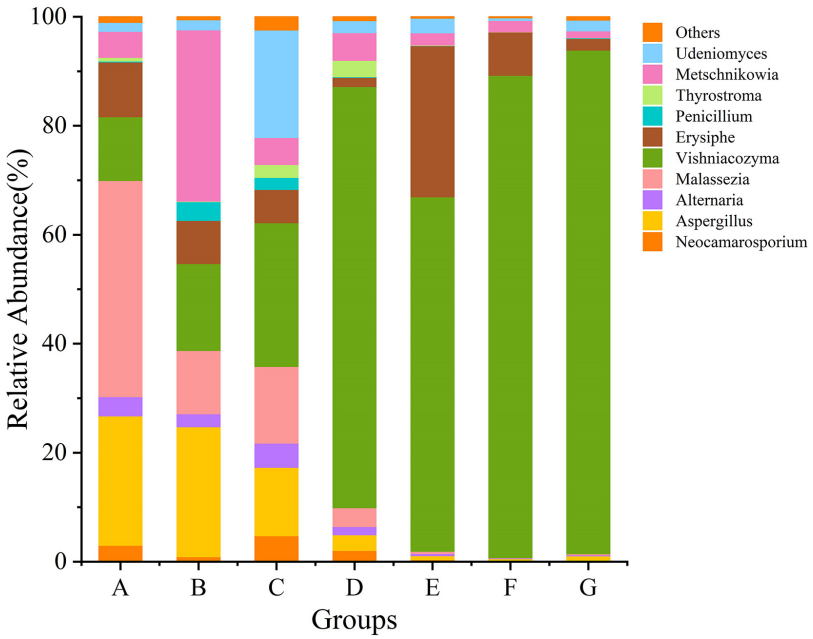

FIGURE 6 | The relative abundance of fungal communities at the genus level.

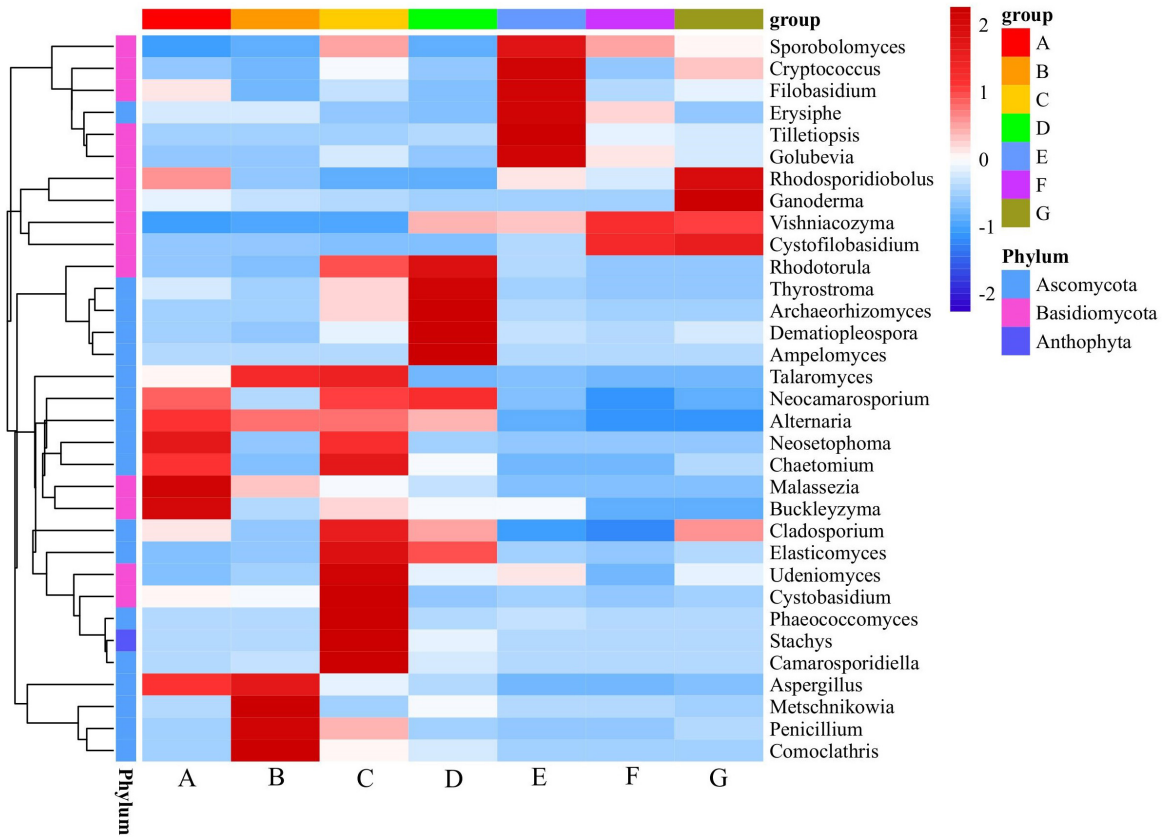

FIGURE 7 | Heatmap of top 35 abundant genera of fungal communities at different developmental stages. Samples are clustered according to the similarity among their constituents and arranged in a horizontal order. In the figure, red represents the more abundant genera in the corresponding group and blue represents the less abundant genera.

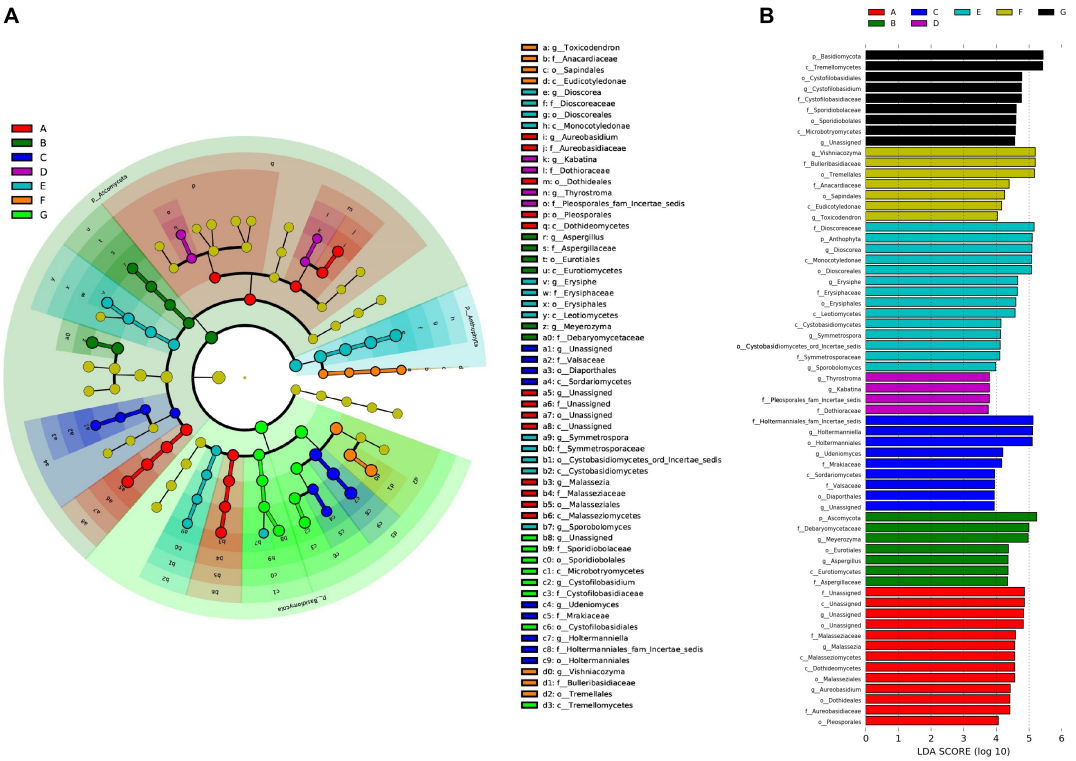

FIGURE 8 | Linear discriminant analysis (LDA) and effect size (LEfSe). **(A)** The bar charts report the taxonomic representation statistically and biologically as determined by LEfSe analysis; **(B)** the linear discriminant analysis (LDA) value distribution histogram.

class levels by their demonstrative microorganisms—with the exception of the D stage, where the distinction is limited to the family level.

Co-occurrence Analyses for Relationships Among Different Microbes

Fungal interactions—usually reflected by co-occurrence correlations—are considered an important factor underpinning the fungal community structures. In the present study, Pearson's correlation coefficients were estimated to investigate the potential beneficial or antagonistic relationships among different fungal genera of grape surfaces. In total, 171 dominant fungal genera were used for co-occurrence network analysis after the unclassified and relatively low abundance genera were removed (**Figure 9**). The generated networks consisted of 96 nodes and 171 edges; here, the nodes represented fungal genera, and the edges represented the positive (green, Pearson's $r > 0.8$) or negative (purple, Pearson's $r < -0.3$) correlations between pairs of genera. The larger the size of the node, the more important is the genera in the fungal community. Based on the network connectivity statistics, fungal genera such as *Vishniacozyma*, *Sporobolomyces*, *Aspergillus*, *Alternaria*, *Erysiphe*, *Toxicodendron*, and *Metschnikowia* were among the hubs that served as the main connecting nodes. Simultaneously, *Vishniacozyma*, *Udeniomyces*, *Aspergillus*, and *Alternaria* were negatively correlated with almost all other fungal genera, whereas *Ampelomyces*, *Rhodotorula*, and *Dematiopleospora* were positively correlated with almost all other fungal genera. In addition, *Metschnikowia* was negatively correlated with *Naganishia* but positively correlated with *Trichoderma*. Notably, the correlation analysis results indicated that *Erysiphe* was correlated positively with *Golubevia*, *Symmetrospora*, and *Tillctiopsis* but negatively with *Neocamarosporium* and *Aspergillus*. A positive correlation was observed between *Pichia* and *Malassezia*.

DISCUSSION

A considerable amount of attention has been focused on the microbial communities associated with wine grapes. However, the changes in the microorganisms inhabiting the grape surface are dynamic over space and time. Previous research has only focused on the harvest-to-ripe stages with a culture-dependent approach; consequently, little is known about the diversity and dynamics among epiphytic fungal communities present on wine grape surfaces across their developmental stages. The culture-independent microbiota studies have provided a reference framework for microbial population diversity and composition on wine grapes and captured the temporal fungal microbial shifts during the phenological stages—as a result increasing the understanding of grape-associated microbial communities. The current study is a very important step into further evaluation of the contributions of microorganisms in the functioning of the

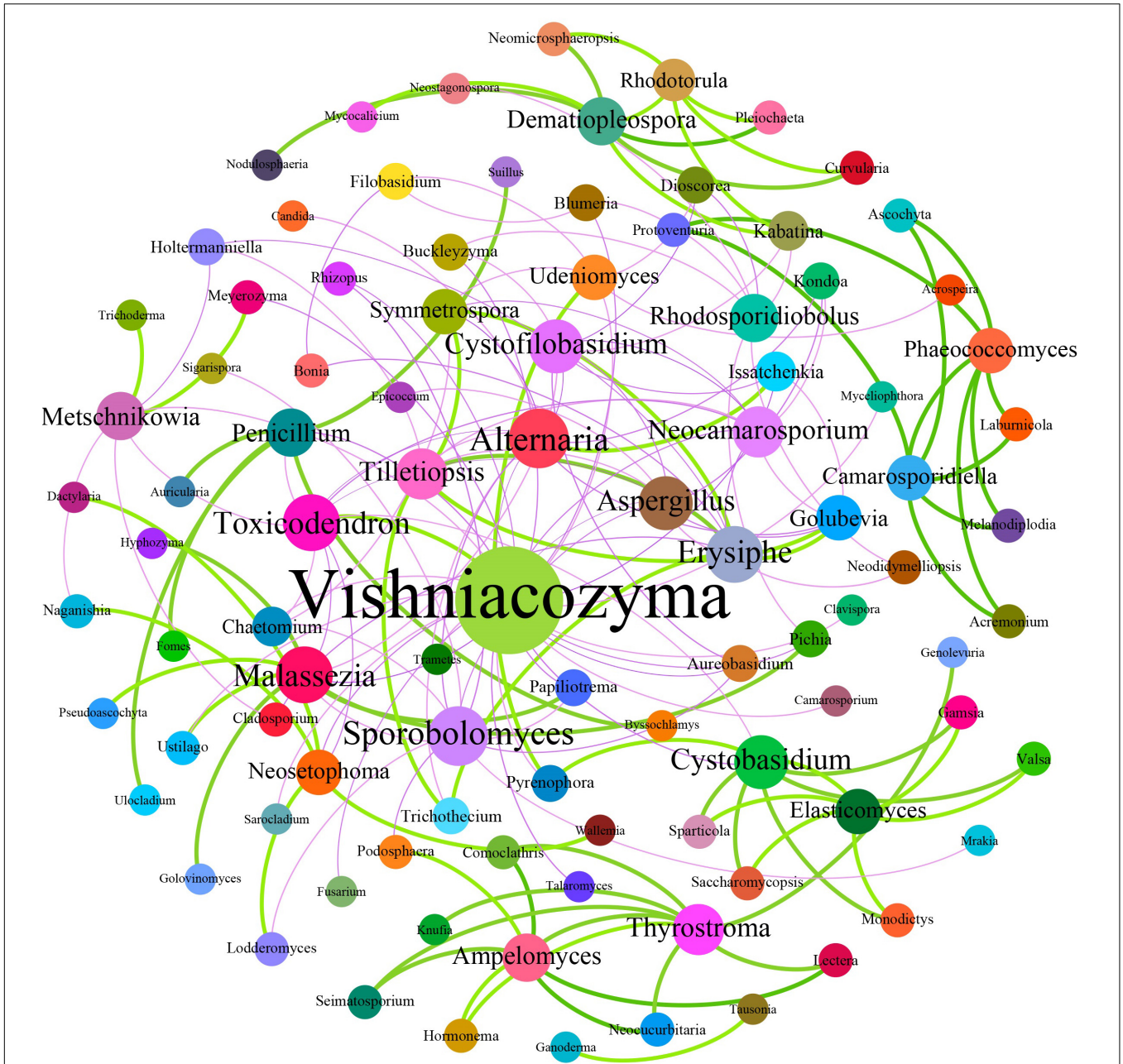

FIGURE 9 | Co-occurrence network among fungi at the genus level. Each dot in the figure represents a species, and the size of the dot indicates the number of related relationships with other species. Solid lines indicate positive correlations; dash lines indicate negative correlations.

vineyard ecosystem and the expansion of potential uses of specific microorganisms to influence grape growth and health.

In general, alpha and beta diversity metrics of wine grape microorganisms have demonstrated that the epiphytic fungal communities are significantly impacted by the mature stage. One hypothesis is that the changes in microbial community are related to the changes in the surface compositions of the grape berries, which include differences in tissue pH and carbon and nitrogen compound contents as well as external factors such as pollen deposits, various organic honeydews, and debris (Janisiewicz et al., 2010; Martins et al., 2014). However, one should not rule out that fungal communities are not randomly combined, but communities with different habitat patterns on the basis of the developmental stages of grapevines.

In the present study, throughout the whole developmental period, the fungal diversity remained relatively constant, even though the number of species tended to decrease. In contrast, Liu and Howell (2021) observed that after the fruit set stage, the fungi diversity of grape berries significantly increased over the remaining ripening process. However, the reasons for these

changes warrant investigation. In general, as demonstrated for grape epiphytes (Jara et al., 2016), the variety of viticulture areas may influence the microbial terroir. Therefore, due to environmental and region fluctuations, only 10 core ASVs of fungal communities continue to exist over time.

Studies have shown that the structural and functional diversity of microbial communities on a wide range of plants (such as *Arabidopsis*, *Medicago*, wheat, maize, pea, and sugar beet) change according to the plant ripening stages (Mougel et al., 2006; Houlden et al., 2008; Micallef et al., 2009). Similarly, in our study, the succession of the microbiome was related to the grape development stages and a "vineyard-specific" distribution was noticed at each stage. This may be the response of grape-related microorganisms to plant development and changing environment. Most distinct community structures of datasets were observed at berry size (**Figure 3**). At the berries still hard and green stage, the grapevine showed highly distinct changes in fungal community diversity (**Figure 2**). Nevertheless, many factors are likely to explain the observed differences.

In grapevine phenology, wine grapes undergo various major biochemical and physiological changes (Conde et al., 2007), which may affect the structure of fungal communities inhabiting a heterogeneous microenvironment and determine the grape quality at harvest. The flowering begin stage is mainly characterized by high ecological interaction with other organisms (such as pollinating insects) (Becher et al., 2018; Zhang et al., 2020). Yeasts such as *Metschnikowia* colonize flowers and produce distinctive scent profiles to enhance floral signaling (Lachance et al., 2001; Becher et al., 2018). The berry stages, such as the C stage, are mainly characterized by physical and chemical changes, such as rapid berry growth both through cell division and expansion (Sun and Xiao, 2015) and increased levels of phenolic compounds because of tartaric acid accumulation (Cuadros-Inostroza et al., 2016). All these factors may have created a more favorable environment for microbial colonization in grapes, and microbial communities became richer at this stage compared with other developmental stages. In particular, *Rhodotorula* that surfaced at this time point demonstrated plant growth-promoting capabilities (Saha and Seal, 2015).

The veraison stage is accompanied by changes on berry color and reduced growth. When the grape is ripe, it shows the greatest size, elasticity, and sugar accumulation (Ben-Hong et al., 2011). In this stage, yeasts likely have the largest surface area available for adherence and probably increased access to nutrients. In our study, the increased abundance of *Cryptococcus*, *Vishniacozyma*, and *Cladosporium* in the G stage suggests that these fungi can withstand high sugar content and low moisture. A study reported that plants can recruit microbes to participate in the key physiological processes and drive microbial assemblages to respond to biotic or abiotic stresses and improve environmental fitness (Turner et al., 2013). Our data may indicate how plant-driven microbes respond to environmental changes.

We also identified characteristic dominant genera typically linked with wine and grape (i.e., *Vishniacozyma, Metschnikowia*, and *Malassezia*) along with several pathogenic fungal genera (*Aspergillus*, *Penicillium*, and *Erysisphe*) (Lorenzini et al., 2016). *Vishniacozyma* was present in all mature stages but was negatively correlated with almost all other fungal genera; this may be because it shows relatively better adaptation to the changes in the grape environment as well as aids suppression and elimination of other characteristic microorganisms, resulting in strong selection (Barata et al., 2012). *Vishniacozyma* is a cosmopolitan yeast and has been isolated from several substrates, such as soil (including Antarctic, Alaska, and Arctic soils) (Tsuji et al., 2019), as well as from wood (Félix et al., 2020) and cold environments (surface of Vidal grapes) (Shi et al., 2020). Nevertheless, its possible impacts on wine quality remain unknown and warrant further investigation, especially with regard to its effects on wine flavor. Furthermore, *Vishniacozyma* have biocontrol effects on the blue molds and gray molds that infect pears (Lutz et al., 2013); our results also suggest a possible antagonistic effect between *Vishniacozyma* and *Erysisphe*. The biocontrol potential of *Vishniacozyma* for grape powdery mildew requires further analysis.

Notably, the abundance of *Aureobasidium* was low in our study, whereas it was the predominant genus in grapes in other studies (Grube et al., 2011; Zhang et al., 2019). In addition, *A. pullulans* have the capacity to adapt well to saprophytes on grape berries; however, it is not widely distributed in Shangri-La and other parts of China (Li et al., 2010; Zhao et al., 2021). In the current study, we detected *Erysisphe*, the richness of which was relatively high in the E stage, which then declined sharply—from 28% in July to 1% in September. This finding is consistent with an earlier report that grape powdery mildew, one of the most harmful fungal diseases, usually occurs in July (Han et al., 2016). This also indicates that grape powdery mildew is quite serious in this area and appropriate preventive measures need to be taken (Amrine et al., 2015). Notably, *B, cinerea*, a well-known necrotrophic fungal pathogen of grapes (Jaspers et al., 2013), was not detected in the current study, possibly due to geographical location (Rivera et al., 2013). This also illustrates that a healthy microbial composition should keep the pathogenic populations at a low or even undetectable levels; this aids in preventing harmful plant diseases.

The relative abundance of *Penicillium* was also high in the B stage (**Figure 7**). Although some *Penicillium* species can cause severe damage to crop, many of them have been reported to be beneficial—preventing plant diseases and inhibiting pathogen activity (Van Wees et al., 2008). *Aspergillus*, which enriches at the early development stages, is a predominant global wine contaminant; it is reported to produce ochratoxin A, which causes human health hazards (Ferrari et al., 2017). Notably, in some organisms, *Alternaria*, considered one of the main mycobiota populations of grapes at harvest, gradually reduces during the berry ripening process (Tournas and Katsoudas, 2005). In particular, *Alternaria* can infect fruit during flowering and immature development by behaving as a biological nutritional pathogen and remaining latent in the outermost layer of the fruit, waiting for suitable conditions to become conducive to disease expression (Prusky et al., 2013). However, contrasting findings indicate that species of *Alternaria* can control the growth of different pathogens such as *Rhizoctonia solani*, *Fusarium*

oxysporum, *B. cinerea*, and *Pseudomonas aeruginosa* (Yu et al., 2011; Ortega et al., 2020).

Biocontrol microbes may provide a sustainable alternative to chemical control of pathogens (Lecomte et al., 2016). In the current study, the relative abundance of *Metschnikowia* and *Rhodotorula* was relatively high in the D stage and that of *Ampelomyces* was relatively high in the B stage (**Figure 7**). These three fungi have beneficial antifungal properties; *Metschnikowia*, *Rhodotorula*, and *Ampelomyces* control common fungal pathogens that cause apple ring rot, cucumber powdery mildew, and grape gray mold blight, respectively (Tian et al., 2004; Zhang et al., 2019). *Cryptococcus*—an effective potential biocontrol agent effective against postharvest pathogens present on fruits (Renouf et al., 2005; Liu et al., 2013; Taylor et al., 2014)—was found predominantly in the E stage.

Taken together, these findings suggest that the beneficial microorganisms and plant pathogens can thrive in a balanced microbial ecosystem. Thus, identifying potential beneficial strains and antagonistic strains that control pathogenic infections is essential.

In conclusion, our study provides in-depth information regarding the differences in the fungal communities on the surface of grapes during the developmental stages. The results illustrate how the fungal microbiota increase in size and how their structure changes during the ripening process. Furthermore, the unclassified microbiota detected in the current study confirmed that the classification of the grape-related fungi needs further exploration and documentation.

In addition, future studies should thus focus on preharvest management practices that can increase the natural abundance of potential biocontrol communities, such as those of *Cryptococcus*, *Vishniacozyma*, and yeast-like fungus. This may result in reduced pesticide costs and postharvest losses due to rot.

In summary, increasing our understanding of microbial ecology and community dynamic change in the vineyard throughout the developmental stages can help improve management techniques for maintaining and producing healthy, high-quality grapes and allowing the expression of the regional character of the wine.

DATA AVAILABILITY STATEMENT

The data presented in the study are deposited in the NCBI repository, accession number PRJNA750856.

AUTHOR CONTRIBUTIONS

LZ collected wine grape samples, compiled the figures and table, and wrote the manuscript. TL and XX conceived the framework of the manuscript. BW conducted the bioinformatic analysis of data and provided advice and constructive critiques. XS supervised the research activities. All authors reviewed the manuscript.

FUNDING

This work was supported by the Science and Technology Research Project of the Xinjiang Production and Construction Corps (No. 2020AB014) and the National Natural Science Foundation of China (No. 31960465).

SUPPLEMENTARY MATERIAL

The Supplementary Material for this article can be found online at: https://www.frontiersin.org/articles/10.3389/fmicb.2021.718261/full#supplementary-material

REFERENCES

Amrine, K. C., Blanco-Ulate, B., Riaz, S., Pap, D., Jones, L., Figueroa-Balderas, R., et al. (2015). Comparative transcriptomics of Central Asian *Vitis vinifera* accessions reveals distinct defense strategies against powdery mildew. *Hortic. Res.* 2:15037. doi: 10.1038/hortres.2015.37

Barata, A., Malfeito-Ferreira, M., and Loureiro, V. (2012). The microbial ecology of wine grape berries. *Int. J. Food Microbiol.* 153, 243–259. doi: 10.1016/j.ijfoodmicro.2011.11.025

Becher, P. G., Hagman, A., Verschut, V., Chakraborty, A., Rozpedowska, E., Lebreton, S., et al. (2018). Chemical signaling and insect attraction is a conserved trait in yeasts. *Ecol. Evol.* 8, 2962–2974. doi: 10.1002/ece3.3905

Ben-Hong, W., Huai-Feng, L., Le, G., Pei-Ge, F., and Shao-Hua, L. (2011). Carbohydrate metabolism in grape cultivars that differ in sucrose accumulation. *Vitis* 50, 51–57.

Bokulich, N. A., Subramanian, S., Faith, J. J., Gevers, D., Gordon, J. I., Knight, R., et al. (2013). Quality-filtering vastly improves diversity estimates from Illumina amplicon sequencing. *Nat. Methods* 10, 57–59. doi: 10.1038/nmeth.2276

Bowers, J. E., and Meredith, C. P. (1997). The parentage of a classic wine grape, Cabernet Sauvignon. *Nat. Genet.* 16, 84–87. doi: 10.1038/ng0597-84

Cadez, N., Zupan, J., and Raspor, P. (2010). The effect of fungicides on yeast communities associated with grape berries. *FEMS Yeast Res.* 10, 619–630. doi: 10.1111/j.1567-1364.2010.00635.x

Callahan, B. J., McMurdie, P. J., Rosen, M. J., Han, A. W., Johnson, A. J., and Holmes, S. P. (2016). DADA2: high-resolution sample inference from Illumina amplicon data. *Nat. Methods* 13, 581–583. doi: 10.1038/nmeth.3869

Capozzi, V., Garofalo, C., Chiriatti, M. A., Grieco, F., and Spano, G. (2015). Microbial terroir and food innovation: the case of yeast biodiversity in wine. *Microbiol. Res.* 181, 75–83. doi: 10.1016/j.micres.2015.10.005

Carmichael, P. C., Siyoum, N., Chidamba, L., and Korsten, L. (2017). Characterization of fungal communities of developmental stages in table grape grown in the northern region of South Africa. *J. Appl. Microbiol.* 123, 1251–1262. doi: 10.1111/jam.13577

Conde, C., Silva, P., Fontes, N., Dias, A., and Gerós, H. (2007). Biochemical changes throughout grape berry development and fruit and wine quality. *Food Glob. Sci. Books* 1, 1–22.

Coombe, B. G. (1995). Growth stages of the grapevine: adoption of a system for identifying grapevine growth stages. *Aust. J. Grape Wine Res.* 1, 104–110. doi: 10.1111/j.1755-0238.1995.tb00086.x

Cuadros-Inostroza, A., Ruíz-Lara, S., González, E., Eckardt, A., Willmitzer, L., and Peña-Cortés, H. (2016). GC-MS metabolic profiling of Cabernet Sauvignon and Merlot cultivars during grapevine berry development and network analysis reveals a stage- and cultivar-dependent connectivity of primary metabolites. *Metabolomics* 12:39. doi: 10.1007/s11306-015-0927-z

Edgar, R. C., Haas, B. J., Clemente, J. C., Quince, C., and Knight, R. (2011). UCHIME improves sensitivity and speed of chimera detection. *Bioinformatics* 27, 2194–2200. doi: 10.1093/bioinformatics/btr381

Félix, C. R., Andrade, D. A., Almeida, J. H., Navarro, H. M. C., Fell, J. W., and Landell, M. F. (2020). *Vishniacozyma alagoana* sp. nov. a tremellomycetes yeast associated with plants from dry and rainfall tropical forests. *Int. J. Syst. Evol. Microbiol.* 70, 3449–3454. doi: 10.1099/ijsem.0.004193

Ferrari, V., Dellacassa, E., Coniberti, A., and Disegna, E. (2017). Role of grapevine vegetative expression on *Aspergillus* spp. incidence and OTA accumulation in wines produced in a temperate humid climate. *Food Addit. Contam. Part A Chem. Anal. Control Expo. Risk Assess.* 34, 299–306. doi: 10.1080/19440049.2016.1252064

Gao, F., Chen, J., Xiao, J., Cheng, W., Zheng, X., Wang, B., et al. (2019). Microbial community composition on grape surface controlled by geographical factors of different wine regions in Xinjiang, China. *Food Res. Int.* 122, 348–360. doi: 10.1016/j.foodres.2019.04.029

Grube, M., Schmid, F., and Berg, G. (2011). Black fungi and associated bacterial communities in the phyllosphere of grapevine. *Fungal Biol.* 115, 978–986. doi: 10.1016/j.funbio.2011.04.004

Haas, B. J., Gevers, D., Earl, A. M., Feldgarden, M., Ward, D. V., Giannoukos, G., et al. (2011). Chimeric 16S rRNA sequence formation and detection in Sanger and 454-pyrosequenced PCR amplicons. *Genome Res.* 21, 494–504. doi: 10.1101/gr.112730.110

Hamad, I., Ranque, S., Azhar, E. I., Yasir, M., Jiman-Fatani, A. A., Tissot-Dupont, H., et al. (2017). Culturomics and amplicon-based metagenomic approaches for the study of fungal population in human gut microbiota. *Sci. Rep.* 7:16788. doi: 10.1038/s41598-017-17132

Han, L., Weng, K., Ma, H., Xiang, G., Li, Z., Wang, Y., et al. (2016). Identification and characterization of *Erysiphe* necator-responsive microRNAs in Chinese wild *Vitis pseudoreticulata* by high-throughput sequencing. *Front. Plant Sci.* 7:621. doi: 10.3389/fpls.2016.00621

Houlden, A., Timms-Wilson, T. M., Day, M. J., and Bailey, M. J. (2008). Influence of plant developmental stage on microbial community structure and activity in the rhizosphere of three field crops. *FEMS Microbiol. Ecol.* 65, 193–201. doi: 10.1111/j.1574-6941.2008.00535.x

Janisiewicz, W. J., Kurtzman, C. P., and Buyer, J. S. (2010). Yeasts associated with nectarines and their potential for biological control of brown rot. *Yeast* 27, 389–398. doi: 10.1002/yea.1763

Jara, C., Laurie, V. F., Mas, A., and Romero, J. (2016). Microbial terroir in Chilean valleys: diversity of non-conventional yeast. *Front. Microbiol.* 7:663. doi: 10.3389/fmicb.2016.00663

Jaspers, M., Seyb, A., Trought, M., and Balasubramaniam, R. (2013). Overwintering grapevine debris as an important source of *Botrytis cinerea* inoculum. *Plant Pathol.* 62, 130–138. doi: 10.1111/j.1365-3059.2012.02631.x

Jiang, B., and Zhang, Z. W. (2012). Comparison on phenolic compounds and antioxidant properties of Cabernet Sauvignon and merlot wines from four wine grape-growing regions in China. *Molecules* 17, 8804–8821. doi: 10.3390/molecules17088804

Kao, C. M., Liao, H. Y., Chien, C. C., Tseng, Y. K., Tang, P., Lin, C. E., et al. (2016). The change of microbial community from chlorinated solvent-contaminated groundwater after biostimulation using the metagenome analysis. *J. Hazard. Mater.* 302, 144–150. doi: 10.1016/j.jhazmat.2015.09.047

Kioroglou, D., Kraeva-Deloire, E., Schmidtke, L. M., Mas, A., and Portillo, M. C. (2019). Geographical origin has a greater impact on grape berry fungal community than grape variety and maturation state. *Microorganisms* 7:669. doi: 10.3390/microorganisms7120669

Lachance, M. A., Bowles, J. M., Kwon, S., Marinoni, G., Starmer, W. T., and Janzen, D. H. (2001). *Metschnikowia lochheadii* and *Metschnikowia drosophilae*, two new yeast species isolated from insects associated with flowers. *Can. J. Microbiol.* 47, 103–109. doi: 10.1139/w00-130

Lecomte, C., Alabouvette, C., Edel-Hermann, V., Robert, F., and Steinberg, C. (2016). Biological control of ornamental plant diseases caused by *Fusarium oxysporum*: a review. *Biol. Control* 101, 17–30. doi: 10.1016/j.biocontrol.2016.06.004

Li, S. S., Cheng, C., Li, Z., Chen, J. Y., Yan, B., Han, B. Z., et al. (2010). Yeast species associated with wine grapes in China. *Int. J. Food Microbiol.* 138, 85–90. doi: 10.1016/j.ijfoodmicro.2010.01.009

Liu, D., and Howell, K. (2021). Community succession of the grapevine fungal microbiome in the annual growth cycle. *Environ. Microbiol.* 23, 1842–1857. doi: 10.1111/1462-2920.15172

Liu, D., Zhang, P., Chen, D., and Howell, K. (2019). From the vineyard to the winery: how microbial ecology drives regional distinctiveness of wine. *Front. Microbiol.* 10:2679. doi: 10.3389/fmicb.2019.02679

Liu, J., Sui, Y., Wisniewski, M., Droby, S., and Liu, Y. (2013). Review: utilization of antagonistic yeasts to manage postharvest fungal diseases of fruit. *Int. J. Food Microbiol.* 167, 153–160. doi: 10.1016/j.ijfoodmicro.2013.09.004

Lorenzini, M., Cappello, M. S., Logrieco, A., and Zapparoli, G. (2016). Polymorphism and phylogenetic species delimitation in filamentous fungi from predominant mycobiota in withered grapes. *Int. J. Food Microbiol.* 238, 56–62. doi: 10.1016/j.ijfoodmicro.2016.08.039

Lutz, M. C., Lopes, C. A., Rodriguez, M. E., Sosa, M. C., and Sangorrin, M. P. (2013). Efficacy and putative mode of action of native and commercial antagonistic yeasts against postharvest pathogens of pear. *Int. J. Food Microbiol.* 164, 166–172. doi: 10.1016/j.ijfoodmicro.2013.04.005

Magoč, T., and Salzberg, S. L. (2011). FLASH: fast length adjustment of short reads to improve genome assemblies. *Bioinformatics* 27, 2957–2963. doi: 10.1093/bioinformatics/btr507

Martins, G., Vallance, J., Mercier, A., Albertin, W., Stamatopoulos, P., Rey, P., et al. (2014). Influence of the farming system on the epiphytic yeasts and yeast-like fungi colonizing grape berries during the ripening process. *Int. J. Food Microbiol.* 177, 21–28. doi: 10.1016/j.ijfoodmicro.2014.02.002

Micallef, S. A., Channer, S., Shiaris, M. P., and Colón-Carmona, A. (2009). Plant age and genotype impact the progression of bacterial community succession in the *Arabidopsis* rhizosphere. *Plant Signal. Behav.* 4, 777–780. doi: 10.1093/jxb/erp053

Mougel, C., Offre, P., Ranjard, L., Corberand, T., Gamalero, E., Robin, C., et al. (2006). Dynamic of the genetic structure of bacterial and fungal communities at different developmental stages of *Medicago truncatula* Gaertn. cv. Jemalong line J5. *New Phytol.* 170, 165–175. doi: 10.1111/j.1469-8137.2006.01650.x

Nones, K., Waddell, N., Wayte, N., Patch, A. M., Bailey, P., Newell, F., et al. (2014). Genomic catastrophes frequently arise in esophageal adenocarcinoma and drive tumorigenesis. *Nat. Commun.* 5:5224. doi: 10.1038/ncomms6224

Novello, G., Gamalero, E., Bona, E., Boatti, L., Mignone, F., Massa, N., et al. (2017). The rhizosphere bacterial microbiota of *Vitis vinifera* cv. Pinot Noir in an integrated pest management vineyard. *Front. Microbiol.* 8:1528. doi: 10.3389/fmicb.2017.01528

Ortega, H. E., Torres-Mendoza, D., and Cubilla-Rios, L. (2020). Patents on endophytic fungi for agriculture and bio- and phytoremediation applications. *Microorganisms* 8:1237. doi: 10.3390/microorganisms8081237

Prusky, D., Alkan, N., Mengiste, T., and Fluhr, R. (2013). Quiescent and necrotrophic lifestyle choice during postharvest disease development. *Annu. Rev. Phytopathol.* 51, 155–176. doi: 10.1146/annurev-phyto-082712-102349

Radovanović, B., and Radovanović, A. (2010). Free radical scavenging activity and anthocyanin profile of Cabernet Sauvignon wines from the Balkan region. *Molecules* 15, 4213–4226. doi: 10.3390/molecules15064213

Rajha, H. N., Darra, N. E., Kantar, S. E., Hobaika, Z., Louka, N., and Maroun, R. G. (2017). A comparative study of the phenolic and technological maturities of red grapes grown in Lebanon. *Antioxidants* 6:8. doi: 10.3390/antiox6010008

Renouf, V., Claisse, O., and Lonvaud-Funel, A. (2005). Understanding the microbial ecosystem on the grape berry surface through numeration and identification of yeast and bacteria. *Aust. J. Grape Wine Res.* 11, 316–327. doi: 10.1111/j.1755-0238.2005.tb00031.x

Rivera, S. A., Zoffolli, J. P., and Latorre, B. A. (2013). Infection risk and critical period for the postharvest control of gray mold (*Botrytis cinerea*) on Blueberry in Chile. *Plant Dis.* 97, 1069–1074. doi: 10.1094/PDIS-12-12-1112-RE

Saha, C., and Seal, A. (2015). Early changes in shoot transcriptome of rice in response to *Rhodotorula mucilaginosa* JGTA-S1. *Genom. Data* 6, 237–240. doi: 10.1016/j.gdata.2015.09.023

Shi, X. W., Chen, Y., Xiao, J., Deng, L., and Wang, B. (2020). Effects of harvest dates on microbial communities of ice grape skins from Xinjiang of China. *Process Biochem.* 98, 202–210. doi: 10.1016/j.procbio.2020.08.002

Sun, Y., and Xiao, H. (2015). Identification of alternative splicing events by RNA sequencing in early growth tomato fruits. *BMC Genomics* 16:948. doi: 10.1186/s12864-015-2128-6

Swami, S. B., Thakor, N. J., and Divate, A. D. (2014). Fruit wine production: a review. *J. Food Res. Technol.* 2, 93–100.

Taylor, M. W., Tsai, P., Anfang, N., Ross, H. A., and Goddard, M. R. (2014). Pyrosequencing reveals regional differences in fruit-associated fungal communities. *Environ. Microbiol.* 16, 2848–2858. doi: 10.1111/1462-2920.12456

Tian, S., Qin, G., and Xu, Y. (2004). Survival of antagonistic yeasts under field conditions and their biocontrol ability against postharvest diseases of sweet cherry. *Postharvest Biol. Technol.* 33, 327–331. doi: 10.1016/j.postharvbio.2004.03.010

Tournas, V. H., and Katsoudas, E. (2005). Mould and yeast flora in fresh berries, grapes and citrus fruits. *Int. J. Food Microbiol.* 105, 11–17. doi: 10.1016/j.ijfoodmicro.2005.05.002

Tsuji, M., Tanabe, Y., Vincent, W. F., and Uchida, M. (2019). *Vishniacozyma ellesmerensis* sp. nov., a psychrophilic yeast isolated from a retreating glacier in the Canadian High Arctic. *Int. J. Syst. Evol. Microbiol.* 69, 696–700. doi: 10.1099/ijsem.0.003206

Turner, T. R., James, E. K., and Poole, P. S. (2013). The plant microbiome. *Genome Biol.* 14:209. doi: 10.1186/gb-2013-14-6-209

Van Wees, S. C., Van der Ent, S., and Pieterse, C. M. (2008). Plant immune responses triggered by beneficial microbes. *Curr. Opin. Plant Biol.* 11, 443–448. doi: 10.1016/j.pbi.2008.05.005

Yu, D., Zhang, J., Tan, G., Yu, N., Wang, Q., Duan, Q., et al. (2019). An easily-performed high-throughput method for plant genomic DNA extraction. *Anal. Biochem.* 569, 28–30. doi: 10.1016/j.ab.2019.01.007

Yu, X., Shentu, X., Dong, S., Hao, P., Bian, Y., and Ma, Z. (2011). *Application of Metabolites of Alternaria alternata 31 in Preventing and Treating Rhizoctonia solani, Fusarium oxysporium, and Botrytis cinerea*. CN 102204570 A. Zhejiang: China National Intellectual Property Administration.

Zetsche, B., Heidenreich, M., Mohanraju, P., Fedorova, I., Kneppers, J., DeGennaro, E. M., et al. (2017). Multiplex gene editing by CRISPR-Cpf1 using a single crRNA array. *Nat. Biotechnol.* 35, 31–34. doi: 10.1038/nbt.3737

Zhang, H., Chen, M., Wen, H., Wang, Z., Chen, J., Fang, L., et al. (2020). Transcriptomic and metabolomic analyses provide insight into the volatile compounds of citrus leaves and flowers. *BMC Plant Biol.* 20:7. doi: 10.1186/s12870-019-2222-z

Zhang, S., Chen, X., Zhong, Q., Zhuang, X., and Bai, Z. (2019). Microbial community analyses associated with nine varieties of wine grape carposphere based on high-throughput sequencing. *Microorganisms* 7:668. doi: 10.3390/microorganisms7120668

Zhao, Y., Sun, Q., Zhu, S., Du, F., Mao, R., Liu, L., et al. (2021). Biodiversity of non-*Saccharomyces* yeasts associated with spontaneous fermentation of Cabernet Sauvignon wines from Shangri-La wine region, China. *Sci. Rep.* 11:5150. doi: 10.1038/s41598-021-83216-x

Conflict of Interest: The authors declare that the research was conducted in the absence of any commercial or financial relationships that could be construed as a potential conflict of interest.

Publisher's Note: All claims expressed in this article are solely those of the authors and do not necessarily represent those of their affiliated organizations, or those of the publisher, the editors and the reviewers. Any product that may be evaluated in this article, or claim that may be made by its manufacturer, is not guaranteed or endorsed by the publisher.

frontiers in Microbiology

ORIGINAL RESEARCH
published: 03 September 2021
doi: 10.3389/fmicb.2021.626920

Oenological Characteristics of Four Non-*Saccharomyces* Yeast Strains With β-Glycosidase Activity

*Tao Qin, Jing Liao, Yingyuan Zheng, Wenxia Zhang and Xiuyan Zhang**

College of Food Science and Technology, Huazhong Agricultural University, Wuhan, China

Non-*Saccharomyces* yeast with β-glucosidase activity might positively contribute to the flavor and quality of wines. The contribution of four non-*Saccharomyces* yeast strains *Issatchenkia terricola* SLY-4, *Pichia kudriavzevii* F2-24, *P. kudriavzevii* F2-16, and *Metschnikowia pulcherrima* HX-13 with β-glucosidase activity to the flavor and quality of wine making was studied. Compared with those of *S. cerevisiae* single fermentation, the four non-*Saccharomyces* yeast strains could grow and consume sugar completely with longer fermentation periods, and with no significantly negative effect on chemical characteristics of wines. Moreover, they produced lower content of C_6 compounds, benzene derivative, and fatty acid ethyl ester compounds and higher content of terpene, β-ionone, higher alcohol, and acetate compounds. Different yeast strains produced different aroma compounds profiles. In general, the sensory evaluation score of adding non-*Saccharomyces* yeast-fermented wine was better than that of *S. cerevisiae*, and *I. terricola* SLY-4 fermentation received the highest one, followed by *P. kudriavzevii* F2-24, *P. kudriavzevii* F2-16, and *M. pulcherrima* HX-13 from high to low. The research results provide a theoretical basis for the breeding of non-*Saccharomyces* yeast and its application in wine making.

Keywords: oenological characteristics, wine, flavor, β-glucosidase, non-*Saccharomyces* yeast

OPEN ACCESS

Edited by:
Kap-Hoon Han,
Woosuk University, South Korea

Reviewed by:
Estéfani García Ríos,
Instituto de Salud Carlos III (ISCIII), Spain
Hee-Soo Park,
Kyungpook National University, South Korea

****Correspondence:***
Xiuyan Zhang
xiuyanzhang73@mail.hzau.edu.cn

Specialty section:
This article was submitted to Food Microbiology, a section of the journal Frontiers in Microbiology

Received: *07 November 2020*
Accepted: *30 July 2021*
Published: *03 September 2021*

Citation:
Qin T, Liao J, Zheng Y, Zhang W and Zhang X (2021) Oenological Characteristics of Four Non-Saccharomyces Yeast Strains With β-Glycosidase Activity. Front. Microbiol. 12:626920. doi: 10.3389/fmicb.2021.626920

INTRODUCTION

It is an established enological practice to use commercial *Saccharomyces cerevisiae* to ferment wine. Pure *S. cerevisiae* fermentation has an easy control fermentation process and a high consistency of product quality between batches, but it is easy to lead poor flavor complexity and varietal aroma characteristics of wine which are mainly contributed by varietal, fermentative, and aging aroma compounds (Pires et al., 2014).

At present, non-*Saccharomyces* yeast is widely accepted because of its ability to produce aroma compounds and other excellent brewing characteristics, which has been used in pure or mixed fermentation with *S. cerevisiae* to overcome the defect of imperfect wine flavor (Parker et al., 2017; Canonico et al., 2019; Plessis et al., 2019; Binati et al., 2020). The varietal aroma characteristics of wine are mainly contributed by the volatile varietal aroma compounds; however, these compounds often exist as non-volatile glycoside precursors and are odorless. The non-volatile glycosides can be hydrolyzed by β-glycosidases and released as volatile compounds

with flavor (Cabrita et al., 2010; García-Carpintero et al., 2011). β-Glycosidase from different resources will affect the category and concentration of volatile varietal aroma compounds (Baffi et al., 2011). Generally, single fermentation of *S. cerevisiae* is weak in liberating these aroma precursors (Boscaino et al., 2019).

Several non-*Saccharomyces* yeast strains have been confirmed to have β-glucosidase activity, including *Hanseniaspora uvarum*, *Pichia fermentans*, *Pichia membranifaciens*, *Wickerhamomyces anomalus*, and *Rhodotorula mucilaginosa*, and they can improve the content of some volatile aroma compounds such as terpenes and benzene derivatives, imparting fruity and floral flavor profile to wine (Sabel et al., 2014; López et al., 2015, 2016; Ovalle et al., 2016; Ma et al., 2017; Sun et al., 2017). Four non-*Saccharomyces* yeast strains *I. terricola* SLY-4, *P. kudriavzevii* F2-24, *P. kudriavzevii* F2-16, and *M. pulcherrima* HX-13 were isolated from vineyards of the Helan Mountain region in Ningxia of China by our research group, which produced 98.51, 76.93, 62.72, and 47.95 U/l β-glucosidase activities, respectively (Wang et al., 2018). Adding crude extraction of β-glucosidases from *I. terricola* SLY-4, *P. kudriavzevii* F2-24, and *M. pulcherrima* HX-13 into must could increase the content of terpenes, esters, and fatty acids and enhance the fruity and floral aroma of wine fermented by *S. cerevisiae*. Wines using different crude β-glucosidase extractions presented distinct volatile compound profiles and varied typical flavor characteristics (Zhang et al., 2020). These results indicated that β-glucosidases from the four non-*Saccharomyces* yeast strains could enhance the content of aroma compounds with different profiles and improve the fruity and floral aroma of wine. However, the positive or negative effects of these four non-*Saccharomyces* yeast strains as main brewing yeast on wine-making are not yet known.

To investigate the effects of pure fermentations of *I. terricola* SLY-4, *P. kudriavzevii* F2-24, *P. kudriavzevii* F2-16, or *M. pulcherrima* HX-13 on flavor complexity and varietal aroma characteristics of wines, the process and the quality of their pure fermentations will be analyzed. Research results will provide some references of using non-*Saccharomyces* yeast strains to improve the flavor complexity and varietal characteristics of wines.

MATERIALS AND METHODS

Strains and Medium

I. terricola SLY-4, *P. kudriavzevii* F2-24, *P. kudriavzevii* F2-16, and *M. pulcherrima* HX-13 were isolated from vineyards of the Helan Mountain region in Ningxia of China. They have been identified through sequence analysis of the 26S rDNA D1/D2 domain and kept in our lab. Reference strains were purchased from the China General Microbiological Culture Collection Center (CGMCC 2.3216 *Issatchenkia terricola*; CGMCC 2.454 *Pichia kudriavzevii*; CGMCC 2.3776 *Metschnikowia pulcherrima*). *Saccharomyces cerevisiae* was a commercial strain Actiflore® F33 (Laffort, France).

Yeast extract peptone dextrose medium (YPD, 10 g/l yeast extract, 20 g/l peptone, 20 g/l glucose, and 20 g/l agar) was used to inoculate preparation and yeast cell count.

Laboratory-Scale Fermentation of Wines

Cabernet Sauvignon grapes from a vineyard of the Helan Mountain region in Ningxia of China were destemmed and crushed into must (239.9 g/l total sugar calculated as glucose and 7.1 g/l total acid calculated as tartaric acid, pH 3.96). Eight hundred milliliters of must was filled into a 1.0–l glass bottle, pasteurized at 68.5°C for 30 min. After adding 50 mg/l SO_2, the must was macerated at 4°C for 12 h, and yeast cells were inoculated at 10^6 CFU/ml and fermented at 20°C without agitation. Each kind of yeast was inoculated in triplicate.

Viable Yeast Cell Counting

Samples were taken during fermentation every day and concurrently diluted onto a YPD plate, then incubated at 28°C for 3 days (Suárez et al., 2007). Colonies on the YPD plate were counted as the viable cells of *S. cerevisiae* or non-*Saccharomyces* yeast. Each sample was analyzed in triplicate from the bottles.

Analytical Determination of Wines

The contents of residual sugar, alcohol, total acid, and volatile acid of wine were analyzed through methods recommended by the International Organization of the Vine and Wine (OIV-MA-AS311-02: R2009, 2009; OIV-MA-AS313-01: R2015, 2015; OIV-MA-AS313-02: R2015, 2015; OIV-MA-AS312-01A: R2016, 2016). The residual sugar contents were expressed as glucose (g/L). The total acid content was expressed as tartaric acid (g/L), and the volatile acid content was expressed as acetic acid (g/L). Each wine sample was measured in triplicates from the bottles.

The extraction of volatile aroma compounds from wine was conducted by headspace solid-phase microextraction with 50/30 μm divinylbenzene carboxen polydimethylsiloxane (DVB/CAR/PDMS) fiber (Supelco, Bellefonte, PA, United States). The extracted volatile compounds were analyzed on an Agilent 6890N gas chromatograph (GC) coupled to an Agilent 5975B mass spectrometer with a DB-5 capillary column (30 m × 0.32 mm × 0.25 μm). An 8-ml sample containing 0.45 g cyclohexanone (internal standard) and 2 g NaCl was put in a 20-ml headspace bottle and stirred by a magnetic bar at 40°C for 15 min. After that, the fiber was exposed to the headspace of bottle for 30 min and immediately desorbed in an injector at 250°C for 3 min. The operating conditions of GC were the following: initial temperature 40°C, increased to 130°C at 3°C/min, then to 250°C at 4°C/min. The injector and detector were set at 250 and 260°C, respectively. The mass spectrometry was operated in electron impact ionization mode at 70 eV, and ion source temperature was 250°C. Detection was carried out in full-scan mode over a range of 30–350 u/s. Compounds were identified by comparing their retention time with MS fragmentation patterns which were obtained from databases Wiley 7.0 and NIST05. All volatile compounds were semi-quantified through the following formula:

$$Compound\ content(mg/mL) = \frac{GC\ peak\ area\ of\ compound \times Quantity\ of\ cyclohexanone\ (mg)}{GC\ peak\ area\ of\ cyclohexanone \times volume\ of\ sample(mL)}$$

Sensory Evaluation of Wines

The sensory evaluation was performed as described by Belda et al. (2015) with modification. Twenty milliliters of wine was poured into wine glasses and presented in random order. The preferences for appearance, aroma (fruity, floral, and green), and taste of the wine were scored from 0 (weak) to 9 (intense) by a well-trained panelist (six females and four males) from Huazhong Agricultural University, respectively. The final score of each sensory characteristic was the mean value of 10 scores given by 10 assessors, respectively.

Data Statistics Processing and Analysis

Data and chart were performed by Microsoft Office 2010 and GraphPad Prism 6.0. One-way ANOVA was completed by SPSS 19.0 software (SPSS Inc., Chicago, IL, United States). Principal component analysis (PCA) was performed by SIMCA-P 14.1 (Umetrics AB, Umea, Sweden).

RESULTS

Growth and Sugar Consumption Kinetics of Yeast Strains During Wine Fermentation

The growth and sugar consumption kinetics of yeast strains indicated that four non-*Saccharomyces* yeast strains could grow normally during wine fermentation (**Figure 1**). Compared with that of *S. cerevisiae* (2.25×10^9 cells/ml), the biomasses of four non-*Saccharomyces* yeast strains were higher. *M. pulcherrima* HX-13 had the highest biomass (11.45×10^9 cells/ml), followed by *I. terricola* SLY-4 (4.8×10^9 cells/ml), *P. kudriavzevii* F2-16 (3.05×10^9 cells/ml), and *P. kudriavzevii* F2-24 (2.8×10^9 cells/ml). Compared with that of *S. cerevisiae* (7 days), the fermentation periods of the four non-*Saccharomyces* yeasts were longer (9–13 days). *M. pulcherrima* HX-13 had the shortest fermentation period (9 days) among the non-*Saccharomyces* yeasts, followed by *I. terricola* SLY-4 (10 days), *P. kudriavzevii* F2-24 (10 days), and *P. kudriavzevii* F2-16 (13 days).

Chemical Characteristics of Wines Fermented by Yeast Strains With β-Glucosidase Activity

The chemical characteristics of wines fermented by different yeast strains showed that all the fermentations contained 2.71–3.64 g/l residue sugar (expressed as glucose), about 12% ethanol (v/v), 5.13–5.44 g/l total acid (expressed as tartaric acid), and 0.23–0.31 g/l volatile acid (expressed as acetic acid) (**Table 1**). These results indicated there was no negative effect on the chemical characteristics of wines.

Volatile Compounds of Wines Fermented by Yeast Strains With β-Glucosidase Activity

The total ion current chromatograms of gas chromatography–mass spectrometry (GC-MS) analysis for all the fermentations indicated that different fermentations had unique chromatogram profiles. Fifty-three kinds of volatile compounds were classified into variety aroma compounds and fermentative aroma compounds. Eleven variety aroma components were clustered into C_6 compound, terpene, norisoprenoid, and benzene derivative compound. Forty-two fermentative aroma components were clustered into compounds of higher alcohol, fatty acid, ester (acetic ester, fatty acid ethyl ester, and other ester), aldehyde, and ketone (**Table 2**).

The effects of non-*Saccharomyces* yeast strains on the aroma compounds were evaluated as follows.

Compared with those of the *S. cerevisiae* single fermentation, the total contents of varietal aroma compounds in non-*Saccharomyces* yeast fermentations were lower (45.49–62.64 mg/l). Among the varietal aroma compounds, lower contents of C_6 compounds (0.21–0.54 mg/l) and benzene derivative compounds (44.68–61.49 mg/l) and higher contents of terpene (0.26–0.89 mg/l) and C_{13}-norisoprenoid compounds (0.01–0.03 mg/l) were produced. Limonene, linalool, citronellol, nerol, β-ionone, phenylethyl alcohol, and phenylethyl acetate were the main odor active variety aroma compounds (OAV > 1) (**Table 2** and **Figure 2**).

Compared with the *S. cerevisiae* single fermentation, the four non-*Saccharomyces* yeast fermentations contained higher contents of fermentative aroma compounds (499.00–636.72 mg/l) (**Table 2** and **Figure 2**), especially higher alcohol (233.21–308.67 mg/l), and ester compounds (250.04–319.98 mg/l), and they produced higher concentrations of acetate compounds (195.87–242.58 mg/l) and lower concentrations of fatty acid ethyl ester compounds (32.11–77.40 mg/l). Isoamyl alcohol, isobutanol, 2-methylpentanol, 1-octanal, ethyl acetate, isobutyl acetate, isoamyl acetate, 2-methylbutyl acetate, ethyl butyrate, ethyl hexanoate, ethyl octanoate, ethyl 9-decenoate, ethyl decanoate, ethyl laurate, isoamyl caprylate, and isoamyl caproate were the main odor active fermentation aroma compounds.

PCA of Volatile Compounds From Wines Fermented by Yeast Strains With β-Glucosidase Activity

A principal component analysis (PCA) was carried out to reveal the correlation and segregation of volatile compounds with different yeast strain fermentations. Here 68.2% of variance was explained, and PC1 and PC2 accounted for 41% and 27.2% of variance, respectively. The *P. kudriavzevii* F2-16 fermentation and the *P. kudriavzevii* F2-24 fermentation were mainly grouped with varietal aroma compounds such as limonene, linalool, citronellol, and some kinds of fermentative aroma compounds such as 1-octanol, 2-methyl-1-butanol, isopentanoic acid, and 2-methylbutyric acid. The *I. terricola* SLY-4 fermentation and the *M. pulcherrima* HX-13 fermentation were closely clustered with various fermentative aroma compounds such as 2,3-butanediol, isoamyl alcohol, isobutyl acetate, acetic acid 2-methyl, ethyl butyrate, octanoic acid, 1-decanol, ethyl decanoate, phenylethyl acetate, and hexanoic acid. *S. cerevisiae* fermentation was grouped with some fermentative aroma compounds such as

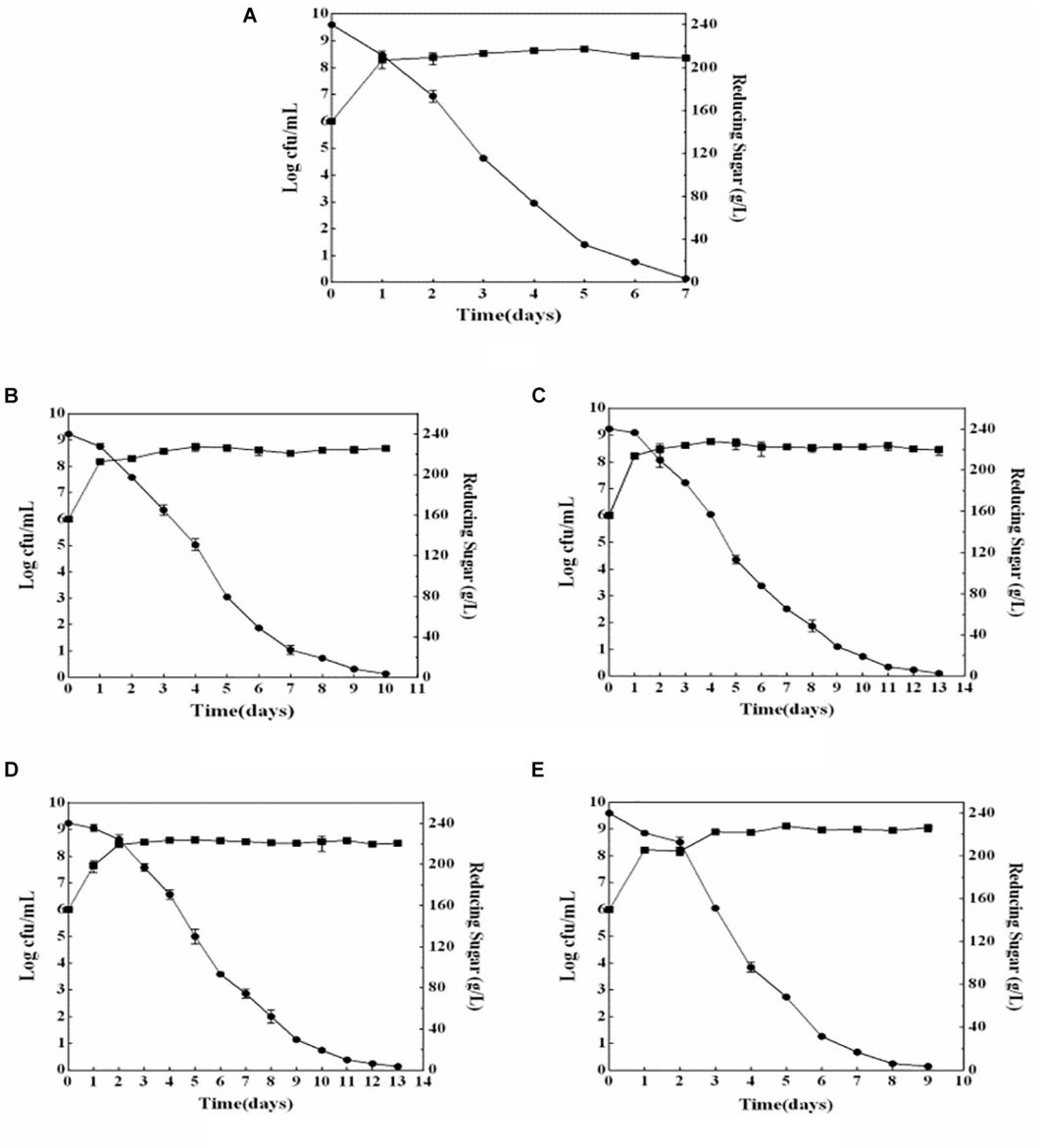

FIGURE 1 | Growth and sugar consumption kinetics of yeast strains during wine fermentation. **(A)** *S. cerevisiae* fermentation; **(B)** *I. terricola* SLY-4 fermentation; **(C)** *P. kudriavzevii* F2-24 fermentation; **(D)** *P. kudriavzevii* F2-16 fermentation; **(E)** *M. pulcherrima* HX-13 fermentation. -■-Growth kinetics of yeast strains -●-Sugar consumption kinetics of yeast strains.

TABLE 1 | Chemical characteristics of wines fermented by yeast with β-glycosidase activity.

Wines	Time (days)	Residual sugar (g/L)	Alcohol content (%, v/v)	Total acid (g/L)	Volatile acid (g/L)
SCw	7	3.57 ± 0.19^{a}	12.85 ± 0.36^{a}	5.44 ± 0.19^{a}	0.23 ± 0.01^{b}
SLY-4w	10	3.64 ± 0.07^{a}	12.91 ± 0.28^{a}	5.44 ± 0.19^{a}	0.31 ± 0.01^{a}
F2-24w	13	2.71 ± 0.07^{b}	12.69 ± 0.08^{a}	5.25 ± 0.19^{b}	0.26 ± 0.01^{b}
F2-16w	13	3.53 ± 0.20^{a}	12.08 ± 0.38^{a}	5.13 ± 0.18^{b}	0.25 ± 0.01^{b}
HX-13w	9	3.50 ± 0.30^{a}	12.96 ± 0.13^{a}	5.31 ± 0.11^{b}	0.24 ± 0.00^{b}

Different inline letters in the same row of values indicate significant differences determined by Duncan test at 95% confidence level.
SCw, S. cerevisiae fermentation; SLY-4w, I. terricola SLY-4 fermentation; F2-24w, P. kudriavzevii F2-24 fermentation; F2-16w, P. kudriavzevii F2-16 fermentation; HX-13w, M. pulcherrima HX-13 fermentation.

TABLE 2 | Volatile compounds in different wines (mg/L).

Compounds	Concentration (mg/L)					Odor threshold	OAV	Odors descriptions
	SCw	SLY-4w	F2-24w	F2-16w	HX-13w			
Varietal aroma	**85.29 ± 12.88^{a}**	**60.16 ± 0.40^{b}**	**45.49 ± 6.18^{c}**	**62.64 ± 0.53^{b}**	**57.89 ± 4.23^{b}**			
C_6 compounds	**0.78 ± 0.04^{a}**	**0.54 ± 0.02^{b}**	**0.21 ± 0.04^{d}**	**0.25 ± 0.01^{d}**	**0.33 ± 0.00^{c}**			
1-Hexanol	0.36 ± 0.05^{a}	0.02 ± 0.01^{c}	0.03 ± 0.01^{c}	0.06 ± 0.02^{c}	0.11 ± 0.01^{b}	8	<0.1	Green, herb
cis-2-Hexen-1-ol	0.42 ± 0.02^{c}	0.52 ± 0.03^{b}	0.19 ± 0.05^{d}	0.20 ± 0.01^{d}	0.23 ± 0.01^{d}	0.4	>0.1	Green, herb
Terpenes	**0.04 ± 0.01^{e}**	**0.26 ± 0.01^{d}**	**0.59 ± 0.01^{b}**	**0.89 ± 0.01^{a}**	**0.33 ± 0.04^{c}**			
Limonene	0.00 ± 0.00^{c}	0.00 ± 0.00^{c}	0.15 ± 0.01^{b}	0.22 ± 0.01^{a}	0.00 ± 0.00^{c}	0.1	>1	Lemon, citrus
Linalool	0.01 ± 0.00^{e}	0.10 ± 0.01^{c}	0.17 ± 0.01^{a}	0.12 ± 0.01^{b}	0.02 ± 0.01^{d}	0.025	>1	Muscat, flowery, fruity
Citronellol	0.02 ± 0.01^{d}	0.09 ± 0.01^{c}	0.17 ± 0.01^{b}	0.42 ± 0.01^{a}	0.17 ± 0.01^{b}	0.01	>1	Citrus
Nerol	0.01 ± 0.00^{d}	0.08 ± 0.02^{c}	0.11 ± 0.01^{b}	0.14 ± 0.02^{a}	0.14 ± 0.03^{a}	0.03	>1	Citrus
C_{13}-Norisoprenoids	**0.00 ± 0.00^{c}**	**0.03 ± 0.01^{a}**	**0.01 ± 0.00^{b}**	**0.02 ± 0.01^{b}**	**0.00 ± 0.00^{c}**			
β-Ionone	0.00 ± 0.00^{c}	0.03 ± 0.01^{a}	0.01 ± 0.00^{b}	0.02 ± 0.01^{b}	0.00 ± 0.00^{c}	$9*10^{-5}$	>1	Raspberry, violet, sweet fruity
Benzene derivatives	**84.51 ± 12.91^{a}**	**59.34 ± 0.41^{b}**	**44.68 ± 6.21^{c}**	**61.49 ± 0.56^{b}**	**57.23 ± 4.27^{b}**			
Benzaldehyde	0.29 ± 0.06^{b}	0.81 ± 0.02^{a}	0.00 ± 0.00^{c}	0.00 ± 0.00^{c}	0.87 ± 0.06^{a}	2	<0.1	
Benzyl alcohol	0.00 ± 0.00^{b}	0.30 ± 0.01^{a}	0.00 ± 0.00^{b}	0.00 ± 0.00^{b}	0.00 ± 0.00^{b}	200	<0.1	Almond, fatty
Phenethyl alcohol	72.16 ± 11.14^{a}	30.99 ± 1.56^{d}	40.35 ± 6.09^{c}	55.14 ± 0.75^{b}	33.24 ± 4.92^{d}	14	>1	Rose, soft tommy
Phenylethyl acetate	12.07 ± 1.71^{c}	27.25 ± 2.00^{a}	4.33 ± 0.12^{d}	6.35 ± 0.20^{d}	23.13 ± 0.59^{b}	0.25	>1	Floral, rose
Fermentative aroma	**404.89 ± 1.45^{d}**	**499.00 ± 9.53^{c}**	**530.83 ± 14.26^{b}**	**524.77 ± 23.19^{b}**	**636.72 ± 12.92^{a}**			
Higher alcohols	**202.03 ± 1.93^{e}**	**233.21 ± 1.86^{d}**	**273.88 ± 7.06^{c}**	**285.47 ± 4.60^{b}**	**308.67 ± 10.16^{a}**			
1-Propanol	2.51 ± 0.17^{c}	6.89 ± 0.02^{b}	2.85 ± 0.49^{c}	8.30 ± 0.41^{a}	0.00 ± 0.00^{d}	306	<0.1	Fresh, alcohol
Isobutyl alcohol	8.06 ± 0.61^{d}	10.73 ± 0.52^{d}	29.50 ± 1.06^{c}	61.01 ± 4.47^{b}	73.57 ± 3.23^{a}	40		Mild sweet, alcohol
1-Butanol	0.41 ± 0.00^{c}	0.85 ± 0.17^{ab}	0.69 ± 0.13^{b}	1.00 ± 0.15^{a}	0.00 ± 0.00^{d}	150	<0.1	Medicinal, fusel, pungency
Isoamyl alcohol	120.46 ± 3.21^{b}	167.28 ± 0.05^{a}	172.69 ± 7.57^{a}	109.57 ± 3.90^{c}	169.06 ± 1.60^{a}	30	>1	Alcohol, harsh, bitter, banana
2-Methyl-1-butanol	68.74 ± 0.50^{b}	45.36 ± 1.20^{c}	66.97 ± 0.00^{b}	102.68 ± 3.11^{a}	64.47 ± 14.99^{b}	65	>0.1	
2,3-Butanediol	0.77 ± 0.04^{c}	1.26 ± 0.01^{b}	0.64 ± 0.19^{c}	1.67 ± 0.21^{a}	1.44 ± 0.02^{b}	120	<0.1	Butter, creamy, chemical
3-Methyl-1-pentanol	0.56 ± 0.10^{a}	0.36 ± 0.01^{b}	0.00 ± 0.00^{c}	0.00 ± 0.00^{c}	0.00 ± 0.00^{c}	0.5	>1	Fusel
1-Octanol	0.27 ± 0.03^{c}	0.50 ± 0.05^{b}	0.44 ± 0.01^{b}	1.26 ± 0.15^{a}	0.14 ± 0.03^{d}	0.9	0.1-1	Waxy
1-Decanol	0.27 ± 0.08^{a}	0.00 ± 0.00^{c}	0.12 ± 0.01^{d}	0.00 ± 0.00^{c}	0.00 ± 0.00^{c}	0.4	0.1-1	Citrus, fatty
Fatty acids	**5.11 ± 0.06^{c}**	**9.16 ± 0.33^{a}**	**4.44 ± 0.14^{d}**	**5.91 ± 0.32^{b}**	**5.28 ± 0.22^{c}**			
Isobutyric acid	0.18 ± 0.01^{b}	0.00 ± 0.00^{c}	0.00 ± 0.00^{c}	0.68 ± 0.03^{a}	0.00 ± 0.00^{c}	8.1	<0.1	Phenol, chemical, fatty
2-Methylbutyric acid	0.32 ± 0.04^{b}	0.00 ± 0.00^{c}	0.29 ± 0.00^{b}	1.26 ± 0.11^{a}	0.00 ± 0.00^{c}	0.25	>1	Cheese
Isopentanoic acid	0.00 ± 0.00^{c}	0.63 ± 0.07^{b}	0.47 ± 0.02^{b}	1.02 ± 0.49^{a}	0.00 ± 0.00^{c}	0.033	>1	Sweaty feet
Hexanoic acid	1.54 ± 0.06^{b}	2.21 ± 0.03^{a}	1.52 ± 0.06^{b}	1.13 ± 0.00^{d}	2.25 ± 0.10^{a}	0.42	>1	Cheese, rancid
Octanoic acid	3.01 ± 0.04^{c}	5.84 ± 0.20^{a}	2.06 ± 0.05^{e}	1.83 ± 0.04^{f}	2.57 ± 0.11^{d}	0.5	>1	Rancid, harsh, cheese, fatty acid
Decanoic acid	0.06 ± 0.00^{cd}	0.48 ± 0.03^{b}	0.11 ± 0.01^{c}	0.00 ± 0.00^{d}	0.46 ± 0.01^{b}	1	<0.1	Unpleasant
Esters	**194.88 ± 3.24^{e}**	**251.99 ± 10.90^{b}**	**250.04 ± 21.92^{b}**	**231.50 ± 19.11^{b}**	**319.98 ± 23.37^{a}**			
Acetic esters	**90.82 ± 3.40^{c}**	**203.12 ± 4.25^{b}**	**217.94 ± 25.24^{ab}**	**195.87 ± 14.59^{b}**	**242.58 ± 17.28^{a}**			

(Continued)

TABLE 2 | Continued

Compounds	Concentration (mg/L)					Odor threshold	OAV	Odors descriptions
	SCw	SLY-4w	F2-24w	F2-16w	HX-13w			
Ethyl acetate	50.46 ± 2.14^{d}	107.46 ± 8.00^{bc}	143.02 ± 10.44^{a}	112.46 ± 11.00^{b}	94.47 ± 11.00^{c}	7.5	>1	Fruity, sweet
Propyl acetate	0.00 ± 0.00^{f}	0.41 ± 0.00^{c}	0.33 ± 0.01^{d}	1.13 ± 0.00^{a}	0.70 ± 0.02^{b}	4.7	<1	Fruity
Isobutyl acetate	0.63 ± 0.07^{d}	1.27 ± 0.15^{c}	0.82 ± 0.05^{d}	2.53 ± 0.40^{b}	10.23 ± 0.26^{a}	1.6	>0.1	Garnetberry, fruity, flowery
Isoamyl acetate	33.70 ± 0.94^{d}	85.91 ± 5.35^{bc}	71.47 ± 14.98^{b}	75.31 ± 3.15^{c}	117.79 ± 6.00^{a}	0.03	>1	Banana
2-Methylbutyl acetate	5.78 ± 2.11^{bc}	7.53 ± 1.32^{b}	2.30 ± 0.12^{d}	4.45 ± 0.05^{c}	19.39 ± 0.00^{a}	0.02–0.05	>1	Fruity
Pentanol acetate	0.00 ± 0.00^{b}	0.18 ± 0.05^{a}	0.00 ± 0.00^{b}	0.00 ± 0.00^{b}	0.00 ± 0.00^{b}			
3-Methylpentyl acetate	0.00 ± 0.00^{b}	0.37 ± 0.07^{a}	0.00 ± 0.00^{b}	0.00 ± 0.00^{b}	0.00 ± 0.00^{b}			
Hexyl acetate	0.19 ± 0.03^{b}	0.00 ± 0.00^{c}	0.00 ± 0.00^{c}	0.00 ± 0.00^{c}	0.00 ± 0.00^{c}	1.5	0.1–1	Pleasant fruity, pear
Octyl acetate	0.06 ± 0.00^{b}	0.00 ± 0.00^{c}	0.00 ± 0.00^{c}	0.00 ± 0.00^{c}	0.00 ± 0.00^{c}			
Fatty acid ethyl esters	**101.42 ± 0.20^{a}**	**48.87 ± 6.65^{c}**	**32.11 ± 3.32^{d}**	**35.63 ± 4.52^{d}**	**77.40 ± 6.09^{b}**			
Ethyl propanoate	0.25 ± 0.02^{d}	0.00 ± 0.00^{e}	0.48 ± 0.02^{c}	1.48 ± 0.25^{a}	1.10 ± 0.06^{b}	1.8–2.1	0.1–1	
Ethyl butyrate	2.35 ± 0.10^{b}	1.81 ± 0.54^{bc}	1.45 ± 0.39^{c}	2.10 ± 0.09^{b}	5.47 ± 0.50^{a}	0.02	>1	Sour fruit, strawberry, fruity
Ethyl hexanoate	44.99 ± 0.34^{a}	12.43 ± 2.10^{d}	11.24 ± 1.09^{d}	10.67 ± 1.22^{d}	31.77 ± 2.32^{b}	0.014	>1	Green apple, fruity, strawberry, anise
Ethyl heptanoate	38.78 ± 0.54^{a}	16.47 ± 1.12^{c}	11.58 ± 1.02^{d}	11.95 ± 0.70^{d}	23.47 ± 2.42^{b}	0.005	>1	Fruity, sweet, anise, wax
Ethyl octanoate	0.06 ± 0.01^{b}	0.00 ± 0.00^{c}	0.00 ± 0.00^{c}	0.00 ± 0.00^{c}	0.00 ± 0.00^{c}	1.3	<0.1	banana
Ethyl non-anoate	1.19 ± 0.06^{a}	0.19 ± 0.03^{c}	0.00 ± 0.00^{c}	0.00 ± 0.00^{c}	0.43 ± 0.02^{b}	0.1	>1	Green, fruity, fatty
Ethyl 9-decenoate	8.09 ± 0.26^{c}	12.39 ± 1.71^{b}	4.67 ± 0.55^{d}	5.06 ± 1.91^{d}	9.65 ± 0.49^{c}	0.1	>1	Fruity, fatty, pleasant, wax flavor
Ethyl decanoate	4.04 ± 0.62^{b}	3.48 ± 0.83^{b}	1.73 ± 0.14^{c}	2.16 ± 0.15^{c}	3.26 ± 0.29^{b}	1.5	>1	Waxy
Ethyl dodecanoate	0.64 ± 0.05^{b}	0.59 ± 0.03^{c}	0.18 ± 0.01^{e}	0.75 ± 0.01^{a}	0.30 ± 0.02^{d}	2	0.1–1	Fatty, butter
Ethyl myristate	0.76 ± 0.03^{b}	0.63 ± 0.18^{b}	0.36 ± 0.09^{c}	0.34 ± 0.08^{c}	1.01 ± 0.01^{a}	100–200	<0.1	Green, fruity
Diethyl succinate	0.30 ± 0.01^{d}	0.90 ± 0.12^{b}	0.44 ± 0.03^{c}	1.14 ± 0.13^{a}	0.98 ± 0.01^{b}	1.5	0.1–1	Fatty
Ethyl palmitate	38.78 ± 0.54^{a}	16.47 ± 1.12^{c}	11.58 ± 1.02^{d}	11.95 ± 0.70^{d}	23.47 ± 2.42^{b}	0.005	>1	Fruity, sweet, anise, wax
Other esters	**2.64 ± 0.04^{a}**	**0.00 ± 0.00^{c}**	**0.00 ± 0.00^{c}**	**0.00 ± 0.00^{c}**	**0.00 ± 0.00^{c}**			
Isoamyl octanoate	1.29 ± 0.06^{a}	0.00 ± 0.00^{c}	0.00 ± 0.00^{c}	0.00 ± 0.00^{c}	0.00 ± 0.00^{c}	0.13	>1	Sweet, cheese
Isoamyl hexanoate	1.35 ± 0.10^{a}	0.00 ± 0.00^{c}	0.00 ± 0.00^{c}	0.00 ± 0.00^{c}	0.00 ± 0.00^{c}			
Carbonyl compounds	**2.89 ± 0.06^{b}**	**4.64 ± 0.16^{a}**	**2.48 ± 0.46^{b}**	**1.90 ± 0.21^{c}**	**2.79 ± 0.51^{b}**			
1-Non-anal	0.17 ± 0.01^{b}	0.00 ± 0.00^{d}	0.27 ± 0.03^{a}	0.00 ± 0.00^{d}	0.00 ± 0.00^{d}	0.015	>1	Waxy
1-Decanal	0.32 ± 0.03^{b}	0.23 ± 0.05^{c}	0.00 ± 0.00^{e}	0.00 ± 0.00^{e}	0.62 ± 0.01^{a}	0.001	>1	Sweet
2,3-Butanedione	0.94 ± 0.02^{d}	3.16 ± 0.05^{a}	1.52 ± 0.07^{b}	1.09 ± 0.06^{c}	1.04 ± 0.05^{c}	0.1	>1	Butter, cheese
2,3-Pentanedione	1.46 ± 0.01^{a}	1.26 ± 0.07^{ab}	0.70 ± 0.36^{c}	0.81 ± 0.27^{bc}	1.14 ± 0.47^{abc}	<0.1	>1	Butter, cheese

Data show average of triplicates ± SD. Different letters indicated differences among wines determined by Duncan test at the 95% confidence level.
SCw, S. cerevisiae fermentation; SLY-4w, I. terricola SLY-4 fermentation; F2-24w, P. kudriavzevii F2-24 fermentation; F2-16w, P. kudriavzevii F2-16 fermentation; HX-13w, M. pulcherrima HX-13 fermentation.
Bold values represent the total content of a class of substances.

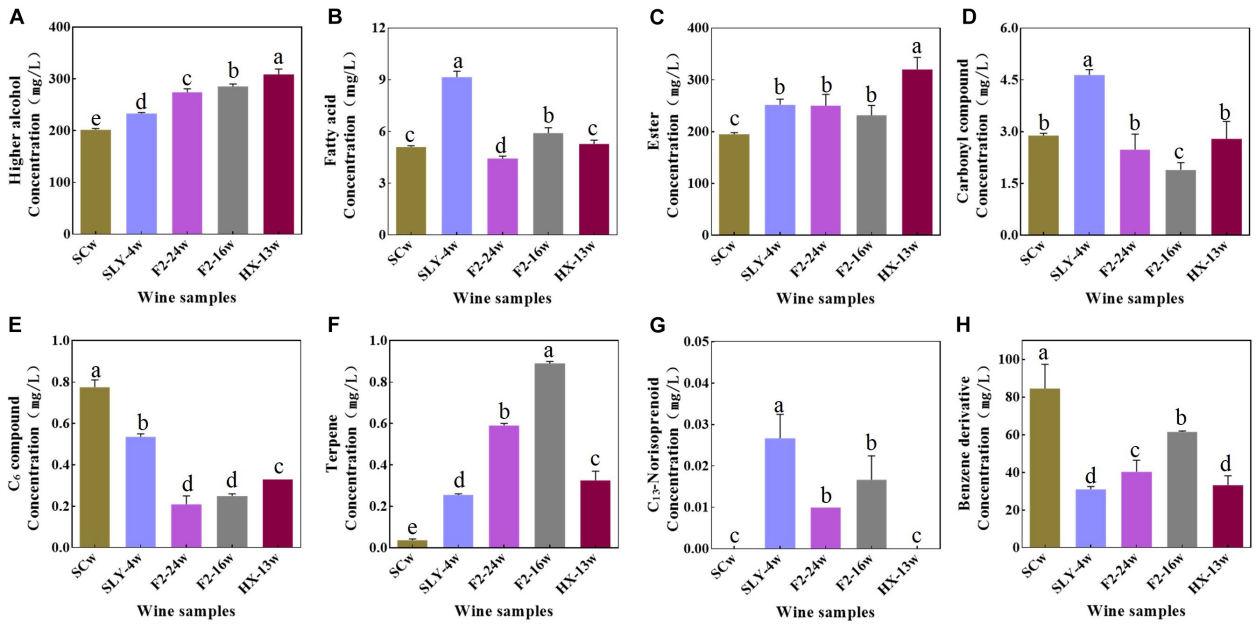

FIGURE 2 | Concentration of aroma compounds in wines fermented by different yeast strains. **(A)** Higher alcohols. **(B)** Fatty acids. **(C)** Esters. **(D)** Carbonyl compounds. **(E)** C_6 compounds. **(F)** Terpenes. **(G)** C_{13}-Norisoprenoids. **(H)** Benzene derivatives; SCw, *S. cerevisiae* fermentation; SLY-4w, *I. terricola* SLY-4 fermentation; F2-24w, *P. kudriavzevii* F2-24 fermentation; F2-16w, *P. kudriavzevii* F2-16 fermentation; HX-13w, *M. pulcherrima* HX-13 fermentation.

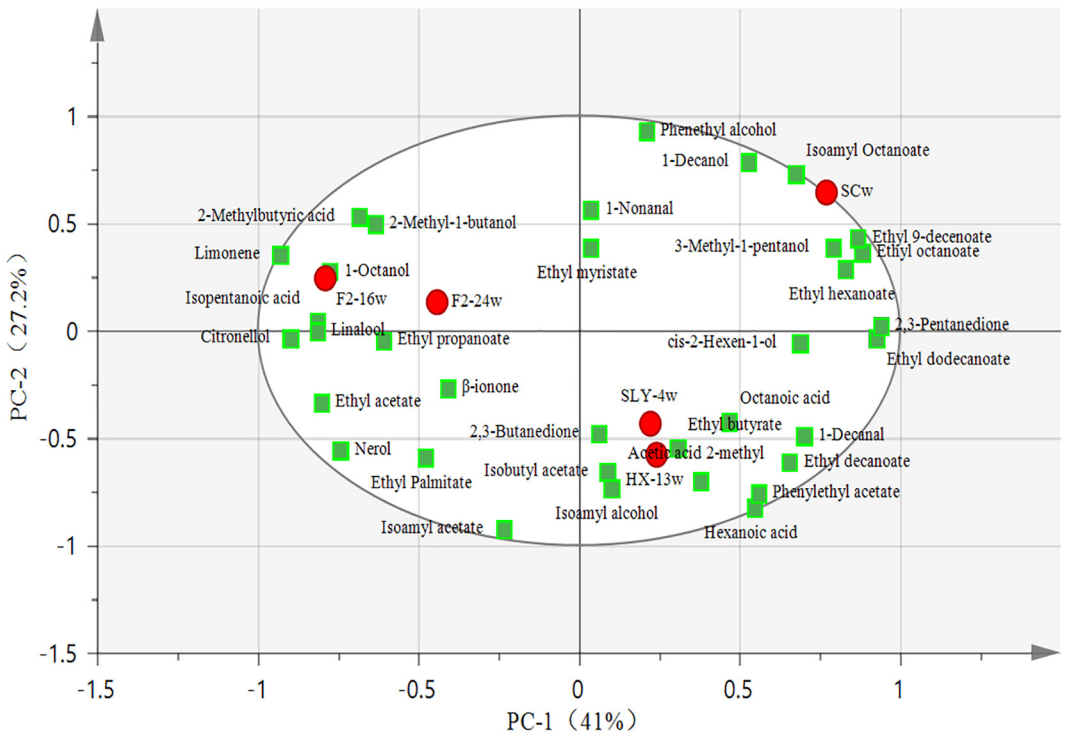

FIGURE 3 | PCA plot of volatile compounds from wines fermented by different yeast strains. ● Wine samples; ■ Aroma compounds; SCw, *S. cerevisiae* fermentation; SLY-4w, *I. terricola* SLY-4 fermentation; F2-24w, *P. kudriavzevii* F2-24 fermentation; F2-16w, *P. kudriavzevii* F2-16 fermentation; HX-13w, *M. pulcherrima* HX-13 fermentation.

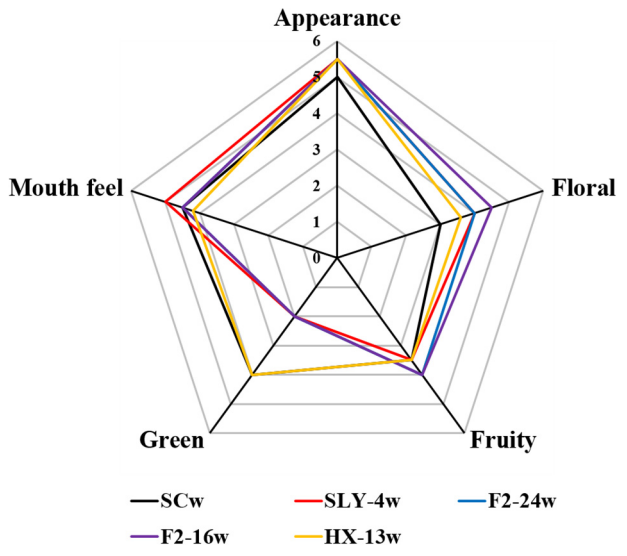

FIGURE 4 | Aroma compounds profiles of wines fermented by different yeast strains with β-glucosidase activity. SCw, *S. cerevisiae* fermentation; SLY-4w, *I. terricola* SLY-4 fermentation; F2-24w, *P. kudriavzevii* F2-24 fermentation; F2-16w, *P. kudriavzevii* F2-16 fermentation; HX-13w, *M. pulcherrima* HX-13 fermentation.

isoamyl octanoate, 3-methyl-1-pentanol, ethyl 9-decenoate, ethyl octanoate, and ethyl hexanoate (**Figure 3**).

Sensory Evaluation of Wines Fermented by Different Yeast Strains With β-Glucosidase Activity

Compared with that of the *S. cerevisiae* single fermentation, all the non-*Saccharomyces* yeast fermentations had no significant difference in appearance, but they had a stronger fruity and floral flavor and a weaker green flavor with exception of *M. pulcherrima* HX-13 fermentation. *I. terricola* SLY-4 fermentation had the best taste, followed by the fermentations of *S. cerevisiae*, *P. kudriavzevii* F2-24, *P. kudriavzevii* F2-16, and *M. pulcherrima* HX-13. The order of total acceptance for the wines from high to low was fermentation of *I. terricola* SLY-4, *P. kudriavzevii* F2-24, *P. kudriavzevii* F2-16, *M. pulcherrima* HX-13, and *S. cerevisiae* (**Figure 4**).

DISCUSSION

Compared with those of the *S. cerevisiae* single fermentation, the four non-*Saccharomyces* yeast strains had higher biomasses and longer fermentation periods which were also reported by Andorrà et al. (2010) and Belda et al. (2015). Those results mean that the four non-*Saccharomyces* yeast strains consumed sugar more slowly than *S. cerevisiae* did, but they could consume it completely.

Compared with *S. cerevisiae*, the four non-*Saccharomyces* yeast strains had no negative effects on the chemical characteristics of wines. Specifically, they produced lower contents of C_6 compounds and benzene derivative and higher contents of terpene, β-ionone, higher alcohol, and ester compounds, these phenomena were also reported by Nyanga et al. (2013); Del Mónaco et al. (2014), Lu et al. (2017), and Sun et al. (2017). Low concentrations of C_6 compounds would reduce the green flavor of wines (Mendez-Costabel et al., 2014; Vilanova et al., 2016), while high contents of terpene, isoprenoid, benzene derivative, ester, and higher alcohol would enhance the fruity and floral flavor of wines (Pretorius and Lambrechts, 2000; Swiegers and Pretorius, 2005; Noguerol-Pato et al., 2012; Sun et al., 2017). The sensory evaluation results of wines indeed indicated that the green flavor of wines was reduced by the four non-*Saccharomyces* yeast strains with exception of *M. pulcherrima* HX-13, and their fruity and floral flavors were enhanced. More importantly, the first report about *M. pulcherrima* could produce high content of varietal aroma compounds in wine. The volatile compound profiles of the four non-*Saccharomyces* yeast fermentations were significantly different from those of *S. cerevisiae* fermentation. Moreover, the volatile compound profiles of *P. kudriavzevii* F2-16 and *P. kudriavzevii* F2-24 fermentations were remarkably different from those of *I. terricola* SLY-4 and *M. pulcherrima* HX-13 fermentations. Different volatile compounds profiles would take different flavor characteristics on wines (Lu et al., 2017; Siebert et al., 2018), which was consistent with sensory evaluation results of wines.

CONCLUSION

Compared with those of *S. cerevisiae* single fermentation, the four non-*Saccharomyces* yeast strains could grow and consume sugar completely and had no significantly negative effect on chemical characteristics of wines. All the four non-*Saccharomyces* yeast strains could improve the flavor and quality of wines. Moreover, different yeast strains produced different aroma compounds profiles and take on different aroma characteristics of wines. The four non-*Saccharomyces* yeast strain fermentations received higher acceptance of sensory evaluation than *S. cerevisiae* did, and *I. terricola* SLY-4 fermentation got the highest sensory evaluation score, followed by *P. kudriavzevii* F2-24, *P. kudriavzevii* F2-16, and *M. pulcherrima* HX-13 fermentation from high to low. However, pure non-*Saccharomyces* yeast fermentation had disadvantages with long fermentation periods and lower content of benzene derivative and fatty acid ethyl ester compounds. To overcome the disadvantages of pure non-*Saccharomyces* yeast fermentation, co-fermentation of several non-*Saccharomyces* yeast strains with different aroma compound profiles, or pure *S. cerevisiae* fermentation of must with addition of complex β-glucosidase (crude or purified) from different non-*Saccharomyces* yeast strains, might be used to further improve the kind of aroma compounds and the flavor complexity of wine and shorten the fermentation period of wine. The research results will provide non-Saccharomyces yeast strains to improve the flavor and quality of wines, and a reference for the selection of other non-*Saccharomyces* yeasts strains with better oenological characteristics.

DATA AVAILABILITY STATEMENT

The original contributions presented in the study are included in the article/supplementary material, further inquiries can be directed to the corresponding author.

AUTHOR CONTRIBUTIONS

XZ and YZ contributed to the experimental design. YZ, WZ, and TQ completed the experiments, performed statistical analysis, and wrote the manuscript. TQ and JL contributed to the experiment verification. JL, YZ, and TQ contributed to the revision of the manuscript. All authors contributed to the article and approved the submitted version.

FUNDING

This research was supported by the National Natural Science Foundation Project of China (31871768) and the Major Science and Technology Program of Ningxia Hui Autonomous Region (2016BZ0601/02/03).

REFERENCES

Andorrà, I., Berradre, M., Rozes, N., Mas, A., Guillamon, J. M., and Esteve-Zarzoso, B. (2010). Effect of pure and mixed cultures of the main wine yeast species on grape must fermentations. *Eur. Food Res. Technol.* 231, 215–224. doi: 10.1007/s00217-010-1272-0

Baffi, M. A., Tobal, T., Henrique, J., Lago, G., Leite, R. S. R., Boscolo, M., et al. (2011). A novel β-glucosidase from. *J. Food Sci.* 76, 997–1002. doi: 10.1111/j.1750-3841.2011.02293.x

Belda, I., Navascués, E., Marquina, D., Santos, A., Calderon, F., and Benito, S. (2015). Dynamic analysis of physiological properties of *Torulaspora delbrueckii* in wine fermentations and its incidence on wine quality. *Appl. Microbiol. Biotechnol.* 99, 1911–1922. doi: 10.1007/s00253-014-6197-2

Binati, R. L., Junior, W. J. F. L., Luzzini, G., Slaghenaufi, D., Ugliano, M., and Torriani, S. (2020). Contribution of non-*Saccharomyces* yeasts to wine volatile and sensory diversity: a study on *Lachancea thermotolerans*, *Metschnikowia* spp. and *Starmerella bacillaris* strains isolated in Italy - sciencedirect. *Int. J. Food Microbiol.* 318:108470. doi: 10.1016/j.ijfoodmicro.2019.108470

Boscaino, F., Ionata, E., Cara, F. L., Guerriero, S., Marcolongo, L., and Sorrentino, A. (2019). Impact of *Saccharomyces cerevisiae* and *Metschnikowia fructicola* autochthonous mixed starter on Aglianico wine volatile compounds. *J. Food Sci. Technol.* 56, 4982–4991. doi: 10.1007/s13197-019-03970-9

Cabrita, M. J., Freitas, A. M. C., Laureano, O., and Stefano, R. D. (2010). Glycosidic aroma compounds of some Portuguese grape cultivars. *J. Sci. Food Agric.* 86, 922–931. doi: 10.1002/jsfa.2439

Canonico, L., Solomon, M., Comitini, F., Ciani, M., and Varela, C. (2019). Volatile profile of reduced alcohol wines fermented with selected non-*Saccharomyces* yeasts under different aeration conditions. *Food Microbiol.* 84, 103247.1–103247.8. doi: 10.1016/j.fm.2019.103247

Del Mónaco, S. M., Barda, N. B., Rubio, N. C., and Caballero, A. C. (2014). Selection and characterization of a Patagonian *Pichia kudriavzevii* for wine deacidification. *J. Appl. Microbiol.* 117, 451–464. doi: 10.1111/jam.12547

García-Carpintero, E. G., Sánchez-Palomo, E., and González-Viñas, M. A. (2011). Aroma characterization of red wines from cv. Bobal grape variety grown in La Mancha region. *Food Res. Int.* 44, 61–70. doi: 10.1016/j.foodres.2010.11.013

López, M. C., Mateo, J. J., and Maicas, S. (2015). Screening of β-glucosidase and β-xylosidase activities in four non-*Saccharomyces* yeast isolates. *J. Food Sci.* 80, C1696–C1704. doi: 10.1111/1750-3841.12954

López, S., Mateo, J. J., and Maicas, S. M. (2016). Characterisation of *Hanseniaspora* isolates with potential aroma-enhancing properties in muscat wines. *S. Afr. J. Enol. Viticult.* 35, 292–303. doi: 10.21548/35-2-1018

Lu, Y., Voon, M. K. W., Chua, J. Y., Huang, D., Lee, P. R., and Liu, S. Q. (2017). The effects of co- and sequential inoculation of *Torulaspora delbrueckii* and *Pichia kluyveri* on chemical compositions of durian wine. *Appl. Microbiol. Biotechnol.* 101, 7853–7863. doi: 10.1007/s00253-017-8527-7

Ma, D., Xia, Y., Wang, Q., Zhang, Y., and Tao, Y. (2017). Performance of selected *P. fermentans* and its excellular enzyme in co-inoculation with *S. cerevisiae* for wine aroma enhancement. *LWT Food Sci. Technol.* 86, 361–370. doi: 10.1016/j.lwt.2017.08.018

Mendez-Costabel, M. P., Wilkinson, K. L., Bastian, S. E. P., Jordans, C., Mccarthy, M., Ford, C. M., et al. (2014). Effect of increased irrigation and additional nitrogen fertilisation on the concentration of green aroma compounds in *Vitis vinifera* L. Merlot fruit and wine. *Aust. J. Grape Wine R.* 20, 80–90. doi: 10.1111/ajgw.12062

Noguerol-Pato, R., González-Álvarez, M., González-Barreiro, C., Cancho-Grande, B., and Simal-Gándara, J. (2012). Aroma profile of Garnacha Tintorera-based sweet wines by chromatographic and sensorial analyses. *Food Chem.* 134, 2313–2325. doi: 10.1016/j.foodchem.2012.03.105

Nyanga, L. K., Nout, M. J. R., Smid, E. J., Teun, B., and Zwietering, M. H. (2013). Fermentation characteristics of yeasts isolated from traditionally fermented masau (Ziziphus mauritiana) fruits. *Int. J. Food Microbiol.* 166, 426–432. doi: 10.1016/j.ijfoodmicro.2013.08.003

OIV-MA-AS313-01: R2015. (2015). *Compendium of International Methods of Wine and Must Analysis. Chemical Analysis: Acids, Total Acidity (Oeno 551/2015)*. Paris: Organisation Internationale de la Vigne et du Vin.

OIV-MA-AS312-01A: R2016. (2016). *Compendium of International Methods of Wine and Must Analysis. Chemical Analysis: Alcohols, Alcoholic Strength by Volume (Resolution Oeno 566/2016)*. Paris: Organisation Internationale de la Vigne et du Vin.

OIV-MA-AS311-02: R2009. (2009). *Compendium of International Methods of Wine and Must Analysis. Chemical Analysis: SUGARS, Glucose and Fructose*. Paris: Organisation Internationale de la Vigne et du Vin.

OIV-MA-AS313-02: R2015. (2015). *Compendium of International Methods of Wine and Must Analysis. Chemical Analysis: Acids, Volatile Acidity*. Paris: Organisation Internationale de la Vigne et du Vin.

Ovalle, S. D., Brena, B., Fariña, L., and Gonzálezpombo, P. (2016). Novel β-glucosidase from *Issatchenkia orientalis*: characterization and assessment for hydrolysis of muscat wine glycosides. *Global J. Biochem. Biotechnol.* 4, 174–183. doi: 10.1016/j.lwt.2017.09.026

Parker, M., Capone, D. L., Francis, I. L., and Herderich, M. J. (2017). Aroma precursors in grapes and wine: flavor release during wine production and consumption. *J. Agric. Food Chem.* 66, 2281–2286. doi: 10.1021/acs.jafc.6b05255

Pires, E. J., Teixeira, J. A., Brányik, T., and Vicente, A. A. (2014). Yeast: the soul of beer's aroma—a review of flavour-active esters and higher alcohols produced by the brewing yeast. *Appl. Microbiol. Biotechnol.* 98, 1937–1949. doi: 10.1007/s00253-013-5470-0

Plessis, H. D., Toit, M. D., Nieuwoudt, H. H., Rijst, M. V. D., and Jolly, N. (2019). Modulation of wine flavor using *Hanseniaspora uvarum* in combination with different *Saccharomyces cerevisiae*, lactic acid bacteria strains and malolactic fermentation strategies. *Fermentation* 5:64. doi: 10.3390/fermentation5030064

Pretorius, I. S., and Lambrechts, M. G. (2000). Yeast and its importance to wine aroma: a review. *South Afr. J. Enol. Viticult.* 21, 97–129. doi: 10.21548/21-1-3560

Sabel, A., Martens, S., Petri, A., König, H., and Claus, H. (2014). *Wickerhamomyces anomalus* as1: a new strain with potential to improve wine aroma. *Ann. Microbiol.* 64, 483–491. doi: 10.1007/s13213-013-0678-x

Siebert, T. E., Barker, A., Pearson, W., Barter, S. R., Ma, D. B. L., Darriet, P., et al. (2018). Volatile compounds related to 'Stone Fruit' aroma attributes in viognier and chardonnay wines. *J. Agric. Food Chem.* 66, 2838–2850. doi: 10.1021/acs.jafc.7b05343

Suárez, R., Suárez-Lepe, J. A., Morata, A., and Calderón, F. (2007). The production of ethylphenols in wine by yeasts of the genera *Brettanomyces* and *Dekkera*: a review. *Food Chem.* 102, 10–21. doi: 10.1016/j.foodchem.2006.03.030

Sun, W. X., Hu, K., Zhang, J. X., Zhu, X. L., and Tao, Y. S. (2017). Aroma modulation of Cabernet Gernischt dry red wine by optimal enzyme treatment strategy in winemaking. *Food Chem*. 245:1248. doi: 10.1016/j.foodchem.2017.11.106

Swiegers, J. H., and Pretorius, I. S. (2005). Yeast modulation of wine flavor. *Adv. Appl. Microbiol*. 57, 131–175. doi: 10.1016/S0065-2164(05)57005-9

Vilanova, M., Genisheva, Z., Graña, M., and Oliveira, J. M. (2016). Determination of odorants in varietal wines from international grape cultivars (Vitis vinifera) grown in NW Spain. *S. Afr. J. Enol. Vitic.* 34, 6502–6506. doi: 10.1073/pnas.87.17.6502

Wang, J., Hu, L. L., Zhang, J. X., Chen, F. S., and Zhang, X. Y. (2018). Screening of wild yeast with high yield β-glycosidase and difference analysis of the enzyme production ability. *Chn. Brw.* 037, 50–53. doi: 10.11882/j.issn.0254-5071.2018.02.011

Zhang, W., Zhuo, X., Hu, L., and Zhang, X. (2020). Effects of crude β-glucosidases from *Issatchenkia terricola*, *Pichia kudriavzevii*, *Metschnikowia pulcherrima* on the flavor complexity and characteristics of wines. *Microorganisms* 8:953. doi: 10.3390/microorganisms8060953

Conflict of Interest: The authors declare that the research was conducted in the absence of any commercial or financial relationships that could be construed as a potential conflict of interest.

Publisher's Note: All claims expressed in this article are solely those of the authors and do not necessarily represent those of their affiliated organizations, or those of the publisher, the editors and the reviewers. Any product that may be evaluated in this article, or claim that may be made by its manufacturer, is not guaranteed or endorsed by the publisher.

frontiers in Microbiology

ORIGINAL RESEARCH
published: 20 September 2021
doi: 10.3389/fmicb.2021.716281

Comparison of the Fermentation Activities and Volatile Flavor Profiles of Chinese Rice Wine Fermented Using an Artificial Starter, a Traditional JIUYAO and a Commercial Starter

*Chen Chen, Zheng Liu, Wenya Zhou, Huaixiang Tian, Juan Huang, Haibin Yuan and Haiyan Yu**

Department of Food Science and Technology, Shanghai Institute of Technology, Shanghai, China

OPEN ACCESS

Edited by:
Xucong Lv,
Fuzhou University, China

Reviewed by:
Yongjun Xia,
University of Shanghai for Science and Technology, China
Sheng Yin,
Beijing Technology and Business University, China

***Correspondence:**
Haiyan Yu
hyyu@sit.edu.cn

Specialty section:
This article was submitted to Food Microbiology, a section of the journal Frontiers in Microbiology

Received: *28 May 2021*
Accepted: *24 August 2021*
Published: *20 September 2021*

Citation:
Chen C, Liu Z, Zhou W, Tian H, Huang J, Yuan H and Yu H (2021) Comparison of the Fermentation Activities and Volatile Flavor Profiles of Chinese Rice Wine Fermented Using an Artificial Starter, a Traditional JIUYAO and a Commercial Starter. Front. Microbiol. 12:716281. doi: 10.3389/fmicb.2021.716281

In this study, an artificial starter culture was prepared using the core microbial species of JIUYAO to produce Chinese rice wine (CRW). The fermentation activity and flavor profiles of CRW samples fermented with traditional JIUYAO, a commercial starter culture, and our artificial starter culture were compared. The optimal protectant combination for lyophilization of the artificial starter was established as 15.09% skim milk, 4.45% polyethylene glycol, 1.96% sodium glutamate, and 11.81% maltodextrin. A comparative analysis revealed that the ethanol content of the three CRW samples was similar. The total acid content of the CRW sample fermented with the artificial starter (7.10 g/L) was close to that of the sample fermented with JIUYAO (7.35 g/L), but higher than that of the sample fermented with the commercial starter (5.40 g/L). An electronic nose analysis revealed that the olfactory fingerprints of the CRW samples fermented with JIUYAO and the artificial starter resembled each other. For both above mentioned samples, the flavor profiles determined by gas chromatography–mass spectrometry indicated some differences in the variety and content of the aroma compounds, but the key odorants (odor activity values $\geq$1), such as isoamyl acetate, ethyl acetate, phenyl alcohol, and isoamyl alcohol, were similar.

Keywords: Chinese rice wine, artificial starter, JIUYAO, flavor profiles, response surface methodology

INTRODUCTION

Chinese rice wine (CRW), which has a high nutritional value and distinctive flavor, has been consumed for centuries (Xu et al., 2015; Huang Z. R. et al., 2018). CRW includes many renowned types, such as Shaoxing, Jimo, and Fujian rice wine (Jiao et al., 2017). The best-known CRW, Shaoxing rice wine, is generally produced using glutinous rice, traditional JIUYAO, and wheat *qu* (Chen et al., 2013). JIUYAO is a mixed starter culture that mainly includes bacteria, molds, and yeast and is responsible for the starch saccharification and fermentation in Shaoxing rice wine brewing (Liu et al., 2018). The microorganisms in JIUYAO are believed to play a crucial role in the fermentation activity and unique flavor formation of Shaoxing rice wine (Xie et al., 2007).

Zhao et al. (2020) revealed that *Proteobacteria* and *Firmicutes* are the dominant bacterial phyla in JIUYAO. Our previous study (Chen et al., 2020) found that only five core species, two from the *Weissella* genus and one each from the *Pediococcus*, *Saccharomycopsis*, and *Rhizopus* genera, play a key role in the flavor formation and fermentation activity of CRW.

Currently, commercial starters that mainly include yeast and *Rhizopus* are widely used in the industrial brewing of CRW (Ferrer-Gallego et al., 2014). Although the fermentation period of CRW brewed with commercial starters is comparable to that of CRW brewed with traditional JIUYAO (Huang et al., 2019), the flavor of the former is inferior due to the limited microbial variety in the commercial starters (Liu et al., 2019). However, as traditional JIUYAO is usually handcrafted, its limitation is the instability of the resulting CRW's quality and flavor profiles across batches (Zhao and Zhang, 2010). Therefore, it would be of great significance to develop an artificial starter culture as a replacement for traditional JIUYAO that could yield CRW batches of high quality and uniform flavor.

A microbial consortium selected as a starter culture should be able to withstand subsequent fermentation. Therefore, lyophilization techniques and low temperatures (refrigeration or freezing) are usually used to stabilize the starter culture (Abadias et al., 2001; Pradelles et al., 2009). Lyophilization is a simple technique to maintain a high number of viable microorganisms in a starter culture inoculum in powder form, as it involves few procedural steps. However, this preservation process can cause cell damage or lead to cell death (Ale et al., 2015). Cell mortality during lyophilization can be minimized by optimizing freeze-drying conditions and using lyoprotectants (Cerrutti et al., 2000; Hubálek, 2003), such as proteins, skim milk, sugars, and other biopolymers (Coulibaly et al., 2016). Although freeze-dried bacterial powder with protectants has been used as a starter culture (Chen H. et al., 2015), its use in place of traditional JIUYAO for CRW brewing has not been documented.

In this study, an artificial starter culture was prepared by combining the core microorganisms from traditional JIUYAO that contribute to the unique flavor of CRW, and then freeze-drying them to powder form using a lyoprotectant combination optimized through a response surface optimization experiment. The fermentation activity and flavor profile of the CRW samples fermented with this artificial starter were compared with those of samples fermented with traditional JIUYAO and a commercial starter culture. The use of such an artificial starter can improve and standardize the fermentation activity and aroma quality of CRW, and further promote the industrial production of traditional CRW.

TABLE 1 | Experimental factor levels of the Box–Behnken design.

Factors	Level		
	−1	0	1
A skim milk (%)	10	15	20
B polyethylene glycol (%)	3	5	7
C sodium glutamate (%)	1.5	2	2.5
D maltodextrin (%)	5	10	15

MATERIALS AND METHODS

JIUYAO, Starter Culture and Lyoprotectants

JIUYAO samples were obtained from Zhejiang Tapai Shaoxing Rice Wine Co., Ltd., Shaoxing city, Zhejiang province, China. The samples were refrigerated at 4°C before being transported to the laboratory. A commercial starter culture composed of *Saccharomyces cerevisiae* and *Rhizopus oryzae* was purchased from a commercial yeast and yeast extract manufacturer in China. Five microbial species, namely *Pediococcus pentosaceus* (CCTCC M 2019323), *Weissella cibaria* (BNCC206838), *W. confusa* (CICC23465), *Saccharomycopsis fibuligera* (CCTCC M 2019324), and *R. arrhizus* (CCTCC M 2019325), were selected and isolated as the core functional microbes from the JIUYAO samples, due to their key role in the fermentation activity and flavor formation of CRW, as determined in our previous study (Chen et al., 2020). To ensure that the samples had the ability to produce ethanol, *S. cerevisiae* (NKCCMR NK3. 00156) was also added to the artificial starter (Chen et al., 2020). The isolated strains were stored at −80°C and used after reactivation by successive subcultures in steamed rice. Briefly, for activation, *W. cibaria*, *W. confusa*, and *P. pentosaceus* (2% vol/vol) were inoculated into MRS broth (Merck, Darmstadt, Germany) and incubated at 37°C for 18 h, whereas *S. fibuligera*, *S. cerevisiae*, and *R. arrhizus* (2% vol/vol) were inoculated in MEB liquid medium (Merck, Darmstadt, Germany) and incubated at 30°C for 24 h. The inoculum concentrations of the individual core bacterial species were determined according to the amount of JIUYAO added to the CRW, the total number of bacterial and fungal colonies in the JIUYAO, and the abundance of core microbial species in JIUYAO as described in our previous study (Chen et al., 2020). The final concentrations of the core microbes that were combined to form the artificial starter culture were *P. pentosaceus* (8.6×10^3 CFU/g), *S. fibuligera* (9.6×10^3 CFU/g), *R. arrhizus* (10.6×10^2 CFU/g), *W. cibaria* (2.2×10^3 CFU/g), *W. confuse* (2.2×10^3 CFU/g), and *S. cerevisiae* (2.0×10^4 CFU/g).

For use as lyoprotectants, skim milk was purchased from Fonterra Ltd. (New Zealand), and polyethylene glycol, sodium glutamate, and maltodextrin of food grade were purchased from WanBang Co. Ltd. (Zhengzhou, Henan Province, China).

Freeze-Drying of the Starter

All of the protectants used in the experiment were dissolved in distilled water to obtain various concentrations. They were sterilized at 115°C for 15 min and stored at 4°C until use.

Different concentrations of the protectant solutions were added to the culture pellets of the core microbes in the ratio 1:1 (vol/vol). After mixing, the samples were pre-frozen at −80°C for 2 h, placed in a vacuum freeze-dryer at −80°C and 0.162 mbar vacuum for 48 h, and finally stored at −20°C until use (Qi et al., 2017).

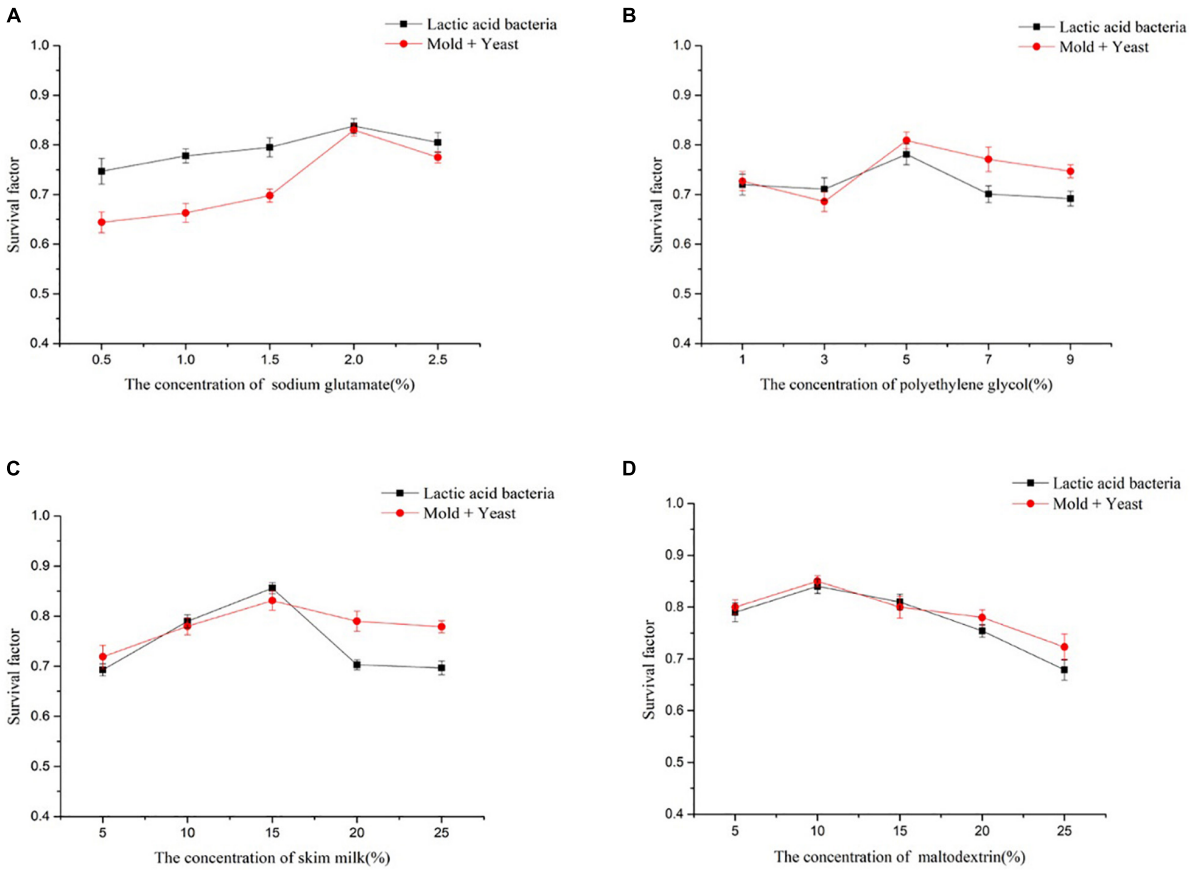

FIGURE 1 | Effects of different concentrations of four lyoprotectants on the survival factor of the artificial starter culture. **(A)** Sodium glutamate, **(B)** polyethylene glycol, **(C)** skim milk, and **(D)** maltodextrin.

TABLE 2 | Regression model analysis of variance.

Source	Sum of squares	Degree of freedom	Mean squared	*F*-value	*p*-Value[a]
Model	0.038	14	2.683×10^{-3}	35.22	< 0.0001***
A	2.621×10^{-3}	1	2.621×10^{-3}	34.40	< 0.0001***
B	6.196×10^{-3}	1	6.196×10^{-3}	81.35	< 0.0001***
C	6.440×10^{-3}	1	6.440×10^{-3}	84.54	< 0.0001***
D	1.927×10^{-3}	1	1.927×10^{-3}	25.30	0.0002**
AB	4.225×10^{-5}	1	4.225×10^{-5}	0.55	0.4687
AC	1.440×10^{-4}	1	1.440×10^{-4}	1.89	0.1908
AD	3.306×10^{-3}	1	3.306×10^{-3}	43.41	< 0.0001***
BC	1.322×10^{-4}	1	1.322×10^{-4}	1.74	0.2088
BD	5.550×10^{-3}	1	5.550×10^{-3}	72.87	< 0.0001***
CD	1.690×10^{-4}	1	1.690×10^{-4}	2.22	0.1585
A^2	9.441×10^{-3}	1	9.441×10^{-4}	123.94	< 0.0001***
B^2	8.653×10^{-3}	1	8.653×10^{-3}	113.61	< 0.0001***
C^2	9.012×10^{-3}	1	9.012×10^{-3}	118.32	< 0.0001***
D^2	8.477×10^{-3}	1	8.477×10^{-3}	111.29	< 0.0001***
Residual	1.066×10^{-3}	14	7.617×10^{-3}		
Lack of fit	8.316×10^{-4}	10	8.316×10^{-5}	1.42	0.3293
Pure error	2.348×10^{-4}	4	5.870×10^{-5}		

[a] ****p < 0.001, extremely significant; **p < 0.01, highly significant; *p < 0.05, significant.*

The lyophilization survival factor (SF_L) was calculated following the formula given by Hubálek (2003):

$$SF_L = 1 - [(\log CFU/mL_{initial} - log\ CFU/mL_{final})/ logCFU/mL_{initial}]$$

where $CFU/mL_{initial}$ is the number of viable cells before lyophilization, and CFU/mL_{final} is the number of viable cells after lyophilization.

Experimental Design for Optimization of the Lyoprotectant Composition

A lyoprotectant is usually added to the target solution of cells before the freeze-drying process. It adds a matrix around the cells that protects them from drying and freezing and increases their survival ability (Abadias et al., 2001). Ten lyoprotectants were selected and mixed thoroughly with the core microbes, and the survival factors of the microbes were determined as an indicator of their survival in our preliminary study (data not shown). Finally, four lyoprotectants with the best protective effects were selected for our experiment: skim milk, polyethylene glycol, sodium glutamate, and maltodextrin. These selected lyoprotectants were diluted to different concentration gradients (skim milk and maltodextrin: 5, 10, 15, 20 and 25%; polyethylene glycol: 1, 3, 5, 7 and 9%; sodium gluconate: 0.5, 1, 1.5, 2 and 2.5%), and their optimal concentrations were determined based on the cell survival factor.

The lyoprotectant composition was further optimized using a four-factor, three-level Box–Behnken design and three levels of the $N = 27$ test with Y (lyophilization survival rate) as the response value. The factor levels are shown in **Table 1**. The following polynomial equation was used:

$$Y = a_0 + a_1A + a_2B + a_3C + a_4D + a_{12}AB + a_{13}AC + a_{14}AD + a_{23}BC + a_{24}BD + a_{34}CD + a_{11}A^2 + a_{22}B^2 + a_{33}C^2 + a_{44}D^2$$

where Y is the predicted response; A, B, C, and D are independent variables representing the concentration of the four protectants skim milk, polyethylene glycol, sodium glutamate, and maltodextrin, respectively; a_0 is the second-order reaction constant; a_1, a_2, a_3, and a_4 are the linear coefficients; a_{11}, a_{22}, a_{33}, and a_{44} are the quadratic coefficients; and a_{12}, a_{13}, a_{14}, a_{23}, a_{24}, and a_{34} are the interaction coefficients (Crowell and Ough, 1979).

CRW Brewing

The main steps in CRW brewing are rice soaking, steaming, cooling, starter addition, and fermentation. Briefly, glutinous rice (100 g) was soaked in 100 mL water for 12 h at 25°C. After steaming the soaked rice for 20 min and then cooling it to 25–30°C, rice fermentation was initiated by adding JIUYAO, the artificial starter, or the commercial starter at a final concentration of 0.002 g/g steamed rice. The fermentation process was performed at 29°C for 30 h. The acid content, ethanol content, and saccharification power were determined as described in our previous study (Chen et al., 2020). All chemical determination experiments were performed in triplicate.

Flash GC Electronic Nose Detection

A HERACLES flash GC electronic nose (Alpha M.O.S., Toulouse, France) equipped with an MXT-5 column and an MXT-1701 column was used for the aroma analysis of the CRW samples. This instrument can perform a complete data analysis owing to its integration with classical gas chromatography (GC) functionalities and electronic nose (e-nose) olfactory fingerprint software.

Briefly, 5 mL of each CRW sample was added to a separate 20-mL vial and incubated at 25°C for 30 min. Hydrogen was circulated at a constant flow rate of 1 mL/min, and 5 mL of headspace gas was injected into the GC port at 200°C. The temperature changes in the GC column were as follows: 50°C for 2 s, a 1°C/s ramp to 80°C, and then a 3°C/s ramp to 250°C with a 15 s hold. The temperature of the detector was 260°C, and each sample was analyzed five times.

Volatile Compound Analysis

The volatile compound profiles of the CRW samples were analyzed using the headspace solid-phase microextraction (HS-SPME)/gas chromatography–mass spectrometry (GC-MS) approach (Yu et al., 2019b). Briefly, 5 mL of each CRW sample was added to 20 μL of internal standard (2-octanol, 410 mg/L) in a 15-mL headspace glass vial. A fiber (50 μm DVB/CAR/PDMS, Supelco Inc., Bellefonte, Pennsylvania, United States) was exposed to the headspace of the glass vial for 50 min at 50°C.

An Agilent 7890 GC instrument was coupled to a 5973C MS detector (Santa Clara, CA, United States). A capillary HP-Innowax column from Agilent Technologies (60 m × 0.25 mm × 0.25 μm) was used to perform the chromatographic separation. After extraction, the fiber was immediately introduced into the GC instrument, and desorption was performed at 250°C for 5 min. The temperature changes were as follows: the initial temperature was maintained at 40°C, increased to 120°C at a rate of 3°C/min, held for 5 min, and then increased to 200°C at a rate of 3°C/min. Helium was used as the carrier gas at a flow rate of 1 mL/min. The transfer line temperature was 250°C. The mass spectrometers were operated in the electron ionization mode at 70 eV, with a scan range of m/z 30–450.

The compounds were identified by comparing their retention indices (RIs) with those reported in the literature and matching their MS spectra with those in the NIST 11 database. The RIs were determined in relation to those of the C_5–C_{30} alkane standards (Sigma-Aldrich, St. Louis, MO, United States). To evaluate the sensory contributions of the compounds to the flavor of the CRW samples, their odor activity values (OAVs) were obtained, given by the ratio of the compound concentration in the sample to the threshold concentration in water (Van Gemert, 2003).

Statistical Analysis

XLSTAT version 7.5 (Addinsoft, New York, NY, United States) was used to analyze the GC-MS data. Design Expert software (version 9, Stat-Ease Inc., Minneapolis, MN, United States) was used for the regression and graphical analysis of the experimental data. The optimal values of the four protectants were calculated

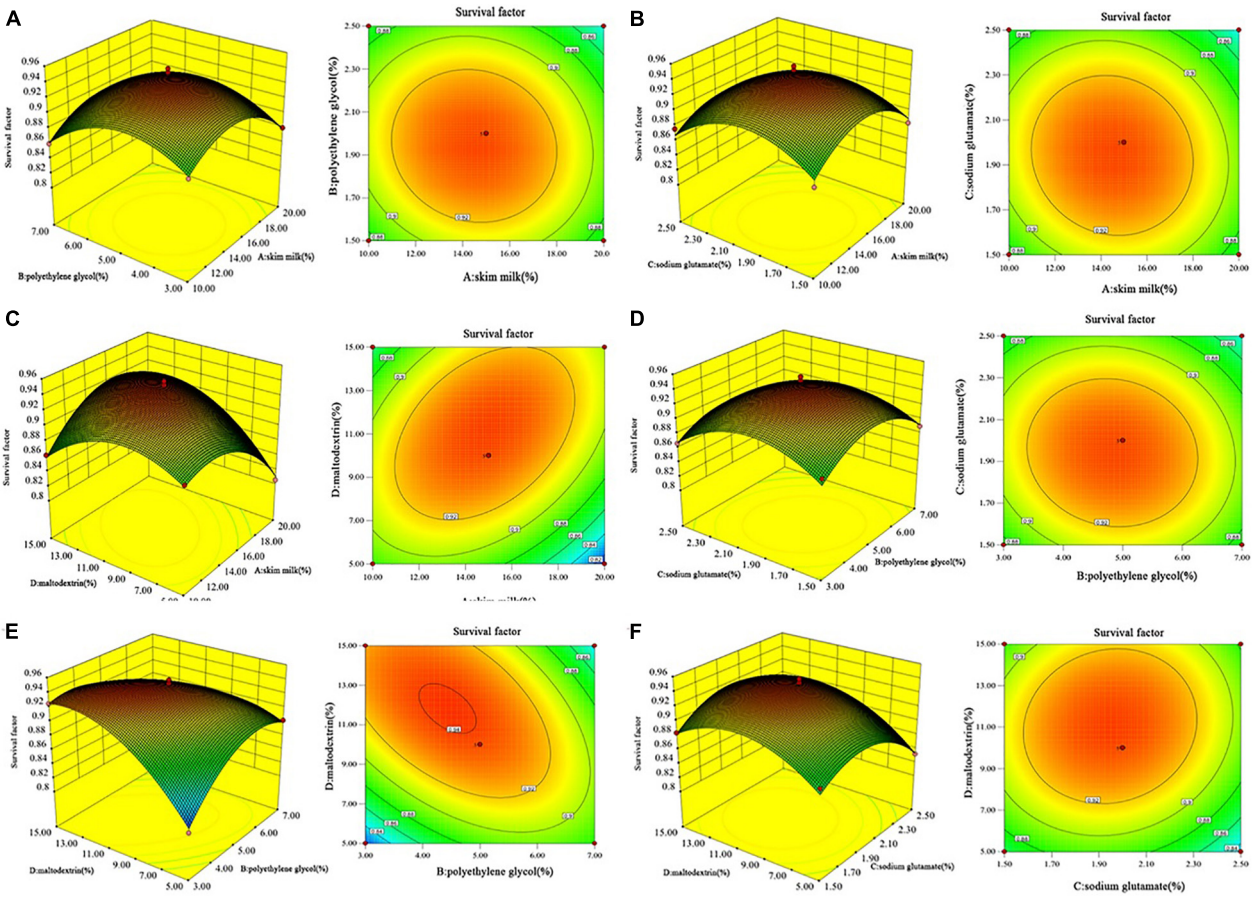

FIGURE 2 | Response surface and contour plots describing the interactive effects of **(A)** skim milk + polyethylene glycol, **(B)** skim milk + sodium glutamate, **(C)** skim milk + maltodextrin, **(D)** polyethylene glycol + sodium glutamate, **(E)** polyethylene glycol + maltodextrin, and **(F)** sodium glutamate + maltodextrin on the survival factor of the artificial starter culture.

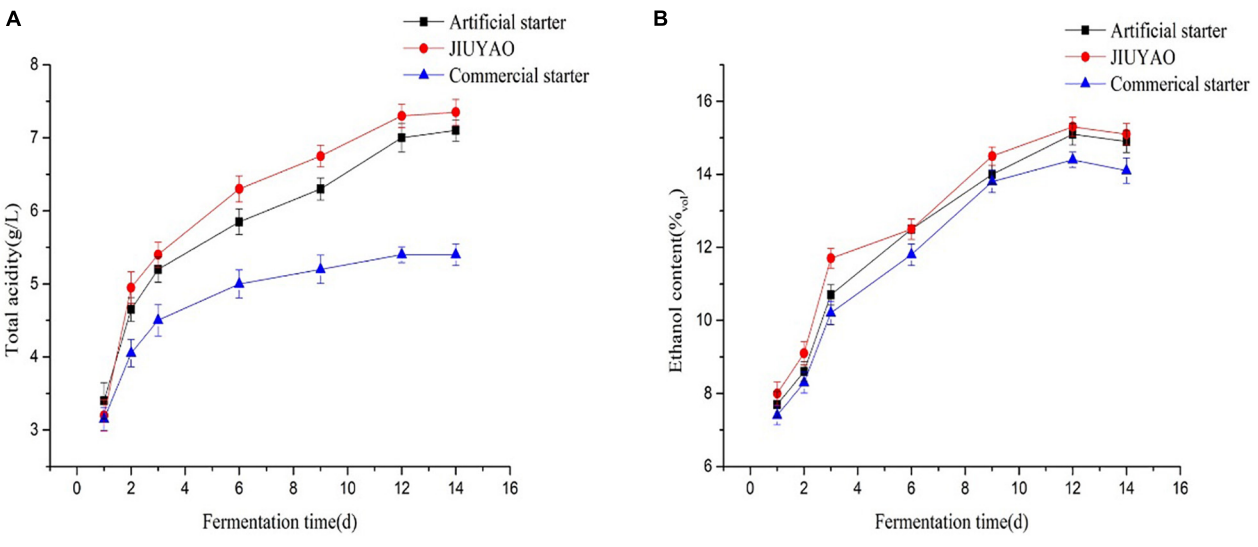

FIGURE 3 | Fermentation performance results of the three Chinese rice wine samples fermented with three different starter cultures. **(A)** Changes in the total acid contents during the fermentation process. **(B)** Changes in the ethanol contents during the fermentation process.

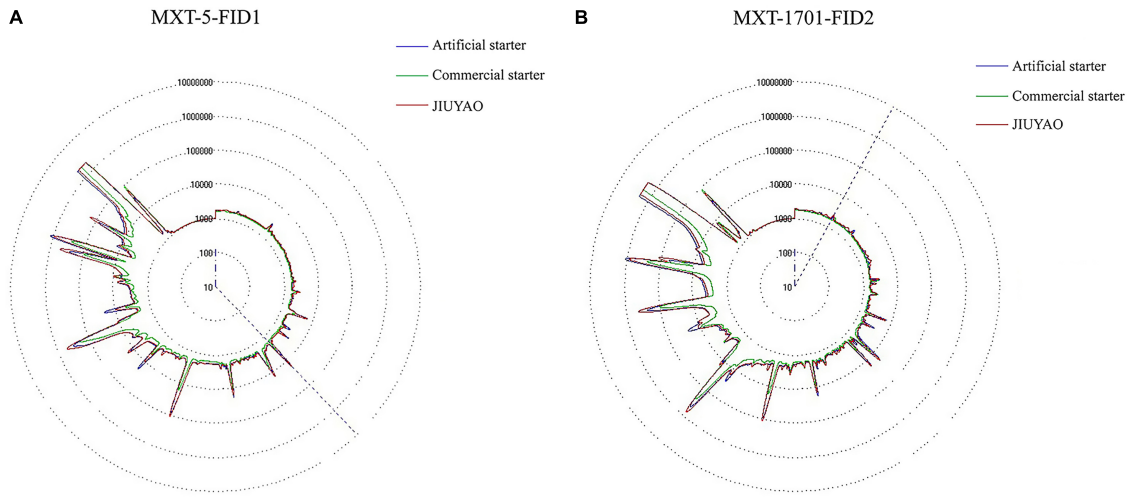

FIGURE 4 | Flavor profile radar chart of three Chinese rice wine samples brewed with three different starter cultures. **(A)** MXT-5-FID and **(B)** MXT-1701-FID.

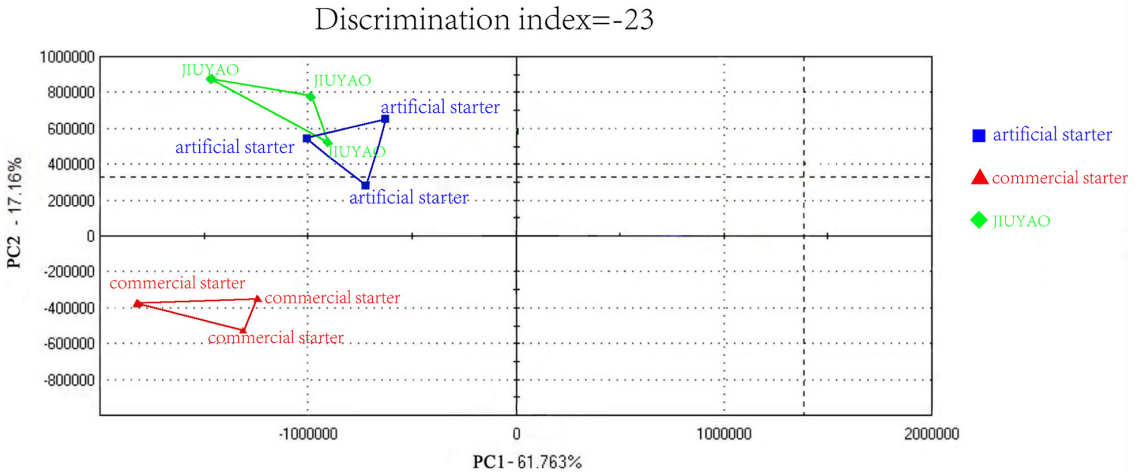

FIGURE 5 | Principal component analysis of the three Chinese rice wine samples brewed with three different starters.

using response surface methodology. The regression equations of the models were evaluated using the *F*-test for the analysis of variance. A principal component analysis was performed using WinMuster version 1.6.2 (Alpha M.O.S., Toulouse, France). Origin version 9.0 (Origin Lab Inc., Hampton, MS, United States) and SPSS version 19.0 (SPSS Inc., Chicago, IL, United States) were used for further data analysis.

RESULTS AND DISCUSSION

Effects of Lyoprotectants on the Survival Factor of the Artificial Starter After Freeze-Drying

Lyophilization has several limitations, such as the formation of ice crystals, altered permeability of the cell membrane, and denaturation and inactivation of sensitive proteins (Yang et al., 2012; Lbg et al., 2020). The role of a lyoprotectant is to prevent these adverse effects. Skim milk, polyethylene glycol, sodium glutamate, and maltodextrin were selected as the protective agents for the artificial starter culture prepared in this study. The results of single-factor experiments indicated that with 15% skim milk, 5% polyethylene glycol, 2% sodium glutamate, or 10% maltodextrin as individual protective agents during freeze-drying, the maximum survival rate of the artificial starter culture was 85.55, 80.94, 83.83, or 85.01%, respectively (**Figure 1**). The survival factor of the artificial starter gradually improved with increasing concentrations of the protective agents, but after a certain concentration, the survival rate remained unchanged or slowly decreased. This phenomenon was in line with the results reported by Chen et al. (2019), who found that extremely high concentrations of protective agents accelerated the repolymerization of

TABLE 3 | Relative contents of volatile compounds in the Chinese rice wine samples fermented by different starter cultures (μg/kg, *n* = 3), as identified by HS-SPME/GC-MS.

No	Compound[a]	Identification[b]	RI		Concentration (μg/kg)		
			Calculate	Reference	A[c]	B	C
1	Ethyl Acetate	RI, MS	898	894	570.78 ± 0.17b[d]	613.63 ± 0.96c	325.68 ± 0.46a
2	Ethyl propionate	RI, MS	969	964	25.92 ± 0.07b	28.23 ± 0.65c	11.86 ± 0.16a
3	Isobutyl acetate	RI, MS	1028	1029	11.59 ± 0.32	7.65 ± 0.16	–[e]
4	Ethyl butyrate	RI, MS	1031	1039	81.71 ± 0.08c	63.16 ± 0.28b	45.29 ± 0.15a
5	Propanoic acid, pentyl ester	MS	1064	–	20.44 ± 0.64	–	–
6	Isobutanol	RI, MS	1086	1092	377.91 ± 0.26c	161.82 ± 0.48b	98.62 ± 0.12a
7	Isoamyl acetate	RI, MS	1119	1126	464.08 ± 0.15	116.15 ± 0.71	–
8	1-Butanol, 3- methyl-, acetate	RI, MS	1135	1129	416.49 ± 0.15b	596.09 ± 0.61c	348.98 ± 0.54a
9	Pentanoic acid, ethyl ester	RI, MS	1140	1142	8.78 ± 0.41	–	62.38 ± 0.48
10	isopentanol	RI, MS	1200	1206	4459.53 ± 10.14	860.82 ± 2.14	–
11	2-methylbutanol	RI, MS	1205	1208	3527.85 ± 0.16	338.94 ± 0.12	–
12	2-Pentylfuran	RI, MS	1234	1235	26.57 ± 0.54	4.62 ± 0.01	–
13	ethyl hexanoate	RI, MS	1238	1241	185.64 ± 0.15a	245.98 ± 0.77b	556.31 ± 0.84c
14	Acetic acid, hexyl ester	RI, MS	1270	1276	14.93 ± 0.18	–	–
15	Ethyl heptanoate	RI, MS	1332	1332	18.24 ± 0.20	3.41 ± 0.02	–
16	1-Hexanol	RI, MS	1365	1361	73.26 ± 0.33	1.8 ± 0.08	–
17	1-Propanol, 3-ethoxy-	RI, MS	1358	1359	65.46 ± 0.34	5.06 ± 0.84	–
18	2-Nonanone	RI, MS	1395	1398	4.65 ± 0.22	–	–
19	acetic acid	RI, MS	1428	1427	82.83 ± 0.15	–	215.89 ± 0.61
20	ethyl caprylate	RI, MS	1436	1441	987.58 ± 0.09	1441.45 ± 1.16	–
21	1-Octen-3-ol	RI, MS	1453	1456	13.53 ± 0.25	29.8 ± 0.21	–
22	furfural	RI, MS	1482	1482	10.42 ± 0.15a	16.08 ± 0.12c	15.56 ± 0.51b
23	1-Hexanol, 2-ethyl-	RI, MS	1502	1484	12.15 ± 0.61	–	–
24	Butanoic acid, 3- hydroxy-, ethyl ester	RI, MS	1516	1522	34.92 ± 0.55	–	–
25	Ethyl nonanoate	RI, MS	1540	1541	84.28 ± 0.40	20.73 ± 0.05	–
26	n-Caprylic acid isobutyl ester	RI, MS	1557	1561	7.59 ± 0.56	5.02 ± 0.03	–
27	Caryophyllene	RI, MS	1593	1594	24.56 ± 0.27	11.12 ± 0.12	–
28	Ethyl decanoate	RI, MS	1640	1643	1021.13 ± 0.11b	1829.47 ± 2.98c	96.07 ± 0.05a
29	Butanoic acid	RI, MS	1655	1652	18.1 ± 0.31	–	–
30	Octanoic acid, 3-methylbutyl ester	RI, MS	1665	1670	–	15.71 ± 0.17	–
31	Hexanoic acid, 3- hydroxy-, ethyl ester	MS	1673	1673	12.32 ± 0.52	–	–
32	Acetophenone	RI, MS	1695	1693	68.63 ± 0.29	–	45.94 ± 0.14
33	1-Decanol	RI, MS	1743	1748	61.47 ± 0.13	7.96 ± 0.23	–
34	Phenethyl acetate	RI, MS	1800	1825	560.16 ± 0.30	351.1 ± 0.24	–
35	Ethyl laurate	RI, MS	1835	1835	197.88 ± 0.10b	161.24 ± 0.14a	536.96 ± 0.11c
36	Pentadecanoic acid, 3-methylbutyl ester	RI, MS	1862	1863	50.11 ± 0.53	8.19 ± 0.06	–
37	Phenylethyl Alcohol	RI, MS	1936	1935	6686.56 ± 0.06b	12940.7 ± 5.17c	1584.71 ± 0.96a
38	Ethyl Oleate	RI, MS	1988	1986	1230.5 ± 0.36c	58.95 ± 0.15a	629.12 ± 21.28b
39	Phenol, 4-ethyl-2-methoxy-	RI, MS	2030	2032	90.28 ± 0.24	7.16 ± 0.11	–
40	Octanoic acid	RI, MS	2040	2039	171.5 ± 0.44	28.28 ± 0.05	–
41	Tetradecanoic acid, ethyl ester	RI, MS	2053	2043	179.69 ± 0.43b	68.65 ± 0.51a	238.36 ± 1.30c
42	Nonanoic acid	RI, MS	2175	2169	45.58 ± 0.39	–	–
43	2-Methoxy-4-vinylphenol	RI, MS	2196	2194	167.85 ± 0.57	–	–
44	Phenol, 4-ethyl-	RI, MS	2200	2202	115.39 ± 0.38c	100.48 ± 0.14b	54.89 ± 0.19a
45	Hexadecanoic acid, ethyl ester	RI, MS	2243	2243	–	964.73 ± 0.56	7756.55 ± 29.48
46	Benzofuran, 2,3-dihydro-	MS	2246	–	89.197 ± 0.48	6.9 ± 0.47	–
47	Ethyl 9-hexadecenoate	RI, MS	2272	2267	53.46 ± 0.60	20.44 ± 0.58	–

(Continued)

TABLE 3 | Continued

No	Compound[a]	Identification[b]	RI		Concentration (μg/kg)		
			Calculate	Reference	A[c]	B	C
48	n-Decanoic acid	RI, MS	2276	2275	92.57 ± 0.19b	115.34 ± 0.29c	53.68 ± 0.10a
49	Phenol, 2,4-bis(1,1-dimethylethyl)-	RI, MS	2320	2321	72.43 ± 0.28	13.09 ± 0.12	–
50	Octadecanoic acid, ethyl ester	RI, MS	2450	2455	205.45 ± 0.35b	33.51 ± 0.28a	597.01 ± 5.47c
51	Linoleic acid ethyl ester	RI, MS	2514	2521	–	31.57 ± 0.17	589.58 ± 14.39

[a]*Aroma compounds detected in the CRW samples.*
[b]*Method of identification: MS, mass spectrum comparison using NIST11.L library; RI, retention index in agreement with literature value.*
[c]*A, B, C are CRW samples fermented with JIUYAO, artificial starter and commercial starter.*
[d]*Values with different letters (a–c) in a row are significantly different using Duncan's multiple comparison tests ($p < 0.05$).*
[e]*Not detected in sample.*

proteins in the cells, resulting in poor survival of the artificial starter.

Predictive Modeling for the Concentration of Protective Agents

To further improve the survival factor of the microbes in the artificial starter, a predictive model was established for the optimal protectant combination comprising skim milk, polyethylene glycol, sodium glutamate, and maltodextrin. Based on the combination of the Box–Behnken design and the response surface method, an empirical quadratic model was selected to establish the correlation between the independent variables and the response of the survival factor, as follows:

$$\begin{aligned} Y = &-0.393 + 0.036A + 0.132B + 0.617C + 0.028D \\ &+ 3.25 \times 10^{-4}AB - 2.40 \times 10^{-3}AC + 1.15 \\ &\times 10^{-3}AD - 5.75 \times 10^{-3}BC - 3.725 \times 10^{-3}BD \\ &+ 2.6 \times 10^{-3}CD - 1.526 \times 10^{-3}A^2 - 9.131 \times 10^{-3}B^2 \\ &-0.149 \times 10^{-3}C^2 - 1.446 \times 10^{-3}D^2 \end{aligned}$$

The *F*-value of the model was 35.22, indicating that this model was significant. The *p*-values of the lack of fit ($p = 0.3293$) and the model ($p < 0.0001$) (**Table 2**) indicated that the actual corresponding survival factor values exhibited a good fit with this model.

The effects of the tested factors on the survival factor were visualized in the response surfaces (**Figure 2**). The interaction terms of the concentrations of skim milk, polyethylene glycol, sodium glutamate, and maltodextrin demonstrated statistical significance ($p < 0.0001$). The survival factor peaked at 0.942 when the concentrations of skim milk, polyethylene glycol, sodium glutamate, and maltodextrin were 15.09, 4.45, 1.96, and 11.81%, respectively. Using this combination, the survival factor increased significantly by approximately 10% relative to the use of single protective agents before optimization. This suggests that the established predictive model could effectively predict the survival factor. Hence, an artificial starter was established with the optimal protectant combination of 15.09% skim milk, 4.45% polyethylene glycol, 1.96% sodium glutamate, and 11.81% maltodextrin. To further verify the predictive value of the response surface optimization, three repeat experiments were performed using the optimal protectant combination. The average value of the survival factor of the artificial starter was 0.931, and the fitting rate of the predicted value was 98.83%, indicating that the predicted value and the actual value had a good fit. Together, these data suggest that the determined optimal protectant composition can significantly improve the survival factor of the artificial starter.

Fermentation Activity Analysis of the CRW Samples Brewed With Different Starters

We compared the fermentation activities of the three CRW samples, each brewed with either traditional JIUYAO, the commercial starter, or the artificial starter prepared with the optimal lyoprotectant composition obtained by the response surface method. Saccharification capacity is a key factor that significantly influences wine fermentation (Yao et al., 2018). JIUYAO showed the highest saccharification capacity at 290 ± 3.2 mg/g h, followed by the artificial starter (275 ± 5.3 mg/g h), while the commercial starter showed the lowest capacity (200 ± 4.6 mg/g h). The fermentation activity (ethanol and acid content) of the three CRW samples during fermentation is shown in **Figure 3**. As CRW is mostly fermented in an open environment, rapid growth of the yeast strains in the starter is required to produce ethanol at the initial stage to inhibit bacterial overgrowth and avoid spoilage (Wu et al., 2015; Yang et al., 2018). The changes in ethanol content during fermentation were similar across the three samples, suggesting comparable ethanol production capacities of all three starter cultures. The total acidity of the wines brewed with JIUYAO and the artificial starter were similar, and were higher than that of the wine brewed with the commercial starter throughout the whole fermentation process. These results suggest that the fermentation activity of the CRW sample fermented with the artificial starter was comparable to that of the sample fermented with JIUYAO, but more vigorous than that of the sample fermented with the commercial starter.

Electronic Nose Measurements

Combining the high-efficiency separation ability of GC and the biological simulation of the sense of smell, the electronic nose can provide a comprehensive aroma profile of volatile flavor compounds (Wu et al., 2012). As shown in **Figure 4**, the

flavor profile radar chart of the CRW samples brewed with the three different starters displays the data intuitively. The overall aroma peak appearance of the samples brewed with JIUYAO and the artificial starter is relatively similar, whereas the peak areas are reduced at multiple positions for the sample fermented with the commercial starter, indicating an overall reduction in aroma intensity. To enable better data discrimination between the three samples, a principal component analysis was performed to identify patterns associated with their individual components (**Figure 5**). The principal components of the CRW samples fermented with the artificial starter and JIUYAO were closer and overlapped in the same quadrant, suggesting similar aroma profiles, whereas those of the CRW sample brewed with the commercial starter appeared in a different quadrant. These results indicate similarities in the aroma profiles between the CRW samples brewed with the artificial starter and JIUYAO, but some differences in the CRW sample brewed with the commercial starter. These differences may be ascribed to the microbial species composition. Five core species isolated from JIUYAO formed the functional microbial species of the artificial starter culture, whereas the commercial starter contained only two functional microbial species, namely *S. cerevisiae* and *R. oryzae*.

Volatile Flavor Compounds of the CRW Samples Fermented With Different Starters

In total, 51 flavor compounds, including 27 esters, 8 alcohols, 1 aldehyde, 4 phenols, 2 ketones, and 5 acids, were detected in the three CRW samples by HS-SPME/GC-MS (**Table 3**). A total of 50, 39, and 20 aroma compounds were identified in the CRW samples fermented with JIUYAO, the artificial starter, and the commercial starter, respectively.

Esters are the most important and common volatile aroma compounds that impart floral and fruity sensory properties to wine (Huang L. et al., 2018), and can be synthesized by yeast and other microorganisms during fermentation (Comuzzo et al., 2006). In the present study, esters formed the largest group of flavor compounds, with 26 and 13 ester compounds detected in the CRW samples fermented with JIUYAO and the artificial starter, respectively. The ester content of the wine fermented with the artificial starter (6685.06 μg/kg) was comparable to that of the wine fermented with JIUYAO (7076.73 μg/kg), but significantly ($p < 0.05$) higher than that of the wine fermented with the commercial starter (4794.15 μg/kg). Notably, isobutyl acetate, n-caprylic acid isobutyl ester, ethyl heptanoate, ethyl nonanoate, phenethyl acetate, and ethyl caprylate were the only esters identified in the CRW samples brewed with JIUYAO and the artificial starter. Thus, these ester compounds may be significantly correlated with the core microbial species used in the artificial starter.

Alcohols formed the second largest category of flavor compounds in the CRW samples, and are known to be the key aroma components of wine, especially brewed rice wine (Wang et al., 2014). Alcohols are produced through the metabolism of sugars and the decarboxylation and dehydrogenation of amino acids (Hernandez-Orte et al., 2008). Nine, eight, and two alcohol compounds were detected in the CRW samples fermented with JIUYAO, the artificial starter, and the commercial starter, respectively. Only two alcohols, namely isobutanol and phenylethyl alcohol, were identified in the wine fermented with the commercial starter. The alcohol content of the CRW samples fermented with JIUYAO and the artificial starter was 15,212.26 and 14,341.84 μg/kg, respectively, but that of the sample fermented with the commercial starter was only 1683.33 μg/kg. These results indicate that the core microorganisms used in the artificial starter could produce considerably more alcohol compounds during CRW fermentation.

To assess the complex olfactory effects of the different aroma compounds, individual OAVs were calculated (Bavcar et al., 2011). As shown in **Table 4**, 14 volatile compounds with OAVs ≥1 were identified in the three CRW samples, including 8 esters, 4 alcohols, 1 acid, and 1 aldehyde. Twelve aroma compounds with OAVs ≥1 were found in the CRW samples fermented with JIUYAO and the artificial starter, but only five were identified in the sample fermented with the commercial starter. Among these compounds, ethyl caprylate, 1-octen-3-ol, ethyl decanoate, ethyl butyrate, furfural, isoamyl alcohol, ethyl propionate, isobutanol, and n-decanoic acid were detected only in the samples brewed with JIUYAO and the artificial starter. These compounds contribute to the pleasant aroma profile of CRW due to their desirable aroma and low odor threshold (Yu et al., 2019a). For example, ethyl butyrate imparts an apple-like aroma to rice wine. Isoamyl alcohol is a powerful aroma agent with a banana flavor, which can improve the taste of wine by reducing the bitter-tasting amino acids (leucine) (Chen Z. et al., 2015). These results, together with those of the electronic nose analysis, indicate that the flavor profile—especially the key aroma compounds—of the

TABLE 4 | OAVs of volatile compounds detected in the three Chinese rice wine samples fermented with three different starter cultures.

No	Compounds	A[a]	B	C	Threshold[c] (μg/kg)
1	Phenylethyl alcohol	111	216	26	60
2	Ethyl caprylate	5	7	–[b]	200
3	Ethyldecanoate	2	3	<1	530
4	Isoamyl acetate	208	298	174	2
5	1-octen-3-ol	5	11	–	2.7
6	Ethyl hexanoate	<1	<1	1	530
7	Ethyl butyrate	1	1	<1	59
8	Ethyl propionate	1	1	<1	29
9	Ethyl acetate	114	123	65	5
10	Furfural	1	2	–	8
11	Ethyl laurate	<1	<1	1	500
12	Isoamyl alcohol	782	689	–	6.1
13	Isobutanol	12	5	–	33
14	n-Decanoic acid	1	2	<1	70

[a] *A, B, C are CRW samples fermented with JIUYAO, the artificial starter and the commercial starter.*

[b] *The OAV was not calculated in the sample.*

[c] *The detection threshold was drawn from the literature (Van Gemert, 2003).*

CRW fermented with the artificial starter is similar to that of the CRW fermented with JIUYAO. Thus, the artificial starter is a potential substitute to JIUYAO to aid the industrial production of high-quality CRW with a stable flavor profile.

CONCLUSION

An artificial starter was prepared for high-efficiency industrial CRW production, and the fermentation activities and flavor profiles of CRW samples fermented with JIUYAO, a commercial starter culture, and our artificial starter culture were compared. The optimal lyoprotectant combination was determined as 15.09% skim milk, 4.45% polyethylene glycol, 1.96% sodium glutamate, and 11.81% maltodextrin, using the response surface optimization method. These three different starters had equivalent fermentation activity in terms of the alcohol content of the fermented CRW samples. The sample brewed with the artificial starter showed similar acid content and volatile compound profiles to those of the sample brewed with JIUYAO. Although the aroma compound content of the CRW sample fermented with the artificial starter was lower than that of the sample fermented with JIUYAO, the same main aroma compounds, such as isoamyl acetate, ethyl acetate, phenyl alcohol, and isoamyl alcohol (OAV $\geq$ 1), were found in both and contributed highly to the flavor of the CRW. Our artificial starter culture is a promising substitute to traditional JIUYAO to aid the industrial production of high-quality CRW with a stable flavor profile. Further studies should be devoted to in-depth analysis of the associations between the core microbes and flavor substances to enhance the activity and stability of the artificial starter during batch production of CRW.

DATA AVAILABILITY STATEMENT

The original contributions presented in the study are included in the article/supplementary material, further inquiries can be directed to the corresponding author/s.

AUTHOR CONTRIBUTIONS

CC wrote the manuscript and performed the statistical analyses. ZL performed the statistical analyses and flash GC electronic nose detection. WZ compared the fermentation activities between different samples. HT determined the flavor profiles of samples by gas chromatography–mass spectrometry. JH and HYua established the optimal protectant combination for lyophilization of the artificial starter. HYu designed the research. All authors contributed to the article and approved the submitted version.

FUNDING

This work was supported by the National Natural Science Foundation of China (32172336) and Capacity Project of Local Colleges and Universities of the Science and Technology Commission of Shanghai, China (21010504100).

ACKNOWLEDGMENTS

The authors are grateful to the Zhejiang Tapai Shaoxing Rice Wine Co., Ltd. for their generous supply of materials for this study.

REFERENCES

Abadias, M., Benabarre, A., Teixidó, N., Usall, J., and ViñAs, I. (2001). Effect of freeze drying and protectants on viability of the biocontrol yeast Candida sake. *Int. J. Food Microbiol.* 65, 173–182. doi: 10.1016/S0168-1605(00)00513-4

Ale, C. E., Otero, M. C., and Pasteris, S. E. (2015). Freeze-drying of wine yeasts and oenococcus oeni and selection of the inoculation conditions after storage. *J. Bioprocess. Biotech.* 5:248.

Bavcar, D., Cesnik, H. B., Cus, F., and Kosmerl, T. (2011). The influence of skin contact during alcoholic fermentation on the aroma composition of Ribolla Gialla and Malvasia Istriana Vitis vinifera (L.) grape wines. *Int. J. Food Sci. Tech.* 46, 1801–1808. doi: 10.1111/j.1365-2621.2011.02679.x

Cerrutti, P., Huergo, M., Galvagno, M., Schebor, C., and Buera, M. (2000). Commercial baker's yeast stability as affected by intracellular content of trehalose, dehydration procedure and the physical properties of external matrices. *Appl. Microbiol. Biot.* 54, 575–580. doi: 10.1007/s002530000428

Chen, C., Liu, Y., Tian, H., Ai, L., and Yu, H. (2020). Metagenomic analysis reveals the impact of JIUYAO microbial diversity on fermentation and the volatile profile of Shaoxing-jiu. *Food Microbiol.* 86, 103321–103326. doi: 10.1016/j.fm.2019.103326

Chen, H., Chen, S., Li, C., and Shu, G. (2015). Response surface optimization of lyoprotectant for lactobacillus bulgaricus during vacuum freeze-drying. *Prep. Biochem. Biotech.* 45, 463–475. doi: 10.1080/10826068.2014.923451

Chen, H., Tian, M., Chen, L., Cui, X., Meng, J., and Shu, G. (2019). Optimization of composite cryoprotectant for freeze-drying Bifidobacterium bifidum BB01 by response surface methodology. *Artif. Cells Nanomed. Biotechnol.* 47, 1559–1569. doi: 10.1080/21691401.2019.1603157

Chen, S., Xu, Y., and Qian, M. C. (2013). Aroma characterization of Chinese rice wine by gas chromatography-olfactometry, chemical quantitative analysis, and aroma reconstitution. *J. Agric. Food Chem.* 61, 11295–11302. doi: 10.1021/jf4030536

Chen, Z., Jia, R., Liu, Z., Zhang, W., Chen, S., Rao, P., et al. (2015). Microbial community structure and dynamics during the traditional brewing of Fuzhou Hong Qu glutinous rice wine as determined by culture-dependent and culture-independent techniques. *Food Control* 57, 216–224. doi: 10.1016/j.foodcont.2015.03.054

Comuzzo, P., Tat, L., Tonizzo, A., and Battistutta, F. (2006). Yeast derivatives (extracts and autolysates) in winemaking: release of volatile compounds and effects on wine aroma volatility. *Food Chem.* 99, 217–230. doi: 10.1016/j.foodchem.2005.06.049

Coulibaly, W. H., N'guessan, K. F., Coulibaly, I., Cot, M., Rigou, P., and Djè, K. M. (2016). Influence of freeze-dried yeast starter cultures on volatile compounds of tchapalo, a traditional sorghum beer from cte d'ivoire. *Beverages* 2:35. doi: 10.3390/beverages2040035

Crowell, E. A., and Ough, C. S. (1979). A modified procedure for alcohol determination by dichromate oxidation. *Am. J. Enol. Vitic.* 30, 61–63.

Ferrer-Gallego, R., Hernández-Hierro, J., Rivas-Gonzalo, J. C., and Escribano-Bailón, M. (2014). Sensory evaluation of bitterness and astringency sub-qualities of wine phenolic compounds: synergistic effect and modulation by aromas. *Food Res. Int.* 62, 1100–1107. doi: 10.1016/j.foodres.2014.05.049

Hernandez-Orte, P., Cersosimo, M., Loscos, N., Cacho, J., Garcia-Moruno, E., and Ferreira, V. (2008). The development of varietal aroma from non-floral grapes by yeasts of different genera. *Food Chem.* 107, 1064–1077. doi: 10.1016/j.foodchem.2007.09.032

Huang, L., Ma, Y., Tian, X., Li, J. M., Li, L. X., Tang, K., et al. (2018). Chemosensory characteristics of regional Vidal icewines from China and Canada. *Food Chem.* 261, 66–74. doi: 10.1016/j.foodchem.2018.04.021

Huang, Z. R., Guo, W. L., Zhou, W. B., Li, L., Xu, J. X., Hong, J. L., et al. (2019). Microbial communities and volatile metabolites in different traditional fermentation starters used for Hong Qu glutinous rice wine. *Food Res. Int.* 121, 593–603. doi: 10.1016/j.foodres.2018.12.024

Huang, Z. R., Hong, J. L., Xu, J. X., Li, L., Guo, W. L., Pan, Y. Y., et al. (2018). Exploring core functional microbiota responsible for the production of volatile flavour during the traditional brewing of Wuyi Hong Qu glutinous rice wine. *Food Microbiol.* 76, 487–496. doi: 10.1016/j.fm.2018.07.014

Hubálek, Z. (2003). Protectants used in the cryopreservation of microorganisms. *Cryobiology* 46, 205–229. doi: 10.1016/S0011-2240(03)00046-4

Jiao, A., Xu, X., and Jin, Z. (2017). Research progress on the brewing techniques of new-type rice wine. *Food Chem.* 215, 508–515. doi: 10.1016/j.foodchem.2016.08.014

Lbg, A., Ahc, A., and Og, B. (2020). Storage stability and sourdough acidification kinetic of freeze-dried Lactobacillus curvatus N19 under optimized cryoprotectant formulation. *Cryobiology* 96, 122–129. doi: 10.1016/j.cryobiol.2020.07.007

Liu, S., Chen, Q., Zou, H., Yu, Y., and Zhang, S. (2019). A metagenomic analysis of the relationship between microorganisms and flavor development in Shaoxing mechanized huangjiu fermentation mashes. *Int. J. Food Microbiol.* 303, 9–18. doi: 10.1016/j.ijfoodmicro.2019.05.001

Liu, Z., Wang, Z., Lv, X., Zhu, X., and Li, N. (2018). Comparison study of the volatile profiles and microbial communities of Wuyi Qu and Gutian Qu, two major types of traditional fermentation starters of Hong Qu glutinous rice wine. *Food Microbiol.* 69, 105–115. doi: 10.1016/j.fm.2017.07.019

Pradelles, R., Vichi, S., Alexandre, H., and Chassagne, D. (2009). Influence of the drying processes of yeasts on their volatile phenol sorption capacity in model wine. *Int. J. Food Microbiol.* 135, 152–157. doi: 10.1016/j.ijfoodmicro.2009.07.019

Qi, K., He, C., Wan, H., Man, H., and Wu, Y. (2017). Response surface optimization of lyoprotectant from amino acids and salts for bifidobacterium bifidum during vacuum freeze-drying. *Acta Univ. Cibiniensis Ser. E Food Technol.* 21, 3–10. doi: 10.1515/aucft-2017-0009

Van Gemert, L. (2003). *Compilations of Odour Threshold Values in Air, Water and Other Media*. Zeist: Oliemans, Punter & Partners B.V.

Wang, P., Mao, J., Meng, X., Li, X., Liu, Y., and Feng, H. (2014). Changes in flavour characteristics and bacterial diversity during the traditional fermentation of Chinese rice wines from Shaoxing region. *Food Control* 44, 58–63. doi: 10.1016/j.foodcont.2014.03.018

Wu, K. N., Tan, B. K., Howard, J. D., Conley, D. B., and Gottfried, J. A. (2012). Olfactory input is critical for sustaining odor quality codes in human orbitofrontal cortex. *Nat. Neurosci.* 15, 1313–1319. doi: 10.1038/nn.3186

Wu, Z., Xu, E., Jie, L., Zhang, Y., Fang, W., Xu, X., et al. (2015). Monitoring of fermentation process parameters of Chinese rice wine using attenuated total reflectance mid-infrared spectroscopy. *Food Control* 50, 405–412. doi: 10.1016/j.foodcont.2014.09.028

Xie, G. F., Li, W. J., Jian, L., Yu, C., Hua, F., Zou, H. J., et al. (2007). Isolation and identification of representative fungi from Shaoxing rice wine Wheat Qu using a polyphasic approach of culture-based and molecular-based methods. *J. Inst. Brew.* 113, 272–279. doi: 10.1002/j.2050-0416.2007.tb00287.x

Xu, E., Jie, L., Wu, Z., Li, H., and Jiao, A. (2015). Characterization of volatile flavor compounds in Chinese rice wine fermented from enzymatic extruded rice. *J. Food Sci.* 80, 1476–1489. doi: 10.1111/1750-3841.12935

Yang, C., Zhu, X., Fan, D., Mi, Y., Luo, Y., Hui, J., et al. (2012). Optimizing the chemical compositions of protective agents for freeze-drying bifidobacterium longum BIOMA 5920. *Chin. J. Chem. Eng.* 20, 930–936. doi: 10.1016/S1004-9541(12)60420-0

Yang, Y. J., Xia, Y. J., Lin, X. N., Wang, G. Q., Zhang, H., Xiong, Z. Q., et al. (2018). Improvement of flavor profiles in Chinese rice wine by creating fermenting yeast with superior ethanol tolerance and fermentation activity. *Food Res. Int.* 108, 83–92. doi: 10.1016/j.foodres.2018.03.036

Yao, L. D., Ju, X., James, T. Y., Qiu, J. Z., and Liu, X. Y. (2018). Relationship between saccharifying capacity and isolation sources for strains of the Rhizopus arrhizus complex. *Mycoscience* 59, 409–414. doi: 10.1016/j.myc.2018.02.011

Yu, H., Xie, T., Xie, J., Ai, L., and Tian, H. (2019b). Characterization of key aroma compounds in Chinese rice wine using gas chromatography-mass spectrometry and gas chromatography-olfactometry. *Food Chem.* 293, 8–14. doi: 10.1016/j.foodchem.2019.03.071

Yu, H., Xie, T., Qian, X., Ai, L., and Tian, H. (2019a). Characterization of the volatile profile of Chinese rice wine by comprehensive two-dimensional gas chromatography coupled to quadrupole mass spectrometry. *J. Sci. Food Agr.* 99, 5444–5456. doi: 10.1002/jsfa.9806

Zhao, G., and Zhang, G. (2010). Effect of protective agents, freezing temperature, rehydration media on viability of malolactic bacteria subjected to freeze-drying. *J. Appl. Microbiol.* 99, 333–338. doi: 10.1111/j.1365-2672.2005.02587.x

Zhao, X., Wang, Y., Cai, W., Yang, M., and Shan, C. (2020). High-throughput sequencing-based analysis of microbial diversity in rice wine koji from different areas. *Curr. Microbiol.* 77, 1–8. doi: 10.1007/s00284-020-01877-9

Conflict of Interest: The authors declare that the research was conducted in the absence of any commercial or financial relationships that could be construed as a potential conflict of interest.

Publisher's Note: All claims expressed in this article are solely those of the authors and do not necessarily represent those of their affiliated organizations, or those of the publisher, the editors and the reviewers. Any product that may be evaluated in this article, or claim that may be made by its manufacturer, is not guaranteed or endorsed by the publisher.

frontiers in Microbiology

ORIGINAL RESEARCH
published: 20 October 2021
doi: 10.3389/fmicb.2021.736525

Correlation Between Microbial Diversity and Volatile Flavor Compounds of *Suan zuo rou*, a Fermented Meat Product From Guizhou, China

Hanyu Wang[1,2,3], *Wei Su*[1,2]*, *Yingchun Mu*[1] and *Chi Zhao*[1,2]

[1] School of Liquor and Food Engineering, Guizhou University, Guiyang, China, [2] Guizhou Key Laboratory for Storage and Processing of Agricultural and Animal Products, Guizhou University, Guiyang, China, [3] Animal Disease Control and Prevention Center of Guizhou Province, Guizhou University, Guiyang, China

Suan zuo rou (*SZR*), a traditional fermented meat from Guizhou province, China, is loved by local people for its unique flavor and nutritional value. However, the microbial communities and related flavor characteristics of *SZR* from different regions of Guizhou are unclear. We studied the correlation between the microbial communities and the physicochemical properties and volatile flavor compounds (VFCs) of 15 *SZR* samples from three regions in Guizhou province. The microbial community structure of *SZR* was determined by high-throughput sequencing and VFCs were identified by headspace-solid phase microextraction combined with gas chromatography-mass spectrometry. The results indicated that the microbial communities of *SZR* varied among the regions, as evidenced by the relative abundance of *Weissella*, *Staphylococcus*, *Brochothrix*, *Kazachstania*, and *Debaryomces*. There were also significant differences in pH, water activity, NaCl, and total volatile basic nitrogen ($P < 0.05$). Based on orthogonal projections to latent structures and Pearson's correlation coefficient, we showed that *Wickerhamomyces*, *Kazachstania*, *Lactobacillus*, *Weissella*, *Brochothrix*, *Debaryomyces*, *Staphylococcus*, *Pediococcus*, *Pichia*, *Candida*, and *Leuconostoc* were highly correlated with 48 VFCs ($|\rho| > 0.8$, $P < 0.05$). Redundancy analysis showed that most of the dominant bacteria were positively related to water activity, whereas *Lactobacillus* was positively related with pH, and negatively related with total volatile basic nitrogen.

Keywords: fermented meat, microbial diversity, volatile flavor compounds, physicochemical properties, correlation

OPEN ACCESS

Edited by:
Wanping Chen,
Georg-August-University Göttingen, Germany

Reviewed by:
Xinping Lin,
Dalian Polytechnic University, China
Huipeng Liang,
Dalian Polytechnic University, China

***Correspondence:**
Wei Su
suwei1886@163.com

Specialty section:
This article was submitted to Food Microbiology, a section of the journal Frontiers in Microbiology

Received: *05 July 2021*
Accepted: *01 October 2021*
Published: *20 October 2021*

Citation:
Wang H, Su W, Mu Y and Zhao C (2021) Correlation Between Microbial Diversity and Volatile Flavor Compounds of Suan zuo rou, a Fermented Meat Product From Guizhou, China. Front. Microbiol. 12:736525. doi: 10.3389/fmicb.2021.736525

INTRODUCTION

Since ancient times, meat products have played an important role in the human diet, providing us with sufficient protein and energy (Mourente and Bell, 2006). Fermentation, a traditional processing technology, is used to preserve food ingredients to extend shelf life and enhance nutritional value, as well as promote the development of the texture and flavor of foods (Liu and Zhou, 2011).

Fermented foods are affected by more complex factors and mechanisms than other types of food, and a wide variety of microorganisms that occur during natural fermentation are responsible for giving cured meat its unique flavor. Li et al. (2019) reported that the unique flavor of fermented meat products comes from a variety of microorganisms harvested during the natural fermentation process, with enzymes in the raw meat closely related to the flavor. Microorganisms are involved in lipid hydrolysis and autoxidation, and hydrolysis of proteins and carbohydrates, which have an impact on flavor formation (Sidira et al., 2016). Microbial catabolism of raw materials is also closely related to the formation of volatile flavor compounds (VFCs) in fermented foods (Yao et al., 2020).

Suan zuo rou (*SZR*) is a traditional natural fermented meat from Guizhou province, with a longer shelf life than fresh meat products. The traditional fermentation process of *SZR* is based on fresh pork, which is sealed in a tank with salt and rice noodles for 1–2 months to ferment under anaerobic conditions. The end product is favored because of its unique flavor, nutritional value, and non-greasy characteristics. Lv et al. (2019b) showed that *Lactobacillus* played a dominant role at the end of fermentation and could inhibit the growth of species with poor acid resistance and spoilage microbes. Several researches mainly focus on the isolation and identification of bacteria, and sensory quality (Chen et al., 2014, 2020; Hu et al., 2017). Another study reporting the natural fermentation process of sour meat has showed that *L. plantarum* may be regarded as an important potential indicator of fermentation maturation and quality (Lv et al., 2019a). The process of *SZR* production, environmental conditions, and regional differences; however, it can lead to different types and metabolic characteristics of microbial flora, and there may be significant differences in the quality and stability of *SZR*. Therefore, it is important to understand the correlation between the microbiota and flavor of *SZR*, and in particular, the relationship between core microorganisms and characteristic flavors. In the past few years, high-throughput sequencing (HTS) has been widely employed in food microbiology, as it offers insights beyond the limitations of traditional culture methods (Zheng et al., 2018). A number of studies have been conducted on the correlation between microbial community and flavor in fermented foods such as sausages (Quijada et al., 2018), Jinhua ham (Wang et al., 2021), traditional white sour soup (Liu et al., 2020), and Pao cai (Kim et al., 2014). However, few studies have yet been carried out for *SZR*.

In this study, the physicochemical properties, bacterial and fungal community structures, and VFCs in *SZR* were analyzed using fermentation feature testing, HTS technology, and headspace-solid-phase microextraction (HS-SPME) combined with gas chromatography-mass spectrometry (GC-MS) analysis, respectively. Furthermore, the redundancy analysis (RDA) and Pearson's correlation coefficient analysis were used to assess the interrelationships between microbial community and physicochemical properties and VFCs in *SZR*, with the aim of providing a theoretical basis for the standardization of production, food quality, and safety control.

MATERIALS AND METHODS

Sample Collection

In total, 15 *SZR* samples were sampled from three different regions in Guizhou province, China, including Zunyi (ZY), Meitan (MT), and Libo (LB). The primary ingredients and processing conditions of samples are listed in **Supplementary Table 1**. Each region of *SZR* was obtained from a local company in five separate lots. Each sample collected weighed 500 g. All *SZR* was produced using a traditional natural fermentation method, fresh pork (purchased in the local market, respectively), washed and sliced, kneaded and decorated with 5% salt and 10% rice flour, plugged the jar mouth with fresh brown leaves, inverted, sealed and naturally fermented for 2 months. And the production process and basic recipe were similar, but with some differing ingredients such as the amount and type of spices. Completely fermented samples were collected, and stored at −80°C until use.

Physiochemical Properties Determination

The pH of the *SZR* was measured according to the method described by Berardo et al. (2016), using a pre-calibrated pH meter (Sabxin SX-620, Shanghai, China) at room temperature. Water activity (a_w) was measured with a water activity meter (Five Easy Plus FE28, Mettler Toledo International Inc., Columbus, OH, United States).

The NaCl content of the samples was tested according to the Chinese national standard (GB5009.44-2016). In brief, 10 g of each sample was added to 50 mL of water at 70°C and boiled for 15 min. After ultrasonic treatment for 20 min, 2 mL of precipitators I and II was added successively [1 mol/L $K_4Fe(CN)_6{\cdot}3H_2O$ and $Zn(CH_3CO_2)_2$, respectively; Sigma-Aldrich Co., St Louis, MO, United States]. After being left to stand for 30 min, 50 mL of filtrate was extracted. Using 1 mL of $K_2Cr_2O_7$ (10%, Shanghai Aladdin Biochemical Technology Co., Ltd., Shanghai, China) as an indicator, the standard titration solution of $AgNO_3$ (0.02 mol/L, Sigma-Aldrich Co.) was titrated for quantification.

The total volatile basic nitrogen (TVB-N) was determined by the semi-micro nitrogen determination method and defined as mg/100 g. In brief, 100 mL of distilled water was added to each 10 g sample, which was shaken and then left to infuse for 30 min. The solution was filtered before use. The receiving agent consisted of 10 mL of 2% H_3BO_3 w/v (Aladdin Co., Ltd.) and mixed indicator (1 g/L methyl red absolute ethanol:1 g/L bromocresol green absolute ethanol in a 1:5 ratio; Macklin Inc., Shanghai, China) This was placed at the lower end of the condensing pipe; 5 mL of filtrate and 5 mL of 1% MgO were then placed in the reaction chamber, which was quickly plugged, and the sample was steam distilled for 5 min. The assay was titrated with 0.01 M HCl (Shanghai Hutian Chemical Co., Ltd., Shanghai, China).

DNA Extraction and Polymerase Chain Reaction Amplification

Total genomic DNA was isolated from samples using the DNeasy PowerSoil Pro Kit (Qiagen, Venlo, Netherlands) according to the

manufacturer's protocol. DNA quality and quantity were assessed using absorbance ratios of 260–280 nm and 260–230 nm. The DNA was then stored at −80°C until further processing. The V3-V4 region of the bacterial 16S rRNA gene was amplified with primers 338F (5′-ACTCCTACGGGAGGCAGCAG-3′) and 806R (5′-GGACTACHVGGGTWTCTAAT-3′) (Jiang et al., 2020). The ITS1 region of the fungi was amplified with the forward primer ITS1F (5′- CTTGGTCATTTAGAGGAAGTAA-3′) and the reverse primer ITS1R (5′-GCTGCGTTCTTCATCGAT GC-3′) (Buée et al., 2010).

Polymerase chain reaction (PCR) amplification was performed using a total volume of 50 μL, which contained 10 μL of buffer, 0.2 μL of Q5® High-Fidelity DNA Polymerase (New England BioLabs Inc., Ipswich, MA, United States), 10 μL High GC Enhancer (New England BioLabs), 1 μL of dNTP, 10 μM of each primer, and 60 ng of genomic DNA. Thermal cycling conditions were as follows: an initial denaturation at 95°C for 5 min, followed by 15 cycles at 95°C for 1 min, 50°C for 1 min, and 72°C for 1 min, with a final extension at 72°C for 7 min. The PCR products from the first step of PCR were purified using VAHTS DNA Clean Beads (Vazyme Biotech Co., Ltd., Nanjing, Jiangsu, China). A second-round of PCR was then performed using a total volume of 40 μL that contained 20 μL of 2 × Phusion High-Fidelity Master Mix (New England BioLabs), 8 μL of ddH_2O, 10 μM of each primer, and 10 μL of PCR products from the first step. Thermal cycling conditions were as follows: an initial denaturation at 98°C for 30 s, followed by 10 cycles at 98°C for 10 s, 65°C for 30 s, and 72°C for 30 s, with a final extension at 72°C for 5 min. Finally, all PCR products were quantified using a Nanodrop™ 2000 spectrophotometer (Thermo Scientific, Wilmington, DE, United States) and pooled together. HTS analysis of bacterial rRNA and fungal ITS1 genes was performed on the purified, pooled sample using the Illumina Hiseq 2500 system (San Diego, CA, United States) (2 × 250 paired ends) at Biomarker Technologies Corporation, Beijing, China.

High-Throughput Sequencing and Sequence Analysis

Raw FASTQ sequencing files obtained from the Illumina platform were quality-filtered with Trimmomatic software (version 0.33) (Bolger et al., 2014) and merged using FLASH software (version 1.2.7) (Magoc and Salzberg, 2011). The USEARCH software (version 11.0[1]) was used to cluster data at a 97% similarity level to obtain operational taxonomic units (OTUs) (Bokulich et al., 2013). OTUs were then taxonomically annotated based on Silva[2] taxonomic databases, setting the comparison threshold at 80%. Lastly, QIIME software (version 4.2) (Edgar et al., 2011) was used to identify and remove the chimeric genes to get the high-quality tag sequences (Caporaso et al., 2010). The alpha diversity indexes, Shannon index curves, and rarefaction curves were evaluated using MOTHUR software (version 1.30) and R software (version 3.6.3[3]) (R Development Core Team, 2009), and beta diversity analysis, principal coordinates analysis (PCoA), and non-metric multidimensional scaling (NMDS) were conducted using QIIME software (Caporaso et al., 2010). To establish the co-occurrence networks of core bacterial and fungal genera, we calculated Pearson's correlation coefficients using R software with the "corrplot" package and applied Gephi software (version 0.9.[4]) for visualization.

Analysis of Volatile Compounds

A TRACE™ 1300 gas chromatograph coupled to a TSQ™ 8000 Evo mass spectrometer (GC-MS, Thermo Electron Corp., Waltham, MA, United States) equipped with a DB-5MS capillary column (30 m length × 0.25 mm inner diameter × 0.25 μm film thickness; Agilent Inc., Santa Clara, CA, United States) and a flame ionization detector (Agilent Inc.) was used for the detection of VFCs in *SZR*, using headspace-solid-phase microextraction-gas chromatography-mass spectrometry (HS-SPME-GC-MS). We used the methods described in Marušić et al. (2014) with modifications. Briefly, each sample (2.5 g) was minced and packed into a 20 mL headspace flask along with a saturated saline mixture (7 mL) and cyclohexanone (20 μL, 20 μg/mL), and then equilibrated in a water bath at 60°C for 20 min. The SPME (50/30 μm DVB/Carboxen/PDMS, Supelco, United States) was exposed in the headspace of the vial at 40°C for 180 min to adsorb VFCs. Then, the fiber was immediately inserted into the GC injector port and heated at 230°C for 5 min. Helium (purity: 99.999%) was used as the carrier gas for GC at a flow rate of 1 mL/min and no shunt mode, with an oven temperature program as follows: initial temperature 40°C for 5 min, increased at a rate of 5°C/min to 150°C, 150°C for 3 min, then increased to 240°C at a rate of 5°C/min and finally 240°C for 5 min. During operation of the mass spectrometer, electron ionization was maintained at 70 eV, ion source temperature at 230°C, and transmission line temperature at 280°C. The full-scan acquisition mode was used, with data collection over the m/z range of 50–450 amu, at a rate of 1 scan/s. The experimental results were compared with the NIST database, and only compounds with probability values greater than 800 were retained. The retention indices of the compounds were calculated using C_7–C_{40} n-alkanes (Sigma-Aldrich, Co.) under the same conditions. Semi-quantification of the aroma compounds was performed according to the following equation (Luo et al., 2008): $C = A_c \times C_{is}/A_{is}$; where C is the relative concentration of VFCs, C_{is} is the final concentration of the internal standard in the sample, A_c is the peak area of VFCs, and A_{is} is the peak area of the internal standard.

Statistical Analysis

Statistical analysis was performed using the Statistical Package for the Social Sciences (SPSS 20.0, IBM Co., Chicago, IL, United States). The data obtained were subjected to one-way analysis of variance (ANOVA), with the significance level defined as $P < 0.05$. Principal component analysis (PCA) and bidirectional orthogonal projections to latent structures (O2PLS) were performed to analyze and screen the main flavor compounds using SIMCA® (version 14.1, Sartorius Stedim Data

[1]http://www.drive5.com/usearch/

[2]https://www.arb-silva.de/

[3]https://www.r-project.org/

[4]https://gephi.org/

Analytics AB, Umeå, Sweden). The RDA of environmental factors and microbial community evolution during *SZR* fermentation was performed using Canoco (version 4.5, Biometris Plant Research International, Wageningen University, Wageningen, The Netherlands). Pearson's correlation was calculated using R to calculate the beneficial or antagonistic relationships between the microbiota and major flavor substances (VIP > 1, $P < 0.05$), and the network was created using Gephi (version 0.9.2[5]). All experiments were completed in quintuplicate, and data are expressed as means ± standard deviations (SD) from the mean.

RESULTS AND DISCUSSION

Physicochemical Analysis

The variations in the physicochemical properties of the *SZR* samples are shown in **Table 1**. The differences in a_w, pH, NaCl, and TVB-N content can be used to compare the quality differences and reflect the microbial status of *SZR* in the three regions. a_w and pH values of the three samples were significantly different ($P < 0.05$) and ranged from 0.9404 to 0.970 and 3.68 to 4.14, respectively. The differences are mainly due to the variation in the relative humidity and local climate during the fermentation process (Kim and Park, 2014). All samples were high-acid fermented meat products. The a_w value of LB was the highest, and that of ZY was the lowest; the lower the a_w value, the more stable the microorganisms, the better the preservation of food, and the higher the quality (Laranjo et al., 2015). LB also had the lowest pH compared to the other samples due to its high a_w value. The change in pH can be attributed to the accumulation of organic acids such as lactic and acetic acids (Juaárez-Castelaán et al., 2019).

TVB-N is considered one of the indicators for evaluating the freshness of meat products (Zhang et al., 2016). By the action of enzymes and bacteria, proteins are broken down to produce ammonia and alkaline nitrogenous substances such as amines, which affect the nutritional value of meat products (Lu et al., 2017). However, higher levels of NaCl can inhibit the growth of TVB-N, thereby retarding spoilage (Wang et al., 2020). Due to the higher NaCl content of MT, its TVB-N value was the lowest compared to the other samples.

Abundance and Diversity of Bacterial and Fungal Microorganisms

HTS was used to obtain 889,303 and 1,051,889 high-quality sequences from the 16S rRNA and ITS1 genes from the 15 *SZR* samples, respectively. The average numbers of effective sequences for fungi and bacteria were 70,126 and 59,287, respectively (**Supplementary Table 2**). In all samples fungal sequences significantly exceeded bacterial sequences; nonetheless, the total number of bacterial OTUs was much higher than that of fungi OTUs. Moreover, the OTU coverage of each sample was higher than 99.99%, indicating that almost all microorganisms were detected in the three samples. The rarefaction curves and Shannon index curves were close to the saturation plateau

[5]https://gephi.org/

TABLE 1 | Physicochemical properties of *SZR* from different regions.

Sample	a_w	pH	NaCl(%)	TVB-N(mg/100 g)
ZY	0.9404 ± 0.002^c	4.14 ± 0.15^a	10.33 ± 0.01^c	20.15 ± 0.01^a
MT	0.9408 ± 0.003^b	4.08 ± 0.44^a	11.60 ± 0.19^a	11.26 ± 0.02^c
LB	0.9470 ± 0.001^a	3.68 ± 0.13^b	11.05 ± 0.55^b	11.62 ± 0.02^b

Values are presented as the mean ± standard deviation of quintuplicate (n = 5). $^{a-c}$*Different letters in the same column represent significant differences (P < 0.05).*

(**Table 2**), indicating that the sequencing data were sufficient for subsequent analysis (**Figures 1A,B**). The results of α-diversity showed that the LB samples had higher bacterial diversity than those from the other two regions, and MT had the highest fungal diversity. NMDS and PCoA, based on the binary Jaccard coefficient, were used to analyze the variability and similarity of the microbial population structure of *SZR* in different regions (**Figures 1C,D**). The results revealed differences in fungal community composition in the three regions but similar bacterial community composition in ZY and MT.

Bacterial and Fungal Communities of *Suan zuo rou*

Next, the sequencing data of fungi and bacteria were classified at both the phylum and genus levels to investigate the community structure in depth (**Figures 2A–D**). At the phylum level, 10 bacterial phyla and 4 fungal phyla were identified in the 15 *SZR* samples (Top 10 relative abundance). Among the bacterial communities, *Firmicutes* and *Proteobacteria* represented more than 90% of each sample sequence, followed by *Cyanobacteria*, *Bacteroidetes*, *Actinobacteria*, *Fusobacteria*, *Chloroflexi*, *Verrucomicrobia*, *Acidobacteria*, and *Tenericutes* (**Figure 2A**). *Firmicutes* dominated in all samples with 89.26%, 92.55%, and 88.61% abundance in ZY, MT, and LB, respectively, whereas the abundances of *Proteobacteria* were 4.05%, 2.81%, and 9.10% in ZY, MT, and LB, respectively (**Figure 2A**). Hu et al. (2020) reported that *Firmicutes* and *Proteobacteria* were also the dominant bacteria in traditional dry sausages from Northeast China. With respect to fungi, *Ascomycota* represented more than 96% of each sample sequence, followed by *Basidiomycota*, *Mortierelomycota*, and *Rozellomycota* (**Figure 2C**). The abundances of *Ascomycota* were 96.53%, 98.15%, and 98.86% in ZY, MT, and LB, respectively, whereas *Rozellomycota* was only detected in ZY and LB with an abundance of 0.01% and 0.0001% (**Figure 2C**), respectively.

At the genus level, 114 bacterial genera were identified in the 15 *SZR* samples. *Lactobacillus*, *Weissella*, *Brochothrix*, *Staphylococcus*, *Psychrobacter*, *Bacillus*, *Leuconostoc*, and *Pediococcus* were the 10 core genera (Top 10 relative abundance), as shown in **Figure 2B**. The highest abundance of *Lactobacillus* (44.95%) was found in LB, followed by MT (41.11%) and ZY (35.34%). *Lactobacillus* can release cytoplasmic enzymes and convert substrates from food matrix into aroma compounds of fermented meat products (Smid and Kleerebezem, 2014), and it has been reported to comprise the vast majority of the bacterial community of fermented meat products, for example, fermented llama meat sausages (Fontana et al., 2016) and chorizo de Leoìn

TABLE 2 | Richness and diversity of bacteria and fungi at different processing stages.

Sample	ACE		Chao1		Simpson		Shannon	
	fungi	bacteria	fungi	bacteria	fungi	bacteria	fungi	bacteria
ZY	104.58 ± 18.79^{a}	147.91 ± 29.08^{a}	100.91 ± 26.81^{a}	149.24 ± 28.13^{a}	0.51 ± 0.16^{a}	0.24 ± 0.02^{a}	1.13 ± 0.43^{a}	1.90 ± 0.27^{b}
MT	90.06 ± 37.02^{a}	148.24 ± 31.51^{a}	93.22 ± 39.86^{a}	149.72 ± 29.94^{a}	0.27 ± 0.04^{b}	0.26 ± 0.02^{a}	1.59 ± 0.21^{a}	1.85 ± 0.17^{c}
LB	104.48 ± 26.46^{a}	139.33 ± 22.36^{a}	89.74 ± 31.32^{a}	145.11 ± 15.66^{a}	0.52 ± 0.12^{a}	0.13 ± 0.01^{b}	1.28 ± 0.37^{a}	2.53 ± 0.11^{a}

Values are presented as the mean ± standard deviation of quintuplicate (n = 5). $^{a-c}$*Different letters in the same column represent significant differences (P < 0.05).*

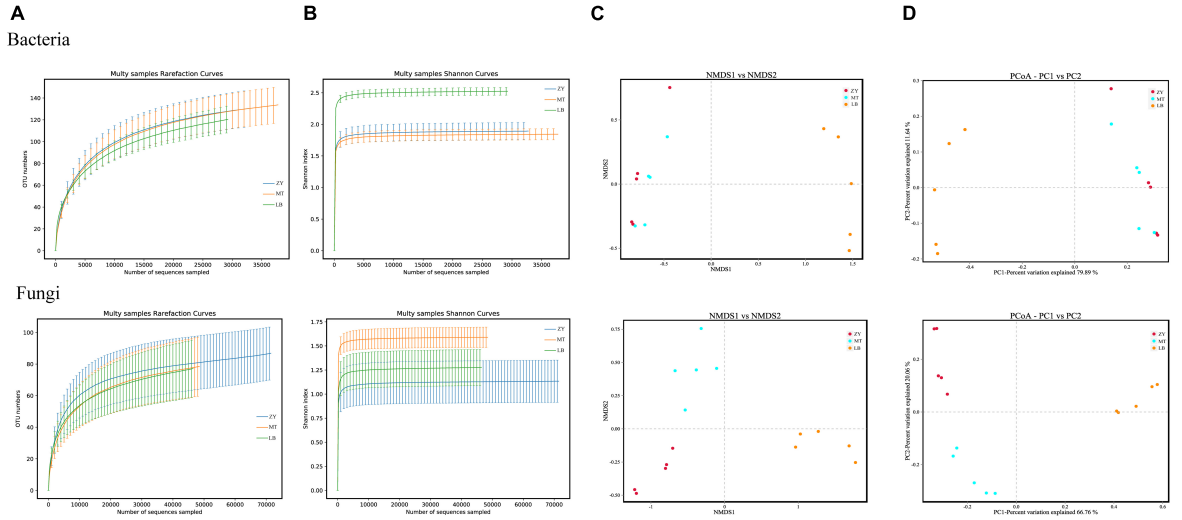

FIGURE 1 | (A) Variations in microbial diversity and community structure of *SZR* in three different regions. rarefaction curves of fungi and bacteria for each sample. **(B)** Shannon index curves of fungi and bacteria for each sample. **(C,D)** NMDS and PCoA score plots of bacteria and fungi.

(Quijada et al., 2018). *Staphylococcus* was detected at a much higher relative abundance in LB (11.15%) than MT (0.33%) and ZY (0.22%), which was consistent with the result of previous study (Lv et al., 2020). *Staphylococcus* is of interest because it have the ability to improve flavor mainly through the metabolism of proteins and lipids (Fonseca et al., 2013). Beneficial bacteria from the genera *Weissella*, *Bacillus*, *Leuconostoc*, and *Pediococcus* were also present in all *SZR* samples in different proportions. In addition, *Brochothrix*, which grows in aerobic or anaerobic environments, and is associated with meat spoilage, was found in LB with an abundance of 22.39% (Odeyemi et al., 2020). This high level of *Brochothrix* in LB may be caused by the fresh raw material and unacceptable hygienic conditions (Casaburi et al., 2014); therefore, care should be taken to detect and inhibit its growth in *SZR* production in the future.

A total of 57 fungal genera were identified in all samples, of which *Kazachstania*, *Debaryomyces*, *Torulaspora*, *Wickerhamomyces*, *Candida*, *Trichoderma*, *Pichia*, *Lactarius*, *Dekkera*, and *Geosmithia* were the most abundant (**Figure 2D**). *Kazachstania* was the major genus in ZY (66.70%), MT (26.14%), and LB (4.16%). In some fermented foods, VFCs, such as ethyl tetradecanoate, are produced by *Kazachstania* during fermentation, and play an important role as a flavoring agent (Tominaga, 2004; Kong et al., 2014). In addition, *Kazachstania* can play a vital part in the regulation of yeast communities, and has been detected in many traditional fermented foods, such as sourdough bread (Lhomme et al., 2015), camembert-type cheese (Bai et al., 2010), and wine (Sun and Liu, 2014). In contrast, *Debaryomyces* was the most abundant in LB (72.65%) and the least abundant in ZY (2.34%). *Debaryomyces* has been widely used as an auxiliary starter, and is a beneficial fungus in Panxian ham (Mu et al., 2019) as well as being important in the fermentation and maturation of sausage (Dalton et al., 1984). Furthermore, Fatichenti et al. (1983) reported that *Debaryomyces* also inhibits putrefactive bacteria. *Wickerhamomyces* has also been reported to show excellent antibacterial activity and antioxidant properties in meat products (Xu et al., 2019), and had the highest content in MT (34.22%), ZY (2.00%), and LB (1.04%). The significant differences in microbial community composition among *SZR* obtained from three different regions could be caused by factors such as raw materials, different ingredients, production environment, fermentation temperature, and relative humidity.

Flavor Compounds Analysis

HS-SPME-GC-MS was used to detect VFCs in the *SZR* samples. In total, 60 VFCs were detected, consisting of 21 alcohols, 17 acids, 8 esters, 5 ketones, 3 aldehydes, 3 phenolic compounds, and 4 others (**Supplementary Table 3**). PCA showed that the differences between PC1 and PC2 were 90.2% and 5.7%,

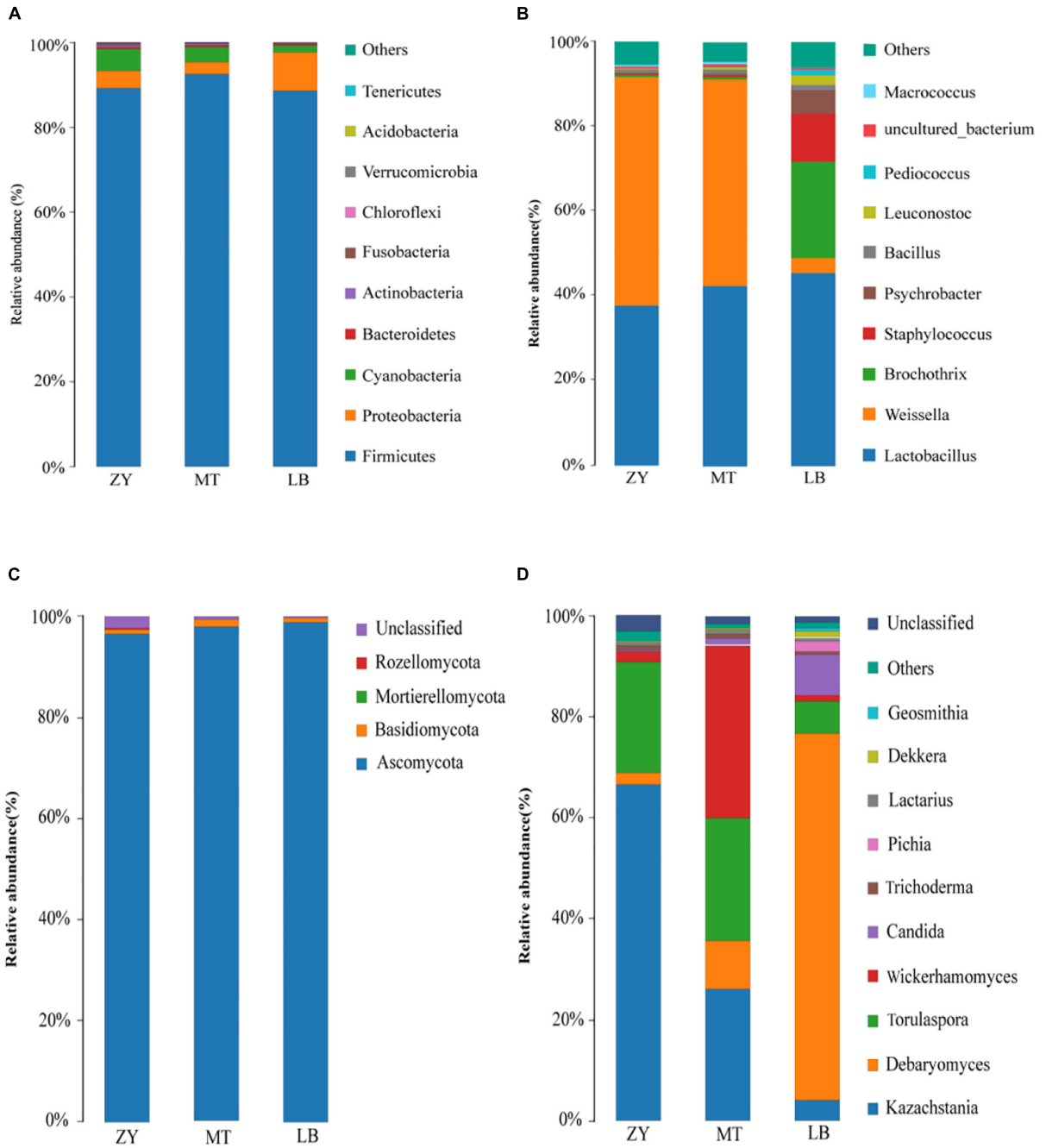

FIGURE 2 | Relative abundance of bacteria at the phylum **(A)** and genus **(B)** level and fungi at phylum **(C)** and genus **(D)** of *SZR* from different regions.

respectively (**Figures 3A,B**). There was a clear separation among ZY, MT, and LB, indicating differences in the flavor of the *SZR* from the three regions.

To better explore the VFCs that lead to the differences between groups, we performed O2PLS discriminant analysis to explore differences in the abundance of VFCs in these samples. Forty-eight types of VFCs were found to be significantly different across samples (VIP $>$ 1, $P < 0.05$). A heat map was generated to investigate the relative quantification of the filtered differential VFCs and their relationship with the characteristics of *SZR* samples from three different regions (**Figure 4**).

Aldehydes are mostly derived from the oxidation of unsaturated fatty acids, while minimal quantities are also generated by the Maillard reaction. These compounds have low perception threshold values and a fruity odor, and are important VFCs in processed meat products (Lorenzo et al., 2014). The hexanal and non-anal detected in this study were also typical of Jinhua ham (Wang et al., 2021). Hexanal is

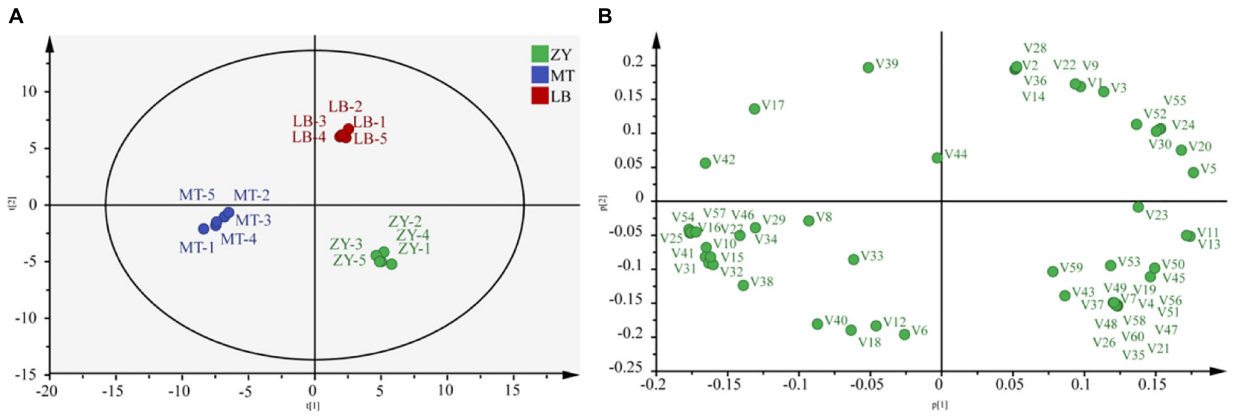

FIGURE 3 | (A) Principal component analysis (PCA) and load diagram **(B)** results for flavor metabolites contents in *SZR* samples.

obtained from the oxidation of n-6 fatty acids (oleic acid and arachidonic acid), which is also associated with grass flavors; however, excessive amounts of hexanal lead to putrefaction odors (Lorenzo et al., 2014). A significantly higher content of 1-nonanal hexanal, which imparts the fruity and green vegetable flavors of meat products, was detected in MT than in the other samples (Ramírez and Cava, 2007).

Esters, which have a particularly fruity flavor, contribute significantly to the formation of flavor qualities in fermented meats and were the main VFC in all *SZR* samples (Sidira et al., 2016). They are usually derived from the esterification of short-chain acids with alcohols (Herranz et al., 2005). Ethyl acetate (fruit and wine aromas), ethyl lactate (fruit aroma), and ethyl caprylate (floral and fruit aromas) were all significantly abundant ($P < 0.05$), with some, such as ethyl acetate and ethyl caprylate, being particularly abundant in the LB sample compared with the other samples. Ethyl benzoate, which can produce pear, apple, and banana aromas that enhance complexity, was also found in LB, which may be attributed to the higher ethanol content during fermentation (Zhao et al., 2020).

Ketones can be produced by lipid autoxidation and microbial metabolism, and are a source of animal flavor and vegetable fat flavor; in fermented meat, a high concentration of ketones can produce floral and spicy flavors (Sanchez-Pena et al., 2005). Methyl ketones are mainly derived from the decarboxylation of β-keto acid or the β-oxidation of saturated fatty acids, providing a certain fermented flavor in sour meat products (Chen et al., 2017). Acetone, 6-methyl-3-heptanone, and 3-octen-2-one were detected at significantly different levels in the three samples ($P < 0.05$), whereas 2,3 octanedione and 4-octanone were only found in the MT and ZY samples.

Volatile acids, which are mainly produced by hydrolysis of phospholipids and triglycerides, lipid oxidation, and the Maillard reaction, also contribute to the aroma and flavor characteristics of fermented meats (Ruiz et al., 2002). Short-chain acids ($C < 6$) have greater implications in VFCs in most samples because of their low perception threshold (Sidira et al., 2016). Acetic acid, propionic acid, isobutyric acid, butyric acid, n-pentanoic acid, and 3-methyl-pentanoic acid were the main short-chain acids found in this study. Long-chain (C14–C18) and medium-chain (C6–C12) acids are products of oxidative degradation of animal fats and are also important reactants formed by ester substances. Octanoic acid is a medium-chain (C6–C12) acid that was detected in the ZY and MT samples. It has an unpleasant smell at high concentrations and a fruity aroma after dilution, but its high threshold does not directly affect the flavor of ZY and MT, which can be inferred for certain other VFCs as well, such as methyl ketones and alcohols (Urbach, 1995).

Alcohols, another important component of *SZR* flavor, are closely related to lipid oxidation, amino acid metabolism, methyl ketone reduction, and microbial reproduction (Lin et al., 2018). Ethanol, 1-pentanol, 1-undecanol, cyclohexanol, 1-Octen-3-ol, linalool, 2,3-butanediol, 1-octanol, and phenethyl alcohol were significant in the *SZR* samples ($P < 0.05$). Phenyl alcohol was the highest in LB, which may be caused by carbohydrate decomposition and hydrate-induced microorganisms (such as yeast *Aspergillus oryzae*). 1-Octen-3-ol, which is oxidized by arachidonic acid and has a low odor threshold value, existed in all the samples but had the highest content in ZY, which had a marked odor of mushroom.

Apart from the above, linalool and terpene alcohol were detected in the 15 samples as components of anise and pepper, as well as *Artemisia argyi* (Summo et al., 2011). Although different manufacturers add a variety of spices, these compounds have a higher threshold value and contribute less to the overall flavor of *SZR* (Shahidi et al., 1986). Small amounts of trichloromethane, cyclopentane, and coconut aldehyde were also detected in MT, ZY, and LB, respectively, the first time these substances have been detected in *SZR*.

Co-occurrence and Exclusion Analyses Revealed the Relationships Between Different Microbes

Microbial interactions are an important factor influencing the structure of microorganisms (Zhang et al., 2018). To understand the symbiotic or antagonistic relationships between different microbial genera, correlation co-occurrence networks

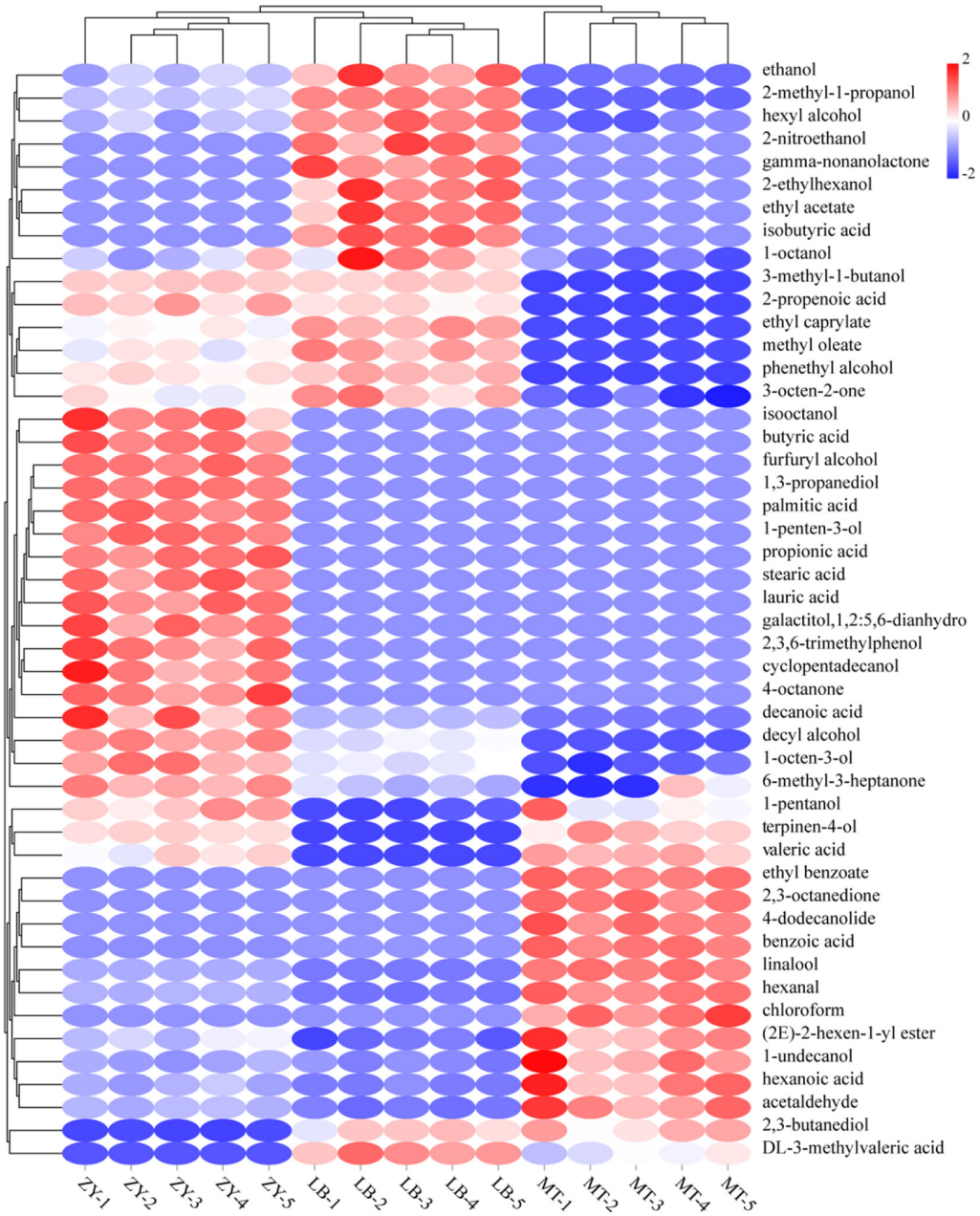

FIGURE 4 | Heat map of changes in differential compounds of *SZR* from three different regions.

between core bacteria and fungi were constructed using Pearson's correlation coefficients and *P*-values (**Figure 5**). Correlation analysis between bacteria and fungi showed that *Brochothrix*, *Staphylococcus*, and *Pediococcus* were positively correlated with *Debaryomyces*, *Candida*, *Pichia*, and *Geosmithia* ($|r| > 0.7$, $P < 0.05$), whereas *Weissella* and *Macrococcus* were negatively correlated with *Debaryomyces* and *Candida* ($|r| > 0.7$, $P < 0.05$). Furthermore, *Staphylococcus*, *Brochothrix*, *Leuconostoc*, and *Pediococcus* together inhibited the growth of *Kazachstania* and *Torulaspora* ($|r| > 0.7$, $P < 0.05$), whereas *Weissella* was positively correlated with *Kazachstania* and *Torulaspora* ($|r| > 0.7$, $P < 0.05$). In addition, *Lactarius* was positively correlated with *Bacillus* and *uncultured_bacterium* ($|r| > 0.7$, $P < 0.05$). Differences among regions were mainly manifested in the relative abundance of *Weissella*, *Brochothrix*, *Staphylococcus*, *uncultured_bacterium*, *Debaryomyces*, *Kazachstania*, and *Torulaspora*, which are the dominant and functional genera known to enhance the aroma profile of fermented foods (Maturano et al., 2015). These findings were consistent with the HTS and microbial co-occurrence network results in our study; however, several microbial genera with high relative abundance, such as *Kazachstania* and

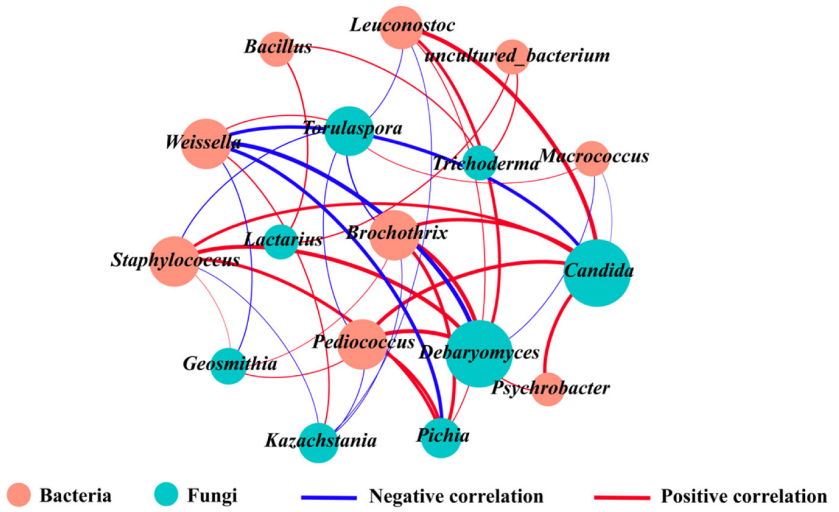

FIGURE 5 | Association network diagram of bacteria and fungi. The orange and green circles refer to bacteria and fungi, respectively, and the red and blue lines refer to positive correlations ($r > 0.7$ and $P < 0.05$) and negative correlations ($r < -0.7$ and $P < 0.05$), respectively. (For interpretation of the references to color in this figure legend, the reader is referred to the web version of this article).

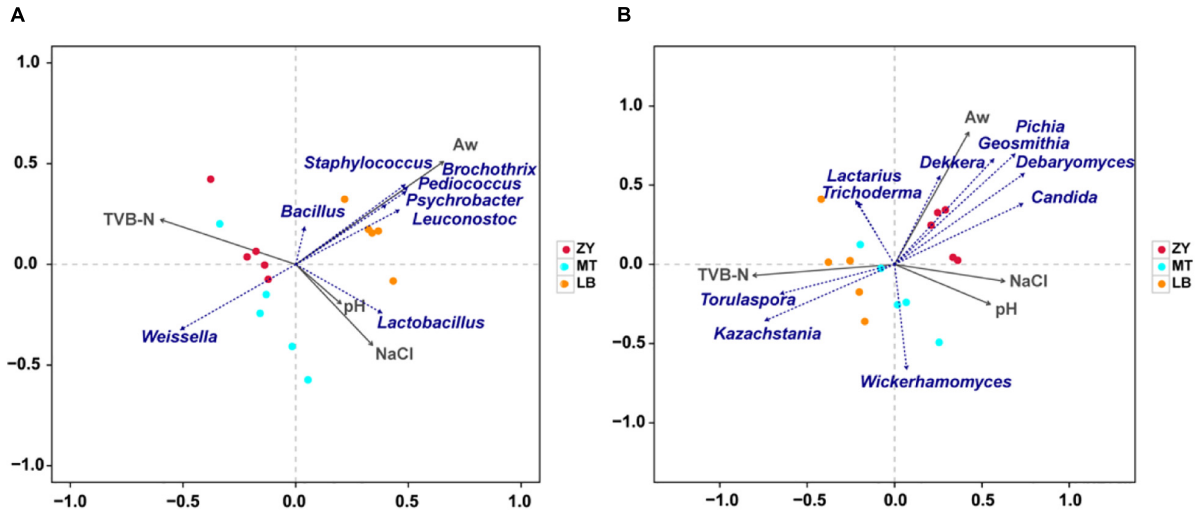

FIGURE 6 | (A) RDA of microorganisms (Top 10 of OTU) and physiochemical properties. Correlation between physiochemical properties and fungal genera. **(B)** Correlations between physiochemical properties and bacterial genera.

Lactobacillus, were unexpectedly eliminated from the microbial correlation network.

Correlations Between Microorganisms and Physiochemical Properties

Physicochemical properties of *SZR* were mainly determined by the production process and fermentation time, which had an obvious influence on the microbial community succession in the food microecological environment (Jung et al., 2014). The correlation between the physicochemical properties and microflora of *SZR* was identified by RDA (**Figure 6**), which showed that the microbial community structure was affected by pH, a_w, NaCl, and TVB-N. In terms of bacteria communities, most of the dominant bacterium were positively related with a_w, with *Staphylococcus*, *Psychrobacter*, *Bacillus*, *Leuconostoc*, *Pediococcus*, and *Macrococcus* showing the strongest positive correlation. Stavropoulou et al. (2018) also reported a significant effect of pH on the community structure of *Staphylococcus* during meat fermentation, and our finding that *Lactobacillus* showed a positive correlation with pH and a negative correlation with TVB-N is consistent with the findings of Zhang et al. (2018), who noticed that *Lactobacillus*, as a facultative anaerobe, has a significant influence on TVB-N (**Figure 6A**).

For fungi, the contribution of a_w to microbial community structure was 97.38%; therefore, it was considered that a_w was the main environmental factor that drove the variation in the

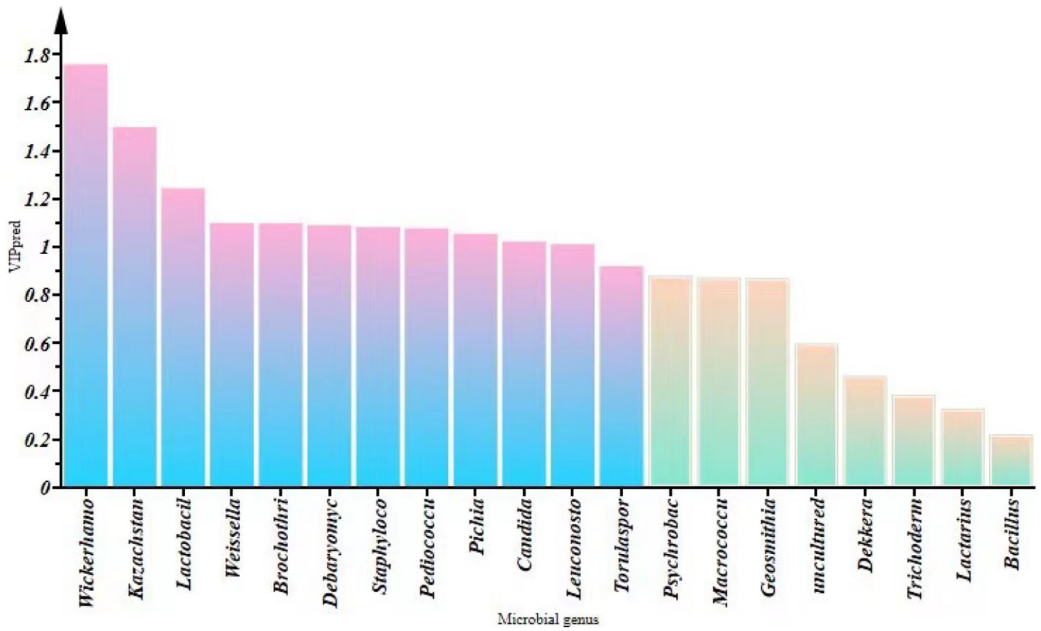

FIGURE 7 | Changes in VIP (pred) values of the top 10 fungi and bacteria by relative abundance at the genus level.

fungus community in *SZR* (**Figure 6B**). *Dekkera* was positively correlated with a_w, converts hydroxycinnamic acids to volatile phenols, which lead to meat spoilage (Lima et al., 2020). Given that the spoilage of meat products is known to depend on the amount of a_w, these results indicate that the effect of a_w on meat spoilage could be linked to the growth and reproduction of *Dekkera* and other fungi (Oelofse et al., 2016). In terms of other fungal genera, *Torulaspora* and *Kazachstania* had a significantly positive correlation with TVB-N, whereas *Lactarius* and *Trichoderma* were negatively correlated with pH and NaCl, indicating that the concentration of NaCl had a greater effect on *Lactarius* and *Trichoderma* than *Dekkera*.

Correlations Between Microorganisms and Volatile Flavor Compounds

We constructed an O2PLS model for VFCs and microorganisms in *SZR* samples from different regions (**Supplementary Figure 1**). The R^2 and Q^2 values of the O2PLS model were 0.983 and 0.891, respectively, which indicate that the O2PLS model has excellent interpretation rate and predictive capability (Triba et al., 2015). The VIP(pred) vector (calculation of variable importance for the projection) was applied to measure the intensity and explanatory ability of the influence of microorganisms on the formation of VFCs (**Figure 7**). A total of 12 microorganisms [VIP(pred) > 1.0], comprising 7 bacteria [VIP(pred):1.242–1.010] and 5 fungi [VIP(pred):1.758–1.021], had an influence on VFCs, of which *Wickerhamomyces*, *Kazachstania*, *Lactobacillus*, *Weissella*, *Brochothrix*, *Debaryomyces*, *Staphylococcus*, *Pediococcus*, *Pichia*, *Candida*, *Leuconostoc*, and *Torulaspora* were the primary influencers.

The interaction of VFCs with microorganisms was evaluated using Pearson's correlation coefficient which showed that different microorganisms exerted different effects on VFCs (**Figure 8**). Based on Pearson's correlation, a total of 5 bacterial and 5 fungal species were screened to be highly correlated with VFCs ($|r| > 0.8, P < 0.05$), namely, *Kazachstania*, *Debaryomyces*, *Wickerhamomyces*, *Candida*, *Pichia*, *Weissella*, *Brochothrix*, *Staphylococcus*, *Leuconostoc*, and *Pediococcus*. *Staphylococcus* plays a crucial role in the formation of the final flavor quality of fermented meat products (Iacumin et al., 2020), and was positively correlated with 8 volatile compounds, namely ethyl acetate, 2-ethylhexanol, isobutyric acid, gamma-non-anolactone, dL-3-methylvaleric acid, ethanol, hexyl alcohol, and 2-methyl-1-propanol, but negatively associated with terpinen-4-ol and valeric acid ($|r| > 0.8, P < 0.05$). This correlation might be related to the involvement of free amino acids produced by *Staphylococcus* owing to the hydrolysis of proteins, which can contribute to the formation of VFCs (Cruxen et al., 2017). In addition, LAB (including *Weissella* and *Leuconostoc*), which are probiotics that have beneficial effects on human health, were related to valeric acid, 1-pentanol, isobutyric acid, 2-ethylhexanol, and hexyl alcohol. They are also widely used as starters in many fermentation processes and might play a pivotal role in flavor development (Göğüş et al., 2004; Leroy et al., 2006). *Leuconostoc* can increase the content of some metabolites such as acids and alcohols (Galle et al., 2010; Xu et al., 2017), so it is not surprising that it is positively correlated with isobutyric acid, ethyl acetate, 2-ethylhexanol, hexyl alcohol, and 2-nitroethanol. In addition, *Pediococcus* was related to ethyl acetate and terpinen-4-ol. These have been widely used in the production of fermented foods because of their role in increasing the content of organic acids, short-chain fatty acids, and esters during food fermentation (Xu et al., 2021), which is consistent with our results.

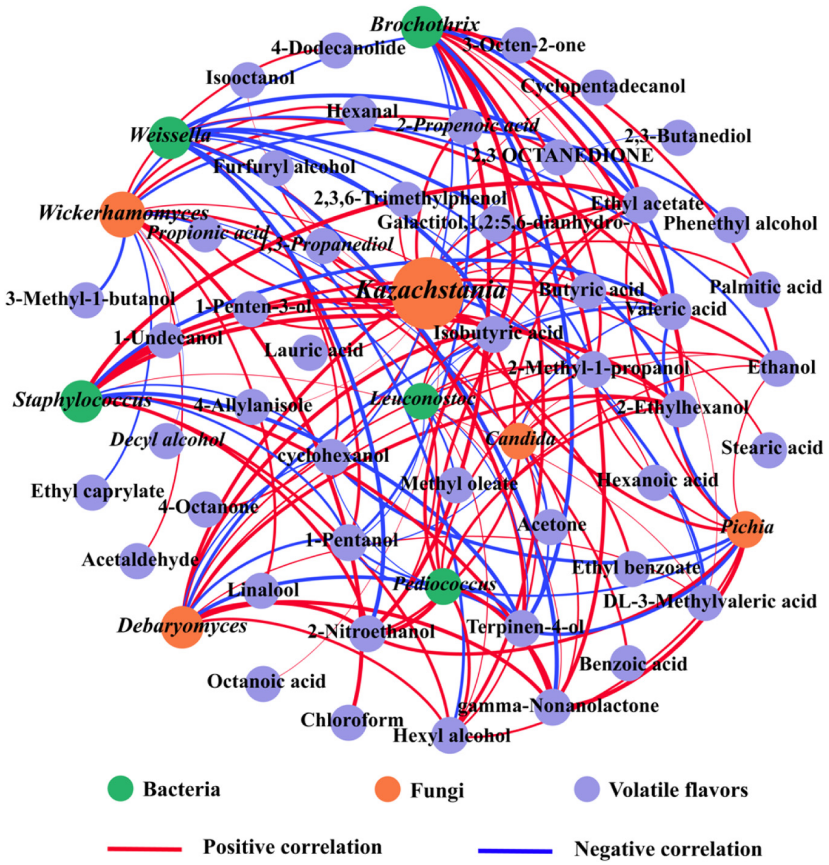

FIGURE 8 | Correlation analyses between microorganisms [VIP(pred) > 1.0] and volatile flavor compounds. Statistically significant ($P < 0.05$) Pearson's correlation coefficient ($|\rho| > 0.8$) indicates the robust correlations. The green, orange and purple circles refer to bacteria, fungi and volatile flavors, respectively, and the red and blue lines refer to positive correlations ($|r| > 0.8$ and $P < 0.05$) and negative correlations ($|r| < -0.8$ and $P < 0.05$), respectively. The size of nodes indicates the degree of connections. The thickness of each connection (edge) between two nodes is proportional to the value of Pearson's correlation coefficient. (For interpretation of the references to color in this figure legend, the reader is referred to the web version of this article).

With regards to fungi, *Kazachstania*, *Debaryomyces*, *Wickerhamomyces*, *Pichia*, and *Candida* are particularly important in fermented meat products and are the main microorganisms in alcohol and glycerol fermentation (Ai et al., 2019). The main VFCs of *SZR* are derived from the breakdown of proteins by yeasts and the conversion of amino acids (Engels et al., 1997). Ethanol, 2-nitroethanol, 2-methyl-1-propanol, hexyl alcohol, 1-pentanol, cyclohexanol, terpinen-4-ol and 2-ethylhexanol showed positive correlation with *Debaryomyces*, *Pichia*, and *Candida*, whereas furfuryl alcohol and cyclopentadecanol were only correlated with *Kazachstania*. Most yeasts were positively correlated with alcohols and esters, and *Debaryomyces* and *Picha* promoted the production of higher alcohols, acetate, and fatty acid esters. *Wickerhamomyces* can promote the Strecker degradation pathway, thereby producing aldehydes that increase the flavor of *SZR* (Bolumar et al., 2003), which is supported by the findings in this study that *Wickerhamomyces* was positively correlated with hexanal and acetaldehyde. Overall, *Weissella*, *Staphylococcus*, *Leuconostoc*, and *Pediococcus* bacteria, and *Kazachstania*, *Debaryomyces*, *Wickerhamomyces*, *Pichia*, and *Candida* fungi were the main sources of VFCs.

CONCLUSION

In this study, we investigated the differences between the microbial communities, VFCs, and physicochemical properties of traditional *SZR* from three different regions of Guizhou province, China. Our findings revealed that the abundance of *Brochothrix* and *Staphylococcus* was significantly higher in LB samples than in ZY and MT samples, whereas that of *Wickerhamomydes* was markedly higher in the MT samples than in ZY and LB samples. Alcohols, acids, and esters were the main VFC found in all the samples. There were significant correlations between 48 volatile compounds and 10 core genera, namely *Wickerhamomyces*, *Kazachstania*, *Lactobacillus*, *Weissella*, *Brochothrix*, *Debaryomyces*, *Staphylococcus*, *Pediococcus*, *Pichia*, *Candida*, and *Leuconostoc*. The demonstration of the relationship among microbial communities, VFCs, and physicochemical properties provides a strong basis for further investigation of

the microbial ecological impact of traditional fermented meat products. Future studies should use multi-omics approaches such as metagenomics, metaproteomics, and metatranscriptomics to study the fermentation mechanisms and metabolic pathways of *SZR* in depth, providing a scientific reference for the industrial production of traditional *SZR* in Guizhou province, China.

DATA AVAILABILITY STATEMENT

The datasets presented in this study can be found in online repositories. The names of the repository/repositories and accession number(s) can be found below: https://www.ncbi.nlm.nih.gov and SRP328727.

AUTHOR CONTRIBUTIONS

HW and WS contributed the experimental design, performed the statistical analysis, and wrote the manuscript. HW, WS, CZ, and YM contributed to manuscript revision, read, and approved the submitted version. All authors contributed to the article and approved the submitted version.

FUNDING

This work was financially supported by 2022 Regional Science Foundation Project: Study on the mechanism of reducing mutton sausage by collaborative fermentation of *P. acidilactici* and *R. oryzae* (32160554); Science and Technology Plan Project of Guizhou Province [(2018)5781]; and Guizhou ecological specialty meat products science and technology innovation talent team [(2020)5004].

ACKNOWLEDGMENTS

We thank Biomarker Technologies Co, Ltd. (Beijing, China) for technical assistance in carrying out the analyses. We would like to thank Editage (www.editage.cn) for English language editing.

SUPPLEMENTARY MATERIAL

The Supplementary Material for this article can be found online at: https://www.frontiersin.org/articles/10.3389/fmicb.2021.736525/full#supplementary-material

REFERENCES

Ai, M., Qiu, X., Huang, J., We, C. D., Jin, Y., and Zhou, R. Q. (2019). Characterizing the microbial diversity and major metabolites of Sichuan bran vinegar augmented by *Monascus purpureus*. *Int. J. Food Microbiol.* 292, 83–90. doi: 10.1016/j.ijfoodmicro.2018.12.008

Bai, M., Qing, M., Guo, Z., Zhang, Y., Chen, X., Bao, Q., et al. (2010). Occurrence and dominance of yeast species in naturally fermented milk from the Tibetan Plateau of China. *Can. J. Microbiol.* 56, 707–714. doi: 10.1139/w10-056

Berardo, A., Devreese, B., De, M. H., Stavropoulou, D. A., Van, R. G., Leroy, F., et al. (2016). Actin proteolysis during ripening of dry fermented sausages at different pH values. *Food Chem.* 221, 1322–1332. doi: 10.1016/j.foodchem.2016.11.023

Bokulich, N. A., Subramanian, S., Faith, J. J., Gevers, D., Gordon, J. I., Knight, R., et al. (2013). Quality-filtering vastly improves diversity estimates from Illumina amplicon sequencing. *Nat. Methods* 10, 57–59. doi: 10.1038/nmeth.2276

Bolger, A. M., Lohse, M., and Usadel, B. (2014). Trimmomatic: a flexible trimmer for Illumina Sequence Data. *Bioinformatics* 30, 2114–2120. doi: 10.1093/bioinformatics/btu170

Bolumar, T., Sanz, Y., Aristoy, M. C., and Toldrá, F. (2003). Purification and properties of an arginyl aminopeptidase from *Debaryomyces hansenii*. *Int. J. Food Microbiol.* 86, 141–151. doi: 10.1016/S0168-1605(03)00069-2

Buée, M., Reich, M., Murat, C., Morin, E., Nilsson, R. H., Uroz, S., et al. (2010). 454 pyrosequencing analyses of forest soils reveal an unexpectedly high fungal diversity. *New Phytol.* 184, 449–456. doi: 10.1111/j.1469-8137.2009.03003.x

Caporaso, J. G., Kuczynski, J., Stombaugh, J., Bittinger, K., Bushman, F. D., and Costello, E. (2010). QIIME allows analysis of high-throughput community sequencing data. *Nat. Methods* 7, 335–336. doi: 10.1038/nmeth.f.303

Casaburi, A., De, F. F., Villani, F., and Ercolini, D. (2014). Activities of strains of Brochothrix thermosphacta in vitro and in meat. *Food Res. Int.* 62, 366–374. doi: 10.1016/j.foodres.2014.03.019

Chen, C., Chen, X., Jiang, M., Rui, X., Li, W., and Dong, M. (2014). A newly discovered bacteriocin from *Weissella hellenica* D1501 associated with Chinese Dong fermented meat (Nanx Wudl). *Food Control* 42, 116–124. doi: 10.1016/j.foodcont.2014.01.031

Chen, Q., Kong, B. H., Han, Q., Xia, X. F., and Xu, L. (2017). The role of bacterial fermentation in lipolysis and lipid oxidation in Harbin dry sausages and its flavour development. *LWT-Food Sci. Technol.* 77, 389–396. doi: 10.1016/j.lwt.2016.11.075

Chen, X., Mi, R., Qi, B., Xiong, S., and Wang, S. (2020). Effect of proteolytic starter culture isolated from Chinese Dong fermented pork (Nanx Wudl) on microbiological, biochemical and organoleptic attributes in dry fermented sausages. *Food Sci. Hum. Well.* 10, 13–22. doi: 10.1016/j.fshw.2020.05.012

Cruxen, C. E. D. S., Funck, G. D., Dannenberg, G. D. S., Haubert, L., Marques, J. D. L., Kroning, I. S., et al. (2017). Characterization of Staphylococcus xylosus LQ3 and its application in dried cured sausage. *LWT-Food Sci. Technol.* 86, 538–543. doi: 10.1016/j.lwt.2017.08.045

Dalton, H. K., Board, R. G., and Davenport, R. R. (1984). The yeasts of british fresh sausage and minced beef. *Antonie Van Leeuwenhoek* 50, 227–248. doi: 10.1007/BF02342134

Edgar, R. C., Haas, B. J., Clemente, J. C., Quince, C., and Knight, R. (2011). UCHIME improves sensitivity and speed of chimera detection. *Bioinformatics* 27, 2194–2200. doi: 10.1093/bioinformatics/btr381

Engels, W. J. M., Dekker, R., Jong, C. D., Neeter, R., and Visser, S. A. (1997). A comparative study of volatile compounds in the water-soluble fraction of various types of ripened cheese. *Int. Dairy J.* 7, 255–263. doi: 10.1016/S0958-6946(97)00003-4

Fatichenti, F., Bergere, J. L., Deiana, P., and Farris, G. A. (1983). Antagonistic activity of *Debaryomyces hansenii* towards Clostridium tyrobutyricum and Cl. butyricum. *J. Dairy Res.* 50, 449–457. doi: 10.1017/S0022029900032684

Fonseca, S., Cachaldora, A., Gómez, M., Franco, I., and Carballo, J. (2013). Effect of different autochthonous starter cultures on the volatile compounds profile and sensory properties of Galician chorizo, a traditional Spanish dry fermented sausage. *Food Control* 33, 6–14. doi: 10.1016/j.foodcont.2013.01.040

Fontana, C., Bassi, D., López, C., Pisacane, V., Otero, M. C., Puglisi, E., et al. (2016). Microbial ecology involved in the ripening of naturally fermented llama meat sausages. A focus on lactobacilli diversity. *Int. J. Food Microbiol.* 236, 17–25. doi: 10.1016/j.ijfoodmicro.2016.07.002

Galle, S., Schwab, C., Arendt, E., and Ganzle, M. (2010). Exopolysaccharide-forming Weissella strains as starter cultures for sorghum and wheat sourdoughs. *J. Agric. Food Chem.* 58, 5834–5841. doi: 10.1021/jf1002683

Göğüş, U., Bozoglu, F., and Yurdugul, S. (2004). The effects of nisin, oil-wax coating and yogurt on the quality of refrigerated chicken meat. *Food Control* 15, 537–542. doi: 10.1016/j.foodcont.2003.08.007

Herranz, B., Hoz, L. D. L., Hierro, E., Fernández, M., and Ordóñez, J. A. (2005). Improvement of the sensory properties of dry-fermented sausages by the addition of free amino acids. *Food Chem.* 91, 673–682. doi: 10.1016/j.foodchem.2004.06.040

Hu, Y., Liu, X., Shan, C., Xia, X., Wang, Y., Dong, M., et al. (2017). Novel bacteriocin produced by *Lactobacillus alimentarius* FM-MM 4 from a traditional Chinese fermented meat Nanx Wudl: purification, identification and antimicrobial characteristics. *Food Control* 77, 290–297. doi: 10.1016/j.foodcont.2017.02.007

Hu, Y., Zhang, L., Liu, Q., Wang, Y., Chen, Q., and Kong, B. H. (2020). The potential correlation between bacterial diversity and the characteristic volatile flavour of traditional dry sausages from Northeast China. *Food Microbiol.* 91:103505. doi: 10.1016/j.fm.2020.103505

Iacumin, L., Osualdini, M., Bovolenta, S., Boscolo, D., Chiesa, L., Panseri, S., et al. (2020). Microbial, chemico-physical and volatile aromatic compounds characterization of Pitina PGI, a peculiar sausage-like product of North East Italy. *Meat Sci.* 163:108081. doi: 10.1016/j.meatsci.2020.108081

Jiang, L., Su, W., Mu, Y., and Mu, Y. C. (2020). Major metabolites and microbial community of fermented black glutinous rice wine with different starters. *Front. Microbiol.* 11:593. doi: 10.3389/fmicb.2020.00593

Juaárez-Castelaán, C., Garciía-Cano, I., Escobar-Zepeda, A., Azaola-Espinosa, A., Aílvarez- Cisneros, Y., and Ponce-Alquicira, E. (2019). Evaluation of the bacterial diversity of Spanish-type chorizo during the ripening process using high-throughput sequencing and physicochemical characterization. *Meat Sci.* 150, 7–13. doi: 10.1016/j.meatsci.2018.09.001

Jung, J. Y., Lee, S. H., and Jeon, C. O. (2014). Microbial community dynamics during fermentation of doenjang-meju, traditional korean fermented soybean. *Int. J. Food Microbiol.* 185, 112–120. doi: 10.1016/j.ijfoodmicro.2014.06.003

Kim, E., Cho, E. J., Yang, S. M., Kim, M. J., and Kim, H. Y. (2014). Novel approaches for the identification of microbial communities in kimchi: MALDI-TOF MS analysis and high-throughput sequencing. *Food Microbiol.* 94:103641. doi: 10.1016/j.fm.2020.103641

Kim, M. S., and Park, E. J. (2014). Bacterial communities of traditional salted and fermented seafoods from jeju island of korea using 16s rRNA gene clone library analysis. *J. Food Sci.* 79, M927–M934. doi: 10.1111/1750-3841.12431

Kong, Y., Wu, Q., Zhang, Y., and Xu, Y. (2014). In Situ analysis of metabolic characteristics reveals the key yeast in the spontaneous and solid-state fermentation process of Chinese light-style liquor. *Appl. Environ. Microbiol.* 80, 3667–3676. doi: 10.1128/AEM.04219-13

Laranjo, M., Agulheiro-Santos, A. C., Potes, M. E., Cabrita, M. J., Garcia, R., Fraqueza, M. J., et al. (2015). Effects of genotype, salt content and calibre on quality of traditional dry-fermented sausages. *Food Control* 56, 119–127. doi: 10.1016/j.foodcont.2015.03.018

Leroy, F., Verluyten, J., and Vuyst, L. D. (2006). Functional meat starter cultures for improved sausage fermentation. *Int. J. Food Microbiol.* 106, 270–285. doi: 10.1016/j.ijfoodmicro.2005.06.027

Lhomme, E., Lattanzi, A., Dousset, X., Minervini, F., De, A. M., Lacaze, G., et al. (2015). Lactic acid bacterium and yeast microbiotas of sixteen French traditional sourdoughs. *Int. J. Food Microbiol.* 215, 161–170. doi: 10.1016/j.ijfoodmicro.2015.09.015

Li, S. Y., Sha, K., Sun, B. Z., Xie, P., Lei, Y. H., Zhang, S. S., et al. (2019). Application of functional microorganisms in fermented meat products. *Meat. Res.* 33, 56–60.

Lima, A. N. D., Rui, M., Campos, F. M., and Couto, J. A. (2020). Survival andand metabolism of hydroxycinnamic acids by *Dekkera bruxellensis* in monovarietal wines. *Food Microbiol.* 93:103617. doi: 10.1016/j.fm.2020.103617

Lin, H. B., Yu, X. Y., Fang, J. X., Lu, Y. H., Liu, P., Xing, Y. G., et al. (2018). Flavor compounds in Pixian broad-bean paste: non-volatile organic acids and amino acids. *Molecules* 23, 1299–1314. doi: 10.3390/molecules23061299

Liu, N., Pan, J. H., Miao, S., and Qin, L. K. (2020). Microbial community in Chinese traditional fermented acid rice soup (rice-acid) and its correlations with key organic acids and volatile compounds. *Food Res. Int.* 137:109672. doi: 10.1016/j.foodres.2020.109672

Liu, S. N., and Zhou, Z. J. (2011). Lactic acid bacteria in traditional fermented Chinese foods. *Food Res. Int.* 44, 643–651. doi: 10.1016/j.foodres.2010.12.034

Lorenzo, J. M., Franco, D., and Carballo, J. (2014). Effect of the inclusion of chestnut in the finishing diet on volatile compounds during the manufacture of dry-cured "lacon" from celta pig breed. *Meat Sci.* 96, 211–233. doi: 10.1016/j.meatsci.2013.07.007

Lu, Q., Tang, X., and Dong, J. (2017). A feasibility quantification study of total volatile basic nitrogen (TVB-N) content in duck meat for freshness evaluation. *Food Chem.* 237, 1179–1185. doi: 10.1016/j.foodchem.2017.06.031

Luo, T., Fan, W., and Xu, Y. (2008). Characterization of volatile and semi- volatile compounds in Chinese rice wines by headspace solid phase microextraction followed by gas chromatography-mass spectrometry. *J. Inst. Brew.* 114, 172–179. doi: 10.1002/j.2050-0416.2008.tb00323.x

Lv, J., Xu, W. H., Ji, C. F., Liang, H. P., Li, S. J., Yang, Z. X., et al. (2020). Relationships between the bacterial diversity and metabolites of a Chinese fermented pork product, sour meat. *Int. J. Food. Sci. Tech.* 56:14905. doi: 10.1111/ijfs.14905

Lv, J., Yang, Z. X., Xu, W. H., Li, S. J., Liang, H. P., Ji, C., et al. (2019b). Relationships between bacterial community and metabolites of sour meat at different temperature during the fermentation. *Int. J. Food Microbiol.* 307:108286. doi: 10.1016/j.ijfoodmicro.2019.108286

Lv, J., Li, C. C., Li, S. J., Liang, H. P., Ji, C. F., Zhu, B. W., et al. (2019a). Effects of temperature on microbial succession and quality of sour meat during fermentation. *LWT* 114:108391. doi: 10.1016/j.lwt.2019.108391

Magoc, T., and Salzberg, S. L. (2011). FLASH: fast length adjustment of short reads to improve genome assemblies. *Bioinformatics* 27, 2957–2963. doi: 10.1093/bioinformatics/btr507

Marušić, N., Vidaček, S., Janči, T., Petrak, T., and Medić, H. (2014). Determination of volatile compounds and quality parameters of traditional istrian dry-cured ham. *Meat Sci.* 96, 1409–1416. doi: 10.1016/j.meatsci.2013.12.003

Maturano, Y. P., Assof, M., Fabani, M. P., Nally, M. C., Jofreé, V., Assaf, L. A. R., et al. (2015). Enzymatic activities produced by mixed Saccharomyces and non-Saccharomyces cultures: relationship with wine volatile composition. *Antonie van Leeuwenhoek* 108, 1239–1256. doi: 10.1007/s10482-015-0578-0

Mourente, G., and Bell, J. G. (2006). Partial replacement of dietary fish oil with blends of vegetable oils (rapeseed, linseed and palm oils) in diets for European sea bass (*Dicentrarchus labrax L.*) over a long term growth study: effects on muscle and liver fatty acid composition and effectiveness of a fish oil finishing diet. *Comp. Biochem. Physiol. B Biochem. Mol. Biol.* 145, 389–399. doi: 10.1016/j.cbpb.2006.08.012

Mu, Y., Su, W., Mu, Y. C., and Jiang, L. (2019). Combined Application of High-Throughput Sequencing and Metabolomics Reveals Metabolically Active Microorganisms During Panxian Ham Processing. *Front. Microbiol.* 10:3012. doi: 10.3389/fmicb.2019.03012

Odeyemi, O. A., Alegbeleye, O. O., Strateva, M., and Stratev, D. (2020). Understanding spoilage microbial community and spoilage mechanisms in foods of animal origin. *Compr. Rev. Food Sci. Food Saf.* 19, 311–331. doi: 10.1111/1541-4337.12526

Oelofse, A., Pretorius, I. S., and Du, T. M. (2016). Significance of Brettanomyces and Dekkera during winemaking: a synoptic review. *S. Afr. J. Enol. Vitic.* 29, 128–144. doi: 10.1145/1346281.1346322

Quijada, N. M., Filippis, F. D., Sanz, J. J., García-Fernández, M. D. C., Rodríguez-Lázaro, D., Ercolini, D., et al. (2018). Different *Lactobacillus* populations dominate in "Chorizo de Leoìn" manufacturing performed in different production plants. *Food Microbiol.* 70, 94–102. doi: 10.1016/j.fm.2017.09.009

R Development Core Team (2009). *R: A Language and Environment for Statistical Computing*. Vienna: R Foundation for Statistical Computing.

Ramírez, R., and Cava, R.,(2007). Volatile profiles of dry-cured meat products from three different iberian x duroc genotypes. *J. Agric. Food Chem.* 55, 1923–1931. doi: 10.1021/jf062810l

Ruiz, J., Garcia, C., Muriel, E., Andr ìes, A. I., and Ventanas, J. (2002). Influence of sensory characteristics on the acceptability of dry-cured ham. *Meat Sci.* 61, 347–354. doi: 10.1016/S0309-1740(01)00204-2

Sanchez-Pena, C. M., Luna, G., Garcia-Gonzalez, D. L., and Aparicio, R. (2005). Characterization of french and spanish dry-cured hams: influence of the volatiles from the muscles and the subcutaneous fat quantified by SPME-GC. *Meat Sci.* 69, 635–645. doi: 10.1016/j.meatsci.2004.10.015

Shahidi, F., Rubin, L. J., D'Souza, L. A., Teranishi, R., and Buttery, R. G. (1986). Meat flavor volatiles: a review of the composition, techniques of analysis, and sensory evaluation. *Crit. Rev. Food Technol.* 24, 141–243. doi: 10.1080/10408398609527435

Sidira, M., Kandylis, P., Kanellaki, M., and Kourkoutas, Y. (2016). Effect of immobilized *Lactobacillus casei* on the evolution of flavor compounds in probiotic dry-fermented sausages during ripening. *Meat Sci.* 100, 41–51. doi: 10.1016/j.meatsci.2014.09.011

Smid, E. J., and Kleerebezem, M. (2014). Production of aroma compounds in lactic fermentations. *Annu. Rev. Food Sci. Technol.* 5, 313–326. doi: 10.1146/annurev-food-030713-092339

Stavropoulou, D. A., Filippou, P., De, S. S., De, V. L., and Leroy, F. (2018). Effect of temperature and pH on the community dynamics of coagulase-negative staphylococci during spontaneous meat fermentation in a model system. *Food Microbiol.* 76, 180–188. doi: 10.1016/j.fm.2018.05.006

Summo, C., Caponio, F., Pasqualone, A., and Gomes, T. (2011). Vacuum-packed ripened sausages: evolution of volatile compounds during storage. *J. Sci. Food Agr.* 91, 950–955. doi: 10.1002/jsfa.4272

Sun, Y., and Liu, Y. (2014). Investigating of yeast species in wine fermentation using terminal restriction fragment length polymorphism method. *Food microbiol.* 38, 201–207. doi: 10.1016/j.fm.2013.09.001

Tominaga, T. (2004). Rapid identification of pickle yeasts by fluorescent PCR and microtemperature-gradient gel electrophoresis. *FEMS Microbiol. Lett.* 238, 43–48. doi: 10.1016/j.femsle.2004.07.015

Triba, M. N., Le, M. L., Amathieu, R., Goossens, C., Bouchemal, N., and Nahon, P. (2015). PLS/OPLS models in metabolomics: the impact of permutation of dataset rows on the K-fold cross-validation quality parameters. *Mol. Biosyst.* 11, 13–19. doi: 10.1039/c4mb00414k

Urbach, G. (1995). Contribution of lactic acid bacteria to flavour compound formation in dairy products. *Int. Dairy J.* 5, 877–903. doi: 10.1016/0958-6946(95)00037-2

Wang, J., Ren, L. Q., and Qian, K. (2020). Study on the changing trend of fish quality of salted carp in storage. *J. Fish. Res.* 42, 70–75. doi: 10.1111/jfbc.12683

Wang, Y., Li, F., Chen, J., Sun, Z., Wang, F., Wang, C., et al. (2021). High-throughput sequencing-based characterization of the predominant microbial community associated with characteristic flavor formation in jinhua ham. *Food Microbiol.* 94:103643. doi: 10.1016/j.fm.2020.103643

Xu, L., Guo, W., Liu, W., Fu, X., and Xu, Y. (2019). Metabolites analysis for cold-resistant yeast (Wickerhamomyces anomalus) strains own antioxidant activity on cold stored fish mince. *Food Chem.* 303:125368. doi: 10.1016/j.foodchem.2019.125368

Xu, X. X., Bi, S., Lao, F., Chen, F., Liao, X. J., and Wu, J. H. (2021). Comprehensive investigation on volatile and non-volatile metabolites in broccoli juices fermented by animal and plant-derived Pediococcus pentosaceus. *Food Chem.* 341:128118. doi: 10.1016/j.foodchem.2020.128118

Xu, Y., Wang, Y. Q., Coda, R., Säde, E., Tuomainen, P., Tenkanen, M., et al. (2017). In situ synthesis of exopolysaccharides by Leuconostoc spp. and Weissella spp. And their rheological impacts in fava bean flour. *Int. J. Food Microbiol.* 248, 63–71.

Yao, Y. P., Zhou, X. Y., Hadiatullah, H., Zhang, J., and Zhao, G. Z. (2020). Determination of microbial diversities and aroma characteristics of Beitang shrimp paste. *Food Chem.* 344:128695. doi: 10.1016/j.foodchem.2020.128695

Zhang, X., Wang, H., Li, M., Wu, N., and Xu, X. (2016). Near-freezing temperature storage (−2°C) for extension of shelf life of chilled yellow-feather broiler meat: a special breed in Asia. *J. Food Process. Pres.* 40, 340–347. doi: 10.1016/j.lwt.2015.07.039

Zhang, Y., Zhu, L., Dong, P., Liang, R., and Xin, L. (2018). Bio-protective potential of lactic acid bacteria: effect of *Lactobacillus sakei* and *Lactobacillus* curvatus on changes of the microbial community in vacuum-packaged chilled beef. *Asian Austral. J. Anim.* 31, 31–41. doi: 10.5713/ajas.17.0540

Zhao, C., Su, W., Mu, Y. C., Jiang, L., and Mu, Y. (2020). Correlations between microbiota with physicochemical properties and volatile flavor components in black glutinous rice wine fermentation. *Food Res. Int.* 138:109800. doi: 10.1016/j.foodres.2020.109800

Zheng, X. J., Liu, F., Li, K. X., Shi, X. W., Ni, Y. Q., Li, B. K., et al. (2018). Dynamic correlations between microbiota succession and flavor development involved in the ripening of Kazak artisanal cheese. *Food Res. Int.* 105, 733–742. doi: 10.1016/j.foodres.2017.12.007

Conflict of Interest: The authors declare that the research was conducted in the absence of any commercial or financial relationships that could be construed as a potential conflict of interest.

Publisher's Note: All claims expressed in this article are solely those of the authors and do not necessarily represent those of their affiliated organizations, or those of the publisher, the editors and the reviewers. Any product that may be evaluated in this article, or claim that may be made by its manufacturer, is not guaranteed or endorsed by the publisher.

frontiers in Microbiology

ORIGINAL RESEARCH
published: 16 December 2021
doi: 10.3389/fmicb.2021.602135

Solid-State Fermentation With *Aspergillus cristatus* Enhances the Protopanaxadiol- and Protopanaxatriol-Associated Skin Anti-aging Activity of *Panax notoginseng*

*Sunmin Lee[1,2], Chagam Koteswara Reddy[1], Jeoung Jin Ryu[3], Seoyeon Kyung[3], Yonghwan Lim[3], Myeong Sam Park[3], Seunghyun Kang[3] and Choong Hwan Lee[1]**

[1]*Department of Bioscience and Biotechnology, Konkuk University, Seoul, Seoul, South Korea,* [2]*Resource Analysis Research Laboratory, Korea Ginseng Corporation, Daejeon, South Korea,* [3]*COSMAX BTI R&I Center, Pangyo inno valley E, 255 Pangyo-ro, Bundang-gu, Seongnam-si, Gyeonggi-do, South Korea*

OPEN ACCESS

Edited by:
Jae-Hyuk Yu, University of Wisconsin-Madison, United States

Reviewed by:
Qing Kong, Ocean University of China, China
Kap-Hoon Han, Woosuk University, South Korea

***Correspondence:**
Choong Hwan Lee
chlee123@konkuk.ac.kr

Specialty section:
This article was submitted to Food Microbiology, a section of the journal Frontiers in Microbiology

Received: *02 September 2020*
Accepted: *17 November 2021*
Published: *16 December 2021*

Citation:
Lee S, Reddy CK, Ryu JJ, Kyung S, Lim Y, Park MS, Kang S and Lee CH (2021) Solid-State Fermentation With Aspergillus cristatus Enhances the Protopanaxadiol- and Protopanaxatriol-Associated Skin Anti-aging Activity of Panax notoginseng. Front. Microbiol. 12:602135. doi: 10.3389/fmicb.2021.602135

A metabolomics approach was used to profile metabolites of *Panax notoginseng* fermented with *Aspergillus cristatus* in two ways, liquid-state fermentation (LF-P) and solid-state fermentation (SSF-P) and examine metabolite markers representing antioxidant activity and skin anti-aging. Protopanaxadiol (PPD) and protopanaxatriol (PPT) contents were higher in SSF-P than in LF-P and showed a multiplicative increase over the fermentation period of four days. PPD and PPT levels also correlated with antioxidant and anti-aging effects in skin, based on the mRNA expression of dermal extracellular matrix components. In the bioactivity validation assays, PPD and PPT significantly improved the expression of type-I collagen, fibrillin-1, and elastin in human dermal fibroblasts from both young and old subjects; these were comparable with the effects of the SSF-P extracts. Overall, our results suggest that changes in the metabolites of *P. notoginseng* fermented with *A. cristatus* enhance the quality and availability of bioactive compounds associated with skin anti-aging.

Keywords: *Panax notoginseng*, *Aspergillus cristatus*, solid-state fermentation, mass spectrometry, protopanaxadiol, protopanaxatriol, skin anti-aging effect

INTRODUCTION

Ample research in recent years has been focused on microbiota-mediated biotransformation (Koppel et al., 2017). Immobilized edible fungi, such as *Aspergillus*, *Monascus*, *Rhizopus*, yeast, and *Mucor,* have also been utilized for biotransformation and efficient, natural bioactive metabolite production in industries (Zang et al., 2017). *Aspergillus cristatus* (synonym: *Eurotium cristatum*), termed as the "Golden Flowers Fungus" because of its yellow cleistothecium color, is a dominant fungal species utilized in the fermentation of Chinese brick tea (Ge et al., 2016; Ren et al., 2017). *A. cristatus* is an inoculum microbe for enhancing bioactivity and producing many

beneficial metabolites because of its various enzymes, such as amylase, α-glucosidase, and β-glucosidase (Lee et al., 2021).

Panax notoginseng is a perennial herb belonging to the genus *Panax* anomaly Araliaceae that is widely used in traditional Chinese medicine. *P. notoginseng* contains a variety of chemical components including saponins, flavonoids, sterols, polysaccharides, amino acids, fatty acids, and various trace elements (Li et al., 2020). Specifically, the root is beneficial to human health due to its anti-atherosclerotic, antioxidant, anti-inflammatory, anti-hyperlipidemic, hypoglycemic, neuroprotective, anti-coagulation, and anti-tumor properties (Wang et al., 2016). Polysaccharides from *P. notoginseng* roots are strongly protective against oxidative stress and have been shown to extend lifespan in *Caenorhabditis elegans* (Feng et al., 2019).

Panax species has been studied using several technologies, including whole-genome sequencing, and high-performance liquid chromatography-mass spectrometry (Yang et al., 2016; Chen et al., 2017; Zhang et al., 2017). Among the different chemical compounds found in *P. notoginseng,* triterpenoid saponins, such as ginsenosides and notoginsenosides, are the major bioactive constituents that are actively utilized for clinical applications. Ginsenosides can be transformed into bioactive compounds, such as ginsenosides Rg3, Rg5, and RK1, by steaming and heating (Kim et al., 2018). Moreover, fermentation of ginsenosides in the presence of intestinal microflora results in the formation of metabolites, such as compound K, ginsenoside Rh1, and PPT (Kim, 2012). Microorganisms not only transform the chemical structure of triterpenoids, but also alter their biological activities. However, the influence of microflora-mediated biotransformation on the bioactivity potential of *P. notoginseng* is not well-understood and requires further studies.

Metabolomics has emerged as a useful and important tool in a variety of research areas, including food science, agriculture, and microbiology. Metabolite profiling can be used for the simultaneous monitoring of all metabolites in a sample to facilitate nutrient analysis and detect the changes in enzyme levels, as well as microbial activities (Lee et al., 2016). In this study, a metabolomics approach was used to evaluate the biochemical events underlying solid-state fermentation of *P. notoginseng* (SSF-P) and investigate the metabolite biomarkers representing the antioxidant activity and skin anti-aging property of *P. notoginseng*.

MATERIALS AND METHODS

Chemicals and Reagents

Potato dextrose agar media (Difco) was purchased from Junsei Chemical Co., Ltd. (Tokyo, Japan). HPLC-grade water, acetonitrile, and methanol were obtained from Fisher Scientific Co., Ltd. (Pittsburgh, PA, United States). Analytical-grade sodium dihydrogen phosphate, sodium chloride, sodium hydroxide, sodium carbonate, disodium hydrogen phosphate, and diethylene glycol were purchased from Junsei Chemical Co., Ltd. (Tokyo, Japan). All remaining analytical-grade reagents and standard compounds used in this study were obtained from Sigma-Aldrich (St. Louis, MO, United States).

Fungal Fermentation of *P. notoginseng*

The fungal culture used in this study (*Aspergillus cristatus* Cosmax-GF) was obtained from Cosmax BTI R&I center (Seongnam, Korea). Before fermentation, raw *P. notoginseng* roots (300 g) were washed with deionized water, soaked for 2 h (45% water content) at room temperature, and autoclaved at 121°C for 60 min. Fermentation of *P. notoginseng* was performed in two ways: solid-state fermentation (SSF-P) and liquid fermentation (LF-P). *A. cristatus* incubated on potato dextrose agar media at 30°C and collected by treated with 0.01% Tween-20 using Neubauer chamber. The final fungal spore was adjusted to approximately 2.0×10^5 colony-forming units (CFUs)/ml. *A. cristatus* (2% v/w) was directly inoculated in *P. notoginseng* roots for solid-state fermentation. In case of liquid fermentation, we put *P. notoginseng* roots in the same amount of water and inoculated *A. cristatus* (2% v/w). After inoculation, the samples were incubated for 8 days at 30°C with 85% humidity. Samples were harvested every 48 h and immediately stored at −80°C until further analyses.

Preparation of Samples

The moisture content of fermented *P. notoginseng* was reduced to less than 12% by drying at 50°C and then pulverized using a mortar and pestle. For sample extraction, each pulverized sample (200 mg) was mixed with aqueous ethanol (1.0 ml, 80%) and sonicated for 60 min in an ultrasonic water bath. After sonication, the sample dispersion was centrifuged at 2370 *g* for 10 min at 4°C, and the supernatant was filtered using a 0.22-μm Milex® (Merck Millipore, Billerica, MA, United States). Then, the sample extracts were dried using a speed vacuum concentrator (Hanil, Seoul, Korea).

For gas chromatography time-of-flight mass spectrometry (GC-TOF-MS) analysis, each sample extract was subjected to two-staged derivatization. First, the oximation step was carried out by dissolving the sample extract with 50 μl of methoxyamine hydrochloride in pyridine (20 mg/ml) and incubated at 30°C for 90 min. Next, the silylation step was performed by adding 50 μl of N-Methyl-N-(trimethylsilyl) trifluoroacetamide (MSTFA) to the sample and the sample was incubated at 37°C for 30 min. Six replicates were analyzed for each sample.

For ultrahigh-performance liquid chromatography quadrupole orbitrap ion trap tandem mass spectrometry (UHPLC-Q-orbitrap-MS) analysis, each dried sample was dissolved in 80% ethanol and used. Six replicates were analyzed for each sample.

Instrumentation

GC-TOF-MS Analysis

GC-TOF-MS analysis for *P. notoginseng* sample extracts was carried out using an Agilent 7890A GC system (Agilent Technologies, Santa Clara, CA, United States) coupled with the Pegasus HT TOF-MS (Leco Corporation, St. Joseph, MI, United States) and an Agilent 7,693 autosampler. The samples were separated on an Agilent Rtx-5MS column (30 m length ×

0.25 mm i.d. × 0.25 μm film thickness; Restek Corp., Bellefonte, PA, United States), and the operational parameters were adapted from a study by Lee et al. (2020).

UHPLC-Q-orbitrap-MS/MS Analysis

UHPLC-Q-orbitrap-MS/MS analysis for *P. notoginseng* sample extracts was performed using a heated electrospray ionization source (Thermo Fischer Scientific Co., Ltd., CA, United States), equipped with a DIONEX UltiMate 3,000 UHPLC system (Ultimate 3,000 RS pump, Ultimate 3,000 RS column compartment, and Ultimate 3,000 RS autosampler; Dionex Corporation, CA, United States). Samples were separated on a hypersil gold C18 selectivity LC column (1.9 μm internal diameter, 50 mm × 2.1 mm; Thermo Fisher scientific Co., Ltd., CA, United States), and the operational parameters were adapted from a study by Lee et al. (2020).

Data Processing and Multivariate Statistical Analysis

The raw data files from GC-TOF-MS and UHPLC-Q-orbitrap-MS/MS were converted into the computable document form (cdf) format using LECO Chroma TOF software v.4.44 (Leco Co., CA, United States) and Thermo Xcalibur v.2.2 (Thermo Fisher Scientific, CA, United States), respectively. After conversion, the converted data files were processed using the MetAlign software package[1] to obtain a data matrix of accurate masses (*m/z*), normalized peak intensities, and retention times. Multivariate statistical analyses were performed using the SIMCA-P$^+$ 12.0 software (Umetrics, Umea, Sweden), to analyze the differences among the metabolomics data of fermented *P. notoginseng* samples. Further, both unsupervised principal component analysis (PCA) and supervised partial least squares discriminant analysis (PLS-DA) were performed on the metabolomic data sets. The metabolites were identified by comparing their retention time and mass fragment patterns with standard compounds, in-house library data, and references.

Bioactivity Assays

ABTS, DPPH, and FRAP assays were done to determine the *in vitro* antioxidant capacities of fermented *P. notoginseng* extracts (1 mg ml^{-1} methanol) by the method described by Lee et al. (2020). Trolox used as positive control in ABTS, DPPH, and FRAP assays. The results are presented as trolox equivalent antioxidant capacity (TEAC) concentration (mm) and as mean value of three analytical replicates.

ABTS Assay

The ABTS antioxidant assay was performed using a stock solution dissolving 7 mm ABTS in 2.45 mm potassium persulfate solution. For analysis, the ABTS solution was diluted in deionized water until an absorbance of 0.7 ± 0.02 (at 750 nm), measured using a spectrophotometer (Thermo Electron, Spectronic Genesys 6, Madison, WI, United States), was obtained. Each sample (20 μl) and diluted ABTS (180 μl) were added into a 96-well plate. The plate was incubated at room temperature for 6 min in the dark, and the absorbance of the samples was measured at 750 nm using a spectrophotometer.

DPPH Assay

For the DPPH assay, the fermented *P. notoginseng* extract (20 μl) was mixed with DPPH solution (180 μl, 0.2 mm in ethanol) in a 96 well plate, followed by incubation for 20 min at room temperature in the dark. The absorbance of the samples, which indicates the levels of DPPH free radicals, was measured at 515 nm using a spectrophotometer.

FRAP Assay

The FRAP assay was performed using a mixture of 10 mm 2,4,6-Tris (2-pyridyl)-s-triazine (TPTZ) solution in 40 mm HCl, 20 mm iron (III) chloride, and 300 mm acetate buffer at pH 3.6 (1:1:10, v:v:v). For the FRAP analysis, the fermented *P. notoginseng* extract (10 μl) was added to the FRAP reagent (300 μl), followed by incubation at room temperature for 6 min. The absorbance of the samples was measured at 570 nm using a spectrophotometer.

Total Phenol Content Assay

The total phenol content (TPC) assay of fermented *P. notoginseng* extracts was performed *via* two steps. First, 20 μl of fermented *P. notoginseng* extract in 80% methanol (1 mg ml^{-1}) was added to 100 μl of 0.2 N Folin-Ciocalteu's phenol reagent, followed by incubation for 5 min at room temperature in the dark. In the next step, 80 μl of 7.5% Na_2CO_3 was added to the samples, and the resulting reaction mixtures were incubated for 60 min. Finally, the absorbance of the samples was measured at 750 nm using a spectrophotometer. The assay results were expressed in terms of the gallic acid equivalent of the activity (μg ml^{-1}) and as the mean value of three analytical replicates.

Cell Cultures

Primary human dermal fibroblast (HDFs) from young (20 y) and old (over 65 y) subjects were purchased from PromoCell (Heidelberg, Germany). The related culture media and DetachKit were also obtained from PromoCell. The HDFs were grown in specific fibroblast medium (Fibroblast Growth Medium 2, PromoCell, Cat no. C-23020) enriched with Supplement Mix/ Fibroblast Growth Medium 2 (PromoCell, Cat no. C-39325) and 1% Penicillin-Streptomycin (PS) at 37°C in a 5% CO_2 incubator. When cultured HDFs reached approximately 80% confluence, they were subsequently cultured or seeded into the appropriate wells for the different treatments.

Real-Time Polymerase Chain Reaction

Total RNA from cell pellets was isolated using TRIzol reagent and quantified using a spectrophotometer. The cDNA was synthesized in a total reaction volume of 20 μl; the reaction mixture contained 2 μg of total RNA, oligo (dT), and reverse transcription premix under the following reaction conditions:

[1]http://www.metalign.nl

45°C for 45 min, followed by 95°C for 5 min. Gene expression was quantified using RT-PCR, and the resultant data were analyzed using the StepOne Plus™ system software (Applied Biosystems, Foster City, CA, United States). RT-PCR amplifications were performed using SYBR Green PCR Master Mix with premixed ROX (Applied Biosystems, Foster City, CA, United States) and primers (Bioneer, Daejeon, Korea) in an ABI 7300 instrument according to the manufacturer's protocol. The reaction conditions were as follows: initiation at 95°C for 10 min, followed by cycling conditions of 95°C for 15 s, 60°C for 30 s, and 72°C for 30 s for 40 cycles. Beta-actin was used as an internal control.

RESULTS

Comparison of the Metabolomes and Bioactivities of *P. notoginseng* Following Liquid Fermentation and Solid-State Fermentation

Metabolite profiling was performed on *P. notoginseng* following LF-P and SSF-P, using GC-TOF-MS and UHPLC-Q-orbitrap-MS combined with multivariate analysis, to determine the metabolites associated with the PCA score plots based on the GC-TOF-MS (**Figure 1A**) and UHPLC-Q-orbitrap-MS (**Figure 1B**; **Supplementary Figure 1**) data sets showed that the different types of fermentation process lead to changes in metabolite distributions of *P. notoginseng*. Among LF-P and SSF-P, the PCA score plots based on GC-TOF-MS and UHPLC-Q-orbitrap-MS analysis were accounted for 61.4% of the total variability (PC1, 39.4%; PC2, 22.0%) and 34.3% of total variability (PC1, 22.8% PC2, 11.5%), respectively. In the next step, considering the differential impacts of the fermentation environment on *P. notoginseng* metabolite distributions, we examined the bioactivities associated with each fermentation procedure. Our results, based on the ABTS, DPPH, FRAP, and TPC assays, showed that the bioactivities following SSF-P were higher than those in case of LF-P on the fourth day of fermentation (**Figures 1C–F**).

Temporal Metabolomes and Bioactivities of *P. notoginseng* Following Solid-State Fermentation

Temporal Metabolomes of *P. notoginseng* Following Solid-State Fermentation

A multivariate statistical analysis was carried out using the GC-TOF-MS and UHPLC-Q-orbitrap-MS data sets to investigate the temporal metabolomes following SSF-P (**Figure 2**). The PCA score plots derived from the GC-TOF-MS (**Figure 2A**) and UHPLC-Q-orbitrap-MS (**Figure 2B**), data sets for the extracts of *P. notoginseng* fermented under different fermentation periods exhibited a clustered pattern. The PCA score plot obtained from GC-TOF-MS analysis represented a total variability of 39.9% (PC1, 31.0%; PC2, 8.9%; **Figure 2A**), whereas the PCA score plots based on the UHPLC-Q-orbitrap-MS data sets (**Figure 2B**) represented a total variability of 37.9% (PC1, 29.5%; PC2, 8.4%). PLS-DA models with variable importance in projection values (VIP > 0.7 values and *value of p* <0.05) were derived from the GC-TOF-MS and UHPLC-Q-orbitrap-MS data sets, respectively. A total of 36 significant discriminant metabolites, including 22 primary and 14 secondary metabolites, were selected for fermented *P. notoginseng* on the basis of the PLS1 and PLS2 components. Overall, three amino acids (GABA, glutamic acid, and pyroglutamic acid), three fatty acids (linoleic acid, oleic acid, and stearic acid), six organic acids (citric acid, fumaric acid, malonic acid, malic acid, gluconic acid, and succinic acid), ten sugar and sugar alcohols (adonitol, erythritol, glycerol, glucuronic acid, glyceryl-glycoside, myo-inositol, ribose, sorbitol, sucrose, and xylose), and 14 triterpenoids (ginsenoside-Rb1, Rb2, Rc, Rd., Rf, Rg2, Rg3, Rh1, glucoginsenoside-Rf, notoginsenoside-R1, -R2, and -R4, protopanaxadiol (PPD), and PPT) were putatively identified. The peak area of identified metabolites was represented by the fold change obtained following normalization to the average fermentation time for each metabolite. We observed a common trend, dependent on the fermentation time, among the metabolic data sets of the extracts of *P. notoginseng* fermented using the two different methods.

Table 1 shows the relative distributions of primary and secondary metabolites in *P. notoginseng*. Specifically, following SSF-P, the levels of many fatty acids (linoleic acid, oleic acid, and stearic acid) showed an increasing trend over the fermentation period. The contents of most sugars and sugar alcohols (adonitol, erythritol, glycerol, glucuronic acid, glyceryl-glycoside, ribose, sorbitol, and xylose) also increased significantly, whereas sucrose levels reduced significantly. Among the selected secondary metabolites, the levels of ginsenosides, including ginsenoside-Rb1, Rb2, Rc, Rd., Rf, ginsenoside-Rg2, Rh1, and notoginsenoside-R1, -R2, and -R4 showed a decreasing trend, whereas the levels of ginsenoside-Rg3 and glucoginsenoside-Rf showed an increasing trend. Finally, the levels of PPD and PPT significantly increased during the fermentation period.

Antioxidant Activities of *P. notoginseng* Following Solid-State Fermentation and Effects of Extracts Obtained Following SSF-P on Skin Aging

Considering the varying impact of the solid-state fermentation time on *P. notoginseng* metabolites, we analyzed antioxidant activities over the fermentation period using the DPPH, ABTS, FRAP, and TPC assays. All these assays revealed that the bioactivities increased significantly with increasing fermentation time (**Supplementary Figure 2**). The effects of fermented *P. notoginseng* on skin aging were investigated using HDFs from subjects belonging to two age groups, the twenties (young) and sixties (old), for investigating the intrinsic aging states of the dermis. The effects of SSF-P extracts on skin aging-associated factors, such as type-I collagen (COLA1), fibrillin-1 (FBN1), and elastin (ELN), were monitored. As shown in **Figure 3**, SSF-P extracts significantly increased the expression of COLA1, FBN1, and ELN in HDFs obtained from both young and old subjects.

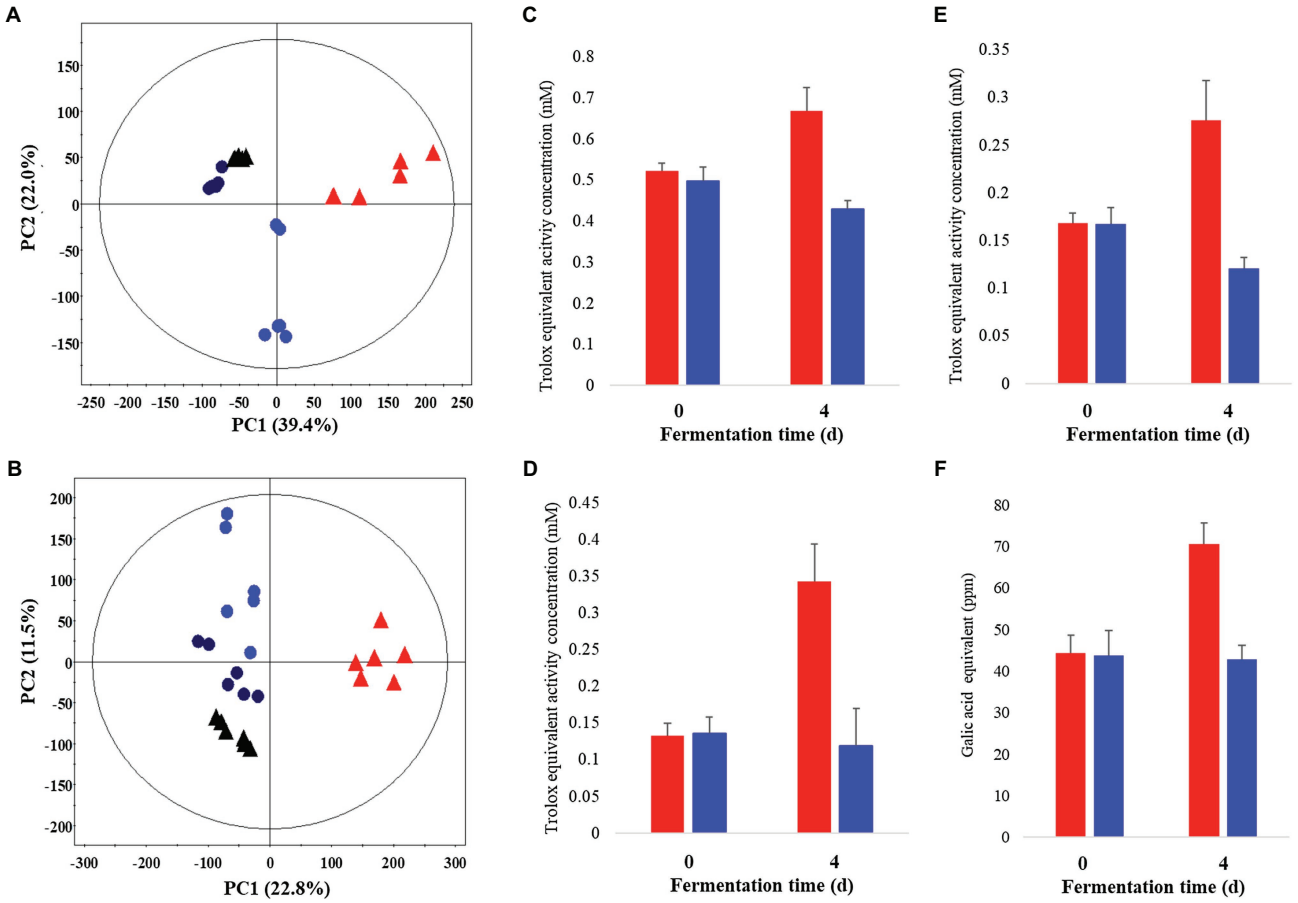

FIGURE 1 | Principal component analysis (PCA) score plot derived from GC-TOF-MS **(A)** and UHPLC-Q-orbitrap-MS **(B)** data sets. Comparison of the bioactivities of *P. notoginseng* during SSF-P and LF-P **(C)** ABTS, **(D)** DPPH, **(E)** FRAP, **(F)** Total phenol contents. ▲, black: day 0 of solid-state fermentation (SSF-P); ▲, red: day 4 of SSF-P; ●, black: day 0 of liquid fermentation (LF-P); ●, blue: day 4 of liquid fermentation (LF-P).

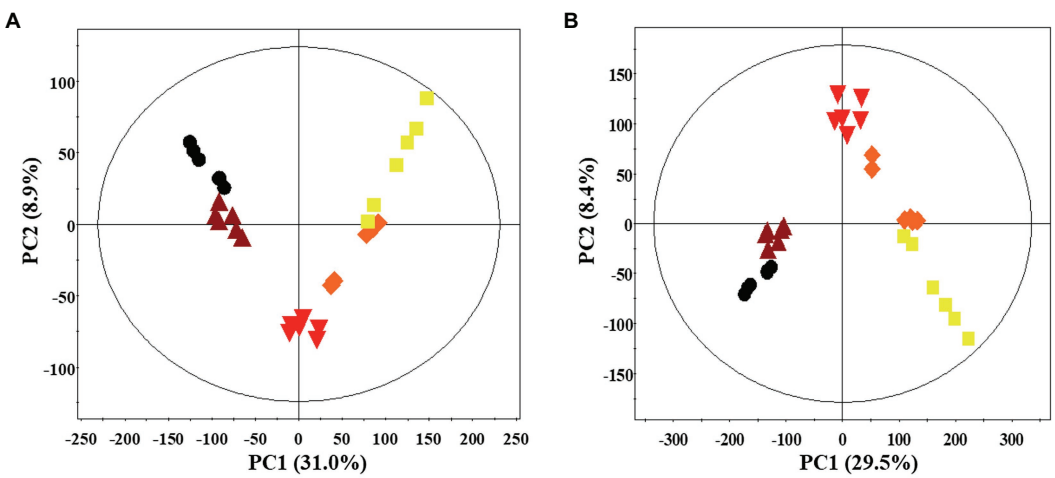

FIGURE 2 | Principal component analysis (PCA) score plot of *P. notoginseng* during SSF-P derived from the GC-TOF-MS **(A)** and UHPLC-Q-orbitrap-MS **(B)** data sets. ●, day 0; ▲, 2 d; ▼, 4 d; ♦, 6 d; ■, 8 d.

TABLE 1 | Relative distributions of metabolites analyzed by GC-TOF-MS and UHPLC-Q-orbitrap-MS in SSF-P (solid-state fermentation *P. notoginseng*) fermented with *A. cristatus.*

	Fermentation time (d)				
	0	**2**	**4**	**6**	**8**
Amino acids					
GABA	1.19	1.19	0.97	0.92	0.74
Glutamic acid	0.71	0.88	1.15	1.23	1.02
Pyroglutamic acid	1.05	1.09	0.99	1.01	0.86
Fatty acids					
Linoleic acid	0.92	1.00	1.02	1.04	1.01
Oleic acid	0.81	0.91	0.99	1.15	1.14
Stearic acid	0.96	1.01	0.96	1.03	1.03
Organic acids					
Citric acid	1.04	1.05	1.05	1.01	0.85
Fumaric acid	0.81	0.84	1.05	1.17	1.13
Malonic acid	1.06	1.07	1.02	1.01	0.84
Malic acid	0.99	1.00	1.01	1.02	0.98
Gluconic acid	1.07	1.04	1.00	0.96	0.94
Succinic acid	0.93	0.97	1.08	1.10	0.92
Sugar & sugar alcohols					
Adonitol	0.93	0.93	1.02	1.00	1.12
Erythritol	0.66	0.75	1.11	1.20	1.29
Glycerol	0.83	0.97	1.04	1.07	1.08
Glucuronic acid	0.80	0.84	1.09	1.12	1.16
Glyceryl-glycoside	0.74	0.82	0.99	1.15	1.30
Myo-inositol	1.02	1.03	0.99	0.98	0.97
Ribose	0.78	0.92	1.12	1.09	1.08
Sorbitol	0.65	0.77	1.17	1.20	1.22
Sucrose	1.17	1.16	1.01	0.90	0.76
Xylose	0.80	0.82	1.04	1.13	1.22
Terpenoids					
Ginsenoside-Rb1	1.08	1.05	1.02	0.90	0.94
Ginsenoside-Rb2	1.32	1.09	1.07	0.89	0.63
Ginsenoside-Rc	1.41	1.05	0.96	0.82	0.76
Ginsenoside-Rd	1.12	1.02	1.03	0.90	0.93
Ginsenoside-Rf	1.21	1.10	1.03	0.86	0.80
Ginsenoside Rg2	1.15	0.99	1.08	0.91	0.87
Ginsenoside Rg3	0.81	0.53	0.89	1.60	1.17
Ginsenoside- Rh1	1.20	1.06	1.03	0.83	0.88
Glucoginsenoside-Rf	0.86	0.76	0.91	1.12	1.36
Notoginsenoside-R1	1.05	1.05	0.99	1.00	0.91
Notoginsenoside-R2	0.96	1.13	1.05	0.96	0.90
Notoginsenoside-R4	1.37	1.15	0.90	0.91	0.68
Protopanaxadiol	0.05	0.05	1.61	1.64	1.65
Protopanaxatriol	0.00	1.24	1.32	1.18	1.25

The values of the table for metabolite levels represent their average fold change values.

Correlation Between Bioactivities and Significant Discriminant Metabolites

The bioactivity of *P. notoginseng* SSF-P extracts is mainly due to its distinct metabolite composition. The spatial distributions of these compounds among different phylogenic groups and plant components are remarkably discriminant.

A Pearson correlation analysis tentatively identified compounds that maximally contributed to the bioactivities of the extracts obtained following SSF-P using *A. cristatus*. The correlation network was evaluated for variables with positive Pearson correlation values (**Figure 4**). Citric acid, glutamic acid, linoleic acid, malic acid, PPD, PPT, ribose, and succinic acid were correlated with COLA1 levels in HDFs from young subjects, while adonitol, PPD, PPT, and ribose correlated with COLA1 levels in HDFs from old subjects. Similarly, citric acid, ginsenoside-Rb2, ginsenoside-Rd, notoginsenoside-R1, and notoginsenoside-R2 correlated with FBN1 levels in HDFs from young subjects, whereas adonitol, glucuronic acid, glycerol, glyceryl-glycoside, PPD, PPT, ribose, sorbitol, and xylose correlated with FBN1 levels in HDFs from old subjects. Finally, glucuronic acid, glycerol, linoleic acid, oleic acid, PPD, PPT, ribose, succinic acid, and sorbitol correlated with ELN levels in HDFs from young subjects, while glutamic acid, glycerol, PPD, PPT,

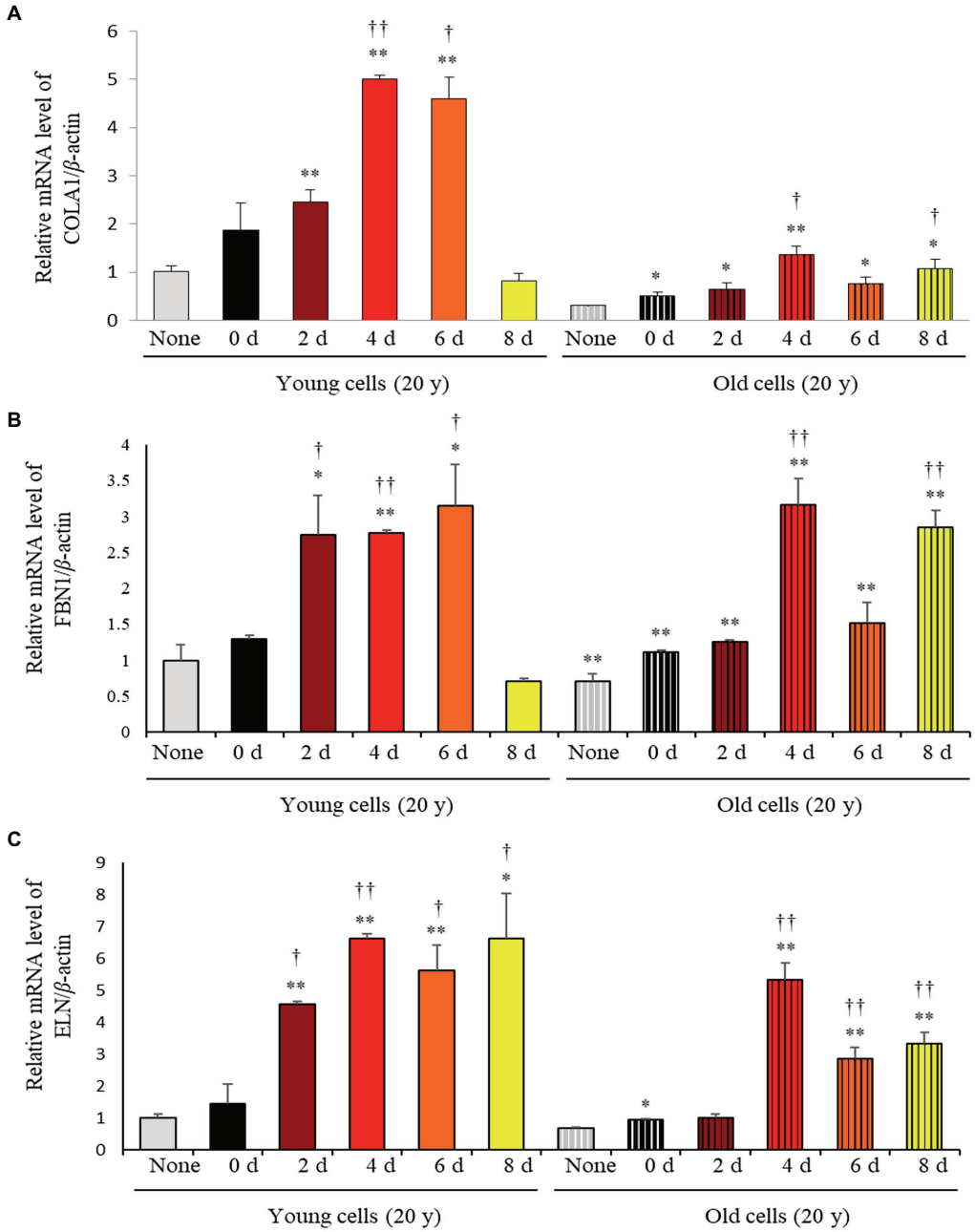

FIGURE 3 | Relative mRNA expression levels of **(A)** COLA1, **(B)** FBN1, and **(C)** ELN in primary normal human dermal fibroblasts (HDFS) incubated with *P. notoginseng* during SSF fermentation. $^{*}p<0.05$, $^{**}p<0.01$ vs. None (Young & old), $^{\dagger}p<0.05$, $^{\dagger\dagger}p<0.0$ vs. SSF-P day (young & old).

ribose, sorbitol, and succinic acid correlated with ELN levels in HDFs from old subjects. PPD, PPT, glucoginsenoside-Rf, and ginsenoside-Rg3 showed positive correlations with the bioactivities measured using the ABTS, DPPH, FRAP, and TPC analyses. Intriguingly, PPD and PPT expressed strong positive correlations with bioactivity measured in all the assays performed and cell-based assays aimed at evaluating skin aging.

Bioactivity Validation of Proposed Metabolites

Based on the results of metabolite profiling and correlation analysis, we hypothesized that the two metabolites PPD and PPT are bioactive components with strong skin anti-aging activity. To confirm the proposed hypothesis, we performed bioactivity validation assays using commercial standards for PPD, PPT, and epigallocatechin gallate (EGCG; used as positive

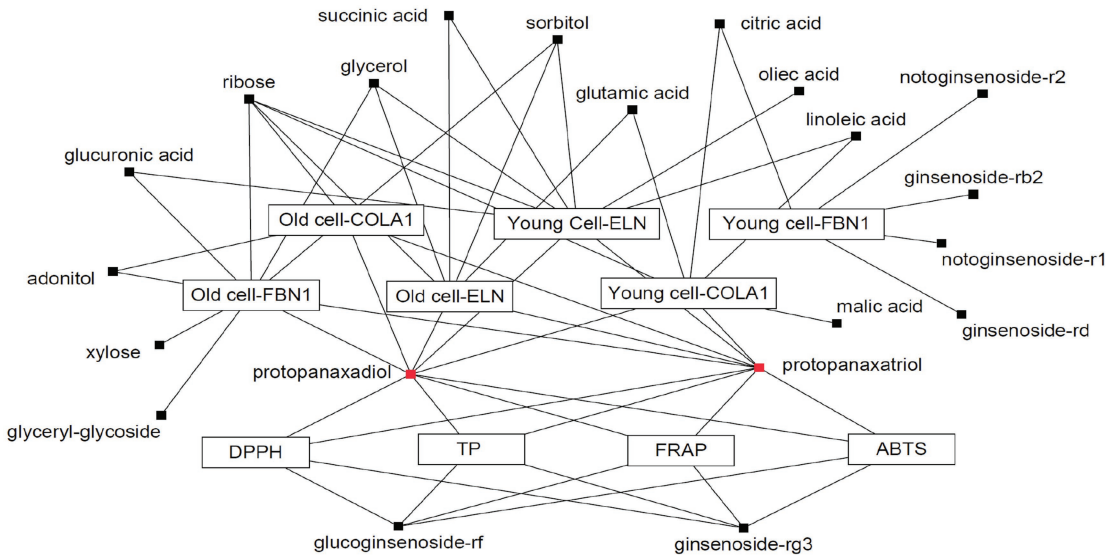

FIGURE 4 | Correlation network between metabolites and bioassays. Box: metabolites; Eclipse: bioassay.

control; **Figure 5**). The EC50 values of standard compounds could not be determined for some bioactivity assays (ABTS, DPPH, and FRAP) due to aggregation of reaction mixture. However, the results of the bioactivity validation analysis showed that both PPD and PPT significantly improved the expression of COLA1, FBN1, and ELN in HDFs from both young and old subjects; these findings were comparable with the effects observed for EGCG and *P. notoginseng* extracts obtained on the 8th day of SSF-P.

DISCUSSION

In this study, untargeted metabolomics was used for evaluating the fermentation of *P. notoginseng* roots with *A. cristatus*. The chemical composition of *P. notoginseng* roots varied significantly over the fermentation period, possibly due to several factors, including the differences in the quantity or activity of enzymes released from *A. cristatus* resulting from the increasing fermentation time or the fermentation procedure. Previously, Son et al. (2018) reported differences in the metabolite levels and bioactivities between solid-state fermentation and submerged fermentation with *Aspergillus oryzae*. In this study, we primarily focused on solid-state fermentation, as higher bioactivity was observed following SSF-P than that following LF-P, along with a distinctive pattern shown by the samples in the PCA score plots. Additionally, numerous studies in the recent years have focused on solid-state fermentation and its applications, including production of enzymes, biomolecules, phenolics, organic compounds, and aromas for food fermentation, pharmaceutical, and cosmetic industries (Soccol et al., 2017).

The multivariate analysis of SSF-P data derived from GC-TOF-MS and UHPLC-Q-orbitrap-MS exhibited a central tendency with increased bioactivities based on the period of fermentation. The levels of PPD-type ginsenosides (Rb1, Rb2, Rc, and Rd), PPT-type ginsenosides (notoginsenoside R1) decreased, whereas the levels of PPD and PPT increased with increasing fermentation period. Using microbial enzymes for the conversion of major ginsenosides in *P. notoginseng* to bioactive components is valuable in the development of ginseng-based products (Wang et al., 2011; Zang et al., 2017). Liu et al. (2010) described that *Aspergillus niger* can convert ginsenoside-Rf into PPT by glycosidase, and the β-glucosidase secreted from *Aspergillus* plays a key role in the hydrolysis of biomass (Sørensen et al., 2011). We have also confirmed the β-glucosidase activity of *A. cristatus* using an enzyme kit (data not shown).

Antioxidant activities, as evaluated by the ABTS, DPPH, FRAP, and TPC assays, as well as mRNA expression levels of genes, such as COLA1, FBN1, and ELN, continuously increased over the period of fermentation. Several plants contain antioxidant compounds, which are involved in the scavenging of free radicals and eliminating the byproducts of metabolism to overcome the typical effects of aging (Mukherjee et al., 2011). It is reported that American ginseng root and berry, as well as Korean ginseng leaf extract, possess antioxidant properties (Wang et al., 2009). Thus, the increase in the levels of antioxidant compounds observed following the SSF-P in this study could prove to be useful in enhancing the nutritional and functional value of *P. notoginseng*. To explore the protective effects of SSF-P on skin aging, the expression levels of aging biomarkers in HDFs exposed to SSF-P extracts were measured by semi-quantitative PCR. Wrinkles, a major feature of skin aging, are primarily a result of molecular modifications of the dermis (Tang et al., 2017), and the extracellular matrix, which consists of collagen, elastin fibers, and fibrillin, is majorly involved in the process of cutaneous aging (Jung et al., 1997).

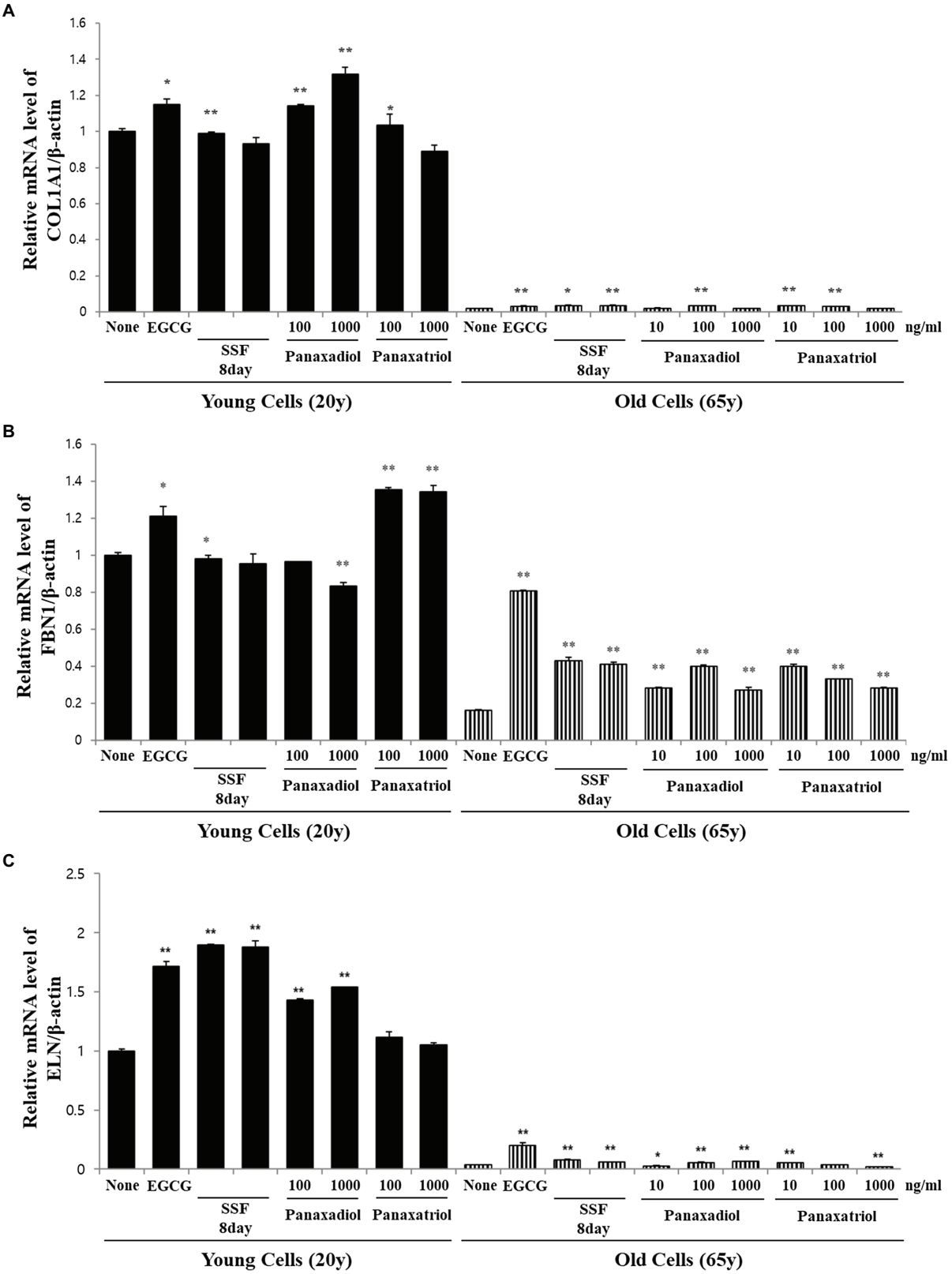

FIGURE 5 | Relative mRNA expression levels of **(A)** COLA1, **(B)** FBN1, and **(C)** ELN in primary normal HDFS treated with protopanaxadiol and protopanaxatriol. $^{*}p<0.05$, $^{**}p<0.01$ vs. None.

Correlation studies and validation assays were performed to identify the bioactivity and efficacy of the identified biomarkers during the fermentation period (**Figure 4**). Among the 36 discriminant metabolites, four saponins, including glucoginsenoside-Rf, ginsenoside Rg3, PPD, and PPT, were positively correlated with antioxidant activity. Ginsenosides represent one of the major bioactive components in white ginseng; they possess powerful antioxidant effects and high bioactivities (Lim et al., 2010). Of the saponins, six metabolites, including notoginsenoside-R2, ginsenoside-Rb2, notoginsenoside-R1, ginsenoside-Rd, PPT, and PPD, were correlated with skin aging effects. Previous studies have suggested that red ginseng extracts have beneficial effects on photoaging and reduce facial wrinkles by improving type-I procollagen gene and protein expression (Cho et al., 2009). Ginsenoside-Rb1, a metabolite of *P. notoginseng*, has anti-aging and hydrating effects and is used in cosmetic products for skin protection (Kim et al., 2018). In this study, we observed that PPD and PPT were positively correlated with both antioxidant activity (measured *via* the ABTS, DPPH, FRAP, and TPC analyses), as well as skin anti-aging effects (based on the increased mRNA expression of COLA1, ELN, and FBN1). Overall, our study identified biomarkers correlated with the antioxidant and anti-aging effects of *P. notoginseng* extracts obtained following SSF-P using *A. cristatus*, based on metabolic bioconversions and the resulting metabolite levels. In the present study, metabolite profiling and integrated bioassays were used to evaluate the biochemical activities characterizing the SSF-P with *A. cristatus* and identify potential metabolite biomarkers for antioxidant activity and skin anti-aging effects. The antioxidant activity and skin anti-aging effects following SSF-P were observed to increase over the fermentation period. In conclusion, we propose protopanaxadiol and protopanaxatriol as biomarkers for bioassays to study *P. notoginseng* fermentation with *A. cristatus*. Thus, our results provide a direction for the efficient fermentation of *P. notoginseng* with *A. cristatus* aimed at the production of bioactive compounds.

DATA AVAILABILITY STATEMENT

The original contributions presented in the study are included in the article/**Supplementary Material**, and further inquiries can be directed to the corresponding author.

AUTHOR CONTRIBUTIONS

CL: conceptualization and supervision. SL: methodology, software, and writing – original draft preparation. CR: validation. JR: investigation. JR, YL, MP, and SK: resources. SK: data curation and project administration. CR and CL: writing – review and editing. SL and SK: visualization. All authors have read and agreed to the published version of the manuscript.

FUNDING

This study was supported by Traditional Culture Convergence Research Program through the National Research Foundation of Korea (NRF) funded by the Ministry of Science, ICT & Future Planning (NRF-2017M3C1B5019303) and the Basic Research Lab Program (Grant no. 2020R1A4A1018648), through the National Research Foundation grant funded by the Ministry of Science and ICT, Republic of Korea.

SUPPLEMENTARY MATERIAL

The Supplementary Material for this article can be found online at: https://www.frontiersin.org/articles/10.3389/fmicb.2021.602135/full#supplementary-material

REFERENCES

Chen, W., Kui, L., Zhang, G., Zhu, S., Zhang, J., Wang, X., et al. (2017). Whole-genome sequencing and analysis of the Chinese herbal plant *Panax notoginseng*. *Mol. Plant* 10, 899–902. doi: 10.1016/j.molp.2017.02.010

Cho, S., Won, C.-H., Lee, D. H., Lee, M.-J., Lee, S., So, S.-H., et al. (2009). Red ginseng root extract mixed with Torilus fructus and Corni fructus improves facial wrinkles and increases type I procollagen synthesis in human skin: a randomized, double-blind, placebo-controlled study. *J. Med. Food* 12, 1252–1259. doi: 10.1089/jmf.2008.1390

Feng, S., Cheng, H., Xu, Z., Feng, S., Yuan, M., Huang, Y., et al. (2019). Antioxidant and anti-aging activities and structural elucidation of polysaccharides from *Panax notoginseng* root. *Process Biochem.* 78, 189–199. doi: 10.1016/j.procbio.2019.01.007

Ge, Y., Wang, Y., Liu, Y., Tan, Y., Ren, X., Zhang, X., et al. (2016). Comparative genomic and transcriptomic analyses of the Fuzhuan brick tea-fermentation fungus *aspergillus cristatus*. *BMC Genomics* 17:428. doi: 10.1186/s12864-016-2637-y

Jung, J.-W., Cha, S.-H., Lee, S.-C., Chun, I.-K., and Kim, Y.-P. (1997). Age-related changes of water content in the rat skin. *J. Dermatol. Sci.* 14, 12–19. doi: 10.1016/S0923-1811(96)00542-7

Kim, D.-H. (2012). Chemical diversity of *Panax ginseng*, *Panax quinquifolium*, and *Panax notoginseng*. *J. Ginseng Res.* 36, 1–15. doi: 10.5142/jgr.2012.36.1.1

Kim, E., Kim, D., Yoo, S., Hong, Y. H., Han, S. Y., Jeong, S., et al. (2018). The skin protective effects of compound K, a metabolite of ginsenoside Rb1 from *Panax ginseng*. *J. Ginseng Res.* 42, 218–224. doi: 10.1016/j.jgr.2017.03.007

Koppel, N., Rekdal, V. M., and Balskus, E. P. (2017). Chemical transformation of xenobiotics by the human gut microbiota. *Science* 356:eaag2770. doi: 10.1126/science.aag2770

Lee, D. E., Lee, S., Jang, E. S., Shin, H. W., Moon, B. S., and Lee, C. H. (2016). Metabolomic profiles of *aspergillus oryzae* and *bacillus amyloliquefaciens* during rice koji fermentation. *Molecules* 21:773. doi: 10.3390/molecules21060773

Lee, H., Lee, S., Kyung, S., Ryu, J., Kang, S., Park, M., et al. (2021). Metabolite profiling and anti-aging activity of Rice Koji fermented with *aspergillus oryzae* and *aspergillus cristatus*: A comparative study. *Meta* 11:524. doi: 10.3390/metabo11080524

Lee, S., Oh, D.-G., Singh, D., Lee, J. S., Lee, S., and Lee, C. H. (2020). Exploring the metabolomic diversity of plant species across spatial (leaf and stem) components and phylogenic groups. *BMC Plant Biol.* 20:39. doi: 10.1186/s12870-019-2231-y

Li, C., Qin, Y., Yang, Q., You, J., Liu, Z., Han, J., et al. (2020). Multivariate quantitative analysis of quality trend based on non-volatile characteristic components in different *Panax notoginseng* samples using HPLC. *J. Pharm. Biomed. Anal.* 182:113127. doi: 10.1016/j.jpba.2020.113127

Lim, S.-I., Cho, C.-W., Choi, U.-K., and Kim, Y.-C. (2010). Antioxidant activity and ginsenoside pattern of fermented white ginseng. *J. Ginseng Res.* 34, 168–174. doi: 10.5142/jgr.2010.34.3.168

Liu, L., Gu, L. J., Zhang, D. L., Wang, Z., Wang, C. Y., Li, Z., et al. (2010). Microbial conversion of rare ginsenoside Rf to 20(S)-protopanaxatriol by *aspergillus Niger*. *Biosci. Biotechnol. Biochem.* 74, 96–100. doi: 10.1271/bbb.90596

Mukherjee, P. K., Maity, N., Nema, N. K., and Sarkar, B. K. (2011). Bioactive compounds from natural resources against skin aging. *Phytomedicine* 19, 64–73. doi: 10.1016/j.phymed.2011.10.003

Ren, C., Tan, Y., Ren, X., Liu, Y., and Liu, Z. (2017). Metabolomics reveals changes in metabolite concentrations and correlations during sexual development of *Eurotium cristatum* (synonym: *aspergillus cristatus*). *Mycosphere* 80, 1626–1639. doi: 10.5943/mycosphere/8/10/3

Soccol, C. R., da Costa, E. S. F., Letti, L. A. J., Karp, S. G., Woiciechowski, A. L., and de Souza Vandenberghe, L. P. (2017). Recent developments and innovations in solid state fermentation. *Biotechnol. Res. Innov.* 1, 52–71. doi: 10.1016/j.biori.2017.01.002

Son, S. Y., Lee, S., Singh, D., Lee, N.-R., Lee, D.-Y., and Lee, C. H. (2018). Comprehensive secondary metabolite profiling toward delineating the solid and submerged-state fermentation of *aspergillus oryzae* KCCM 12698. *Front. Microbiol.* 9:1076. doi: 10.3389/fmicb.2018.01076

Sørensen, A., Lübeck, P. S., Lübeck, M., Teller, P. J., and Ahring, B. K. (2011). β-Glucosidases from a new species can substitute commercial β-glucosidases for saccharification of lignocellulosic biomass. *Can. J. Microbiol.* 57, 638–650. doi: 10.1139/w11-052

Tang, R., Samouillan, V., Dandurand, J., Lacabanne, C., Lacoste-Ferre, M.-H., Bogdanowicz, P., et al. (2017). Identification of ageing biomarkers in human dermis biopsies by thermal analysis (DSC) combined with Fourier transform infrared spectroscopy (FTIR/ATR). *Skin Res. Technol.* 23, 573–580. doi: 10.1111/srt.12373

Wang, T., Guo, R., Zhou, G., Zhou, X., Kou, Z., Sui, F., et al. (2016). Traditional uses, botany, phytochemistry, pharmacology and toxicology of *Panax notoginseng* (Burk.) FH Chen: A review. *J. Ethnopharmacol.* 188, 234–258. doi: 10.1016/j.jep.2016.05.005

Wang, H., Peng, D., and Xie, J. (2009). Ginseng leaf-stem: bioactive constituents and pharmacological functions. *Chin. Med.* 4:20. doi: 10.1186/1749-8546-4-20

Wang, D. M., Yu, H. S., Song, J. G., Xu, Y. F., Liu, C. Y., and Jin, F. X. (2011). A novel ginsenosidase from an *aspergillus* strain hydrolyzing 6-O-multi-glycosides of protopanaxatriol-type ginsenosides, named ginsenosidase type IV. *J. Microbiol. Biotechnol.* 210, 1057–1063. doi: 10.4014/jmb.1101.01044

Yang, W., Qiao, X., Li, K., Fan, J., Bo, T., Guo, D.-A., et al. (2016). Identification and differentiation of *Panax ginseng*, *Panax quinquefolium*, and *Panax notoginseng* by monitoring multiple diagnostic chemical markers. *Acta Pharm. Sin. B* 6, 568–575. doi: 10.1016/j.apsb.2016.05.005

Zang, Y., Guo, N., Jiao, J., Wang, X., Gai, Q., Xu, W., et al. (2017). Application of magnetically immobilized edible fungus for the biotransformation of *Panax notoginseng* saponin Rb1 to Rd and Rg3. *J. Chromatogr. B* 1061, 306–313. doi: 10.1016/j.jchromb.2017.07.038

Zhang, D., Li, W., Xia, E.-H., Zhang, Q.-J., Liu, Y., Zhang, Y., et al. (2017). The medicinal herb *Panax notoginseng* genome provides insights into ginsenoside biosynthesis and genome evolution. *Mol. Plant* 10, 903–907. doi: 10.1016/j.molp.2017.02.011

Conflict of Interest: The authors declare that the research was conducted in the absence of any commercial or financial relationships that could be construed as a potential conflict of interest.

Publisher's Note: All claims expressed in this article are solely those of the authors and do not necessarily represent those of their affiliated organizations, or those of the publisher, the editors and the reviewers. Any product that may be evaluated in this article, or claim that may be made by its manufacturer, is not guaranteed or endorsed by the publisher.

frontiers | Frontiers in Microbiology

REVIEW
published: 08 April 2022
doi: 10.3389/fmicb.2021.664850

Interaction and Application of Molds and Yeasts in Chinese Fermented Foods

Qilin Yang[1], Hongli Yao[1], Shuangping Liu[1,2,3] and Jian Mao[1,2,3]**

[1] National Engineering Research Center of Cereal Fermentation and Food Biomanufacturing, Jiangnan University, Wuxi, China, [2] Jiangnan University (Shaoxing) Industrial Technology Research Institute, Shaoxing, China, [3] National Engineering Research Center of Huangjiu, Zhejiang Guyuelongshan Shaoxing Wine Co., Ltd., Shaoxing, China

Fermentation is an ancient food preservation and processing technology with a long history of thousands of years, that is still practiced all over the world. Fermented foods are usually defined as foods or beverages made by controlling the growth of microorganisms and the transformation of raw and auxiliary food components, which provide the human body with many beneficial nutrients or health factors. As fungus widely used in traditional Chinese fermented foods, molds and yeasts play an irreplaceable role in the formation of flavor substances and the production of functional components in fermented foods. The research progress of molds and yeasts in traditional Chinese fermented foods from traditional to modern is reviewed, including the research on the diversity, and population structure of molds and yeasts in fermented foods. The interaction between fermenting mold and yeast and the latest research results and application development prospects of related industries were discussed.

Keywords: fermented food, molds, yeasts, application, interaction

OPEN ACCESS

Edited by:
Wanping Chen,
University of Göttingen, Germany

Reviewed by:
Hiroshi Kitagaki,
Saga University, Japan
Lixin Luo,
South China University of Technology, China

****Correspondence:***
Shuangping Liu
liushuangping668@126.com
Jian Mao
maojian@jiangnan.edu.cn

Specialty section:
This article was submitted to Food Microbiology, a section of the journal Frontiers in Microbiology

Received: *06 February 2021*
Accepted: *28 December 2021*
Published: *08 April 2022*

Citation:
Yang Q, Yao H, Liu S and Mao J (2022) Interaction and Application of Molds and Yeasts in Chinese Fermented Foods. Front. Microbiol. 12:664850. doi: 10.3389/fmicb.2021.664850

INTRODUCTION

Traditional fermented food has a long history and is widely distributed in the world. Many countries and regions have local characteristics of traditional fermented food which is indispensable delicacies on the table, such as Chinese spirits, soy sauce and fermented bean curd, Japanese natto and sake, Korean pickles, Italian salami sausage, Caucasia kefir milk, Turkish Tarhana, African garri, as well as bread, cheese, and yogurt from many western countries (**Table 1**). Due to the different geographical environments and life styles, traditional fermented foods from different countries or regions has their own characteristics in production form, flavor and nutritional value (Hesseltine and Wang, 1967).

As fungi widely used in fermented food, molds, and yeasts play an irreplaceable role in the formation of flavor substances and the production of functional components in fermented food. Traditional fungal fermentation leading to the production of foods and beverages is an ancient bioprocess, but it is still practiced worldwide to date. In Europe, yeast are extensively involved in the brewing of beers and wines. *Penicillium* spp. are used to ripen cheeses and meats. In East Asia, there are a variety of fermented foods produced by molds or yeasts, which have profoundly shaped the eating habits of the locals. *Aspergillus oryzae (Asp. oryzae)* is used for brewing soy sauce, miso, sake, ginger, etc. *Monascus* spp. are used to produce red mold rice. Various molds or yeasts play an important role in the production of fermented bean curd, huangjiu, Chinese liquor, tempeh, and

TABLE 1 | Main classification of fermented food in the world.

Category	Main fermented food	Main distribution areas	References
Alcoholic beverages	Baijiu, *Huangjiu*, Beer, Wine, Sake,	All over the world	Soni and Dey, 2014; Tamang et al., 2016
Grain	Bread, Pasta, Ogi, Tape, Ketan	All over the world	Campbell-Platt and Geoffrey, 1994; Tamang et al., 2016
Beans	Soy sauce, Natto, Douchi, Sufu	Asia	Nagai et al., 2010
Milk	Yogurt, Cheese, Kefir	Europe, North America, Middle East	Campbell-Platt and Geoffrey, 1994
Meat	Sausage, Ham, Suanyu, Smelly, Mandarin Fish	Europe, North America, China	Holck et al., 2017
Fermented vegetables	Pickles, Suancai, Kimchi	All over the world	Tamang and Kailasapathy, 2010b
Fishes	Fish sauce	East Asia, Southeast Asia, Europe	Liu et al., 2017
Rhizome	Gari, Fufu, Cingwada, Tape, Tapai Ubi	Africa, Southeast Asia	El and Montet, 2014
Others	Vinegar, Pixian, Broad, Bean paste, Black bean, Pidan	Asia	Wang and Fung, 1996; Mo et al., 2008; Wang et al., 2016

so on (**Figure 1**). *Qu* (Koji) as a fermentation starter is the soul behind these fermented foods, which is composed of cooked grains inoculated with a fermentation culture. The invention of *Qu* embodies the wisdom of the ancient working people without the concept of modern microbiology, which has potentially become an important part of local culture. However, many fermented foods from molds and yeasts have not been widely recognized yet.

Although traditional fungal fermentation has great economic and practical significance in food production, its core problem is that products and fermentative fungi have strong regional characteristics, which also leads to the relative lack of systematic comparison of related research on local characteristics. Therefore, this paper reviews the research history of molds and yeasts from traditional to modern, the diversity, population structure, functional characteristics and the development of analytical technology of molds and yeasts in fermented food, introduces some new research achievements and problems encountered through the role and characteristics of molds and yeasts in all kinds of fermented food, and discusses the fermentation molds and yeasts and related industries. The development prospect of the new technology. It is hoped that this topic can provide a communication platform for the research and application of different types of fermented fungi, and also provide a global perspective for the application of molds and yeasts in fermented food production in China.

HISTORY OF FERMENTED FOOD PRODUCTION IN CHINA

The wide application of microbial cultures represented by yeast in daily life is one of the characteristics of Chinese culture. In nature, yeasts grow on the surface of fruits (especially berries). These fruits will naturally ferment into wine when they fall to a place that does not leak. Therefore, fruit wine has long existed in nature. Many countries around the world have legends that monkeys love to drink, and there are also historical records of monkeys drinking. To be sure, fruit wines existed long before mankind. Inspired by natural phenomena, mankind has long known the use of fruit to make wine. In addition, in ancient times, humans domesticated a variety of wild animals into domestic animals, and the milk of domestic animals began to be drunk by humans (Tamang and Kailasapathy, 2010a). There are fewer yeasts that ferment lactose in milk than those that ferment glucose in fruits, but there are still enough yeasts to ferment milk into wine. After humans drink livestock milk, they have surplus. The surplus milk is first fermented by lactic acid bacteria into yogurt, and then fermented by yeast into milk wine. Therefore, many nomads will brew dairy wine. It is more complicated to use grain to make wine. The starch in the grain must be hydrolyzed into sugar, and then yeast can ferment the sugar into wine (Farnworth and Edward, 2003). Glucoamylase, which hydrolyzes starch, is rich in grain sprouts. The sprouts are soaked in water, the glucoamylase in the sprouts will hydrolyze the starch into sugar, so the yeasts present on the sprouts will ferment and make it into wine. Under natural conditions, this kind of grain wine will be widely produced everywhere (Steinkraus, 2004). When the Chinese ancestors began agricultural production, the climate was different from now, when the weather was hot and humid, which was suitable for the reproduction of mold. The grains that people store are not only easy to sprout, but also easy to mold. There are many glucoamylases in molds, which can hydrolyze starch into sugar. Over time, humans have begun to purposefully make grains moldy. This moldy grain is *Qu* (for fermented foods, *Qu* is also unique). *Qu* foam can be fermented into wine in water. The ancestors of the Chinese people discovered the mold first, cultivated it and used it first, and then spread it to Asian countries, which occupies an important position in the history of winemaking in the world. Play a great role in promoting social progress (Cheng, 2014).

The famous Japanese microbiologist Kenichiro Sakaguchi believes that China's creation of *Qu*, the use of mold to make wine, and the promotion of it to East Asia are as important as China's four major inventions. Why was the use of microorganisms particularly successful in China thousands of years ago? The main reason is that China's farming era started relatively early, and it is also affected by the monsoon (Monsoon) climate. According to Zhu Kezhen's research, on the east coast of Eurasia between 20 and 40° north latitude, the summer is controlled by the sinking airflow on the west side of the subtropical high The sinking air absorbs a large amount of water vapor from the

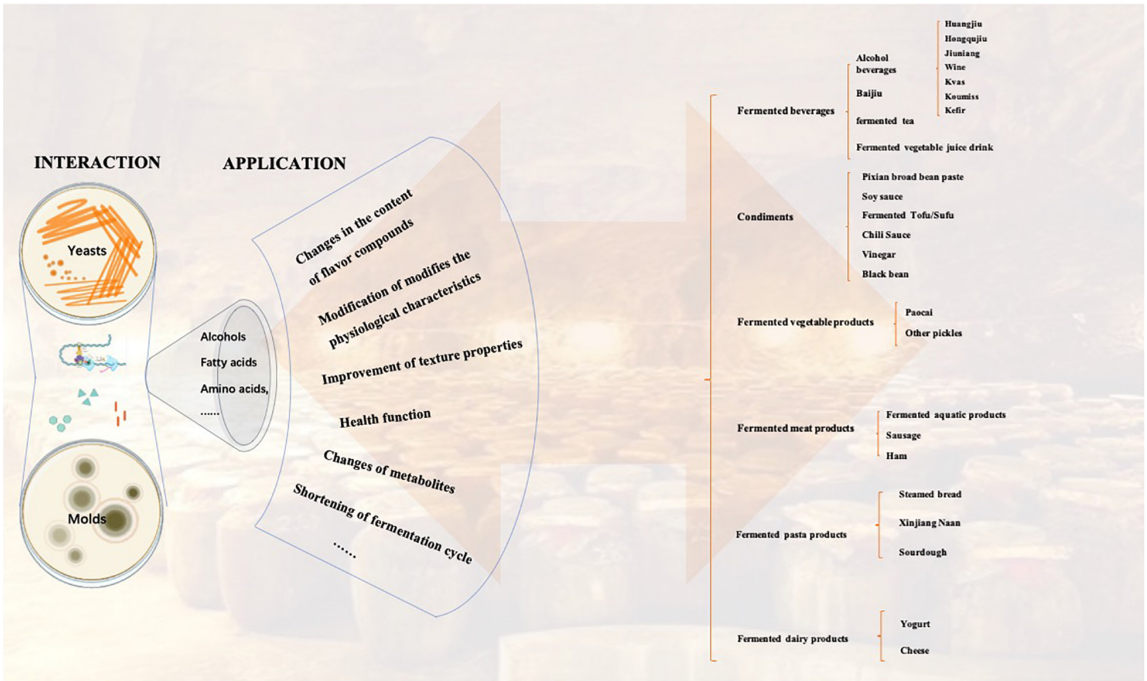

FIGURE 1 | Distribution and classification of traditional fermented foods in China.

warm and wet sea surface, thus bringing abundant precipitation. Formed a humid subtropical climate. Due to the strong contrast between the sea and the land, a unique monsoon climate is formed here. Its notable feature is that it rains in summer and is dry in winter, and the rainfall is concentrated in summer. High temperature and high humidity are naturally suitable for the growth of microorganisms. Therefore, since ancient times, China has referred to the first "C" day after the awn planting as "molding," and the first day after Xiaoshu as "molding,"0 that is, from June 6–15 to July 8–19. For a period of time, there was a rainy season in eastern China with a long rainy period and concentrated rainfall. During this period, food utensils are prone to mold, so a warning is given in the almanac. At the same time, Zhu Kezhen also conducted an in-depth study of China's paleo-climate changes and pointed out that in the first 2000 years (from the Yangshao culture in the primitive clan era to the Anyang Yin Ruins in the slave society) in China, the annual average for most of the time was The temperature is about 2°C higher than it is now. The temperature in January was 3∼5°C higher than it is now. Therefore, at that time, the area suitable for the growth of microorganisms would be wider, so most of the "*Qu*" recorded in ancient documents we know today were created in the first 2000 years (Hsieh, 1976).

Qu is a fermentation agent containing a large number of living bacteria and enzymes made by cultivating microorganisms with grains or by-products of grain processing. Since the Zhou Dynasty in 841 BC, there have been written records of fermented foods, and most of them used *Qu* as a starter. The earliest form of *Qu* should be germinated and moldy grain seeds (Wang, 2016). After a long period of use and improvement, before the Zhou Dynasty, there was the so-called "*Qu Yi*," that is, grain *Qu* covered with *Aspergillus* spores, because the strains were relatively high. The simplicity and color are single and bright, indicating that the microorganisms in the *Qu* at this time should be mainly *Asp. oryzae* that produces yellow spores, and of course yeasts are indispensable. Since molds were grown on scattered grains to make *Qu* at that time, they are now called "*San Qu*." In the Han dynasty, "*Bing Qu*" was popular, because more kinds of microorganisms could multiply inside the "*Bing Qu,*" which made the microbial composition in the *Qu* more abundant. First of all, there are more yeasts. More importantly, *Rhizopus* is easier to grow inside the *Qu* than *Aspergillus*, and bacteria with strong ability to produce lactic acid and decompose proteins are also easier to occupy a place in the *Qu*. Later, wild herbs were added to the *Qu*, which provided the yeast with vitamins and other nutrients, which made it grow more vigorously, so that my country's unique alcoholic double fermentation process of saccharification and fermentation was formed. Because of the diversity of the microbial flora of *Qu*, not only saccharification and alcohol fermentation, but also the decomposition of protein and fat by other microorganisms, as well as the formation of various biochemical metabolites, make the ingredients in the wine extremely complex and unique (Yang, 2013). The flavor. However, due to the development of *Qu* making technology, especially through the continuous continuation of the "*Mu Qu*" process with fine *Qu*, the utilization effect of *Qu* has been continuously improved. Make *Qu* a means to enrich good bacteria, and make *Qu* a form of long-term preservation of good bacteria. Many excellent pure strains used in modern fermentation industries in China and Japan, many of which are

obtained by selecting and breeding after being separated from *Qu* (Zhang, 2001).

In 1929, Wei Yanshou reported a new species of Mucor isolated from fermented bean curd in *Science*. In 1932, Chen Jusheng began to isolate 15 strains of yeast and several species of *Aspergillus* from Nanjing and other places of wine and medicine, and to conduct morphological and physiological studies on them. In the early 1930s, he also contributed to the improvement of my country's traditional soy sauce brewing process during his stay at the Central Industrial Laboratory. For example, he isolated *Asp. oryzae* with strong protease activity from soy sauce and successfully used it to make pure *Qu* to brew soy sauce, which attracted the attention of domestic brewing circles. In 1937, Jin Peisong observed various *Aspergillus*, *Rhizopus* and yeast isolated from *Qu* from all over China to observe their color under ultraviolet light, which is easy to identify their types. In 1956, Fang Xinfang began to study the classification and important physiological characteristics of Rhizopus isolated from *Xiaoqu*, and determined that *Rhizopus* is the main saccharifying bacteria of *Xiaoqu*. With the development of the fermentation industry, the research on the technology and its core microorganisms is gradually moving toward modernization, mechanization, thoroughbredness and intelligence.

Chinese *Jiu Qu* has a long history, diverse types, unique functions, and each has its own merits (Wan, 2007; Zhu, 2011). The use of *Qu* is a great invention of Chinese ancestors, and it is a precious scientific and cultural heritage of the motherland. "*Shu Jing Shuo Ming*": "If you make wine, you will only be able to squeeze tillers." This is the earliest written record of the ancients on the wine making of *Jiu Qu*. The use of *Qu* is the characteristic of Chinese winemaking, and it spreads to Japan, Vietnam and other Asian countries, and it is also the watershed of the world's eastern and western wine culture. For the core microorganisms in the fermentation process, mold and yeast, and their role in the fermentation process, it is an important subject so far, and there are many mysteries.

THE DISCOVERY OF MOLDS AND YEASTS OF TRADITIONAL FERMENTED FOODS IN CHINA

Fermented food contains rich microbial resources because of the open system of the fermentation. After a long period of evolution, a large number of excellent microbial resources have been retained. The study of microorganisms in fermented food is an important way to deepen the understanding of the molecular mechanism of fermentation process. Therefore, in recent years, a great deal of analysis has been performed for the succession and diversity of microorganisms in the fermentation process of traditional fermented food. In fermented food, the application of denaturing gradient gel electrophoresis (DGGE) and high-throughput sequencing (HGS) in traditional pure culture methods has broken the limitation of traditional culture methods, making the microbial community map of fermented food more clear and accurate (Muyzer et al., 1998).

In the past, microorganisms were known mainly through traditional culturable methods, which is to first isolate and purify the microorganisms, and then identify the species of the isolated strains. According to the diversity of yeasts in Italian traditional fermented olives, 117 strains of yeasts were isolated, of which 87 strains belonged to *Saccharomyces cerevisiae* (*S. cerevisiae*), and the rest were *Pichia galeiformis*, *Candida* and so on (Tofalo et al., 2013). However, this method has great limitations, time-consuming and laborious, and can only detect a limited number of microbial species, which cannot accurately determine the microbial composition of the fermentation system. In the past decade, with the wide application of modern molecular microbial ecology technology based on PCR-DGGE technology and high-throughput sequencing technology, people's understanding of microbial species and microbial succession in the manufacturing process of traditional fermented food has undergone a qualitative leap (Liu et al., 2012).

At present, in the field of traditional fermented food, there are few reports on the integration and analysis of the data generated by different ensemble platforms. With the gradual reduction of sequencing cost and the continuous improvement of sequencing accuracy, the acquisition of abundant accurate data will no longer be the threshold to limit the research. The more important problem that researchers need to solve is how to analyze the vast amount of data deeply and effectively according to biological problems, so as to completely analyze the types and functions of microorganisms in the brewing system. The research progress of mold and yeast composition in microbial community of traditional fermented food is shown in **Table 2**. The main fungi in traditional fermented food in China are *Rhizopus*, *Mucor, Aspergillus*, *Penicillium*, while *Saccharomyces*, *Candida*, *Coccidioides*, etc. For example, the fermentation bacteria of huangjiu include *Mucor*, *Rhizopus*, *Aspergillus niger* (*Asp. niger*), *Monascus*, *Aspergillus flavus* (*Asp. flavus*), and other molds, as well as yeast such as *Trichosporon* and *Candida*. The dominant fungi (>1% abundance) were *Saccharomyces* and *Aspergillus*, and *Saccharomyces* accounts for 11.34–25.01% of the whole microbiota (Liu et al., 2019).

In recent years, research on the composition of mold and yeast in the microbial community of traditional fermented foods has developed rapidly. Therefore, the study of its function also lays a foundation for the study of the safety, flavor quality, and nutrition of the corresponding fermented food. The scientific connotation of mold and yeast in traditional fermented food needs to be further analyzed and its application value needs to be further explored.

FUNCTION OF MOLD AND YEAST IN TRADITIONAL FERMENTED FOOD

The fermentation system of traditional fermented food is composed of one or more microorganisms. In the traditional fermentation process, the microorganisms involved in metabolism are uniformly enriched in their respective places of origin to form a complete and complex structural system. As the traditional fermentation process is formed in the natural

TABLE 2 | Research advances in studying microbial community composition and function of traditional fermented foods.

Traditional fermented food		Main fermentation microorganisms	References
Fermented beverages	Shaoxing Huangjiu Wheat Qu	*Saccharomyces*; *Aspergillus*, etc. *Rhizopus*, *Rhizomucor*, *Aspergillus*, *Penicillium*, etc.	Bokulich et al., 2016; Bourrie et al., 2016; Zheng and Han, 2016; Cai et al., 2018; Wang et al., 2018; Wei et al., 2018; Gao and Zhang, 2019; Guo et al., 2019; Liu et al., 2019; Tang et al., 2019; Chen et al., 2020; Liu Z. et al., 2020; Nejati et al., 2020
	Jiuyao	*Saccharomycopsis*, *Rhizopus*, *Aspergillus*, etc.	
	Hongqujiu	*Wickerhamomyces anomalus*, *S. cerevisiae*, *Monascus purpureus*, *Xeromyces bisporus*, etc.	
	Hongqu	*Monascus*, *Rhizopus*, *Asp. niger*, *Asp. flavus*, *S. cerevisiae*, etc.	
	Jiuniang	*R. oryzae*, *R. microsporus*, *Asp. niger*, *Asp.* candidus, *Mucor indicus*, *Mucor circinelloides*, *Saccharomycopsis fibuligera, S. cerevisiae*, *Pichia sp*., *Pichia burtonii*, *Candida glabrata*, *C. metapsilosis*, *C. rugosa*, *C. tropicalis*, *Kodamaea ohmeri*, etc.	
	Wine	*Saccharomyces*, *Kloeckera apiculate, Candida, Metschnikowia, Hanseniaspora, Schizosaccharomyces, Hansenula, Debaryomyces, Zygosaccharomyces Hanseniaspora*, *Issatchenkia*, *Rhodotorula*, *Penicillium*, *Cladosporium*, *Botrytis*, *Sporobolomyces*, *Aspergillus*, *Cryptococcus*, *Pichia*, etc.	
	Koumiss	*Kluyveromyces marxianus*, *Kazachstania unispora*, *Dekkera anomala*, *S. cerevisiae*, *Trichosporon asahii*, *Penicillium carneum*, *Pichia membranifaciens*, etc.	
	Kefir	*Kluyveromyces marxianus*, *Dekkera anomalus*. *Kazachstania unispora*, *Kazachstania turicensis*, *Kluyveromyces marxianus, S. cerevisiae*, *Dekkera anomala*, *Asp. Amstelodami,* etc.	
	Baijiu	*Rhizopus, Aspergillus, Mucor, Absidia, Rhizomucor, Penicillium; S. cerevisiae, Pichia, Zygosaccharomyces, Schizosaccharomyces, Saccharomycopsis,* etc.	
Fermented tea	Kombucha; Oolong tea; Pu'er tea; Dark tea (Fu-Brick Tea); Black tea	*Penicillium*, *Aspergillus Saccharomyces, Yarrowia,* etc.	
	Soy sauce	*Aspergillus*, *Zygosaccharomyces rouxii, Candida*, etc.	Marsh et al., 2014; Huang et al., 2017; Li et al., 2018; Rui et al., 2019; Arıkan et al., 2020
Condiments	Vinegar	*Eurotium, Monascus,Asp. Pichia, Saccharomyces*, etc.	Lindner et al., 2008; Nie et al., 2017; Yunping et al., 2018
	Fermented Tofu/Sufu	*Aspergillus*, *Monascus*, etc.	
	Paocai	*Pichia, S. cerevisiae*, etc.	
Fermented vegetable products	Sausage, Panxian Ham, Jinhua Ham, Xuanwei Ham, Suanyu, Smelly mandarin fish, Fermented shrimp paste	*Aspergillus*, *Penicillium S. cerevisiae Virgibacillus halodenitrificans*, *Asp.s niger*. *Pichia gilliermondii*, etc.	Patra et al., 2016
Fermented meat products	Steamed bread	*S. cerevisiae*, *Cyberlindnera jadini*, *Wickerhamomyces anomalus*, *Candida tropicalisstrain*, *R. oryzae*, *Torulaspora delbruecki*, *Candida humilis*, etc.	Aquilanti et al., 2007; Połka et al., 2015; Duan et al., 2016; Lv et al., 2019; Wang et al., 2019
Fermented pasta products	Sour dough	*S. cerevisiae*, *S. exiguus*, *Candida milleri*, *Pichia norvegensis*, *Hansenul anomala*, *Candida krusei*, etc.	Bai et al., 2010; Ercolini et al., 2013; Zhang et al., 2019
	Yogurt, Cheese	*Aspergillus*, *Galactomyces; Kluyveromyces*, *Torulaspora*, etc.	

environment, different regional environment, climate and other factors will make the flavor of fermented food different, and the role of microflora is also different. Fermented food and beverages are organisms produced by the activities of microorganisms, mainly yeasts, molds, and bacteria. Fungi (yeast and mold) play an important role in traditional fermented food (Tamang and Kailasapathy, 2010a).

YEAST

Yeast plays an important role in the production of many fermented foods. About 21 major genera with several species of functional yeasts have been reported from fermented food and beverages which include *Brettanomyces*, *Candida*, *Cryptococcus*, *Debaryomyces*, *Galactomyces*, *Geotrichum*, *Hansenula*, *Hanseniaspora*, *hyphopichia*, *Kluyveromyces*, *Metschnikowia*, *Pichia*, *Rhodotorula*, *Saccharomyces*, *Saccharomycodes*, *Saccharomycopsis*, *Schizo saccharomyces*, *Torulopsis*, *Trichosporon*, *Yarrowia*, and *Zygosacchartztorius* (Aidoo, 1986; Hesseltine, 1991, 2003; Nout and Aidoo, 2010).

Yeast has a direct or indirect relationship with alcohol fermentation, higher alcohols, esters, organic acids and so on, which has a great impact on the flavor of products. Among them, *S. cerevisiae* is the most widely used in fermented foods such as bread and alcoholic drinks. In the fermentation process, *S. cerevisiae* mainly converts small molecular sugars into ethanol and carbon dioxide, and can also metabolize a

small amount of other flavor substances. For example, alcohol fermentation is mainly a process in which yeast converts glucose into alcohol and carbon dioxide. Glucose produces pyruvate through the EMP pathway. Pyruvate dehydrogenase catalyzes pyruvate to acetaldehyde, which is then reduced to ethanol by alcohol dehydrogenase. In the process, other by-products are also produced in addition to alcohol and carbon dioxide, such as glycerol, amyl alcohol, isoamyl alcohol, butanol, isobutanol, and other higher alcohols (collectively referred to as fusel oil) and a variety of esters and so on. Alcohol has a refreshing aroma, higher alcohols have a certain flavor, glycerol has a refreshing sweet taste, these alcohols are also the premise of the formation of esters.

MOLDS

There are relatively few molds in fermented food and beverages, including *Actinomycetes*, *Mucor*, *Rhizopus*, *Amylomyces*, *Monascus*, *Neurospora*, *Aspergillus,* and *Penicillium* (Hesseltine, 1991; Hesseltine, 2003; Nout and Aidoo, 2010). The main role of these molds in fermented food is to produce a variety of enzymes (Tamang, 2010). For example, protease (acidic, neutral, alkaline), amylase, glutamidase, pectinase, hemicellulase, and cellulase can use starch, oligosaccharide and monosaccharide as carbon source, and protein, amino acid and urea as nitrogen source. Maltose can effectively induce *Asp. oryzae* to secrete various hydrolytic enzymes, such as *Asp. oryzae* to secrete α-amylase, *Asp. Niger,* and *Asp. nigrum* to produce Glucoamylase and so on. Starchy raw materials are degraded into small molecular sugars such as dextrin, maltose and glucose under the action of amylase and glucoamylase. On the one hand, they promote the growth of bacteria, yeasts and other microorganisms, and further metabolize to produce alcohols, organic acids and other flavor substances. On the other hand, some monosaccharides, oligosaccharides, and polysaccharides that can't be decomposed increase the nutritional value of the products. Protein raw materials are decomposed into peptides, amino acids and other functional and flavor substances by protease. At the same time, these small molecular substances also contribute to the growth and metabolism of bacteria and yeast (Tamang, 2010). Therefore, deepening the understanding of mold and yeast in fermented food is helpful to promote the progress of fermented food.

INTERACTION BETWEEN MOLD AND YEAST IN TRADITIONAL FERMENTED FOODS

In the production of traditional fermented food, not only the microorganisms are closely related to the environment in the fermentation process, but also the ecological relationship among microorganisms is very complex. The synergism and antagonism among microorganisms have a profound impact on the formation of the final flavor of fermented food and the generation of new substances. With the progress of systems biotechnology, the complex interactions among microorganisms are studied at multi-level by using multi-group technology as an important means. Genomics, transcriptome, proteomics, and metabonomics reveal a series of changes in the life process of microorganisms at the levels of DNA, RNA, protein and metabolites, respectively, which is helpful to a comprehensive and in-depth understanding of the complex interactions among microorganisms. The application of these techniques further reveals the physiological mechanism of interactions among different microbial populations, and provides theoretical guidance for the directional regulation and application of microorganisms. For example, *Aspergillus* was the main strain producing tea fuscin in the early stage, while *Mucor* and *S. cerevisiae* were also involved in the production of tea fuscin in the later stage (Li et al., 2018). *Pseudomonas* and *Aspergillus* are important strains for the production of methoxyphenols (Li et al., 2018). In the production of alcohols, *Aspergillus* was the main production strain in the initial stage, and *Bacillus*, *Cunninghamia lanceolata*, *Lhasa and Listeria monocytogenes* played a role in the later stage. For instance, the succession of *Staphylococci* on cheese skin is mainly driven by biological factors. It can promote the growth of beneficial staphylococci by strengthening specific molds, so as to inhibit the reproduction of potential pathogens in cheese production (Kastman et al., 2016). So the analysis of the interaction of molds and yeasts in traditional fermented food will help to: (1) deeply understand the law of community succession and analyze the fermentation mechanism; (2) find out the source of flavor substances; (3) through microbial interaction, inhibit the growth of harmful microorganisms or the production of harmful metabolites to ensure the safety of traditional fermented food. Deepening the understanding of the interaction between microorganisms in traditional fermented food is helpful to enhance the formation of flavor substances or control the production of bad flavor substances from the source of fermentation.

The fermentation agents currently in use are mainly yeasts and some molds. These microorganisms have evolved over tens of millions of years (Papadimitriou et al., 2015). Through the acquisition and deletion of genes, they can obtain the corresponding niche in the biological environment of fermented food. These characteristic microorganisms in fermented food are separated and used as starters to ensure the stability of the food. However, the microorganisms involved in the natural fermentation process of food are mostly complex and diverse (Smid and Lacroix, 2013). Diverse microorganisms change their own functional characteristics through interactions, thereby changing the species composition and functions of the entire microbial system in the entire fermented food system, which will ultimately affect the quality and safety of fermented food. A detailed understanding of these interactions is a prerequisite for optimizing and controlling the quality of fermented foods. Therefore, clarifying the mechanism of the interaction between microorganisms in fermented foods can help people develop new starters of mixed strains, better regulate the parameters of the fermentation process, and produce stable and excellent fermented foods.

With the analysis of the microbial community structure of a large number of brewed foods, the core microorganisms in the production process of different brewed foods have gradually been identified, and the deep-level microbial interaction has received more and more attention, but

there is still a lack of microbial interactions in traditional Chinese brewed foods (Hong et al., 2016). In-depth study of the mechanism of action. Microbial interaction is becoming a new direction for in-depth analysis of the production mechanism of traditional brewed food. At present, researchers are paying more and more attention to the research of co-enzyme mechanism in brewed food, mainly focusing on the traditional fermented food (Nie et al., 2017). Research on interaction mechanism, quality formation, maintenance, and deterioration mechanism under processing conditions (Wolfe and Dutton, 2015). Xu Yan found that the complementary metabolism of yeast and lactic acid bacteria during liquor fermentation is the basis for the formation of sulfur-containing flavor substances (Liu et al., 2017). Liu et al. (2015) found that microbial co-fermentation can significantly increase the concentration of flavor substances in huangjiu. There are a large number of metabolites in huangjiu that can regulate the physiological functions of fungi, β-phenethyl alcohol, tyrosol, chromanol, and farnesol. For example, the fungal metabolite farnesol can inhibit The cell division of *S. cerevisiae* is in the G1 phase and reduces the content of diglycerides, thereby inhibiting the proliferation of *S. cerevisiae*. To perfectly analyze the formation mechanism of the interaction between the two bacteria, it must be from four levels: functional phenotype, metabolic level, transcription level, and gene level In-depth elucidation of the functional complementarity, metabolic interaction and transcriptional interaction between the two bacteria and the identification of key genes (Albuquerque and Casadevall, 2012).

For example, the brewing of huangjiu uses wheat *Qu* and mother of wine as starters to form a double-sided fermentation process at room temperature while saccharification and fermentation, while wine and beer, which are the world's three major ancient wines, can only be fermented on one side (Chen and Xu, 2013). The core of this process difference is huangjiu (Liu S. et al., 2020). The use of microbial interaction makes the decomposition of raw materials and the formation of flavors proceed simultaneously, realizing the efficient division of labor and coordination of complex community metabolism: (1). The component modules of different sources and functions are functioned by different strains, which facilitates functional partitioning, avoids cross-effects, and does not increase the metabolic burden Completion of complex work at the same time; (2). The degradation of raw materials and the synthesis of flavor are carried out simultaneously, which avoids the inhibition of microbial metabolism due to high sugar content; (3). The degree of fermented alcohol (18–21°) is much higher than that of wine and beer (<14°). The concentration and abundance of substances are significantly improved, and the production efficiency is significantly improved.

Huangjiu brewing is an open and complex fermentation process. The microorganisms involved mainly come from malt, yeast and the production environment (He et al., 2017). The microorganisms include bacteria, molds and yeasts, especially *Aspergillus* and yeast, which participate in the process of huangjiu brewing. The whole process of saccharification and liquefaction, alcohol fermentation and flavor formation play a vital role in the quality of huangjiu. The brewing process of huangjiu is a bilateral fermentation process in which solid and liquid coexist. The decomposition of raw materials and the utilization of substrates are carried out simultaneously. In the whole fermentation process, yeast and *Aspergillus* are the most important microorganisms. The fermentation process involves the growth of microorganisms, the degradation of brewing materials, the consumption of oxygen, the utilization of substrates, and the accumulation of ethanol organic acids. In the process of huangjiu brewing, the main yeast is *S. cerevisiae*, which plays a role in producing alcohol and flavor (Wu et al., 2015). Some studies have found the existence of Pichia in both manual *Qu* and cooked wheat *Qu* using traditional microbial isolation and culture technology. *Saccharomycopsis fibuligera* was found to be an absolute predominance in huangjiu medicine. In the fermentation process, the mold secretes enzymes for saccharification and liquefaction while the yeast is fermented. In brewing, the mold provides abundant enzymes and becomes an essential brewing microorganism. Studies have pointed out that the molds in the huangjiu brewing process are mainly derived from wheat *Qu* microorganisms. Chen Jianyao and others have used traditional microbial separation. Researches have pointed out that *Asp. oryzae* and *S. cerevisiae* coexist in the early stage of white wine fermentation, which is crucial for saccharification and fermentation, ethanol and flavor substances. Importantly, different ratios of *Asp. oryzae* and *S. cerevisiae* have different effects, and multiple strains will affect the diversity of glucoamylase production and thus have a synergistic effect on yeast production of ethanol (Wang et al., 2020).

In general, there are various types of interactions between microorganisms, and the interaction mechanism is complex. The formation of the nutritional and sensory qualities of fermented foods does not only rely on the action of a single microorganism, but also the interaction between different microorganisms and their metabolites, and finally forms a unique fermented food. The study of the interaction between important microorganisms, mold and yeast is of great significance for understanding the fermentation mechanism of traditional fermented foods and the study of filling interactions.

APPLICATION OF MICROBIAL CO-FERMENTATION REGULATION IN FERMENTED FOOD PRODUCTION

The analysis of microbial community structure of traditional fermented food and the study of microbial interaction laid a good theoretical foundation for understanding its brewing mechanism at the system level, constructing an efficient and controllable mixed strain fermentation system, and realizing efficient and directional production of products. On this basis, the researchers put forward the application of functional microbial co-culture in fermented food production. The advantages of microbial co-culture have been gradually explored and valued by people, especially in recent years, there have been many successful reports on reforming traditional fermentation process,

improving product quality and safety, shortening fermentation cycle and so on.

Co-fermentation plays a very positive role in improving the taste and favor of fermented food. For example, different proportions of *Bacillus licheniformis* and *S. cerevisiae* were inoculated into sorghum extract and fermented, and then the volatile components of the product were analyzed. The results showed that co- fermentation had almost no effect on the growth of *S. cerevisiae,* but had a certain inhibitory effect on the growth of *B. licheniformis*. Under the condition of co-fermentation, the amount of ethanol and flavor compounds produced by *S. cerevisiae* increased significantly, including four fatty acids and their corresponding two esters, one terpene, and five aromatic compounds. At the same time, sixteen kinds of flavor compounds in the product were increased by the addition of *B. licheniformis*, which showed that co-fermentation had a positive effect on the flavor of fermented food (Zha et al., 2018).

Changes in the Content of Flavor Compounds

Compared with single fermentation, the co-fermentation of *S. cerevisiae* Y3401 and *Wickerhamomyces anomalus* Y3604 produced more ethyl acetate and increased the content of other flavor compounds such as β-phenylethanol and phenylethyl acetate (Fan et al., 2019). The co-fermentation of non-*S. cerevisiae* (*Hanseniaspora opuntiae*, *Hanseniaspora uvarum, and Torulaspora delbrueckii*) and *S. cerevisiae* had lower ethanol content and total acidity, higher volatile aroma components, especially higher alcohols and esters, which was an effective way to improve the sensory quality of fruit wine (Hu et al., 2020). Compared with the single fermentation of *S. cerevisiae,* the co-fermentation of *S. cerevisiae* by *Issatchenkia terricola* SLY-4 and *Pichia kudriavzevii* F2-24 had lower volatile acidity and higher content of aroma components, which improved the flavor and quality of wine. At the same time, sequential co-fermentation is more conducive to the improvement of wine flavor and quality than simultaneous co-fermentation, because the content of esters is higher, and the content of C6 compounds, benzene derivatives, higher alcohols, and fatty acids is lower (Shi et al., 2019).

Modification of Modifies the Physiological Characteristics

The yeast *S. cerevisiae*, which is incapable of synthesizing glucosylceramide (GlcCer), adapted to alkaline and ethanol tolerance conditions after exposure to GlcCer from *Qu* cereal cultured with *Asp. kawachii*, and modifies its flavor profile (Kazutaka et al., 2015). In nitrogen gas-sparging anaerobic culture of *S. sake* Kyokai No. 7, supplementing the basal synthetic medium with phosphatidylcholine enhanced the yeast growth and fermentative activity, whereas adding ergosteryl oleate enhanced alcohol-endurability. Supplementation with both phosphatidylcholine and ergosteryl oleate promoted the yeast growth, fermentative activity and alcohol-endurability of cells (Hayashida and Ohta, 1980). These novel insights demonstrate a new mechanism of cooperation between microbes in food fermentation and a new technical approach for the modification of fermentation.

Improvement of Texture Properties

Extracellular polysaccharides (EPS) produced by *Lactic acid bacteria* (LAB) and organic acids produced by *Propionic acid bacteria* (PAB) are used to enhance the texture and extend the shelf life of baked products. The extracellular polysaccharide co-cultured with *Weissella confuse* 11GU-1 and *Propionibacterium freudenreichii* JS15 had synergistic effect on wheat dough and bread texture (Tinzl-Malang et al., 2015). The multi starter fermentation system of LAB and yeast was used to obtain new type of acidified goat milk (AGM), which reduced the relative content of free octanoic acid in AGM, promoted the forming of more aroma in AGM, covered up the fishy smell of goat and made AGM have pleasant flavor. It provides a new choice for people who are hypersensitive to milk protein but do not like the goat flavor of goat milk (Huang et al., 2020).

Health Function

Edible yeast, *Lactobacillus plantarum* (*L. plantarum*) and Mucor were used in traditional fermentation of three food materials with wheat dough, pickled Chinese cabbage and Mao-tofu, respectively. These microorganisms are able to enhance OPPs dissipation in these fermented food materials, and yeast and Mucor are more potent than *L. plantarum* to degrade OPPs (Zhou et al., 2015). Soybean co-fermentation with different microorganisms (*Bifidobacterium*, *B. subtilis,* and *Rhizopus oligosporus*) in a specific order has higher nutritional value than single fermentation (Puri et al., 2015). *S. cerevisiae var. Boulardii* (S.B.) strain has no negative effect on beer aroma, and adding S.B. strain into the mixed starter can improve antioxidant activity and polyphenol content (Angela et al., 2018). When *Seabuckthorn* was co-fermented with *S. cerevisiae* and *Aesculus orientalis*, the content of the ascorbic acid decreased by 14% (Negi and Dey, 2013). The combined action of *Asp. oryzae* MAO103 and *A. oryzae* MAO104 from Meju, which is a traditional fermented soybean starter in Korea, reduced the mutagenic ability of base substitution of aflatoxin and significantly inhibited the production of aflatoxin by *Asp. flavus* (Lee et al., 2016). *L. plantarum* Shanghai brewing 1.08 and *Zygosaccharomyces rouxii* CGMCC 3791 were inoculated into pickled cabbage and radish, and fermented for 8 days. During the fermentation, the content of nitrite in the system decreased continuously, while its content in the natural fermentation group increased at first and then decreased slightly. The results showed that co-fermentation could effectively inhibit the formation of nitrite and reduce its content in sauerkraut (Wu et al., 2013).

Changes of Metabolites

S. cerevisiae SY1 could not produce ethanol in milk fermentation, but the ethanol production was higher when co-cultured with *L. plantarum* ZL1 (Kuda et al., 2016). By using it to hydrolyze the pretreated biomass, engineered *S. cerevisiae* 424A makes to the co-fermentation of xylose and glucose (mainly glucose and xylose) to ethanol, which can reduced the investment cost. Compared with single hydrolysis, co-fermentation (SHCF) can

save energy and increase ethanol yield by reducing the inhibition of terminal products (Jin et al., 2012).

Shortening of Fermentation Cycle

The fermentation cycle of Chinese traditional fermented fish products (CTFPs) co-fermented by *L. plantarum* 120, *S. cerevisiae* 2018 and *Staphylococcus xylosus* 135 was shortened, and the contents of total volatile base nitrogen, trimethylamine, dimethylamine, nitrite, and N-nitrosodimethylamine (NDMA) were significantly lower than those of natural fermentation samples (Liao et al., 2018).

CONCLUSION AND PERSPECTIVES

As a traditional food with a long history, traditional fermented food is widely spread, and has a variety of health functions on human body. The industrialization level of traditional fermented food in all over the world is not high. There is little knowledge and experience in the production of fermented food for reference. At the same time, the product quality is unstable, and there are many potential safety hazards. Mold and yeast, as important microorganisms in fermented food, not only can form complex flora structure in the fermentation process, but also can produce complex and diverse flavor components. Its growth and metabolism process can improve food structure and texture.

Traditional culturable methods and molecular microbial ecology methods are difficult to systematically analyze the structure and function of such complex microbial flora. In the face of such challenges, microbiome technology which is based on microbiology, functional genomics, metabonomics, bioinformatics, and systems biology, has developed rapidly in recent years. It can reveal how the natural inoculation of microbial flora affects the food fermentation process, and also determine the safety, flavor characteristics, the quality and nutritional function of traditional fermented food (WileyBlackwell, 2013).

The study of molds and yeasts in traditional fermented food will be beneficial to analyze their metabolic mechanisms and complex interactions during the fermentation. This review can provide some new opinions for the research of microorganisms in fermented food, and it can also provide some theoretical guidance for the upgrading and transformation of the industrialization of traditional fermented food. Therefore, the application value of complex and diverse molds and yeasts needs to be further explored (Adams and Mitchell, 2002).

DEVELOPING THE RESOURCE OF MOLDS AND YEASTS

The production technology of traditional fermented food has been inherited for thousands of years, which is also the process of microbial domestication. And the microorganisms in the brewing system may co-evolve with human beings. The physiological and metabolic characteristics of some domesticated microorganisms may be different from those of undomesticated microorganisms in nature (Bing et al., 2014). For example, it was identified for a bifunctional lipase gene of glyceresterase phospholipase with high catalytic activity and substrate applicability in *Rhizopus chinensis* (a common fungus in *Qu*). The application of protein engineering modification greatly improves the thermal stability of lipase, reduces the production cost, and fills the blank of industrial production of lipase (Yu et al., 2009). *ARO8* gene in deficient yeast strains can significantly improve the ability of glucose conversion to β-phenylethanol (Romagnoli et al., 2015). At present, culturable methods are often used to excavate the microbial resources of fermented food. In the future, it is necessary to establish the culturable method of the difficult culture microorganism. Traditional fermented food microbial germplasm resources and gene resources will be deeply explored to provide new microorganisms, enzymes and gene elements for modern biotechnology industry.

QUALITY CONTROL AND OPTIMIZATION OF TRADITIONAL FERMENTED FOOD

Using tyrosine as substrate, the *A. oryzae* 3.042 was adaptively evolved, the content of tyrosine in soybean paste fermented by *Asp. oryzae* decreased from 6.49 to 6.14 mg/g ($p < 0.05$). After optimization, its content decreased to 5.67 mg/g (Niu et al., 2018). *Meyerozyma* and *Candida* were added to *Aspergillus* type Douchi so that the content of all amino acids, organic acids and the percentage of unsaturated fatty acids were significantly increased. The results further indicated that the co-fermentation could improve the flavor components of *Douchi* (He et al., 2019). Therefore, the rational use of the interaction between mold and yeast and other microorganisms has important guiding value for the directional and efficient control of microbial flora metabolism, which also has far-reaching significance for the improvement of product quality. In the near future, we believe that the continuous progress and development of mold and yeast in fermented food will help to improve the quality, stability, and safety of fermented food.

MICROBIAL INTERACTION IS BECOMING A NEW DIRECTION TO ANALYZE THE MECHANISM OF TRADITIONAL FERMENTED FOOD PRODUCTION

Microbial interactions are widespread in nature, especially in fermented foods. The growth of microorganisms also has a certain impact on the formation of flavor substances, such as yeast and mold at the late stage of sausage fermentation, it has been reported that the interaction between yeast and mold, yeast and bacteria has an important influence on the flavor of liquor, and the interaction of these microorganisms endows fermented food with rich taste and mouthfeel. Study of traditional fermented food fermentation of yeast and mold in the process of interaction,

cannot only clarify the ebb and flow of yeast and mold in the process of fermentation, also helps to parse and factors which influence the growing phenomenon of interaction mechanism, so as to provide certain guidance for the fermentation process, has important scientific significance and application value.

AUTHOR CONTRIBUTIONS

QY carried out the initial literature review and wrote the initial manuscript. JM and SL provided expertise and insight relating to fermented food. HY revised the manuscript and checked it. All authors read and approved the final manuscript.

FUNDING

This work was financially supported by the National Natural Science Foundation of China (32072205 and 22138004), and Sichuan Key Research and Development Project(2021YFS0337), and the first phase of the connotation construction of the 14th Five-Year Plan of Tibetan medicine (2021ZYYGH008).

REFERENCES

Adams, M., and Mitchell, R. (2002). Fermentation and pathogen control: a risk assessment approach. *Int. J. Food Microbiol.* 79, 75–83. doi: 10.1016/S0168-1605(02)00181-2

Aidoo, K. E. (1986). Lesser-known fermented plant foods. *Trop. Sci.* 26, 249–258.

Albuquerque, P., and Casadevall, A. (2012). Quorum sensing in fungi–a review. *Med. Mycol.* 50, 337–345. doi: 10.3109/13693786.2011.652201

Angela, C., Rossana, R., Angela, P., Gabriella, S., Rocchina, P., Marianna, Z., et al. (2018). Use of *Saccharomyces cerevisiae* var. boulardii in co-fermentations with *S. cerevisiae* for the production of craft beers with potential healthy value-added. *Int. J. Food Microbiol.* 284, 22–30. doi: 10.1016/j.ijfoodmicro.2018.06.028

Aquilanti, L., Santarelli, S., Silvestri, G., Osimani, A., Petruzzelli, A., and Clementi, F. (2007). The microbial ecology of a typical Italian salami during its natural fermentation. *Int. J. Food Microbiol.* 120, 136–145. doi: 10.1016/j.ijfoodmicro.2007.06.010

Arıkan, M., Mitchell, A. L., Finn, R. D., and Gürel, F. (2020). Microbial composition of Kombucha determined using amplicon sequencing and shotgun metagenomics. *J. Food Sci.* 85, 455–464. doi: 10.1111/1750-3841.14992

Bai, M., Qing, M., Guo, Z., Zhang, Y., Chen, X., Bao, Q., et al. (2010). Occurrence and dominance of yeast species in naturally fermented milk from the Tibetan Plateau of China. *Can. J. Microbiol.* 56, 707–714. doi: 10.1139/w10-056

Bing, J., Han, P.-J., Liu, W.-Q., Wang, Q.-M., and Bai, F.-Y. (2014). Evidence for a far East Asian origin of lager beer yeast. *Curr. Biol.* 24, R380-1. doi: 10.1016/j.cub.2014.04.031

Bokulich, N. A., Collins, T. S., Masarweh, C., Allen, G., Heymann, H., Ebeler, S. E., et al. (2016). Associations among wine grape microbiome, metabolome, and fermentation behavior suggest microbial contribution to regional wine characteristics. *mBio* 7, e00631–16. doi: 10.1128/mbio.00631-16

Bourrie, B. C. T., Willing, B. P., and Cotter, P. D. (2016). The microbiota and health promoting characteristics of the fermented beverage kefir. *Front. Microbiol.* 7:647. doi: 10.3389/fmicb.2016.00647

Cai, H., Zhang, T., Zhang, Q., Luo, J., Cai, C., and Mao, J. (2018). Microbial diversity and chemical analysis of the starters used in traditional Chinese sweet rice wine. *Food Microbiol.* 73, 319–326. doi: 10.1016/j.fm.2018.02.002

Campbell-Platt, and Geoffrey (1994). Fermented foods - a world perspective. *Food Res. Int.* 27, 253–257. doi: 10.1016/0963-9969(94)90093-0

Chen, C., Liu, Y., Tian, H., Ai, L., and Yu, H. (2020). Metagenomic analysis reveals the impact of JIUYAO microbial diversity on fermentation and the volatile profile of Shaoxing-jiu. *Food Microbiol.* 86:103326. doi: 10.1016/j.fm.2019.103326

Chen, S., and Xu, Y. (2013). Effect of 'wheat Qu' on the fermentation processes and volatile flavour-active compounds of Chinese rice wine (Huangjiu). *J. Inst. Brewing* 119, 71-77.

Cheng, G. (2014). Present situations of the utilization of microbes in Chinese Jiuqu. *Liquor Mak. Sci. Technol.* 3, 122–124. doi: 10.13746/j.njkj.2014.03.033

Duan, S., Hu, X., Li, M., Miao, J., Du, J., and Wu, R. (2016). Composition and metabolic activities of bacterial community in shrimp sauce at the flavor forming stage of fermentation as revealed by metatranscriptome and 16S rRNA gene sequencing. *J. Agric. Food Chem.* 64:2591. doi: 10.1021/acs.jafc.5b05826

El, S. A., and Montet, D. (2014). *African Fermented Foods: Historical Roots and Real benefits*. Boca Raton, FL: CRC Press

Ercolini, D., Pontonio, E., De Filippis, F., Minervini, F., La Storia, A., Gobbetti, M., et al. (2013). Microbial ecology dynamics during rye and wheat sourdough preparation. *Appl. Environ. Microbiol.* 79, 7827–7836. doi: 10.1128/aem.02955-13

Fan, G., Teng, C., Xu, D., Fu, Z., and Pual, X. (2019). Enhanced production of ethyl acetate using co-culture of *Wickerhamomyces anomalus* and *Saccharomyces cerevisiae*. *J. Biosci. Bioeng.* 128, 564–570. doi: 10.1016/j.jbiosc.2019.05.002

Farnworth, and Edward (2003). *[Functional Foods and Nutraceuticals] Handbook of Fermented Functional Foods Volume 20034675 | | The History of Fermented Foods* (Boca Raton, FL: CRC Press), 1–25. doi: 10.1201/9780203009727.

Gao, W., and Zhang, L. (2019). Comparative analysis of the microbial community composition between Tibetan kefir grains and milks. *Food Res. Int.* 116, 137–144. doi: 10.1016/j.foodres.2018.11.056

Guo, L., Ya, M., Guo, Y. S., Xu, W. L., Li, C. D., Sun, J. P., et al. (2019). Study of bacterial and fungal community structures in traditional koumiss from Inner Mongolia. *J. Dairy Sci.* 102, 1972–1984. doi: 10.3168/jds.2018-15155

Hayashida, S., and Ohta, K. (1980). Effects of phosphatidylcholine or ergosteryl oleate on physiological properties of *Saccharomyces* sake. *Agric. Biol. Chem.* 44, 2561–2567. doi: 10.1271/bbb1961.44.2561

He, B., Li, H., Hu, Z., Zhang, Y., Sun, M., Qiu, S., et al. (2019). Difference in microbial community and taste compounds between Mucor-type and Aspergillus-type Douchi during koji-making. *Food Res. Int.* 121, 136–143. doi: 10.1016/j.foodres.2019.03.031

He, G. Q., Liu, T. J., Sadiq, F. A., Gu, J. S., and Zhang, G. H. (2017). Insights into the microbial diversity and community dynamics of Chinese traditional fermented foods from using high-throughput sequencing approaches. *J. Zhejiang Univ. Sci. B* 18, 289–302. doi: 10.1631/jzus.B1600148

Hesseltine, C. W. (1991). Zygomycetes in food fermentations. *Mycologist* 5, 162–169. doi: 10.1016/s0269-915x(09)80475-8

Hesseltine, C. W., and Wang, H. L. (1967). Traditional fermented foods. *Biotechnol. Bioeng.* 9, 275–288. doi: 10.1002/bit.260090302

Hesseltine, W. C. (2003). Microbiology of oriental fermented foods. *Annu. Rev. Microbiol.* 37, 575–601. doi: 10.1146/annurev.mi.37.100183.003043

Holck, A., Axelsson, L., Mcleod, A., Rode, T. M., and Heir, E. (2017). Health and safety considerations of fermented sausages. *J.Food Qual.* 2017:9753894 . doi: 10.1155/2017/9753894

Hong, X., Chen, J., Liu, L., Wu, H., Tan, H., Xie, G., et al. (2016). Metagenomic sequencing reveals the relationship between microbiota composition and quality of Chinese Rice Wine. *Sci. Rep.* 6:26621. doi: 10.1038/srep26621

Hsieh, C.-M. (1976). Chu K'o-chen and China's climatic changes. *Geograp. J.* 142, 248–256. doi: 10.2307/1796599

Hu, L., Liu, R., Wang, X., and Zhang, X. (2020). The sensory quality improvement of citrus wine through co-fermentations with selected non-*Saccharomyces* yeast strains and *Saccharomyces cerevisiae*. *Microorganisms* 8:323. doi: 10.3390/microorganisms8030323

Huang, K. Y., Chang, T. H., Jhong, J. H., Chi, Y. H., Li, W. C., Chan, C. L., et al. (2017). Identification of natural antimicrobial peptides from bacteria through metagenomic and metatranscriptomic analysis of high-throughput transcriptome data of Taiwanese oolong teas. *BMC Syst. Biol.* 11:131. doi: 10.1186/s12918-017-0503-4

Huang, Z., Huang, L., Xing, G., Xu, X., Tu, C., and Dong, M. (2020). Effect of co-fermentation with *Lactic Acid* bacteria and *K. marxianus* on physicochemical and sensory properties of goat milk. *Foods* 9:299. doi: 10.3390/foods9030299

Jin, M., Gunawan, C., Balan, V., Lau, M. W., and Dale, B. E. (2012). Simultaneous saccharification and co-fermentation (SSCF) of AFEXTM pretreated corn stover for ethanol production using commercial enzymes and *Saccharomyces cerevisiae* 424A(LNH-ST). *Bioresourc. Technol.* 110, 587–594. doi: 10.1016/j.biortech.2012.01.150

Kastman, E. K., Kamelamela, N., Norville, J. W., Cosetta, C. M., Dutton, R. J., and Wolfe, B. E. (2016). Biotic interactions shape the ecological distributions of Staphylococcus species. *mBio* 7, e01157–16.

Kazutaka, S., Tomoya, S., Hiroshi, H., Niroshan, J. L., Miyo, H., Mikako, Y., et al. (2015). Glucosylceramide contained in koji mold-cultured cereal confers membrane and flavor modification and stress tolerance to *Saccharomyces cerevisiae* during coculture fermentation. *Appl. Environ. Microbiol.* 81:3688. doi: 10.1128/AEM.00454-15

Kuda, T., Sarengaole, Takahashi, H., and Kimura, B. (2016). Alcohol-brewing properties of acid- and bile-tolerant yeasts co-cultured with lactic acid bacteria isolated from traditional handmade domestic dairy products from Inner Mongolia. *LWT Food Sci. Technol.* 65, 62–69. doi: 10.1016/j.lwt.2015.07.065

Lee, K. R., Yang, S. M., Cho, S. M., Kim, M., and Chung, S. H. (2016). *Aflatoxin* B1 detoxification by *Aspergillus oryzae* from Meju, a traditional Korean fermented soybean starter. *J. Microbiol. Biotechnol.* 27. doi: 10.4014/jmb.1607.07064

Li, Z., Feng, C., Luo, X., Yao, H., Zhang, D., and Zhang, T. (2018). Revealing the influence of microbiota on the quality of Pu-erh tea during fermentation process by shotgun metagenomic and metabolomic analysis. *Food Microbiol.* 76, 405–415. doi: 10.1016/j.fm.2018.07.001

Liao, E., Xu, Y., Jiang, Q., and Xia, W. (2018). Effects of inoculating autochthonous starter cultures on N -nitrosodimethylamine and its precursors formation during fermentation of Chinese traditional fermented fish. *Food Chemistry* 271, 174–181. doi: 10.1016/j.foodchem.2018.07.186

Lindner, J. D. D., Bernini, V., Lorentiis, A. D., Pecorari, A., Neviani, E., and Gatti, M. (2008). Parmigiano Reggiano cheese: evolution of cultivable and total lactic microflora and peptidase activities during manufacture and ripening. *Dairy Sci. Technol.* 88, 511–523. doi: 10.1051/dst:2008019

Liu, J., Wu, Q., Wang, P., Lin, J., Huang, L., and Xu, Y. (2017). Synergistic effect in core microbiota associated with sulfur metabolism in spontaneous Chinese liquor fermentation. *Appl. Environ. Microbiol.* 83:e01475-17. doi: 10.1128/aem.01475-17

Liu, S. P., Mao, J., Liu, Y. Y., Meng, X. Y., Ji, Z. W., Zhou, Z. L., et al. (2015). Bacterial succession and the dynamics of volatile compounds during the fermentation of Chinese rice wine from Shaoxing region. *World J. Microbiol. Biotechnol.* 31, 1907–1921. doi: 10.1007/s11274-015-1931-1

Liu, S., Chen, Q., Zou, H., Yu, Y., and Zhang, S. (2019). A metagenomic analysis of the relationship between microorganisms and flavor development in Shaoxing mechanized huangjiu fermentation mashes. *Int. J. Food Microbiol.* 303, 9–18. doi: 10.1016/j.ijfoodmicro.2019.05.001

Liu, S., Hu, J., Xu, Y., Xue, J., Zhou, J., Han, X., et al. (2020). Combined use of single molecule real-time DNA sequencing technology and culture-dependent methods to analyze the functional microorganisms in inoculated raw wheat Qu. *Food Res. Int.* 132:109062. doi: 10.1016/j.foodres.2020.109062

Liu, W., Bao, Q., Jirimutu, Qing, M., Siriguleng, Chen, X., et al. (2012). Isolation and identification of lactic acid bacteria from Tarag in Eastern Inner Mongolia of China by 16S rRNA sequences and DGGE analysis. *Microbiol. Res.* 167, 110–115. doi: 10.1016/j.micres.2011.05.001

Liu, Z., Wang, Z., Sun, J., and Ni, L. (2020). The dynamics of volatile compounds and their correlation with the microbial succession during the traditional solid-state fermentation of Gutian Hong Qu glutinous rice wine. *Food Microbiol.* 86:103347. doi: 10.1016/j.fm.2019.103347

Lv, J., Li, C., Li, S., Liang, H., Ji, C., Zhu, B., et al. (2019). Effects of temperature on microbial succession and quality of sour meat during fermentation. *LWT* 114:108391. doi: 10.1016/j.lwt.2019.108391

Marsh, A. J., O"Sullivan, O., Hill, C., Ross, R. P., and Cotter, P. D. (2014). Sequence-based analysis of the bacterial and fungal compositions of multiple kombucha (tea fungus) samples. *Food Microbiol.* 38, 171–178. doi: 10.1016/j.fm.2013.09.003

Mo, H., Zhu, Y., and Chen, Z. (2008). Microbial fermented tea – a potential source of natural food preservatives. *Trends Food Sci. Technol.* 19, 124–130.

Muyzer, G., Brinkhoff, T, Nübel, U, Santegoeds, C, Schäfer, H, Wawer, C. (1998). "Denaturing gradient gel electrophoresis (DGGE) in microbial ecology," in *Molecular Microbial Ecology Manual*, eds A. D. L. Akkermans, J. D. V. Elsas, F. J. D. Bruijn (Dordrecht: Kluwer Academic Publishers), 1–27.

Nagai, T., Staatz, J. M., Bernsten, R. H., Sakyi-Dawson, E. O., and Annor, G. A. (2010). Locally processed roasted-maize-based weaning foods fortified with legumes: factors affecting their availability and competitiveness in accra, ghana. *Afr. J. Food Agric. Nutr. Dev.* 9, 1945–1965. doi: 10.18697/ajfand.30.3425

Negi, B., and Dey, G. (2013). Effects of co-fermentation by *Saccharomyces cerevisiae* and Issatchenkia orientalis on sea buckthorn juice. *Int. J. Food Sci. Nutr.* 64, 508–513. doi: 10.3109/09637486.2012.759182

Nejati, F., Junne, S., and Neubauer, P. (2020). A big world in small grain: a review of natural milk kefir starters. *Microorganisms* 8:192. doi: 10.3390/microorganisms8020192

Nie, Z., Zheng, Y., Xie, S., Zhang, X., Song, J., Xia, M., et al. (2017). Unraveling the correlation between microbiota succession and metabolite changes in traditional Shanxi aged vinegar. *Sci. Rep.* 7:9240. doi: 10.1038/s41598-017-09850-6

Niu, C., Min, S., Jia, Y., Zhao, J., and Li, Q. (2018). Adaptive evolution of *Aspergillus oryzae* 3.042 strain and process optimization to reduce the formation of tyrosine crystals in broad bean paste. *J. Food Biochem.* 43:e12716. doi: 10.1111/jfbc.12716

Nout, M. J. R., and Aidoo, K. E. (2010). "Asian Fungal Fermented Food," in *Industrial Applications. The Mycota (A Comprehensive Treatise on Fungi as Experimental Systems for Basic and Applied Research)*, ed. M. Hofrichter, 10. (Berlin: Springer).

Papadimitriou, K., Pot, B., and Tsakalidou, E. (2015). How microbes adapt to a diversity of food niches. *Curr. Opin. Food Sci.* 2, 29–35. doi: 10.1016/j.cofs.2015.01.001

Patra, J. K., Das, G., Paramithiotis, S., and Shin, H. S. (2016). Kimchi and other widely consumed traditional fermented foods of Korea: a review. *Front. Microbiol.* 7:1493. doi: 10.3389/fmicb.2016.01493

Połka, J., Rebecchi, A., Pisacane, V., Morelli, L., and Puglisi, E. (2015). Bacterial diversity in typical Italian salami at different ripening stages as revealed by high-throughput sequencing of 16S rRNA amplicons. *Food Microbiol.* 46, 342–356. doi: 10.1016/j.fm.2014.08.023

Puri, A., Mir, S. R., and Panda, B. P. (2015). Effect of sequential bio-processing conditions on the content and composition of vitamin K2 and isoflavones in fermented soy food. *J. Food Sci. Technol.* 52, 8228–35. doi: 10.1007/s13197-015-1903-3

Romagnoli, G., Knijnenburg, T. A., Liti, G., Louis, E. J., Pronk, J. T., and Daran, J. M. (2015). Deletion of the *Saccharomyces cerevisiae ARO8 gene*, encoding an aromatic amino acid transaminase, enhances phenylethanol production from glucose. *Yeast* 32, 29–45. doi: 10.1002/yea.3015

Rui, Y., Wan, P., Chen, G., Xie, M., Sun, Y., Zeng, X., et al. (2019). Analysis of bacterial and fungal communities by Illumina MiSeq platforms and characterization of Aspergillus cristatus in Fuzhuan brick tea. *LWT Food Sci. Technol.* 110, 168–174. doi: 10.1016/j.lwt.2019.04.092

Shi, W.-K., Wang, J., Chen, F.-S., and Zhang, X.-Y. (2019). Effect of *Issatchenkia terricola* and *Pichia kudriavzevii* on wine flavor and quality through simultaneous and sequential co-fermentation with *Saccharomyces cerevisiae*. *LWT* 116:108477.

Smid, E. J., and Lacroix, C. (2013). Microbe–microbe interactions in mixed culture food fermentations. *Curr. Opin. Biotechnol.* 24, 148–154. doi: 10.1016/j.copbio.2012.11.007

Soni, S., and Dey, G. (2014). Perspectives on global fermented foods. *Br. Food J.* 116, 1767–1787.

Steinkraus, K. H. (2004). "Origin and history of food fermentations," in *Handbook of Food & Beverage Fermentation Technology*, eds Y. H. Hui, L. M. Goddik, A. S. Hansen, J. Josephsen, W. K. Nip, P. S. Stanfield, et al. (New York, NY: Marcel Dekker). 1–7.

Tamang, J. (2010). *Diversity of Fermented Foods*. Boca Raton, FL: CRC Press. doi: 10.1515/znc-2010-3-409

Tamang, J. P., Koichi, W., and Holzapfel, W. H. (2016). Review: diversity of microorganisms in global fermented foods and beverages. *Front. Microbiol.* 7:377. doi: 10.3389/fmicb.2016.00377

Tamang, J., and Kailasapathy, K. (2010a). *Fermented Foods and Beverages of the World*. Boca Raton, FL: CRC Press. 247–261. doi: 10.1201/EBK1420094954

Tamang, J., and Kailasapathy, K. (2010b). Fermented vegetable products. 149–190. doi: 10.1201/EBK1420094954

Tang, Q., He, G., Huang, J., Wu, C., Jin, Y., and Zhou, R. (2019). Characterizing relationship of microbial diversity and metabolite in Sichuan Xiaoqu. *Front. Microbiol.* 10:696. doi: 10.3389/fmicb.2019.00696

Tinzl-Malang, S. K., Rast, P., Grattepanche, F., Sych, J., and Lacroix, C. (2015). Exopolysaccharides from co-cultures of *Weissella confusa* 11GU-1 and *Propionibacterium freudenreichii* JS15 act synergistically on wheat dough and bread texture. *Int. J. Food Microbiol.* 214, 91–101. doi: 10.1016/j.ijfoodmicro.2015.07.025

Tofalo, R., Perpetuini, G., Schirone, M., Suzzi, G., and Corsetti, A. (2013). Yeast biota associated to naturally fermented table olives from different Italian cultivars. *Int. J. Food Microbiol.* 161, 203–208. doi: 10.1016/j.ijfoodmicro.2012.12.011

Wan, W. C. (2007). Discussion on the meaning, the manifestation and the development trend of Chinese wine culture. *Liquor Mak. Sci. Technol.* 5.

Wang, B., Wu, Q., Xu, Y., and Sun, B. (2020). Synergistic effect of multiple saccharifying enzymes on alcoholic fermentation for chinese baijiu production. *Appl. Environ. Microbiol.* 86:e00013-20. doi: 10.1128/aem.00013-20

Wang, J., and Fung, Y. D. (1996). Alkaline-fermented foods: a review with emphasis on pidan fermentation. *Crit. Rev. Microbiol.* 22, 101–138.

Wang, M. Y., Yang, J. G., Zhao, Q. S., Zhang, K. Z., and Su, C. (2018). Research progress on flavor compounds and microorganisms of maotai flavor Baijiu. *J. Food Sci.* doi: 10.1111/1750-3841.14409

Wang, X., Wang, S., and Zhao, H. (2019). Unraveling microbial community diversity and succession of Chinese Sichuan sausages during spontaneous fermentation by high-throughput sequencing. *J. Food Sci. Technol.* 56, 3254–3263. doi: 10.1007/s13197-019-03781-y

Wang, Z. (2016). Brief introduction to the development of the production technology of liquor starter in ancient China. *Liquor Mak. Sci. Technol.* 2.

Wang, Z.-M., Lu, Z.-M., Shi, J.-S., and Xu, Z.-H. (2016). Exploring flavour-producing core microbiota in multispecies solid-state fermentation of traditional Chinese vinegar. *Sci. Rep.* 6:26818. doi: 10.1038/srep26818

Wei, Z., Changqing, Z., and Huibo, L. (2018). Diversity and function of microbial community in chinese strong-flavor baijiu ecosystem: a review. *Front. Microbiol.* 9:671. doi: 10.3389/fmicb.2018.00671

WileyBlackwell (2013). *Comprehensive Reviews in Food Science and Food Safety*. Hoboken, NJ: WileyBlackwell.

Wolfe, B. E., and Dutton, R. J. (2015). Fermented foods as experimentally tractable microbial ecosystems. *Cell* 161, 49–55. doi: 10.1016/j.cell.2015.02.034

Wu, C., Zheng, J., Huang, J., and Zhou, R. (2013). Reduced nitrite and biogenic amine concentrations and improved flavor components of Chinese sauerkraut via co-culture of *Lactobacillus plantarum* and *Zygosaccharomyces rouxii*. *Ann. Microbiol.* 64, 847–857. doi: 10.1007/s13213-013-0724-8

Wu, Q., Chen, B., and Xu, Y. (2015). Regulating yeast flavor metabolism by controlling saccharification reaction rate in simultaneous saccharification and fermentation of Chinese Maotai-flavor liquor. *Int. J. Food Microbiol.* 200, 39–46. doi: 10.1016/j.ijfoodmicro.2015.01.012

Yang, L. (2013). Wine ceremony to lead healthy development of Chinese wine culture. *Liquor Mak. Sci. Technol.* 4.

Yu, X.-W., Wang, L.-L., and Xu, Y. (2009). Rhizopus chinensis lipase: gene cloning, expression in Pichia pastoris and properties. *J. Mol. Catal. B Enzym.* 57, 304–311. doi: 10.1016/j.molcatb.2008.10.002

Yunping, Z., Feifei, Z., Chengnan, Z., Li, Y., Guangsen, F., Youqiang, X., et al. (2018). Dynamic microbial succession of Shanxi aged vinegar and its correlation with flavor metabolites during different stages of acetic acid fermentation. *Sci. Rep.* 8:8612. doi: 10.1038/s41598-018-26787-6

Zha, M., Sun, B., Wu, Y., Yin, S., and Wang, C. (2018). Improving flavor metabolism of *Saccharomyces cerevisiae* by mixed culture with *Wickerhamomyces anomalus* for Chinese Baijiu making. *J. Biosci. Bioeng.* 126, 189–195. doi: 10.1007/s10295-015-1647-0

Zhang, G., Zhang, W., Sadiq, F. A., Sakandar, H. A., and Guoqing, H. (2019). Microbiota succession and metabolite changes during the traditional sourdough fermentation of Chinese steamed bread. *Cyta J. Food* 17, 172–179. doi: 10.1080/19476337.2019.1569166

Zhang, P. Z. (2001). Chinese wine culture-the origin and development of wine. *China Brew.* 38:43. doi: 10.3969/j.issn.0254-5071.2001.01.015

Zheng, X.-W., and Han, B.-Z. (2016). Baijiu, Chinese liquor: history, classification and manufacture. *J. Ethn. Foods* 3, 19–25. doi: 10.1016/j.jef.2016.03.001

Zhou, X.-W., Liu, H.-F., and Zhao, X.-H. (2015). The potencies of three microorganisms to dissipate four organophosphorus pesticides in three food materials during traditional fermentation. *J. Food Sci. Technol.* 52, 7353–7360. doi: 10.1007/s13197-015-1848-6

Zhu, L. L. (2011). Comparative study of wine culture in China and Japan. *J. Jishou Univers.* 32, 124–127. doi: 10.3969/j.issn.1007-4074.2011.05.027

Conflict of Interest: SL and JM were employed by the company Zhejiang Guyuelongshan Shaoxing Wine Co., Ltd.

The remaining authors declare that the research was conducted in the absence of any commercial or financial relationships that could be construed as a potential conflict of interest.

Publisher's Note: All claims expressed in this article are solely those of the authors and do not necessarily represent those of their affiliated organizations, or those of the publisher, the editors and the reviewers. Any product that may be evaluated in this article, or claim that may be made by its manufacturer, is not guaranteed or endorsed by the publisher.

Advantages of publishing in Frontiers

OPEN ACCESS
Articles are free to read for greatest visibility and readership

FAST PUBLICATION
Around 90 days from submission to decision

HIGH QUALITY PEER-REVIEW
Rigorous, collaborative, and constructive peer-review

TRANSPARENT PEER-REVIEW
Editors and reviewers acknowledged by name on published articles

Frontiers
Avenue du Tribunal-Fédéral 34
1005 Lausanne | Switzerland

Visit us: www.frontiersin.org
Contact us: frontiersin.org/about/contact

REPRODUCIBILITY OF RESEARCH
Support open data and methods to enhance research reproducibility

DIGITAL PUBLISHING
Articles designed for optimal readership across devices

FOLLOW US
@frontiersin

IMPACT METRICS
Advanced article metrics track visibility across digital media

EXTENSIVE PROMOTION
Marketing and promotion of impactful research

LOOP RESEARCH NETWORK
Our network increases your article's readership